EXECUTIVE SUMMARY of "C-SMART: a wearable solution to cataracts"

Cataracts is one of the leading causes of preventable blindness worldwide, resulting in an increased level of intraocular light scattering (see Fig. 1), reducing the contrast of retinal images impairing vision. Cataracts can develop at any age due to variety of causes such as falls, UV exposure, or smoking, and they can also be present from birth. However, most cataract cases are linked to the natural aging process of the crystalline lens. According to Statista, a trusted global statistics portal, about 70% of individuals over the age of 65 suffer from cataracts, **affecting approximately 700 million people worldwide**. Left untreated, cataracts are responsible for approximately 51% of the cases of blindness globally, according to the latest study by the World Health Organization. Furthermore, this number is projected to rise in the coming years as life expectancy continues to increase, which makes **ocular cataracts a major health issue**.

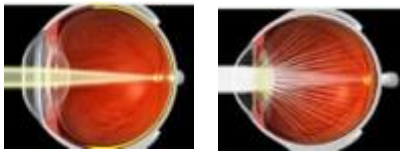

Figure 1: *Schematic of light propagation in a healthy eye (left) and cataractous eye (right). Credit: www.corkeyeclinic.com*

The ONLY treatment for eye cataracts is surgery, where the cataract-affected lens is removed, and then replaced with an intraocular lens. Currently, cataract surgery is typically a safe surgery, with a remarkable 97-98% success rate. However, **it is the only, and invasive, solution.** Due to this invasive nature, despite its effectiveness and ability to restore vision, **cataract surgery is not universally recommended or available for all patients**. This is particularly the case for infants with congenital cataracts, where surgery complications are common, being at a higher risk of blindness. It is not suitable either for patients with other ocular pathologies as corneal or retinal diseases, people with certain chronic diseases or medication, etc. Additionally, **cataract surgery is not equally accessible to the world's population**. Especially in low and middle-income countries (88% of world's population according to The World Bank), people might not have access to a surgeon who can operate cataracts or the financial means to do so. However, being the only existing solution means that people who cannot undergo surgery, will certainly become blind in the coming years.

Figure 2*: Idea sketch on corrector glasses based on Augmented Reality platform.*

The goal of this proposal is the development of the technology and first prototype of the Cataract's smart glasses (C-SMART), a wearable device capable of correcting vision for cataracts patients in an all-optical approach, thus avoiding surgery. This approach will be based on a similar concept to the Augmented Reality (AR) glasses. Here, the AR screen will display a real-time video of the exterior (as shown in Fig.2), wavefront-corrected for vision through cataracts by a miniaturized optical system on the glasses side, enabling a small form-factor for a definitive wearable solution for cataractous vision. If cataracts were corrected by smart glasses, it could revolutionize the lives of not only the community unable to undergo surgery but also of everyone who would prefer to avoid the surgery. Similar to the situation with myopia, where the success rate of surgery is quite high (around 98%), a significant majority of myopic individuals (approximately 80%) opt for non-invasive options like glasses or contact lenses over surgical procedures. The **intended outcomes of this project** are the development of the first prototype of the Cataracts smart glasses, a wearable device for the optical correction of cataracts. A wavefront measurement desktop device will also be developed, for the high-speed measurement of the cataract correction profile and glasses calibration.

The feasibility of this approach is supported by previous proof-of-concept experiments detailed in the full proposal, where we examined light scattering in ex-vivo human cataractous lenses and performed the wavefront correction through such lenses, forming wide-angular images through cataracts. The signal-to-noise-ratio of the focus spot through the cataractous crystalline lens was improved by 80-fold, demonstrating the potential of this technique for controlling light in real human cataractous lenses. We also demonstrated that the wavefront measurement and correction can be done non-invasively, using light reflected from the eye as feedback. In parallel, we have successfully miniaturized the technology required for the wavefront correction, in the form of wearable devices. These proofs of concept demonstrate that there is no physical limitation to the non-invasive (all-optical) correction of cataracts. **Now the open question is: Can Optics and Photonics with the existing technology handle this challenge to make it a practical solution?** I am convinced that, if granted, this project will make this optical solution to cataracts a reality, becoming a global change of paradigm.

C-SMART glasses: a wearable solution to cataracts

Cataracts – a global (and lifelong) visual condition

Cataracts are a common eye condition characterized by lens degradation due to natural protein aggregation. This results in the clouding of the lens and increased light scattering, **leading to blurry vision** [1, 2]. Cataracts can develop at any age due to variety of causes and it can also be present from birth. However, most cataract cases are linked to the natural aging process of the crystalline lens, affecting approximately **70% of individuals over the age of 65**, that is, **700 million people worldwide,** according to Statista. As life expectancy rises, the number of people affected by cataracts is expected to rise globally, positioning ocular cataracts as a major health issue. When cataracts cause visual impairment, **the only solution is a surgical intervention**. Left untreated, cataracts are responsible for approximately 51% of the cases of blindness globally, according to the latest study by the World Health Organization. That is, if a surgical intervention is not possible**, the only alternative is blindness.**

Nowadays cataract surgery is typically a safe procedure, with a remarkable success rate of 97-98%. After cataract removal, an Intraocular Lens (IOL) is injected through a small incision (1-3 mm). Yet, like any surgery, it is not free of risks (e.g. retinal detachment, corneal edemas) [2, 3]. Additionally, this surgery is not universally recommended nor accessible. This is especially true for children with congenital cataracts, with about 30% developing glaucoma and other issues like visual axis opacification soon after surgery [4]. Cataract surgery is not recommended either for those with preexisting ocular pathologies like corneal or retinal diseases or certain chronic conditions or medications. However, surgery is the only available solution, meaning that infants and individuals with these clinical conditions cannot benefit from this reliable yet invasive treatment. This places them at a significant risk of developing blindness if no action is taken. Furthermore, cataract surgery is not equally accessible to the global population. In low and middle-income countries, approximately 7% and 81% of the world's total population (according to the World Bank), many individuals may lack the financial resources or access to surgeons [5,6]. Nonetheless, as the sole existing solution, individuals with these conditions or from these countries may be unable to benefit from this single resource, condemning them to blindness in the years to come.

The big challenge addressed by this project is the development of a non-surgical alternative to cataract surgery based on smart glasses, for the optical correction of cataracts. This alternative would help people who are unsuitable for surgery, or with limited access, to improve vision and avoid blindness. Furthermore, it will also offer an alternative to all those suffering from cataracts that would prefer a non-surgical solution to cataracts, avoiding potential complications that surgery might entail.

To date, most cataract research has primarily focused on enhancing surgical techniques, improving the quality of Intraocular Lenses (IOLs), extending post-operative visual range, exploring new IOL materials, and related aspects [2,3]. Nevertheless, the challenges associated with surgery have prompted research groups worldwide to explore alternative approaches. These alternatives have predominantly concentrated on the development of novel pharmacotherapies, with the goal of chemically dissolving cataracts, albeit with limited success in human trials thus far [7]. It was not until recently that the concept of a non-surgical optical correction for cataracts emerged, pioneered by Professor Artal's group [8], which ingeniously merged two originally distinct domains: complex photonics and visual optics. This innovation now represents the state-of-the-art of the approaches developed in this proposal.

State of the art: optical correction of cataracts

Until recently, the optical correction of cataracts had been considered something close to science fiction. This was due to the historic difficulty in understanding light scattering behaviour, and above all, the control of light scattering. In fact, imaging through light-scattering media is still a challenge of big interest in different fields. In recent years, **Wavefront Shaping (WS) techniques have emerged as an excellent tool to improve imaging through scattering media** by spatially modulating the light wavefront, thus controlling the global propagation of light [9]. Any propagating light wave is characterized by the shape of

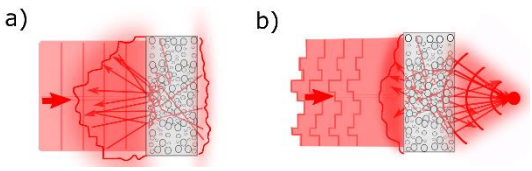

***Figure 1**: Schematic of light propagation into a scattering media before (a) and after (b) WS techniques to focus light on the other side of the scattering medium.*

its wavefront, a two-dimensional surface connecting different positions of the wave with equal phase. The WS technique is based on the coherent control of the light wavefront incident on the scattering medium, where its local amplitude or phase can be modified (and thus light interference), to end up modifying the overall propagation of light macroscopically through such media (Fig. 1).

In visual optics, **the Point Spread Function (PSF) is used to evaluate the quality of eye's optics**. Any disturbance to the eye's PSF will translate into a visual disturbance. Cataracts causes intraocular scattering in the eye lens, therefore affecting the eye's PSF [1]. The retinal image (or any image in general) is given by the convolution of the real object and the eye's PSF (or imaging system's PSF). Equally, by improving the PSF, we improve imaging.

When the eye's lens develops cataracts, the eye's PSF (a sharp peak for young and healthy eyes [1]) flattens, impairing vision. Given that the **eye's PSF is deteriorated by light scattering, it is possible to use WS techniques to control the scattered light**, thus improving the eye's PSF. It is important to note two aspects at this point: first, WS have demonstrated to be efficient at focusing light through scattering materials with optical densities 5 times those found in human cataracts [10], so it is expected to work even with the apparently fully opaque cataracts. Second, approximately after the age of 45, when presbyopia appears, the crystalline lens is rigid, so the scattering occasioned by cataracts in elder patients is static to a good degree, only changing over the period of months/years, as cataracts keep developing. These two factors facilitate the optical-correction approach, meaning that WS techniques would be able to correct cataracts of any opacity degree and that only a static cataract correction should be displayed by correcting smart glasses, making the wearable device easier to develop and calibrate.

When the optimized wavefront leading to the optimal (sharpest) PSF is loaded on the spatial light modulator, the image of the object becomes sharper, consequently improving vision through cataracts. The use of WS to improve the eye´s PSF was initially simulated, obtaining promising results when optimizing the eye's PSF through simulated cataracts [8]. I recently pushed this work forward by demonstrating for the first time how WS can improve the eye's PSF in a cataract's model in a double-pass, that is, in a completely non-invasive configuration [11] using fluorescent feedback mimicking the lipofuscin protein at the retinal pigmented epithelium. We also characterized the behaviour of light scattering in ex-vivo cataractous human crystalline lenses. In particular we studied the optical scattering properties of cataracts, as their optical memory effect, transmitted-image contrast, or the objective straylight parameter to classify the scattering strength of cataracts [12].

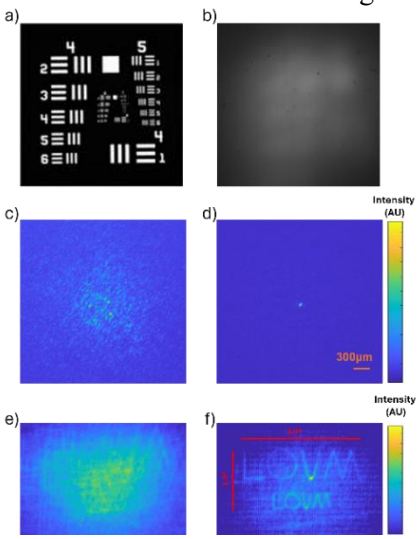

***Figure 2**: a) Object to be imaged through human lenses. b) Image of object in (a) through the cataractous human lens. Panels c) and d) show the PSF of the cataractous lens before and after wavefront optimization, respectively. Panels e) and f) show the image reconstruction with the non-optimized and optimized PSFs, respectively.*

Further advancing in this direction and aided by the knowledge of cataract's scattering, we combined the WS techniques with imaging using a raster-scanning approach for image display, demonstrating the imaging capabilities of the cataract-correction system, as shown in Fig.2. Here **we demonstrated, for the first time, the possibility of optimizing the PSF and extended images through cataracts, using ex-vivo human crystalline lenses and wavefront shaping techniques**. In this experiment, yet unpublished, we used highly opaque cataracts, unable to form a clear image (Fig.2a,b). We successfully optimized the PSF of this lens, with a focus SNR ~80 (Fig.2c,d), with its corresponding imaging improvement (Fig.2e,f), enabling image formation in an otherwise opaque lens, that would make the patient clinically-blind. Although these results can be considerably improved in several aspects, this proof of concept demonstrates that retinal-image restoration through cataracts is possible using WS.

In practice, wavefront shaping is achieved using Spatial Light Modulators (SLMs) as wavefront correctors. These are electronic devices, typically working in reflection, that enable the spatial manipulation of both phase and/or amplitude of the wavefront. The wavefront manipulation for vision correction and simulation based on adaptive optics was developed long time ago [13], with the existence of commercial desktop devices for those purposes (VAO, Voptica SL, Spain). Common SLMs used for wavefront modulation include Liquid Crystal on Silicon (LCoS), Digital Micromirror Devices

(DMD), and deformable mirrors. Two key considerations for our application are optimization speed (to be performed while the eye is stationary) and cost-effectiveness for wearable devices. For cost-effectiveness, Vertical Aligned LCoS is the best choice, designed for LCD micro-displays, offering significantly lower prices than other LCoS alternatives. Although primarily not designed for phase modulation, we have demonstrated recent work has demonstrated their potential in phase modulation tasks, including vision correction [14,15]. Feedback-based wavefront shaping is one of the most robust approaches in low signal-to-noise conditions, as it will be our case. State-of-the-art methodologies for faster iterative wavefront optimization include the use of micro-electro-mechanical system (MEMS) based mirror arrays [16], obtaining up to 4.1kHz rates, the use of binary DMDs in phase modulation [17] or the use of Grating Light Valves [18], reducing the optimization time to 2.4 milliseconds.

Project goal and work packages

The goal of this proposal can be divided into three main Aims or Work Packages contributing to the global goal of the project:

- **Aim 1** (WP1): High-speed performance of cataract's wavefront measurement, and wavefront corrector calibration, including high-speed hardware and software development.
- **Aim 2** (WP2): C-Smart glasses development, including pupil control and integrated software.
- **Aim 3** (WP3): Development of a desk-top device for real-time cataract's wavefront measurement (*WAMES*) for patients measurement and C-SMART glasses calibration.

Methodology and Workplan

WP1: In this WP we will **implement the complete cataract correction system on the optical bench focusing on high-speed performance.** As per today, we have the system fully working on the optical bench for artificial eyes, however the measurement of the cataract's wavefront phase takes too long, in the order of 10 minutes. Although for static eyes this speed is ok, when transitioning to real patients this speed needs to be drastically accelerated. As mentioned before, this is possible and has been done before in the literature [16-18], however, we need faster modulators, which will be purchased with the allocated budget of this project, if granted. Therefore, in this work package **the optimization algorithm will be optimized in speed**, to perform the cataract's wavefront measurement in real-time.

Currently the optical system is equipped with a Digital Micromirror Device as SLM, a green laser (532nm) and 2D fast steering mirror for image drawing by raster scanning. In this work package the laser and fast steering mirror will be substituted by a **Maxwellian display based on three lasers (RGB),** to display full-colour images, for which we will use the commercial augmented reality display RETISSA Display II from QD Laser (Japan), enabling us to optimize white images instead of monochromatic ones. Finally, a **highly sensitive photodetector** typically used for retinal imaging (H9305-02, Hamamatsu, Japan) will be integrated, for testing the system with real retinas and cataractous lenses, which will also help the speeding up of the wavefront optimization process.

The last task on this work package will be to include a corrector module, integrating an extra modulator only used for correction in an auxiliary optical path, independent from the modulator performing the optimization measurement. This corrector modulator will be the same that later on will be used in the C-SMART glasses, an economical device without special speed requirements, since a static wavefront is required for the correction. We will **study how to best perform the calibration of the phase wavefront between the different modulators** (the high-speed and expensive modulator for measurement and the economical and low speed one for correction). The figure of merit for the calibration will be the optimized PSF, the SNR of the peak should be equal using the corrector module.

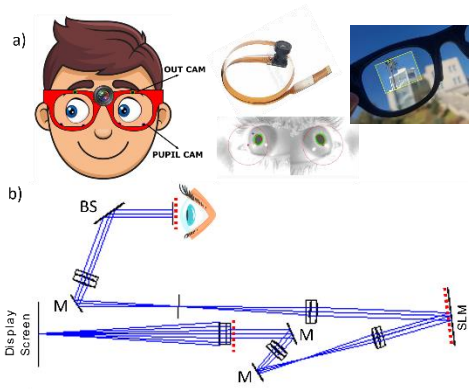

***Figure 3**: a) Schematic of the C-SMART glasses appearance, highlighting the position of the front and pupil cameras. On the right side, a cartoon simulating the vision these glases, with the augmented reality screen showing the corrected video-see-through. B) Optical design of the the C-SMART glasses, with two 4f systems conjugating the eye pupil plane with the SLM and display pupil.*

WP2: In this work package we will develop the **first prototype of the C-SMART glasses** using economical components. These glasses will be based on a phase SLM

and an RGB laser-based Maxwellian display (RETISSA Display II, QD Laser, Japan) streaming a video-see-through image of the outside, delivered by a small front camera (Fig.3a). The device will also be equipped with pupil cameras and infrared LEDs for pupil illumination, giving information about gaze direction to the system under any illumination condition.

The optical correction of cataracts is carried out in several steps, first the front camera captures the outside world, which is displayed with no latency by the RGB display screen, as in schematic of Fig. 3b. This light wavefront is then modulated by an SLM in the typical configuration of an adaptive optics visual corrector or simulator [13], inputting the cataract correction wavefront to the incident light (previously measured with a desktop/table top system). The SLM is optically conjugated with the eye pupil plane, finally sending to the eye the cataract-corrected-video image of the exterior. This image is finally delivered to the subject by a beam splitter (BS), which combines the direct see-through images and the corrected-video-image, as in Fig.3a. Different tests for evaluating the imaging and correction capabilities of the glasses will be performed. The case for the glasses will be 3D printed. A custom software integrating the information from the pupils, front camera, RGB display and SLM will be developed to have all these elements properly synchronized.

If time permits, the beam splitter combiner will be substituted by an RGB waveguide from Dispelix, in particular the Dispelix Selva offering 40º of FOV display. Initially the system will only correct for far vision, and if time permits, an extra 1D MEMs mirror and compact translation stage will be placed for vergence control, enabling accommodation and correction at all-distances [19].

WP3: In this work package, **the high-speed measurement system will be integrated into a desktop mobile platform** for the cataract's wavefront measurement and scattering characterization (*WAMES*). This system will be equipped with a joystick and a chinrest, to enhance the measurement process for subjects, as shown in Fig.4. It will also serve as a platform for connecting the C-SMART glasses to perform wavefront correction calibration of the smart glasses. Calibration tests of the wavefront correction with the smart glasses will be performed. A gaze fixation light will be used for this task (FIX LED in Fig.4), to ensure that correction is performed for the same gaze direction than correction. The system will also have the same Maxwellian display (LBS: Laser Beam Scanning system) than the glasses, to ensure an efficient wavefront correction, which strongly depends on the laser wavelength. Scattering characterization will be carried out by using the Optical Integration Method [20], by using a camera imaging the retinal plane (PSF CAM in Fig.4). Initial measurements will be taken with ex-vivo human cataractous lenses and retinas, obtained by our long-term collaborators from Hospital "Virgen de la Arrixaca". After the initial tests, the system will be moved to the Hospital to test real patients, evaluating the C-SMART glasses performance, as well as the perceived enhancement in visual acuity or contrast sensitivity.

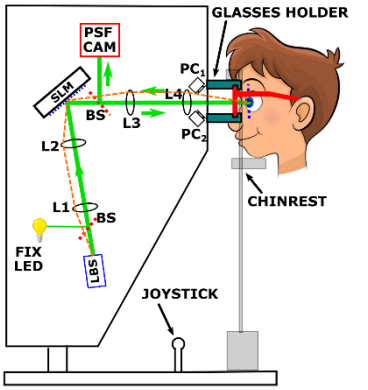

Figure 4: *Schematic of WAMES system, with the glasses holder system for C-SMART glasses calibration.*

Main IMPACT and OUTCOMES of the project

The main outcomes of this project, expected to cause a significant technical impact in the field's state of art are:

1) The development of **the first optical system to ever correct vision through cataracts in real patients**, paving the way for the optical correction of other ocular diseases based on light scatter.
2) Development of **the first working prototype of cataract's smart glasses (*C-SMART*)**, setting the basis for a commercial device, becoming the **first and only non-surgical alternative to cataract surgery**.

The **potential social impact of the project is extremely significant**, given that, if granted, with this project we will develop for the first time a non-surgical correction to cataract, with the **potential of contributing with our work to the future eradication of preventable cataract's blindness**. Due to the high impact cataracts have worldwide, this project has the **potential of changing the life of millions of people globally**, when cataract surgery is not recommended or available and for those who prefer to avoid surgery. The technology development carried out in this project has the potential to be successfully transferred also to other visual affections as corneal opacification, opening new opportunities that had not been addressed yet due to the lack of appropriate technology and approaches.

Risk contingency plan of the project

Due to the innovative and multidisciplinary character of this proposal, which brings together state-of-the-art smart glasses technology, complex photonics and visual sciences, risks are necessarily present. There are **three principal risks** to take care of: **first**, that the wavefront measurement and correction cannot be performed in real-time. We will devote 12 months to this task, to allow enough time for problem solving, as well as holding collaborations with expert personnel with expertise in computer engineering, physics and electrical engineering, which will minimize the risk. Even if that is not enough, the pupil tracking software will allow to pause and resume wavefront measurement, ensuring success, even with slow functioning. **Second**, the optimized PSF signal-to-noise ratio (SNR) is too small to improve imaging through cataracts. According to our simulations [11] a SNR of 80 significantly improves imaging, and we are confident of achieving SNR improvements much larger than that, as we have done preliminarily, and has been widely done in the literature. **Third**, the corrector modulator might be too slow for wavefront correction. The intended modulator has a refresh rate of 100Hz, and cataracts remain static for several months, meaning that the same correction should be valid for several months, after which a re-calibration should be done using the *WAMES* system.

References

[1] Artal, P. (2017). *Handbook of visual optics. Volume 1*. CRC Press.
[2] Liu, Y. C. *et al.* (2017). Cataracts. *The Lancet*, *390*(10094), 600-612.
[3] Davis, G. (2016). The evolution of cataract surgery. *Missouri medicine*, *113*(1), 58.
[4] Lenhart, P. D., & Lambert, S. R. (2022). Current management of infantile cataracts. *Survey of Ophthalmology*, *67*(5), 1476-1505.
[5] Wang, W. *et al.* (2017). A global view on output and outcomes of cataract surgery with national indices of socioeconomic development. *Investigative ophthalmology & visual science,* 58(9), 3669-3676.
[6] Resnikoff, S. *et al.* (2020). Estimated number of ophthalmologists worldwide (International Council of Ophthalmology update): will we meet the needs?. British Journal of Ophthalmology, 104(4), 588-592.
[7] Heruye, S. H., *et al.* (2020). Current trends in the pharmacotherapy of cataracts. *Pharmaceuticals*, *13*(1), 15.
[8] Arias, A. and Artal, P. (2020). Wavefront-shaping-based correction of optically simulated cataracts. *Optica, 7*(1), 22-27.
[9] Vellekoop, I.M. and Mosk, A.P. (2007) Focusing coherent light through opaque strongly scattering media. *Opt. Lett*. 32(16), 2309-2311.
[10] Liu, Y., *et al.* (2018). Time-reversed ultrasonically encoded optical focusing through highly scattering ex vivo human cataractous lenses. *Journal of Biomedical Optics, 23*(1), 010501-010501.
[11] Paniagua-Díaz, *et al.* (2021). Double-pass wavefront shaping for scatter correction in a cataract's model. *Optics Express*, *29*(25), 42208-42214.
[12] Paniagua-Diaz, A. M., *et al*. (2023). Optical memory effect of excised cataractous human crystalline lenses. *Biomedical Optics Express*, *14*(2), 639-650.
[13] Marcos, S., *et al*. (2022). Adaptive optics visual simulators: a review of recent optical designs and applications. *Biomedical Optics Express*, *13*(12), 6508-6532.
[14] A. Arias, *et al.* (2020) "Phase-only modulation with two vertical aligned liquid crystal devices". Optics Express, **28**, 34180-34189
[15] A. M. Paniagua-Diaz, *et al.* (2022) "Vertical-aligned liquid crystal devices for ocular wavefront correction and simulation". Optical Engineering, **61**, 121806.
[16] Blochet, B., *et al.* (2017) "Focusing light through dynamical samples using fast continuous wavefront optimization". Opt. Lett. 42, 4994–4997.
[17] Conkey, D. B., *et al*. High-speed scattering medium characterization with application to focusing light through turbid media. Opt. Express 20, 1733–1740 (2012).
[18] Tzang, O., *et al*. (2019). Wavefront shaping in complex media with a 350 kHz modulator via a 1D-to-2D transform. *Nature Photonics*, *13*(11), 788-793.
[19] Sager, S., *et al.* (2024, March). A binocular adaptive optics visual simulator with convergence control. In *Ophthalmic Technologies XXXIV* (Vol. 12824, pp. 155-157). SPIE.
[20] Ginis, H. S., *et al.* (2011). Wide-Angle Point Spread Function of the Human Eye: An Optical Procedure to Measure Scatter. *Investigative Ophthalmology & Visual Science*, *52*(14), 5274-5274.

Guiding cancer therapies with light

Executive summary for health challenge

Challenge. Even with modern therapies, patients with advanced stages of cancer often face drug resistance, a phenomenon in which cancer cells are intrinsically immune to anticancer drugs or acquire immunity during therapy. Hence, drug resistance renders cancer therapy futile. Unfortunately, since many cancers are detected and treated at advanced stages, *drug resistance is a major contributor to the mortality of cancer patients*. Cutaneous melanoma – a malignancy that accounts for over 80% of deaths related to skin cancer – not only epitomizes drug resistance but also exposes the lack of adequate methods for addressing it. The molecular testing (analysis of genetic material) of recurrent melanoma tumors is the clinical standard for identifying the genes that drive the malignancy and the mutations linked with drug resistance. Molecular testing guides targeted therapies against these oncogenes, effectively shrinking tumors during the early stages of therapy.

However, despite apparent success, most melanoma patients develop drug resistance and succumb to cancer. By relying solely on the genetic mechanisms of drug resistance, the clinical standard for guiding therapies neglects the morphofunctional properties of the tumor microenvironment (***TME***) – a key driver of drug resistance. The clinical standard delivers incomplete information about drug resistant tumors, leading to ineffective treatments. *This deficiency contributes to over 65,000 annual deaths* of melanoma patients worldwide and *highlights a global need for methods that fully elucidate the mechanisms of drug resistance*.

Biophotonics solution. By imaging the TME, nonlinear optical microscopy can identify the specific biochemical and structural properties of melanoma that support drug resistance. Yet, state-of-the-art systems face three main limitations that hinder their clinical success: ***i***) Bulky, inefficient, and expensive laser infrastructure restricts them to specialized labs. ***ii***) Narrowband detection schemes reduce the specificity of imaging platforms. ***iii***) Limited contrast palettes fail to provide complementary signals, compromising the ability to discern pathological states.

This project will overcome these limitations through two key technological innovations: a compact, cost-effective laser source capable of producing the necessary radiation for parallel excitation of all relevant nonlinear signals, and a novel multichannel detector that shifts the detection scheme from narrowband to broadband. These innovations are encapsulated in spectrally-resolved nonlinear optical microscopy (***SRNOM***), a translatable imaging platform that co-registers vibrational and emission spectra to achieve superior analytical power. Because these spectroscopic fingerprints are molecule-specific, *SRNOM spatially resolves the composition of specimens in a label-free and non-destructive fashion*, delivering images with intrinsic chemical contrast. SRNOM will identify the features that furnish drug-resistant tumors, reveal morphofunctional mechanisms that govern drug resistance, and enable effective guided therapies against melanoma in clinics.

Impact. The success of this project has three implications on human health: ***i)*** SRNOM could establish a new clinical paradigm for guiding melanoma therapies. By interrogating the TME prior to treatment, SRNOM, in concert with molecular testing, could predict the response to therapy, pointing clinical oncologists to more effective drug combinations. ***ii)*** SRNOM could routinely assess melanoma tumors, evaluating the progress of therapy without biopsies. ***iii)*** SRNOM could quantify the effects of drugs on preclinical models, supporting drug discovery efforts. Therefore, by leveraging novel optical technology, *this project could lead to cancer therapies guided by light*.

Introduction and background

Cutaneous melanoma is an aggressive form of skin cancer that efficiently metastasizes, leading to poor survival rates, becoming the deadliest skin cancer[1]. The incidence rate of this malady has consistently increased worldwide, with a 27% rise in the annual diagnosis of invasive melanoma cases over the past decade (2013 – 2023)[2]. While conventional cancer treatments fail to treat metastatic melanoma, targeted therapies hold potential by blocking the specific genetic and molecular mechanisms that support cancer growth. Sadly, most melanoma patients subjected to targeted therapies face drug resistance and suffer the deadly relapse of cancer[3–5].

Drug resistance is the main challenge of modern treatments for advanced melanoma. Current efforts for identifying resistance focus on the genetic and epigenetic mechanisms driving this phenomenon[3]. These efforts use molecular testing, including genomic, proteomic, and functional analysis of biopsies or body fluids (blood or urine), to reveal the genes and pathways that dictate the response of tumors to drugs[6–8]. Molecular testing determines the molecular signatures and genotypes underlying drug resistance. These predictive factors are crucial for defining treatment strategies, enabling targeted therapies to use drugs that block the specific genetic and molecular mechanisms supporting melanoma. Because molecular testing enables targeted therapies to extend the patients' lives or, in some cases, cure the disease, it is the clinical standard for guiding treatment decisions. Despite the success of molecular testing, the response of melanoma to targeted therapies is transient in over half of patients, leading to several deadly relapses. Hence, *comprehensive assessment of drug-resistant melanoma is still missing in clinical oncology*[9–11].

While genetic and epigenetic factors are relevant mechanisms of drug resistance, the tumor microenvironment (***TME***) plays an equally important role[12]. Consider, for example, the effects induced by the abnormally high acidity of the TME, a condition that leads to the trapping of drugs with basic pH before reaching their target. Another source of TME-induced drug resistance stems from the extracellular matrix, the structure that procures mechanical support to cells, which in tumors becomes so dense that it prevents drugs from diffusing into neoplasms. Additional properties of the TME that drive drug resistance include hypoxia, vascular irregularities, cellular heterogeneity, metabolic alteration, and soluble species within the tumor milieu that interfere with the intended effect of drugs[13–15]. Manifestly, the TME is a critical factor in drug resistance[16].

Problem statement and objective of the project

The problem with established techniques for assessing resistance in melanoma is that they *neglect the spatial properties of the TME, missing the microscopic heterogeneity* of the chemistry, structure, and function of tumors[17–20]. By ignoring the TME, the clinical standard provides an incomplete picture of melanoma, preventing clinical oncologists from selecting drugs that arrest cancer progression without undergoing resistance. This limitation calls for methods capable of *revealing the properties of the TME in real-time and directly from the skin of patients*, methods that would deliver adjuvant feedback to molecular testing, leading to a holistic view of drug-resistant melanoma. This feedback would steer targeted therapies toward the most effective drugs against melanoma, allowing treatments tailored to the current pathological state of the TME.

Therefore, *the objective of this project is to develop a clinically translatable optical technology for TME screening* (***Aim 1***). From chemical images, this technology will identify the spectroscopic signatures related to the morphofunctional properties of melanoma cells and tumors in both resistant and non-resistant states (***Aim 2***), enabling the prediction of drug resistance in melanoma tumors (***Aim 3***). Thus, *this project could clear the next hurdle of targeted therapies*.

Implementation

By analyzing the intrinsic spectroscopic signatures of the TME, imaging techniques can discriminate the pathological states of tumors, distinguishing resistant from non-resistant states[21–23].This *discriminatory power would enable the prediction of drug resistance*. Nonlinear optical microscopy, which merges spectroscopy and imaging, offers a powerful tool for screening the TME. This modality charts specimens using light originating from the nonlinear response of native biomolecules in tissues to ultrashort pulse lasers, allowing fast chemical imaging at subcellular resolution in a label-free and nondestructive manner. By simultaneously detecting these signals, a nonlinear microscope attains complementary contrasts that enable analytical chemical imaging.

These contrasts include multiphoton and vibrational signals [24–31]. The multiphoton signals are second harmonic generation (SHG), third harmonic generation (THG), and multiphoton-absorption fluorescence (MPAF). SHG and THG reveal architectural features of tissues[32–35], while MPAF uncovers key biochemical properties, notably metabolism and homeostasis[36–41]. The exemplary vibrational signal is coherent anti-Stokes Raman scattering (CARS), a process that relies on the vibration of chemical bonds to expose DNA, proteins, carotenoids, and lipids, thus mapping tissues with molecular contrast[28,42–45]. Therefore, *nonlinear signals could reveal the spectroscopic profiles of the TME in drug-resistant and non-resistant states, elucidating the mechanisms underlying drug resistance*.

While nonlinear signals could predict drug resistance, state-of-the-art nonlinear microscopes exhibit three limitations that prevent this feat in clinical settings:

i) ***Bulky and expensive infrastructure:*** Modern microscopes require various lasers or additional optical devices for driving all the contrasts. This requirement increases the cost, dimensions, and complexity of the systems, thus constraining the microscopes to specialized laser labs.

ii) ***Narrowband detection:*** By capturing a few spectral bands, modern microscopes discard the information encoded in the spectra. This scheme (unchanged since the 1990s[46,47]) reduces the analytical power of nonlinear microscopy and its capacity to discern pathological states.

iii) ***Lack of complementarity:*** Modern microscopes measure either multiphoton or vibrational signals, revealing only molecular or structural features, resulting in an incomplete profile.

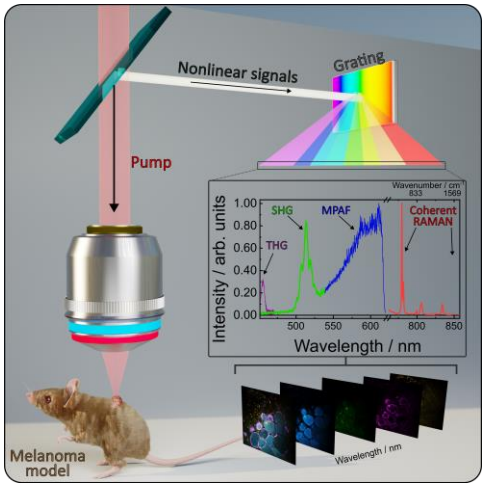

Figure 1*. Concept of SRNOM: breaking the narrowband paradigm of nonlinear microscopy to exploit the spectroscopic power of the nonlinear signals. The insets show data from mouse kidney.*

This project aims to overcome these limitations by developing spectrally resolved nonlinear optical microscopy (***SRNOM***). This translatable and cost-effective platform features a novel laser source and a broadband detection scheme to drive and measure the spectra of all the nonlinear signals, *enabling investigations of drug-resistant melanoma with full analytical power* (Figure 1).

The execution of this project will take place at the Beckman Institute for Advanced Science and Technology and the Cancer Center at Illinois (CCIL). As a Beckman fellow, I have access to all the necessary resources, equipment, and infrastructure for the successful implementation of the project, including state-of-the-art imaging systems, computational tools, and animal facilities.

Technological outcomes

This project will deliver SRNOM along with the two technological innovations driving it: ***i)*** the *LAser source for VIbrational and Multiphoton analytical contrasts* (***LAVIM***) and ***ii)*** the *MultiChannel Detector of spectral nonlinear Signals* (***MCDS***). LAVIM eliminates the need for bulky and expensive lasers, while MCDS enables broadband detection, *enabling a comprehensive and synergistic contrast palette suited for clinical applications*. Figure 2 shows the scheme of SRNOM.

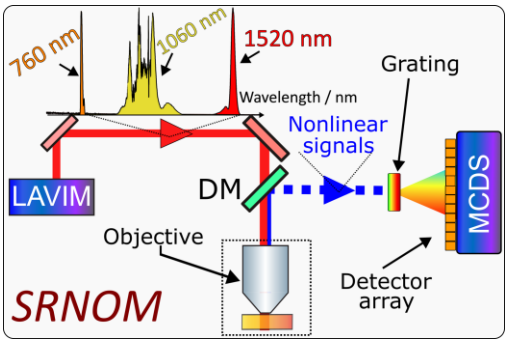

Figure 2 *SRNOM schematic. DM: Dichroic.*

Laser source for vibrational and multiphoton analytical contrasts (LAVIM)

SRNOM will use LAVIM, a compact and cost-effective source. LAVIM – *a system that I devised, built, and tested* – provides the spectral support and power needed for driving all the signals of the nonlinear contrast palette (Figure 3 (a)). LAVIM builds on a solid-state oscillator, leveraging supercontinuum generation[48] and Type 0 (quasi-) phase matching[49]. This simple design results in a laser source with almost four times less cost and size compared to current solutions.

LAVIM exhibits excellent noise performance. It matches the noise level of commercial solid-state optical parametric oscillators (OPOs) and easily outperforms fiber-based systems. Evidence of this is the relative intensity noise (RIN) of LAVIM and other laser sources used in nonlinear microscopes (Figure 3 (b)). The RIN is a metric for how noisy a laser is at a given modulation frequency (the closer to zero, the noisier the source[50]). LAVIM's low noise enables the fast acquisition required for high-speed imaging.

Upon tuning the position of a crystal, LAVIM also delivers radiation within 1200 to 1700 nm (Figure 3 (c)), light that suffers less tissue-scattering, enabling deep tissue explorations[51]. Finally, due to its versatile spectral capabilities, LAVIM can provide the frequency detuning for probing molecular vibrations in the full Raman spectrum[52]. *My preliminary data validates the capacity of LAVIM to drive nonlinear signals (Figure 3 (d-e)), demonstrating its potential to revolutionize the field of nonlinear microscopy*.

By delivering several spectral bands with a single laser, LAVIM enables the parallel excitation of all the relevant nonlinear signals, offering an unprecedented contrast palette for observing the TME with new colors. *This potential can help me establish a new research niche and propel me toward an independent career, applying this source to investigate cancer*.

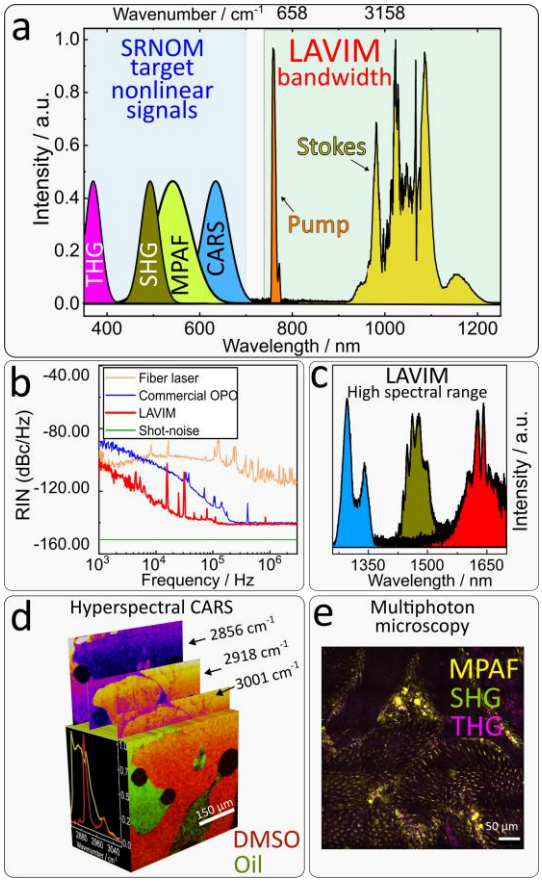

Figure 3 *a) Lower spectral range of LAVIM for driving SRNOM. b) RIN traces at 1030 nm. c) Higher spectral range of LAVIM for deep tissue imaging. d) Hyperspectral CARS of a DMSO-Oil mixture. e) Multiphoton imaging of mouse testis.*

Multichannel detector of spectral nonlinear signals (MCDS)

Nonlinear optical microscopes have been operating with a narrowband scheme for over 30 years[46,47]. This scheme, which hinders the specificity of nonlinear microscopy, stems from a lack of detectors sensitive enough to capture the weak nonlinear signals at high speeds. While CCD/CMOS[30,53] chips can detect the spectra of these signals, their low transfer rates prevent fast hyperspectral imaging. To address this obstacle, SRNOM will use MCDS, a system that combines arrays of photomultiplier tubes, a multichannel high-speed digitizer, and the lock-in technique. MCDS will allow spectral acquisition of nonlinear contrasts, *breaking the narrowband paradigm* and enabling the full analytical power and complementary nature of nonlinear microscopy.

MCDS adapts an analog lock-in amplification technique I previously used to detect pump-probe and stimulated Raman[29,54,55] signals into the digital domain for homodyne multiphoton and vibrational detection. This approach, facilitated by the low noise of LAVIM, will detect even the weakest spectral signals, resulting in a fast and ultrasensitive spectrometer for nonlinear optical microscopy. This stage of the project will capitalize on the vast expertise of scientists in my home institution, the Beckman Institute for Advanced Science and Technology, including researchers developing biophotonics (Prof. Stephen A. Boppart) and ultrasound technology (Prof. Michael Oelze). Serendipitously, the latter has extensive experience with ultrafast multichannel detection.

Because it transcends the narrowband paradigm and enables the investigation of tissues with unprecedented chemical specificity, *MCDS, along with LAVIM, will not only establish me as a leading developer of imaging technologies but also drive new discoveries in cancer research*.

Cancer research outcomes – predicting drug resistance in melanoma animal models *in vivo*.

This project will explore the potential of SRNOM for predicting drug resistance in melanoma. Upon successful completion, it will shed new light on the still obscure role of the TME in drug-resistant melanoma and provide a new tool to predict it. Thus, this project will deliver fundamental insights into drug resistance mechanisms and the means to anticipate them. Therefore, *the most relevant outcome of this project is the prediction of drug resistance in melanoma tumors*. By developing and validating the SRNOM technology, this project lays the foundations for clinical experiments, i.e., predicting melanoma drug resistance in humans, and paves the way for a new paradigm in determining treatment choices, choices that could improve the survival of patients.

To achieve this predictive capability, mice with melanoma tumors in resistant and non-resistant states will receive targeted therapy[56]. SRNOM will image the tumors sprouting on the animals, producing time-dependent maps of the TME in both states. This imaging will reveal the impact of therapy on the tumors by recording the structural transformation, alongside the biochemical and dynamic changes of the TME.

SRNOM will identify the spectral and spatial profiles of resistant and non-resistant states, delivering data that will train a deep neural network (DNN)[57,58] to recognize these characteristic profiles. Once trained, *the DNN will be able to discriminate between tumors in these states (Figure 4), enabling the prediction of drug resistance by optically screening the TME*.

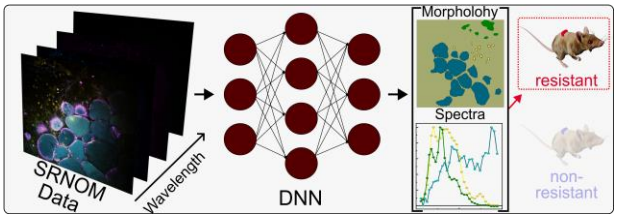

Figure 4 *A DNN will use SRNOM data to identify resistant and non-resistant tumors, predicting drug resistance in melanoma.*

This stage of the project will leverage the infrastructure of the CCIL and the expertise of researchers, including Profs. Erik R. Nelson and Chitra Subramanian, who specialize in cancer therapies. Their teams will oversee the melanoma models and treatments, as well as advise me on the biological interpretation of the data. The support from the CCIL will sustain the cancer research component of the project, ensuring the resources and guidance to execute it.

Finally, these experiments and their outcomes will give me *skills in preclinical practices along with the credentials for establishing myself as a relevant scientist* in the field of cancer research.

Impact

This project will supply unprecedented imaging technology to support the fight against melanoma, a cancer that causes several deaths worldwide every year. While the main goal is to address a global health challenge, this project will achieve it by advancing optical technologies. Therefore, this project would have technological and human health implications, simultaneously impacting my professional life. Below, I describe the anticipated impacts in each of these domains.

Technological impact. *SRNOM encapsulates the technological impact of the proposal*. On the one hand, its novel laser source (LAVIM) produces the radiation needed for simultaneously driving all the nonlinear contrasts, generating this light in a compact and cost-effective platform. Contrary to conventional systems, this source permits both parallel excitation of the nonlinear signals and clinical translation. On the other hand, its detector (MCDS) shifts the detection scheme from the narrowband to the broadband regime, not only driving forward a stagnated nonlinear microscopy field but also harnessing the full spectroscopic nature of the nonlinear signals. These innovations take SRNOM beyond the state-of-the-art in nonlinear microscopy, endowing it with the analytical power and portability required for predicting resistance in clinics.

Health impact. *This project aims to address the next hurdle of clinical oncology* against melanoma: drug resistance. SRNOM will reveal the pathological state of the TME, providing. the missing piece of information to fully characterize this phenomenon. The preclinical approach proposed paves the way for clinical applications, where a comprehensive view of resistance prior to treatments will allow oncologists to choose the best drugs to treat melanoma, thus maximizing therapy efficacy. Since SRNOM enables routine assessments of tumors, oncologists will no longer wait until the patient is cured or succumbed to cancer to evaluate the intervention. The possibility to repeat screenings would provide feedback to tailor the therapies to the ever-evolving state of the TME, enhancing the effectiveness of interventions and improving patient survival. Thus, *this project could establish a new clinical standard for guiding cancer therapies with light*.

Career development impact. *The Optica Foundation Challenge could be a catalyst for my career*. The program prize would give me the economic means to develop the proposed technology, thus establishing my research niche. The execution of the project would give me cancer research skills and the chance to produce work that could be published in top-tier journals – the SRNOM implementation in Optica and the prediction of resistance in Nature Cancer. Therefore, this project could give me credentials in both biophotonics and cancer research, *propelling me toward an independent research career*. Finally, receiving the Optica Foundation Challenge award would be an extraordinary honor that would galvanize my career, supporting advances in nonlinear microscopy and cancer research for a lasting impact.

References

1. Thompson, J. F., Scolyer, R. A. & Kefford, R. F. Cutaneous melanoma. *The Lancet* **365**, 687–701 (2005).
2. Melanoma Research Alliance. Melanoma Statistics. *https://www.curemelanoma.org/about-melanoma/melanoma-101/melanoma-statistics-2* (2024).
3. Winder, M. & Virós, A. Mechanisms of Drug Resistance in Melanoma. in 91–108 (2017). doi:10.1007/164_2017_17.
4. Long, G. V. *et al.* Adjuvant Dabrafenib plus Trametinib in Stage III *BRAF* -Mutated Melanoma. *New England Journal of Medicine* **377**, 1813–1823 (2017).
5. Kozar, I., Margue, C., Rothengatter, S., Haan, C. & Kreis, S. Many ways to resistance: How melanoma cells evade targeted therapies. *Biochimica et Biophysica Acta - Reviews on Cancer* vol. 1871 313–322 Preprint at https://doi.org/10.1016/j.bbcan.2019.02.002 (2019).
6. Harris, T. J. R. & McCormick, F. The molecular pathology of cancer. *Nat Rev Clin Oncol* **7**, 251–265 (2010).
7. Hunt, J. L. Applications of molecular testing in surgical pathology of the head and neck. *Modern Pathology* **30**, S104–S111 (2017).
8. Scaini, M. C. *et al.* A multiparameter liquid biopsy approach allows to track melanoma dynamics and identify early treatment resistance. *NPJ Precis Oncol* **8**, 78 (2024).
9. Sabnis, A. J. & Bivona, T. G. Principles of Resistance to Targeted Cancer Therapy: Lessons from Basic and Translational Cancer Biology. *Trends in Molecular Medicine* vol. 25 185–197 Preprint at https://doi.org/10.1016/j.molmed.2018.12.009 (2019).
10. Goldie, J. H. Drug resistance in cancer: A perspective. *Cancer and Metastasis Reviews* **20**, 63–68 (2001).
11. Dagogo-Jack, I. & Shaw, A. T. Tumour heterogeneity and resistance to cancer therapies. *Nat Rev Clin Oncol* **15**, 81–94 (2018).
12. Villanueva, J. & Herlyn, M. Melanoma and the tumor microenvironment. *Curr Oncol Rep* **10**, 439–446 (2008).
13. Naser, R., Fakhoury, I., El-Fouani, A., Abi-Habib, R. & El-Sibai, M. Role of the tumor microenvironment in cancer hallmarks and targeted therapy (Review). *International Journal of Oncology* vol. 62 Preprint at https://doi.org/10.3892/IJO.2022.5471 (2023).
14. Kaemmerer, E., Loessner, D. & Avery, V. M. Addressing the tumour microenvironment in early drug discovery: a strategy to overcome drug resistance and identify novel targets for cancer therapy. *Drug Discovery Today* vol. 26 663–676 Preprint at https://doi.org/10.1016/j.drudis.2020.11.030 (2021).

15. Mackenzie, N. J. *et al.* Modelling the tumor immune microenvironment for precision immunotherapy. *Clinical and Translational Immunology* vol. 11 Preprint at https://doi.org/10.1002/cti2.1400 (2022).

16. Egeblad, M., Nakasone, E. S. & Werb, Z. Tumors as Organs: Complex Tissues that Interface with the Entire Organism. *Dev Cell* **18**, 884–901 (2010).

17. Garraway, L. A. & Jänne, P. A. Circumventing Cancer Drug Resistance in the Era of Personalized Medicine. *Cancer Discov* **2**, 214–226 (2012).

18. Gajewski, T. F. The Next Hurdle in Cancer Immunotherapy: Overcoming the Non–T-Cell–Inflamed Tumor Microenvironment. *Semin Oncol* **42**, 663–671 (2015).

19. Russo, M. *et al.* Tumor Heterogeneity and Lesion-Specific Response to Targeted Therapy in Colorectal Cancer. *Cancer Discov* **6**, 147–153 (2016).

20. Sarmento-Ribeiro, A. B., Scorilas, A., Gonçalves, A. C., Efferth, T. & Trougakos, I. P. The emergence of drug resistance to targeted cancer therapies: Clinical evidence. *Drug Resistance Updates* **47**, (2019).

21. Zwielly, A., Gopas, J., Brkic, G. & Mordechai, S. Discrimination between drug-resistant and non-resistant human melanoma cell lines by FTIR spectroscopy. *Analyst* **134**, 294–300 (2009).

22. Ebenezar, J., Pu, Y., Liu, C. H., Wang, W. B. & Alfano, R. R. Diagnostic Potential of Stokes Shift Spectroscopy of Breast and Prostate Tissues — A Preliminary Pilot Study. *Technol Cancer Res Treat* **10**, 153–161 (2011).

23. Hope, C. K., Billingsley, K., de Josselin de Jong, E. & Higham, S. M. A Preliminary Study of the Effects of pH upon Fluorescence in Suspensions of Prevotella intermedia. *PLoS One* **11**, e0158835 (2016).

24. You, S. *et al.* Intravital imaging by simultaneous label-free autofluorescence-multiharmonic microscopy. *Nat Commun* **9**, (2018).

25. Tu, H. *et al.* Stain-free histopathology by programmable supercontinuum pulses. *Nat Photonics* **10**, 534–540 (2016).

26. Cheng, J.-X. & Xie, X. S. Vibrational spectroscopic imaging of living systems: An emerging platform for biology and medicine. *Science (1979)* **350**, aaa8870–aaa8870 (2015).

27. Evans, C. L. & Xie, X. S. Coherent Anti-Stokes Raman Scattering Microscopy: Chemical Imaging for Biology and Medicine. *Annual Review of Analytical Chemistry* **1**, 883–909 (2008).

28. Vanna, R. *et al.* Vibrational imaging for label-free cancer diagnosis and classification. *La Rivista del Nuovo Cimento* **45**, 107–187 (2022).

29. De la Cadena, A., Valensise, C. M., Marangoni, M., Cerullo, G. & Polli, D. Broadband stimulated Raman scattering microscopy with wavelength-scanning detection. *Journal of Raman Spectroscopy* jrs.5816 (2020) doi:10.1002/jrs.5816.

30. Valensise, C. M. *et al.* Removing non-resonant background from CARS spectra via deep learning. *APL Photonics* **5**, (2020).

31. De la Cadena, A. *et al.* Simultaneous label-free autofluorescence multi-harmonic microscopy driven by the supercontinuum generated from a bulk nonlinear crystal. *Biomed Opt Express* **15**, 491 (2024).

32. Smith, D. R., Winters, D. G. & Bartels, R. A. Submillisecond second harmonic holographic imaging of biological specimens in three dimensions. *Proceedings of the National Academy of Sciences* **110**, 18391–18396 (2013).

33. Murray, G. *et al.* Aberration free synthetic aperture second harmonic generation holography. *Opt Express* **31**, 32434 (2023).

34. Masihzadeh, O. *et al.* Third harmonic generation microscopy of a mouse retina. *Mol Vis* **21**, 538–547 (2015).

35. Hu, C. *et al.* Harmonic optical tomography of nonlinear structures. *Nat Photonics* **14**, 564–569 (2020).

36. Xu, C. & Webb, W. W. *Measurement of Two-Photon Excitation Cross Sections of Molecular Fluorophores with Data from 690 to 1050 Nm*. *J. Opt. Soc. Am. B* vol. 13 (1996).

37. Xu, C. & Webb, W. W. Multiphoton Excitation of Molecular Fluorophores and Nonlinear Laser Microscopy. in *Topics in Fluorescence Spectroscopy* 471–540 (Springer US, Boston, MA, 2002). doi:10.1007/0-306-47070-5_11.

38. Xu, C. & Wise, F. W. Recent advances in fibre lasers for nonlinear microscopy. *Nature Photonics* vol. 7 875–882 Preprint at https://doi.org/10.1038/nphoton.2013.284 (2013).

39. Kobat, D., Horton, N. G. & Xu, C. In vivo two-photon microscopy to 1.6-mm depth in mouse cortex. *J Biomed Opt* **16**, 106014 (2011).

40. Lakowicz, J. R. *Topics in Fluorescence Spectroscopy*. *Springer* vol. 2 (Springer US, 2002).

41. Croce, A. C. & Bottiroli, G. Autofluorescence spectroscopy and imaging: A tool for biomedical research and diagnosis. *European Journal of Histochemistry* **58**, 320–337 (2014).

42. Cheng, Ji-Xin Min, Wei Ozeki, Yasuyuki Polli, D. *Stimulated Raman Scattering Microscopy: Techniques and Applications*. (Elsevier, 2021).

43. Cheng, J.-X. & Xie, X. S. Coherent Anti-Stokes Raman Scattering Microscopy: Instrumentation, Theory, and Applications. *J Phys Chem B* **108**, 827–840 (2004).

44. Lee, H. J. *et al.* Assessing Cholesterol Storage in Live Cells and C. elegans by Stimulated Raman Scattering Imaging of Phenyl-Diyne Cholesterol. *Sci Rep* **5**, 7930 (2015).

45. Lu, F.-K. *et al.* Label-free DNA imaging in vivo with stimulated Raman scattering microscopy. *Proceedings of the National Academy of Sciences* **112**, 11624–11629 (2015).

46. Denk, W., Strickler, J. H. & Webb, W. W. Two-photon laser scanning fluorescence microscopy. *Science* **248**, 73–6 (1990).

47. Zumbusch, A., Holtom, G. R. & Xie, X. S. Three-dimensional vibrational imaging by coherent anti-stokes raman scattering. *Phys Rev Lett* **82**, 4142–4145 (1999).

48. Dudley, J. M., Genty, G. & Coen, S. Supercontinuum generation in photonic crystal fiber. *Rev Mod Phys* **78**, 1135–1184 (2006).

49. Hum, D. S. & Fejer, M. M. Quasi-phasematching. *C R Phys* **8**, 180–198 (2007).

50. Paschotta, R. RP Photonics Encyclopedia. *Article on 'Relative Intensity Noise'* https://www.rp-photonics.com/relative_intensity_noise.html (2021).

51. Hontani, Y., Xia, F. & Xu, C. Multicolor three-photon fluorescence imaging with single-wavelength excitation deep in mouse brain. *Sci Adv* **7**, 3531–3548 (2021).

52. Polli, D., Kumar, V., Valensise, C. M., Marangoni, M. & Cerullo, G. Broadband coherent Raman scattering microscopy. *Laser Photon Rev* **12**, 1800020 (2018).

53. Vernuccio, F. *et al.* Fingerprint multiplex CARS at high speed based on supercontinuum generation in bulk media and deep learning spectral denoising. *Opt Express* **30**, 30135 (2022).

54. Sciortino, G. *et al.* Four-Channel Differential Lock-in Amplifiers With Autobalancing Network for Stimulated Raman Spectroscopy. *IEEE J Solid-State Circuits* **56**, 1859–1870 (2021).

55. De La Cadena, A. *et al.* Broadband stimulated Raman imaging based on multi-channel lock-in detection for spectral histopathology. *APL Photonics* **7**, (2022).

56. Larkin, J. *et al.* Combined Vemurafenib and Cobimetinib in BRAF -Mutated Melanoma . *New England Journal of Medicine* **371**, 1867–1876 (2014).

57. Zhou, Z.-H. A brief introduction to weakly supervised learning. *Natl Sci Rev* **5**, 44–53 (2018).

58. Shi, J. *et al.* Weakly Supervised Identification and Localization of Drug Fingerprints Based on Label-Free Hyperspectral CARS Microscopy. *Anal Chem* **95**, 10957–10965 (2023).

Optica Foundation Challenge 24: Executive Summary

TerRaman - A Raman Scattering Tool for Depth-Resolved Soil Monitoring

For millennia, it has been understood that poor soil health precludes a bountiful harvest. However, it wasn't until the start of the First World War that human civilization appreciated the dire need for synthetic fertilizers. Even after Fritz Haber won the 1918 Nobel Prize for the process of ammonia distillation, efficient distribution of synthetic fertilizers was sparse due to inconsistent or unavailable soil monitoring practices. Today, nearly half of Earth's population depends on synthetic fertilizers for agriculture, yet soil erosion, pollution, and drought still plague the industry. Additionally, a large portion of carbon credits and other economic incentives are capriciously awarded to companies and communities despite a lack of evidence for tangible results such as soil carbon capture (C-fix) and methane reduction. **As sustainability efforts abound, accurate measurement and identification of soil conditions will become critical to the efficient allocation of resources, whether biochemical or monetary.**

Despite the recent globalization of many crops, the majority are still only feasible in certain climates and soil conditions. Therefore, a single standard soil composition does not exist. Accurate monitoring requires several measurements such as moisture level, inorganic nutrient content, and organic content, including microorganisms or pollutants.Current methods rely on separate modalities for moisture, mineral, and organic content, many of which require consumables, processing, and analysis at centralized facilities. Wide-field measurements using drones, such as UV or reflectance spectroscopy, capture only surface-level information or, at best, low-resolution information about irrelevant minerals. Furthermore, drone assessment is infrequent and inaccessible to most small farms. By harnessing the power of inelastic scattering of monochromatic light (Raman Scattering), we can quantitatively assess water absorption and organic and inorganic vibrational modes using only optical tools.

The TerRaman platform is a conceptualized spinout of previous successful work in the biomedical space. Our group has recently made tremendous strides in analyzing drug constituents, small metabolites, and living tissues with this platform. Given its versatility and ability to separate and quantify a wide range of molecular moieties, the **TerRaman has the potential to analyze all of the most pertinent compounds in soil, such as carbon content, mineral nutrients, microplastics, oils, pesticides, and water.** There are three inherent barriers for the application of Raman scattering in this space: depth-resolved real-time measurements, fluorescence-background removal, and multi-component quantitation. To overcome these barriers, we seek funding to prototype a multi-level fiber-optic stake capable of assessing spatial distributions of soil components in the field, as well as a multi-wavelength laser source and iterative discrete wavelet transform (IDWT) based deep learning models to generate fluorescence-free Raman spectra. We are currently in the process of translating this technology to the environmental space by securing lab and prototyping facilities at ClimateHaven, an environmentally focused incubator for research and discovery. If we are successful, the TerRaman holds significant potential for ensuring the efficient use of biochemical and monetary resources. Whether improving agricultural productivity or enhancing carbon capture, biochemical and economic inputs are essential. **By providing accurate, continuous soil monitoring ensures that these inputs are used judiciously, enhancing their efficacy and reducing waste. Successful translation of basic biomedical Raman scattering research can support sustainable farming practices and environmental stewardship, ultimately benefiting the global community.**

Optica Foundation Challenge 24: Full Proposal

TerRaman - A Raman Scattering Tool for Depth-Resolved Soil Monitoring

The need for accurate, continuous soil monitoring has become increasingly critical in modern agriculture and environmental management. Soil health is the foundation of agricultural productivity, and its monitoring is essential for crop yield optimization and sustainability. Accurate soil monitoring allows for the precise application of fertilizers, pesticides, and other biochemical resources, leading to cost savings and reduced environmental impact. Studies have shown that tailored nutrient management, based on real-time soil data, can significantly increase crop yields while minimizing the overuse of fertilizers [1]. This precision agriculture approach not only improves the economic returns for farmers but also mitigates the adverse effects of nutrient runoff, which can lead to water pollution and eutrophication in nearby water [2].

Carbon capture is another area where accurate soil monitoring is essential. Soil acts as a significant carbon sink, and practices such as no-till farming, cover cropping, and organic amendments can enhance soil carbon sequestration [3,4]. By accurately measuring soil carbon levels, farmers and land managers can implement practices that maximize carbon storage (C-fix), thereby contributing to climate change mitigation. Moreover, accurate soil carbon measurement is crucial for verifying carbon credits, which are traded in carbon markets as part of global efforts to reduce greenhouse gas emissions [5].The ability to provide verifiable data on soil carbon levels can unlock substantial monetary incentives for farmers, making sustainable practices economically viable.

Table 1. Summary of soil analysis methods. Recent developments in basic Raman Scattering research are highlighted.

	Traditional Soil Sampling and Lab Analysis	Soil Testing Kits	Electrical Conductivity Meters	Moisture Sensors (Electromagnetic or Neutron Based)	TerRaman
Cost Efficiency	✗	✓	✓	✓	✓
Time Efficiency	✗	✗	✓	✓	✓
Specificity and Sensitivity	✓	✗	✗	✓	✓
Effective Depth Profiling	✓	✗	✗	✓	✓
Fluorescence Background Removal	✗	N/A	N/A	N/A	✓
High Multi-parameter Capability	✓	✓	✗	✗	✓

There are already several methods of soil assessment, but as shown in Table 1 above, each carry their own disadvantages such as requiring separate tests for different soil parameters [6–9]. These can be time-consuming and require contractor analysis. In contrast, Raman scattering, a technique based on the inelastic scattering of monochromatic light, remains underutilized in this space. When a laser interacts with molecules, especially the easily polarizable carbon-based particles of interest, it induces vibrations in the molecules, which scatter the light at different wavelengths **(Fig. 1)** [10,11]. This scattered light, known as the Raman spectrum, provides a molecular fingerprint of the soil's composition. Raman scattering can detect various soil components, including organic biota, inorganic nutrients, and contaminants, with high specificity and sensitivity in a single analysis[12].

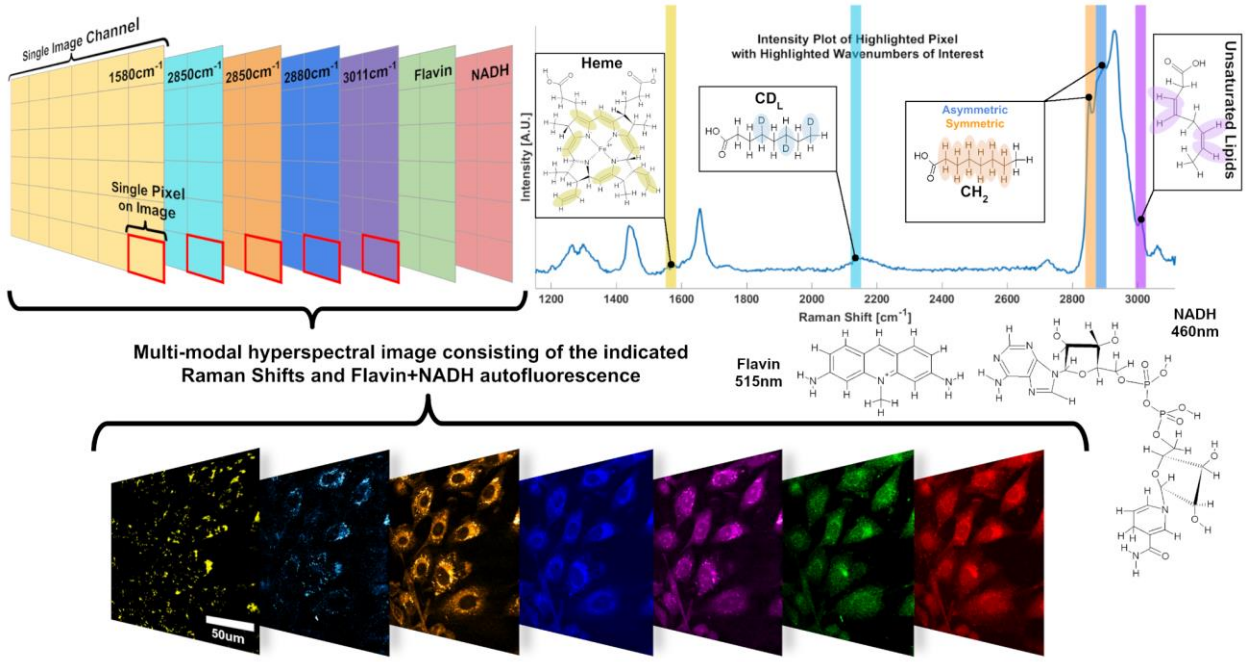

Fig. 1 Illustration of Raman Scattering concept, applied to biological samples. Raman Scattering can be applied both chemometrically, in the form of a spectrum, and spatially, in the form of a selective image of a specific rho-vibrational mode. Taken with permission from Fung, A. et al. *Front. In Onc.* 2022 [10].

A significant advantage of Raman scattering is its ability to provide detailed molecular information without the need for extensive sample preparation or the use of consumables. This makes it an efficient and cost-effective method for continuous soil monitoring. Recently, Raman spectroscopy was integrated with water testing devices, enabling real-time detection of microplastics in water [13]. Additionally, Raman scattering can enhance the verification of carbon credits, with an estimated market size of USD $800B, by providing accurate measurements of soil carbon content [14]. This can facilitate the efficient and transparent trading of carbon credits, promoting sustainable land management practices and contributing to global carbon reduction goals.

Problem Statement/ Objective

As highlighted in Table 1, three key developments in Raman-based soil evaluation that may bridge the inherent gap between Raman Scattering and the environmental domain are: depth resolved measurements, fluorescence background removal, and multi-component signal decomposition. Recent publications from our group have demonstrated early success in biological

tissues, however more work must be done to establish this method in the field. **Through this translation and development of optical Raman Scattering technology, we aim to develop a robust, real-time, and comprehensive soil monitoring tool that can significantly enhance agricultural productivity, facilitate efficient resource allocation, and support global sustainability efforts.**

Outcomes

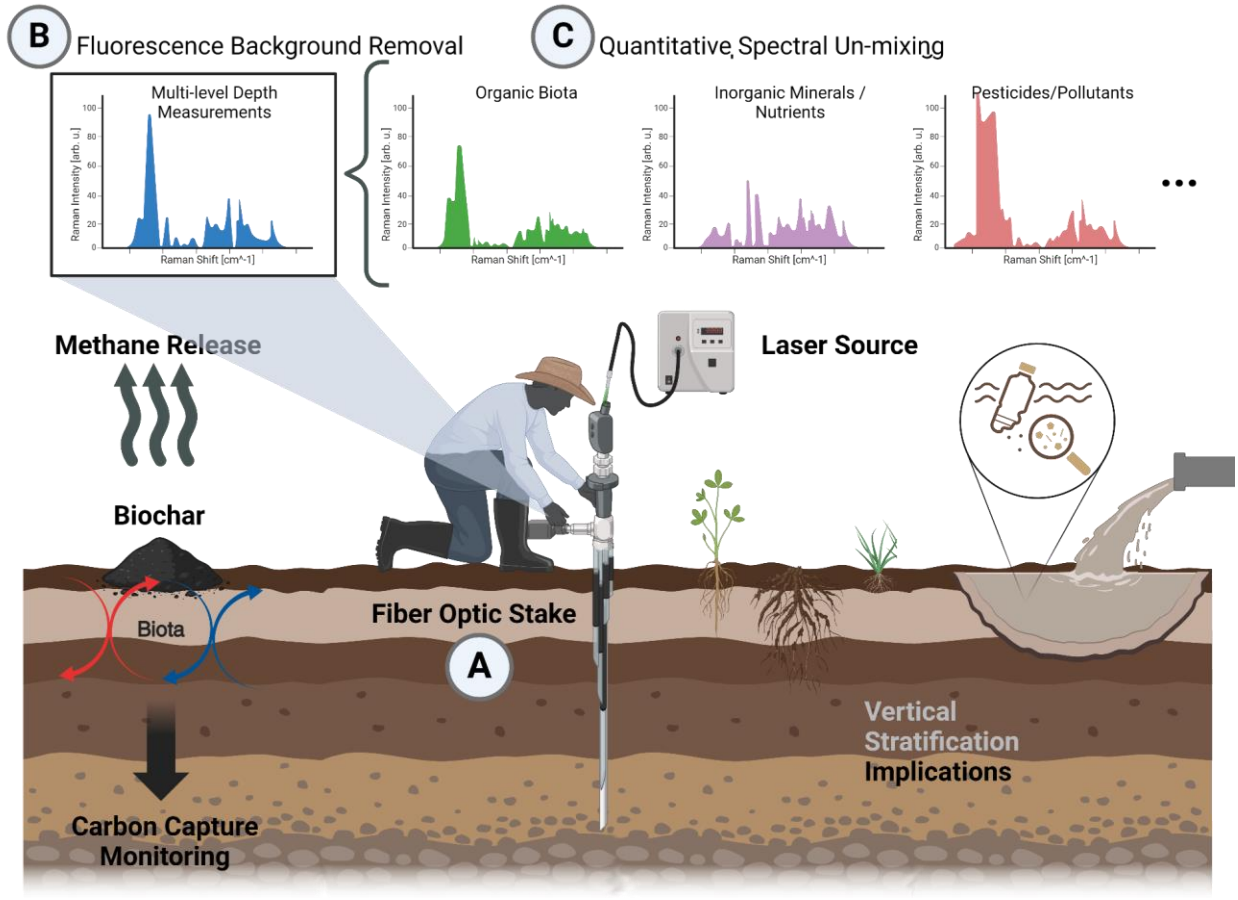

Fig. 2 Summary of problem statement and objectives. (A) Development of a fiber optic stake to asses multi-level depth-resolved Raman Spectral measurements to assess vertical stratification of soil content including organic biota and related carbon fixation, microplastic and oil pollution, water band absorbance, fertilizer and pesticide penetration. **(B)** Development of fluorescence background removal algorithms. **(C)** Signal decomposition to unmix critical components quantitatively. Created with license in BioRender.

The successful completion of this project will address the critical challenges of depth-resolved measurements, fluorescence background removal, and signal decomposition in Raman spectral analysis. First, understanding the vertical distribution of soil components such as top-soil nutrients, water-level, and pollutants is crucial for optimizing crop yields, especially in varying agricultural conditions. This knowledge is crucial to the efficient application of resources and irrigation practices. To tackle this, we will prototype an optical fiber stake that can be driven into the earth to capture multi-level spectral measurements (**Fig. 2A**). Necessary components are an optically clear protective sheath, and Gradient-index (GRIN) lenses to slightly extend the working distance [15–17]. This stake will enable depth-resolved analysis, providing comprehensive data on soil composition at various depths. Such detailed insights are essential for managing soil health

and optimizing resource use, ultimately supporting better crop management and sustainable farming practices.

Next, some soils contain a high fluorescence background, which can obscure the Raman signal and complicate analysis. To address this, we are developing background-removal algorithms that will process the Raman spectra in real-time, eliminating fluorescence interference and enhancing the clarity of the measurements (**Fig. 2B**). In addition, we aim to test far UV wavelength lasers to avoid excitation of native fluorescent compounds and therefore contaminating quantum yield. This innovation will ensure that the Raman signal is accurately interpreted, leading to precise quantification of soil components.

Signal decomposition is another vital aspect of Raman spectral analysis. Accurate assessment of compounds of interest, such as minerals, nutrients, and pollutants, depends on the ability to unmix complex spectra into their constituent components (**Fig. 2C**). Our novel unmixing method, Penalized Reference Matching (PRM), offers a significant advancement over current algorithms [18]. PRM is computationally faster and more robust than pseudo-inverse matrix multiplication-based or multivariate curve resolution-based algorithms, providing more reliable results in less time (**Fig. 3**) [18]. This method will allow us to isolate and quantify various soil components, enhancing the overall effectiveness of our soil monitoring technology. This capability is particularly valuable where timely and accurate soil information is crucial for making informed decisions on resource allocation, whether surrounding arable land, polar ice caps, or extraterrestrial bodies. It is also practical because this algorithm allows for any Raman spectrum to serve as a reference standard, including complex mixtures of chemicals such as pesticides.

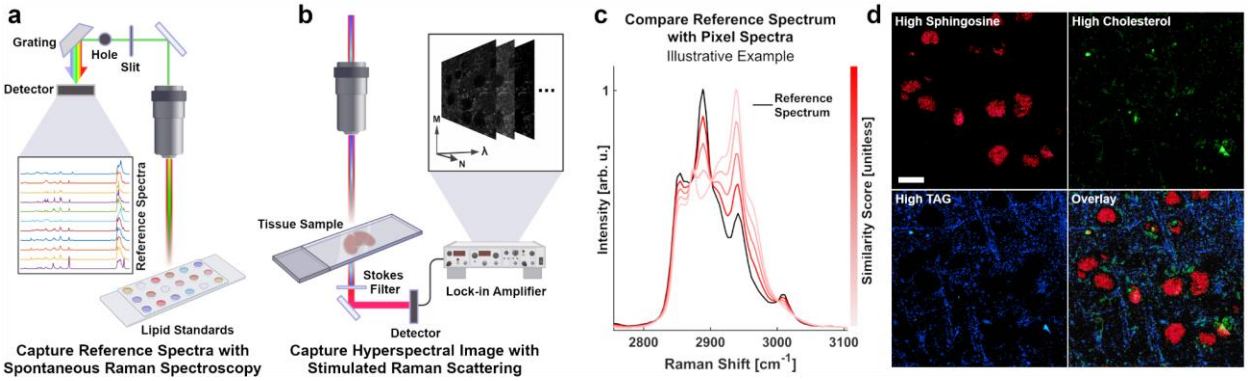

Fig. 3 Summary of PRM concept, as applied to biological specimens. (A) A lipid subtype standard is analyzed by spontaneous Raman spectroscopy and preprocessed to generate a reference spectrum. **(B)** A sample is imaged using SRS to generate a HSI. **(C)** Each pixel of the HSI is a vector of intensity values that represent the Raman spectrum at that pixel. These spectra are compared using spectral angle mapping and illustrate how dissimilar spectra have a lower cosine similarity. **(D)** An example of a mouse brain sample with thresholded similarity scores with respect to sphingosine, cholesterol, and TAG. Pixel intensities are scaled to their similarity scores. Taken with permission from Fung, A., Zhang, W., Li, Y., et al. *Nat. Methods.* 2024.

Much of this basic research has been successfully developed for the biomedical space, where Raman Scattering has been used to analyze drug constituents, small metabolites, and living tissues. While the theoretical foundations are solid, translating this technology into a viable prototype for environmental applications poses unique challenges and opportunities. Unlike biomedical research, which often attracts significant funding from entities like the NIH, environmental applications require specific adaptations and targeted support to realize their full potential. Therefore, this proposal seeks critical funding to bridge this gap and translate our advanced Raman Scattering technology into a practical, field-deployable tool for soil monitoring.

In summary, the integration of Raman scattering into soil monitoring systems holds significant potential for ensuring the efficient use of biochemical and monetary resources. By addressing these challenges and achieving these outcomes, this project will significantly enhance soil monitoring capabilities, leading to more efficient resource use, improved agricultural productivity, and greater environmental sustainability. The TerRaman platform will provide farmers, environmental scientists, and policymakers with a powerful tool to manage soil health and contribute to global sustainability efforts. Whether improving agricultural productivity or enhancing carbon capture, biochemical and economic inputs are essential. By providing accurate, continuous soil monitoring ensures that these inputs are used judiciously, enhancing their efficacy and reducing waste. Successful translation of basic biomedical Raman scattering research can support sustainable farming practices and environmental stewardship, ultimately benefiting the global community.

References

[1] Sabatini, A., Leoni, A., Goncalves, G., Zompanti, A., Marchetta, M. V., Cardoso, P., Grasso, S., Di Loreto, M. V., Lodato, F., Cenerini, C., Figuera, E., Pennazza, G., Ferri, G., Stornelli, V. and Santonico, M., "Microsystem Nodes for Soil Monitoring via an Energy Mapping Network: A Proof-of-Concept Preliminary Study," Micromachines **13**(9), 1440 (2022).

[2] Aryal, J. P., Sapkota, T. B., Krupnik, T. J., Rahut, D. B., Jat, M. L. and Stirling, C. M., "Factors affecting farmers' use of organic and inorganic fertilizers in South Asia," Environ. Sci. Pollut. Res. Int. **28**(37), 51480–51496 (2021).

[3] Jenkins, C. R., Cook, P. J., Ennis-King, J., Undershultz, J., Boreham, C., Dance, T., de Caritat, P., Etheridge, D. M., Freifeld, B. M., Hortle, A., Kirste, D., Paterson, L., Pevzner, R., Schacht, U., Sharma, S., Stalker, L. and Urosevic, M., "Safe storage and effective monitoring of CO2 in depleted gas fields," Proc. Natl. Acad. Sci. U. S. A. **109**(2), E35–E41 (2012).

[4] "Environmental Integrity Carbon Capture, Use, and Sequestration.", .

[5] "Why transparency is key to scaling carbon removal.", World Econ. Forum, 9 October 2023, <https://www.weforum.org/agenda/2023/10/why-transparency-is-key-to-scaling-carbon-removal/> (24 May 2024).

[6] Ouyang, A., "Soil Moisture: Why Important, What Challenges, How to Measure & More," Latest Open Tech Seeed (2022).

[7] "Basics of irrigation scheduling.", <https://extension.umn.edu/irrigation/basics-irrigation-scheduling> (24 May 2024).

[8] "S1 TITAN Handheld XRF Analyzer.", <https://www.bruker.com/en/products-and-solutions/elemental-analyzers/handheld-xrf-spectrometers/S1-TITAN.html> (24 May 2024).

[9] "SoilOptix.", Deveron.

[10] Fung, A. A., Hoang, K., Zha, H., Chen, D., Zhang, W. and Shi, L., "Imaging Sub-Cellular Methionine and Insulin Interplay in Triple Negative Breast Cancer Lipid Droplet Metabolism," Front. Oncol. **12** (2022).

[11] Fung, A. A. and Shi, L., "Mammalian cell and tissue imaging using Raman and coherent Raman microscopy," 6, WIREs Syst. Biol. Med. **12**(6), e1501 (2020).

[12] Zarei, M., Solomatova, N. V., Aghaei, H., Rothwell, A., Wiens, J., Melo, L., Good, T. G., Shokatian, S. and Grant, E., "Machine Learning Analysis of Raman Spectra To Quantify the Organic Constituents in Complex Organic–Mineral Mixtures," Anal. Chem. **95**(43), 15908–15916 (2023).

[13] Qian, N., Gao, X., Lang, X., Deng, H., Bratu, T. M., Chen, Q., Stapleton, P., Yan, B. and Min, W., "Rapid single-particle chemical imaging of nanoplastics by SRS microscopy," Proc. Natl. Acad. Sci. **121**(3), e2300582121 (2024).

[14] "Global Carbon Markets Get Bigger, Even as Trading Dips.", BloombergNEF (2023).

[15] Lindlein, N. and Herzig, H. P., "Design and modeling of a miniature system containing micro-optics," Gradient Index Miniat. Diffractive Opt. Syst. II **4437**, 1–13, SPIE (2001).

[16] Udd, E. and Spillman, W. B., eds., [Fiber optic sensors: an introduction for engineers and scientists, 2nd ed], John Wiley & Sons, Hoboken, N.J (2011).

[17] Murata, H., [Handbook of optical fibers and cables, 2nd ed], M. Dekker, New York (1996).

[18] Zhang, W., Li, Y., Fung, A. A., Li, Z., Jang, H., Zha, H., Chen, X., Gao, F., Wu, J. Y., Sheng, H., Yao, J., Skowronska-Krawczyk, D., Jain, S. and Shi, L., "Multi-Molecular Hyperspectral PRM-SRS Imaging," 2022.07.25.501472 (2022).

Breaking Reciprocity of Thermal Light Through Nanophotonics for Solar Harvesting at the Thermodynamic Limit

Executive Summary

- Title: Breaking Reciprocity of Thermal Light Through Nanophotonics for Solar Harvesting at the Thermodynamic Limit

- The pertinent global challenge we are seeking to address using optics and photonics belongs to the **environmental** challenge category.

- Solar energy represents a renewable resource with enormous potential to reduce greenhouse gas emissions. However, as a global challenge, their current efficiencies are still far from their thermodynamic limit. The proposed project aims to address the photonic challenge associated with pushing the efficiency of solar energy harvesting to their thermodynamic limit. The high efficiency will bring tremendous environmental and economic benefits.

- As an effective approach to harvesting solar energy, solar thermophotovoltaics (STPVs) promise theoretical efficiency higher than the Shockley-Quiesser limit of single-junction solar cells by utilizing the full spectrum of solar energy. Despite the attractive high efficiencies, existing STPV systems all suffer from exergy destruction resulting from unavoidable back emission from the intermediate layer to the sun caused by reciprocity. Here, we propose to break the reciprocity of thermal light transport to enable nonreciprocal STPV systems that can completely eliminate the back emission and funnel all emission coming from the sun to the cell. In doing so, the efficiency can be improved to as high as 93.3%, significantly higher than traditional STPVs. We propose to study the required nonreciprocal radiative properties to realize a high-performance system in practice. We plan to design a photonic crystal structure with time-reversal breaking materials to create the nonreciprocal properties. With perimetric optimization, we propose to eventually show the first-ever experimental demonstration of nonreciprocal thermal light transport effect. Our results will demonstrate unrealized possibilities for thermal radiation control and pave the way for a new high-performance energy harvesting technique for solar energy.

Breaking Reciprocity of Thermal Light Through Nanophotonics for Solar Harvesting at the Thermodynamic Limit

a. Problem Statement and Objective

This project aims to demonstrate for the first time a reciprocity-breaking effect for thermal light, a technology enabler for single-junction solar cells to achieve record-breaking efficiencies. Solar cells represent the most popular way to utilize sunlight. However, its conversion efficiency is limited to the so-called Shockley-Queisser limit[1] because only the above-bandgap photons can be absorbed and converted to electricity in solar cells. Solar thermophotovoltaics (STPV) is an attractive technology that overcomes these limitations by utilizing the full spectrum of sunlight. As depicted in Fig. 1a, instead of letting the sunlight illuminate the solar cells directly, full-spectrum sunlight is firstly absorbed by a black intermediate layer to heat up the layer to a high temperature. Thermal radiation from the backside of the intermediate layer is absorbed in a TPV cell and converted to electricity. In doing so, one can significantly improve the conversion efficiency[2]. STPVs are actively being commercialized as the next-generation solar energy harvesting technology[3,4].

However, traditional STPVs have a detrimental disadvantage since the intermediate layer in conventional STPVs is reciprocal. Reciprocity guarantees that, while the intermediate layer receives the sunlight, there is unavoidable thermal emission from the top side of the intermediate layer towards the sun, as shown by the purple arrows on top of the emitter in Fig. 1a. This is the well-known Kirchhoff's law of thermal radiation[5,6]. Since the emission towards the sun cannot be harvested and is essentially lost, this back emission represents a primary intrinsic loss mechanism[7].

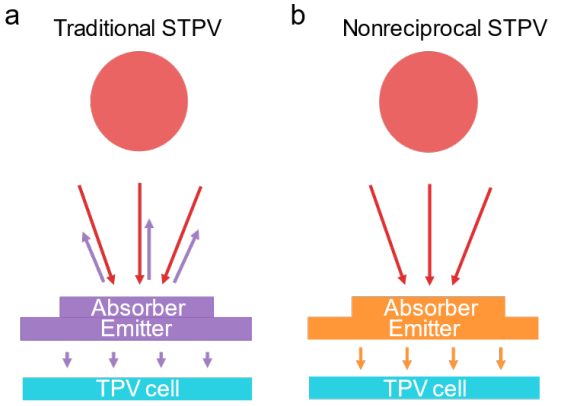

Fig. 1. (a) Traditional STPV with a reciprocal intermediate layer. (b) Proposed NSTPV with a nonreciprocal intermediate layer. In both plots, the intermediate layers consist of an absorber facing the sun and an emitter facing the STPV cell.

Recently, we proposed a **novel nonreciprocal thermal light transport effect** that allows one to break Kirchhoff's law and enable a nonreciprocal solar thermophotovoltaic (NSTPV) system that eliminates the back emission of the intermediate layer towards the sun[8,9], as depicted in Fig. 1b. In NSTPVs, all the emissions from the intermediate layer can be directed to the cell. Such nonreciprocal functionality, therefore, brings a higher photon flux to the thermophotovoltaic cell, resulting in more electric power and higher efficiency. **The PI's group introduced this concept in a recent work[8], which is reported by numerous news media worldwide as a breakthrough for solar energy harvesting.** We have shown that the nonreciprocal STPV system can reach the ultimate efficiency of solar energy harvesting, the Landsberg limit (93.3%). More interestingly, when a single-junction solar cell is used as the TPV cell, our nonreciprocal STPV system can have an amazingly high record-breaking efficiency beyond 60%[6] (the current record is held by NREL's GaAs cell with an efficiency of 30.8 %[10]). Therefore, demonstrating the required thermal light transport provides a clear pathway to revolutionize the traditional wisdom of how single-junction solar cells are used. **In this project, we propose to fabricate the nonreciprocal intermediate layer and provide direct experimental evidence of the nonreciprocal thermal light transport effect for the first time, paving the way for solar energy harvesting at the thermodynamic limit.**

b. Significance and Impact

Nonreciprocal thermal radiative transport has a direct impact on achieving the urgently needed solar energy harvesting technologies with the ultimate efficiency that can generate tremendous economic and environmental impacts. The codes and experimental metrology method gained through this research can be expanded to facilitate benchmarking a broader class of photon-mediated energy harvesting and conversion systems. The results point out the pathway to use topological and magnetic materials for energy applications and pave the way to bring super-efficient solar energy harvesting technologies to the industry.

c. Literature Review and Preliminary Results

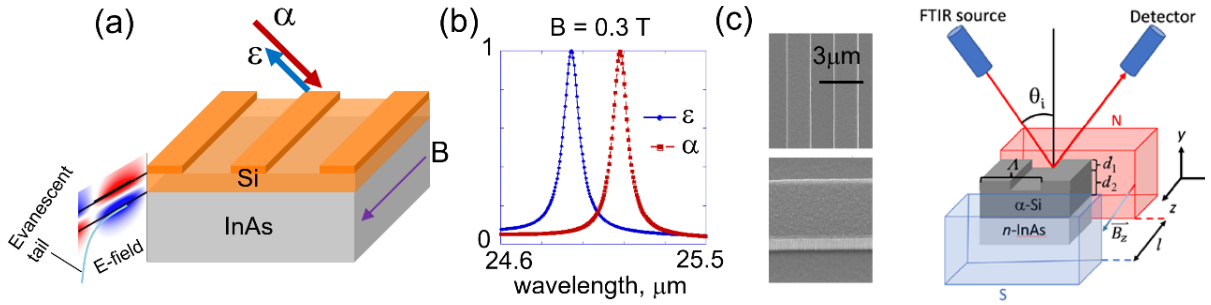

Fig. 2 PI's preliminary work[11,12]: (a and b) A nanophotonics-enhanced nonreciprocal thermal emitter and (c) its experimental demonstration. In (a), the orange material is silicon (Si) and the field distribution is for the electric field (E-field). In (c), the grating is amorphous Si (a-Si).

Recently, the PI demonstrated a pathway to break Kirchhoff's law and achieve strong nonreciprocal thermal emission through periodic grating structures made of magneto-optical materials[11,12]. The key is to use gratings to create strong confinement effects that are sensitive to the applied *B*-field. The PI conducted a thermal emitter design[11] shown in Fig. 2a, which consists of a Si grating atop an InAs substrate. The evanescent tail of the guided optical mode, which represents a highly confined mode in the dielectric grating, extends to the InAs layer. When *B*-field is applied, the evanescent tail of the guided mode is perturbed, resulting in a strong nonreciprocal response. As shown in Fig. 2b, the directional emissivity (*e*) and absorptivity (*a*) spectra are completely not overlapped with each other, indicating a violation of Kirchhoff's law. Based on this design, the PI demonstrated a strong nonreciprocal effect in experiment[9] using **neodymium permanent magnets** (Figs. 2c and 3). We directly measure the emissivity and absorptivity of the structure using reflection and emission spectroscopy. When $B = 0$, the structure is reciprocal and the emissivity and absorptivity contour in Fig. 3a are essentially the same. However, when B = 1T, reciprocity is broken and the emissivity and absorptivity show a contrast which is enhanced by the excitation of the guided modes (the red bands in Fig. 3b).

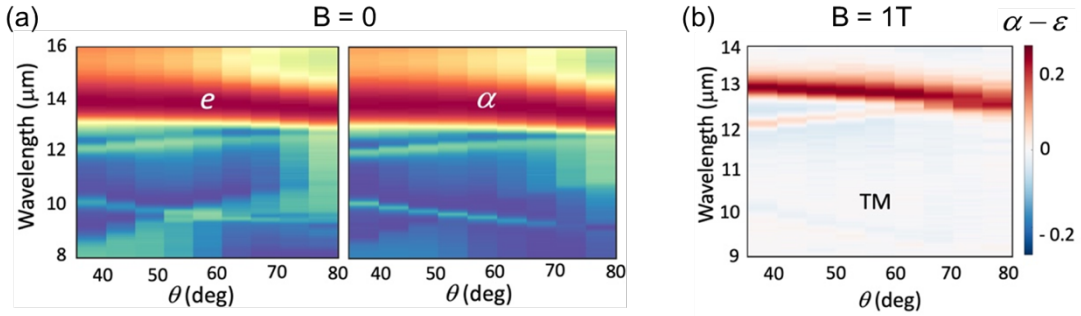

Fig. 3. PI's preliminary work[9]: (a) emissivity and absorptivity contour with no B field applied, i.e., reciprocal. (b) the contrast between emissivity and absorptivity with B = 1T, which breaks the reciprocity of the system.

d. Applicant Expertise

The PI Dr. Bo Zhao has authored over 40 publications in the thermal radiation field, including book chapters for Annual Review of Heat Transfer[13] and Handbook of Thermal Science and Engineering Radiative Heat Transfer[14] and one patent on near-field photon transport[15]. Several of his works were recognized as "highly cited" or selected as journal covers[16-19]. Zhao is among the authors who pioneered the early works on nonreciprocal thermal radiation, including showcasing the pathway for achieving nonreciprocal thermal emission using only 0.3-T magnetic field[11,12], strong nonreciprocal thermal emission from topological magnetic Weyl semimetals[20], and multiport nonreciprocal thermal emitters[21]. Zhao also has extensive experience in nanophotonics for enhanced photon transports, including absorption enhancement[17,22], coherent thermal radiation[16,23-25], and photon tunneling

enhancement[26-28]. The PI's experience will serve as the foundation for studying nonreciprocal thermal radiation in this project.

e. Approach

Proposed Work 1: Design and fabricate the nonreciprocal intermediate layer. In order to realize nonreciprocal thermal light transport, we propose to design and experimentally measure the needed wavelength-selective nonreciprocal radiative properties. Building on our previous successes[11,20], we propose to use magneto-optical materials and apply an external magnetic field to do so. In Fig. 4a, we show the desired nonreciprocal properties: when light is incident from the top, the layer can totally absorb it, but light is only emitted toward the bottom. We have published a preliminary design of a photonic structure that can achieve this function near 10 μm infrared range[29]. In the design, only one type of magneto-optical material is used, and therefore, the effect does not have a wide wavelength range. Here we propose to use

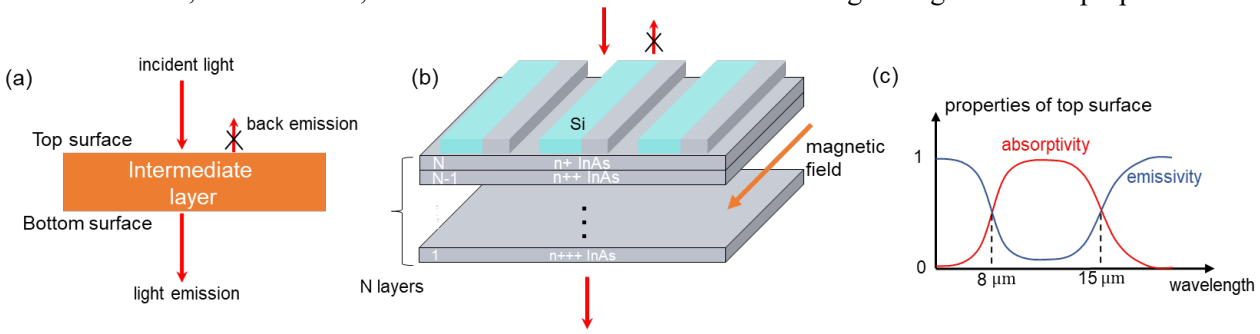

Fig. 4. (a) Nonreciprocal properties the intermediate layer has. (b) Proposed device to achieve the desired nonreciprocal properties in the infrared range of thermal light. The arrows show the magnetic field. (c) Expected nonreciprocal properties.

multiple magneto-optical materials with different doping levels to extend the wavelength range of the nonreciprocal behavior. Our design is shown in Fig. 4b, which is a design based on our preliminary results. The rationale behind this design is that each layer of the magneto-optical material can provide the desired nonreciprocal effect in a desired narrow wavelength range. By changing the doping levels, the nonreciprocal effects provided by each layer can be coupled and expanded to a broad wavelength range. Such extension of effect in wavelength range has been shown to be feasible both theoretically and experimentally[30]. Through geometric optimization, we aim to design a structure with radiative properties shown in Fig. 4c, which is the wavelength range most of the thermal emission from a near-room-temperature hot body falls within. We will fabricate and characterize the device using the facilities fully available at the University of Houston and the PI's lab.

Proposed Work 2: Experimentally demonstrate the nonreciprocal thermal transport effect. Using the fabricated nonreciprocal layer, we propose to do a proof-of-concept demonstration of the nonreciprocal thermal light transport effect. Our proposed experimental setup is shown in Fig. 5. A blackbody at an elevated temperature slightly above room temperature is used to provide the thermal emission, which is captured by the intermediate layer. While receiving the emission from the blackbody, the intermediate also emits thermal emission to the light detector, a InAs cell. Our control experiment is shown in Fig. 5a, where the intermediate layer does not experience a magnetic field. In this case, the layer behaves as a conventional device with back emission to the blackbody, as indicated by the dashed arrows. When the magnetic field is turned on, as shown in Fig. 5b, the intermediate layer becomes nonreciprocal, and the back emission from the layer to the blackbody can be suppressed. Therefore, we expect to observe an increase in temperature of the intermediate layer due to the nonreciprocal effect and a higher photocurrent in the InAs cell. For better comparison in the experiments, the intermediate layer will be put into a vacuum chamber to eliminate the heat transfer due to convection. Thermometers will be attached to the intermediate layer to monitor its temperature. A spectrometer will be used to monitor the electrical detection from the deuterated triglycine sulfate (DTGS) detector, which has excellent detectivity in the mid-infrared. We expect to see higher

temperature readings and higher power detected from the DTGS detector in the setup shown in Fig. 5(b) compared to (a).

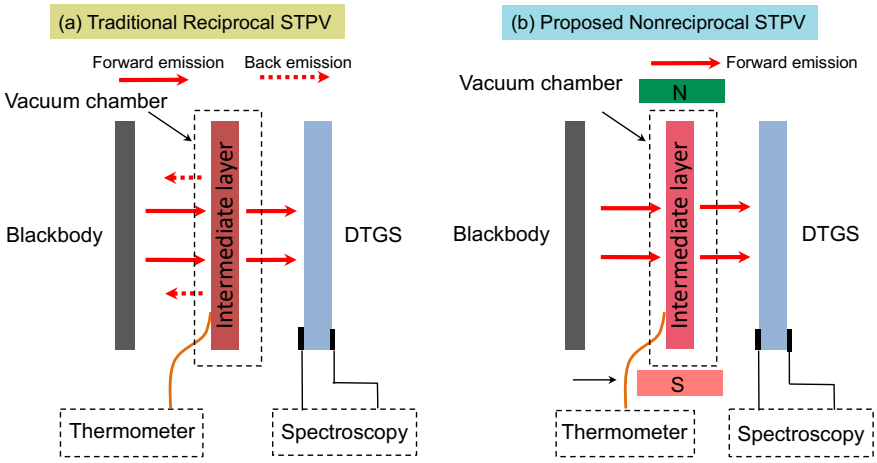

Fig. 5. Our experimental plan. (a) The reciprocal system without an applied magnetic field. (b) The nonreciprocal system with a magnetic field applied by magnets. The temperature of the intermediate layer and the power produced in the InAs cell are monitored in both cases as a direct justification of the nonreciprocal effect.

f. Expected Outcomes and Products

We summarize our expected outcomes and products with the following two milestones. The timeline of all activities is detailed in the timeline document.

Milestone 1 Design and demonstrate nonreciprocal radiative properties (ms 1.1) design nonreciprocal intermediate layer based on magneto-optical materials with high emissivity and absorptivity contrast > 0.9 (ms 1.2) numerically demonstrate the pathway to achieve bandwidth-tunable nonreciprocal radiative properties using magneto-optical materials (ms 1.3) experimentally characterize the nonreciprocal radiative properties in the magneto-optical nanophotonic structure

Milestone 2 Experimentally demonstrate the nonreciprocal thermal transport effect (ms 2.1) calibrate the current-voltage response of the InAs cell (ms 2.2) test the reciprocal system and nonreciprocal system (ms 2.3) optimize the system to highlight the nonreciprocal effect

g. Risk Migration

In case that magneto-optical material cannot provide a satisfying nonreciprocal effect, we will then use magnetic Weyl semimetals such as Co_2MnAl[31] with different doping levels from our collaborators (Prof. Ziqiang Mao at the Pennsylvania State University) to provide the broadband nonreciprocal effect.

h. References

[1] W. Shockley and H. J. Queisser, "Detailed Balance Limit of Efficiency of P-N Junction Solar Cells," *Journal of Applied Physics*, vol. 32, no. 3, pp. 510-519, 1961.
[2] E. Rephaeli and S. Fan, "Absorber and Emitter for Solar Thermo-Photovoltaic Systems to Achieve Efficiency Exceeding the Shockley-Queisser Limit," *Optics Express*, vol. 17, no. 17, p. 15145, 2009.
[3] Zero-Emissions Industrial Heat & Power. https://antoraenergy.com/technology (accessed 1/15/2024).
[4] Thermophotovoltaics Market Size & Share to Hit US$ 17.4 million by 2031, Garnering 6.7% CAGR: TMR Report. https://www.prnewswire.com/news-releases/thermophotovoltaics-market-size--share-to-hit-us-17-4-million-by-2031--garnering-6-7-cagr-tmr-report-301969225.html (accessed 1/15/2024).
[5] J. R. Howell, M. P. Menguc, K. Daun, and R. Siegel, *Thermal Radiation Heat Transfer*. 7th ed.; CRC Press: Florida (2021).
[6] S. Fan, "Thermal Photonics and Energy Applications," *Joule*, vol. 1, no. 2, pp. 264-273, 2017.
[7] Y. Wang, H. Liu, and J. Zhu, "Solar Thermophotovoltaics: Progress, Challenges, and Opportunities," *APL Materials*, vol. 7, no. 8, p. 080906, 2019.

[8] S. Jafari Ghalekohneh and B. Zhao, "Nonreciprocal Solar Thermophotovoltaics," *Physical Review Applied*, vol. 18, no. 3, p. 034083, 2022.
[9] K. J. Shayegan, S. Biswas, B. Zhao, S. Fan, and H. A. Atwater, "Direct Observation of the Violation of Kirchhoff's Law of Thermal Radiation," *Nature Photonics*, vol. 17, no. 10, pp. 891-896, 2023.
[10] Best Research-Cell Efficiency Chart. https://www.nrel.gov/pv/cell-efficiency.html (accessed 7/13/2022).
[11] B. Zhao, Y. Shi, J. Wang, Z. Zhao, N. Zhao, and S. Fan, "Near-Complete Violation of Kirchhoff's Law of Thermal Radiation with a 0.3T Magnetic Field," *Optics Letters*, vol. 44, no. 17, pp. 4203-4206, 2019.
[12] K. J. Shayegan, B. Zhao, Y. Kim, S. Fan, and H. A. Atwater, "Nonreciprocal Infrared Absorption Via Resonant Magneto-Optical Coupling to InAs," *Science Advances*, vol. 8, no. 18, p. eabm4308, 2022.
[13] B. Zhao and S. Fan, "Chemical Potential of Photons and Its Implications for Controlling Radiative Heat Transfer," *Annual Review of Heat Transfer*, vol. 23, no., pp. 397-431, 2020.
[14] B. Zhao and Z. M. Zhang, Design of Optical and Radiative Properties of Surfaces. In *Handbook of Thermal Science and Engineering*, Kulacki, F. A., Ed. Springer International Publishing: Cham, 2017; pp 1-46.
[15] S. Fan, B. Zhao, S. Assawaworrarit, P. Santhanam, and M. Orenstein, Apparatuses and Methods Involving DC Voltage Conversion Using Photonic Transformers. Google Patents: 2022.
[16] B. Zhao, L. P. Wang, Y. Shuai, and Z. M. Zhang, "Thermophotovoltaic Emitters Based on a Two-Dimensional Grating/Thin-Film Nanostructure," *International Journal of Heat and Mass Transfer*, vol. 67, no. 0, pp. 637-645, 2013.
[17] B. Zhao, J. M. Zhao, and Z. M. Zhang, "Enhancement of near-Infrared Absorption in Graphene with Metal Gratings," *Applied Physics Letters*, vol. 105, no. 3, p. 031905, 2014.
[18] B. Zhao and Z. M. Zhang, "Perfect Absorption with Trapezoidal Gratings Made of Natural Hyperbolic Materials," *Nanoscale and Microscale Thermophysical Engineering*, vol. 21, no. 3, pp. 123-133, 2017.
[19] B. Zhao and Z. M. Zhang, "Perfect Mid-Infrared Absorption by Hybrid Phonon-Plasmon Polaritons in hBN/Metal-Grating Anisotropic Structures," *International Journal of Heat and Mass Transfer*, vol. 106, pp. 1025-1034, 2017.
[20] B. Zhao, C. Guo, C. A. C. Garcia, P. Narang, and S. Fan, "Axion-Field-Enabled Nonreciprocal Thermal Radiation in Weyl Semimetals," *Nano Letters*, vol. 20, no. 3, pp. 1923-1927, 2020.
[21] B. Zhao, J. Wang, Z. Zhao, C. Guo, Z. Yu, and S. Fan, "Nonreciprocal Thermal Emitters Using Metasurfaces with Multiple Diffraction Channels," *Physical Review Applied*, vol. 16, no. 6, p. 064001, 2021.
[22] B. Zhao, J. M. Zhao, and Z. M. Zhang, "Resonance Enhanced Absorption in a Graphene Monolayer Using Deep Metal Gratings," *Journal of the Optical Society of America B*, vol. 32, no. 6, pp. 1176-1185, 2015.
[23] B. Zhao and Z. M. Zhang, "Strong Plasmonic Coupling between Graphene Ribbon Array and Metal Gratings," *ACS Photonics*, vol. 2, no. 11, pp. 1611-1618, 2015.
[24] B. Zhao, J.-H. Song, M. Brongersma, and S. Fan, "Atomic-Scale Control of Coherent Thermal Radiation," *ACS Photonics*, vol. 8, no. 3, pp. 872-878, 2021.
[25] B. Zhao and Z. M. Zhang, "Study of Magnetic Polaritons in Deep Gratings for Thermal Emission Control," *Journal of Quantitative Spectroscopy and Radiative Transfer*, vol. 135, pp. 81-89, 2014.
[26] B. Zhao and Z. M. Zhang, "Enhanced Photon Tunneling by Surface Plasmon–Phonon Polaritons in Graphene/Hbn Heterostructures," *Journal of Heat Transfer*, vol. 139, no. 2, pp. 022701-022701-8, 2016.
[27] B. Zhao, B. Guizal, Z. M. Zhang, S. Fan, and M. Antezza, "Near-Field Heat Transfer between Graphene/Hbn Multilayers," *Physical Review B*, vol. 95, no. 24, p. 245437, 2017.
[28] G. T. Papadakis, B. Zhao, S. Buddhiraju, and S. Fan, "Gate-Tunable near-Field Heat Transfer," *ACS Photonics*, vol. 6, no. 3, pp. 709-719, 2019.
[29] Y. Park, V. S. Asadchy, B. Zhao, C. Guo, J. Wang, and S. Fan, "Violating Kirchhoff's Law of Thermal Radiation in Semitransparent Structures," *ACS Photonics*, vol. 8, p. 2417, 2021.
[30] M. Liu, S. Xia, W. Wan, J. Qin, H. Li, C. Zhao, L. Bi, and C.-W. Qiu, "Broadband mid-infrared non-reciprocal absorption using magnetized gradient epsilon-near-zero thin films," *Nature Materials*, vol. 22, no. 10, pp.1196-1202, 2023.
[31] P. Li, J. Koo, W. Ning, J. Li, L. Miao, L. Min, Y. Zhu, Y. Wang, N. Alem, C.-X. Liu, Z. Mao, and B. Yan, "Giant Room Temperature Anomalous Hall Effect and Tunable Topology in a Ferromagnetic Topological Semimetal Co_2MnAl," *Nature Communications*, vol. 11, no. 1, p. 3476, 2020.

Executive summary Optica Foundation Challenge

Applicant: Junior Prof. Carlos Doñate Buendía, University Jaume I, Spain

Category: Health

Stereolitography 3D printed custom and low-cost bactericidal dentures by laser generated Ag_2WO_4 nanoparticles additivation

The proposed project addresses a fundamental problem in nowadays society, universal health access. Specifically, **dental health costs limit its access to low-income population and countries**, resulting in reduced well-being, sickness, and even death. Implants, crowns, and dentures costs still represent a barrier for their extended employment. One of the sources of the high costs comes from the necessity of fabricating custom dental prosthetics for each patient, not allowing serial production. To overcome this limit, a **photonics-based 3D printing** technique as stereolitography (SLA) is proposed **to produce dentures** with complex custom geometries and low production costs.

Another problem linked to **dental prosthetic** is the proliferation of bacterias and the **risk of infection**. Dentures represent a reservoir of microorganisms that can derive into stomatitis or infections. In fact, 70% of dentures wearers suffer from denture stomatitis. To treat infection problematics, antibiotic protocols are developed. However, this solution is limited due to the emergence of antibiotic resistant superbugs. To address it, the employment of **laser irradiated Ag_2WO_4 particles to provide bactericidal properties to dentures** is proposed.

Overall, in the current project a complete photonics based approach is designed to produce dentures with bactericidal properties by the formulation and SLA printing of resins containing laser generated Ag_2WO_4 particles with enhanced bactericidal properties.

The proposed methodology can be explained in three steps, represented in the scheme below. First, the **irradiation of Ag_2WO_4 particles dispersed in the dental resin**, a commercial flexible resin to produce dentures. The irradiation is carried out by laser fragmentation in liquids (LFL), it enhances the Ag_2WO_4 bactericidal effects and facilitates the particle dispersion. Then, the **Ag_2WO_4-resin is employed for SLA** after detailed characterization of the Ag_2WO_4 particle stability in the resin, the viscosity and wettability. Finally, the **produced dentures are characterized by tensile, hardness, bactericidal, and biocompatibility** tests to evaluate their suitability for in-vivo applications.

The proposed approach aims to overcome the current main drawbacks of dental prosthetics. On the one side, high costs that difficult general population access to basic dental health treatments. On the other side, infection and bacteria proliferation and the subsequent loss of patient well-being and extra dental health treatment costs.

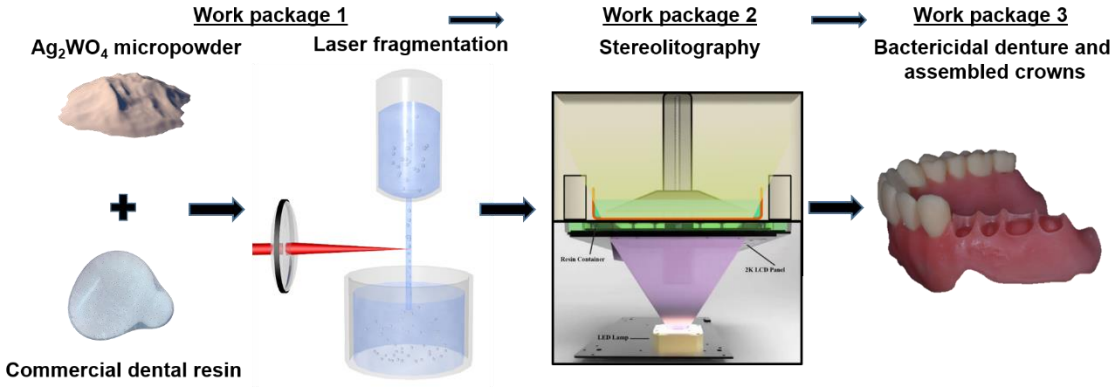

Project Proposal Optica Foundation Challenge

Applicant: Junior Prof. Carlos Doñate Buendía, University Jaume I, Spain

Category: Health **Anticipated total duration of the project: 24 months**

Stereolitography 3D printed custom and low-cost bactericidal dentures by laser generated Ag_2WO_4 nanoparticles additivation

1 Literature review and problem statement

Photonics and nanotechnology are considered strategic areas for research and innovation in advanced materials by the European Commission. The development of new technologies based these fields is key for the development of human society lifestyle in the following decades. For instance, improving imaging and treatments in medicine, material fabrication and processing, or green energy harvesting systems and other fields, are essential for facilitating a sustainable human growth. Laser-irradiation is one of the most active frontiers in the development of optics. It combines the frontier achievements of photonics and nanotechnology to be a powerful tool for the fast synthesis of nanomaterials for electrochemical applications due to the advantages of low cost, high accuracy, easy preparation, and high yield [1]. It can realize many new functions on the basis of local electromagnetic interaction, being an indispensable key science and technology in the 21st century. Laser as synthetic and microfabrication technique and provide the advantages of fast, scalable, environment friendly, and cost effective approach permitting in situ processing [2]. Compared with the traditional synthesis and microfabrication techniques, laser-assisted processing techniques enable direct synthesis of nanomaterials in both gas and liquid media with environment friendliness and less energy loss. Pulsed laser ablation in liquids (PLAL), is located at the intersection of photonics and nanotechnology, representing a green synthesis technique of advanced materials from metallic, ceramic, organic, and alloy nanoparticles [3]. A focused laser beam with high energy directly irradiates a precursor sample, allowing for rapid heating, melting, reacting, and cooling to generate a new active material. The high-power pulsed laser-assisted synthesis of nanomaterials in liquids provides many degrees of parameter control (i.e., pulsed laser power, wavelength, reaction time duration, laser pulse repetition rate, and solvent) and numerous advantages over traditional physical and chemical synthetic methods, such as simplicity, high purity, avoid by-products and toxicity, and no need for surfactants and reducing agents. This is an appropriate approach to produce cost-effective smart materials for effective applications such as health, energy and environmental processes [4]. This versatility is a key feature for the development and technological applications of advanced materials.

Among metal oxides that confer antimicrobial characteristics, Ag-based materials have gained prominence, including Ag-based semiconductors [5,6]. Particularly noteworthy is silver tungstate (Ag2WO4), owing to its versatility, easy fabrication, high stability, and potent antimicrobial activity [7]. Its robust antimicrobial capacity is attributed to the semiconductor's ability to generate reactive oxygen species (ROS), even in the dark, and the gradual release of Ag+ ions [8]. Specifically, the formation of Ag nanoparticles on Ag2WO4 with bactericidal properties has been demonstrated, as well successfully produced composite materials comprising Ag2WO4 and chitosan by electron beam and femtosecond irradiation, demonstrating high antimicrobial efficacy against fungi, and bacteria, and viruses [9,10].

Oral diseases are considered by the World Health Organization (WHO) as a major health burden for many countries that affect people throughout their lifetime, causing pain, discomfort, and even death [11]. Diseases as dental caries, periodontal, or dental trauma can

lead to tooth loss or gums degradation, reducing the affected person wellbeing, and requiring the employment of prosthesis or implants. This worldwide problematic further affects low- and middle-income countries and society sectors [12] due to the costly access to dental care [13].

The impact of dental implants can be assessed in few numbers, its annual global market is estimated at around 12-18 million implants, with more than 200 million patients having received an implant in the last two decades [14]. However, implants, and dentures costs still represent a barrier for their extended employment in several countries and parts of society [13]. One of the sources of the high costs comes from the necessity to fabricate a custom implant for each patient, not allowing serial production. To overcome this limit, photonics-based 3D printing techniques have been employed to produce dentures, achieving complex geometries and low-cost custom parts [15]. Within the broad spectrum of 3D printing techniques, stereolitography (SLA) provides key advantages for prosthetic manufacturing cost reduction. SLA is based on the photopolymerization of a liquid resin that turns into a solid under UV light illumination. The low energy photopolymerization threshold of the resins allows the employment of low cost UV sources such as LEDs. The light modulator used to spatially control the layer-by-layer photopolymerization of the resin can be a LCD display, reaching resolutions of 20 μm. The employment of general consumer technology reduces the overall cost of standard SLA devices to hundreds of dollars. Besides, there already exist commercial dental resins suitable for dentures [16]. Overall, SLA printing offers an excellent perspective to reduce production costs of dental parts, prospectively facilitating access to such essential goods to a broader worldwide population percentage.

An additional problem arising after incorporation of the dental pieces to the patient are infections resulting in peri-implantitis. It occurs in 3% of the patients [17,18], which results in approximately 6 million people affected in the last two decades. As another example, 70% of dentures wearers suffer from denture stomatitis [19]. To prevent infection problematics, antibiotic protocols have been developed [18]. Nevertheless, this solution presents also limitations when the emergence of antibiotic resistant superbugs is considered. To address it, the employment of inorganic particles exhibiting bactericidal properties such as Ag or Cu has been proposed [10]. However, when incorporated into dentures, the elemental metals can suffer from leaching, increasing their concentration in the media to toxic levels [19]. To control the release of the bactericidal Ag, the employment of Ag_3PO_4 has been proposed, proving that the composite can be integrated in a scaffold providing bactericidal properties without cytotoxicity, and even allowing cell proliferation [21]. Hence, inorganic particles have been shown effective as bactericidal agent [22]. However, the addition of bactericidal particles to SLA dental resins has been only recently tested for elemental metals, and oxides, mostly focusing on their effect over the mechanical properties of the printed parts and not providing extra bactericidal properties [23]. Preliminary work from the applicant [5,24] confirmed that high intensity laser irradiation of Ag_2WO_4 microparticles in air leads to the formation of Ag nanoparticles bonded to the original composite [7]. The Ag nanoparticles formed, provide bactericidal, antifungal, and antitumor properties to the irradiated material, with specificity and biocompatibility with healthy human cells (BALB/3T3) [9]. Even SARS-CoV-2 deactivation has been demonstrated by the applicant employing a laser irradiated chitosan/Ag_2WO_4 composite [5]. Consequently, laser irradiated Ag_2WO_4 represents an interesting material to provide antiseptic properties to denture manufacturing dental resins employed in SLA.

Overall, a complete photonics based approach is proposed to produce dentures with bactericidal properties by the formulation and printing of new SLA resins containing laser generated Ag_2WO_4 particles. This approach aims to overcome the current main drawbacks of dental parts. On the one side, high costs that difficult general population access to these dental

health treatments. On the other side, infection and bacteria proliferation and the subsequent patient well-being and health treatment costs.

2 Objectives

Photonics related additive manufacturing (AM) techniques provide the required design freedom and represent a growing industrial market. In this context, the focus of the present project is the development and application of photopolymer dental materials modified by the addition of laser generated Ag/α-Ag2WO4 nanoparticles to provide the AM printed custom dentures with enhanced bactericidal properties towards mitigation of oral disease complications. The specific objectives are intended to provide broader worldwide access to dental parts by reducing production costs and to address human wellbeing and resources losses arising from bacteria development and infections in dentures:

1) The **adaptation of nanoparticle additivated resins** as base materials **in SLA**, allowing the production of **custom dentures with novel functionalities** at reduced costs, making them more accessible for low-income countries.
2) **The production of bactericidal and biocompatible dentures** by the formulation of new Ag_2WO_4-resins printed by SLA.

3 Outcome

WP1 – Dental resin additivation with laser generated Ag_2WO_4 nanoparticles

A laser based procedure to prepare Ag_2WO_4 nanoadditivated dental resins will be studied. The process will be compared with direct mixing of the Ag_2WO_4 micropowder with the resin, and direct mixing of air irradiated Ag_2WO_4 with the resins. The effect of Ag_2WO_4 laser fragmentation on the stability and the bactericidal response of the particles will be evaluated.

WP1.1 – Laser fragmentation (LFL) of Ag_2WO_4 microparticles

Direct addition of Ag_2WO_4 powders to the SLA resins could result in agglomeration of the material and sedimentation before printing. This would affect the homogeneous distribution of the particles in the printed part, generating local variations of the mechanical and bactericidal properties that can result in the fracture of the part or infection risk increase in specific areas. The novel procedure proposed in this project is based on the initial mixing of Ag_2WO_4 microparticles with the dental resins, Fig. 1a. The mixture is ultrasonically dispersed, and irradiated in a liquid flow configuration, Fig. 1b. The irradiated particles with increased bactericidal properties will gain stability in the resin due to surface coverage with the photopolymer functional groups. To avoid degradation of the resin (printed at 405 nm) during laser irradiation, the laser source employed will be a 1064 nm ps laser (4 MHz, 10 ps, 60 W).

WP1.2 – Ag_2WO_4 additivation of the dental resin

The in-situ laser irradiated Ag_2WO_4-resins in WP1.1 will be compared in terms of particle stability, and viscosity (WP1.3), as well as mechanical, bactericidal, and biocompatibility properties (WP3), with 1) the base Ag_2WO_4 microparticles added to the resin, and 2) the Ag_2WO_4 powder irradiated in air and mixed with the resin. The mixing process for the initial and irradiated in air Ag_2WO_4 will be performed by direct mixing and ultrasonic dispersion.

WP1.3 – Optical and rheological characterization of additivated resins

The effect of Ag_2WO_4 particles addition to the resin will be evaluated by the influence on its optical and flow properties. The measurements described will be performed to the Ag_2WO_4-resins prepared in WP 1. 1) Denture resin with Ag_2WO_4 particles; 2) Denture resin with Ag_2WO_4 particles irradiated in air; 3) Laser irradiated Ag_2WO_4-resin.

The optical properties will be characterized by UV-Vis spectrophotometry (StellarNet Inc.). The stability of the optical properties, absorption peaks wavelengths, and intensity, provide information of the laser interaction on the resin and the dispersed Ag_2WO_4 particles.

To evaluate the influence of the Ag_2WO_4 particles and laser irradiation methodology on the flow properties of the resulting additivated resins, contact angle (sessile drop method) and viscosity measurements (rotational rheometry) will be conducted. These parameters are especially relevant for the processability of the resulting resins by SLA keeping the maximum spatial resolution, process reproducibility, and mechanical performance of the printed parts.

WP2 – Photonics based 3D printing (SLA) of additivated dental parts

Within this work package, the prepared Ag_2WO_4 resins will be processed by SLA (Elegoo Mars 2) to produce test samples for characterization, WP 2.1. In WP 2.2, tensile tests, disks, and dentures will be printed employing the Ag_2WO_4-resins produced in WP1, Fig. 1c.

WP 2.1: SLA printing of tensile tests and disks for optimization and characterization

The influence of the 405 nm LED light employed in the SLA system on the Ag_2WO_4-resins will be evaluated in WP 3.2 to confirm that bactericidal enhancement of the Ag_2WO_4 particles can be achieved in-situ during SLA. A strong synergy with WPs 1.3 and 3 will be required at this point to optimize the processing parameters and achieve simultaneously high printing spatial resolution, repeatability of the process, and maximum bactericidal effect.

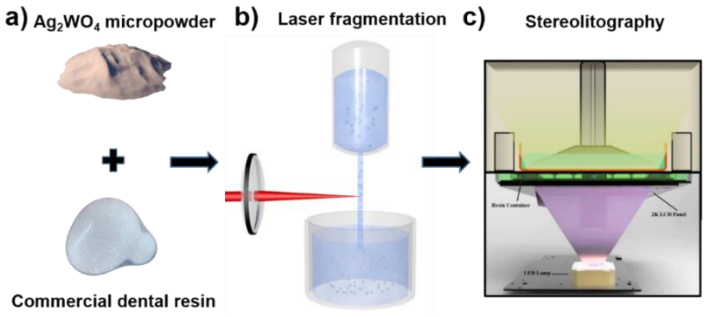

Figure 1. a) Ag_2WO_4 commercially available micropowder and dental resin mixed for laser irradiation in b). b) Laser fragmentation setup in a flow jet configuration to ensure uniform irradiation of the particles and promote a homogeneous bactericidal effect enhancement. c) Stereolitography (SLA) setup with a 405 nm LED and LCD employed to process the laser irradiated Ag_2WO_4-resins, bottom image reproduced from [25].

WP 2.2: SLA printing of additivated flexible dentures

The flat geometries proposed in WP 2.1 will be replaced by the intended denture models for the additivated flexible resin. Different complete and partial dentures from open 3D repositories will be printed to confirm the advantage that SLA provides for the production of custom parts with complex geometries.

WP 3: Bactericidal and mechanical characterization of the printed dental parts

To quantify the effect of the Ag_2WO_4 particles and the laser irradiation over the performance of the printed dental parts, mechanical and bactericidal characterization is required.

WP 3.1: Hardness and tensile testing of the printed parts

Tensile test (DIN 53504:2017-03) and hardness tests (DIN ISO 48-4:2021-02) will be performed. The samples exhibiting values below (<20%) the provider specifications will be discarded. The LFL samples are expected to exhibit better performance due to the Ag_2WO_4 size reduction and dispersion, contributing to a reduced part porosity and density increase.

WP 3.2: Antimicrobial and biocompatibility tests

The antimicrobial tests will be performed for C. Albicans, E. Coli, and MRSA, the most common bacteria present in dentures. Besides, to be able to prospectively qualify the produced parts for in-vivo employment, biocompatibility with oral cells is required. Hence,

alamarBlue™ assay and an MTT assay will be performed to ensure that the printed parts exhibit no toxicity that could damage the denture user.

4 Impact

The funds required to develop the project include the purchase of the necessary Ag_2WO_4 micropowders, the dental resins, and a SLA processing station fully dedicated to the printing of dental resins. Furthermore, material for analytics and optics are included in the budget. The UV-Vis, contact angle, viscosity, mechanical, bactericidal and biocompatibility tests can be performed with the already available devices in the group and close groups at the University Jaume I. The technician full time contract and part-time contract is envisioned to produce major evidences of the project outcomes and setting up the printing and characterization methodologies proposed, representing a fundamental advance in the applicant's current early career stage to start his independent career. The proposed project cannot be currently funded by any funding scheme within Spain due to the preliminary state. The results achieved within the Optica challenge project would allow to apply for European funds after finishing the project. The expected outcomes of the project can be summed up as:

1) Qualification of **laser fragmentation in liquid** approach for the **in situ nanoparticle additivation of SLA resins** with enhanced **bactericidal properties.**
2) Establishment of a photonics-driven printing protocol for the generation of **custom dentures with bactericidal properties and reduced cost.**

The project outcomes address a fundamental problem in nowadays society, universal health care access. Specifically, dental health costs limit the access to low-income population and countries, resulting in reduced well-being, sickness, and even death. The photonics-driven qualification of lower cost approaches to generate dentures offer a possibility to improve dental health for the general population. Furthermore, the bactericidal properties of the generated dentures are envisioned to further reduce health risks as infection, and bacteria proliferation. Overall, it represents a strong benefit for a situation that a significant part of the population faces during their lives, the requirement of a denture.

5 References

[1] V. Nair, J. Yi, D. Isheim, et al., Sci. Adv. 6 (2020).
[2] H. Palneedi, J.H. Park, D. Maurya, et al., Adv. Mater. 30 (2018) 1705148.
[3] D. Zhang, B. Gökce, S. Barcikowski, Chem. Rev. 117 (2017) 3990–4103.
[4] L. Zhao, Z. Liu, D. Chen, et al., Nano-Micro Lett. 2021 131. 13 (2021) 1–48.
[5] P. Fabiana, S. Pereira, A.C. Alves De Paula E Silva, et al., Sci. Reports 2022 121. 12 (2022) 1–18.
[6] B.N.A. da S. Pimentel, F.H. Marin-Dett, M. Assis, et al., Front. Bioeng. Biotechnol. 10 (2022) 826123.
[7] N.G. MacEdo, T.R. MacHado, R.A. Roca, et al., ACS Appl. Bio Mater. 2 (2019) 824–837.
[8] C.V.G. Pellissari, C.E. Vergani, E. Longo, et al., J. Nanomater. 2020 (2020).
[9] M. Assis, T. Robeldo, C.C. Foggi, et al., Sci. Rep. 9 (2019) 1–15.
[10] N.L. Haro Chávez, E.D. de Avila, et al., Colloids Surfaces B Biointerfaces. 170 (2018) 505–513.
[11] M.A. Peres, L.M.D. Macpherson, R.J. Weyant, et al., Lancet. 394 (2019) 249–260.
[12] G.H. Gilbert, R. Paul duncan, B.J. Shelton, Health Serv. Res. 38 (2003) 1843–1862.
[13] E. Bernabé, M. Masood, M. Vujicic, BMC Public Health. 17 (2017) 1–8.
[14] B. Klinge, M. Lundström, M. Rosén, et al., Clin. Oral Implants Res. 29 (2018) 145–151.
[15] L. Lin, Y. Fang, Y. Liao, et al., Adv. Eng. Mater. 21 (2019) 1801013.
[16] A. Della Bona, V. Cantelli, V.T. Britto, et al., Dent. Mater. 37 (2021) 336–350.
[17] O. Camps-Font, P. Martín-Fatás, A. Clé-Ovejero, et al., J. Periodontol. 89 (2018) 1165–1173.
[18] R. Tabrizi, F. Mobin, M. Dehghanpour, et al., J. Cranio-Maxillofacial Surg. 50 (2022) 293–297.
[19] P. Ramburrun, N.A. Pringle, A. Dube, et al., Materials (Basel). 14 (2021) 3167.
[20] M. Cao, S. Wang, J. Hu, et al., Adv. Sci. 9 (2022) 2103721.
[21] K. Hayashi, M. Shimabukuro, K. Ishikawa, ACS Appl. Mater. Interfaces. 14 (2022) 3762–3772.
[22] C. Zhao, W. Liu, M. Zhu, et al., Bioact. Mater. 18 (2022) 383–398.
[23] M.M. Gad, A.M. Al-Thobity, Jpn. Dent. Sci. Rev. 57 (2021) 46–53.
[24] T.R. Machado, N.G. Macedo, M. Assis, et al., ACS Omega. 3 (2018) 9880–9887.
[25] A. Al Rashid, S.A. Khan, S. G. Al-Ghamdi, et al., J. Mater. Res. Technol. 14 (2021) 910–941.

Wide Field-of-View Mid-IR Wildfire Detection Enabled by Fisheye Metalens

PI: Carlos A. Rios Ocampo | University of Maryland College Park

Executive summary

Wildfires are one of the most destructive natural disasters worldwide. They alone caused 150 billions in US$ losses in 2022 throughout the Americas, but more importantly, losses in human lives, irreversible damage to ecosystems, and health threats due to poor air quality. The USA and Colombia (country of origin of the PI) accounted for ~26% and 12% of the wildfires, respectively. Some due to natural disasters and unvoluntary accidents, but others, like in the case of Colombia, due to the deliberate destruction of the Amazon Forest for illegal farming. Regardless the cause, early detection enables a fast reaction to suppress fires when still manageable.

Detecting wildfires has inspired the development of novel technologies, yet several open challenges remain ahead towards finding accurate and cost-effective solutions—the 2024 XPrize Wildfire challenge is an example of how imperative is to find solutions. While artificial intelligence combined with the internet of things have provided novel software tools to improve the detection of fires, several challenges remain on the hardware side given the complex task of monitoring vast extensions of land in a timely, efficient, and accurate manner.

This program tackles this challenge as part of the Optica Foundation Challenge in the category *Environment*. We aim to pioneer a lightweight, low-cost, and wide field-of-view (FOV) metalens for efficient and reliable detection of early-stage wildfires. Moreover, we aim to develop a thin-film narrow-band filter to, in addition, image only at 3.9 μm wavelength to avoid false positives that arise from Earth's and humans' radiation and parasitic reflections (e.g. from bodies of water). Our approach combines innovative optics and fire protection engineering to optimize the area that an unmanned aerial vehicle (UAV) can scan in a single flight, and the accuracy of mid-infrared detection of fires. Upon success, this optical system will significantly facilitate the detection of wildfires in early stages and thus, support fast suppression protocols.

Our approach is a hardware solution to wildfire detections and could enhance the artificial intelligence initiatives on the software counterpart by providing more data per deployed UAV. Moreover, our approach will provide a single solution to all the reasons why glass-based fisheye lenses are not commonly used in UAVs: size, weight (of special importance in small UAVs), and cost. Lastly, a mid-IR camera with wide FOV can be broadly used in other contexts, such as remote chemical sensing, robotic control, automotive sensing, and consumer electronics.

Wide Field-of-View Mid-IR Wildfire Detection Enabled by Fisheye Metalens

PI: Carlos A. Rios Ocampo | University of Maryland College Park

Overview and Objectives

In this program, we aim to pioneer a lightweight, low-cost, and wide field-of-view metalens for efficient and reliable detection of early-stage wildfires. Moreover, we aim to develop a thin-film narrow-band filter to, in addition, image only at 3.9 μm wavelength to avoid false positives that arise from Earth's and humans' radiation and parasitic reflections (e.g. from bodies of water).[1] Our approach combines innovative optics and fire protection engineering to optimize the area that an unmanned aerial vehicle (UAV) can scan in a single flight, and the accuracy of mid-infrared detection of fires. Upon success, this optical system will significantly facilitate the detection of wildfires in early stages and thus, support fast suppression protocols. Our approach is a hardware solution to wildfire detections and will enhance the artificial intelligence initiatives on the software counterpart by providing more data per deployed UAV.

While we focus on tackling an environmental challenge, our approach is broadly compatible with other applications, such as remote chemical sensing, robotic control, automotive sensing, and consumer electronics. This proposal responds to the Optica Foundation Challenge in the category *Environment*.

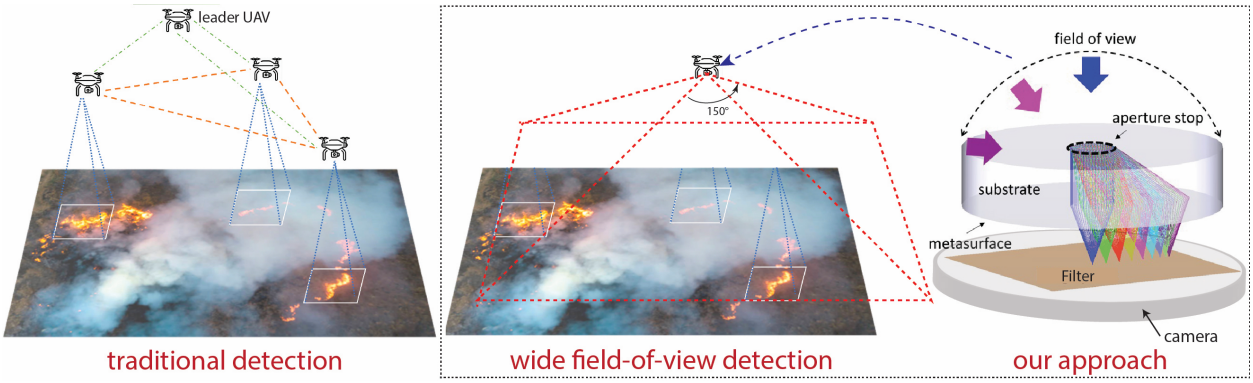

Fig. 1. Traditional detection including several coordinated UAVs to image a large area vs. our approach with a single UAV with wide FOV. Right: Schematic design of the flat fisheye metalens, filter, and camera. Image adapted from Ref. [2].

Problem statement

Wildfires are one of the most destructive natural disasters worldwide.[2,3] They alone caused 150 billions in US$ losses in 2022 throughout the Americas, but more importantly, losses in human lives, irreversible damage to ecosystems, and health threats due to poor air quality.[3–5] The USA and Colombia (country of origin of the PI) accounted for ~26% and 12% of the wildfires, respectively. Some due to natural disasters and unvoluntary accidents, but others, like in the case of Colombia, due to the deliberate destruction of the Amazon Forest for illegal farming.[6] Regardless the cause, early detection enables fast reaction to suppress fires when still manageable.

Detecting wildfires has inspired the development of novel technologies, yet several open challenges remain ahead towards finding accurate and cost-effective solutions —the 2024 XPrize Wildfire challenge is an example of how imperative is to find solution.[7] While artificial intelligence combined with the internet of things have provided novel software tools to improve

the detection of fires,[4] several challenges remain on the hardware side given the complex task of monitoring vast extensions of land in a timely, efficient, and accurate manner.

Background

Current approaches to monitor wildfires include satellite imaging, which can cover vast areas from continents to countries with Geosynchronous Earth Orbit (GEO) or Low-Earth Orbit (LEO) satellites, respectively[3]. The main disadvantages of this technology are the cost and spatial resolution, thus, not spotting wildfires in early stages. Another common technology uses mid-infrared (mid-IR) cameras on drones, at the cost of efficiency, given the limited flight autonomy and restrictions in the use of the space (e.g., the US has a limitation of 400 ft flying altitude for drones.) In this proposal, we tackle the challenge of expanding the area an UAV can image, and thus, the amount of data it collects in a single flight. We do so by expanding the vision of typically 20°-30° in commercial forward-looking infrared (FLIR) cameras (or up to 80° with $25k+ cameras[8]) to a target of 150° (although, virtually near-180° is possible) using fisheye metalens technologies.[9]

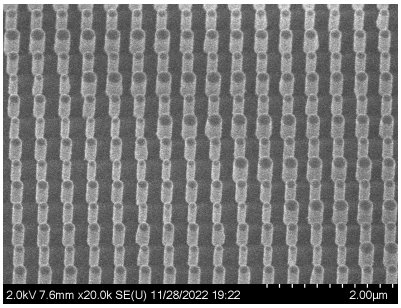

Fig. 2. a-Si metalens fabricated by 2Pi Optics.

Wide field of view metalens: Metasurfaces are artificial planar (or 2.5D) platforms with sub-wavelength thickness and elements called meta-atoms that perform unprecedented optical modulation.[10,11] A metalens is a specific metasurface design to mimic the behavior of conventional "bulky" lenses, but more interestingly, to surpass their response in terms of aberration corrections and multiple functionalities in a single lens.[12,13] Ours is a specific case of a metalens extending on what conventional optics can do by achieving arbitrary FOV with no coma aberration. Fig. 1 shows the baseline configuration of the fisheye lens, which comprises a single piece of flat transparent substrate with an input aperture positioned on the front surface and a metalens positioned on the back surface. Light beams incident on the input aperture at different angles of incidence (AOIs) are refracted to the backside metalens and then focused. When the metalens phase function ϕ fulfills the following closed-form solution all focal spots across the entire panoramic FOV will fall on the same image plane while minimizing coma aberration[14]:

$$\phi(r) = \frac{2\pi}{\lambda} \cdot \int_0^r \left(\frac{nr}{\sqrt{r^2 + L^2}} + \frac{r-h}{\sqrt{f^2 + (r-h)^2}} \right) \cdot dr, \quad (1)$$

where r, λ, n, L, and f denote the radial position from the lens center, wavelength, substrate refractive index, substrate thickness, and effective focal length, respectively. h is the image height (focal spot position) at AOI = θ and it can be given in a differential form:

$$\frac{dh}{d\theta} = \left[\left(\frac{L \sin\theta}{\sqrt{n^2 - \sin^2\theta}} - h \right)^2 + f^2 \right] \cdot \frac{\cos\theta}{f^2}. \quad (2)$$

This finding is significant because it indicates that a flat substrate, when decorated with a single-layer metalens, can be transformed into a fisheye lens with near-180˚ diffraction-limited FOV. Moreover, the planar focal surface enables considerably simplified optical system architectures.

Our collaborators at MIT (Prof. Juejun Hu) and the startup 2Pi Optics have extensive experiences with the proposed metalens fabrication process. Fig. 2 shows one example of a-Si metalens indicating excellent pattern fidelity with outstanding wide FOV, shown in Fig. 3.

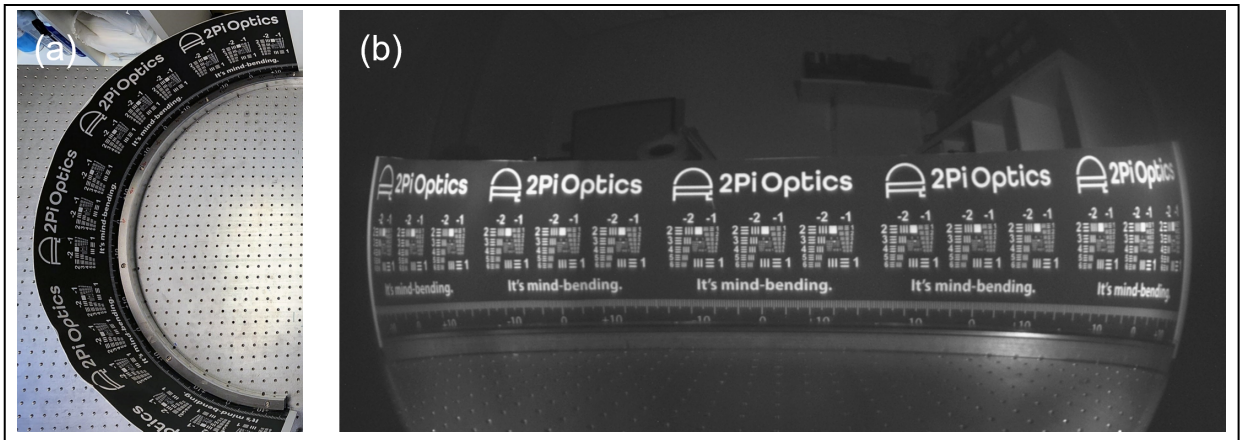

Fig. 3. Experimental demonstration of a fisheye metalens at 940 nm. (a) setup and (b) an image captured by a metalens + camera system. (Courtesy of 2Pi Optics).

Thin-film optical filters: Narrow band wavelength filters have been widely researched and applied in optical technology.[15] Thin-film approaches are of particular interest given their simple fabrication with conventional deposition methods, such as sputtering. Bragg structures and Fabry-Perot cavities are examples of such filtering thin-film coatings. More recently, Fano-resonant optical coatings have gained space in the field given the simplicity and compactness of the multilayer stack, which achieves narrow-band transmissive modes with just four ultra-thin layers (three of which are absorptive), in a task that Bragg-like structures need several more layers to achieve.[16,17] Such structures achieve Fano resonances by coupling two resonating cavities: a typical Fabry-Perot cavity, and an absorptive cavity comprising a thin lossy material (see Fig. 4). One of the outstanding aspects of such a technology is the simple fabrication process that allows integration to virtually any substrate. Moreover, by careful material selection, Fano resonances can be achieved in different optical windows, from UV to mid-infrared, with conventional, cheap, and easy to deposit amorphous materials and metals. In this proposal, the PI will leverage his previous demonstrated experience developing both tunable Fabry-Perot [18] and Fano-resonant optical coatings[17] to achieve a high transmission and narrow band (~50nm) filter center at 3.9 μm wavelength. 3.9 μm is chosen given that all fires emit at this wavelength, while no other significant source of noise is present, i.e. black body radiation from planet Earth, humans, and-or animals, and reflections from bodies of water or other common materials on the surface.[1,3]

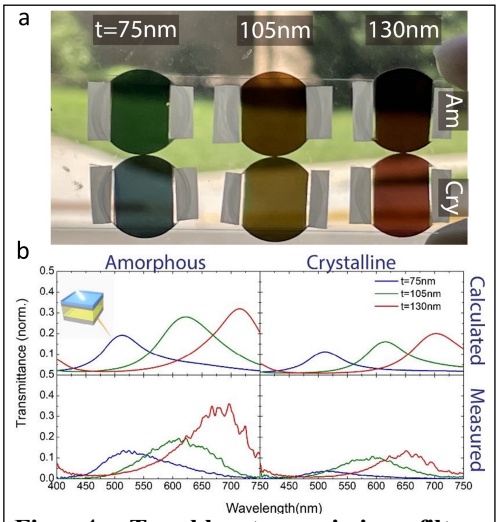

Fig. 4. Tunable transmissive filters demonstrated by PI.[17] **a.** Sb_2Se_3/Ag/ITO/Ag stacks with varying ITO thickness *t*. **b.** Spectra of devices in a, for the amorphous and crystalline states of Sb_2Se_3.

Measurements with controlled fires: The Department of Fire Protection Engineering at UMD counts with a variety of unique facilities to perform measurements with fires of different powers and sizes in controlled environments. Fig. 5 shows a fire hood capable of housing fires with heat release rates up to 700 kW (continuous) or 1.5 MW (peak, 30 second duration) and footprints of up to 2 m × 2 m. This facility has been used in the past for commercial partners researching fires in enclosures (up to 3.5 cubic meters), fire whirls, pool fires, and combustion + firebrand

generation from trees, among others. Fig. 5b shows a 1.8 m Fraser Fir tree tested in the facility (peak heat release rate ~ 1 MW). Importantly, such facilities count with ample space to host optical characterization experiments, which this proposal will leverage to image fires from different angles to test the FOV of our metalenses.

Fig. 5. UMD's Fire hood and example of a burning tree.

Work Plan

The project will support a PhD student, who will design and fabricate the metalens, as well as performing the experimental measurements. We will leverage the PI's group's expertise in nanofabrication and nanophotonics, but also collaborations with experts in the different areas to articulate this multidisciplinary project and guarantee its success. Specifically, we will leverage an existing collaboration with 2Pi Optics—a startup pioneering fisheye metalenses, and Prof. Juejun Hu (MIT), who will support our design efforts and inform our nanofabrication processes. Moreover, we will harness the unique facilities of the University of Maryland (UMD), which hosts one of the few Fire Protection Engineering Departments in the USA. We will collaborate with Prof. Fernando Rafán Montoya to perform experiments in controlled environments. The project will be divided in three thrust areas that we will pursue in parallel during a period of 12 months (see separate timeline file):

Thrust 1: Design and fabrication of wide FOV metalens: In this task, we will build the flat fisheye metalens operating at 3.9 μm, a wavelength that is critical in detection the first instances of fire. We will design a metalens following the principles of a technology exclusively licensed to 2Pi Optics[19] but never demonstrated at this wavelength. The metalens prototype will be fabricated in shared university cleanroom facilities at UMD's NanoCenter. We will use amorphous silicon (a-Si) or PbTe as platforms for high-index meta-atoms. To do so, we will deposit a-Si films via plasma enhanced chemical vapor deposition or PbTe using thermal evaporation and then patterned using electron beam lithography and plasma etching. After metalens patterning, a layer of SU-8 epoxy will be spin-coated to enhance ruggedness of the nano-post meta-atoms. SU-8 is chosen here since our collaborators have found that it can completely fills in the spacing between meta-atoms without leaving any residual air pockets, and produce a flat, fully planarized top surface suitable for subsequently bonding integration. The fabricated metalens samples will be systematically characterized to assess their performances and provide insights on improvements to be made in subsequent fabrication iterations. The tests to be performed on the metalens include bulk transmission and focusing efficiency measurements, point spread function (PSF) profiling, Strehl ratio quantification, and modulation transfer function (MTF) evaluation. All these tests will be performed at different angles of incidence (AOIs) throughout the FOV using small fires as light sources at UMD's Fire protection facilities.

Risks and mitigations: the main risk in our approach is achieving the correct high aspect ratio meta-atoms for the metalens. While we count on vast cleanroom experience, if the metalens is not achieved, we will rely on our collaborators to perform the fabrication with their proven techniques but following our design. Another aspect to consider is the image "accumulation" at the edges of the camera sensor (see Fig. 3). However, our main goal is detecting the wildfires, not necessarily to get a high-resolution image of them. In addition, once detecting a signal from fire, the camera can be rotated to point towards that direction for a clearer image.

Thrust 2: Design and fabrication of thin-film optical filter*:* we will buy a modified FLIR camera with direct access to the sensor, to which we will attach our metalens and filter. We will follow previously demonstrated alignment and integration protocols by our collaborators. With the complete camera setup, we will use the facilities at the Department of Fire Protection Engineering at UMD to perform the experimental testing of our optical device. We will use small, controlled fires with varying powers and a rotational stage to capture images from different angles. The response of our optical systems and provide feedback for the design optimization of our metalens.

Risks and mitigations: the main risk identified in this task is attaching the filter to either the metalens or the mid-IR camera, we will mitigate this risk by fabricating several samples and testing their integration without compromising the system's performance. In the worst scenario, we can test our approach without the filter.

Task 3: Integration to a FLIR camera and controlled-environment tests: We will buy a modified FLIR camera with direct access to the sensor, to which we will attach our metalens and filter. We will follow previously demonstrated alignment and integration protocols by our collaborators at 2Pi Optics. With the complete camera setup, we will use the facilities at the Department of Fire Protection Engineering at UMD. Where we will set up and experiment where small, controlled fires can be imaged from several moving angles and thus, characterize the response of our optical system.

Risks and mitigations: The biggest risk is damaging the sensor during the metalens integration. Given the high cost of FLIR cameras, we will first test our approach on second hand visible CCD cameras with the goal of finding the correct integration method while guaranteeing that the CCD works as intended.

Expected Outcomes

Our expectations for a one-year seed funding are ambitious, given our accumulated experience in this type of device. We anticipate:

- Demonstrating a wide field-of-view metalens, advancing conventional 20°-30° FOV to a target of 150° (our approach has previously demonstrated field-of-view of over 170°).
- Demonstrating and integrating a 3.9 μm wavelength filter to avoid false positives.
- Integrating the metalens and filter to a modified commercial mid-IR camera.
- Developing a characterization method for mid-IR cameras plus metalens in controlled fire experiments.

Moreover, we expect insightful exchanges and fruitful collaborations from other scientists in the OPTICA network and pursuing further funding opportunities to take our approach to a full-scale field demonstration.

Impact

This project pursues a unique cross-disciplinary approach spanning nanophotonics and fire protection engineering, which will boost the performance of conventional mid-IR imaging sensors in UAVs. Upon success, this optical system will significantly facilitate the detection of wildfires in early stages—when they are easier to suppress—by maximizing the area an UAV can image during its short fly time. Moreover, our approach will directly tackle all the reasons why glass-based fisheye lenses are not commonly used in UAVs: size, weight (of special importance in small UAVs), and cost. Lastly, a mid-IR camera with wide FoV can be broadly used in other contexts, such as chemical sensing and also in other unmanned vehicles for autonomous navigation.

References

1. NASA. GOES-R Fire Detection and Characterization. *https://www.goes-r.gov/education/docs/fs_fire.pdf*.
2. Lattimer, B. Y. *et al.* Use of Unmanned Aerial Systems in Outdoor Firefighting. *Fire Technology* vol. 59 Preprint at https://doi.org/10.1007/s10694-023-01437-0 (2023).
3. Boroujeni, S. P. H. *et al.* A comprehensive survey of research towards AI-enabled unmanned aerial systems in pre-, active-, and post-wildfire management. *ArXiv* **2401.02456**, (2024).
4. Bushnaq, O. M., Chaaban, A. & Al-Naffouri, T. Y. The Role of UAV-IoT Networks in Future Wildfire Detection. *IEEE Internet Things J* **8**, (2021).
5. Alexiou, S., Papanikolaou, I., Schneiderwind, S., Kehrle, V. & Reicherter, K. Monitoring and Quantifying Soil Erosion and Sedimentation Rates in Centimeter Accuracy Using UAV-Photogrammetry, GNSS, and t-LiDAR in a Post-Fire Setting. *Remote Sens (Basel)* **16**, (2024).
6. Rodríguez-de-Francisco, J. C. *et al.* Post-conflict transition and REDD+ in Colombia: Challenges to reducing deforestation in the Amazon. *For Policy Econ* **127**, (2021).
7. XPrize Wildfires 2024. *https://www.xprize.org/prizes/wildfire*.
8. Wide field of view commercial FLIR camera example. *https://www.flircameras.com/flir-a-series-a615-230.htm*.
9. Shalaginov, M. Y. *et al.* Single-Element Diffraction-Limited Fisheye Metalens. *Nano Lett* **20**, (2020).
10. Hail, C. U., Michel, A. K. U., Poulikakos, D. & Eghlidi, H. Optical Metasurfaces: Evolving from Passive to Adaptive. *Adv Opt Mater* **7**, 1–29 (2019).
11. Arbabi, A. & Faraon, A. Fundamental limits of ultrathin metasurfaces. *Sci Rep* **7**, 43722 (2017).
12. Park, J. S. *et al.* All-Glass 100 mm Diameter Visible Metalens for Imaging the Cosmos. *ACS Nano* **18**, (2024).
13. Liu, W., Cheng, H., Tian, J. & Chen, S. Diffractive metalens: from fundamentals, practical applications to current trends. *Advances in Physics: X* vol. 5 Preprint at https://doi.org/10.1080/23746149.2020.1742584 (2020).
14. Yang, F. *et al.* Understanding wide field-of-view flat lenses: an analytical solution [Invited]. *Chinese Optics Letters* **21**, 023601 (2023).
15. MacLeod, H. A. Thin-Film Optical Filters. *Thin-Film Optical Filters* (2001) doi:10.1201/9781420033236.
16. ElKabbash, M. *et al.* Fano-resonant ultrathin film optical coatings. *Nat Nanotechnol* **16**, (2021).
17. Huang, Y.-S. *et al.* Tunable structural transmissive color in fano-resonant optical coatings employing phase-change materials. *Mater Today Adv* **18**, 100364 (2023).
18. Ríos, C., Hosseini, P., Taylor, R. A. & Bhaskaran, H. Color Depth Modulation and Resolution in Phase-Change Material Nanodisplays. *Advanced Materials* **28**, 4720–4726 (2016).
19. Shalaginov, M. Y. *et al.* Single-Element Diffraction-Limited Fisheye Metalens. *Nano Lett* **20**, 7429–7437 (2020).

Name of Challenge Project: Next-Generation holographic imaging for in situ detection of Autofluorescent Microplastics in water

The global challenge of microplastic (MPs) pollution poses significant threats to ecosystems and human health, necessitating innovative solutions for accurate assessment and mitigation. In recent years, the pervasive presence of MPs in the environment has emerged as a pressing global concern. These tiny plastic particles, ranging from a few millimeters to nanometers in size, have been found in various ecosystems, including oceans, rivers, and even in the air we breathe. The potential detrimental impacts of MPs on marine life, terrestrial ecosystems, and human health underscore the urgent need for effective monitoring and mitigation strategies. This proposal addresses this challenge by leveraging lensless holographic imaging technology to develop the required tools for *autofluorescent MPs underwater detection in situ*. Detecting MPs with intrinsic fluorescence offers numerous advantages. Firstly, it eliminates the need for exogenous labels or external dyes, simplifying sample preparation and reducing potential artifacts. This approach is cost-effective and minimizes interference with biological samples, ensuring accurate results. Moreover, the long-term stability of intrinsic fluorescence ensures consistent and reliable results over time. These advantages yield a promising solution for MPs underwater assessment *in situ* where controlled laboratory settings cannot be guaranteed.

This solution involves the development of what will be the first high-sensitivity holographic microscope tailored specifically to address the challenges of in situ assessment of underwater autofluorescent MPs. This Next-Generation approach, characterized by its high sensitivity to weak autofluorescent signals, a wide field of view (>20mm^2), and submicrometer spatial resolution, aims to significantly enhance the microscope's detection capabilities beyond current performance levels. Achieving this improvement entails optimizing sensing instruments, refining the optical path, adjusting lensless configurations, and enhancing the signal-to-noise ratio. Furthermore, the project will explore excitation light sources and optical filters to maximize sensitivity while minimizing background noise across various in-field conditions. Validation and calibration procedures will be conducted, involving extensive testing in both controlled laboratory settings and real-world environmental conditions, such as water bodies used as sources for human consumption. The overarching goal of this project is to provide an alternative solution for MPs assessment, empowering researchers and environmental authorities with a potent tool to combat the threat of plastic pollution.

This project intersects with both the "**Health**" and "**Environment**" categories of the OPTICA Foundation Challenge call, addressing the need for advanced technologies to monitor MPs pollution in water. The project is poised to have *significant impacts* across multiple domains:

(1) In the short term, the project aims to enhance the detection and quantification of MPs, providing accurate and timely assessments for environmental monitoring programs. This solution offers an additional and complementary approach to MP assessment, augmenting existing methods.
(2) Looking towards the long term, the implemented instrument holds the potential to revolutionize global environmental monitoring practices. By enabling more widespread and effective detection of MPs, it has the capacity to significantly reduce the overall environmental and health impacts of plastic pollution on a global scale.
(3) The data generated by the instrument developed in this project will equip policymakers and regulatory agencies with the information and insights necessary to craft more precise and targeted regulations and policies aimed at mitigating plastic pollution. This aligns with the overarching goal of addressing the identified global challenge of MP pollution.

Name of Challenge Project: Next-Generation holographic imaging for in situ detection of Autofluorescent Microplastics in water

Literature Review

Microplastics (MPs), plastic particles ranging in size from a few millimeters (5 mm) to nanometers, have become a global environmental concern [1]. In 2019, approximately 368 million metric tons of plastics were manufactured worldwide [2]. MPs can originate from primary sources, such as microbeads in personal care products, or from secondary sources, resulting from the breakdown of larger plastics [3] They have been found in various ecosystems, including oceans and rivers [3]. Given the critical role of water bodies in the ecosystem, focusing research on MPs in aquatic environments is essential for understanding the extent of this pollution. Researchers estimate that there are approximately 24.4 trillion MPs in the world's upper oceans [4]. Human exposure to MPs has also been detected, with tiny plastic fibers found deep inside the placenta [5] and in peripheral blood lymphocytes [6], among other cases. While the health implications are still uncertain, addressing this planetary pollution requires collective efforts and informed action.

Detection and quantification of MPs are complex due to their diverse origins, sizes, shapes, and chemical compositions. Traditional methods such as visual sorting, density separation, and chemical digestion are often labor-intensive and lack sensitivity for smaller particles [7]. Advanced analytical techniques like Raman spectroscopy [8], Fourier-transform infrared spectroscopy (FTIR) [9], and pyrolysis-gas chromatography/mass spectrometry (Pyr-GC/MS) [10] are employed to identify and quantify MPs. However, these methods require sophisticated equipment and extensive sample preparation, making *in situ* measurements often impractical. Therefore, there is a pressing need for more efficient, sensitive, and reliable methods to enhance the proper assessment of MPs, especially for small and complex particles that evade detection by conventional means [9]. Targeting MPs in water bodies specifically is crucial, as it represents a major pathway through which MPs spread and impact various ecosystems and human health.

One promising approach involves leveraging the intrinsic fluorescence properties of certain MPs. Polymers such as polyethylene (PE), polypropylene (PP), polyethylene terephthalate (PET), and polystyrene (PS) exhibit intrinsic (auto) fluorescence when exposed to specific wavelengths of light (see Table 1) [11]. By relying on this inherent fluorescence, several benefits emerge, including the potential detection of MPs without the need for exogenous labels or external dyes, thereby simplifying sample preparation and reducing potential artifacts in the implemented systems [12]. This approach is particularly beneficial for analyzing water samples, where simplifying the detection process can significantly enhance the accuracy and efficiency in underwater conditions.

Polymer	**Excitation Wavelength**	**Emission Wavelength**
PET	325 nm - 305 nm	345 nm - 365 nm
PP	265 nm - 265 nm	285 nm and (main maxima)
PS	265 nm	315 nm (most intense)

Polymer	Excitation Wavelength	Emission Wavelength
PE	285 nm	305 nm

Detection of MPs using intrinsic fluorescence has been demonstrated in controlled laboratory settings [12]. Techniques such as fluorescence microscopy [7] and spectroscopy [8] are employed to identify and quantify these MPs based on their unique fluorescence signatures. In these environments, some reports use high-sensitivity cameras and specific excitation and emission filters to detect and analyze the weak fluorescence signals emitted by MPs [11]. Calibration with known standards and the use of appropriate controls are essential to differentiate MPs from background fluorescence and other artifacts. These methods provide valuable insights into the distribution, concentration, and types of MPs in various samples, paving the way for improved pollution assessment and mitigation strategies.

However, translating laboratory-oriented methods to *in situ* detection of MPs presents significant challenges. Water samples in *in situ* conditions are often complex, containing a mixture of organic matter, sediments, and other particulates that can interfere with fluorescence signals [13]. Additionally, external conditions such as varying pH, salinity, and temperature can affect the fluorescence properties of MPs, leading to potential inaccuracies in detection and quantification. *In situ* underwater detection requires robust, portable, highly sensitive and efficient systems capable of operating in diverse conditions.

Problem Statement/Objective

As previously mentioned, MPs are widespread in the environment, especially in aquatic ecosystems, raising concerns about their impact on both ecosystems and human health [3]. Accurately assessing and characterizing MPs, particularly in underwater *in situ* conditions, presents significant challenges [9]. One promising solution to address these challenges is to detect MPs with intrinsic fluorescence. By relying on this inherent fluorescence, several benefits emerge [12]. First, there is no need for exogenous labels or external dyes, simplifying sample preparation and reducing potential artifacts. Second, it is cost-effective since no additional fluorophores need to be purchased or applied. Third, intrinsic fluorescence minimizes interference with biological samples, ensuring accurate results. This is achieved through the specificity of fluorescence spectra, which allows for precise identification and differentiation of microplastics. Fourth, this approach aligns well with environmentally friendly practices when assessing MPs in underwater samples. Finally, the long-term stability of intrinsic fluorescence ensures consistent results over time. Therefore, detecting MPs by measuring their intrinsic fluorescence promises the implementation of *in situ* systems, addressing the need for accurate assessment and characterization of MPs.

Conventional microscopy systems, while effective in controlled laboratory settings, fall short when deployed in the field due to their bulkiness, complexity, and vulnerability to environmental conditions [3]. Hence, a primary technical challenge is to design a portable system capable of seamless transportation and deployment across diverse environmental contexts. Such a system would enable timely *in situ* analysis, eliminating the need for sample transportation. Additionally, another significant challenge is that conventional 2D imaging methods, like brightfield or fluorescence microscopy, offer limited insights into the 3D distribution of MPs [14]. Understanding their spatial arrangement within complex samples, such as water, soil, or sediments, is crucial for comprehensive analysis and accurate quantification. Therefore, a technique that enables volumetric assessment, capturing the true

3D nature of MPs, is imperative. From a technical standpoint, obtaining 3D information allows for precise localization and characterization of MPs within the sample volume, facilitating a more thorough understanding of their distribution and interaction with the surrounding environment.

Holographic microscopy (HM) [15] presents a solution for addressing the challenges of MP assessment. By capturing both amplitude and phase information from the samples, HM enables precise plane-by-plane volumetric information recovery. The advantages of HM are twofold: firstly, certain configurations of these systems offer large field-of-view imaging which is crucial for assessing MPs in field samples [16]. Secondly, properly configured holographic systems achieve submicrometer resolution, facilitating detailed imaging of MPs [17]. However, there is a notable gap in the literature regarding holographic microscopes with fluorescence sensitivity. The proposed methods suffer from bulkiness and impracticality for fieldwork due to their large optical components and complex setups, making them cumbersome to handle outside controlled laboratory environments [18]. Additionally, they tend to be expensive, further limiting their accessibility and widespread use. Consequently, there an urgent necessity for a more agile solution that upholds high sensitivity while being portable and adaptable to various field conditions.

In this context, Lensless holographic microscopy (LHM) emerges as an intriguing and promising alternative [19]. These systems eliminate the need for lenses, resulting in a compact and lightweight implementation. LHM systems are inherently portable, making them ideal for *in situ* measurements [20]. Furthermore, Lensless approaches, being holography-based methods, as stated before, provide volumetric information, crucial for assessing MPs within complex matrices. Additionally, LHM systems are simple and require fewer optical components, thereby reducing costs and making this approach practical for widespread deployment [21]. However, a scientific challenge persists in the proper utilization of LHM for the recovery of weak autofluorescence signals from MPs: the limited sensitivity of the methods remains a hurdle.

To achieve the required high-sensitivity capability of LHM methods, three primary issues must be addressed. First, enhancing the sensitivity of the detectors is crucial to maximize signal detection. By exploring innovative approaches, the performance of the sensors must be optimized, ensuring they capture weak autofluorescence signals emitted by MPs effectively. This optimization process will involve experimenting with different sensor configurations and employing techniques to boost sensitivity. Secondly, optimizing the optical path is essential for minimizing losses and maximizing light collection. Efficient light transmission through the system ensures that the maximum amount of signal reaches the detectors, contributing to improved sensitivity. Finally, noise reduction is paramount to maintaining a high signal-to-noise ratio. By minimizing background noise and other sources of detrimental artifacts, the system can effectively distinguish weak signals from unwanted noise, further enhancing its sensitivity to MPs. Addressing these challenges collectively will pave the way for the development of *Next-Generation* LHM systems for microplastic detection.

This project aims to create a portable, high-sensitivity holographic microscope customized for *in situ* autofluorescent microplastic underwater assessment. By integrating LHM with fluorescence sensitivity, and addressing the techniques sensitivity challenges, the project's aim is to engineer a versatile tool proficient in volumetric imaging, achieving submicrometer resolution, and ensuring the reliable detection of autofluorescent MPs in acoustic ecosystems.

Outcome(s)

Development of a lensless holographic system for autofluorescent MPs measurement: This project will provide the first LHM system with optical sensitivity tailored for the detection of autofluorescent MPs. This system will provide critical insights into the required optical filters for fluorescent detection, appropriate light excitation sources, and their integration into the system. Additionally, it will establish optimal optical configurations to balance the trade-off between field of view and spatial resolution. The findings will be reported in an OPTICA open-access journal (as required by the call guidelines) and presented at an OPTICA-organized event.

Novel proposal for in situ MP underwater assessment: This outcome includes the development of a novel in situ assessment method for MPs that complements existing detection and quantification techniques. It involves a high-throughput screening method using microfluidic systems and customized *lab-on-a-chip* technology. The project will also produce a mechanical design for *in situ* measurements that guarantees optical performance, mechanical stability, and reliability under underwater conditions. The findings will be reported in an OPTICA open-access journal (as required by the call guidelines) and presented at an OPTICA-organized event.

Comprehensive dataset of MP images in real case scenarios: The project will generate a dataset of intensity and phase images of MPs present in actual water bodies, focusing on water collection and treatment processes before human consumption. The local company handling the water supply and sanitation in Medellín, Colombia, will provide access to their water bodies for the project. The generated dataset will facilitate the detection of MPs at different stages of water treatment in a real experimental scenario, enhancing the understanding of MP distribution and behaviour in natural water systems.

Training of graduate students: As outlined in the work plan, two graduate students will be involved in the proposed research projects. They will receive training in both the scientific aspects of the technology and its application, thereby contributing to the development of highly trained professionals in this field and addressing the global challenge of MP pollution.

Impacts

Short-term impacts: The development of a portable, high-sensitivity holographic microscope for *in situ* autofluorescent MP underwater assessment will enhance MP detection and quantification, benefiting environmental monitoring programs with accurate and timely assessments. By integrating LHM with fluorescence sensitivity, the project will advance ecosystem monitoring technology, with findings published and presented to foster further research and innovation. Involving graduate students will provide hands-on experience and training in cutting-edge technology, producing skilled professionals to address MP pollution and contributing to workforce development in this critical area.

Long-term impacts: The implementation of the proposed system has the potential to transform environmental monitoring practices worldwide, enabling more widespread and effective detection of MPs and thereby reducing the overall environmental and health impacts of plastic pollution. Furthermore, the data generated by this project can inform policymakers and regulatory agencies about the extent of MP contamination and the effectiveness of existing mitigation strategies, potentially leading to the development of more stringent regulations and policies aimed at reducing plastic pollution. The success of this project could also spur further innovations in LHM and related fields, inspiring advancements in other areas of environmental

science and technology. Additionally, by demonstrating the feasibility and benefits of detecting MPs through intrinsic fluorescence without the need for exogenous labels, the project promotes more sustainable and environmentally friendly research practices, aligning with global efforts to minimize the environmental footprint of scientific activities. Finally, the enhanced environmental monitoring facilitated by this technology will directly contribute to several Sustainable Development Goals (SDGs), including SDG 6 (Clean Water and Sanitation) and SDG 14 (Life Below Water), among others, by addressing the threats posed by plastic pollution to marine and terrestrial ecosystems.

References

1. J. P. G. L. Frias and R. Nash, Mar Pollut Bull **138**, 145 (2019).
2. statista, "Annual production of plastics worldwide from 1950 to 2022," .
3. G. Lamichhane, A. Acharya, R. Marahatha, B. Modi, R. Paudel, A. Adhikari, B. K. Raut, S. Aryal, and N. Parajuli, International Journal of Environmental Science and Technology **20**, 4673 (2023).
4. M. Eriksen, L. C. M. Lebreton, H. S. Carson, M. Thiel, C. J. Moore, J. C. Borerro, F. Galgani, P. G. Ryan, and J. Reisser, PLoS One **9**, e111913 (2014).
5. A. Ragusa, A. Svelato, C. Santacroce, P. Catalano, V. Notarstefano, O. Carnevali, F. Papa, M. C. A. Rongioletti, F. Baiocco, S. Draghi, E. D'Amore, D. Rinaldo, M. Matta, and E. Giorgini, Environ Int **146**, 106274 (2021).
6. H. Çobanoğlu, M. Belivermiş, E. Sıkdokur, Ö. Kılıç, and A. Çayır, Chemosphere **272**, 129805 (2021).
7. V. Hidalgo-Ruz, L. Gutow, R. C. Thompson, and M. Thiel, Environ Sci Technol **46**, 3060 (2012).
8. C. F. Araujo, M. M. Nolasco, A. M. P. Ribeiro, and P. J. A. Ribeiro-Claro, Water Res **142**, 426 (2018).
9. J. C. Prata, J. P. da Costa, A. C. Duarte, and T. Rocha-Santos, TrAC Trends in Analytical Chemistry **110**, 150 (2019).
10. E. Fries, J. H. Dekiff, J. Willmeyer, M.-T. Nuelle, M. Ebert, and D. Remy, Environ Sci Process Impacts **15**, 1949 (2013).
11. J. Gratzl, T. M. Seifried, D. Stolzenburg, and H. Grothe, Environmental Science: Atmospheres (2024).
12. S. Morgana, B. Casentini, V. Tirelli, F. Grasso, and S. Amalfitano, TrAC Trends in Analytical Chemistry **172**, 117559 (2024).
13. E. Nicolai, R. Pizzoferrato, Y. Li, S. Frattegiani, A. Nucara, and G. Costa, Water (Basel) **14**, 3235 (2022).
14. V. Bianco, D. Pirone, P. Memmolo, F. Merola, and P. Ferraro, ACS Photonics **8**, 2148 (2021).
15. M. Kim K, (2012), **2**.
16. A. Greenbaum, Y. Zhang, A. Feizi, P. L. Chung, W. Luo, S. R. Kandukuri, and A. Ozcan, Sci Transl Med (2014).
17. C. D. Depeursinge, A. M. Marian, F. Montfort, T. Colomb, F. Charrière, J. Kühn, E. Cuche, Y. Emery, and P. Marquet, in *Fringe 2005* (Springer-Verlag, n.d.), pp. 308–314.
18. J. Rosen and G. Brooker, Nat Photonics **2**, 190 (2008).
19. P. Piedrahita-Quintero, C. Trujillo, and J. García-Sucerquia, (n.d.).
20. H. Tobon-Maya, S. Zapata-Valencia, E. Zora-Guzmán, C. Buitrago-Duque, and J. Garcia-Sucerquia, Appl Opt **60**, A205 (2021).
21. M. J. Lopera and C. Trujillo, Opt Lett **47**, 2862 (2022).

Quantum-entangled Photon-pairs On-chip based on Layered Integrated Semiconductors (q-POLIS)

What are entangled photons? The importance of quantum technologies and their impact on scientific research and society are growing at an impressive pace. As the 20th century technology has been shaped by electronic and photonic devices (the first quantum revolution), a completely new class of applications based on our ability to detect and manipulate single quantum objects (the second quantum revolution) will characterize the 21st century. Many applications of quantum technologies, including quantum information, computing, cryptography, spectroscopy and sensing, require the use of **entangled photon pairs**. One of the most efficient approaches for entangled photon pair generation is via the parametric second-order **nonlinear process** known as **spontaneous parametric down-conversion (SPDC)**, in which a high energy pump photon annihilates into the sum of signal and idler photons in a nonlinear crystal. The quantum superposition of signal and idler states generates entangled states of light, which constitute the basic building block of a quantum processor.

Entangled photon sources currently have macroscopic size. The maximum efficiency of a nonlinear process is achieved by minimizing the wave vector mismatch, achieving the so-called **phase matching** condition. **Typical phase-matched nonlinear crystals**, *e.g.*, β-barium borate and periodically poled lithium niobate, have **moderate second-order nonlinearities** ($\chi^{(2)}$=1-30pm/V) but can reach **high nonlinear efficiencies** due to their **large thickness** (millimeter/centimeter). However, such macroscopic thickness required to reach useful efficiencies **limits further technology development and on-chip integration.**

What role can two-dimensional materials play in the miniaturization paradigm? The miniaturization and on-chip integration paradigm, which has dominated the world of electronics, is now shifting to the field of photonics. The discovery of graphene, a one-atom-thick sheet of carbon atoms, opened research on other two-dimensional materials, like semiconducting **transition metal dichalcogenides (TMDs)**, *e.g.*, MoS_2. TMDs are van der Waals layered materials which are having a **transformative impact on nonlinear optics**, because of their **huge optical nonlinearity ($\chi^{(2)}$~100-1000 pm/V)**. From the first report of second harmonic generation from monolayer TMDs, many other parametric nonlinear processes have been observed, *e.g.*, sum-frequency, optical parametric amplification, third and higher order harmonics, four wave mixing and, very recently, also the generation of entangled photon pairs via SPDC.

Despite the giant nonlinearity, **the nonlinear efficiency** ($\propto[\chi^{(2)}]^2z^2$) **of monolayer TMDs is still limited by their sub-nanometer thickness** z. Such efficiency can be boosted by increasing the propagation length through the medium, *i.e.*, by increasing the TMD thickness z. However, the most studied 2H polytype is centrosymmetric in crystals with an even number of layers, resulting in a vanishing second-order nonlinearity. Recently **this limitation has been circumvented using a different crystalline phase, the non-centrosymmetric 3R polytype**. Using 3R-MoS_2 flakes, nonlinear efficiencies have been increased by ~10^4-10^5x compared to monolayers.

Pushing towards even higher conversion efficiencies, however, **requires phase-matching** the nonlinear interactions. Very recently the realization of **periodically poled 3R-stacked TMDs (PPTMDs)** has enabled quasi-phase-matched second harmonic generation and SPDC. Thanks to their superior nonlinearity, PPTMDs finally provide (i) **similar conversion efficiencies as standard bulk crystals** but **within micron thicknesses** and (ii) **SPDC coincidence-to-accidental-ratio (CAR)>350**, outperforming any SPDC source based on bare van der Waals flakes reported to date.

On-chip entangled photon sources. Despite efficient, ultracompact, broadband and programmable entangled photon sources based on layered semiconductors are now finally available, **integrating them on chip** is essential for new photonic quantum technologies required to address rising demands for fast and energy-efficient quantum processing, and it still **remains an open *challenge***.

q-POLIS wants to solve this *challenge*, **implementing entangled photon pair sources based on nano-engineered 3R-TMDs directly onto universal silicon photonics circuitry**. Producing photon pairs directly on chip will be an enabling technology for next-generation quantum photonic devices, bypassing the loss associated with coupling each photon onto the chip, which scales exponentially with the number of photons produced. Thus, integrating **TMD-based entangled photon sources** could address a major bottleneck in photonic quantum computing, impacting the **future of secure quantum operations**, creating entirely **new digital protocols and technologies**, and **enabling significant advances in computing speed, with drastically lower energy dissipation**.

Quantum-entangled Photon-pairs On-chip based on Layered Integrated Semiconductors (q-POLIS)

q-POLIS in a nutshell

Many applications of quantum technologies, including quantum information, computing, cryptography, spectroscopy and sensing, require the use of **entangled photon pairs**[1]. One of the most efficient approaches for EPP generation is via the parametric second-order nonlinear process known as **Spontaneous Parametric Down-Conversion (SPDC)**, in which a high energy photon, *i.e.*, the pump, annihilates into an *entangled photon pair*, *i.e.*, signal and idler photons[2].

Typical nonlinear crystals employed for the generation of EPPs have **moderate second-order nonlinearities ($\chi^{(2)}$ = 1-30 pm/V)** but can reach **high nonlinear conversion efficiencies** due to their **large thickness** (millimeter/centimeter). However, such macroscopic thickness does not easily allow on-chip integration of these materials. **Generating entangled photon pairs via SPDC on-chip is indeed a goal not feasible with the existing bulk crystal systems.** The **miniaturization and on-chip integration paradigm**, which has dominated the world of electronics, is now shifting to the field of photonics, with the development of all-optical integrated circuits[4], essential for new photonic technologies required to address rising demands for fast and energy-efficient **quantum processing**[5].

My project "Quantum-entangled Photon-pairs On-chip based on Layered Integrated Semiconductors" (q-POLIS) aims at bridging this gap, **realizing integrated entangled photon sources based on van der Waals layered materials**, like **transition metal dichalcogenides (TMDs)**, which have recently emerged as promising platforms for integrated nonlinear optics, thanks to their **huge second-order nonlinearity ($\chi^{(2)}$ = 100-1000 pm/V)**[6]. **TMDs indeed promise similar conversion efficiencies as standard bulk crystals but within micron thicknesses**. Producing photon pairs directly on chip will be an enabling technology for next-generation photonic quantum devices, bypassing the loss associated with coupling each photon onto the chip, which scales exponentially with the number of photons produced. Thus, integrating **TMD-based entangled photon sources** could address a major bottleneck in photonic quantum computing, **impacting the future of secure quantum operations, creating entirely new digital protocols and technologies, and enabling significant advances in computing speed, with drastically lower energy dissipation**.

Literature Review

The importance of quantum technologies and their impact on scientific research and society are growing at an impressive pace. As the 20th century technology has been shaped by electronic and photonic devices (first quantum revolution), completely new applications based on our ability to detect and manipulate single quantum objects (second quantum revolution) will characterize the 21st century. Many applications of quantum technologies, including quantum information, computing, cryptography, spectroscopy and sensing, require the use of **entangled photon pairs (EPPs)**.

One of the most efficient approaches for EPP generation is using **SPDC, a parametric second-order nonlinear optical process** in which a photon with energy $\hbar\omega_3$ (pump) is annihilated in two photons with energies $\hbar\omega_1$ (signal) and $\hbar\omega_2$ (idler), satisfying energy conservation ($\hbar\omega_1 + \hbar\omega_2 = \hbar\omega_3$)[2]. SPDC is the time-reverse process of sum-frequency generation, in which two photons $\hbar\omega_1$ and $\hbar\omega_2$ are annihilated and a photon at higher energy $\hbar\omega_3$ is generated. Second harmonic (SH) generation is the particular case of sum-frequency generation, in which the two photons have the same frequency ω and generate a new photon at the SH frequency 2ω. In all these nonlinear processes, the **efficiency is maximized** by minimizing the wave vector mismatch $\Delta k = k_3 - k_2 - k_1$, where k_1, k_2, k_3 are the wave vectors of the interacting fields[3], **achieving the so-called phase matching condition** ($\Delta k = 0$). In the following we consider the case for SH, but identical considerations apply for SPDC.

In a second-order nonlinear process under **non-phase-matched conditions**, the SH intensity periodically oscillates with the crystal thickness, with a semi-period equal to the **coherence length** $L_c = \pi/\Delta k$, due to constructive/destructive interference between pump and SH fields, which propagate inside the nonlinear crystal with different refractive indexes, thus different speeds (Fig.1). Under birefringent phase-matching conditions the interacting fields have orthogonal polarizations and propagate along a suitable direction that guarantees $\Delta k = 0$[7], allowing for the SH intensity to grow quadratically with the thickness z of the nonlinear medium. While birefringent phase matching is simple and effective, it can only be applied to a limited number of nonlinear crystals, such as the prototypical β-barium borate, which display comparatively low $\chi^{(2)}$ values of the order of a few pm/V.

An alternative to birefringent phase matching is **quasi-phase matching**, which introduces periodic

phase shifts of π between the pump and the second-harmonic every coherence length L_c (Fig.1) to re-establish the proper phase relationship and restore the quadratic growth of the the SH intensity with the propagation length ($\propto z^2$)[8]. Quasi-phase matching is typically achieved in ferroelectric crystals, like **lithium niobate**, by the so-called **periodic poling**, which consists in inverting the sign of the nonlinearity $\chi^{(2)}$ every coherence length L_c (Fig.1). The invention of **quasi-phase matching has represented a breakthrough in nonlinear optics because it has enabled the use of nonlinear crystals with higher $\chi^{(2)}$, of the order of 20-30 pm/V**, for which birefringent phase matching cannot be achieved[9]. Periodically poled lithium niobate enabled the highest SH efficiencies[10], optical parametric amplifiers and oscillators, and entangled photon pairs via SPDC, representing the current gold standard for nonlinear frequency conversion.

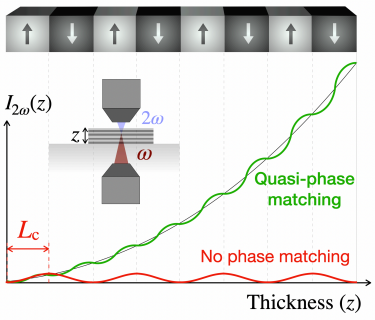

Figure 1 | Thickness-dependent SH in quasi-phase-matching (Δk=0) and no phase-matching (Δk≠0) conditions.

Typical **phase-matched nonlinear crystals**, like β-barium borate or periodically poled lithium niobate, possess **moderate nonlinearities ($\chi^{(2)}$ = 1-30 pm/V)** but can reach **high conversion efficiencies** due to their **large thickness** (millimeter/centimeter). However, such macroscopic thickness limits further technology development and integration, making the generation of **entangled photon pairs via SPDC on-chip not feasible with the existing bulk nonlinear crystals.**

The discovery of graphene, a one-atom-thick sheet of carbon atoms, opened research on other van der Waals materials, like **semiconducting TMDs**, *e.g.*, MoS_2. Similar to graphene, TMDs can be thinned down, *e.g.*, by mechanical exfoliation, to the 2D monolayer limit[11,12]. Mono- and few-layer crystals can then be stacked into vertical heterostructures with tailored optical properties and arbitrary twist-angles, leading to the emergence of new physics and unlocking new technological applications[13]. Van der Waals materials are also having a **transformative impact** on **nonlinear optics,** because of their **huge optical nonlinearity ($\chi^{(2)}$~100-1000 pm/V)**, up to 1000x higher than standard bulk crystals[14]. From the first report of second harmonic from monolayer TMDs[15], a plethora of nonlinear processes have been observed, *e.g.*, sum-frequency, optical parametric amplification[16], third and higher order harmonics, four wave mixing and, recently, also SPDC[17].

Despite the giant nonlinearity $\chi^{(2)}$, **the SH conversion efficiency** ($I_{2\omega}/I_\omega \propto [\chi^{(2)}]^2 z^2$) **of monolayer TMDs is still limited by their sub-nm thickness** z. Such efficiency can be boosted by increasing the propagation length through the medium, *i.e.*, by increasing the TMD thickness z. However, the most studied 2H polytype is centrosymmetric for crystals with an even number of layers, resulting in a vanishing second order nonlinearity. Recently **we have circumvented this limitation using a different crystalline phase, the non-centrosymmetric 3R polytype**[18]. By measuring thickness-dependent SH in 3R-MoS_2, we have shown that its coherence length at 1520nm is L_c~500nm[19]. Additionally, at L_c we have reported record enhancement of the conversion efficiency: 10^4-10^5 higher than a monolayer, resulting in an overall conversion efficiency $I_{2\omega}/I_\omega \sim 10^{-6}$[19,20]. **The generation of entangled photons from 3R-MoS_2 via SPDC has also been demonstrated**, with polarization-entangled Bell states with fidelity as high as 96%[21].

Pushing towards higher SH conversion efficiencies, comparable to bulk nonlinear crystals ($I_{2\omega}/I_\omega \sim 1-10\,\%$), **requires phase-matching the nonlinear interactions.** Very recently I conceived, designed and realized engineered stacks of 3R-stacked semiconductors to demonstrate **quasi-phase-matched SH and SPDC in periodically poled 3R-stacked transition metal dichalcogenides (PPTMDs)[22]**, illustrated in Fig. 2.

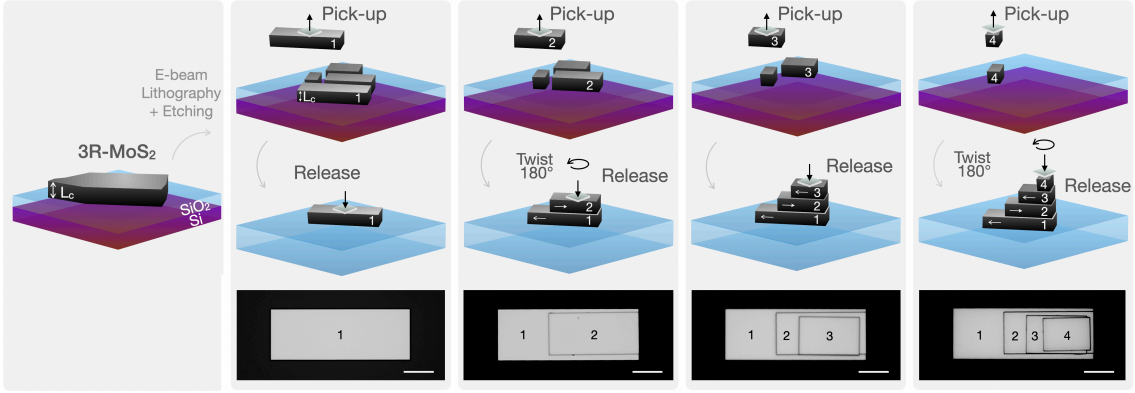

Figure 2: Procedure schematics used to fabricate periodically poled transition metal dichalcogenides (PPTMDs) by etching a 3R-MoS_2 flake, followed by pick-up, twisting and release. Sample micrographs below, scale bar 10 μm.

In PPTMDs we achieve (1) **SH conversion efficiencies close to $I_{2\omega}/I_{\omega} \sim 0.1\,\%$, over only 3 µm thickness**, and (2) **coincidence-to-accidental-ratio (CAR) >350**, *i.e.*, two-orders of magnitude larger than any other SPDC source based on bare van der Waals flakes[17,21]. This work has extraordinary consequences from both fundamental and applied viewpoints, as it **initiates the field of *phase-matched nonlinear optics with layered semiconductors*** and finally **bridges macroscopic and microscopic nonlinear optics,** providing **macroscopic efficiencies over microscopic thicknesses**.

Problem Statement/Objective

Despite efficient, ultracompact, broadband and programmable entangled photon sources based on layered semiconductors are now finally available[22], **integrating them on chip** is essential for new on-chip photonic quantum technologies required to address rising demands for fast and energy-efficient quantum processing, and it still **remains an open *challenge***. q-POLIS wants to solve this *challenge*, **implementing entangled photon pair sources based on nano-engineered 3R-TMDs directly onto universal silicon photonics circuitry**.

As periodically poled lithium niobate crystals enabled the largest efficiencies over millimeter-thick lengths, 3R-TMDs will represent another breakthrough for nonlinear optics, as they will unlock **macroscopic efficiencies over micrometer thicknesses, directly on chip**. Beyond PPTMDs for quasi-phase-matched SPDC, also **programmable metastructures with 3R-TMDs** will be realized. Leveraging on the local field enhancement metastructures could achieve **similar efficiencies of PPTMDs**, but this time pushing it **down to sub-wavelength thicknesses**. The operating frequency can be easily tuned in the **visible or near infrared** range, simply by **changing the slab thickness** and the **metastructure geometry,** enabling **next-generation on-chip integrated low-dimensional and frequency tunable EPPs.** Producing photon pairs directly on chip could address a major bottleneck in quantum photonics, as it would bypass the loss associated with coupling each photon onto the chip (scaling exponentially with the number of photons produced). In turns, it would shrink the size of **quantum processors** from tens of centimeters down to the size of optical chips, *i.e.*, few **millimeters.**

The term ‘q-POLIS’, from the greek ‘πόλις’ (‘city’), represents the project ambition of creating a *quantum* city. Like in a real city essential amenities and services are located close to each other for efficiency and accessibility, q-POLIS aims at integrating on-chip entangled photon pairs, *i.e.*, the missing on-chip building block of a quantum processor, mirroring the organization and convenience of a city but in the quantum technology realm.

Outcomes

q-POLIS is a multidisciplinary project with well-defined and quantifiable goals: to design and realize integrated entangled photon sources based on nanoscale-engineered van der Waals materials. Its main outcomes, which reflect the logical development steps, are:

1. Design and realization of nano-structured TMD-based entangled photon sources using two main platforms: periodically poled structures and metasurfaces.

2. On-chip integration of TMD-based entangled photon sources on silicon photonics platforms using thin claddings, directional couplers and tapering.

This proposal represents a disruptive innovation in integrated nonlinear and quantum optics, which will result in the **first implementation of fully integrated entangled photon sources**, leveraging on the extreme nonlinearity of TMDs.

Outcome 1 — Design and realization of nanostructured TMD-based EPP sources.

Periodically-poled 3R-stacked transition metal dichalcogenides (PPTMDs). q-POLIS will start off by tackling the controlled nanoscale engineering of 3R-TMDs, the go-to materials in view of their unique nonlinear and quantum properties. I will focus on operation wavelengths in the relevant telecom band (*i.e.*, 1550 nm), designing crystals that are ready to be integrated into standard on-chip silicon photonics platforms based on silicon oxide (SiO_2) and silicon nitride (SiN) circuitry. Since SH and degenerate SPDC photon energies are identical and time-reversible, modeling and initial characterization will focus on the experimentally more straight-forward SH process. To design PPTMDs, q-POLIS will benefit from the collaboration with Prof. A. Marini, from Università dell’Aquila (Italy), a leader in the field of analytical calculations of the nonlinear response of low-dimensional crystals, and specifically TMDs. Following the methodology that I developed[22], **to realize PPTMDs operating at 1550 nm, the coherence length L_c will be first measured** by thickness-dependent SH in multilayers of 3R-MoS_2. Like the conventional 2H phase, 3R-TMD flakes can be exfoliated from their bulk counterpart following the well-established scotch-tape technique. High quality bulk 3R crystals are now commercially available from several companies, *e.g.*, HQ

Graphene. q-POLIS will benefit the collaboration with Prof. P. J. Schuck and Prof. J. Hone, who lead worldwide recognized laboratories for 2D material processing at Columbia University (USA). The sample preparation will be carried out in their cleanroom facilities, equipped with optical and atomic force microscopes, electron beam lithography systems, etching systems and probe stations that will allow us to exfoliate, search, characterize, pattern and stack TMD flakes into PPTMDs (Fig.2). I have a proven expertise at fabricating/characterizing TMDs, having worked on 2D materials since 2016.

3R-metasurfaces. A complementary strategy to enhance light-matter nonlinear interaction includes the possibility to pattern **nano-structured metasurfaces**, to enable local field enhancement for more efficient nonlinear processes [23]. q-POLIS also aims at designing and realizing nonlinear 3R-metasurfaces. For the metasurface design (for both SH and SPDC), q-POLIS will benefit from the collaboration with Prof. A. Alù, from City University of New York (USA), a worldwide recognized scientist in the field of metamaterials. I will then imprint the optimum calculated design directly on 3R-MoS_2 flakes, by direct patterning and etching. Leveraging the high refractive index of 3R-MoS_2 (ranging between 4 and 5.5) to squeeze the mode volume, and the periodic trenches to maximize the mode overlap between the pump and the SH/SPDC, I aim at fabricating sub-diffractive nanostructures directly on 3R-MoS_2 flakes using a modified CMOS-like scalable process, to achieve at least two orders of magnitude nonlinear enhancement compared to the unpatterned flake. Starting from 3R-MoS_2 slabs which already provide 10^4-10^5 stronger nonlinear emission compared to a monolayer, the further two-order of magnitude enhancement provided by the patterned **metasurface will enable macroscopic conversion efficiencies** but this time **over sub-wavelength-thick active metamaterial**.

To fully characterize SPDC from PPTMDs and metasurfaces and prove polarization entanglement [21] between signal and idler photons, I will perform **quantum tomographic measurements**. In quantum state tomography the entangled photons are projected onto various polarization bases using a combination of quarter waveplates, half waveplates and linear polarizers. Photons are detected using single-photon detectors and coincidences obtained via photon-counting electronics. By performing projections on different basis states, the density matrix of the quantum state can then be determined.

Outcome 2 — Integration of TMD-based EPPs on silicon photonics chips.

q-POLIS will be concluded by tackling the core objective of the proposal: integrating on chip the optimally designed and nano-engineered 3R-TMD platforms. I aim at integrating 3R-MoS_2 crystals on standard silicon photonics chips, for mainstream compatibility and straight forward extension to large-scale all-optical on-chip processing, establishing new protocols for TMD integration.

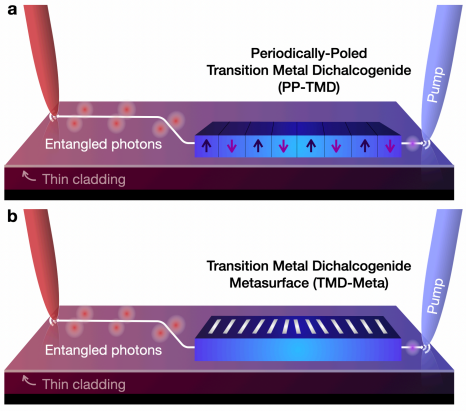

Figure 3: Scheme of the integrated entangled photon sources based on periodically poled crystals and metasurfaces made of 3R-TMDs.

I will first perform and optimize coupling with individual 3R-MoS_2 flakes. I aim at coupling TE modes [19,20] from the silicon waveguide to the TMD through evanescent field coupling, *i.e.*, by placing the TMD crystal on top of the waveguide. Since SiO_2/SiN waveguides are typically cladded with a >1 μm fused silica protection layer, with a thickness comparable to or higher than the mode size supported by the waveguide, we aim at **thinning the cladding down to ~50 nm** via controlled deposition and etching, in order to **achieve efficient light coupling (>20%)** into the flake. To improve coupling even further, prior to the flake transfer on-chip we also aim at tapering the flake via lithography and etching. To selectively in- and out-couple different frequencies we will introduce tailored grating couplers, with optimized pitch, as well as directional couplers. To design, realize and optimize the silicon photonic circuit on top of which perform the TMD integration, q-POLIS will benefit the collaboration with Prof. M. Lipson at Columbia University, a worldwide leader in the field of integrated photonics. Following efficient integration of individual 3R-MoS_2 flakes, I will then proceed integrating PPTMDs (Fig.3a) and metasurfaces (Fig.3b). Once on-chip integration has been achieved, to fully characterize the generated polarization quantum state, I will perform **quantum tomographic measurements** out-coupling the SPDC emission in free-space. **This measurement will allow full monitoring and optimization of the quantum state, generated by PPTMDs and metasurfaces on the chip**. Achieving successful integration of 3R-TMD platforms will represent a milestone in the field on integrated optics, as it will enable the **first on-chip, programmable, micrometer long/thick classical and quantum light source**.

Impact

Exploiting the concepts of **quantum superposition**, **quantum interference** and **quantum entanglement**, quantum technologies hold the promise of disruptive conceptual and technological advances in computation, communications, sensing and simulations. Several groundbreaking applications are already beginning to appear: **quantum computers**, based on either superconducting circuits[24] or photonic circuits[25], have demonstrated a quantum advantage in accomplishing specific operations, and promise to solve key societal problems, *e.g.*, design of new drugs, weather forecasting, modeling of financial markets; **quantum key distribution** enables two parties to exchange a secret key while detecting an eavesdropper, allowing secure communications, and has already been demonstrated over satellites[26]; **quantum sensing** can be used in a variety of metrological applications, from biomedical imaging to mineral prospecting to precision navigation; **quantum squeezing** is used in the LIGO interferometer to detect gravitational waves[27]. In view of this huge untapped potential, many governments have launched billion-worth research programs such as the European Quantum Flagship and the Quantum Leap efforts from the US National Science Foundation. At the same time, an increasing number of quantum start-ups are appearing on the market, aimed at providing commercial solutions for the essential building blocks of quantum technologies as well as complete systems for quantum computing, key distribution and sensing.

Several platforms have been proposed to implement quantum states, including superconducting junctions, trapped ions, trapped neutral atoms and spins in semiconductors. Among these solutions, **light stands out due to its unique properties**: it exhibits quantum effects at room temperature, exceptionally low noise, and strong entanglement between the photons. **Quantum photonics has therefore become a key player in the quantum revolution**. Like classical photonic technologies, which started with discrete optical components and rapidly evolved towards photonic integrated circuits (PICs), integrated quantum photonics will come more and more into the spotlight. Quantum PICs (qPICs) will offer several advantages with respect to their discrete counterparts, such as small footprint, high stability, portability, and enhanced light-matter interactions due to the strong spatial confinement of light. Standard passive integrated optics components, such as waveguides, splitters, directional couplers and resonators, can be readily fabricated in qPICs using established material platforms such as silicon nitride and lithium niobate, leveraging the advanced manufacturing technologies developed for the semiconductor industry, which enable large-scale, low-cost and reproducible fabrication. However, a **key outstanding challenge** is the **integration of quantum light sources. Producing photon pairs directly on chip** could address a major bottleneck in quantum photonics, as it would **bypass the loss associated with coupling each photon onto the chip** (scaling exponentially with the number of photons produced). In turns, it would shrink the size of **quantum processors** from tens of centimeters down to the size of optical chips, *i.e.*, few **millimeters. q-POLIS precisely addresses this gap** by **developing on-chip integrated entangled photon sources**.

Layered semiconductors, and particularly TMDs, will revolutionize opto-electronics and nanotechnology by enabling completely novel functionalities. In view of their quantum properties, TMDs will provide access to new products that will confer information and communication functionalities to traditionally non-electronic products. In addition to a scientific and technological impact, the implementation of quantum technologies with TMDs, that do not require cumbersome low-temperature experimental conditions to operate, **could also be key to bringing energy efficient quantum technology to the market**. The reduction of energy consumption on large-scale devices can lead to significant cuts in CO_2 emissions.

As an Early Career Scientist, I aim to advance my academic career, gaining independence and leadership as PI by establishing my own research group. I envision to **initiate a novel nonlinear quantum nano-optics branch based on engineered layered materials, with q-POLIS serving as a cornerstone of this new chapter in my career**. Although its goals are ambitious, q-POLIS is also founded on solid grounds, and I believe my proven expertise in the field of nonlinear optics and layered materials perfectly fits the ideal profile to lead this project and *solve this Challenge*. q-POLIS will be instrumental in helping me to achieve research independence and to foster excellence in my scientific profile. The *Challenge* resources provided by the Optica Foundation will be essential to achieve these interdisciplinary scientific goals, independently, and to enhance my success in securing future projects. In addition, the professional relationships I will cultivate with the other Challenge Awardees of 2024 and of the past years will enrich my international network with a diverse and young community of scientists. Building such a solid support ground among one another will create more opportunities for us, collectively, to become successful young group leaders in the near future.

References

1. P. G. Kwiat, K. Mattle, H. Weinfurter, A. Zeilinger, A. V. Sergienko, and Y. Shih, “New High-Intensity Source of Polarization-Entangled Photon Pairs”, Phys. Rev. Lett. 75, 4337 (1995).
2. A. Anwar, C. Perumangatt, F. Steinlechner, T. Jennewein, and A. Ling, “Entangled photon-pair sources based on three-wave mixing in bulk crystals”, Rev. Sci. Instrum. 92, 041101 (2021).
3. C. Manzoni and G. Cerullo, “Design criteria for ultrafast optical parametric amplifiers,” J. Opt. 18, 103501 (2016).
4. S. Y. Siew, B. Li, F. Gao, H. Y. Zheng, W. Zhang, P. Guo, S. W. Xie, A. Song, B. Dong, L. W. Luo, C. Li, X. Luo, and G.-Q. Lo, "Review of Silicon Photonics Technology and Platform Development," J. Lightwave Technol. 39, 4374-4389 (2021).
5. E. Pelucchi, G. Fagas, I. Aharonovich et al., “The potential and global outlook of integrated photonics for quantum technologies”, Nat. Rev. Phys. 4, 194–208 (2022).
6. O. Dogadov, C. Trovatello, B. Yao, G. Soavi, and G. Cerullo, “Parametric Nonlinear Optics with Layered Materials and Related Heterostructures”, Laser & Photonics Rev. 16, 2100726 (2022).
7. R. W. Boyd, Nonlinear Optics, Academic Press, Boston (2020).
8. M.M. Fejer, D.H. Jundt, R.L. Byer, and G.A. Magelh, “Quasi-phase-matched second harmonic generation: tuning and tolerances”, IEEE J. Quantum Electron. 28, 2631 – 2654 (1992).
9. A. Boes et al., “Lithium niobate photonics: Unlocking the electromagnetic spectrum”, Science 379, eabj4396 (2023).
10.S. Suntsov, C.E. Rueter, D. Brueske and D. Kip, “Watt-level 775 nm SHG with 70% conversion efficiency and 97% pump depletion in annealed/reverse proton exchanged diced PPLN ridge waveguides”, Opt. Express. 29, 11386–11393 (2021).
11.S. Manzeli, D. Ovchinnikov, D. Pasquier, O.V. Yazyev and A. Kis, “2D transition metal dichalcogenides”, Nat. Rev. Mater. 2, 17033 (2017).
12.S. Dal Conte, C. Trovatello, C. Gadermaier, and G. Cerullo, “Ultrafast Photophysics of 2D Semiconductors and Related Heterostructures,” Trends in Chemistry 2, 28–42 (2020).
13.K. S. Novoselov et al., “2D materials and van der Waals heterostructures”, Science 353, aac9439 (2016).
14.K. Yao et al. “Continuous Wave Sum Frequency Generation and Imaging of Monolayer and Heterobilayer Two-Dimensional Semiconductors”, ACS Nano 14, 708-714 (2020).
15.L.M. Malard, T.V. Alencar, A. P.M. Barboza, K.F. Mak, and A.M. de Paula, “Observation of intense second harmonic generation from MoS2 atomic crystals”, Phys. Rev. B 87, 201401(R) (2013).
16.C. Trovatello et al. “Optical parametric amplification by monolayer transition metal dichalcogenides”, Nat. Photon. 15, 6 (2021).
17.Q. Guo, X.Z. Qi, L. Zhang et al., “Ultrathin quantum light source with van der Waals NbOCl2 crystal”, Nature 613, 53–59 (2023).
18.J. Shi et al. “3R MoS2 with Broken Inversion Symmetry: A Promising Ultrathin Nonlinear Optical Device”, Adv. Mater. 29, 1701486 (2017).
19. X. Xu, C. Trovatello, F. Mooshammer , Y. Shao , S. Zhang , K. Yao , D. N. Basov , G. Cerullo , and P. J. Schuck “Towards compact phase-matched and waveguided nonlinear optics in atomically layered semiconductors”, Nat. Photon. 16, 698–706 (2022).
20.F. Mooshammer, X. Xu, C. Trovatello et al. “Enabling Waveguide Optics in Rhombohedral-Stacked Transition Metal Dichalcogenides with Laser-Patterned Grating Couplers”, ACS Nano 18, 4118-4130(2024).
21. M. A. Weissflog et al. “A Tunable Transition Metal Dichalcogenide Entangled Photon-Pair Source”, arXiv preprint arXiv:2311.16036 (2023).
22. C. Trovatello et al., "Quasi-phase-matched up-and down-conversion in periodically poled layered semiconductors", arXiv preprint arXiv:2312.05444 (2023).
23. G. Li, S. Zhang, and T. Zentgraf, “Nonlinear photonic metasurfaces”, Nat. Rev. Mater. 2, 17010 (2017).
24. F. Arute, K. Arya, R. Babbush et al., “Quantum supremacy using a programmable superconducting processor”, Nature 574, 505–510 (2019).
25. H.-S. Zhong et al., “Quantum computational advantage using photons”, Science 370, 1460-1463 (2020).
26. J. Yin et al., “Satellite-based entanglement distribution over 1200 kilometers”, Science 356, 1140-1144 (2017).
27. L. McCuller et al. “Frequency-Dependent Squeezing for Advanced LIGO”, Phys. Rev. Lett. 124, 171102 (2020).

Executive Summary:

In-situ nanoparticle monitoring and analysis using modulated light patterns.

Our environment contains a multitude of micro and nano-sized particles, from man-made particulate matter such as microplastics to smoke and exhaust pollutants as well as air- and water-borne pathogens. Depending on the type of particle and its concentration, this can greatly affect human health, especially in densely populated areas. Standard measurement methods rely on concentration of particulate matter via filters and measuring optical transparency, weight, or mechanical resonance. However, their resolution is limited to micron sized particles. Dynamic light scattering based methods and photoacoustic methods have been able to measure size distributions in the nanometre scale. However, these rely on ensembles of nanoparticles and only measure size distributions or only target certain materials. Condensation particle counters can measure single nanoparticles and combined with a differential mobility analyser provides size discrimination. They can also be bulky and require consumable working fluids with related high operation costs. In all cases, discerning nanoparticle materials properties requires laboratory analysis.

The goal of this project is to develop a method for in-situ measurement of single nanoparticles at low concentration, including the detection of single nanoparticles, measurement of their size in the range of 10's of nm to 100's of nm, and spectroscopic characterisation. Developing such a method will fill an urgent need to better understand and monitor the types of nanoparticles present in our environment, to identify pollutants, for early detection of pathogens, etc., in an economical manner. The innovations being explored to achieve this goal are based on using modulated light patterns to measure nanoparticle velocity, position, and size, with methods adapted from single molecule localisation microscopy as well as techniques from x-ray beam monitoring and flow cytometry. Further, infrared absorption spectroscopy on single nanoparticles will be employed using a novel, compact, and simple spectrometer within the same optical system that is robust to vibrations. This will allow not only size measurement, but also basic materials characterisation and classification, such as the identification of air- and water-borne viruses. The device will integrate microfluidic systems to control nanoparticle distribution and flow rate, while recent developments in fabrication techniques for rapid prototyping of micro-optical systems will be used and incorporated into the system for optical illumination and measurement as well as microchannel integration.

Current technologies can only count and measure nanoparticle size distributions. Being able to not only measure single nanoparticle sizes more precisely but also their spectral absorption will allow better nanoparticle classification and identification, leading to breakthroughs in environmental monitoring by providing us with real-time understanding of the nano-world surrounding us. Such an in-situ measurement device will find applications in, for example, monitoring water sources for nano-plastics, monitoring transit hubs such as airports for airborne pathogens, monitoring industrial processes for pollutants such as soot, etc. By adapting and synthesising latest developments in micro-optics fabrication and compact spectrometer design, such a method for in-situ nanoparticle monitoring and analysis will be realised, helping us detect and prevent diseases transmitted by environmental nanoparticles in order to safeguard our health.

Proposal name: In-situ nanoparticle monitoring and analysis using modulated light patterns.

Literature review:

Micro and nanoparticles surround us, and can be found in our environment in the air we breathe and water we drink [1]. These nanoparticles can be a cause of concern for human health, both directly via ingestion or inhalation, and indirectly by affecting the ecosystem [2]. Mitigating this risk requires understanding the type of nanoparticle and its origins, for example whether they are biologically active (such as airborne viruses) or inorganic but toxic (such as heavy metals) or increasingly common (such as certain nano-plastics) [1,3,4]. Nanoparticle size is particularly important in the context of human health as toxicity is correlated with surface area [5,6]. Furthermore, a nanoparticle's materials properties, such as whether it is an inorganic compound or a bioactive pathogen [7–9] will inform the required response necessary to mitigate health risks.

In-situ and on-line detection and monitoring of nanoparticles (< 1 μm size) with size discrimination typically rely on electrical charging for size separation followed by detection. For example, a scanning mobility particle sizer, the gold standard for aerosol counting, relies on a differential mobility analyser to separate nanoparticles based on their electrical mobility followed by a condensation particle counter which grows each nanoparticle via nucleation in a supersaturated vapour to be counted optically. However, this method can involve bulky equipment and consumable working fluids, driving up operational costs [10]. Impactors and filters are used for particles larger than a few microns while dynamic light scattering can be used for nanometre sized particles, however, both require a large ensemble of particles and cannot measure single particles. For in-situ nanoparticle characterisation, time-of-flight aerosol mass spectroscopy can be used, however the equipment can be bulky and expensive [11,12].

Recent developments in microsystems engineering have resulted in new concepts for single nanoparticle detection, sizing, and analysis. Mechanical resonances of cantilevers were used to detect single nanoparticles and measure their mass [13,14]. Plasmonic [15,16] and dielectrophoretic [17] trapping have been used to trap nanoparticles within a sensing region (e.g., for surface enhanced Raman spectroscopy). Further, confinement of nanoparticles within a small volume was used to enhance nanoparticle tracking analysis measurements [18] while optical confinement was used to enhance light-matter interactions to improve signal-to-noise ratio [19,20].

Meanwhile, in the field of microscopy, structured illumination microscopy [21] and super-resolution microscopy using patterned illumination [22] have improved imaging resolution significantly, down to a few nanometres. By using modulated light patterns, single fluorescing emitters have been tracked at nm resolution [23]. Similarly, developments in 3D printing of optical components has allowed production of customised structured light fields for point-spread-function engineering [24]. This presents an opportunity to synthesize these cross-disciplinary ideas and apply them to environmental nanoparticle monitoring. By using state-of-the-art 2-photon lithography for micro-optical component fabrication integrated with microfluidic channels, a compact design for nanoparticle sizing and spectroscopy will be explored. This is based on aerodynamic particle sizing [25] and conventional flow cytometry [26] where a nanoparticle traverses a region with two light beams, giving both size and velocity information. The novelty is that by using an interference pattern the size can be determined with greater accuracy, while by using broadband illumination and measuring velocity, spectroscopy can be performed to enable nanoparticle characterisation.

Problem statement/objective:

The aim of the project is to measure, in-situ, the size and absorption spectrum of single nanoparticles. This will involve **a)** the use of modulated light patterns in a confined microfluidic channel with controlled flow rates to measure the size of single nanoparticles and **b)** the use of light-fields with custom wavelength distribution in space to perform absorption spectroscopy on a nanoparticle moving at a measured speed. In order for in-situ measurements, the device must be able to operate in the field

with a simple concept to keep costs low and measurements robust. To achieve this, the latest methods in micro-fabrication and 3D printing of micro-optics and micro-fluidics will be used.

Consider a single nanoparticle moving with a constant velocity (Fig. 1a). By illuminating it with a sinusoidal light pattern, for example via the interference pattern from counterpropagating coherent light beams, some of its properties can be measured. If the nanoparticle movement direction is known, such as via a continuous laminar flow inside a long microfluidic channel with a sheath fluid, the speed of the nanoparticle as it traverses the interference pattern can be measured based on the modulated scattered light, similar to aerodynamic particle sizing. Detection limits depend on the speed of the nanoparticle compared to the detector/camera speed. For a nanoparticle speed of ~1 m/s, an avalanche photodetector with MHz response is sufficient to measure a signal and determine speed [27].

For fast moving nanoparticles and/or relatively slow photodetectors, the interference pattern itself can be moved. By tracking the phase of the light pattern, e.g. via electro-optic modulators or relatively inexpensive thermo-optic modulators, such that the known light pattern travels near the speed of the nanoparticle, the modulated scattered light signal can be measured easily, and the speed calculated from the scattered signal frequency (Fig. 1a). This is analogous to single molecule tracking with patterned illumination, used in super-resolution microscopy to triangulate the location of single emitters [22,23,28]. Furthermore, the scattered light's modulation contrast (Fig. 1a) and average light intensity (Fig. 1b) can indicate Rayleigh scattering cross-section and thus nanoparticle size [27]. Following [27], the modulation contrast, M (denoted M.C. in Fig. 1a), is given by:

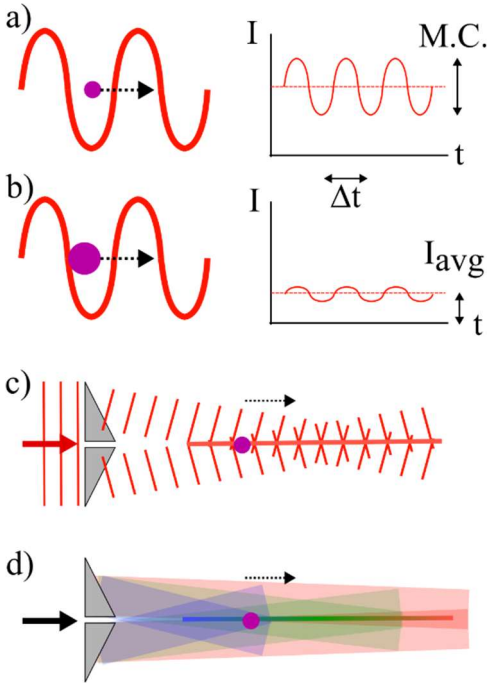

Figure 1: a) Nanoparticle inside a modulated light pattern produces a modulated intensity signal with frequency and modulation contrast (M.C.) indicating speed and size. b) Average intensity can also be measured. c) One way to produce intensity fringes using a Bessel beam. d) Broadband Bessel beam acts like calibrated wavelength source for spectroscopy.

$$M = \frac{1}{1-(2d/p)^2}\cos(\pi d/p) \quad (1)$$

where p is the periodicity or pitch of the illumination interference pattern and d is the nanoparticle size. Similarly, the Rayleigh scattering cross-section, σ_S, which is related to the scattered light intensity, is given by:

$$\sigma_S \approx 90\frac{d^2}{\lambda^4}\delta n^2 \quad (2)$$

where λ is the illumination wavelength and δn is the refractive index difference between the nanoparticle and the fluid medium. Following the equations above, and for illumination light in the visible wavelength, nanoparticle detection size ranges from tens of nm to hundreds of nm [27]. This method has previously been used for in-line monitoring of x-ray beam sizes in synchrotron facilities [29]. The benefit of using modulated light is that measurement sensitivity and signal-to-noise ratio can be vastly improved via filtering and lock-in amplification, and hence fluorescence labelling might be avoided. Without the need for specimen preparation, in-situ measurements can thus be taken.

For the production of counterpropagating waves inside a micro-fluidic cavity containing the specimen, various methods can be used, such as high-NA microscope objective or prism-based light illumination [27]. Recently, fabrication methods for rapid prototyping of micro-optical elements have been developed, allowing miniaturisation of optical systems [30]. By using miniaturised micro-mirrors, waveguides, or Bessel beams (Fig. 1c), precise interference patterns can be produced, with phase control via electro-optic or thermo-optic modulators. For example, axicons can be used to produce long, non-

diffracting Bessel beams with a modulating intensity pattern in the core (Fig. 1c). The contrast of this modulated pattern can be increased by counterpropagating another beam via a mirror or a second axicon. By then using broadband illumination light, the interference pattern can be engineered such that different wavelength components are diffracted to specific regions along the path of the nanoparticle (Fig. 1d). If the nanoparticle velocity and initial position are known (such as via measurements using the modulated light patterns above) and on-axis and off-axis detectors are used to record the absorbed and scattered light signals respectively, the absorption spectrum of the nanoparticle can be recovered via deconvolution. The benefit of this arrangement is not only simplicity but also due to a smaller number of moving parts, such as reference mirrors, and smaller micro-metre distances between optical elements the system is more robust to vibrations, making it suitable for field spectroscopy. Of particular interest is short-wavelength infrared spectral region as many molecular transitions and absorption features occur in this range for organic and polymeric materials.

Micro-optics fabrication processes have been developed by the applicant using 2-photon lithography, allowing production of modulated light beams integrated with miniaturised systems. Fig. 2a shows scalar diffraction simulations [31] of optical propagation of axicon produced Bessel beam (top), where the length of the beam can be extended by a precisely angled axicon (middle) or encasing the axicon in a second refractive-index-matched resin (bottom) allowing relaxation of fabrication tolerances [24] from a 1° axicon to a 20° axicon. Fig. 2b shows simulation and experimental results of using this technique to fabricate a 2 mm diameter 3D printed spiral phase plate producing a vortex beam (unpublished), while fig. 2c shows a 3D printed micro-optical mirror facet at the end of a fibre ferrule (unpublished). This micro-optics fabrication technology can be adapted to produce the modulated illumination patterns within an integrated miniaturised device necessary for this proposal. Apart from the Bessel beam configuration mentioned above, and in order to mitigate project risks, a waveguide/micro-prism system will also be designed and evaluated (Fig. 3), with the advantage of better integration for micro-fluidic flow at the expense of more complicated optics design. The same concept of multi-material high-resolution 2-photon lithography will be used to produce precise waveguides and prisms to generate the required interference patterns.

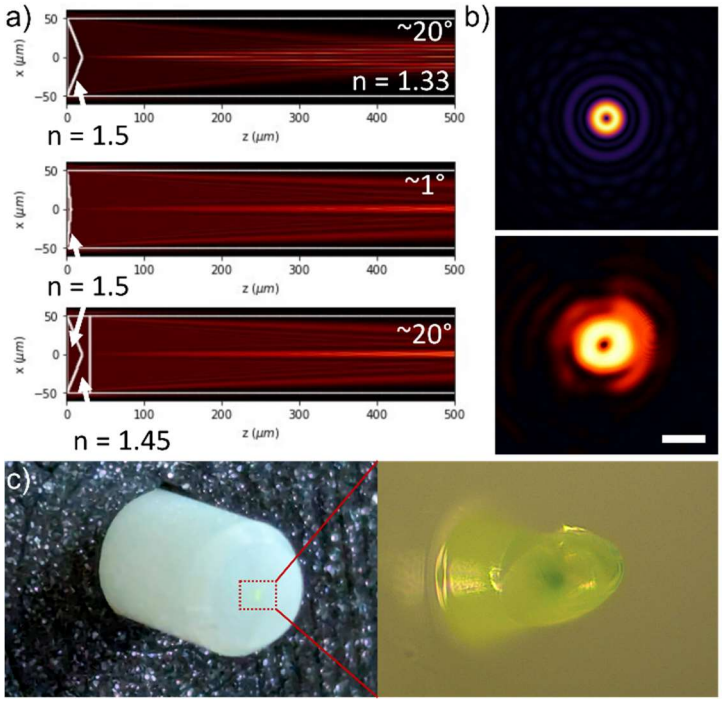

Figure 2: a) Simulations of axicon producing a Bessel beam. The beam length can be extended by fabricating a multi-material axicon. b) Simulation and experimental result of m = 1 spiral phase plate producing a vortex beam (scale bar = 200 μm). c) Micro-optic mirror with attached lens printed on the end of an optical fibre ferrule. The element has approximate dimensions of ~100 μm x ~200 μm.

In summary the concept relies on using a microfluidic channel to impart a constant velocity on a nanoparticle specimen via a sheath fluid. Because of its constant velocity, and the fact that the nanoparticle will pass through regions of defined wavelengths and modulated light patterns, its size and absorption spectrum can be measured. By miniaturisation using state-of-the-art micro-optics fabrication, costs can be kept low, and a compact device be realised for field use. The specific milestones set to achieve this aim are demonstration of a tabletop system for size and velocity measurement, translation into a miniaturised device, and finally integration of spectroscopy (see Timeline). To mitigate risks, multiple designs will be evaluated, and the scheme demonstrated first on a tabletop system.

Nanoparticle tracking using widefield microscopy will be used to ensure microfluidic system produces constant flowrates. Miniaturisation will be based on existing microfabrication processes developed by the applicant. In case scattered signal is insufficient, fluorescent markers will be used to troubleshoot the system while cavity mirrors will be used to improve modulation contrast of the illuminating pattern [27]. For spectroscopy, in case scattered signal is insufficient, instead of a broadband light-source, a tunable light-source with sufficient temporal coherence to produce interference patterns will be used and swept in wavelength, allowing combination of both pattern modulation and multiple wavelength excitation.

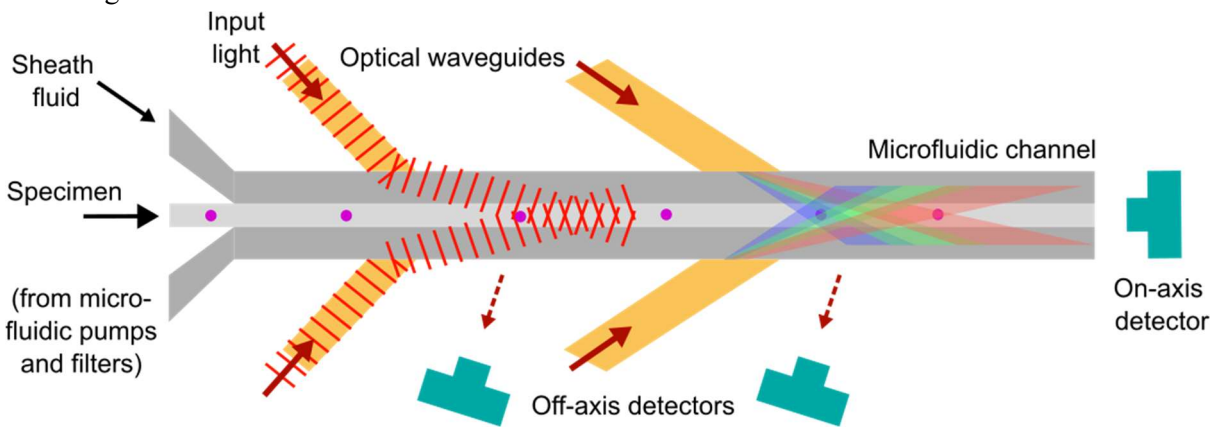

Figure 3: Alternative concept for in-situ nanoparticle size measurement and absorption spectroscopy.

Outcomes:

This project will explore a novel synthesis of microfluidic flow and patterned light to monitor and analyse nanoparticle properties. A tabletop system will first be designed and constructed as proof-of-principle, followed by translation of the concept into a chip-based miniature device using state-of-the-art microfabrication. Outcomes will include a prototype device for measuring single nanoparticle size and materials properties at technology readiness levels (TRL) 4/5, in preparation for systems integration at TRL 6. The developed prototype will allow measurement of calibration nanoparticles such as plastic nano-beads, metallic nano-spheres, and nanoparticles coated with various biological materials such as proteins, in a laboratory setting. By demonstrating the robustness of the concept, future integration into a field-ready prototype (including pre-filtering and automated fluid handling) can be explored possibly with industrial partners under industry linkage schemes and funding opportunities. This might include international air-monitoring or air-conditioning manufacturers as well as system integrators such as building and infrastructure engineers. Such a prototype can also lead to custom instruments for a range of scientific and industrial projects such as water-quality monitoring and flow cytometry in the pharmaceutical sector.

Currently, in-situ nanoparticle analysis is very challenging, where specimens must typically be collected and analysed in a laboratory using bulky and expensive tools such as mass spectrometers, electron microscopes, and chemical analyses. The outcomes of this project will lead to a breakthrough in how single nanoparticles can be identified in-situ and in real-time, in a variety of environments. This will open the door to real-time monitoring of the nanoparticles in our environment, ranging from pollutants to pathogens, organic matter, nano-plastics, soot, and so on.

Another outcome is the development of a laboratory platform for microfluidic handling of nanoparticles integrated with modulated illumination and microscopy imaging. This platform will allow further concepts for nanoparticle analysis to be explored. For example, using the sheath fluid at a different refractive index as a light-guide, light can be confined within the nanoparticle stream, enhancing light-matter interactions for improved scattering intensities allowing the tracking of sub-10 nm particles [18,19,32].

State-of-the-art microfabrication techniques will be used to fabricate the devices in this project. Some of those methods, such as multi-material printing for refractive-index-matched optical elements, micro-lens elements, and integration with miniature systems such as optical fibres have been developed or used by the applicant. New related methods will form part of project outcomes, such as micro-optics for short-wavelength infrared spectroscopy, micro-optics/micro-fluidics design integration, and incorporation of thermo-optic resistive heating elements for light phase control. The applicant has over 10 years' microfabrication experience and is in an excellent position to develop novel fabrication processes that could be useful in a variety of applications.

This seed funding will also provide the applicant, as an early-career researcher in applied optics and nanoscience who recently returned to Australia despite several career interruptions, to establish an experimental laboratory and solid track-record for independent research. This will allow the applicant to further explore their interests in multidisciplinary research at the intersection of applied optics, nanotechnology, and imaging and spectroscopy for foundational challenges of the future.

Impact:

Much of our environment is invisible to us. This includes the myriad of microparticles and nanoparticles that surround us both in air and water, with both natural and man-made origins. These can include viruses and pathogens such as Zika and SARS, inorganic micro/nanoprecipitates originating from industrial processes, and naturally occurring nano-particulates. Detecting these nanoparticles in-situ is possible but classifying them requires laboratory analysis of their chemical composition and size, which can be time-consuming. With the increasing concern over polluting microparticles in our environment such as microplastics and incidental nanoplastics [3], industrial byproducts such as engineered nanomaterials, as well as concern over active pathogens that spread illness as highlighted by the recent pandemic, there is an urgent need for in-situ real-time measurement, analysis, and classification of the nano-objects in our environment.

In order to solve this problem, this project will explore a method for in-situ characterisation of nanoparticles including their size and absorption spectrum. The innovations to achieve this aim will be applying miniaturised micro-optical and micro-fluidic systems together with control over illumination patterns and nanoparticle flowrates to measure velocity, size, and absorption within a compact, robust, and inexpensive device suitable for field measurements. It is envisaged that such low-cost devices will permit spatially dense measurement coverage and provide real-time data on environmental nanoparticles. This will allow a breakthrough in how we quantify and measure the nano-environment surrounding us, warning us about potential hazards that could impact human and ecological health.

References:

1. Scientific committee on emerging and newly identified health risks (SCENIHR), "The appropriateness of existing methodologies to assess the potential risks associated with engineered and adventitious products of nanotechnologies (modified opinion after public consultation)," (2006).
2. S. Smita, S. K. Gupta, A. Bartonova, M. Dusinska, A. C. Gutleb, and Q. Rahman, "Nanoparticles in the environment: assessment using the causal diagram approach," Environ Health **11**, S13 (2012).
3. J. Gigault, H. El Hadri, B. Nguyen, B. Grassl, L. Rowenczyk, N. Tufenkji, S. Feng, and M. Wiesner, "Nanoplastics are neither microplastics nor engineered nanoparticles," Nat. Nanotechnol. **16**, 501–507 (2021).
4. M. Bundschuh, J. Filser, S. Lüderwald, M. S. McKee, G. Metreveli, G. E. Schaumann, R. Schulz, and S. Wagner, "Nanoparticles in the environment: where do we come from, where do we go to?," Environ Sci Eur **30**, 6 (2018).
5. F. Serita, H. Kyono, and Y. Seki, "Pulmonary Clearance and Lesions in Rats after a Single Inhalation of Ultrafine Metallic Nickel at Dose Levels Comparable to the Threshold Limit Value.," INDUSTRIAL HEALTH **37**, 353–363 (1999).
6. O. Schmid and T. Stoeger, "Surface area is the biologically most effective dose metric for acute nanoparticle toxicity in the lung," Journal of Aerosol Science **99**, 133–143 (2016).
7. J. S. Kutter, D. De Meulder, T. M. Bestebroer, P. Lexmond, A. Mulders, M. Richard, R. A. M. Fouchier, and S. Herfst, "SARS-CoV and SARS-CoV-2 are transmitted through the air between ferrets over more than one meter distance," Nat Commun **12**, 1653 (2021).
8. J. V. Puthussery, D. P. Ghumra, K. R. McBrearty, B. M. Doherty, B. J. Sumlin, A. Sarabandi, A. G. Mandal, N. J. Shetty, W. D. Gardiner, J. P. Magrecki, D. L. Brody, T. J. Esparza, T. L. Bricker, A. C. M. Boon, C. M. Yuede, J. R. Cirrito, and R. K. Chakrabarty, "Real-time environmental surveillance of SARS-CoV-2 aerosols," Nat Commun **14**, 3692 (2023).
9. M. Pan, J. A. Lednicky, and C. -Y. Wu, "Collection, particle sizing and detection of airborne viruses," J Appl Microbiol **127**, 1596–1611 (2019).
10. H. Lee, S.-J. Yook, and K.-H. Ahn, "Effects of exponentially decaying and growing concentrations on particle size distribution from a scanning mobility particle sizer," Aerosol Science and Technology **54**, 1135–1143 (2020).
11. F. Drewnick, S. S. Hings, P. DeCarlo, J. T. Jayne, M. Gonin, K. Fuhrer, S. Weimer, J. L. Jimenez, K. L. Demerjian, S. Borrmann, and D. R. Worsnop, "A New Time-of-Flight Aerosol Mass Spectrometer (TOF-AMS)—Instrument Description and First Field Deployment," Aerosol Science and Technology **39**, 637–658 (2005).
12. C. C. Harper, Z. M. Miller, M. S. McPartlan, J. S. Jordan, R. E. Pedder, and E. R. Williams, "Accurate Sizing of Nanoparticles Using a High-Throughput Charge Detection Mass Spectrometer without Energy Selection," ACS Nano **17**, 7765–7774 (2023).
13. M. M. Daryani, T. Manzaneque, J. Wei, and M. K. Ghatkesar, "Measuring nanoparticles in liquid with attogram resolution using a microfabricated glass suspended microchannel resonator," Microsyst Nanoeng **8**, 92 (2022).
14. S. Schmid, M. Kurek, J. Q. Adolphsen, and A. Boisen, "Real-time single airborne nanoparticle detection with nanomechanical resonant filter-fiber," Sci Rep **3**, 1288 (2013).
15. K. B. Crozier, "Plasmonic Nanotweezers: What's Next?," ACS Photonics **11**, 321–333 (2024).
16. S. L. Kitaw, Y. S. Birhan, and H.-C. Tsai, "Plasmonic surface-enhanced Raman scattering nano-substrates for detection of anionic environmental contaminants: Current progress and future perspectives," Environmental Research **221**, 115247 (2023).
17. C. T. Ertsgaard, M. Kim, J. Choi, and S.-H. Oh, "Wireless dielectrophoresis trapping and remote impedance sensing via resonant wireless power transfer," Nat Commun **14**, 103 (2023).
18. T. Wieduwilt, R. Förster, M. Nissen, J. Kobelke, and M. A. Schmidt, "Characterization of diffusing sub-10 nm nano-objects using single anti-resonant element optical fibers," Nat Commun **14**, 3247 (2023).
19. L. Kohler, M. Mader, C. Kern, M. Wegener, and D. Hunger, "Tracking Brownian motion in three dimensions and characterization of individual nanoparticles using a fiber-based high-finesse microcavity," Nat Commun **12**, 6385 (2021).

20. S. Spindler, J. Ehrig, K. König, T. Nowak, M. Piliarik, H. E. Stein, R. W. Taylor, E. Garanger, S. Lecommandoux, I. D. Alves, and V. Sandoghdar, "Visualization of lipids and proteins at high spatial and temporal resolution via interferometric scattering (iSCAT) microscopy," J. Phys. D: Appl. Phys. **49**, 274002 (2016).
21. R. Heintzmann and T. Huser, "Super-Resolution Structured Illumination Microscopy," Chem. Rev. **117**, 13890–13908 (2017).
22. J. Cnossen, T. Hinsdale, R. Ø. Thorsen, M. Siemons, F. Schueder, R. Jungmann, C. S. Smith, B. Rieger, and S. Stallinga, "Localization microscopy at doubled precision with patterned illumination," Nat Methods **17**, 59–63 (2020).
23. F. Balzarotti, Y. Eilers, K. C. Gwosch, A. H. Gynnå, V. Westphal, F. D. Stefani, J. Elf, and S. W. Hell, "Nanometer resolution imaging and tracking of fluorescent molecules with minimal photon fluxes," Science **355**, 606–612 (2017).
24. R. Orange kedem, N. Opatovski, D. Xiao, B. Ferdman, O. Alalouf, S. Kumar Pal, Z. Wang, H. von der Emde, M. Weber, S. J. Sahl, A. Ponjavic, A. Arie, S. W. Hell, and Y. Shechtman, "Near index matching enables solid diffractive optical element fabrication via additive manufacturing," Light Sci Appl **12**, 222 (2023).
25. P. A. Baron, "Calibration and Use of the Aerodynamic Particle Sizer (APS 3300)," Aerosol Science and Technology **5**, 55–67 (1986).
26. M. Rieseberg, C. Kasper, K. F. Reardon, and T. Scheper, "Flow cytometry in biotechnology," Applied Microbiology and Biotechnology **56**, 350–360 (2001).
27. T. Shintake, "Proposal of Absolute Nanometer Size Measurement in Flow Cytometry Based on Laser Interferometry," (2021).
28. P. van Velde, B. Rieger, T. Hinsdale, jelmer Cnossen, D. Fan, S. Hung, D. Grunwald, and C. Smith, "ZIMFLUX: Single molecule localization microscopy with patterned illumination in 3D," Opt. Express (2023).
29. T. Shintake, "Proposal of a nanometer beam size monitor for e+e− linear colliders," Nuclear Instruments and Methods in Physics Research Section A: Accelerators, Spectrometers, Detectors and Associated Equipment **311**, 453–464 (1992).
30. L. Siegle, S. Ristok, and H. Giessen, "Complex aspherical singlet and doublet microoptics by grayscale 3D printing," Opt. Express **31**, 4179 (2023).
31. L. M. Sanchez Brea, "Diffractio, python module for diffraction and interference optics," (2019).
32. R. W. Taylor and V. Sandoghdar, "Interferometric Scattering Microscopy: Seeing Single Nanoparticles and Molecules via Rayleigh Scattering," Nano Lett. **19**, 4827–4835 (2019).

Optically guided intraoperative assessment of surgical margins in cancer

One in every three people will develop cancer in their lifetime, meaning almost every person in the world has been affected either directly or indirectly by the disease. In 90% of cancer cases, solid tumors are responsible, for which the most common method of treatment is surgical excision. Unfortunately, however, it is estimated that up to 20% of these procedures do not result in full removal of the tumor, leaving the cancer free to continue to grow and lowering the odds of survival for the patient. In this challenge, we would like to **imagine what could happen if the surgeon was able to leave the operating room confident that they had removed the entirety of the tumor, every time.**

We propose to build a multimodal polarization-sensitive optical coherence tomography (PS-OCT) system with microscope-level resolution, specifically for the purpose of intraoperative cancer cell detection. The system will be cart-based, capable of sitting within the operating theater so that specimens can be imaged immediately following excision. If the surface of the excised tissue still contains cancer, the surgeon can then go on to excise further until negative margins are found. In the long term, we envision that this method of intraoperative imaging will replace the current gold standard of post-operative histopathology, where patients must currently wait a week on average for the results.

While optical imaging more broadly is increasingly demonstrating its power in diagnostics, we believe that our solution addresses the issue in a manner which is reliable, fast, and inexpensive:

Superior resolution. Axial resolution in PS-OCT is proportional to the square of the central wavelength of the light source. By bringing the wavelength down into the visible light range, we will improve the axial resolution by an order of magnitude. The lateral resolution on the other hand is dictated by the imaging optics like in traditional microscopy. By using visible light, we can share the same objective lens kits as microscopy uses, resulting in cellular-scale imaging across wide fields of view.

Speed and simplicity. There is currently no optical method of intraoperative margin assessment that has made it past the research phase. We believe that this is, in part, due to the high complexity of the systems that are typically developed for this purpose. Our solution will be built to reduce all complexity of operation, with automated scanning and classification, so the only input required from the user is to place the tissue to be investigated face-down on the scanner and press a “go” button.

Lower cost. The blue light SLED used as the primary light source in this work is an order of magnitude cheaper than the visible-light sources (supercontinua) that have been proposed for microscopy-like OCT resolution in the past. This will make the device cheaper to roll out in the future – not only to the tertiary-care-providing institutions. Also, since this optical imaging technique requires very little manual input, it will reduce the cost of human resources required to perform routine histopathology.

This study is intended to be a proof-of-concept demonstration of the ability of a blue light OCT system and its extensions to provide cellular level histopathology-like analysis of an excised tumor surface. If successful, it will be the first in a fleet of intraoperative OCT-based imaging techniques developed in the lab, all serving the goal of removing every last cancer cell.

This application falls under the “Health” subcategory of the Optica Foundation Challenge.

Cancer is responsible for one in every six deaths worldwide [1], but many cancers can be cured if they are treated early enough. In the case of solid tumors, which represent approximately 90% of adult cancers [2], surgical resection is the most common and most effective method of treatment [3]. Unfortunately, however, complete surgical resection is challenging as the surgeons have few visual cues to indicate infiltration zones, and it is estimated that up to 20% of all cancer surgeries fail to completely remove the tumor, but this number could actually be as high as 60% for some cancers [4]. The clinical gold standard for assessing the success of tumor removal is to examine the excised tissue using histopathology. As described in Fig. 1 (top row), histopathology involves several steps of tissue preparation before being embedded, sectioned and stained for imaging through a slide scanner.

While accurate, the many steps involved require experienced technicians to be on site to perform this, and typically patients have to wait approximately one week or more for results [5]. In the case where the excised tumor surface was found to contain tumor cells, known as a positive surgical margin, the patient must either undergo a second surgery, experience laser ablation therapy, or take the “wait and see” approach to assess if the tumor starts to regrow. In cancer, early treatment is key, and these unnecessary delays in treatment lead to poorer survival outcomes [6].

If a surgeon had access to surgical margin information during the procedure, they would be able to ensure that the whole tumor is removed. In recognition of this and the limitations associated with histopathology, attention has recently turned to optical methods to provide an intraoperative alternative, allowing the surgeon to act on positive margins before the surgery’s conclusion.

Intraoperative optical detection of cancerous cells

There has been recent success in intraoperative tumor margin assessment using fluorescent imaging probes, where a fluorescent tracer is administered prior to surgery either via injection or orally [7,8], however the addition of exogeneous contrast agents in this way is not suitable for use on all patients. Fluorescent signal is also proportional to the number of cancerous cells in the tissue, which means that the infiltration zone “glows” only very dimly, which can still result in tumor being missed [9]. Reaching histopathology-level resolution, Stimulated Raman spectroscopy has demonstrated its ability to classify the major histopathologic classes of brain tumors and also identify potential zones of infiltration based on the intrinsic vibrational properties of tissues [10]. However, the high complexity of this system makes it incredibly expensive and therefore prohibitive to mass rollout beyond neurosurgery. Hyperspectral imaging, where the field is imaged across a range of wavelengths, is another imaging modality that has shown promise in tumor margin identification [11]. While initial results have shown high accuracies of tumor detection in breast cancer [12], hyperspectral imaging lacks depth resolution and hence information about the 3D morphology of the cells is lost, as is information about the distance from the tumor cell to the surface.

From two to three dimensions

A natural imaging technique to turn to for depth-resolved optical imaging contrast is optical coherence tomography (OCT) [13]. Based on low-coherence interferometry, OCT is an inherently three-dimensional imaging modality that has approached near real-time visualization in recent years [14]. There have been several studies that have demonstrated the ability of OCT to differentiate healthy from cancerous tissue based on backscattered

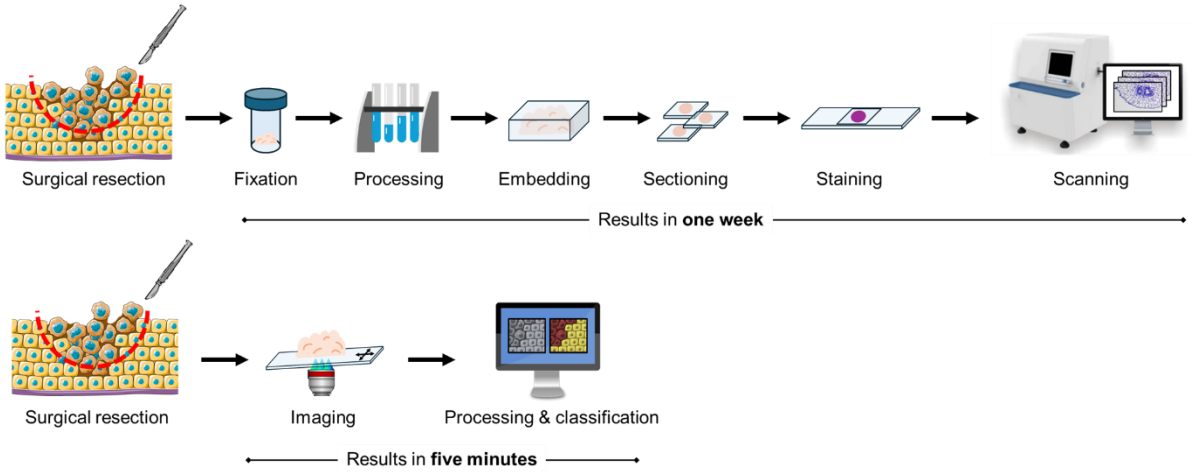

Figure 1. *The gold standard method of tumor margin assessment is histopathology, represented in the top row. This process is laborious, expensive and slow. Our proposed optical-imaging-based method, represented in the bottom row, would allow intraoperative assessment of the tumor margin, allowing the surgeon to resect more tissue in case a positive margin is identified.*

intensity contrast; healthy cells and cancer cells have different attenuation properties [15-17]. This allows maps of tissue type to be generated and visualized, ready for interpretation.

Traditional OCT is conducted in the near-infrared region, as these wavelengths provide a good trade-off between adequate imaging resolution (~10 μm) while maintaining a penetration depth down to around 2 mm. To improve the resolution, shorter wavelengths are needed, i.e., the visible light region. Visible light OCT boasts axial resolutions on the order of 1 μm [18] and, when coupled with microscopy-like objective lenses, reaches submicron lateral resolution. This means it is capable of 3D mapping on a cellular level, and can give clear tissue discrimination between tumor and healthy tissue, with the infiltration zones sitting neatly in between the two [19].

Attenuation vs. fiber orientation as a contrast mechanism

What traditional OCT is not sensitive to, however, is sample orientation. To visualize orientation, we need to extend the capability of an OCT system to be polarization-sensitive (PS) by illuminating a sample with light of a known polarization state and using PS detection methods to measure any changes that occur to that state [20]. In doing this, it is possible to measure phase retardation, which is a measure of the birefringence, or “orderedness”, of the sample with respect to the incoming light beam; and optic axis orientation, which provides a 2D vector field of fiber orientation. This provides exquisite contrast for any tissue that has a defined microstructural orientation, such as collagen, muscle or nerve [21]. An example of collagen alignment revealed by PS-OCT can be found in Fig. 2.

In solid tumors, the cancer cells surround themselves with type I collagen fibers, which form the majority of the tumor microenvironment [22]. Understanding the growth patterns of these collagen fibers may be cruicial for understanding tumor progression. However, unlike the type II collagen fibers in Fig. 2 that tend to grow in parallel to one another (found in articular cartilage), type I fibers can change direction very quickly, and so cellular-level resolution is needed to understand the directionality. To date, polarimetric imaging of type I collagen fibers has been largely limited to two dimensions [23].

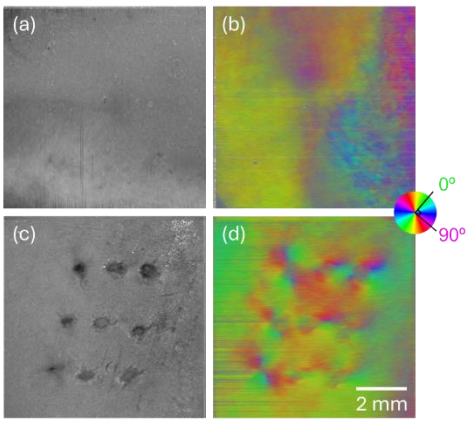

Figure 2. *OCT images of healthy (a-b) and laser-damaged (c-d) articular cartilage. The intensity-based structural images (a,c) give no information regarding the fiber structure. PS-OCT imaging, on the other hand, shows the variation in preferred collagen fiber alignment. Smooth transitions in fiber orientation occur naturally in healthy cartilage (b). The radial patterns in (d) indicate the reorganization of the collagen fiber microstructure around the laser ablation holes during healing. (Unpublished data from ongoing work)*

Toward a solution

We believe that a cellular-resolution 3D imaging system with polarization sensitivity would be the ideal combination for intraoperative tumor margin assessment, and constructing and validating such a system is the theme of this proposal.

Objective. In this project, we seek to overcome the limitations of traditional histopathology by providing an optical alternative for cancer detection that can be used intraoperatively.

A blue light PS-OCT system will be constructed, specifically tailored to the problem of positive margin detection. A schematic of the final system can be found in Fig. 3, and the two-part construction of the system is described in Specific Aims 1 and 2. The following features make this the ideal imaging system for this application:

1) The axial resolution of an optical coherence tomography system is dependent on the wavelength of the light, so using blue light instead of the traditional near-infrared reduces the axial resolution by an order of magnitude at the same bandwidth [24].
2) At shorter wavelengths, phase retardation occurs faster in oriented tissues (collagen). This means that a blue-light PS-OCT system is inherently more sensitive than those at longer wavelengths, e.g., in the near-infrared.
3) The only penalty for these improvements is a shallower penetration depth when compared to near-infrared light. However, as we are only looking at the tumor margin and not deeper into the sample, this is not a concern here. If additional penetration

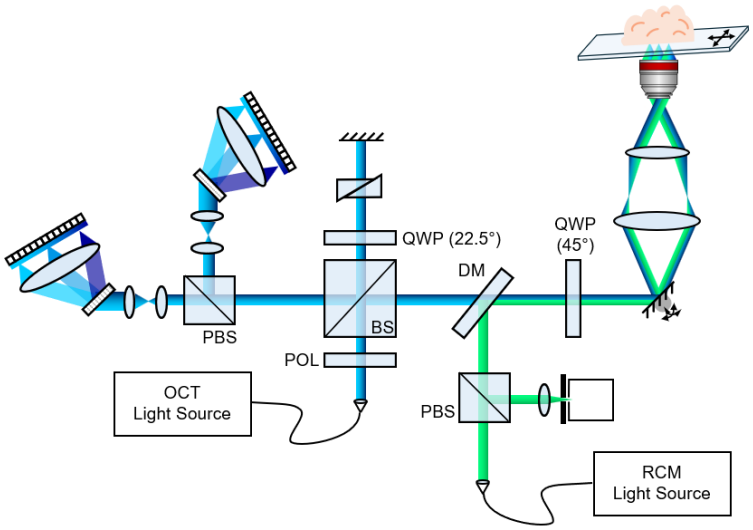

Figure 3. *The proposed multimodal PS-OCT and scanning RCM system. An OCT light source centered at 450 nm can share scanning and imaging optics with the 560-nm RCM channel. The paths are combined at the entrance to the scanner using a dichroic mirror (DM). BS: Beamsplitter. PBS: Polarizing beamsplitter. POL: Polarizer. QWP: Quarter-wave plate.*

depth is needed, we can amplify the power further as the laser beam will be enclosed and *ex vivo* tissue is not subject to the same power limitations as *in vivo* tissue.

4) A reflectance confocal microscopy (RCM) channel will be included at only a small additional system complexity (adding just a light source, beamsplitter and detector) to provide fully co-registered imaging with a previously validated technique.
5) The system will be cart-based in preparation for seamless integration into the operating theater, and the automated imaging will be microscope-like, familiar to the user and requiring very little manual input.
6) To image the sample at several magnifications, like in microscopy, a microscope objective turret will be integrated into the system containing magnifications ranging from 4x to 40x.
7) Using a blue light SLED as the light source reduces the PS-OCT system costs greatly and makes it possible to replicate this system for a larger study following this one.

As described in Specific Aim 3, the data produced by the system will be fed into a machine learning algorithm for automated classification of tissue into cancerous or non-cancerous, at a cellular level, using tissue samples sourced from the Human Research Tissue Bank at Cambridge University Hospital under the University of Cambridge Human Tissue Act Research Licence.

Intended outcomes

At the conclusion of this pilot project, we will have demonstrated that, with automated sample scanning and classification, it is possible to perform tumor margin assessment based on blue light PS-OCT in under five minutes. We will have demonstrated this in two cancer types. In addition to this data-driven outcome, this project will also result in an outcome from a technical perspective: this will be the first demonstration of blue light PS-OCT, which we believe will have the highest PS-sensitivity to date owing to its short wavelength.

As part of this project, a databank of fully deidentified co-registered cellular-level OCT, PS-OCT and RCM images will be made available open-source. These images will be the first of their kind and other researchers may benefit from using them as training data, or simply for understanding more about the 3D micro- and macrostructure of collagen fibers in the tumor microenvironment.

It is important to note that this system is intended to be the first in a fleet of OCT-based intraoperative tumor detectors, fueled by their low cost and high sensitivity. This is not just a single system for research purposes, but rather a pilot system for a much larger project. As such, this system will be designed in a manner that has user friendliness at its core, with upgrades to the system also being very simple if there are additional application-specific needs for other cancers in the future.

Making an impact

Everybody knows somebody who has been affected by cancer, and no patient or their loved ones want to hear that their resection was incomplete, one week later. Beyond the clear emotional toll that this takes on the patient, it also usually results in a second surgery which carries a huge additional burden to the healthcare system. If the surgeon could leave the operating theater sure that no positive margins remain, the need for additional surgery would

simply vanish. We hope that this study may serve as a first step in eliminating these unnecessary procedures, improving the quality of life for cancer patients and their families.

Managing anxiety caused by biopsy result waiting times. In this project, we are focusing on tumor margin assessment, as survival and reoperation outcomes are highly dependent upon this. However, this system will also be capable of providing intraoperative biopsy results, reducing the amount of time a patient must wait to hear the results about whether they have cancer or not. It has been well documented that anxiety rates increase while awaiting biopsy results [25] and rollout of a system such as this could help prevent improve the mental health of patients during a stressful time.

Looking ahead

Although the study proposed as part of this work will be conducted on biobank-sourced tissues, the system that we will construct for imaging will be cart-based and all tissue contact surfaces will be sterilizable. This means that, following a successful ethics board approval, we will be ready to take this technology directly into the operating theater for intraoperative imaging as the next step toward fully automated margin assessment, and a larger grant application to do just that will be submitted using the preliminary data generated in this work.

References

[1] World Health Organization (2022). *Cancer*. [online] World Health Organization. Available at: https://www.who.int/news-room/fact-sheets/detail/cancer.

[2] Butcher, L., 2008. Solid tumors: Prevalence, economics, and implications for payers and purchasers. *Biotechnology Healthcare*, *5*(1), p.20.

[3] Sullivan, R., Alatise, O.I., Anderson, B.O., Audisio, R., Autier, P., Aggarwal, A., Balch, C., Brennan, M.F., Dare, A., D'Cruz, A. and Eggermont, A.M., 2015. Global cancer surgery: delivering safe, affordable, and timely cancer surgery. *The Lancet Oncology*, *16*(11), pp.1193-1224.

[4] Piper, M.L., Wong, J., Fahrner-Scott, K., Ewing, C., Alvarado, M., Esserman, L.J. and Mukhtar, R.A., 2019. Success rates of re-excision after positive margins for invasive lobular carcinoma of the breast. *NPJ Breast Cancer*, *5*(1), p.29.

[5] Cancer.net. (2013). *Biopsy*. [online] Available at: https://www.cancer.net/navigating-cancer-care/diagnosing-cancer/tests-and-procedures/biopsy.

[6] Hanna, T.P., King, W.D., Thibodeau, S., Jalink, M., Paulin, G.A., Harvey-Jones, E., O'Sullivan, D.E., Booth, C.M., Sullivan, R. and Aggarwal, A., 2020. Mortality due to cancer treatment delay: systematic review and meta-analysis. *BMJ*, *371*.

[7] Koch, M., de Jong, J.S., Glatz, J., Symvoulidis, P., Lamberts, L.E., Adams, A.L., Kranendonk, M.E., Terwisscha van Scheltinga, A.G., Aichler, M., Jansen, L. and de Vries, J., 2017. Threshold analysis and biodistribution of fluorescently labeled bevacizumab in human breast cancer. *Cancer Research*, *77*(3), pp.623-631.

[8] Tummers, Q.R., Hoogstins, C.E., Gaarenstroom, K.N., de Kroon, C.D., van Poelgeest, M.I., Vuyk, J., Bosse, T., Smit, V.T., van de Velde, C.J., Cohen, A.F. and Low, P.S., 2016. Intraoperative imaging of folate receptor alpha positive ovarian and breast cancer using the tumor specific agent EC17. *Oncotarget*, *7*(22), p.32144.

[9] de Wit, J.G., Vonk, J., Voskuil, F.J., de Visscher, S.A., Schepman, K.P., Hooghiemstra, W.T., Linssen, M.D., Elias, S.G., Halmos, G.B., Plaat, B.E. and Doff, J.J., 2023. EGFR-targeted fluorescence molecular imaging for intraoperative margin assessment in oral cancer patients: a phase II trial. *Nature Communications*, *14*(1), p.4952.

[10] Hollon, T.C., Pandian, B., Adapa, A.R., Urias, E., Save, A.V., Khalsa, S.S.S., Eichberg, D.G., D'Amico, R.S., Farooq, Z.U., Lewis, S., Petridis, P.D. et al. 2020. Near real-time intraoperative brain tumor diagnosis using stimulated Raman histology and deep neural networks. *Nature Medicine*, *26*(1), pp.52-58.

[11] Zhang, Y., Wu, X., He, L., Meng, C., Du, S., Bao, J. and Zheng, Y., 2020. Applications of hyperspectral imaging in the detection and diagnosis of solid tumors. *Translational Cancer Research*, *9*(2), p.1265.

[12] Kho, E., de Boer, L.L., Van de Vijver, K.K., van Duijnhoven, F., Vrancken Peeters, M.J.T., Sterenborg, H.J. and Ruers, T.J., 2019. Hyperspectral imaging for resection margin assessment during cancer surgery. *Clinical Cancer Research*, *25*(12), pp.3572-3580.

[13] Bouma, B.E., de Boer, J.F., Huang, D., Jang, I.K., Yonetsu, T., Leggett, C.L., Leitgeb, R., Sampson, D.D., Suter, M., Vakoc, B.J., Villiger, M. and Wojtkowski, M., 2022. Optical coherence tomography. *Nature Reviews Methods Primers*, *2*(1), p.79.

[14] Li, J.D., Viehland, C., Dhalla, A.H., Trout, R., Raynor, W., Kuo, A.N., Toth, C.A., Vajzovic, L.M. and Izatt, J.A., 2023. Visualization of surgical maneuvers using intraoperative real-time volumetric optical coherence tomography. *Biomedical Optics Express*, *14*(7), pp.3798-3811.

[15] Lichtenegger, A., Gesperger, J., Kiesel, B., Muck, M., Eugui, P., Harper, D.J., Salas, M., Augustin, M., Merkle, C.W., Hitzenberger, C.K., Widhalm, G., Woehrer, A and Baumann B., 2019. Revealing brain pathologies with multimodal visible light optical coherence microscopy and fluorescence imaging. *Journal of Biomedical Optics*, *24*(6), pp.066010-066010.

[16] Yuan, W., Kut, C., Liang, W. and Li, X., 2017. Robust and fast characterization of OCT-based optical attenuation using a novel frequency-domain algorithm for brain cancer detection. *Scientific Reports*, *7*(1), p.44909.

[17] Aleksandrova, P.V., Zaytsev, K.I., Nikitin, P.V., Alekseeva, A.I., Zaitsev, V.Y., Dolganov, K.B., Reshetov, I.V., Karalkin, P.A., Kurlov, V.N., Tuchin, V.V. and Dolganova, I.N., 2024. Quantification of attenuation and speckle features from endoscopic OCT images for the diagnosis of human brain glioma. *Scientific Reports*, *14*(1), p.10722.

[18] Harper, D.J., Augustin, M., Lichtenegger, A., Eugui, P., Reyes, C., Glösmann, M., Hitzenberger, C.K. and Baumann, B., 2018. White light polarization sensitive optical coherence tomography for sub-micron axial resolution and spectroscopic contrast in the murine retina. *Biomedical Optics Express*, *9*(5), pp.2115-2129.

[19] Gesperger, J., Lichtenegger, A., Roetzer, T., Salas, M., Eugui, P., Harper, D.J., Merkle, C.W., Augustin, M., Kiesel, B., Mercea, P.A., Widhalm, G., Woehrer, A and Baumann B., 2020. Improved diagnostic imaging of brain tumors by multimodal microscopy and deep learning. *Cancers*, *12*(7), p.1806.

[20] De Boer, J.F., Hitzenberger, C.K. and Yasuno, Y., 2017. Polarization sensitive optical coherence tomography–a review. *Biomedical Optics Express*, *8*(3), pp.1838-1873.

[21] Tang, P., Kirby, M.A., Le, N., Li, Y., Zeinstra, N., Lu, G.N., Murry, C.E., Zheng, Y. and Wang, R.K., 2021. Polarization sensitive optical coherence tomography with single input for imaging depth-resolved collagen organizations. *Light: Science & Applications*, *10*(1), p.237.

[22] Hsu, K.S., Dunleavey, J.M., Szot, C., Yang, L., Hilton, M.B., Morris, K., Seaman, S., Feng, Y., Lutz, E.M., Koogle, R. and Tomassoni-Ardori, F., 2022. Cancer cell survival depends on collagen uptake into tumor-associated stroma. *Nature Communications*, *13*(1), p.7078.

[23] Liu, B., Yao, Y., Liu, R., Ma, H. and Ma, L., 2019. Mueller polarimetric imaging for characterizing the collagen microstructures of breast cancer tissues in different genotypes. *Optics Communications*, *433*, pp.60-67.

[24] Drexler, W., Morgner, U., Ghanta, R.K., Kärtner, F.X., Schuman, J.S. and Fujimoto, J.G., 2001. Ultrahigh-resolution ophthalmic optical coherence tomography. *Nature Medicine*, *7*(4), pp.502-507.

[25] Wilson, M., Rankin, K., Ludi, D. and Sweeny, K., 2022. Emotional, cognitive, and physical well-being during the wait for breast biopsy results. *Psychology & Health*, pp.1-20.

Green and Affordable Energy Harvesting Using Laser Sculptured Moist-Electric Generators

PI: Daozhi Shen, Shanghai Jiao Tong University, dzshen@sjtu.edu.cn

Category: Environment

The Challenge − ***The world faces two energy problems: most of our energy production still produces greenhouse and polluted gas emissions, and hundreds of millions of people lack access to energy entirely.*** The global harmful emissions, most of which is caused by the production of energy, lead to climate change and further responsible for drought, wildfires, flooding, poverty displacement, food insecurity, health risks, and species loss. So far, anthropogenic activities have caused about 1.0 °C of global warming above the pre-industrial level and this is likely to reach 1.5 °C between 2030 and 2052 if the current emission rates persist. In 2018, the world encountered 315 cases of natural disasters which are mainly related to the climate. Approximately 68.5 million people were affected, and economic losses amounted to $131.7 billion. Ongoing increase in temperature and natural disasters cause some species to migrate further inland or upland, resulting in fragmented, isolated populations and local extinctions. To bring emissions down towards net-zero will be one of the world's biggest challenges in the years ahead. But the world has another global energy problem that is just as big: hundreds of millions of people lack access to sufficient energy entirely, with terrible consequences to themselves and the environment. According to the report by the International Energy Agency, there are almost one billion of people around the world living without electricity, while they are most affected by climate change. For example, Africa accounts for less than 3% of the world's energy-related carbon dioxide emissions to date and has the lowest emissions per capita of any region. But Africans are disproportionately experiencing the negative effects of climate change, including water stress, reduced food production, increased frequency of extreme weather events and lower economic growth. ***The world needs solutions for the twin problems by developing green and affordable energy technology***.

Proposed Project − This research proposal addresses the urgent global energy problems of greenhouse gas emissions and lack of access to energy. The atmosphere has long been recognized as a sink of electrical power, and water vapor or moisture is abundant almost everywhere, even in the very dry area such as desert. The annual energy power involved in the natural water cycle is up to 6×10^{15} W, three orders of magnitude higher than the annual energy consumption of human beings. ***By harnessing the abundant moisture in the atmosphere, this project aims to develop green and affordable energy harvesting technology using laser-sculptured moist-electric generators (MEGs)***. The proposed MEGs will utilize active materials with abundant channels and functional groups, obtained from lab-free materials such as cloth, paper, wood, food, and cork, through a controllable laser sculpture technique. The research objectives can be summarized as follows: 1. **Develop a laser sculpture technique** to fabricate active materials with abundant channels and functional groups from lab-free materials, enabling the conversion of these materials into graphene-like nanomaterials. 2. **Investigate the interfacial force-electric-thermal coupling process** to gain a deep understanding of the moisture-induced electricity mechanism. 3. **Build generators** and the generators will be tested in various ambient conditions and geographic locations on Earth, including deserts, forests, and mountains.

Outcomes −The potential impacts of this research are significant including: ***Low greenhouse and polluted gas emission*****:** moisture energy harvesting technology produces extremely low greenhouse and polluted gas emission because it purely relies on the absorbance and discordance of water process. Electricity from MEGs is directly from various forms of water, significantly expanding the ability to harvest energy from the natural water cycle and reducing the greenhouse and polluted gas emission. ***Energy accessibility in poverty areas*****:** moisture, water in the gaseous state, is ubiquitous geographically in nature, including most poor areas. Meanwhile, the scalable fabrication method through laser direct writing also makes the MEG devices cost-effective. The effective harvesting of moisture energy through our proposed MEG technology provides a promising solution to electricity crisis in poverty areas. ***Environmental monitoring*****:** The electricity output is directly related to the environmental parameters such as humidity level, the generators themselves can be used as humidity sensors without external power supply. In addition, the electricity generated form moisture also can be used for powering sensors for monitoring temperature, toxic gas, and light. Thus, the self-powered environmental monitoring systems without external power supply are possible through the MEG technology.

Green and Affordable Energy Harvesting Using Laser Sculptured Moist-Electric Generators

PI: Daozhi Shen, Shanghai Jiao Tong University, dzshen@sjtu.edu.cn

Category: Environment

Introduction

The world faces two energy problems: most of our energy production still produces greenhouse and polluted gas emissions, and hundreds of millions of people lack access to energy entirely [1]. The global harmful emissions, most of which is caused by the production of energy, lead to climate change and further responsible for drought, wildfires, flooding, poverty displacement, food insecurity, health risks, and species loss [2,3]. So far, anthropogenic activities have caused about 1.0 °C of global warming above the pre-industrial level and this is likely to reach 1.5 °C between 2030 and 2052 if the current emission rates persist [4]. In 2018, the world encountered 315 cases of natural disasters which are mainly related to the climate [5]. Approximately 68.5 million people were affected, and economic losses amounted to $131.7 billion, of which storms, floods, wildfires and droughts accounted for approximately 93% [6]. Ongoing increase in temperature and natural disasters cause some species to migrate further inland or upland, resulting in fragmented, isolated populations and local extinctions [7]. To bring emissions down towards net-zero will be one of the world's biggest challenges in the years ahead.

But the world has another global energy problem that is just as big: hundreds of millions of people lack access to sufficient energy entirely, with terrible consequences to themselves and the environment. According to the report by the International Energy Agency (IEA), there are almost one billion of people around the world living without electricity, while they are most affected by climate change [8]. For example, Africa accounts for less than 3% of the world's energy-related carbon dioxide emissions to date and has the lowest emissions per capita of any region [9]. But Africans are disproportionately experiencing the negative effects of climate change, including water stress, reduced food production, increased frequency of extreme weather events and lower economic growth. The world needs solutions for the twin problems by developing green and affordable energy technology.

The atmosphere has long been recognized as a sink of electrical power, as water covers 71% of the Earth's surface, and water vapor or moisture is abundant almost everywhere, even in the very dry area such as desert, no matter day and night [10]. The atmosphere contains approximately 1.3×10^4 cubic kilometers of water, mainly in the form of vapor and droplets. Within a relatively small area, water is evenly distributed in the air. The conversion of water form from one to another involves tremendous energy exchange with environment. Specifically, one single gram of water evaporates or condenses, converting 2.6 kJ of energy, which is equivalent to the energy contained in an AAA battery [11]. And the annual energy power involved in the natural water cycle is up to 6×10^{15} W, three orders of magnitude higher than the annual energy consumption of human beings [12]. As the water vapor (moisture) resource is clean and sustainable, and most importantly, accessible worldwide including undeveloped countries or remote areas, harvesting energy from ambient moisture then shows potential to provide a promising solution for the twin energy problems the world faced today.

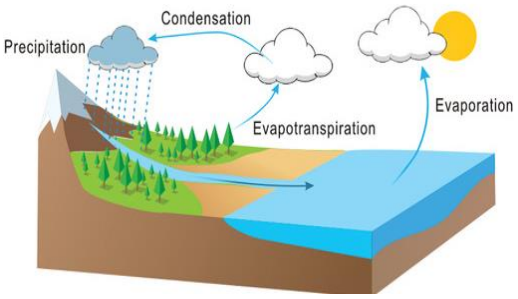

The hydrological cycle on Earth involves tremendous energy exchange with environment, showing great promise for sustainable and green energy.

Problem Statement

The opportunities for moisture-enabled electricity generation have been usually overlooked for a long time. The possibilities for electricity generation are facilitated by the electrification of water in response to changes in phase but experiments directed toward the harvesting of this charge to generate electrical power from atmospheric water vapor have been only recently been reported [13]. The moisture energy harvesting can be achieved mainly by: 1) doing work driven by reversible deformation of moisture-responsive materials and 2) ion diffusion driven by moisture-induced gradient energy. The first method converts environmental humidity changes into mechanical shifts of moisture-responsive

materials, further driving piezoelectric or magnetoelectric generators to output electricity. The latter method is to drive ion migration by moisture-induced gradient energy, in which the chemical potential changes of water from gas to liquid or the phase. Either way the nanomaterials with functional groups are need to yield electricity output because there needs relatively high specific area and active sites to interact with water molecular in ambient moisture [14].

Nanomaterials with high specific area due to reduced size are usually used for constructing moist-electric generator (MEG). Qu's group reported the first graphene-based MEG in 2015 and propelled its development with substantive works[13]. The applicant (Prof. Daozhi Shen) also had made significant contribution to developing efficient metal-oxide-nanowire-based MEGs for harvesting ambient moisture energy and pioneering their self-powered wearable electronic applications [15–17]. However, the current MEGs fabrication is costly and the materials used are not eco-friendly enough. For example, the graphene materials used were fabricated through strong acid chemical reaction with low productivity [18]. Metal oxide nanowires were grown through dangerous hydrothermal method in sealed autoclave with high inner pressure for days [15]. Some polymer-based MEGs show high output, but the materials synthesis includes serious pollution issues and the devices themselves may be harmful to both humans and environment, which does not meet the requirement of green and sustainable life. In addition, the highest energy conversion efficiency is 1~2%, still low compared with typical energy conversion technologies [19]. The primary reason is the lacked in-depth understanding of the interfacial force-electric-thermal coupling process and mechanism of moisture-induced electricity generation.

Despite the ambient moisture source is green and ubiquitously accessible, the current MEGs for moisture energy harvesting are not yet green and affordable. Thus, in order to let moist-electricity offer a potential solution for two energy problems, cost-effective and lab-free active materials, together with efficient and scalable fabrication method are necessary. Building affordable generators capable of harvesting green moisture energy eventually with fundamental insight of understanding interfacial process is also essential.

Goals

The main goal of this proposal is to establish an effective protocol for addressing two energy problems globally by harvesting green energy from ubiquitous moisture source through low-cost and environmental-friendly generators sculptured by laser from lab-free materials, with three specific objectives to:

(1) Develop controllable laser sculpture technique for generators with active materials containing abundant channels and functional groups from lab-free materials like cloth, paper, wood, food and cork, etc.;

(2) Investigate the interfacial force-electric-thermal coupling process for deeply understanding moisture-induced electricity mechanism in order to guide the materials fabrication and device design for energy conversion efficiency enhancement;

(3) Build affordable generators capable of harvesting green moisture energy with scalable electricity output based on the low-cost laser sculpture technique from environmental-friendly materials, with output density higher than 1 W/m^2, and conduct test in different regions, including deserts, forests, and mountains, etc.

This research program ultimately aims at the understanding between the feasibility of laser sculptured nanomaterials and the moisture electric generation for affordable and green energy harvesting practice, with possibilities of providing novel solutions for continued growth twin energy problems on the help of advanced optical technology.

Laser sculpture, an advanced photonics-based technology, can provide a unique approach for moisture-electric generators fabrication in a low-cost and environmental-friendly way. Laser shows powerful to sculpture almost any carbon-atom-rich and lab-free materials, including cross-linked polymers, cloth, paper, wood, food and cork, with the capability of converting them into graphene-like nanomaterials [20], which can be further used for efficiency moisture-electric generator construction due to high specific area and active sites. Laser-based processes can largely reduce the fabrication time and simplify the manufacturing process by avoiding two or more steps for manipulation, placement, and integration of materials. Laser engineering can not only use high power irradiation to obtain scalable

modification efficiently, but also selectively engrave nanostructured materials with high resolution by providing local high-temperature and high-pressure environments in a controllable way, without additional use of harmful chemical processes. As the affordable energy from clean and sustainable moisture source can be harvested in a low-cost and environmental way, the proposed moisture-electric generators sculptured by laser offers a promising solution to address the two energy problems globally.

Research Design

Task 1. One major task is to develop laser sculpture technique to obtain active materials containing abundant channels and functional groups from lab-free materials. Direct induction of the graphene will be developed through one-step graphitization process by converting carbon precursors into graphene-like flakes under the irradiation of low-cost lasers such as CO_2 laser. In this context, lab-free materials including cloth, paper, wood, food and cork will be used for providing carbon precursors and directly converted into graphene flakes. To increase the hydrophobic surface states, oxygen plasma may be used for posttreatment. As the graphitization is strong related to thermal process, different laser power densities and photonic energies will be used to tune the graphene transformation and adjust the sheet conductivity. Furthermore, the different graphene structures such as porous sheets and fibers will be obtained by changing the laser focal conditions. High speed scanning will be adopted to patterning the active materials and electrodes in a scalable production way. This task will be done in the first 4 months.

Task 2. To understand the interfacial process for interaction between water molecules and nanomaterials surface, charge transfer at the water-material interface will be stimulated using the cross-scale dynamic simulation method. The influence of various factors including surface properties, channel size, temperature, and humidity on the water molecular migration will be considered in the simulation, together with the influential effects on electricity output will be explored. The active materials characterization and geometrical dimensions before and after interaction with water molecules will be examined by advanced analytical instruments such as Raman spectroscopy, scanning electron microscopy (SEM), transmission electron microscopy (TEM), atomic force microscopy (AFM) and X-ray photoelectron spectroscopy (XPS). Both inert and active electrodes will be used for building device geometry and the electricity output will be compared to check the role of electrochemical reaction during electricity generation. This task will be done in the following 3 months.

Task 3. In the third task, we will use the laser sculptured active materials to build the prototypes of generators that can efficiently harvest ambient moisture energy. Both planner and sandwiched device structures with active materials between two electrodes will be built from the output of Tasks 1 and 2, with electricity generation driven by reversible deformation of moisture-responsive materials and ion diffusion driven by moisture-induced gradient energy, respectively, when interact with moisture. To increase the overall voltage or current output, a number of generators can be connected together in series or in parallel, respectively. The devices will be tested in various ambient conditions including highly moist and dry environment, sunlight, cloudy and night times to show the capability of versatile output. To demonstrate that the device can provide accessible energy in undeveloped regions or remote areas, the output of generators prototype will be also tested in different regions on Earth, including deserts, forests, and mountains. This task is arranged to be done in the last 5 months.

This project requires a range of skills, tools, and expertise in optics, materials, mechanicals, chemistry and electronics. This project comprises Daozhi Shen (material/electrical scientist, PI), Honghao Zhang (optics/mechanical scientist, PDF), and Linglan Guo (material/chemical developer, PhD student) at the Shanghai Jiao Tong University (SJTU). We have also initiated a collaboration with material/mechanical scientists from (Prof. Norman Zhou and Dr. Xiaoye Zhao) University of Waterloo (UW) for sharing materials and device tests. We have already built the ultrafast laser and CO_2 laser scanning system with micro/nano fabrication capability, as well as the electrical test platform. This concerted effort and multidisciplinary approach provides an excellent starting point for completing this project in 12 months.

Outcomes

The potential impacts of this research are significant, and they include:

Low greenhouse and polluted gas emission: Unlike the conventional fossil energy, the moisture energy harvesting technology produces extremely low greenhouse and polluted gas emission because it purely relies on the absorbance and discordance of water process. Through the electric coupling between

water and materials, electricity from MEGs is directly from various forms of water, significantly expanding the ability to harvest energy from the natural water cycle and reducing the greenhouse and polluted gas emission.

Energy accessibility in poverty areas: Moisture, water in the gaseous state, is ubiquitous geographically in nature, including most poor areas. The effective harvesting of moisture energy through our proposed MEG technology provides a promising solution to electricity crisis in poverty areas. Meanwhile, the scalable fabrication method through laser direct writing also makes the MEG devices cost-effective. Thus, the energy and electricity in poverty areas becomes affordable.

Environmental monitoring: The electricity output is directly related to the environmental parameters such as humidity level, the generators themselves can be used as humidity sensors without external power supply. In addition, the electricity generated form moisture also can be used for powering sensors for monitoring temperature, toxic gas, and light. Thus, the self-powered environmental monitoring systems without external power supply are possible through the MEG technology.

Broader Impact

Problems associated with energy issues including global warming, polluted air and water, poverty displacement, and species loss represent unprecedented challenges to our society and planet. The world needs solutions for the twin energy problems by developing green and affordable energy technology, which requires the strong collaboration between researchers with different expertise including physics, chemistry, material/mechanical/electronic science and engineering, with the global participations. The proposed project helps to cement new collaborative relationship among PIs with different academic backgrounds, institutions, and industries (AquaSensing) and will aid in fostering the broader international collaborative team across different countries. This study will demonstrate the fact that, with the help of advanced optics and photonics, global environmental challenges and threats can potentially be solved by embracing wide collaboration and efforts across countries and regions.

Reference Cited

(1) The world's energy problem. Our World in Data. https://ourworldindata.org/worlds-energy-problem (Accessed 2024-04-06).
(2) Jansson, J. K.; Hofmockel, K. S. *Nat. Rev. Microbiol.* **2020**, *18* (1), 35–46.
(3) Yue, X.-L.; Gao, Q.-X. *Adv. Climate Change Res.* **2018**, *9* (4), 243–252.
(4) Fawzy, S.; Osman, A. I.; Doran, J.; Rooney, D. W. *Environ. Chem. Lett.* **2020**, *18* (6), 2069–2094.
(5) UNCCS (2019) Climate action and support trends, United Nations Climate Change Secretariat. https://unfccc.int/sites/default/files/resource/Climate_Action_Support_Trends_2019.pdf. (Accessed 2024-04-06).
(6) UNEP (2019) Emissions gap report. UN Environment Program, Nairobi. https://wedocs.unep.org/bitstream/handle/20.500.11822/30797/EGR2019.pdf?sequence=1&isAllowed=y. (Accessed 2024-04-06).
(7) Román-Palacios, C.; Wiens, J. J. Recent Responses to Climate Change Reveal the Drivers of Species Extinction and Survival. *Proc. Natl. Acad. Sci. U.S.A.* **2020**, *117* (8), 4211–4217.
(8) Access to electricity – SDG7: Data and Projections – Analysis. IEA. https://www.iea.org/reports/sdg7-data-and-projections/access-to-electricity (Accessed 2024-04-06).
(9) IEA. https://www.iea.org/news/global-energy-crisis-shows-urgency-of-accelerating-investment-in-cheaper-and-cleaner-energy-in-africa (Accessed 2024-04-06).
(10) Shen, D.; Duley, W. W.; Peng, P.; Xiao, M.; Feng, J.; Liu, L.; Zou, G.; Zhou, Y. N. *Adv. Mater.* **2020**, *32* (52), 2003722.
(11) Stephens, G. L.; Li, J.; Wild, M.; Clayson, C. A.; Loeb, N.; Kato, S.; L'ecuyer, T.; Stackhouse, P. W.; Lebsock, M.; Andrews, T. *Nat. Geosci.* **2012**, *5* (10), 691–696.
(12) Huang, Y.; Cheng, H.; Qu, L. *ACS Mater. Lett.* **2021**, *3* (2), 193–209.
(13) Zhao, F.; Cheng, H.; Zhang, Z.; Jiang, L.; Qu, L. *Adv. Mater.* **2015**, *27* (29), 4351–4357.
(14) Zhao, X.; Shen, D.; Duley, W. W.; Tan, C.; Zhou, Y. N. *Adv. Energy Sus. Res.* **2022**, *3* (4), 2100196.

(15) Shen, D.; Xiao, M.; Zou, G.; Liu, L.; Duley, W. W.; Zhou, Y. N. *Adv. Mater.* **2018**, *30* (18), 1705925.
(16) Shen, D.; Xiao, Y.; Zou, G.; Liu, L.; Wu, A.; Xiao, M.; Feng, J.; Hui, Z.; Duley, W. W.; Zhou, Y. N. *Adv. Mater. Technol.* **2020**, *5* (1), 1900819.
(17) Shen, D.; Xiao, M.; Xiao, Y.; Zou, G.; Hu, L.; Zhao, B.; Liu, L.; Duley, W. W.; Zhou, Y. N. *ACS Appl. Mater. Interfaces* **2019**, *11* (15), 14249–14255.
(18) Huang, Y.; Cheng, H.; Yang, C.; Zhang, P.; Liao, Q.; Yao, H.; Shi, G.; Qu, L. *Nat. Commun.* **2018**, *9* (1), 1–8.
(19) Zhang, Z.; Li, X.; Yin, J.; Xu, Y.; Fei, W.; Xue, M.; Wang, Q.; Zhou, J.; Guo, W. *Nat. Nanotechnol.* **2018**, *13* (12), 1109–1119.
(20) Chyan, Y.; Ye, R.; Li, Y.; Singh, S. P.; Arnusch, C. J.; Tour, J. M. *ACS Nano* **2018**, *12* (3), 2176–2183.

Executive summary-health category

Development of Robotic Microscopy for rapid and cost-effective malaria diagnosis

Malaria is one of the most serious public health challenges globally, despite current therapeutics having high efficacy rates when administered timely. Most concerning is that the fight against malaria has stalled. There were 230 million cases in 2015 (the baseline year of the global technical strategy for malaria 2016-2030) and 247 million cases in 2020. The barrier to malaria eradication is the lack of early diagnosis of the infected population. Current malaria diagnostics can be classified into three categories with specific strengths and weaknesses: 1) highly sensitive molecular-based techniques which use PCR. These are slow and demand the use of sophisticated equipment, expensive reagents, and a highly trained workforce; 2) Rapid Diagnostic Tests (RDTs) are relatively fast in comparison to optical microscopy but less sensitive (100-200 parasite μL^{-1}). Besides, the majority of them target the *Plasmodium falciparum* histidine-rich protein 2 *(pfhrp-2*) biomarker, and recent studies have shown the deletion of *pfhrp-2* which causes false negatives and threatens malaria control strategies. 3) Optical microscopy, the gold standard method for diagnosis. This involves examining stained blood smear samples under a microscope. It can detect up to 5-20 parasite μL^{-1}, however, the results vary significantly based on the expertise of the technician or health care provider, and it is labor and time intensive.

None of the three methods offers a definitive solution to early detection. Prompt treatment is crucial in preventing severe illness, complications, and deaths associated with malaria. To boost the fight against malaria, new approaches for diagnostics must be adopted to enhance the sensitivity, accuracy of detection besides being rapid and affordable. While research and development efforts are ongoing to improve and develop these and other malaria diagnostic methods, microscopy (the gold standard method for diagnosis) is likely to remain a vital tool in malaria diagnosis due to its proven effectiveness, cost-effectiveness, and established specialists in many malaria-endemic regions. Therefore, we think offering a solution within microscopy will likely offer a faster way to integrate new techniques in malaria diagnosis. Enhancing early screening and reducing the disease burden.

In this study, we propose to develop an affordable robotic configuration for imaging malaria by detecting the presence of hemozoin (Hz). Affordable, open-source, 3D-printed microscope like OpenFlexure microscope (OFM) will be modified to incorporate magneto-optic imaging capability. Leveraging on the magneto-optical physical properties of malaria pigment Hz, we will develop a phase-locked mode combining magneto-optical control, thus fully exploiting the Hz features to maximize sensitivity. To allow full automation of the detection assay, we will use a classification algorithm to accurately identify and categorize malaria-infected cells from the microscopy images. We can thus overcome the limitations of traditional microscopy and improve malaria diagnostics in terms of accuracy, efficiency, and accessibility.

Development of Robotic Microscopy for rapid and cost-effective malaria diagnosis

Introduction

Malaria is one of the most serious public health challenges globally. According to World Health Organization (WHO), there were 247 Million reported cases and 625,000 Malaria related deaths in 2020. This was a 10% increase from 2019[1]. Interestingly, current malaria therapeutics have nearly 100% efficacy if administered timely. Of concern is that progress against malaria fight has stalled since 2015 (the baseline year of the global technical strategy for malaria 2016-2030). In that year, there was an estimated 230 million Malaria cases [2, 3]. The barrier to malaria eradication being the lack of early diagnosis of the infected population. Early detection and prompt treatment are crucial in preventing severe illness, complications, and deaths associated with malaria.

Currently, malaria diagnostics can be classified into three categories: immunological-based, molecular-based techniques, and optical microscopy [4-6]. Immunological diagnostic kits are commonly referred to as Rapid Diagnostic Tests (RDTs). They are relatively fast, cost-effective, and user-friendly. However, they are less sensitive, and the majority target histidine-rich protein 2 (*pfhrp-2*) [7, 8]. Recent studies have shown the deletion of *pfhrp-2* genes which causes false negatives and threatens malaria control strategies [9-11]. In any case, the use of *pfhrp-2* biomarker limits the use of the RDTs in monitoring disease progression, and evaluating the efficacy of the interventions due to its persistence in the bloodstream long after malarial infection [12-14]. The molecular-based techniques uses Polymerase Chain Reaction (PCR) to probe and amplify the *Plasmodium* parasites' genetic material (either DNA or RNA) present in the blood to detectable levels. The technique is highly sensitive but slow and demands the use of sophisticated equipment, expensive reagents, and a highly trained workforce. Optical microscopy is the gold standard method for the diagnosis of the disease. It involves examining stained blood smear samples under a light microscope. The process is labor and time intensive and the reliability of the results depends on the expertise of the technician or health care provider. To boost the fight against malaria, new approaches for diagnostics must be adopted to enhance the sensitivity, and accuracy of detection besides being rapid and affordable.

Literature Review

Various methods have been proposed to overcome the challenges of the three methods highlighted above. For example, electrochemical biosensors for Malaria detection which offer high sensitivity [15-18] and have been demonstrated capable of rapid detection [19, 20], allowing timely initiation of treatments. However, electrochemical biosensors often require complex fabrication processes which can increase the cost of production and limit their accessibility [21].

Optical-based techniques have also been proposed for Malaria diagnostics. These techniques leverage optical principles such as fluorescence, luminescence, optical fiber, photonics, and Surface Plasmon Resonance (SPR). Optical techniques offer theoretically higher levels of sensitivity[22]. For example, the cloning and expression of fluorescent malaria parasite protein probes were shown in the fabrication of fluorescent-based biosensors for measuring the amount of heme in cells[23]. In principle, there is fluorescence quenching during the heme binding[24-26]. Nevertheless, the method is limited by the short life span of the fluorophores and the photostability of the fluorophores[27]. Other methods reported include the use of the FRET-based heme sensor[24] and the noninvasive and rapid photoacoustic technique [28]. The major drawback of the photoacoustic technique is the attenuation of the signal before reaching the transducer, resulting in poor SNR. To suppress the noise and enhance the detected signal, specialized technology must be employed, which makes the setup complex and expensive.

The SPR technique relies on the variations in the refractive index of the plasma resonance material, in the SPR angle. This is coupled with the reflectance intensity, caused by the interaction between the biomaterial targets[29-32]. Briand *et al.*[29] used hemoglobin-polyacrylic acid as a bio-recognition target for a gold-coated SPR based sensor for rapid heme detection. This biosensor acted by extracting the heme, followed by heme-

free hemoglobin exposure to samples containing heme that interact with the bio recognition element. Though the SPR-based Malaria biosensors are highly sensitive, have high resolution and can allow real-time measurements, they are motion-sensitive and depend on the development of light detectors with a high signal-to-noise ratio[33, 34].

Another approach for malaria diagnosis is to utilize the changes in both the magnetic and optical properties of the infected red blood cells (iRBCs). Since, they exhibit a high magnetic anisotropy and have optical dichroism properties because of hemozoin (HZ) which is a Malaria byproduct. Based on this principle, various configurations have been proposed. Ranging from the polarizing optical microscopy [35-39] and cellphone-based imaging. Cellphone-based methods are particular appealing because of their portability. However, the methods fail to account for all Hz due to the random orientation of the Hz crystals. Besides, the method requires phones with advanced cameras imaging capabilities, making them expensive. Due to strong paramagnetic behavior of Hz, responding to low magnetic field strengths, magneto-optic-based techniques have also been proposed [40-42]. The method can detect parasite densities as low as less than 10 parasites/mL [43]. Majority of the studies using this method were done under laboratory conditions. However, recent studies by Arndt *et al* [44] has shown the method has great potential as a malaria biosensor with 82% and 84% sensitivity and specificity respectively. Importantly, the parasite density correlated well with the quantitative magneto-optical signal.

Problem Statement

The magneto-optical method has the potential to revolutionize malaria diagnosis given the linear correction between parasite load and Hz. However, the works reported on Hz detection uses linear magnetic fields. Use of linear magnetic fields offers less control and precision in manipulating Hz because force is applied in a single direction. This limits the ability to finely adjust the position and orientation of Hz. In addition, linear magnetic fields often result in non-uniform force distribution across the paramagnetic material.

Besides, the proposed diagnosis techniques require extensive training for medical specialists to ensure accurate usage and interpretation of results. The need for such training can be a significant barrier in resource-limited settings, where healthcare workers are already stretched thin. Secondly, adopting new diagnostic techniques would necessitate a substantial shift in health policy, including updates to diagnostic protocols, investment in new equipment, and ongoing support for training and maintenance. This shift could be met with resistance due to the entrenched nature of current practices and the high initial costs involved. Therefore, while alternative diagnostic techniques for malaria hold promise, the transition from microscopy to these new methods must be carefully managed.

Proposed project

Microscopy remains the gold standard method for diagnosis and, is likely to remain a vital tool in malaria diagnosis due to its proven effectiveness, cost-effectiveness, and established specialists in many malaria-endemic regions. Therefore, we think offering a solution within microscopy will likely offer a faster way to integrate new techniques in malaria diagnosis. In this work, we propose to use a rotating magnetic field for the following reasons:

(i) Provide more precise and versatile control over the orientation and movement of paramagnetic materials
(ii) Create more homogeneous and uniform magnetic environments
(iii) Increasing the number of magnetic poles raises the degrees of freedom of magnetic force application[45].

We believe a rotating magnetic field will not only enhance the sensitivity and specificity of the system, but will also lower the limit of detection. We will adopt the open source OpenFlexure microscope (OFM) configuration [46-48] on which we have previous experience (through a previous networking grant at the

University of Cambridge, UK), and develop it for affordable polarized microscopy by incorporating polarizers and cellophane sheet half waveplate (HWP). The imaging module will be phase-locked with the sinusoidal input driving the rotating magnetic field to acquire images at the maximum contrast. Machine learning will be utilized to enhance image analysis and automate the system.

Aim of Study

To develop an affordable robotic microscope to leverage on the magnetic and optical features of Hz for rapid and stain-free malaria diagnostics. The specific objectives will be:

(i) Design an imaging phase-locked system integrated with a time-dependent magnetic field based on the OpenFlexure microscope (OFM).
(ii) Develop machine learning models to automate the system.
(iii) Testing and comparison of the performance of the setup with standard methods
(iv) Conduct a clinical trial in small populations in Nyanza region, Kenya (Migori Teaching and Referral Hospital, and Jaramogi Oginga Odinga Teaching and Referral Hospital).

Outcome(s)

The development of robotic microscopy for rapid and cost-effective malaria diagnosis will led to several significant outcomes, contributing to improved healthcare, particularly in regions with high malaria prevalence. Here are the key outcomes:

a. Developed protocols and designs for imaging and quantifying magnetic-optical properties in malaria-infected RBCs which will have the following benefits:
   (i) Reduced time required to diagnose malaria compared to traditional manual microscopy. Automated systems will analyze blood samples quickly and provide results within minutes.
   (ii) High accuracy in the detection of malaria parasites. This will eliminate human error and fatigue, which are common in manual microscopy, leading to more consistent and reliable diagnoses.
   (iii) The development of portable and user-friendly robotic microscopy systems will improved access to malaria diagnostics in remote and resource-limited areas. The automation means that the systems can be operated with minimal training, broadening the reach of effective malaria diagnosis.
   (iv) The system can be integrated with telemedicine platforms, allowing remote experts to review and confirm diagnoses. This integration is particularly beneficial in areas lacking specialist healthcare professionals, ensuring that accurate diagnoses can be made even in isolated locations.
   (v) The system systems can be expanded to collect and store diagnostic data, which can be used for epidemiological studies. This data can help track malaria prevalence, identify outbreaks early, and inform public health interventions and policy decisions.
b. Report on the performance of the device both in the lab and clinical trials.
c. Enhanced capacity for Kenyan researchers in designing and fabrication of affordable optical biosensors.
d. Dissemination of research findings

Impact

The development of the robotic microscope will lead to the creation of a new diagnostic platform for Malaria by providing rapid, stain-free, and accurate diagnosis. This will significantly reduce the time the health care personnel requires for staining the samples and scanning for parasites using a light microscope. Meaning, more patients could be tested at the same time. Besides, microscopy is the gold standard method for malaria diagnosis, and offering affordable and rapid solutions within the platform will be very appealing to policymakers and biomedical companies. This can generate significant revenue from the sale of these products and encourage more research on expanding the robotic microscope for other applications. Finally, the collaboration with Prof. Pietro Cicuta and colleagues in the Cavendish Laboratory at the University of Cambridge UK will help build capacity for Kenyan researchers in designing and fabrication of affordable biosensors. Finally, the project will support two MSc female students to bridge the gap of women in the field of Optics and Photonics particularly in developing countries.

References

1. Organization, W. H., *World malaria report 2022*. World Health Organization: 2022.
2. Organization, W. H., *Global technical strategy for malaria 2016-2030*. World Health Organization: 2015.
3. World Health, O., *World malaria report 2015*. World Health Organization: Geneva, 2015.
4. Makler, M. T.; Palmer, C. J.; Ager, A. L., A review of practical techniques for the diagnosis of malaria. *Annals of tropical medicine and parasitology* **1998,** *92* (4), 419-434.
5. Vo, Q. H.; Le, X.-H.; Le, T.-H., A deep learning approach in detection of malaria and acute lymphoblastic leukemia diseases utilising blood smear microscopic images. *Vietnam Journal of Science, Technology and Engineering* **2022,** *64* (1), 63-71.
6. Wongsrichanalai, C.; Barcus, M. J.; Muth, S.; Sutamihardja, A.; Wernsdorfer, W. H., A review of malaria diagnostic tools: microscopy and rapid diagnostic test (RDT). *Defining and Defeating the Intolerable Burden of Malaria III: Progress and Perspectives: Supplement to Volume 77 (6) of American Journal of Tropical Medicine and Hygiene* **2007**.
7. Sivaradjy, M.; Hamide, A.; Krishnamoorthy, S.; Rajkumari, N.; Mohan, V.; Sharmila, F. M., Assessment of Plasmodium falciparum histidine rich protein 2 and/3 (pfhrp 2&/pfhrp 3) gene deletion or mutation in Plasmodium falciparum positive blood samples in a tertiary care centre in South India. *Journal of Parasitic Diseases* **2022,** *46* (3), 729-743.
8. Kaaya, R. D.; Kavishe, R. A.; Tenu, F. F.; Matowo, J. J.; Mosha, F. W.; Drakeley, C.; Sutherland, C. J.; Beshir, K. B., Deletions of the Plasmodium falciparum histidine-rich protein 2/3 genes are common in field isolates from north-eastern Tanzania. *Scientific reports* **2022,** *12* (1), 5802.
9. Molina-de la Fuente, I.; Pastor, A.; Herrador, Z.; Benito, A.; Berzosa, P., Impact of Plasmodium falciparum pfhrp2 and pfhrp3 gene deletions on malaria control worldwide: a systematic review and meta-analysis. *Malaria Journal* **2021,** *20* (1), 1-25.
10. Gatton, M. L.; Chaudhry, A.; Glenn, J.; Wilson, S.; Ah, Y.; Kong, A.; Ord, R. L.; Rees-Channer, R. R.; Chiodini, P.; Incardona, S., Impact of Plasmodium falciparum gene deletions on malaria rapid diagnostic test performance. *Malaria journal* **2020,** *19* (1), 1-11.
11. Mukkala, A. N.; Kwan, J.; Lau, R.; Harris, D.; Kain, D.; Boggild, A. K., An update on malaria rapid diagnostic tests. *Current infectious disease reports* **2018,** *20*, 1-8.
12. Piper, R.; Lebras, J.; Wentworth, L.; Hunt-Cooke, A.; HouzÃ, S.; Chiodini, P.; Makler, M., Immunocapture diagnostic assays for malaria using Plasmodium lactate dehydrogenase (pLDH). *The American journal of tropical medicine and hygiene* **1999,** *60* (1), 109-118.
13. Krampa, F. D.; Aniweh, Y.; Kanyong, P.; Awandare, G. A., Recent advances in the development of biosensors for malaria diagnosis. *Sensors* **2020,** *20* (3), 799.
14. Markwalter, C. F.; Davis, K. M.; Wright, D. W., Immunomagnetic capture and colorimetric detection of malarial biomarker Plasmodium falciparum lactate dehydrogenase. *Analytical Biochemistry* **2016,** *493*, 30-34.
15. Jain, P.; Das, S.; Chakma, B.; Goswami, P., Aptamer-graphene oxide for highly sensitive dual electrochemical detection of Plasmodium lactate dehydrogenase. *Analytical Biochemistry* **2016,** *514*, 32-37.
16. Figueroa-Miranda, G.; Feng, L.; Shiu, S. C.-C.; Dirkzwager, R. M.; Cheung, Y.-W.; Tanner, J. A.; Schöning, M. J.; Offenhäusser, A.; Mayer, D., Aptamer-based electrochemical biosensor for highly sensitive and selective malaria detection with adjustable dynamic response range and reusability. *Sensors and Actuators B: Chemical* **2018,** *255*, 235-243.
17. Dutta, G.; Nagarajan, S.; Lapidus, L. J.; Lillehoj, P. B., Enzyme-free electrochemical immunosensor based on methylene blue and the electro-oxidation of hydrazine on Pt nanoparticles. *Biosensors and Bioelectronics* **2017,** *92*, 372-377.
18. Hemben, A.; Ashley, J.; Tothill, I. E., Development of an Immunosensor for PfHRP 2 as a Biomarker for Malaria Detection. *Biosensors* **2017,** *7* (3), 28.

19. Singh, P.; Chatterjee, M.; Chatterjee, K.; Arun, R. K.; Chanda, N., Design of a point-of-care device for electrochemical detection of P.vivax infected-malaria using antibody functionalized rGO-gold nanocomposite. *Sensors and Actuators B: Chemical* **2021,** *327*, 128860.
20. Dutta, G.; Lillehoj, P. B., Wash-free, label-free immunoassay for rapid electrochemical detection of PfHRP2 in whole blood samples. *Scientific Reports* **2018,** *8* (1), 17129.
21. Fan, R.; Andrew, T. L., Perspective—Challenges in developing wearable electrochemical sensors for longitudinal health monitoring. *Journal of The Electrochemical Society* **2020,** *167* (3), 037542.
22. Zherebtsova, A. I.; Dremin, V. V.; Makovik, I. N.; Zherebtsov, E. A.; Dunaev, A. V.; Goltsov, A.; Sokolovski, S. G.; Rafailov, E. U., Multimodal optical diagnostics of the microhaemodynamics in upper and lower limbs. *Frontiers in physiology* **2019,** *10*, 416.
23. Wißbrock, A.; Imhof, D., A tough nut to crack: intracellular detection and quantification of heme in malaria parasites by a genetically encoded protein sensor. *ChemBioChem* **2017,** *18* (16), 1561-1564.
24. Abshire, J. R.; Rowlands, C. J.; Ganesan, S. M.; So, P. T.; Niles, J. C., Quantification of labile heme in live malaria parasites using a genetically encoded biosensor. *Proceedings of the National Academy of Sciences* **2017,** *114* (11), E2068-E2076.
25. Ragavan, K.; Kumar, S.; Swaraj, S.; Neethirajan, S., Advances in biosensors and optical assays for diagnosis and detection of malaria. *Biosensors and Bioelectronics* **2018,** *105*, 188-210.
26. Xu, S.; Liu, H.-W.; Chen, L.; Yuan, J.; Liu, Y.; Teng, L.; Huan, S.-Y.; Yuan, L.; Zhang, X.-B.; Tan, W., Learning from artemisinin: bioinspired design of a reaction-based fluorescent probe for the selective sensing of labile heme in complex biosystems. *Journal of the American Chemical Society* **2020,** *142* (5), 2129-2133.
27. Villena Gonzales, W.; Mobashsher, A. T.; Abbosh, A., The progress of glucose monitoring—A review of invasive to minimally and non-invasive techniques, devices and sensors. *Sensors* **2019,** *19* (4), 800.
28. Lukianova-Hleb, E. Y.; Campbell, K. M.; Constantinou, P. E.; Braam, J.; Olson, J. S.; Ware, R. E.; Sullivan, D. J.; Lapotko, D. O., Hemozoin-generated vapor nanobubbles for transdermal reagent-and needle-free detection of malaria. *Proceedings of the National Academy of Sciences* **2014,** *111* (3), 900-905.
29. Briand, V. A.; Thilakarathne, V.; Kasi, R. M.; Kumar, C. V., Novel surface plasmon resonance sensor for the detection of heme at biological levels via highly selective recognition by apo-hemoglobin. *Talanta* **2012,** *99*, 113-118.
30. Chaudhary, V. S.; Kumar, D.; Kumar, S., Gold-immobilized photonic crystal fiber-based SPR biosensor for detection of malaria disease in human body. *IEEE Sensors Journal* **2021,** *21* (16), 17800-17807.
31. Wu, F.; Singh, J.; Thomas, P. A.; Ge, Q.; Kravets, V. G.; Day, P. J.; Grigorenko, A. N., Ultrasensitive and rapid detection of malaria using graphene-enhanced surface plasmon resonance. *2D Materials* **2020,** *7* (4), 045019.
32. Sikarwar, B.; Sharma, P. K.; Srivastava, A.; Agarwal, G. S.; Boopathi, M.; Singh, B.; Jaiswal, Y. K., Surface plasmon resonance characterization of monoclonal and polyclonal antibodies of malaria for biosensor applications. *Biosensors and Bioelectronics* **2014,** *60*, 201-209.
33. Piliarik, M.; Homola, J., Surface plasmon resonance (SPR) sensors: approaching their limits? *Optics express* **2009,** *17* (19), 16505-16517.
34. Caucheteur, C.; Guo, T.; Albert, J., Review of plasmonic fiber optic biochemical sensors: improving the limit of detection. *Analytical and bioanalytical chemistry* **2015,** *407* (14), 3883-3897.
35. Pirnstill, C. W.; Coté, G. L., Malaria diagnosis using a mobile phone polarized microscope. *Scientific reports* **2015,** *5* (1), 13368.
36. Yu, Z.; Li, Y.; Deng, L.; Luo, B.; Wu, P.; Geng, D., A high-performance cell-phone based polarized microscope for malaria diagnosis. *Journal of Biophotonics* **2023**, e202200290.
37. Maude, R. J.; Buapetch, W.; Silamut, K., A simplified, low-cost method for polarized light microscopy. *The American journal of tropical medicine and hygiene* **2009,** *81* (5), 782.

38. Gordon, P.; Venancio, V. P.; Mertens-Talcott, S. U.; Coté, G., Portable bright-field, fluorescence, and cross-polarized microscope toward point-of-care imaging diagnostics. *Journal of Biomedical Optics* **2019,** *24* (9), 096502-096502.
39. Cho, S.; Kim, S.; Kim, Y.; Park, Y., Optical imaging techniques for the study of malaria. *Trends in biotechnology* **2012,** *30* (2), 71-79.
40. McBirney, S. E.; Chen, D.; Scholtz, A.; Ameri, H.; Armani, A. M., Rapid diagnostic for point-of-care malaria screening. *ACS sensors* **2018,** *3* (7), 1264-1270.
41. Kumar, R.; Verma, A. K.; Shrivas, S.; Thota, P.; Singh, M. P.; Rajasubramaniam, S.; Das, A.; Bharti, P. K., First successful field evaluation of new, one-minute haemozoin-based malaria diagnostic device. *EClinicalMedicine* **2020,** *22*, 100347.
42. Valdivia, H. O.; Thota, P.; Braga, G.; Ricopa, L.; Barazorda, K.; Salas, C.; Bishop, D. K.; Joya, C. A., Field validation of a magneto-optical detection device (Gazelle) for portable point-of-care Plasmodium vivax diagnosis. *Plos one* **2021,** *16* (6), e0253232.
43. Orbán, Á.; Butykai, Á.; Molnár, A.; Pröhle, Z.; Fülöp, G.; Zelles, T.; Forsyth, W.; Hill, D.; Müller, I.; Schofield, L., Evaluation of a novel magneto-optical method for the detection of malaria parasites. *PloS one* **2014,** *9* (5), e96981.
44. Arndt, L.; Koleala, T.; Orbán, Á.; Ibam, C.; Lufele, E.; Timinao, L.; Lorry, L.; Butykai, Á.; Kaman, P.; Molnár, A., Magneto-optical diagnosis of symptomatic malaria in Papua New Guinea. *Nature Communications* **2021,** *12* (1), 969.
45. Koczula, K. M.; Gallotta, A., Lateral flow assays. *Essays in biochemistry* **2016,** *60* (1), 111-120.
46. Board, S. A., OpenFlexure: an open-source 3D printed microscope.
47. Grant, S. D.; Cairns, G. S.; Wistuba, J.; Patton, B. R., Adapting the 3D-printed Openflexure microscope enables computational super-resolution imaging. *F1000Research* **2019,** *8*.
48. Stirling, J.; Sanga, V. L.; Nyakyi, P. T.; Mwakajinga, G. A.; Collins, J. T.; Bumke, K.; Knapper, J.; Meng, Q.; McDermott, S.; Bowman, R. In *The OpenFlexure project. the technical challenges of co-developing a microscope in the UK and Tanzania*, 2020 IEEE Global Humanitarian Technology Conference (GHTC), IEEE: 2020; pp 1-4.

Category: Environment
Title: Spectral radiance mapping to characterize the ecological impacts of light pollution

The global challenge

The accessibility and growing demand for electric lighting have a large-scale impact on natural habitats. Unfortunately, the electric light at night (LAN) can cause negative consequences, such as disrupting ecosystems, confusing migratory patterns, altering predatory-prey relations, causing stress, and interrupting the entrainment of circadian rhythms of many species. The negative effects of LAN (light pollution) is often quantified using photometric and colorimetric measures. Despite the complexity of spectral impact of light sources on the environment, research suggests that light source spectra influences arachnida, aves, instecta, mammalia, and reptiles in predictable manners. However, ecological research studies still use photometric (i.e., illuminance, luminance) and colorimetric (i.e., correlated color temperature) measures, which are based on human visual sensitivity. In addition, photometric and colorimetric measurements are performed using either spot measurements or satellite images. While these measurement methods have merits, they have limitations in accurately evaluating the ecological impacts of light pollution.

Proposed project and relation to the "Environment" category

Characterizing the impacts of light pollution on several species requires a holistic measurement approach in spectral and spatial dimensions. The proposed research project aims to characterize optical radiation using a spectral imaging radiance colorimeter and assess the outcomes compared to spot (e.g., handheld spectroradiometer) and remote (satellite) measurements. By utilizing spectral radiance mapping techniques, I aim to provide a holistic understanding of how different light spectra impact ecological processes. This project aligns with the Environment category of the Optica Foundation Challenge, as it addresses the urgent need for innovative solutions to mitigate the ecological effects of light pollution. A test field will be identified, and light pollution of a large field of view will be characterized using radiance imaging colorimeter to simulate realistic field conditions. The variation between the traditional and proposed measurement methods will be evaluated, and a new metric for light pollution will be developed using the data generated in this project.

Capability to address the challenge and intended outcomes

The project's capability and application lie in its ability to provide valuable insights into the ecological impacts of light pollution beyond human perception. By developing a comprehensive light pollution assessment method that considers spectral characteristics, we can better understand the effects of electric lighting on wildlife behavior, habitat disruption, and ecosystem functioning. This project has the potential to inform conservation efforts, guide outdoor lighting policies, and promote the development of sustainable lighting practices to preserve biodiversity and mitigate the ecological consequences of light pollution on a global scale. New light pollution metric and measurement methods comparison will be disseminated to relevant bodies, such as the Council for Optical Radiation Measurements, the International Commission on Illumination, and International Dark-Sky Association. The development of a holistic light pollution metric will also help ecological researchers find acceptability thresholds and guide outdoor lighting standards and recommendations, such as Model Lighting Ordinance (MLO), LEED Sustainable Sites program, the International Commission on Illumination (CIE) recommendations, and standards, such as the Australian New Zealand Standard AS/NZS 4282:2019 Control of the obtrusive effects of outdoor lighting.

2024 Optica Foundation Challenge
Category: Environment
Title: Spectral radiance mapping to characterize the ecological impacts of light pollution
Name: Dorukalp Durmus
Affiliation: Pennsylvania State University

1. Literature review

1.1 Negative impacts of light pollution

Light is imperative to achieve viable conditions for human activity at night, such as transportation, work, commerce, and leisure. The use of outdoor lighting is beneficial for commercial and cultural endeavours, especially in urban environments, but electric light at night (LAN) also reduces darkness which may be necessary for the ecology and some animals. For the outdoor lighting to be sustainable it should fulfil the functional needs of the users, be cost- and energy-efficient, and result in minimal environmental impact. The use of outdoor lighting during night-time can result in various unwanted and harmful side-effects (often collectively referred to as light pollution). The unwanted effects of the use of outdoor LAN include:

- Increase in human-made sky glow (the diffuse luminance of the night sky),[1]
- Degradation of ground-based astronomical observatories operating in the optical range and a decreased ability to observe the stars due to the brightening of the night sky,[2]
- Increase in obtrusive light causing nuisance and discomfort glare for humans,
- Adverse health outcomes, such as circadian disruption, mood effects, and increased breast cancer incidence risk in humans,[3]
- Disturbances and negative impacts on species, ecosystems, and wildlife.[4]

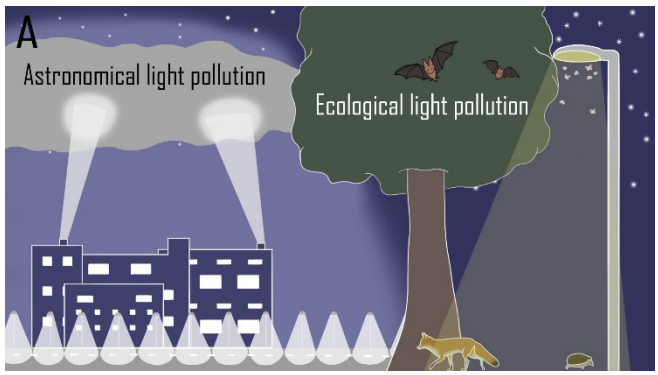

Fig. 1. Electric light at night can cause astronomical and ecological light pollution.[5]

The unwanted side-effects are measured through response variables and vary significantly depending on the research discipline and the study objects. In astronomy, the

[1] Kyba, C., Tong, K. P., Bennie, J., Birriel, I., Birriel, J. J., Cool, A., ... & Gaston, K. J. (2015). Worldwide variations in artificial skyglow. *Scientific Reports*, 5(1), 1-7.
[2] Riegel, K. W. (1973). Light Pollution: Outdoor lighting is a growing threat to astronomy. *Science*, 179(4080), 1285-1291.
[3] Durmus D., Tengelin, M. N., & Jägerbrand, A. K. (2022) Investigating the methods and health outcomes of research studies on light pollution and human physiology and behaviour: a systematic review, 17th International Symposium on Science & Technology of Lighting, Toulouse, France.
[4] Sanders, D., Frago, E., Kehoe, R., Patterson, C., & Gaston, K. J. (2021). A meta-analysis of biological impacts of artificial light at night. *Nature Ecology & Evolution*, 5(1), 74-81.
[5] Jägerbrand, A. K., Tengelin, M. N., & Durmus, D. (2022) An overview of the adverse effects of outdoor light at night and the research methods used in different areas. 2022 Conference Proceedings of Lux Europa. Prague.

response variable can be sky brightness or upward emitted light. For impacts on human health, the response variable can be human behaviour or various health outcomes (e.g., sleep quality, melatonin suppression or risk of cancer). In ecology, the response variable is usually restricted to appropriate study variables for the specific species, the spatial scale or ecosystem of the investigation. Characterizing the ecological impacts of light pollution requires considering species' spectral sensitivity to optical radiation. The spectral sensitivities can help characterize their visual response (i.e., brightness perception) to natural and electrical lighting. Some species may require darkness to hunt or hide from predators, find mating partners, or forage. Electric light at night with spectral distributions that are different than natural light sources (e.g., moonlight) may cause disruption to biological cycles of many species.

1.2 Light pollution measurement methods

Methods used in ecological light pollution studies are plentiful because of the large number of organisms that are studied. For example, LAN impact on birds have been studied through observational studies in the field that correlated bird responses (e.g., migration) to satellite-based light measurements or to ground-based measurements, but also through controlled indoor experiments or through experiments using bird enclosures outdoor. Bio-loggers attached on birds can help correlated exposure of LAN to movement patters. The effects of LAN on insects (or invertebrates) have been studied in observational studies, often by comparing the number of trapped insects, with and without lighting (often using light as a source of attraction for the insects), or by introducing different kinds of interventions in unlit or lit areas. Insect responses have also been studied by introducing LAN in previously unlit areas in manipulative field experiments and observing the responses.

Bats have only been studied through field experiments. Observational studies have been performed that compares bat movements and frequency of activity without any intervention. Field experiments varies much in their design, but some use already lit areas for introducing interventions (e.g., altered light sources, light intensity, or light distribution) and others use previously unlit areas to introduce LAN and study impacts on behaviour. Fish responses to LAN can be studied in field experiments, mesocosms, enclosures or in laboratory studies. Field experiments can be conducted to study both lit or unlit conditions with or without interventions. Use of mesocosms, enclosures or laboratory environments can improve the scientific reliability of the study since it is more controlled, and the influence of external factors can be minimized.

Responses of plants can be investigated through controlled field experiments manipulating various lighting conditions. Studies can also be performed as observations in unlit or lit areas with or without interventions. Tree phenology can be correlated with satellite-based measurements or with ground-based measurements. Similarly, turtles have mainly been studied in their natural habitats and in the field. Studies are often observations of behaviour before/after interventions have been introduced. Studies focuses on hatchlings, but adult turtles have also been under investigation. On the other hand, responses of rats, mice and rodents have been investigated in controlled laboratory studies where lighting manipulations can be fully controlled and measured. Field experiments of mice and rats in natural environments or in more controlled enclosures have also been performed. Response variables includes behaviour, ecological relevant variables and physiological measurements.

Many ecological studies are conducted without including data on environmental factors that may influence the results. Especially field experiments are very poor in reporting the lighting condition, for example light source, light intensity, and light distribution.[5] Only a few studies report enough information on light distribution to be able to repeat the study. Light sources are often mentioned but rarely with enough information to replicate the study. For example, the spectral power distribution (SPD) of the light sources are rarely reported. Even

during controlled conditions, measurement details are not often clearly stated or reported. In addition, exposure levels for organisms are rarely reported.

These ecological studies often characterize the lighting conditions using photometric measures, such as illuminance (unit: lux). Illuminance, the total luminous flux incident on a surface per unit area, does not quantify the light reflected from surfaces and it is based on human visual sensitivity to optical radiation. The human spectral sensitivity to optical radiation is assessed using the photopic luminous efficiency function, which peaks at 555 nm. However, most other animals (e.g., mammals except old and new world monkeys, insects, birds) have different photoreceptor spectral sensitivities due to evolutionary reasons, such as detecting flowers or fruits.[6] Some animals can even detect optical radiation beyond light, such as ultraviolet and infrared radiation. Therefore, the use of photometric measures (i.e., illuminance, luminance) is limited at best, and might mislead researchers, conservators, and lighting designers in their efforts in protecting natural habitats. In addition, the typical illuminance and luminance meters can only perform point measurements (a single point in time). A single point measurement does not fully characterize the visual scene in an outdoor setting but taking more measurements can be cumbersome and time intensive with these devices. Therefore, alternative methods should be used to characterize the lighting conditions of a field of view of a large area.

1.3 Satellite images

An alternative approach to photometric spot-measurements is extracting light exposure information from satellite images. Ground-based measurements include astronomical photometry and spectroscopy at large observatories, wide-field photometry using all-sky cameras with fish-eye lenses, narrow angle measurements (typically in only one band) using sky quality meters. Naked eye observations of stellar objects where citizen observations can be used to get large coverage of the observations. For light emitted through the earth atmosphere, remote sensing is carried out with radiance measurements by satellite-based sensors and photographs taken from NASA's International Space Station.

In earlier studies, mostly telescopes and naked eye observations were used in ecological research. From the year 2000 and onwards satellite-based radiometry has been used in the studies of light pollution, starting with the Defense Meteorological Satellite Program (DMSP) Operational Linescan System and later with the higher resolution of the monthly cloud-free night-time imagery from the Suomi National Polar-Orbiting Partnership (Suomi NPP), Visible Infrared Imaging Radiometer Suite (VIIRS) Day/Night Band, and most recently the Chinese satellite Jilin-1, claiming to have a spatial resolution below 1 m. With the development of wide-angle photometry, from 2010 and onwards the number of studies using camera-based measurements have increased.[5]

LAN measured by satellite is often correlated to urbanization, noise levels, and air pollution. In outdoors, it was found that satellite-based radiance measurements were useful when estimating the ground exposure, although luminance values from The New World Atlas had a better correlation with ground measurements considering the full sky. However, both the satellite image composites, and the estimated zenith brightness levels were found to smooth out local spatial variations as measurements performed on the ground have shown a much larger variation between high and low exposure sites when total exposure is considered.[7]

Although, satellite measurements of sky brightness can provide a broad analysis of a larger geographical area, it has limitations. For example, the process of sky glow and the measurement of the sky brightness is highly influenced by meteorological conditions. In

---

[6] Osorio, D., & Vorobyev, M. (2008). A review of the evolution of animal colour vision and visual communication signals. *Vision Research*, *48*(20), 2042-2051.

[7] Simons, A. L., Yin, X., & Longcore, T. (2020). High correlation but high scale-dependent variance between satellite measured night lights and terrestrial exposure. *Environmental Research Communications*, 2(2), 021006.

astronomical studies, different units are used depending on the experimental technique. It is common to report the sky brightness in the astronomical magnitude system mag/arcsec^2. This can be approximately compared to luminance in mcd/m^2, but the different measurement techniques and bands used make it difficult to compare results from different studies. Another important limitation of the satellite images is the spectral sensitivity of the radiometers in the satellite (i.e., between 500 nm and 900 nm), which does not include a substantial portion of short wavelength energy that animals, including humans, are sensitive.

1.4 Spectral radiance imaging

The limitations of photometric and satellite measures can be balanced by utilizing spectral radiance measurements captured through imaging systems. Spectral radiance imaging is the method of collecting radiometric data from a scene using a calibrated camera. Spectral radiance imaging is a subset of remote imaging, where electromagnetic radiation emitted or reflected from surfaces are measured. This method enables large field-of-view scanning and imaging for remote sensing and surveillance, with early applications focusing on the relationship between electromagnetic radiation and water,[8] complex vegetation,[9] and climate variability.[10] Today, spectral imaging cameras can be purchased to measure the radiometric quantities that are far more relevant for ecological and environmental research.

2. Problem statement / objective

The growing population and the increase in urbanization has rapidly expanded the human reach into the natural habitats. This increase comes at a price for the ecological environments and its inhabitants. Light, a key factor for human vision, can disrupt other species' biological cycles. Current methods of quantifying the negative impacts of light pollution is limited. The objective of this project is to evaluate the performance of spectral radiance imaging for a faster and accurate measurement of the lit night environment. The data collected in this study will be also used to develop new metrics to quantity the ecological impacts of light pollution.

3. Outcomes

The primary outcome of this project is the development and confirmation of a novel method to accurately assess the impact of light pollution. Through rigorous experimentation and data analysis, I will refine the approach to spectral radiance mapping and validate its effectiveness in quantifying the ecological effects of artificial lighting. By employing mathematical modeling techniques, I aim to optimize the estimation of radiometric quantities, providing researchers with precise and reliable data for assessing light pollution levels in diverse environments.

Furthermore, the project will result in the creation of a comprehensive light pollution metric that accounts for the spectral characteristics of light sources and the irradiance of the visual scene. This metric will offer a nuanced understanding of how different light spectra influence ecological processes, facilitating targeted interventions to mitigate the adverse effects of light pollution on biodiversity. By integrating spectral information into the assessment

---

[8] Curran, P. J., & Novo, E. M. M. (1988). The relationship between suspended sediment concentration and remotely sensed spectral radiance: a review. *Journal of Coastal Research*, 351-368.

[9] Goward, S. N., Cruickshanks, G. D., & Hope, A. S. (1985). Observed relation between thermal emission and reflected spectral radiance of a complex vegetated landscape. *Remote sensing of Environment*, *18*(2), 137-146.

[10] Iacono, M. J., & Clough, S. A. (1996). Application of infrared interferometer spectrometer clear sky spectral radiance to investigations of climate variability. *Journal of Geophysical Research: Atmospheres*, *101*(D23), 29439-29460.

framework, I aim to enhance the accuracy and relevance of light pollution evaluations, empowering stakeholders to make informed decisions about outdoor lighting practices and policies.

Moreover, to foster collaboration and knowledge-sharing within the research community, the data generated through this project will be made openly accessible online. By providing access to the datasets and methodology, I aim to encourage other researchers to develop their own approaches for assessing light pollution and evaluating the proposed metrics and measurement methods. This open-access initiative will promote transparency and reproducibility in scientific inquiry, catalyzing further advancements in the field of ecological light pollution research and fostering interdisciplinary collaboration towards sustainable lighting solutions.

In summary, the outcomes of this project will not only contribute to our understanding of the ecological impacts of light pollution but also provide valuable tools and resources for researchers, policymakers, and practitioners striving to address this pressing environmental issue. Through the development of innovative assessment methods and the dissemination of open-access data, I seek to catalyze positive change in outdoor lighting practices and promote the conservation of biodiversity in light-polluted ecosystems.

4. Impact

The project outputs will directly impact the practice of lighting design and illumination engineering. There are currently several outdoor lighting standards that aim to limit the light exposure on unwanted areas to limit the negative consequences of light pollution. The International Commission on Illumination (CIE) "CIE 150:2017 Guide on the limitation of the effects of obtrusive light from outdoor lighting installations,"[11] the Model Lighting Ordinance (MLO) published jointly by the International Dark Sky Association and the Illuminating Engineering Society (IES), Leadership in Energy and Environmental Design (LEED) Light pollution reduction Sustainable Sites (SS8), and Australian and New Zealand Standards (AS/NZS) 4282:2019 Outdoor Lighting Obtrusive Effects[12] are some of the most prominent examples. However, these standards still utilize photometric measures and are often limited to negative impacts on humans (e.g., glare).

Leveraging my connections with standards bodies and technical expertise, I will actively engage with stakeholders to enhance existing guidelines by incorporating the metrics developed through the outcomes of this research proposal. By advocating for the integration of spectral radiance mapping and the new light pollution metric into outdoor lighting standards, I aim to ensure that these standards effectively address the ecological impacts of light pollution beyond human perception.

Through dedicated service work and collaboration with industry stakeholders, the results of this research will be translated into actionable recommendations and guidelines, facilitating immediate real-world impact. By influencing the revision and adoption of outdoor lighting standards, this project will contribute to the development of sustainable lighting practices that minimize the ecological footprint of artificial illumination. Ultimately, the integration of spectral radiance mapping and the new light pollution metric into lighting design and engineering practices will promote biodiversity conservation and support efforts to create environmentally responsible built environments.

[11] CIE (2017) 150:2017 Guide on the limitation of the effects of obtrusive light from outdoor lighting installations. CIE: Austria, Vienna.
[12] AS/NZS (2019) 4282:2019 Outdoor Lighting Obtrusive Effects. Standards Australia.

Ultrasensitive Nanophotonic Analysis of Sebum as a Non-Invasive Source of Biomolecular Information: Toward biophotonic diagnostics based on skin surface lipids *–Executive summary*

***The challenge*.** The skin surface lipidome contains information from the human body's metabolic and biochemical processes. Hence, sebum (an oily substance produced by sebaceous glands in the skin) represents an innovative source of biomolecular information. Chromatographic methods and mass spectrometry are the most common analytical techniques employed in sebum analysis. These analytical techniques often need bulky equipment and highly trained personnel. In addition, they generally require organic solvents and time-consuming extraction procedures. Hence, these analytical techniques are challenged by technological features offered by the next generation of diagnostic devices, including environmental friendliness, easy-to-sample collection, high sensitivity, and the capability to operate at the point of care. In addition, the limitations of current analytical/extraction methodologies, may hinder the discovery of new biomarker candidates in sebum. In fact, sebum can contain specific biosignatures offered by biomolecules expressed in relatively low concentrations that are yet to be systematically identified.

***Proposed project*.** The overarching objective of the *Challenge Project* is to embark on an innovative journey by integrating ultrasensitive surface-enhanced Raman spectroscopy (SERS) substrates with portable technologies (e.g., handheld Raman equipment). The ultimate goal is to perform direct analysis of sebum in a simple fashion (e.g. from a simple skin swab from volunteers and avoiding the usage of reagents), thereby revealing unexplored biosignatures by SERS. Using flexible nanoplasmonic patches, SERS analysis of sebum will be carried out (our team has previously developed ultrasensitive flexible 3D SERS substrates made of silver/gold nanoparticles, graphene oxide and nanopaper, which are also eco-friendly). As a control, non-plasmonic sebum collection substrates will also be analyzed using Raman spectroscopy. Upon judicious optimization, the sebum of at least 30 healthy volunteers will be analyzed via SERS and Raman, respectively. The resulting spectral signatures will be analyzed and compared to determine those Raman fingerprints arising from SERS and absent in conventional Raman; for instance, using spectral library matching. In the last stage, in a pilot translational setting, to investigate the potential biomedical relevance of the approach, the sebum of at least 10 volunteers undergoing a neurodegenerative disease (ex., Parkinson's Disease or Alzheimer's Disease) will be also analyzed.

Intended outcomes. By executing this project, we will not only simplify sebum analysis, but also provide an innovative nanophotonic approach to discover SERS biofingerprints in a readily available biofluid. The resulting SERS biofingerprints could be linked with specific metabolic and biochemical processes occurring in the human body, thereby providing an innovative platform for noninvasive diagnostics and catalyzing the advancement of technologies devoted to healthcare. Importantly, the spectra generated in this project will be deposited in a publicly available database, ensuring the thoroughness and transparency of our research process, and thereby sharing new insights with the scientific community. This project will provide pioneering research on the advantageous analysis of sebum using nanophotonics, lay the foundations of biophotonic diagnostics based on sebum analysis, and boost advances in the next generation of molecular sensors, biomedical research, and democratized healthcare. In addition, combining this type of biophotonic diagnostics with digital technologies such as artificial intelligence could give rise to innovative smart spectral diagnostics. This project has, therefore, the potential to facilitate an innovative platform for personalized, noninvasive, and preventive healthcare, especially at the point of need.

Ultrasensitive Nanophotonic Analysis of Sebum as a Non-Invasive Source of Biomolecular Information: Toward biophotonic diagnostics based on skin surface lipids

Literature Review. The outermost epidermal layer of the skin is a barrier that safeguards skin integrity and offers a protective coating made of lipids. Such a coating prevents desiccation and the loss of moisture to the external environment. It also protects against external aggressions and invaders such as pathogenic agents, allergens and ultraviolet radiation.[1] Skin surface lipids is a complex mixture of free fatty acids and neutral lipids, arising from both skin removal and sebaceous secretion, particularly triglycerides (20–60%), wax esters (23–29%), squalene (10–14%), free fatty acids (5–40%), small amounts of cholesterol and cholesterol esters (1–5%), as well as diglycerides (1–2%).[2]

Metabolic and biochemical processes occurring in the human body may be reflected in the skin surface lipidome. As a consequence, lipidomic analysis of sebum may allow for the identification of biomarkers that are related to specific health statuses such as neurological disorders (Parkinson's disease and Alzheimer's disease),[3–5] type 2 diabetes,[6] COVID-19 infection,[7] self-perceived skin sensitivity,[8] and ethanol consumption.[9] In addition, sebum can also contain inflammatory biomarkers (cytokines, namely, IL-1α and IL-1RA, IL-6, IL-8, TNF-α, INF-γ, IL-33, IL-1β and G-CSF).[10]

While sebum can be an interference in electrochemical sensors,[11] considering the aforementioned context and from the viewpoint of biophotonics, sebum represents an innovative source of biomolecular information that could be exploited to perform non-invasive molecular diagnostics. **Table 1** summarizes representative literature reporting the analysis of sebum with different scopes and aims. As observed in Table 1, chromatographic techniques, followed by mass spectrometry are the most common analytical techniques employed in sebum analysis. These analytical techniques often need bulky equipment and highly trained personnel. In addition, they generally require organic solvents as well as time-consuming extraction procedures.

“Raman spectroscopy is a highly specific optical technique that can identify molecules based on their chemical bonds and their unique vibrational modes. These modes are associated with different light frequencies created after incident monochromatic light gains or loses energy through inelastic scattering, also known as Raman scattering, after its discovery by Chandrasekhara V. Raman in 1928. Despite its high analytical specificity, Raman spectroscopy applications are highly constrained by the weak signal produced during such a light-matter interaction, since only one photon between 10^6-10^{10} is Raman scattered. Nevertheless, surface-enhanced Raman spectroscopy (SERS) overcomes this limitation.”[12] As far as we know, employing organic solvents and laborious extraction procedures, sebum has been analyzed using Raman spectroscopy.[13] Moreover, a proof-of-concept developed in Eden Morales-Narváez’s laboratory demonstrated the feasibility to perform sebum analysis using ultrasensitive surface enhanced Raman spectroscopy (SERS) substrates without any sample treatment and from a simple skin swab from a couple of volunteers.[14]

Table 1. Representative literature reporting the analysis of sebum using different techniques.

Analytical Technique | Region of collection	**Scope** | Extraction method or media	**Reference**
Paper Spray Ionization Ion Mobility Mass Spectrometry | *Mid-back of participants*	Biomarkers for the Diagnosis of Parkinson’s Disease | *Direct transfer via touch and roll*	3
Gas chromatography-mass spectrometry | *Central region of the forehead*.	Biomarkers for the Diagnosis of Parkinson’s Disease and Alzheimer’s Disease | *Acetone, methanol, isopropanol mixture*	4
Liquid chromatography-mass spectrometry | *Upper back of participants*	Biomarkers for the Diagnosis of Parkinson’s Disease | *Methanol*	5
Ultra-high performance liquid chromatography-quadrupole tandem time-of-flight mass spectrometry and weighted gene co-expression network analysis | *Right side of the foreheads of participants*	Biomarkers for Type 2 Diabetes | *Chloroform methanol, acetone, and isopropanol*	6
Ultraperformance liquid chromatography–quadrupole time-of-flight mass spectrometry | *Right cheek of participants*	Biomarkers related to self-perceived skin sensitivity | *Chloroform and methanol*	8
Gas Chromatography-Mass Spectrometry | *Center of the forehead of participants*	Ethanol consumption | *A mixture of acetone/hexane*	9
Immunoassay / *Pelvic region of participants*	Inflammatory biomarkers | *Phosphate buffered saline+ 0.1% dodecyl maltoside*	10
High-pressure liquid chromatography–atmospheric pressure chemical ionisation–mass spectrometry | *Forehead of participants*	Forensic context: identification of sex and ethnicity | *Hexane and a mixture of chloroform/methanol.*	15
Liquid chromatography-mass spectrometry | *Right side of the upper back of participants*	Lipidome biosignature upon COVID-19 infection | *Methanol*	7
High-temperature gas chromatography/mass spectrometry **Raman** | *Forehead of participants*	Differences in terms of geographical localization | *Diethyl ether and isooctane.*	13
Surface enhanced **Raman** spectroscopy / *Forehead of participants*	Proof-of-concept | *Skin swab with a flexible SERS substrate*	14

Problem Statement/Objective. By means of a series of technological features, such as environmental friendliness, easy-to-sample collection, high sensitivity and the capability to operate at the point-of-care, the next generation of diagnostic devices is intended to facilitate personalized, non-invasive and preventive healthcare.[16,17] However, the realization of this type of diagnostics remains a challenge, where nanophotonics and biophotonics can play a crucial role.

Sebum can contain specific biosignatures offered by biomolecules expressed in relatively low concentrations and therefore they have not been identified until now by current analytical/extraction methodologies, which may hinder the discovery of new biomarker candidates in sebum. The main objective of the proposal is to integrate ultrasensitive SERS substrates with portable technologies (e.g. a handheld Raman equipment), with the ultimate goal of performing direct analysis of sebum in a simple fashion (e.g. from a simple skin swab from volunteers and avoiding the usage of reagents), thereby revealing unexplored SERS biosingatures systematically.

We will realize this *Challenge Project* by using flexible nanoplasmonic patches enabling SERS analysis. Our team has previously developed ultrasensitive flexible 3D SERS substrates made of silver/gold nanoparticles, graphene oxide and nanopaper, which are also eco-friendly.[14,18] As a control, non-plasmonic sebum collection substrates will also be analyzed using Raman spectroscopy. Upon judicious optimization, sebum of at least 30 healthy volunteers will be analyzed via SERS and Raman, respectively. The resulting spectral signatures will be analyzed and compared to determine those Raman fingerprints arising from SERS and absent in conventional Raman (for instance, using statistical tests and/or spectral library matching; ex., KnowItAll Software). Eventually, in a pilot translational setting, to investigate the potential biomedical relevance of the approach, the sebum of at least 10 volunteers undergoing a neurodegenerative disease (ex., Parkinson's Disease or Alzheimer's Disease) will be also analyzed. Ethical approval to collect sebum samples from human volunteers will be submitted in the Ethics Committee of the Center for Applied Physics and Advanced Technology with Delegated Authority, National Autonomous University of Mexico (Universidad Nacional Autónoma de México, UNAM). The overall vision is depicted in **Figure 1**.

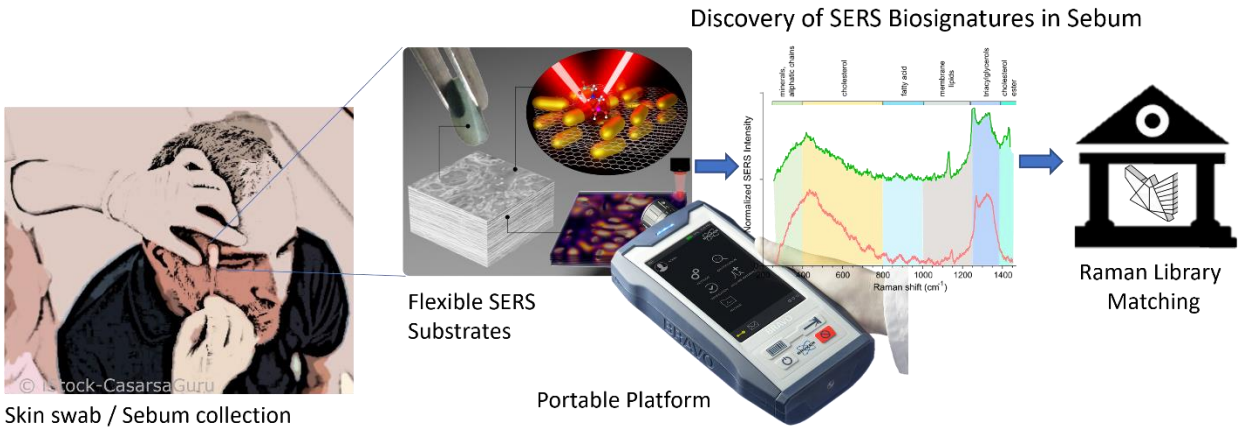

Figure 1. Toward biophotonic diagnostics based on skin surface lipids.

Outcome(s). Sebum is an emerging source of biomolecular information that can revolutionize non-invasive molecular diagnostics. By executing this project, we will not only simplify sebum analysis, but also provide an innovative nanophotonic approach to discover SERS biofingerprints in a readily available biofluid. The resulting SERS biofingerprints could be related with specific metabolic and biochemical processes occurring in the human body, thereby providing an innovative platform for spectral diagnostics and catalyzing the advancement of technologies devoted to healthcare. Importantly, the spectra generated in this project will be deposited in a publicly available database, ensuring the thoroughness and transparency of our research process, and thereby sharing new insights with the scientific community.

Impact. This project will provide pioneering research on the advantageous analysis of sebum using nanophotonics, lay the foundations of biophotonic diagnostics based on sebum analysis and boost advances in the next generation of molecular sensors, biomedical research, as well as democratized healthcare.

In addition, the combination of this type of biophtonic diagnostics with digital technologies such as artificial intelligence could give rise to innovative smart spectral diagnostics.[12] This project has therefore the potential to facilitate an innovative platform for personalized, non-invasive and preventive healthcare, especially at the point-of-need.

References

(1) Mijaljica, D.; Townley, J. P.; Spada, F.; Harrison, I. P. The Heterogeneity and Complexity of Skin Surface Lipids in Human Skin Health and Disease. *Progress in Lipid Research* **2024**, *93*, 101264. https://doi.org/10.1016/j.plipres.2023.101264.

(2) Assi, A.; Michael-Jubeli, R.; Jacques-Jamin, C.; Duplan, H.; Baillet-Guffroy, A.; Tfayli, A. Skin Surface Lipids Photo-Oxidation: A Vibrational Spectroscopy Study. *Journal of Raman Spectroscopy* **2023**, *54* (5), 487–500. https://doi.org/10.1002/jrs.6504.
(3) Sarkar, D.; Sinclair, E.; Lim, S. H.; Walton-Doyle, C.; Jafri, K.; Milne, J.; Vissers, J. P. C.; Richardson, K.; Trivedi, D. K.; Silverdale, M.; Barran, P. Paper Spray Ionization Ion Mobility Mass Spectrometry of Sebum Classifies Biomarker Classes for the Diagnosis of Parkinson's Disease. *JACS Au* **2022**, *2* (9), 2013–2022. https://doi.org/10.1021/jacsau.2c00300.
(4) Briganti, S.; Truglio, M.; Angiolillo, A.; Lombardo, S.; Leccese, D.; Camera, E.; Picardo, M.; Di Costanzo, A. Application of Sebum Lipidomics to Biomarkers Discovery in Neurodegenerative Diseases. *Metabolites* **2021**, *11* (12). https://doi.org/10.3390/metabo11120819.
(5) Sinclair, E.; Trivedi, D. K.; Sarkar, D.; Walton-Doyle, C.; Milne, J.; Kunath, T.; Rijs, A. M.; de Bie, R. M. A.; Goodacre, R.; Silverdale, M.; Barran, P. Metabolomics of Sebum Reveals Lipid Dysregulation in Parkinson's Disease. *Nature Communications* **2021**, *12* (1), 1592. https://doi.org/10.1038/s41467-021-21669-4.
(6) Li, H.; Ma, Y.; Feng, N.; Wang, W.; He, C. Exploration of Potential Biomarkers for Type 2 Diabetes by UPLC-QTOF-MS and WGCNA of Skin Surface Lipids. *Clin Cosmet Investig Dermatol* **2022**, *15*, 87–96. https://doi.org/10.2147/CCID.S347245.
(7) Spick, M.; Longman, K.; Frampas, C.; Lewis, H.; Costa, C.; Walters, D. D.; Stewart, A.; Wilde, M.; Greener, D.; Evetts, G.; Trivedi, D.; Barran, P.; Pitt, A.; Bailey, M. Changes to the Sebum Lipidome upon COVID-19 Infection Observed via Rapid Sampling from the Skin. *EClinicalMedicine* **2021**, *33*, 100786. https://doi.org/10.1016/j.eclinm.2021.100786.
(8) Ma, Y.; Cui, L.; Tian, Y.; He, C. Lipidomics Analysis of Facial Lipid Biomarkers in Females with Self-Perceived Skin Sensitivity. *Health Science Reports* **2022**, *5* (3), e632. https://doi.org/10.1002/hsr2.632.
(9) González-Illán, F.; Ojeda-Torres, G.; Díaz-Vázquez, L. M.; Rosario, O. Detection of Fatty Acid Ethyl Esters in Skin Surface Lipids as Biomarkers of Ethanol Consumption in Alcoholics, Social Drinkers, Light Drinkers, and Teetotalers Using a Methodology Based on Microwave-Assisted Extraction Followed by Solid-Phase Microextraction and Gas Chromatography-Mass Spectrometry. *Journal of Analytical Toxicology* **2011**, *35* (4), 232–237. https://doi.org/10.1093/anatox/35.4.232.
(10) Jayabal, H.; Abiakam, N. S.; Filingeri, D.; Bader, D. L.; Worsley, P. R. Inflammatory Biomarkers in Sebum for Identifying Skin Damage in Patients with a Stage I Pressure Ulcer in the Pelvic Region: A Single Centre Observational, Longitudinal Cohort Study with Elderly Patients. *International Wound Journal* **2023**, *20* (7), 2594–2607. https://doi.org/10.1111/iwj.14131.
(11) Yang, M.; Sun, N.; Lai, X.; Wu, J.; Wu, L.; Zhao, X.; Feng, L. Paper-Based Sandwich-Structured Wearable Sensor with Sebum Filtering for Continuous Detection of Sweat pH. *ACS Sens.* **2023**, *8* (1), 176–186. https://doi.org/10.1021/acssensors.2c02016.
(12) Horta-Velázquez, A.; Arce, F.; Rodríguez-Sevilla, E.; Morales-Narváez, E. Toward Smart Diagnostics via Artificial Intelligence-Assisted Surface-Enhanced Raman Spectroscopy. *TrAC Trends in Analytical Chemistry* **2023**, *169*, 117378. https://doi.org/10.1016/j.trac.2023.117378.
(13) Rime MICHAEL-JUBELI; Ali TFAYLI; Jean BLETON; Arlette BAILLET-GUFFROY. Chemometric Approach for Investigating the Skin Surface Lipids (SSLs) Composition: Influence of Geographical Localization. *European Journal of Dermatology* **2011**, *21* (2), 63–71. https://doi.org/10.1684/ejd.2011.1263.
(14) Rodríguez-Sevilla, E.; Álvarez-Martínez, J. U.; Castro-Beltrán, R.; Morales-Narváez, E. Flexible 3D Plasmonic Web Enables Remote Surface Enhanced Raman Spectroscopy. *Advanced Science* **2024**, *n/a* (n/a), 2402192. https://doi.org/10.1002/advs.202402192.
(15) Shetage, S. S.; Traynor, M. J.; Brown, M. B.; Chilcott, R. P. Sebomic Identification of Sex- and Ethnicity-Specific Variations in Residual Skin Surface Components (RSSC) for Bio-Monitoring or Forensic Applications. *Lipids in Health and Disease* **2018**, *17* (1), 194. https://doi.org/10.1186/s12944-018-0844-z.
(16) Land, K. J.; Boeras, D. I.; Chen, X.-S.; Ramsay, A. R.; Peeling, R. W. REASSURED Diagnostics to Inform Disease Control Strategies, Strengthen Health Systems and Improve Patient Outcomes. *Nature Microbiology* **2019**, *4* (1), 46–54. https://doi.org/10.1038/s41564-018-0295-3.
(17) Hosseinifard, M.; Naghdi, T.; Morales-Narváez, E.; Golmohammadi, H. Toward Smart Diagnostics in a Pandemic Scenario: COVID-19. *Frontiers in Bioengineering and Biotechnology* **2021**, *9*, 510. https://doi.org/10.3389/fbioe.2021.637203.
(18) Rodríguez-Sevilla, E.; Vázquez, G. V.; Morales-Narváez, E. Simple, Flexible, and Ultrastable Surface Enhanced Raman Scattering Substrate Based on Plasmonic Nanopaper Decorated with Graphene Oxide. *Advanced Optical Materials* **2018**, *6* (19), 1800548. https://doi.org/10.1002/adom.201800548.
(19) Jayabal, H.; Bader, D. L.; Worsley, P. Development of an Efficient Extraction Methodology to Analyse Potential Inflammatory Biomarkers from Sebum. *Skin Pharmacology and Physiology* **2023**, *36* (1), 38–50. https://doi.org/10.1159/000528653.

Project Title: Fabrication of Bioplastic Diffraction Gratings Based on Chitosan/Silica Nanoparticles from Crab Shell Waste and Coal Fly Ash.

Project Summary:

Dwindling natural resources has led to creative and efficient methods for using materials typically considered waste. Recycling waste materials for various purposes necessarily involves environmental issues such as toxicity, sustainability, and cost-effectiveness that need to be properly addressed. The Philippines produces more than 250,000 metric tons of seafood waste annually. In seafood production, 35% to 40% of waste is in the form of discarded shells which, if incorrectly disposed of, cause environmental pollution in coastal areas. Repurposing crab waste as a raw material for bioplastic components is promising, with shells having a chitin content of 10 to 72%, suitable for chitosan extraction. Further, the Philippines has several coal fire power plants producing thousands of tons of waste material including fly ash when improperly disposed can harm the environment. This waste may contain contaminants like boron, selenium, and arsenic. Utilizing coal fly ash as a source of sodium silicate will reduce waste disposal. This current work is aligned with Sustainable Development Goal 12 of the United Nations on ensuring sustainable consumption and production patterns and SDG 13 on urgent action to combat climate change and its impacts. Repurposing crab shell waste and coal fly ash will help ensure a sustainable source of raw materials from what is tagged as waste. It will help reduce the emission of pollution in the air and the accumulation of contaminants in soil and water affecting the environment.

Recently, I fabricated a Bioplastic Diffraction gratings from chitosan extracted from crab shell waste. Using the soft lithography technique, I successfully replicated the groove lines from the commercial gratings with a density of 600 and 1200 lines/mm. The diffraction experiment and power efficiency result are comparable with the performance of the commercial grating. Indeed it is the first step to producing lightweight, cheaper, and biodegradable diffraction gratings for industrial use and converting wastes into valuable products. Further, with the modified chemical extraction method, I produced chitosan from crab shell waste with approximately 93% Degree of Deacetylation. In 2023, when my first paper on ***"Chitosan from crab shell waste for soft lithography of bioplastic diffraction gratings"*** was published in Applied Optics caught the attention of the scientific community and featured in various online platforms in both local and international media. The method of extraction of chitosan from marine waste and the process of fabricating a bioplastic diffraction grating is now under evaluation by the Intellectual Property of the Philippines (IPOPhil) for possible patent protection. This led to winning the **Most Outstanding Graduate Student Research Award** in the **School of Science and Engineering, Ateneo de Manila University**. This idea won the **Best Paper Award (1st Place)** and **Best Presenter Award (2nd Place)** titled ***"Chitosan diffraction grating from crab shell wastes: Turning South East Asia's marine waste into an optical biopolymer with industrial value"*** during the **1st ASEAN Region 6 Research Conference** hosted by **CHED Region VI**. The success of this project is useful not only to the scientific community but more specifically to the fisher folks community and seafood industry engaging with crabs, and protecting the environment. This time my training in nano synthesis is useful in extracting sodium silica from coal fly ash and synthesizing it to silica nanomaterial.

One of my goals is to establish an **Advanced Physics, Photonics Laboratory, and Emerging Technology (APPLETech)** to prepare the university to offer a **Bachelor of Science in Physics** program. As far as my knowledge, there is no university offering this program in the Region. I desire to transfer the skills and knowledge learned in space science technology application research and development to aspiring researchers in the field of Physics. Bringing science to the community and protecting the environment through innovative technology using raw materials from waste.

I. Title: Fabrication of Bioplastic Diffraction Gratings Based on Chitosan from Crab Shell Waste Combined with Silica Nanoparticles from Coal Fly Ash

II. Literature Review

To accomplish the research objectives, a review of related literature is first performed. These previous studies give insight into the motivation and applications of this current research.

1. Chitosan and Extraction Method

One of the most prevalent biopolymers in crustaceans, insects, fungi, and mollusks is chitin [1]. When deacetylated, chitin, a polymer of N-acetyl-D- glucosamine, becomes chitosan. Due to the presence of primary and secondary hydroxyl groups on each repeating unit as well as the amine group on each deacetylated unit, chitosan is chemically more active than chitin [2]. These reactive groups are easily modified chemically to change chitosan's mechanical and physical properties. It is greatly helpful that chitin and chitosan have amine groups since they allow for specific biological processes and the utilization of modifying reactions [3]. These polysaccharides' excellent properties, such as biocompatibility, biodegradability, bioactivity, bioresorptivity, non-toxicity, and high adsorption, make them useful and essential biomaterials, attracting a great deal of industrial attention as potential alternatives to synthetic polymers [4].

In general, there are two methods for producing chitosan: chemical and biological [5]. Chemical methods of chitosan preparation primarily consist of three stages of reaction: demineralization (the vast majority of recent literature reports using HCl at concentrations of up to 10% w/v to remove $CaCO_3$ from the shell by reacting for 2-3 hours with agitation), deproteinization (removing the protein and other organic components other than chitin from the shell by reacting with a heated alkali solution, such as 1% - 10% (w/w) aqueous NaOH solution, at temperatures ranging from 65 to 100 °C for 0.5 to 12 hours), and deacetylation (chitin to chitosan conversion using a 40% - 50% (w/w) heated alkali solution, such as NaOH solution) [6]. Because demineralization is a much easier reaction than deproteinization, most recently published literature adopted processes that used those steps in that order: demineralization followed by deproteination and deacetylation. If demineralization is used prior to deproteinization, it can create more surface area on the shell material by dissolving $CaCO_3$ and accelerating the deproteinization reaction, which occurs later in the process [5]. Despite this, some earlier studies have instead used the process where deproteinization is carried out first, i.e. via the steps of deproteinization → demineralization → deacetylation, but executing the process in this particular order has not been perceived to lead to any significant difference in the quality and yield of the chitin produced [7].

To prepare chitosan from crustacean byproducts, biological methods (such as enzymatic methods and fermentation methods) are also available. Enzymatic methods use the same demineralization mechanism as chemical methods, namely the use of acid to remove the $CaCO_3$ in the shell, as previously discussed [8,9]. This method substitutes enzymes for the deproteinization and deacetylation reactions at lower temperatures, typically between 25 °C and 59 °C [9]. For enzymatic deproteinization, various proteinases have been developed, and these enzymes are typically extracted from microbes or fish entrails, such as sardinella (*Sardinella aurita*) and grey triggerfish (*Balistes capriscus*) intestines [8,10]. Likewise, deacetylases can also be extracted from fish intestines or microbes [11- 12], for instance, Alcalase® obtained from *Bacillus licheniformis* [5]. Microorganisms that have been genetically modified have also been reported as a source of enzymes for deproteinization and deacetylation reactions [13].

2. Silica Nanoparticle Synthesis from Coal Fly Ash

Fly ash is a fine ash transported upward with flue gases and may be collected by a powerful electrostatic precipitator before reaching the atmosphere [14]. This material contains hazardous environmental contaminants such as boron and selenium [15]. The Philippines produces almost 1.4 metric tons of coal fly ash each year, an amount expected to increase by 10% annually. Millions of tons of this waste material are also produced in countries like Japan, China, USA, and South Africa. Promisingly, fly ash may be repurposed as a source of rare earth elements (REEs) and converted into valuable products [16].

Recently, this waste material became the focus of research due to its high content of Silicon (Al) and Aluminum (Al) which could be viable sources of purified silica and alumina suitable for various industrial applications. The silica nanoparticles are used in thin film substrates, electrical and thermal insulators, and adsorbents [17]. Leaching is the conventional way of extracting hazardous elements in REEs like coal fly ash [18]. A simple, affordable, and less energy intensive method of sodium silica is available, such as the use of NaOH [19]. Hydrochloric acid (HCl) has also been commonly used because it limits silica dissolution that interferes with coal fly ash extraction and filtration through the formation of silica gel [20].

3. Soft Lithography

Hard lithography techniques are now the most commonly used patterning techniques for micro- and nano-structuring of various surfaces. These techniques primarily employ e-beam, x-ray, ultraviolet, or visible light to pattern a photoresist, either through a mask or directly through scanning techniques. The depletion of the resist allows for etching and substrate patterning. The main drawback of these methods is their high equipment cost.

In the 1990s, Whitesides et al. introduced unique non-photolithographic micropatterning approaches utilizing versatile molds or stamps to overcome this disadvantage [21]. These techniques, collectively known as “soft lithography,” enable low-cost patterning for laboratory use by using a previously patterned stamp instead of “hard” radiation (UV/Vis, x-ray, or e-beam). Another development is the use of an elastomer such as PDMS as a flexible material for stamp preparation. Masking and molding processes were developed in addition to pure stamping methods. Soft lithography techniques offer quick, simple, and inexpensive tools for lab-scale surface micro- and nanostructuring. Large and non-planar (rough or curved) areas, on the other hand, can be treated with a variety of “ink” materials [22]. Partial surface protection by a monolayer is another field of application for microcontact printing. In this case, the deposited molecules protect the surface from etchants or other similar substances. Microcontact printing provided the first way to form various high-resolution patterns using standard laboratory equipment without the need for expensive facilities.

Microcontact printing's advantages have been adapted to replica molding, which has been used for a vast scope of structured surfaces such as compact disks (CDs), diffraction gratings, and holograms [23]. While these techniques are based on molding a suitable material (usually a thermoplastic polymer) against a rigid mold, the use of elastomers makes it easier to form tailored microstructures. As a result, nanoimprint lithography (NIL) was developed, which enables surface patterning with feature heights as low as a few micrometers. Chou et al. first described NIL as a process in which a rigid stamp is pressed onto a PMMA layer on a rigid silicon substrate while being lightly thermally treated [24]. This method could provide an appropriate alternative for photolithographic resist patterning with comparable resolution. In order to speed up the capillary flow of the ink solution from the other side of the stamp, Tvingstedt et al. employed a technique in 2007 that involves extracting air with a syringe from one side of the channels between the patterned stamp and the pre-activated substrate [25]. Unfortunately, the technique needs connected cavities to enable full infiltration. The invention of a variety of soft lithography technologies, all

of which used an elastomeric stamp or mold as a patterning tool, was made possible by straightforward and inexpensive stamp preparation and handling methods. These include hybrid optical/soft lithography techniques, and microfluidic methods.

III. Project Statement/Objectives

The specific objectives of this project are:

1. Extract and characterize chitosan from crab shell waste.
2. Extract and characterize sodium silicate from coal fly ash and synthesis of silica nanoparticles.
3. Soft lithography fabrication of bioplastic diffraction gratings based on chitosan-silica nanoparticle composites.
4. Characterize fabricated bioplastic gratings.
5. Perform diffraction experiments using a laser source with the fabricated bioplastic gratings.

IV. Outcome

The target outputs in this study are:

1. Chitosan powder extracted from crab shell wastes with approximately 90% Degree of Deacetylation.
2. Sodium silicate and silica nanoparticles with high purity.
3. Bioplastic diffraction gratings prototypes fabricated from a chitosan-silica nanoparticles composite.
4. Data on mechanical and optical properties of fabricated bioplastic diffraction gratings.
5. Data on diffraction performance of fabricated bioplastic diffraction gratings.
6. At least one journal article published by Optica.

V. Impact

The results of this research will verify the potential of chitosan as a base material for diffractive elements imprinted microscopic structures. Much promise is seen in further research on repurposing waste materials for fabricating optical devices and promoting sustainability in optical manufacturing. Conventional gratings are made of glass and metal films, whereas chitosan gratings are lightweight and biodegradable, allowing the development of disposable spectrometers. Lightweight and inexpensive spectrometers based on chitosan could be applied as a single-use analytical tool for fieldwork.

References

[1] D.E. Azofeifa, H.J. Arguedas and W.E. Vargas, “Optical properties of chitin and chitosan biopolymers with application to structural color analysis,” *Optical Materials* 35, 175-183(2012).

[2] V.G.L Souza, A.L. Fernando, J.R.A. Pires, P.F. Rodrigues, A.A.S. Lopes and F.M. Braz Fernandes, “Physical properties of chitosan films incorporated with natural antioxidants,” *Industrial Crops and P Products* 107, 565-572(2017).

[3] R. A. Guerrero and S. J. C. Oliva, “Optical wavelength tuning via actuation of a fluidic grating,” *Opt. Eng.* 53(2), 025104 (2014).

[4] S. Ahmed and S. Ikram, Chitosan: Derivatives, Composites and Applications, first ed. John Wiley & Sons, Incorporated, Hoboken, NJ, 2017.

[5] D. Eileh-Ali-Komi and M.R. Hamblin,”Chitin and chitosan: production and application of versatile Biomedical nanomaterials,” Int. J. Adv. Res. 4(3), 411(2016).

[6] H.K. No and S.P. Meyers, “Preparation and characterization of chitin and chitosan – a review, Journal of Aquatic Food Product Technology 4(2), 27-52(1995).
[7] D.A. do Vale, et. al., “Chitosan-based edible films produced from crab-uca (*Ucides cordanus*) wastes, physiochemical, mechanical and antimicrobial properties,” Journal of Polymers and the Environment Springer Nature (2020).
[8] J. Vasquez, I. Rodriguez-Amado, M. Montemayor, J. Fraguas, M. Gonzales and M. Murado, “Chondroitin sulfate, hyaluronic acid and chitin/chitosan production using marine waste source: characteristics, applications and eco-friendly processes: a review,” Marine Drugs 11(3), 747-774(2013).
[9] V. Veugogal, “Green processing of seafood biomass towards blue economy,” Current Research in Environmental Sustainability 4, 100164(2022).
[10] H. Tan, Z. Lim. N. Muhamad and F. Liew, “Potential economic value of chitin and its derivatives as major biomaterials of seafood waste, with particular reference to South East Asia,” Journal of Renewable Materials 10(4), 909-938(2022).
[11] S.K. Kim, “Chitin, chitosan, oligosaccharides and their derivatives: biological activities and applications, CRC Press, Boca Raton, FL, 2011.
[12] P. Charoenvuttitham, J. Shi and G.S. Mittal, “Chitin extraction from black tiger shrimp (*Penaeus monodon*) waste using organic acids,” Sep. Sci. Technol. 41(6), 1135-1153(2006).
[13] C.A.M. Ruiz and H.F.Z. Corrales, “Chitosan derivatives and their biomedical applications, Biological Activities and Application of Marine Polysaccharides 87, (2017).
[14] Koloa MT, Khandakera MU, Amina YM, Abdullah WHB, Bradley DA, Alzimami KS. Assessment of health risk due to the exposure of heavy metals in soil around mega coal-fired cement factory in Nigeria. Results Phys. 11:755–62 (2018).
[15] Klinger, J.M. Rare Earths Frontiers: From Terrestrial Subsoils to Lunar Landscapes; Cornell University Press New York, NY, USA, 2017.
[16] Dahan, A.M.E.; Alorro, R.D.; Pacaña, M.L.C.; Baute, R.M.; Silva, L.C.; Tabelin, C.B.; Resabal, V.J.T. Hydrochloric Acid Leaching of Philippine Coal Fly Ash: Investigation and Optimisation of Leaching Parameters by Response Surface Methodology (RSM). Sustain. Chem. 3, 76–90 (2022).
[17] Zaky, R.R., Hessien, M.M., El-Midany, A.A., Khedr, M.H., Abdel-Aal, E.A., El-Barawy, K.A.: Preparation of silica nanoparticles from semi-burned rice straw ash. Powder Technol. 185, 31–35 (2008).
[18] Valeev, D.; Mikhailova, A.; Atmadzhidi, A. Kinetics of iron extraction from coal fly ash by hydrochloric acid leaching. Metals 8, 533 (2018)
[19] Fertani-Gmati, M., Jemal, M.: Thermochemical and kinetic investigations of amorphous silica dissolution in NaOH solutions. J. Therm. Anal. Calorim. 123, 757–765 (2016).
[20] Seredin, V.V.; Dai, S. Coal deposits as potential alternative sources for lanthanides and yttrium. Int. J. Coal Geol. 94, 67–93 (2012).
[21] G. Whitesides and A. Kumar, “Features of gold having micrometer to centimeter dimensions can be formed through a combination of stamping with an elastomeric stamp and an alkanethiol ink.” Appl. Phys. Lett 63, 2002-2004 (1993).
[22] Y. Xia and G. Whitesides, “Soft lithography,” Annu. Rev. Mater. Sci. 28, 153-184 (1998).
[23] M.C. Hutley, Diffraction Gratings, Academic Press, Inc., New York, 57(1982).
[24] S. Y. Chou, P. R. Krauss and P. J. Renstrom, “Imprint of sub-25 nm vias and trenches in polymers,” *Appl. Phys.Lett.* 67, 3114–3116 (1995).
[25] S. Y. Chou and P. R. Krauss, “Imprint lithography with sub-10 nm feature size and high throughput.” *Microelectron. Eng.* 35, 237–240(1997).

Revolutionizing Optical Communication: Noise Reduction in Microcavities via Nonlinear Optics

PI: Dr. Elham Heidari (she/her) el.heidari@ufl.edu, University of Florida, USA

Optica Foundation Challenge: Information

Introduction: Kerr comb generation holds significant promise in advancing optical telecommunications by providing a versatile platform for generating high-quality frequency combs with a wide range of applications. These include precise optical clock synchronization, coherent communication systems, and ultrafast data transmission. However, current challenges persist in optimizing the performance of Kerr combs for telecommunications applications, particularly in mitigating the impact of noise sources such as thermal fluctuations and environmental disturbances. Additionally, the integration of Kerr combs into existing optical networks requires careful consideration of factors such as compatibility with standard telecommunications components and scalability to meet the demands of future network architectures. Addressing these challenges will be crucial for unlocking the full potential of Kerr comb technology in enhancing the efficiency and reliability of optical telecommunications systems.

Integrated optical frequency combs are poised to transform real-world applications by extending precise metrological capabilities from the lab to practical settings. However, these innovative devices are challenged by their sensitivity to stochastic thermal fluctuations, which notably impact the frequency noise of both the individual comb teeth and the overall repetition rate, with these effects intensifying as the cavity size is reduced.

Novelty: To tackle these issues, we employ a technique that involves phase-locking the cavity soliton to an externally introduced reference. Traditional methods primarily combat thermal fluctuations by modifying the physical system, which can increase complexity and decrease efficiency. In contrast, this work uses an all-optical strategy to align the phase of cavity solitons with an externally injected reference pump laser. This method (Kerr induced synchronization) stabilizes the microcomb by making it less susceptible to internal noise fluctuations and limits the impact of external noise sources such as the frequency noise of the pump lasers. The key innovation is its ability to sustain microcomb performance regardless of cavity size, which could broaden the applicability of microcombs due to its simplicity and effectiveness.

Proposed research: Our main objective is to illustrate the process of using a second reference laser to initiate the synchronization of the microcomb and its function in reducing noise. Although the increased light power may result in higher levels of heat and noise, this approach efficiently circumvents inherent cavity sounds. The microcomb will demonstrate little noise, principally constrained by the laser noise, and even without any external control, it outperforms thermo-refractive noise. This study demonstrates that the size of the cavity is no longer a constraint when it comes to constructing low-noise microcombs. Instead, the focus has shifted towards improving noise suppression in the Kerr-induced synchronized domain by manipulating the lifetime of photons.

The initial phase of this research involves a detailed elucidation of the problem statement, subsequently advancing toward the formulation and refinement of proposed solutions.

Impact: Minimizing thermal noise in ring resonators has significant implications for industry and society. In quantum technology, it boosts the reliability and efficiency of quantum communication systems, enhancing data security. For quantum computing, it extends coherence times and improves quantum gate accuracy, leading to more powerful computers and advancements in cryptography, material science, and simulations. Enhanced sensitivity in quantum sensing and metrology allows for precise measurements, benefiting healthcare diagnostics and environmental monitoring. This precision is crucial for breakthroughs in gravitational wave detection and dark matter research. Additionally, improving the quality factor of photonic circuits fosters high-quality photonic integration, resulting in efficient, compact devices in telecommunications, sensors, and consumer electronics, driving innovation and economic growth.

Optica Foundation Challenge: Information

I. Literature Review

The significance of size reduction in micro ring resonators is paramount for the advancement of integrated photonic systems, particularly regarding their scalability, cost-efficiency, and enhanced functional performance. Miniaturized resonators facilitate the integration of a greater number of photonic components on a single semiconductor substrate, thereby augmenting the functional density and complexity of photonic integrated circuits (PICs) without an increase in physical footprint. Simultaneously, attaining a high-quality factor (Q-factor) in these miniaturized resonators is imperative, as it directly influences the resonator's performance by minimizing optical losses and enhancing the sharpness of the resonance [**1-3**]. A high Q-factor ensures prolonged confinement of light within the resonator, thereby markedly improving sensitivity and precision in applications such as optical sensing, filtering, and wavelength division multiplexing. Consequently, the confluence of size reduction and high-Q factors is essential for the progression of integrated photonics, enabling the development of more compact, efficient, and high-performance photonic devices. However, as micro ring resonators are scaled down, thermorefractive noise (TRN) becomes a significant challenge [**4-6**]. TRN arises from fluctuations in the refractive index due to temperature changes, significantly impacting precision optical applications like micro resonator s and optical frequency combs. These random thermal fluctuations affect the phase and frequency of light within the material, compromising the stability and coherence of signals, especially in Kerr soliton generation [**7**]. Micro resonators are particularly susceptible to TRN due to their small size and high surface-to-volume ratio, which amplify the effects of localized heating from absorbed pump light and environmental temperature changes. The tight confinement of light in smaller resonators increases local heat generation, further impacting the refractive index. High Q factors in these resonators, while beneficial for processes like soliton formation, also amplify noise due to repeated light-material interactions. Strategies to mitigate TRN include temperature stabilization systems, selecting materials with low thermo-optic coefficients, and optimizing resonator geometry to minimize thermal impacts. These approaches are crucial for maintaining the stability and coherence of optical outputs in high-precision applications. Furthermore, integrating advanced thermal management techniques and employing innovative material engineering can further enhance the robustness of micro ring resonators against TRN, paving the way for the next generation of ultra-compact, high-performance photonic devices.

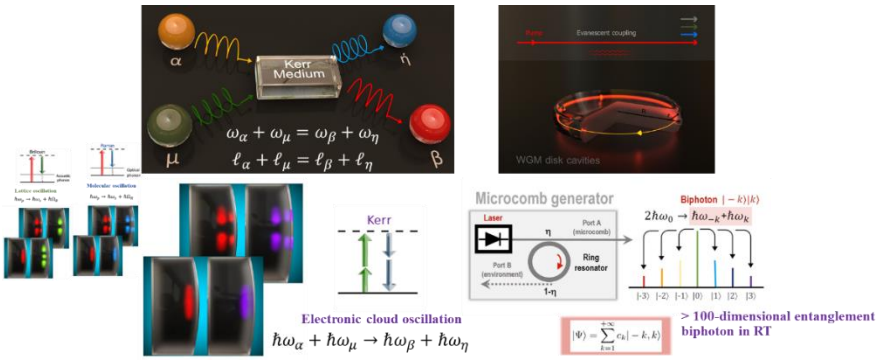

Fig.1 Illustration of four-wave mixing in different resonator models: Depicts the nonlinear Kerr effect in microresonators, leading to new frequency generation. Various resonator designs, including whispering-gallery-mode (WGM) disk cavities, enable efficient frequency conversion, high-dimensional entanglement, and biphoton generation for advanced quantum technologies.

II. Problem Statement/Objective

Kerr comb generation holds significant promise in advancing optical telecommunications by providing a versatile platform for generating high-quality frequency combs with applications such as precise optical

clock synchronization, coherent communication systems, and ultrafast data transmission. These frequency combs, characterized by equidistant spectral lines, are essential for optical arbitrary waveform generation, dense wavelength division multiplexing (DWDM), and high-precision metrology. However, current challenges persist in optimizing the performance of Kerr combs for telecommunications applications, particularly in mitigating the **impact of noise sources such as thermal fluctuations and environmental disturbances**. These noise sources introduce phase and amplitude noise, which degrade the signal quality and coherence of the comb lines, posing significant hurdles for achieving the desired performance metrics in practical settings [**8-10**]. Additionally, the integration of Kerr combs into existing optical networks requires careful consideration of factors such as **compatibility with standard telecommunications components**, including erbium-doped fiber amplifiers (EDFAs), wavelength-selective switches (WSS), and photodetectors, as well as scalability to meet the demands of future network architectures. This necessitates the development of robust packaging techniques and thermal management solutions to ensure stable operation under varying environmental conditions. Moreover, the drive towards silicon photonics integration necessitates overcoming material and fabrication challenges to achieve low-loss waveguides and efficient nonlinear interactions in CMOS-compatible platforms. Addressing these challenges will be crucial for unlocking the full potential of Kerr comb technology in enhancing the efficiency and reliability of optical telecommunications systems.

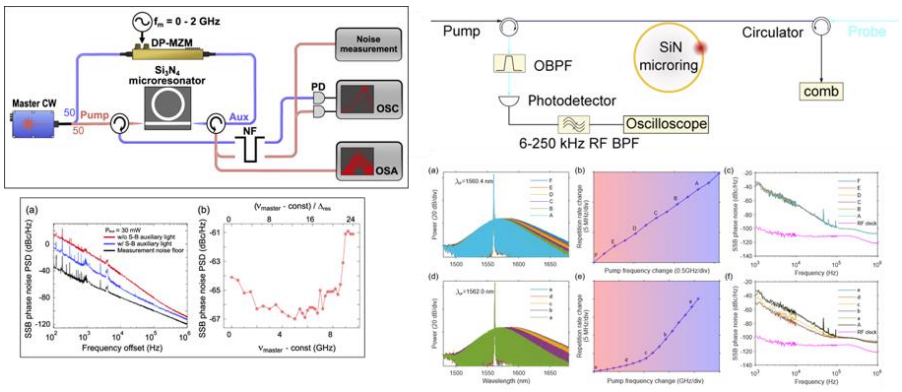

Fig. 2 (a) Setup for sideband-based auxiliary light system, (b) result for sideband-based auxiliary light system (c) Setup for laser-cooling system (d) Comparative study of the self-cooling of soliton microcombs. The top panel depicts the case without self-cooling effect, where the pump only excites a TE mode, (a)-(c) stand for the optical spectra, the repetition frequency, and the singe side band (SSB) phase noise of the down converted repetition frequency of the soliton microcombs at different pump detuning, respectively. (d)-(f) same for the case with self-cooling, where the pump is coupled to TE and TM modes simultaneously [12].

Integrated optical frequency combs, known as microcombs, are poised to transform real-world applications by extending precise metrological capabilities from the lab to practical settings. These devices leverage high-Q micro resonator s to achieve broad and coherent frequency combs through four-wave mixing (FWM) processes [**11**]. However, these devices are challenged by their sensitivity to stochastic thermal fluctuations, which significantly impact the frequency noise of both the individual comb teeth and the overall repetition rate. This frequency noise arises from TRN and thermo-optic effects, which cause variations in the refractive index due to temperature fluctuations. These effects are particularly pronounced as the cavity size is reduced, leading to higher surface-to-volume ratios and increased susceptibility to thermal perturbations. Furthermore, the high confinement of optical fields in micro resonator s results in localized heating, exacerbating the impact of TRN. Mitigating these thermal noise sources requires advanced thermal stabilization techniques, such as integrating microheaters with feedback control systems, employing materials with low thermo-optic coefficients, and optimizing the resonator design to minimize thermal sensitivity. Additionally, improving the precision of comb stabilization techniques, such as Pound-

Drever-Hall (PDH) locking and optical phase-locked loops (OPLL), is essential for achieving the desired performance. By addressing these technical challenges, microcombs can realize their full potential in applications ranging from coherent optical communications and precision spectroscopy to frequency synthesis and metrology, thereby transforming the landscape of integrated photonics.

The optical sidebands from electro-optic modulators (EOM) have been used to mitigate thermal effects that disrupt performance and explores thermal control strategies for Kerr micro resonator soliton combs [**12**]. The sideband-based (S-B) auxiliary light systems stabilize the soliton comb and expand its effective range over 10GHz w/o microheaters, eliminating the need for an auxiliary laser and reducing phase noise. (**Fig.2**). The setup uses an external-cavity diode laser (ECDL) divided into pump and auxiliary paths. The auxiliary path generates S-B auxiliary light, integrated with the pump light in the micro resonator, maintaining nearly constant detuning and enhancing stability. While this method simplifies the setup and reduces the need for microheaters, it involves complex and potentially expensive modulating equipment. The high cost and complexity of the EOMs and associated electronics pose significant barriers to practical implementation. Additionally, the scalability of this approach to different micro resonator s and other applications may be limited. The necessity for precise modulation and integration of auxiliary light adds layers of technical difficulty, which could hinder widespread adoption. The approach's reliance on specialized components makes it less accessible and potentially limits its use in a broader range of photonic systems. The technique of thermal noise reduction in soliton microcombs via laser self-cooling [**13**] offers significant benefits, including a simple and reliable method to mitigate low-frequency thermal noise, improve coherence, and narrow optical linewidths. the transverse electric (TE) mode for soliton generation and the transverse magnetic (TM) mode for cooling. This method extends the soliton existence range in pump frequency from 1.6 GHz to 4.2 GHz and reduces phase noise at a 10 kHz offset by over 10 dB. The process excites two cavity modes in silicon nitride micro resonator.

However, it has drawbacks: the cooling laser can introduce frequency noise into the comb lines, sideband modulation or pump-induced stimulated Brillouin scattering may affect comb purity, and the method requires precise stabilization of cooling and pump lasers to avoid detuning fluctuations. Additionally, it is slightly less effective than using an auxiliary laser for suppressing low-frequency noise.

By employing methods such as material selections, thermal management, passive thermal insulation, the impact of thermorefractive noise on the performance of ring resonators can be significantly mitigated, leading to more stable and precise optical systems.

III. Novelty: To tackle the issues of sensitivity to noise and scalability issues, a technique will be employed that involves phase-locking the cavity soliton to an externally introduced reference. Traditional methods primarily combat thermal fluctuations by modifying the physical system, which can increase complexity and decrease efficiency. In contrast, this approach uses an all-optical strategy to align the phase of cavity solitons with an externally injected reference pump laser. This method stabilizes the microcomb by making it less susceptible to internal noise fluctuations and limits the impact of external noise sources such as the frequency noise of the pump lasers. The key innovation is its ability to sustain microcomb performance regardless of cavity size, which could broaden the applicability of microcombs due to its simplicity and effectiveness.

Proposed Research: The initial phase of this research involves a detailed elucidation of the problem statement, subsequently advancing toward the formulation and refinement of proposed solutions. Each task within the scope of this research is succinctly outlined below.

Task 1. Attenuation of Noise in Integrated Optical Frequency Combs: This task focuses on demonstrating the effectiveness of Kerr-induced synchronization (KIS) in attenuating internal noise sources

in integrated optical frequency combs. By implementing this technique, the comb's reliance on external pump noise is increased, thereby enhancing the stability and performance of optical communication systems.

Task 2. Reduction of Repetition Rate Noise: With KIS-enabled microcombs, there is a notable improvement in the repetition rate noise performance, even when using free-running lasers. This significant reduction in noise is expected to enhance the precision of optical frequency measurements, which are critical in communication systems.

Task 3. Improvement of Individual Comb Tooth Linewidths: The project includes an in-depth analysis of how individual comb tooth linewidths are maintained at an order of magnitude comparable to that of the pump lasers. This is vital for applications such as optical frequency synthesis and spectroscopy, which require high spectral purity.

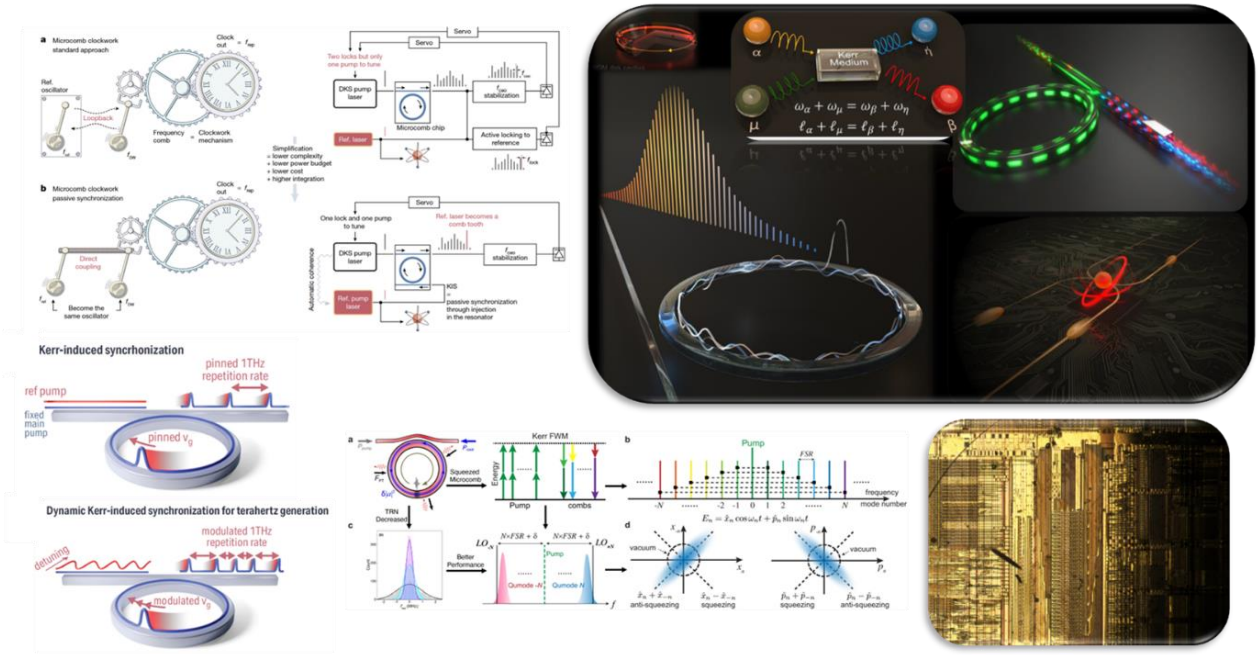

Fig. 3 The current optical clock [14] links a stabilized reference laser with a microcomb tooth using active feedback, which is complex for chip integration. A simpler method uses passive Kerr nonlinearity, injecting the reference laser into the DKS micro resonator for synchronization, reducing complexity and improving stability.

Task 4. Engineering Photonic Lifetime for Noise Reduction: This task involves optimizing photon lifetime through the design of micro-resonator coupling structures to further reduce the noise floor of microcombs. The engineering of these photonic structures is crucial for achieving low-noise performance in compact, integrated optical systems. We anticipate that the reduction in size, weight, and power consumption (SWaP) of these micro resonators by incorporation of KIS into optical microcombs (to decrease the thermal noise) will facilitate their use in field applications, potentially transforming areas like optical communications, environmental monitoring, and biomedical diagnostics. Further enhancements in KIS technology are expected to achieve even lower noise levels and improved stability, positioning these devices as essential elements in advanced photonic systems. Additionally, future research will likely concentrate on refining integration techniques and exploring novel materials and structural designs to boost the performance and practical utility of Kerr combs in diverse applications.

Outcome: The outcome of reducing thermal noise, particularly thermorefractive noise, in a ring resonator

will be transformative across multiple domains. In quantum communication, this advancement will enable more secure and faster networks, enhancing data privacy and protection. In quantum computing, it will lead to more powerful, error-resistant quantum computers, driving breakthroughs in cryptography, material science, and complex simulations. Improved sensitivity in quantum sensing and metrology will yield more precise measurements, benefiting healthcare with better diagnostics and environmental monitoring with more effective pollutant detection. This will also support groundbreaking research in gravitational wave detection and dark matter studies, expanding our understanding of the universe. Additionally, the enhanced quality factor of photonic circuits will foster the development of more efficient and compact devices, spurring innovation in telecommunications, sensors, and consumer electronics. Overall, these advancements will drive significant technological progress, economic growth, and societal benefits.

Impact: Reducing thermal noise, particularly thermorefractive noise, in a ring resonator has profound impacts on both industry and society. For the quantum technology sector, this enhancement translates to more reliable and efficient quantum communication systems, **improving data security and enabling faster**, more secure information exchange. In the realm of quantum computing, extended coherence times and high-fidelity quantum gates lead to more powerful and **accurate quantum computers**, **accelerating advancements** in fields such as **cryptography, material science, and complex system simulations**. **Enhanced sensitivity in quantum sensing** and metrology provides more precise measurements, benefiting industries like healthcare with better diagnostic tools, and environmental monitoring with more accurate detection of pollutants. In gravitational wave detection and dark matter research, this precision supports groundbreaking discoveries, **expanding our understanding of the universe**. Additionally, improving the quality factor of photonic circuits fosters the development of high-quality photonic integration, leading to more efficient and miniaturized devices in telecommunications, sensors, and various consumer electronics, ultimately driving innovation and economic growth across multiple sectors.

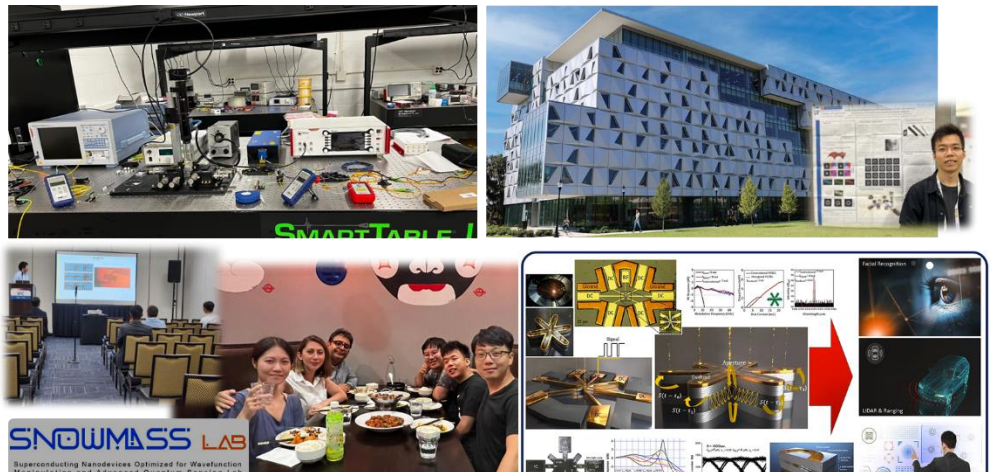

Fig. 4 The related measurement setup for this project is in the new ECE building, Malachowski Hall. Also, there are pictures of students and collaborators at conferences such as CLEO 2024, IPC 2023, and other research-related events within the PI's group.

(PI) Dr. Elham Heidari and her team have played a crucial role in progressing technology from basic research to practical advancements and real-world applications. The team prioritizes technology transition to ensure that as soon as a technology advances, it smoothly moves towards its use in important industries.

References:

1. S. A. Diddams, K. Vahala, and T. Udem, Science 369, eaay3676 (2020).
2. Lu, X., Moille, G., Rao, A., Westly, D. A. & Srinivasan, K. Efficient photoinduced second-harmonic generation in silicon nitride photonics. Nat. Photonics 15, 131–136 (2021).
3. N. Picqu´e and T. W. H¨ansch, Nature Photonics 13, 146 (2019).
4. G. Huang, E. Lucas, J. Liu, A. S. Raja, G. Lihachev, M. L. Gorodetsky, N. J. Engelsen, and T. J. Kippenberg, Physical Review A 99, 061801 (2019).
5. J. Lim, A. A. Savchenkov, E. Dale, W. Liang, D. Eliyahu, V. Ilchenko, A. B. Matsko, L. Maleki, and C. W. Wong, Nature Communications 8, 8 (2017).
6. F. Lei, Z. Ye, ´ O. B. Helgason, A. F¨ul¨op, M. Girardi, V. T-Company, Nature Communications 13, 3161 (2022).
7. C. Panuski, D. Englund, and R. Hamerly, Physical Review, X 10, 041046 (2020).
8. Z. Ye, F. Lei, K. Twayana, M. Girardi, P. A. Andrekson, and V. Torres- Company, “Integrated, ultra-compact high-Q silicon nitride microresonators for low-repetition-rate soliton microcombs,” Laser & Photon. Rev
9. G. Moille, X. Lu, A. Rao, Q. Li, D. A. Westly, L. Ranzani, S. B. Papp, M. Soltani, and K. Srinivasan, Phys. Rev. Appl. 12, 034057 (2019).
10. T. E. Drake, J. R. Stone, T. C. Briles, and S. B. Papp, Nat. Photonics 14, 480 (2020).
11. Y. K Chembo, E. Heidari, C. R Menyuk, “A perspective on nonlinear, microwave, and quantum photonics with Kerr microcombs” Appl. Phys. Lett. 123(24) 2023.
12. K. Nishimoto, K. Minoshima, T. Yasui, and N. Kuse, "Thermal control of a Kerr microresonator soliton comb via an optical sideband, Optics Letters, vol. 47(2) pp. 281–284 (2022)
13. F. Lei, Z. Ye, and Others, "Thermal noise reduction in soliton microcombs via laser self-cooling," Optics Letters, 47 (3) pp. 513–516 (2022).
14. G. Moille, M. Leonhardt, D. Paligora, N. Englebert, F. Leo, et.al. “Parametrically driven pure-Kerr temporal solitons in a chip-integrated microcavity” Nat. Photon (2024) doi.org/10.1038/s41566-024-01401-6.

EXECUTIVE SUMMARY

Home-use wearable blue light therapeutic wrap with built-in diffuse reflectance spectroscopic biosensor for simultaneous treatment and real-time monitoring of neonatal jaundice (HEALTH).

Background

The birth of a child is one of the most incredible and rewarding events to see, but it is not necessarily the greatest experience for the newborn. Among numerous types of biological stresses, physiological and, in rare cases, pathological events cause neonatal jaundice, which has a global frequency of roughly 80% and usually requires hospital readmission within the first two weeks of life. As a result, more than half of all births require readmission for jaundice therapy. These readmissions at only a few days postpartum are taxing on both the baby and the mother, and they pose several challenges to families, service providers, and governments, particularly in low- and middle-income countries (LMICs), where government facilities are frequently used with inadequate resources. In these countries, neonatal wards are often overcrowded, and the incidence of nosocomial and iatrogenic illnesses is high, putting neonates at risk of getting potentially fatal hospital-acquired diseases and, in some circumstances, resulting in preventable deaths.

We have therefore designed a wearable blue-light phototherapy baby wrap with built-in real-time monitoring of bilirubin levels for remote neonatal jaundice treatment. Our goal is to develop this portable device that will take away the need for hospitalization for the majority of neonatal jaundice cases and enable the millions of babies born each year to have the opportunity for home treatment, saving the millions of mothers the burden of returning to the hospital while recovering from labor or surgical wounds, relieving financial burdens on families, and improving service delivery in LMICs.

Project Detail

Our design incorporates phototherapy of jaundice using blue light-emitting diodes (LEDs) delivering a narrow band of light between 420 and 470 nm, with simultaneous monitoring of therapeutic response using diffuse reflectance spectroscopic (DRS) biosensing technology computed with multiple regression analysis for real-time optical measurement of bilirubin levels. Micro-sized LEDs suited for fabrication in a baby-size body wrap covering only the back and limbs will be manufactured on a thin, hypoallergenic, breathable non-conductor fabric to provide simultaneous therapy and monitoring for home usage. As a wearable device, it will provide continuous physical touch for mother-infant heat transfer and tactile-kinesthetic stimulation (TKS), both of which are critical electrophysiological phenomena required for immunological, hormonal, and other physiological benefits for both mother and baby. Furthermore, the positioning of the wrap covers a wider surface area of blood perfusion, enabling quicker response and recovery rates. The completion of this project will result in the deployment of a product at technology readiness level (TRL) 7. The findings will also be disseminated through journal publications and conference presentations to advance the use of optics and photonic technologies for remote disease management.

Impact

This innovation takes advantage of the advances in optics and photonics to reduce neonatal hospital readmission and save the lives of millions of babies who are at risk of acquiring jaundice complications, other preventable secondary disorders, and avoidable deaths. No infant deserves to be hospitalized a few days after birth, and no woman should return to the hospital so soon after giving birth for such a treatment that can be administered at home. This solution will have a far-reaching influence on LMICs, where governments strive to offer healthcare with limited resources. These countries will greatly benefit from minimizing the number of neonatal admissions, which will free up space and resources for other disorders that certainly require hospitalization. Moreover, with rising indebtedness, healthcare finance is facing serious issues in third-world countries, exacerbated by the COVID-19 economic recession. Thus, moving forward, healthcare solutions that reduce costs in these countries are not only necessary but critical. Hence, our innovation addresses significant challenges faced by babies, mothers, families, clinical staff, and governments alike, delivering both short-term and long-term benefits that will safeguard a better healthcare system for everyone.

PROPOSAL

Home-use wearable blue light therapeutic wrap with built-in diffuse reflectance spectroscopic biosensor for simultaneous treatment and real-time monitoring of neonatal jaundice (HEALTH).

1. BACKGROUND

Childbirth is one of the most fulfilling events to witness, but it is not necessarily the greatest experience for the newborn. Among the many biological stresses that newborns face, high hemoglobin levels and a shortened red blood cell (RBC) lifespan result in high amounts of bilirubin, a byproduct of hemoglobin degradation, in the blood (i.e., neonatal hyperbilirubinemia). This is aggravated by the immaturity of the liver in the early days of life, making it unable to effectively conjugate and remove the bilirubin at the rate it is produced. This results in severe neonatal hyperbilirubinemia, which appears as a yellowish discoloration of the skin and sclera, referred to as neonatal physiological jaundice. Pathological jaundice, unlike physiological jaundice, is rare and occurs when jaundice is caused by underlying pathologies such as blood group incompatibility between baby and mother, glucose-6-phosphate dehydrogenase (G6PD) deficiency, delivery complications, and other congenital disorders[1]. Whether physiological or pathological, neonatal jaundice usually necessitates hospital readmission for treatment, which is burdening for both the baby and the mother and presents numerous challenges to families, service providers, and governments, particularly in low- and middle-income countries (LMICs).

2. LITERATURE REVIEW

2.1 Global incidence and prevalence

Neonatal jaundice is the most prevalent medical condition in newborns, the most frequent reason for medical intervention, and the leading cause of hospital readmission in the first two weeks of life[2]. Essentially, premature newborns are at a higher risk of physiological jaundice; however, healthy infants have episodes of hyperbilirubinemia, which cause clinically significant jaundice requiring medical attention. While pathological jaundice is usually more acute and severe at presentation, the most common form of the disease is prolonged physiologic hyperbilirubinemia, in which bilirubin levels may continue to be elevated for weeks or even months and may reach hazardous concentrations, resulting in life-threatening conditions that may affect the functioning of vital organs such as the brain. Depending on the severity, complications may include kernicterus (bilirubin encephalopathy), abnormal audio-evoked response (aBAER), or death, if not managed well. While there is no actual variation in jaundice prevalence according to race, region, or socioeconomic status, the consequences and outcomes differ dramatically between wealthy countries and LMICs. Similarly, due to this distinction, the burdens, while important in each context, vary.

2.2 Treating Neonatal Jaundice

The increase in bilirubin levels caused by physiological stresses is usually a benign, transitory condition; therefore, most occurrences are short-lived, and bilirubin levels can return to normal with minimum intervention. However, treatment is usually recommended to prevent the severity of the disease and its complications. Severe pathologic cases necessitate treatment of the primary pathology in addition to removing the bilirubin, whereas physiological jaundice and some milder aspects of pathological cases are treated solely by clearing the bilirubin and lowering it to normal serum levels.

The most commonly utilized therapies are phototherapy and exchange transfusions. Although most hospitals follow their standards for phototherapy versus exchange transfusion, particularly in preterm infants, phototherapy is the first-line treatment for neonatal jaundice in standard practice, and it is aimed at reducing the risk of bilirubin toxicity by isomerization, which mimics liver conjugation to convert the nonpolar water-insoluble bilirubin to a water-soluble excretable isomer. Continuous bilirubin level monitoring during treatment is also standard practice to observe the response to therapy and determine when normal levels are achieved, allowing therapy to be concluded. Treatment duration often ranges from one night to many days or weeks, depending on the severity of jaundice at presentation, response rates, and other clinical factors.

2.3 Challenges faced by the baby and mother

The majority of readmissions for jaundice treatment occur within the first two weeks after birth. It is at this time that the baby requires constant mother-baby touch for heat transfer and tactile-kinesthetic stimulation (TKS), both of which are vital electrophysiological phenomena that are necessary for immunological, hormonal, and other physiological benefits for both baby and mother and psychosomatic development for the baby[3,4]. The lack of contact for several hours or days hurts the baby's development with immediate and delayed consequences. For the mother, this lack of contact also affects milk production, a consequence of which is undernutrition and feeding problems for the baby. Besides, putting the baby in a phototherapy incubator has several disadvantages, including a slow response rate and longer hospital stays, because of the detachment from the mother, which makes babies irritable and mothers anxious, thereby necessitating frequent removal of the baby from the incubator to feed and caress. Furthermore, being admitted to the hospital when mothers are still recovering from labor or surgical wounds is both physically and psychologically demanding, especially if postpartum stress disorders are present.

2.4 Economic burden to families and governments.

While challenges affecting the baby and mother are universal, those faced by families, service providers, and governments are contextual and vary for different socioeconomic regions. Hospital readmissions affect families differently based on their financial status, medical insurance coverage, and whether they use private or public hospitals. In each context, some financial strain is felt from dealing with medical bills. In LMICs, most families use public hospitals, and because most LMICs have limited resources and understaffing, this burden falls on the already struggling governments. Studies have shown that in these countries, failure to manage neonatal jaundice due to limited resources results in preventable complications and avoidable neonatal deaths[5]. A recent meta-analysis of the global prevalence of severe neonatal jaundice showed that the highest percentage of severe cases, complications, and deaths were observed in the African and South-East Asian regions[6].

To date, attempts to resolve these health system challenges involve pleas to wealthier economies for donations and loans, and this approach has a negative economic bearing on LMIC governments[7]. It is quite counterintuitive that most debt, including that taken to address health challenges, ends up negatively impacting the health systems. A recent financial study of the growing debt in LMICs in 2019, showed that 54 LMICs spent more on servicing their debt to foreign creditors than on financing their health services during the COVID pandemic[8]. Moreover, as reported in the same study, the COVID-19 economic slump worsened the financial status of these countries, further threatening to crowd out essential health spending. Hence, rethinking possible solutions for health systems in LMICs as well as curating a contextualized approach that solves the problem by reducing spending as opposed to getting more debt is not only necessary but critical.

2.5 Overcrowding and the risk of nosocomial and Iatrogenic infections.

Overcrowding is another serious challenge in LMICs. A review of infectious disease outbreaks in infants hospitalized at low-resource neonatal wards in South Africa showed that neonatal units were at high risk of nosocomial infection outbreaks owing to overcrowding, understaffing, and shared equipment, with a 7% recorded mortality rate from these infections[9]. This and other studies[10] have noted that the actual negative impact of overcrowding is under-reported in sub-Saharan Africa, and the negative impact could be more detrimental than reported*. Nosocomial infections i.e., infections acquired during the process of receiving health care that were not present during the time of admission, are frequent in overcrowded wards and common ones include skin infections, urinary tract infections (UTIs), meningitis, and sepsis, caused by bacteria, viruses, fungi, or several of these combined[11]. Moreover, limited access to phototherapy leads to the presentation of severe jaundice at admission, which, by standard practice, is treated using exchange transfusion, posing more risk of iatrogenic infections.

* Having worked in and visited different government hospitals in southern Africa, the author can affirm by experience and observation the under-representation of the impact of overcrowding in neonatal wards in these areas.

3. PROBLEM STATEMENT

Hospital readmissions due to neonatal jaundice pose a significant global health challenge. The consequences of these admissions are far-reaching, causing physical stresses and suffering for both the mother and the infant. The economic implications for families are strenuous, and the impact is particularly profound in LMICs, where government facilities are often utilized with limited resources. Overcrowding is common in these countries, with a high prevalence of nosocomial and iatrogenic infections. These readmissions, therefore, only put babies at unnecessary risk of contracting life-threatening hospital-acquired diseases. All this is largely due to the current state of phototherapy devices, which can only be administered in a hospital setting, as well as health management policies that have not yet embraced the concept of remote disease management due to its apparent impracticality. However, with innovation, phototherapy can be administered and monitored at home if home-friendly devices are available. By rethinking the delivery of phototherapy to avoid readmissions, we can make a significant impact on global health, reducing the burden of neonatal jaundice, and especially for LMICs, resolving a multitude of problems.

4. OBJECTIVES

We have therefore designed a wearable blue-light phototherapy baby wrap with built-in real-time monitoring of bilirubin levels for at-home neonatal jaundice treatment. Our goal is to develop this portable device that will take away the need for hospitalization for the majority of neonatal jaundice cases and enable the millions of babies born each year to have the opportunity to undergo treatment in the comfort of their homes, saving the millions of mothers the burden of returning to the hospital a few days after giving birth, relieving the financial burden for families, and improving service delivery in LMICs. To achieve this goal, we have set out three main objectives in the following order:

- Fabrication of the device using our preconceived design: The design consists of blue light emitting diodes (LEDs) that will deliver phototherapy, and a Diffuse Reflectance Spectroscopic (DRS) biosensing system, which will monitor the therapeutic response in real-time. Micro-sized LEDs and ultra-portable parts will be used and fabricated on a thin, fordable, and wearable non-conductor fabric housing. The DRS biosensor will be configured to take three-point measurements at hourly intervals and use a computed multi-regression analysis to capture the rate of bilirubin isomerization.

- Characterization of the device: In the second objective we will evaluate the optical properties of the device using mathematical formulas to assess power outputs, fluence rates, irradiance, reflectance/scattering coefficients, and the performance of the device *in vitro* using spectrum analysis, functional characterization, and the rate of bilirubin conjugation *ex vivo* utilizing hyperbilirubinemia in artificial mimics prepared on plastic gel phantoms.

- Proof of concept (POC) assessment: The final goal will be to evaluate the wrap's acceptability, usability, and effectiveness through a POC study with invited and consenting participants. For this purpose, ethical clearance will be sought from the institutional review board and access will be granted by hospital management at Charlotte Maxeke Academic Hospital in Johannesburg. Both parents will be required to provide consent for their and their babies' participation.

5. OUTCOMES

Completing these three objectives will result in the deployment of a product at technology readiness level (TRL) 7 at the end of the project. In objective one, the major outcome is a fully produced wrap that is ready to use. The principal outcome of objective two is a record of its performance through the use of calculations and analyzers. The final goal will verify its practical functionality, usability, and acceptability. This wearable infant wrap with therapeutic blue LEDs and a DRS monitoring system suited for home-use will be the first of its kind on the medical device market, as well as the first to recommend remote jaundice treatment in LMICs.

As a TRL 7 product, this outcome lays the groundwork for the next endeavor, which is potential commercialization. TRL 7 goods are commercialization-ready according to the TRL standard utilized globally, and our prospective aim is to use these findings for two major functions. First, we will use the report to acquire funds for commercial production of the wrap, allowing the product to reach the market faster, while we perform follow-up research to complete TRLs 8 and 9. Second, we will utilize our research to engage governments, particularly in LMICs, beginning with Southern Africa, to consider including remote phototherapy in their healthcare management policies.

Finally, the outcome of this research will yield a scientific paper, planned for submission to Biomedical Optics Express, an Optica Publishing Group journal. This paper will discuss the entire process from conceptualization, fabrication, and POC testing to contribute knowledge regarding the role and benefits of concurrent treatment and monitoring of the therapeutic response for remote management of neonatal jaundice. The findings will also be presented at various conferences, including the annual conference of the South African Institute of Physics (SAIP), and Frontiers in Optics + Laser Science (FiO LS). A conference proceeding will also be issued for FiO LS, summarizing the technology used in this device.

6. IMPACT

6.1. Increasing the availability and usability of phototherapy for neonatal Jaundice

With this home-friendly phototherapy wrap, we are increasing both the availability and usability of phototherapy. Not only will the device be more accessible, but it will also be more effective in treating jaundice due to the use of focused LEDs, which deliver a narrow band of blue light at a calculated therapeutic dose. Moreover, allowing home therapies is more convenient for both the infant and the mother and will enable treatment in the comfort of home, allowing the baby to cope swiftly while providing the mother with enough time, space, and privacy to deal with post-partum wounds and stress. Its design as a wearable wrap will enable mother-infant interaction during therapy to avoid the baby's developmental problems while also reducing the parents' anxiety.

Its positioning on the back and limbs covers a wider surface area of blood perfusion, enabling quicker response and recovery rates, and also prevents light exposure to the baby's eyes as opposed to the use of a clinical incubator, where eye damage is most likely to occur when the eye mask is not correctly covering the eyes. Making phototherapy more available and effective in this way has the potential to largely replace exchange transfusions in LMICs, lowering the risk of iatrogenic infections from unsafe transfusions. Nosocomial infections are also prevented if therapy is delivered at home. This increased availability of phototherapy will therefore resolve several challenges that currently do not have a solution.

6.3 Advancing photonic biosensors for monitoring and assessing therapy responses.

The DRS biosensing technology in this device will monitor and assess the therapeutic response in real-time with continuous updates of the rate of jaundice clearing. This feature will enable the ease of use of the device, with simple instructions for parents to read progress without the need for a healthcare provider. Parents will be able to track progress, and where the jaundice is not clearing at an acceptable rate or if, for some reason, it increases, a beeping prompt will be triggered to catch the attention of parents, who will then seek medical guidance via phone from the attending nurse on call. Furthermore, this non-invasive transcutaneous biosensing technology eliminates the need for blood tests, making monitoring safer and more convenient. To date, many biosensing technologies have been studied; however, the DRS technology made possible by miniature, ultra-portable spectrometers is more suitable for fabrication in this design, besides its sensitivity and accuracy. Our innovation therefore will promote the use of miniature, ultra-portable biosensing technology, which, beyond its applications in monitoring bilirubin response to phototherapy, will be pertinent to more applications in the field.

6.4 Increasing healthcare affordability in 3rd world countries.

One of the most significant impacts of home therapy will be its role in increasing the affordability of jaundice treatments for both individuals who use private services and governments that provide healthcare. By removing the need for admission, families will be relieved of the financial burden, clinical staff will be alleviated of workload, and where governments provide resources, as is the case in LMICs, fewer budgets will be required for neonatal health. In these countries, especially at a time when healthcare budgets are affected by increasing international debt, home therapy will enable the redirecting of resources and space (i.e., neonatal wards) to babies with more in-hospital-requiring illnesses. For the first time, this solution will trigger healthcare providers and governments alike to start considering remote therapies for qualifying ailments. Hence, beyond saving the lives of millions of children, the saved resources and the mindset change will offer a lasting financial solution for healthcare systems in third-world countries. Long-term, this mindset change will potentially have an impact on healthcare policy, providing a means for health financial planning that entails decreasing expenditures to avoid excessive debt in LMICs.

6.5 Advancing optics and photonics-based healthcare solutions

Many cutting-edge solutions in healthcare exist in the subject of physics, but because medicine and healthcare are traditionally biochemical and pharmaceutical, most scientists choose to look for healthcare solutions in these traditional sciences. Despite several discoveries about critical electrophysiological processes and the significance of photobiology in human physiology, traditional medical sciences remain mostly biochemical. Our solution, which employs optics and photonics principles, contributes to the small pool of biophysics healthcare investigations and widens the door for more scientists to pursue greater solutions in the field of biophysics, particularly since optical solutions and photonics provide the majority of the needed healthcare solutions. Our product and the rationale behind it will be shared with the broader scientific community, engaging like-minded scientists to ask even better questions and find solutions using optics and photonics.

7. SUMMARY

Home therapies, where applicable, are an indispensable solution to resolving a multitude of challenges. Our new device leverages innovations in optics and photonics to save the lives of millions of newborns at risk of developing complications of jaundice, other preventable secondary diseases, and avoidable deaths. Most especially, LMICs will benefit immensely from reducing the number of neonatal hospitalizations to free up space and resources for other diseases that certainly require hospitalization. All this will be made possible by this quest to fabricate a wearable blue-light phototherapy baby wrap with built-in real-time monitoring of bilirubin levels for at-home neonatal jaundice treatment. This solution addresses critical challenges faced by babies, mothers, families, clinical staff, and governments alike. Moreover, this innovative baby wrap has the potential to drastically improve our approach to jaundice management and will influence policy around remote therapies to improve health systems in LMIC and people's lives elsewhere. Hence, this innovation will deliver both short-term and long-term benefits that will safeguard a better healthcare system for everyone.

8. REFERENCES

1. Singh SK, et al. *Clin Epidemiol Glob Health* 2016;4(2):95-100. doi:10.1016/j.cegh.2016.03.006
2. Hansen TWR. *Pediatr Med*. 2021;4:18-18. doi:10.21037/pm-21-4
3. Purificação MMD. *Eyes on Health Sciences V.02*. 1st ed. 2024. doi:10.56238/sevened2024.001-025
4. Abedi F, et al. *Bodyw. Mov. Ther.* 2018;22(2):308-312. doi:10.1016/j.jbmt.2017.08.005
5. Bhutani VK, et al. *Pediatr Res*. 2013;74(S1):86-100. doi:10.1038/pr.2013.208
6. Diala UM, et al. *JCM*. 2023;12(11):3738. doi:10.3390/jcm12113738
7. Law SH, et al. *Econ Model*. 2021;98:26-40. doi:10.1016/j.econmod.2021.02.004
8. Federspiel F, et al. *Glob Health Action*. 2022;15(1):2072461. doi:10.1080/16549716.2022.2072461
9. Dramowski A, et al. *Int J Infect Dis*. 2017;57:79-85. doi:10.1016/j.ijid.2017.01.026
10. Rothe C, et al. *J Hosp Infect.* 2013;85(4):257-267. doi:10.1016/j.jhin.2013.09.008
11. Wang L, et al.*Med Sci Monit*. 2019;25:8213-8220. doi:10.12659/MSM.917185

Improving the health safety in drug and agrochemical development with optofluidic chiral molecule separation (CHIMOS)

Life's biochemical intricacies involve molecules exhibiting chirality, possessing left- and right-handed forms, with distinct biological activities concerning toxicology, metabolism, and pharmacology. Concerns over health and environmental impacts arise due to the asymmetric behaviours of chiral molecules, prominent in pharmaceuticals and agrochemicals. Developing robust analytical techniques capable of discriminating stereoisomers is crucial for safer industrial practices for human health and environmental protection.
Existing sensing technologies struggle to distinguish stereoisomers effectively, lacking versatility and widespread applicability. CHIMOS aims to address these challenges by devising an approach capable of identifying chiral compounds through separation and detection of stereoisomers in a single workflow and device.

The project focuses on employing chiral light combined with heat engineering to generate achiral and chiral-specific axial and lateral forces, enhancing the interaction strength between optothermal fields and chiral molecules. By leveraging advancements in spatial light modulation and microfluidic architecture, CHIMOS aims to optimize protocols for precise collection, sorting, and detection within a compact chip design. Furthermore, the integration of well-established instruments and technologies will facilitate a rapid translation and adoption of the platform in industrial sectors such as pharmaceuticals where workflow compliance is crucial.

A key innovation of the CHIMOS approach lies in its synergistic combination of various concepts and methods. By integrating structured light to control fluid motion and enhance electromagnetic fields coupling with molecules through plasmonic nanostructures, the platform offers unparalleled control and precision in chiral molecule analysis. Validation efforts will involve rigorous testing of the platform's capabilities using state-of-the-art force spectroscopy techniques and advanced fluid dynamics imaging, such as circular dichroism spectroscopy, digital holographic microscopy, and optical diffraction tomography.

Ultimately, CHIMOS aspires to not only address the existing challenges in chiral molecule analysis but also to catalyze a paradigm shift in this field. By providing a versatile, cost-effective, and user-friendly solution applicable across a wide range of compounds, the platform holds immense potential to transform industries reliant on precise molecular recognition. Through innovation and collaboration, CHIMOS aims to empower researchers and practitioners to unlock new frontiers in chiral chemistry, ultimately improving the health safety and environmental impact through the usage of more effective chiral molecules.

Improving the health safety in drug and agrochemical development with optofluidic chiral molecule separation (CHIMOS)

1. Literature Review

Life exhibits chirality: essential biological components like nucleotides and amino acids exist in both left- and right-handed forms. Stereoisomers, molecules with chiral centers, share identical chemical structures but often display distinct biological activities including toxicology, metabolism, and pharmacology. These asymmetric biochemical behaviours raise significant concerns regarding the use of chiral molecules due to potential health and environmental impacts [1]. Pharmaceuticals and agrochemicals are major sectors employing such molecules, with numerous chiral chemicals involved in intermediate industrial processes such as discovery, production, use, disposal, recycle, among others. The growing demand for safer, eco-friendly industrial practices necessitates robust analytical techniques capable of discriminating and quantifying stereoisomers. Various methods leverage the asymmetric properties of chiral molecules, including their interaction with light (chiroptical effects [2-4]), chemical reactivity (asymmetric catalysis, redox reactions [5]), and movement in solid/liquid mediums (chromatography [6]), among others. Chromatography, for instance, has shown the possibility of manipulating enantiomers in liquid environments, by focusing them inside a microfluidic channel in the presence of a global thermal and electric gradients [7]. By introducing chiral selectors into a buffer solution with temperature-dependent ionic strength, chiral separation becomes achievable.

More recently, the field of optofluidics proved that a high-degree of control over the motion of particles and the surrounding fluid can be simultaneously achieved by combining the powerful capabilities of optics with microfluidics [8]. While optics, in particular nanophotonics, enables the precise control over small objects including molecules, microfluidics provides the capabilities to manipulate fluid flows at large scale [9,10]. Such light-based approaches often involve nanofabricated plasmonic structures such as nano-apertures that squeeze the light beyond the diffraction-limit thereby inducing optical forces relevant for the trapping of single molecules and proteins [11,12]. By selecting optimal designs for advanced optical materials, chiral light fields can be generated enabling the manipulation of chiral objects, including particles and molecules [13-15]. Light-induced plasmon resonances also induce significant heating in the surrounding fluid, creating opto-thermal fields that have been exploited for the manipulation of single molecules via thermophoretic and thermo-osmotic fluid flows [16,17]. However, the application of local optically-induced thermal gradients on chiral particles has not been experimentally demonstrated yet, although simulations have shown significant effects on the thermophoresis of asymmetric particles such as rods and micro-turbines [18-20].

2. Problem Statement/Objective

Existing sensing technologies struggle to effectively distinguish stereoisomers without resorting to time-consuming and expensive methods tailored to the specific analyte. Moreover, many established techniques mandate labeling the analyte or utilizing other chiral mediums/selectors tailored to the analyte under investigation. However, employing specific chiral agents compromises the development of user-friendly methods applicable to a broad range of chiral molecules. Put simply, current methodologies lack versatility and widespread applicability. The discrimination, recognition, and quantification of chiral molecules remain significant challenges. **CHIMOS aims to address these challenges by devising an approach capable of identifying chiral compounds through the separation and detection of stereoisomers in a single workflow and device.** Building upon research into the interaction between chiral optothermal light fields and chiral molecules, our objective is to progress towards the development of a functional system with TRL 4. Our method will operate in liquid mixtures without the need for labelling or specific chiral agents, making it suitable for diverse compounds across the market. We foresee that our device will possess the capability to detection nM concentrations coupled with a discrimination efficiency up to 10^5. This implies that it can detect one isomer when its concentration is 100,000 times lower than the other, starting from standard market compounds (mM concentrations).

Key elements of this project are:

- Employ chiral light combined with heat engineering to generate large optical and thermophoretic forces overcoming Brownian motion in liquid samples. These forces will push chiral molecules towards opposite directions thus enabling their sorting and separation
- Develop a comprehensive microfluidic architecture and optimised protocols for spatial light modulation for collection, sorting and detection within a single chip design.
- Exploitation of market-ready instruments and technologies to foster rapid translation and the development of new instrumentations to fully exploit the innovations introduced.

Goal: The development of an advanced optofluidic platform utilizing optical forces and thermal effects, to efficiently separate and extract chiral molecules.

The platform will be based on a combination of plasmonic and dielectric nanostructured materials whose optical and thermal properties can be locally addressed via spatial light modulation of a focused laser beam. By taking profit of these tailored states, we will engineer an approach to produce both achiral axial optothermal forces and chiral specific axial and lateral forces (see Fig. 1). While achiral axis forces are used to drive all molecules towards the interface where optothermal fields are strongest, only chiral specific axial and lateral forces allow for controlled separation based on chirality. The main focus lies on the generation of such axial forces to selectively deliver stereoisomers into two different microfluidic channels from where they can be extracted in bulk.

Measurable Objective: The generation of optical and thermal forces which are of opposite directions for distinct stereoisomers in the order of at least 1 pN for molecules <10 kDa. For the duration of this project, we aim at reaching a separation efficiency of 10^3 (starting from equal concentrations, 1:1).

The innovation of our approach lies in a synergetic exploitation of various concept and methods. Specifically, it leverages structured light to generate precise thermal landscapes for fluid motion control and to enhance the coupling of the electromagnetic field with molecules, particularly by integrating Orbital Angular Momentum (OAM).

To achieve this goal, we utilize a combination of chiroptical light fields and thermal gradients, facilitating broad manipulation across the entire length scale of the optofluidic device (~1mm). Initially, we assess the separation efficiency of enantiomers using diverse sizes and compositions of chiral nanoparticles before progressing to molecules of commercial interest. Employing high laser fluence (100 mW/μm^2) generates significant heating at the plasmonic interface, which can be harnessed to further control fluid and molecule motion. Precise modulation of local temperature changes, facilitated by efficient light-to-heat conversion via plasmonic materials, results in microfluidic flows whose shape, direction, and velocity are meticulously controlled by adjusting the optical properties of the light beam. Optical Diffraction Tomography (ODT) [22] and Digital Holographic Microscopy (DHM) [10] provide detailed oversight of optically induced fluid changes. We will measure the separation efficiency of enantiomers using dielectric nanostructures that locally amplify their circular dichroism (CD) signal (by about 100x as previously demonstrated in our group [21]). This enables the differentiation of various molecular counterparts by measuring the differential absorption of left and right circularly polarized light. To validate the effectiveness of the proposed platform, we fabricate and extensively test the optofluidic platform using force spectroscopy techniques and 3D fluid dynamics imaging capabilities.

3. Outline of tasks

To reach the final goal, we propose a synergic approach working in 3 steps, i.e. sorting, separation, and detection.

1. Molecular sorting by optical and thermal forces enhanced by structured light and temperature engineering.
2. Separation by optofluidic protocols into different compartments of the chip.
3. Detection of CD signals from enantiomers enhanced by chiral light and dielectric nanostructures.

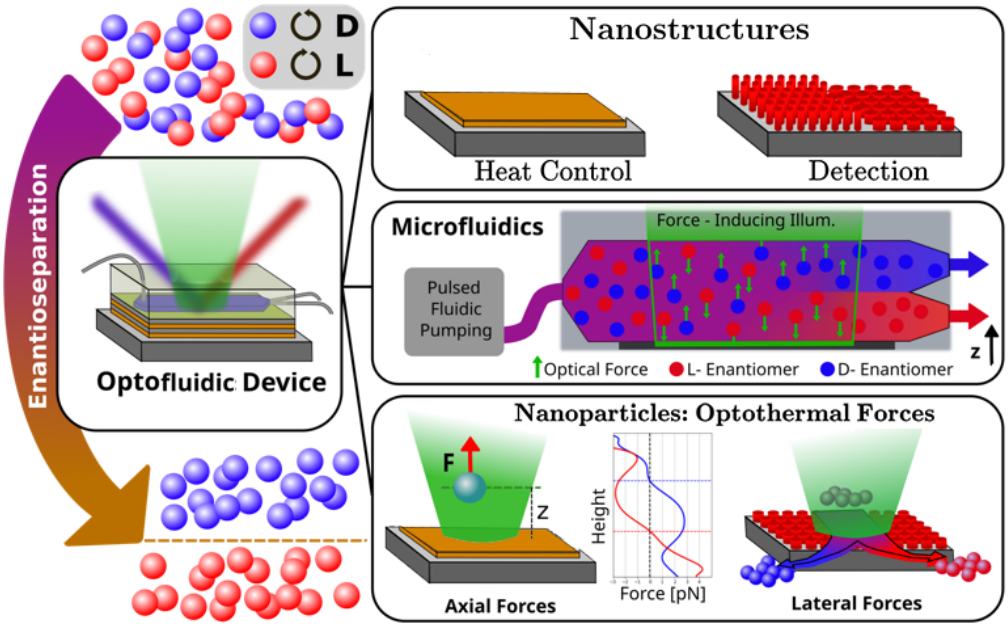

Figure 1: Optofluidic separation of enantiomers. The platform will consist of an optothermal forces generating plasmonic nanostructure in an optofluidic chip. **Top** The nanostructures will consist of plasmonic surfaces for heat control (left) and nanopillars of different sizes for detection of CD signals. **Middle** The microfluidic device will flow a racemic mixture over the nanostructure, utilizing optical forces and light-induced thermal gradients to separate enantiomers, which are extracted from different outflow ports. The efficiency of the separation method will be tested by analyzing CD spectroscopy data. **Bottom** The combined axial and lateral optothermal forces are used for achiral trapping, and chiral enantiomer separation.

Sorting and separation are achieved by combining capturing forces and sorting forces, indicated in Fig.1 as axial and lateral forces, respectively. Capturing forces arise from optothermal forces driven by strong optical and thermal gradients, leading to fluid flows that have a capture range in the order of tens of µm (indicated in blue, on the right side). These forces are the same for both enantiomers and are used to collect molecules and enrich their concentration to relevant numbers followed by sorting. By playing with the chirality of light generating asymmetric optical and thermal effects, we can selectively choose which enantiomer has to be captured and delivered to the collection chamber. Notably, selective separation will facilitate the discrimination of the enantiomers (left vs. right) thus increasing sensitivity of the method. Here, the type and quantity of sorted molecules will be identified subsequently using circular dichroism which is significantly enhanced in the presence of dielectric nanostructures [21].
The project will greatly benefit from the recently initiated collaboration with the Nanoplasm group of Prof. Giuseppe Strangi at Case Western Reserve University, who will support us with their expertise on designing chiral light fields structures through advanced optical materials [14].

The work is split into 3 work packages (defined as aims below) focusing on each subtask, i.e. sorting, separation, and detection, before combining them into a single workflow optofluidic device.

3.1 Timeline Description

For a detailed description of the individual aims, timeline, and associated deliverables and milestones, please refer to the Optica Foundation Challenge Timeline Template attached to the proposal.

3.2 Risk Mitigation

Risks (Likelihood, Impact)	WP	Risk Mitigation Strategy
Concentration of molecules near surface is low (Medium, Medium).	1	Use stronger chiral light fields in the presence of hyperbolic metamaterials produced by our collaborator [13].
Convection-based transport can not efficiently deliver sorted particles to detection chamber (Medium, Low).	1	Use conventional microfluidic pumping instead.

Risks (Likelihood, Impact)	WP	Risk Mitigation Strategy
The CD signal in the presence of dielectric nanopillars is not strong enough for the detection of enantiomers (Medium, High).	1	Use commercially available CD spectrometers to test signal strength. Then, improve previous nanopillars design [21] to increase signal.
Nanostructures for detection interfere with the manipulation of chiral molecules (Medium, Low).	2	Extract particles through additional microfluidic outlets.
Not all functionalities can be incorporate on chip due to interference between tasks (Low, Medium).	3	Employ commercial alternatives (such as solutions by on-campus startup ENANTIOS, ETH) and enable plugin of chip within a single device.

4. Outcomes

All the identified market needs necessitate novel technological advancements to enhance chiral sensing capabilities. Given the intricate and varied nature of chiral compounds across different sectors, devising a single universal approach poses significant challenges. For instance, the quality control protocols in industrial chemical plants for agrochemicals vary substantially from those in pharmaceutical drug discovery departments. **With the aim of introducing a market-ready optofluidic method with broad applicability, we outline the following key target requirements:**

- The ability to handle a wide range of enantiomers without relying on chiral mediators for analyte recognition or capture (label-free).
- Compatibility with small sample volumes in the range of 10 µL - 1 mL.
- A dynamic detection range for chiral molecule concentrations between 10 mM to 10 pM.
- Capability to separate and differentiate stereoisomers when their composition is at 10 parts per million (ppm), in compliance with legal standards, i.e., detecting the presence of one isomer with a concentration 10^5 times lower than the other isomer.

Crucially, our focus is on developing a functional optofluidic device, where the associated methodologies for material fabrication are commercially available and scalable. This includes considerations for technology development that align with existing industrial protocols. Additionally, we anticipate gaining fundamental insights into the optothermal manipulation of chiral molecules, which will be considered for publication in scientific journals.

5. Impact

The global market size for chiral chemicals reached $78.6 billion in 2023 (source: www.factmr.com and www.imarcgroup.com). With a compound annual growth rate (CAGR) exceeding 12%, it is projected to surpass $220 billion by 2033. This growth is fueled by strong demand from the pharmaceutical and agrochemical sectors, which are the primary drivers of this market. The pharmaceutical industry's need for chiral chemicals is particularly significant, both for new drug development and the synthesis and discovery of chiral compounds. Notably, **56% of currently used drugs are chiral molecules, with 88% of the recent drugs marketed as racemic mixtures,** comprising equimolar proportions of two stereoisomers. Despite identical chemical structures, most isomers of chiral drugs demonstrate notable differences in biological activities such as pharmacology, toxicology, pharmacokinetics, and metabolism. An illustrative instance of a chiral drug is dopa, or dihydroxy-3,4 phenylalanine, a precursor of dopamine utilized in treating Parkinson's disease. Initially administered in racemic form (d,l-dopa), its d-isomer was found to cause severe toxicity (agranulocytosis). Consequently, only the levorotary form, known as L-Dopa, is used in therapeutics. Hence, promoting chiral separation and analysis of racemic drugs in the pharmaceutical industry and clinical settings is crucial for eliminating unwanted isomers, thereby enhancing treatment efficacy and therapeutic control for patients.

Regulatory bodies like the U.S. FDA and the European EMA prioritize drug safety and efficacy, placing pharmaceutical companies under growing pressure to develop drugs with precise stereochemistry. Chiral chemicals are instrumental in meeting these stringent regulatory standards, facilitating the synthesis of chiral drugs with consistent stereochemistry. This approach minimizes the

risk of unexpected side effects and ensures patient safety. **Compliance with these regulations is imperative for pharmaceutical firms, making the utilization of chiral chemicals indispensable.**

An alternative approach involves synthesizing only the desired enantiomer while sidestepping the production of its counterpart, a process known as asymmetric synthesis. This method constitutes 40% of the current market value (30 billion/year in 2023, projected to exceed 80 billion by 2033). However, it is exceptionally intricate and inevitably necessitates the use of pure enantiomeric compounds as reactants, failing to resolve the reliance on chiral chemicals for synthesis. Consequently, the majority of chiral chemicals exist as racemic mixtures, constituting half of the market value associated with separation methods (40 billion/year in 2023, anticipated to exceed 100 billion by 2033), with liquid chromatographic techniques being the most prevalent. Regardless of the application field or market (separation, synthesis, development, and use), **the ability to quantify absolute or relative chiral concentrations is pivotal.**

The absence of effective technologies not only impacts the market but also raises significant environmental concerns. The production and utilization of chiral chemicals release highly volatile compounds into the environment, posing risks to human health and various organisms. Environmental regulations impose strict limits on the release of production waste, with a **maximum allowable content of volatile compounds set at 90 parts per million (ppm)**, further constraining the growth of the chiral chemicals market.

Similarly, in the **agrochemical sector,** chiral pesticides and herbicides are extensively utilised for their enhanced efficacy and reduced environmental impact. Farmers are increasingly adopting chiral agrochemicals to safeguard crops, enhance yields, and minimize ecological harm. Chiral chemicals offer a pathway to develop more precise and efficient agricultural products, enabling the creation of compounds that selectively target pests or weeds while preserving beneficial organisms. As global agriculture endeavors to achieve greater sustainability and efficiency, the demand for chiral chemicals in this sector is anticipated to steadily increase. **Europe and North America lead in both chiral chemicals production and consumption, owing to their well-established pharmaceutical and agrochemical industries.** Prominent European companies include BASF (Germany), Solvias AG (Germany), and Johnson Matthey (UK). However, Asia-Pacific countries are emerging as significant contenders, propelled by economic growth and expanding healthcare sectors.

Given the current market landscape, significant advancements are expected in the near future, driven by escalating consumer demands and regulatory requirements. **Quality control procedures across various industrial domains, such as food and drug production and waste analysis in industrial facilities, alongside challenges posed by chiral pollution, remain unresolved.** Presently, there are over 1500 known chiral pollutants, including pesticides, polychlorinated biphenyls, polyaromatic hydrocarbons, brominated flame retardants, phenols, personal care products, and pharmaceuticals. More than a thousand additional products are slated for commercialization in the next decade, potentially exposing people and the environment to these compounds. **The current landscape, coupled with existing market needs, necessitates effective methods for detecting and quantifying chiral compounds. Without these essential tools, legislators cannot adequately establish regulatory frameworks across all industrial sectors.** Consequently, unchecked market expansion for chiral compounds may pose significant risks to both the environment and public health.

References

[1] Caldwell, J., 1996. Importance of stereospecific bionalytical monitoring in drug development. *Journal of chromatography A*, *719*(1), pp.3-13.

[2] Solomon, M.L., Saleh, A.A., Poulikakos, L.V., Abendroth, J.M., Tadesse, L.F. and Dionne, J.A., 2020. Nanophotonic platforms for chiral sensing and separation. *Accounts of chemical research*, *53*(3), pp.588-598.

[3] Forbes, K.A. and Andrews, D.L., 2018. Optical orbital angular momentum: twisted light and chirality. *Optics letters*, *43*(3), pp.435-438.

[4] Bégin, J.L., Jain, A., Parks, A., Hufnagel, F., Corkum, P., Karimi, E., Brabec, T. and Bhardwaj, R., 2023. Nonlinear helical dichroism in chiral and achiral molecules. *Nature Photonics*, *17*(1), pp.82-88.

[5] Ward, T.J. and Ward, K.D., 2012. Chiral separations: a review of current topics and trends. *Analytical Chemistry*, *84*(2), pp.626-635.

[6] Stalcup, A.M., 2010. Chiral separations. *Annual Review of Analytical Chemistry*, *3*, pp.341-363.

[7] Balss, K.M., Vreeland, W.N., Phinney, K.W. and Ross, D., 2004. Simultaneous concentration and separation of enantiomers with chiral temperature gradient focusing. *Analytical chemistry*, *76*(24), pp.7243-7249.

[8] Fan, X. and White, I.M., 2011. Optofluidic microsystems for chemical and biological analysis. *Nature photonics*, *5*(10), pp.591-597.

[9] Yang, S., Hong, C., Zhu, G., Anyika, T.H., Hong, I. and Ndukaife, J.C., 2024. Recent Advances in Nanophotonics for Optofluidics. *arXiv preprint arXiv:2404.04685*.

[10] Ciraulo, B., Garcia-Guirado, J., de Miguel, I., Ortega Arroyo, J. and Quidant, R., 2021. Long-range optofluidic control with plasmon heating. *Nature Communications*, *12*(1), p.2001.

[11] Ndukaife, J.C., Kildishev, A.V., Nnanna, A.G.A., Shalaev, V.M., Wereley, S.T. and Boltasseva, A., 2016. Long-range and rapid transport of individual nano-objects by a hybrid electrothermoplasmonic nanotweezer. *Nature nanotechnology*, *11*(1), pp.53-59.

[12] Sanders, R., Liu, Y. and Zheng, Y., 2022. Towards Single-Molecule Chiral Sensing and Separation. In *Single Molecule Sensing Beyond Fluorescence* (pp. 271-293). Cham: Springer International Publishing.

[13] Sreekanth, K.V., Alapan, Y., ElKabbash, M., Ilker, E., Hinczewski, M., Gurkan, U.A., De Luca, A. and Strangi, G., 2016. Extreme sensitivity biosensing platform based on hyperbolic metamaterials. *Nature materials*, *15*(6), pp.621-627.

[14] Lininger, A., Palermo, G., Guglielmelli, A., Nicoletta, G., Goel, M., Hinczewski, M. and Strangi, G., 2023. Chirality in light–matter interaction. *Advanced Materials*, *35*(34), p.2107325.

[15] Tkachenko, G. and Brasselet, E., 2014. Optofluidic sorting of material chirality by chiral light. *Nature communications*, *5*(1), p.3577.

[16] Duhr, S. and Braun, D., 2006. Optothermal molecule trapping by opposing fluid flow with thermophoretic drift. *Physical review letters*, *97*(3), p.038103.

[17] Fränzl, M. and Cichos, F., 2022. Hydrodynamic manipulation of nano-objects by optically induced thermo-osmotic flows. *Nature communications*, *13*(1), p.656.

[18] Gardin, A. and Ferrarini, A., 2019. Thermo-orientation in fluids of arbitrarily shaped particles. *Physical Chemistry Chemical Physics*, *21*(1), pp.104-113.

[19] Yang, M., Liu, R., Ripoll, M. and Chen, K., 2014. A microscale thermophoretic turbine driven by external diffusive heat flux. *Nanoscale*, *6*(22), pp.13550-13554.

[20] Tan, Z., Yang, M. and Ripoll, M., 2017. Anisotropic thermophoresis. *Soft matter*, *13*(40), pp.7283-7291.

[21] Garcia-Guirado, J., Svedendahl, M., Puigdollers, J. and Quidant, R., 2019. Enhanced chiral sensing with dielectric nanoresonators. *Nano letters*, *20*(1), pp.585-591.

[22] Vasista, A.B., Ciraulo, B., Schmidt, F., Arroyo, J.O. and Quidant, R., 2024. Non–steady state thermometry with optical diffraction tomography. *Science Advances*, *10*(12), p.eadk5440.

Executive Summary

An Open Source Digital Twin for Intelligent Multi-band and Multi-Core Flexible Optical Networks

Optica Foundation Challenge Category: ***Information***

Farhad Arpanaei, University Carlos III de Madrid (UC3M), 28911 Leganes, Madrid, Spain

Email: farhad.arpanaei@uc3m.es

Introduction: The project addresses the evolving landscape of telecommunications, where traditional optical networks struggle to meet increasing demands for high-speed data transmission. Multi-band and multi-core technologies offer solutions, but their complexity requires advanced real-time planning tools. A digital twin as a service (DTaaS), replicating the network virtually, provides a platform for testing new architectures and protocols. Leveraging machine learning (ML) in the intelligent optical network, the DTaaS enables predictive analytics and autonomous optimization. Open-source principles empower collaboration, reducing costs and accelerating technology deployment. Additionally, proactive energy management strategies, optimize network configurations, reducing energy consumption and operational costs.

Objective: The project has three main objectives: (i) Develop a comprehensive DTaaS framework for multi-band and multi-core intelligent flexible optical networks, enabling testing and validation of new network architectures and protocols. (ii) Facilitate collaborative research and innovation through open-source principles, fostering a vibrant community and accelerating technology development. (iii) Optimize network performance and reduce operational costs through proactive energy management strategies, leveraging ML algorithms for predictive analytics and autonomous optimization, contributing to the sustainability of telecommunications infrastructure.

Plan: The 24-month project integrates optical network planning, ML, and physical layer modeling, culminating in proof of concept validation. Collaboration between UC3M, Telefonica in Madrid, University of Bristol (UOB) in Bristol, UK, Chalmers University of Technology in Sweden, and University of Virginia in USA drives the project forward. The plan entails developing synthesized and experimental datasets, planning tools, and ML algorithms by collaborating with Chalmers University of Technology and University of Virginia. Subsequently, validation will occur at Telefonica and University of Bristol, based on the Lab and real-word research networks. The primary focus of the first year is on simulation and emulation development, while the second year aims to integrate the developed DTaaS with real-world test beds and field trial at Telefonica and UOB. The project's goals include producing six high-impact journal papers such as Optica, Optics Express, Journal of Communication and Optical Networking, and Journal of Lightwave, and eight conference papers.

Impact: (i) The project greatly enhances the development and optimization of telecommunications infrastructure, resulting in more efficient and reliable optical networks. (ii) Embracing open-source principles encourages collaboration, speeding up innovation, and cutting costs. (iii) Proactive energy management, powered by ML machine learning algorithms, reduces energy consumption and operational costs, promoting the sustainability of telecommunications infrastructure and minimizing the environmental impact of optical networks.

OPTICA FOUNDATION CHALLENGE 2024

Category: Information

PROPOSAL

An Open Source Digital Twin for Intelligent Multi-band and Multi-Core Flexible Optical Networks [TWINCORE]

Name of the Principal Investigator (PI): Farhad Arpanaei (Ph.D.), University Carlos III de Madrid

1 Literature Review

The development of optical networks has become imperative due to the exponential growth of IT technologies and the escalating need to handle vast amounts of IP traffic [1]. As digital transformation accelerates across industries, the demand for high-speed, reliable, and scalable communication infrastructure intensifies [2]. Optical networks, leveraging the power of fiber optics, offer unmatched bandwidth capabilities, essential for supporting data-heavy applications such as cloud computing, video conferencing, and the Internet of Things [3]. These networks ensure low latency and high throughput, meeting the critical requirements of modern applications that rely on real-time data processing and seamless connectivity [4]. Consequently, investing in advanced optical networking technology is crucial to sustain the burgeoning digital ecosystem and maintain competitive advantage in a data-driven world [5].

Expanding the bandwidth in optical networks by utilizing multiband approaches beyond the traditional C-band (including S, E, O, and U-bands) is a cost-effective strategy [6]. This method maximizes the use of existing fiber optic infrastructure, thereby reducing the need for new fiber installations and significantly lowering capital expenditures [7]. Technological advancements, such as improved optical amplification and Dense Wavelength Division Multiplexing (DWDM), have made it feasible to use these additional bands effectively [8]. These innovations allow for greater bandwidth without substantial additional costs. Moreover, this approach provides a scalable solution for future network growth, ensuring that the network can meet increasing data demands without frequent and costly upgrades [9]. By distributing traffic across multiple bands, networks can also enhance service quality, reduce congestion, and improve signal reliability, making this a future-proof strategy that offers both immediate and long-term benefits [10].

Multi-core fibers offer a multitude of advantages, particularly in the context of multiband optical networks [11]. By integrating multiple cores within a single fiber, these innovative solutions significantly enhance data transmission capacity and efficiency [12]. With the exponential growth of data traffic, especially in the era of cloud computing, IoT, and 5G, traditional single-core fibers are becoming increasingly limited in their ability to meet the escalating demands for bandwidth. Multi-core fibers mitigate this challenge by enabling parallel data transmission through distinct cores, effectively multiplying the fiber's data-carrying capacity [13]. This not only boosts network performance but also enhances scalability and flexibility, crucial for accommodating future technological advancements and evolving user needs. Thus, for operators seeking to optimize network capabilities and stay ahead in the rapidly evolving telecommunications landscape, transitioning to multi-core fibers is not just advantageous but imperative.

The digital twin (DT) paradigm, as outlined in [14], heralds a transformative approach to engineering and maintenance strategies. Digital twin technology has gained significant attention in various domains, including optical networks, due to its potential to revolutionize network management, optimization, and performance monitoring [15, 16]. In the context of optical networks, a DT is a virtual replica of the physical network infrastructure, continuously updated with real-time data to mirror its behavior and enable advanced analytics, simulations, and predictive maintenance [17]. DT offers a wide range of applications in optical networks, including network design, planning, provisioning, optimization, fault detection, and performance monitoring [18]. By integrating real-time data from network elements such

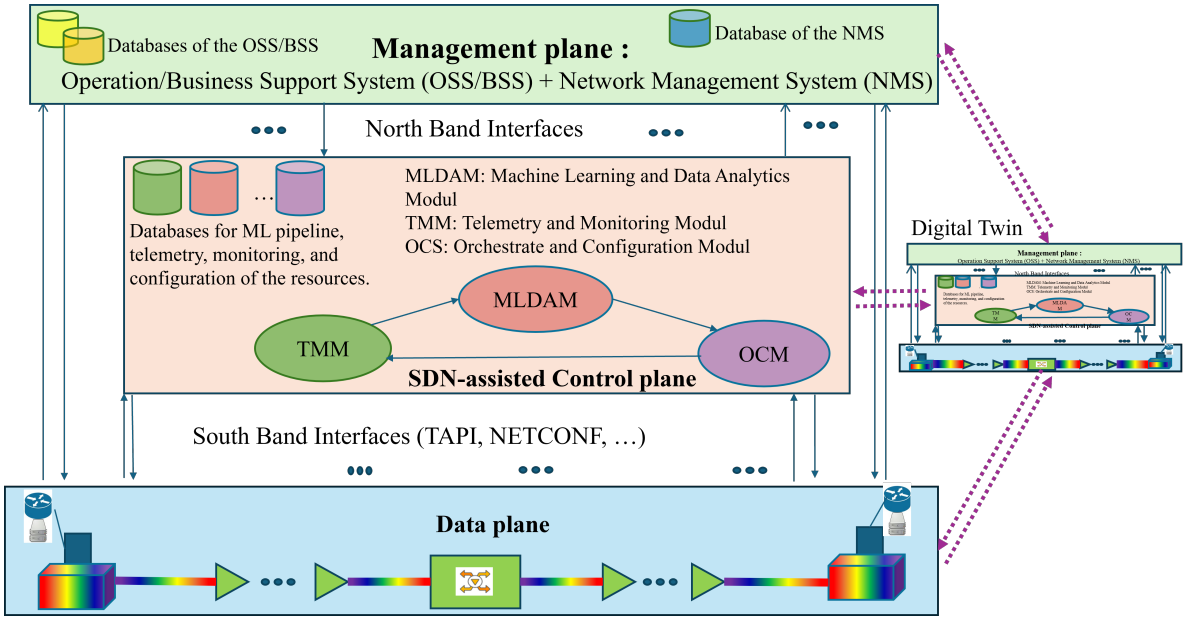

Figure 1: Physical and digital twins of an intelligent optical network's plane.

as optical switches, transceivers, and fiber links, digital twins provide network operators with a holistic view of network behavior and facilitate proactive decision-making [19]. Moreover, digital twins enable the testing of new network configurations and services in a virtual environment before deployment, minimizing risks and optimizing resource utilization [20].

In conclusion, the adoption of digital twin technology in optical networks offers numerous benefits, including cost reduction, complexity management, agility enhancement, accuracy improvement, and energy efficiency. By providing network operators with a comprehensive and dynamic view of network behavior, digital twins empower them to make informed decisions, optimize resource allocation, and ensure the reliable and efficient operation of optical networks in the face of evolving technological and market challenges. On the contrary, over the past three years, numerous works have emerged leveraging digital twin (DT) technology. However, the absence of an open-source platform tailored for this purpose remains a notable gap in the field. Addressing this gap could serve as a pivotal reference point for advancing research and industry initiatives in this domain. The primary objective of this project is to establish such a platform through collaborative efforts involving four academic institutions and one industry sector. In the subsequent section, detailed discussions on the implementation of the project will encompass methodologies, anticipated outcomes, and potential impacts. Additionally, the attachments provide insight into the project budget and its scheduling.

2 Problem Statement and Objectives

In this section, our methodology and targets are discussed, explaining the system model and the main components of the digital twin at different layers of the multi-band multi-core intelligent optical network (ION). We then demonstrate how Digital Twin as a Service (DTaaS) can enable the ION to function as an autonomous, self-healing, low-margin [21], and zero-touch network for the next-generation optical network infrastructure of the telecom operator.

2.1 Problem Statement

Figure 1 illustrates the three main planes of the IONs, including the management plane, control plane, and data plane. The management plan function within the FCAPS (Fault, Configuration, Accounting, Performance, Security) standard is primarily associated with Configuration Management [22]. This

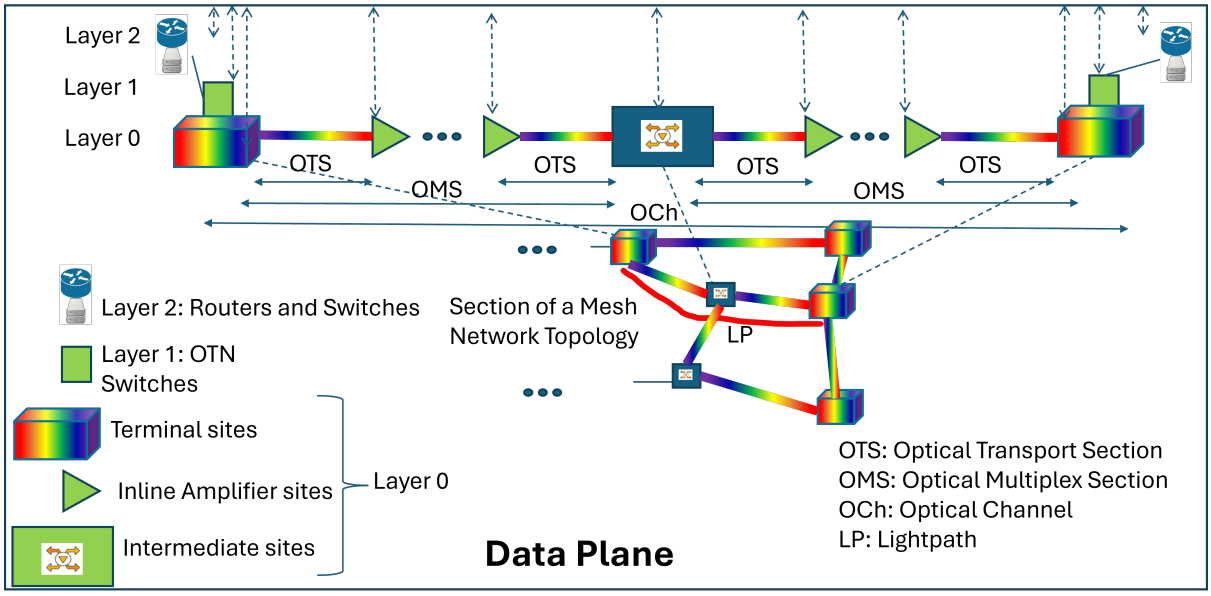

Figure 2: Data plane architecture.

function is responsible for network configuration and reconfiguration, ensuring that hardware and software configurations are optimally set up and modified as needed. It includes maintaining an accurate inventory of all network components, documenting their configurations, versions, and locations. Provisioning services is another critical aspect, which involves setting up and maintaining network services according to predefined policies and service level agreements (SLAs). Additionally, the management plan oversees change management, systematically handling and documenting changes to the network to prevent negative impacts on performance or security. It also ensures that configuration data is regularly backed up and can be restored in case of failures, supporting network continuity and quick recovery from disruptions. Compliance management is another vital role, ensuring that the network configuration adheres to industry standards, regulatory requirements, and internal policies through regular audits and assessments. Overall, the management plan function within FCAPS Configuration Management ensures that the network's configuration is well-maintained, documented, and optimized to support operational goals and service requirements.

The SDN-based control plane of an ION leverages Software-Defined Networking (SDN) principles to provide dynamic, automated, and centralized management of network resources [16]. This control plane decouples the control logic from the underlying hardware, enabling more flexible and efficient network operations. By utilizing a centralized SDN controller, the network can intelligently route traffic, optimize resource allocation, and quickly adapt to changing network conditions and demands. As shown in Figure 1, key components include a Telemetry and Monitoring Module (TMM) for real-time data collection and analysis, and an Orchestrator and Configuration Module (OCM) for managing network configurations and orchestrating resources. Machine learning and data analytics module (MLDAM) are integrated into the control plane, with databases supporting the ML pipeline to enhance predictive analytics and automated decision-making. These databases collect and process telemetry data to provide insights that drive network optimization and fault management. The SDN-based control plane, with its programmability and automation capabilities, reduces the need for manual interventions, enabling rapid deployment of new services and applications. Through its centralized control and holistic view of the network, it significantly improves the agility, scalability, and overall performance of intelligent optical networks.

The data plane of an ION encompasses three critical layers: Layer 2 (packet and/or label switching), Layer 1 (frame switching, such as SDH/OTN frames), and Layer 0 (wavelength switching). The details of data plane are depicted in Figure 2. This plane includes a variety of equipment across the IP and opti-

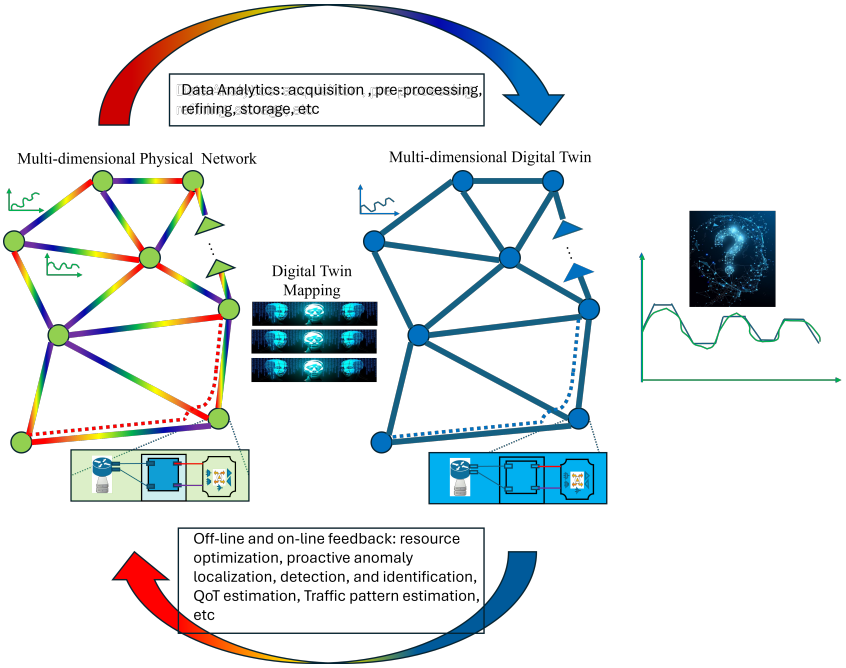

Figure 3: Digital twin closed loop and visualization of the digital twin as a service (DTaaS).

cal layers. At Layer 2, packet and label switching are managed by routers and switches, which handle the efficient forwarding of data packets. Layer 1 involves frame switching with Optical Transport Network (OTN) switches, which manage OTN frames to ensure reliable and high-capacity transport of data. Layer 0 focuses on wavelength switching, utilizing optical cross-connects and wavelength-selective switches to dynamically route wavelengths across the network. Additional essential components in the data plane include transceivers, amplifiers, digital gain equalizers, multiplexers, and demultiplexers. As illustrated in Figure 2, these elements work together to carry lightpaths (LPs) from the source to the destination across multiple layers and domains. The primary function of this plane is to ensure seamless and efficient data transport, leveraging the strengths of each layer to optimize network performance and resource utilization in a multi-layer, multi-domain environment.

The Digital Twin Closed Loop (DTCL) concept, as defined by the [17], involves creating a seamless integration between a real-world network and its digital twin counterpart. The digital twin replicates all components of the physical network, but in a virtual or logical form. Each hardware component, such as EDFAs (erbium-doped fiber amplifiers) and ROADM (Reconfigurable Optical Add-Drop Multiplexer), is represented by a corresponding software component that mimics its functionality. The DTCL operates continuously, querying real-world network hardware and databases every 15 minutes to update the mirrored databases and virtual components within the digital twin.

As represented in Figure 3, in this closed-loop system, data from the real-world network is read, preprocessed, refined, and stored in the corresponding databases of the digital twin. The Advanced AI-enabled modules within the digital twin then use this data for tasks such as quality of transmission analysis [23, 24], resource optimization, and failure detection, allowing the digital twin to function as a Digital Twin as a Service (DTaaS). Unlike the real-world network, where hardware negotiation requires specific APIs in the north and southbound interfaces (such as TAPI, Netconf, gRPC, RESTful, and OpenFlow), the digital twin operates through digital interactions, eliminating the need for these APIs.

The DTaaS then provides optimized services back to the real-world network. However, ensuring the accuracy of data acquisition and processing is a significant challenge and risk in this system model. To mitigate this risk, more accurate physical layer modeling and data analytics models based on neural networks and machine learning algorithms will be employed to reduce errors and enhance the reliability of the digital twin.

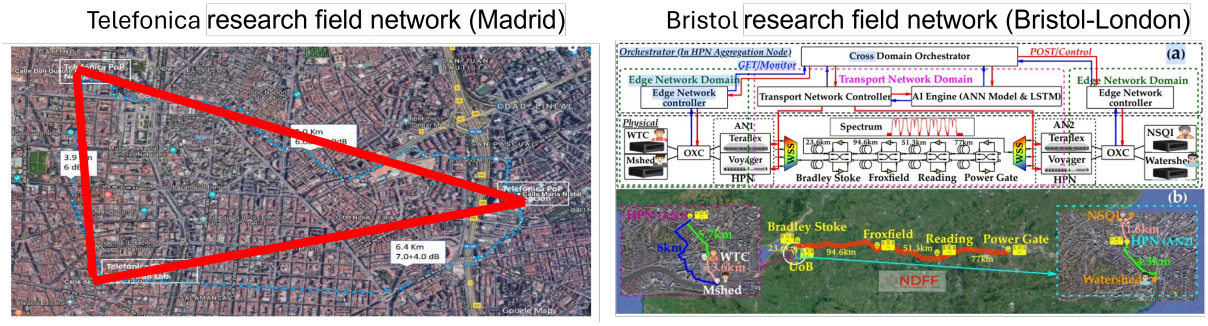

Figure 4: Research field networks in Spain [26] and the UK [27].

3 Outcomes

Our open-source project called ***TWINCORE*** leveraging Digital Twins as a Service (DTaaS) in optical networks aims to significantly reduce costs, manage complexity, enhance agility, and improve energy efficiency. By optimizing resource allocation, minimizing downtime, and streamlining maintenance activities through predictive maintenance, DTaaS helps identify cost-effective solutions for network expansion and upgrades. It simplifies network complexity with a unified platform for monitoring, analysis, and optimization, using advanced analytics and machine learning to automate tasks, detect anomalies, and recommend optimal configurations. DTaaS enhances agility by enabling rapid experimentation, testing, and deployment of new services, with virtualization and SDN capabilities allowing dynamic adjustments and resource allocation. Real-time data and advanced modeling techniques provide insights into network health and performance, while predictive analytics forecast future behavior and recommend preemptive measures. Additionally, DTaaS contributes to energy efficiency by optimizing resource utilization, reducing idle capacity, and implementing energy-efficient protocols, ensuring a robust and sustainable network infrastructure.

4 Impact

The TWINCORE project aims to make a significant impact by introducing the first open-source digital twin for intelligent optical networks, expanding beyond the capabilities of existing tools like GNPy, which is limited to QoT estimation [25]. By sharing our digital twin with the community, we enable researchers worldwide to access datasets and modules online, fostering collaboration and further development. TWINCORE is pioneering in its application of advanced technologies such as multi-band and multi-core fibers, setting a new standard for digital twins in the field. This project not only provides a valuable resource for academic research but also has the potential to drive innovation and efficiency in the telecommunications industry. Three high-ranking universities in Europe, i.e., UNiversity Carloss III de Madrid (UC3M), Chalmers University of Technology in Sweden, University of Bristol, along with the University of Virginia in the United States, are participating in the TWINCORE project. All partners are aligned with the objectives of advancing multi-band multi-core intelligent optical networks (please, see the references). The principal investigator [28] from UC3M leads the project alongside two collaborators at UC3M. Dr. Shuangyi Yan [29] and a PhD student from the University of Bristol, and Prof. Paolo Monti [30] and Dr. Carlos Natalino [31], along with a postdoctoral researcher and a PhD student from Chalmers University of Technology. Dr. Juan Pedro Fernández-Palacios from Telefonica [32] and Prof. Maite Brandt-Pearce [33], along with a PhD student from the University of Virginia, also contribute to the project. This collaborative effort not only spans multiple disciplines but also bridges academia with industry. The utilization of test beds and research field networks is crucial for the success of this project. Figure 4 illustrates the research field networks in Spain and the UK that support this endeavor.

References

[1] P. Harvey, "Looking ahead: Gen ai could amplify optical opportunities," *Light Reading*, 2023. [Online]. Available: https://www.lightreading.com/optical/looking-ahead-gen-ai-could-amplify-optical-opportunities/a/d-id/785432

[2] J. Lee, S. Kumar, and H. Kim, "Optimizing optical network infrastructure to meet rising ip traffic demands," *IEEE Communications Magazine*, vol. 62, no. 4, pp. 45–53, 2024. [Online]. Available: https://ieeexplore.ieee.org/document/9355123

[3] R. Shore, "Infinera 2024 predictions: Illuminating the future - what 2024 will bring for optical networking," *VMblog*, 2024. [Online]. Available: https://vmblog.com/archive/2024/01/05/infinera-2024-predictions-illuminating-the-future.aspx

[4] T. F. Mode, "Optical networking in 2024 - lighting the way forward," *The Fast Mode*, 2024. [Online]. Available: https://www.thefastmode.com/expert-opinion/30687-optical-networking-in-2024-lighting-the-way-forward

[5] Corning, "Broadband trends and industry predictions 2024," *Corning*, 2024. [Online]. Available: https://www.corning.com/worldwide/en/innovation/corning-research/broadband-trends-and-industry-predictions-2024.html

[6] **Farhad Arpanaei**, J. M. Rivas-Moscoso, I. De Francesca, J. A. Hernandez, A. Sanchez-Macian, M. R. Zefreh, D. Larrabeiti, and J. P. Fernandez-Palacios, "Enabling seamless migration of optical metro-urban networks to the multi-band: unveiling a cutting-edge 6d planning tool for the 6g era," *Journal of Optical Communications and Networking*, vol. 16, no. 4, pp. 463–480, 2024.

[7] T. Hoshida, V. Curri, L. Galdino, D. T. Neilson, W. Forysiak, J. K. Fischer, T. Kato, and P. Poggiolini, "Ultrawideband systems and networks: Beyond C + L-band," *Proceedings of the IEEE*, vol. 110, no. 11, pp. 1725–1741, 2022.

[8] N. Deng, L. Zong, H. Jiang, Y. Duan, and K. Zhang, "Challenges and enabling technologies for multi-band wdm optical networks," *Journal of Lightwave Technology*, vol. 40, no. 11, pp. 3385–3394, 2022.

[9] **Farhad Arpanaei**, J. M. Rivas-Moscoso, J. A. Hernández, J. P. Fernández-Palacios, and D. Larrabeiti, "Migration strategies from c-band to C+L-band/multi-fiber solutions in optical metropolitan area networks," in *49th European Conference on Optical Communications (ECOC 2023)*, vol. 2023, 2023, pp. 1531–1534.

[10] D. Uzunidis, E. Kosmatos, C. Matrakidis, A. Stavdas, and A. Lord, "Strategies for upgrading an operator's backbone network beyond the c-band: Towards multi-band optical networks," *IEEE Photonics Journal*, vol. 13, no. 2, pp. 1–18, 2021.

[11] W. Klaus, P. J. Winzer, and K. Nakajima, "The role of parallelism in the evolution of optical fiber communication systems," *Proceedings of the IEEE*, vol. 110, no. 11, pp. 1619–1654, 2022.

[12] **Farhad Arpanaei**, N. Ardalani, H. Beyranvand, and S. A. Alavian, "Three-dimensional resource allocation in space division multiplexing elastic optical networks," *Journal of Optical Communications and Networking*, vol. 10, no. 12, pp. 959–974, 2018.

[13] P. J. Winzer, D. T. Neilson, and A. R. Chraplyvy, "Fiber-optic transmission and networking: the previous 20 and the next 20 years," *Opt. Express*, vol. 26, no. 18, pp. 24 190–24 239, Sep 2018. [Online]. Available: https://opg.optica.org/oe/abstract.cfm?URI=oe-26-18-24190

[14] E. Glaessgen and D. Stargel, "The digital twin paradigm for future NASA and U.S. Air Force vehicles," in *53rd AIAA/ASME/ASCE/AHS/ASC Structures, Structural Dynamics and Materials Conference*, 2012.

[15] Y. Song, M. Zhang, Y. Zhang, Y. Shi, S. Shen, B. Guo, S. Huang, and D. Wang, "Implementing digital twin in field-deployed optical networks: Uncertain factors, operational guidance, and field-trial demonstration," *IEEE Network*, vol. 38, no. 1, pp. 38–45, 2024.

[16] R. Vilalta, L. Gifre, R. Casellas, R. Muñoz, R. Martínez, A. Mozo, A. Pastor, D. López, and **Fernández-Palacios, Juan Pedro**, "Applying digital twins to optical networks with cloud-native sdn controllers," *IEEE Communications Magazine*, vol. 61, no. 12, pp. 128–134, 2023.

[17] C. Zhou, H. Yang, X. Duan, D. Lopez, A. Pastor, Q. Wu, M. Boucadair, and C. Jacquenet, "Digital Twin Network: Concepts and Reference Architecture," Internet Engineering Task Force, Internet-Draft draft-zhou-nmrg-digitaltwin-network-concepts-07, Mar. 2022, work in Progress. [Online]. Available: https://datatracker.ietf.org/doc/draft-zhou-nmrg-digitaltwin-network-concepts/07/

[18] Q. Zhuge, X. Liu, Y. Zhang, M. Cai, Y. Liu, Q. Qiu, X. Zhong, J. Wu, R. Gao, L. Yi, and W. Hu, "Building a digital twin for intelligent optical networks [invited tutorial]," *Journal of Optical Communications and Networking*, vol. 15, no. 8, pp. C242–C262, 2023.

[19] D. Wang, Y. Song, Y. Zhang, X. Jiang, J. Dong, F. N. Khan, T. Sasai, S. Huang, A. P. T. Lau, M. Tornatore, and M. Zhang, "Digital twin of optical networks: A review of recent advances and future trends," *Journal of Lightwave Technology*, pp. 1–28, 2024.

[20] Y. Wu, M. Zhang, L. Zhang, J. Li, X. Chen, and D. Wang, "Dynamic network topology portrait for digital twin optical network," *Journal of Lightwave Technology*, vol. 41, no. 10, pp. 2953–2968, 2023.

[21] M. Mehrabi, H. Beyranvand, M. J. Emadi, and **Farhad Arpanaei**, "Efficient statistical qot-aware resource allocation in eons over the c+l-band: a multi-period and low-margin perspective," *Journal of Optical Communications and Networking*, vol. 16, no. 5, pp. 577–592, 2024.

[22] I. T. Union, *Telecommunications Management Network (TMN) - Concepts and Applications*, ser. Recommendation M.3400. ITU-T, 2000, fCAPS Standard. [Online]. Available: https://www.itu.int/rec/T-REC-M.3400-200002-I

[23] M. A. Amirabadi, M. H. Kahaei, S. A. Nezamalhosseini, **Farhad Arpanaei**, and A. Carena, "Deep neural network-based qot estimation for smf and fmf links," *Journal of Lightwave Technology*, vol. 41, no. 6, pp. 1684–1695, 2023.

[24] **Farhad Arpanaei**, N. Ardalani, H. Beyranvand, and B. Shariati, "Qot-aware performance evaluation of spectrally–spatially flexible optical networks over fm-mcfs," *Journal of Optical Communications and Networking*, vol. 12, no. 8, pp. 288–300, 2020.

[25] S. Shen, H. Li, A. Tyrovolas, Y. Teng, R. Nejabati, **Yan, Shuangyi**, and D. Simeonidou, "End-to-end qot predictions enhanced by gnpy-based digital twin with network telemetry," in *2024 Optical Fiber Communications Conference and Exhibition (OFC)*, 2024, pp. 1–3.

[26] V. Martin, A. Aguado, J. P. Brito, A. L. Sanz, P. Salas, D. R. López, V. López, A. Pastor-Perales, A. Poppe, and M. Peev, "Quantum aware sdn nodes in the madrid quantum network," in *2019 21st International Conference on Transparent Optical Networks (ICTON)*, 2019, pp. 1–4.

[27] R. Yang, H. Li, Y. Teng, S. Shen, R. Wang, R. Oliveira, R. Nejabati, S. Yan, and D. Simeonidou, "Field trial demonstration of ai-engine driven cross-domain rerouting and optimisation in dynamic optical networks," in *49th European Conference on Optical Communications (ECOC 2023)*, vol. 2023, 2023, pp. 1726–1729.

[28] **Farhad Arpanaei**, "Google scholar profile," 2024, https://scholar.google.se/citations?hl=en&user=mrBClQwAAAAJ&view_op=list_works&sortby=pubdate.

[29] **Shuangi Yan**, "Google scholar profile," 2024, https://scholar.google.com/citations?hl=en&user=3t8Tn_MAAAAJ&view_op=list_works&sortby=pubdate.

[30] **Paolo Monti**, "Google scholar profile," 2024, https://scholar.google.se/citations?hl=en&user=zkftV60AAAAJ.

[31] **Carlos Natalino**, "Google scholar profile," 2024, https://scholar.google.se/citations?hl=en&user=Yk0VpAkAAAAJ.

[32] **Juan Pedro Fernández-Palacioso**, "Google scholar profile," 2024, https://www.linkedin.com/in/juan-fernandez-palacios-520ba542/?originalSubdomain=es.

[33] **Maite Brandt-Pearce**, "Google scholar profile," 2024, https://scholar.google.com/citations?hl=en&user=KFLFbWoAAAAJ&view_op=list_works&sortby=pubdate.

ENHANCING SURGICAL PRECISION: AUTOMATED SESORRS FOR IMPROVED TUMOR DETECTION AND RESECTION– EXECUTIVE SUMMARY (HEALTH)

CHALLENGE

Glioblastoma multiforme (GBM) is one of the most formidable challenges in oncology. GBMs are the most aggressive forms of brain tumors and are associated with a poor median survival rate of only 14–16 months post-diagnosis and a 5-year survival rate of less than 5%. Due to the infiltrating nature of GBM, as well as the challenges associated with drug delivery and late-stage diagnosis, treatment of the disease is challenging. Surgical resection followed by adjuvant radio-chemotherapy the is the main therapeutic option with very few alternative treatment options. Studies have shown that more efficient tumor resection can lead to better prognosis, however current image-guided surgical techniques such as fluorescence-guided surgery (FGS) are limited in their ability to evaluate the required resection margin, or depth of tumor invasion. Surface enhanced spatially offset resonance Raman spectroscopy (SESORRS) is an emerging optical approach which can image through depths far superior to current optical imaging approaches such as fluorescence. SESORRS can acquire high spatial and spectral information through depths not currently possible in clinical image-guided surgery.

PROPOSED PROJECT AND CATEGORY

Central hypothesis: While FGS is showing promise in the clinic for supporting image-guided resection of tumors including GBM, its ability to detect deeper seated tumors is limited. **Overall goal:** The goal of this project is to establish and provide a new automated technological approach for the detection, evaluation of tumor invasion, and identification of residual tumor cells on or beneath the resection bed. Ultimately, patients with GBM could benefit from portable, low-cost, biopsy free imaging, and improved image-guided evaluation and resection of GBM in real-time. We will address this health-related challenge through three specific aims (SAs) as outlined below.

SA1: Integrate an *xyz* automated translation stage and CMOS camera with imaging spectrometer and SORS probe.

SA2: Validate automated SORS imaging using calibration standards and optical phantoms.

SA3: Evaluate the benefit using of automated SESORS for image-guided surgical resection of GBM in comparison with clinically approved approaches.

IMPACT

While progress in the image-guided resection of GBM has been achieved, there is still an urgent need to develop more efficient surgical navigational tools to improve progression-free survival in patients. To the best of our knowledge, automated SORS imaging, with or without the use of SERRS contrast agents, has not been published. More importantly, no one has applied SESORRS imaging for image-guided resection of tumors or compared it with clinically approved optical surgical navigation approaches such as fluorescence. We expect that the research outlined here will provide proof-of-concept data demonstrating the potential benefit of SESORRS imaging in comparison to FGS, for image guided resection of tumors on, or beneath the resection bed, in mouse models harboring GBMs. It is well established that early detection, as well efficient tumor resection, correlates with improved prognosis in patients. Although we have chosen to focus on developing an approach for image-guided resection of GBM, the development of more effective imaging technologies and contrast agents is vital for the treatment, and management, of all types of cancer. Taken together, we will build a tool that has the potential to drastically improve cancer detection in a clinical setting and lay the foundation for future development and application of automated SESORRS imaging for the assessment of additional solid tumors, e.g., breast cancer. I am highly qualified to lead and execute this research project however I also am hopeful that the unique environment of Dana-Farber Cancer Institute, as well as the novelty, and clinical relevance of this research area, will appeal to the next generation of scientists of whom I am eager to train.

LITERATURE REVIEW AND BACKGROUND:

Glioblastoma Multiforme (GBM): Despite notable advances in the detection and treatment of cancer, high grade gliomas such as glioblastoma multiforme (GBM), present as one of the most formidable challenges in oncology[1,2]. GBMs are the most aggressive forms of brain tumors and are associated with a poor median survival rate of only 14–16 months post-diagnosis and a 5-year survival rate of less than 5%[2]. Due to the heterogeneous and infiltrating nature of GBM, as well as challenges associated with drug delivery to the brain and late-stage diagnosis, treatment of the disease is challenging. Currently, surgical resection of the tumor followed by adjuvant radio-chemotherapy the is the main therapeutic option with very few alternate treatment options[1–4].

Image guided surgery in the management of glioblastoma:

The recurrence of GBM following surgical resection is seen in approximately 80% of patients, indicating ineffective surgical resection at the ROI. It is well established that complete resection of the tumor mass accounts for better prognosis, with some studies reporting that an extent of GBM resection greater than 98% is necessary for better prognosis[2,4]. Other studies have demonstrated that the majority of GBMs reoccur locally within 1-2 cm of the resection margin, indicating incomplete surgical resection[2,4]. While improvements in diagnostic imaging, and pathological analysis have had a positive outcome on patient survival, current image guided surgical techniques such as white light (WL) and fluorescence, remain limited in their ability to image the microscopic infiltration of GBM. Contrast agents (CAs) have been shown to be useful in supporting image-guided resection of GBM however 5-aminolevulinic acid (5-ALA) is currently the only FDA-approved agent for fluorescence guided surgery (FGS) of GBM. Oral administration of 5-ALA results in metabolism into protoporphyrin IX (peak excitation 400–410 nm, peak emission 635 nm), which accumulates in high-grade GBMs. Studies have demonstrated that using 5-ALA in FGS results in improved resection and progression-free survival in patients[5]. However, owing to the limitations of visible light probes, if malignant tissue is obscured by 1 mm of tissue, no fluorescence is observed thus leading to insufficient resection of diseased tissues[4–6]. The use of surface-enhanced resonance Raman scattering (SERRS) CAs has also been shown to be useful in image-guided surgical detection of infiltrating margins and microscopic foci in several cancers including GBM[7–12]. Currently, fluorescence probes lead the way in image guided surgical applications, however both fluorescence and traditional SERRS approaches are only able to image superficial lesions of interest[3–5]. Moreover, fluorescence imaging suffers from photobleaching and intrinsic autofluorescence. Surgical resection is stopped once the surgeon is confident all malignant lesions have been removed, however there is a likely possibility that deep-seated, microscopic lesions remain. Currently, this can only be evaluated with further removal of potentially healthy tissue. An opportunity therefore exists for a new image-guided surgical navigational tool that can non-invasively identify deeper-seated, and residual microscopic lesions of GBM through significantly larger depths of tissue than what can be achieved using current practices. Surface enhanced spatially offset resonance Raman spectroscopy (SESORRS) is an emerging technique which can image through depths far superior to current optical imaging approaches such as fluorescence[13–16]. SESORRS can provide real-time molecular information and can acquire high spatial and spectral information to achieve new levels of detail not currently possible in clinical optical cancer imaging. The goal of this project is to

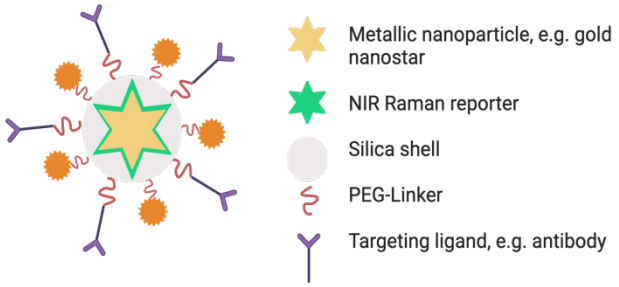

Figure 1: Schematic representing SERRS CAs.

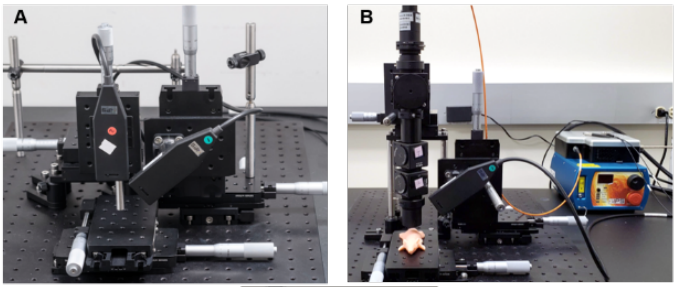

Figure 2: (A) 1st generation SORS set up. (B) 2nd generation SORS set up.

provide and establish a new automated technological approach for the detection, evaluation of tumor invasion, and identification of residual tumor cells on the resection bed *in vivo*.

SERRS contrast agents for the imaging of GBM. Optical contrast can enable characterization, staging, surgical navigation, and post-operative follow up. SERRS CAs consist of a gold nanoparticle core (diameter 120 nm) functionalized with a Raman reporter, encased in a silica shell (20 nm thickness) (Fig. 1)[12,17,18]. These are then functionalized with polyethylene glycol (PEG) to improve biodistribution and minimize uptake by the reticuloendothelial system[31]. By tracking their unique "fingerprint" spectra, SERRS CAs can be used to image tumors since they target cells with high specificity *in vivo*, e.g. through the use of targeting ligands such as antibodies[11,19–21]. Untargeted SERRS CAs have also consistently been shown to accumulate in solid tumors due to the enhanced permeability and retention (EPR) effect [9,10,18,22,23]. Our lab has demonstrated the reliable detection of a large variety of different tumor types *in vivo* (including GMBs) and their microscopic extensions using SERRS NPs[10,11,20,21,21]. SESORRS relies, in part, on the signal intensity of the SERRS agents which must be strong enough to overcome intrinsic tissue scattering. We have developed cutting-edge SERRS NPs which exhibit a detection threshold as low as 100 attomolar, a sensitivity so far unparalleled and superior to any other imaging method. I spent both my graduate and postdoctoral training designing efficient and selective SERRS CAs for SESORRS imaging[17,22,24–30]. I have screened several reporter molecules and have selected optimal IR 792 as the resonant Raman reporter to be used in this project.

SERRS and SESORRS Imaging: SERRS imaging is a non-destructive and sensitive technique, capable of providing successful delineation of tumor margins on a microscopic level[11,14,21,24]. However, while the detection of Surface enhanced resonance Raman scattering (SERRS) contrast agents (CAs) is sensitive and specific, their detection using traditional Raman imaging strategies is limited since these approaches fail to probe through large depths of tissue (typically only depths of a few mm are possible, similar to near-infrared fluorescence). Spatially offset Raman spectroscopy (SORS) utilizes the phenomenon of photon migration to collect Raman signal from much greater depths[13,14]. Unlike traditional Raman spectroscopy methods, SORS is achieved by offsetting the collection optics from the point of laser excitation, i.e., the laser is delivered separately to the sample and the scattered photons are collected through a separate collection probe at a spatial offset from the point of laser excitation[13,14] (Fig. 2). SERRS CAs have been detected in tissue phantoms through 5 cm of tissue using a SORS approach[31]. SESORRS (the use of SORS to detect SERRS CAs) offers the potential to image cancer with high contrast *in vivo* at depths far superior to what can currently be achieved using other optical imaging approaches. We recently reported

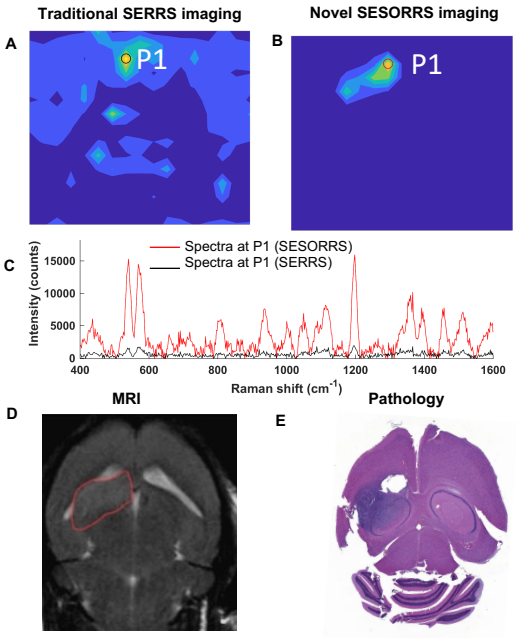

Figure 3. (A) Traditional SERRS imaging of GBM in vivo. (B) SESORRS approach using the same mouse. (C) Comparison spectra at P1. (D) MRI. (E) Histopathology. Reproduced from Ref 16.

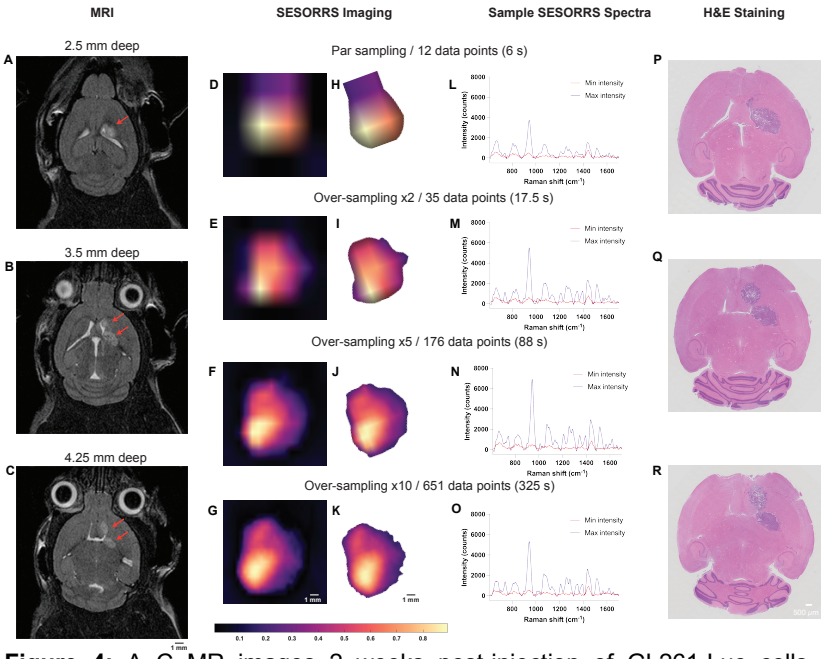

Figure 4: A–C MR images 2 weeks post-injection of GL261-Luc cells confirms the presence of a tumor at depths of 2.5 mm, 3.5 mm, and 4.25 mm respectively demonstrating the emergence of a secondary tumor region at greater depths within the brain. D-G In vivo SESORRS imaging performed using a spatial offset of 1.5 mm, using (D) par sampling frequency (12 data points) (E) over- sampling frequency of: 2 (35 data points), (F) 5 (176 data points), and (G) 10 (651 data points). The respective times taken to acquire each image are also shown. H–K Background removal of areas of non-intensity from the SESORRS images. Images were rotated to match the orientation of the MR images. L–O SESORRS spectra taken at the point of minimum and maximum intensity from the respective SESORRS image using a par sampling frequency and an oversampling frequency of 2, 5 and 10 respectively indicating uptake of SERRS CAs. P–R H&E stained 5 μM section of the brain confirming the presence of a tumor and the emergence of a secondary tumor region. Reproduced from Ref 22.

the very first demonstration of SESORRS for the *in vivo* imaging of any disease[16]. This was achieved by explicitly targeting integrins overexpressed on the tumor vasculature, angiogenic endothelial cells and tumor cells in a clinically relevant genetically engineered mouse model of GBM. In comparison to traditional SERRS imaging (Fig. 3A), SESORRS (Fig 3B) provided clear delineation of the tumor margin as confirmed by MRI and histology, Fig. 3D and E)[16]. In addition, SESORRS imaging generated one order of magnitude higher signal than a traditional SERRS imaging approach (Fig. 3C). While these data enabled us to report the first demonstration of SESORRS for the *in vivo* imaging of cancer, this approach used long acquisition and accumulation times which is unfavorable for *in vivo* applications[16,22]. Therefore, we engineered and optimized a purpose built SORS collection probe to improve light collection efficiency by increasing: (i) lens NA from 0.2 to 0.34, (ii) probe working distance from 9 mm to 40 mm, (iii) fiber NA from 0.2 to 0.34, and (iv) fiber diameter from 100 μm to 400 μm (Fig. 2B) [22]. Furthermore, by accounting for laser spot size, we also developed a method for rapidly detecting the bulk tumor and delineating tumor margins *in vivo*. To determine our sampling frequency, which refers to the number of data point spectra obtained for each image, we considered the laser spot size of the elliptical beam (6 × 4 mm). Then, after administering SERRS contrast agents *in vivo*, we performed SESORRS imaging on a GL261-Luc mouse model of GBM at four distinct sampling frequencies: par-sampling frequency (12 data points collected), and over-frequency sampling by factors of 2 (35 data points collected), 5 (176 data points collected), and 10 (651 data points collected). *In vivo* SESORRS imaging of a GBM mouse model showed a 300% improvement in SNR compared to previous SORS systems, with lower power density (13.8 mW/mm^2 versus 6 mW/mm^2) and shorter integration times (15 s in previous work compared with only 0.5 s our latest report)[22]. Mapping of the mouse head and identifying regions of interest within as few as 12 spectra (6 s total acquisition time) was achieved, with higher sampling frequencies providing greater certainty and improved delineation of ROIs[22], Fig. 4D-K. Interestingly, and perhaps more importantly, our SESORRS approach enabled the detection of secondary ROIs (tumors) deeper within the brain as confirmed by MRI and H&E staining (Fig.4 A-C, Fig.4 P-R), thus suggesting the suitability of SESORRS as an intraoperative imaging approach for the detection and imaging of deep-seated tumors, particularly within the

brain[22]. Therefore, we believe that our approach offers an opportunity to navigate larger areas of tissues in shorter time frames than previously reported, identify regions of interest on the surface and more importantly, deep-seated tumors that may not be visible using traditional techniques[22]. Thus, we hypothesize that it could be possible to apply SESORRS imaging using a par-sampling frequency to scan large areas of tissue to identify ROIs where the malignant tissues are present, then, using a higher-sampling frequency approach, e.g. 5, delineate that same ROI with greater certainty and identify the presence of potentially deeper-seated lesions in real time.

PROBLEM AND OBJECTIVES

Central hypothesis: While fluorescence guided surgery (FGS) is showing promise in the clinic for supporting surgical resection of multiple tumor types including GBM, its ability to detect deeper seated, microscopic foci is limited. **Overall goal:** The goal of this project is to establish and provide a new automated technological approach for the detection, evaluation of tumor invasion, and identification of residual tumor cells on or beneath the resection bed. Ultimately, patients with GBM could also benefit from portable, low-cost, biopsy free imaging and evaluation of GBM. We will address this goal through three specific aims (SAs):

SA1: Integrate an *xyz* automated translation stage and CMOS camera with imaging CCD and SORS probe.

SA2: Validate automated SORS Imaging using calibration standards and optical phantoms.

SA3: Evaluate the benefit using of automated SESORRS for image-guided surgical resection of GBM in comparison with clinically approved approaches.

OUTCOMES AND FUTURE DIRECTIONS

Upon completion of this project we will have designed, built, optimized, and evaluated an automated SORS imaging device, validated its efficiency using previously published calibration standards, and developed calibration models that directly correlate spatial offset and depth with Raman intensity from SERRS CAs. Following evaluation of our bench-top *in vivo* imaging system we will have determined the efficiency of automated SESORRS to support image-guided resection of GBM and detect microscopic foci on or beneath the resection bed and compared it against clinically approved image-guided approaches such as 5-ALA (fluorescence) and white-light. These results will enable us to understand if SESORRS could serve as a viable, complementary technique, for the characteristic assessment and improvement in the resection of GBM *in vivo* and enable us to predict the success of automated SORS imaging in combination with SERRS CAs for potential clinical translation, forming the basis for at least two publications.

The aims outlined in this proposal are realistic to the funding timeline however there are additional follow-up studies that will be addressed in parallel with, or after, the proposed research:

1) In SA2 we propose to develop a RMSE calibration model to determine the depth at which SERRS CAs are located at using *ex vivo* phantoms. Using MRI, H&E staining, as well as our automated SESORRS imaging system which will enable us to pinpoint where exactly on the mouse spectra is being obtained, we will validate this calibration model *in vivo* using varying concentrations of SERRS CAs administered to multiple cohorts of mice bearing different tumors types. Given that the uptake of SERRS CAs depends on several factors including tumor necrosis, route of administration, tumor location, and whether the SERRS CAs are functionalized with a targeting ligand, we will validate our approach using multiple models of cancer including GBM and colorectal cancer out with this proposal. We may also explore the use of AI and Monte Carlo simulations to validate our models. In this case we would seek a collaborator for guidance.

2) Although not discussed here, my lab is currently investigating the efficiency of a SORS endoscope for the assessment of pre-malignant and malignant lesions of colorectal cancer and the real-time imaging and assessment of polyp invasion into the colon wall. Future work may focus on integrating both the automated SORS imaging device outlined here, together with the SORS endoscope for bulk tumor imaging and subsequent validation and assessment of difficult to reach areas using the handheld endoscope.

3) While we have focused on developing an automated SORS imaging device for the detection of GBM, my team may investigate the feasibility of automated SORS imaging for the detection, and image guided resection of other solid tumors, e.g., melanoma and breast cancer.
4) While we expect to show the advantage of SESORRS imaging for the resection of deep-seated tumors over clinically approved approaches, e.g., fluorescence, we ultimately believe that SESORRS imaging would serve a complementary optical imaging approach to FGS. Thus, we may investigate using fluorescence imaging for real-time assessment and imaging of surface-based tumors, and then integrate it with SESORRS imaging for the detection of deeper-seated lesions that would otherwise go unnoticed.
5) We chose 5-ALA as a fluorescence CA due to its FDA approval for FGS of GBM however future work could also explore the potential of using molecularly specific fluorescent NIR or NIR-II contrast agents, e.g., antibodies labelled with NIR or NIR-II dyes, in combination with SESORRS imaging. This would be carried out by utilizing a short-wave infrared (SWIR) camera. Future work may also focus on integrating a SWIR camera into our SORS imaging system for multimodal imaging.

IMPACT

To the best of our knowledge, image-guided resection using SESORRS has not been published, and no one has compared the benefit of SESORRS imaging for image-guided resection to clinically approved optical surgical navigation tools, such as fluorescence. We expect that the research outlined here will provide proof-of-concept data demonstrating the potential benefit of SESORRS imaging to support the image guided resection of tumors on, or beneath the resection bed in mouse models harboring GBMs in comparison to clinically approved FGS approaches, thus helping to support the likelihood of clinical translation. I will continue to combine my expertise in the design of SERRS CAs and SORS imaging with that of oncological colleagues and engineers to develop innovative approaches for the intra-operative detection of GBM and strengthen the translational relevance of my research. It is well established that early detection, as well efficient tumor resection correlates with improved prognosis. While progress has been achieved, there is still an urgent need to develop more efficient surgical navigational tools to improve survival rates. Although we have chosen to focus on developing an approach for image-guided resection of GBM, the development of more efficient imaging technologies and CAs is vital for the treatment, and management, of all types of cancer. Taken together, we will build a tool that has the potential to drastically improve cancer detection in a clinical setting and lay the foundation for future application of automated SESORRS imaging for the assessment of other solid tumors, e.g., breast cancer.

In addition to developing a technology that could considerably improve the efficiency of image-guided resection of cancer, these data will also allow me to prepare a strong portfolio for additional funding, e.g., funding from the National Institute of Health and the Department of Defense that will further seek to facilitate the clinical translation of this technique. Moreover, as a Harvard Medical School teaching affiliate, Dana-Farber Cancer Institute (DFCI) provides the unique and world-class environment required to fully execute the work outlined in this proposal. DFCI researchers have full access to several core facilities including the Lurie Family Imaging Center (pre-clinical small animal imaging), The Molecular Pathology Core Laboratory, and the Confocal and Light Microscopy Core, all of which will support this project. I was the first to report the application of SESORRS for *in vivo* imaging of any disease and thus have a unique understanding on how to apply it for cancer imaging. I also have extensive experience in understanding the synthesis, biodistribution, and properties of SERRS CAs for *in viv*o applications. While I am highly qualified to lead and mange this research proposal, I am hopeful that the unique environment, novelty, and clinical relevance of this research, will appeal to the next generation of scientists. I am confident that funding from this project will enable to me to recruit and train the next generation of scientists and engineers of whom I am eager to train.

REFERENCES

1. Lee JYK, Thawani JP, Pierce J, Zeh R, Martinez-Lage M, Chanin M, Venegas O, Nims S, Learned K, Keating J, Singhal S. Intraoperative Near-Infrared Optical Imaging Can Localize Gadolinium-Enhancing Gliomas During Surgery. Neurosurgery. United States; 2016 Dec;79(6):856–871. PMCID: PMC5123788
2. Bonosi L, Marrone S, Benigno UE, Buscemi F, Musso S, Porzio M, Silven MP, Torregrossa F, Grasso G. Maximal Safe Resection in Glioblastoma Surgery: A Systematic Review of Advanced Intraoperative Image-Guided Techniques. Brain Sci. Switzerland; 2023 Jan 28;13(2). PMCID: PMC9954589
3. Azari F, Zhang K, Kennedy GT, Chang A, Nadeem B, Delikatny EJ, Singhal S. Precision Surgery Guided by Intraoperative Molecular Imaging. J Nucl Med. United States; 2022 Nov;63(11):1620–1627. PMCID: PMC9635678
4. Palmieri G, Cofano F, Salvati LF, Monticelli M, Zeppa P, Perna GD, Melcarne A, Altieri R, La Rocca G, Sabatino G, Barbagallo GM, Tartara F, Zenga F, Garbossa D. Fluorescence-Guided Surgery for High-Grade Gliomas: State of the Art and New Perspectives. Technol Cancer Res Treat. United States; 2021 Dec;20:15330338211021605. PMCID: PMC8255554
5. Cho SS, Sheikh S, Teng CW, Georges J, Yang AI, De Ravin E, Buch L, Li C, Singh Y, Appelt D, Delikatny EJ, Petersson EJ, Tsourkas A, Dorsey J, Singhal S, Lee JYK. Evaluation of Diagnostic Accuracy Following the Coadministration of Delta-Aminolevulinic Acid and Second Window Indocyanine Green in Rodent and Human Glioblastomas. Mol Imaging Biol. United States; 2020 Oct;22(5):1266–1279. PMCID: PMC7667706
6. Vahrmeijer AL, Hutteman M, van der Vorst JR, van de Velde CJH, Frangioni JV. Image-guided cancer surgery using near-infrared fluorescence. Nat Rev Clin Oncol. England; 2013 Sep;10(9):507–518. PMCID: PMC3755013
7. Kircher MF, de la Zerda A, Jokerst JV, Zavaleta CL, Kempen PJ, Mittra E, Pitter K, Huang R, Campos C, Habte F, Sinclair R, Brennan CW, Mellinghoff IK, Holland EC, Gambhir SS. A brain tumor molecular imaging strategy using a new triple-modality MRI-photoacoustic-Raman nanoparticle. Nat Med. United States; 2012 Apr 15;18(5):829–834. PMCID: PMC3422133
8. Karabeber H, Huang R, Iacono P, Samii JM, Pitter K, Holland EC, Kircher MF. Guiding brain tumor resection using surface-enhanced Raman scattering nanoparticles and a hand-held Raman scanner. ACS Nano. United States; 2014 Oct 28;8(10):9755–9766. PMCID: PMC4212801
9. Andreou C, Neuschmelting V, Tschaharganeh DF, Huang CH, Oseledchyk A, Iacono P, Karabeber H, Colen RR, Mannelli L, Lowe SW, Kircher MF. Imaging of Liver Tumors Using Surface-Enhanced Raman Scattering Nanoparticles. ACS Nano. United States; 2016 May 24;10(5):5015–5026. PMCID: PMC4884645
10. Harmsen S, Rogalla S, Huang R, Spaliviero M, Neuschmelting V, Hayakawa Y, Lee Y, Tailor Y, Toledo-Crow R, Kang JW, Samii JM, Karabeber H, Davis RM, White JR, van de Rijn M, Gambhir SS, Contag CH, Wang TC, Kircher MF. Detection of Premalignant Gastrointestinal Lesions Using Surface-Enhanced Resonance Raman Scattering-Nanoparticle Endoscopy. ACS Nano. United States; 2019 Feb 26;13(2):1354–1364. PMCID: PMC6428194
11. Harmsen S, Huang R, Wall MA, Karabeber H, Samii JM, Spaliviero M, White JR, Monette S, O'Connor R, Pitter KL, Sastra SA, Saborowski M, Holland EC, Singer S, Olive KP, Lowe SW, Blasberg RG, Kircher MF. Surface-enhanced resonance Raman scattering nanostars for high-precision cancer imaging. Sci Transl Med. United States; 2015 Jan 21;7(271):271ra7. PMCID: PMC4414254

12. Harmsen S, Wall MA, Huang R, Kircher MF. Cancer imaging using surface-enhanced resonance Raman scattering nanoparticles. Nat Protoc. England; 2017 Jul;12(7):1400–1414. PMCID: PMC5694346
13. Matousek P, Clark IP, Draper ERC, Morris MD, Goodship AE, Everall N, Towrie M, Finney WF, Parker AW. Subsurface probing in diffusely scattering media using spatially offset Raman spectroscopy. Appl Spectrosc. United States; 2005 Apr;59(4):393–400. PMID: 15901323
14. Nicolson F, Kircher MF, Stone N, Matousek P. Spatially offset Raman spectroscopy for biomedical applications. Chem Soc Rev. England; 2021 Jan 7;50(1):556–568. PMCID: PMC8323810
15. Dey P, Vaideanu A, Mosca S, Salimi M, Gardner B, Palombo F, Uchegbu I, Baumberg J, Schatzlein A, Matousek P, Stone N. Surface enhanced deep Raman detection of cancer tumour through 71 mm of heterogeneous tissue. Nanotheranostics. Australia; 2022;6(3):337–349. PMCID: PMC9194587
16. Nicolson F, Andreiuk B, Andreou C, Hsu HT, Rudder S, Kircher MF. Non-invasive In Vivo Imaging of Cancer Using Surface-Enhanced Spatially Offset Raman Spectroscopy (SESORS). Theranostics. Ivyspring International Publisher; 2019;9(20):5899–5913.
17. Andreiuk B, Nicolson F, Clark LM, Panikkanvalappil SR, Kenry, Rashidian M, Harmsen S, Kircher MF. Design and synthesis of gold nanostars-based SERS nanotags for bioimaging applications. Nanotheranostics. Australia; 2022;6(1):10–30. PMCID: PMC8671966
18. Zavaleta CL, Smith BR, Walton I, Doering W, Davis G, Shojaei B, Natan MJ, Gambhir SS. Multiplexed imaging of surface enhanced Raman scattering nanotags in living mice using noninvasive Raman spectroscopy. Proc Natl Acad Sci U S A. United States; 2009 Aug 11;106(32):13511–13516. PMCID: PMC2726370
19. Eremina OE, Czaja AT, Fernando A, Aron A, Eremin DB, Zavaleta C. Expanding the Multiplexing Capabilities of Raman Imaging to Reveal Highly Specific Molecular Expression and Enable Spatial Profiling. ACS Nano. United States; 2022 Jul 26;16(7):10341–10353. PMID: 35675533
20. Huang R, Harmsen S, Samii JM, Karabeber H, Pitter KL, Holland EC, Kircher MF. High Precision Imaging of Microscopic Spread of Glioblastoma with a Targeted Ultrasensitive SERRS Molecular Imaging Probe. Theranostics. Australia; 2016;6(8):1075–1084. PMCID: PMC4893636
21. Oseledchyk A, Andreou C, Wall MA, Kircher MF. Folate-Targeted Surface-Enhanced Resonance Raman Scattering Nanoprobe Ratiometry for Detection of Microscopic Ovarian Cancer. ACS Nano. United States; 2017 Feb 28;11(2):1488–1497. PMCID: PMC5502101
22. Nicolson F, Andreiuk B, Lee E, O'Donnell B, Whitley A, Riepl N, Burkhart DL, Cameron A, Protti A, Rudder S, Yang J, Mabbott S, Haigis KM. In vivo imaging using surface enhanced spatially offset raman spectroscopy (SESORS): balancing sampling frequency to improve overall image acquisition. npj Imaging. 2024 Apr 3;2(1):7.
23. Kircher MF, de la Zerda A, Jokerst JV, Zavaleta CL, Kempen PJ, Mittra E, Pitter K, Huang R, Campos C, Habte F, Sinclair R, Brennan CW, Mellinghoff IK, Holland EC, Gambhir SS. A brain tumor molecular imaging strategy using a new triple-modality MRI-photoacoustic-Raman nanoparticle. Nat Med. United States; 2012 Apr 15;18(5):829–834. PMCID: PMC3422133
24. Kenry, Nicolson F, Clark L, Panikkanvalappil SR, Andreiuk B, Andreou C. Advances in Surface Enhanced Raman Spectroscopy for in Vivo Imaging in Oncology. Nanotheranostics. Australia; 2022;6(1):31–49. PMCID: PMC8671959
25. Surface-enhanced Resonance Raman Scattering Nanoprobe Ratiometry for Detecting Microscopic Ovarian Cancer via Folate Receptor Targeting. United States; 2019.

26. Nicolson F, Andreiuk B, Andreou C, Hsu HT, Rudder S, Kircher MF. Non-invasive In Vivo Imaging of Cancer Using Surface-Enhanced Spatially Offset Raman Spectroscopy (SESORS). Theranostics. Australia; 2019;9(20):5899–5913. PMCID: PMC6735365
27. Nicolson F, Jamieson LE, Mabbott S, Plakas K, Shand NC, Detty MR, Graham D, Faulds K. Multiplex imaging of live breast cancer tumour models through tissue using handheld surface enhanced spatially offset resonance Raman spectroscopy (SESORRS). Chem Commun (Camb). England; 2018 Jul 26;54(61):8530–8533. PMID: 30010164
28. Nicolson F, Jamieson LE, Mabbott S, Plakas K, Shand NC, Detty MR, Graham D, Faulds K. Through tissue imaging of a live breast cancer tumour model using handheld surface enhanced spatially offset resonance Raman spectroscopy (SESORRS). Chem Sci. England; 2018 Apr 21;9(15):3788–3792. PMCID: PMC5939614
29. Nicolson F, Jamieson LE, Mabbott S, Plakas K, Shand NC, Detty MR, Graham D, Faulds K. Towards establishing a minimal nanoparticle concentration for applications involving surface enhanced spatially offset resonance Raman spectroscopy (SESORRS) in vivo. Analyst. England; 2018 Nov 5;143(22):5358–5363. PMID: 30325368
30. Nicolson F, Jamieson LE, Mabbott S, Plakas K, Shand NC, Detty MR, Graham D, Faulds K. Surface enhanced resonance Raman spectroscopy (SERRS) for probing through plastic and tissue barriers using a handheld spectrometer. Analyst. England; 2018 Dec 3;143(24):5965–5973. PMID: 30225477
31. Stone N, Kerssens M, Lloyd GR, Faulds K, Graham D, Matousek P. Surface enhanced spatially offset Raman spectroscopic (SESORS) imaging – the next dimension. Chem Sci. The Royal Society of Chemistry; 2011;2(4):776–780.

Executive Summary for Health Challenge

NOD-GMG - Nanoscale Optomechanical Detection of Gene Mutations in Glioma

Dr. Giovanna Palermo, NLHT Lab - Physics Department University of Calabria and CNR NANOTEC Rende CS – Italy

What is the unmet need?

Sensor technology offers a tremendous opportunity in medical research and clinical diagnostics to specifically detect small numbers of low molecular weight biomolecules relevant for infectious and lethal diseases. In recent years, various label-free technologies for detection of cancer biomarkers and viruses have been developed. However, early disease diagnostics, tracking of disease progression and evaluation of treatments require a radical innovation to deliver high specificity, sensitivity, diffusion-limited transport and accuracy for both nucleic acids and proteins. Worldwide, the vast majority of research groups are focused on the exploration of strategies to enhance the sensitivity of biosensors - all the way down to single molecule detection - whereas the selectivity and the specificity of the biorecognition process relies primarily upon the chemical affinity only. In this project, the question we ask is how to move the specificity to an entirely new level and what solutions we may implement to face this limit that for too long has been considered difficult to achieve.

In particular, the diagnosis of neoplasia in the central nervous system is based on clinical symptoms, radiologic imaging, and invasive biopsy. There is an unmet need for the quantitative detection of biomarkers in biofluids of brain tumor patients to complement clinical examination and neuroradiographic images findings, and obviate the need for invasive neurosurgical procedures. Mutations in the Isocitrate Dehydrogenase (IDH) genes 1 and 2 are present in most of human World Health Organization grade II and III gliomas. The mutated enzymes have a neomorphic activity that results in elevated production of metabolite D-2-Hydroxyglutarate (D-2HG) in the tumors.

What is being proposed to meet this need?

The objective of NOD-GMG project is to boost the specificity and develop a transformative biosensing technology based on nanostructured metasurfaces for liquid biopsy to detect and separate tandemly chiral biomolecules.

Along these lines NOD-GMG project aims to conduct a fundamental study to develop nanophotonic platform, based on dielectric/plasmonic metasurfaces, to separate optomechanically chiral biomolecules related to low-grade (LGG) and high grade glioma (HGG) patients.

The research hypothesis is that electromagnetic fields generated by metasurfaces can enable a precise optomechanical spatial control of submicrometric polarizable particles. By engineering epsilon-near-zero (ENZ) metasurfaces, we aim to achieve waves that exhibit “static-like” spatial distributions, while temporally they are dynamic. One consequence is the possibility of levitation of electrically-polarized chiral particles in the vicinity of ENZ substrates (axial forces). Such metasurfaces can also be nanopatterned with hybrid metal-dielectric nanostructures to imbue transversal field gradients and/or chiral optical activity (transversal forces).

What are the expected outcomes?

In **NOD-GMG** project we want to demonstrate that D-2HG can be detected through an optical platform in the biofluids of glioma patients with mutated IDH1/2, supporting its further development as a clinical test for diagnosis and follow-up.

What will be the real-world impact of this project?

The breakthrough objective of **NOD-GMG** project is to demonstrate that early and accurate analysis can be achieved using a non-invasive ‘liquid biopsy’ approach, by uniquely implementing Key Enabled Technologies: nanoscience, physical optics, artificial intelligence, and medicine.

Proposal for Health Challenge

(NOD-GMG) Nanoscale Optomechanical Detection of Gene Mutations in Glioma.

Dr. Giovanna Palermo, NLHT Lab - Physics Department University of Calabria and CNR NANOTEC Rende CS – Italy

Literature Review and Objectives:

Sensor technologies have become crucial in medical research and clinical diagnostics for enabling the detection of small numbers of low molecular weight biomolecules relevant to diagnose and monitor diseases. However, to radically improve early disease diagnostics, tracking of disease progression and evaluation of treatments, sensing technologies require a paradigm shift to address the daunting problem of ultrahigh specificity and accuracy to recognize the chirality (handedness) of nucleic acids and/or proteins. Liquid biopsy (LB) is considered the most advanced diagnostic assay since it allows low invasiveness and wide spectrum biomedical analysis. Nonetheless, workflows remain complicated with technological limitations in terms of specificity at both nucleic acid and protein levels. Translation from research to clinical applications remains costly, limited by variability/reproducibility and lack of standardized protocols for sample preparation. Although it has developed a sensing technology to detect ultra-low molecular weight molecules with a limit of detection <1pg/ml [1], highly specific sensory systems to detect structural changes in proteins or single base mutations in nucleic acids have not yet been developed. Recent studies show that single base mutations result in changes of the handedness of biomolecules of clinical relevance.

Chirality exists at all scales: Cells gain a substantial fitness advantage by either increasing the magnitude of their chirality or switching to the opposite handedness. So far, in medicine, stereochemistry has occupied a major role in drug design and development since chiral properties are crucial in the determination of the pharmacological actions of compounds [2,3]. More recently, the chirality of metabolites or small molecules which are end products of cell metabolism has gained increased attention in cancer research [4]. It has been shown that mutations in enzymes could favor the production of new endogenous chiral metabolites that allow cells to acquire new properties thus promoting cancer development and progression [5]. As an example, mutations in isocitrate dehydrogenase 1 (IDH1) and 2 (IDH2) genes [6] are characterizing both low-grade (LGG) and high-grade glioma (HGG) patients. The neomorphic activity of the mutated IDH1/2 enzymes results in the elevated production of the right D-enantiomer of 2-Hydroxyglutarate (2HG) locally in the brain tissue and systemically in biofluids[7]. IDH1/2 mutation is present in 80% of LGG and in 10% of HGG and, in both, is considered a diagnostic, prognostic and predictive biomarker [8,9]. The development of a sensory system able to detect, with high sensitivity and specificity, the level of chiral biomarkers as the IDH1/2 mutations and/or D-2HG will result in a promising technological achievement for diagnosis and follow-up. Motivated by these striking examples, we started to investigate whether chirality - being a product of natural mutations rather than a historical accident - could allow to elevate the specificity of the biorecognition process to an unprecedented level.

Metamaterials can be manufactured with specific electromagnetic properties, one of those being the capability to exert a repulsive force on an electric radiating dipole, resulting in levitation. This phenomenon, which was inspired as a classical analogue to levitated magnets in proximity of superconductors (Meissner effect), provides a new approach in opto-mechanics to manipulate electrically polarizable particles in the presence of optical fields[10].

Remarkably, photonic metamaterials [11] have been proposed for separation processes based on repulsive-attractive interactions enabling optomechanical control of nano- and micro-particles[12]. The field of metamaterials has provided ample opportunities for scientists and technologists to design material platforms with unique characteristics in manipulating and structuring light[13-14].
More recently, it has been explored how metamaterials platforms, in particular epsilon-near-zero (ENZ) substrates, can influence optical force on nano- and microscale polarizable particles in the vicinity of such substrates. Through numerical simulations and experimental investigations, it has been studied how the ENZ-based substrate can affect the direction (attractive and repulsive) and the strength of the optical force on such particles.
The development of optomechanics based on optical tweezers [15] has stimulated the exploitation of optical forces and torques in several research areas, such as biophysics, nanotechnology, complex fluids, microrheology and microfluidics. Optical tweezers are a powerful tool to study forces and torques on physical systems both at the micro and the nanoscale, down to the femtoN range. Recently, chirality-dependent optical forces have been probed, aiming at obtaining enantiomeric separation at the micro- and nanoscale[16-20]. Circularly polarized light selectively interacts with chiral particles having similar helicity[16], inducing trapping and rotation, due to the transfer of spin angular momentum from the trapping beam. The extension to nano or even molecular scale is currently a hot research topic[17-20], allowing, in principle, the study of the handedness of a single, isolated chiral nanoparticle. While extensive theoretical modeling has predicted the ability to use optomechanical forces for separation of chiral objects [17-19,21], the experimental realization has yet to be achieved.

The objective of NOD-GMG project is to demonstrate that highly selective enantiomeric separation can be achieved using optomechanical forces on ad hoc designed planar and nanopatterned metasurfaces. To pursue this goal we will be probing levitation forces as well as lateral forces on chiral biomarkers related to low-grade (LGG) and high-grade glioma (HGG).

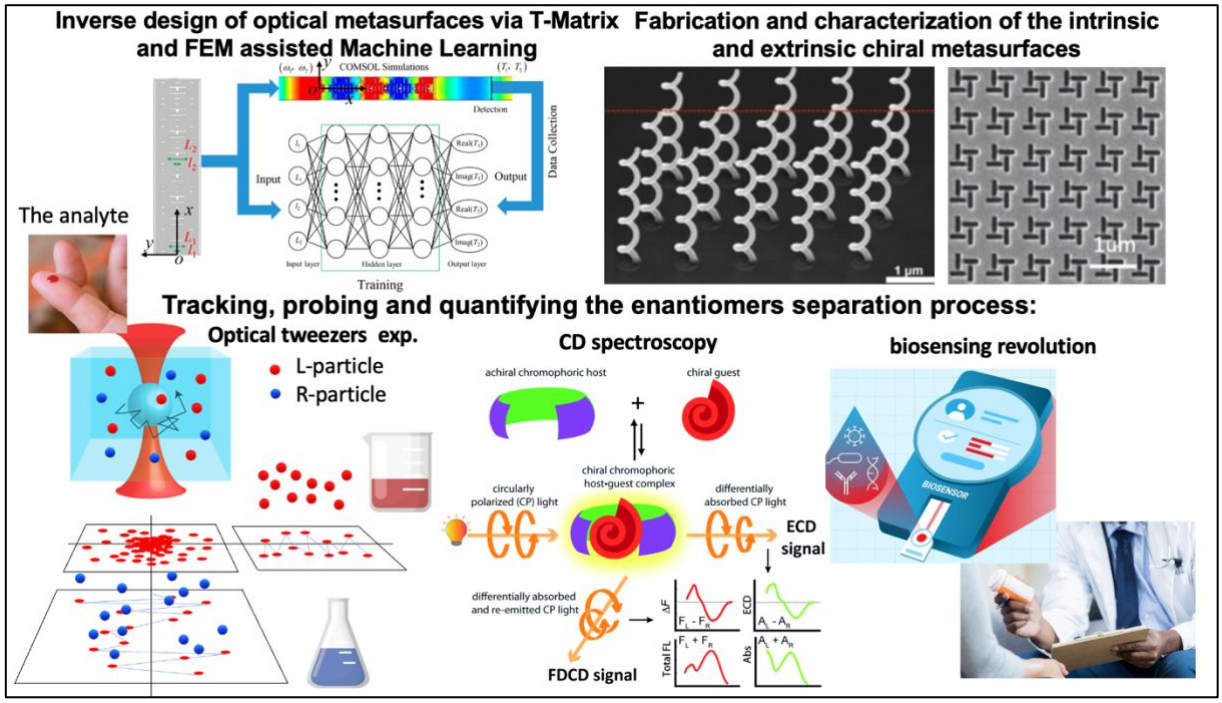

Proposal for Health Challenge

Illustration of the structure of the project: Top left panel: Use of machine learning to inverse design optical metasurfaces. The neural network training is done via T-Matrix data. Top right panel: Optical Metasurfaces routinely fabricated and characterized. Bottom panel: Illustration of the experimental techniques used to track, probe (optical tweezers) and quantify (circular dichroism (CD) and Fluorescence detection circular dichroism spectroscopy (FDCD)) the separation process that will be used to the research of the chiral biomarkers IDH1/2.

The main objectives of NOD-GMG project are distinct, but interconnected:

Objective 1: Design of a novel optical enantioselective platform based on nanostructured metasurfaces, including characterization of optimally chiral electromagnetic fields and their interactions with chiral molecular and supramolecular structures. The difference in the effective refractive index of chiral samples exposed to left- and right-handed optimally chiral fields is expected to be up to 10^6 times greater than those observed in optical polarimetry.

Objective 2: Fabrication and characterization of the inverse designed nanostructured metasurfaces. The central objective is to implement a process of selective separation of chiral analytes by means of optomechanical forces generated on nanostructured metasurfaces. The separation aims to discern chiral molecules, sorting them by their handedness within a wide range of size and chiral polarizability. The locally increased twisting of light polarization occurring under chiral conditions induces intense light-chiral matter interactions, causing the separation of enantiomeric excesses, thereby enabling ultra-specific chiro-selective separation. In particular, our objective is to reach an enantiopurity above 90% by separating chiral molecules with different size (5 nm – 1 μm), and chiral polarizability χ as small as 10^{-21} cm^3.

Objective 3: The final objective is to quantify the efficiency and the selectivity of the separation methods by analyzing CD spectroscopy data. The CD spectroscopy analysis will be performed by collecting fractions of solution after exiting the flow cell and performing CD spectroscopy in the aliquots afterwards, we will characterize the selectivity of the separation. The platform will be tested for the separation and quantification of isocitrate dehydrogenase 1 (IDH1) and 2 (IDH2) genes, first from racemic solutions prepared ad-hoc and followed by LB samples from low-grade (LGG) and high-grade glioma (HGG) patients.

Outcomes:

There are three intellectual merits to this proposal:

1. This research will develop inverse designed sensing platforms based on chiral metasurfaces to enhance light – chiral matter interactions to manipulate optomechanically chiral biomolecules.
2. The complementary methods used will find more general applications in materials science and energy research. Specifically, the behavior of chiral nano-objects interacting with chiral electromagnetic fields is not well understood, particularly for low polarizability systems.
3. This research may enable high selectivity and throughput separation methods of biomolecules of relevance for the diagnosis and the prognosis of lethal diseases as glioblastoma, by identifying the chirality of biomarkers.

Proposal for Health Challenge

Impact:

NOD-GMG is a project with transformational impact and true potential in healthcare, pharmaceutical industry and environmental science. Embedded in its combined technologies is a radical new approach to discriminate enantiomeric excess of chiral analytes and biomarkers of clinical importance. The results will definitely contribute to the advancement of knowledge in the framework of nanophotonic platform to induce chiro-selective optical forces.

The project will have a significant scientific & technological impact on four Key Enabling Technologies (KETs): Nanotechnology, Advanced Materials, Biotechnology, Advanced Manufacturing & Processing, and Medicine. The short-term program is devoted to investigate how opto-mechanics enables analytes separation at molecular level to elevate to an entirely new level the specificity in biosensing processes. The project is expected to put the foundations for a long-term objective, which aims to deliver a platform that detects in real time handedness gene mutations in precision medicine. Notwithstanding the project's total focus on the role of enantioselectivity through optomechanical forces, the advancements will clearly find significant new opportunities in healthcare and environmental challenges. The next level of specificity based on chiral sign recognition of nucleic acids and peptides could also prove highly valuable for monitoring the spread of pandemic infectious disease and other forms of cancer. The consequent diagnostic platforms will introduce new paradigms in clinical diagnosis and treatment decisions, improving patient's life expectancy, with lower health care costs through the combination of higher accuracy and fast readout times, aided by deep machine learning protocols.

Future social and economic impact will be truly global. Diagnostics currently costs the EU €126 billion in 2020, with health care accounting for €51 billion (40%). Across the EU, health-care costs of cancer disease were equivalent to €102 per citizen; unsurprising given that the average cost for lethal diseases treatment per patient is a staggering €30K. The platform performance objective is to significantly outperform current technologies, while delivering improved patient outcomes at reduced health care costs. Success will lead to a unique new platform of importance in the in-vitro diagnostic field, which will pull in supporting R&D investment and growth of the European diagnostics sector, in particular for SMEs. A strong social impact is ensured through delivery of new, cost-effective and reliable liquid biopsy technology for improved diagnosis and tracking of socially important lethal diseases, including infectious diseases. Last but not least, an important expected impact of the project will be the involvement and mentoring of early stage EU researchers in a demanding but rewarding cross-disciplinary research activities and learning, including science, engineering of advanced materials, and biotechnologies, that will accelerate innovation and translation into nanoscience and human technologies.

Use of Research Infrastructures:

The research activities will be carried out in the CNR NANOTEC laboratories "Beyond Nano" and in the Nanoscience Laboratory for Human Technologies (NLHT) of the Physics Department of University of Calabria.
The CNR NANOTEC laboratories "Beyond Nano" have facilities for fabrication (DLW workstation - Photonic Professional GT, Nanoscribe GmbH) and characterization of materials and devices for emerging photonics and optoelectronic technologies as Variable Angle Spectroscopic Ellipsometry, Time resolved spectroscopy, Near-field scanning optical microscopy (NSOM).

NLHT have state-of-the-art research laboratories that are connected with a larger and active research network with ultimate infrastructures that will allow them to accomplish all tasks and objectives proposed in this project. NLHT at UNICAL is a fully renovated and functional 270 square meters Nanobiophotonics and Plasmonics research laboratory. The laboratory includes last generation optical benches for bio-spectroscopy and bio-sensing experiments, CD biospectroscopy, , Transient Absorption Spectroscopy, an optical tweezers setup equipped with a white laser source.

Aim of the clinical part will be to take advantage of the population of glioma patients treated and followed by the Neurosurgery Department of Udine to define whether identification and quantification of circulating factors (IDH1/2 mutation in ctDNA and D-2HG) can predict glioma presence and recurrence.

Bibliopraphy:

1. Sreekanth, K. V., Alapan, Y., ElKabbash, M., Ilker, E., Hinczewski, M., Gurkan, U. A., ... & Strangi, G. (2016). Extreme sensitivity biosensing platform based on hyperbolic metamaterials. Nature materials, 15(6), 621-627
2. Nguyen, L. A., He, H., & Pham-Huy, C. (2006). Chiral drugs: an overview. International journal of biomedical science: IJBS, 2(2), 85.
3. Alkadi, H., & Jbeily, R. (2018). Role of Chirality in Drugs: An Overview. Infectious Disorders Drug Targets, 18(2), 88-95.
4. Thamim, M., & Thirumoorthy, K. (2020). Chiral discrimination in a mutated IDH enzymatic reaction in cancer: A computational perspective. European Biophysics Journal, 49(7), 549-559.
5. Dang, L., White, D. W., Gross, S., Bennett, B. D., Bittinger, M. A., Driggers, E. M., ... & Su, S. M. (2009). Cancer-associated IDH1 mutations produce 2-hydroxyglutarate. Nature, 462(7274), 739-744.
6. Yan, H., Parsons, D. W., Jin, G., McLendon, R., Rasheed, B. A., Yuan, W., ... & Bigner, D. D. (2009). IDH1 and IDH2 mutations in gliomas. New England journal of medicine, 360(8), 765-773.
7. Kalinina, J., Ahn, J., Devi, N. S., Wang, L., Li, Y., Olson, J. J., ... & Van Meir, E. G. (2016). Selective detection of the D-enantiomer of 2-hydroxyglutarate in the CSF of glioma patients with mutated isocitrate dehydrogenase. Clinical Cancer Research, 22(24), 6256-6265.
8. Louis, D. N., Perry, A., Reifenberger, G., Von Deimling, A., Figarella-Branger, D., Cavenee, W. K., ... & Ellison, D. W. (2016). The 2016 World Health Organization classification of tumors of the central nervous system: a summary. Acta neuropathologica, 131, 803-820.
9. Cancer Genome Atlas Research Network. (2015). Comprehensive, integrative genomic analysis of diffuse lower-grade gliomas. New England Journal of Medicine, 372(26), 2481-2498.
10. Rodríguez-Fortuño, F. J., Vakil, A., & Engheta, N. (2014). Electric levitation using ϵ-near-zero metamaterials. Physical review letters, 112(3), 033902.
11. Solomon, M. L., Saleh, A. A., Poulikakos, L. V., Abendroth, J. M., Tadesse, L. F., & Dionne, J. A. (2020). Nanophotonic platforms for chiral sensing and separation. Accounts of chemical research, 53(3), 588-598.
12. Kiasat, Y., Donato, M. G., Hinczewski, M., ElKabbash, M., Letsou, T., Saija, R., ... & Engheta, N. (2023). Epsilon-near-zero (ENZ)-based optomechanics. Communications Physics, 6(1), 69.
13. Palermo, G., Lio, G. E., Esposito, M., Ricciardi, L., Manoccio, M., Tasco, V., ... & Strangi, G. (2020). Biomolecular sensing at the interface between chiral metasurfaces and hyperbolic metamaterials. ACS applied materials & interfaces, 12(27), 30181-30188.
14. Palermo, G., Sreekanth, K. V., Maccaferri, N., Lio, G. E., Nicoletta, G., De Angelis, F., ... & Strangi, G. (2020). Hyperbolic dispersion metasurfaces for molecular biosensing. Nanophotonics, 10(1), 295-314.
15. Jones, P., Maragó, O., & Volpe, G. (2015). Optical tweezers. Cambridge: Cambridge University Press.
16. Donato, M. G., Hernandez, J., Mazzulla, A., Provenzano, C., Saija, R., Sayed, R., ... &

Cipparrone, G. (2014). Polarization-dependent optomechanics mediated by chiral microresonators. Nature communications, 5(1), 3656.

17. Donato, M. G., Hernandez, J., Mazzulla, A., Provenzano, C., Saija, R., Sayed, R., ... & Cipparrone, G. (2014). Polarization-dependent optomechanics mediated by chiral microresonators. Nature communications, 5(1), 3656.
18. Canaguier-Durand, A., Hutchison, J. A., Genet, C., & Ebbesen, T. W. (2013). Mechanical separation of chiral dipoles by chiral light. New Journal of Physics, 15(12), 123037.
19. Patti, F., Saija, R., Denti, P., Pellegrini, G., Biagioni, P., Iatì, M. A., & Maragò, O. M. (2019). Chiral optical tweezers for optically active particles in the T-matrix formalism. Scientific reports, 9(1), 29.
20. Ali, R., Pinheiro, F. A., Dutra, R. S., Rosa, F. S., & Neto, P. A. M. (2020). Enantioselective manipulation of single chiral nanoparticles using optical tweezers. Nanoscale, 12(8), 5031-5037.
21. Pellegrini, G., Finazzi, M., Celebrano, M., Duò, L., Iatì, M. A., Maragò, O. M., & Biagioni, P. (2019). Superchiral surface waves for all-optical enantiomer separation. The Journal of Physical Chemistry C, 123(46), 28336-28342.

Revolutionizing Photonic Integrated Circuits: Achieving a 10,000-Fold Size Reduction with ITO

PI: Dr. Hamed Dalir (hamed.dalir@ufl.edu), Florida Semiconductor Institute, Electrical and Computer Engineering Department, University of Florida

Objectives: The increasing demand for advanced artificial intelligence (AI) hardware stems from the necessity for improved efficiency, speed, and scalability, areas where conventional electronic methods like application-specific integrated circuits (ASICs) face challenges. Photonic accelerators offer significant potential in addressing these constraints, providing enhancements in power economy, processing speed, and overall performance of AI applications. Indium Tin Oxide (ITO) active devices are at the forefront of this advancement, exhibiting superior performance compared to traditional Mach-Zehnder Interferometer (MZI) modulators, boasting near-diffraction-limit capabilities, low insertion loss, and remarkable modulation depth. Furthermore, our innovative slot detector technology, with its compact footprint and high-speed operation, meets the demanding speed requirements critical for advanced AI applications.

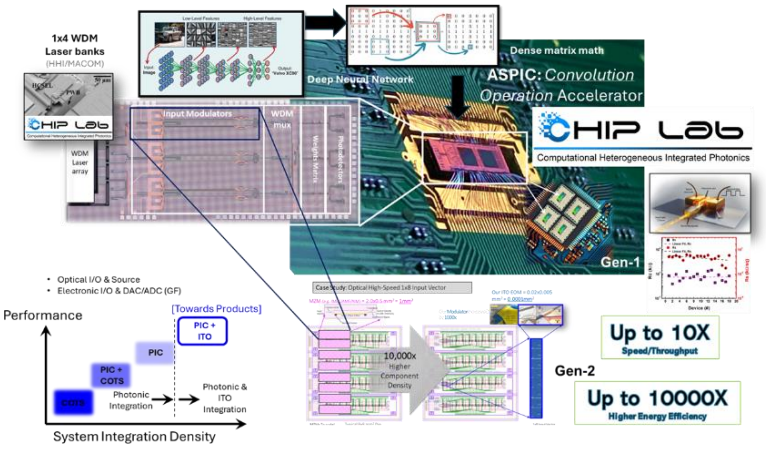

Problem Statement: As PICs progress, they face new obstacles in the areas of dense integration, electronic-photonic integration (EIC-PIC), packaging, and system-level design metrology. Despite the potential of PICs for commercial use, their production efficiencies are currently lower than those of Complementary Metal-Oxide-Semiconductor (CMOS) technology owing to their substantial device size. This underscores the pressing need for advancements in fabrication processes, design methodologies, and quality control measures to meet and exceed industry standards.

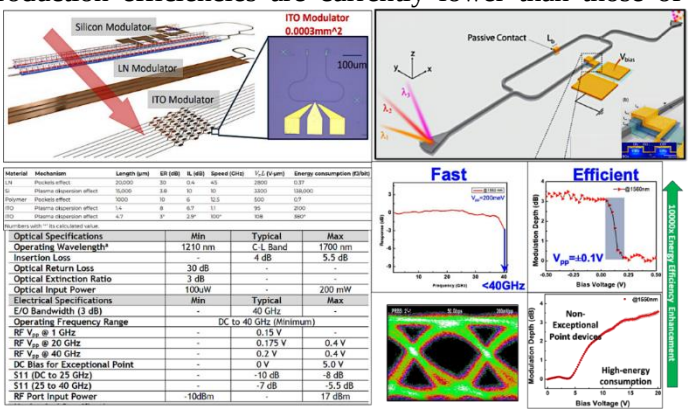

Optical Specifications	Min	Typical	Max
Operating Wavelength*	1210 nm	C-L Band	1700 nm
Insertion Loss		4 dB	5.5 dB
Optical Return Loss	30 dB	-	-
Optical Extinction Ratio	3 dB	-	-
Optical Input Power	100uW	-	200 mW
Electrical Specifications	**Min**	**Typical**	**Max**
E/O Bandwidth (3 dB)	-	40 GHz	-
Operating Frequency Range		DC to 40 GHz (Minimum)	
RF V_{pp} @ 1 GHz	-	0.15 V	-
RF V_{pp} @ 20 GHz	-	0.175 V	0.4 V
RF V_{pp} @ 40 GHz	-	0.2 V	0.4 V
DC Bias for Exceptional Point	-	0 V	5.0 V
S11 (DC to 25 GHz)	-	-10 dB	-8 dB
S11 (25 to 40 GHz)	-	-7 dB	-5.5 dB
RF Port Input Power	-10dBm	-	17 dBm

Novelty: Transition to compact photonics for AI hardware: This figure contrasts traditional MZI modulators with our novel ITO device, which drastically reduces size and lowers insertion loss to 0.5 dB with a 3-dB modulation depth at 100mV. Achieving a device density 10,000 times greater than Lithium Niobate, our technology also supports 100 Gbps operational speeds. Enhanced integration is achieved through photonic wire bonding, significantly advancing photonic AI applications.

Heterogeneous Integration & Processing of ITO for Energy Efficient Photonic Active Devices: We use novel techniques like "critical coupling" mechanism. This technique enables us to have a figure of merits (FOM) of 30 dB/V (extinction ratio/bias voltage) for switching in free carrier-and coupling based modulators. The effective index-sensitive coupling mechanism here provides an efficient modulation technique boosting up the operational energy consumption enhancement by 10,000x.

Broader Impact: In addition to scientific and technological impacts, the project aims addressing the national shortage of skilled labor in the semiconductor industry and enhancing US competitiveness in the global market. Through collaborative efforts and community engagement, the project aims to cultivate a sustainable domestic workforce while promoting diversity and inclusivity within the Florida semiconductor industry, thereby contributing to national security and technological leadership.

I. Literature Review

Advanced artificial intelligence (AI) hardware is needed to improve efficiency, speed, and scalability, which conventional electronics methods like application-specific integrated circuits (ASICs) are struggling to achieve. Despite their capabilities, ASICs have energy and expandability issues, which photonic accelerators can address [**1**]. Photonic technologies provide an attractive option that boosts power efficiency, processor speed, and AI performance. AI hardware must improve its processing power to handle increasingly complex computations. Photonic technology is led by compact, efficient Indium Tin Oxide (ITO) active devices. These devices outperform Mach-Zehnder Interferometer (MZI) modulators. When driven at 100mV, they have near-diffraction-limit capabilities, 0.5 dB insertion loss, and 3 dB modulation depth at 40 GHz [**2**]. These devices also outperform conventional techniques by **10,000** and sophisticated technologies by 1,000 in device density. Our novel slot detector, with a footprint of 1um^2, sub voltage energy efficiency, and a frequency of 30 GHz and 300 GHz [**3**], meets the speed requirements for most artificial intelligence applications. Combining these devices with lasers advances photonic integration by employing photonic wire bonding (PWB) in distributed feedback (DFB) [**4**] and even flip-chip vertical-cavity surface-emitting laser (VCSEL) [**5**]. This integration heralds the next generation of photonic integrated circuits (PICs) [**6**]. However, renowned foundries like AIMs Photonics in the US have placed environmental limits on operating devices, which is hindering their development and adoption. The constraint emphasizes the necessity for a pilot effort that examines photonic technology's boundaries in AI hardware and ensures that the next generation of AI hardware is produced within a framework that supports **scalability and trust**.

II. Problem Statement/Objective

As PICs progress, they face new obstacles in the areas of dense integration, electronic-photonic integration (EIC-PIC), packaging, and system-level design metrology. Despite the potential of PICs for commercial use, their production efficiencies are currently lower than those of complementary metal-oxide-semiconductor (CMOS) technology owing to **their substantial device size**. This underscores the pressing need for advancements in fabrication processes, design methodologies, and quality control measures to meet and exceed industry standards. To address these challenges, a co-design approach integrating materials, devices, and systems is pivotal. Photonic Accelerators (PA) are a groundbreaking advancement in the realm of AI hardware, offering transformative potential for accelerating AI computations. By co-designing material properties alongside device structures, higher integration densities, superior signal integrity, and enhanced functionality can be achieved within compact footprints [**7-8**]. Lasers, modulators, photodetectors, and DFB lasers in PA encounter specific obstacles that limit their capability [**9**]. Co-design is used for heterogenous integration (HI) difficulties including temperature management and silicon photonics. Problems with lasers For Si-PICs, Indium Phosphide (InP) lasers with output power above 20 mW and continuous-wave (CW) operation are popular. Their enormous footprint exceeding 0.5 mm^2 hinders dense integration, scalability, and cost. GaAs lasers, used in PICs for data transmission, have smaller footprints (50-300 μm^2). InP and GaAs lasers need additional downsizing to provide better integration densities, performance, and cost advantages in next-generation PICs. PICs need electro-optic modulators, yet footprint size is a problem. Lithium niobate ($LiNbO_3$) modulators have excellent efficiency (>80%) but large footprints (>500 μm^2). PICs with high integration density and power efficiency are difficult to make due to their size. Micro-disk modulators using whispering gallery mode resonators provide low footprints of 10 μm^2 and are promising for compactness [**10**]. Larger Mach-Zehnder designs often have higher modulation efficiency and bandwidth than ultra-compact ones [**11**]. The balance between miniaturization, performance, and energy efficiency across varied modulator designs and material substrates is a continuing PIC research and development goal. PIC photodetectors, which convert optical signals into electrical impulses, have footprint size issues. AIM photonics, IMEC, AMF, and other Germanium (Ge) and Silicon (Si) photodetectors have great responsivity and speed but different footprints. Ge PIN photodetectors combined with waveguides have great responsivity and speed, but they need sophisticated production procedures that are incompatible with CMOS technology. Monolithically integrated Ge photodetectors on Silicon-On-Insulator (SOI) substrates have high responsivities (>1 A/W) in the optical communication

wavelength range, although their footprints sometimes surpass 100 μm^2. In contrast, silicon-based integrated photodetectors such lateral pin diodes and avalanche photodiodes have achieved tremendous downsizing, with footprints as tiny as 10 μm^2 and exceeding 0.8 A/W. New III-V materials, such as InGaAs, have allowed small, efficient waveguide-integrated photodetectors with footprints below 10 μm^2 and good responsivities, although the footprint remains a hurdle for all. The fundamental physics of design and the rising costs of producing, assembling, incorporating, and aligning lasers on the chip make laser integration in silicon photonics difficult. More laser channels and bandwidth increase the challenges. This scenario illustrates the limitations of current technology and production methods, stressing the need for creative ways to overcome the inherent obstacles of incorporating efficient laser sources into silicon-based photonic circuits. Modern photonic components including lasers, innovative materials, CMOS technology, creating nanophotonic structures, pursuing heterogeneous integration, and using improved production processes. These research thrusts seek to build small and efficient photonic components to create high-performance, highly integrated PICs for a variety of applications. **This study proposes** unprecedented device density and performance enhancements to overcome existing constraints in AI hardware. By leveraging unique Indium Tin Oxide (ITO) active devices and slot detectors, the suggested technique increases device density 10,000 times over traditional Lithium Niobate (LN) modulators and 1,000 times over current technology. Our novel ITO device offers a transformative shift in AI hardware by drastically reducing size and achieving a device density 10,000 times greater than Lithium Niobate. It also lowers insertion loss to 0.5 dB with a 3dB modulation depth at 100mV, supports operational speeds of 30 GHz scalable beyond 100 GHz, and significantly advances photonic AI applications. Enhanced integration through photonic wire bonding further propels the potential of compact photonics in AI hardware, potentially revolutionizing power efficiency, data processing rates, and scalability.

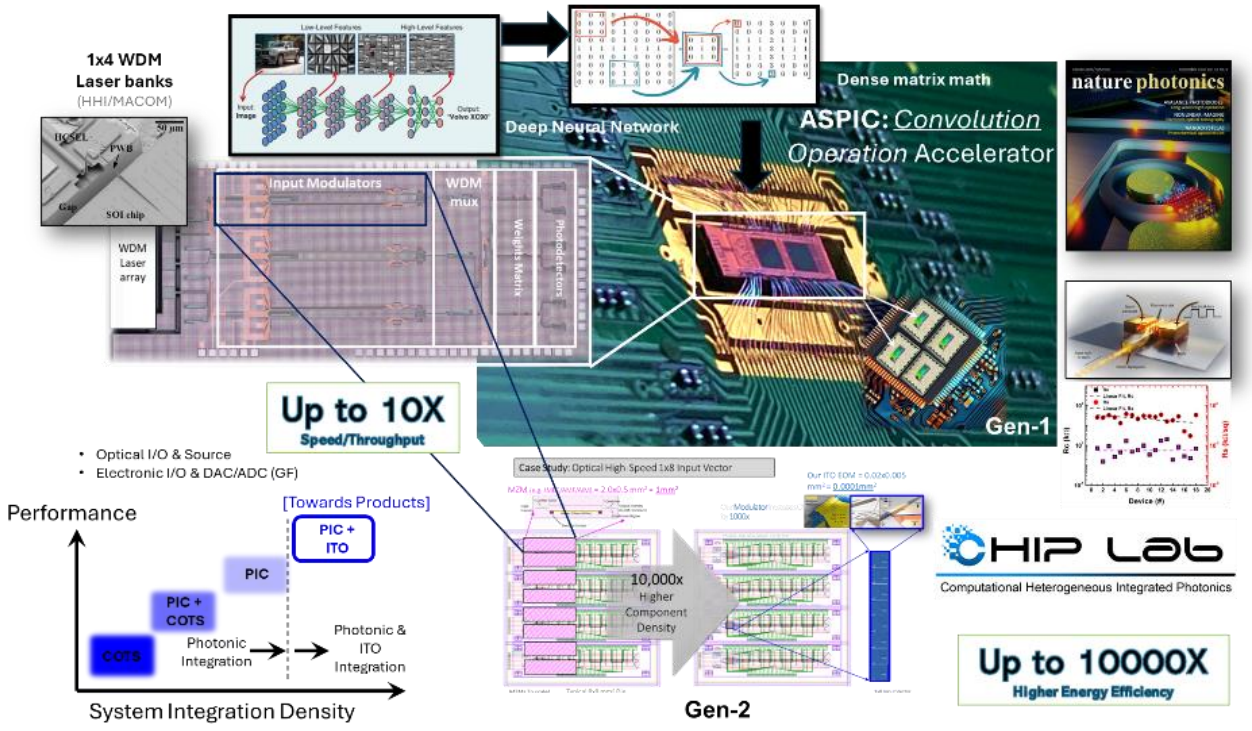

Figure 1: Transition to Compact Photonics for AI hardware: This figure contrasts traditional Mach-Zehnder Interferometer modulators with our novel ITO device, which drastically reduces size and lowers insertion loss to 0.5 dB with a 3dB modulation depth at 100mV. Achieving a device density 10,000 times greater than Lithium Niobate, our technology also supports 30 GHz operational speeds, scalable beyond 100 GHz. Enhanced integration is achieved through photonic wire bonding, significantly advancing photonic AI applications.

III. Outline of Tasks/Work Plan

Task 1: Heterogeneous Integration: On-chip Lasers for AI Hardware: CHIP Lab is advancing silicon photonics through the integration of semiconductor lasers, specifically 1550 nm DFB lasers for silicon platforms. The project aims to integrate light sources into silicon-based electronics using PWB technology to address ultra-compact device packaging and reduce integration losses. The goal is to enhance optical computing, high-speed data transport, and sensor technologies by reducing integration losses and maintaining high Side Mode Suppression Ratios (SMSR). Initial results show integration losses at 1.7 dB, with an objective to reduce this to 0.9 dB while upholding an SMSR of 55 dB. CHIP Lab focuses on integrating sophisticated laser sources and electrical components into Silicon Photonics devices, addressing the challenges of silicon's indirect bandgap and the complexities of incorporating III-V materials. Using heterogeneous materials and 2.5D technology at the Back End of Line (BEOL), the lab aims to expand the functionality and performance of photonic devices. Leveraging advanced technologies like PWB, CHIP Lab aims to set new standards for efficiency and scalability in Silicon Photonics, pushing the boundaries of the field with a goal of minimizing insertion losses to 0.5 dB.

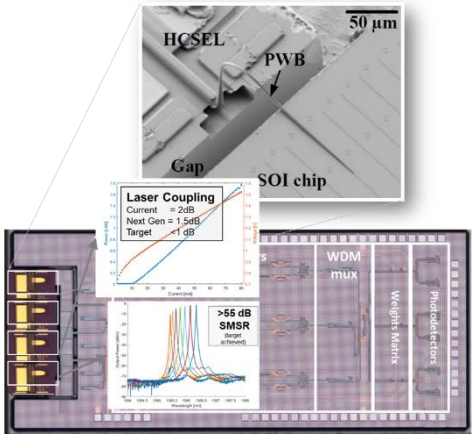

Figure 2: Overview of Laser Integration Techniques on Silicon Photonics (SiPh) Achieving a SMSR of 55dB for the DFB laser, Demonstration of the cascading capability of multiple lasers. Attainment of an insertion loss as minimal as 2dB.

Task 2: Processing of ITO for Energy Efficient Photonics Integrated Circuits: For photonic devices and thin film contacts, our ITO integration technology uses atomic layer deposition (ultra-thin, high-quality film) and sputtering deposition (high and complex conformality). We employ UV-Vis-NIR spectroscopy to measure ITO thin film transmittance and absorbance at various wavelengths. We use spectroscopic micro-ellipsometry to determine the optical constants of the generated ITO thin films, allowing accurate film thickness and refractive index adjustment for optoelectronic device applications (ENZ, carrier tuning, optical index tuning). Electrical conductivity, carrier concentration, and mobility of developed ITO thin films (high-speed >40GHz devices) are measured using Hall effect and four-point probe methods. An in-house thermal annealing recipe lets our researchers study post-annealing effects on electrical and optical characteristics and project device reliability parameters (athermal operation >100ºC). Conductive atomic force microscopy (C-AFM)

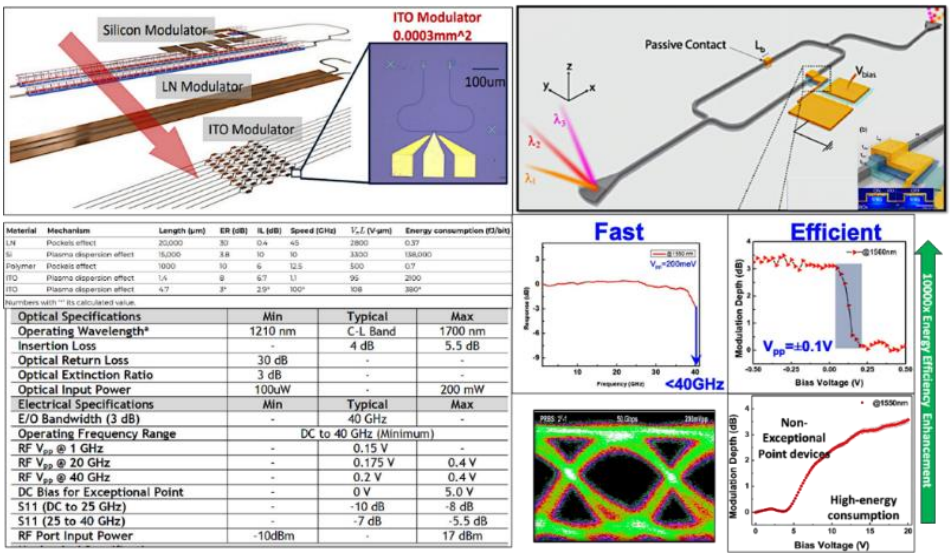

Material	Mechanism	Length (µm)	ER (dB)	IL (dB)	Speed (GHz)	$V_\pi L$ (V·µm)	Energy consumption (fJ/bit)
LN	Pockels effect	20,000	30	0.4	45	2800	0.37
Si	Plasma dispersion effect	15,000	3.8	10	10	3300	138,000
Polymer	Pockels effect	1000	10	6	125	500	0.7
ITO	Plasma dispersion effect	1.4	8	6.7	1.1	99	2100
ITO	Plasma dispersion effect	4.7	3*	2.9*	100*	108	380*

Numbers with '*' its calculated value.

Optical Specifications	Min	Typical	Max
Operating Wavelength*	1210 nm	C-L Band	1700 nm
Insertion Loss	-	4 dB	5.5 dB
Optical Return Loss	30 dB	-	-
Optical Extinction Ratio	3 dB	-	-
Optical Input Power	100uW	-	200 mW
Electrical Specifications	**Min**	**Typical**	**Max**
E/O Bandwidth (3 dB)	-	40 GHz	-
Operating Frequency Range	DC to 40 GHz (Minimum)		
RF V_{pp} @ 1 GHz	-	0.15 V	-
RF V_{pp} @ 20 GHz	-	0.175 V	0.4 V
RF V_{pp} @ 40 GHz	-	0.2 V	0.4 V
DC Bias for Exceptional Point	-	0 V	5.0 V
S11 (DC to 25 GHz)	-	-10 dB	-8 dB
S11 (25 to 40 GHz)	-	-7 dB	-5.5 dB
RF Port Input Power	-10dBm	-	17 dBm

Figure 3: The current global and national market trends for ITO. The inclusion of ITO in PIC components strongly aligns with the semiconductor and material development in United States as seen in the chart above.

can map electrical characteristics at the nanoscale, showing film conductivity and flaws that affect device performance. SEM and TEM provide high-resolution imaging of film shape and grain boundaries, helping optimize deposition settings for desired film qualities. Nanoscale surface roughness, morphology, and topography are characterized using AFM. Critical coupling mechanism and dynamic insertion loss isolation (-5dB to -1dB) are unique methods. We can switch free carrier- and coupling-based modulators with a chip-chip 3dB extinction ratio using these methods. An efficient modulation strategy using the index-sensitive coupling mechanism increases operating energy usage by 10000x. Due to its transparency, ITO material interaction over photonic components preserves system symmetry and passive photonic component effective coupling requirements. With its optical index tuning characteristics, ITO can scale devices down by ~1000x compared to platforms based on Si, lithium niobate, and SiN.

Task 3: Monolithic Atomically Thin Film Photodetectors for Compact & Energy Efficient PICs: For photonic chip energy efficiency, speed, and footprint, optoelectronic device design demands material design improvements. The necessity to overcome silicon CMOS and silicon photonic 2D scaling limitations drives this requirement [12-13]. Co-designing alternative materials and device design paradigms to develop semiconductor technology maintains Moore's Law [14]. To solve this problem, we provide a physical model for a plasmonic-enhanced photodetector integrated with 2D materials to demonstrate device and material co-design. This technique lets photonic computing devices like photonic tensor core computers use 2D-based plasmonic photodetectors. This method might allow dimensional scaling and energy-efficient computation by using 2D materials' thin structure and efficient carrier transport [15]. These materials can also be incorporated into 3D nano systems, which might change computer systems by enhancing energy efficiency and data processing. In our breakthrough study, slot width greatly affected the frequency response of plasmonic slot photodetectors of 15 nm, 30 nm, 60 nm, and 120 nm slot widths (**Figure 4**). These devices showed 3dB roll-off frequencies of 30 GHz, 10 GHz, 2.5 GHz, and 200 MHz at 1 V bias, showing that smaller slots increase frequency responses. Our slot design significantly minimizes transit lengths for photo-excited carriers, increasing drift velocity ($v = \mu E$) due to reduced electrode distance (L) and stable $MoTe_2$ in-plane carrier mobility (μ). We found that the plasmonic slot design reduces carrier transit distance to a few nanometers, enabling device speeds limited only by RC time. Because few-layer MoTe2 has a carrier mobility of 0.01 cm^2/Vs, we predict an ideal device speed of 100 GHz. TMDC-based photodetector technology is developing toward ultra-high-speed optoelectronic devices, as shown in **Figure 4.** We will focus on numerous crucial areas to enhance TMDC-based plasmonic slot photodetectors' frequency responsiveness from 30 to 100 GHz. Optimize $MoTe_2$'s in-plane carrier mobility to 0.01 cm^2/Vs. We will research material engineering strategies to decrease defects and increase $MoTe_2$ crystal quality.

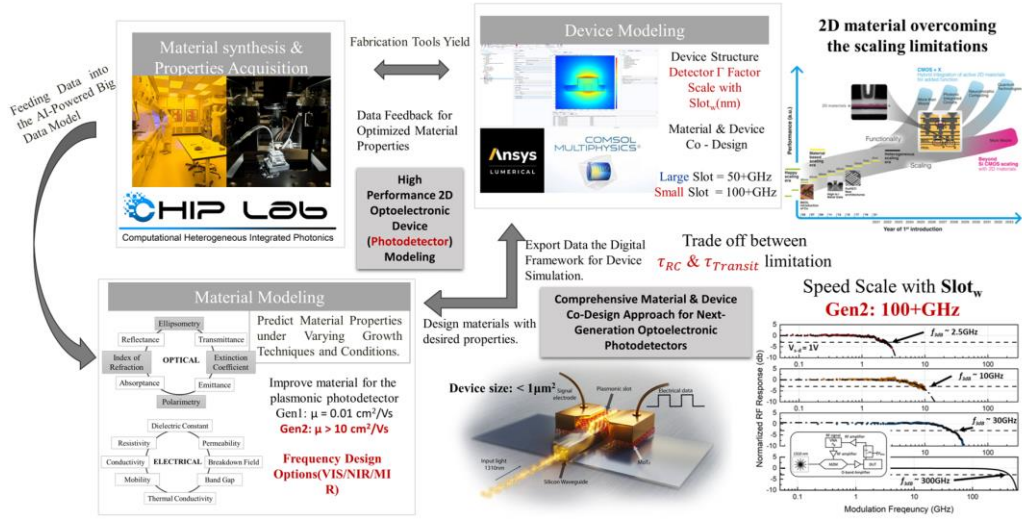

Figure 4: Illustration of our holistic photodetector modeling strategy, aimed at advancing beyond the scaling constraints of traditional silicon-based technologies using 2D materials. This approach facilitates further miniaturization and enhances performance in electronic and optoelectronic devices.

Task 4: Dense Integrated Photonic Accelerator for Large Bandwidth & Low Power Computing:

We are finally proposing an integrated photonic computing accelerator surpassing traditional silicon photonic technology. It features an on-chip integrated source, high-speed, compact, and energy-efficient ITO based Mach-Zehnder modulators (MZM) and microring resonators (MRM), along with high-performance 2D material-based plasmonic photodetectors.

Our ongoing research indicates that the integration of high-performance optoelectronic components is essential for advancing the capabilities of these computing systems.

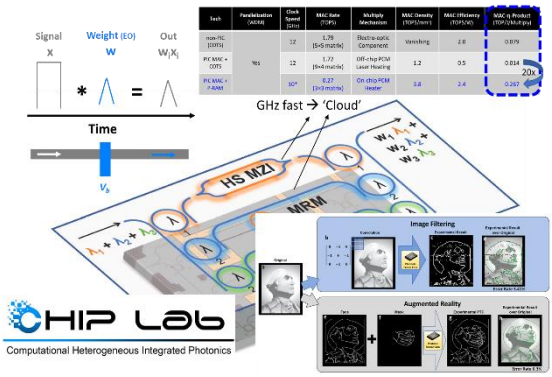

Figure 5: Schematic of the Integrated Photonic Computing Accelerator.

IV. What are the Outcomes& Impacts (Science & Technology & Community)?

The proposed project aims to pioneer novel material structures optimized for photonic applications through a co-design approach, integrating materials science with device engineering and system-level considerations. This interdisciplinary approach will lead to the discovery of new phenomena and the development of innovative material structures tailored specifically for photonic applications. The project's advanced knowledge of PICs and their potential in photonic computing, particularly in enabling high-speed and energy-efficient information processing, promises to significantly advance our understanding of PICs and their broader applications. This research will have profound impacts across various domains, benefiting researchers and engineers in material science, hardware design, artificial intelligence, computer vision, physical inspection, and hardware testing. Moreover, the project aims to develop scalable, reliable, and highly energy-efficient system-on-chip solutions, fostering a deeper appreciation of the value and interconnectedness of components across diverse fields. In terms of the semiconductor industry, the project's outcomes will offer advanced material integration techniques, co-design methodologies, and on-chip laser integration methods, enhancing performance efficiency, testing quality, and overall effectiveness. These advancements will not only benefit chip designers and manufacturers but also critical components in other sectors such as transportation, military, and computing. On a societal level, the project seeks to bolster consumer confidence in the safety and reliability of electronic equipment by emphasizing the importance of physical inspection. Furthermore, by addressing the national shortage of skilled labor in the semiconductor industry through workforce training initiatives, the project aims to cultivate a sustainable domestic workforce, thereby bolstering US competitiveness in the global market and enhancing national security.

(PI) Dr. Hamed Dalir and the entire team have been instrumental in advancing technology from fundamental research to applied innovations and further into practical applications. With a strong focus on the transition of technology, the team ensures that as soon as a technology evolves, there is a seamless progression towards its application in relevant fields.

References:

1. Feldmann, et al., “Parallel convolutional processing using an integrated photonic tensor core” Nature 589,52–58 (2021).
2. Amin, et al., “0.52 V mm ITO-based Mach-Zehnder modulator in silicon photonics” APL Photonics 3, 126104 (2018).
3. Gui, et al., “100 GHz micrometer-compact broadband monolithic ITO Mach–Zehnder interferometer modulator enabling 3500 times higher packing density” Nanophotonics 11, 4001–4009 (2022).
4. Sugavanam, et al., “Spectral correlations in a random distributed feedback fibre laser,” Nature Communications 8 (5 2017).
5. Lu, et al., “Flip-chip integration of tilted VCSELs onto a silicon photonic integrated circuit,” Optics Express 24, 16258 (7 2016).
6. Katumba, et al., “Low-loss photonic reservoir computing with multimode photonic integrated circuits,” Scientific reports 8(1), 2653 (2018).
7. Wang, et al., “Integrated lithium niobate electro-optic modulators operating at cmos-compatible voltages,” Nature 562(7725), 101–104 (2018).
8. Li, et al., “Co-design of a differential transimpedance amplifier and balanced photodetector for a sub-pj/bit silicon photonics receiver,” Optics Express 28(9), 14038–14054 (2020).
9. Feldmann, et al., “Parallel convolutional processing using an integrated photonic tensor core,” Nature 589(7840), 52–58 (2021).
10. Kumar, et al., “Quantum states of higher-order whispering gallery modes in a silicon micro-disk resonator,” JOSA B 37(8), 2231–2237 (2020).
11. Haffner, et al., “All-plasmonic mach–zehnder modulator enabling optical high-speed communication at the microscale,” Nature Photonics 9(8), 525–528 (2015).
12. Lindenmann, et al., “Photonic wire bonding: a novel concept for chip-scale interconnects,” Optics express 20(16), 17667–17677 (2012).
13. Wong, “The end of the road for 2d scaling of silicon cmos and the future of device technology” in [76th (DRC)], 1–2, IEEE (2018).
14. Huang, et al., “2d semiconductors for specific electronic applications: from device to system,” npj 2D Materials and Applications 6(1), 51 (2022).
15. Liu, et al. Two-dimensional materials for next-generation computing technologies. Nature Nanotechnology 15, 545–557 (2020).

Executive Summary

MEms-based Cascaded flat Optics (MECO) for universal optical modulation

Category: Information

PI: Haoning Tang, UC Berkeley, Cory Hall, Berkeley, CA 94720, hat431@g.harvard.edu

Introduction: The growing demand for advanced optical information technologies, including display, communications, and computing, necessitates adaptive components that support real-time, reconfigurable control of optical responses in multiple dimensions. Recent research in flat optics has significantly reduced the size of optical components such as sensors and detectors. However, a major limitation of passive flat optics is their inherent rigidity, which confines them to a limited set of functionalities in processing optical information. Current free-space on-chip flat optics devices lack multidimensional tunability. The recent development of tunable flat optics, which utilizes external stimuli on resonant subwavelength scatterers, enables dynamic control over the wavefront of light. Nonetheless, these tunable flat optics still lack the multidimensional controllability of electromagnetic wave properties due to the absence of tunability across multiple degrees of freedom. **This project aims to develop a 'universal' tunable flat optics solution that provides independent and continuous control over multiple characteristic properties of light for deterministic optical information processing.**

Objective and outcomes: We propose strategies for realizing this goal, specifically using our recently developed microelectromechanical system (MEMS)-based Cascaded Flat Optics (MECO) platform. This platform offers multiple mechanical degrees of freedom for various layers of flat optics, such as relative twist angle, gap, translational displacement, and tilting angle between different layers (Tang et al., arXiv:2312.09089; arXiv:2311.12030, 2023). The MECO platform serves as a programmable transfer element that can encode arbitrary functions and perform complex tasks using a single dynamic component with universal tunability to multidimensional optical properties. In this proposal, we will: (1) Discuss five multidimensional control architectures involving frequency, direction, polarization, spatial and spatiotemporal orbital angular momentum, and field intensity. We aim to harness these controls and integrate them into a wide range of functions, including filtering, beam-steering, multiplexing, and switching. This is particularly relevant for applications such as free-space communications, analog computing, and holographic displays that require enhanced information processing capabilities. (2) Use the MECO platform to explore fundamental physics properties such as photon-material interactions with unparalleled cavity modulation and precision. We aim to achieve robust control over structures at quantum-relevant length scales, which is crucial for harnessing quantum effects. This capability will facilitate the discovery of innovative methods to manipulate single photons or entangle photons, applicable in quantum computing.

Plan: The project will span 12 months and include optical modeling, fabrication, and measurement, as well as MEMS modeling, fabrication, and characterization. The MECO platform will be fabricated on a wafer scale at the Marvell Nanofabrication Laboratory at UC Berkeley. All measurements will be conducted at UC Berkeley, utilizing tunable CW, ultra-fast laser sources, and a home-built MEMS characterization kit in PI Tang's lab. We will acquire an additional lens kit, polarization optics, Photomultiplier tubes, and a spectrometer to build and characterize our setup. We will collaborate with Prof. Shanhui Fan from Stanford University on the theoretical modeling of cascaded flat-optics design, with Prof. Eric Mazur from Harvard University on the measurement of second harmonic generation, and with Prof. Evelyn Hu from Harvard University on III-V material fabrication.

Impact: Efficient and versatile on-chip manipulation of optical responses in multiple dimensions will facilitate their widespread use in a variety of applications, such as free-space communications (including 6G and IoT), analog computing, remote sensing, holographic displays, and quantum computing, which presents significant opportunities for the optics community. Additionally, the MECO platform enables researchers to investigate fundamental physical properties with unmatched cavity modulation precision at quantum-relevant scales, which is essential for single-photon manipulation in quantum communication. Lastly, given their large-scale CMOS compatibility and compact footprint, the MECO platform is not limited to single-pixel multidimensional information processing but also extends to row-column and perimeter operation.

MEms-based Cascaded flat Optics (MECO) for universal optical modulation

Dr. Haoning Tang, UC Berkeley, Department of Electrical Engineering and Computer Science

LITERATURE REVIEW

Flat optics[1–10], such as metasurface and photonic crystal slabs, are engineered as two-dimensional arrays of nanoscale resonant structures that manipulate light at a subwavelength scale, altering its fundamental properties such as phase,[11–15] polarization,[8] wavelength,[5,16,17] and momentum.[18] However, a critical drawback of passive flat optics is their inherent rigidity; once manufactured, their properties cannot be tuned, confining them to a set of predetermined functionalities. In contrast, the large demand for advanced optical applications, such as imaging, communications, LiDAR, remote sensing, and computing, calls for adaptive components that support real-time, reconfigurable wavefront customization.[19–22] Recent advancements in active, reconfigurable flat optics have made a significant leap in the field of optical modulation. Dynamic control over the optical response of the flat optics is then obtained upon application of an external stimulus, including field-effect tuning[23–27], electro-optical tuning[27–35], thermo-optical tuning[36,37], electrochemical tuning[38], structural changes in phase change materials[39–50] and liquid crystals[51–58], all-optics modulation[59–64], and mechanical deformation[65–75]. These external stimuli can change the resonant properties of subwavelength scatterers, dynamically controlling the wavefront of light at visible and near-infrared wavelengths. The ability to dynamically control optical responses in flat optics unlocks a multidimensional design space, which can be exploited by developing nanophotonic structures for arbitrary light manipulation.

PROBLEM STATEMENT/OBJECTIVE

However, current tunable flat optics typically allow only active and continuous control over the amplitude and phase of light from each nanostructure, limiting their use in multi-channel signal processing. Several key questions emerge regarding the development of universal tunable flat optics: How can we have universal tunable flat optics that enable more dynamic, independently addressable, and comprehensive control over all constitutive properties of light? Can these optics serve as programmable elements to encode functions and perform complex tasks, integrating them into applications like free-space communications (including 6G and IoT),[15,76] analog computing,[77] and holographic displays? [2,78–81] Several constraints exist in terms of addressing these key questions. First, from a design perspective, conventional flat optics are often limited to one-dimensional spatial modulation on the guided-mode resonances and extended modes.[82] Second, multidimensional control is constrained by the nature of external stimuli, and current technology primarily allows modulation across an entire array,[83–85] limiting the functionality of single-chip devices.[86] Therefore, advanced strategies to overcome interference between electromagnetic modes and ensure directed phase control, necessitating extensive multiphysics analysis and design, are essential for realizing these capabilities. Electrostatic MEMS-based mechanical modulation involves complex designs and offers modulation speeds from several kHz to GHz. The MEMS modulation gives rise to a wide-range optical response suitable for controlling multiple properties. It offers precise control, works across various temperatures and magnetic fields, and is compatible with thin-film and quantum materials.[69,87] These features make MEMS-tunable cascaded flat optics a promising approach for enabling multi-dimensional control at the single-unit cell level, allowing controllable interference between neighboring nanostructures within and across layers.

The tunability of advanced cascaded flat optics mainly stems from dynamically adjusting far- or near-field interactions between layers.[88–93] State-of-the-art devices typically manipulate far-field coupling, where layer separation exceeds the wavelength. Each layer modulates light propagation independently, combining to produce the optical effect. Examples include varifocal and Alvarez lenses,[94–100] tunable beam steering,[98,101–103] and more. However, many such devices operate sub-optimally due to oversized interlayer gaps or remain theoretical simulations. Achieving the desired overall function by directly adding the phase profiles of each layer is challenging due to the suboptimal gap sizes between layers, which are neither infinitely small nor equal to the Talbot length, requiring precise alignment and motion control.[104,105] Efforts to precisely control gap sizes in static cascaded flat optics through microfabrication have led to devices that support multiwavelength achromatic functions or minimize monochromatic aberrations with gaps close to or smaller than a wavelength.[91,92,106–108] Moreover, efforts have also been made in static cascaded flat optics to control the relative layer positions, such as creating moiré patterns or superlattices, while maintaining

small vertical gaps smaller than the operating wavelength for effective near-field coupling. [69,87,109–124] The guided mode and evanescent field in each layer couple simultaneously. While fine-tuning the topology and geometry of these resonant structures can significantly modulate the coupling behavior, changing the relative positions of different layers also disrupts system symmetry, enhancing mode coupling and phase accumulation. This approach adds functionalities such as anisotropic propagation,[125–128] beamforming,[115] tunable nanocavities,[121,129–131] tunable filters,[112,113] spatial light modulation,[101,117,132,133], and spatiotemporal light modulation.[109]

OUTCOMES

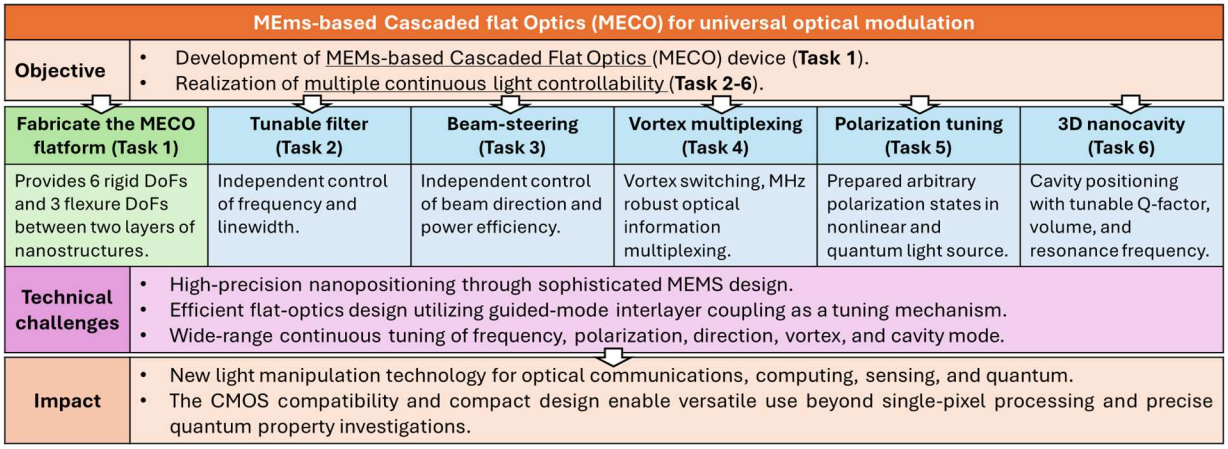

Figure 1 Overview of our proposal: Objective, tasks, challenge, and impact.

Achieving multidimensional control of universal optical properties in cascaded flat-optics requires active manipulation of optical layers with any relative position. The main challenges include precise layer alignment, parallelism, nanoscale motion control, and compact integration. Current MEMS-flat optics designs do not offer nanometer-scale controllability in multidimensions,[65,67,68,71,94,97,134–136] and using a motion stage often fails to maintain parallelism and stability. Our recent research shows that electrostatic MEMS, with their multidimensional nanoscale precision, have significant potential to address these issues.[69,137] Building on prior results, we propose to use our recently developed MEms-tunable Cascaded flat Optics (MECO) platform that resolves the problems of low integrability and limited tunability in existing tunable cascaded metasurface devices (Fig. 1). The MECO platform integrates six rigid bodies and two flexural degrees of freedom (DoFs) in a single MEMS flat optics device, allowing for active manipulation of far-field, near-field, symmetry, topology, effective index, and nonlinearity of the meta-structures. This design enables independent control of various optical properties, including frequency, phase, intensity, direction, spatial, and temporal light. Unlike systems that depend on optical matrices, The MECO platform consolidates multiple functionalities into a single pixel, with modulation speeds ranging from several kHz to GHz. Additionally, it can be combined with other modulation methods, such as electrical, thermal, and optical modulation. This proposal outlines strategies for achieving universal light control using the MECO platform. We identify key challenges in mechanical control architecture and tunable cascaded flat optics design and applications.

Mechanical control architecture. Conventional flat optics are dielectric or metal nanostructures with small elasticity, which can be regarded as rigid bodies. They have six DoFs, which can be specified with three orthogonal coordinates and x, y, z, and three angles of rotation, θ_x, θ_y, and θ_z (Fig. 2a). Movement of the body is defined by three translations, inplane translation Δx, Δy, and vertical translation Δz, and three rotations, the inplane tilting $\Delta\theta_x$, $\Delta\theta_y$ and twisting $\Delta\theta_z$. In comparison, flexure flat optics, such as polymer nanostructures or nanostructures embedded in the elastic substrate, have three additional mechanical DoFs: stretch and compression Δg (Fig. 2b) and bending $\Delta\sigma$ (Fig. 2c). The spacing between unit cells can be directly changed. MEMS electrostatic actuators will be used to control both rigid body and flexure DoFs, which offer a fast response, zero backlash (hysteresis), and compatibility with a wide range of environments and are ideal for low-power, on-chip cascaded flat optics devices. The MECO platform achieves both rigid-body and flexure DoF of a layer of flat optic through a coupling design of vertical actuators, translational actuators, and rotary actuators (Fig. 2c-e). The basic operation of our designed electrostatic vertical

actuators involves a parallel plate capacitor setup with a fixed plate and a movable plate that displaces perpendicularly to a fixed platform, controlled by an external voltage V_z (Fig. 2c). This action allows the vertical actuator to provide motion in the z-direction (Δz=0-5μm) and tilt motions ($\Delta\theta_x$, $\Delta\theta_y$=0-3°). We designed the translational actuators that operate on a similar principle, where the movable plate moves horizontally in response to external voltages V_x or V_y, enabling motion in the x and y directions (Δx, Δy=0-20μm) (Fig. 2d). This mechanism also allows for stretching, compressing (Δg), and bending ($\Delta\sigma$) motions in flat optics by varying V_x and V_y positively and negatively. The rotary actuators (Fig. 2e), also use the actuation force from parallel capacitors. Our design breaks the capacitor into as many smaller capacitors as possible. One ends up either in a `comb' design or a `teeth' design. This design allows for constructing a stepper motor-like mechanism around a rotary core[138], optimizing force and range for rotation ($\Delta\theta_z$=0-60°), corresponding to in-plane twisting. Multidimensional control of cascaded flat optics requires tunability in multiple DoFs. Therefore, the basic actuators above need to be coupled together. We designed an inter-stage electrical network with vias to allow each actuator to operate independently while collectively driving the flat optics, minimizing crosstalk between actuators. Other layers of flat optics can be wafer bonded to the active flat optics layer, allowing the relative position between the two layers to be tuned arbitrarily (Fig. 2f). This integration strategy, when combined with devices like photonic crystal surface-emitting lasers (PCSELs),[12,139] metalenses,[140] and space plates,[141] aims to enable previously inaccessible on-chip applications such as miniaturized tunable lasers[142] and miniaturized atomic clocks[143,144].

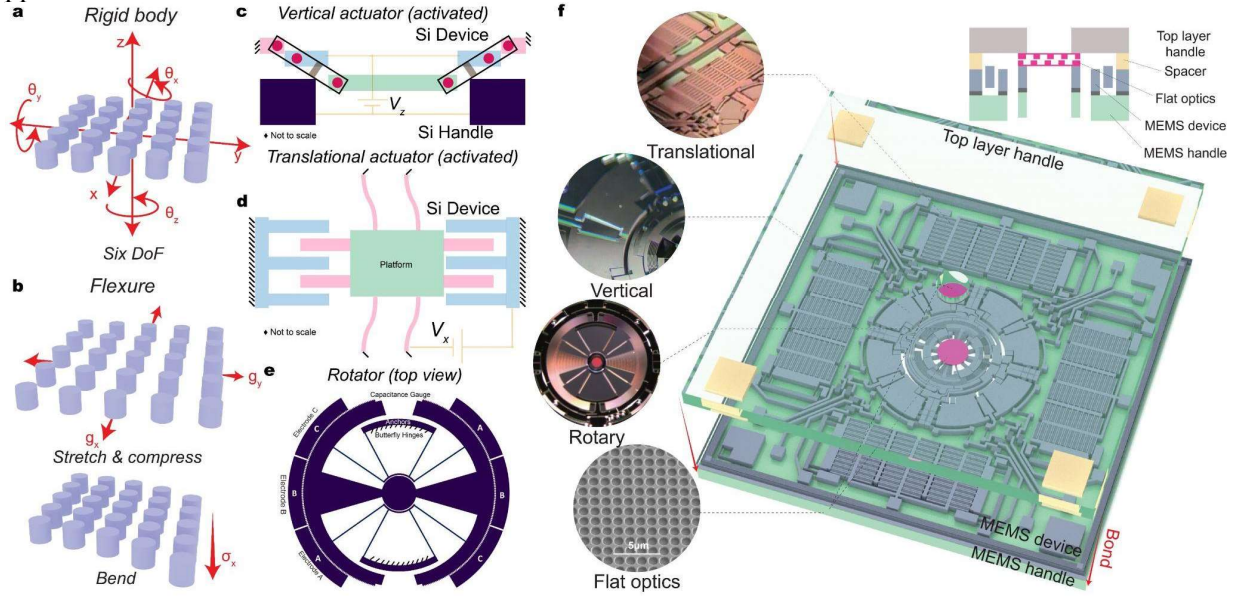

Figure 2 Mechanical degrees of freedom (DoFs) of MECO platform. (a) Three-dimensional rigid bodies have six DoF, which can be specified with three orthogonal coordinates, x, y, z, and three angles of rotation, θ_x, θ_y, and θ_z. (b) Flat optics as flexures can obtain three DoF through MECO: in-plane stretch and compression (g_x and g_y) and bending (only σ_x is represented). (c-h) Principle of the vertical actuator, translational actuator, and rotary stepper. (c) The vertical actuator is driven by a voltage V_z. (d) The translational actuator is driven by a voltage V_x. (e) Rotary actuator with three-phase electrode driven by micro-stepping voltage waveform. (f) Illustration and microscope image of a MECO flatform featuring three basic actuators (translational, vertical, and rotary) coupled together. One layer of flat optics is fabricated at the core of the MEMS, and another layer is fabricated on the top capping layer (made transparent for illustration), wafer-bonded to the bottom layer. All cascaded flat optics layers are suspended in a window.

MECO for multidimensional light manipulation. We propose using MEMS-enabled tuning DoFs in combination with cascaded flat optics to develop multifunctional devices. We have already developed a MEMS-tunable twisted bilayer photonic crystal (PhC) and demonstrated the modulation of bandstructure, frequency, and polarization by tuning twist angle ($\Delta\theta_z$) and vertical gap (Δz). This work led to a chip-based single-pixel sensor that simultaneously resolves hyperspectral and hyperpolarimetric images.[69] Triggered by this successful demonstration, we also propose the following devices. In the following section, we will show how we use *one MECO device for multiple purposes in light modulation*.

Purpose A. Frequency and linewidth modulation (tunable filter). Color filtering is a key function in applications such as sensors and optical communication devices. Yet, there are many challenges in using a

flat optics structure with one tunable DoF to create a tunable narrow-band filter. It is difficult to independently tune frequency and linewidth while maintaining high transmission simultaneously in a miniaturized device.[145–148] We aim to use MECO to develop an ideal tunable filter that fully controls broadband wavelength and linewidth, leveraging the DoFs of $\Delta\theta_z$ and Δz in bilayer cascaded flat optics. Our initial simulations (Fig.3a) demonstrate the ability to tune the band frequency response over a 100nm range around the telecom wavelength, maintaining constant linewidth and reflection, allowing for independent frequency and linewidth tuning.

Purpose B. Direction and frequency modulation (Beam-steering). Free-space beam steering is important for applications like LiDAR and telecommunications. Typical methods involve phased array design, requiring intricate control over many active components.[136] Other methods that avoid complicated phase control rely on wavelength tuning.[149] A compact free-space beam steering device that takes input from and sends the output to the free space is highly desired but absent. We propose demonstrating such a device based on tuning the $\Delta\theta_z$, Δx, and Δz of the two designed cascaded flat optics slabs. Our preliminary simulations (Fig. 3b) show that these slabs can be rotated in-plane to diffract incident light at various angles up to ±87° while maintaining the same wavelength, with 80% power efficiency across a wide angle range that is unaffected by polarization. This wide-range tunability and power efficiency cannot be achieved with state-of-the-art free space beam steering devices.[98,101–103]

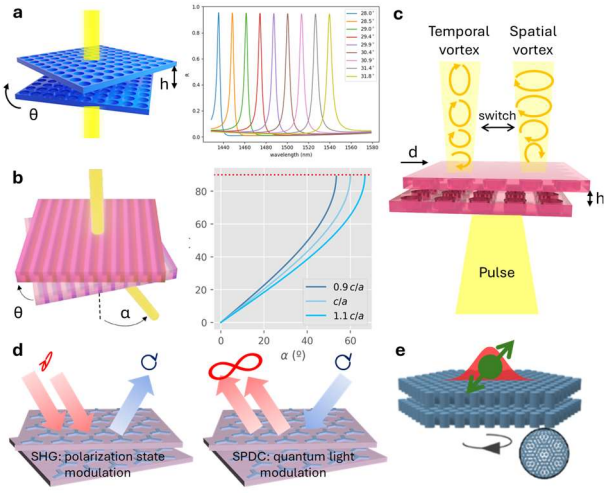

Figure 3 Proposed tunable cascaded flat optics devices based on the MECO platform. (a) Tunable filter that tunes the wavelength and linewidth independently. (b) Ultra-wide Field of view beam-steering. (c) Modulation of spatial and spatiotemporal vortex beam through symmetry breaking. (d) The tunable nonlinear and quantum light source for arbitrary polarization and entangled states. (e) 3D cavity for single photon lasing and manipulation.

Purpose C. Spatial and spatiotemporal vortex light modulation. The bilayer cascaded flat optics have shown potential in tailoring chiral-optical effects and elliptical polarizations and creating robust vortex beams.[101,109,117,132,133] Recently, we showed theoretically that the bilayer tunability around topological optical singularities allows precise control of arbitrary polarization states in momentum space[150], bound-state-in-continuum,[69,132,150] spatial[117] and spatiotemporal[109] orbital angular momentum, and unidirectional radiation[109]. While this modulation type is still far from being explored, the experiment remains unrealized due to the lack of a precision tuning approach. We propose to use the MECO platform to enhance this capability through its ability to disrupt the σz-, rotation-, and mirror-symmetry of electromagnetic modes. We will further advance this research by developing a high-speed MECO platform with a modulation speed ranging from MHz to GHz, which allows the nano-scale spatial modulation that significantly alters different topological vortices (Fig. 3c). By matching the modulation speed with the laser rep-rate, we will multiplex each pulse with different topologically protected information. The high-speed multiplexing of optical vortices will be combined with the imaging capability in nonlocal flat optics to develop the time-varying optical holography device.[151,152] The actuation rate can potentially exceed the laser linewidth (typically under 1 MHz), enabling the generation of additional frequency harmonics.

Purpose D. Arbitrary polarization states. Nonlinear optical frequency conversion is pivotal in classical and quantum information processing, where phase matching is necessary. Such phase matching can be achieved through several different mechanisms, including the use of anisotropy or the use of a proper waveguide geometry design. The cascaded flat optics system introduces an additional DoF for phase matching. We recently found that, in a system with C_3 rotational symmetry, twisting adds a nonlinear Pancharatnam-Berry phase term to the second harmonic polarization increased by $3\theta_z$, which, along with the Δz and cavity interference, tune the nonlinear phase drastically around topological singularities.[87] This controllability applies to any harmonic order nonlinearity in structures with varying symmetries.[153,154] Reversely, the spontaneous parametric down-conversion process produces entangled photon pairs, where the bell states

and entanglement entropy can also be fully modulated through $\Delta\theta_z$ and Δz as well. This extensive tunability works in all wavelength ranges. We propose to realize such on-chip tunable nonlinear and entangled photon-pair sources through the combination of the MECO platform flat optics based on Silicon Nitride (Fig. 3d). The result will lead to new mechanisms for arbitrary ultrafast and entangled photon switching and develop applications in quantum logic gating[155–157] and optical auto-correlation.[158]

Purpose E. Facilitating quantum interconnects with bespoke modes in 3D nanocavities. A general problem in nanophotonics is the limited precision in positioning single emitters within the high-field intensity region. While conventional Fabry-Perot cavities offer high Q-factors, they come with large mode volumes and limited achievable Purcell enhancement, emitter directionality, and polarization. Cascaded flat optics introduce innovative opportunities in emitter-photonic interfaces. Such a system unlocks unconventional dynamic nanocavities, including tunable chiral cavities,[133,159–161] tunable flat-band localization cavities,[121,129,162,163] tunable frequency cavities,[110–112,164] tunable structural light cavities,[117,132,150] and tunable anisotropic cavities.[122,124,127] We propose to use the MECO platform to customize the tuning of cascaded flat optics nanocavities, creating specific electromagnetic field environments for single-photon emitters and other optical materials. We anticipate two primary scientific pursuits: (1) The exploration of methods to tune the high-field positioning, polarization, orbital angular momentum, emission lifetime, and optical coherence of single-photon emitters, and (2) the enhancement of the chiral light-matter interaction in chirality-preserving nanocavities.[165,166] For (1), we will study the integration of III-V quantum dots and defects in diamonds through the MECO platform. A specific first cavity design relies on the twist-angle ($\Delta\theta_z$) tuning between two opposing III-V semiconductor PhC slabs (Fig. 3e)[112,129]. At a so-called 'magic' twist angle, the band structure of the material exhibits high-Q flat bands, giving rise to momentum-free trapping of Bloch waves in both transverse and vertical directions. The position of superlattice localization can be changed through translational displacement (Δx, Δy), providing positional control over the high-field region. This capability will be harnessed to show tunable coupling with spatially varied quantum emitters. These 3D nanocavities should not cause extra dephasing, with anticipated Purcell factors nearing 10^3 that enable highly coherent single-photon emission. We will establish a fully controllable emitter-photonic interface that paves the way for applications like spectrally-selective enhancement of biexciton or single-exciton emission in quantum dots[167,168] and tailored emission directivity and polarization in single-photon emitters.[169] For (2), the design of arbitrary bilayer flat-optics cavities at low temperatures is a unique approach to access bespoke states of exciton-polaritons with optical chirality. Several recent works propose 3D tunable bilayer meta-optical cavities that preserve chirality and possess high Q-factors and degrees of circular polarization.[165,166] Such structures generally require precise (several nanometers) positioning of the two substrates with respect to each other, which we will realize through the MECO platform. The integration of gain materials, e.g., semiconducting polymers of perovskite nanoplatelets, can form chiral exciton-polaritons,[170] expected to possess high chiroptical activity in addition to other well-known exotic effects common to exciton-polaritons, including spatially-coherent emission,[171] Bose-Einstein-Condensation,[172] polariton-lasing,[173] single-photon optical non-linearities, bi-stability, optical limiter behavior,[174] and long-range coherent energy transport.[175]

IMPACTS

The active control of the optical response in multidimensions presents significant opportunities for our society as a bottleneck solution to the lack of wide tunability in the current on-chip tunable device. No other multidimensional tunable flat optics devices exist. The MECO platform provides a pathway for multidisciplinary researchers to design universal tunable on-chip optical devices, which is particularly interesting for many imaging and communication applications requiring enhanced information processing capability. The MECO platform will empower researchers to explore fundamental physics properties such as topological photonics and photon-material interactions with multiple cavity modulation and precision. It also achieves robust control over structures at scales of quantum-relevant lengths and facilitates the manipulation of single photons or entangled photons applicable in quantum computing. The MECO platform will critically impact education and workforce development. We expect it to be used in the research training of at least 1-2 Ph.D. students/year. Integration with several optics courses at Berkeley is permitted, which will be disseminated for democratized access. Undergraduate and high school students will participate in all research phases through NSF REU and Berkeley's URAP programs.

REFERENCES

1. Kildishev, A. V., Boltasseva, A. & Shalaev, V. M. Planar photonics with metasurfaces. *Science* **339**, 1232009 (2013).
2. Nikolov, D. K. *et al.* Metaform optics: Bridging nanophotonics and freeform optics. *Sci Adv* **7**, (2021).
3. Yu, N. & Capasso, F. Flat optics with designer metasurfaces. *Nat. Mater.* **13**, 139–150 (2014).
4. Capasso, F. The future and promise of flat optics: a personal perspective. *Nanophotonics* **7**, 953–957 (2018).
5. Chen, W. T., Zhu, A. Y. & Capasso, F. Flat optics with dispersion-engineered metasurfaces. *Nature Reviews Materials* **5**, 604–620 (2020).
6. Lawrence, M., Barton, D. R., 3rd & Dionne, J. A. Nonreciprocal Flat Optics with Silicon Metasurfaces. *Nano Lett.* **18**, 1104–1109 (2018).
7. Kuznetsov, A. I. *et al.* Roadmap for Optical Metasurfaces. *ACS Photonics* **11**, 816–865 (2024).
8. Zhao, Y. & Alù, A. Manipulating light polarization with ultrathin plasmonic metasurfaces. *Phys. Rev. B Condens. Matter* **84**, 205428 (2011).
9. Lin, D., Fan, P., Hasman, E. & Brongersma, M. L. Dielectric gradient metasurface optical elements. *Science* **345**, 298–302 (2014).
10. Urbas, A. M. *et al.* Roadmap on optical metamaterials. *J. Opt.* **18**, 093005 (2016).
11. Forbes, A. Structured matter creates toroidal structured light. *Light Sci Appl* **11**, 230 (2022).
12. Sroor, H. *et al.* High-purity orbital angular momentum states from a visible metasurface laser. *Nat. Photonics* **14**, 498–503 (2020).
13. He, C., Shen, Y. & Forbes, A. Towards higher-dimensional structured light. *Light Sci Appl* **11**, 205 (2022).
14. Choudhury, S. *et al.* Pancharatnam–berry phase manipulating metasurface for visible color hologram based on low loss silver thin film. *Adv. Opt. Mater.* **5**, 1700196 (2017).
15. Zhao, Z., Wang, J., Li, S. & Willner, A. E. Metamaterials-based broadband generation of orbital angular momentum carrying vector beams. *Opt. Lett.* **38**, 932–934 (2013).
16. Liu, C. *et al.* Photon Acceleration Using a Time-Varying Epsilon-near-Zero Metasurface. *ACS Photonics* **8**, 716–720 (2021).
17. Pang, K. *et al.* Adiabatic Frequency Conversion Using a Time-Varying Epsilon-Near-Zero Metasurface. *Nano Lett.* **21**, 5907–5913 (2021).
18. Lustig, E. *et al.* Photonic time-crystals - fundamental concepts [Invited]. *Opt. Express* **31**, 9165–9170 (2023).
19. Saha, S., Shah, D., M. Shalaev, V. & Boltasseva, A. Tunable metasurfaces: Controlling light in space and time. *Opt. Photonics News* **32**, 34 (2021).
20. Sasikala, V. & Chitra, K. All optical switching and associated technologies: a review. *J. Opt.* **47**, 307–317 (2018).
21. Zhang, Z. *et al.* Recent Advances in Reconfigurable Metasurfaces: Principle and Applications. *Nanomaterials (Basel)* **13**, (2023).
22. Abdelraouf, O. A. M. *et al.* Recent Advances in Tunable Metasurfaces: Materials, Design, and Applications. *ACS Nano* **16**, 13339–13369 (2022).
23. Shah, D., Kudyshev, Z. A., Saha, S., Shalaev, V. M. & Boltasseva, A. Transdimensional material platforms for tunable metasurface design. *MRS Bull.* **45**, 188–195 (2020).
24. Huang, Y.-W. *et al.* Gate-Tunable Conducting Oxide Metasurfaces. *Nano Lett.* **16**, 5319–5325 (2016).
25. Ju, L. *et al.* Graphene plasmonics for tunable terahertz metamaterials. *Nat. Nanotechnol.* **6**, 630–634 (2011).
26. Papadakis, G. T. & Atwater, H. A. Field-effect induced tunability in hyperbolic metamaterials. *Phys. Rev. B Condens. Matter* **92**, 184101 (2015).
27. Anopchenko, A., Tao, L., Arndt, C. & Lee, H. W. H. Field-Effect Tunable and Broadband Epsilon-Near-Zero Perfect Absorbers with Deep Subwavelength Thickness. *ACS Photonics* **5**, 2631–2637 (2018).

28. Benea-Chelmus, I.-C. *et al.* Electro-optic spatial light modulator from an engineered organic layer. *Nat. Commun.* **12**, 5928 (2021).
29. Cheng, Z. *et al.* On-chip silicon electro-optical modulator with ultra-high extinction ratio for fiber-optic distributed acoustic sensing. *Nat. Commun.* **14**, 7409 (2023).
30. Shirmanesh, G. K., Sokhoyan, R., Wu, P. C. & Atwater, H. A. Electro-optically Tunable Multifunctional Metasurfaces. *ACS Nano* **14**, 6912–6920 (2020).
31. Wu, P. C., Sokhoyan, R., Shirmanesh, G. K., Cheng, W.-H. & Atwater, H. A. Near-infrared active metasurface for dynamic polarization conversion. *Adv. Opt. Mater.* **9**, 2100230 (2021).
32. Forouzmand, A. *et al.* Tunable all-dielectric metasurface for phase modulation of the reflected and transmitted light via permittivity tuning of indium tin oxide. *Nanophotonics* **8**, 415–427 (2019).
33. Park, J., Kang, J.-H., Liu, X. & Brongersma, M. L. Electrically Tunable Epsilon-Near-Zero (ENZ) Metafilm Absorbers. *Sci. Rep.* **5**, 15754 (2015).
34. Park, J. *et al.* Dynamic thermal emission control with InAs-based plasmonic metasurfaces. *Sci Adv* **4**, eaat3163 (2018).
35. Yao, Y. *et al.* Electrically tunable metasurface perfect absorbers for ultrathin mid-infrared optical modulators. *Nano Lett.* **14**, 6526–6532 (2014).
36. Lewi, T., Evans, H. A., Butakov, N. A. & Schuller, J. A. Ultrawide Thermo-optic Tuning of PbTe Meta-Atoms. *Nano Lett.* **17**, 3940–3945 (2017).
37. Lee, B. S. *et al.* On-chip thermo-optic tuning of suspended microresonators. *Opt. Express* **25**, 12109–12120 (2017).
38. Thyagarajan, K., Sokhoyan, R., Zornberg, L. & Atwater, H. A. Millivolt Modulation of Plasmonic Metasurface Optical Response via Ionic Conductance. *Adv. Mater.* **29**, (2017).
39. Chu, C. H. *et al.* Active dielectric metasurface based on phase-change medium (Laser Photonics Rev. 10(6)/2016). *Laser Photon. Rev.* **10**, 1063–1063 (2016).
40. Zhang, Y. *et al.* Broadband transparent optical phase change materials for high-performance nonvolatile photonics. *Nat. Commun.* **10**, 4279 (2019).
41. Shalaginov, M. Y. *et al.* Reconfigurable all-dielectric metalens with diffraction-limited performance. *Nat. Commun.* **12**, 1225 (2021).
42. Zhang, Y. *et al.* Electrically reconfigurable non-volatile metasurface using low-loss optical phase-change material. *Nat. Nanotechnol.* **16**, 661–666 (2021).
43. Kim, Y. *et al.* Phase Modulation with Electrically Tunable Vanadium Dioxide Phase-Change Metasurfaces. *Nano Lett.* **19**, 3961–3968 (2019).
44. Ding, F., Yang, Y. & Bozhevolnyi, S. I. Dynamic metasurfaces using phase-change chalcogenides. *Adv. Opt. Mater.* **7**, 1801709 (2019).
45. Tittl, A. *et al.* A Switchable Mid-Infrared Plasmonic Perfect Absorber with Multispectral Thermal Imaging Capability. *Adv. Mater.* **27**, 4597–4603 (2015).
46. Wuttig, M., Bhaskaran, H. & Taubner, T. Phase-change materials for non-volatile photonic applications. *Nat. Photonics* **11**, 465–476 (2017).
47. Kats, M. A. *et al.* Vanadium Dioxide as a Natural Disordered Metamaterial: Perfect Thermal Emission and Large Broadband Negative Differential Thermal Emittance. *Phys. Rev. X* **3**, 041004 (2013).
48. Jeyasingh, R. *et al.* Ultrafast characterization of phase-change material crystallization properties in the melt-quenched amorphous phase. *Nano Lett.* **14**, 3419–3426 (2014).
49. Chaudhary, K. *et al.* Polariton nanophotonics using phase-change materials. *Nat. Commun.* **10**, 4487 (2019).
50. Raeis-Hosseini, N. & Rho, J. Metasurfaces Based on Phase-Change Material as a Reconfigurable Platform for Multifunctional Devices. *Materials* **10**, (2017).
51. Badloe, T. *et al.* Liquid crystal-powered Mie resonators for electrically tunable photorealistic color gradients and dark blacks. *Light Sci Appl* **11**, 118 (2022).
52. Izdebskaya, Y. V., Yang, Z., Shvedov, V. G., Neshev, D. N. & Shadrivov, I. V. Multifunctional Metasurface Tuning by Liquid Crystals in Three Dimensions. *Nano Lett.* **23**, 9825–9831 (2023).
53. Zhuang, X. *et al.* Active terahertz beam steering based on mechanical deformation of liquid crystal

elastomer metasurface. *Light Sci Appl* **12**, 14 (2023).
54. Dolan, J. A. *et al.* Broadband Liquid Crystal Tunable Metasurfaces in the Visible: Liquid Crystal Inhomogeneities Across the Metasurface Parameter Space. *ACS Photonics* **8**, 567–575 (2021).
55. Lininger, A. *et al.* Optical properties of metasurfaces infiltrated with liquid crystals. *Proc. Natl. Acad. Sci. U. S. A.* **117**, 20390–20396 (2020).
56. Gorkunov, M. V. *et al.* Double-sided liquid crystal metasurfaces for electrically and mechanically controlled broadband visible anomalous refraction. *Nanophotonics* **11**, 3901–3912 (2022).
57. Li, J., Yu, P., Zhang, S. & Liu, N. Electrically-controlled digital metasurface device for light projection displays. *Nat. Commun.* **11**, 3574 (2020).
58. Nouman, M. T. *et al.* Vanadium dioxide based frequency tunable metasurface filters for realizing reconfigurable terahertz optical phase and polarization control. *Opt. Express* **26**, 12922–12929 (2018).
59. Shaltout, A., Liu, J., Shalaev, V. M. & Kildishev, A. V. Optically active metasurface with non-chiral plasmonic nanoantennas. *Nano Lett.* **14**, 4426–4431 (2014).
60. Shcherbakov, M. R. *et al.* Ultrafast all-optical tuning of direct-gap semiconductor metasurfaces. *Nat. Commun.* **8**, 17 (2017).
61. Iyer, P. P. *et al.* Sub-picosecond steering of ultrafast incoherent emission from semiconductor metasurfaces. *Nat. Photonics* **17**, 588–593 (2023).
62. Shaltout, A. M., Shalaev, V. M. & Brongersma, M. L. Spatiotemporal light control with active metasurfaces. *Science* **364**, (2019).
63. Shaltout, A. M. *et al.* Spatiotemporal light control with frequency-gradient metasurfaces. *Science* **365**, 374–377 (2019).
64. Clerici, M. *et al.* Controlling hybrid nonlinearities in transparent conducting oxides via two-colour excitation. *Nat. Commun.* **8**, 15829 (2017).
65. Zhao, X., Duan, G., Li, A., Chen, C. & Zhang, X. Integrating microsystems with metamaterials towards metadevices. *Microsyst Nanoeng* **5**, 5 (2019).
66. Ou, J.-Y., Plum, E., Zhang, J. & Zheludev, N. I. An electromechanically reconfigurable plasmonic metamaterial operating in the near-infrared. *Nat. Nanotechnol.* **8**, 252–255 (2013).
67. Arbabi, E. *et al.* MEMS-tunable dielectric metasurface lens. *Nat. Commun.* **9**, 812 (2018).
68. Dirdal, C. A. *et al.* MEMS-tunable dielectric metasurface lens using thin-film PZT for large displacements at low voltages. *Opt. Lett.* **47**, 1049–1052 (2022).
69. Tang, H. *et al.* On-Chip Multidimensional Dynamic Control of Twisted Moiré Photonic Crystal for Smart Sensing and Imaging. *arXiv [physics.optics]* (2023).
70. Zhang, X. *et al.* Reconfigurable Metasurface for Image Processing. *Nano Lett.* **21**, 8715–8722 (2021).
71. He, S., Yang, H., Jiang, Y., Deng, W. & Zhu, W. Recent Advances in MEMS Metasurfaces and Their Applications on Tunable Lens. *Micromachines (Basel)* **10**, (2019).
72. Xu, L. *et al.* Kirigami Nanocomposites as Wide-Angle Diffraction Gratings. *ACS Nano* **10**, 6156–6162 (2016).
73. Shyu, T. C. *et al.* A kirigami approach to engineering elasticity in nanocomposites through patterned defects. *Nat. Mater.* **14**, 785–789 (2015).
74. Lee, C.-W., Choi, H. J. & Jeong, H. Tunable metasurfaces for visible and SWIR applications. *Nano Converg* **7**, 3 (2020).
75. He, Q., Sun, S. & Zhou, L. Tunable/Reconfigurable Metasurfaces: Physics and Applications. *Research* **2019**, 1849272 (2019).
76. Zhao, Z. *et al.* Experimental demonstration of 16-Gbit/s millimeter-wave communications link using thin metamaterial plates to generate data-carrying orbital-angular-momentum beams. in *2015 IEEE International Conference on Communications (ICC)* 1392–1397 (IEEE, 2015).
77. Wang, Z. *et al.* Metasurface on integrated photonic platform: from mode converters to machine learning. *Nanophotonics* **11**, 3531–3546 (2022).
78. Ha, Y., Smirnov, V., Glebov, L. & Rolland, J. P. Optical modeling of a holographic single-element head-mounted display. in *Helmet- and Head-Mounted Displays IX: Technologies and Applications*

vol. 5442 254–260 (SPIE, 2004).
79. Cakmakci, O. & Rolland, J. Head-worn displays: A review. *J. Display Technol.* **2**, 199–216 (2006).
80. Rolland, J. P. *et al.* Freeform optics for imaging. *Optica* **8**, 161 (2021).
81. Cheng, F. *et al.* Mechanically tunable focusing metamirror in the visible. *Opt. Express* **27**, 15194–15204 (2019).
82. Shastri, K. & Monticone, F. Nonlocal flat optics. *Nat. Photonics* **17**, 36–47 (2022).
83. Weigand, H. *et al.* Enhanced Electro-Optic Modulation in Resonant Metasurfaces of Lithium Niobate. *ACS Photonics* **8**, 3004–3009 (2021).
84. Malek, S. C., Overvig, A. C., Shrestha, S. & Yu, N. Active nonlocal metasurfaces. *Nanophotonics* **10**, 655–665 (2021).
85. Saha, S., Dutta, A., DeVault, C., Shalaev, V. M. & Boltasseva, A. Ultrafast tunable metasurface with transparent conducting oxide antenna array. in *Conference on Lasers and Electro-Optics* (OSA, Washington, D.C., 2018). doi:10.1364/cleo_qels.2018.fth4m.4.
86. Park, J. *et al.* All-solid-state spatial light modulator with independent phase and amplitude control for three-dimensional LiDAR applications. *Nat. Nanotechnol.* **16**, 69–76 (2021).
87. Tang, H. *et al.* An on-chip platform for multi-degree-of-freedom control of two-dimensional quantum and nonlinear materials. *arXiv [cond-mat.mes-hall]* (2023).
88. Fernández-Hurtado, V., García-Vidal, F. J., Fan, S. & Cuevas, J. C. Enhancing Near-Field Radiative Heat Transfer with Si-based Metasurfaces. *Phys. Rev. Lett.* **118**, 203901 (2017).
89. Balli, F., Sultan, M., Lami, S. K. & Hastings, J. T. A hybrid achromatic metalens. *Nat. Commun.* **11**, 3892 (2020).
90. Yang, B., Liu, T., Guo, H., Xiao, S. & Zhou, L. High-performance meta-devices based on multilayer meta-atoms: interplay between the number of layers and phase coverage. *Sci Bull (Beijing)* **64**, 823–835 (2019).
91. Avayu, O., Almeida, E., Prior, Y. & Ellenbogen, T. Composite functional metasurfaces for multispectral achromatic optics. *Nat. Commun.* **8**, 14992 (2017).
92. Zhou, Y. *et al.* Multilayer Noninteracting Dielectric Metasurfaces for Multiwavelength Metaoptics. *Nano Lett.* **18**, 7529–7537 (2018).
93. Shaltout, A. M., Kim, J., Boltasseva, A., Shalaev, V. M. & Kildishev, A. V. Ultrathin and multicolour optical cavities with embedded metasurfaces. *Nat. Commun.* **9**, 2673 (2018).
94. Arbabi, E. *et al.* MEMS-tunable dielectric metasurface lens Nat. *Commun* **9**, 812 (2018).
95. Colburn, S., Zhan, A. & Majumdar, A. Varifocal zoom imaging with large area focal length adjustable metalenses. *Optica, OPTICA* doi:10.1364/OPTICA.5.000825.
96. Colburn, S. & Majumdar, A. Simultaneous Achromatic and Varifocal Imaging with Quartic Metasurfaces in the Visible. *ACS Photonics* **7**, 120–127 (2020).
97. Han, Z., Colburn, S., Majumdar, A. & Böhringer, K. F. MEMS-actuated metasurface Alvarez lens. *Microsyst Nanoeng* **6**, 79 (2020).
98. Wang, C. *et al.* Tunable beam splitter using bilayer geometric metasurfaces in the visible spectrum. *Opt. Express* **28**, 28672–28685 (2020).
99. Wei, Y. *et al.* Compact optical polarization-insensitive zoom metalens doublet. *Adv. Opt. Mater.* **8**, 2000142 (2020).
100. Qian, Y., Hu, B., Du, Z. & Liu, J. Reinforced design method for moiré metalens with large spacing. *Opt. Express* **29**, 26496–26508 (2021).
101. Cai, X. *et al.* Dynamically controlling terahertz wavefronts with cascaded metasurfaces. *Adv. Photonics* **3**, (2021).
102. Che, X. *et al.* Generalized phase profile design method for tunable devices using bilayer metasurfaces. *Opt. Express* **29**, 44214 (2021).
103. Zhang, L. *et al.* Highly Tunable Cascaded Metasurfaces for Continuous Two-Dimensional Beam Steering. *Adv. Sci.* **10**, e2300542 (2023).
104. Wen, J., Zhang, Y. & Xiao, M. The Talbot effect: recent advances in classical optics, nonlinear optics, and quantum optics. *Adv. Opt. Photon., AOP* doi:10.1364/AOP.5.000083.
105. Kim, M.-S., Scharf, T., Menzel, C., Rockstuhl, C. & Herzig, H. P. Talbot images of wavelength-

scale amplitude gratings. *Opt. Express* **20**, 4903–4920 (2012).
106. Zhou, Y. *et al.* Multifunctional metaoptics based on bilayer metasurfaces. *Light Sci Appl* **8**, 80 (2019).
107. Arbabi, A. *et al.* Miniature optical planar camera based on a wide-angle metasurface doublet corrected for monochromatic aberrations. *Nat. Commun.* **7**, 13682 (2016).
108. Groever, B., Chen, W. T. & Capasso, F. Meta-Lens Doublet in the Visible Region. *Nano Lett.* **17**, 4902–4907 (2017).
109. Ni, X. *et al.* Three-Dimensional Reconfigurable Optical Singularities in Bilayer Photonic Crystals. *Phys. Rev. Lett.* **132**, 073804 (2024).
110. Lou, B., Wang, B., Rodríguez, J. A., Cappelli, M. & Fan, S. Tunable guided resonance in twisted bilayer photonic crystal. *Sci Adv* **8**, eadd4339 (2022).
111. Lou, B. & Fan, S. Tunable Frequency Filter Based on Twisted Bilayer Photonic Crystal Slabs. *ACS Photonics* **9**, 800–805 (2022).
112. Tang, H. *et al.* Experimental probe of twist angle-dependent band structure of on-chip optical bilayer photonic crystal. *Sci. Adv.* **9**, eadh8498 (2023).
113. Lou, B. *et al.* Theory for Twisted Bilayer Photonic Crystal Slabs. *Phys. Rev. Lett.* **126**, 136101 (2021).
114. Guo, C., Guo, Y., Lou, B. & Fan, S. Wide wavelength-tunable narrow-band thermal radiation from moiré patterns. *Appl. Phys. Lett.* **118**, 131111 (2021).
115. Liu, S. *et al.* Moiré metasurfaces for dynamic beamforming. *Sci Adv* **8**, eabo1511 (2022).
116. Wang, P. *et al.* Localization and delocalization of light in photonic moiré lattices. *Nature* **577**, 42–46 (2020).
117. Zhang, T. *et al.* Twisted moiré photonic crystal enabled optical vortex generation through bound states in the continuum. *Nat. Commun.* **14**, 6014 (2023).
118. Du, L. *et al.* Moiré photonics and optoelectronics. *Science* **379**, eadg0014 (2023).
119. Yu, D. *et al.* Moiré lattice in one-dimensional synthetic frequency dimension. *Phys. Rev. Lett.* **130**, 143801 (2023).
120. Krasnok, A. & Alù, A. Low-Symmetry Nanophotonics. *ACS Photonics* **9**, 2–24 (2022).
121. Dong, K. *et al.* Flat bands in magic-angle bilayer photonic crystals at small twists. *Phys. Rev. Lett.* **126**, 223601 (2021).
122. Hu, G., Zheng, C., Ni, J., Qiu, C.-W. & Alù, A. Enhanced light-matter interactions at photonic magic-angle topological transitions. *Appl. Phys. Lett.* **118**, 211101 (2021).
123. Oudich, M. *et al.* Photonic analog of bilayer graphene. *Phys. Rev. B Condens. Matter* **103**, 214311 (2021).
124. Hu, G. *et al.* Topological polaritons and photonic magic angles in twisted α-MoO3 bilayers. *Nature* **582**, 209–213 (2020).
125. Hu, G., Wang, M., Mazor, Y., Qiu, C.-W. & Alù, A. Tailoring Light with Layered and Moiré Metasurfaces. *TRECHEM* **3**, 342–358 (2021).
126. Chen, J. *et al.* A perspective of twisted photonic structures. *Appl. Phys. Lett.* **119**, 240501 (2021).
127. Hu, G., Krasnok, A., Mazor, Y., Qiu, C.-W. & Alù, A. Moiré Hyperbolic Metasurfaces. *Nano Lett.* **20**, 3217–3224 (2020).
128. Zheng, J.-P. *et al.* Focusing Micromechanical Polaritons in Topologically Nontrivial Hyperbolic Metasurfaces. *Adv. Mater.* e2311599 (2024).
129. Tang, H. *et al.* Modeling the optical properties of twisted bilayer photonic crystals. *Light Sci Appl* **10**, 157 (2021).
130. Tang, H., Ni, X., Du, F., Srikrishna, V. & Mazur, E. On-chip light trapping in bilayer moiré photonic crystal slabs. *Appl. Phys. Lett.* **121**, 231702 (2022).
131. Nguyen, D. X. *et al.* Magic configurations in moiré superlattice of bilayer photonic crystals: Almost-perfect flatbands and unconventional localization. *Phys. Rev. Research* **4**, (2022).
132. Huang, L., Zhang, W. & Zhang, X. Moiré Quasibound States in the Continuum. *Phys. Rev. Lett.* **128**, 253901 (2022).
133. Zhang, J. C. *et al.* Nanoimprint meta-device for chiral imaging. *Adv. Funct. Mater.* (2023)

doi:10.1002/adfm.202306422.
134. Roy, T. *et al.* Dynamic metasurface lens based on MEMS technology. *APL Photonics* **3**, 021302 (2018).
135. John, D. D. *et al.* Single-Mode and High-Speed 850nm MEMS-VCSEL. *Lasers Congress 2016 (ASSL, LSC, LAC)* Preprint at https://doi.org/10.1364/assl.2016.ath5a.2 (2016).
136. Wang, Y. *et al.* 2D broadband beamsteering with large-scale MEMS optical phased array. *Optica* **6**, 557 (2019).
137. Mazur, E. & Tang, H. Photonic Crystals with a Twist. in *CLEO 2023* (Optica Publishing Group, Washington, D.C., 2023). doi:10.1364/cleo_si.2023.sth1h.5.
138. Stranczl, M., Sarajlic, E., Fujita, H., Gijs, M. A. M. & Yamahata, C. High-Angular-Range Electrostatic Rotary Stepper Micromotors Fabricated With SOI Technology. *J. Microelectromech. Syst.* **21**, 605–620 (2012).
139. Morita, R., Inoue, T., De Zoysa, M., Ishizaki, K. & Noda, S. Photonic-crystal lasers with two-dimensionally arranged gain and loss sections for high-peak-power short-pulse operation. *Nat. Photonics* **15**, 311–318 (2021).
140. Khorasaninejad, M. *et al.* Metalenses at visible wavelengths: Diffraction-limited focusing and subwavelength resolution imaging. *Science* **352**, 1190–1194 (2016).
141. Reshef, O. *et al.* An optic to replace space and its application towards ultra-thin imaging systems. *Nat. Commun.* **12**, 3512 (2021).
142. Azzam, S. I. *et al.* Ten years of spasers and plasmonic nanolasers. *Light Sci Appl* **9**, 90 (2020).
143. Martinez, G. D. *et al.* A chip-scale atomic beam clock. *Nat. Commun.* **14**, 3501 (2023).
144. Knappe, S. *et al.* A chip-scale atomic clock based on ^{87}Rb with improved frequency stability. *Opt. Express* **13**, 1249–1253 (2005).
145. Horie, Y., Arbabi, A., Arbabi, E., Kamali, S. M. & Faraon, A. Wide bandwidth and high resolution planar filter array based on DBR-metasurface-DBR structures. *Opt. Express* **24**, 11677–11682 (2016).
146. Xie, Z.-W., Yang, J.-H., Vashistha, V., Lee, W. & Chen, K.-P. Liquid-crystal tunable color filters based on aluminum metasurfaces. *Opt. Express* **25**, 30764–30770 (2017).
147. Che, Y., Wang, X., Song, Q., Zhu, Y. & Xiao, S. Tunable optical metasurfaces enabled by multiple modulation mechanisms. *Nanophotonics* **9**, 4407–4431 (2020).
148. McClung, A., Samudrala, S., Torfeh, M., Mansouree, M. & Arbabi, A. Snapshot spectral imaging with parallel metasystems. *Sci Adv* **6**, (2020).
149. Tao, J. *et al.* Beam-steering metasurfaces assisted coherent optical wireless multichannel communication system. *Nanophotonics* **12**, 3511–3518 (2023).
150. Qin, H. *et al.* Arbitrarily polarized bound states in the continuum with twisted photonic crystal slabs. *Light Sci Appl* **12**, 66 (2023).
151. Rai, M. R., Vijayakumar, A. & Rosen, J. Superresolution beyond the diffraction limit using phase spatial light modulator between incoherently illuminated objects and the entrance of an imaging system. *Opt. Lett.* **44**, 1572–1575 (2019).
152. Pan, Y. *et al.* Edge extraction using a time-varying vortex beam in incoherent digital holography. *Opt. Lett.* **39**, 4176–4179 (2014).
153. Li, G. *et al.* Continuous control of the nonlinearity phase for harmonic generations. *Nat. Mater.* **14**, 607–612 (2015).
154. Tymchenko, M. *et al.* Gradient Nonlinear Pancharatnam-Berry Metasurfaces. *Phys. Rev. Lett.* **115**, 207403 (2015).
155. Shi, S. *et al.* High-fidelity photonic quantum logic gate based on near-optimal Rydberg single-photon source. *Nat. Commun.* **13**, 4454 (2022).
156. Crespi, A. *et al.* Integrated photonic quantum gates for polarization qubits. *Nat. Commun.* **2**, 566 (2011).
157. LaBorde, M. L., Rogers, A. C. & Dowling, J. P. Finding broken gates in quantum circuits–exploiting hybrid machine learning. in *Frontiers in Optics / Laser Science* (OSA, Washington, D.C., 2020). doi:10.1364/fio.2020.ftu8d.4.

158. Gliserin, A., Chew, S. H., Kim, S. & Kim, D. E. Complete characterization of ultrafast optical fields by phase-preserving nonlinear autocorrelation. *Light Sci Appl* **11**, 277 (2022).
159. Wu, Z. & Zheng, Y. Moiré Chiral Metamaterials. *Advanced Optical Materials* **5**, 1700034 (2017).
160. Wu, Z., Chen, X., Wang, M., Dong, J. & Zheng, Y. High-Performance Ultrathin Active Chiral Metamaterials. *ACS Nano* **12**, 5030–5041 (2018).
161. Lin, X. *et al.* Chiral Plasmons with Twisted Atomic Bilayers. *Phys. Rev. Lett.* **125**, 077401 (2020).
162. Lin, H.-M., Lu, Y.-H., Chang, Y.-J., Yang, Y.-Y. & Jin, X.-M. Direct observation of a localized flat-band state in a mapped moiré Hubbard photonic lattice. *Phys. Rev. Appl.* **18**, (2022).
163. Fu, Q. *et al.* Optical soliton formation controlled by angle twisting in photonic moiré lattices. *Nat. Photonics* **14**, 663–668 (2020).
164. Sunku, S. S. *et al.* Photonic crystals for nano-light in moiré graphene superlattices. *Science* **362**, 1153–1156 (2018).
165. Gautier, J., Li, M., Ebbesen, T. W. & Genet, C. Planar chirality and optical spin–orbit coupling for chiral Fabry–Perot cavities. *ACS Photonics* **9**, 778–783 (2022).
166. Voronin, K., Taradin, A. S., Gorkunov, M. V. & Baranov, D. G. Single-handedness chiral optical cavities. *ACS Photonics* **9**, 2652–2659 (2022).
167. Borri, P. *et al.* Ultralong dephasing time in InGaAs quantum dots. *Phys. Rev. Lett.* **87**, 157401 (2001).
168. Patton, B., Langbein, W. & Woggon, U. Trion, biexciton, and exciton dynamics in single self-assembled CdSe quantum dots. *Phys. Rev. B Condens. Matter* **68**, 125316 (2003).
169. Lodahl, P. *et al.* Chiral quantum optics. *Nature* **541**, 473–480 (2017).
170. Wang, Y. *et al.* Spin-Polarization-Induced Chiral Polariton Lasing at Room Temperature. *ACS Photonics* **10**, 1936–1943 (2023).
171. Deng, H., Solomon, G. S., Hey, R., Ploog, K. H. & Yamamoto, Y. Spatial coherence of a polariton condensate. *Phys. Rev. Lett.* **99**, 126403 (2007).
172. Balili, R., Hartwell, V., Snoke, D., Pfeiffer, L. & West, K. Bose-Einstein condensation of microcavity polaritons in a trap. *Science* **316**, 1007–1010 (2007).
173. Christopoulos, S. *et al.* Room-temperature polariton lasing in semiconductor microcavities. *Phys. Rev. Lett.* **98**, 126405 (2007).
174. Sanvitto, D. & Kéna-Cohen, S. The road towards polaritonic devices. *Nat. Mater.* **15**, 1061–1073 (2016).
175. Hou, S. *et al.* Ultralong-Range Energy Transport in a Disordered Organic Semiconductor at Room Temperature Via Coherent Exciton-Polariton Propagation. *Adv. Mater.* **32**, e2002127 (2020).

Scalable room-temperature quantum computing based on nonlinearities in microcavities (Executive summary)

Quantum computing leverages **parallel information processing** based on quantum mechanics, leading to exponential speed improvements for specific tasks compared to classical computers. Yet, prevalent quantum systems like superconducting qubits, trapped ions, neutral atoms, and silicon quantum dots necessitate cryogenic cooling or high-vacuum chambers to mitigate the relentless deleterious influence of the environment. Photons, as light quanta, naturally evade environmental effects, presenting a promising avenue for achieving universal quantum computing at room temperature and atmospheric conditions. **This positions photons as the key to democratizing quantum computing, akin to how silicon semiconductors revolutionized classical computing**. However, the historical challenge remains: the absence of single-photon level photon-photon interactions, impeding the realization of this transformative vision.

In this project, we propose a configuration of interconnected optical microcavities exhibiting robust $\chi^{(2)}$ nonlinearity as a viable solid-state platform for achieving high-precision quantum computing at room temperature. Leveraging the intense nonlinearity inherent in the materials, we disrupt the harmonic nature of cavity energy levels, enabling the fulfillment of essential criteria—such as well-defined qubit states with prolonged coherence times, qubit initialization, single- and two-qubit operations, and qubit readout—with superior efficiency and accuracy. Notably, this represents the pioneering instance of a large-scale qubit operating at room temperature, encompassing over 10^{10} atoms within a single qubit. Furthermore, this CMOS-compatible scalable design is poised for realization in the near future, given the rapid advancements in high-Q cavity fabrication techniques using nonlinear materials.

Given the current state of quantum control technologies, achieving this ambitious goal requires substantial technological accumulation and simplification of theoretical approaches in order to develop this direction into a competitive research field in quantum computing. In current stage, our team has developed a throughout detailed theoretical scheme to realize this aim (which has been submitted to Nature). Moreover, we have developed the most advanced nano-fabrication technologies on both LiNbO3 and III-V semiconductors crucial for fabricating a novel scalable qubit. As this project spans two years, it is expected to achieve two milestone objectives: i) room-temperature single-photon source based on photon blockade, and ii) strong coupling between microcavity modes to form a qubit, and its coherent operations.

Scalable room-temperature quantum computing based on nonlinearities in microcavities

Introduction

Quantum computing harnesses the rule of quantum mechanics to deliver a huge leap forward in computation to solve certain problems. Very recently, we have witnessed the strong supports of quantum supreme by quantum sampling tasks [1,2], multipartite entanglement preparation [3-6] for noisy intermediate-scale quantum (NISQ) applications, etc. However, unrelenting hazardous effect of environment grievously hinders the scalability and development of quantum computing. To combat it, most of the physical system must be cooled to cryogenic temperature to protect the coherence of quantum hardware, either by sophisticated laser cooling [7,8] or by expensive refrigerators [9,10]. This makes quantum computers costly and impractical for future's applications.

A long sought-after goal here is to directly realize a universal quantum computer at room temperature. Extensive efforts have been devoted into this direction [11-19]. Among all candidates, photon [11-15] is a prominent alternative to realize this enormous goal since it perfectly decouples with environment and thus is potentially free from decoherence at room temperature. However, this also prohibits an interaction between photons, while such an interaction is essential for scalable quantum computing. The lack of high-fidelity photon-photon gate is the main bottleneck of current photonic quantum computing with single photons.

Literature brief review

In 2001, a pioneering work by Knill, Laflamme, and Milburn (KLM) [20] demonstrated that single photons, linear optical elements and projective measurements are sufficient for universal quantum computing. However, the prohibitively large overhead of a nondeterministic two-photon gate renders KLM scheme daunting for physical implementation [21]. For a deterministic photon-photon logic gate, it's strongly believed that nonlinearity should be added to linear optics for scalable quantum computing. To this end, several alternative ways are developed to obtain strong nonlinearity for deterministic two-photon gate, including electromagnetically induced transparency (EIT) using atomic ensembles [22], strongly coupled atom-cavity system (also called Duan-Kimble scheme) [23], Rydberg blockade [24,25], chiral quantum optics in waveguide [15], and natural occurring nonlinearities in materials [11-13,26].

Nevertheless, all previous methods face a number of limitations to make two-

photon quantum gate with high efficiency and fidelity simultaneously. For example, EIT faces a great challenge to realize photon-photon interaction at a single-photon level [27]. An experiment based on Duan-Kimble scheme showed a photon-photon gate with an efficiency of 4.8% and a fidelity of 76.2% [28], which suffers from inefficient photon storage and retrieval during whole process, and the gate fidelity is limited by precision of spin characterization. Same issues happen to several recent experiments utilizing Rydberg blockade [29-31]. By storing single photons to a long-lived Rydberg state, the efficiency of single-photon storage and retrieval has been improved to 39% [30]. Even so, the average efficiency is only ~40%, which is far away from the threshold of quantum error correction. Until now, the former four approaches are unrealistic to realize quantum computing at room temperature. For the latter one, it has been commented that realizing high-fidelity two-photon gate faces many challenges due to causal, noninstantaneous nature of the nonlinear response both in second- and third-order nonlinear medium.

Problem statement & Objectives

In this project, we propose that a series of coupled microcavities with strong second-order nonlinearity provide a reliable and realistic physical system to implement a scalable room-temperature quantum computing. Owing to the strong $\chi^{(2)}$ nonlinear susceptibility, the harmonicity of microcavity can be broken so that one and only one photon can inject in. This so-called photon blockade in strong coupling regime enables all key elements for scalable quantum computing—well-designed qubit with long coherent time, qubit initialization, single- and two-qubit logic gates, and high-fidelity readout. The distinctive features of our work include (i) this is the first solid-state qubit based on macroscopic quantum effects meanwhile working at room temperature, (ii) the dominant error in our system—loss—can be detectable and erased, (iii) the final qubits can be measured by a nondemolition mean, and (iv) all elements can be integrated on a single chip working at room temperature under atmospheric condition.

For the second-harmonic generation (SHG) in a microring, the Hamiltonian of the system can be written as $H = \omega_a a^\dagger a + \omega_b b^\dagger b + g(a^2 b^\dagger + a^{\dagger 2} b)$, where ω_a and ω_b are the frequency of pump light and its second harmonic generation, the photon-photon interaction strength is denoted as g. If g is larger than the loaded dissipation rate κ of the microcavity, the harmonicity will be broken such that a two-level system formed by vacuum and the first excited state is well isolated (see Fig. 1a). This effect is very similar in superconducting qubits, both are based on the anharmonicity of cavities due to the strong nonlinear effects of devices. the main difference is that superconducting qubits works at microwave frequency while our system is for optical wavelength. This brings a remarkable advantage of our system over superconducting qubits---free from decoherence at room temperature.

Based on this two-level system, we can realize room-temperature quantum computing with either flying photon qubits or solid-state qubits. Here, we do not intend to provide any further details on this. However, it is worth noting that this project explores a completely new field of physics, named as **quantum nonlinear optics** [32]. Compared to traditional linear optics and nonlinear optics, quantum nonlinear optics allows photon-photon interaction at single photon level, without neither post-selections in linear optics nor strong pumping of light field.

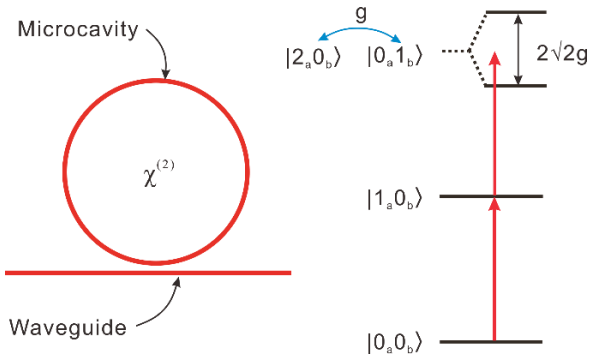

Figure 1. A microring cavity with strong $\chi^{(2)}$ nonlinearity can break the harmonicity of the cavity, thus forms a two-level system for quantum computing.

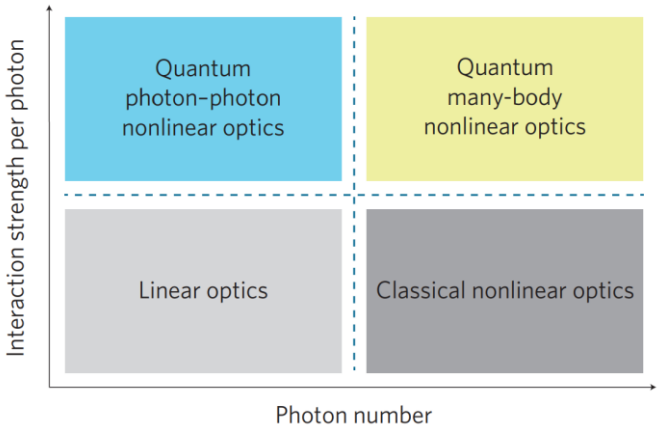

Figure 2. Comparison of quantum nonlinear optics and conventional linear optics, nonlinear optics. From [32].

This is the first macroscopic qubit working at room temperature, containing more than 10^{10} atoms in a single qubit. This CMOS-compatible scalable scheme can be carried out within next few years in view of rapid development of high-Q cavity fabrication on nonlinear materials. Given the current state of quantum control technologies, achieving this ambitious goal requires substantial technological accumulation and simplification of theoretical approaches in order to develop this direction into a competitive research field in quantum computing. As this project spans two years, it is expected to achieve two milestone objectives:

1. room-temperature single-photon source based on photon blockade, and
2. strong coupling between microcavity modes.

Outline of tasks

This project will span two years. The main focus of the first year's work is to mature and streamline the nano fabrication process. This process will take around seven months to optimize all parameters to improve the quality factor of microrings. After that, we will develop various quantum control technologies to achieve controllable cavity modes and develop a cavity-cavity coupling system. The assessment criteria include observing unconventional photon blockade phenomena in the weak coupling regime with high Q-factor and high nonlinear coefficients, as well as preparing single-photon sources.

The focus of the second year's work is primarily centered around achieving a strong coupling system with high Q-factor and high nonlinear coefficients through technological innovation and iteration. Based on this system, the objectives include demonstrating single-photon source experiments and two-qubit gate operations using different encoding schemes. Further experiments aim to enhance the scalability of the system and demonstrate error-correcting codes and scalable quantum computing achieved through optical nonlinear systems.

Impact

The deterministic interaction between single photons is recognized as a great challenge in the field of photonic quantum computing. The breakthrough of this project will not only hold the potential to revolutionize the field of optical quantum computing but also paves the way for a new discipline called quantum nonlinear optics, which will have a profound impact on fundamental research. In some sense, this project's room-temperature optical quantum computing can be considered as "room-temperature superconducting quantum computing," with similarities both in principles and performance. In the future, room-temperature quantum computing will undoubtedly become an important branch, not only contributing to fundamental research but also providing a more feasible and cost-effective research path for quantum computing.

References:

1. H.-S. Zhong, H. Wang, *et al.*, *Science* **370**,1460 (2020).
2. F. Arute *et al.*, *Nature* **574**, 505 (2019).
3. X.-L. Wang, *et al*., *Phys. Rev. Lett*. **120**, 260502 (2018).
4. C. Song, *et al.*, *Science* **365**, 574 (2019).
5. A. Omran, *et al*., *Science* **365**, 570 (2019).
6. I. Pogorelov, *et al*., *PRX Quantum* **2**, 020343 (2021).
7. D. Leibfried, R. Blatt, C. Monroe, and D. Wineland, *Rev. Mod. Phys*. **75**, 281

(2003).
8. C. Gross and I. Bloch, *Science* **357**, 995 (2017).
9. J. Clarke and F. K. Wilhelm, *Nature* **453**, 1031 (2008).
10. F. A. Zwanenburg, *et al*., *Rev. Mod. Phys.* **85**, 961 (2013).
11. N. K. Langford *et al*., *Nature* **478**, 360 (2011).
12. M. Heuck, K. Jacobs, and D. R. Englund, *Phys. Rev. Lett.* **124**, 160501 (2020).
13. M. Li *et al*., *Phys. Rev. Appl.* **13**, 044013 (2020).
14. S. Krastanov *et al*., *Nat. Commun.***12**, 1 (2021).
15. Z. Chen *et al*., *Phys. Rev. A* **103**, 052610 (2021).
16. G. Balasubramanian *et al*., *Nat. Mater.* **8**, 383 (2009).
17. K. Bader *et al*., *Nat. Commun*. **5**, 1 (2014).
18. N. Y. Yao *et al*., *Nat. Commun*. **3**, 1 (2012).
19. E. Herbschleb *et al*., *Nat. Commun*. **10**, 1 (2019).
20. E. Knill, R. Laflamme, and G. J. Milburn, *Nature* **409**, 46 (2001).
21. P. Kok *et al*., *Rev. Mod. Phys.* **79**, 135 (2007).
22. M. Fleischhauer, A. Imamoglu, and J. P. Marangos, *Rev. Mod. Phys.* **77**, 633 (2005).
23. L.-M. Duan and H. Kimble, *Phys. Rev. Lett.* **92**, 127902 (2004).
24. A. V. Gorshkov *et al*., *Phys. Rev. Lett.* **107**, 133602 (2011).
25. S. Das *et al*., *Phys. Rev. A* **93**, 040303 (2016).
26. I. L. Chuang and Y. Yamamoto, *Phys. Rev. A* **52**, 3489 (1995).
27. M. Bajcsy *et al*., *Phys. Rev. Lett.* **102**, 203902 (2009).
28. B. Hacker, S. Welte, G. Rempe, and S. Ritter, *Nature* **536**, 193 (2016).
29. D. Tiarks *et al*., *Nat. Phys.* **15**, 124 (2019).
30. T. Stolz *et al*., *Phys. Rev. X* **12**, 021035 (2022).
31. J. Vaneecloo, S. Garcia, and A. Ourjoumtsev, *Phys. Rev. X* **12**, 021034 (2022).
32. D. E. Chang, V. Vuletić, and M. D. Lukin, *Nat. Photon.* **8**, 685 (2014).

Probing intracranial epileptic biomarkers using silicon photonic biosensors

Category: Health

Dr. Jesus Maldonado Vazquez, Department of Neurosurgery, Yale University

Project Summary

There is an urgent need to understand the biochemical fundamentals of ictogenesis and epileptogenesis to allow earlier and better-directed pharmacotherapy and surgical approaches for epilepsy. One significant challenge in treating epilepsy is a lack of accurate diagnosis due to our limited knowledge of the disorder and inefficient diagnostic technology. Current diagnostic modalities include electroencephalogram (EEG), magnetoencephalogram (MEG), CT (computed tomography), PET (positron emission tomography), MRI (magnetic resonance imaging), and fMRI. While there has been tremendous growth in our knowledge through the use of EEG, intracranial EEG, and structural and functional imaging in epilepsy, our ability to follow conjoint changes in neurochemistry with fine temporal resolution is limited. There are no implantable devices that can detect chemical cues in epileptic brains in-vivo. In the past decade, many researchers have explored the implications of a wide range of techniques for developing biosensors for neurochemical detection. The three main ones are: separation-based, electrochemical-based, and optical-based. Separation-based techniques are cumbersome and expensive and require highly skilled operators to perform the experiment. Electrochemical-based techniques are suitable for the detection of some neurotransmitters, and it is extremely difficult to monitor non-electroactive neurotransmitters such as GABA because neither an oxidase nor a dehydrogenase is available for GABA. These techniques also suffer from poor sensitivity and low temporal and spatial resolution.

Our proposal centers around a silicon photonic device based on loop-terminated Mach-Zehnder interferometric (LT-MZI) configuration for rapid and accurate brain biomarker detection. Photonic biosensors offer a promising alternative to conventional tools due to their high sensitivity, short response time, excellent specificity, and multiplexed analyzing and integration capabilities. They hold significant potential as a future compact neuromonitoring tool. We aim to develop a real-time multianalyte photonic sensing system that can provide an analysis of biomarkers associated with epilepsy. The key advantage of our photonic system is its potential to be used as an implantable optical probe, a point-of-care (POC) system, and to monitor multiple compounds in real-time, rapidly with high accuracy and ease of operation, thereby potentially revolutionizing epilepsy diagnosis.

Impact of this project: This research aims to utilize an innovative photonic neuroprobe to better understand the complex functions of the human brain, which remains one of the challenges of neuroscience. Our photonic neuroprobe will contribute to finding effective treatments for diseases such as epilepsy, Parkinson's, depression, and schizophrenia. In addition, this sensor will help to provide individual treatment for each patient, leading to more effective interventions.

Proposal title: Probing intracranial epileptic biomarkers using silicon photonic biosensors.

Category: Health

Dr. Jesus Maldonado Vazquez

Epilepsy

For many years we have understood that functional electrophysiological networks in the brain are associated with and served by prominent neurotransmitters, biochemicals, and other metabolites[1-3]. Examples are the excitatory/inhibitory relationship of glutamate and GABA where their imbalance is a frequent hypothesis underlying causality in epilepsy and in psychiatric problems, especially depression which is a prominent comorbidity of epilepsy [4,5]. Likewise, a balanced noradrenergic and cholinergic system is associated with memory modulation along with emotional networks which also may be deranged in anxiety and depression[6]. Most of this evidence comes from animal studies using pharmacologic manipulation often associated with microdialysis which provides offline relatively slow measurements of the intracerebral biochemical milieu and most often from a single point. Despite these limitations, microdialysis has provided us with data, for example, regarding glutamate and the branch chain amino acids (BCAAs) role in deranged epileptogenic networks and in predicting seizure onset [7]. Despite significant progress, real-time *in-vivo* monitoring of changes in neurotransmitters in dynamic brain processes, such as disease progression and response to pharmacologic, cognitive, behavioral, and neuromodulation therapies has not been achieved.

The number of known neurotransmitters exceeds 100, and based on their chemical structure they are classified as amino acids, monoamines, neuropeptides, purines, and gasotransmitters [8]. Gamma-aminobutyric acid (GABA) and glutamate are two key neurotransmitters that play important roles in brain function. GABA, discovered in 1950, has been established as the main inhibitory neurotransmitter, which is widely distributed in the central nerve system [9]. In-*vivo*, real-time, or near-real-time measurements of GABA in biological fluids are important because changes in GABA concentrations have been implicated in many neurological and psychiatric disorders, such as epilepsy, schizophrenia, anxiety, and bipolar disorders. In addition, GABAergic neurons are critically involved in oscillatory network activities that underlie sleep-wake cycles and cognitive function [10-13]. Glutamate is the main excitatory neurotransmitter in the central nervous system. It is involved in many brain functions, including sensory perception, motor control, learning, memory formation, higher-level cognition, and behavior [14-17]. As a result, changes in glutamate signaling or processing are involved in the pathophysiology of various neurological and neurodegenerative disorders. Glutamate is rapidly removed from the synaptic cleft by excitatory amino acid transporters (EAATs) to prevent glutamate-mediated excitotoxicity. Therefore, it is important to understand how glutamatergic activity is regulated, not only because much of the brain energy is spent on sustaining synaptic activity at the glutamatergic synapse but also because of glutamate's critical role in brain function at normal and disease-related levels [18-20]. Also, the excitatory and inhibitory relationship of glutamate and GABA plays an important role in brain function. Their imbalance is a frequent hypothesis underlying causality in epilepsy and in psychiatric disorders, especially depression which is a prominent comorbidity of epilepsy [21].

Current Technology for Neurochemicals Detection and Limitations

The current detection methods for neurotransmitters can be classified into four categories: (1) Analytical chemistry techniques (ACT), including high-performance liquid chromatography (HPLC). In HPLC, the sample is injected into a chromatography column (stationary phase) and forced through the column using the flow of liquid (mobile phase). Various stationary and mobile phases can be used in a sample to separate a wide range of chemicals, including neurotransmitters. HPLC is often coupled with mass spectrometry (MS), which significantly increases the specificity and sensitivity (signal-to-noise) of the technique. However, most ACT technologies have limited spatial and temporal resolution, high cost, and require complex instruments, time-consuming sample preparation, and maintenance and operation of the instrumentation. (2) Electrochemical detection [22], including voltammetry and amperometry. This technology consists of a three-electrode configuration (working, counting, and reference electrodes), and either the voltage difference between the working electrode and the counter electrode or the current flow from the working electrode to the counter electrode is measured to estimate the concentration of neurotransmitters. With the development of novel nanofabrication process methods, this technology is now low-cost, easy to use, and allows real-time sensing. However, it may suffer from low sensitivity and low selectivity (specificity) for neurotransmitters, such as GABA because neither an oxidase nor a dehydrogenase is available for GABA. (3) Microdialysis [23], a well-known technology that has been used for over three decades. Although it can be used to detect multiple neurotransmitters including acetylcholine, neuropeptides, and amino acids, the temporal resolution is not high enough for real-time or near real-time study of brain dynamics and brain function. (4) Optical sensing includes surface-enhanced Raman spectroscopy [24], fluorescence [25], near-infrared spectroscopy [26], optical fiber-based biosensors [27], and surface plasmon resonance (SPR)[28,29]. In this technology small variations in neurotransmitter concentration are converted to a readable optical signal. This optical signal can be defined as changes in optical intensity, light spectrum, or light polarization and is delivered to an appropriate detector for reading and further analysis. Among all-optical sensing methods, fiber optic SPR biosensing has been considered one of the most promising techniques for the high performance, robustness, label-free, and rapid detection of neurochemicals. However, the transfer of the optical signals through an optical fiber presents a challenge for the *in-vivo* use of this technology. This is primarily due to the high probability of damage to the optical fiber (breaking) and, thus, the degradation of optical signals.

To this end, we propose a silicon photonic device for rapid and accurate brain biomarker detection (Figure 1). Photonic biosensors represent a promising alternative to conventional tools based on their high sensitivity, short response time, excellent specificity, and multiplexed analyzing and integration capabilities. They have enormous potential as a future compact neuromonitoring tool. We will develop a real-time multiplexing silicon photonic sensing system to provide an analysis of biomarkers associated with epilepsy. This system's strength lies in its versatility—it can serve as an implantable optical probe or a point-of-care (POC) unit—and its ability to monitor various neurochemicals simultaneously, offering rapid, high precision, high sensitivity, and user-friendliness in operation.

The development of this sensing platform follows three phases. First, we will design and fabricate a prototype system as a portable point-of-care unit with a loop-terminated Mach-Zehnder interferometric (LT-MZI) sensor and microfluidics. Next, we will use the system to measure biomarkers, including glutamate, GABA, and lactate in buffer and artificial cerebral

spinal fluid (aCSF), a biofunctionalization method will be developed for each neurochemical, and the results will be validated with mass-spectroscopy. After thorough benchtop testing, our goal is to transition the photonic system into an implantable format for trials in rodent models. We discuss the four aims in the following section.

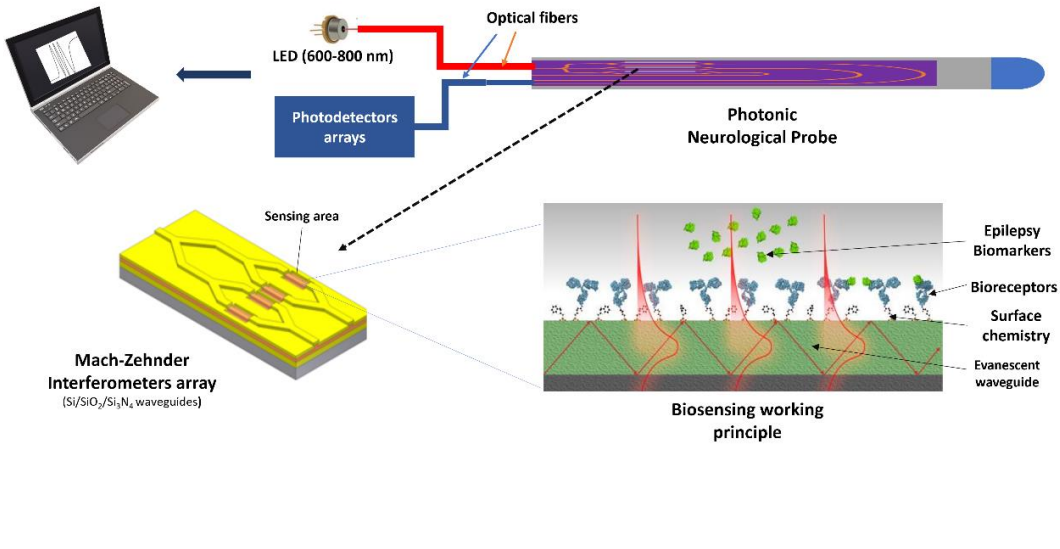

Figure 1. A schematic of the Photonic NeuroProbe device. General view of the main components and the biosensing principle. The diagnostic probe employs a looped optical waveguide structure and specifically designed surface chemical functionalization. Light transmits via the waveguide to the sensing area and interacts with the biomolecules. Biomarker detection is based on the principle that electrically polarized biomolecules on the waveguide would alter the light's refractive index. Thus, comparing the incident and outgoing lights discovers biomarkers and their concentration.

Specific aims

Specific Aim 1 (Months 1-6): Design and fabrication of the photonic neuroprobe: We will design and fabricate the silicon photonic device for measurement of glutamate, GABA, and lactate. a cleanroom foundry will be used to fabricate MZI sensors. A novel MZI configuration based on a Loop-Terminated waveguide will be used. Devices will be designed and optimized for nanostructures, material properties, and layout to achieve the expected performance (sensitivity in the picomolar to femtomolar range and reproducibility). A final design is planned, including dozens of nanophotonic neuroprobes into a wafer substrate. Each photonic neuroprobe will contain up to 3-4 independent MZI waveguide sensing devices. An optical characterization of the photonic neuroprobe, which allows the simultaneous analysis of the devices, will be done to determine the performance. The photonic sensors will be tested in a benchtop optical set-up that incorporates all the necessary components (i.e., light sources, optical parts, electronics, data processing, and software). In addition, a microfluidic system will be accurately designed and integrated into the nanophotonic sensor. Finally, the photonic sensors will be evaluated in terms of sensitivity, selectivity, and response time.

Specific Aim 2 (Months 6-12): Perform benchtop evaluations of the sensitivity and specificity of GABA, glutamate, and lactate photonic sensors: GABA, glutamate, and lactate detections will be performed by using specific bioreceptors (enzymes, antibodies, aptamers) immobilized on the surface of the photonic biosensor. Quality tests of the bioreceptor molecules in terms of affinity and specificity will be done to select those with better performance. Immobilization of bioreceptors would be challenging because it leads to a decrease in their activity. Thus, the biofunctionalization of the bioreceptors will be optimized to enhance the interaction with high sensitivity. With the optimal surface chemistry in terms of stability and reproducibility, individual bioassays for each biomarker in buffer solution will be performed with the photonic platform to obtain the optimal features. Finally, the photonic biosensors will be performed in aCSF. The results of the photonic sensors will be compared with gold-standard mass spectrometry to evaluate the analytical performance of the photonic neuroprobe in complex fluids.

Specific Aim 3 (months 13-18): Test the photonic neuroprobe sensors in rodents and validate with mass-spectrometry. We will perform measurements of all biomarkers using the photonic system developed in Aim 2 in rodents, with the results being validated with "gold standard" mass spectrometry measurements to evaluate the analytical performance of the photonic sensors in an animal model system. An animal model will be used to evaluate each biomarker (GABA, glutamate, and lactate) as a proof of concept. Collaborative efforts with the Eid laboratory at Yale will facilitate the in-vivo examination of the device's performance within rat brains.

Intended Outcomes

We plan to develop a new silicon photonic neuroprobe to monitor neurochemicals related to epilepsy and validate the system using gold-standard technology. This photonic technology will facilitate the study of fundamental mechanisms of brain function, providing reliable techniques for understanding normal and pathological brain activity. Real-time and in-vivo simultaneous detection of GABA, Lactate, and glutamate will significantly improve treatment and research, potentially leading to cures for epilepsy and other brain diseases.

Impact of this project

This project aims to utilize an innovative photonic neuroprobe to better understand the complex functions of the human brain, which remains one of the challenges of neuroscience. Our photonic neuroprobe will contribute to finding effective treatments for diseases such as epilepsy, Parkinson's, depression, and schizophrenia. In addition, this sensor will help to provide individual treatment for each patient, leading to more effective interventions.

References

1. Duman RS, Sanacora G, Krystal JH. Altered Connectivity in Depression: GABA and Glutamate Neurotransmitter Deficits and Reversal by Novel Treatments. *Neuron* 2019; **102**(1): 75-90.
2. Morgane P, Galler J, Mokler D. Morgane PJ, Galler JR, Mokler DJ. A review of systems and networks of the limbic forebrain/limbic midbrain. Prog Neurobiol 75: 143-160. *Progress in neurobiology* 2005; **75**: 143-60.
3. Spencer SS. Neural Networks in Human Epilepsy: Evidence of and Implications for Treatment. *Epilepsia* 2002; **43**(3): 219-27.

4. Çavuş I, Romanyshyn JC, Kennard JT, et al. Elevated basal glutamate and unchanged glutamine and GABA in refractory epilepsy: Microdialysis study of 79 patients at the yale epilepsy surgery program. *Annals of Neurology* 2016; **80**(1): 35-45.
5. Eid T, Gruenbaum SE, Dhaher R, Lee T-SW, Zhou Y, Danbolt NC. The Glutamate–Glutamine Cycle in Epilepsy. In: Schousboe A, Sonnewald U, eds. The Glutamate/GABA-Glutamine Cycle: Amino Acid Neurotransmitter Homeostasis. Cham: Springer International Publishing; 2016: 351-400.
6. Dalmaz C, Introini-Collison IB, McGaugh JL. Noradrenergic and cholinergic interactions in the amygdala and the modulation of memory storage. *Behavioural Brain Research* 1993; **58**(1): 167-74.
7. Gruenbaum SE, Chen EC, Sandhu MRS, et al. Branched-Chain Amino Acids and Seizures: A Systematic Review of the Literature. *CNS Drugs* 2019; **33**(8): 755-70.
8. Kovacs GL. The Endocrine Brain: Pathophysiological Role of Neuropeptide-Neurotransmitter Interactions. *EJIFCC* 2004; **15**(3): 107-12.
9. Petroff OA. GABA and glutamate in the human brain. *Neuroscientist* 2002; **8**(6): 562-73.
10. Castro VHC, Valenzuela CLL, Sanchez JCS, et al. An Update of the Classical and Novel Methods Used for Measuring Fast Neurotransmitters During Normal and Brain Altered Function. *Curr Neuropharmacol* 2014; **12**(6): 490-508.
11. Meldrum BS. Epilepsy and gamma-aminobutyric acid-mediated inhibition. *Int Rev Neurobiol* 1975; **17**: 1-36.
12. Ling W, Shoptaw S, Majewska D. Baclofen as a cocaine anti-craving medication: A preliminary clinical study. *Neuropsychopharmacol* 1998; **18**(5): 403-4.
13. Fuchs EC, Zivkovic AR, Cunningham MO, et al. Recruitment of parvalbumin-positive interneurons determines hippocampal function and associated behavior. *Neuron* 2007; **53**(4): 591-604.
14. Jamain S, Betancur C, Quach H, et al. Linkage and association of the glutamate receptor 6 gene with autism. *Mol Psychiatry* 2002; **7**(3): 302-10.
15. van der Zeyden M, Oldenziel WH, Rea K, Cremers TI, Westerink BH. Microdialysis of GABA and glutamate: analysis, interpretation and comparison with microsensors. *Pharmacol Biochem Behav* 2008; **90**(2): 135-47.
16. Watkins JC, Evans RH. Excitatory amino acid transmitters. *Annu Rev Pharmacol Toxicol* 1981; **21**: 165-204.
17. Pena F, Tapia R. Seizures and neurodegeneration induced by 4-aminopyridine in rat hippocampus in vivo: role of glutamate- and GABA-mediated neurotransmission and of ion channels. *Neuroscience* 2000; **101**(3): 547-61.
18. Armbruster M, Hanson E, Dulla CG. Glutamate Clearance Is Locally Modulated by Presynaptic Neuronal Activity in the Cerebral Cortex. *Journal of Neuroscience* 2016; **36**(40): 10404-15.
19. Attwell D, Laughlin SB. An energy budget for signaling in the grey matter of the brain. *J Cereb Blood Flow Metab* 2001; **21**(10): 1133-45.
20. Sheldon AL, Robinson MB. The role of glutamate transporters in neurodegenerative diseases and potential opportunities for intervention. *Neurochem Int* 2007; **51**(6-7): 333-55.
21. Cavus I, Romanyshyn JC, Kennard JT, et al. Elevated Basal Glutamate and Unchanged Glutamine and GABA in Refractory Epilepsy: Microdialysis Study of 79 Patients at the Yale Epilepsy Surgery Program. *Ann Neurol* 2016; **80**(1): 35-45.
22. Wang B, Wen X, Cao Y, et al. An implantable multifunctional neural microprobe for simultaneous multi-analyte sensing and chemical delivery. *Lab on a Chip* 2020; **20**(8): 1390-7.
23. Lee WH, Ngernsutivorakul T, Mabrouk OS, et al. Microfabrication and in Vivo Performance of a Microdialysis Probe with Embedded Membrane. *Analytical Chemistry* 2016; **88**(2): 1230-7.
24. Moody AS, Payne TD, Barth BA, Sharma B. Surface-enhanced spatially-offset Raman spectroscopy (SESORS) for detection of neurochemicals through the skull at physiologically relevant concentrations. *Analyst* 2020; **145**(5): 1885-93.
25. Kruss S, Salem DP, Vuković L, et al. High-resolution imaging of cellular dopamine efflux using a fluorescent nanosensor array. *Proceedings of the National Academy of Sciences* 2017; **114**(8): 1789-94.
26. Moreau F, Yang R, Nambiar V, Demchuk AM, Dunn JF. Near-infrared measurements of brain oxygenation in stroke. *Neurophotonics* 2016; **3**(3): 031403.
27. Sharma PS, Choudhary K, Gupta VK, Raghuwanshi SK, Kumar S. Optical fiber-based LSPR biosensor for enhanced dopamine detection: advancing personalized healthcare: SPIE; 2024.
28. Amiri M, Dadfarnia S, Haji Shabani AM, Sadjadi S. Non-enzymatic sensing of dopamine by localized surface plasmon resonance using carbon dots-functionalized gold nanoparticles. *Journal of Pharmaceutical and Biomedical Analysis* 2019; **172**: 223-9.
29. Pathak A, Gupta BD. Ultra-selective fiber optic SPR platform for the sensing of dopamine in synthetic cerebrospinal fluid incorporating permselective nafion membrane and surface imprinted MWCNTs-PPy matrix. *Biosensors and Bioelectronics* 2019; **133**: 205-14.

Near-Field Microwave-Based Plasmonic Nanoneedle for Monitoring Water in Plants

Water scarcity is a pressing issue globally, with climate change and unsustainable water usage exacerbating the problem. Even regions with abundant water reserves, such as South America, are beginning to feel the impact. The presence of diverse biomes in Brazil, such as the Amazon rainforest and the "Cerrado", plays a crucial role in addressing water challenges. The frequency of extreme climate events like wildfires, heatwaves, and floods, due to the exacerbated growth and accumulation of greenhouse gas levels, underscores the urgent need for immediate action. The water cycle is complex and poorly understood, because it is highly challenging to analyze the water content variation with high precision. Understanding the water cycle, as well as the adaptability of plants to adverse events like what we experience today, is essential, especially in complex ecosystems like the Amazon and the "Cerrado". Field-based vegetation monitoring is carried out in two ways: manually through sample collection that is subsequently analyzed in the laboratory and in situ using water potential meters, which provide an approximate value and are highly susceptible to temperature, considerably limiting their action. Implementing new technologies to study water behaves within the vegetation, and its impact on taxonomic and functional diversity, water dynamics in the soil, and response to polluting agents is not just essential, but it could be a game-changer in our fight against water scarcity and its impact on biodiversity and water stress. To address this critical need, this proposal presents a groundbreaking and innovative platform to better understand the behavior of water in plants and how vegetation responds to changes in water availability (in the soil and atmosphere) on a daily and seasonal scale, as well as the impact that water variation has on tree performance and how climate changes contribute to a collective deterioration of vegetation in the various ecosystems. As an alternative for this purpose, we propose a microwave-based plasmonic nano-needle platform, which combines plasmonics, optics, microwaves, and electronics to obtain a highly precise and stable analysis and monitoring system.

This proposal aims to develop plasmonic nanoneedles for real-time analysis and monitoring of water content in plants through near-field generation using microwave radiation. Thanks to the properties of water in this range of the spectrum, that is, extremely high relative permittivity, it will be possible to extract discretized information from its content with high precision and reliability. This platform will comprise a hybrid microwave–optic system, which offers several advantages over existing methods, as detailed previously. It will convert the generated optical signal to the frequency of operational interest, bringing the best optics and microwaves to a single platform. This integration will enhance the sensitivity and accuracy of the system, allowing for more precise and reliable measurements. Initially, we will focus our research on a single topic, the water analysis and monitoring in the vegetation, however, this platform will have the potential to analyze the xylem and phloem variations in plants, evaluate the control of the sap flow, analyze the increase or reduction of water in the vegetation, and even monitor carbon dioxide concentrations absorbed during photosynthesis.

The successful execution of this proposal will result in a technology that surpasses all current vegetation analysis and monitoring methods. This innovative approach, integrating optics and microwaves, will continue to grow and strengthen, opening new paths for diverse applications. The dissemination of our research results through leading scientific publications and conferences will foster a global exchange of knowledge. Finally, our findings will significantly advance our understanding of the water cycle, potentially influencing public policies for environmental conservation.

Near-Field Microwave-Based Plasmonic Nanoneedle for Monitoring Water in Plants

1. Literature review / Problem statement / Objectives

Water is a finite resource, part of a natural cycle that allows recycling, ensuring the constant renewal of natural reservoirs like rivers, lakes, groundwater, and aquifers. It is important to remember that water cannot be formed on the surface of the Earth but arrived on our planet millions of years ago. In a simplified way, these reservoirs are replenished with rainwater, absorbed by the soil, preserves, evaporates, transpires, and falls as rain. However, the increasing frequency of droughts and environmental imbalances have significantly reduced the amount of water available for human consumption and the maintenance of life on the planet, underscoring the urgency of the issue.

Water scarcity threatens the health and development of communities around the world. Climate change, changes in vegetation cover, and indiscriminate use of water intensify the problem, pushing governments to find more innovative and collaborative ways to address water stress. This problem is present throughout the planet; however, in Fig. 1, we can see that the region with the least water stress is South America, with a percentage below 10%. The reasons are obvious: the presence of the six Brazilian biomes (Amazônia, Caatinga, Cerrado, Mata Atlântica, Pampa, and Pantanal), which contribute enormously in the most diverse ways to water issues, as well as the natural reserves of neighboring countries.

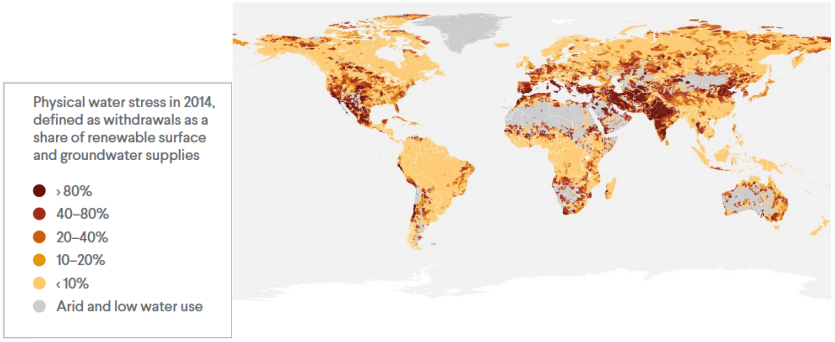

Fig. 1. Water stress around the globe[1]

The Amazon rainforest, a treasure trove of biodiversity, plays a unique role in our planet's health. It stores an astounding amount of carbon, equivalent to 15-20 years of CO2 emissions (150-200 Pg C), and provides a cooling effect that stabilizes the climate on Earth. The forest's contribution of up to 50% of the rainfall in the region is a lifeline for moisture supply across South America[2]. However, the emission of greenhouse gasses by human activities is accelerating global warming, leading to degenerations that ecosystems are struggling to cope with. It is crucial to understand that our actions are directly contributing to this crisis.

Every day, we are confronted with news about climate change and its devastating impact on our society. The frequency of events such as wildfires in Greenland, extreme heat waves shattering records in Europe, and torrential rains causing extreme flooding in Latin America, coupled with the alarming levels of greenhouse gasses in the atmosphere, serve as a stark reminder of the imminent catastrophe our planet is hurtling towards. The urgency of the situation demands immediate action.

One of the main actions to be taken is to understand the problem, and in this context, understanding the water cycle and the behavior of plants and their adaptability to events that potentiate water stress is essential. The water cycle in the Amazon rainforest and the “Cerrado” (a vast tropical savanna ecoregion in Brasil) ecosystems, two of the most biodiverse regions on the planet, is particularly complex and poorly understood. For this reason, new technologies must

[1] Source: National Geographic; Navajo Water Project; UNICEF; World Resource Institute.
[2] Flores, B.M., Montoya, E., Sakschewski, B. *et al.* Critical transitions in the Amazon forest system. *Nature* **626**, 555–564 (2024).

be implemented to understand how water behaves within the vegetation and its impact on taxonomic and functional diversity, water dynamics in the soil, and response to polluting agents, among others.

Currently, field-based vegetation monitoring in the Amazon and the "Cerrado" is carried out manually through sample collection that is subsequently analyzed in the laboratory. The results are an approximation and provide limited information about the tree's status. The available devices on the market for plant water analysis are very limited. Among the most notable is the ICT International Psychrometer, which, as the manufacturer reports on its website, is a unique, non-destructive, standalone, and in situ logging device[3]. However, it is costly, making its use on a wide scale difficult; and limited to measuring plant water potential.

Plasmonic nanostructures are pivotal in recent transformative breakthroughs spanning biosensing[4], waveguiding[5], imaging[6], energy harvesting[7], and beyond[8]. Rooted in surface plasmon polaritons, these nanostructures exploit the resonant coupling of optical fields with surface charge density oscillations on metal surfaces, enabling the confinement, enhancement, and localization of light at subwavelength scales. Such resonances foster innovation across diverse domains, facilitating the development of high-performance optical devices that surpass the diffraction limit[9].

In this context, as an alternative to better understand the behavior of water in plants, we propose implementing a microwave-based plasmonic nano-needle platform capable of monitoring water content variation in trees in the Amazon and "Cerrado" ecosystems. Our proposal offers several benefits, including real-time data collection and extremely high precision, and despite being an invasive monitoring platform, the nanometric size of the nano-needle significantly reduces the impact on trees during the measurements. Through this technology, it will be possible to evaluate the increase or reduction of water in the trees.

Knowing the behavior of water in plants will provide information that will be crucial during decision-making in the process of preserving the various biomes. Similarly, with the reduction of water in the vegetation due to droughts and considering the large number of thunderstorms in this environment, we can assume that trees are more susceptible to being burned when drier, generating wildfires in the region and causing deforestation. Additionally, extreme droughts alone can already cause widespread tree mortality. By implementing our proposed technology, we can monitor these water dynamics not only effectively but also potentially predict and prevent such events, thereby contributing to preserving these vital ecosystems.

1.1. Objective

Develop and implement a novel microwave photonics platform based on a plasmonic nano-needle device for real-time analysis of water variation in plants. Our proposal aims to revolutionize the detection of subtle variations in plants´ water content through a high-tech platform that makes it a powerful tool for predicting performance and understanding how vegetation responds to changes in water availability (in the soil and atmosphere) on a daily and seasonal scale. In addition, it has the potential to provide information that allows a better understanding of the impact that water variation has on tree performance and how climate changes contribute to a

[3] https://ictinternational.com/product/psy1-psychrometer-for-plant-water-potential/
[4] Wang, X. et al. 3d hybrid trilayer heterostructure: Tunable au nanorods and optical properties. ACS Appl. Mater. Interfaces 12, 45015–45022 (2020).
[5] Ono, M. et al. Ultrafast and energy-efficient all-optical switching with graphene-loaded deep subwavelength plasmonic waveguides. Nat. Phot. 14, 37–43 (2020).
[6] Okamoto, H., Kamada, S., Yamaguchi, K., Haraguchi, M. & Okamoto, T. Experimental confirmation of self-imaging effect between guided light and surface plasmon polaritons in hybrid plasmonic waveguides. Scientific Reports 12, 17943 (2022).
[7] Dhiman, M. Plasmonic nanocatalysis for solar energy harvesting and sustainable chemistry. J. Mater. Chem. A 8, (2020).
[8] Rizal, C., Shimizu, H. & Mejía-Salazar, J. R. Magneto-optics effects: New trends and future prospects for technological developments. Magnetochemistry 8 (2022).
[9] Gramotnev, D. K. & Bozhevolnyi, S. I. Plasmonics beyond the diffraction limit. Nature Photonics 4, 83–91 (2010).

collective deterioration of vegetation in various biomes, as well as predict and prevent events such as wildfires and tree mortality due to extreme droughts in the Amazon and Cerrado ecosystems.

1.2. Outcomes

- Development and implementation of a novel microwave photonics platform based on a plasmonic nano-needle device for real-time analysis of water content variation in plants.
- Implementing a plasmonic system based on nanoneedles will allow obtaining a tool that, despite being invasive, will significantly reduce the damage induced to the plant. This is a completely different approach to anything currently used.
- Revolutionizing the detection of subtle variations in plants' water content.
- Comprehensive testing and validation of the platform's ability to detect subtle changes in plant water availability, ensuring its reliability and robustness.
- Platform integration into field monitoring systems for real-world application.
- Training researchers in photonics and microwaves applied to solving environmental problems will strengthen our community in this specific field.

1.3. Preliminary results

We have been investigating various effects in near-field microwaves, and the various studies have allowed us to explore the applicability of these effects in impedance microscopy using radiation with a wavelength of 0.1m. Through our experiments, we were able to observe the spontaneous formation of a 2nm diameter water nano meniscus, which, thanks to its high relative permittivity ($\varepsilon r = \varepsilon/\varepsilon 0 \approx 80$ at 3GHz), allowed the focusing of the electric field in a metal tip with 10um in height and 8um at the top (Fig. 2a). The effect above is then responsible for allowing the visualization of surfaces with a resolution down to 1nm. This work was published in Nature Communication[10].

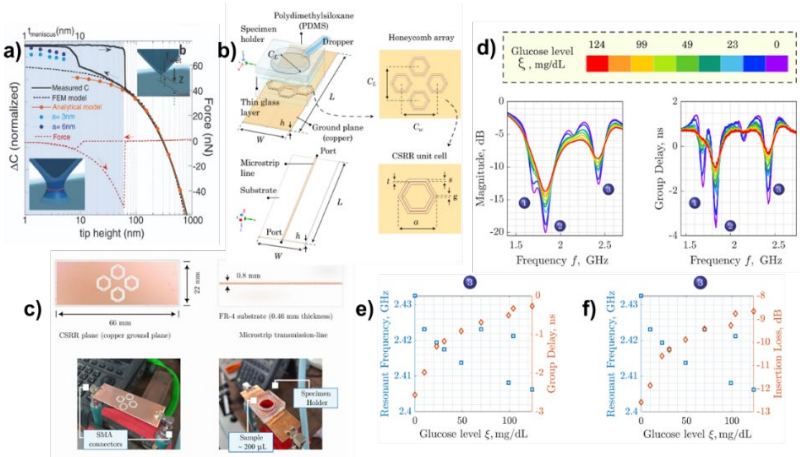

Fig. 2. a. Capacitance with and without water meniscus[10]. (b-c) Honeycomb-based near-field microwave device[11]. (d-e-f) Measurement of blood glucose variation[11].

Taking advantage of the principle of operation of the near-field in microwave systems, in the master's thesis of my student Reinaldo José Velasquez Gomez, we study the variation of the electromagnetic response in a microwave system in aqueous media[11]. We modeled a complementary split-ring resonator integrating the FDTD numerical method and an Artificial Neural Network to optimize the sections that compose it. This device demonstrated excellent

[10] Ohlberg, D. A. A., Ramirez, J. C., *et al.*, The limits of near field immersion microwave microscopy evaluated by imaging bilayer graphene moiré patterns. Nat. Comm., **12**, 8–13. (2021).
[11] Reinaldo José Velasquez Gomez. Microwave-based Complementary Split-ring Resonator for Detection of Variations In Aqueous Media. Master's Thesis. Electrical Engineering Graduate Program (PPGEE) – Universidade Federal de Minas Gerais (UFMG). (2024). Advisor: Jhonattan Cordoba Ramirez.

performance in monitoring the amount of water in a container and detecting variations in low glucose concentrations in the blood of the individuals evaluated, as seen in Fig. 2. It is important to highlight that glucose is the main component of the elaborate sap, which is composed of organic compounds produced in the leaves through photosynthesis.

As shown in Fig. 2, the non-invasive response thanks to the near-field generated, is interesting to develop our proposal. However, as presented in Fig. 3, the response of the capacitance in direct contact with the analyzed sample improves by 50%-a significant increase in sensitivity, and the conductance in direct interaction with a dielectric sphere improves by 4000%-a dramatic enhancement in the ability to detect and monitor of water content variation in plants.

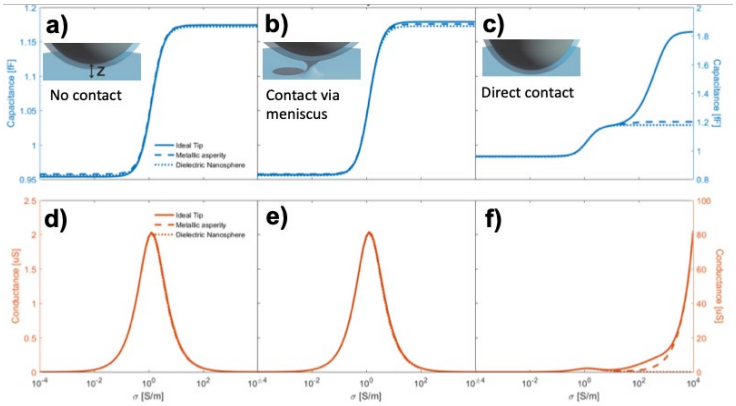

Fig. 3 Simulated capacitance (a-b-c) and conductance (d-e-f) in the MIM for non-contact with a 1nm gap, contact through a 1nm radius water meniscus with 1nm thick, and direct contact.

Other works developed by our group have demonstrated the electromagnetic response of pyramidal structures. With their unique geometry, these structures enhance the interaction of light with the sample, leading to enhanced Raman signals and localized plasmon. This has been particularly useful in applications including Tip-Enhanced Raman Spectroscopy (TERS) [12,13], and Surface-Enhanced Raman Spectroscopy (SERS), as well as applications that focus on improving high-intensity plasmon-polariton interaction[14]. The previously mentioned devices were evaluated in some bio-detection processes, demonstrating very high sensitivity. This is because the pyramidal structure favors the movement of electrons at its vertices.

1.4. Hypothesis

Based on the information provided, we hypothesized that the utilization of microwave radiation around 3GHz, in combination with a highly efficient plasmonic device based on a pyramidal shape (nano-needle) and a photonic system for the generation and processing of the required microwave signals, has the potential to revolutionize the detection and monitoring of subtle variations, such as changes in water content in plants. Despite being invasive, this innovative approach does not harm the plants analyzed due to the proposed nanometric dimensions; in addition, it could significantly enhance our ability to understand and analyze the impact of water variation and how climate changes contribute to the collective deterioration of vegetation in various biomes.

1.5. Methodology

We will develop the proposal using the following methodology: it will be divided into four work packages (WP1 to WP4), each aimed at achieving specific objectives.

---

[12] Portes, A., Ramirez, J. C. *et al.*, Electro-optical properties of a graphene device on a tip-enhanced Raman spectroscopy system. Optics Letters, **49**(4), 871. (2024). (Editor's Pick)
[13] Nadas, R. B., Ramirez, J. C., et al., Spatially Coherent Tip-Enhanced Raman Spectroscopy Measurements of Electron − Phonon Interaction in a Graphene Device. Nano Letters. (2023).
[14] Marques, T. E. M., Ramirez, J. C. et al., Tunable Surface Plasmon-Polaritons Interaction in All-Metal Pyramidal Metasurfaces: Unveiling Principles and Significance for Biosensing. arxiv.org/abs/2405.12428

- WP1: Development of the plasmonic nano-needle device integrated with the microwave photonics platform for real-time monitoring of water content variation in plants. This WP will involve modeling and optimization of the plasmonic nanoneedles using FEM and FDTD numerical methods. Subsequently, we should proceed with manufacturing the plasmonic nano-needles and the implementation of the experimental setup responsible for converting the generated optical signal to the frequency of operational interest.
- WP2: Once the device is ready, we can conduct comprehensive testing and validate the platform's ability to detect sap concentration and composition changes. This will involve conducting laboratory tests to analyze the system's plasmonic response obtained at frequencies around 2.5 - 3GHz.
- WP3: We will calibrate our platform using an in situ water potential meter. Because they are susceptible to temperature, the calibration process will be carried out in a controlled environment. At the same time, we will study the impact of temperature on the variability of our calibration standard. We will instantly measure water content in the leaf or stem of different trees with different wood properties to get an idea of how some of these parameters influence this measurement.
- WP4: We will adapt our bench test system for use in field studies. As part of this WP, native plants in the Amazon and Cerrado biomes will be processed and analyzed.

This platform could be adapted into a portable system for performing real-time monitoring studies *in situ* over a certain period, allowing us to analyze the impact of water content variations on vegetation performance. In addition, by integrating this technology with a pattern recognition system and machine learning, it will be possible to predict models to anticipate events such as wildfires and tree mortality due to extreme droughts in the Amazon and Cerrado ecosystems. These are some of the future work established after the successful completion of this project.

2. Impact

2.1. Originality

The microwave photonics platform based on a plasmonic nano-needle device for analysis and monitoring of water in plants is a groundbreaking and innovative approach to understanding how vegetation responds to changes in water availability (in the soil and atmosphere) on a daily and seasonal scale, as well as the impact that water variation has on tree performance and how climate changes contribute to a collective deterioration of vegetation in various biomes. Importantly, it ensures non-damage, preserving the plants´ integrity due to the nanometric dimensions of the proposed device. In addition, this platform enables real-time data collection with high precision and has the potential to enhance our understanding of the impact of sap compound variations on the water cycle in diverse biomes. It also has the potential to predict and prevent events such as wildfires and tree mortality caused by extreme droughts. Integrating this technology into field monitoring systems will revolutionize how we monitor and preserve vital ecosystems like the Amazon and Cerrado, potentially leading to more effective and targeted conservation efforts.

2.2. Impact

The proposed research, though challenging, is of paramount importance. It is a journey into the unknown, and with the aid of highly sensitive platforms like the one we propose, we aim to shed light on how environmental degradation impacts plant behavior in complex biomes such as the Amazon and the “Cerrado” and in the adaptability of plants under water stress. By addressing these crucial questions, we can uncover other factors that endanger the future of the forests and, subsequently, water security on our planet, making our potential contribution invaluable in the collective efforts for environmental conservation.

Cavity Electro-Optics for Efficient Integrated Circuits Beyond 100 Gigahertz

This proposal aims to tackle pressing global challenges in information technology by utilizing cutting-edge photonic integrated circuits.

The primary objective of this research initiative is to deploy ultra-efficient photonic integrated circuits operating at high frequencies, extending into the THz domain, a frontier yet to be fully explored. This endeavor seeks to address two enduring challenges: 1) enhancing the efficiency of photonic integrated circuits employing electro-optic (Pockels) effects, and 2) overcoming obstacles at high frequencies in the THz gap, demonstrating signal generation and detection beyond 100 GHz.

Achieving these ambitious aims hinges on the utilization of cavity electro-optics, integrating emerging nonlinear optical materials with exceptionally high electro-optic coefficients onto silicon photonic chips. This integration will involve the meticulous design and fabrication of optical and THz cavities to enhance field confinement while minimizing losses. Two strategies are proposed to overcome limitations in efficiency at high frequencies: 1) optimizing THz cavity design using an innovative "dual cavity" concept for superior field confinement, and 2) utilizing superconducting materials to mitigate losses in THz integrated circuits. Anticipated outcomes of this research include the development of a THz-optic frequency conversion photonic chip with record-high efficiency, facilitating room-temperature THz signal generation, manipulation and detection monolithically, which remains a technical challenge so far.

Another objective of this research is to create the first-ever superconducting THz integrated photonic device on a chip. With full capabilities for high-frequency signal generation, manipulation, and detection, this device will provide a groundbreaking platform to investigate exciting fundamental questions, including the performance of superconducting materials at high frequencies, the dynamics of Cooper pairs dissociation and recombination, and the control/readout of qubits in a high-frequency Josephson junction. These advancements will pave the way for future developments in quantum computing and information processing.

In summary, the proposed research not only promises to yield powerful chip-scale devices for fundamental research at high frequencies but also anticipates advancements in sensing capabilities within the THz domain. This transformative impact extends to various applications, including wireless communication, LiDAR technology, non-invasive imaging, and beyond. Overall, this research endeavor holds immense potential to enhance the efficiency and functionality of photonic and quantum devices, driving innovation across telecommunications, quantum computing, and sensing technologies. The integration of novel materials and sophisticated cavity designs constitutes critical steps towards realizing high-performance, scalable photonic and quantum systems, making this work highly relevant and impactful in both academic and industrial settings.

Cavity Electro-Optics for Efficient Integrated Circuits Beyond 100 Gigahertz

1. Literature review: the development of photonic integrated circuits (PIC)

The monolithic integration of electronic circuits has revolutionized our lives since the last century.[1] Exploiting linear and nonlinear optical phenomena, photonic integrated circuits (PIC) have rapidly transitioned from academic research to widespread applications. One extremely successful platform is silicon-on-insulator (SOI) with CMOS technology compatibility. Over the past two decades, SOI devices have achieved significant advancements, including light amplification and lasing,[2,3] data interconnects,[4] and communications systems.[5] Silicon nitride (SiN) is another CMOS-compatible integrated photonic platform which allows efficient optical pumping due to its weaker two-photon absorption, and low-loss waveguides and resonators.[6] These characteristics make SiN suitable for applications like optical frequency combs[7] and parametric amplifiers.[8]

Lithium niobate (LiNbO3) is notable for its large nonlinear-optic, electro-optic, and piezo-electric coefficients, making it an attractive material for generating and manipulating electromagnetic waves.[9] Using similar methodologies, LiNbO3 has been transformed into lithium niobate-on-insulator (LNOI) structures, emerging as a superior platform for ultrahigh-speed, low-voltage photonic integrated devices such as modulators[10] and more[11,12]. Very recently, lithium tantalate (LiTaO3) has also been introduced to photonic integrated circuits. With a similar structure and properties to LiNbO3 but featuring lower fabrication costs, weaker photorefractive effects[13], and lower losses at microwave frequencies,[14,15] LiTaO3 shows promise for future volume manufacturing.[13] Demonstrations on this platform include electro-optic modulators[16] and soliton microcombs.[13]

Other disruptive materials for the next generation of photonic integrated circuits include silicon-carbide,[17] gallium phosphide[18] and more. Among these, optical nonlinear polymers stand out due to their ultra-high nonlinear optical coefficient,[19] and other key advantages such as flexibility and processability in integrated circuits.[20,21] Combining the benefits of silicon technology (low cost, easy micro-nanofabrication, and integration with existing semiconductor manufacturing technologies) with the versatility of organic materials, the silicon-organic hybrid (SOH) platform has enabled numerous potential applications, including low-consumption high-speed modulators,[22] laser sources,[23] and quantum transduction.[24]

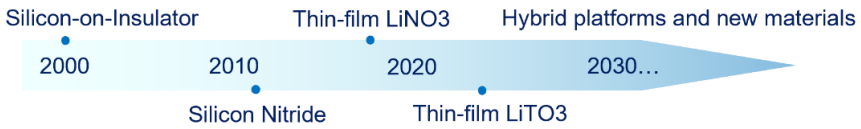

Figure 1. Emerging materials for "next generation" integrated photonics.

2. Challenges in next generation PIC, proposed solutions and objectives

Challenge #1: High-efficiency electro-optic frequency conversion on a chip. The interaction of two electromagnetic waves in nonlinear optical materials leads to frequency conversion through the electro-optic effect (Pockels effect), which has drawn extensive attention in imaging and spectroscopy applications.[25] With the growing demands for optical networks linking various information processing nodes over long distances,[26] frequency conversion is of escalating significance for coherently mapping quantum states between different frequency domains. To improve electro-optic conversion efficiency, cavity electro-optics has been proposed[27,28] and demonstrated[29,30] for direct signal transduction, which has the potential for better efficiency and less added noise[31] compared to the non-direct optomechanical systems.[32–34] However, electro-optic chips for frequency conversion still face a longstanding challenge – low efficiency, recently reaching only 1-2%[29,30] or even much lower[35] due to factors such as the small electro-optic coefficient of the nonlinear optical material or small single-photon coupling rates caused by large optical and microwave mode volumes.

Solutions and objectives: Our solution to this issue is twofold. First, we need to maximize the electro-optic coupling efficiency using emerging materials with higher χ^2 coefficients. Emerging

nonlinear optical polymers, which possess χ^2 coefficients 10-100 times higher than state-of-the art materials like $LiNbO_3$, play a key role in this. Second, by combining these polymers with mature silicon photonic technologies, we will seamlessly incorporate them into photonic circuits with minimized mode volumes at micro-scale. This will substantially improve the electro-optic coupling strength in on-chip devices. In the proposed research we will systematically investigate and optimize hybrid Si-organic circuits, aiming to demonstrate an on-chip device with unprecedented electro-optic coupling efficiency.

Challenge #2: High-frequency signal generation/detection beyond 100GHz on PIC. THz technologies have become increasingly impactful in chemical and biological research,[36,37] due to their superior ability to probe fundamental vibrational modes of molecules within this frequency range. However, the development of crucial components operating within the 100 GHz to 10 THz frequency range, such as continuous wave and pulsed sources, detectors, amplifiers, and waveguides, remains in a rudimentary stage.[38] These limitations hinder important applications in daily life, such as wireless communications, LiDAR system for autonomous vehicles, and noninvasive imaging. A significant limitation is the prominence of ohmic losses as the resonance frequency increases from the microwave domain to higher frequencies[39] due to the skin effect.[40]

Solutions and objectives: Our solution to this issue involves two main strategies. First, we focus on optimizing the design of THz cavities to achieve extraordinary field confinement and enhancement. We propose the concept of a "THz dual cavity", where a THz antenna cooperates with a coplanar waveguide (CPW) cavity to provide extra enhancement of the THz field, as introduced in section 3.1. Second, mitigating losses in THz integrated circuits is a top priority. We aim to employ superconducting materials for THz cavities and test their performance at THz domain. By implementing these strategies, we aim to achieve quantum-limited electro-optic coupling efficiency. This research holds the promise of revolutionizing the design and implementation of efficient high-frequency integrated circuits for future classical and quantum applications in the THz domain.

Challenge #3: High-frequency superconducting circuits for quantum information. Microwave superconducting circuits currently stand as the leading platform for quantum computing. Increasing the operating frequency of current microwave quantum circuits to the THz level offers several advantages: 1) it allows faster operation, and smaller footprints for large-scale integration; 2) it enhances the tolerance to thermal perturbations, enabling the maintenance of quantum states at higher temperatures (e.g., a few kelvin instead of few millikelvin Despite being a long-desired pursuit in the quantum science community, efforts to investigate high-frequency quantum circuits remain sparse, with recent breakthroughs reaching only 20GHz.[41] This falls far short of the THz domain, primarily due to the underdevelopment of THz technologies.

Proposed solution: We plan to use ultra-efficient photonic integrated circuits to address this open question. By harnessing cavity electro-optics within PICs, we anticipate achieving THz generation, waveguiding, and detection on the same chip with unprecedented efficiency. This method opens up new avenues for investigating and deploying THz quantum circuits, laying the groundwork for future breakthroughs in quantum computing and information processing.

3. Research plan

Phase #1: Efficient signal generation and detection using hybrid Si-organic circuits

Concept of cavity electro-optics. As illustrated in Figure 2(a), the resonant frequency of the optical cavity is modulated by changes in the refractive index of the electro-optic medium, induced by an electrical field confined within the THz cavity. This process produces Stokes and anti-Stokes sidebands through wave mixing in the electro-optic medium (Figure 2b), which will then be sensitively detected using mature optoelectronic instruments. Achieving high electro-optic conversion efficiency requires meticulous design of the electro-optic system, evaluated by two key figures of merit: 1) the electro-optic coupling rate $g_{eo}(\omega_P) = \frac{1}{2} n_{NLO}^2 \cdot r_{33} \cdot \omega_P \cdot \sqrt{\frac{\hbar\Omega}{2\varepsilon_{THz} V_{THz}}} \cdot \Gamma_c$,[31] a measure of the rate at

which sideband optical photons are generated through electro-optic coupling, determined by the mode volume of the confined THz field V_{THz} and THz-optic mode overlapping Γ_c, and 2) the total frequency conversion efficiency $\eta = \frac{n_{SB}}{n_{THz}} = \frac{\kappa_{opt,ex}\kappa_{THz,ex}}{\kappa_{opt}\kappa_{THz}} \frac{4C}{[1+C]^2}$ with cooperativity $C = n_p \frac{4{g_{eo}}^2}{\kappa_{opt}\kappa_{THz}}$,[35] which describes the competition between photon generation, readout and losses.

In our current design, we utilize silicon ring resonators as the optical cavity to confine a continuous-wave pump (@1.55 μm), while the THz cavity takes the form of a LC circuit or antenna, as shown in Figure 2(c). Simulations of such optical and THz cavities are shown in Figure 2(d) and (e) respectively.

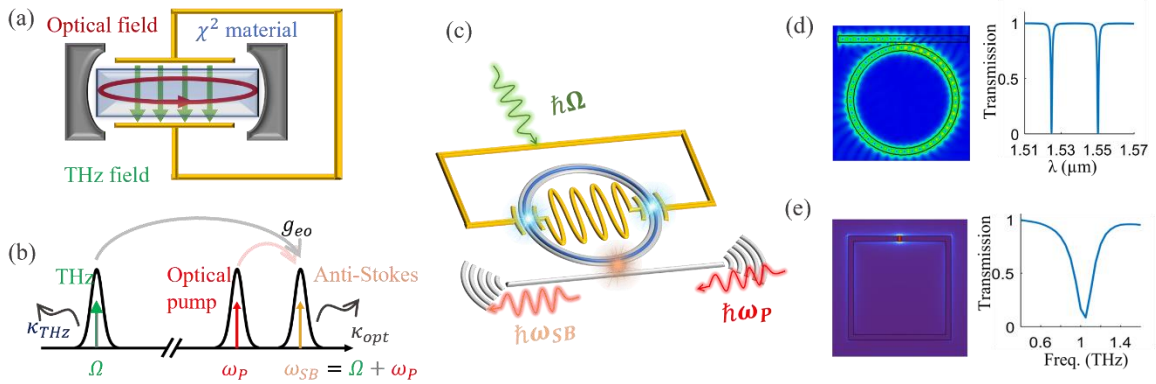

Figure 2. (a) schematic of the electro-optic cavity. (b) Principal of THz-optic frequency conversion. (c) Examples of designed photonic circuits on a silicon chip with a THZ antenna. (c) Simulation of an exemplary electric field distribution (left) and transmission (right) in the optical ring resonator. (d) Simulations of electrical fields confined in the capacitive gap of a THz split ring resonator (left) and its transmission spectrum (right).

Integration of high-efficiency χ^2 materials in PIC. From the expression of g_{eo}, a high electro-optic coefficient r is essential for efficient electro-optic coupling. Emerging molecules JRD1[42] exhibit remarkable electro-optic coefficients of several hundreds of pm/V, surpassing those of other promising materials such as lithium niobate by 10-100 times. This organic material also features excellent characteristics including thermal stability, slow ageing rate, low acoustic losses, and the ability to create compact structures with nanoscale footprints. The current design incorporates the integration of JRD1 polymer into silicon photonic circuits, as illustrated in Figure 2(c), where the ring resonator is configured as a slot waveguide (Figure 3a). Thus, optical fields will propagate in the 100 nm wide slot full of JRD1, maximizing field confinement and light-matter interaction (Figure 3c). Optical losses within the system are another crucial aspect to consider. Silicon photonic waveguides have a typical loss of 2.7 dB/cm, while preliminary studies (Figure 3d) show that JRD1 exhibits also low loss characteristics of about 5 dB/cm at 1550nm. This suggests the potential for constructing low-loss silicon-organic slot ring waveguides, with Q factor easily exceeding 10000 and a significant field enhancement (Figure 3b). For the optical cavity, we need to engineer the free spectral range (FSR) in such a way that the sideband photon $\hbar\omega_{SB}$ is supported by the resonance mode of the ring resonator for superior signal-to-noise ratios. Additionally, we will investigate different fabrication strategies for achieving smooth sidewalls in the slot ring to reduce scattering losses.

Dual cavities for enhanced THz confinement and THz-optic interaction. Inspired by the successful superconducting transmission line in circuits QED,[43] we design THz coplanar waveguide (CPW) cavity where THz field can be well-confined inside (Figure 4a-c). Building upon this design, we have further developed the concept of a THz dual cavity (Figure 4e), incorporating a bowtie antenna to capture THz irradiation and a CPW cavity carefully designed to match the resonance of the antenna, thereby enhancing the confined THz field. Figure 4(d) illustrates the simulation results of a conventional bowtie antenna, with a narrow gap of only 1μm which allows for a field enhancement of 1000. This design also facilitates a strong overlap between the optical and THz fields on the nonlinear optical

medium (Figure 3e-g), resulting in an extraordinary electro-optic coupling rate g_{eo} approaching 100MHz, surpassing even the recently reported plasmonic configurations.[31] Furthermore, Figure 4(e) showcases the field confinement in the dual cavity, where an additional factor of 3-4 enhancement in the amplitude is achieved (equating to a factor of 10 in terms of intensity or photon numbers), as compared in Figure 4(f).

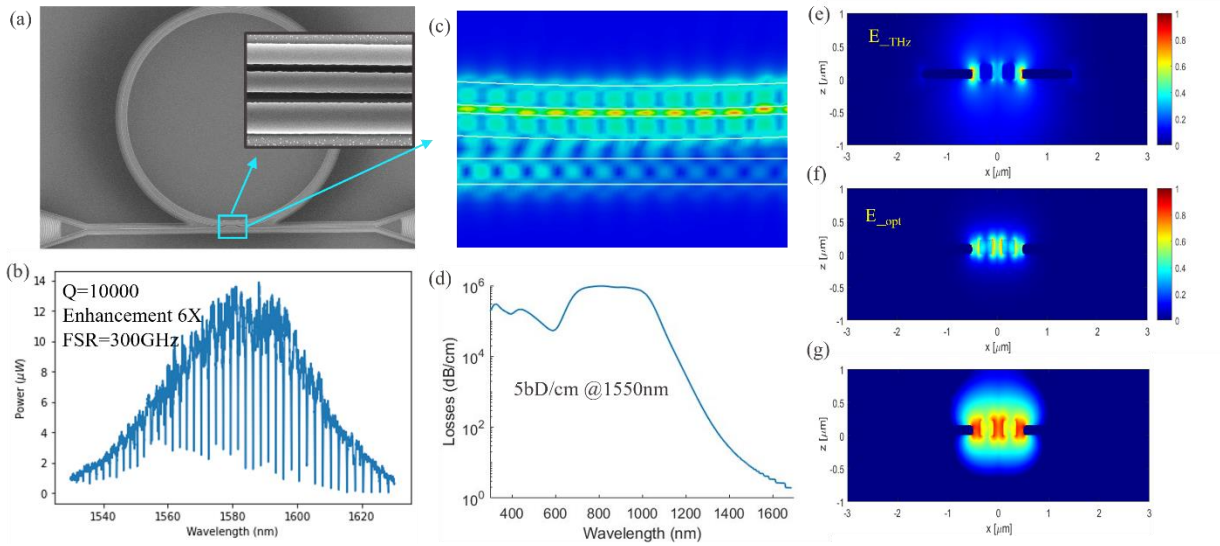

Figure 3. (a) SEM of fabricated slot ring waveguide. (b) Transmission measurements of the slot ring. (c) Simulation of evanescent coupling region. (d) Optical losses of JRD1. (e-g) Simulation of field confinement for THz mode (e) and optical mode (f) respectively. The strong overlap of the two mode is depicted in (g).

Anticipated results in Phase #1: Efficient THz signal detection and generation on PICs. We anticipate creating THz silicon-organic PIC for the THz-optic frequency conversion on a chip with record-high efficiency, enabled by the optimized fields confinement and interaction in ultrahigh electro-optic coefficients nonlinear optical medium. The research aims to implement chip-scale THz sensors characterized by high efficiency and rapid operation at room temperature, meeting the demands of applications in wireless communication, LiDAR technology, THz imaging, and beyond.

Phase #2: Superconducting THz integrated circuits for quantum information

Design and fabrication of superconducting THz cavities. The superconducting material to investigate is Nb or NbN, which exhibits a high critical temperature typically around 15 K, and a gap frequency reaching 1.2 THz.[44] Figure 4(g) showcases a preliminary lift-off result of Nb deposition on a sapphire substrate by electro-beam evaporation. Structures with critical dimensions of 500 nm can already be well implemented successfully in the current test. In the Laboratory of Hybrid Photonics at EPFL, we are in the process of establishing an optical experimental system combined with a dilution refrigerator, as depicted in Figure 4(h). This setup will facilitate cryogenic investigations in quantum regimes within the THz frequency range. By conducting these experiments, we aim to understand and benchmark the performance of emerging materials at high frequencies. This research marks a pivotal stride towards the development of superconducting THz integrated circuits for quantum information processing.

Stretched goal: fundamental study of THz superconducting circuits. The on-chip superconducting THz-optic system realized in previous steps can simultaneously serve as a platform for fundamental studies of quantum electrodynamics at the THz domain. With capabilities of on-chip signal generation, detection, and modulation that have never been accessible before, this platform offers exciting opportunities to explore various fundamental questions, including the performance of superconducting materials at high frequencies, dynamics of Cooper pairs dissociation and recombination, and control/readout of quantum states in a THz Josephson junction These THz

superconducting circuits, unexplored until now, hold tremendous potential for groundbreaking research fields such as THz quantum computing.

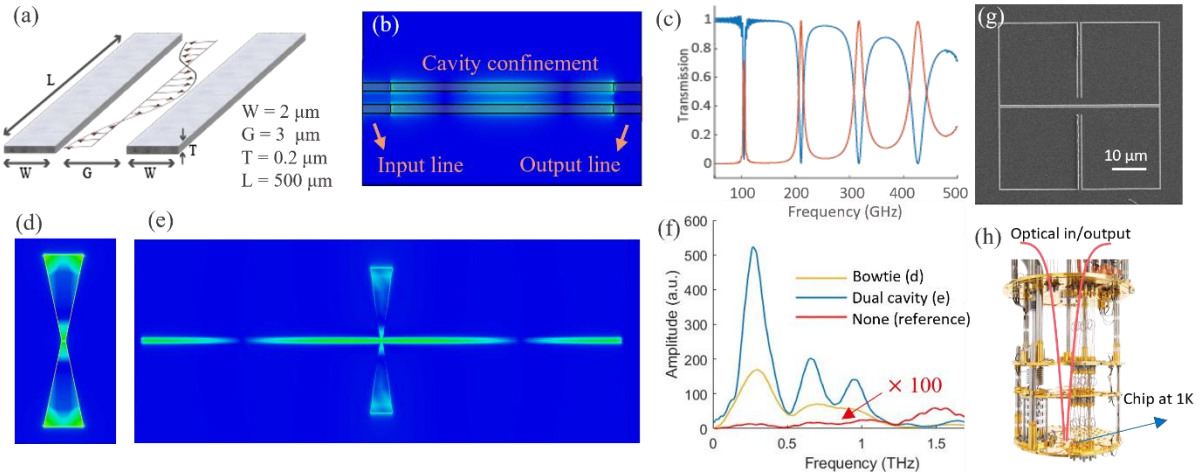

Figure 4. (a) Schematic of THz CPW cavity. (b) Simulation of field confinement in the THz CPW cavity. (c) Simulation results of S11 and S21 of CPW cavity. (d) Simulation of electrical fields confined by a simple bowtie antenna at around 250 GHz. (e) Simulation of electrical fields confined in THz dual cavity. (f) Simulation of amplitudes of confined THz fields in bowtie antenna (yellow), dual cavity (blue) and reference case without any metallic structure. (g) lift-off result of Nb resonator deposition on sapphire substrate. (h) Dilution fridge with optical input and output channels for cryogenic study.

Anticipated results in Phase 2: Superconducting THz PIC for quantum information. By the end of the second research phase, we anticipate gaining profound insights into the cryogenic behavior of THz superconducting materials. Additionally, we aim to create the first-ever superconducting THz integrated photonic device on a chip, equipped with full capabilities of high-frequency signal generation, modulation, and detection. This device will facilitate THz-optic frequency conversion with unprecedented efficiency, reaching the single-photon level. This breakthrough will unlock a broad spectrum of applications in both classical and quantum domains. We believe this research will illuminate a brand-new approach to designing and implementing efficient high-frequency integrated circuits for future classical and quantum applications in the THz domain.

4. Relevance and impact

This proposal aims to establish cutting-edge interdisciplinary research in THz photonic integrated circuits, cavity electro-optics, and quantum superconducting circuits. Phase 1 focuses on developing highly efficient THz signal detection and generation on photonic integrated circuits. This will be achieved by leveraging high electro-optic coefficient materials like JRD1 and designing novel dual THz cavities for strong field enhancement. This innovation could revolutionize applications in wireless communication, LiDAR technology, and THz imaging by offering superior performance with compact, low-cost devices. Phase 2 extends the impact by exploring superconducting THz integrated circuits for quantum information. By fabricating and characterizing superconducting THz cavities, this research aims to achieve unprecedented electro-optic coupling efficiencies and facilitate the development of on-chip systems capable of quantum state manipulation and readout. This has profound implications for quantum computing, as it could lead to new methods of controlling and detecting quantum states at THz frequencies.

Overall, this research holds the potential to significantly enhance the efficiency and functionality of photonic and quantum devices, driving innovation across multiple fields including telecommunications, quantum computing, and advanced sensing technologies. The integration of novel materials and the development of sophisticated cavity designs are crucial steps towards realizing high-performance, scalable photonic and quantum systems, making this work highly relevant and impactful in both academic and industrial contexts.

5. Bibliography

1. Celler, G. K. & Cristoloveanu, S. Frontiers of silicon-on-insulator. *J Appl Phys* **93**, 4955–4978 (2003).
2. Pavesi, L., Dal Negro, L., Mazzoleni, C., Franzò, G. & Priolo, F. Optical gain in silicon nanocrystals. *Nature 2000 408:6811* **408**, 440–444 (2000).
3. Foster, M. A. *et al.* Broad-band optical parametric gain on a silicon photonic chip. *Nature 2006 441:7096* **441**, 960–963 (2006).
4. Alduino, A. & Paniccia, M. Wiring electronics with light. *Nat Photonics* **1**, 153–155 (2007).
5. Thomson, D. *et al.* Roadmap on silicon photonics. *Journal of Optics* **18**, 073003 (2016).
6. Pfeiffer, M. H. P. *et al.* Photonic Damascene process for integrated high-Q microresonator based nonlinear photonics. *Optica* **3**, 20 (2016).
7. Brasch, V. *et al.* Photonic chip–based optical frequency comb using soliton Cherenkov radiation. *Science (1979)* **351**, 357–360 (2016).
8. Riemensberger, J. *et al.* A photonic integrated continuous-travelling-wave parametric amplifier. *Nature 2022 612:7938* **612**, 56–61 (2022).
9. Boes, A. *et al.* Lithium niobate photonics: Unlocking the electromagnetic spectrum. *Science (1979)* **379**, (2023).
10. Wang, C. *et al.* Integrated lithium niobate electro-optic modulators operating at CMOS-compatible voltages. *Nature* **562**, 101–104 (2018).
11. Zhang, M. *et al.* Broadband electro-optic frequency comb generation in a lithium niobate microring resonator. *Nature* **568**, 373–377 (2019).
12. He, M. *et al.* High-performance hybrid silicon and lithium niobate Mach–Zehnder modulators for 100 Gbit s−1 and beyond. *Nat Photonics* **13**, 359–364 (2019).
13. Wang, C. *et al.* Lithium tantalate photonic integrated circuits for volume manufacturing. *Nature* (2024) doi:10.1038/s41586-024-07369-1.
14. Jacob, M. V. *et al.* Temperature Dependence of Permittivity and Loss Tangent of Lithium Tantalate at Microwave Frequencies. *IEEE Trans Microw Theory Tech* **52**, 536–541 (2004).
15. Yang, R.-Y., Su, Y.-K., Weng, M.-H., Hung, C.-Y. & Wu, H.-W. Characteristics of coplanar waveguide on lithium niobate crystals as a microwave substrate. *J Appl Phys* **101**, (2007).
16. Keith Powell, X. L. D. A. L. M. N. S. M. L. Stable electro-optic modulators using thin-film lithium tantalate. *ArXiv* (2024).
17. Lukin, D. M. *et al.* 4H-silicon-carbide-on-insulator for integrated quantum and nonlinear photonics. *Nat Photonics* **14**, 330–334 (2020).
18. Wilson, D. J. *et al.* Integrated gallium phosphide nonlinear photonics. *Nat Photonics* **14**, 57–62 (2020).
19. Kieninger, C. *et al.* Ultra-high electro-optic activity demonstrated in a silicon-organic hybrid modulator. *Optica* **5**, 739 (2018).
20. Leuthold, J. *et al.* Silicon Organic Hybrid Technology—A Platform for Practical Nonlinear Optics. *Proceedings of the IEEE* **97**, 1304–1316 (2009).
21. Steglich, P. *et al.* Silicon-organic hybrid photonics: Overview of recent advances, electro-optical effects and CMOS-integration concepts. *Journal of Physics: Photonics* (2021) doi:10.1088/2515-7647/abd7cf.
22. Palmer, R. *et al.* Low Power Mach–Zehnder Modulator in Silicon-Organic Hybrid Technology. *IEEE Photonics Technology Letters* **25**, 1226–1229 (2013).
23. Korn, D. *et al.* Lasing in silicon–organic hybrid waveguides. *Nature Communications 2016 7:1* **7**, 1–

9 (2016).
24. Witmer, J. D. *et al.* A silicon-organic hybrid platform for quantum microwave-to-optical transduction. *Quantum Sci Technol* **5**, 034004 (2020).
25. Barh, A., Rodrigo, P. J., Meng, L., Pedersen, C. & Tidemand-Lichtenberg, P. Parametric upconversion imaging and its applications. *Adv Opt Photonics* **11**, 952 (2019).
26. Lauk, N. *et al.* Perspectives on quantum transduction. *Quantum Sci Technol* **5**, 020501 (2020).
27. Tsang, M. Cavity quantum electro-optics. *Phys Rev A (Coll Park)* **81**, 063837 (2010).
28. Tsang, M. Cavity quantum electro-optics. II. Input-output relations between traveling optical and microwave fields. *Phys Rev A (Coll Park)* **84**, 043845 (2011).
29. Fan, L. *et al.* Superconducting cavity electro-optics: A platform for coherent photon conversion between superconducting and photonic circuits. *Sci Adv* **4**, (2018).
30. Xu, Y. *et al.* Bidirectional interconversion of microwave and light with thin-film lithium niobate. *Nat Commun* **12**, 4453 (2021).
31. Benea-Chelmus, I.-C. *et al.* Electro-optic interface for ultrasensitive intracavity electric field measurements at microwave and terahertz frequencies. *Optica* **7**, 498 (2020).
32. Forsch, M. *et al.* Microwave-to-optics conversion using a mechanical oscillator in its quantum ground state. *Nat Phys* **16**, 69–74 (2020).
33. Mirhosseini, M., Sipahigil, A., Kalaee, M. & Painter, O. Superconducting qubit to optical photon transduction. *Nature* **588**, 599–603 (2020).
34. Roelli, P., Galland, C., Piro, N. & Kippenberg, T. J. Molecular cavity optomechanics as a theory of plasmon-enhanced Raman scattering. *Nat Nanotechnol* **11**, 164–169 (2016).
35. Han, X., Fu, W., Zou, C.-L., Jiang, L. & Tang, H. X. Microwave-optical quantum frequency conversion. *Optica* **8**, 1050 (2021).
36. Nagatsuma, T., Ducournau, G. & Renaud, C. C. Advances in terahertz communications accelerated by photonics. *Nature Photonics 2016 10:6* **10**, 371–379 (2016).
37. Tonouchi, M. Cutting-edge terahertz technology. *Nature Photonics 2007 1:2* **1**, 97–105 (2007).
38. Rajabali, S. & Benea-Chelmus, I.-C. Present and future of terahertz integrated photonic devices. *APL Photonics* **8**, (2023).
39. Jin, B. *et al.* Low loss and magnetic field-tunable superconducting terahertz metamaterial. *Opt Express* **18**, 17504 (2010).
40. Laman, N. & Grischkowsky, D. Terahertz conductivity of thin metal films. *Appl Phys Lett* **93**, (2008).
41. Anferov, A., Harvey, S. P., Wan, F., Simon, J. & Schuster, D. I. Superconducting Qubits Above 20 GHz Operating over 200 mK. (2024).
42. Dalton, L. R. *et al.* Perspective: Nanophotonic electro-optics enabling THz bandwidths, exceptional modulation and energy efficiencies, and compact device footprints. *APL Mater* **11**, 50901 (2023).
43. Blais, A., Grimsmo, A. L., Girvin, S. M. & Wallraff, A. Circuit quantum electrodynamics. *Rev Mod Phys* **93**, 025005 (2021).
44. Kawamura, J. *et al.* Low-noise submillimeter-wave NbTiN superconducting tunnel junction mixers. *Appl Phys Lett* **75**, 4013–4015 (1999).

Multi-gas sensing hollow-core fiber-based platform with power-over-fiber capabilities

Jonas H. Osório

Department of Physics, Federal University of Lavras, Lavras, Brazil

Category: Environment

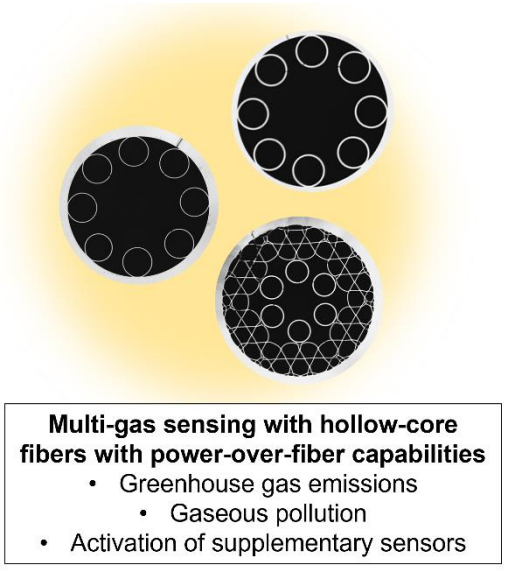

The development of devices able to monitor multiple gas species is a pressing need in environmental science. Although this need motivated the study of a great set of gas sensors, selectively and remotely detecting multiple gas species using a single platform lingers as a challenging task. This project proposes the realization of a multi-gas sensing platform endowed with power-over-fiber capabilities using fiber-enhanced Raman spectroscopy (FERS) and ultralow-loss hollow-core photonic crystal fibers (HCPCFs). Performing FERS with such fibers will allow enlarging the interaction lengths to potentially achieve lower detection limits for greenhouse gases and gaseous pollutants sensing. Furthermore, the use of HCPCFs, known for their ability to transmit high-power optical beams, introduces a novel dimension to environmental sensing. Through power-over-fiber (PoF) schemes, complementary electrical sensors can be activated, enhancing the platform's versatility by enabling assessments of parameters such as temperature, pressure, and humidity. Thus, the proposed platform represents a significant advancement in environmental sensing, promising enhanced efficacy and broader applicability in gathering data for environmental assessments.

The outcomes of my project will yield both scientific and practical achievements. Scientifically, my endeavors will delve into understanding HCPCF properties, including modal content, polarization characteristics, and sources of loss. Practically, the development and application of these sensors will enable the detection and quantification of greenhouse emissions and gaseous pollutants. This contribution aligns with broader community efforts towards a sustainable future by furnishing stakeholders engaged in production, monitoring, and control activities with an effective means of assessing multi-gas environments. The development of the proposed multi-gas HCPCF sensors will hence highly impact the scenario of environmental monitoring systems and, therefore, significantly contribute to the efforts regarding environment preservation. This has the potential to supply information on the environmental conditions capable of guiding strategic discussions on environmental conservation and climate change assessment. Furthermore, given Brazil's strategic importance in global environmental discourse, owing to its abundant natural resources and imperative for environmental monitoring, the amplification of this project's impact is noteworthy. Following laboratory characterization, the developed devices will be deployed in on-the-field applications across diverse environments such as urban and rural areas, plantations, livestock production sites, and forests, further magnifying their significance.

Optica Foundation Challenge – Proposal

Category: environment

Multi-gas sensing hollow-core fiber-based platform with power-over-fiber capabilities

Prof. Jonas Henrique Osório

Department of Physics, Federal University of Lavras, Lavras, Brazil

The development of devices able to monitor multiple gas species is a pressing need in environmental science. Indeed, although this has driven extensive research on a great set of gas sensors, selectively and remotely detecting multiple gas species using a single platform lingers as a challenging task. In this framework, my project proposes the realization of multi-gas fiber-enhanced Raman spectroscopy (FERS) with newly demonstrated hollow-core photonic crystal fibers (HCPCFs) displaying ultralow loss in the short-wavelength range. Performing FERS with such new fibers, which stand nowadays as the lowest loss fiber optics guiding in the visible range, will allow enlarging the interaction lengths of the current systems and achieve lower detection limits for greenhouse gases and gaseous pollutants sensing. Additionally, this platform enables setting up power-over-fiber (PoF) configurations thanks to the HCPCFs' capability of successfully transmitting and delivering high-power optical beams. This offers a new dimension to the realization of environmental sensing as it allows for the activation of complementary electrical sensors for temperature, pressure, and humidity assessment, thereby enhancing the platform's versatility. Therefore, the platform I propose herein promises a significant advancement in environmental sensing with enhanced efficacy and broader applicability in gathering data for environmental assessments.

Literature review

Bountiful results have been achieved by the gas sensors research community in the latest years both regarding the demonstration of the sensing schemes and their corresponding performances. Indeed, these efforts have been highly motivated by the pressing need for the development of such devices, which became of paramount importance to medical and industrial applications, as well as to environmental science (*e.g.*, for the detection of greenhouse emissions and gaseous pollutants).

Among the different gas sensing approaches, optical methods appear as highly promising ones as they afford excellent selectivity, sensitivity, and very low detection limits whilst keeping the possibility of being set in compact, lightweight, and electromagnetic interference-immune setups. Thus, techniques such as laser absorption and photothermal spectroscopies [1, 2] have been investigated and successfully applied

to the detection of different gas species. Although these techniques can provide superior performances, they are typically designed to probe single gas molecules. Alternatively, if one wishes to perform multiple gas sensing using the latter, the complexity of the experimental setups can greatly increase, as multiple optical sources might be needed to assess the different absorption lines of the gases under study.

In this context, Raman spectroscopy [3] emerges as a potent alternative to the realization of multi-gas sensing as it is able to detect the molecules' spectral fingerprints and, hence, afford a highly selective measurement for the study of complex gas mixtures while using a single optical source. Despite its potentialities for the detection of multiple gases, the Raman scattering cross-sections of gases are diminutive (typically in the order of 10^{-27} cm^2), hence entailing feeble Raman signals. To circumvent this limitation, resonant or multi-pass configurations have been approached [4].

Hollow-core photonic crystal fibers (HCPCFs), in turn, appear as an excellent alternative for the realization of Raman scattering-based gas sensing. This is so because HCPCFs, special optical fibers exhibiting an internal microstructure that defines a void core, can simultaneously act as performant waveguides and hosts for gas molecules. This capability readily allows for significantly increasing the interaction length between the optical fields and the analyte gas molecules, hence heightening the Raman signals and enabling the development of sensors with smaller detection limits. Due to the latter, one typically refers to the Raman spectroscopy experiments using HCPCFs as fiber-enhanced Raman spectroscopy (FERS). Similarly to free-space configurations, FERS has allowed the development of gas sensors with sub-ppm detection limits [5, 6]. Noteworthily, as they rely on fiber optics, FERS sensors enable the realization of remote gas detection measurements, an advantage over free-space setups.

In this framework, we observe that HCPCF technology has experienced intense development in recent years. Amid the important results in the area, we find my recent work that demonstrated the fabrication of record low-loss HCPCFs guiding in the visible and ultraviolet wavelength ranges [7]. My fibers display, in fact, the lowest loss figures in the visible and ultraviolet considering all fiber optics as they lie below the silica Rayleigh scattering limit (a fundamental hindrance for loss decreasing in solid-core fibers). Therefore, the availability of these new-generation ultralow-loss HCPCFs stands as the core of my grant proposal since applying such fibers as a platform for FERS opens a promising path for demonstrating gas sensors with better performances. This is so because their reduced loss enables the utilization of longer fibers to enhance the measured signals and potentially reduce the detection limits.

Additionally, my recent research has also demonstrated the potential of HCPCFs as promising platforms for power-over-fiber (PoF) applications [8]. PoF systems use optical fibers to deliver high-power beams for activating electrical systems. In turn, HCPCFs, thanks to their outstanding capability to efficiently transmit and deliver high-power optical beams, emerge as excellent candidates for PoF integration. Therefore, HCPCF technology offers a pathway to establish sensing configurations endowed with PoF capabilities, presenting itself as an opportunity to integrate complementary electrical sensors into a fibered platform for a comprehensive environmental assessment. Through this integration, one enables the collection of data on gas composition and supplementary parameters such as temperature and humidity levels.

Therefore, my project proposes to pursue the demonstration of multi-gas sensors with better performances than those reported hitherto and with PoF capabilities to

seamlessly integrate complementary sensors for comprehensive environmental assessment. The efforts of my project will hence focus on deploying these advanced sensors for detecting greenhouse gas emissions and gaseous pollutants. The development of this project in Brazil, a country with salient importance to climate change scenario due to its great availability of natural resources and the critical need for environment preservation, will enhance the impact of the efforts to be devoted to my research. Moreover, the broader impact of these advancements extends beyond environmental monitoring, with potential applications in industries, agriculture, and livestock production. Moreover, future applications may also encompass the characterization of liquid samples, offering potential utility in critical areas such as water quality monitoring.

Problem statement/Objective

The development of multi-gas sensors for environment monitoring is a pressing need for environmental science. In this framework, this project's objective is to develop multi-gas sensors with power-over-fiber capabilities based on Raman spectroscopy and new-generation HCPCFs with ultralow loss in the short-wavelength range. The devices I will develop within the context of this project will therefore be applied in monitoring greenhouse gas emissions (*e.g.*, methane and carbon dioxide) and gaseous pollution detection, such as hydrogen sulfide. Additionally, the devices will incorporate electrical sensors, activated by optical beams, to assess parameters such as temperature, atmospheric pressure, and humidity.

Fig. 1 displays representative diagrams of my project's aims and actions. As indicated in the introduction, my recent work [7] demonstrated HCPCFs with record low-loss figures in the visible and ultraviolet ranges (typical HCPCFs' cross-sections are shown in Fig. 1). The availability of such new-generation HCPCF allows proposing the realization of Raman spectroscopy of gaseous samples to attain multi-gas sensors with better performance than those reported up to date. I mention that I keep with me several samples of these fibers, which are readily available for being employed in this project. Additionally, I mention that I coordinate the Multiuser Laboratory of Optics and Photonics (LaMOF) at the Department of Physics at the Federal University of Lavras, which encompasses the fundamental infrastructure for the realization of my project.

As represented in Fig. 1, the initial tests will take place in a laboratory environment by accounting for the Raman spectra of known gas species at known concentrations (in single-gas and multi-gas scenarios) to determine the response of the sensors and obtain an adequate calibration of the latter. In this context, I will study the proposed platform using different fiber lengths and light coupling conditions to evaluate the optimum configuration for the sensor operation. Additionally, by using appropriate lasers and photovoltaic converters (PV), the developed gas sensor will also act as a PoF platform to activate supplementary electrical sensors to monitor parameters such as temperature, atmospheric pressure, and humidity levels. The data gathered from the optical gas sensor and complementary electrical sensors will be consolidated in a user-friendly interface to provide valuable information for having a broad characterization of the tested environment. My effort, therefore, will generate a prototype that will include the optical fiber-based multi-gas sensor and the electrical sensors powered by the beams

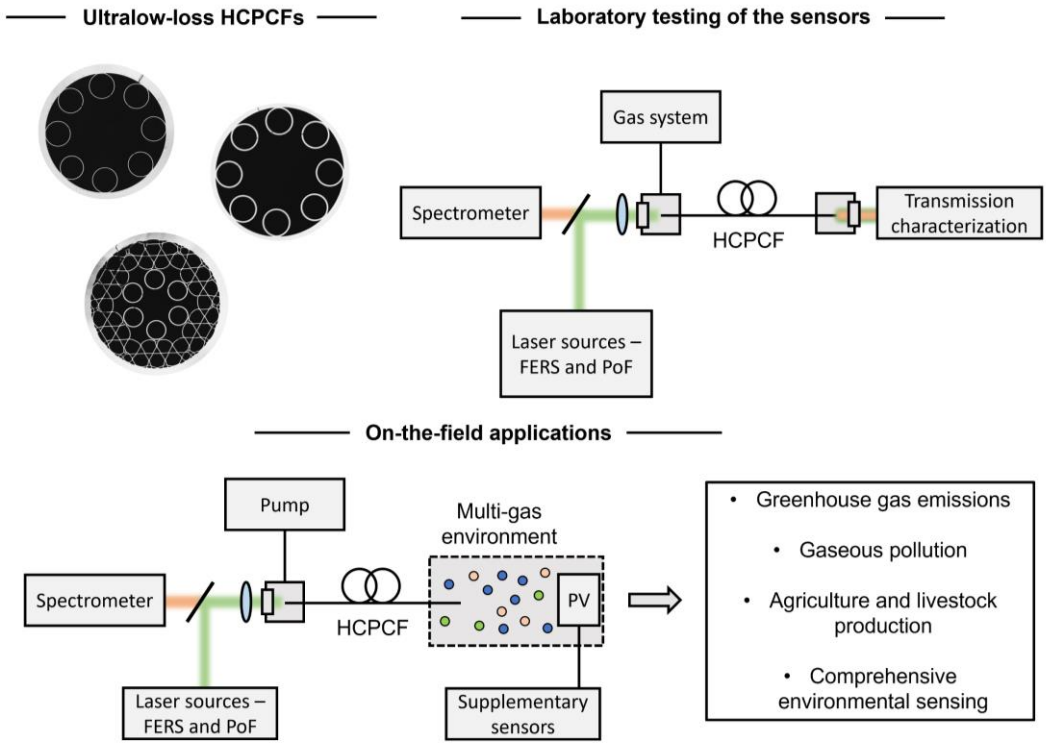

Fig. 1. *Diagram of the project activities, which will encompass the use of ultralow-loss HCPCFs for the development of multi-gas sensors based on FERS with PoF capabilities. The tests will evaluate the sensor response under laboratory-controlled conditions and in on-the-field applications involving greenhouse gas emission and gaseous pollution monitoring.*

transmitted by the very same fiber. The fiber will hence act as the gas reservoir, the sensor itself, and a transmission medium for optically activating the electrical sensors.

Finally, following the laboratory testing of the sensors, I will approach on-the-field applications. In this context, one of the HCPCF ends will be placed into real-world environments of interest (*e.g.*, urban environment and agriculture sites) and a pump will be used to fill the fiber with the gaseous sample to be assessed. It is expected that the developed sensors will enable remote detection and quantification of gaseous pollution and greenhouse gas quantities in the studied environments besides an account of supplementary environmental parameters such as temperature, atmospheric pressure, and humidity levels.

Outcomes

The outcomes of this project will encompass both scientific and practical achievements. From the scientific viewpoint, the activities to be developed within the scope of my project will allow delving into HCPCF properties – modal content, polarization characteristics, and sources of loss –, to identify the most suitable configuration for the sensors' operation. Indeed, although there are previous studies in the literature regarding FERS in HCPCF, the latter are mostly related to the applications themselves. Thus, more comprehensive studies on the impact of HCPCF properties on sensing performance are highly desirable. Hence, one can expect that my efforts will generate relevant scientific papers on the subject.

From a practical point of view, the development and application of the sensors will allow for demonstrating devices able to detect and quantify greenhouse gases and gaseous pollutants. This will contribute to the broad community efforts on environment preservation towards a better future for humanity and will provide the society actors involved in productive, monitoring, and controlling actions with an effective means for assessing multi-gas environments using a simple configuration.

Additionally, this grant will act as seed funding for the consolidation of the research line proposed in this project at the University of Lavras. This is highly beneficial as obtaining substantial financial resources for initiating a research line in Brazil is very challenging due to strict economic conditions. The funding by Optica, therefore, will allow me to consolidate the infrastructure for the development of HCPCF-based multi-gas sensors in Brazil and enable future advancements via local funding.

Impact

The development of the multi-gas HCPCF-based sensor with PoF capabilities I propose herein will impact the broad scenario of environmental monitoring systems and supply the social actors with an efficient means for remotely assessing multi-gas compositions in environments of interest. The endeavors to be devoted to this project will, therefore, significantly contribute to community efforts regarding environment preservation by providing a means for attaining data on greenhouse emissions and gaseous pollution. This, together with other techniques, has the potential of supplying information on the environmental conditions hence guiding discussions on the strategies for environmental conservation and climate change assessment.

Additionally, being Brazil a country with strategic importance to the world's environmental issues due to its wide availability of natural resources and urgent need for environmental monitoring, I highlight that the development of my project has the potential of having amplified repercussions of its gas sensing results, as the developed devices will be, after laboratory characterization, employed in on-the-field applications in areas of interests such as urban and rural environments, plantations, livestock production sites, and forests. This direct field application highlights the practical utility and broader relevance of my research, positioning it as a significant contributor to addressing pressing environmental challenges on both local and global scales.

References

[1] C. Liu & L. Xu, "*Laser absorption spectroscopy for combustion diagnosis in reactive flows: a review*," Applied Spectroscopy Reviews 54, 1 (2019).
[2] S. E. Bialkowski *et al.* "*Photothermal spectroscopy methods*," John Wiley & Sons (2019).
[3] E. Smith & G. Dent, "*Modern Raman spectroscopy: a practical approach*," John Wiley & Sons (2019).
[4] M. Hippler, "*Cavity-enhanced Raman spectroscopy of natural gas with optical feedback cw-diode lasers*," Analytical Chemistry 87, 15, 7803-7809 (2015).
[5] A. Knebl *et al.* "*Fiber enhanced Raman gas spectroscopy*," TRAC 103, 230-238 (2018).
[6] T. W. Kelly *et al.* "*Sub-ppm gas phase Raman spectroscopy in an anti-resonant hollow core fiber*," Optics Express 30, 43317-13329 (2022).
[7] J. H. Osório *et al.* "*Hollow-core fibers with reduced surface roughness and ultralow loss in the short-wavelength range*," Nature Communications 14, 1146 (2023).
[8] J. H. Osório *et al. "Hollow-core photonic crystal fibers for power-over-fiber systems,"* Optical Fiber Technology 73, 103041 (2022).

Deep Optics Modulo Imager for Single Shot High Dynamic Range Imaging

Executive Summary for Optica Foundation Challenge: Information

Jorge Bacca, Universidad Industrial de Santander, Colombia, jbacquin@uis.edu.co

In today's optically driven world, High Dynamic Range (HDR) imaging is essential for accurately capturing and processing visual data across a wide range of intensities, enhancing the quality and reliability of visual information, and allowing improvements in diverse decision-making processes. However, current methods for expanding dynamic range often rely on capturing multiple images at varying exposures, complicating their utilization in dynamic scenes. One single-shot HDR solution integrates encoded-optical elements with reconstruction algorithms to encode bright regions into Low Dynamic Range (LDR) multiplexed measurements. However, this leads to an ill-posed reconstruction process because of the single free parameter—the height map of the encoded-optical element—resulting in spatial resolution sacrifices. On the other hand, a promising solution to this challenge lies in the modulo camera, employing self-reset pixels to analogically wrap the signal in continuous time, thus expanding the intensity range capabilities. While this camera provides an alternative to single-shot HDRs, the acquired measurement presents image discontinuities that need to be restored with reconstruction algorithms, with current methods demanding the satisfaction of band-limited requirements regarding the problem of the ambiguity of image edges and wrapping edges, which may not always be fully satisfied for real-world images.

Therefore, the main objective of the project is to develop a Deep Optics Modulo Imager, integrating optical-encoding elements with modulo sensors to modify the reconstruction requirement to enable high-quality HDR imaging in a single capture. Specifically, our focus lies in jointly optimizing the free parameters of the optical-encoding elements with the parameters of a reconstruction algorithm to obtain optimal modulo measurements that allow the HDR image reconstruction. The outcome will be a prototype with accompanying reconstruction algorithms, rigorously tested and refined for real-world applications.

The successful implementation of the Deep Optics Modulo Imager has the potential to revolutionize single-shot HDR imaging, offering more efficient and accurate visual data capture. The development of this research could make a significant impacts across diverse fields, including surveillance, autonomous driving, and medical imaging. By providing intensity details of scenes, it could improve detection, classification and tracking tasks, thereby advancing both optical imaging technology and information science.

1. Title: Deep Optics Modulo Imager for Single Shot High Dynamic Range Imaging

Name of participant: Jorge Bacca, Universidad Industrial de Santander, Colombia, jbacquin@uis.edu.co

2. Literature Review:

High Dynamic Range (HDR) Imaging consists of a set of imaging techniques to accurately represent a wide range of intensity levels, spanning from bright sunlight to deep shadows. HDR imaging stands in contrast to conventional cameras, which typically offer only an 8-bit depth representation per channel, limiting their ability to capture the full spectrum of brightness in a scene. While HDR in static scenes can usually be achieved using multiple exposure times [1], [2], dynamic scenes present additional challenges as robust exposure alignment is needed. HDR can be addressed by complex multi-sensor imaging systems [3], varying the exposure time at pixel level [4], or using a spatially-variant gain sensor [5]. However, these alternatives introduce additional limitations such as bulky or complex imaging systems, calibration problems, and limited image resolution [6]. Hence, recent efforts have been conducted to treat HDR reconstruction from a single image capture by introducing deep neural networks, optical-encoding elements, or modulo-based image sensors.

Single-shot HDR reconstruction using deep neural networks involves directly learning a reconstruction operator, which transforms a Low Dynamic Range (LDR) image into an HDR image through a black-box inverse mapping process [7]. This alternative can be used in standard cameras without additional constraints or assumptions in the imaging acquisition system [6], [8]. For instance, authors in [6] proposed a hybrid dynamic range autoencoder that transforms the LDR image into a non-linear compact representation and then feeds it into an HDR decoder network to reconstruct an HDR image. Other works such as [9], proposed multiscale CNNs where local CNN branches aim to learn high-frequency details. In contrast, the dilatation branch provides large information from larger pixels neighborhoods, and a third branch provides overall information by learning the global context of the input. However, these methods lack a mathematical or recovery foundation supporting the information associated with the original HDR scene, which results in generating plausible reconstructions in low-light regions but fails to accurately reconstruct saturated regions.

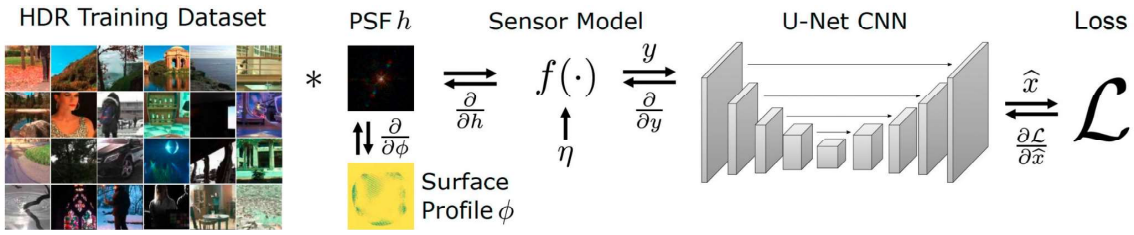

Figure 1. Deep Optics for Single-Shot HDR Imaging [9]. Using a training dataset, the optical-encoding element can be jointly optimized with the network parameters to perform HDR reconstruction using an E2E approach.

Single-shot HDR imaging based on optical-encoding elements surpasses black-box neural networks by incorporating optical-encoding elements. These optical encoding elements induce alterations in the image formation model, allowing the encoding of the brightest pixel values into nearby pixels [10], [11]. Consequently, the spatial-coded LDR image and the optical transfer function of the imaging system are fed to an HDR decoder for

reconstructing the HDR image. For instance, authors in [10], propose incorporating a cross-screen filter mounted in front of a lens where bright image regions are encoded into specially shaped glare patterns. Subsequently, post-processing is employed to remove the glare patterns, enabling HDR reconstruction. Other works such as [11][12] include diffractive optical elements as a lens where the height maps of the lens and the HDR reconstruction algorithm are jointly optimized into an end-to-end (E2E) learning optimization scheme, as shown in Fig. 1, maximizing the information passed from the HDR image to the spatial coding LDR image. However, in practical scenarios, the spatially invariant property of the diffractive optical elements introduces strong spatial degradations, where the reconstruction process becomes significantly ill-posed, evidenced by a loss of spatial image resolution and image artifacts.

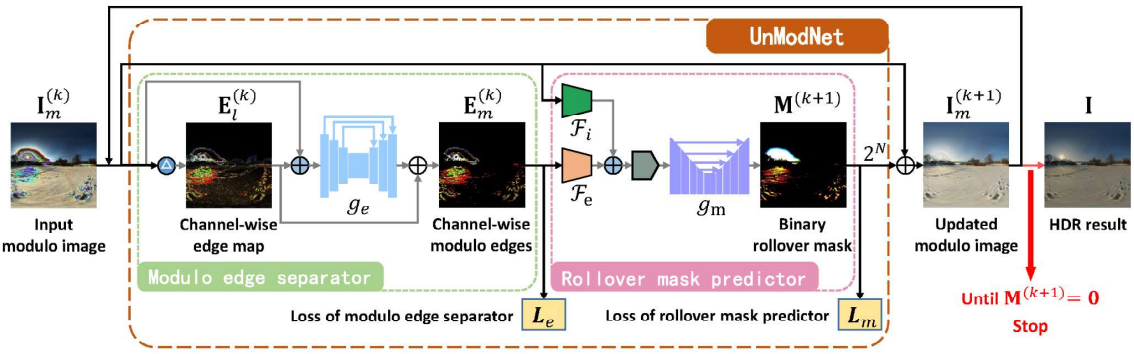

Figure 2. Single-shot HDR using modulo images and deep learning [13]. The modulo image enters the network, where the number of times each pixel was wrapped is iteratively estimated to obtain the HDR image.

Single-shot HDR using modulo image sensors encodes information regarding all image intensities by resetting/wrapping the current intensity pixel value when it reaches the maximum level instead of saturating it [14], [15]. Modulo sensors offer the potential to enhance DR capabilities by indirectly sensing an unlimited intensity range. In this scenario, HDR image reconstruction relies on an unwrapping inverse problem, wherein the missing information corresponds directly to the number of times each pixel has been wrapped, in ideal scenarios (noiseless). There are various alternatives to feasibly implement a modulo camera, including the use of digital focal plane arrays (DFPAs), smart-vision sensors such as SCAMP-5, commercial smart-vision cameras such as SONY IMX500, or employing an array of modulo ADCs that wrap the image in continuous time [16]. Furthermore, by making assumptions about the nature of the image and noise models, it becomes feasible to ensure exact recovery [17]. Therefore, several works on HDR reconstruction algorithms based on modulo sensors have been proposed. These include adapting existing phase unwrapping algorithms for the case of natural images [18], directly estimating the missing unwrapping levels map from quantization noise measurements [19] or from logarithmic modulo samples [20], and employing iterative binary roll-over estimation using deep neural networks [13], as shown in Fig. 2. Current methods demand satisfaction of band-limited requirements, regarding the problem of the ambiguity of image edges and wrapping edges [21], which may not always be fully satisfied in real-world images.

Moreover, current literature focuses on addressing the challenges of acquiring HDR images from single-shot captures, utilizing neural networks, specially designed optical elements, or modulo sensors. However, these efforts have largely proceeded independently, highlighting

a significant gap that requires attention through a comprehensive analysis of the strengths and weaknesses inherent in each approach.

3. Problem Statement.

In today's optically driven world, HDR imaging plays a critical role in accurately capturing and processing visual information across a wide range of intensities. From surveillance systems and autonomous vehicles to medical imaging and environmental monitoring, HDR imaging ensures the fidelity and reliability of critical visual data. At each application, HDR techniques enable precise visualization across a broad spectrum of brightness levels, thereby enhancing our understanding and decision-making capabilities across diverse fields. However, current state-of-the-art solutions for expanding dynamic range involve acquiring multiple images at varying exposure levels and subsequently fusing them using computational methods, leading to inefficiencies and limitations, particularly in dynamic scenes. As a result, there is a growing interest in single-shot high dynamic range imaging solutions.

One current approach involves designing encoded-optical elements jointly with reconstruction algorithms to encode the bright parts into low dynamic range (LDR) multiplexed measurements. However, the reconstruction process becomes significantly ill-posed because of the only free parameter—the height map of a diffractive optical element—leading to sacrifices in spatial resolution. Conversely, a promising solution to this challenge lies in the modulo camera, offering single-shot HDR capabilities by employing self-reset pixels to analogically wrap the signal in continuous time, thereby expanding the intensity range capabilities. Nevertheless, this camera introduces discontinuities in the acquired measurements, necessitating restoration through reconstruction algorithms. Current methods demand satisfaction of band-limited requirements, regarding the problem of the ambiguity of image edges and wrapping edges, which may not always be fully satisfied in real-world images.

The introduction of optical-encoding elements in the image formation model of modulo sensors could have the potential to modify the sensed signal by accomplishing the reconstruction requirements of unwrapping reconstruction and mitigating the natural image discontinuities. Consequently, this research proposal poses the following question: How can the Single-Shot Deep Optics Modulo Imager address the challenges posed by high dynamic range real-world scenes while simultaneously ensuring high-fidelity reconstruction and spatial resolution preservation?

4. Objectives.

General Objective: To design and implement an optical-computational encoded modulo imager for single-shot high dynamic range imaging

Aim 1: To establish the image formation model of a Deep Optics Modulo Imager: This aim involves designing and formulating the image formation model for the Deep Optics Modulo Imager. It includes mathematically modeling wave-front propagation through optical-encoded elements such as diffractive optical elements acting as lenses, along with a modulo sensor. Specifically, based on the selected optical-encoded elements, these will define the optical-encoded free parameters to posteriorly be optimized jointly with the HDR

reconstruction algorithm. By precisely outlining the optical principles governing the imaging process, this aim sets the groundwork for subsequent development phases.
Lead time: Over 1-6 months

Aim 2: To develop an end-to-end deep learning-based computational model: This aim involves creating and simulating an end-to-end computational model using deep learning methodologies. The model will parameterize the free parameters of the optical-encoded element, along with a fully differentiable image formation operator. Furthermore, the aim includes developing an optimization-based HDR reconstruction algorithm for wrapped images. Furthermore, it involves integrating optical design with the reconstruction algorithm through joint optimization of the optical parameters and reconstruction parameters to obtain optimal modulo measurements that allow the HDR image reconstruction.
Lead time: Over 6-14 months

Aim 3. To implement and validate a prototype of the Deep Optics Modulo Imager. This aim focuses on the practical implementation and validation of a prototype Deep Optics Modulo Imager. It involves fabricating the designed optical-encoded elements and integrating them with a compatible modulo sensor. Additionally, it encompasses calibrating the integrated system to ensure expected functionality. Through extensive validation exercises conducted across diverse scenarios covering varying noise levels and quantization errors, this aim is to ascertain the functionality and reliability of the prototype in capturing high dynamic range images.
Lead time: Over 14-24 months

5. Outcome.
Through this project, we aim to develop the Deep Optics Modulo Imager, integrating optical-encoding elements and a modulo sensor, to enable single-shot high dynamic range imaging. Furthermore, we will establish an optimization strategy for designing optics and reconstruction parameters within an end-to-end framework. The project will culminate in the creation of a portable prototype, suitable for demonstration at Optica conferences and collaboration with partners. The outcomes of this project will include quantifying the performance of our Deep Optics Modulo Imager and showcasing its capabilities for high-fidelity imaging in various scenarios. Finally, it is expected to share the results obtained in at least:

- Two (2) scientific articles in Optica magazines.
- Two (2) Optica Conferences.

6. Impact.
The successful implementation of a technology capable of extending the high dynamic range of images with a single shot has the potential to revolutionize various fields where accurate visual data is desired. In fields such as surveillance and security, this advancement could significantly enhance the detection and identification of objects in challenging lighting conditions, thus reinforcing overall safety and security measures. Similarly, in autonomous vehicles, where fast and accurate interpretation of the enviroment is paramount, single-shot high dynamic range imaging can improve obstacle detection and navigation, ultimately enhancing road safety, especially at night. Additionally, in medical imaging, the ability to capture a wider range of intensities in a single shot could lead to improved diagnostic accuracy and treatment planning, benefiting patient outcomes. Moreover, in scientific

research and environmental monitoring, this technology could facilitate the precise analysis of complex visual data, aiding in the study of phenomena ranging from climate change to celestial events. Overall, the impact of this type of technology extends across various sectors, offering enhanced capabilities for data acquisition, analysis, and decision-making, thereby advancing both optical imaging technology and information science as a whole.

7. Bibliography

[1] E. Reinhard, “High Dynamic Range Imaging,” in *Computer Vision: A Reference Guide*, Cham: Springer International Publishing, 2020, pp. 1–6.

[2] P. E. Debevec and J. Malik, “Recovering High Dynamic Range Radiance Maps from Photographs,” in *Seminal Graphics Papers: Pushing the Boundaries, Volume 2*, 1st ed., vol. 2, New York, NY, USA: Association for Computing Machinery, 2023, pp. 643–652.

[3] J. Kronander, S. Gustavson, G. Bonnet, A. Ynnerman, and J. Unger, “A unified framework for multi-sensor HDR video reconstruction,” *Signal Processing: Image Communication*, vol. 29, no. 2, pp. 203–215, Feb. 2014.

[4] S. K. Nayar and T. Mitsunaga, “High dynamic range imaging: spatially varying pixel exposures,” in *Proceedings IEEE Conference on Computer Vision and Pattern Recognition. CVPR 2000 (Cat. No.PR00662)*, IEEE, 2000, pp. 472–479 vol.1.

[5] S. Hajisharif, J. Kronander, and J. Unger, “Adaptive dualISO HDR reconstruction,” *EURASIP Journal on Image and Video Processing*, vol. 2015, no. 1, p. 41, Dec. 2015.

[6] G. Eilertsen, J. Kronander, G. Denes, R. K. Mantiuk, and J. Unger, “HDR image reconstruction from a single exposure using deep CNNs,” *ACM Trans. Graph.*, vol. 36, no. 6, pp. Nov. 2017.

[7] L. Wang and K.-J. Yoon, “Deep Learning for HDR Imaging: State-of-the-Art and Future Trends,” *IEEE Trans. Pattern Anal. Mach. Intell.*, vol. 44, no. 12, pp. 8874–8895, Dec. 2022.

[8] Y.-L. Liu *et al.*, “Single-image HDR reconstruction by learning to reverse the camera pipeline,” in *Proceedings of the IEEE/CVF conference on computer vision and pattern recognition*, 2020,

[9] D. Marnerides, T. Bashford-Rogers, J. Hatchett, and K. Debattista, “ExpandNet: A Deep Convolutional Neural Network for High Dynamic Range Expansion from Low Dynamic Range Content,” *Comput. Graph. Forum*, vol. 37, no. 2, pp. 37–49, May 2018.

[10] M. Rouf, R. Mantiuk, W. Heidrich, M. Trentacoste, and C. Lau, “Glare encoding of high dynamic range images,” in *CVPR 2011*, IEEE, Jun. 2011, pp. 289–296.

[11] C. A. Metzler, H. Ikoma, Y. Peng, and G. Wetzstein, “Deep optics for single-shot high-dynamic-range imaging,” *Proc. IEEE Comput. Soc. Conf. Comput. Vis. Pattern Recognit.*, pp. 1372–1382, Aug. 2019.

[12] Q. Sun, E. Tseng, Q. Fu, W. Heidrich, and F. Heide, “Learning rank-1 diffractive optics for single-shot high dynamic range imaging,” *Proc. IEEE Comput. Soc. Conf. Comput. Vis. Pattern Recognit.*, pp. 1383–1393, Jun. 2020.

[13] C. Zhou *et al.*, “Unmodnet: Learning to unwrap a modulo image for high dynamic range imaging,” *Adv. Neural Inf. Process. Syst.*, vol. 33, pp. 1559–1570, 2020.

[14] H. Zhao, B. Shi, C. Fernandez-Cull, S.-K. Yeung, and R. Raskar, “Unbounded High Dynamic Range Photography Using a Modulo Camera,” in *2015 IEEE International Conference on Computational Photography (ICCP)*, IEEE, Apr. 2015, pp. 1–10.

[15] A. Bhandari, F. Krahmer, and R. Raskar, “On unlimited sampling,” in *2017 International Conference on Sampling Theory and Applications (SampTA)*, IEEE, Jul. 2017, pp. 31–35.

[16] A. Bhandari, F. Krahmer, and T. Poskitt, “Unlimited Sampling From Theory to Practice: Fourier-Prony Recovery and Prototype ADC,” *IEEE Trans. Signal Process.*, vol. 70, 2022.

[17] A. Bhandari, F. Krahmer, and R. Raskar, “On Unlimited Sampling and Reconstruction,” *IEEE Trans. Signal Process.*, vol. 69, pp. 3827–3839, 2021.

[18] J. Bacca, B. Monroy, and H. Arguello, “Deep Plug-and-Play Algorithm for Unsaturated Imaging,” in *ICASSP 2024 - 2024 IEEE International Conference on Acoustics, Speech and Signal Processing (ICASSP)*, IEEE, Apr. 2024, pp. 2460–2464.

[19] A. Bhandari and F. Krahmer, “HDR Imaging From Quantization Noise,” in *2020 IEEE International Conference on Image Processing (ICIP)*, IEEE, Oct. 2020, pp. 101–105.

[20] H. M. So, J. N. P. Martel, G. Wetzstein, and P. Dudek, “MantissaCam: Learning Snapshot High-dynamic-range Imaging with Perceptually-based In-pixel Irradiance Encoding,” in *2022 IEEE International Conference on Computational Photography (ICCP)*, IEEE, Aug. 2022, pp. 1–12.

[21] Y. Lu, X. Wang, and X. Zhang, “Weighted least-squares phase unwrapping algorithm based on derivative variance correlation map,” *Optik* , vol. 118, no. 2, pp. 62–66, Feb. 2007.

Meta spectral imaging for wildfire monitoring

Wildfires are an increasingly severe global issue, exacerbated by climate change and impacting ecosystems, human health, and economies. Traditional wildfire monitoring systems, which rely on multispectral imaging from satellites and airplanes, face significant challenges such as high energy consumption, extensive data volume, and poor thermal stability. This project seeks to address these challenges by developing innovative systems that combine metasurface-based hyperspectral imaging with neuromorphic optical processing, offering a new approach to satellite-based forest fire monitoring.

Our approach leverages metasurfaces—ultra-thin, sub-wavelength structures capable of precise light manipulation. These metasurfaces enable one-shot hyperspectral imaging, capturing detailed spectral data across a wide range of wavelengths without the need for moving parts. This innovation significantly enhances the speed and resolution of wildfire detection, allowing for the rapid identification of fire hotspots, smoke plumes, and other critical indicators of wildfire activity.

In addition to the advanced imaging capabilities, we integrate neuromorphic optical processing through multiplane light conversion meta-optics. This integration forms an inbuilt optical neural network that processes spectral images in real-time with minimal latency and energy consumption. By performing optical neural computations directly on the spectral data, we reduce the computational load and data transmission requirements, facilitating efficient onboard data processing and communication with ground stations.

The project's primary objectives for the next two years focus on three main areas:

- Thermal infrared hyperspectral imaging for fire spot detection, where we will use metasurfaces to detect fire spots within the 8-14μm atmospheric window by optimizing point spread functions for multiple wavelengths and compressively reconstruct the spectral images.
- Neuromorphic pre-processing of spectral images, where we will employ multiplane light conversion based on reflective metasurfaces, performing complex linear transformations to preprocess the spectral images, thus reducing data bandwidth requirements and number of detectors in the array.
- Near-infrared multispectral imaging for vegetation detection, where we aim to design metasurfaces that differentiate between burned and healthy vegetation, enhancing our ability to assess fire damage and vegetation health.

The outcomes of this project will include the development of high-resolution, real-time imaging systems, successful fabrication and testing of metasurface prototypes, and dissemination of research findings through high-impact scientific publications and conferences. Additionally, we anticipate establishing research collaborations and securing further financial support to sustain and expand our research efforts.

The impact of this project extends beyond technological advancements. Enhanced wildfire monitoring capabilities will enable quicker detection and response, potentially mitigating the devastating effects of wildfires. The lightweight, thermally stable metasurface-based systems will reduce operational costs and extend the lifespan of satellite monitoring systems. Improved wildfire monitoring will have significant environmental and economic benefits, helping to protect ecosystems, human health, and property.

By addressing the critical need for advanced wildfire monitoring technologies, this project aims to revolutionize how we detect and respond to wildfires. Our innovative approach promises to contribute significantly to the global effort to manage and mitigate the impacts of climate change and natural disasters.

Meta spectral imaging for wildfire monitoring

This project aims to develop paradigm-shifting systems that combine metasurface-based hyperspectral imaging and real-time neuromorphic optical processing for satellite-carried forest fire monitoring. Here, the meaning of *meta spectral imaging* is two-fold: on the one hand, it employs a one-shot hyperspectral imaging system enabled by metasurfaces; on the other hand, the functionality of the system is beyond conventional imaging or computation imaging – it has an inbuilt optical neural network based on multilayer meta-optics for the low-latency and energy-efficient all-optical neuromorphic pre-processing of the spectral image, minimizing the overhead for onboard computation and data communication.

Background/Problem Statement

Wildfires are a growing global concern, worsened by climate change and increasingly affecting ecosystems, human health, and economies. The situation's urgency necessitates robust monitoring systems, often space-borne or airplane-based and typically reliant on multispectral imaging. Traditional satellite-carried wildfire monitoring systems suffer from the following main problems [1]:

- Large onboard energy consumption and instability associated with the moving parts for scanning-based spectral imaging.
- Fluctuations in the atmospheric transparent windows that reduces the sensitivity, resolution, and reliability of the detection.
- A huge amount of imagery data presents a challenge in downloading the data from the satellite as well as processing the data in real time.
- Conventional optics are bulky and heavy and exhibit poor thermal stability in hush environments of space.

These issues constitute bottlenecks in current satellite-based wildfire monitoring devices, making them extremely difficult to operate in real-time and provide timely alerts to forest fires at an early stage.

Metasurfaces composed of judiciously designed sub-wavelength structures, offer unprecedented capabilities in manipulating light in all degrees of freedom, from spatial to spectral to polarization. In fact, metasurfaces are extremely suitable for tackling all the above challenges associated with conventional satellite-carried wildfire monitoring devices for the following reasons:

- Highly resonant features of metasurfaces can be easily utilized to achieve one-shot multi-spectral or even hyper-spectral imaging systems across a wide wavelength range, with no need for any moving parts.
- Multilayer metasurfaces can perform a wide range of linear transformations for the neuromorphic pre-processing of the multi-spectral images, minimizing the data bandwidth requirement for communication with the ground.
- Unlike bulk optics that have a volume, ultra-thin metasurfaces have the advantage of miniaturization with good thermal stability and are, therefore, highly suitable for space-related applications.

By harnessing these capabilities, our project will develop one-shot hyperspectral imaging systems that can capture a wide range of spectral data in a single snapshot. This approach significantly enhances the speed and resolution of imaging, enabling rapid identification of fire hotspots, smoke plumes, and other critical indicators of wildfire activity. Unlike traditional

sensors that require multiple exposures or scanning mechanisms, our meta-optic-based hyperspectral imaging can provide instantaneous and comprehensive spectral information, crucial for timely wildfire response. The combination of meta-optic elements and neuromorphic optical processing represents a paradigm shift in wildfire monitoring technology.

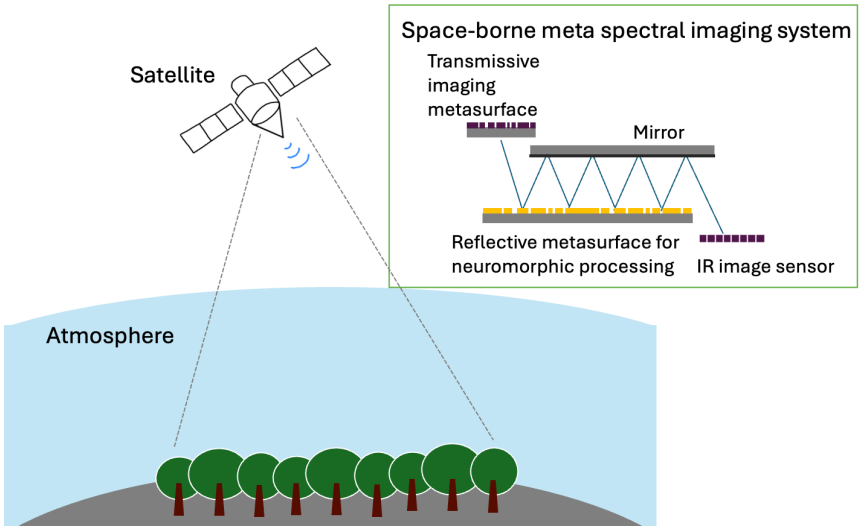

Figure 1 Conceptual sketch of the space-borne meta spectral imaging system for wildfire monitoring

I personally experienced three of the world's most disastrous forest fires in the past five years, including the 2019–2020 Australian wildfire season when I was a PhD student at the Australian National University in Canberra, Australia, the 2020 California wildfires right after I became a postdoctoral scholar at Stanford University in California, US, and the 2023 Canadian wildfires right after I started a faculty position at McGill University in Montreal, Canada. Such experiences especially motivated me to utilize my optics and photonics expertise to help tackle the global challenge of increasingly severe wildfires. However, **since my primary research program and publication track records are on quantum and topological photonics, it is very hard for me to obtain financial support to seed my research on wildfire monitoring and climate change.** By applying for the Optical Challenge program, I aim to partially switch my research to tackling this global challenge of wildfires, the outcome of which will enable a new long-term research program in my research group, secure other financial support based on the established track record through this project and establish potential collaborations with relevant research institutions and teams.

Literature review

Current wildfire monitoring relies heavily on satellite and aerial imaging systems using multispectral cameras. These systems face challenges such as high energy consumption, large data volumes, and limited thermal stability [1]. Hyperspectral imaging captures a wide spectrum of light across many bands, providing detailed information about the material properties and composition of objects in the scene. Traditional hyperspectral imaging systems are bulky and require scanning mechanisms, which are unsuitable for real-time applications and space deployment [2].

Metasurfaces composed of sub-wavelength resonators are capable of manipulating light with high precision [3]. They have revolutionized optical technologies by replacing traditional bulk optics with ultra-thin, planar components. Recent advancements have demonstrated metasurfaces' ability to control various aspects of light, including phase, amplitude, frequency, and polarization, making them ideal for compact, efficient optical systems. While metasurfaces are in the process of replacing many of the conventional optics, such as lenses, structured light

illumination for facial recognition, and polarization cameras, their application in space technology and environmental remote sensing remains largely under-explored. Metasurface-based hyperspectral imaging holds great potential to play a transformative role in such applications by enabling one-shot acquisition of hyperspectral data without moving parts, significantly reducing size, weight, and power consumption [4,5].

Neuromorphic optical processing leverages the principles of neural networks using optical components. This approach offers significant advantages in speed and energy efficiency by performing computations with light instead of electrons. Optical neural networks have shown promise in various applications, including image recognition and data compression, due to their ability to perform parallel processing with extremely low latency and energy consumption. They are particularly suitable for applications where the task is fixed (i.e. no need of reconfiguration once the device is designed and fabricated). Integrating neuromorphic processing with metasurface technology enables the creation of advanced imaging systems capable of real-time data analysis. Multilayer metasurfaces can be designed to implement complex linear transformations required for optical neural networks, providing a compact and efficient solution for onboard data processing.

Objectives

The proposed research project has a *long-term vision* to revolutionize wildfire detection and monitoring through the development of advanced meta-optic elements for multi-spectral imaging and neuromorphic optical processing.

The *short-term objectives* for the next two years focus on the following three thrusts:

1) Thermal infrared spectral imaging for fire spot detection
2) Neuromorphic pre-processing of computational spectral images
3) Near-infrared (NIR) multi-spectral imaging for vegetation detection

The detail on each objective is described as follows:

Objective 1: Thermal infrared hyperspectral imaging for fire spot detection

In this objective, we aim to use the atmospheric transparent window of $8-14\mu m$ to detect fire spots based on one-shot multi-spectral imaging enabled by a dielectric metasurface. The metasurface will be designed to operate in the transmission mode, and we will use inverse design to jointly optimize the point spread function (PSF) of the metasurface for computationally imaging multiple wavelengths chosen in $8-14\mu m$, ensuring that the PSFs for different wavelengths are highly incoherent. Then, by reading out the image from an infrared image sensor, we can computationally reconstruct the images for each of the chosen wavelengths, taking advantage of the typical sparsity nature of fire-spot images.

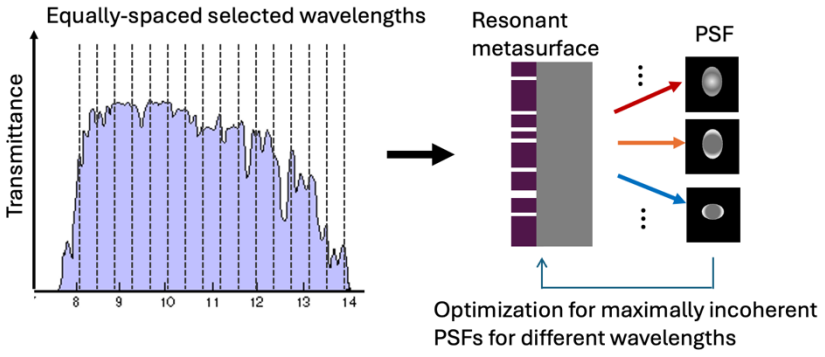

Figure 2 Inverse design of thermal hyperspectral imaging metasurface

We will base our inverse design [6] on GPU optimized finite domain time difference solver [7] and latest frequency domain solvers such as augmented partial factorization [8], a solver that can calculate the scattering matrix of a large-scale metasurface in an extremely fast manner. We have tested such solvers when we did other works related to metasurface for quantum photonics. These solvers enable the combination of the simulation of the entire structure or a large-size unit cell of the metasurface with the optimization algorithm. The optimization will be based on gradient descent.

We will prototype the metasurface using amorphous-silicon-on-glass structures using top-down fabrications and characterize the wavelength-dependent PSFs. As we have expertise in fabricating metasurfaces for optical wavelengths, it is straightforward to scale to 8-14 μm where the minimum feature size is larger. Then, we will perform proof-of-principle experiments with emulated fire spots to test the capability of our metasurfaces. We will demonstrate the robustness of our multi-spectral imaging system against fluctuations in transparent windows by adding dynamical IR filtering.

Objective 2: Neuromorphic pre-processing of computational spectral images

In this objective, we will design reflective metasurfaces that use multiplane light conversion to form an optical neural network for the pre-processing of the computational spectral images. By reflecting light multiple times from the metasurface before it is sent to the image sensor, we can achieve a wide range of linear transformations. Compared to using a multilayer metasurface design, such a configuration features the simplicity of having only one piece of metasurface and hence is potentially more stable and presents less challenges in the alignment. The pre-processed image will have an advantage over the bare image produced by the imaging-metasurface in Objective 1: Instead of generating many frames of raw image data, here the photonic neural network can generate a pre-processed data that is minimum necessary for reconstructing a fire-spot image. Thereby we also no longer need a large array of IR detectors.

Objective 3: Near-infrared (NIR) multi-spectral imaging for vegetation detection

In this objective, we aim to inversely design resonant metasurfaces for multispectral computational imaging that is optimized for vegetation detection, i.e. obtaining images that can be processed to indicate areas that are burned in contrast to areas that are still covered by healthy vegetation.

We will achieve this goal by designing a dielectric imaging metasurface that is highly transmissive only for a few signature wavelengths. For the NIR that can be used with a silicon-based image sensor, the metasurface will need to at least achieve two-wavelength images – one as a reference wavelength around 690 nm, where the reflectance of healthy vegetation is the same as the burned ones, and we will also choose a few other NIR wavelengths that can exhibit a pronounced contrast in reflectance, e.g. around 750 nm. The design will also be based on PSF engineering for different wavelengths. For such evaluation-purpose imaging, we will only use a few wavelengths while focusing on an excellent imaging resolution. The PSFs will all be designed to be nearly optimal for computational image reconstruction.

Outcomes

The proposed project on meta spectral imaging for wildfire monitoring is expected to yield several significant outcomes:

Development of Advanced Imaging Systems: Creation of a one-shot hyperspectral imaging system enabled by metasurfaces, capable of capturing detailed spectral data in a single snapshot

without the need for moving parts. This system will significantly enhance the speed and resolution of wildfire detection.

Integration of Neuromorphic Optical Processing: Implementation of an optical neural network using multilayer meta-optics, enabling real-time, low-latency, and energy-efficient processing of spectral images. This will reduce the computational overhead and data bandwidth requirements for satellite communication.

Prototyping and Validation: Successful fabrication and testing of metasurfaces for thermal infrared and near-infrared imaging. The prototypes will demonstrate the robustness and effectiveness of the metasurface-based imaging systems in identifying fire spots, smoke plumes, and vegetation health.

Publication and Dissemination: Dissemination of research findings through high-impact scientific journals and conferences. The results will contribute to the broader scientific community's understanding of metasurface applications in environmental monitoring and remote sensing.

Collaboration and Funding: Establishment of collaborations with relevant research institutions and teams focused on wildfire monitoring and climate change. The project will also lay the groundwork for securing additional financial support for long-term research in this domain.

Impact

The successful completion of this project will have a profound impact on wildfire monitoring and response, with several key implications:

Enhanced Early Detection and Response: The advanced hyperspectral imaging and neuromorphic processing capabilities will enable rapid and accurate identification of wildfire hotspots, smoke plumes, and vegetation health. This will facilitate timely alerts and interventions, potentially reducing the scale and damage of wildfires.

Energy and Cost Efficiency: The metasurface-based imaging systems are ultra-thin, lightweight, and thermally stable, making them ideal for space deployment. The reduction in onboard energy consumption and elimination of moving parts will lower operational costs and increase the lifespan of satellite monitoring systems.

Environmental and Economic Benefits: Improved wildfire monitoring will help mitigate the devastating effects of wildfires on ecosystems, human health, and economies. Early detection and intervention can save lives, protect property, and preserve natural resources.

Technological Advancement: The integration of metasurface technology with neuromorphic optical processing represents a paradigm shift in remote sensing and environmental monitoring. The project's outcomes will drive innovation in optical technologies, with potential applications beyond wildfire monitoring, including climate change studies, natural disaster management, and agricultural monitoring.

Educational and Research Opportunities: The project will provide valuable training and research opportunities for students and early-career researchers in optics, photonics, and environmental science. It will also raise awareness of the critical role of advanced optical technologies in addressing global challenges such as climate change and natural disasters.

Overall, this project aims to revolutionize wildfire monitoring through cutting-edge optical technologies, delivering tangible benefits to society and the environment.

References

1. S. Veraverbeke, P. Dennison, I. Gitas, G. Hulley, O. Kalashnikova, T. Katagis, L. Kuai, R. Meng, D. Roberts, and N. Stavros, "Hyperspectral remote sensing of fire: State-of-the-art and future perspectives," Remote Sens. Environ. **216**, 105–121 (2018).
2. K. Thangavel, et al., "Autonomous Satellite Wildfire Detection Using Hyperspectral Imagery and Neural Networks: A Case Study on Australian Wildfire," Remote Sens. **15**, 720 (2023).
3. A. I. Kuznetsov, et al., "Roadmap for Optical Metasurfaces," ACS Photonics **11**, 816–865 (2024).
4. F. Yesilkoy, et al., "Ultrasensitive hyperspectral imaging and biodetection enabled by dielectric metasurfaces," Nat. Photonics **13**, 390–396 (2019).
5. C. H. Lin, S. H. Huang, T. H. Lin, and P. C. Wu, "Metasurface-empowered snapshot hyperspectral imaging with convex/deep (CODE) small-data learning theory," Nat. Commun. **14**, 1–10 (2023).
6. Z. Lin, et al., "End-to-end metasurface inverse design for single-shot multi-channel imaging," Opt. Express **30**, 28358 (2022).
7. T. W. Hughes, M. Minkov, V. Liu, Z. Yu, and S. Fan, "A perspective on the pathway toward full wave simulation of large area metalenses," Appl. Phys. Lett. **119**, 150502 (2021).
8. H. Lin, Z. Wang, and C. W. Hsu, "Fast multi-source nanophotonic simulations using augmented partial factorization," **2**, (2022).

Executive Summary

Scalable-manufactured, Decorative, Temperature-adaptive Radiative Window Films for All-season Passive Energy Saving of Glass Skyscrapers

OPTICA Foundation Challenge: Environment

PI: Kaichen Dong (dkc22@sz.tsinghua.edu.cn)

Tsinghua Shenzhen International Graduate School, Tsinghua University, China

Introduction: Global warming is a growing threat to society, which is caused by greenhouse gas emissions from ever-increasing energy consumptions. Glass skyscrapers are energy-greedy giants in modern cities: their large-area glass windows and facades offer poor thermal insulation against temperature variations throughout the year, while their complicated heating, ventilation, and air-conditioning (HVAC) systems require prodigious energy to maintain an optimal indoor temperature. For example, the Al Hamra Tower in Kuwait City (height: 413 m), consumes 116.6 MWh of electricity per day, equivalent to 82.6 ton of CO_2 emission. Existing solutions include expensive double-paned low-emissivity glass windows priced at \$70-310/sqft, which yet offer inadequate thermal insulation. Thus, economical and energy-efficient technologies are urgently desired to further reduce the HVAC energy consumption in glass skyscrapers.

Photonic radiative cooling materials have been considered as the next generation of energy-efficient building envelope, with maximum thermal emissivity that can passively mitigate the energy consumption for cooling the buildings. However, the problem of overcooling has been overlooked: they continue to radiate heat from buildings even at low temperatures, leading to unwanted heating load penalties in winter. Recently, temperature-adaptive radiative coatings successfully addressed this problem by self-switching thermal radiation along with temperature changes. Unfortunately, they are still limited by problems such as opaqueness, small size, high costs, and poor appearance. The goal of this project is to develop economical photonic window films with temperature-adaptive thermal emissivity for smart passive thermal regulation of glass skyscrapers.

Objectives: Our research objectives are to develop practical temperature-adaptive radiative window (TARW) films based on flexible photonic metamaterials and phase-change nanomaterials: (1) Temperature-adaptive thermal emissivity around 22 ºC with a large emissivity modulation depth ($\Delta\varepsilon$>0.5); visible transparency ($T_{non\text{-}colored}$>60%) with rich color selection (>10 color options). (2) Scalable economical manufacturing with high throughput (>10 m/hour) and low costs (<\$2/sqft) for roll-to-roll nanoimprinted flexible photonic metamaterials. (3) Robustness against UV irradiation and thermal cycles. (4) Experimental demonstrations and energy-saving calculations.

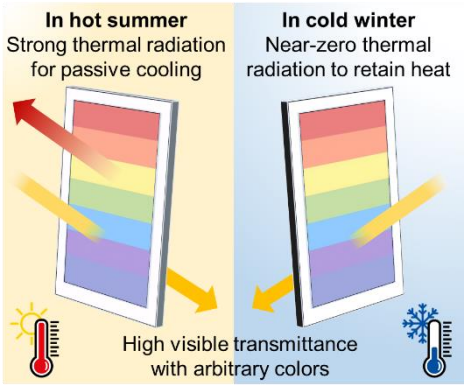

Figure: Proposed low-cost, colored transparent TARW films on glass.

Impacts: This project will lead to an economical photonic solution to the gigantic HVAC energy consumption by worldwide glass skyscrapers. Our innovative TARW films will cool down glass windows in summer as normal radiative coolers, and passively switch to a low-emissivity, heat-retaining mode in winter. This will provide year-round reduction of the HVAC energy consumption and greenhouse gas emissions of glass skyscrapers. Moreover, TARW films can be easily installed to the external surface of glass windows and facades with aesthetic advantages. Additionally, this project's impacts will easily extend beyond skyscrapers, ranging from various resident houses to vehicles with large glass roofs. Energy-poverty populations will also benefit from this affordable smart material for thermal comfort in extreme weather events.

In conclusion, our research project holds significant promise for drastically decreasing the energy consumption and greenhouse gas emissions of glass skyscrapers and significantly contributing to the worldwide efforts to fight global warming.

Proposal

Scalable-manufactured, Decorative, Temperature-adaptive Radiative Window Films for All-season Passive Energy Saving of Glass Skyscrapers

OPTICA Foundation Challenge: Environment

PI: Kaichen Dong (dkc22@sz.tsinghua.edu.cn)
Tsinghua Shenzhen International Graduate School, Tsinghua University, China

1. Literature Review

1.1 Global Warming and Skyscrapers' Energy Consumption

Global warming is endangering everyone in a way that has never been so grievous before. Crises including extreme weather, sea-level rise, hurricanes, and wild fires are witnessed frequently in recent years, leading to numerous climate refugees and economic losses [1]. Human activities associated with excess burning of fossil fuels are among the main drivers of global warming via greenhouse gas emissions [2]. On the other hand, our modern society has an ever-increasing need for energy and hundreds of millions of people in the world are still suffering from energy poverty [3]. Therefore, it is extremely important to develop innovative technologies to reduce energy consumption for long-term sustainability. Building operations, which account for 30% of global final energy consumption and 26% of global energy-related emissions, are in pressing need for energy-efficient technologies [4]. Notably, the heating, ventilation and air conditioning (HVAC) system is typically the most energy-consuming element and concentrating 38% of the total energy consumption in a building [5].

Among all buildings, skyscrapers with glass curtain walls are energy-greedy giants: For example, in New York City (Fig. 1A), the annual electricity consumption of a skyscraper may be several thousand times of that used by a residential building [6]. The Empire State Building consumes 196 MWh of electricity per day with 43-ton CO_2 emissions [7]. The prodigious HVAC power consumption in skyscrapers mainly comes from large-area glass windows and facades with poor thermal insulation against large temperature variations throughout the year. For example, even if windows only covering 15%-25% of the building envelop, they could easily contribute to 40%-70% of the total heat loss of the building [8]. Existing solutions include expensive double-paned windows with low-emissivity coatings at a cost of $70-310/sqft, but their thermal insulation is still insufficient [9]. Thus, energy-efficient retrofit technologies are urgently desired to further reduce the all-season HVAC energy consumption in glass skyscrapers.

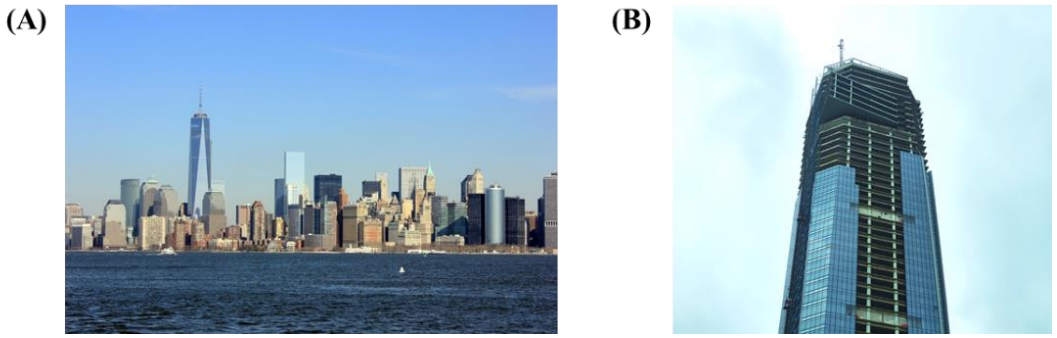

Figure 1. Skyscrapers in modern cities. (A) Skyscrapers in New York City, U.S. **(B)** A glass skyscraper under construction in Shenzhen, China. Modern skyscrapers are only enveloped by glass curtain walls with rather limited thermal insulation.

1.2 Temperature-adaptive Photonic Radiative Cooling

Photonic radiative cooling, featured with nearly ideal thermal emissivity and solar reflectance, is one promising green technology to passively reduce the energy consumption of air conditioning in buildings (Fig. 2A and 2B) [10]. Based on Planck's law of blackbody radiation, those radiative coolers

passively cool down buildings by emitting heat into the cold universe. Meanwhile, solar heating effect is minimized for diurnal cooling. Thanks to the great advances in photonics, high-performance radiative coolers started to emerge since 2014, which are mostly based on artificial, deep-subwavelength photonic nanostructures [11]. In the past ten years, we have witnessed the fast development of scalable-manufactured photonic radiative coolers, such as microparticle-embedded flexible coatings [12], porous polymers [13], and structural materials [14].

Nevertheless, further improvements are required for photonic radiative coolers. Though the above implementations are all excellent static coolers in summer, they continue to radiate heat in cold weather when space heating is needed. As a result, static photonic radiative coolers cause over-cooling problems in winter and exacerbate heating energy consumption [15], which has been verified by real-world tests and applications. Note that space and water heating almost account for half of global energy use in buildings [16]. To eliminate the unwanted heating load penalties, actively switchable radiative coolers were invented, whose thermal emissivity can be switched "ON" for cooling and "OFF" for heat-retaining. Most demonstrations in this field utilized active approaches for switching, including mechanical actuation [17], electrical actuation [18], and flip-over Janus membranes [19].

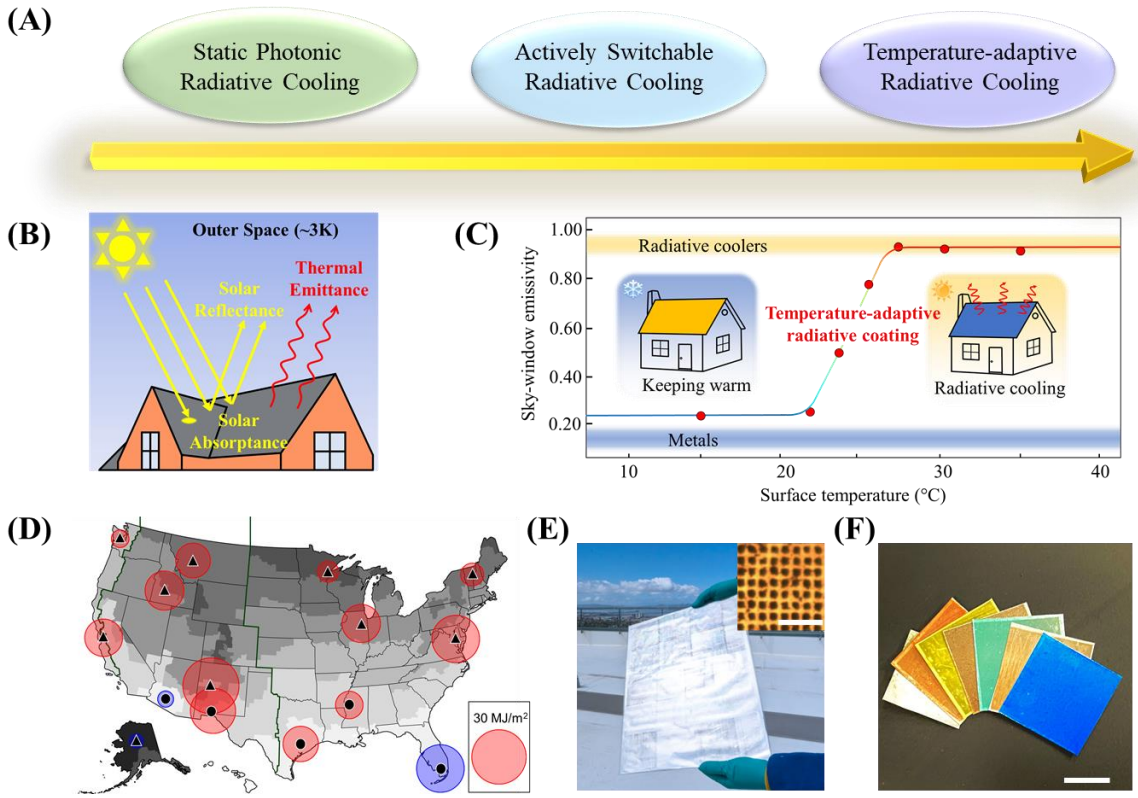

Figure 2. Temperature-adaptive radiative coatings (TARCs). (A) Roadmap of photonic radiative coolers [15]. **(B)** Schematic of (static) photonic radiative cooling [15]. **(C)** Thermal emissivity of TARC as a function of surface temperature [20]. **(D)** Year-round space-conditioning source energy saving advantage of TARC over locally best performing roofs in U.S. cities (red and blue circles indicate positive and negative values) [20]. **(E)** Roll-to-roll fabricated opaque TARC [21]. Inset: a microscopic image of the photonic metamaterial structure in TARC. Scale bar: 20 μm. **(F)** Colored opaque TARCs [21]. Scale bar: 1 cm.

To fully eliminate the energy requirements for the "ON/OFF" switching process, and to facilitate deployment and long-term applications, temperature-adaptive radiative coatings (TARCs) were invented very recently (Fig. 2C) [20]. One representative technology is our temperature-sensitive flexible metamaterial based on the thermally driven phase change of vanadium dioxide (VO_2), whose

phase-change temperature can be tailored by doping. As such, TARC delivers high radiative cooling power with thermal emissivity up to 0.90 exclusively for high-temperature conditions. When the surface temperature drops below a preset switching temperature, TARC automatically switches its thermal emissivity to 0.20 without external energy input or user intervention, thus retaining heat for the building to prevent over-cooling. Energy simulations using real climate database reveal the energy-saving advantages of TARC over all existing roof coatings (including static photonic radiative coolers) in 80% climate zones of U.S., leading to a paradigm shift in this research field (Fig. 2D). However, this prototype of TARC is far from practical application due to its small size and expensive microfabrication costs. In 2023, we demonstrated a low-cost colored TARC crafted from recyclable materials with a high-throughput roll-to-roll process (Fig. 2E and 2F) [21]. It is estimated that, compared with locally most energy-efficient roofs, one house in San Francisco whose 1700-sqft roof is covered by TARC will save 12.63 GJ each year, equivalent to the elimination of 2.49-ton CO_2 emission. Nevertheless, this colored TARC is opaque with poor appearance, severely limiting its deployment on glass skyscrapers for all-season energy saving of HVAC energy consumption.

2. Problem Statement and Objectives

TARC can help regulate the exterior surface temperature of buildings against environmental temperature variations, thus reducing their HVAC power consumption. However, the opaqueness and poor appearance of TARC severely hamper this cutting-edge green technology from practical installation onto skyscrapers. The objective of this project is to develop economical temperature-adaptive radiative window (TARW) films as a next-generation TARC technology for smart passive thermal regulation of glass skyscrapers (Fig. 3).

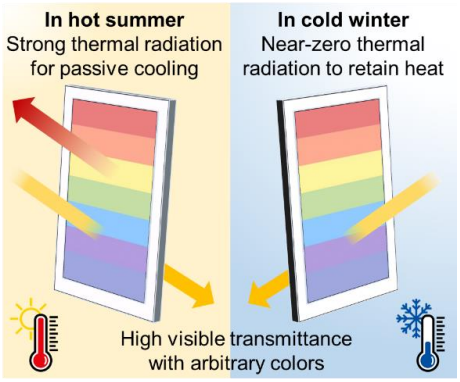

Figure 3. Proposed low-cost, colored, transparent TARW films on glass. The red and yellow arrows indicate thermal emission and solar light, respectively.

3. Tasks with Work Plans

3.1 Development of Temperature-adaptive Radiative Window Films (8 Months)

(1) High visible transparency with decorative colors. The visible transparency of TARW films is of critical importance to their deployment on glass windows and facades without impeding magnificent views of surrounding environment or ample natural light. Hence, both the photonic structural materials and mechanical supporting materials in TARW films should be highly transparent. Moreover, colored transparent window films are always demanded by customers for decorative or aesthetic reasons. Technological measures to color TARW films without affecting its temperature-adaptive thermal emissivity will also be developed in this project. Our research is targeted at developing noncolored TARW films with >60% average transparency in the wavelength range of 380-700 nm. For colored TARW films, the 380-700 nm wavelength transparency can be arbitrarily designed in the range of 30%-60% with >10 color options.

(2) Temperature-adaptive thermal emissivity. Passive radiative coolers operate in the atmospheric transparency window of 8-13 μm wavelength (also coined as “sky window”). In order to help skyscrapers passively maintain more manageable interior building temperatures in all seasons, the sky-window emissivity of TARW films should be high in hot weather for strong radiative cooling, and low in cold weather for heat-retaining. Therefore, the modulation depth of sky-window emissivity is the core technical parameter of TARW films, determining its year-round energy-saving performance. This project is aiming at developing noncolored and colored TARW films with a >0.5 modulation depth of sky-window emissivity. According to World Health Organization’s Guidelines [22], the switching temperature for TARW films will be designed around 22 ºC in order to help achieve optimal human thermal comfort in skyscrapers with minimum HVAC energy consumption.

3.2 Scalable Manufacturing at Low Costs (6 Months)

The proposed TARW films should be readily upgraded for commercialization, so large-area manufacturing at low costs is a mandatory aim of this project. Similar to commercial window films [23], TARW films will also be produced using the roll-to-roll processing technology with key technical innovations including: (1) judicious selection of component materials, which should all be roll-to-roll processable and economical. (2) high-precision and high-throughput nanoimprinting technology to mass-produce infrared photonic metamaterials with phase-change nanomaterials. (3) mature laminating procedures with high yields. Our research will enable roll-to-roll manufactured TARW films with high throughput (>10 m/hour), low costs (<$2/sqft), and micrometer-scale thickness.

3.3 Durability against UV Irradiation and Thermal Cycles (6 Months)

Two major reasons for window film deterioration are ultraviolet (UV) irradiation and thermal cycles. Firstly, UV irradiation from the sun gradually breaks down the organic chemicals in window films, leading to an inevitably fading process. In order to prolong the lifespan of TARW films, UV-resistant materials will be investigated and added for enhanced robustness against UV irradiation. Secondly, since TARW films will be installed onto the external surfaces of skyscrapers, exposure to extreme temperature swings will be another fatal environmental aging factor. The interlayer bonding strength in a TARW film has to be large enough to survive a large number of thermal cycles. The proposed TARW films will be able to survive 1,000 hours of xenon lamp irradiance and 1,000 thermal cycles between 10 ^{o}C and 60 ^{o}C without significant decrease in their thermal regulation performance.

3.4 Experimental Demonstrations with Energy-saving Calculations (4 Months)

The passive thermal regulation capability of TARW films on glass will be verified by outdoor experiments. Model skyscrapers will be 3D printed and glass windows will be installed on them. Four groups of windows will be tested simultaneously: single-paned windows with TARW films, single-paned windows without TARW films, double-paned windows with TARW films, and double-paned windows without TARW films. The 24-hour records of the interior building temperatures will be compared and analyzed. Energy-saving calculations of TARW films for skyscrapers will be conducted using EnergyPlus simulation [24], where adiabatic approximation, real climate parameters using TWY3 weather files, and building thermal inertia will be included.

4. Outcomes

The completion of this project will yield an innovative smart radiative coating for zero-power thermal regulation of glass skyscrapers. The resultant TARW film is a light-weighted, flexible membrane with enhanced durability and can be scalable manufactured at low costs. Moreover, the installation of transparent TARW films onto the external surfaces of glass windows and facades will allow natrual light in and an unobstructed view out (Fig. 4A and 4B). Optional colors of TARW films further meet various decorative and aesthetic requirements. When the environment is hot, the TARW film is able to effectively cool down the (external) glass via passive thermal radiation. As the temperature drops below a preset switching temperature, the TARW film automatically switches to a low-emissivity mode and help the (external) glass keep warm. The above emissivity-switching process is enabled by the incorporated temperature-sensitive phase-change nanomaterials, whose infrared response is amplified by the subwavelength photonic structures imprinted in the TARW film. Therefore, the smart thermal regulation capablity of TARW film is totally automatic without any electricity input or user intervention.

The smart thermal regulation performance of TARW film is compatible with multi-paned windows, which, optionally with low-emissivity coating(s) and/or trapped gas, are designed for better thermal insulation (Fig. 4C and 4D). Since the low-emissivity coating(s) is not deposited onto the external surface of the outside glass [25], the installation of TARW films onto existing multi-paned windows will not affect its thermal insulation performance. Specifically speaking, the TARW film modulates the

temperature of outside glass and further boosts the energy-efficiency of multi-paned windows.

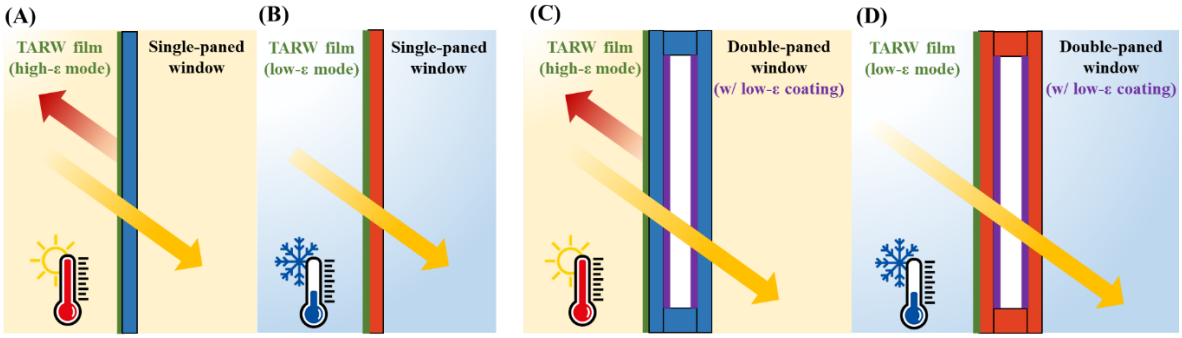

Figure 4. Energy-saving scenarios for TARW films. (A, B) TARW films installed on single-paned windows in a hot environment (A) and a cold environment (B). **(C, D)** TARW films installed on double-paned windows in a hot environment (C) and a cold environment (D). The red and yellow arrows indicate thermal emission and solar light, respectively. The green and purple coatings indicate TARW films and low-emissivity coatings, respectively.

5. Impacts

The implementation of this project will lead to significant impacts on photonic technology, building industry, modern society, and global environment.

(1) Photonic technology. The development of TARW films is a transdisciplinary research pursuing a real-world energy-saving technology based on temperature-sensitive photonic metamaterials and phase-change nanomaterials. This project will not only lead to the invention of transparent TARC for the first time, but also create a low-cost, nanoimprinting fabrication approach for large-scale photonic metamaterials. We envision a future where the contribution of photonic technologies to energy-efficient society will be widely acknowledged by the world.

(2) Building industry. With the uprising concern of global climate change, the world is seeking for economical solutions to the energy challenge of glass skyscrapers, especially those aged skyscrapers. For example, it was estimated that replacing all 6,514 windows of the Empire State Building with energy-efficient new models would cost $20 million in the year of 2009. Our proposed TARW film is a suprisingly cheap building envelope material for skyscrapers that has never existed before, triggering a pradigm shift of the building industry.

(3) Modern society. This project's impacts will easily extend beyond skyscrapers, ranging from various resident houses to vehicles with large glass roofs, making widespread impacts on the modern society. Furthermore, energy-poverty populations will also benefit from this affordable smart technology for thermal comfort in extreme weather events.

(4) Global environment. The proposed TARW film will be widely adopted to reduce the energy consumption and greenhouse gas emissions from HVAC systems in skyscrapers. Owing to the thousands of energy-greedy skyscrapers in the world, it is expected that TARW films will significantly alleviate global warming with a collosal impact on the global environment.

References

[1] United Nations. What is Climate Change? (https://www.un.org/en/climatechange/what-is-climate-change)

[2] U.S. Environment Protection Agency. Sources of Greenhouse Gas Emissions. (https://www.epa.gov/ghgemissions/sources-greenhouse-gas-emissions)

[3] Our World in Data, Global Change Data Lab. The world's energy problem. (https://ourworldindata.org/worlds-energy-problem)

[4] Tracking Buildings. International Energy Agency. (https://www.iea.org/energy-system/buildings)

[5] M. González-Torres, et al. A review on buildings energy information: Trends, end-uses, fuels and drivers. Energy Reports 8 (2022): 626-637.

[6] B. Howard, et al. Spatial distribution of urban building energy consumption by end use. Energy and Buildings 45 (2012): 141-151.

[7] New York State Energy Research and Development Authority. ESRT: Case Study. (https://knowledge.nyserda.ny.gov/display/EBP/ESRT+Case+Study)

[8] S. T. Tam and P. Meisen. Skyscraper Green Retrofits Guide. California, USA: Global Energy Network Institute (GENI) (2011).

[9] Architectural Digest. Cost of Double-Pane Windows | 2024 Guide (https://www.architecturaldigest.com/reviews/windows/double-pane-windows-cost).

[10] S. Fan and W. Li. Photonics and thermodynamics concepts in radiative cooling. Nature Photonics 16.3 (2022): 182-190.

[11] A. Raman, et al. Passive radiative cooling below ambient air temperature under direct sunlight. Nature 515 (2014): 540–544.

[12] Y. Zhai, et al. Scalable-manufactured randomized glass-polymer hybrid metamaterial for daytime radiative cooling. Science 355.6329 (2017): 1062-1066.

[13] J. Mandal, et al. Hierarchically porous polymer coatings for highly efficient passive daytime radiative cooling. Science 362.6412 (2018): 315-319.

[14] T. Li, et al. A radiative cooling structural material. Science 364.6442 (2019): 760-763.

[15] K. Dong, and J. Wu. Radiative cooling, what's next? Next Energy 1.1 (2023): 100003.

[16] International Energy Agency. Why is heating important? (https://www.iea.org/energy-system/buildings/heating).

[17] X. Li, et al. Integration of daytime radiative cooling and solar heating for year-round energy saving in buildings. Nature Communications 11.1 (2020): 6101.

[18] X. Tao, et al. A bistable variable infrared emissivity device based on reversible silver electrodeposition. Advanced Functional Materials 32.32 (2022): 2202661.

[19] H. Qiao, et al. Scalable and durable Janus thermal cloak for all-season passive thermal regulation. Device 1.1 (2023).

[20] K. Tang, K. Dong, J. Li, et al. Temperature-adaptive radiative coating for all-season household thermal regulation. Science 374.6574 (2021): 1504-1509.

[21] J. Li, K. Dong, et al. Printable, emissivity-adaptive and albedo-optimized covering for year-round energy saving. Joule 7.11 (2023): 2552-2567.

[22] World Health Organization. WHO Housing and Health Guidelines. (https://www.ncbi.nlm.nih.gov/books/NBK535294/)

[23] ClimatePro. Window Film Faqs: How Is Window Film Made? (https://www.climatepro.com/blog/window-film-faqs-how-is-window-film-made/)

[24] U.S. Department of Energy's Building Technologies Office. EnergyPlus. (https://energyplus.net/)

[25] B. Mempouo, et al. Novel window technologies and the code for sustainable homes in the UK. International Journal of Low-Carbon Technologies 5.4 (2010): 167-174.

Distributed fiber optic Hydrogen leak detector

Applicant: Dr. Korina Hartmann, United Fiber Sensing B.V., The Hague, The Netherlands

Category: Environment

Challenge

Global warming is a pressing challenge, with countries covering 88% of global emissions committed to net zero goals. Hydrogen is vital in the future energy mix, and pipelines are recognized as a cost-effective transportation solution, leading to numerous pure hydrogen or blended hydrogen with natural gas (NG) grid projects. However, hydrogen's wide flammability range (4% - 75%) and leak potential pose significant safety risks. Although generally considered environmentally benign, recent studies show hydrogen emissions can be potent indirect greenhouse gases, highlighting the need for reliable, real-time leak detection systems for large-scale applications. Optic sensors which are 100% free from electronics offer intrinsic safety and a reliable performance. Current technologies for continuous monitoring are inadequate, with traditional point sensors offering limited coverage and few fiber optic methods suggesting feasible distributed solutions.

Project

The project aims to develop and demonstrate a hydrogen leak detection system capable of continuously detecting gaseous hydrogen leaks over distances spanning several tens of kilometers. This system will be deployed along hydrogen transport infrastructure using commercially available Distributed Fiber Optic Temperature Sensing (DTS) instruments. Trace amounts of hydrogen induce a detectable temperature change at leakage points, using Raman DTS technology. This innovative fiber optic sensor system provides fully distributed sensing without the need for separate point-based hardware, operating passively along the sensor's length. The hydrogen-sensitive coating for the fiber optic sensor is based on patented technology invented by Dr. Hartmann. The next development step focuses on employing Raman DTS technology for real distributed sensing over unprecedented distances. The system's target requirements include a spatial resolution of <1 meter, a detection limit of 0.1% hydrogen, a linear response to hydrogen concentrations between 0-4%, and a detection response time of <30 seconds. The project plans to refine the hydrogen-sensitive coating for direct application onto optical fibers during manufacturing in the draw tower. This research will be multi-disciplinary, combining advanced chemistry with specialty fiber manufacturing processes. Key topics include optimizing fiber draw speed, curing time and temperature of the coating, and assessing optical fiber characteristics such as micro-bends induced by the coating.

Outcome and Impact

The result of the project will be a unique, first of its kind, laboratory demonstration of a distributed fiber optic hydrogen leak detection system. Meeting the target system requirements on spatial resolution, limit of detection, linearity and response time will enable real-time, distributed sensing over several kilometers. As such the project will make a significant contribution towards the safety aspects associated with the use of hydrogen in production, storage and foremost transport of hydrogen. The use of hydrogen in the battle against global warming is on the agenda of almost all major countries across the globe, emphasizing the relevancy and potential impact of this project. This scalable detection system will be cost-effective, leveraging existing production techniques and off-the-shelf Raman DTS systems, thus facilitating the perception of safety in society associated with the use of hydrogen, decrease escalation risks of hydrogen leakages and in turn will reduce insurance costs.

Distributed fiber optic Hydrogen leak detector

Applicant: Dr. Korina Hartmann, United Fiber Sensing B.V., The Hague, Netherlands
Duration: 18 months
Category: Environment

Literature review

Hydrogen is a crucial and versatile energy carrier for a sustainable energy future, yet its flammability over a wide concentration range (4% - 75%) and potential for leaks pose significant safety challenges. Therefore, accurate and reliable hydrogen detection is essential. Traditional hydrogen sensing techniques, such as gas chromatography mass spectrometry and specific ionization gas pressure sensors, involve ion-pair extraction and mass spectrometry quantification, achieving detection levels down to parts per million. However, these methods are time-consuming, costly, require skilled operators, necessitate off-site analyses, and depend on matrix-matched calibration standards that are not readily available. To overcome these limitations, alternative hydrogen detection methods have been explored, including electrochemical, catalyst-based, and resistance-based sensors. Despite their utility, these electronic-based sensors consume power and pose safety risks due to potential electrical sparks. A more advanced solution necessitates innovative sensors that are fully passive and capable of detecting leaks along entire pipelines extending several kilometers. Optical technology offers several inherent advantages over electrical measurement methods. These include being inherently explosion-proof, providing faster response times, experiencing less signal degradation, being more robust, having a lower total cost of ownership (TCO), being smaller in size, and enabling multi-parameter sensing. Consequently, optical fiber sensors represent a promising approach for enhancing hydrogen leak detection, ensuring both safety and efficiency in hydrogen infrastructure.

Numerous fiber optic technologies have been studied for hydrogen sensing. A comprehensive overview of these technologies is available in various reviews [1] [2]. Most efforts have focused on developing detectors for discrete point sensors. To enhance hydrogen detection, many sensor embodiments use metal or metal oxide coatings that strongly interact with hydrogen at room temperature (RT), such as palladium (Pd) and tungsten trioxide (WO_3). Palladium selectively absorbs hydrogen, forming palladium hydride (PdH_x) even at room temperature. The formation of PdH_x induces changes in the lattice constant, refractive index, density, and stress, affecting acoustic wave propagation through the Pd surface layer. Grating-type fiber optic sensors exploit these strain changes and are widely studied. However, stabilization of these sensors takes minutes or hours, making them unsuitable for leak detection. WO_3 also forms hydrogen bronzes at RT, resulting in a detectable color change. Fast response times, in the order of seconds, can be achieved by decorating WO_3 with a metal catalyst such as Pd or platinum (Pt), which facilitates an exothermic reaction with hydrogen. Caucheteur *et al.* demonstrated that covering a Fiber Bragg Grating (FBG) with a WO_3 layer doped with Pt results in fast response times, high sensitivity, reversibility, and the capability for frequency multiplexing [3]. This sensor can detect hydrogen concentrations well below the explosion limit of 4 vol%, making it highly effective for safety applications.

Among the various fiber optic methods, only a few published concepts mention the potential for truly distributed solutions. Some distributed concepts rely on hydrogen molecules diffusing into the silica glass, measuring the induced optical attenuation in the fiber. For example, Delepine-Lesoille *et al.* proposed such solutions, which are promising for slowly evolving hydrogen environments like nuclear storages but are too slow for applications such as transport of pure or Natural Gas blended

hydrogen (H_2NG) using pipelines [4]. Other research papers claim potential for fully distributed solutions. Early work by Sumida *et al.* used evanescent field sensing on the colour change of WO_3:Pt fiber coating, a technology that is inherently lossy and limited to short-length sensing [5]. Recent work by Chen *et al.* probed hydrogen-induced strain changes in a Pd/Cu coated section of fiber using Rayleigh backscattering, achieving 1 cm resolution over a 2-meter fiber [6]. However, resistive heating of the coating was needed to increase sensitivity, resulting in a complex and expensive solution with safety concerns in a hydrogen atmosphere. Yang *et al.* used stimulated Raman scattering to detect and locate the presence of hydrogen in hollow-core photonic crystal fibers, a technology that relies on the gas being present inside the fiber and can at best be considered quasi-distributed, likely making it prohibitively complex and expensive [7]. Wang *et al.* probed a fiber with acoustically induced traveling long-period gratings (LPGs), a technology greatly limited in length due to the acoustic damping of silica [8].

Objectives

In recent years, an increasing number of countries have committed to achieving net zero emissions. By April 2022, 131 countries, accounting for 88% of global greenhouse gas emissions, had announced net zero targets. As hydrogen gains prominence as a clean energy carrier, its use has expanded across transportation, energy storage, and industrial processes. However, hydrogen's inherent flammability and potential for leaks pose significant safety challenges, making accurate and reliable detection paramount. Beyond safety concerns, large-scale hydrogen leak detection is critical due to recent findings that hydrogen emissions, traditionally considered benign, can act as potent indirect greenhouse gases when released into the atmosphere [9]. This underscores the need for advanced hydrogen sensing methodologies that combine high performance, reliability, and safety.

The use of hydrogen as an energy carrier needs substantial investment in transport infrastructure, including pipelines, conversion, liquefaction units, and storage facilities, which increases initial capital requirements. The most practical and economically viable strategy for ensuring comprehensive transportation and widespread adoption of hydrogen is through the (re)use of existing natural gas grids. Currently, the global pipeline of hydrogen pilot projects is still in its early stages. The United States has developed a clean energy strategy, released in September 2022, which includes numerous recently announced projects investigating the mixing of hydrogen with natural gas in pipelines. While most hydrogen injection projects into natural gas grids are still in the early development stages, some have successfully operated with hydrogen blend levels for several years [10]. The European Commission's hydrogen and decarbonized gas package, published in December 2021, underscores the critical role of hydrogen pipeline infrastructure in promoting market competition, supply security, and demand security. Similarly, China, the world's largest hydrogen producer, has introduced standards for low-carbon, clean, and renewable hydrogen energy within its Hydrogen Alliance.

The project aims to develop and demonstrate a hydrogen leak detection system capable of continuously detecting gaseous hydrogen leaks over long distances, spanning several tens of kilometers. This system will be deployed along hydrogen transport pipelines and networks, including H_2NG networks, as well as in compressor housings and Hydrogen Refueling Stations (HRS).

The detection system will use commercially available instruments for Distributed fiber optic Temperature Sensing (DTS). When trace amounts of hydrogen are present, they induce a temperature change at the leakage point, detectable using Raman DTS technology as illustrated in Figure 1.

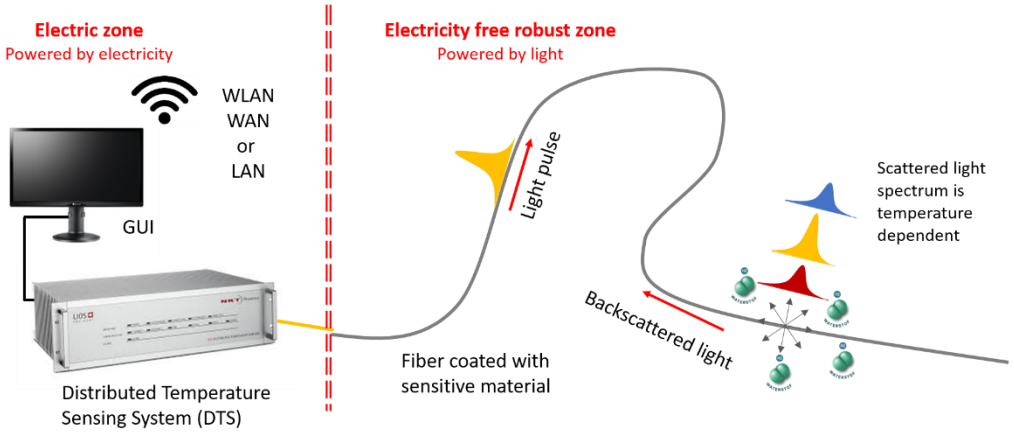

Figure 1 Distributed monitoring design. The optical fiber is coated with the sensitive material along the needed detection length. Hydrogen reacts exothermally with the sensitive coating detectable by Raman-DTS.

This novel fiber optic sensor system will provide fully distributed sensing without the need for separate point-based sensing hardware, operating passively along the sensor's length. The hydrogen-sensitive coating for the fiber optic sensor is based on the patented hydrogen leak detector technology invented by Dr. Hartmann. Dr. Hartmann has successfully developed a fiber optic hydrogen leak detector for point sensing using two uniform Fiber Bragg Gratings (FBGs) written in a photosensitive single-mode optical fiber. The first FBG is coated with WO_3:Pt, while the second FBG is uncoated to discriminate between temperature variations and hydrogen effects. Typical sensor responses are shown in Figure 2. By daisy-chaining multiple detectors, multi-point sensing on a single fiber is achieved.

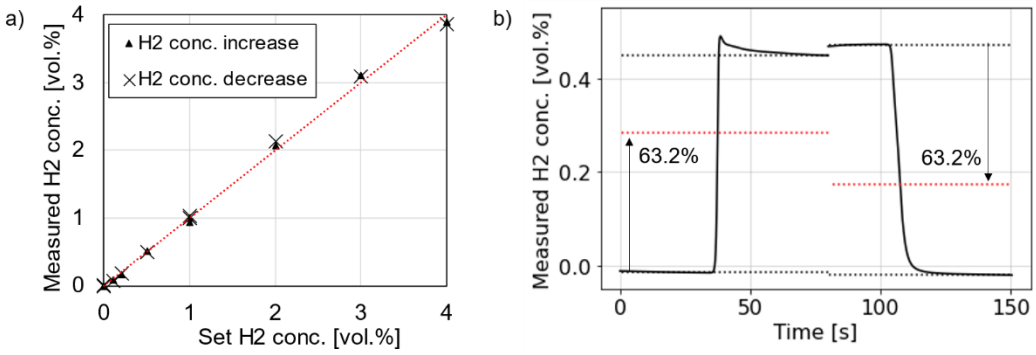

Figure 2 (a)Measured hydrogen concentration induced by the developed sensitive coating applied over 2 cm of optical fiber with a Fiber Bragg Grating at different hydrogen concentrations in air and its linear fit in red. (b) Measured hydrogen concentration over time from 0-0.5 vol.%. 63.2% of the final value is marked in red. These sensor characteristics are expected to be replicated by the developed distributed sensor.

The next step in the development of novel fiber optic hydrogen leak detection equipment is focused on employing Raman DTS technology to achieve real distributed sensing along unprecedented distances. Target requirements of such a system include a spatial resolution of <1 meter, limit of detection at 0.1% hydrogen and a linear response to hydrogen concentrations between 0-4% and a detection response time <30 seconds. The application of the development is the monitoring of pipelines for hydrogen and will have a profound impact on public safety in rural areas but also impact financial and environmental aspects. To achieve this goal, Dr. Hartmann plans to continue her development of the hydrogen sensitive coating such that it can be applied directly onto an optical fiber during the manufacturing process in the draw tower. The research of Dr. Hartmann will have a multi-

disciplinary character combining state-of-the-art chemistry with specialty fiber manufacturing processes. Parameters such as fiber draw speed, curing time and temperature of the novel coating and optical fiber characteristics such as micro-bends induced by the coating are among the topics of the planned research. In addition, demonstration of the technology in a laboratory setting is included in the project plan. The ambition of Dr. Hartmann is to demonstrate the distributed fiber optic hydrogen leak detection system and verify the aforementioned target system requirements on spatial resolution, limit of detection, linearity and response time.

Outcomes

The result of the project will be a unique, first of its kind, laboratory demonstration of a distributed fiber optic hydrogen leak detection system. As such the project will make a significant contribution towards the safety aspects associated with the use of hydrogen in production, storage and foremost transport of hydrogen. The use of hydrogen in the battle against global warming is on the agenda of almost all major countries across the globe, emphasizing the relevancy and potential impact of Dr. Hartmann's current and future work.

Impact

Environment

Global warming is one urgent challenge we are confronted with in our times. Countries that cover 88% of the global greenhouse emissions committed to the Net zero emission goals. Hydrogen has an established place in the energy mix of the future and the use of pipelines for transportation has been recognized as a suitable and cost effective solution and is manifested in national strategies around the world giving rise to ample H_2NG gas grid projects. Hydrogen is generally considered to have minimal environmental impact, however recent studies show that hydrogen emissions appear to be a very potent indirect greenhouse gas when released to the atmosphere. This adds to the urgency of finding a reliable hydrogen leak detection system that can, in real time, indicate the location and severity of leaks in large scale applications. In addition, when blending hydrogen with natural gas, a small hydrogen leak can be used as an early warning system and mitigates the risk of severe methane leakages.

Science

Current technologies for continuous leak detection monitoring are not satisfactory for meeting the industrial and public area requirements. This becomes obvious when considering the pipeline infrastructure on a (multi-)national scale and the ambition to use such infrastructure for pure hydrogen or blended hydrogen with NG. State of the art hydrogen leak detection are traditional point sensors with limited coverage. Cutting-edge Raman DTS in combination with an optical fiber that can directly sense the presence of hydrogen will enable real-time distributed sensing of hydrogen along distances of several kilometers.

Safety

Hydrogen has a high flammability across a large concentration range (4% - 75%) and its leak potential pose safety challenges. The distributed system allows safeguarding large hydrogen infrastructure. The fast responsiveness to concentrations way below the Lower Explosion Limit (LEL) of 4% hydrogen is a crucial parameter for the success. Detection of hydrogen leakages in pipelines transversing rural areas will increase the safety of the local community. In fact, such a system will increase the perception of safety in society associated with the use of hydrogen, decrease escalation risks of hydrogen leakages and in turn will reduce insurance costs.

Cost effectiveness

The proposed detection system, unlike the current state-of-the-art, is scalable and will effectively enforce the widespread adaptation of continuous monitoring of hydrogen which has the potential to drastically lower the total monitoring costs. The project proposes adaption of existing fiber optic draw

tower production techniques which, if successful, will result in a cost-effective scalable production method of kilometers of hydrogen sensitive optical fiber. In addition, existing off-the-shelf Raman DTS systems will be used in the project limiting the required scope of the work and shortening the route to commercial success.

References

[1] C. Shen and e. al., "Review of the Status and Prospects of Fiber Optic Hydrogen Sensing Technology," *Chemosensors,* vol. 11, no. 9, p. 473, 2023.

[2] A. Pathak and e. al., "Recent Advances in Optical Hydrogen Sensor including Use of Metal and Metal Alloys: A Review," *Photonics,* vol. 10, no. 2, p. 122, 2023.

[3] C. e. a. Caucheteur, "Hybrid fiber gratings coated with a catalytic sensitive layer for hydrogen sensing in air," *Optics Express,* vol. 16, no. 21, p. 16854, 2008.

[4] S. Delepine-Lesoille and e. al., "Distributed Hydrogen SensingWith Brillouin Scattering in Optical Fibers," *IEEE Photonics Technology Letters,* vol. 24, no. 17, p. 1475, 2012.

[5] S. Sumida and e. al., "Distributed hydrogen determination with fiber-optic sensor," *Sensors and Actuators B: Chemical,* vol. 108, no. 1-2, p. 508, 2005.

[6] T. Chen and e. al., "Distributed hydrogen sensing using in-fiber Rayleigh scattering," *Applied Physics Letters,* vol. 100, no. 19, p. 191105, 2012.

[7] F. Yang and e. al., "Towards label-free distributed fiber hydrogen sensor with stimulated Raman spectroscopy," *Optics Express,* vol. 27, no. 9, p. 12869, 2019.

[8] D. Wang and e. al., "Fully Distributed Fiber-Optic Hydrogen Sensing Using Acoustically Induces Long-Period Grating," *IEEE Photonics Technology Letters,* vol. 23, no. 11, p. 733, 2011.

[9] Y. Najjar and e. al., "Hydrogen Leakage Sensing and Cotrol: (Review)," *Biomedical Journal Science and Technology,* vol. 21, no. 5, p. 16228, 2019.

[10] B. Erdener, "A review of technical and regulatory limits of hydrogen blending in natural gas pipelines," *International Journal of Hydrogen Energy,* vol. 48, no. 14, p. 5595, 2022.

Executive Summary: 'Multispectral Freeform Imaging Spectrometer Enhancing Climate Change Monitoring'

Space-based spectrometers are of high importance for Earth observation and greenhouse gas sensing, providing vital information for climate and climate change monitoring. Currently, an ongoing trend towards miniaturization and the use of cost-effective small satellites can be observed, while wide field-of-view (FOV) imaging is considered to offer a huge potential by enabling to capture global data. We pursue the development of a novel freeform pushbroom imaging spectrometer, covering the visible, near-infrared and thermal wavelength ranges, and focusing light onto 2D detectors, providing both spatial and spectral information. To date, a nominal design of the freeform imaging spectrometer has been achieved, showing a full field-of-view of 120°, nearly reaching Earth observation from limb to limb from an altitude of about 700 km, while fitting in a compact design (95 x 50 x 50 mm^3). The visible (400 – 1100 nm), near-infrared (1100 – 1700 nm) and thermal (8 – 14 μm) spectrometer channels show a spatial nadir resolution of 3.5 km, 3.7 km and 6.3 km, and a spectral resolution of 1 nm, 1.3 nm and 28 nm, respectively. The full optical design comprises 9 freeform mirrors, described using XY polynomials up to the 6th order, in combination with 3 diffraction gratings, resulting in a highly challenging and costly design for manufacturing and characterisation.

In this proposal, **we pursue the realisation of a laboratory demonstrator of the freeform imaging spectrometer, starting from the nominal design towards tolerancing and stray light analysis, manufacturing, characterisation and laboratory demonstration**. First, the current nominal design needs to be optimized towards a manufacturable design taking into account an extensive tolerance and stray light analysis, and applying a design for manufacturing approach. Second, the manufacturing of the freeform mirrors and the diffraction gratings will be tackled using ultraprecision diamond tooling, followed by the characterisation of the manufactured components using metrology tools in a cleanroom environment. Finally, the realization and characterization of a laboratory demonstrator is targeted. Key challenges are expected with respect to the advanced freeform optics manufacturing and alignment, which will be tackled using Brussels Photonics extreme optics pilot line, present within the engineering faculty of the Vrije Universiteit Brussel. Realisation of this demonstrator setup will ease the path towards further development and integration within future space missions by creating visibility in the field while easing the processes to apply for larger European-funded projects.

The topic fits within the scope of the Optics Foundation Challenge on Environment, requiring a multi-disciplinary approach, combining **multispectral imaging, freeform optical design and advanced manufacturing, benefitting the measurement and monitoring of climate change using satellites**. We are confident that the freeform imaging spectrometer will pave the way towards improved Earth observation and climate monitoring due to its unprecedented wide field-of-view and its extended wavelength range. This extended wavelength range, covering the visible, near-infrared and thermal wavelength bands, not only enables accurate **monitoring of greenhouse gases**, but also allows differentiation between the reflected and thermally emitted Earth radiation, benefitting the measurement of the **Earth Energy Imbalance (EEI)**, which is used as a measure for climate change. Our challenge furthermore requires innovative research and technology related to the **advanced manufacturing** of freeform optical mirrors and their integration into the compact design. Consequently, we believe the **freeform imaging spectrometer will be driving both technological developments and Earth science, benefiting future space missions, and contributing to an improved climate measurement and monitoring, benefitting all of us.**

Proposal: 'Multispectral Freeform Imaging Spectrometer Enhancing Climate Change Monitoring'

Literature review: introduction and state-of-the-art

Space-based spectrometers are of high importance for Earth observation and greenhouse gas sensing, providing vital information for climate and climate change monitoring, while offering a global coverage and daily revisit times [1]. Scientific and technological efforts have been made over the past decades to improve the monitoring accuracy. Initially, space-spectrometers tended to use a whiskbroom configuration, scanning the Earth perpendicularly to their line of motion, as was the case for the Global Ozone Monitoring Experiment (GOME and GOME-2) [2,3], the Greenhouse Gases Observing Satellite (GOSAT) [4], and the SCanning Imaging Absorption spectroMeter for Atmospheric CartograpHY (SCIAMACHY) [5]. The main drawback of these configurations is the presence of a moving mirror, leading to a low signal intensity and efficiency due to the point-by-point imaging method, driving the transition to wide field-of-view (FOV) pushbroom configurations. The Ozone Monitoring Instrument (OMI) was the first wide FOV spectrometer using the pushbroom (staring) configuration [6], and was patented in 1998. OMI covers the 270 nm – 500 nm spectral range, features a swath of 2600 km, and has a spatial resolution of 13 km x 24 km. Today, the Tropospheric Monitoring Instrument (TROPOMI) is considered as a state-of-the-art wide field-of-view space-based spectrometer, developed within the framework of the ESA Copernicus space mission and launched in 2017 on the Sentinel-5 Precursor satellite [7,8]. TROPOMI comprises a telescope followed by a multi-channel spectrometer, benefitting from freeform optics. The instrument features an FOV of 107°, a resolution of 7 km x 7 km, and covers spectral bands from UV to SWIR (270 nm – 495 nm (UV/VIS), 710 nm –775 nm (NIR), and 2305 nm – 2385 nm (SWIR) [7,8]. An ongoing **trend towards miniaturization and the use of cost-effective small satellites** can be observed, while also extended wide field-of-view imaging is considered to offer a huge potential by enabling to capture global data. Freeform optics has been indicated as an enabling technology, allowing to decrease the mass and volume of the optical system while enhancing system performance [9,10].

We aim to improve the state-of-the-art space-spectrometers by targeting an **enlarged FOV of 120°**, enabling Earth observation from limb to limb at an altitude of 700 km, by considering an **extended wavelength range** covering the visible (VIS), near-infrared (NIR) and thermal wavelength bands, and by miniaturizing the design to fit within a single CubeSat Unit. The extended wavelength range enables an **improved monitoring of the greenhouse gases, while also allowing to study both the reflected and thermally emitted Earth radiation**, benefitting the measurement of the Earth Energy Imbalance (EEI). Miniaturisation of the design is indispensable in view of the use of cost-effective small satellites, which can be individually considered or used in satellite constellations.

A nominal design of our novel wide FOV imaging spectrometer has been successfully achieved, comprising of 2 main parts: (1) a telescope that collects light within the FOV of 120° and sends it to the spectrometer entrance slit (Figure 1), and (2) a 3-channel spectrometer that diffracts and focuses the light onto 2D detectors comprising the spatial information in one dimension and the spectral information in the other (Figures 1-4). The imaging telescope comprises two freeform mirrors, mounted off-axis, including an aperture stop located at the focal point of the secondary mirror, and guides the light to the spectrometer entrance slit. An initial design of the telescope has been successfully manufactured and realized in a laboratory proof-of-principle setup [11]. Following the spectrometer entrance slit, a freeform collimating mirror is present, guiding the light to the 3-channel spectrometer, covering the visible (400 nm – 1100 nm), near-infrared (1100 nm – 1700 nm) and thermal (8 μm – 14 μm) spectral bands. Each of the 3 channels comprises 2 freeform mirrors. A fold design approach is used to enable the full optical system to fit within one CubeSat unit. To optimize the used space, a transmission grating is used in the visible channel (Figure 2), while a reflection diffraction grating is used in the near-infrared and thermal channels (Figures 3,4). The total design comprises 9 freeform mirrors, each described using

XY polynomials up to the 6th order. All three channels show a nearly diffraction-limited performance, as indicated by the spot diagram (Figures 2-4), leading to an excellent spatial and spectral resolution as indicated in Table 1. The optical design and analysis were performed using Ansys Zemax OpticsStudio. To our knowledge, our novel design shows the **widest FOV that has ever been realized for space-based telescopes**, nearly reaching Earth observation from limb to limb from an altitude of about 700 km, while fitting in a **compact design** (95 x 50 x 50 mm³).

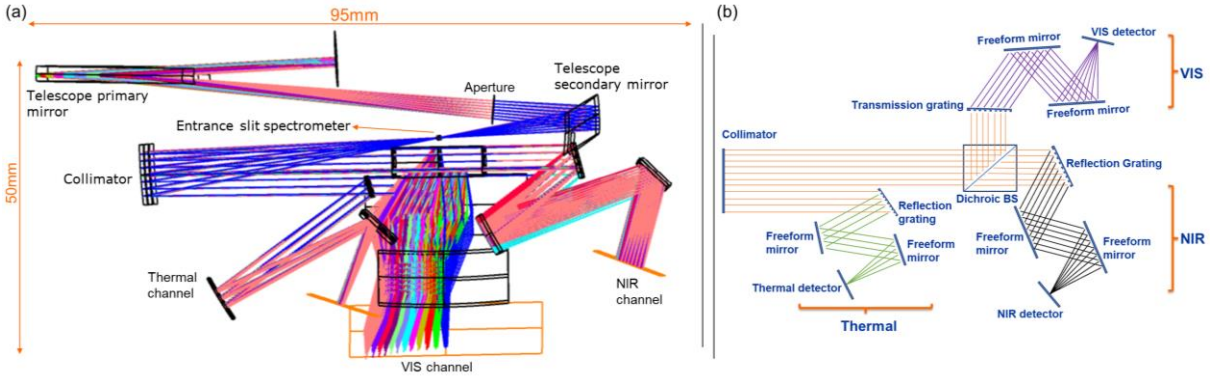

Figure 1: Freeform imaging spectrometer design, comprising the freeform telescope and 3-channel spectrometer design: (a) full design, (b) structure of the 3-channel spectrometer, starting from the collimator mirror.

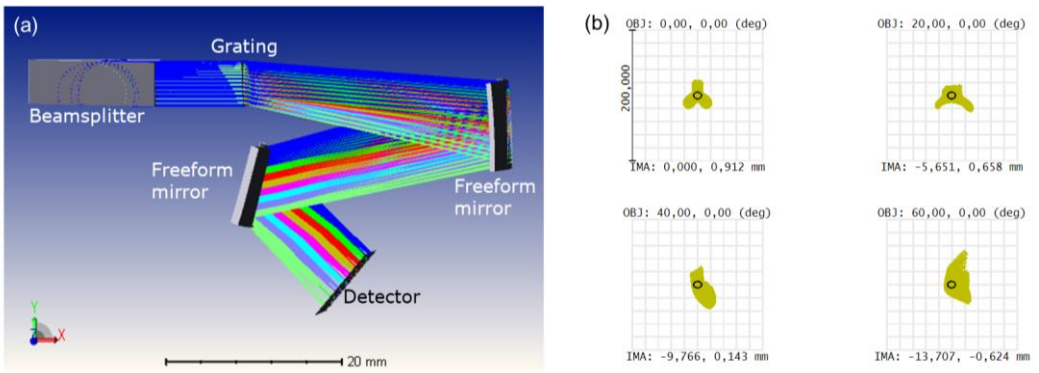

Figure 2: Visible (400 – 1100 nm) spectrometer design: (a) layout; (b) spot diagram at 700 nm for field angles of 0° (on-axis), 20°, 40° and 60° showing a nearly diffraction-limited performance. A similar performance is achieved for the other wavelengths.

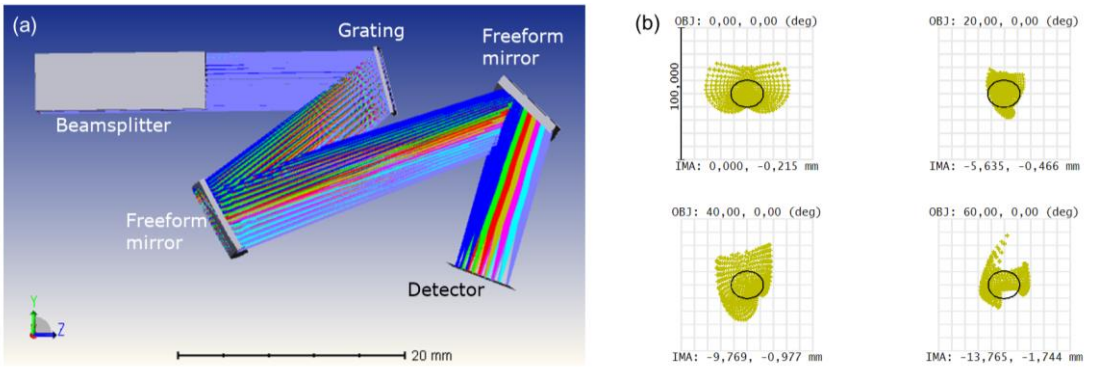

Figure 3: Near-infrared (1100 - 1700 nm) spectrometer design: (a) layout; (b) spot diagram at 1400 nm for field angles of 0° (on-axis), 20°, 40° and 60° showing a nearly diffraction-limited performance. A similar performance is achieved for the other wavelengths.

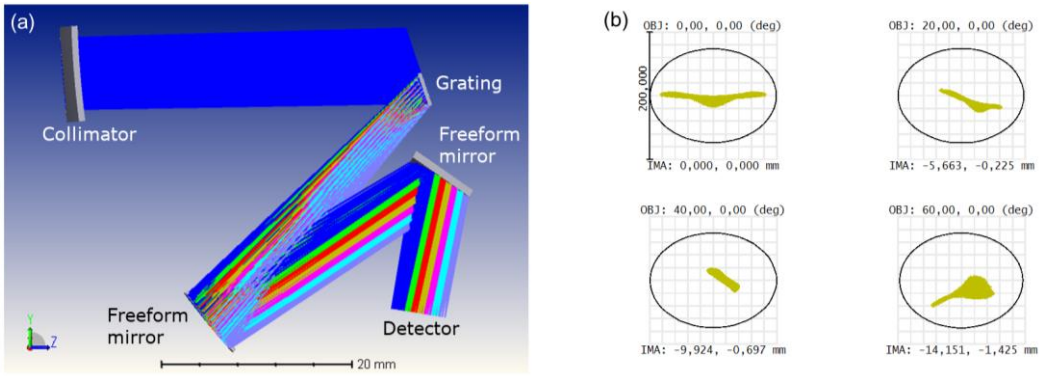

Figure 4: Thermal (8 – 14 µm) spectrometer design: (a) layout; (b) spot diagram at 11 µm for field angles of 0° (on-axis), 20°, 40° and 60° showing a diffraction-limited performance. A similar performance is achieved for the other wavelengths.

Table 1: Simulated spatial and spectral resolution of the 3-channel spectrometer design.

	Spatial resolution at nadir	Spatial resolution at FOV 60°	Spectral resolution at nadir	Spectral resolution at FOV 60°
Visible channel	3.5 km	5.1 km	1 nm	1.5 nm
Near-infrared channel	3.7 km	6.1 km	1.3 nm	2.2 nm
Thermal channel	6.3 km	9.5 km	28 nm	43 nm

Objective

This proposed OPTICA Foundation Challenge targets to develop a laboratory demonstrator of the fully presented multispectral imaging spectrometer design, comprising 9 freeform mirrors and 3 diffraction gratings. Starting from the current optimized nominal design, this requires tackling the following 4 tasks and their related challenges:

(1) **Optimization of the nominal design considering manufacturing tolerances and stray light**, applying a design for manufacturing approach. Tolerance analysis will be performed, evaluating both surface and element tolerances, including manufacturing defects on the surface shapes and mechanical misalignments respectively, and using a statistical Monte Carlo analysis. Additionally, a sensitivity analysis will be included, indicating the worst offenders and thus most significant contributors to the performance, enabling their mitigation during the alignment of the demonstrator setup. Following, a stray light analysis will be performed in the non-sequential mode, facilitating optimization of the mechanical layout and indicating the required positioning of baffles between the channels, after which a computer-aided design (CAD) of the laboratory setup will be created.

(2) **Manufacturing of the freeform mirrors and diffraction gratings.** The freeform mirrors and the diffraction gratings will be manufactured in-house at the VUB B-PHOT Photonics Innovation Centre, benefitting from Brussels Photonics (B-PHOT) extreme optics pilot line, present within the engineering faculty of the Vrije Universiteit Brussel (VUB). The freeform mirrors will be manufactured in aluminium, given its suitable broadband use. Preshaping of the freeform mirrors will be performed using a 5-axis Milling Machine (Röders TEC RXP601DSHZ2), starting from the blank material and generating a preliminary shape. The optical finishing of the mirrors and the manufacturing of the gratings will be tackled using 5-axis ultraprecision diamond tooling (Nanotech 350FG), ensuring an optical surface quality.

(3) **Characterisation and validation of the individually manufactured components**, using in-house metrology tools in a cleanroom environment at the VUB B-PHOT Brussels Photonics Innovation Centre. The freeform mirror profile will be assessed using a Coordinate Measurement Machine (CMM - Werth Video Check UA 400x400x200 3D) and a non-contact 3D optical profiler (Taylor Hobson Luphoscan 420 HD). The surface roughness will be examined using a white-light Interferometer (Bruker Contour GT-I). The grating profile will be characterized with an Atomic Force Microscope (Bruker Dimension Icon).

(4) **Laboratory demonstrator setup and performance evaluation**. A laboratory demonstrator will be realized, first considering the telescope in combination with each of the 3 spectral channels separately, and followed by the mounting and evaluation of the full design. The components will be precisely mounted using a combination of standard opto-mechanics and custom mounts. Translation stages with micrometer actuators will facilitate the alignment of critical components. Subsequent characterization of the design will build on the present expertise related to the characterization of imaging systems [12]. For each of the 3 spectrometer channels, the image resolution will be determined by measuring the Modulation Transfer Function using a slanted edge approach, and the spectral resolution will be evaluated using calibrated light sources. The design tolerances will be experimentally determined, impacting the future integration of the components within the CubeSat.

Risk mitigation

Based on the experience gained from the realisation of a first version of the freeform telescope, we believe the stated challenges are feasible. The manufacturing and characterisation of the freeform mirrors and diffraction gratings will significantly benefit from VUB B-PHOTs state-of-the-art pilot line for freeform optics, which has been previously successfully applied for e.g. the realisation of diffraction gratings, a freeform mirror for ultra short-throw projection, a freeform beam-shaping lens for laser-cutting applications, and freeform mirrors for head-up displays. The in-house manufacturing is considered as an important advantage, enabling a close collaboration with the manufacturing technology experts. As soon as the components for one subpart of the setup are available (telescope, visible channel, near-infrared channel or thermal channel), a subpart of the full setup will already be mounted, evaluated and compared to the simulations, enabling early identification of potential defects or re-optimization needs, which can then be addressed through a manufacturing iteration.

A highly challenging alignment of the mirrors is anticipated, both during the manufacturing process and during the assembly of the laboratory setup. This will be managed by the implementation of alignment features within the design. Custom mounts may be used to facilitate the alignment, which can be 3D printed within the Photonics Innovation Centre.

A total project duration of 18 months is envisioned (see also the Timeline), accounting for manufacturing lead times and allowing for iterations in the manufacturing process. To enable these iterations, the different tasks will be partly performed in parallel.

Outcome

As main outcome, a **laboratory demonstrator of the full freeform imaging spectrometer** is targeted, including a comprehensive evaluation of its performance in terms of imaging quality (Modulation Transfer Function and resolution), spectral resolution, power budget, and efficiency. Additionally, a practical assessment will be made on the design and mounting tolerances, necessary for further development and integration. This laboratory demonstrator is expected to play a pivotal role in the future development of the imaging spectrometer and eventually satellite. The challenging nominal design and its high prototyping costs are currently hampering the development chain, causing difficulties in attracting space industry partners and/or to secure ESA funding. We believe that receiving

the OPTICA Foundation recognition will not only boost the technological developments, but will also allow to gain visibility in the field of space optical instruments and enable to reach out to the space industry.

Impact

The development of the laboratory demonstrator of the 3-channel wide-field-of-view space-based spectrometer is expected to **pave the way towards larger space projects and its integration onboard of a small satellite at Low-Earth-Orbit**, at an altitude of 700 km, driving future space missions that enable improved Earth observation and greenhouse gas sensing.

For the realisation of the satellite, the use of a SmallSat platform can be considered (such as a PROBA technology demonstration mission), or alternatively the satellite could be considered as a companion to other Earth-observing missions, as e.g. the Earth Climate Observatory (ECO) [13,14]. ECO is one of the four selected mission ideas for the ESA Earth Explorer 12 mission and aims to measure the difference between incoming solar radiation and outgoing terrestrial radiation using a satellite constellation, where each satellite comprises four wide field-of-view radiometers. Our proposed 3-channel spectrometer would enable an enhanced interpretation and measurement of the greenhouse gases. The Royal Observatory of Belgium has already shown interest in the spectrometer design as a potential CubseSat companion to the ECO satellite.

Climate and climate change are controlled by complex and delicate mechanisms, impacted by essential climate variables linked to the Earth radiation budget and greenhouse gases in the atmosphere. Our proposed 3-channel imaging spectrometer is expected to **advance the state-of-the-art pushbroom spectrometer designs** by offering an extended wavelength range (Figure 5) and an extremely wide field-of-view, combined with a good spatial resolution < 10 km at nadir for each of the 3 channels. The extended wavelength range enables to improve greenhouse gas sensing while considering both the reflected and emitted Earth radiation, where the latter thermal radiation is currently not monitored by OMI and TROPOMI. The extended FOV of 120° enables a nearly limb to limb observation from an altitude of about 700 km and is, to our knowledge, the widest FOV that has ever been realized for a space-based telescope.

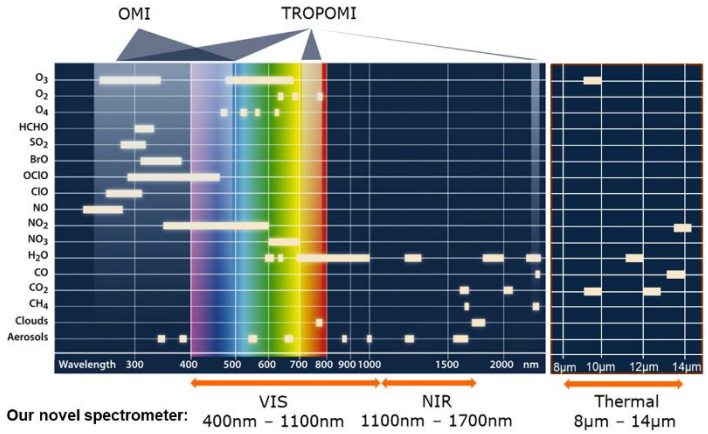

Figure 5: Indication of the extended wavelength range that can be achieved with our proposed 3-channel spectrometer, and the corresponding greenhouse gasses impacting the spectrum. (adapted from [8]).

Summarized, we believe our proposed design paves the way for future space missions, enabling an improved Earth observation and greenhouse gas sensing, advancing climate change monitoring while contributing to the Sustainable Development Goals (SDGs), and particularly Climate Action, leading to an enhanced climate mitigation, benefitting all of us.

References

1. H. Boesch, Y. Liu, J. Tamminen, D. Yang, P. I. Palmer, H. Lindqvist, Z. Cai, K. Che, A. Di Noia, L. Feng, J. Hakkarainen, I. Ialongo, N. Kalaitzi, T. Karppinen, R. Kivi, E. Kivimäki, R. J. Parker, S. Preval, J. Wang, A. J. Webb, L. Yao, and H. Chen, "Monitoring greenhouse gases from space," Remote Sens (Basel) **13**, (2021).

2. J. P. Burrows, M. Weber, M. Buchwitz, V. Rozanov, A. Ladsta¨tter, L. Ladsta¨tter-Weißenmayer, A. Richter, R. Ru¨, R. Debeek, R. Hoogen, K. Bramstedt, K.-U. Eichmann, M. Eisinger, and D. Perner, "The Global Ozone Monitoring Experiment (GOME): Mission Concep and First Scientific Results," J Atmos Sci **56**, (1998).

3. R. Munro, R. Lang, D. Klaes, G. Poli, C. Retscher, R. Lindstrot, R. Huckle, A. Lacan, M. Grzegorski, A. Holdak, A. Kokhanovsky, J. Livschitz, and M. Eisinger, "The GOME-2 instrument on the Metop series of satellites: Instrument design, calibration, and level 1 data processing - An overview," Atmos Meas Tech **9**, 1279–1301 (2016).

4. T. Hamazaki, Y. Kaneko, A. Kuze, and K. Kondo, "Fourier transform spectrometer for Greenhouse Gases Observing Satellite (GOSAT)," in *Enabling Sensor and Platform Technologies for Spaceborne Remote Sensing* (SPIE, 2005), Vol. 5659, p. 73.

5. H. Bovensmann, J. P. Burrows, M. Buchwitz, J. Frerick, S. Noe, V. V Rozanov, K. V Chance, and A. P. H Goede, "SCIAMACHY: Mission Objectives and Measurement Modes," J Atmos Sci **56**, (1998).

6. P. F. Levelt, G. H. J. Van Den Oord, M. R. Dobber, A. Mälkki, H. Visser, J. De Vries, P. Stammes, J. O. V. Lundell, and H. Saari, "The ozone monitoring instrument," IEEE Transactions on Geoscience and Remote Sensing **44**, 1093–1100 (2006).

7. D. Nijkerk, B. van Venrooy, P. Van Doorn, R. Henselmans, F. Draaisma, and A. Hoogstrate, "The TROPOMI Telescope," in *International Conference on Space Optics ICSO* (SPIE, 2012).

8. J. P. Veefkind, I. Aben, K. McMullan, H. Förster, J. de Vries, G. Otter, J. Claas, H. J. Eskes, J. F. de Haan, Q. Kleipool, M. van Weele, O. Hasekamp, R. Hoogeveen, J. Landgraf, R. Snel, P. Tol, P. Ingmann, R. Voors, B. Kruizinga, R. Vink, H. Visser, and P. F. Levelt, "TROPOMI on the ESA Sentinel-5 Precursor: A GMES mission for global observations of the atmospheric composition for climate, air quality and ozone layer applications," Remote Sens Environ **120**, 70–83 (2012).

9. J. P. Rolland, M. A. Davies, T. J. Suleski, C. Evans, A. Bauer, J. C. Lambropoulos, and K. Falaggis, "Freeform optics for imaging," Optica **8**, 161 (2021).

10. W. Jahn, M. Ferrari, and E. Hugot, "Innovative focal plane design for large space telescope using freeform mirrors," Optica **4**, 1188–1195 (2017).

11. L. Schifano, M. Vervaeke, D. Rosseel, J. Verbaenen, H. Thienpont, S. Dewitte, F. Berghmans, and L. Smeesters, "Freeform Wide Field-of-View Spaceborne Imaging Telescope: From Design to Demonstrator," Sensors **22**, (2022).

12. L. Smeesters, J. Verbaenen, L. Schifano, M. Vervaeke, H. Thienpont, G. Teti, A. Forconi, and F. Lulli, "Wide-Field-of-View Multispectral Camera Design for Continuous Turfgrass Monitoring," Sensors **23**, (2023).

13. L. Schifano, F. Duerr, F. Berghmans, S. Dewitte, and L. Smeesters, "Towards a demonstrator setup for a wide-field-of-view visible to near-infrared camera aiming to characterize the solar

radiation reflected by the Earth," in *Optics, Photonics and Digital Technologies for Imaging Applications VII* (Proc. SPIE, 2022).

14. L. Schifano, L. Smeesters, T. Geernaert, F. Berghmans, and S. Dewitte, "Design and analysis of a next-generation wide field-of-view Earth radiation budget radiometer," Remote Sens (Basel) **12**, 1–19 (2020).

EXECUTIVE SUMMARY:
A sensing toolbox based on polarimetric spectroscopy for continuous real-time monitoring of blood biomarkers

Prof. Dr. phil. Lilian Witthauer

Global Challenge:
The global challenge addressed by this proposal is the need for comprehensive, real-time metabolic monitoring to improve personalized healthcare and facilitate early disease detection. Current methods for clinical metabolomics are complex, costly, bulky, and time-consuming, providing only snapshot assessments of an individual's metabolic state. These methods, such as liquid and gas chromatography (GC), mass spectrometry (MS), and nuclear magnetic resonance spectroscopy (NMR) require extensive sample preparation and trained personnel, restricting their usability to disease aetiology and discovery. To also address therapy and management of diseases, continuous, real-time metabolic monitoring is necessary. Sensor-based, real-time metabolomics would be transformative for precision personalized medicine, offering continuous insights compared to the end-point diagnostics provided by traditional GC-MS and NMR metabolomics. This shift would enable more dynamic and responsive healthcare interventions, significantly improving disease management and patient outcomes.

The Proposed Project:
This project, fitting into the health category of the OPTICA foundation challenge, aims to develop a polarimetric spectroscopy-based toolbox for the sensitive, specific, continuous and real-time tracking of blood biomarkers. Polarimetric spectroscopy leverages the optical rotation properties of chiral molecules and spectroscopic fingerprinting in the visible and near-infrared range to detect various metabolites in the human body. The proposed project will integrate this technology into a photonic integrated circuit (PIC), with the future goal of creating an implantable device capable of delay-free continuous metabolite monitoring. The 2-year project will be executed through three primary aims:

- Monte Carlo Simulation: Perform optical simulations to optimize the design parameters, component placement, and signal detection of the polarimetric spectroscopy system.
- PIC Design and Fabrication: Design and fabricate a miniaturized PIC that incorporates the polarimetric spectroscopy setup, focusing initially on glucose monitoring with the potential to expand to other metabolites.
- In Vitro Tests: Conduct in vitro studies to evaluate the PIC's optical, mechanical, and biochemical performance, assessing its sensitivity and accuracy in detecting glucose.

Outcomes & Impact:
The project will result in a first prototype of a PIC tailored for real-time continuous glucose monitoring, with the potential for future multi-metabolite sensing capabilities. The implementation of a sensor based on polarimetric spectroscopy has only recently become feasible, thanks to advances in complex algorithms and the availability of miniaturizable hardware necessary for this technology.
The broader impact of this project extends to the management of chronic diseases beyond diabetes, including cardiovascular, inflammatory, and metabolic disorders. By enabling continuous monitoring of multiple metabolites, the device will facilitate early disease detection, personalized treatment, and improved patient outcomes. For instance, monitoring biomarkers such as lactate, cholesterol, and cytokines can provide early warnings and better management of ischemic events, metabolic stress, and disease progression, ultimately enhancing the efficacy of treatments and reducing healthcare costs. The proposed project not only advances continuous real-time monitoring of blood biomarkers but also contributes to the understanding and development of effective polarization management strategies in PICs.

RESEARCH PLAN
A sensing toolbox based on polarimetric spectroscopy for continuous real-time monitoring of blood biomarkers

Prof. Dr. phil. Lilian Witthauer
Department of Diabetes, Endocrinology, Nutritional Medicine and Metabolism, Inselspital, Bern University Hospital, University of Bern, Bern, Switzerland
lilian.witthauer@unibe.ch

1. Literature Review

Human physiology and pathology imprint a distinctive chemical signature into the bloodstream. This fingerprint, composed of a vast array of small molecules known as metabolites, holds immense potential to inform personalized medicine. By analyzing these metabolites, we can gain valuable insights into an individual's health, disease susceptibility, and response to treatment [1], [2]. Despite the advancements in metabolomics - the science of decoding these metabolites - there remains a **significant challenge to leverage metabolomic data for immediate clinical use. There exists no method for the real-time, sensitive, and specific tracking of a diverse set of metabolites over a large concentration range in everyday environments**. The proposed project addresses this gap. Current methods for clinical metabolite analysis involve complex procedures that are not only costly and time-consuming but also require extensive sample preparation and the expertise of trained personnel. These methods, such as liquid and gas chromatography [3], [4], nuclear magnetic resonance spectroscopy [5] and mass spectrometry [4] while precise, are hardly scalable for real-time or continuous personalized diagnostics. Thus, assessing clinically relevant parameters typically offers only a snapshot at a singular timepoint. Continuous monitoring of metabolites for real-time metabolomics via sensors remains elusive. One exception in clinical practice is the management of diabetes, where continuous glucose monitoring devices (CGM) [6] have become the standard of care. A CGM device is composed of a sensor, a transmitter, and a monitor (e.g., smartphone) that lets the person view the glucose levels. Commercial continuous glucose monitors include models from Dexcom, Medtronic, Abbott, and Ascensia and measure the glucose levels in the interstitial fluid of the subcutaneous tissue. This is either done via a minimally invasive needle-like sensor or with a small implant (only Eversense). Except for the Eversense system, all CGM devices use amperometric sensors relying on the enzymatic reaction between glucose oxidase and glucose as originally proposed by Clark [7] and have accuracies of 8-10 %. This reaction generates hydrogen peroxide, which is then oxidized at an electrode, producing a current proportional to glucose concentration [8]. The measurement principle of the Eversense sensor is based on a fluorophore (anthracene) that is bound to a polymer and has an appended ortho-aminomethylphenylboronic acid that serves as a glucose receptor (indicator) [9], [10]. In the absence of glucose, electron transfer occurs between the tertiary amines and the anthracene causing quenching of the fluorescence. When a glucose molecule binds to the boronic acid, weak boron-nitrogen bonds are formed resulting in reduced quenching and a fluorescence proportional to the glucose concentration. These systems have made significant advancements in metabolic monitoring, however, commercial solutions are currently limited to sensing of glucose. Besides glucose, the first companies (Abbott, SIBIONICS) have announced continuous ketone sensors [11], [12]. In addition, non-medical consumer-grade lactate monitoring devices (K'Watch Athlete) have recently come to the market. Apart from the announced system by Abbott and a sensor recently introduced in nature biomedical engineering [13] current methods for measuring ketones and lactate are largely separate from glucose monitoring, requiring additional devices. To close this gap and to allow multiplexing of several metabolites further advancements in sensing technologies going beyond current electrochemical sensors are needed.
Expanding beyond diabetes, the demand for continuous monitoring in healthcare settings continues to grow, driven by the need for early detection, personalized treatment, and

improved patient outcomes. Sensing additional metabolites such as cortisol, glucagon, growth hormone, epinephrine, and incretin hormones, could allow for a more holistic perspective of metabolic and cardiovascular health [14]. A holy grail for multi-metabolite monitoring is certainly a non-invasive device, however, methods based on various optical technologies including infrared spectroscopy, Raman spectroscopy, fluorescence spectroscopy, optical coherence tomography, polarimetry, and photoacoustic spectroscopy have not been successful so far [8] mainly due to poor accuracy, consistency issues, adverse effects, and poor hardware adaptability. On the other hand, two implantable devices based on near-infrared spectroscopy have shown promising results for glucose, however, while the device by Anima [15], was discontinued the Indigo device is still in early development. Additionally, results from other technologies, such as single-molecule sensing based on free particle motion have recently been published in Nature Communications [16]. The existence of these projects highlights the pressing need for a comprehensive sensing solution that can enable real-time metabolomics in a resilient, scalable, and cost-effective way.

2. Problem Statement/Objective

Despite the critical role metabolites play in understanding physiological states and disease processes, current diagnostic methods are ill-equipped for real-time continuous monitoring of a broad spectrum of metabolites. GC-MS, NMR technology are not miniaturizable, which significantly limits their use as on-body applicability, and current sensors have not yet been optimized for effective multi-metabolite detection.

This project aims to fill this significant gap by developing a **polarimetric spectroscopy-based toolbox for the sensitive, specific, and real-time tracking of blood biomarkers.** This toolbox will have metabolite-specific and customizable sensor options for personalized healthcare by enabling continuous and adaptable monitoring and assessment of an individual's health status and response to treatments. Polarimetric spectroscopy combines the measurement of optical rotation of chiral substances with the advantages of spectroscopic fingerprinting. Many molecules in the human body are known to be chiral (sugars, amino acids, nucleotides and nucleic acids, cholesterol, cortisol, testosterone, epinephrine, melatonin, etc.); this chirality affects the light transmitted through a sample containing chiral molecules by rotating the light's polarization. The polarization rotation φ depends on the specific rotation α of the chiral molecule, its concentration c, and the path length l that light travels through via the equation $\phi = [\alpha]^T_{\lambda,pH} \cdot c \cdot l$. In the concentration range of metabolites in the human blood, the induces rotation change is small, i.e. in the order of millidegrees. Thus, to extract a signal from the multitude of background contributions a modulation of the polarization is necessary. In a recent study we were able to show that the modulation can be done through polarization switching using the setup shown in Fig. 1. A laser diode module (4.5 mW at 532 nm) together with a Glan-Thompson polarizer (GTP) was used to generate a linearly polarized beam. The

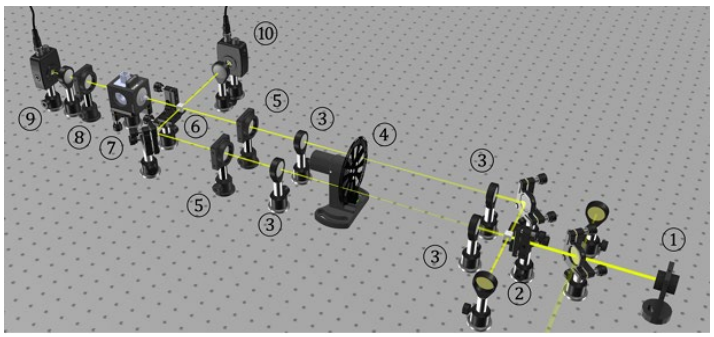

Figure 1: Schematics of the experimental setup (1) Light source, (2) Beamsplitter, (3) Telescope system, (4) Chopper, (5) Polarizer, combiner, (7) Sample, (8) Analyzer, (9) Signal detector, (6) Beam (10) Reference detector.

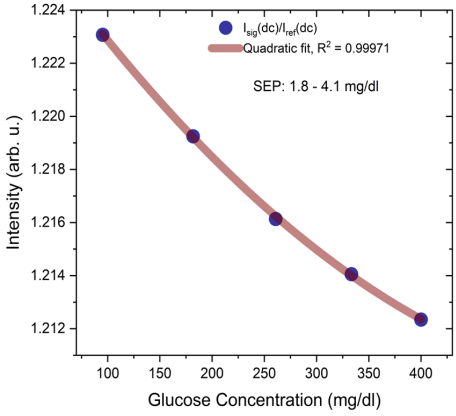

Figure 2: Relationship between glucose concentration and intensity measurements

beam was divided into two arms via a beam splitter. An optical chopper was used to create pulsed beams with a temporal delay between the two arms. Each of the beams was guided through a GTP that was set to +1 and -1 degrees, respectively (0 is perpendicular to the table plane). The two beams were recombined using a beam splitter resulting in a beam with square-wave modulated polarization. An additional GTP acted as an analyzer and the beam intensity was measured with a photodiode. The resulting intensity for a chiral sample (aqueous glucose solution) depends quadratically on the glucose concentration (Fig 2.), the results are currently under review for publication in Biomedical Optics Express.

By conducting this measurement at different wavelengths in the visible and near-infrared range, we can further expand the sensitivity and specificity of this measurement technology to different molecules. In the near-infrared (NIR) range (750-2500 nm), many molecules absorb light that matches the frequency of their vibrational and rotational motions (periodic motion of atoms in a molecule, stretching and bending of intramolecular bonds). When the molecule is in its ground state, such a vibration is called a fundamental vibration, when more energy is absorbed by the molecule, overtones can be excited. The corresponding NIR spectra of different metabolites thus show many peaks corresponding to different functional groups of the molecule. **The analysis of these spectra requires advanced algorithmic processing, which has only recently become feasible.**

Recent advancements in Photonic Integrated Circuits (PIC), will allow us to integrate the polarimetric-spectroscopy-based setup into an implantable miniature device that will be able to measure metabolite concentrations in blood in real time without any delay. The real-time sensing in blood will be achieved by an extravascular implant on the vessel wall. The proximity to the blood without being directly in the bloodstream (increased risk for thrombosis) itself seems to be the ideal trade-off between invasiveness and a precise, delay-free measurement. Possible implantation sites could be at a superficial blood vessel (for example vena radialis or carotid artery). Veins have the advantage of being very thin-walled (see-through), however, arteries offer more stability and less vasoconstriction and dilatation effects.

The implantation on the vessel wall is expected to induce only minimal foreign body response [15], [17] and hence would allow for a long implantation time (potentially 8-10 years) and a stable signal with only few calibrations. Surgical implantation at superficial blood vessels are well known from other devices such as the barostim device [17], [18], [19], [20], [21]. Depending on the exact sensor location only the sensor head could be implanted, and a readout unit could either be wireless on the skin or could be placed under the skin near the implant (Fig.3).

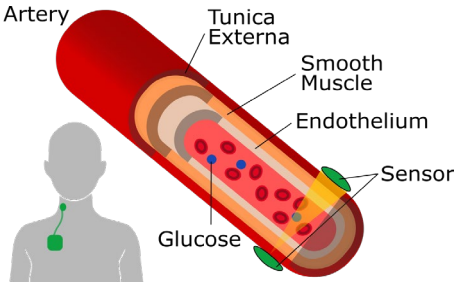

Figure 3: Possible embodiment for the implantable sensor.

This two-year project will make a significant contribution to the overarching goal of an extravascular implant by conducting the following three aims:

Aim 1: Monte Carlo Simulation

Under Aim 1 we will perform optical simulations of the polarimetric spectroscopy system to find the correct design parameters such as geometry and components and identify potential challenges in detecting and quantifying blood biomarkers. For the simulation, we plan to use existing Monte Carlo simulation tools such as Pol-MC [22] or PyTissueOptics [23].

Objectives:

a) Path Length Optimization:
   - Develop simulations to determine the maximum allowable path length to minimize depolarization effects.
   - Analyze the relationship between path length and signal-to-noise ratio (SNR).

b) Scattering Effects:
   - Model the influence of scattering on the polarimetric signal.

- Evaluate the impact of different types of tissues and blood compositions on signal integrity.

c) Component Placement and Signal Optimization:
   - Identify which components of the system need to be implanted versus those that can remain external.
   - Optimize the placement of components to balance invasiveness and signal quality.
   - Simulate various configurations to determine the optimal arrangement of components to maximize signal strength and accuracy.

Aim 2: PIC Design and Fabrication

Based on the benchtop prototype and the results from the simulation under Aim 1, we will design and fabricate a PIC that integrates the polarimetric spectroscopy setup into a miniaturized device with the potential to be integrated into an implantable device in the future.

Objectives:

a) Design Specifications:
   - Develop design specifications for the PIC, focusing on a two-chip system with implantable and non-implantable parts.
   - The initial design will focus on single-wavelength measurements for glucose, with provisions for future upgrades to multi-band measurements to accommodate additional metabolites.

b) Polarization Management:
   - Design and implement a polarization management system. The polarization angle of the light will be tuned by modifying the light splitting ratio among the two Grating Couplers, e.g. a tunable Mach Zehnder Interferometer (MZI). Alternatively, the polarization modulation can be achieved by combining a tunable coupler with a phase shifter to control the phase delay. A similar concept has shown success in transforming path entanglement into polarization entanglement [24].
   - Integrate anti-reflection coatings and nanostructures to minimize unwanted light scattering.

c) Fabrication:
   - Collaborate with CSEM and the Optical Nanomaterial Group at ETH Zurich for the fabrication of the PIC on a Lithium Niobate (LNOI) platform.
   - Ensure the fabricated PIC meets the design specifications and is suitable for in vitro testing.

Aim 3: In Vitro Tests

Lastly, we will conduct in vitro studies to evaluate the optical, mechanical, and physiochemical responses of the PIC prototype, and assess its sensitivity and accuracy in detecting and quantifying glucose.

Objectives:

a) Optical and Mechanical Evaluation:
   - Assess the optical performance of the PIC, including polarization modulation and signal detection capabilities.
   - Evaluate the mechanical optical stability and durability of the PIC under simulated physiological conditions.

b) Sensitivity and Accuracy Testing:
   - Use synthetic and real blood samples spiked with different glucose concentrations to test the sensitivity and accuracy of the PIC in detecting glucose.
   - Compare the PIC's performance with current standard methods.

3. Outcome(s)

Specific Outcome Aim 1: A detailed simulation report outlining the optimal design parameters, component placement, and potential challenges, providing a solid foundation for

the subsequent design and fabrication of the Photonic Integrated Circuit (PIC).
Specific Outcome Aim 2: A fabricated PIC prototype ready for in vitro testing, demonstrating the feasibility of real-time continuous glucose monitoring with the potential for expansion to other biomarkers.
Specific Outcome Aim 3: An evaluation report demonstrating the PIC prototype's performance, sensitivity, and accuracy, with recommendations for further optimization during the next prototype cycle
General Outcome: The outcome of the project is a first prototype of a photonic integrated circuit tailored to real-time, continuous and delay-free monitoring of glucose with the intention to perform further research to sense multiple blood biomarkers.

4. Impact

Multi-metabolite monitoring offers a promising approach to **diagnosing and managing chronic diseases**, including metabolic disorders, cardiovascular disease, nerve injury, inflammatory disease, and tumors. For instance, **diabetes** affects more than 537 million people worldwide. Despite advancements in insulin therapy, CGM, and adjunct therapies, only about a quarter of people with diabetes achieve target glucose ranges. Insulin therapy's complexity, coupled with risks of hypoglycemia and weight gain, underscores the need for a broader metabolic understanding. Factors like carbohydrate, fat, and fiber content, along with fluctuations in regulatory hormones such as cortisol and glucagon, impact glucose levels and insulin requirements. These variations, influenced by stress, illness, and physical activity, challenge accurate insulin sensitivity prediction. Current CGM systems, relying solely on glucose measurements, struggle to adapt quickly to these changing needs. Monitoring additional metabolites such as ketones and lactate alongside glucose would allow closed-loop systems to detect metabolic shifts early, ensuring precise insulin dosing and timely interventions to prevent severe complications such as hypoglycemia and Diabetic Ketoacidosis. This approach would reduce the need for hospitalizations, including ICU stays. By enabling tighter glycemic control, long-term diabetes complications could be reduced, and related healthcare costs lowered. Beyond diabetes, multi-metabolite monitoring can significantly impact the management of other diseases. In **cardiovascular disease**, monitoring biomarkers such as lactate, cholesterol, and triglycerides can provide early warnings of ischemic events or metabolic stress, enabling timely interventions to prevent heart attacks or strokes. For **inflammatory diseases** and **tumors**, tracking metabolites like cytokines and oncometabolites can help in assessing disease progression and response to therapy, allowing for more personalized and effective treatment plans. Additionally, in cases of nerve injury, metabolites like neuropeptides and neurotransmitters can provide insights into the extent of injury and recovery progress, guiding rehabilitation strategies.
To summarize, multi-metabolite monitoring supports personalized treatment strategies tailored to individual metabolic profiles and lifestyle factors, enhancing treatment efficacy, patient satisfaction, and overall quality of life. Our sensing toolbox will enhance diagnostic capabilities by providing a rapid, accurate tool for early disease detection and monitoring, benefiting a wide range of chronic conditions beyond diabetes. Besides enabling real-time blood biomarker monitoring, the project contributes to the understanding of polarization management in PICs. The results from this project will be published in reputable journals such as Biomedical Optics Express, and Nature Biomedical Engineering. Additionally, we will present at conferences such as the OPTICA Sensors Conference and the IEEE EMBS Annual Conference.
In addition to the research output, the project will provide **educational resources and hands-on experience in the development of photonic sensing technologies for students** and junior researchers at the University of Bern. Furthermore, the project will help me establish my research group in sensing and monitoring, making a **significant contribution towards fulfilling my tenure conditions.**

Bibliography

[1] F. Danzi *et al.*, "To metabolomics and beyond: a technological portfolio to investigate cancer metabolism," *Signal Transduct. Target. Ther.*, vol. 8, no. 1, pp. 1–22, Mar. 2023, doi: 10.1038/s41392-023-01380-0.

[2] A. Zhang, H. Sun, G. Yan, P. Wang, and X. Wang, "Metabolomics for Biomarker Discovery: Moving to the Clinic," *BioMed Res. Int.*, vol. 2015, p. 354671, 2015, doi: 10.1155/2015/354671.

[3] S. T. Kong, H.-S. Lin, J. Ching, and P. C. Ho, "Evaluation of dried blood spots as sample matrix for gas chromatography/mass spectrometry based metabolomic profiling," *Anal. Chem.*, vol. 83, no. 11, pp. 4314–4318, Jun. 2011, doi: 10.1021/ac200662s.

[4] C. A. Crutchfield, S. N. Thomas, L. J. Sokoll, and D. W. Chan, "Advances in mass spectrometry-based clinical biomarker discovery," *Clin. Proteomics*, vol. 13, p. 1, Jan. 2016, doi: 10.1186/s12014-015-9102-9.

[5] D. S. Wishart *et al.*, "NMR and Metabolomics—A Roadmap for the Future," *Metabolites*, vol. 12, no. 8, p. 678, Jul. 2022, doi: 10.3390/metabo12080678.

[6] O. Didyuk, N. Econom, A. Guardia, K. Livingston, and U. Klueh, "Continuous Glucose Monitoring Devices: Past, Present, and Future Focus on the History and Evolution of Technological Innovation," *J. Diabetes Sci. Technol.*, vol. 15, no. 3, pp. 676–683, May 2021, doi: 10.1177/1932296819899394.

[7] L. C. Clark and C. Lyons, "Electrode systems for continuous monitoring in cardiovascular surgery," *Ann. N. Y. Acad. Sci.*, vol. 102, no. 1, pp. 29–45, 1962, doi: 10.1111/J.1749-6632.1962.TB13623.X.

[8] W. V. Gonzales, A. Mobashsher, and A. Abbosh, "The Progress of Glucose Monitoring—A Review of Invasive to Minimally and Non-Invasive Techniques, Devices and Sensors," *Sensors*, vol. 19, no. 4, p. 800, Feb. 2019, doi: 10.3390/s19040800.

[9] T. D. James, K. R. A. S. Sandanayake, and S. Shinkai, "A Glucose-Selective Molecular Fluorescence Sensor," *Angew. Chem. Int. Ed. Engl.*, vol. 33, no. 21, pp. 2207–2209, Nov. 1994, doi: 10.1002/ANIE.199422071.

[10] T. D. James, K. R. A. S. Sandanayake, R. Iguchi, and S. Shinkai, "Novel Saccharide-Photoinduced Electron Transfer Sensors Based on the Interaction of Boronic Acid and Amine," *J Am Chem Soc*, vol. 117, pp. 8982–8987, 1995.

[11] S. Alva, K. Castorino, H. Cho, and J. Ou, "Feasibility of Continuous Ketone Monitoring in Subcutaneous Tissue Using a Ketone Sensor," *J. Diabetes Sci. Technol.*, vol. 15, no. 4, pp. 768–774, Jul. 2021, doi: 10.1177/19322968211008185.

[12] H. Teymourian *et al.*, "Microneedle-Based Detection of Ketone Bodies along with Glucose and Lactate: Toward Real-Time Continuous Interstitial Fluid Monitoring of Diabetic Ketosis and Ketoacidosis," *Anal. Chem.*, vol. 92, no. 2, pp. 2291–2300, Jan. 2020, doi: 10.1021/acs.analchem.9b05109.

[13] F. Tehrani *et al.*, "An integrated wearable microneedle array for the continuous monitoring of multiple biomarkers in interstitial fluid," *Nat. Biomed. Eng.*, vol. 6, no. 11, Art. no. 11, Nov. 2022, doi: 10.1038/s41551-022-00887-1.

[14] A. Zeigerer, R. Sekar, M. Kleinert, S. Nason, K. M. Habegger, and T. D. Müller, "Glucagon's Metabolic Action in Health and Disease," *Compr. Physiol.*, vol. 11, no. 2, pp. 1759–1783, Apr. 2021, doi: 10.1002/cphy.c200013.

[15] J. I. Joseph, M. C. Torjman, and P. J. Strasma, "Vascular Glucose Sensor Symposium," *J. Diabetes Sci. Technol.*, vol. 9, no. 4, pp. 725–738, Jun. 2015, doi: 10.1177/1932296815587938.

[16] A. D. Buskermolen *et al.*, "Continuous biomarker monitoring with single molecule resolution by measuring free particle motion," *Nat. Commun.*, vol. 13, no. 1, p. 6052, Oct. 2022, doi: 10.1038/s41467-022-33487-3.

[17] S. J. Wilks *et al.*, "Non-clinical and pre-clinical testing to demonstrate safety of the barostim neo electrode for activation of carotid baroreceptors in chronic human implants," *Front. Neurosci.*, vol. 11, no. AUG, Aug. 2017, doi: 10.3389/FNINS.2017.00438/FULL.

[18] CVRx, “Barostim baroreflex activation therapy.”
[19] J. R. Costa *et al.*, “Percutaneous implantation of endoprostheses in the carotid arteries,” *Arq. Bras. Cardiol.*, vol. 80, no. 1, pp. 77–82, Jan. 2003, doi: 10.1590/S0066-782X2003000100007.
[20] B. Marie *et al.*, “Carotid versus femoral access for transcatheter aortic valve replacement: comparable results in the current era,” *Eur. J. Cardiothorac. Surg.*, vol. 60, no. 4, pp. 874–879, Oct. 2021, doi: 10.1093/EJCTS/EZAB109.
[21] P. Overtchouk and T. Modine, “Alternate access for TAVI: Stay clear of the chest,” *Interv. Cardiol. Rev.*, vol. 13, no. 3, pp. 145–150, 2018, doi: 10.15420/ICR.2018.22.1.
[22] D. Côté and I. A. Vitkin, “Robust concentration determination of optically active molecules in turbid media with validated three-dimensional polarization sensitive Monte Carlo calculations,” *Opt. Express*, vol. 13, no. 1, p. 148, Jan. 2005, doi: 10.1364/OPEX.13.000148.
[23] “DCC-Lab/PyTissueOptics.” DCC-Lab, Apr. 24, 2024. Accessed: May 13, 2024. [Online]. Available: https://github.com/DCC-Lab/PyTissueOptics
[24] L. Olislager *et al.*, “Silicon-on-insulator integrated source of polarization-entangled photons,” *Opt. Lett.*, vol. 38, no. 11, p. 1960, Jun. 2013, doi: 10.1364/OL.38.001960.

Microcomb-driven Communication Link with 100Tb/s Data Rate and Energy-efficient Operation

Optica 20th Anniversary Challenge: Information
Lin Chang, School of Electronics, Peking University, Beijing 100871, China;
linchang@pku.edu

The ever-growing data traffic of the internet, fueled by recent advancements in AI and big data, is imposing significant challenges on optical communication infrastructures. Over the last few years, remarkable efforts have been dedicated to increase the capacity of communication links, particularly exploring the massively parallel wavelength division multiplex (WDM) communications. However, conventional approach employing laser arrays as the light source suffers from drawbacks in stability and coherency, resulting in substantial power consumption in both wavelength multiplexing and digital signal processing (DSP).

Recently, microcomb has attracted a lot of attentions as a promising candidate to overcome this problem. One microcomb can provide hundreds of equally-spaced wavelengths, which can support high-capacity communication. However, previous microcomb-based communications rely on bulky and power-hungry pump lasers, thereby causing a disadvantage in terms of energy efficiency.

In this project, we propose to develop a fully chip-based and power-efficient microcomb to drive communication links. We will leverage self-injection locking technology, which enables coherent microcomb generation by laser-diode pumping, without relying on any bulky equipment or auxiliary electronics. Based on ultra-high Q S_3N_4 microresonators ($Q > 2.6 \times 10^8$) manufactured by CMOS foundry, we can achieve high coherence between each comb line, whose linewidth can reach Hz level. Furthermore, the self-injection locking technique enables the generation of a dark pulse, allowing for a conversion efficiency exceeding 80%, which can overcome the energy efficiency problem of microcombs used in previous communication systems.

At the system level, we propose a novel WDM coherent communication architecture that fully leverages the advantage of microcombs in massive parallelization and high coherence. This communication system will incorporate over 150 channels, **covering C+L+S band**, with each channel capable of supporting high-order coherent modulation formats, which leads to **beyond 100 Tb/s aggregate data rate**. Importantly, such high capacity is achieved with significantly improved energy-efficiency: the equal spacing of comb lines **eliminates the need for wavelength control**; more importantly, the constant phase relation among different comb lines can significantly **reduce 99% of coherent DSP**, leading to **less than 1pJ/bit energy efficiency**. With these advantages, we envision a high-capacity, power-efficient communication system which should have a profound impact on the future of the telecom and datacenters.

Microcomb-driven Communication Link with 100Tb/s Data Rate and Energy-efficient Operation

Literature Review

The ever-growing data traffic of the internet, fueled by recent advancements in AI and big data, is imposing significant challenges on optical communication infrastructures. Over the last few years, remarkable efforts have been dedicated to increasing the capacity of communication links, including the exploration of massive wavelength division multiplex (WDM) systems, higher channel bandwidths, as well as higher-order communication modulation formats. However, these approaches come at the expense of increased hardware requirements and power consumption: For WDM systems, expanding the channel number often involves adding more individual lasers, which makes precise wavelength control a critical task [1]; for an individual channel, high-bandwidth and high-format transmission requires extensive digital signal processing (DSP), particularly for coherent communications [2].

One promising solution to address the energy-efficiency problem of high-capacity communication is using an optical frequency comb to drive the communication link. A comb consists of multiple equally distributed frequency lines, which can support the massive parallelization for WDM in a single source. Importantly, the recent development of microcomb provides a path to achieve OFC generation on a chip [3], leading to numerous demonstrations of microcomb-driven, high-capacity communication systems. In 2014, Joerg Pfeifle et al. reported the first experimental demonstration of coherent data transmission using 20 microcomb channels, achieving a total data stream of 1.44 Tbit s^{-1} [4]. In 2017, by interleaving two dissipative Kerr solitons (DKS) combs, Pablo Marin-Palomo et al. used a total of 179 comb line carriers to achieve an aggregate line rate of 55.0 Tbit s^{-1} transmitted over a distance of 75 km [5]. In 2020, a high spectral efficiency of 10.4 bits/Hz was realized by using a high modulation format of 64 QAM with a low comb-free spectral range (FSR) spacing of 48.9 GHz in the report of Bill Corcoran et al. [6]. In 2022, Yong Geng et al. used coherence-cloned Kerr soliton microcombs to show the ability of the DKS microcomb coherence to simplify traditional digital signal processing algorithms [7]. In 2022, our group demonstrated a microcomb-driven silicon photonic link with 50 Gbaud PAM4 format and an aggregate bit rate of 2 Tbit s^{-1}[8].

Problem statement/Objective

Despite remarkable progress, the practical implementation of microcombs for real-world applications remains elusive. One big challenge is the integration. Although microresonators for comb generation can be integrated on-chip nowadays, their pumping lasers are usually bench-top ones. Particularly, for coherent communication, a narrow linewidth pump laser is essential, which is usually bulky and expensive. Additionally, the conversion efficiency poses another difficulty. The most commonly used coherent comb state, bright soliton, exhibits a conversion efficiency of around 1-2%, resulting in a main disadvantage in energy efficiency for communications using microcomb. Meanwhile, the

converted power is distributed to combs lines unevenly, which further degrades the effective wall plug efficiency.

To address these challenges, we propose to develop WDM coherent communication technologies based on fully chip-based, power-efficient microcombs. We will use our recently developed self-injection locking technology, which enables coherent microcomb generation by laser-diode pumping, without relying on any bulky equipment or auxiliary electronics. Moreover, to further improve energy efficiency, we will leverage the highly coherent nature of comb lines to remove all the coherent DSP consumption. This combination will lead to a 100 Tb/s-capacity, energy-efficient communication system, as shown in Fig.1A.

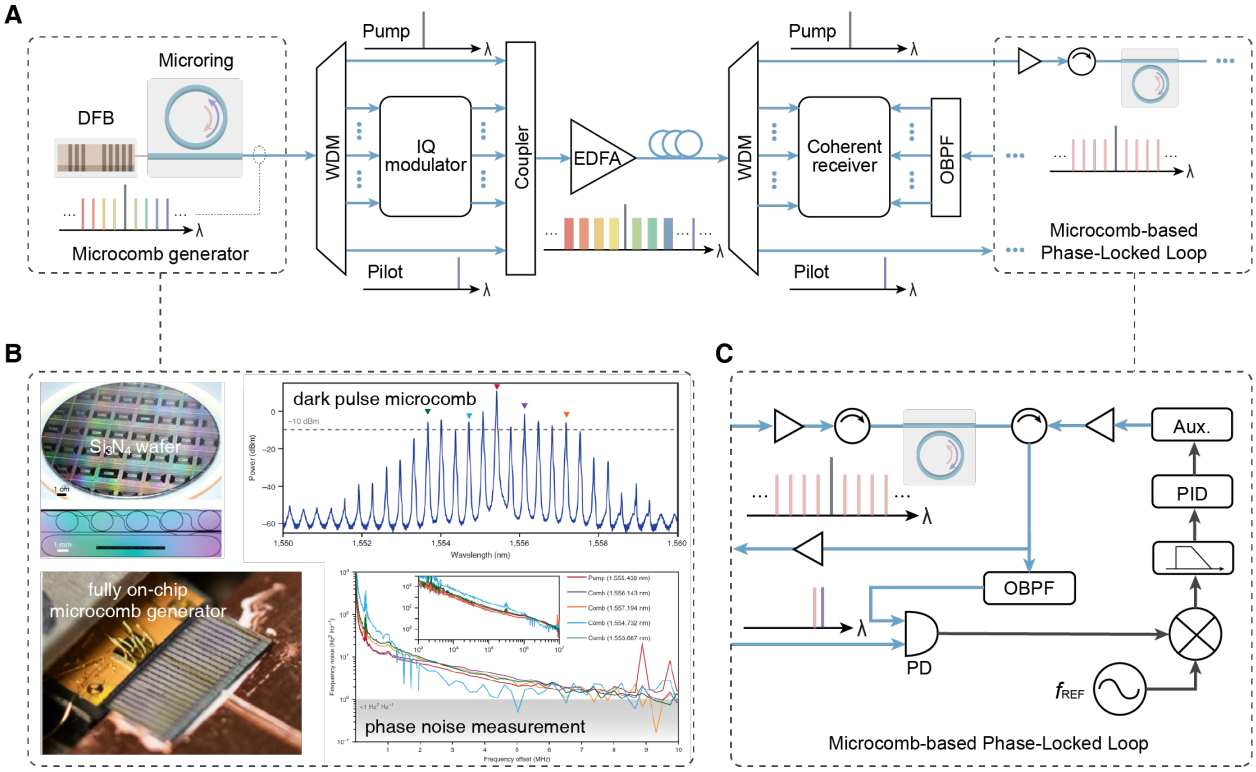

Fig. 1 (A) Proposed microcomb-based, power-efficient coherent communication link; (B) Fully on-chip, energy-efficient coherent microcomb generation based on wafer-scale CMOS Si_3N_4 production; (C) Microcomb-based phase locked loop for reducing DSP consumption.

Outline of tasks

This project comprises two main tasks: At the device level, we will develop a fully chip-based microcomb generator that has a **near-unity nonlinear conversion efficiency** and flat envelope; At the system level, we will construct a new microcomb-based coherent communication link with high capacity much higher than those of any integrated photonic link so far. The high coherence of the microcomb will lead to **no wavelength control** and **nearly no coherent DSP consumption** for the system, significantly improving the energy efficiency. A detailed description is given below:

1.Fully chip-based, power-efficient microcomb generation

To achieve an operationally simple, fully chip-based microcomb, there are two challenges to overcome: the complexity of tuning schemes and feedback loops used in conventional microcomb pumping setups, and the high-power requirement for the pump laser. In this work, we will address this problem by using an ultra-high-Q microresonator and applying the self-injection locking strategy for microcomb generation (Fig.1B) based on the technologies recently developed by our team.

Microresonators with ultra-high Q are based on a wafer-scale, CMOS foundry fabrication process for Si_3N_4 [9]. The thickness of Si_3N_4 will be selected to achieve the balance between high Q and dispersion engineering flexibility for broad-band comb generation. In fabrication, advanced lithography and etching have been well developed, ensuring low scattering loss from the sidewall of waveguides. The Si_3N_4 is deposited by low pressure chemical vapor deposition (LPCVD) and later treated by high temperature annealing to outgas the N-H for absorption reduction. Combining these strategies, we have demonstrated a Q factor of microresonator beyond 2.6×10^8, which is one of the highest numbers achieved in integrated photonics. Such high Q characteristic dramatically relieves the pump power requirement: for a 30 GHz microcomb, the power to generate a coherent comb is below 20 mW, a level well within the capabilities of commercial distributed feedback (DFB) lasers.

To get rid of the complex control/feedback procedures for microcomb generation, we will adopt the self-injection locking scheme here[10]. The laser diode will be directly coupled to the microresoantor without an isolator in between. Under the reflection from the high Q resonator induced by Rayleigh scattering, the pump laser can be locked to the resonance of the cavities automatically when the laser frequency and the resonance mode are within a certain bandwidth. This mechanism enables the direct generation of coherent microcomb by simply powering the laser on, making it a turnkey operation. Moreover, the self-injection locking scheme significantly reduces the linewidth of the pump laser, whose coherence can be transferred to all comb lines. Through the ultra-high-Q resonator, we have successfully achieved Hertz-level linewidth for all comb lines, surpassing the performance of commercial bench-top narrow linewidth lasers.

Another critical challenge to overcome is conversion efficiency. In this project, instead of using well-studied bright solitons, we will explore the generation of a dark pulse state. Since the dark pulse is operated at the blue detuning side of the resonance of the cavity, it can support more effective pump coupling and therefore higher conversion efficiencies. Through proper dispersion engineering by tailoring the geometry, the generated comb spectrum can have a flat plateau covering the tens of nm range, which is suitable for WDM purposes by eliminating the spectrum shaping filters.

2.High-capacity, power-efficient coherent communication link

The self-injection locked microcomb source provides hundreds of comb lines for a WDM communication link, while the high coherence of each comb line allows for higher order

modulation formats compared with widely used DFB laser. Since the spacing between comb lines is equal, microcomb gains a significant advantage in massive parallelization without wavelength control, leading to considerable power saving than the DFB arrays. The stable repetition frequency between comb lines also enables a smaller guard band, further improving the efficiency of spectrum utilization. Furthermore, the constant phase relation among comb lines provides the opportunity to significantly reduce the DSP resources, which previously was a power-intensive part in communication links.

Fig. 1A shows the architecture of our system, we employ a WDM to separate comb lines into different channels as hundreds of carriers, which are further encoded by different IQ modulators. A WDM coupler combines these modulated signals with an uncoded pump laser signal and a pilot tone. All of them are transmitted to the receiver through fiber. By leveraging the phase stability and coherence among different wavelengths, we can achieve significant power savings in DSP while maintaining a high-order coherent modulation format, without incurring any noticeable increase in bit error rate.

At the receiver, we clone a microcomb as the local oscillator (Fig.1C): the conveyed pump signal is amplified through a low-noise Erbium-doped Fiber Amplifier (EDFA) to generate a dark pulse in the receiver microresonator, which may have a slightly different soliton repetition rate compared with the transmit microresonator. The transmitted pilot comb line and the corresponding mode index comb line from the receiver resonator are filtered out and directed to a fast photodiode to be phase-locked using an optical phase-lock loop (OPLL). The resulting error signal is sent back to the auxiliary laser, allowing for feedback control of the laser power. Consequently, this process synchronizes both the pump laser wavelength and the repetition rate. All symbols are decoded by beating different comb lines with corresponding data channels.

By utilizing coherence-cloned microcombs to generate local oscillator (LO) lasers, we eliminate the need for frequency offset estimation in the digital signal processing (DSP) process, as the optical phase-lock loop (OPLL) provides a reliable reference clock. Additionally, all cloned microcombs maintain low phase noise characteristics, simplifying carrier phase estimation in each individual channel. By capitalizing on the coherence among microcombs, we can minimize the carrier phase estimation to only one channel, benefiting all carriers collectively. This strategy will save most of the DSP consumption for coherent communication.

Outcome

This project is expected to have the following outcomes:

At the device level, we will achieve fully on-chip, energy-efficient microcomb generation. The expected pump-to-optical conversion efficiency will be **higher than 80%**. The generated spectrum of the comb will cover the **C+L+S band**, leading to more than 100 nm span and more than 150 comb lines.

At the system level, we will achieve a communication link with more than 150 channels, and the single channel rate is more than 700 Gb/s. The expected aggregate rate will reach **100 Tb/s**. There will be **no wavelength control** required for the link. The coherent DSP consumption will be **99% smaller** compared with those of coherent links using DFB arrays. The energy-efficiency will be **better than 1 pJ/bit**.

Impact

This project will lead to a profound impact on future communication technologies. It will bring microcomb to wide deployment for practical use in communications and thus revolutionize the existing WDM architectures. By significantly improving the channel numbers and reducing the DSP power consumption, this strategy will pave the way for high-capacity, energy-efficient communications in future telecom and data-centers.

[1] R. Nagarajan et al., "InP Photonic Integrated Circuits," in IEEE Journal of Selected Topics in Quantum Electronics, vol. 16, no. 5, pp. 1113-1125, Sept.-Oct. 2010, doi: 10.1109/JSTQE.2009.2037828.

[2] M. Yoshida, T. Kan, K. Kasai, T. Hirooka, K. Iwatsuki and M. Nakazawa, "10 Channel WDM 80 Gbit/s/ch, 256 QAM Bi-Directional Coherent Transmission for a High Capacity Next-Generation Mobile Fronthaul," in Journal of Lightwave Technology, vol. 39, no. 5, pp. 1289-1295, 1 March1, 2021, doi: 10.1109/JLT.2020.3034417.

[3] Chang, L., Liu, S. & Bowers, J.E. Integrated optical frequency comb technologies. Nat. Photon. 16, 95–108 (2022). https://doi.org/10.1038/s41566-021-00945-1

[4] Pfeifle, J., Brasch, V., Lauermann, M. et al. Coherent terabit communications with microresonator Kerr frequency combs. Nature Photon 8, 375–380 (2014). https://doi.org/10.1038/nphoton.2014.57

[5] Marin-Palomo, P., Kemal, J., Karpov, M. et al. Microresonator-based solitons for massively parallel coherent optical communications. Nature 546, 274–279 (2017). https://doi.org/10.1038/nature22387

[6] Corcoran, B., Tan, M., Xu, X. et al. Ultra-dense optical data transmission over standard fibre with a single chip source. Nat Commun 11, 2568 (2020). https://doi.org/10.1038/s41467-020-16265-x

[7] Geng, Y., Zhou, H., Han, X. et al. Coherent optical communications using coherence-cloned Kerr soliton microcombs. Nat Commun 13, 1070 (2022). https://doi.org/10.1038/s41467-022-28712-y

[8] Shu, H., Chang, L., Tao, Y. et al. Microcomb-driven silicon photonic systems. Nature 605, 457–463 (2022). https://doi.org/10.1038/s41586-022-04579-3

[9] Jin, W., Yang, QF., Chang, L. et al. Hertz-linewidth semiconductor lasers using CMOS-ready ultra-high-Q microresonators. Nat. Photonics 15, 346–353 (2021). https://doi.org/10.1038/s41566-021-00761-7

[10] Shen, B., Chang, L., Liu, J. et al. Integrated turnkey soliton microcombs. Nature 582, 365–369 (2020). https://doi.org/10.1038/s41586-020-2358-x

Executive Summary

Title of the proposal: Ultrafast Logic Gates and High-Density Information Coding: a Disruptive Platform for Lightwave Electronics
Category: Information

Introduction: Modern electronic devices, such as diodes and transistors, are the cornerstone of our digital life. These devices operate based on the collective movement of electrons, which can be turned "on" and "off" at a frequency measured in gigahertz (10^9 Hz, i.e. 10^-9 second). This speed dictates the information processing capabilities of devices like computers and cell phones. For example, gigahertz is also a commonly used unit to describe the speed of computers central processing units (CPUs). As a general rule, the higher the processing units speed, the higher the performance of the computer.

In the past decades, research in terahertz (10^{12}) electronic and hybrid electronic-photonic systems has flourished. Despite these advancements, researchers remain undeterred to launch their footsteps toward the higher level— petahertz (10^{15} Hz, PHz), corresponding to the electron dynamics at the sub-femtosecond timescale.

Challenge: Lightwave electronics offer a way to study sub-femtosecond electron dynamics but face three main challenges. First, they require either bulk dielectric materials (i.e. mm scale) or complex nanostructures. Second, they depend on intricate optical setups, such as carrier-envelope phase manipulation or timing delays between laser pulses, making integrating with tabletop photonic devices difficult. Third, it is easy to "switch on" in the femtosecond scale to a new electronic state whereas the "switch off" takes picoseconds at resonant conditions. Even if the femtosecond on/off switch can be realized, the signal processing is limited by the repetition rate of the electronic or optical device.

Objective: I intend to develop a theoretical framework and establish proof-of-concept experiments for an all-optical controlled tabletop processor, which will extend the information coding capacity to the next level and realize ultrafast chirality logic gates via the following two objectives:

Objective 1 (enhancing information coding capacity via the high-harmonic generation): I will achieve an optical transistor with higher information coding capacity through the high harmonic generation process. Each frequency line in the harmonic spectrum acts as a signal pixel, diverging from conventional transistors where only one digital signal is decoded within a signal repetition rate.

Objective 2 (ultrafast chirality logic gate): I will capitalize on chirality to develop an ultrafast logic gate. Leveraging the angular momentum carried by incident light, the emitted nonlinear spectrum contains information on both incidence light and material chirality. By adhering to momentum and energy conservation, certain harmonic orders are prohibited. This prohibited emission serves as the "off"/"0" state, while emissions allowed by conservation laws represent the "on"/"1" state.

Outcome: The proposed scheme has three major advantages. First, since the concept is all-optical-controlled, the emitted signal only lasts as long as the driving pulse duration i.e. femtosecond, leading to immediate "on" and "off" states. Second, the emitted harmonic spectrum lines supply more than 1 bit (bit number is equal to the number of harmonics) per pulse, extending the information coding capacity to a new level. Lastly, the scheme proposed utilizes planar structures and a simple driving pulse, freeing the implementation from complicated driving pulse shape manipulation.

The proposed project is dedicated to advancing open science. Consequently, all numerical packages created will be openly shared with user guides, on open platforms such as GitHub. Manuscripts will be uploaded on ArXiv. I believe these efforts will boost the related research in the scientific community, foster early engagement with frontier scientific research among young students, and ignite their passion for science at an early age. These will have a far-reaching impact beyond the Optica Foundation Challenge program duration.

Ultrafast Logic Gates and High-Density Information Coding: a Disruptive Platform for Lightwave Electronics

1 Literature Review

Research aim: Using 2D Weyl semimetals to enable ultrafast chiral logic gate and revolutionize information processing to petahertz level.

Modern electronic devices, such as diodes and transistors, are the foundation of our daily digital life. These devices operate based on the collective movement of electrons, which can be turned on and off at a frequency measured in gigahertz (10^9 Hz) [1, 2]. For example, gigahertz is also a commonly used unit to describe the speed of computers' central processing units. As a general rule, the higher the processing units' speed the higher the computer's performance. In the past decades, research in terahertz (10^{12} Hz) electronics and hybrid electronic-photonic systems have flourished [3]. Recently, first step has been taken to advance optoelectronics to the PHz (10^{15} Hz, PHz) realm.

Lightwave electronics, as a relatively young field, opens a door for probing attosecond electron dynamics without involving attosecond pulses. Generally, near-infrared pulses with the carrier wave cycle period ~ 3 fs are used as the driving fields. In the interaction process, the subwave cycle (i.e., subfemtosecond optically controlled gate) ionizes the electron around the peak of the field. Depending on the relative emission time of the electron compared to the peak of the electric field (hundred attoseconds sooner/later than the peak), the electron can gain/lose energy, which realizes attosecond control of the electron dynamics and the resulting nonlinear emission [4].

Lightwave electronics enable the unique possibility to explore quantum solid-state properties, topological phase, and quantum coherence, which are beyond the reach of todays conventional electronics [5, 6]. In addition, it paves the way toward real-life applications, such as ultrafast optoelectronics in signal processing [7, 8, 9, 10, 11], enhancing solar-cell energy capturing efficiency [12], and advancing high-resolution spectroscopy [13]. In particular, **the state-of-the-art of lightwave electronics for signal processing are:**
— In the past decades, ultrafast optical switches have been realized via various methods such as photonic crystal, nanocavities, and plasmonics [14].
— In 2014, Li et. al. proposed a graphene modulator with ∼ps response time [15].
— Later on in 2019, an ultrafast optical switch at ∼30 femtosecond, was realized using ∼1mm thick GaP film [16].
— Recently in 2023, using Lithium Niobate, Guo et. al. achieved ∼2.6 pJ output pulse energy with a wide range of tunability of the frequency comb via the carrier-envelope-offset control, enabling ultrafast photonics and data communication [17].

All of the aforementioned results have achieved ultrafast optoelectronics. However, these achievements necessitate either bulk dielectric materials (i.e. mm scale) or complicated nanostructure. Moreover, it is easy to "switch on" in the femtosecond scale to a new electronic state whereas the "switch off" takes picoseconds for resonant excitation owing to the nature of phonon relaxation [18, 19]. Even if the switch on/off can be realized at the femtosecond scale, the signal processing bottleneck shifts to the repetition rate of electronic or optical devices (see Fig. 1a). Furthermore, achieving femtosecond control necessitates intricate optical configurations, involving the manipulation of either the carrier-envelope phase or the timing delay between two laser pulses. In addition, most existing research focuses on the electronic current generated via the femtosecond pulse, while little use has been made of the chiral material response. I will leverage the high-harmonic generation process to realize an all-optical controlled compact processor.

2 Problem Statement/Objective

My proposal is related to the following ideas about signal processing [8, 9, 10, 11]. The theoretical concept will be developed in Prof. Brabec's group at the University of Ottawa. The experimental implementation will be realized in Prof. Vampa's group, at the National Research Council Ottawa. Here, I intend to extend the information coding capacity to the next level and to realize ultrafast chirality logic gates using 2D Weyl semimetals (WSMs). In particular, the proposed research ambition will be achieved via the following two objectives:

Objective 1 (enhancing information coding capacity via the high-harmonic generation):

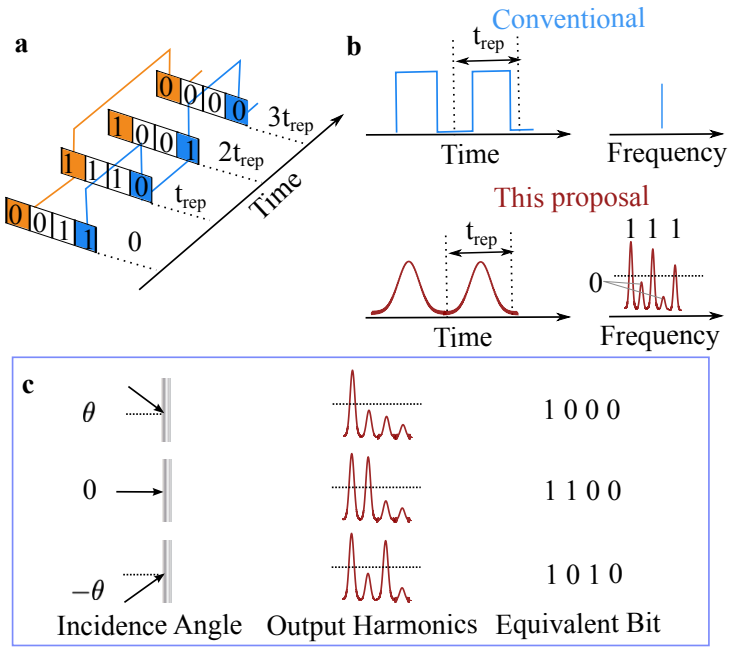

Figure 1: The illustration of objective 1 is presented in panel **a**, where the signal processing inside a computer is shown. The repetition rate is denoted by t_{rep}. Panel **b** compares conventional signal processing and the proposed scheme. Data encoding examples are shown in panel **c**.

In this objective, I aim to increase the information coding capacity through the high-harmonic generation process. Specifically, I am working towards realizing an **optical transistor**. A conventional transistor amplifies or switches electrical signals [20]. The switch functionality registers a 0/1 signal by an off/on state triggered by the voltage. Instead of the electronic signal, the optical transistor is triggered by femtosecond optical signals. In this objective, each harmonic spectral line serves as an information bit. As a result, the number of harmonics determined the number of possible bits per pulse. This contrasts conventional schemes where one digital signal is transferred within the signal pulse in a repetition rate window. Leveraging harmonic spectra can substantially amplify information processing capacity (see Fig. 1**b**). Thus improving the limit set by at best GHz optical repetition rates.

Furthermore, this endeavor seeks to simplify the signal modification processes. In previous work, the lightwave electronic dynamics are controlled by electric field waveform either obtained via fine-tuning the carrier-envelope phase of the driving pulse or implementing the multi-color configuration (combining different frequencies of the driving pulse) [21, 22, 23].

However, this proposal circumvents direct manipulation of the incident electric field waveform. Instead, by choosing the angle of incidence, the electric fields transmitted into the WSM are modified, i.e. the WSM experiences different trigger signals [24](applicant's work). In addition, WSM heterostructures can be leveraged for designing the harmonic spectrum responses [25](applicant's work). Consequently, the resulting harmonic spectra are modified (Fig.1**c**). As a result, **by removing all the direct operations on the driving pulse, I aim to achieve a compact, femtosecond, all-optical controlled high-density information coding scheme.**

Objective 2 (ultrafast chirality logic gate):

This objective capitalizes on chirality to develop **ultrafast logic gate** [11]. In Fig. 2, the XNOR logic gate is shown as an example. Other types of logic gates could be realized via the same principles [8, 9, 10]. Leveraging the angular momentum carried by incident light, the emitted

nonlinear spectrum contains information on both incidence light and material chirality. By adhering to momentum and energy conservation, certain harmonic orders are prohibited. As shown in Fig. 2, when input driving fields exhibit opposite chirality e.g., one left circularly polarized and the other right circularly polarized the output is prohibited [11, 26]. This prohibition serves as the "off"/"0" state, while emissions allowed by conservation laws represent the "on"/"1" state.

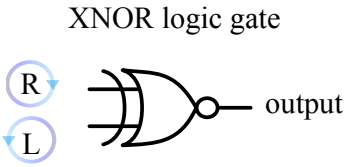

Input		output
R	R	1
L	L	1
R	L	0
L	R	0

Figure 2: A XNOR logic gate is shown as an example. "R" and "L" represent right- and left-hand side polarization, respectively.

My proposal hinges on two properties of Weyl semimetals (WSMs): the extreme nonlinearity and the chiral response. (i) Extreme nonlinearity: 2D WSMs belong to a class of newly discovered quantum materials. Generally, WSMs exhibit remarkable nonlinearity, often exceeding conventional materials by order of magnitude [27, 28] [29](applicant's work), attributed to their exceptionally high electron mobility ($\sim 10^6$m/s) [30]. This facilitates access to electron nonlinear responses even at moderate electric field strengths. Several 2D WSMs have been experimentally discovered such as WTe_2 Cr_2C, VI_3, $PtCl_3$, and $NbIrTe_4$ monolayers [31, 32, 33], which are ready to be explored and implemented. Specifically, Objective 1 can be achieved via 2D WSM heterostructures. With careful design of the photonic structure, such as adjusting the separation between layers or employing diverse materials in combination, one can observe distinct responses across various frequency ranges, i.e. different harmonics orders. Since the entire structure forms different boundary conditions, leading to markedly different optical responses [25, 34](applicant's work).

(ii) Chiral response: for WSM to exist, it is necessary to break either spatial inversion symmetry, time-reversal symmetry, or both. In momentum space, the points where valence and conduction bands cross are Weyl nodes, around which electrons behave as massless fermions [35]. Weyl nodes appear in pairs with opposite chirality. In Fig. 3 zoomed-in panel, one pair of Weyl nodes separated by 2**b** in the momentum space is shown. When the Weyl nodes with opposite chirality merge i.e. nodes separation $\mathbf{b} = \mathbf{0}$, the chirality at two nodes cancels out. In this situation, two Weyl nodes reduce to Dirac nodes, and the material behaves as graphene [36]. Owing to momentum conservation, optical transitions induced by right-handed circularly polarized photons with angular momentum $+1$ are permissible on one of the Weyl nodes but prohibited on the other depending on the chirality of the Weyl fermions [37, 38, 39, 40]. These properties enable allowed and prohibited harmonic emissions, serving as the foundation of the harmonic spectrum manipulation and logic gate for the abovementioned objectives.

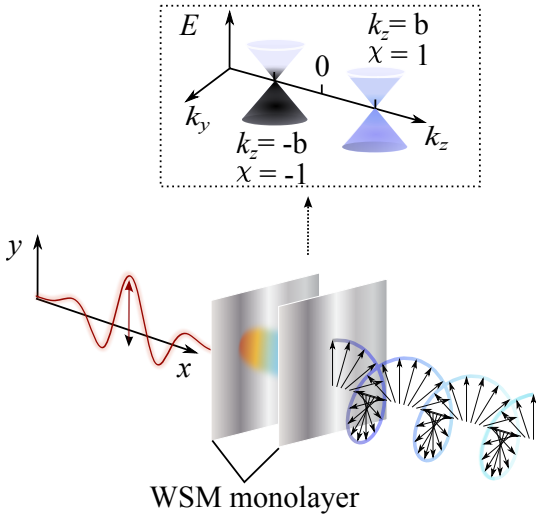

Figure 3: Illustration of the proposed 2D Weyl semimetal heterostructure. The zoomed-in panel indicates one pair of Weyl nodes separated by 2**b** along k_z in the momentum space.

As a result, there are three major advantages of the proposed 2D WSM scheme. Firstly, since the proposed concept is all-optical-controlled, the emitted signal only lasts as long as the driving pulse duration i.e. femtosecond [41], leading to an immediate "on" and "off" states. Secondly, the emitted harmonic spectrum lines supply more than 1 bit (bit number is equal to the number of harmonics) per pulse, extending the information coding capacity to a new level.

Lastly, the scheme proposed utilizes planar structures and a simple driving pulse. It does not require complicated driving pulse shape manipulation, freeing the implementation from the two-color or carrier-envolope manipulation of the driving pulse. Thus, some of the weaknesses of ultrafast optoelectronic schemes, discussed in the introduction, are being addressed.

3 Outcome

An optical computer consists of 3 components i.e. optical processor, optical data transfer, and optical storage. This proposal aims to tackle the aspect of optical processors using the high-harmonic generation process. The data transfer can be achieved by optical fibers [42]. The harmonic spectra can be analyzed by the 2D Fourier optical co-process [43], where the signal is measured using a conventional CMOS or CCD image sensor. The concept of optical processors rests on several new ideas: (i) simple manipulation, and (ii) spectral control. This proposal aims to establish the theoretical framework for optical processors and to experimentally demonstrate a proof-of-concept harmonic processor.

Methods for simple manipulation: I will utilize the unique material properties of the WSMs i.e. intrinsic time-reversal symmetry or inversion symmetry breaking, where the optical responses of the WSMs to photons with $+\mathbf{k}$ and $-\mathbf{k}$ momenta are not the same [24, 34] (applicant's work). In other words, the transmission coefficients from air to the material change based on both the polarization direction and the angle of incidence. By adjusting the angle of incidence, one can transition between circular, elliptical, and linear polarization states. [24] (applicant's work). As a result, the entire waveform modification can be replaced by incidence angle modification, resulting in far easier manipulation compared to conventional carrier-envelope or multi-color control. Specifically, the electric field manipulation is achieved via the first-order response of the material. The analyses are based on the transfer matrix method [44, 45] [24, 34] (applicant's work).

Milestones: The outcome of this method is the semi-analytical model for electric field waveform manipulation, which serves as the initial condition for nonlinear light-matter interaction. This will largely reduce the computational cost, and give design guidelines to experiments for the optimal electric field format of a given heterostructure.

Methods for harmonic spectral control: The electronic dynamics and the emitted electric field dynamics must be taken into account interactively. The incident pulse induced electronic motions inside the WSMs are described via the tight-binding model [46, 47]. The output of the light-driven electronic dynamics is the nonlinear current, which enters the Maxwell equations as a radiation source.

Milestones: The outcome is a full 3D numerical model of the nonlinear process inside the WSMs heterostructure. It can be used to design the emitted spectrum at a given harmonic order, resulting in the signal bit control.

Numerical methods: The nonlinear current together with the electric field propagation can be solved by finite-difference time-domain method on a Yee grid [48, 49][29, 50, 51, 52] (applicant's work), where the Euler method can be used for the numerical update.

The entire numerical package will be optimized on a high-performance cluster. The host institute has access to high-performance computing centers at the Digital Research Alliance of Canada, providing excellent hardware (e.g. CPU Intel Xeon Gold 6248 processor) and access to more than 100 nodes. The data point on each spatial pints x and y can be computed in parallel via OpenMP [29, 50, 51] (applicant's work).

Experimental conditions: We will perform experiments of the proposed idea at the National Research Council Ottawa, which also gives us access to the Joint Centre for Extreme Photonics. Regarding sensibility and precise measurements, the existing lab facilities are capable of single pule and single photon experiments [53, 54]. In terms of strong field physics, extremely high-intensity ($>10^{12}\mathrm{W/cm^2}$) femtosecond lasers are ready to be used for ionization and XUV

attosecond pulses related research [55, 56]. The combined theoretical and experimental efforts from the host groups have already led to various fruitful results in high-harmonic generation [57, 58, 59, 60].

Extended results: The outcomes of the proposed optical transistor and optical logic gate enable the exploration of the time-resolving transient optical response of the 2D WSMs at a sub-femtosecond scale. This will enhance the fundamental understanding of light-matter interaction. The extension of information coding using the harmonic spectral lines can realize extremely high repetition rate signal processing. For example, if we can manipulate 10 harmonic spectral lines, the information capacity extended is $2^{10} = 1024$ times larger. In addition, this all-optical platform takes a forward step towards the single photon device which supports the transformation of information coding from bit to qubit.

4 Impact

Impact on Scientific Community: Modern solid-state electronics use voltage control on a nanosecond time scale (10^{-9}) [2]. This speed dictates the processing capabilities of devices like computers and cell phones. One of the best commercially available processors, AMD EPYC 9654 for example, operates at 2.6GHz [61]. Optical laser at the standard infrared wavelength could reach $\sim$10GHz or even more than 100GHz [17, 62] repetition rate, prompting exploration into faster information processing via all-optical processors. My proposal harnesses material science advancements to pioneer optical transistors and logic gates, envisioning them as the future of information processing. The proposed compact, all-optical-controlled devices leverage light for faster, more efficient processing, potentially surpassing existing logic devices by at least an order of magnitude. The proposed idea introduces additional dimensions for information storage, aligning with quantum optical storage's potential [63].

Impact on Society: The proposed scheme only requires simple planer structures. Thus, it is potentially easy for large-scale manufacturing. It will lead to lower costs, making this innovation accessible to small companies and labs. Since the proposed research opens up new possibilities for future electronics, it may open new job markets, and increase the impact of lightwave electronics.

I strongly support open-access science and am eager to convey that science is fun and accessible to everyone. Thus all numerical packages developed (Output 1.1, Output 2.1 mentioned in Timeline) will be publicly available on the GitHub repository (https://github.com/LuWang-Physics) with instructions/licenses to suggest how others can use them. The data generated will follow the FAIR (Findable, Accessible, Interoperable, Reusable) data principles. The experimental groups can use the numerical packages to guide/verify their experiments. Theoretical groups can extend their research based on the open-source numerical frame developed. The numerical models can be developed with interactive interfaces, which allow non-specialists to benefit from them, fostering early engagement with frontier scientific research among young students and igniting their passion for science. These will have a far-reaching impact beyond the Optica Foundation Challenge program duration.

Impact on Personal Development: Determined to be a professor, obtaining the Optica Foundation Challenge fund will be a milestone in my academic career. The proposed research will help me to form a more comprehensive understanding of light-matter interaction and will undoubtedly shape me into a leader in the field. The fund will support me in proposing possible future directions related to optical information coding, which will enrich the existing studying of lightwave electronics. During the 2-year research, I will acquire the ability for budget management, enhance my communication skills via establishing joint projects with group leaders around the world, and develop a grand vision for science by collaborating with multidisciplinary scientists. These necessary skills will shape me into an independent group leader in the next career step.

References

[1] R. J. Trew, "High-frequency solid-state electronic devices," *IEEE transactions on electron devices*, vol. 52, no. 5, pp. 638–649, 2005.

[2] M. T. Hassan, "Lightwave electronics: Attosecond optical switching," *ACS Photonics*, vol. 11, 2024.

[3] K. Sengupta, T. Nagatsuma, and D. M. Mittleman, "Terahertz integrated electronic and hybrid electronic–photonic systems," *Nature Electronics*, vol. 1, no. 12, pp. 622–635, 2018.

[4] E. Goulielmakis, V. S. Yakovlev, A. L. Cavalieri, M. Uiberacker, V. Pervak, A. Apolonski, R. Kienberger, U. Kleineberg, and F. Krausz, "Attosecond control and measurement: lightwave electronics," *Science*, vol. 317, no. 5839, pp. 769–775, 2007.

[5] F. Krausz and M. I. Stockman, "Attosecond metrology: from electron capture to future signal processing," *Nature Photonics*, vol. 8, no. 3, pp. 205–213, 2014.

[6] S. Y. Kruchinin, F. Krausz, and V. S. Yakovlev, "Colloquium: Strong-field phenomena in periodic systems," *Reviews of Modern Physics*, vol. 90, no. 2, p. 021002, 2018.

[7] F. Bonaccorso, Z. Sun, T. Hasan, and A. Ferrari, "Graphene photonics and optoelectronics," *Nature photonics*, vol. 4, no. 9, pp. 611–622, 2010.

[8] N. Saito, P. Xia, F. Lu, T. Kanai, J. Itatani, and N. Ishii, "Observation of selection rules for circularly polarized fields in high-harmonic generation from a crystalline solid," *Optica*, vol. 4, no. 11, pp. 1333–1336, 2017.

[9] F. Langer, M. Hohenleutner, U. Huttner, S. W. Koch, M. Kira, and R. Huber, "Symmetry-controlled temporal structure of high-harmonic carrier fields from a bulk crystal," *Nature photonics*, vol. 11, no. 4, pp. 227–231, 2017.

[10] N. Rana, M. Mrudul, and G. Dixit, "Generation of circularly polarized high harmonics with identical helicity in two-dimensional materials," *Physical Review Applied*, vol. 18, no. 6, p. 064049, 2022.

[11] Y. Zhang, Y. Wang, Y. Dai, X. Bai, X. Hu, L. Du, H. Hu, X. Yang, D. Li, Q. Dai *et al.*, "Chirality logic gates," *Science Advances*, vol. 8, no. 49, p. eabq8246, 2022.

[12] C. S. Ponseca Jr, P. Chabera, J. Uhlig, P. Persson, and V. Sundstrom, "Ultrafast electron dynamics in solar energy conversion," *Chemical reviews*, vol. 117, no. 16, pp. 10 940–11 024, 2017.

[13] D. A. Zimin, V. S. Yakovlev, and N. Karpowicz, "Ultra-broadband all-optical sampling of optical waveforms," *Science Advances*, vol. 8, no. 51, p. eade1029, 2022.

[14] Z. Chai, X. Hu, F. Wang, X. Niu, J. Xie, and Q. Gong, "Ultrafast all-optical switching," *Advanced Optical Materials*, vol. 5, no. 7, p. 1600665, 2017.

[15] W. Li, B. Chen, C. Meng, W. Fang, Y. Xiao, X. Li, Z. Hu, Y. Xu, L. Tong, H. Wang *et al.*, "Ultrafast all-optical graphene modulator," *Nano letters*, vol. 14, no. 2, pp. 955–959, 2014.

[16] G. Grinblat, M. P. Nielsen, P. Dichtl, Y. Li, R. F. Oulton, and S. A. Maier, "Ultrafast sub–30-fs all-optical switching based on gallium phosphide," *Science advances*, vol. 5, no. 6, p. eaaw3262, 2019.

[17] Q. Guo, B. K. Gutierrez, R. Sekine, R. M. Gray, J. A. Williams, L. Ledezma, L. Costa, A. Roy, S. Zhou, M. Liu *et al.*, "Ultrafast mode-locked laser in nanophotonic lithium niobate," *Science*, vol. 382, no. 6671, pp. 708–713, 2023.

[18] M. Caputo, L. Khalil, E. Papalazarou, N. Nilforoushan, L. Perfetti, A. Taleb-Ibrahimi, Q. Gibson, R. J. Cava, and M. Marsi, "Dynamics of out-of-equilibrium electron and hole pockets in the type-ii weyl semimetal candidate wte 2," *Physical Review B*, vol. 97, no. 11, p. 115115, 2018.

[19] G. B. Osterhoudt, Y. Wang, C. A. Garcia, V. M. Plisson, J. Gooth, C. Felser, P. Narang, and K. S. Burch, "Evidence for dominant phonon-electron scattering in weyl semimetal wp 2," *Physical Review X*, vol. 11, no. 1, p. 011017, 2021.

[20] M. Andreev, S. Seo, K.-S. Jung, and J.-H. Park, "Looking beyond 0 and 1: principles and technology of multi-valued logic devices," *Advanced Materials*, vol. 34, no. 51, p. 2108830, 2022.

[21] C. Heide, T. Eckstein, T. Boolakee, C. Gerner, H. B. Weber, I. Franco, and P. Hommelhoff, "Electronic coherence and coherent dephasing in the optical control of electrons in graphene," *Nano Letters*, vol. 21, no. 22, pp. 9403–9409, 2021.

[22] C. Heide, T. Boolakee, T. Eckstein, and P. Hommelhoff, "Optical current generation in graphene: Cep control vs. ω+ 2ω control," *Nanophotonics*, vol. 10, no. 14, pp. 3701–3707, 2021.

[23] T. Higuchi, C. Heide, K. Ullmann, H. B. Weber, and P. Hommelhoff, "Light-field-driven currents in graphene," *Nature*, vol. 550, no. 7675, pp. 224–228, 2017.

[24] L. Wang, "Nonreciprocal electromagnetic wave manipulation via a single reflection," *Advanced Photonics Research*, vol. 4, no. 12, p. 2300194, 2023.

[25] L. Wang, M. F. Ciappina, T. Brabec, and X. Liu, "Table-top tunable chiral photonic emitter," *arXiv preprint arXiv:2402.02715*, 2024.

[26] O. Kfir, P. Grychtol, E. Turgut, R. Knut, D. Zusin, D. Popmintchev, T. Popmintchev, H. Nembach, J. M. Shaw, A. Fleischer *et al.*, "Generation of bright phase-matched circularly-polarized extreme ultraviolet high harmonics," *Nature Photonics*, vol. 9, no. 2, pp. 99–105, 2015.

[27] L. Wu, S. Patankar, T. Morimoto, N. L. Nair, E. Thewalt, A. Little, J. G. Analytis, J. E. Moore, and J. Orenstein, "Giant anisotropic nonlinear optical response in transition metal monopnictide weyl semimetals," *Nature Physics*, vol. 13, no. 4, pp. 350–355, 2017.

[28] S. Patankar, L. Wu, B. Lu, M. Rai, J. D. Tran, T. Morimoto, D. E. Parker, A. G. Grushin, N. Nair, J. Analytis *et al.*, "Resonance-enhanced optical nonlinearity in the weyl semimetal taas," *Physical Review B*, vol. 98, no. 16, p. 165113, 2018.

[29] L. Wang, J. Lim, and L. J. Wong, "Highly efficient terahertz generation using 3d dirac semimetals," *Laser & Photonics Reviews*, vol. 16, no. 10, p. 2100279, 2022.

[30] C. Shekhar, A. K. Nayak, Y. Sun, M. Schmidt, M. Nicklas, I. Leermakers, U. Zeitler, Y. Skourski, J. Wosnitza, Z. Liu *et al.*, "Extremely large magnetoresistance and ultrahigh mobility in the topological weyl semimetal candidate nbp," *Nature Physics*, vol. 11, no. 8, pp. 645–649, 2015.

[31] Y. Zhang, J. van den Brink, C. Felser, and B. Yan, "Electrically tuneable nonlinear anomalous hall effect in two-dimensional transition-metal dichalcogenides wte2 and mote2," *2D Materials*, vol. 5, no. 4, p. 044001, 2018.

[32] W. Meng, X. Zhang, Y. Liu, L. Wang, X. Dai, and G. Liu, "Two-dimensional weyl semimetal with coexisting fully spin-polarized type-i and type-ii weyl points," *Applied Surface Science*, vol. 540, p. 148318, 2021.

[33] J. Zhang, T. Zhang, L. Yan, C. Zhu, W. Shen, C. Hu, H. Lei, H. Luo, D. Zhang, F. Liu *et al.*, "Colossal room-temperature terahertz topological response in type-ii weyl semimetal nbirte4," *Advanced Materials*, vol. 34, no. 42, p. 2204621, 2022.

[34] L. Wang, F. J. G. de Abajo, G. T. Papadakis *et al.*, "Maximal violation of kirchhoff's law in planar heterostructures," *Physical Review Research*, vol. 5, no. 2, p. L022051, 2023.

[35] B. Yan and C. Felser, "Topological materials: Weyl semimetals," *Annual Review of Condensed Matter Physics*, vol. 8, pp. 337–354, 2017.

[36] S. A. Yang, "Dirac and weyl materials: fundamental aspects and some spintronics applications," in *Spin*, vol. 6, no. 02. World Scientific, 2016, p. 1640003.

[37] Q. Ma, S.-Y. Xu, C.-K. Chan, C.-L. Zhang, G. Chang, Y. Lin, W. Xie, T. Palacios, H. Lin, S. Jia *et al.*, "Direct optical detection of weyl fermion chirality in a topological semimetal," *Nature Physics*, vol. 13, no. 9, pp. 842–847, 2017.

[38] N. Yoshikawa, K. Ogawa, Y. Hirai, K. Fujiwara, J. Ikeda, A. Tsukazaki, and R. Shimano,

"Non-volatile chirality switching by all-optical magnetization reversal in ferromagnetic weyl semimetal co3sn2s2," *Communications Physics*, vol. 5, no. 1, p. 328, 2022.

[39] F. Nematollahi, S. A. O. Motlagh, J.-S. Wu, R. Ghimire, V. Apalkov, and M. I. Stockman, "Topological resonance in weyl semimetals in a circularly polarized optical pulse," *Physical Review B*, vol. 102, no. 12, p. 125413, 2020.

[40] Z. Ji, G. Liu, Z. Addison, W. Liu, P. Yu, H. Gao, Z. Liu, A. M. Rappe, C. L. Kane, E. J. Mele *et al.*, "Spatially dispersive circular photogalvanic effect in a weyl semimetal," *Nature materials*, vol. 18, no. 9, pp. 955–962, 2019.

[41] H. Hübener, M. A. Sentef, U. De Giovannini, A. F. Kemper, and A. Rubio, "Creating stable floquet–weyl semimetals by laser-driving of 3d dirac materials," *Nature communications*, vol. 8, no. 1, p. 13940, 2017.

[42] J. Limpert, F. Roser, D. N. Schimpf, E. Seise, T. Eidam, S. Hadrich, J. Rothhardt, C. J. Misas, and A. Tunnermann, "High repetition rate gigawatt peak power fiber laser systems: challenges, design, and experiment," *IEEE Journal of Selected Topics in Quantum Electronics*, vol. 15, no. 1, pp. 159–169, 2009.

[43] A. J. Macfaden, G. S. Gordon, and T. D. Wilkinson, "An optical fourier transform coprocessor with direct phase determination," *Scientific reports*, vol. 7, no. 1, p. 13667, 2017.

[44] T. G. Mackay and A. Lakhtakia, "The transfer-matrix method in electromagnetics and optics," *Synthesis lectures on electromagnetics*, vol. 1, no. 1, pp. 1–126, 2020.

[45] D. W. Berreman, "Optics in stratified and anisotropic media: 4× 4-matrix formulation," *Josa*, vol. 62, no. 4, pp. 502–510, 1972.

[46] R. Chen, C.-Z. Chen, J.-H. Sun, B. Zhou, and D.-H. Xu, "Phase diagrams of weyl semimetals with competing intraorbital and interorbital disorders," *Physical Review B*, vol. 97, no. 23, p. 235109, 2018.

[47] S. Kourtis, J. Li, Z. Wang, A. Yazdani, and B. A. Bernevig, "Universal signatures of fermi arcs in quasiparticle interference on the surface of weyl semimetals," *Physical Review B*, vol. 93, no. 4, p. 041109, 2016.

[48] K. Yee, "Numerical solution of initial boundary value problems involving maxwell's equations in isotropic media," *IEEE Transactions on antennas and propagation*, vol. 14, no. 3, pp. 302–307, 1966.

[49] J. Lim, Y. S. Ang, F. J. G. de Abajo, I. Kaminer, L. K. Ang, and L. J. Wong, "Efficient generation of extreme terahertz harmonics in three-dimensional dirac semimetals," *Physical Review Research*, vol. 2, no. 4, p. 043252, 2020.

[50] L. Wang, T. Kroh, N. H. Matlis, and F. Kärtner, "Full 3d+ 1 modeling of tilted-pulse-front setups for single-cycle terahertz generation," *JOSA B*, vol. 37, no. 4, pp. 1000–1007, 2020.

[51] L. Wang, A. Fallahi, K. Ravi, and F. Kärtner, "High efficiency terahertz generation in a multi-stage system," *Optics express*, vol. 26, no. 23, pp. 29 744–29 768, 2018.

[52] L. Wang, G. Tóth, J. Hebling, and F. Kärtner, "Tilted-pulse-front schemes for terahertz generation," *Laser & Photonics Reviews*, vol. 14, no. 7, p. 2000021, 2020.

[53] N. Couture, M. Lippl, W. Cui, A. Gamouras, N. Y. Joly, and J.-M. Ménard, "Performance analysis of tabletop single-pulse terahertz detection at rates up to 1.1 mhz," *Physical Review Applied*, vol. 21, no. 5, p. 054020, 2024.

[54] D. J. J. Fandio, A. Vishnuradhan, E. K. Yalavarthi, W. Cui, N. Couture, A. Gamouras, and J.-M. Ménard, "Zeptojoule detection of terahertz pulses by parametric frequency upconversion," *Optics Letters*, vol. 49, no. 6, pp. 1556–1559, 2024.

[55] H. Liu, C. Guo, G. Vampa, J. L. Zhang, T. Sarmiento, M. Xiao, P. H. Bucksbaum, J. Vučković, S. Fan, and D. A. Reis, "Enhanced high-harmonic generation from an all-dielectric metasurface," *Nature Physics*, vol. 14, no. 10, pp. 1006–1010, 2018.

[56] M. Sivis, M. Taucer, G. Vampa, K. Johnston, A. Staudte, A. Y. Naumov, D. Villeneuve, C. Ropers, and P. Corkum, "Tailored semiconductors for high-harmonic optoelectronics,"

Science, vol. 357, no. 6348, pp. 303–306, 2017.

[57] Á. Jiménez-Galán, C. Bossaer, G. Ernotte, A. M. Parks, R. E. Silva, D. M. Villeneuve, A. Staudte, T. Brabec, A. Luican-Mayer, and G. Vampa, "Orbital perspective on high-harmonic generation from solids," *Nature Communications*, vol. 14, no. 1, p. 8421, 2023.

[58] G. Vampa and T. Brabec, "Merge of high harmonic generation from gases and solids and its implications for attosecond science," *Journal of Physics B: Atomic, Molecular and Optical Physics*, vol. 50, no. 8, p. 083001, 2017.

[59] G. Vampa, T. Hammond, N. Thiré, B. Schmidt, F. Légaré, C. McDonald, T. Brabec, and P. Corkum, "Linking high harmonics from gases and solids," *Nature*, vol. 522, no. 7557, pp. 462–464, 2015.

[60] G. Vampa, B. Ghamsari, S. Siadat Mousavi, T. Hammond, A. Olivieri, E. Lisicka-Skrek, A. Y. Naumov, D. Villeneuve, A. Staudte, P. Berini *et al.*, "Plasmon-enhanced high-harmonic generation from silicon," *Nature Physics*, vol. 13, no. 7, pp. 659–662, 2017.

[61] A. E. 9654. (2022) Amd epyc 9654. [Online]. Available: https://www.amd.com/en/products/cpu/amd-epyc-9654

[62] M. Mangold, C. A. Zaugg, S. M. Link, M. Golling, B. W. Tilma, and U. Keller, "Pulse repetition rate scaling from 5 to 100 ghz with a high-power semiconductor disk laser," *Optics express*, vol. 22, no. 5, pp. 6099–6107, 2014.

[63] Y. Lei, F. K. Asadi, T. Zhong, A. Kuzmich, C. Simon, and M. Hosseini, "Quantum optical memory for entanglement distribution," *Optica*, vol. 10, no. 11, pp. 1511–1528, 2023.

Agriphotonic Technique for Sustainable Agriculture: Reducing Human Footprint Through Whitefly Pest Management

Author: Luis Miguel Gomes Abegão, Ph.D. || **Category:** Environment

The use of insecticides and pesticides in crop production can significantly impact environmental pollution. Water pollution, soil contamination, non-target species, residue accumulation, and resistance development are examples of the human footprint consequences of controlling crop pests. This real-world issue is among the highest challenges the science community must solve. On one hand, one must provide food for an increasing world population; on the other hand, humanity must drastically decrease its footprint. A solution for this real-world issue is replacing pesticides with novel biocompatible techniques to control crop pests. An agriphotonic technique, based on laser, able to control crop pests without harming the plant's development or affecting non-target species can help tackle this global problem.

Several species of whiteflies are considered pests in agriculture. For example, the whitefly *Bemisia tabaci* (biotype MEAM1) is one of the most relevant insect pests of crops worldwide once it is present in all continents. *Bemisia tabaci* can colonize plants belonging to many plant families and adapt highly to different environments. Moreover, they have a rapid selection of insecticide-resistant populations, which makes them a threat to food security, especially in developing countries.

The main objective of this proposal is to develop a prototype of a future commercial agriphotonic device for pest control. This device will use a novel biocompatible technique based on a laser. Such a technique has already been tested in the laboratory, showing that it is able to achieve 100% mortality of *Bemisia tabaci* without affecting the plant's development [1].

The proposal's objective will be achieved concurrently by conducting a science investigation and technology implementation, as illustrated in Figure 1. The first will focus on how different optical parameters will affect the mortality of whitefly species not yet studied and the plant's development after laser irradiation, and the latter will focus on the prototype development. It is important to emphasize that the strong collaboration between the author's proposal and the Brazilian Agricultural Research Corporation (Embrapa) will trigger a high-level success for the proposed strategy.

In summary, this proposal intends to develop a prototype of a future commercial agriphotonic device, based on a laser, for whitefly pest management. The success of this proposal will be capable of providing a new biocompatible technique for pest control to small- and large-scale farmers, which can decrease environmental pollution by reducing the usage of conventional pesticides. Moreover, if accepted, this proposal will unlock new possibilities and perspectives, paving the way for a new startup company in Agriphotonics.

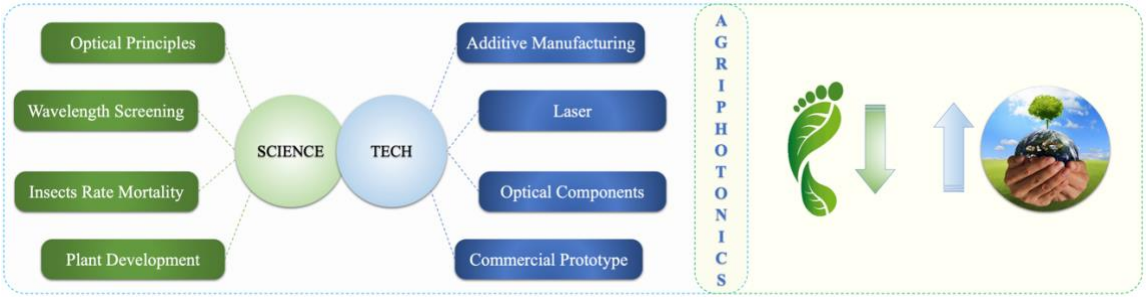

Figure 1. Diagram showcasing the proposal's integration. The left side represents the science and technology elements needed to develop the photonic device prototype. The right side illustrates the proposal's goal, i.e., reducing the human footprint and pursuing a better, more sustainable world using Agriphotonics.

[1] Zaidem, A., Silva, L., Ferreira, A., Carvalho, M., Ragni, M., **Abegão, L.**, & Pinheiro, P. (2023, May). New Biocompatible Technique Based on the Use of a Laser to Control the Whitefly Bemisia tabaci. In *Photonics* (Vol. 10, No. 6, p. 636). MDPI.

PROPOSAL SUBMISSION

Title: Agriphotonic Technique for Sustainable Agriculture: Reducing Human Footprint Through Whitefly Pest Management

Author: Luis Miguel Gomes Abegão, Ph.D.

Category: Environment

---

1. Literature Review

The use of insecticides and pesticides in crop production can significantly impact environmental pollution. Water pollution, soil contamination, residue accumulation, non-target species, and pest resistance development are examples of the human footprint consequences of controlling crop pests, which have been pointed out, discussed, and reported since 1986 [1-7]. The economic impact of using insecticides and pesticides in crop production is also a complex issue with both positive and negative implications. On one hand, the chemicals used are essential for protecting crops from pests and diseases, thereby ensuring higher yields and greater economic returns for farmers. On the other hand, the negative environmental impact is enormous. In fact, pesticides increased agricultural productivity and reduced crop losses in the United States, as reported in 2005 by Pimentel et al. [8]. However, the same study also highlighted the environmental and health costs associated with pesticide use, which can result in additional economic burdens in the long term. Therefore, a balance between maximizing crop productivity and minimizing the negative externalities of pesticide use is crucial for achieving sustainable agricultural practices that consider economic and environmental factors. This real-world issue is among the most significant challenges humanity must solve [9-12], and Optica will have the chance to help significantly with this proposal's approval, which proposes a photonics-based prototype to decrease environmental pollution by reducing the usage of conventional pesticides.

There is a multitude of insect pest species encompassing many insects' orders, such as Acari (Mites), Coleoptera (beetles), Diptera (flies), and Hemiptera (True Bugs). The latter order contains several whitefly species that threaten different types of crops [13-16]. For example, the whitefly *Bemisia tabaci* (biotype MEAM1) [17] is one of the most relevant insect pests of crops worldwide once it is present in all continents, particularly in the Americas [18]. This insect species belongs to the Aleyrodidae family and is known for its ability to infest a wide range of host plants, including many economically important crops. The biotype MEAM1, also known as the "Middle East-Asia Minor 1" or the "*Bemisia B*" biotype, is particularly noteworthy due to its invasiveness and adaptability, making it a significant concern for agricultural systems globally. This whitefly species is known to transmit numerous plant viruses, including begomoviruses, criniviruses, and torradoviruses [19]. These viruses can cause devastating crop diseases, leading to reduced yields and significant economic losses. For example, in the United States, was reported losses of over 200 million dollars yearly in cotton

production caused by this whitefly biotype [20]. Similarly, in the Andes, substantial yield losses and economic damages were caused by *Bemisia tabaci* MEAM1 in yellow potatoes and tomato crops [21]. In Brazil, common bean crops are also strongly affected by *Bemisia tabaci* [22].

Sustainable agriculture urges reducing insecticide applications as a pest control method; therefore, insect control methods based on innovative and clean tools such as electromagnetic (EM) radiation can be a valuable option to reduce the human footprint. Ultraviolet (UV) light is the best-known EM radiation to have lethal effects on most organisms. However, it is well known that UV light is highly damaging to biological systems because it can induce various mutagenic and cytotoxic DNA alterations. For example, in 2014, Dáder et al. showed that UV-B (~280-315 nm) radiation might have lethal effects on plants, so they decided to work with UV-A (~315-400 nm), which is not absorbed by native DNA but can still damage cell constituents, such as lipids, proteins, and even DNA, by increasing the synthesis of reactive oxygen species (ROS). There are few reports with precise data on the effect of EM radiation within the visible (VIS) spectral window on insect mortality. In 2021, Gaetni et al. showed that laser emission in the VIS and IR spectral regions could be a potential biocompatible technique for pest control [23]. And the most recent study (2023) was made by Zaidem et al., demonstrated that a laser emission center at 445 nm can achieve 100% mortality on the 3rd instar nymphs of *Bemisia tabaci* without harming the plants' development [24]. These two particular and recent studies have shown the massive potential of VIS light emitted by a laser to become an agriphotonic technique for sustainable agriculture, with excellent chances to reduce the human footprint.

2. Problem Statement/Objective

As described in the previous section, the problem is that using insecticides and pesticides in crop production can significantly impact environmental pollution. Conventional pest control methods often involve applying chemical substances that can adversely affect the ecosystem. These chemicals can seep into the soil, contaminate water sources, harm non-target organisms, and contribute to the development of pesticide resistance in pests. A sustainable and environmentally friendly alternative to pest control methods is vital to ensure agricultural ecosystems' long-term health and balance.

The main objective of this proposal is to consolidate the feasibility and effectiveness of using laser technology as an alternative approach for pest control in crop production, i.e., as an agriphotonic technique for sustainable agriculture. By employing lasers, it is possible to target specific pests without harming beneficial insects, birds, or other organisms within the ecosystem. This approach aims to minimize environmental collateral damage while effectively managing pest populations. Therefore, the proposal's objective will be achieved concurrently by conducting a science investigation (basic research) and technology implementation (product development), as illustrated in Figure 1. The first will focus on how different optical parameters will affect the mortality of whitefly species not yet studied and the plant's development after laser irradiation, and the latter will focus on the prototype

development, generating a portable photonic prototype to be used in the field. It is important to emphasize that this proposal's author built a simplified bench version (hardware and software) of the photonic prototype version proposed in this project, as depicted in Figure 3 of the published work by Zaidem et al. [24]. The strong collaboration between the author's proposal and the Brazilian Agricultural Research Corporation (Embrapa) will trigger a high-level success for the proposed strategy due to knowledge synergy. Finally, the proposal's project also will focus on advancing scientific and technological knowledge and provides a valuable opportunity to prepare and train undergraduate personnel in optics and photonics.

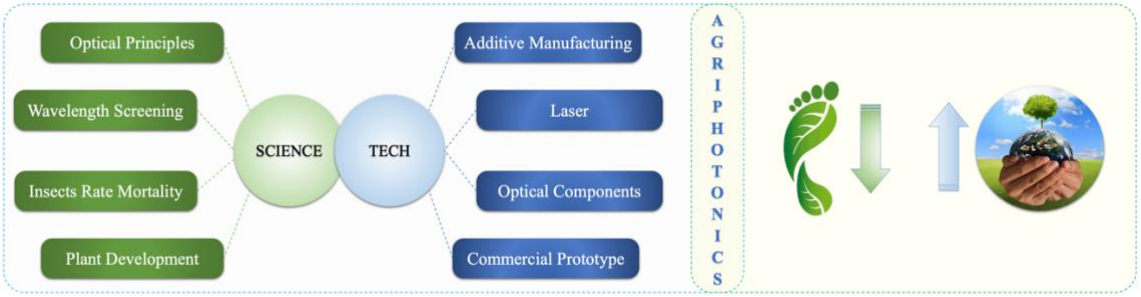

Figure 1. Diagram showcasing the proposal's integration. The left side represents the science and technology elements needed to develop the photonic device prototype. The right side illustrates the proposal's goal, i.e., reducing the human footprint and pursuing a better, more sustainable world using Agriphotonics.

3. Outcome

The primary anticipated outcome of this proposal is the development and commercialization of a photonic-based prototype for pest management, specifically targeting the whitefly species Bemisia tabaci on common bean crops. This prototype will leverage laser technology to achieve effective pest control without harming plant development, reducing reliance on chemical pesticides. Below a simplfied list of key deliverables:

a) A **patented** photonic-based prototype designed for field use;

b) Several **publications** of scientific research in **Optica journals** detailing the findings and technological advancements;

c) Enhanced knowledge and training **opportunities for undergraduate students** involved in the project, fostering a new generation of experts in optics and photonics.

d) **Community outreach** and education through Optica's **Student Chapter**, promoting the Agriphotonics concept in schools and public seminars, raising awareness of sustainable agricultural practices.

4. Impact

By adopting the proposed agriphotonic technique for pest control, we can positively impact the environment and reduce our reliance on harmful chemicals. This approach seeks to foster ecological balance, preserve biodiversity, and safeguard the health of ecosystems. Furthermore, this transformational shift towards a more sustainable and resilient agricultural sector will have far-reaching benefits that extend to farmers, consumers, and the overall well-being of our planet. Therefore, this project is expected to have several profound impacts, such as:

a) **Environmental Impact:** The proposed technology will decrease soil and water contamination, protect non-target species, and mitigate the development of pesticide resistance in pests by reducing the need for chemical pesticides. Such impact will contribute to preserving biodiversity and promoting ecological balance;

b) **Agricultural Impact:** The proposed system, with its low-cost, effective, and user-friendly nature, will be accessible to both small and large-scale farmers. This innovation will not only support sustainable agricultural practices but also potentially increase crop yields, leading to more abundant and affordable food for consumers and reducing losses due to pests, thereby improving farmers' livelihoods;

c) **Economic Impact:** The commercialization of the photonic-based prototype holds the potential to stimulate significant economic growth. It can create new market opportunities and jobs, particularly in the field of Agriphotonics. The development of a startup company based on this technology could drive innovation and economic development in the agricultural sector, contributing to a more robust and sustainable economy;

d) **Educational and Social Impact:** The project will provide significant educational benefits by training students in cutting-edge technologies and engaging the broader community through educational outreach. This will enhance scientific literacy and inspire future innovations in sustainable agriculture.

By achieving these outcomes, the proposal will contribute to a transformational shift towards a more sustainable and resilient agricultural sector, benefiting farmers, consumers, and the overall well-being of the planet.

References

1. Papendick, R.I., L.F. Elliott, and R.B. Dahlgren, *Environmental consequences of modern production agriculture: How can alternative agriculture address these issues and concerns?* American Journal of Alternative Agriculture, 1986. **1**(1): p. 3-10.
2. Holden, P.W. and N.R. Council, *Pesticides and groundwater quality: Issues and problems in four states*. 1986: National Academies Press.
3. Iyaniwura, T.T., *Non-target and environmental hazards of pesticides.* Reviews on environmental health, 1991. **9**(3): p. 161-176.
4. Krieger, R.I., J.H. Ross, and T. Thongsinthusak, *Assessing human exposures to pesticides.* Reviews of environmental contamination and toxicology, 1992: p. 1-15.
5. Edwards, C.A., *The impact of pesticides on the environment*, in *The pesticide question: Environment, economics, and ethics*. 1993, Springer. p. 13-46.
6. Koh, D. and J. Jeyaratnam, *Pesticides hazards in developing countries.* Science of the total environment, 1996. **188**(1): p. S78.
7. van der Werf, H.M., *Assessing the impact of pesticides on the environment.* Agriculture, Ecosystems & Environment, 1996. **60**(2-3): p. 81-96.
8. Pimentel, D., *Environmental and economic costs of the application of pesticides primarily in the United States.* Environment, development and sustainability, 2005. **7**: p. 229-252.
9. Özkara, A., D. Akyıl, and M. Konuk, *Pesticides, environmental pollution, and health*, in *Environmental health risk-hazardous factors to living species*. 2016, IntechOpen.
10. Carvalho, F.P., *Pesticides, environment, and food safety.* Food and energy security, 2017. **6**(2): p. 48-60.
11. AL-Ahmadi, M.S., *Pesticides, anthropogenic activities, and the health of our environment safety*, in *Pesticides-use and misuse and their impact in the environment*. 2019, IntechOpen.
12. Boudh, S. and J.S. Singh, *Pesticide contamination: environmental problems and remediation strategies.* Emerging and eco-friendly approaches for waste management, 2019: p. 245-269.
13. Martin, J., *An identification guide to common whitefly pest species of the world (Homopt Aleyrodidae).* International Journal of Pest Management, 1987. **33**(4): p. 298-322.
14. Morales, F.J., *Tropical whitefly IPM project.* Advances in virus research, 2006. **69**: p. 249-311.
15. Horowitz, A.R., Y. Antignus, and D. Gerling, *Management of Bemisia tabaci whiteflies*, in *The Whitefly, Bemisia tabaci (Homoptera: Aleyrodidae) interaction with geminivirus-infected host plants: Bemisia tabaci, host plants and geminiviruses*. 2011, Springer. p. 293-322.
16. Shah, M.M.R., S. Zhang, and T. Liu, *Whitefly, host plant and parasitoid: A review on their interactions.* Asian Journal of Applied Science and Engineering, 2015. **4**(1): p. 48-61.
17. LIU, S.-s., J. Colvin, and P.J. De Barro, *Species concepts as applied to the whitefly Bemisia tabaci systematics: how many species are there?* Journal of Integrative Agriculture, 2012. **11**(2): p. 176-186.
18. Barbosa, L.d.F., et al., *Indigenous American species of the Bemisia tabaci complex are still widespread in the Americas.* Pest Management Science, 2014. **70**(10): p. 1440-1445.
19. Fiallo-Olivé, E., et al., *Transmission of begomoviruses and other whitefly-borne viruses: Dependence on the vector species.* Phytopathology, 2020. **110**(1): p. 10-17.
20. Naranjo, S.E., *Impacts of Bt transgenic cotton on integrated pest management.* Journal of agricultural and food chemistry, 2011. **59**(11): p. 5842-5851.
21. Rincon, D.F., et al., *Economic injury levels for the potato yellow vein disease and its vector, Trialeurodes vaporariorum (Hemiptera: Aleyrodidae), affecting potato crops in the Andes.* Crop Protection, 2019. **119**: p. 52-58.
22. Inoue-Nagata, A.K., M.F. Lima, and R.L. Gilbertson, *A review of geminivirus diseases in vegetables and other crops in Brazil: current status and approaches for management.* Horticultura Brasileira, 2016. **34**: p. 8-18.
23. Gaetani, R., et al., *Sustainable laser-based technology for insect pest control.* Scientific Reports, 2021. **11**(1): p. 11068.
24. Zaidem, A., et al. *New Biocompatible Technique Based on the Use of a Laser to Control the Whitefly Bemisia tabaci*. in *Photonics*. 2023. MDPI.

Tunable Quantum Meta Networks: towards a new generation of information - **QMetaNet**

QMetaNet propose robust, practical single photon emission and multi photon correlation from devices that can be fabricated at scale and would be readily deployable without the current restrictions on operation temperature, brightness or durability. Practical quantum devices will require fundamental and technological advances to discover new paths for quantum correlations and new ways to manipulate quantum states in matter that eschew cryogenics. Aiming to manipulate entanglement via quantum networks based on meta-arrays of single emitters coupled to nanostructures, supporting extremely high single photon emission rates in the weak coupling regime and achieving strong coupling when plasmonic resonances are coupled with excitons.

Metamaterials are adept at manipulating the amplitude, phase, polarization, frequency and other degrees of freedom of electromagnetic waves in the classical regime, QMetaNet project will investigate metamaterials that could similarly manipulate quantum states: meaning controlling single photon interactions with an array of nanoparticle nodes acting as quantum meta-atoms. Porposing a metasurface array of cavity-coupled single-emitters (nodes) for nonclassical photon generation. Manipulating the spacing between nodes in the array should impact the coupling and coherence of dipole-dipole interactions, adjusting between sub-and super luminal regimes. Ultimately this could lead to new paths for multiphoton correlations in robust, room-temperature technology, advancing the nascent field of quantum networks for information applications.

Measuring the spatiotemporal information of spontaneous emission lifetimes enhancements of single emitters coupled to the nanostructures, opening possibilities for fine control of quantum devices and single-photon sources at nanoscale precision. Use a new metamaterial nanofabrication technique that produces plasmonic 3D hollow truncated nanocones with precise, repeatable features across several cm^2, demonstrating excellent scalability of nanodevices. By combining quantum optics expertise with this novel nanofabrication technique, QMetaNet poised to harness this platform for enhanced photon emission and forge new paths for quantum multi photon correlations. Exploring the tunability of these interactions to switch among different n-photon emission pathways by changing the polarization and angle of incident light, and geometry parameters of the network. Such tunable meta-networks could enable high-fidelity quantum state generation, not achievable in conventional nonlinear crystals and single-emitter fluorescence. The significant designed freedom of these nanostructures enables various tailorable functionalities: 1) Purcell-factor enhancement to shorten emission lifetime for a brighter single photon source 2) strong coupling between exciton and plasmonic modes for enhanced light-matter interaction, and 3) potential meta-networks of quantum nodes made from these nanostructure arrays.

By changing the spacing between nodes in the network QMetaNet project aims to control the coupling and coherence in the dipole-dipole interactions obtaining tunable control of sub- and super-luminal regimes. With long-term goal to investigate experimentally the collective decay dynamics of atoms with a generic multilevel structure coupled to light modes and discover new paths of multiphoton correlations. Studying the interference between different transitions and the resulting entanglement. By measuring changes in decay rates, investigating the super-radiant decay of multilevel meta-atoms in the network.

Tunable Quantum Meta Networks: towards a new generation of information
QMetaNet

Light is a powerful information carrier both at the classical and quantum levels which has led to a wide range of technological developments allowing the controlled manipulation of light emission, absorption and propagation thanks to specifically designed materials. Photons are ideal for carrying quantum information: they can travel long distances with low transmission losses and experience minimal decoherence. Practical quantum devices will require fundamental and technological advances to discover new paths for quantum correlations and new ways to manipulate quantum states in matter that eschew cryogenics. The QMetaNet project aims to manipulate entanglement via quantum networks based on meta-arrays of single emitters coupled to nanostructures, supporting extremely high single photon emission rates in the weak coupling regime and achieving strong coupling when plasmonic resonances are coupled with excitons [1-8].

The manipulation and coherent control of arrays of interacting quantum systems are at the heart of the next generation of quantum science and technologies. Realizations of new correlated states and ways to control qubits will innovation and challenging new approaches for realization of such arrays in quantum networks [2,3] for quantum internet and quantum computer. Entangling the electronic states of coherently interacting emitters is challenging since it requires both a coupling strength larger than the coherence decay rate (implying nanometric distances between the emitters) and quasi-degenerate optical transitions detuned by less than their coupling strength [1]. In the past decades, few works have demonstrated coherent coupling of emitters, and these have mainly been in cryogenic environments. Here I propose a new concept: control coupled emitter networks via metamaterial effects and control the coherent coupling that produces entangled sub- and superradiant states by changing the distance between the nodes in the meta network [9]. Each node will be composed of a “meta-atom” within a unit cell supporting a large density of photonic states and therefore a single photon emission lifetime as low as picoseconds at room temperature, the decay rate will be tailored with metamaterial separation with coupled quantum emitters.

Single photons are a key enabler in emerging quantum technologies including secure quantum communications, quantum computing, quantum internet and new ways to detect very small fields with quantum sensing. Each application has distinct requirements of the generated single photons, but a key parameter to control is the rate of a single-photons, determined by its spontaneous emission lifetime. This spontaneous emission lifetime can be modified by the local photonic density of states in the vicinity of the emitter [1]. Quantum technologies thus rely on better understanding this light-matter interaction in the quantum regime. Reliable tuning of the spontaneous emission of photons is a major milestone towards controlling how quickly and where an excited quantum emitter may release a single photon, as well as the properties of the emitted photon. Metal-based nanophotonic materials make possible nanoscale tuning of electromagnetic fields, accelerating the quantum transitions in atoms, which can in turn give rise to incredibly fast and bright quantum light sources [7]. The strong enhanced plasmonic fields that hollow metal nanostructures have been used in many applications such as sensing, SERS, photo thermal ablation (PTA) of cancer, drug delivery, and catalysis over the years with performances better than their solid counter parts.

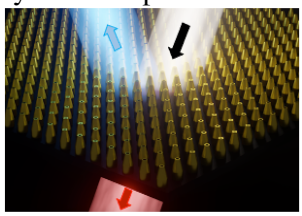

Objectives. The QMetaNet project will explore room-temperature quantum devices operating at the single-photon level, with functionalities that can be tailored by changing different parameters of a meta-network of quantum nodes composed of quantum emitters efficiently coupled to nanoparticles that presents high density of states photonic states [2,3]. Compared with most devices that have achieved enhanced light-matter interactions, this nanodevices have scalability with preserved quantum properties from nanoscale to centimeter-scale extent of the sample [1]. Quantum emitters will be placed in a controlled manner within a nanolattice with perfect and uniform control of nanoparticle position and orientation. This project is inspired by my earlier results where I developed a noninvasive quantum nanometrology technique for precisely localizing quantum emitters coupled to nanostructured materials [17]. In these works, we studied how the local density of states (LDOS) of a hollow nanocone significantly enhanced the spontaneous emission lifetime of an emitter localized to nano-scale precision [7,17]. This unique metamaterial platform supports extraordinary,

enhanced field enhancement to shorten the spontaneous emission lifetimes down to picoseconds in an open environment at room temperature of emitters of natural lifetimes of tens of nanoseconds. In preliminary results I also demonstrated experimentally that strong light-matter interaction between a single exciton and a plasmon mode could be achieved in these structures when the plasmonic field enhancement is optimized, thus producing hybrid modes. The QMetaNet project will focus on study how the interaction between multiple meta-atoms and photons leads to the generation of highly entangled photon states. With control the single-photon interaction with a network of nodes composed of nanoparticles acting as quantum meta-atoms. By changing the spacing between nodes in the network we will aim to control the coupling and coherence in the dipole-dipole interactions obtaining tunable control of sub- and super-luminal regimes. The long-term goal is to investigate experimentally the collective decay dynamics of atoms with a generic multilevel structure coupled to light modes and discover new paths of multiphoton correlations. Studying the interference between different transitions and the resulting entanglement. By measuring changes in decay rates, we will study the super-radiant decay of multilevel meta-atoms in the network [9].

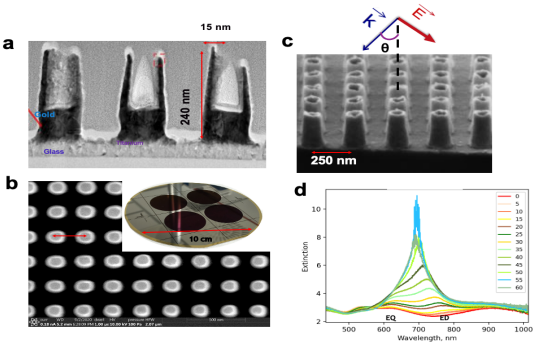

Fig. 1 a-b Images of metamaterial fabricated at a wafer scale sample. d. Plasmonic modes in function of the angle of illumination.

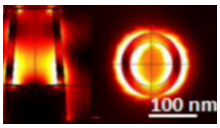

The Network and the Node: Despite the high losses of plasmonic modes, a properly engineered structure can create strong electromagnetic fields (hotspots) in confined nano volumes. Among the various geometries possible for light control with plasmonic nanomaterials, hollow nanostructures offer a more homogeneous distribution of strong field enhancement and reduced LSPR absorption-related quenching thanks to the plasmon hybridization mechanism. A hollow geometry is a promising plasmonic structure with enhanced properties vs. their solid counterparts. Conversely, 3D geometries are difficult to achieve, especially at the wafer scale while maintaining good reproducibility. I propose to couple quantum emitters to a nanomaterial featuring hollow plasmonic truncated gold cones regularly distributed on a square nanolattice that can be manufactured up to centimeter sizes (Fig. 1a-c) while maintaining the unit cell dimension and nanoparticle orientation. We will study experimentally and numerically how various parameters of the unit cell of the metamaterial modify the local electromagnetic environment experienced by the nearby quantum emitters. This platform furthermore can achieve electromagnetic properties that sharply vary with position at the nanometric level. We will study how a quantum emitter located along the hollow 3D plasmonic structure exhibits a spontaneous emission lifetime enhancement that depends on the position and orientation of the single emitter. **Hollow cone array fabrication and characterization**. In collaboration with University of Twente that I established with MESA+ Institute, we fabricated different metamaterials lattice separation and lattice configuration.

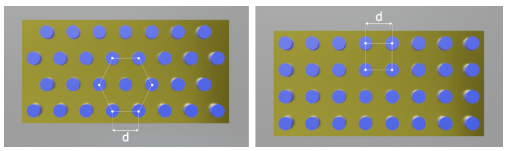

We will explore a significant number of metamaterials samples with different hollow truncated nanocone dimensions and develop the protocols for nanometric control of nanosources. Simulations and experimental results will inform what array dimensions will be desireable for testing the coupling of the collective response of the meta-nodes and single photon emitters. The QMetaNet project will extend this previous collaboration to a realization of the coupling of quantum emitters and the quantum characterization of the networks. We will develop further devices with our established nanofabrication recipe and refine the fabrication process accordingly with the optimal parameters calculated for different coupling regimes [8,17]. **Positioning and studying different Quantum Nodes: Stable Single emitters at room temperatures.** We will study different possible quantum emitters that preserve their quantum behavior at room temperature, characterizing their response to the polarization of the illumination, photon correlation function, spontaneous emission lifetime, radiation pattern with different polarization structures, and spectral broadening. Different excitation and emission wavelengths will be used to couple the emitters at desirable wavelengths determined by the network separation. We aim to optimize our findings at telecommunication wavelengths. Applying a unique

technique to nanolocalized the quantum emitters, in a collaboration that I recently established with University of Technology of Troyes (UTT) in France, for the realization of this proposed QMetaNet project, we will use smart nano-polymers that allows us to address these issues. The smart nature of the polymer is twofold. First, it is a photopolymer that reticulates at the plasmonic hot spot of the metal nanoparticle, allowing one to keep the memory of the selected electromagnetic sites. This memory is spatially anisotropic and decides the distance between the plasmonic nanostructure and the future nano-emitter to be attached. Second, it is chemically pre- functionalized to electrostatically recognize the nano-emitter that can get selectively attached to the pre-designed sites.

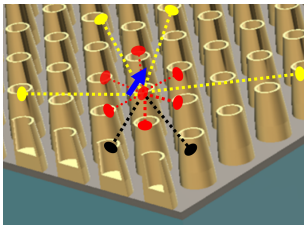

Fundamental studies of meta network connectivity. The local environment of a single emitter can be probed by studying changes in its emission properties. The rate at which an emitter can convert its excited-state energy into a photon increases as more photon states are available to radiate into, which is quantified by the local density of states (LDOS), or its dimensionless counterpart (i.e. normalized to the LDOS of free space), which is known as the Purcell factor [1]. We will perform full-wave numerical simulations for different positions of the dipole along the hollow conical pillar metamaterial with its dipole moment oriented along one of the three-coordinate axis, x, y, z to investigate the different coupling extent along the network when one node is illuminated by a single dipole emitter. Figure 4 shows calculations of a dipole placed on top of the 15 nm ring of the truncated hollow cone. We considered different orientations of the dipole moment and observed that when the dipole is oriented along the longitudinal axis. We will extend our calculations to telecom wavelengths and to the different meta networks separations. We will perform calculations to study the eigenvalues that this structure presents and the coupling modes that can be achieved when a single particle is illuminated and coupled to its neighbors via the metamaterial effect. The parameters we will explore to control this network connectivity are as follows**.** *The Node:* Angle of illumination, addition Layer, ring thickness, refractive index. *The Network:* Different periodicity**,** lattice arrangement: hexagonal, square, kagome and honeycomb.

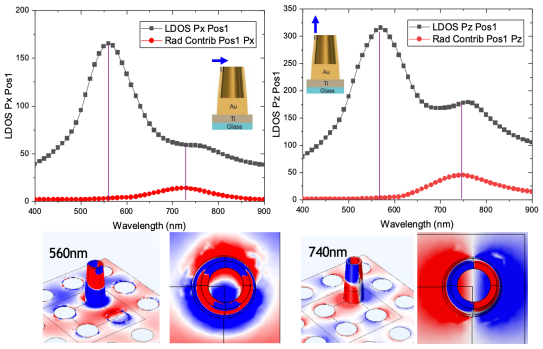

Figure 4 Calculations of enhanced local density of states in a metamaterial with 250 nm square lattice.

Measurements at the super resolution level of the spontaneous emission lifetime modification when the nodes are coupled such that d<<λ. I will apply a non-invasive quantum nanometrology technique at the single-molecule level to study the highly modified spontaneous emission lifetime of quantum emitters along 3D nano fields in the meta network. We will apply far- field super resolution fluorescence microscopy (SRM) to image light-matter interaction beyond the Abbe diffraction limit in the weak-coupling regime, which will be describe in relation to the LDOS as in my recent publication [7]. We will demonstrate nanometer-scale far-field imaging of picosecond lifetime enhancement experienced by single emitters coupled to an array of gold hollow conical nanopillars at room temperature. Motivated by our previous study where we obtained lifetime reduction factors of more than 80 in a unit cell study [17]. Such a hollow geometry supports scalable 3D electromagnetic modes and generates very high field enhancement bringing high spontaneous emission decay-rate enhancements, which furthermore depend strongly both on the position of the emitter and on the illumination angle. We will use far-field lifetime detection coupled to super-resolution single-molecule microscopy to recover and correlate both the excited state lifetime in the picosecond range and the position of each molecule at the nanometer scale in a noninvasive manner, as the measurement does not rely on the use of a tip scanned across the sample (such tips are known to modify the LDOS) [1]. Although the emitters are densely distributed across the material, they will be illuminated one at a time with a focus beam, and we will observe the map of the Purcell factor on a nanometer distance scale extended along the interaction region within the network. Our findings combining SMR with

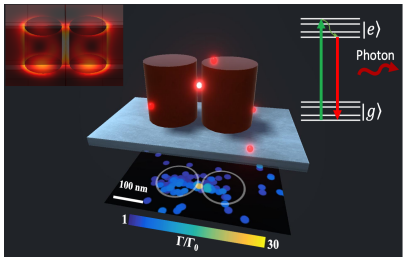

Fig.5 Example of super-resolved decay rate map of single emitter on nano antenna [7].

nanophotonics will lay the groundwork for the manipulation of several other processes based on light-matter interactions, with far reaching implications for both fundamental and applied research opening new avenues for quantum nanotechnologies, optical devices and quantum sensing, gas sensing, and biosensing [7, 17]. We previously demonstrated super-resolved localization of single molecules with enhanced emission performance, spontaneous emission lifetime enhancement, with enhancement not only in the total decay rate but also in the radiative decay rate at all the position around the 3D hollow nanostructure (Fig. 6) [17]. Our findings show a new material platform that can enhance quantum yield of emitters and at the position of molecules around nano fields show enhanced lifetimes and picosecond

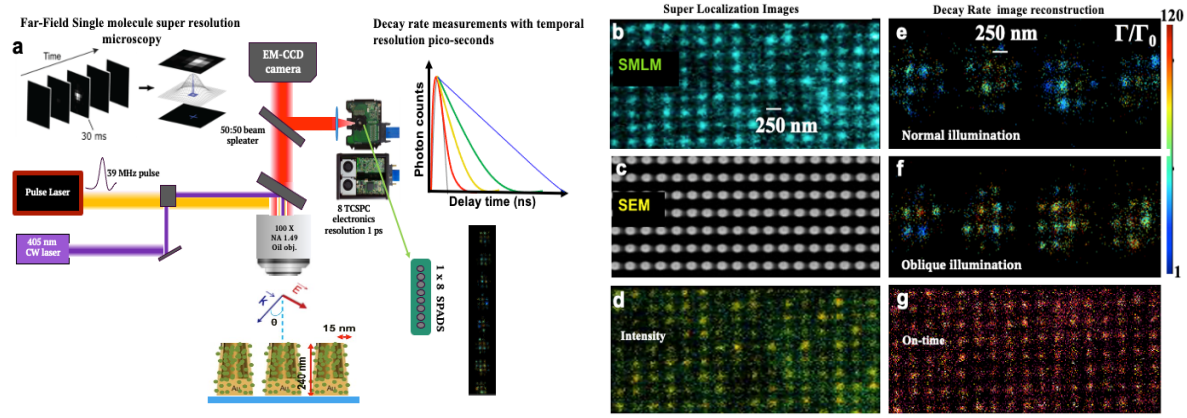

Fig. 6. Experimental setup for super-resolved Purcell factor maps. Results of nano resolved maps of enhanced properties of single emitters coupled to the metamaterial network under wide field illumination. [17]

emission rates at non-cryogenic temperatures. All this occurs in a wafer scale device, where the enhancement of the quantum emitter emission rate can be extended in the centimetre dimension but yet with a nanoscale dimensions geometry in a nano lattice performing as a scalable quantum sensing platform.

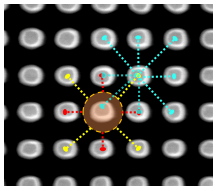

Extent in the meta network scattering at single Node illumination. Tailored light fields at the nanoscale act as multi-purpose tools for the in-depth optical investigation at the single particle level. By tightly focusing vector beams, the field landscape illuminating the single node can be engineered, thus enabling measurements of position dependent resonance spectra and radiation patterns. Vector beams with a polarization state changing about the optical axis, for example under tight focusing, azimuthally and radially polarized vector beams, can be implemented to control the photonic modes excited in the single node illumination and to observe the extent of the meta connection with the neighbor nodes. We will study the extent in the meta network of the photonic mode when single particle is illuminated, changing the wavelength of illumination, with the configuration shown in Fig 8. Running the experiment wavelength-by-wavelength allows us to observe the resonance condition of the unit cells, and, at longer wavelengths, the coupled modes of the meta network. Our aim is to operate our meta network from visible to telecom wavelengths.

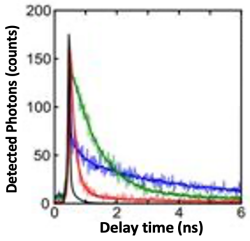

Fig. 7. Measured decay curves of emitters placed at different positions of the node.

Study of the strong coupling from single particle illumination to network connectivity. To reach the so-called strong coupling regime a favorable electromagnetic environment is required to support the interaction i.e. strong and confined fields, the initial constituents hybridize and form mixed light/matter states called polaritons. Strong coupling has been intensively studied with a variety of plasmonic systems (SPP, localized SP) and various kinds of excitons [1]. Motivated by our unpublished

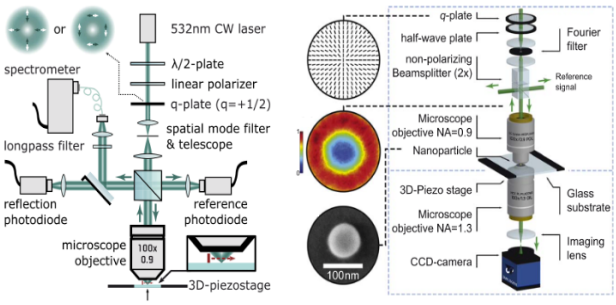

Figure 8. Examples of our experimental array of focused beam illuminated single particle [25, 2 6].

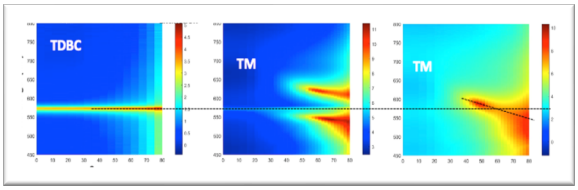

Figure 9. Experimental results of extinction spectral curves in function of angle showing strong coupling of exciton and plasmon.

preliminary results of coupling J-aggregates excitons (TDBC Fig. 9) to the hollow plasmonic structure that presents very strong coupling to excitons when the illumination angle is increased and the longitudinal plasmonic resonances presents super high field enhancement. Here we will investigate in detail numerically and experimentally how the coupling strength is affected by the threshold of filed concentration in the local regime. Contrary with previous works were mainly colloidal random oriented and dimension nanoparticles has been using as quantum cavities [27, 28], the proposed nano device as unique qualities, such as reproducibility of the effect along the cm scale, maintaining the same dimensions and orientation along with uniformly separated particles. We will carry on numerical calculations of TDBC molecules coupled to the hollow the plasmonic meta-Net to study the field distribution in the upper (UP) and lower polaritons (LP) and the effect of the angle of illumination in the UP and LP. **Illumination with Heralded Photons: multi-photon correlations.** We will measure the strength of photon-plasmon, photon-photon and photon-electron interaction. We will investigate the correlations when a single node is illuminated by a heralded single-photon as it scatters into the meta network [1-3]. Our group has experience investigating exotic single photon interactions with plasmonic modes [18]. This could reveal important clues to the potential interactions between coupled nodes and therefore the paths through which single photon states could travel and maintain coherence. Apart of the study of quantum emitters network, we will study the quantum behavior of the localized surface plasmons itself as was done previously with surface plasmons polaritons [19,20]**. Tunable Subluminal and superluminal regimes radiation via network nodes separation.** Trapping the quantum emitters in the host matrix with fixed positions and orientations that set their coupling strength, the degree of superposition in the quantum states can be tuned only by adjusting their resonance wavelengths, or the interseparation in the lattice. The QMetaNet project aims to manipulate this degree of superposition by changing the lattice arrange of the individual nodes and their separation at different illumination conditions. We will measure the spontaneous emission lifetime of the sub-and superradiance regimes for various degrees of superposition [16,17,9]. We will measure multicorrelated states, in different nodes of the network. With both classical light and heralded photon illumination from single node illumination to wide field excitation of the emitters. Tailoring the quantum metamaterial functionalities, we will study different network, starting with hexagonal and square arrange of different periodicity, measuring the change in radiation patterns and coupling modes.

Conclusion: Overall, the development of environmentally robust single photon emitters and their coherent interaction with nanostructured elements is crucial for advancing multiple fields of science and technology, offering opportunities for breakthroughs in quantum internet, sensing, computing and advanced materials research [1-7,9-24]. Quantum information could benefit from the development of stable qubits from reliable single photon sources. This has well-established implications for decryption by the rapid factoring of large numbers, but could also be applied to complex optimization problems, such as resource allocation and scheduling, for improved strategic planning. As single photon probing can provide precise information on the electrical or optical responses of a material, the implications for advanced materials research must also be seriously considered. The proposed QMetaNet project with different and impactful tasks to develop in the next two year will lead to a plethora of new venues for fundamentals and quantum applications. If successful, several new concept will be coined in this work, as well as new ways for solving current challenges and limitations in the development of realistic quantum non-cryogenic devices for new generation of information. We anticipated new discoveries beyond our current imagination thanks to our observables in this unique experiment to be developed.

[1] Bozhevolnyi, S. I., Martin-Moreno, L., & Garcia-Vidal, F. (2018). Quantum Plasmonics. Springer.

[2] Bekenstein, R., Pikovski, I., Pichler, H., Shahmoon, E., Yelin, S. F., and Lukin, M. D. (2020). Quantum metasurfaces with atom arrays. Nature Physics 16, 676-681 https://www.nature.com/articles/s41567-020-0845-5

[3] Li, L., Liu, Z., Ren, X., Wang, S., Su, V., Chen, M., Chu, C., Kuo, Y., Liu, B., Zang, W., Guo, G., Zhang, L., Wang, Z., Zhu, S. and Tsai D. (2020). Metalens-array-based high-dimensional and ultiphoton quantum source. Science 368, 1487-1490. https://www.science.org/doi/10.1126/science.aba9779

[4] Archambault, A., Marquier, F., Greffet, J., & Arnold, C. (2010). Quantum theory of spontaneous and stimulated emission of surface plasmons. Physical Review B, 82(3). https://doi.org/10.1103/physrevb.82.035411

[5] You, J. B., Xiong, X., Bai, P., Zhou, Z. K., Ma, R. M., Yang, W. L. et.al. (2020). Reconfigurable photon sources based on quantum plexcitonic systems. Nano Letters, 20(6), 4645-4652. https://doi.org/10.1021/acs.nanolett.0c01562

[6] Birnbaum, K. M., Boca, A., Miller, R., Boozer, A. D., Northup, T. E., & Kimble, H. J. (2005). Photon blockade in an optical cavity with one trapped atom. Nature, 436(7047), 87-90. https://doi.org/10.1038/nature03804

[7] Córdova-Castro, R. M, van Dam, B., Lauri, A., Maier, S. A., Sapienza, R., De Wilde, Y., Izeddin, I. and Krachmalnicoff, V. (2024). Single-emitter super-resolved imaging of radiative decay rate enhancement in dielectric gap nanoantennas. Light: Science and Applications, 13,7 https://www.nature.com/articles/s41377-023-01349-2

[8] Jonker, D., Jafari, Z., Winczewski, J.P., Eyovge, C., Berenschot, J.W., Tas, N.R., Gardeniers, J.G.E., De Leon, I. and Susarrey-Arce, A. (2021). A wafer-scale fabrication method for three-dimensional plasmonic hollow nanopillars. Nanoscale advances, 3(17), 4926-4939. https://doi.org/10.1039/D1NA00316J

[9] Trebbia, J. B., Deplano, Q., Tamarat, P. and Lounis, B. (2022), Tailoring the superradiant and subradiant nature of two coherently coupled quantum emitters. Nature communications, 13, 2962. https://www.nature.com/articles/s41467-022-30672-2

[10] Altewischer, E., Van Exter, M. P., & Woerdman, J. P. (2002). Plasmon-assisted transmission of entangled photons. *Nature*, *418*(6895), 304-306. https://doi.org/10.1038/nature00869

[11] Archambault, A., Marquier, F., Greffet, J., & Arnold, C. (2010). Quantum theory of spontaneous and stimulated emission of surface plasmons. Physical Review B, 82(3). https://doi.org/10.1103/physrevb.82.035411

[12] You, C., Hong, M., Bhusal, N., Chen, B., Quiroz-Juárez, M. A., Mostafavi, F., Guo, J., De León, I., De J León-Montiel, R., & Magaña-Loaiza, O. S. (2021). Observation of the modification of quantum statistics of plasmonic systems. Nature Communications, 12(1). https://doi.org/10.1038/s41467-021-25489-4

[13] Huck, A., Smolka, S., Lodahl, P., Sørensen, A. S., Boltasseva, A., Janoušek, J., & Andersen, U. L. (2009). Demonstration of Quadrature-Squeezed Surface Plasmons in a Gold Waveguide. Physical Review Letters, 102(24).

[14] Heeres, R., Kouwenhoven, L. P., & Zwiller, V. (2013). Quantum interference in plasmonic circuits. *Nature Nanotechnology*, *8*(10), 719-722. https://doi.org/10.1038/nnano.2013.150

[15] Vest, B., Dheur, M., Devaux, É., Baron, A., Rousseau, E., Hugonin, J., Greffet, J., Messin, G., & Marquier, F. (2017). Anti-coalescence of bosons on a lossy beam splitter. *Science*, *356*(6345), 1373-1376. https://doi.org/10.1126/science.aam9353

[16] Zavatta, A., Viciani, S., & Bellini, M. (2004). Quantum-to-Classical Transition with Single-Photon-Added Coherent States of Light. *Science*, *306*(5696), 660-662. https://doi.org/10.1126/science.1103190

[17] Córdova-Castro, R.M., Vaddi, Y., Cabriel, C., Jonker, D., Zapata-Herrera, M., Krasavin, A., Susarrey-Arce, A., Sapienza, R., De Wilde, Y., Krachmalnicoff, V., Zayats, A., R. Carminaty, I Izeddin and R. W. Boyd. (2023). Single-Emitter Photon Emission Rate Enhancement with Nanomaterials at the Super-Resolution Level. *Frontiers in Optics* https://doi.org/10.1364/FIO.2023.JTu4A.52

[18] Magaña-Loaiza, O., De Leon, I., Mirhosseini, M., Ficler, R., Safari, a., Mick, U., McIntyre, B., Banzer, P., Rodenburg, b., Leuchs, G. and Boyd, R. W. (2016). Exotic looped trajectories of photons in three-slit interference. Nat Commun 7, 13987 (2016). https://doi.org/10.1038/ncomms13987

[19] Safari, A., Fickler, R., Giese, E., Magaña-Loaiza, O. S., Boyd, R. W., & De León, I. (2019). Measurement of the Photon-Plasmon Coupling Phase Shift. Physical Review Letters, 122(13). https://doi.org/10.1103/physrevlett.122.133601

[20] Hong, M., Dawkins, R. B., Bertoni, B., You, C., & Magaña-Loaiza, O. S. (2024). Nonclassical near-field dynamics of surface plasmons. *Nature Physics*. https://doi.org/10.1038/s41567-024-02426-y

[21] Flayac, H., & Savona, V. (2017). Unconventional photon blockade. Physical Review A, 96(5), 053810. https://doi.org/10.1103/PhysRevA.96.053810

[22] Dirmeier, T., Tiedau, J., Khan, I., Ansari, V., Müller, C. R., Silberhorn, C., et.al. (2020). Distillation of squeezing using an engineered pulsed parametric down-conversion source. Optics Express, 28(21), 30784-30796. https://doi.org/10.1364/OE.402178

[23] Chang, D. E., Vuletić, V., & Lukin, M. D. (2014). Quantum nonlinear optics—photon by photon. Nature Photonics, 8(9), 685-694. https://doi.org/10.1038/nphoton.2014.192

[24] Snijders, H. J., Frey, J. A., Norman, J., Flayac, H., Savona, V., Gossard, A. C., ... & Löffler, W. (2018). Observation of the unconventional photon blockade. Physical review letters, 121(4), 043601. https://doi.org/10.1103/PhysRevLett.121.043601

[25] Bauer, T., Banzer, P., Bauchard, F., Orlov, S., Marruacci, L., Santamato, E., Boyd, R.W., Karimi, E. and Leuchs, G. (2019). Multi-twist polarization ribbon topologies in highly confined optical fields. New Journal of Physics, 21, 053020. https://iopscience.iop.org/article/10.1088/1367-2630/ab171b

[26] Groshe, S., Hunermann, Richard., Sarau, G., Christiansen, S., Boud, R.W., Leuchs, G. and Banzer, P. (2020). Towards polarization-based excitation tailoring for extended Raman Spectroscopy. Optics Express, 10239. https://opg.optica.org/oe/fulltext.cfm?uri=oe-28-7-10239&id=429446

[27] Liu, R., Zhou, Z., Yu, Y., Zhang, T., Wang, H., Liu, G., Wei, Y., Chen, H. and Wang X. (2017). Strong- Light-Matter Interactions in Single Open Plasmonic Nanocavities at the Quantum Optics Limit. Physical Review Letters, 118, 237401. https://journals.aps.org/prl/abstract/10.1103/PhysRevLett.118.237401

[28] Dovzhenko, D. S., Ryabchuk, S. V., Rakovich, Y. and Nabiev, R. (2018). Light-matter interaction in the strong coupling regime: configurations, conditions and applications. Nanoscale, 10, 3589. https://pubs.rsc.org/en/content/articlelanding/2018/nr/c7nr06917k

Executive Summary

QOSY: Quantum-Optic Silicon: Device Efficiency and Applications

Mariana F. Ramos (Scientist), AIT Austrian Institute of Technology

Challenge: In today's digital age, cloud services are omnipresent, offering immense benefits to industries and professionals alike. Despite their popularity, grave concerns regarding the security within the underlying datacentres persist. Traditional security measures are grounded on the belief that data within the datacentre perimeter is secure, and only external connections require robust encryption. However, this assumption is failing to account for potential internal threats, an emerging concern considering the fact that 85% of total traffic is internal to the datacentre. In light of this, a paradigm shift towards a zero-trust model - where no datacentre resource is inherently trusted - is necessary. Therefore, to secure the intra data center communication links, Quantum Key Distribution (QKD) the most secure cryptographic key exchange method should be employed. The challenge lies in fitting QKD into a much smaller scale to allow seamless integration with processors and storage, all while maintaining massive data transfer rates.

Solution: QOSY aims to create a highly compact (sub-mm^2) and cost-effective QKD system by developing an all-silicon PIC based QKD transmitter. Although silicon is widely available in the chip industry, it lacks a built-in light source due to its indirect semiconductor bandgap. Therefore, current silicon-based photonic ICs rely on complex and costly hetero-integration with III-V semiconductors like InP or hybrid integration with III-V chiplets to provide optical power. Our approach targets an optically active all-silicon solution seamlessly integrated with microelectronic systems, ensuring natural inherent information theoretical security (ITS). This paves the way for the integration of ITS through QKD into everyday scenarios. It ensures the protection of vital public infrastructure such as transportation and energy grids from cyber threats, while further ensures the security of wireless communications, including contactless payments, through short-range free-space optical connections, and also reinforces the safeguarding of medical data transmission and processing within data centres.

Current QKD system developments employing photonic integrated circuits rely on heterogeneous co-integration with a complex die-level assembly, including precise alignment of waveguides. Furthermore, the current focus in QKD system development resides on performance improvements in terms of secure-key rate (SKR), even though one-time pad encryption is deemed impossible (1 secure bit required for 1 classical data bit) and the NIST limit (one new 256-bit AES key is needed every 64 GB of data) is already considered. In this second case, which is considered for practical QKD deployment, a SKR of 1 Mb/s would be sufficient to secure 2000 Tb/s. It would therefore make more sense to strike trade-offs between QKD simplicity and performance (i.e. SKR), especially when considering commodity-like applications. This is where the all-silicon approach can clearly outperform traditional QKD systems.

Impact: Our simplified monolithic silicon solution can create new application domains and therefore new markets for QKD. Together with its unique ITS-grade security compared to other crypto primitives like PQC and PLS, our approach offers significant cost advantages over QKD contenders: (i) Silicon IC technology is a mature, fast and well-developed process. (ii) The seamless co-integration of electronics and photonics eliminates the need for external interfaces and bonding efforts, effectively reducing the footprint and increasing security. (iii) There is no hetero- or hybrid integration of III-V materials necessary. This would also reduce the environmental effects of our technological approach (United Nations SDG #12). Silicon is a readily and abundantly available material compared to raw III-V materials (like In, Ga or As). Together with the intended small size of <1 mm2 of the QKD engine, it is clearly a more sustainable and environmentally friendly solution. Although there is a small amount of Germanium necessary for co-doping of the GeSi light source and potential receiver SPADs, its impact is strongly reduced compared to the vast material needed to supply III-V wafer substrates for III-V gain material manufacturing.

1 Problem statement/objective

In today's digital age, cloud services are omnipresent, offering immense benefits to industries and professionals alike. Despite their popularity, grave concerns regarding the security within the underlying datacentres persist. Traditional security measures are grounded on the belief that data within the datacentre perimeter is secure, and only external connections require robust encryption. However, this assumption is failing to account for potential internal threats, an emerging concern considering the fact that 85% of total traffic is internal to the datacentre. In light of this, a paradigm shift towards a zero-trust model - where no datacentre resource is inherently trusted - is necessary, especially considering a more formidable threat on the horizon: quantum computing. This emerging technology is bolstered by substantial investments (exceeding $1 billion since 2020) and a surge in research and development, evidenced by over 66,000 scientific papers and more than 4,000 patent families filed in the past four years. As the number of qubits continues to grow, it's only a matter of time before current encryption methods become insecure, particularly since the quantum advantage has already been demonstrated [1]. As a response to this threat, quantum physics offers Quantum Key Distribution (QKD), an information-theoretically secure (ITS) key generation method grounded in the laws of nature rather than the computational complexity of mathematical problems. The development of QKD systems began 40 years ago when Bennett and Brassard introduced the secure BB84 protocol. Over the past four decades, QKD has evolved into commercial rack-scale products now securing long-haul and metro-scale networks to enforce perimeter security [2]. However, these systems mainly rely on bulk optics, making them unsuitable for short-reach or intra-facility networks due to their size and cost. Instead, non-ITS technologies like post-quantum cryptography (PQC) and physical-layer security (PLS) are used [3], even though their long-term security remains unproven. For QKD to be widely adopted in environments such as datacenters, industrial settings, public infrastructure, IoT devices, and mobile phones, it must achieve significant reductions in system size, complexity, and cost. This calls for a broadly accessible, low-complexity QKD solution that tears down existing barriers to deployment, making it feasible for QKD to be integrated into critical but presently untapped commodity-flavored application domains.

We introduce an all-silicon approach that provides cost-effective and highly compact QKD system. Silicon, being abundant both in availability and adoption-wise, is the top choice for the chip industry. However, due to its indirect semiconductor bandgap, silicon cannot generate light, making monolithic photonic-electronic integrated circuits unfeasible. This requires the expensive and complex hetero-integration of III-V semiconductor dies (such as Indium Phosphide, InP) to compensate for silicon's optically passive nature. In QOSY, we demonstrate that a quasi-direct bandgap can enable a silicon light-source, fully compatible with integrated QKD solutions. This innovation allows us to significantly simplify chip-scale QKD assembly, making it seamlessly integrable into silicon-centric microelectronic systems. This represents a paradigm shift, making QKD as accessible and widespread as microelectronics. Ultimately, this will allow end-users and the general public to employ the highest level of security for everyday personal and professional activities. QOSY's ambition aims even higher—to demonstrate that the same chip can be used for quantum protocols beyond QKD, such as oblivious transfer, unlocking powerful new possibilities for secure multiparty computation applications, initiating a groundbreaking journey to revolutionize quantum security and elevate the standards of data protection.

2 Literature review

State-of-the-art demonstrations of chip-scale QKD transmitters or receivers build on a wide range of integration platforms [4-10]. They follow a purely photonics-oriented approach to unlock unique performance advantages. None of the demonstrations (see table) features a *monolithic integration scheme compatible with electronic-photonic co-integration to gracefully blend quantum-optics with microelectronic commodities.* Even though monolithic InP integration has been demonstrated for QKD, this chiplet solution would have to be co-packaged with a silicon electronic ASIC, again rendering the entire system as too costly for commodity applications. Other works, which leverage on the silicon ecosystem for photonic integration, require an external light source or again, a hybrid integration with

InP for this purpose, involving complex assembly due to precise waveguide-to-waveguide alignment and additional wiring. Monolithic InP QKD or hybrid III-V/Si QKD solutions further necessitate hermitic packaging. None of the existing approaches is therefore competitive enough for low-cost mass applications.

Work	Principle / Protocol	PIC platform	Light source	QKD state encoder	Performance	Form-factor	Electronic upgrade?
[4]	**DV**: BB84,COW	InP	InP, tunable	phase / int. modulator	345 kb/s	2 × 6 mm^2	× external
[5]	**CV**-QKD	InP	× external	I/Q modulator	2.3 Mb/s	6 × 12 mm^2	× external
[6]	**DV**: BB84 time-bin	Si + $LiNbO_3$	× external	asymmetric MZI	10 kb/s	Si: 2.3×0.6 cm^2 LN: 3.8×0.1 cm^2	× external
[7]	**CV**-QKD	InP + SiN	InP / Si_3N_4	× ext. I/Q modulator	ξ = 5.8%SNU	2.4 × 1.3 mm^2	× external
[8]	**MDI**-QKD	InP	monol. InP	phase modulator / MZI	12kb/s	6 × 2 mm^2	× external
[9]	**DV**: COW	InP	monol. InP	phase modulator + VOA	6 kb/s	4 × 2 mm^2	× external
[10]	**DV**: time-bin decoy BB84	Hybrid Si + InP	InP	phase encoding + multi-level OOK	235 kb/s	2 × 6 mm^2	× external
QOSY	**DV**: pol. encoded BB84	monolithic SOI	monolithic silicon	I/Q pol. encoder	1 kb/s	4.2 × 0.4 mm^2 ✓ non-hermetic	✓ possible

To position silicon at the core of our photonic-integrated QKD circuit, we employ a quasi-direct bandgap in a GeSi junction. Although previous attempts on silicon-based light emitters have failed due to poor emission characteristics, making them unsuitable for telecom applications, QKD only requires signal launched at the level of a single photon per symbol to leverage the unique properties of quantum physics. This matches perfectly with our GeSi light source. Recent work with die-level [11] and waveguide-based GeSi light emitters [12] has shown that we can achieve a photon number of $\mu = 0.25$ photons per symbol at a transmitter rate of 1 GHz, surpassing the required launch of $\mu = 0.1$ photons per symbol (around -80 dBm) to accommodate Poissonian photon statistics in discrete-variable QKD. Additionally, our emitter operates at 1550 nm, fully compatible with WDM technology. For quantum state preparation in the QKD transmitter we use the polarization-based BB84 protocol, by employing a dual-polarization inphase/quadrature for polarization modulation [11]. Since our GeSi source currently emits broadband and incoherent light, spectral filtering is required to prevent signal depolarization during fiber transmission. Although this reduces the output power of the QKD transmitter and requires further design adjustments to optimize the spectral characteristics of the silicon light source, we can already generate secure keys at a rate of 0.37 kb/s. This rate is sufficient to secure a classical channel with a capacity of up to 745 Gb/s according to NIST standards, meeting the demands of commodity applications.

An implementation of the complete QKD transmitter circuit on a silicon photonic platform is shown in Fig. 1, and it could potentially be reduced to a footprint of less than 1 mm^2 (Silicon light sources from the ERC StG COYOTE). In comparison, a state-of-the-art InP QKD transmitter has the size of 2x4 mm2 [9]. Moreover, an opto-electronic BiCMOS implementation for a quantum random number generator (QRNG) has been demonstrated as feasible in [13]. This advancement could lead to a simplified monolithic all-silicon QKD transmitter that includes an integrated QRNG engine. Such a system would be fully compatible with microelectronics, enabling integration virtually anywhere. Seamless integration with electronics, for instance, through 3D wafer bonding,

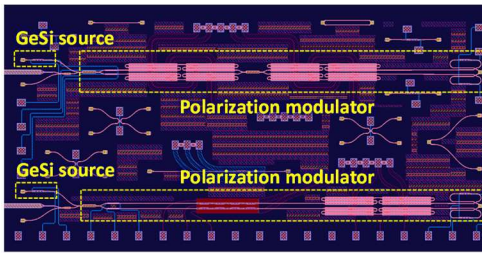

Fig. 1. Prototype PIC of a world's first all-silicon QKD transmitter.

removes critical interfaces like exposed die-to-die bond wires. This approach elegantly addresses the exposure of intermediate interfaces through a purely silicon-centric photonic-electronic integration scheme. The decision to exclusively focus on simplifying the QKD transmitter, while excluding the QKD receiver, is driven by the unidirectional channel layout of QKD systems. In such systems, only one subsystem—either the transmitter or the receiver—needs to be simplified as the distributed network element, while the more complex component can be centralized, similar to cloud-based access or 6G networks. The QKD receiver, equipped with single-photon detectors (SPADs), is inherently the more complex element. However, recent advances in GeSi SPAD technology [14] hold the potential to reduce the receiver's complexity by replacing InGaAs SPADs over time. This would create a silicon-centric approach for both the transmitter and receiver, eventually leading to a more balanced and symmetric complexity distribution within the QKD link.

3 Outcome (s)

Through rigorous exploration and experimentation, this project aims to yield a wealth of valuable outcomes in the realm of QKD technology. Firstly, we anticipate the development of a detailed set of use cases, meticulously outlining the most promising deployment scenarios for the all-silicon QKD transmitter. These use cases will categorize deployment contexts based on environmental and operational requirements, providing a clear framework for subsequent testing and evaluation stages. Secondly, our efforts will culminate in the establishment of a comprehensive laboratory test-bed, facilitating the rigorous evaluation of QKD system components. This setup, equipped with precise alignment tools and environmental controls, will simulate various operating conditions, ensuring accurate capture of key performance metrics such as secure key rate (SKR) and quantum bit error rate (QBER). Through back-to-back performance evaluations, we aim to glean insights into the characteristics of the silicon light source and identify optimal operating conditions for the QKD system. Furthermore, our project endeavours to benchmark QOSY's QKD approach in real-world contexts. This comprehensive evaluation, conducted on an expanded test-bed setup, will consider classical data traffic and various coexistence conditions, measuring SKR and QBER under specified network characteristics. Additionally, we will assess the QKD transmitter in protocols beyond QKD, such as oblivious transfer for secure multi-party computation applications. Resource allocation based on performance estimations will optimize the QKD system for the most impactful use cases, ultimately leading to the development of a comprehensive blueprint for post-project exploitation of the all-silicon Commodity-QKD technology. This blueprint will delineate strategies for integrating QKD into diverse network environments, showcasing its broad applicability across various scenarios and protocols.

- *Catalog of Promising Deployment Scenarios for the All-Silicon QKD Transmitter* - The project will yield a detailed set of use cases outlining the most promising deployment scenarios for the all-silicon QKD transmitter. These use cases will categorize deployment contexts based on environmental and operational requirements. Each scenario will undergo thorough analysis to understand its unique security needs, operational constraints, and performance expectations. These defined use cases will provide a clear framework for subsequent testing and evaluation stages.
- *Robust Laboratory Test-Bed for Comprehensive QKD System Evaluation* - The project will establish a comprehensive laboratory test-bed for rigorous evaluation of the QKD system components. This setup will feature precise alignment tools and environmental controls to simulate various operating conditions. Calibration of measurement instruments will ensure accurate capture of key performance metrics such as secure key rate (SKR) and quantum bit error rate (QBER). Back-to-back performance evaluations will provide insights into the silicon light source characteristics and optimal operating conditions for the QKD system. Analysis of operational limits will identify potential weaknesses and strategies for mitigation, ensuring system robustness under diverse conditions.

- *Benchmarking QOSY's QKD Approach and Beyond* - The project will benchmark QOSY's QKD approach in real-world contexts outlined in Aim 1. This evaluation will be conducted on an expanded test-bed setup, considering classical data traffic and various coexistence conditions. Performance evaluation will measure SKR and QBER under specified network characteristics, aiming to achieve secure key generation sufficient to protect classical data capacities in telecom and datacom-driven applications. Additionally, the QKD transmitter will be evaluated in protocols beyond QKD, such as oblivious transfer for secure multi-party computation applications. Resource allocation based on performance estimations will optimize the QKD system for the most impactful use cases. The outcome will be a comprehensive blueprint for post-project exploitation of the all-silicon Commodity-QKD technology, detailing strategies for integrating QKD into diverse network environments and showcasing its broad applicability across various scenarios and protocols.

4 Impact

The implementation of quantum-optics and QKD in electronics-friendly silicon IC solutions promises widespread societal benefits, aligning with the UN's Sustainable Development Goals (SDGs). This technology facilitates personal health monitoring and remote interactions across various platforms, including both wired and wireless applications. By securing data transmissions through free-space optical key exchanges, it enables secure living and remote work opportunities, particularly crucial in the context of the Covid19 pandemic. Furthermore, its integration into IoT scenarios improves data security and confidentiality, promoting democracy and digital inclusion. Additionally, QKD solutions play a vital role in safeguarding critical infrastructure against cyberattacks and ensuring uninterrupted service provision. Moreover, transitioning to silicon from III-V semiconductor materials reduces environmental footprint, aligning with sustainability goals. Overall, this technology offers a multifaceted approach to address societal challenges while promoting sustainable development. This innovative approach unlocks new application domains, offering significant economic benefits. By leveraging all-silicon solutions, it addresses market gaps where existing QKD or alternative solutions fall short. These silicon-based innovations offer advantages like streamlined design processes, seamless integration with electronic components, and simplified assembly methods, leading to substantial cost savings compared to traditional approaches. The cost advantages of our approach are illustrated in Fig. 2, comparing them to the most competitive monolithic QKD transmitter developed on InP [9], resulting in a remarkable 73% reduction in costs. Moreover, compared to the best-of-breed hybrid III/V-on-Si solution, our approach maintains a significant 42% cost advantage. However, it's important to note that our Commodity-QKD transmitter operates at a lower secure-key rate (SKR), which means the cost advantage varies depending on the classical data capacity requiring security. This relationship is analysed in Fig. 2, where our all-silicon QKD approach demonstrates an advantage for classical capacities of up to 8000 Gb/s/λ, enabling us to drive down costs in the commodity regime (Ξ).

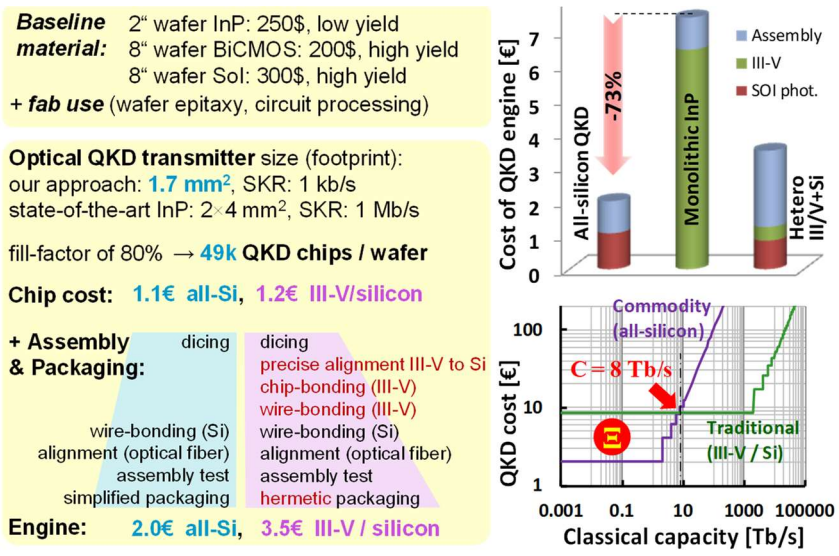

Fig. 2. QKD transmitter cost using all-silicon and traditional PICs [10].

At the core of every photonic circuit is its light source, which in this case is achieved through a quasi-direct bandgap of a SiGe junction. While research has shown that strained SiGe junctions or optically pumped silicon lasers can produce faint broadband light emissions, the telecom industry has shifted towards hetero-integration methods that offer significantly higher output power levels above 0 dBm. However, quantum circuits require power levels that are 8-9 orders of magnitude lower, making C-band (1550 nm) SiGe light emitters a viable option for single-photon QKD transmitter operation. The successful demonstration of an all-silicon QKD transmitter PIC will pave the way for Commodity-QKD technology. QKD's unidirectional nature allows for asymmetric complexity distribution along the optical link, necessitating either a low form-factor, low-cost transmitter, or receiver. In QOSY, the more challenging C-band single-photon avalanche photodetectors (SPAD) will be centralized at a cost-shared location. This leaves the compact (1.7 mm²) all-silicon QKD transmitter as the only distributed network element. Additionally, recent advances in SiGe near-infrared SPAD development promise a monolithic approach for QKD receivers in the near future [14-15], potentially transforming these into a commodity and enabling even simpler link configurations without cost-shared elements.

Notably, QOSY aims for a significant reduction in complexity rather than achieving premium-grade performance. This approach is practical since QKD-based encryption relies on rapid AES-key renewal under the NIST limit. For a Secure Key Rate (SKR) of 1 kb/s provided by low-complexity QKD, the classical data capacity that can be secured under this limit is 20 Tb/s. In the context of 6G requirements, this capacity translates to approximately 20 wired access or fronthaul connections. Therefore, a balance between simplicity and secure-key generation rate is essential for the development of Commodity-QKD.

5 Bibliography

[1] H. Zhong et al, Science **370**, 1460 (2020)
[2] Q. Zhang et al, Opt. Expr. **26**, 24260 (2018)
[3] I. Djordjevic, Entropy **24,** 935 (2022)
[4] P. Sibson et al, Nature Comm. 8, 13984 (2017)

[5] J. Aldama et al, Proc. OFC **M1I.3**, San Diego, USA (2023)
[6] X. Li et al, Chin. Phys. B. **31**, 6, (2022)
[7] L. Li et al, Photon. Res. **11**, 504 (2023)
[8] H. Semenenko et al, Optica **7**, 238 (2020)
[9] A. Trenti et al, J. Lightwave Technol. **40**, 7485 (2022)
[10] T. K. Paraiso et al, Nat. Photonics **15**, 850 (2021)
[11] F. Honz et al, J. Sel. Topics in Quantum Electron. **30**, 6600109 (2024)
[12] F. Honz et al, Opt. Fiber Comm. Conf., **M4H.4** (2024)
[13] A. Khanmohammadi et al., Phot. J. **7**, 7500113 (2015)
[14] L.F. Llin et al, Opt. Lett. **45**, 6406 (2020)
[15] J. F. Tasker et al., Sci. Adv.**10**,eadk6890(2024)

Zhuldybina, Mariia

Terahertz Technology for Efficient Recycling of Plastics

Plastic production has soared from just two million tonnes in 1950 to over 450 million tonnes today, highlighting its importance due to its low cost, versatility, and utility in diverse applications such as construction, home appliances, medical instruments, and food packaging. Despite these benefits, the mismanagement of plastic waste—through inadequate recycling, incineration, or poor landfill practices—transforms this valuable material into a significant environmental pollutant. Each year, approximately one to two million tonnes of plastic end up in our oceans, severely impacting wildlife and ecosystems.

The challenge of plastic waste management is compounded by the difficulties in sorting plastics for recycling, especially colored plastics like black plastics, which are particularly problematic. These plastics are less desirable for recycling due to the carbon black pigment used, which absorbs significant amounts of light, making it difficult for optical sorting technologies to identify and separate them effectively. As a result, black plastics often end up as unrecyclable mixed waste, further lowering their economic and environmental value. The widespread use of these plastics, especially in single-use packaging, has led to an increase in plastic waste, with only a small fraction being recycled, thus posing substantial environmental challenges.

Current sorting technologies, such as NIR and SWIR spectroscopy, struggle with black plastics due to their low reflectance and flat spectral profiles. In response, the project explores the use of terahertz (THz) technology, which shows promise in overcoming these limitations. THz time-domain spectroscopy (THz-TDS) and continuous wave (CW) THz spectroscopy are evaluated for their ability to penetrate materials and distinguish between different polymer types based on unique spectral fingerprints, regardless of color.

The project is structured around three focused objectives: first, to assess the effectiveness of THz technology for identifying black plastics, comparing its performance with current infrared-based methods which struggle with high carbon content plastics. The second objective involves developing optimized THz-based sorting algorithms, which includes creating a comprehensive database of THz spectral fingerprints for various polymers. This data will be used to train machine learning models that classify polymers accurately, aiming for seamless integration into existing recycling operations. The third objective is the implementation of single-frequency THz systems in recycling facilities to test the practical application of this technology. This involves setting up, calibrating, and refining THz systems to enhance the sorting process, ensuring they align with the operational standards of modern recycling facilities.

The anticipated outcomes of employing THz technology are multifaceted. Primarily, it is expected to significantly enhance the efficiency and accuracy of the recycling process, aligning with broader global objectives aimed at minimizing resource depletion and reducing environmental impact. The successful integration of THz technology would not only improve recycling rates but also influence broader industry practices, providing a benchmark for the adoption of new technologies in waste management. Additionally, the project supports public policy initiatives geared towards a circular economy, advocating for standards that facilitate easier sorting and recycling of plastics at the infrastructure level. Ultimately, by enabling more effective recycling solutions, the project contributes to significant reductions in landfill waste, thereby offering a sustainable approach to managing the environmental challenges posed by black plastics. This holistic approach underscores the project's potential to deliver substantial benefits in environmental conservation and resource management, marking a significant advancement in tackling the recycling challenges of today.

Terahertz Technology for Efficient Recycling of Plastics

Literature Review:

Plastic production has surged dramatically over the past 70 years, rising from just two million tonnes in 1950 to over 450 million tonnes today. This exponential growth underscores the immense value plastic has brought to our lives as a cheap, versatile, and sterile material used in countless applications, from construction and home appliances to medical instruments and food packaging. However, when plastic waste is mismanaged – not recycled, incinerated, or properly contained in sealed landfills – this valuable material becomes a major environmental pollutant. Each year, an estimated one to two million tonnes of plastic enter our oceans, causing significant harm to wildlife and ecosystems [1].

In recent years, the consumption of plastics has reached unprecedented levels, particularly in packaging applications [2]. The convenience, versatility, and cost-effectiveness of plastics have made them indispensable in various industries. However, this widespread use has led to a significant increase in plastic waste, posing substantial environmental challenges. In 2018, only Canadians threw away **4.4 million** tonnes of plastic waste, only 8 percent of which was recycled [3]. One of the critical issues in managing polymer waste is related to the diverse range of plastic colors. Colorless or white plastics hold the highest market value as recycled products, as they can be easily sorted and re-colored to suit various applications. In contrast, colored plastics, especially black ones, are more challenging to sort with current sorting technologies which leads often to unrecyclable mixed plastic waste have lower economic value because their color limits their recyclability [4]. Black plastics can generally only be recycled into black plastic products, making them less desirable from a recycling perspective. The coloration of plastics results from the presence of organic or inorganic colorants, which can influence the recycling process, depending on their properties and the recycling methods used. Efficient mechanical recycling is currently the most sustainable approach to plastic recycling, emphasizing the separation of different polymer types to obtain high-quality secondary raw materials. Automated sorting of polymers is increasingly performed using sensor-based technologies, such as optical sensors operating in the Near-Infrared and Short-Wave Infrared (NIR and SWIR) spectral ranges. NIR spectroscopy has demonstrated its capability to classify various polymer types from different waste sources, significantly contributing to improved plastic recycling [5]. The technique relies on the interaction of NIR light (wavelengths between 780 nm and 2500 nm) with the material. Polymers absorb NIR light at specific wavelengths corresponding to their molecular vibrations, creating a spectral fingerprint unique to each type of plastic. These spectral fingerprints are then used to identify and sort the polymers. However, a significant challenge arises when dealing with black-colored plastics. The strong light absorption of black plastics, primarily due to carbon black pigmentation, leads to low reflectance and flat spectra in the NIR range. As a result, NIR-based technologies struggle to classify black plastics by polymer type. SWIR spectroscopy, operating in the 1,000 nm to 2,500 nm range, extends the capabilities of NIR by providing better penetration and sensitivity for certain materials. Similar to NIR, SWIR spectroscopy relies on the specific absorption characteristics of polymers in the SWIR range. While it offers improved performance over NIR in some cases, SWIR still faces challenges with black plastics due to the same issues of light absorption and low reflectance caused by carbon black [6]. Black plastics account for a substantial portion of household plastic waste, particularly in single-use packaging. Carbon black, used as a common colorant in black plastics, offers various advantages, including cost-effectiveness, color stability, and resistance to environmental factors. It is widely employed in outdoor applications and products requiring strength, conductivity, or thermal stability. Despite its benefits, the presence of black plastics in the recycling stream poses significant challenges, necessitating effective sorting based on polymer type at recycling facilities [7]. Several

approaches have emerged to address the sorting of post-consumer black plastic waste. Several approaches have emerged to address the sorting of post-consumer black plastic waste, one of which is the use of Mid-Infrared (MIR) technology. MIR operates in the 2,500 nm to 25,000 nm range and is less influenced by surface morphology and color, including black color. MIR spectroscopy can identify the unique absorption bands of polymers, making it a promising candidate for sorting black plastics. However, the effectiveness of MIR technology in industrial plastic sorting requires further research and validation [8].

In order to meet the stringent demands of achieving a 100% recycling cycle, new sensor concepts are currently being explored. Traditional system approaches, particularly those utilizing hyperspectral cameras in the infrared region, exhibit limitations, especially when it comes to sorting black plastics. However, the lower terahertz (THz) frequency range appears to offer a promising solution for sorting black plastics, primarily due to the unique properties of THz light [9]. THz time-domain spectroscopy (THz-TDS) involves generating short pulses of THz radiation and measuring the time it takes for the pulses to pass through or reflect off a material. This technique provides detailed information about the material's absorption and refractive index across the THz spectrum. THz-TDS can penetrate non-metallic materials and provide distinct spectral fingerprints for different polymers, including black plastics. However, it often requires complex post-processing to interpret the data, which can be a limitation for rapid industrial applications [10]. CW-THz spectroscopy, on the other hand, uses a continuous THz source and is simpler in terms of data acquisition and analysis compared to THz-TDS. This method is particularly advantageous for identifying and sorting black plastics because THz waves can penetrate materials regardless of color or pigmentation, providing clear differentiation between polymer types. CW-THz technology can potentially be integrated into existing recycling facilities to enhance the sorting efficiency of black plastics.

Project objectives:

To address this challenge, the primary goal of this challenge is **to assess the feasibility and potential benefits of utilizing continuous waves (CW) terahertz (THz) technology for the characterization and sorting of recycled black plastics**. The anticipated outcome is the formulation of a strategic development plan aimed at enhancing product circularity within the recycling industry. To accomplish this, three distinct interrelated objectives have been established:

Objective 1: Evaluate the Effectiveness of THz Technology for Black Plastic Identification

The primary objective of this project is to assess the feasibility and efficiency of using terahertz (THz) technology, including both time-domain spectroscopy (THz-TDS) and continuous wave (CW) THz spectroscopy, for the identification and sorting of black plastics. This involves a comprehensive investigation into the capabilities of THz technology to accurately differentiate between various types of black plastics based on their unique spectral fingerprints. The evaluation will include a comparative analysis of THz technology against traditional NIR, SWIR, and MIR-technologies to determine its relative advantages and limitations in real-world recycling environments.

Objective 2: Develop and Optimize THz-Based Sorting Algorithms

Building upon the results from the first objective, the second objective focuses on the development and optimization of machine learning algorithms for the automated sorting of black plastics using THz spectral data. This involves creating a robust database of THz spectral fingerprints for various black plastic polymers and training machine learning models to classify

these polymers with high accuracy. The goal is to refine these algorithms to ensure they are efficient, reliable, and capable of being integrated into existing recycling facility operations, thereby enhancing the overall efficiency and accuracy of the sorting process [11].

Objective 3: Implement and Test Single-Frequency THz Systems Using Commercial Tools

The final objective is to develop and implement practical strategies for integrating single-frequency THz technology into existing recycling frameworks, using commercially available tools. This involves selecting suitable commercial single-frequency THz systems and developing a cost-effective, scalable solution that can be seamlessly incorporated into industrial recycling facilities. The project will address potential challenges such as system compatibility, throughput rates, and operational costs. Additionally, this objective includes pilot testing the integrated THz-based sorting system in real-world conditions to validate its performance and making necessary adjustments to ensure the technology can be successfully adopted on a large scale.

Methodological Approach:

This challenge will be realized at École de technology supérieure (ÉTS). The project will start with an in-depth review of existing literature related to THz technology applications in material characterization, particularly within the context of plastics recycling and the challenges posed by black pigments. A diverse range of black plastic samples commonly encountered in recycling streams will be collected with the preliminary focus on: High-Density Polyethylene (HDPE), Low-Density Polyethylene (LDPE) and Polypropylene (PP) as commodity polymers as well as Acrylonitrile Butadiene Styrene (ABS) Black, High Impact Polystyrene (PS), and Polyoxymethylene (POM) as engineering polymers. These polymers are representative of plastic waste encountered in different applications, especially packaging which is the main generator of plastic waste.

To collect spectroscopy information for this project, our team will use the available resources at ÉTS. First of all, Nicolet 6700 FT-IR Spectrometer from Thermo Fisher Scientific will be used, which is available at the Open Characterization Laboratory at ÉTS. On the other side, being a member of Microelectronics and Communications Research Lab (LaCIME), M. Zhuldybina has access to the unique instrument from TOPTICA Photonics Inc: TeraScan1550 (THz-FDS) and TeraFlashPro (ultra-rapid THz-TDS). These are tabletop THz systems. TeraScan1550 system with a tuning range extending up to 2.7 THz and TeraFlash Pro operating from 0.1 THz to 6 THz.

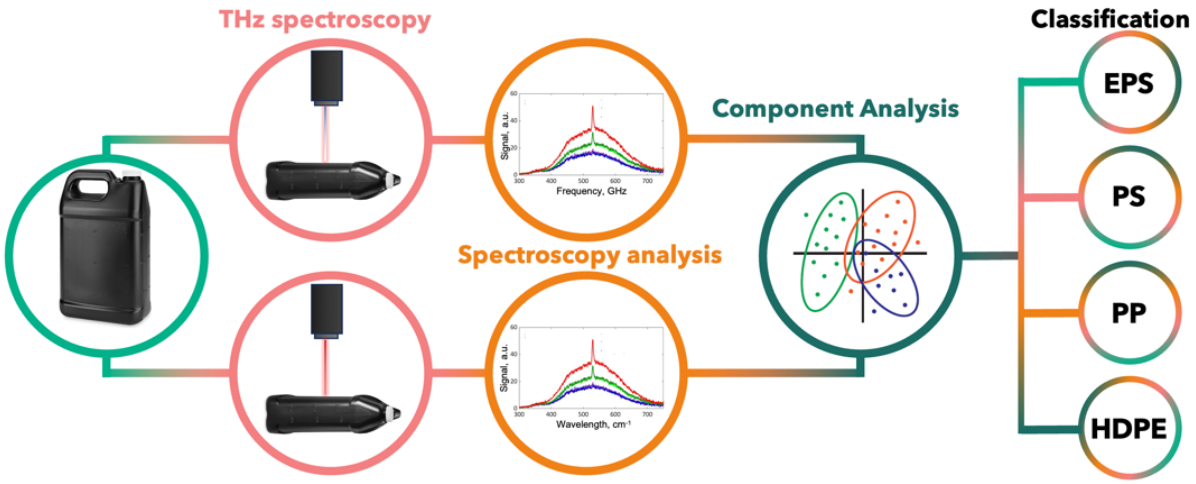

Figure 1 Schematic demonstration of project realization steps. The name of classified polymers can be varied.

Further, comprehensive comparative studies will be conducted to assess the difference in characterizing recycled black plastics using FTIR and THz instruments. The extracted transmission spectra will be evaluated, and a database containing the information about the transmission lines corresponding to various polymers will be created. It is expected that the C-H groups especially stretching vibration mode CH, CH_2 and CH will have a particular fingerprint in THz range.
To achieve the last objective, the team will acquire equipment from Eravant, which provides a compact CW THz solution for the range of 110-170 GHz. This system will be specifically tested and evaluated for its effectiveness in recycling black pigment plastic. To create a realistic testing environment, the team will set up a simulated recycling line that mimics industrial conditions. This setup will involve several steps. First, the Eravant THz CW system, known for its compact design, will be installed on a mock conveyor belt system that imitates the actual sorting lines used in recycling facilities. The team will then develop a custom bricolage to integrate the THz system into the simulated line. This will include designing mounts, supports, and interfaces to ensure the THz system can effectively scan and analyze black plastic waste as it moves along the conveyor. Next, the system will be tested with a variety of black plastic samples to assess its ability to accurately identify and sort different polymers. Key performance metrics will include sorting accuracy, processing speed, and system reliability. Based on the initial testing results, the team will make necessary adjustments to optimize the system's performance. This may involve fine-tuning the positioning of the THz equipment, enhancing the machine learning algorithms, or improving the physical setup of the simulated line. The final step will be to evaluate the feasibility of scaling the single-frequency THz system for full-scale industrial use. This will include an analysis of cost-effectiveness, integration challenges, and potential modifications required for deployment in actual recycling facilities.

Outcomes:

This project stands at the nexus of materials science, spectroscopy, and recycling technology, harnessing the distinctive capabilities of THz technology to address a pressing issue in the recycling sector—the identification and sorting of black plastics. The systematic investigation and benchmarking of THz technology against conventional methods promise to deliver substantial scientific insights and practical improvements to the recycling industry. The primary goal is to elevate the use of THz technology for sustainable recycling practices, significantly boosting the precision and efficiency of plastic recycling processes. This enhancement aligns with broader global efforts to mitigate resource depletion and minimize environmental damage, aiming to set new benchmarks for recycling efficacy that could be universally adopted.

Impact:

In terms of impact and influence on the industry, this project and the resulting transfer and valorization activities offer an opportunity to continue reflections within Quebec's recycling industries and sorting centres about the opportunities/potential offered by new technologies, such as THz, to increase plastic recycling rates. The proposed project also aims to raise awareness and hold companies, and more broadly those working in engineering, accountable for the environmental impact of decisions made during product development. More broadly, the project aims to equip the next generation by proposing methods, tools, and sharing our results to fuel their personal reflections.

From an environmental perspective and in the long term, this project aims to create drastically environmental impacts by reducing the amount of waste, often destined for landfill. The

produced waste can be reduced; hence, it is imperative to implement the creation of a suitable solution to divert them from landfilling. Using the novel inspection tool, it will be possible to sort the black plastic in a more efficient way and to keep black plastic in the circular economy and stopping it from unnecessarily going to landfill.

From a public policy perspective, the project supports circular economy initiatives via standardization of plastic color codes for simple sorting process in recycling infrastructure. The obtained results can be transferred to a producer for waste export regulations and encourage manufacturers to design products with recyclability in mind. Incentives will be offered to organizations and businesses engaged in innovative recycling solutions, such as THz technology integration.

References:

[1] Plastic Pollution - Our World in Data, https://ourworldindata.org/plastic-pollution
[2] Bonifazi, G., et al. "Black Plastic Waste Classification by Laser-Induced Fluorescence Technique Combined with Machine Learning Approaches." Waste and Biomass Valorization (2023): 1-12.
[3] Canadians share their views on better plastics labelling and tracking plastic products nationally, Government of Canada, 2023
[4] Turner, Andrew. "Black plastics: Linear and circular economies, hazardous additives and marine pollution." Environment international 117 (2018): 308-318.
[5] Araujo-Andrade, Cuauhtémoc, et al. "Review on the photonic techniques suitable for automatic monitoring of the composition of multi-materials wastes in view of their posterior recycling." Waste Management & Research 39.5 (2021): 631-651.
[6] Nogo, Kosuke, et al. "Identification of black microplastics using long-wavelength infrared hyperspectral imaging with imaging-type two-dimensional Fourier spectroscopy." Analytical Methods 13.5 (2021): 647-659.
[7] Gabriel, Djoko Sihono, and Jimmy Maulana. "Impact of plastic labelling, coloring and printing on material value conservation in the products of secondary recycling." Key Engineering Materials 773 (2018): 384-389.
[8] Signoret, Charles, et al. "Alterations of plastics spectra in MIR and the potential impacts on identification towards recycling." Resources, Conservation and Recycling 161 (2020): 104980.
[9] Bhuvanesh, N., et al. "Experimental modelling and analysis of semi-automated waste black plastic materials sorter." Materials Today: Proceedings 45 (2021): 2029-2033.
[10] Cielecki, Paweł Piotr, et al. "Identification of black plastics with terahertz time-domain spectroscopy and machine learning." *Scientific Reports* 13.1 (2023): 22399.
[11] Küter, Andries, et al. "THz imaging for recycling of black plastics." Technisches Messen 85.3 (2018): 191-201

Towards objective monitoring of Parkinson's disease progress and reaction to cures: optimizing deep-brain stimulation effects with retinal eye-tracker (Health Challenge)

Parkinson's disease, a growing global concern with no cure, presents a significant health challenge to the aging population. While Deep Brain Stimulation (DBS) offers some patient relief, optimizing its effectiveness for each patient remains a hurdle due to the need of extensive subjective assessments. This project proposes a novel solution: using a high-precision retinal eye tracker to assess eye movements in Parkinson's disease patients.

Eye movement abnormalities are a common feature of Parkinson's disease and hold promise as both diagnostic and treatment monitoring tools. Our retinal eye tracker offers a distinct advantage over existing technologies. It boasts superior accuracy and eliminates the need for patient cooperation, making it ideal for clinical settings.

Our project unfolds in two phases. Phase 1 establishes a baseline by recording eye movements during visual tasks in healthy controls and Parkinson's disease patients. This data will create a foundation for differentiating Parkinson's disease patients from healthy individuals. In Phase 2, conducted in a clinical setting, we will assess how DBS parameter adjustments affect eye movements in Parkinson's disease patients. By analyzing these changes, we aim to identify the optimal DBS settings for each individual, maximizing symptom reduction while minimizing side effects.

The successful outcome of this project has the potential to revolutionize Parkinson's disease management. We envision developing an objective and non-invasive diagnostic tool for Parkinson's disease based on eye movement analysis. Additionally, this project will pave the way for optimizing DBS therapy, leading to targeted symptom control, improved quality of life for patients, and potentially reduced healthcare costs. Furthermore, the ability to detect Parkinson's disease earlier through eye movement analysis could lead to earlier intervention strategies, potentially slowing disease progression and improving long-term patient outcomes. Finally, the success of this project could have broader implications for the field of neurodegenerative diseases by establishing eye movements as a valuable tool for diagnosis and treatment optimization in other neurological conditions.

By funding this project, you will contribute significantly to advancements in Parkinson's disease diagnosis and therapy, ultimately improving the lives of patients battling this debilitating, incurable disease.

Towards objective monitoring of Parkinson's disease progress and reaction to cures: optimizing deep-brain stimulation effects with retinal eye-tracker

Parkinson's disease: a major global health concern

Global aging trends are driving a significant increase in neurodegenerative diseases, with Parkinson's disease (PD) being a critical concern. The World Health Organization reports a doubling of PD cases in the past 25 years, reaching 8 million people worldwide [1]. This highlights the urgent need for research and improved management strategies as the aging population faces an increasingly growing burden from Parkinson's disease. At present, no cure exists for Parkinson's disease.

Parkinson's disease is characterized by neuron loss in the *substantia nigra* of the brain. This region of the brain is crucial for movement coordination, including eye movements [4]. Consequently, beyond the familiar core motor symptoms like tremor, rigidity, and bradykinesia, roughly 75% of Parkinson's disease patients exhibit concomitant eye movement abnormalities [5].

These impairments primarily involve saccades, which are rapid eye shifts, and smooth pursuit, the action of tracking moving objects. Parkinson's disease patients demonstrate decreased saccadic speed, amplitude, and frequency, particularly during complex visual tasks [6-10]. Additionally, patients exhibit increased latency in memory-guided saccades as well as antisaccade tasks -- or the resisting of reflexive eye movements [11]. Smooth pursuit is also compromised, with reduced gain (eye vs. visual target velocity) and accuracy [12, 13]. Moreover, Parkinson's disease patients show reduced fixation stability and increased microsaccades, or tiny eye flicks, even while fixating on a stationary point [14]. These eye movement disorders hold promise as both biomarkers for PD and for differentiating it from other neurodegenerative diseases [15-17]. Furthermore, analysis of eye movements in Parkinson's disease extends beyond aiding early diagnosis. It serves as a valuable tool to monitor disease progression and assess treatment efficacy.

Deep Brain stimulation: a non-pharmacological therapeutic approach

State of the art implantable pulse generators currently allow sending delicately crafted electric signals to the cerebral regions responsible for the control of body movements. Deep Brain Stimulation (DBS) offers significant relief for Parkinson's patients by disrupting abnormal brain activity, reducing motor and non-motor symptoms including eye movement disorders [18, 19]. It improves saccade latency, smooth pursuit accuracy and fixation stability [20-22]. DBS is a promising therapy for inhibiting brain activity associated to Parkinson's disease, akin to cardiac defibrillators and pacemakers, which inhibit abnormal electric activity in the heart and regulate its pulse.

Optimizing DBS therapy is a crucial step in its path to its effective use in Parkinson's disease. In particular, research suggests that a tailored set of parameters can further improve patient outcomes [23-26]. Currently, the primary challenge for DBS lies in efficiently selecting the most effective stimulation settings for every patient in four particular parameters: electrode sequence, signal frequency, amplitude and pulse width [27]. The present trial-and-error approach is not only time-consuming for both patients and doctors, but it also requires multiple clinic visits and subjective assessments [28, 29]. Additionally, improper settings can lead to ineffectiveness or contribute to adverse effects, including depression and other mental disorders, as well as eye movement issues [30-32].

Developing objective and non-invasive methods for optimal DBS parameter selection is therefore a pressing need to improve patient care and treatment efficacy in Parkinson's disease.

Advanced eye-tracking: the key to clinical success

A novel retinal eye tracker developed at Nicolaus Copernicus University offers one solution to optimize DBS therapy for Parkinson's disease. Unlike the most effective competing technology of video-based trackers which require patient cooperation and calibration, our scanning laser retinal tracker is capable of measuring eye movements using retinal blood vessel location, which obviates the need for calibration and enables straightforward clinical assessment for non-communicative patients [33]. In particular, our technology boasts superior precision (up to 0.0005°) and accuracy (up to 0.02°) when compared with state-of-the-art commercially available video trackers (0.06° and 0.25° respectively) [34, 35]. Additionally, its integrated LED display allows presenting visual tasks to assess fixations, saccades, and smooth pursuit – all crucial for monitoring DBS effectiveness in Parkinson's disease. By precisely capturing the subtle changes in eye movements related to DBS parameter adjustments, this retinal tracker holds promise for objective and efficient DBS optimization, improving patient care and treatment outcomes.

This project investigates the use of a novel retinal eye tracker to assess eye movements in Parkinson's disease (PD) and optimize DBS therapy. Phase one involves recording eye movements during visual tasks in healthy controls and symptomatic patients. This process aims to create a baseline library of eye movement patterns to differentiate patients with symptoms from healthy, control individuals. Phase two, conducted in a clinical setting with the support of neurosurgeons, will quantitatively assess the actual impact of DBS parameter adjustments on eye movements in pathologically significant patients. By observing the effect of parameter value scans, we aim to identify the optimal DBS settings for each patient, with the goal of maximizing symptom reduction and minimizing side effects.

In order to facilitate these studies, our existing retinal tracker prototype requires major modifications to be adapted for use with elderly patients with physical limitations, who make up a significant portion of the typical patient population. Technical upgrades required include enhanced optical system for better retinal imaging and displaying complex visual tasks beyond simple "follow-the-dot" paradigms. Likewise, suitable chin and headrest stability for accurate measurements in spite of severe motor impairment will enable the assessment of patients with a range of symptoms. These refinements will significantly improve eye movement data collection, reducing patient and doctor time commitment.

Ultimately, our high-precision retinal tracker will enable the detection of delicate eye movement changes, contributing to early PD diagnosis, but also to serving as a clinical guide in DBS parameter adjustments for personalized treatment.

Outcome

This project holds significant promise for revolutionizing the use of DBS therapy for Parkinson's disease by leveraging our novel retinal eye tracking technology as a tool for objective and personalized treatment optimization. By meticulously analyzing these patterns using the high-precision retinal tracker, the project aims to identify distinct eye movement characteristics associated with Parkinson’s disease. This newfound knowledge will pave the way for the development of an accessible, non-invasive and objective diagnostic tool for Parkinson’s disease, potentially leading to clinical therapeutic intervention.

The project's significance extends beyond optimizing DBS therapy for existing patients. The high accuracy of the retinal tracker, offers the exciting potential for earlier diagnosis. By accurately identifying these early-stage biomarkers, clinicians might be able to intervene with treatment strategies that could slow disease progression and improve long-term patient outcomes. This project represents a significant step forward in the development of a successful therapy for Pakinson’s disease and holds immense promise for improving the lives of patients battling this debilitating, incurable neurodegenerative disease.

Impact

The potential impact of this project's outcome is nothing short of transformative. Designing an effective, noninvasive therapy for Parkinson's disease could lead to significant improvements in patient outcomes. Namely:

- **Targeted Symptom Reduction**: By precisely pinpointing optimal DBS settings for each patient, clinicians could achieve specific, targeted symptom control. This translates to potentially reducing the tremors, rigidity, and gait disturbances, hallmarks of Parkinson's disease, while minimizing the risk of debilitating side effects like dysarthria and dyskinesias.

- **Improved Quality of Li**fe: Effective symptom control directly translates to an improved quality of life for patients. With better control over their motor functions, patients can regain independence and participate more actively in daily activities.

- **Streamlined Treatment**: Earlier diagnosis and more targeted DBS therapy could lead to significantly reduced healthcare costs associated with managing Parkinson's disease progression and its complications. Additionally, a non-invasive diagnostic tool could streamline the diagnostic process, lessening economic the burden on patients and national healthcare systems.

- **Earlier Diagnosis and Intervention**: By cataloguing ophthalmic biomarkers that allow for the early detection for Parkinson's disease, clinicians could potentially intervene with early treatment strategies that slow disease progression and improve long-term patient outcomes. Early intervention could in turn significantly impact the course of the disease and potentially delay the onset of more severe symptoms.

- **Broader Applications in clinical neurology**: The success of this project could have broader implications for the field of neurodegenerative diseases. The concept of using eye movements as a biomarker for diagnosis and treatment optimization has the potential to be applied to other neurological conditions. This new diagnostic tool could open new avenues in research and lead to significant future advancements in the overall management of other neurodegenerative diseases.

Overall, the successful outcome of this project has the potential to revolutionize DBS therapy for Parkinson's disease, leading to a future with earlier diagnosis, more effective treatment, and improved quality of life for patients battling this debilitating disease.

Literature Review

1. "Parkinson disease," https://www.who.int/news-room/fact-sheets/detail/parkinson-disease.

4. G. E. Vázquez-Vélez and H. Y. Zoghbi, "Parkinson's Disease Genetics and Pathophysiology," Annu. Rev. Neurosci. 44(Volume 44, 2021), 87–108 (2021).

5. R. A. Armstrong, "Visual Symptoms in Parkinson's Disease," Park. Dis. 2011, e908306 (2011).

6. F. Chan *et al.*, "Deficits in saccadic eye-movement control in Parkinson's disease," Neuropsychologia 43(5), 784–796 (2005).

7. C. Helmchen *et al* "Role of anticipation and prediction in smooth pursuit eye movement control in Parkinson's disease," Mov. Disord. 27(8), 1012–1018 (2012).

8. Y. Yu *et al*, "Response times for reflexive saccades correlate with cognition in parkinson's disease, not disease severity or duration," Front. Neurol. 13, (2022).

9. M. Gorges, E. H. Pinkhardt, and J. Kassubek, "Alterations of eye movement control in neurodegenerative movement disorders," J. Ophthalmol. 2014, 658243 (2014).

10. H. Matsumoto *et al.*, "Small saccades restrict visual scanning area in Parkinson's disease," Mov. Disord. Off. J. Mov. Disord. Soc. 26(9), 1619–1626 (2011).

11. R. Rodríguez-Labrada *et al.*, "Eye Movement Abnormalities in Neurodegenerative Diseases," in Eye Motility (IntechOpen, 2019).

12. M. Bareš *et al.*, "The effect of apomorphine administration on smooth pursuit ocular movements in early Parkinsonian patients," Parkinsonism Relat. Disord. 9(3), 139–144 (2003).

13. K. Frei, "Abnormalities of smooth pursuit in Parkinson's disease: A systematic review," Clin. Park. Relat. Disord. 4, 100085 (2021).

14. P. Tsitsi *et al.*, "Fixation Duration and Pupil Size as Diagnostic Tools in Parkinson's Disease," J. Park. Dis. 11(2), 865–875 (2021).

15. S. Farashi, "Analysis of vertical eye movements in Parkinson's disease and its potential for diagnosis," Appl. Intell. 51(11), 8260–8270 (2021).

16. C. A. Antoniades and M. Spering, "Eye movements in Parkinson's disease: from neurophysiological mechanisms to diagnostic tools," Trends Neurosci. 47(1), 71–83 (2024).

17. E. H. Pinkhardt *et al.*, "Differential diagnostic value of eye movement recording in PSP-parkinsonism, Richardson's syndrome, and idiopathic Parkinson's disease," J. Neurol. 255(12), 1916–1925 (2008).

20. A. Yugeta *et al*, "Effects of STN stimulation on the initiation and inhibition of saccade in Parkinson disease," Neurology 74(9), 743–748 (2010).

21. M. H. Nilsson *et al*, "Subthalamic deep brain stimulation improves smooth pursuit and saccade performance in patients with Parkinson's disease," J. Neuroengineering Rehabil. 10, 33 (2013).

22. H. a. C. Wark *et al.*, "A case report on fixation instability in Parkinson's disease with bilateral deep brain stimulation implants," J. Neurol. Neurosurg. Psychiatry 79(4), 443–447 (2008).

23. J. Roediger *et al*, "StimFit—A Data-Driven Algorithm for Automated Deep Brain Stimulation Programming," Mov. Disord. 37(3), 574–584 (2022).

24. J. Volkmann *et al*, "Introduction to the programming of deep brain stimulators," Mov. Disord. Off. J. Mov. Disord. Soc. 17 Suppl 3, S181-187 (2002).

25. M. Fabbri *et al.*, "Deep brain stimulation fine-tuning in Parkinson's disease: Short pulse width effect on speech," Parkinsonism Relat. Disord. 87, 130–134 (2021).

26. T. Xie *et al.*, "Effect of low versus high frequency stimulation on freezing of gait and other axial symptoms in Parkinson patients with bilateral STN DBS: a mini-review," Transl. Neurodegener. 6(1), 13 (2017).
27. G. Deuschl *et al.*, "Deep brain stimulation: postoperative issues," Mov. Disord. Off. J. Mov. Disord. Soc. 21 Suppl 14, S219-237 (2006).
28. D. N. Anderson *et al.*, "Optimized programming algorithm for cylindrical and directional deep brain stimulation electrodes," J. Neural Eng. 15(2), 026005 (2018).
29. W. G. Ondo and H. Bronte-Stewart, "The North American Survey of Placement and Adjustment Strategies for Deep Brain Stimulation," Stereotact. Funct. Neurosurg. 83(4), 142–147 (2005).
30. K. Hunka *et al.*, "Nursing Time to Program and Assess Deep Brain Stimulators in Movement Disorder Patients," J. Neurosci. Nurs. 37(4), 204 (2005).
31. M. Z. Zarzycki and I. Domitrz, "Stimulation-induced side effects after deep brain stimulation – a systematic review," Acta Neuropsychiatr. 32(2), 57–64 (2020).
32. J. F. Baizabal-Carvallo and J. Jankovic, "Movement disorders induced by deep brain stimulation," Parkinsonism Relat. Disord. 25, 1–9 (2016).
33. M. M. Bartuzel *et al.*, "High-resolution, ultrafast, wide-field retinal eye-tracking for enhanced quantification of fixational and saccadic motion," Biomed. Opt. Express 11(6), 3164–3180 (2020).
34. "Tobii Customer Portal," https://connect.tobii.com.
35. "EyeLink 1000 Plus," https://www.sr-research.com/eyelink-1000-plus/.

Wavefront shaping of ultrashort ultraviolet pulses with metasurfaces for the chirality study of biomolecules

Optica Foundation Challenge: Environment

PI: Maryna L. Meretska, Karlsruhe Institute of Technology (KIT)
maryna.meretska@kit.edu

1. Introduction

Ultraviolet (UV) light has been important since living organisms started to populate our planet. The UV part of the sun's spectrum governs many biochemical processes in nature. Exposure to ultraviolet light triggers vitamin D production in humans and other animals. DNA strongly absorbs UV light, leading to harmful mutations and sometimes causing skin cancer. UV light is routinely used for disinfection purposes. Some organisms developed a photoreactivation process that reverses the detrimental influences of UV light on DNA. Photosynthesis is a remarkable process in which plants use sunlight to convert carbon dioxide and water into carbohydrates and oxygen with 100% efficiency. Understanding and controlling the dynamics of photochemical reactions may pave the way to designing highly efficient absorbers of greenhouse gasses or lead to bioinspired solar cells.

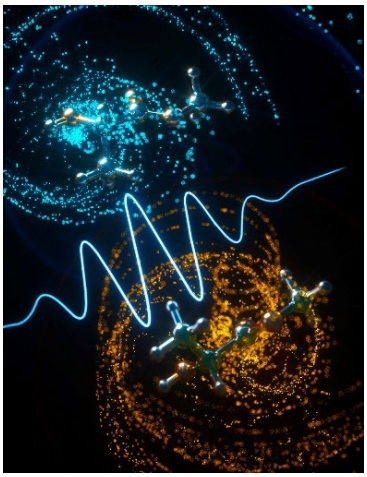

Image credit: Ella Maru Studio, Inc.

The introduction of ultrashort pulse technology, which was awarded the Nobel Prize, provided tools for investigating the dynamics of chemical processes at their intrinsic timescale. It led to several breakthroughs that unraveled electron-driven phenomena in both condensed and soft matter. Despite significant advancements in the field, studying the dynamics of biomolecules remains challenging due to the lack of advanced optical components that can operate in the UV part of the spectrum. This project aims to develop metasurface-assisted techniques to study the electron dynamics of neutral biomolecules with ultrashort UV pulses.

2. Objective

We propose using optical metasurfaces combined with an advanced ultrashort UV pulse light source to realize novel, highly sensitive measurement techniques to study chiral neutral biomolecules. Optical metasurfaces are collections of engineered sub-wavelength nanostructures on a substrate that can manipulate light on demand at the subwavelength scale. Our proposed setup comprises a light source that generates ultra-broadband UV pulses and an achromatic metasurface that shapes UV pulses. The shaped light is used to illuminate the chiral molecule of choice. The developed setup will allow the probe of previously inaccessible electron dynamics in chiral neutral biomolecules.

3. Plan

The project duration is expected to be 24 months. In the first 12 months, the development and initial characterization of metasurface for UV pulses will be performed. The next 12 months will be dedicated to measuring the electron dynamics of chiral neutral biomolecules in collaboration with Prof. Calegari's group. Her group pioneered the broadband ultrashort UV pulse light source and has extensive expertise in measuring the electron dynamics of chiral molecules.

4. Significance

We introduce a new toolkit for studying the neutral chiral molecules using a novel light source of ultrashort UV pulses combined with a metasurface that can generate structured light. The unique collaboration between Meretska and Calegari lab will allow us to demonstrate experimentally novel techniques for chirality discrimination of biomolecules. **With the availability of these tools, the proposed project offers a key step toward understanding and controlling photochemical reactions for a sustainable future.**

Wavefront shaping of ultrashort ultraviolet pulses with metasurfaces for the chirality study of biomolecules

Optica Foundation Challenge: Environment
PI: Maryna L. Meretska, Karlsruhe Institute of Technology (KIT)
maryna.meretska@kit.edu

1. Introduction

Observing events in time is an indispensable tool of science that has been used throughout humanity's history. As technology develops, events at increasingly higher speeds can be recorded, allowing new and exciting possibilities to gain insight into the world. The development of laser technologies allows for the generation of short light pulses to resolve the dynamics of chemical reactions[1]. The state-of-the-art techniques produce attosecond pulses for observing electronic motion and can provide an understanding of the first steps of chemical reaction dynamics. **This project aims to experimentally demonstrate the methodology to study electron dynamics in neutral chiral molecules using all-dielectric metasurfaces.**

2. Problem statement

The introduction of ultrashort pulse technology, which was awarded the Nobel Prize[1], revolutionized the investigation of chemical processes at their intrinsic timescale[1,2], leading to several breakthroughs that unraveled electron-driven phenomena in both condensed and soft matter. For example, attosecond pulses in the extreme ultraviolet (XUV) and soft X-rays have been used to investigate the electron dynamics of ionized targets. They are unsuitable for studying neutral biomolecules due to their high photon energy[3,4] (> 15 eV). The ultrafast optics community is currently making efforts to produce few-femtosecond pulses in the ultraviolet (UV) and vacuum-UV spectral regions[5], where the photon energy is lower than most molecular ionization potentials (<10 eV). Such pulses, with their potential to open a route to investigating UV-induced dynamics in the neutral states of biomolecules that can also be triggered by natural light, could ultimately lead to the development of schemes for photochemical control at the electron time scale[6].

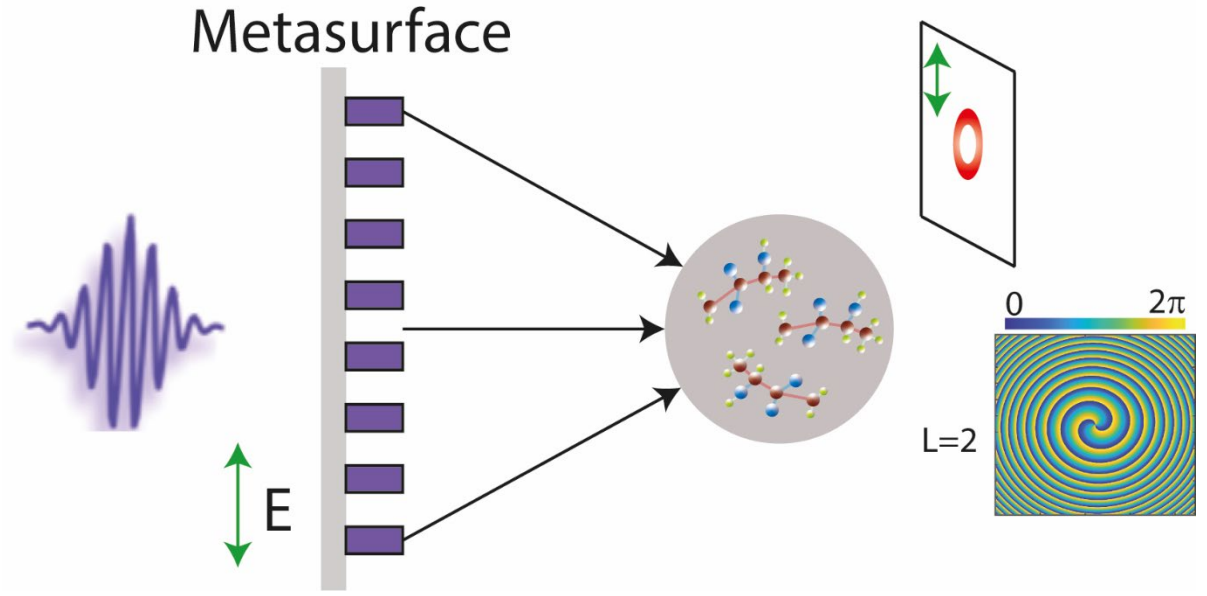

Fig. 1. Schematic of the proposed measurement setup for neutral chiral biomolecules. Linearly polarized ultrashort pulse propagates through an achromatic metasurface, generating an orbital angular momentum beam. The cross-section of the beam is shown in the top right corner. The beam illuminates biomolecules. The phase profile of the metalens with orbital angular momentum (L=2) is shown in the bottom right corner. The proposed setup will allow for the implementation of new techniques to probe molecular chirality with high-sensitivity

Many examples from nature underscore the critical need for understanding and manipulating photochemical reactions in biology using ultrashort UV pulses[5]. The ultraviolet part of the Sun's spectrum strongly influences the chemistry of life. Exposure to ultraviolet light triggers vitamin D production in humans and other animals. DNA strongly absorbs UV light, leading to harmful mutations and sometimes causing skin cancer. Some organisms use a photoreactivation process that reverses the detrimental influences of UV light on DNA. Photosynthesis is a remarkable process in which plants use sunlight to convert carbon dioxide and water into carbohydrates and oxygen with 100% efficiency.

Despite significant advancements in the field, studying the dynamics of chiral reacting biomolecules remains challenging[7]. Many advanced techniques have been developed to resolve the issues. The most common technique exploits the effect of circular dichroism (CD), which results in a tiny difference between the absorption of circularly polarized light by the enantiomers of a chiral molecule. However, this technique produces a low signal. Many efforts have been made to develop more sensitive techniques for chiral discrimination. These techniques include[7] microwave three-wave mixing, Coulomb-explosion imaging, high-harmonic generation (HHG) in weakly elliptical and bicircular laser pulses, and time-resolved photoelectron CD (TR-PECD).

The lack of commercially available optical components for advanced wavefront control hinders further development of new sensitive techniques for chiral discrimination and control. Promising techniques exploiting the spin and orbital angular momentum of ultrashort and broadband light pulses have been predicted to be highly sensitive[8], but the experimental demonstration remains unachievable. **To realize these novel approaches to studying neutral chiral biomolecules, achromatic polarization optics that can operate in the UV region is required.**

3. Objective

We propose using achromatic optical metasurfaces combined with an advanced ultrashort UV pulse light source to realize novel, highly sensitive measurement techniques to study chiral neutral biomolecules. Optical metasurfaces are collections of engineered sub-wavelength nanostructures on a substrate that can manipulate light on demand. This technology has demonstrated phase, amplitude, and polarization control of light[9–13], enabling ultra-compact, lightweight optical systems, including polarimeters[14,15] imagers, and spectrometers[16] that can operate at various spectral ranges.
Our proposed setup consists of a light source that generates ultra-broadband UV pulses developed in Prof. Calegari's group[17,18], followed by an achromatic metasurface that generates a vortex beam. The shaped light will be used to illuminate the chiral molecule of choice. The developed setup will allow the probe of previously inaccessible electron dynamics in chiral neutral biomolecules[19].

4. Approach

4.1 Broadband UV light source

Producing UV radiation with a duration of a few femtoseconds presents technological challenges due to the ultra-broadband nature of the spectra and its strong sensitivity to chromatic dispersion. This typically requires using nonlinear gas media with minimal dispersion properties compared to highly dispersive nonlinear crystals. An emerging gas-based approach involves using multi-cycle near-infrared (NIR) femtosecond pulses for ultraviolet generation through soliton dynamics in hollow-core fibers[20], offering high spectral tunability. Another method is via third-harmonic generation of NIR pulses in a highly pressurized glass cell filled with noble gas, as the Prof. Calegari group demonstrated[17,18]. They achieved the broadest and shortest UV pulses to date with a near-octave spanning spectral bandwidth between 220 to 320 nm (Fig. 2(a)). The sub-2fs time duration of these UV pulses enables the investigation of UV-induced phenomena with unprecedented temporal resolution[21]. This light source will be combined with the metasurface to generate a broadband orbital angular momentum UV light.

4.2 Metalens design

It has been demonstrated that optical metasurfaces provide advanced wavefront control for light in the UV part of the spectrum[22]. Focusing metalenses[22], self-accelerating beam generator, Airy beam generator, auto-focusing Airy optical vortex generators, holograms, and spin-multiplexed metasurfaces, optical spin latices[23] have been demonstrated to operate in the UV part of the spectrum. Moreover, many approaches to designing achromatic metasurfaces in the wavelength range from visible to mid-infrared spectrum have been demonstrated[24]. We will combine these advances in metasurface technologies to develop a broadband achromatic focusing optical vortex generator.

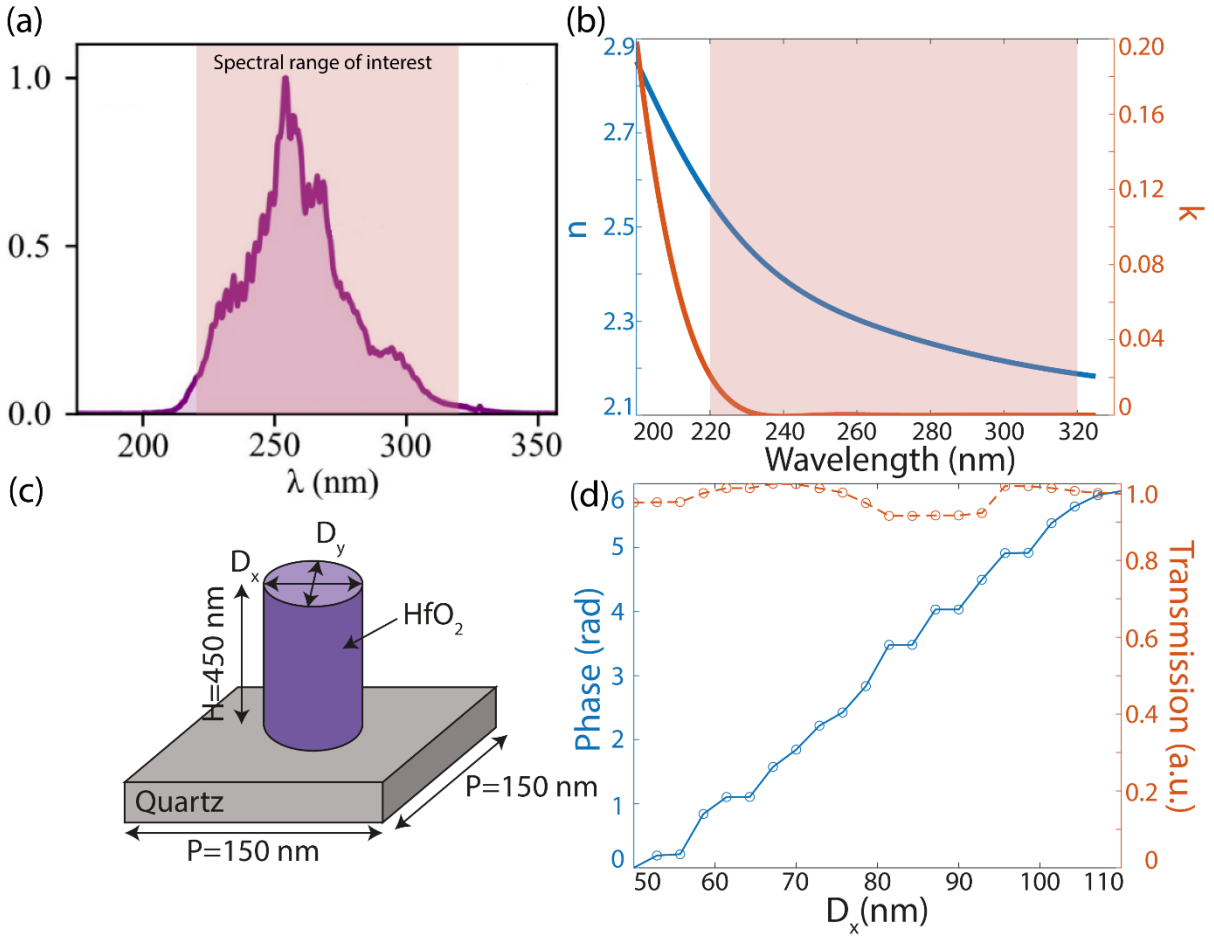

Fig. 2 (a) The spectrum generated by a UV light source developed by Prof. Calegari's group. The spectral range of interest is outlined in red. (b) Refractive index of HfO_2. The red region indicates the wavelength range of interest[22]. (c) The nanofin geometry schematic with key dimensions that are indicated in the image. (d) The exemplary library of nanofins for λ=265 nm, where D_x is sweeped and D_y=50 nm is fixed.

The first step in metasurface design is to choose the material for the nanofabrication of the metasurface. The main challenge at the UV part of the spectrum is the availability of materials with high refractive index and low absorption, as well as established nanofabrication techniques for the material of choice. In the literature, various materials such as HfO_2[22], Nb_2O_5[25], MgO[26], Si_3N_4[27], and AlN[23] have been explored to realize metasurfaces in UV. Considering the spectral extent of the light source used in this project, HfO_2 will be the material of choice, as it has the lowest absorption for the spectral range of interest (see Fig. 2(b)), and it can be patterned using a well-established atomic layer deposition technique (ALD).

The next step is choosing the metaatom geometry and generating a library of metaatoms. The generated library should consider the metaatoms' multiwavelength response to achieve an achromatic response from the designed metasurface. Fig. 2(d) shows an example of a generated metaatom library at the

wavelength λ=265 nm illuminated by linearly polarized light. The metaatom of choice is HfO_2 nanofins on a glass substrate with a height of 450 nm, a unit cell size of 150 nm, and a diameter on the x-axis varying from D_x=50 to 110 nm, where the diameter on the y-axis is kept fixed D_y=50 nm (see Fig. 2(c)). The defined range of radiuses of the nanofin provides full 0-2pi phase coverage for a given wavelength and polarization, satisfying central design requirements.

Once the multi-wavelength library is created, the metasurfaces can be designed by matching the intended phase profile with the metaatom phase response at each wavelength.

4.3 Nanofabrication

The fabrication workflow is identical to the well-established process of fabricating TiO_2 metasurfaces, which is well described in the literature[11,15] The nanofabrication of metalens is performed in three steps. In the first step, the metasurface design is fabricated in the ebeam resist. Then, HfO_2 is deposited using the low-temperature atomic layer deposition (ALD) technique, followed by the etching of excessive HfO_2 and removal of the resist.

4.4 Optical testing

The metasurface's initial optical testing will be performed at Meretska Lab using a continuous-wave (CW) UV laser that covers the wavelength of interest. The transmission setup consisting of the light source, metasurface, objective, and UV camera will be assembled. The intensity distribution behind the metasurface will be recorded by moving the objective along the lens's optical axis. The resulting 2D intensity map should reveal the OAM light beam.

In the next step, Prof. Calegari's group will test the metasurface. Her group has extensive expertise in developing measurement tools for the dynamics of chemical processes in chiral molecules. Recently, Prof. Calegari's group pioneered a new class of experiments by mapping in real time the ultrafast electronic dynamics induced by UV-excitation of chiral molecules[19]. The work revealed the impact of coherent electronic excitation on the molecular chiral response and identified the production of chiral current driven by electronic motion, providing a key element for enantio-sensitive photochemical control.

5. Significance

We introduce a new toolkit for studying the neutral chiral molecules using a novel light source of ultrashort UV pulses combined with an achromatic metasurface that can generate orbital angular momentum carrying light. The unique collaboration between Meretska and Calegari lab will allow us to demonstrate experimentally novel techniques for chirality discrimination of biomolecules. **With the availability of these tools, the proposed project offers a key step toward understanding and controlling photochemical reactions for a sustainable future.**

6. References

1. Mourou, G. Nobel Lecture: Extreme light physics and application. *Rev Mod Phys* **91**, 030501 (2019).
2. Nisoli, M., Decleva, P., Calegari, F., Palacios, A. & Martín, F. Attosecond Electron Dynamics in Molecules. *Chem Rev* **117**, 10760–10825 (2017).
3. Calegari, F. *et al.* Ultrafast electron dynamics in phenylalanine initiated by attosecond pulses. *Science* **346**, 336–339 (2014).
4. Månsson, E. P. *et al.* Real-time observation of a correlation-driven sub 3 fs charge migration in ionised adenine. *Commun Chem* **4**, 73 (2021).
5. Wanie, V., Colaizzi, L., Cartella, A., Trabattoni, A. & Calegari, F. Advances of ultraviolet light sources: towards femtosecond pulses in the few-cycle regime. in *Emerging Laser Technologies for High-Power and Ultrafast Science* (IOP Publishing, 2021). doi:10.1088/978-0-7503-2536-3ch5.
6. Calegari, F. & Martin, F. Open questions in attochemistry. *Commun Chem* **6**, 184 (2023).
7. Svoboda, V. *et al.* Femtosecond photoelectron circular dichroism of chemical reactions. *Sci Adv* **8**, 2811 (2022).
8. Ayuso, D., Ordonez, A. F. & Smirnova, O. Ultrafast chirality: the road to efficient chiral measurements. *Physical Chemistry Chemical Physics* **24**, 26962–26991 (2022).

9. Kai, Y. *et al.* High-power laser beam shaping using a metasurface for shock excitation and focusing at the microscale. *Opt Express* **31**, 31308 (2023).
10. Ossiander, M. *et al.* Metasurface-stabilized optical microcavities. *Nat Commun* **14**, 1114 (2023).
11. Lim, S. W. D. *et al.* Point singularity array with metasurfaces. *Nat Commun* **14**, 3237 (2023).
12. Palermo, G. *et al.* All-Optical Tunability of Metalenses Permeated with Liquid Crystals. *ACS Nano* **16**, 16539–16548 (2022).
13. Ossiander, M. *et al.* Extreme ultraviolet metalens by vacuum guiding. *Science* **380**, 59–63 (2023).
14. Rubin, N. A. *et al.* Matrix Fourier optics enables a compact full-Stokes polarization camera. *Science* **365**, (2019).
15. Zaidi, A. *et al.* Metasurface-enabled single-shot and complete Mueller matrix imaging. *Nat Photonics* 1–9 (2024) doi:10.1038/s41566-024-01426-x.
16. Faraji-Dana, M. *et al.* Compact folded metasurface spectrometer. *Nat Commun* **9**, 4196 (2018).
17. Wanie, V. *et al.* Ultraviolet supercontinuum generation using a differentially-pumped integrated glass chip. *Journal of Physics: Photonics* **6**, 025005 (2024).
18. Galli, M. *et al.* Generation of deep ultraviolet sub-2-fs pulses. *Opt Lett* **44**, 1308 (2019).
19. Wanie, V. *et al.* Capturing electron-driven chiral dynamics in UV-excited molecules. *ArXiv* (2023) doi:10.1038/s41586-024-07415-y. (accepted in Nature)
20. Travers, J. C., Grigorova, T. F., Brahms, C. & Belli, F. High-energy pulse self-compression and ultraviolet generation through soliton dynamics in hollow capillary fibres. *Nat Photonics* **13**, 547–554 (2019).
21. Wanie, V. *et al.* Ultraviolet supercontinuum generation using a differentially-pumped integrated glass chip. *Journal of Physics: Photonics* **6**, 025005 (2024).
22. Zhang, C. *et al.* Low-loss metasurface optics down to the deep ultraviolet region. *Light Sci Appl* **9**, 55 (2020).
23. Yu, X. *et al.* Generation of stable ultraviolet optical ring lattices using monolithic AlN metasurfaces for cooling atoms. *Opt Mater Express* **14**, 1201 (2024).
24. Chen, W. T., Zhu, A. Y. & Capasso, F. Flat optics with dispersion-engineered metasurfaces. *Nat Rev Mater* **5**, 604–620 (2020).
25. Ahmed, H., Rahim, A. A., Maab, H., Ali, M. M. & Naureen, S. Polarization insensitive all-dielectric metasurfaces for the ultraviolet domain. *Opt Mater Express* **10**, 1083 (2020).
26. Ali, F. & Aksu, S. A hybrid broadband metalens operating at ultraviolet frequencies. *Sci Rep* **11**, 2303 (2021).
27. Shafqat, M. D., Mahmood, N., Zubair, M., Mehmood, M. Q. & Massoud, Y. Highly Efficient Perfect Vortex Beams Generation Based on All-Dielectric Metasurface for Ultraviolet Light. *Nanomaterials* **12**, 3285 (2022).

Executive Summary

SISTER-PV: Storage-Integrated Solar ThERmoPhotoVoltaics

Category Environment

As humanity strives to achieve carbon neutrality by 2050, renewable energy sources like solar power become increasingly crucial. While PV systems have dominated the market due to lower costs and modularity, their intermittent energy production necessitates significant storage capacities. Concentrated solar power (CSP) offers an advantage over PV by storing energy as heat, enabling on-demand electricity generation. However, it is limited to utility-scale and can only operate up to temperatures around 500°C. Thermophotovoltaics (TPV), which uses the PV effect to convert thermal radiation from any hot source into electric power, is a breakthrough technology to replace conventional heat engines for heat-to-electricity conversion with high-temperature sources (over 1000°C). Unlike dynamic engines, the performance of TPV devices is independent of scale, and they offer better reliability and lower maintenance costs thanks to the absence of moving parts or working fluids. TPV is an increasingly active research field, owing to developments in material science and devices, which have led to impressive experimental results and several startups.

Storage-Integrated Solar TPV (SISTPV) technology combines the modularity of PV cells with the energy storage of CSP. **The SISTER-PV project aims to develop this novel energy solution, a sibling of PV cells**, by integrating TPV technology with solar absorption and thermal energy storage. Specifically, it focuses on an **innovative approach for solar absorption, exploring direct absorption in partially or fully transparent phase-change materials (PCMs) as the energy storage material.** The project will leverage the unique capabilities of the PROMES research lab in France, which specializes in high-temperature operations using concentrated sunlight.

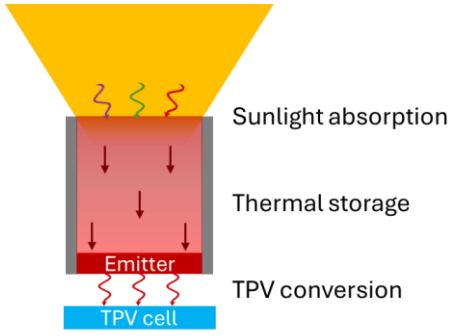

Three key goals will be pursued within the SISTER-PV project:

1. **Modeling SISTPV Systems with transparent PCMs**: Develop a fully coupled SISTPV model integrating heat transfer, sunlight absorption, and TPV power generation to identify a pathway towards 10+% efficiency.
2. **Characterizing Transparent PCMs**: Investigate the optical properties of phase-change materials (PCMs) like MgF_2 in both solid and liquid states above 1000°C.
3. **Integrating PCMs into SISTPV**: Implement and test transparent PCMs within an existing SISTPV prototype to assess durability and demonstrate electricity production with TPV cells.

The SISTPV technology has the potential to **revolutionize energy production and storage by offering a scalable and efficient solar energy solution**. It addresses the need for sustainable energy systems, contributing to global efforts to **reduce greenhouse gas emissions**. The project will generate valuable intellectual property and publications, fostering further research and development in this field. Promising results will help secure additional funding and collaborations, ultimately aiming to scale up the prototype towards commercial dimensions and achieve efficiencies comparable to current solar cells.

In conclusion, the SISTER-PV project represents a significant step forward in the quest for sustainable and reliable energy solutions, with the potential to make a profound impact on both the environment and energy markets globally.

Proposal

SISTER-PV: Storage-Integrated Solar ThERmoPhotoVoltaics

Category Environment

Literature review

Immediate coordinated action is required to secure a livable and sustainable future, as humanity must achieve carbon neutrality by 2050 to limit global warming below 1.5°C [1]. Solar cells, which directly generate electricity from sunlight through the ***photovoltaic (PV)*** effect (**Fig. 1(a)**), hold a central place in this plan. However, the transition towards an energy mix dominated by renewable sources implies ***intermittent energy production*** with little dispatchability. As a result, colossal energy storage capacities will be necessary to meet the energy demand, with time scales ranging from a few hours to a few days [2]. Indeed, the energy storage capacity is expected to grow 15-fold by 2030 relative to 2021 [3].

An alternative solar technology, known as ***concentrated solar power (CSP)***, harvests sunlight directly as thermal energy. In a solar power tower (**Fig. 1(b)**), heliostats on the ground focus sunlight onto a receiver on top of a tower. The heat is transferred and stored in molten salts at a few hundred degrees, which are used to run a steam turbine. Both CSP and PV systems currently offer a similar year-averaged efficiency of around 20%. However, the levelized cost of electricity is much lower for PV. This is partly because the modularity of PV makes it deployable at all scales (from kW to GW), while CSP is only viable at the utility-scale (over 10MW) as the turbine efficiency decreases for lower power. **As a result, PV has overtaken most of the solar energy market in the past 10 years** [4]**.**

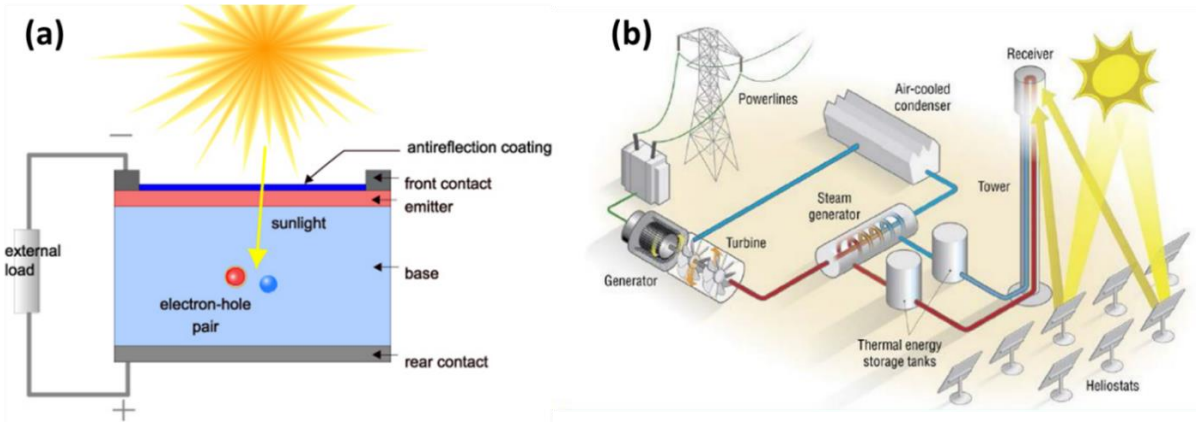

Figure 1: (a) A photovoltaic (PV) solar cell directly generates electricity from sunlight (image from pveducation.org). (b) A concentrated solar power (CSP) plant generates heat from sunlight, which is then converted into electricity using a turbine (image from energy.gov).

However, **CSP offers one crucial advantage compared to PV conversion: the integrated ability to store energy as heat and produce electricity on demand**. Indeed, thermal energy storage can be both dense and cheap, with costs below 10€/kWh, more than an order of magnitude lower than for Li-ion batteries [5]. Furthermore, **solar thermal technologies could significantly outperform PV** for high concentrations due to a much higher **theoretical efficiency limit of 85%**, versus 41% for single-junction solar cells [6]. To improve the prospects of solar thermal technologies, their operation temperature should be drastically enhanced, from ~500ºC to well over 1000ºC. To do so, material and engineering constraints on the solar receiver, storage medium, and heat engine must be addressed.

A promising way to enable **high-temperature and modular energy conversion** is to replace the steam turbine of CSP systems with ***thermophotovoltaic (TPV) cells***, a technology that uses the PV effect to convert the thermal radiation from any hot source into electric power [7]. The photons radiated by the thermal emitter are absorbed in a semiconductor, generating electron-hole pairs that can be extracted to produce electric power (**Fig. 2(a)**). Unlike dynamic engines, the performance of TPV devices is independent of scale, and they offer better reliability and lower maintenance costs thanks to the **absence of moving parts or working fluids**. Furthermore, they strongly benefit from operating at very high temperatures [8,9]. TPV has been an increasingly active research field in the past decade, owing to developments in material science and devices [10–12], leading to impressive experimental results (**Fig. 2(b)**) [13]. Indeed, several experiments have recently demonstrated TPV efficiencies above 30% [14–17], and even above 40% for temperatures above 2000ºC [18]. Following this rapid progress, TPV technology is already out of the lab, with 3 start-ups developing commercial solutions: Antora Energy [19], Fourth Power [20] and Thermophoton [21]. **However, all these systems rely on thermal batteries which are heated electrically rather than with sunlight.**

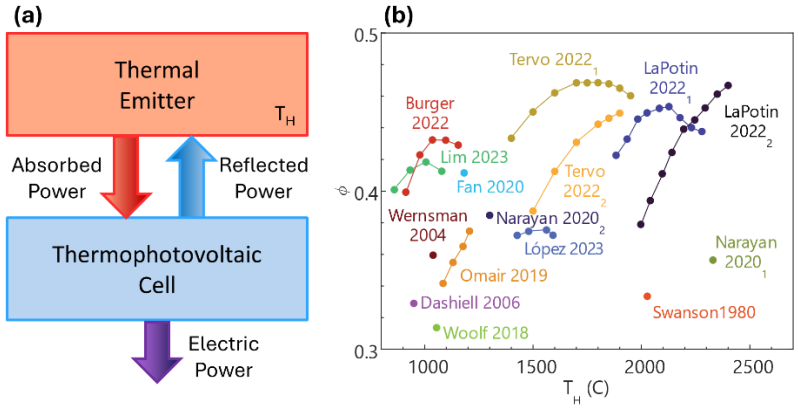

Figure 2: (a) Schematic of a TPV system. (b) Figure of merit ϕ defined as the performance relative to the thermodynamic limit for the best TPV experiments reported so far, as a function of the emitter temperature T_H. Adapted from Giteau et al. *[21]*.

Solar TPV (STPV), where an absorber heats up by collecting concentrated sunlight on one side and emits photons towards a TPV cell on the other side, has long been suggested for its potential to approach the 85% solar efficiency limit [22]. The first experiment was reported in 2013 [23]. Since then, despite significant progress on the numeric [24,25] and experimental [26,27] fronts, **the efficiency record is only 8.4%** [28]. Additionally, **all STPV experiments have so far considered direct solar-to-electricity energy conversion, neglecting storage.**

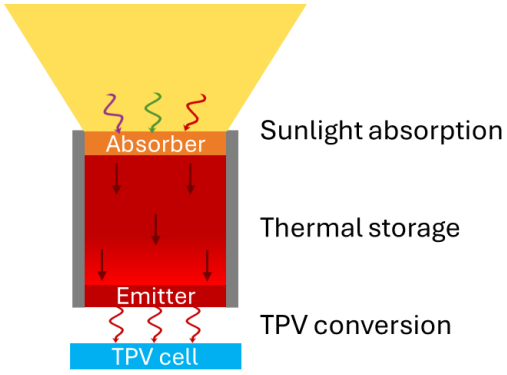

Figure 3: Sketch of a general SISTPV system

A system that combines sunlight absorption, thermal storage, and TPV electricity generation, called ***storage-integrated solar TPV (SISTPV)***, was first suggested in 2013 [29], inspired by an earlier work [30]. A SISTPV system can fundamentally be decomposed into several parts (**Fig. 3**). Sunlight is concentrated by a parabola onto a surface with high absorptivity in the solar spectrum, generating heat. This heat is transferred to a material in which it can be stored. To produce electricity, the heat is radiated by a surface with high emissivity in the infrared towards a low-bandgap TPV cell which converts thermal radiation into electricity.

Problem statement and objective

Why is there a 10x discrepancy between the theoretical limit and the efficiency record for STPV systems? And why have no complete SISTPV systems been reported to date? The main reason is that developing this technology requires a wide combination of expertise. First, a high-concentration system must be able to **focus sunlight several thousands of times**. Second, the system should **absorb all incoming sunlight while minimizing emission losses**. Third, the thermal storage unit must provide **high energy density** to enable overnight storage capacity. Fourth, the energy conversion process must be optimized, requiring **dedicated TPV cells** with characteristics significantly different from solar PV cells. Finally, the entire system must be designed to work at **very high temperatures**, which have not been previously considered for energy applications.

Since March 2024, I have been working as a postdoctoral researcher at PROMES, a research lab located in the South of France, part of CNRS (National Scientific Research Center) to tackle this broad challenge. The research conducted at PROMES focuses on **achieving very high temperatures using concentrated sunlight** for energy production and other applications. As such, the lab aggregates a unique set of tools to characterize and simulate materials and devices at very high temperatures under concentrated illumination [31]. This includes numerous solar concentration systems of various sizes, including a 6 kW vertical apparatus with a **concentration of 4500 suns** (**Fig. 4(a,b)**).

I am currently developing, on this 6 kW system, **a prototype that absorbs sunlight to store it at temperatures between 1000ºC and 1500ºC** (**Fig. 4(c)**). In particular, I am targeting **thermal energy storage as latent heat in the solid-liquid phase transition of a *phase-change material (PCM),*** initially focusing on ferroaluminum alloys. Compared to sensible heat in a solid or liquid, latent heat storage is particularly appealing for TPV conversion which does not require a working fluid, as it allows operating around a fixed temperature, enabling higher efficiency [32]. Also, latent heat storage generally offers higher energy densities, especially for materials with a very high melting temperature [5]. Furthermore, I was recently awarded a **research scientist (tenured) position at PROMES starting January 2025**, pending a final validation from CNRS in July. My general research project aims at **identifying and implementing innovative solutions to enable high-performance SISTPV systems**. As a first step, il will insert a TPV cell at the back of the prototype in **Fig. 4(c)** to **demonstrate, for the first time, a fully functional SISTPV system**.

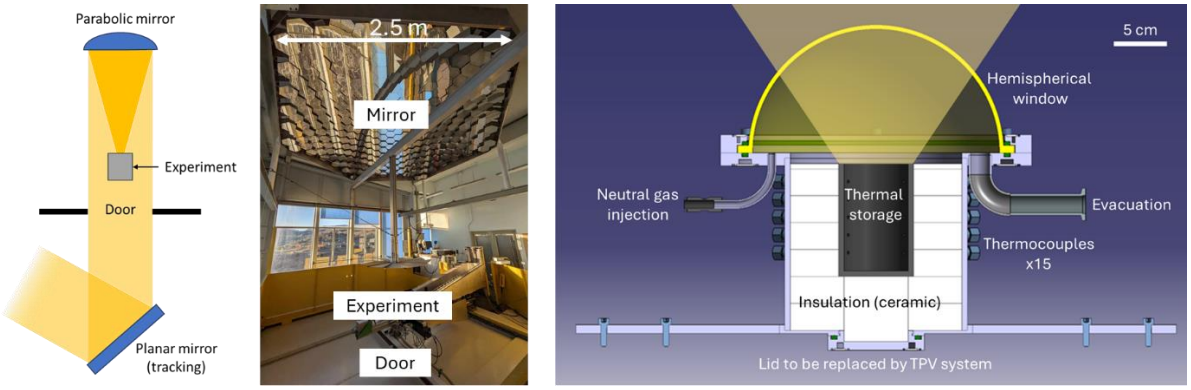

Figure 4: (a) Schematic and (b) picture of the 6 kW vertical solar concentrator system at PROMES. (c) Sketch of the thermal storage prototype currently developed at PROMES.

Photonics and optics have a critical role to play for SISTPV due to the radiative heat transfers involved both for solar absorption and TPV conversion. In particular, **angular and spectral engineering of the optical properties of the absorber, emitter, and TPV cell are aspects I have significant experience with** [33–35] and will apply to optimize SISTPV performance.

The SISTER-PV project targets the development of SISTPV technology, the younger sibling of solar cells. Specifically, it focuses on an **innovative approach for solar absorption with a large potential upside**. Typically, solar absorbers are solid materials that absorb sunlight and transfer heat to a circulating fluid underneath. SISTPV does not require a working fluid, so it not only allows but uniquely benefits from using high-temperature PCMs to store heat with high energy density at a stable temperature. One problem that arises is to make sure heat gets transferred through the PCM to fully exploit the storage capacity and minimize thermal losses. Indeed, in the prototype illustrated in **Fig. 4(c)**, the heat is absorbed at the top and must travel through the PCM, before being radiated towards the TPV cells at the bottom. This configuration creates a **temperature gradient through the system which can be detrimental to the performance and limits the possibility to upscale** (**Fig. 5(a)**).

To tackle this issue, two complementary strategies can be employed. The first is to improve heat transfer through the PCM, by selecting materials with high conductivity (as I am currently exploring with metallic alloys) and taking advantage of natural or forced convection. The second is to ensure heat absorption occurs as close as possible to the TPV emission area. This implies **optimizing the geometry of the system**, such as the shape of the storage medium and the position of the TPV cells. But this can also be addressed by **engineering optically where light gets absorbed**.

Within the SISTER-PV project, I will investigate the possibility of direct sunlight absorption in the storage PCM, without an intermediate absorber. One first advantage of this approach is that it removes the thermal resistance between the absorber and storage material. However, the main appeal of this strategy lies in the implementation of **partially or fully transparent PCMs**. **With a fully transparent PCM, absorption occurs on the inner walls of the crucible, completely reversing the thermal behavior of the system** (**Fig. 5(b)**). Alternatively, **by embedding absorbing microparticles within a transparent PCM, sunlight absorption can be homogeneous through the PCM**, minimizing the temperature gradient. Finally, more exotic optical behavior depending on the PCM phase (a PCM transparent only in the liquid or in the solid phase in certain spectral bandwidths) can lead to **optical trapping of the thermal radiation** and greatly reduce emission losses towards the sky.

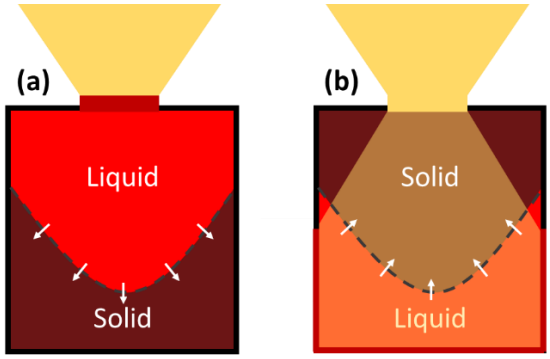

Figure 5: (a) Temperature gradient in the thermal storage unit when considering absorption occurs in a solar absorber above the PCM. The back surface remains colder until the whole PCM is melted (b) With a transparent PCM, sunlight travels through the storage material to directly heat the side walls, drastically modifying the temperature profile.

The main objective of the project is to explore the potential **benefits of implementing partially or fully transparent PCMs for SISTPV technology**. The core of the research will be conducted between January and December 2025. To assist me in this project, I will recruit a postdoctoral researcher for a duration of 12 months. I note that in the unlikely event that my CNRS position was not validated, I would still be able to conduct the SISTER-PV project by using the personnel budget allocation for my salary.

Outcomes

The detailed workflow is presented in the timeline document.

Aim 1: Model SISTPV systems with transparent PCMs

- Develop a 2D axisymmetric model of heat transfer within the transparent PCM and its walls.
- Integrate the code with sunlight absorption and TPV power generation to obtain a fully coupled description of the heat exchanges in the system and their impact on energy production.
- Determine the optimal optical properties of partially transparent PCMs.
- Identify a pathway towards 10+% efficiency with minimal modifications of the prototype.

Aim 2: Characterize transparent PCMs

- Develop a methodology to characterize the optical properties of PCMs in the liquid phase.
- Measure the optical properties of 1+ PCM (MgF_2) as a function of temperature in both phases.
- Inject the obtained data into the model (Aim 1).

Aim 3: Integrate the PCMs into a SISTPV system

- Implement 1+ transparent PCM within a graphite crucible in the SISTPV prototype.
- Track the temperature and phase of the PCM with time using a combination of optical and thermal characterization tools.
- Perform 10+ fusion cycles to test the durability of the PCM.
- Compare the data with the models (Aim 1) to identify additional relevant physical phenomena.
- Integrate a TPV cell to demonstrate power generation and compare it to the solar absorber case.

Impact

There is no doubt that SISTPV technology can bring a profound change in energy production and storage by offering modular solar energy production with integrated thermal storage. The unique skillset and experimental facilities available at laboratory PROMES, my theoretical and technical background, and the ongoing research I am conducting on the topic form an ideal combination to make the SISTER-PV project a success.

SISTPV technology remains largely unexplored and has a high potential for generating valuable outputs in terms of publications and intellectual property, a process I already have experience with [36,37]. Results will be communicated widely, in particular through interviews and featured articles for non-technical science media, which I have been invited to multiple times [38–41]. I also note that I already have a **patent and publication in preparation on the engineering of radiative properties using PCMs**, which this project will be able to build upon.

Promising results will help secure future funding to explore a broad space of partially transparent PCMs in collaboration with material science laboratories. Future goals would be to build a material database of high-temperature optical properties, to achieve efficiencies above 20% with SISTPV technology so it is comparable to that of solar cells, and to scale up the prototype towards commercial dimensions.

In terms of broader impact, the SISTER-PV project can help stimulate the renewable energy and storage market by providing a reliable and efficient solar energy solution capable of operating around the clock. It could drastically help reduce greenhouse gas emissions and environmental degradation by avoiding the need for fossil fuels or materials such as lithium and noble metals. The technology's social impact could also be significant, as it is particularly well suited for regions with high solar insolation but limited access to stable power grids.

References

[1] IPCC, 2022: Climate Change 2022: Mitigation of Climate Change., in Contribution of Working Group III to the Sixth Assessment Report of the Intergovernmental Panel on Climate Change (Cambridge University Press, 2022).

[2] P. Albertus, J. S. Manser, and S. Litzelman, Long-Duration Electricity Storage Applications, Economics, and Technologies, Joule **4**, 21 (2020).

[3] Global Energy Storage Market to Grow 15-Fold by 2030, https://about.bnef.com/blog/global-energy-storage-market-to-grow-15-fold-by-2030/.

[4] IRENA (2021), Renewable Power Generation Costs in 2021, Executive Summary, Abu Dhabi., n.d.

[5] A. Datas, Ultra High Temperature Thermal Energy Storage for Dispatchable Power Generation, in Encyclopedia of Energy Storage, edited by L. F. Cabeza (Elsevier, Oxford, 2022), pp. 141–150.

[6] M. A. Green, Third Generation Photovoltaics Advanced Solar Energy Conversion (Springer, Berlin; Heidelberg, 2003).

[7] A. Datas and R. Vaillon, Chapter 11 - Thermophotovoltaic Energy Conversion, in Ultra-High Temperature Thermal Energy Storage, Transfer and Conversion, edited by A. Datas (Woodhead Publishing, 2021), pp. 285–308.

[8] T. Burger, C. Sempere, B. Roy-Layinde, and A. Lenert, Present Efficiencies and Future Opportunities in Thermophotovoltaics, Joule **4**, 1660 (2020).

[9] A. Datas and A. Martí, Thermophotovoltaic Energy in Space Applications: Review and Future Potential, Solar Energy Materials and Solar Cells **161**, 285 (2017).

[10] A. Licht, N. Pfiester, D. DeMeo, J. Chivers, and T. E. Vandervelde, A Review of Advances in Thermophotovoltaics for Power Generation and Waste Heat Harvesting, MRS Advances **4**, 2271 (2019).

[11] R. Sakakibara, V. Stelmakh, W. R. Chan, M. Ghebrebrhan, J. D. Joannopoulos, M. Soljacic, and I. Čelanović, Practical Emitters for Thermophotovoltaics: A Review, JPE **9**, 032713 (2019).

[12] A. Datas, M. Francoeur, M. Shimizu, and R. Vaillon, Advances in Thermophotovoltaics: Materials, Devices, and Systems, Solar Energy Materials and Solar Cells **240**, 111711 (2022).

[13] M. Giteau, M. F. Picardi, and G. T. Papadakis, Thermodynamic Figure of Merit for Thermophotovoltaics, JPE **14**, 042402 (2024).

[14] D. Fan, T. Burger, S. McSherry, B. Lee, A. Lenert, and S. R. Forrest, Near-Perfect Photon Utilization in an Air-Bridge Thermophotovoltaic Cell, Nature **586**, 7828 (2020).

[15] T. Burger, B. Roy-Layinde, R. Lentz, Z. J. Berquist, S. R. Forrest, and A. Lenert, Semitransparent Thermophotovoltaics for Efficient Utilization of Moderate Temperature Thermal Radiation, PNAS **119**, e2215977119 (2022).

[16] E. J. Tervo et al., Efficient and Scalable GaInAs Thermophotovoltaic Devices, Joule **6**, 2566 (2022).

[17] J. Lim, B. Roy-Layinde, B. Liu, A. Lenert, and S. R. Forrest, Enhanced Photon Utilization in Single Cavity Mode Air-Bridge Thermophotovoltaic Cells, ACS Energy Lett. **8**, 2935 (2023).

[18] A. LaPotin et al., Thermophotovoltaic Efficiency of 40%, Nature **604**, 7905 (2022).

[19] Antora Energy, https://antoraenergy.com.

[20] Fourth Power, https://gofourth.com/.

[21] Thermophoton, http://www.thermophoton.com/.

[22] N.-P. Harder and P. W. Würfel, Theoretical Limits of Thermophotovoltaic Solar Energy Conversion, Semicond. Sci. Technol. **18**, S151 (2003).

[23] A. Datas and C. Algora, Development and Experimental Evaluation of a Complete Solar Thermophotovoltaic System, Progress in Photovoltaics: Research and Applications **21**, 1025 (2013).

[24] A. S. Rana, M. Zubair, Y. Chen, Z. Wang, J. Deng, M. T. S. Chani, A. Danner, J. Teng, and M. Q. Mehmood, Broadband Solar Absorption by Chromium Metasurface for Highly Efficient Solar Thermophotovoltaic Systems, Renewable and Sustainable Energy Reviews **171**, 113005 (2023).

[25] G. Hou, Z. Lin, Q. Wang, Y. Zhu, J. Xu, and K. Chen, Integrated Silicon-Based Spectral Reshaping Intermediate Structures for High Performance Solar Thermophotovoltaics, Solar Energy **249**, 227 (2023).
[26] A. Lenert, D. M. Bierman, Y. Nam, W. R. Chan, I. Celanović, M. Soljačić, and E. N. Wang, A Nanophotonic Solar Thermophotovoltaic Device, Nature Nanotech **9**, 2 (2014).
[27] M. Shimizu, A. Kohiyama, and H. Yugami, High-Efficiency Solar-Thermophotovoltaic System Equipped with a Monolithic Planar Selective Absorber/Emitter, JPE **5**, 053099 (2015).
[28] R. Bhatt, I. Kravchenko, and M. Gupta, High-Efficiency Solar Thermophotovoltaic System Using a Nanostructure-Based Selective Emitter, Solar Energy **197**, 538 (2020).
[29] A. Datas, D. L. Chubb, and A. Veeraragavan, Steady State Analysis of a Storage Integrated Solar Thermophotovoltaic (SISTPV) System, Solar Energy **96**, 33 (2013).
[30] D. L. Chubb, B. S. Good, and R. A. Lowe, Solar Thermophotovoltaic (STPV) System with Thermal Energy Storage, AIP Conference Proceedings **358**, 181 (1996).
[31] PROMES, https://www.promes.cnrs.fr/en/infrastructure-solaire/moyens-solaires/.
[32] A. Datas, A. López-Ceballos, E. López, A. Ramos, and C. del Cañizo, Latent Heat Thermophotovoltaic Batteries, Joule **6**, 418 (2022).
[33] M. Giteau, M. Sarkar, M. P. Ayala, M. T. Enders, and G. T. Papadakis, Design Rules for Active Control of Narrowband Thermal Emission Using Phase-Change Materials, Phys. Rev. Appl. **19**, L051002 (2023).
[34] M. Sarkar, M. Giteau, M. T. Enders, and G. T. Papadakis, Lithography-Free Directional Control of Thermal Emission, Nanophotonics **13**, 763 (2024).
[35] M. Giteau, Y. Oteki, K. Kitahara, N. Miyashita, R. Tamaki, and Y. Okada, Resonant Absorption for Multilayer Quantum Well and Quantum Dot Solar Cells, JPE **12**, 022203 (2022).
[36] M. Giteau, S. Almosni, and J.-F. Guillemoles, Hot-Carrier Multi-Junction Solar Cells: A Synergistic Approach, Appl. Phys. Lett. **120**, 213901 (2022).
[37] S. Almosni, M. Giteau, J.-F. Guillemoles, and D. Suchet, CELLULES SOLAIRES MULTI-JONCTIONS A PORTEUR CHAUD, (n.d.).
[38] Decoding Thermophotovoltaic Efficiency, https://spie.org/news/decoding-thermophotovoltaic-efficiency.
[39] S. Shaheen, Solar Cells Combining Hot Carriers and Multijunctions: Synergies and Insights from Maxime Giteau, Samy Almosni, and Daniel Suchet, JPE **12**, 032202 (2022).
[40] Reaching beyond Efficiency Limits, https://www.pv-magazine.com/2022/06/02/reaching-beyond-efficiency-limits/.
[41] A. Piccone, Combining Hot-Carrier and Multijunction Solar Cells Increases Efficiency, Lowers Cost, Scilight **2022**, 211106 (2022).

Executive Summary| Category: Environment

Energy-efficient sensor for continuous and real-time monitoring of greenhouse gas emissions

1. The Challenge: A major challenge the world is facing today is the intensive emission of greenhouse gases and air pollutants from industry, agriculture, and urban traffic. These emissions contribute to global warming and serious health problems, resulting in substantial societal costs. Greenhouse gases such as CO_2 comprising 76% and CH_4 comprising 16% are identified as the primary environmental pollutants today, which contributes to current climate crisis. A recent study finds that damage to farming, infrastructure, productivity, and health from climate change will cost an estimated $38 trillion per year by 2050. Emissions from intensive livestock production significantly contribute to global warming and various other environmental issues. Livestock's impact on global warming primarily from CH_4 emissions resulting from animal metabolism. NH_3 emissions from livestock manure contribute to several effects including adverse human health impacts and premature deaths due to fine particle formation. Farming is the primary source of ammonia (NH_3) emissions, responsible for over 50% of global NH_3 emissions. Approximately half of this NH_3 emission becomes an environmental pollutant. Additionally, agriculture ranks as the second highest contributor to CH_4 emissions, accounting for up to 31% of total emissions in the US and recognized as one of the key contributors to global warming. A recent report suggests that **Florida Everglades has become a greenhouse gas emissions hotspot** leading to global warming, climate change, and more frequent hurricanes in this area. Despite their significance, tracing and monitoring greenhouse gases in the parts-per million (ppm) level in real-time with high sensitivity and selectivity remains challenging. Therefore, the development of a low cost and reliable gas sensor capable of real-time monitoring these emissions is extremely significant.

2. Objective: The proposed effort will address the critical need for a new family of energy-efficient, compact, and cost-effective all fiber-based gas sensor for real-time monitoring of multi-species greenhouse gases (NH_3, CO_2, and CH_4) with high sensitivity, selectivity, and reliability. The proposed device is based on a unique concept: "Laser-based Absorption Spectroscopy" (**Figs. 1(a-c)**). A critical objective of this project is to build an all-fiber based gas sensor in the telecommunication window. Operating in the telecommunication wavelength regime offers the advantage of accessing high-quality, cost-effective components due to the advanced and matured optical telecommunication technology. As a result, the overall system development costs much less than comparable commercial systems.

3. Outcome: The proposed research is a unique combination of ultra-low loss near-IR fiber design and fabrication, experimental demonstrations, and prototype system assembly. The outcome of the proposal is expected to be a prototype of an all fiber-based energy-efficient, compact, reliable, and cost-effective gas sensor for multi-species gas sensing (**Fig. 1(c)**). A detection limit in the order of parts-per-million (ppm) can be obtained with an average measuring time of less than 5 s or even less with unprecedented sensitivity, selectivity and detection limit.

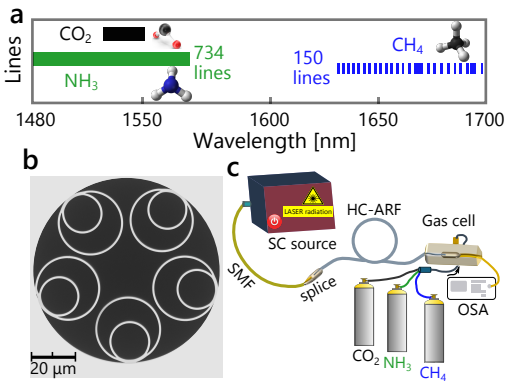

Fig. 1: (a) Molecular absorption lines of CO_2, NH_3, and CH_4. (b) SEM image of HC-ARF with a record loss of 0.79 dB/km at 1 μm, single-mode, and bend insensitive. (c) Prototype of continuous measurement of multi-species gas sensing.

4. Capability and Impact: Success in program goals will have broader societal and economical impacts since the proposed sensor will have direct impact on the industrial and agricultural sector. The success of this project can lead to "**Lab to Technology and Market**" towards commercialization, and will have positive-impact to trace and monitor greenhouse gases. The proposed sensor is of great interest for spectroscopy, environmental sensing, and medical diagnostics. Thus, funding from this proposal is vital for fully exploring its commercial potential, laying a solid foundation for market entry, and driving innovative solutions for societal benefit.

Project Description| Category: Enviroment

PI: Md Selim Habib, Florida Institute of Technology, Melbourne, USA, mhabib@fit.edu

Energy-efficient sensor for continuous and real-time monitoring of greenhouse gas emissions

1. The Challenge

The emission of extensive greenhouses gases such as carbon dioxide (CO_2), methane ($CH4$), nitrous oxide (N_2O) and ammonia (NH_3), and air pollutants from industry, intensive agriculture, and urban traffic are causing global warming and serious health problems. According to World Economic Forum, a new study finds that over the past 20 years, extreme weather events globally, like hurricanes, floods and heat waves, have cost an estimated $2.8 trillion. Due to greenhouse effect the average global temperature has already increased by about 1.2^0c since pre-industrial times. This warming trend is driving climate change, leading to rising sea levels, more frequent and severe heatwaves. For example, a growing evidence suggests that **Florida Everglades has become a greenhouse gas emissions hotspot**. This is due to draining the water and exposing the peat has made the region a significant source of greenhouse gas emissions, which are warming the global climate and contributing to impacts like hotter temperatures, rising seas and more damaging hurricanes [1]. In addition, gaseous emissions from intensive livestock production contribute to global warming and several other environmental challenges. The livestock contribution to global warming is mainly due to emissions of methane (CH_4) from animal metabolism as well as manure storage and application. Emission of CH_4 from livestock manure contribute to **(i)** human health effects and premature deaths due to fine particle formation, **(ii)** eutrophication of aquatic ecosystems, and **(iii)** acidification of soils through nitrification. Agriculture is the second highest contributor to CH_4 emission, accounting for up to 31% of total emission in the US for example [2]. The emission of CH_4 is considered among the primary contributors to earth warming [3]. In addition, monitoring of CH_4 concentrations in water is of high importance in many areas, such as fishery and water treatment plants, where rapid changes in concentrations could result in serious complications. In fishery, low levels of CH_4 concentration can expose the fish to bacterial infection and a high concentration can have lethal effects. However, controlling and legislating guidelines on greenhouse gases is hindered by the lack of cost-effective, sensitive and selective gas detection systems. Moreover, tracing and monitoring greenhouse gases in the ppm level in real-time with high sensitivity and selectivity remains challenging. Therefore, the development of a low cost and reliable gas sensor capable of continuously detecting and monitoring these emissions is **extremely significant**.

Solution: The proposed effort will address the critical need for a new family of energy-efficient, compact, and cost-effective all fiber-based gas sensor for real-time monitoring of multi-species greenhouse gases (NH_3, CO_2, and CH_4) with high sensitivity, selectivity, and reliability. The proposed device is based on a unique concept: "Laser-based Absorption Spectroscopy". For any optical fiber sensor to be practical and deployable, it is necessary for it to be compact and all-fiberized. A critical objective of this project is to build an all fiber-based gas sensor in the telecommunication window. Operating in the telecommunication wavelength regime offers the advantage of accessing high-quality, cost-effective components due to the advanced and matured optical telecommunication technology. As a result, the overall system development costs much less than the available commercial systems. Another critical objective of this project is to surmount the challenge of creating an efficient near-IR waveguiding medium that enables strong light-matter interactions with greenhouse gases (NH_3, CO_2, and CH_4). To accomplish this, the PI will utilize a novel fiber medium: **"hollow-core anti-resonant fiber (HC-ARF)"**, as it is currently the only viable solution that offers low-loss, low bend loss, and single-mode transmission [4–8]. The HC-ARF is the heart of this project, which acts as high-quality "gas-cell". HC-ARF provides exceptionally precise and well-controlled light-matter interactions, which are unattainable in any type of waveguides [9]. This unique capability holds significant promise for the development of novel applications in many emerging areas, and therefore, would be extremely impactful.

2. Literature Review and Rationale

In this section, a brief overview of the various gas sensing techniques will be discussed. Recently, several articles have been published on various gas sensors for various applications such as automobile gas emission monitoring [10], fire alarms [11], inspection of dairy products for food industries [12], etc. Most of these gas sensors are developed to target specific gases and although some of the sensors have reached commercialization, they still lack the ability for monitoring other gases such as NH_3 and CH_4. For example, sensors used for fire and smoke detectors are mostly based on photoelectric or air ionization effects, where a change in the density of air in the gas chamber triggers the alarm. Oxide semiconductors have been widely studied for gas sensing, and a major setback has been the issue of selectivity [13] and operational temperature. In attempts to increase the selectivity, dopants and additives have been used to modulate the selectivity to some extent [14] but the operational temperature still goes as high as 300^0c for detection at 1000 ppm level. A more versatile, highly sensitive and selective system is necessary for the detection and monitoring of ammonia in the atmosphere. Gas absorption spectroscopy offers a strong advantage in terms of selectivity. By utilizing the unique absorption spectrum of molecules, it is possible to target a specific gas, and the sensitivity of the system can be improved by enhancing the light-matter interaction. To this end, hollow-Core anti-resonant fibers (HC-ARFs) have attracted huge attention by virtue of their promise to deliver a unique range of optical properties that are simply not possible with conventional solid-core fiber types. In HC-ARFs, 99.99% of the power in the optical mode is confined within the hollow-core. This gives the provision of ultra-low (a tunable) optical nonlinearity, excellent power handling capabilities, low latency, and even offers the prospect of ultra-low losses, both at conventional wavelengths (e.g., around 1550 nm) and at longer wavelengths into the mid-IR where solid-core silica fibers fail [15]. Above all, the possibility of light-matter interaction within the core of these fibers is of great importance for gas sensing applications. This technology has also recently enabled their use for extreme gas-based nonlinear optics covering the extreme UV to mid-IR region [16].

In this project, the PI will demonstrate the detection of NH_3, CO_2, and CH_4 using a ultra-low loss and single-mode HC-ARF platform. In addition, the PI will investigate the absorbance of NH_3, CO_2, and CH_4 for different fiber lengths and gas-filling time. The proposed system is based on an all fiber configuration thus enhancing its robustness. The system is expected to exhibit highly repeatability and will have a response time of <5 s under only 0.5 bar pressure above the atmospheric pressure. The system can be readily tuned to target other gas molecules with absorption bands in the near-IR.

3. Key Challenges

(1) One of the key challenges of this project is to identify an efficient and versatile near-IR transmission medium with low-loss and tailored optical properties, which overlaps with the absorption spectra with NH_3, CO_2, and CH_4. **(2)** Another challenge is tracing atmospheric greenhouse gases in the ppm level in real-time with high sensitivity and selectivity–the PI will address these challenges during this project.

4. Preliminary Results

Fiber loss characterization: The PI has performed extensive FEM simulations and loss characterizations based on recently fabricated HC-ARFs to ensure that HC-ARF can guide light in the near-IR (1480–1700 nm). **Fig. 1(a)** shows the SEM image of a 5-tube nested HC-ARF. The fibers were fabricated in-house at CREOL, UCF based on the numerically optimized design

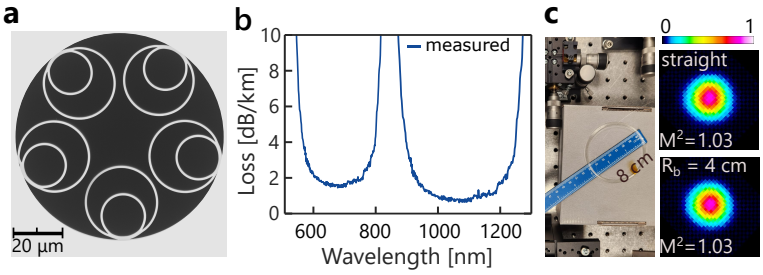

Fig. 1: SEM image and loss characterization. (a) SEM image of 5-tube nested HC-ARF, (b) loss spectra of nested HC-ARF, and (c) HC-ARF bend measurement (8cm bend diameter) with measured near-field profiles.

parameters provided by the PI. The PI's research students actively participated at CREOL in the clean room activities, fiber preform preparation, fabrication and characterization. It is noteworthy that in the U.S., "HC-ARFs can exclusively be fabricated at CREOL with a ultra low-loss of 0.79 dB/km, record power delivery of 2.2 KW, and beam quality (M^2) of 1.03 at 1080 nm [17]" and their modeling with advanced FEM-code is limited to PI's group. The fiber has a core diameter, D_c = 23 μm, average nested tube ratio $d/D \approx 0.5$, tube thickness, t_1/t_2 = 780 nm$\pm$10 nm, and gap separation between tubes, g = 2 μm. The fiber parameters are chosen ensuring the maximum transmission, according to [18]: $\lambda_m = 4t\frac{\sqrt{n^2-1}}{2m+1}, m = 0, 1, 2, ...$, where n is the glass index and t is the tube thickness. The measured loss spectra is shown in **Fig. 1(b)**. **The HC-ARF exhibits broadband ultra-low loss guidance from UV to near-IR with a record measured loss of $\sim$0.79 dB/km at 1030 nm**. The measured mode-field profiles for straight and bend fiber are shown in **Fig. 1(c)**. The mode-field confirms excellent mode-fields with near diffraction limited single-mode beam (M^2 = 1.03). The measured bend loss remains below 1 dB/km for bend diameters around 8 cm and confirms very stable mode-field profiles upon tight bending (see **Fig. 1(c)**). The fiber in **Fig. 1(a)** is optimized at 1030 nm. The PI will design and fabricate the fiber for the maximum transmission in the spectral range: 1480–1700 nm.

Ammonia (CH_4) gas detection: Recently, we reported a compact all fiber system that constitutes an hollow-core band-gap fiber (HC-PBGF) for detection of trace ammonia molecules [16]. The HC-PBGF with central transmission band at 1550 nm is used to target the $V_1 + V_3$ ammonia absorption band. Using a home-built supercontinuum source, spectrum analyzer, a telecom SMF-28 fiber, ferrule and mating sleeves, a compact all fiber system was developed that allows for effective gas detection. The enhanced light-gas interaction in the 20 μm core HC-PBGF allows for accurate monitoring of the ammonia based on absorption spectroscopy. The proposed system is robust, cost-effective and based on readily available commercial components which proffer solutions to the challenges faced in existing gas sensors. Ammonia molecules were detected in less than 5 seconds response time using a few meters of HC-PBGF with high repeatability. The preliminary findings of the ammonia gas detection will aid in developing sensors for detecting multiple gas-species. Overall, the measured beam quality, loss values, and ammonia gas detection are "highly promising", which provide PI confidence to investigate tailored light-gas interactions to achieve multi-species gas sensing.

5. Objectives: The objectives of this proposal are

Objective 1: Investigate, Design and Optimize near-IR Guiding HC-ARFs: The PI will conduct a comprehensive investigation, design, and optimization of a versatile and customized next-generation HC-ARF with record low-loss and tailored optical properties in the near-IR regime: 1480–1700 nm. The primary goal is to design HC-ARFs with ultra-low loss and bend loss, and single-mode transmission. To achieve this goal, the guiding and loss mechanism of HC-ARFs with random structural perturbations will be investigated with finite-element modeling (FEM), and Monte-Carlo technique for the first time.

Objective 2: Fabricate and Characterize near-IR guiding HC-ARFs: The PI intends to fabricate ultra-low loss HC-ARF with transmission from 1480 to 1700 nm. The optimized design parameters obtained through extensive investigations using FEM, and Monte-Carlo technique in **objective 1** that will be used to fabricate HC-ARFs at CREOL, UCF (PI's long-term collaborator). The fiber will be provided at no cost and will be characterized in the PI's lab. The characterization of HC-ARF includes: **(a)** SEM imaging to check the fiber dimension and symmetry, and **(b)** loss measurements. Finally, the fiber length will be optimized to a desired value for enhanced light-gas interactions.

Objective 3: Develop the Sensor for Real-Time Monitoring of Greenhouse Emission: The end goal of this project is to develop the first-of-its-kind energy-efficient, compact, fast, reliable, and sensitive fiber-based gas sensor for greenhouse gas detection. This will be achieved by utilizing a versatile and customized HC-ARF, which will be deployed in a stand-alone device incorporating supercontinnum (SC) source, HC-ARF, optical spectrum analyzer, and a few optical components.

6. Experimental Plan

SC laser characterization: In this project, the characterization of SC laser is crucial so that it overlaps the absorption with the CO_2, NH_3, and CH_4. A relatively easy-to-build fiber-coupled, in-house made SC laser will be used for the experiment (the PI will collaborate with Dr. Christos Markos, DTU Electro). The SC laser uses a directly modulated telecom-range diode laser based amplifier (MLT-PLR-OEM20, Manlight) operating at 1550 nm as a pump laser with 3.2 ns pulse duration. The pump laser is driven by an external pulse generator (TG2000, AIM-TTi), which is tunable from 30 kHz to 100 kHz. This tunability is vital for our application because the peak power is consequential in determining the broadening of the SC spectrum. The pulses from the laser are used to pump a standard dispersion-shifted fiber (DSF) (DCF4, Thorlabs) with a ZDW close to 1550 nm; this means our pump is very close to the ZDW, which is essential for standard SC generation [20]. The fiber output of the pump laser will be directly spliced using a commercial splicer (FSM-100P+, Fujikura) on to the DSF so as to maximize the coupling efficiency and also for the ease of handling.

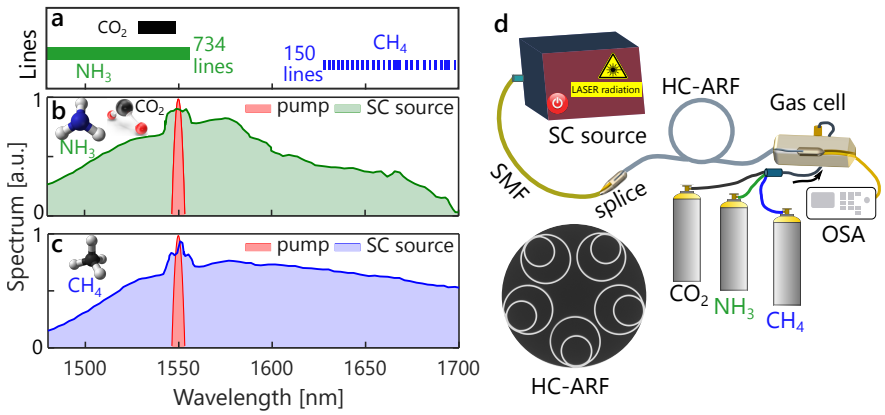

Fig. 2: SC laser characterization and experimental setup: (a) Simulation of molecular absorption lines of CO_2, NH_3, and CH_4 [19]. (b) SC generated for NH_3 and CO_2 sensing, overlaid with measured NH_3 and CO_2 absorbance (c) SC spectrum for CH_4 sensing, overlaid with measured absorbance of CH_4. (d) Schematic of multi-species gas sensing set up: The SMF from the laser is mechanically spliced to an HC-ARF, the other end of the HC-ARF is also mechanically spliced, and placed in a sealed gas-cell. Two mass flow controllers (MFCs: (EL-Flow, Bronkhorst) will be used to control the flow from N_2 and either CH_4 or NH_3. The fiber SEM image is shown in **Fig. 2(d)**.

Fiber characterization: In order to avoid back reflections from the end facet of the output fiber, the output fiber will be angle cleaved - setting a cleaving angle of about 8 degrees in the tension cleaver (CT-100, Fujikura). The angle-cleaved end of the fiber will be placed in the ferrule inside the gas-cell shown in **Fig. 2(d)**. Then the other end of the ferrule will be glued with an epoxy glue. Another ferrule of same dimensions will be used for HC-ARF, here, the facet of the fiber will be flat-cleaved because there is no issue of back reflection since the core is hollow (air). The HC-ARF is fixed into the ferrule similarly with epoxy; the two connectorized fibers will be mated with a mating-sleeve connector (Thorlabs, ADAF1). The mechanical splice will be adjusted carefully to obtain high coupling efficiency between the two fibers while still maintaining some gap between the two ends to facilitate gas diffusion into the HC-ARF. This procedure will be performed carefully under optical microscope for higher precision. The PI predicts that a gap of 80 µm between the SMF and the HC-ARF will give a coupling efficiency of 70% while maintaining sufficient path for gas diffusion. The procedure will be performed again at the other end of the HC-ARF, where an optical patch cable will be mechanically spliced to the HC-ARF and then connected to either an optical spectrum analyzer (OSA) for spectral characterization.

Output spectrum characterization: The output spectrum of the SC will be tailored to match the absorption bands of the species by switching between the settings. For NH_3 and CO_2 detection, the PI will use a repetition rate of 30 kHz and a seed current of 1700 mA to increase the power spectral density (PSD) below the pump, since the region of interest is about 1480 nm to 1550 nm (**Figs. 2(a–b)**). For CH_4 detection, the PI will use a repetition rate of 91 kHz and a seed current of 3200 mA, to increase the PSD above 1610nm, since this is the region of interest for CH_4 (**Fig. 2(a)** and **Fig. 2(c)**).

Sensor Diffusion Time: The diffusion of the gas into the fiber is a crucial factor in this experiment. Recently, we have measured the diffusion time with a small core fiber of 20 µm. The diffusion time of $<$5 s and $<$8 s for 10 cm and 45 cm fiber lengths, respectively were measured for ammonia gas [16]. The PI expects that the diffusion time will be much lower due to the large core dimension [16].

Sensor Response Time, Detection Limit, and Sensitivity: In the proposed system, the response time will be quantified by measuring the duration it takes for the gas to enter the HC-ARF, traverse the entire fiber, and exit from it, expecting response time of $<$5 s. A detection limit in the order of parts-per-million (ppm) can be obtained with an average measuring time of less than 5 s or even less is attainable with the proposed configuration. The sensor performance will be evaluated using Allan-Werle analysis [21]. The sensitivity and light-gas sample interactions can be enhanced by using a longer fiber length, which will be explored in this project. It is worth mentioning that use of long-piece of fiber will not increase the response time drastically, since a relatively large core diameter will be used. For maintaining a compact footprint, the fiber will be coiled with a small bend radius, thanks to the HC-ARF design, which exhibits low bend loss. The PI will leverage his expertise to miniaturize the proposed device through optimizing the fiber length and coiling the fiber for a small footprint for real-world applications towards a trustworthy sensor.

Sensor Reliability, Selectivity, and Size: For any sensor, reliability is important; i.e., it must give consistent results when being used repeatedly. It is expected that the proposed sensor will be highly repeatable based on our recent investigations [16], that shows consistent characteristics, thereby confirming its repeatability, unlike the metal oxides [21], and other techniques available today. Attaining sensor selectivity holds significant importance when employing spectroscopic techniques for gas sensing. The PI intends to investigate these effects experimentally during this project. In summary, the proposed device is compact and cost-effective which requires a few optical components. The device can fit comfortably on a small table or easy portability for real-time monitoring of multi-species gases.

7. Outcome

The project will deliver a compact, cheap, and all fiber-based gas sensor for multi-species gas detection (NH_3, CO_2, and CH_4) based on readily available and off-the-shelf optical components. All the above-mentioned milestones are very ambitious and of high technological and scientific interest and will be considered thus for publications in high profile international journals (Optics Letters/Express) and conferences (CLEO/FiO, USA). The key results of the project will be considered for patenting and could lead to commercialization of all fiber-based gas sensor, and will have positive-impact in the industrial and agricultural sectors. Thus, funding from this proposal is vital for fully exploring its commercial potential, laying a solid foundation for market entry, and driving innovative solutions for societal benefit.

8. Impact

This project will be a bridge between laboratory knowledge and urgent environmental demand to provide a cutting-edge technological solution for a better detection of multi-species greenhouse gases. Technologically, this project could lead to a compact, cost-effective and all fiber-based real-time monitoring gas sensor with unprecedented sensitivity, selectivity and detection limit. Success in program goals will have broader societal and economical impacts since the proposed sensor will have access to more researchers with lower cost. There is an enormous demand for the development of such devices in the industrial and farming sectors. Thus, transitioning the technology to the industry would be naturally facilitated through existing collaborations with companies engaged in building all fiber-based gas sensor and would increase partnerships between academia, industry, and others. Overall, this proposal directly addresses a problem of critical importance to the nation and society, which could create strategic partnerships between academia and industry that turn concepts and ideas into solutions that meet critical needs for society and help us all live more healthy, comfortable, and productive lives.

References Cited

[1] "Winrock website:." https:https://winrock.org/wp-content/uploads/2023/07/EAA-carbon-assessment-PEER-REVIEW.pdf.

[2] D. Chianese, C. Rotz, and T. Richard, "Simulation of methane emissions from dairy farms to assess greenhouse gas reduction strategies," *Transactions of the ASABE*, vol. 52, no. 4, pp. 1313–1323, 2009.

[3] S. C. Neubauer and J. P. Megonigal, "Moving beyond global warming potentials to quantify the climatic role of ecosystems," *Ecosystems*, vol. 18, pp. 1000–1013, 2015.

[4] F. Poletti, "Nested antiresonant nodeless hollow core fiber," *Optics Express*, vol. 22, no. 20, pp. 23807–23828, 2014.

[5] M. S. Habib, J. Antonio-Lopez, C. Markos, A. Schülzgen, and R. Amezcua-Correa, "Single-mode, low loss hollow-core anti-resonant fiber designs," *Optics Express*, vol. 27, no. 4, pp. 3824–3836, 2019.

[6] M. S. Habib, C. Markos, and R. Amezcua-Correa, "Impact of cladding elements on the loss performance of hollow-core anti-resonant fibers," *Optics Express*, vol. 29, no. 3, pp. 3359–3374, 2021.

[7] H. Sakr, Y. Hong, T. Bradley, G. Jasion, J. Hayes, H. Kim, I. Davidson, E. N. Fokoua, Y. Chen, K. Bottrill, N. Taengnoi, N. V. Wheeler, P. Petropoulos, D. J. Richardson, and F. Poletti, "Interband short reach data transmission in ultrawide bandwidth hollow core fiber," *Journal of Lightwave Technology*, vol. 38, no. 1, pp. 159–165, 2020.

[8] G. T. Jasion, H. Sakr, J. R. Hayes, S. R. Sandoghchi, L. Hooper, E. N. Fokoua, A. Saljoghei, H. C. Mulvad, M. Alonso, A. Taranta, T. Bradley, I. Davidson, Y. Chen, D. Richardson, and F. Poletti, "0.174 dB/km hollow core double nested antiresonant nodeless fiber (DNANF)," in *2022 Optical Fiber Communications Conference and Exhibition (OFC)*, pp. 1–3, IEEE, 2022.

[9] P. S. J. Russell, P. Hölzer, W. Chang, A. Abdolvand, and J. Travers, "Hollow-core photonic crystal fibres for gas-based nonlinear optics," *Nature Photonics*, vol. 8, no. 4, pp. 278–286, 2014.

[10] G. A. Bishop, J. R. Starkey, A. Ihlenfeldt, W. J. Williams, and D. H. Stedman, "Ir long-path photometry: a remote sensing tool for automobile emissions," *Analytical Chemistry*, vol. 61, no. 10, pp. 671A–677A, 1989.

[11] T. Ueda, T. Nagano, H. Okawa, and S. Takahashi, "Zirconia-based amperometric sensor using la–sr-based perovskite-type oxide sensing electrode for detection of no2," *Electrochemistry communications*, vol. 11, no. 8, pp. 1654–1656, 2009.

[12] E. N. Carmona, V. Sberveglieri, and A. Pulvirenti, "Detection of microorganisms in water and different food matrix by electronic nose," in *2013 Seventh International Conference on Sensing Technology (ICST)*, pp. 699–703, IEEE, 2013.

[13] M. Aslam, V. Chaudhary, I. Mulla, S. Sainkar, A. Mandale, A. Belhekar, and K. Vijayamohanan, "A highly selective ammonia gas sensor using surface-ruthenated zinc oxide," *Sensors and Actuators A: Physical*, vol. 75, no. 2, pp. 162–167, 1999.

[14] G. Uozumi, M. Miyayama, and H. Yanagida, "Fabrication of a cuo-infiltrated zno composite and its gas sensing properties," *Journal of materials science*, vol. 32, pp. 2991–2996, 1997.

[15] A. I. Adamu, M. Habib, C. R. Petersen, J. Lopez, B. Zhou, A. Schülzgen, M. Bache, R. Amezcua-Correa, O. Bang, and C. Markos, "Deep-UV to mid-IR supercontinuum generation driven by mid-IR ultrashort pulses in a gas-filled hollow-core fiber," *Scientific Reports*, vol. 9, no. 1, pp. 1–9, 2019.

[16] A. I. Adamu, M. K. Dasa, M. S. Habib, R. Amezcua-Correa, O. Bang, and C. Markos, "Towards an all-fiber system for detection and monitoring of ammonia," in *Frontiers in Biological Detection: From Nanosensors to Systems XI*, vol. 10895, pp. 14–21, SPIE, 2019.

[17] M. Cooper, J. Wahlen, S. Yerolatsitis, D. Delgado, D. Parra, B. Tanner, P. Ahmadi, O. Jones, M. S. Habib, I. Divliansky, J. Antonio-Lopez, A. Schülzgen, and R. Amezcua-Correa, "2.2 kW single-mode narrow-linewidth laser delivery through a hollow-core fiber," *Preprint*, 2023.

[18] W. Belardi and J. C. Knight, "Hollow antiresonant fibers with reduced attenuation," *Optics Letters*, vol. 39, no. 7, pp. 1853–1856, 2014.

[19] C. Hill, I. E. Gordon, R. V. Kochanov, L. Barrett, J. S. Wilzewski, and L. S. Rothman, "Hitranonline: An online interface and the flexible representation of spectroscopic data in the hitran database," *Journal of quantitative spectroscopy and radiative transfer*, vol. 177, pp. 4–14, 2016.

[20] J. M. Dudley, G. Genty, and S. Coen, "Supercontinuum generation in photonic crystal fiber," *Reviews of modern physics*, vol. 78, no. 4, p. 1135, 2006.

[21] A. I. Adamu, M. K. Dasa, O. Bang, and C. Markos, "Multispecies continuous gas detection with supercontinuum laser at telecommunication wavelength," *IEEE Sensors Journal*, vol. 20, no. 18, pp. 10591–10597, 2020.

Title: Machine Learning assisted Wearable Multiwavelength NIR Spectroscopy Module for Cardiovascular Risk Monitoring in various environments.

Cardiovascular diseases (CVDs) are the most prevalent and significant health challenges facing the global population. It has reached epidemic proportions, leading to substantial economic burdens, loss of productivity, and increased mortality rates. These diseases are chronic and requires long term monitoring. Cardiovascular diseases are aggrieved by various conditions. A significant strain is caused by the local environment conditions like ventilation, altitude level, etc., which affects the respiratory health. As respiratory and cardiovascular system are interdependent, the strain on respiratory health has affects on cardiovascular and vice versa. Hence, monitoring of local/indoor environment along with cardiovascular health is critical. The proposed project aims to develop a NIR (Near-Infrared) spectroscopy module, wearable and equipped with multiwavelength capabilities, for non-invasive prediction and detection of cardiovascular risk. The machine learning algorithms will combine the data of various sensor and provide accurate understanding on the nature of the cardiovascular problem. This device will significantly impact healthcare by enabling personalized monitoring, timely diagnosis, and proactive management of the associated risk.

Objective:
The multiwavelength NIR spectroscopy module will interact with the skin's surface, and underlying tissues and blood vessels. The gas sensing module will track the local environment condition like O2 and CO2 levels. The device will be combine the specific spectral patterns from individual and the local environmental factors to understand the cause and later track progress of cardiovascular disease. The spectral patterns will be a combination of both chemical changes like cholesterol levels, blood viscosity, O2 levels from various regions, etc., and physical changes in blood pressure and heart rate.

1. **Compact and Wearable Design:** The primary objective is to design a compact and user-friendly NIR spectroscopy module that can be easily worn on the skin and monitor chemical and physical parameters associated with cardiovascular diseases. The device will be non-intrusive and comfortable, allowing for continuous monitoring and seamless integration into users' daily lives.
2. **Integration with environmental effects to predict and track the damage:** The integration of O2 / CO2 sensing module will provide further insights into the effects of local ambient conditions to the cardiovascular system. Especially those living in non-ventilated environments and for individuals living/working at high altitudes.
3. **Multisensor data integration for ML assisted data analysis:** By integrating multiwavelength capabilities and gas sensing modules, the module will be able to provide various conditions relevant to cardiovascular diseases. This enhanced specificity will enable accurate detection and differentiation of various conditions, leading to better management and control of the disease. It will also help with incorporating the effects of local environment and skin conditions in the analysis.
4. **Database development:** One of the major challenges with success of such non-invasive devices is unavailability of good reference data. The work will help in creating a database which will be helpful for future researchers in improving the work.

Timely intervention based on the cardiovascular risk level can prevent or delay the progression of heart-related issues. The information of the local conditions will help in better understanding of the cause of variation in cardiovascular parameters**.** Users will be motivated to adopt healthier lifestyle choices based on real-time health data. The data will provide the doctors information to provide personalized treatment based on the individual’s local conditions.

Title: Machine Learning assisted Wearable Multiwavelength NIR Spectroscopy Module for Cardiovascular Risk Monitoring in various environments

Section 1: Background and Literature Review

Cardiovascular diseases (CVD) affect millions of people and present serious healthcare issues. Cardiovascular diseases are the leading cause of increased medical costs and death worldwide. Cardiovascular diseases encompass a range of conditions affecting the heart and blood vessels, including coronary artery disease, heart failure, and stroke. A majority of cardiovascular diseases are associated with lifestyle and environmental conditions. There are various chemical and physical indicators for monitoring cardiovascular risk. Cholesterol and triglycerides are some of the chemical indicators, and blood pressure, blood viscosity and heart rate variability are some physical indicators of cardiovascular diseases. CVD share several risk factors, including unhealthy diets, physical inactivity, tobacco use, poor environmental conditions straining the heart and excessive alcohol consumption. Early detection and management of cardiovascular diseases are crucial to reducing the associated healthcare costs, improving patients' quality of life, and ultimately decreasing the mortality rates related to these conditions.

Another important but usually ignored factors for predicting strain on the heart is environmental conditions. The environmental conditions like oxygen and CO2 levels, increases the strain on the heart as cardiovascular and respiratory conditions affect each other. Higher CO2 levels in the ambient living or work conditions can increase the load on the heart to maintain O2 concentration in the body. The environment conditions like high altitude where the air is thinner making the availability of O2 lesser during breathing, also has significant effect on the cardiovascular system by thickening the blood, higher HRV, etc. This increases the strain on the heart. These environmental conditions are also helpful in tracking the prognosis or predicting cardiovascular issues for those with existing medical conditions.

The conventional standard monitoring method for cardiovascular disease starts with ECG, and detection of biochemical biomarkers. Though ECG provide a better view to indicate problems in various regions of the heart. It misses out the effect of blood viscosity and other parameters. Also, for continuous ECG monitoring, chest straps with electrodes are available, it is inconvenient for users to wear them, making them limited to professional athletes and hospital settings. There are many fitness bands and smartwatches that help with continuously monitoring physical parameters like Heart rate variability but do not provide information about the other important factors like blood viscosity, cholesterol, etc. Also, none of the consumer grade wearable device provide information about the environmental conditions, and map it to the monitoring of vital parameters.

A promising method for non-invasive, continuous monitoring of blood and cardiovascular markers is NIR spectroscopy. NIR wavelength based non-invasive biomarkers detection have decent accuracy for cholesterol detection and blood viscosity measurements. One of the limitations of such a method is it either focuses on only cholesterol and completely ignores other chemical and physical parameters for tracking. For physical parameters monitoring, IR wavelengths can help understand the blood viscosity conditions at various skin depths, blood pressure and the heart rate variability. Mutli-wavelength sampling can help with normalization and removing the effect of other interfering factors. For this, the selection of appropriate wavelengths and tuned algorithms or models are needed for calibration. The NIR monitoring

can also help with detection of O2 and CO2 levels by selecting the ratio of appropriate wavelengths.

To understand the effect of mutli-wavelength data from multiple parameters is not easy to process. Here, various machine learning algorithms helps with predictions and generating inferences and risk factors, which will be useful for consumer grade device as well as for doctors for understanding the impact of various environment.

This project aims to combine multi-wavelength to make multiplexing of both chemical and physical biomarkers feasible, as well as compensate for variations due to sweat, skin type, and local environment. A reliable reference database and real-time algorithms are needed to achieve the required specificity.

References:

1. I. Yusoff *et al, "Non invasive cholesterol meter using Near Infrared sensor",* 2015 Innovation & Commercialization of Medical Electronic Technology Conference (ICMET), https://doi.org/10.1109/ICMETC.2015.7449581.
2. Naeije R. *"Physiological adaptation of the cardiovascular system to high altitude",* Prog Cardiovasc Dis. 2010 May-Jun;52(6):456-66. doi: 10.1016/j.pcad.2010.03.004. PMID: 20417339.
3. Neth MR, Idris A, McMullan J, Benoit JL, Daya MR. A review of ventilation in adult out-of-hospital cardiac arrest. J Am Coll Emerg Physicians Open. 2020 Apr 28;1(3):190-201. doi: 10.1002/emp2.12065. PMID: 33000034; PMCID: PMC7493547.
4. Jing Zhang, Fenfen Lei, Mingliang Li, Tao Pan, Lijun Yao, Jiemei Chen, "Spectral noise-to-signal ratio priority method with application for visible and near-infrared analysis of whole blood viscosity", Spectrochimica Acta Part A: Molecular and Biomolecular Spectroscopy, 219, 2019, 427-435. DOI: 10.1016/j.saa.2019.04.028

Section 2: Problem Statement/Objective

The prevalence of cardiovascular diseases has reached alarming levels worldwide, leading to significant economic burdens and increased mortality rates. Despite advances in medical technology, early and non-invasive detection methods remain limited.

- The primary objective of our project is to design and create a compact, wearable NIR spectroscopy module with multiwavelength capabilities. This module will continuously monitor cardiovascular risk factors, including cholesterol and triglycerides, and the measurement of physical parameters like blood viscosity, HR variability and blood pressure. Along with the direct cardiovascular markers, it will also monitor indirect but influencing parameters like local O_2/CO_2 levels which can help with monitoring at all altitudes. The device aims to improve disease management, reduce healthcare. costs, and enhance overall patient outcomes by providing real-time health insights.
    - To achieve the above objectives:
        - Optimum NIR wavelength has to be selected.
        - Position of LEDs has to be optimised.

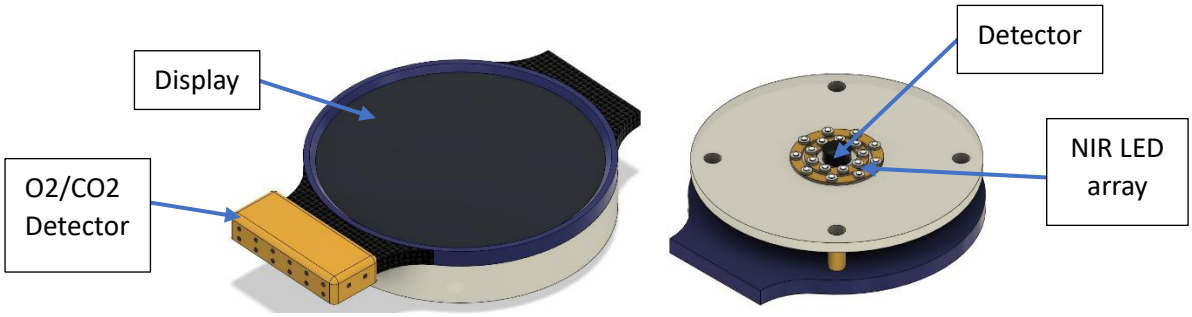

Figure 1: Representative images of the device with watch-type form factor with LED array on the back and O_2/CO_2 sensor modules on the wrist band.

- The secondary objective is to create a database of signals from the skin at various NIR wavelengths and standard values to help the global research community use it to build new Machine learning algorithms with better accuracy.

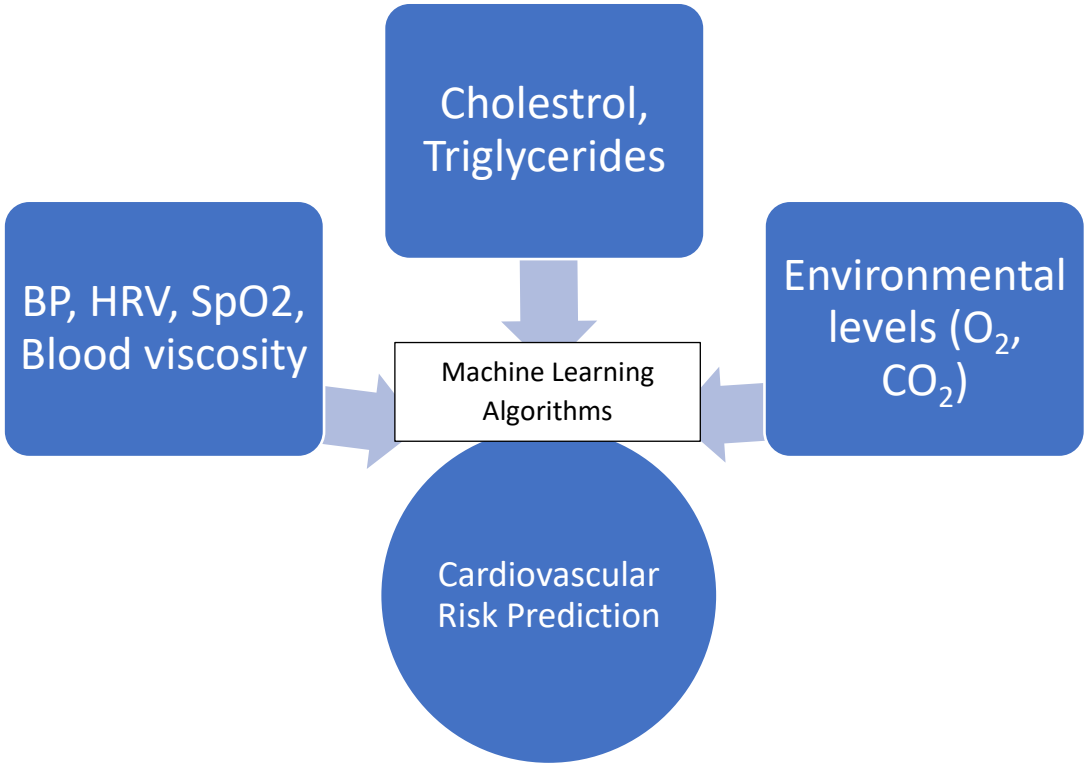

Figure 2: Multi-sensor input from multiwavelength NIR sensors for predicting cardiovascular risk.

- As the device considers environmental factors, it can help individuals living at various altitudes for personalized data, which is different from individual living at low altitudes.

Section 3: Outcomes

The expected outcomes of the project include:

1. **Compact and Wearable NIR Spectroscopy Module:** The primary objective is to design a compact and user-friendly NIR spectroscopy module that can be easily worn on the skin and monitor chemical and physical risk parameters associated with cardiovascular diseases. The device will be non-intrusive and comfortable, allowing for continuous monitoring and seamless integration into users' daily lives.
2. **Multiwavelength Functionality:** By integrating multiwavelength capabilities, the module will be able to interact with specific biomarkers relevant to cardiovascular diseases. This enhanced specificity will enable accurate detection and differentiation of these conditions, leading to better management and control of the disease. It will also help incorporate the effects of the local environment and skin conditions in the analysis.
3. **Database development:** One of the significant challenges with the success of such non-invasive devices is good algorithms. But, that is dependent on the unavailability of good reference data. The work will help create a database that will be helpful for future researchers in further developing such NIR-based non-invasive devices.
4. **Tracking impact of local living conditions:** The local living conditions like poor ventilation has not received proper monitoring in the health domain. So, data of environmental levels, can help with better prediction and analysis of the problem.
5. **Real-Time Health Monitoring:** Integration of machine learning algorithms to provide real-time health insights, empowering users to manage their conditions proactively.
6. **Validated Calibration Models for various altitudes:** Calibration models are based on extensive datasets validated against traditional laboratory measurements for robust and accurate results.

Section 4: Impact

The proposed technology has the potential to make a significant impact:

1. **Improved Disease Management:** Early and non-invasive detection will allow for timely intervention and personalized treatment plans, leading to better management of cardiovascular diseases.
2. **Economic Benefits:** The wearable module can reduce healthcare costs by minimizing complications, hospitalizations, and the need for frequent clinic visits.
3. **Enhanced Quality of Life:** Continuous health monitoring will enable users to make informed lifestyle choices, improving overall well-being.
4. **Accessible Healthcare:** In many parts of the world, healthcare is not easily accessible due to a limited number of doctors in the population or the far-off or few healthcare centers from the villages or countryside. The proposed continuous wearable device can help track chronic diseases which require care and monitoring. The data can be shared with the doctor to decide about the further course of treatment.

5. **Screening Device:** The device can also be used for screening purposes for public health monitoring purposes.
6. **Helps in further research:** The database and open-source design will help enhance the accessibility and accuracy of such devices and support a global support environment.

Section 5: Conclusion

The development of a wearable multiwavelength NIR spectroscopy module for cardiovascular disease monitoring can revolutionize healthcare by providing a cost-effective, non-invasive, and real-time monitoring solution for individuals living at all altitudes. It will also incorporate information of effect of poor ventilation, local conditions, altitudes, etc., in monitoring/predicting the cardiovascular risk. We have currently tested wavelengths from 800 nm to 1650 nm for initial testing in a circular configuration. The proposed project aims to build upon the existing literature and address the limitations of previous research, ultimately leading to better disease management and improved health outcomes for individuals worldwide. Also, the database of responses of different NIR wavelengths generated would be a valuable resource for the global research community.

EXECUTIVE SUMMARY

Reducing Battery Wastage with Wavefront-Corrected Adaptive Terahertz Tomography

Global Challenge: Environment

Background

One of the key strategies to net zero is decarbonization of passenger vehicles as well as other upcoming technologies such as IOT and medical devices, reducing electronic waste by increasing the energy storage lifecycle. It is projected that the global demand for lithium-ion batteries from a current 700 GWh to 4.7TWh by 2030. This rounds about to 70 million batteries being currently being produced and will scale to production of 470 million batteries. Currently, gigafactories hold a capacity of 10-40GWh per year of batteries. The cost of scrappage can be significant, especially for a Gigafactory reliant on high-volume production to maintain profitability. The cost of materials consumed accounts for 75% of the price of lithium-ion battery cell production. Cell production losses can be high, and a scrap rate of up to 30% is not uncommon due to poor quality. The anticipated increase in numbers in the coming years highlights the importance of prioritizing decarbonization in battery manufacturing. This involves implementing sustainable practices aimed at minimizing waste and prolonging the life cycle of batteries. Enhancing quality control methods throughout production will assist Gigafactory operators in identifying the underlying causes of battery defects.

Challenge

Lacking structural integrity can lead to overcharging, pumping in far more energy than the cell intends to which cause a significant safety concern. Optimization of these processes and identifying defects early with nondestructive (NDE) inspection may minimize battery waste. Therefore, analytical methods are crucial for assessing parameters such as porosity, thickness uniformity, surface roughness, delamination, and swelling in battery packs, especially for thin, rapidly moving, coated electrodes. Current imaging methods face limitations in resolution and depth penetration, especially when dealing with materials that are not transparent in the visible light spectrum. THz radiation, with its ability to penetrate various non-metallic materials and provide high-resolution imaging, presents a promising solution. However, challenges such as wavefront distortions, environmental variability, and limited depth resolution need to be addressed

Application and Impact

The proposed project aims to develop an innovative Terahertz (THz) tomography technique with adaptive control to tackle these challenges. For layered structures, the THz time-of-flight time domain spectroscopy will enable micron-level depth information, allowing the system to quantitatively characterize materials that are opaque in the visible spectrum and of varying thicknesses. By measuring the arrival time of pulses reflected from surface and sub-surface layers, the technique can reveal uneven coatings and interface defects. The adaptive control is facilitated through real-time control of a deformable mirror tailored for terahertz regime. This mirror ensures an adjustable beam path, maintaining consistent signal quality, rectifying turbulence induced by environmental factors such as temperature and humidity variations, and achieving optimal focus at varying depths. This technique will enable precise imaging and analysis of battery structures, allowing for early detection and correction of defects, ultimately enhancing battery safety and efficiency while minimizing waste.

Reducing Battery Wastage with Wavefront-Corrected Adaptive Terahertz Tomography

Background

One of the key strategies to net zero is decarbonization of passenger vehicles as well as other upcoming technologies such as IOT and medical devices, reducing electronic waste by increasing the energy storage lifecycle. It is projected that the global demand for lithium-ion batteries will go from a current 700 GWh to 4.7TWh by 2030 [1]. This rounds about to 70 million batteries being currently being produced and will scale to production of 470 million batteries. Currently, gigafactories hold a capacity of 10-40GWh per year of batteries. The cost of scrappage can be significant, especially for a Gigafactory reliant on high-volume production to maintain profitability. The cost of materials consumed accounts for 75% of the price of lithium-ion battery cell production. Cell production losses can be high, and a scrap rate of up to 30% is not uncommon due to poor quality [2]. The anticipated increase in numbers in the coming years highlights the importance of prioritizing decarbonization in battery manufacturing. This involves implementing sustainable practices aimed at minimizing waste and prolonging the life cycle of batteries. Enhancing quality control methods throughout production will assist Gigafactory operators in identifying the underlying causes of battery defects. A simplified understanding of a battery's internal structure comprises key components: the cathode, anode, electrolyte, and separator, which are assembled to form a cell. Following this, cells are combined to create modules. Each layer undergoes a specific preparation process before stacking. A majority of the electrode manufacturing processes are roll-to-roll of very thin metal foils as shown in figure 1.

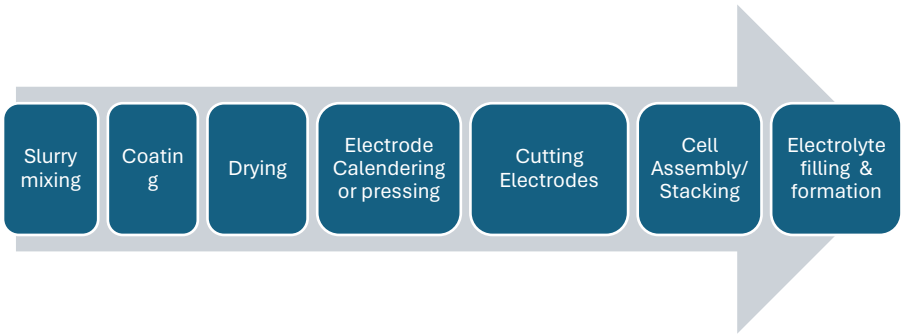

Figure 1: Li-Ion Battery Manufacturing Process Steps

Introduction to the proposed technology

Lacking structural integrity can lead to overcharging, pumping in far more energy than the cell intends to which causes a significant safety concern. Optimization of these processes and identifying defects early with nondestructive (NDE) inspection may minimize battery waste. Therefore, analytical methods are crucial for assessing parameters such as porosity, thickness uniformity, surface roughness, delamination, and swelling in battery packs, especially for thin, rapidly moving, coated electrodes.

THz technology has witnessed immense progress, driven by advancement in efficient emitters, detectors and femtosecond laser systems. These developments have propelled the field into diverse applications, including quality inspection across various industries such as automatic paint coating, paper and plastic production [3] and medical imaging [4]. Many practical applications harness the remarkable capabilities of THz radiation (0.1-10THz) such as efficient transmission through materials and distinct spectral characteristics of chemical

compounds. While THz technology has made significant strides in these areas, the development of wavefront analysis and correction devices remains limited.

The proposed project aims to develop an innovative THz tomography technique with adaptive control to tackle these challenges. The depth information is obtained through ‘time-of-flight’ time spectroscopy measurements. A micron-level resolution can be achieved when a single-cycle THz pulses reflect from layers with varying transparency, which differs from the visible range and complements white-light interferometry. The THz pulses are generated via photoconductive conversion of 800nm near-infrared pulses with a pulse duration of 100fs. The reflected pulses will have varying amplitudes (Fresnel coefficients) and time delays (phase shifts) due to the different refractive indices of materials in a battery pack, thus offering clear temporal information about the interfaces. Given its time-resolved nature, the technique encompasses a wide bandwidth, enabling it to access a broad spectrum of THz frequencies, from very low to high. The adaptive control is facilitated by a deformable mirror that offers real-time monitoring and adjustment of the beam path, with further details provided in the 'Wavefront Correction' section. This technique will enable precise imaging and analysis of battery structures, allowing for early detection and correction of defects, ultimately enhancing battery safety and efficiency while minimizing waste.

Wavefront Correction

THz time domain pulsed imaging offers a distinctive 3D image of the sample by utilizing the time-of-flight of the reflected THz pulses. However, wavefront distortions can impact the phase and amplitude data even before the THz beam interacts with the sample (see Figure 2). More insights into aberrations in conventional THz optical setups employing broadband off-axis parabolic mirrors are available in the cited paper [5]. Consequently, wavefront distortion presents a notable limitation for THz imaging, affecting the focus, depth, and spatial resolution of the resulting images.

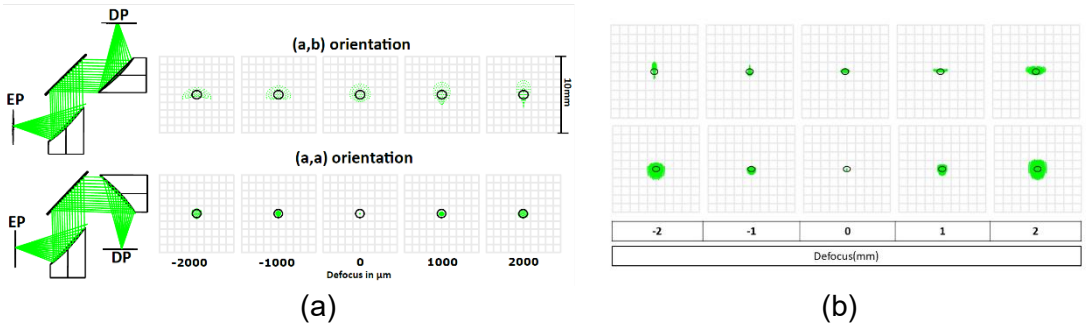

Figure 2: Zemax ray tracing and aberration analysis: (a) Reflection module with fold-mirror used in a conventional THz imaging (b) Mismatched focal length off-axis parabolic mirrors (in a 2”/3”/3”/2” sequence). The rays cover a range about 2 times wider than the diffraction-limited size at 1THz exceeding the air disk (black circle) limit.

The latest progress in beam shaping [6] and polarization control [7] is expanding the potential of THz imaging by integrating wavefront manipulation techniques. Yet, without precise understanding of the initial wavefront shape generated by the interaction of the THz beam with various optical components, these advancements are somewhat restricted [8,9]. It is anticipated that wavefront-corrected THz adaptive technology offers many advantages over other optical technologies such as optical coherence tomography and X-ray tomography, given that these have limited penetration depth and low spatial resolution. The penetration depths of THz radiation vary depending on the material, with plastics, for example, being transparent to it. This characteristic makes THz imaging advantageous in cases where battery packs

contain dense opaque layers that hinder visibility under visible light. Moreover, being non-ionizing and non-destructive, it has a lower environmental impact and may be more sustainable for long-term quality control applications. Developing a THz tomography system with deformable mirror ensures an adjustable beam path, maintaining consistent signal quality, rectifying turbulence induced by environmental factors such as temperature and humidity variations, and achieving optimal focus at varying depths.

Current deformable mirror devices are unsuitable for THz frequencies due to their limited stroke range (6-10μm), making them viable only for frequencies exceeding 10THz. The objective will be to design the device that can work in the lower THz frequency range <5THz. By developing and integrating deformable mirror devices for THz wavefront analysis and correction, in a reflection geometry, it is possible to achieve dynamic depth-resolved imaging. The adaptive control will operate in a closed-loop configuration, continually receiving feedback and adjusting the beam path to achieve a desired wavefront shape. The system employs an electro-optic detection scheme to measure the amplitude and phase of the THz waves, while changes in the wavefront shape are monitored by capturing the intensity of the probe beam (at 800nm) using a CMOS camera (see Figure 3).The design of the deformable mirror involves a thin film reflective membrane controlled by actuators, which exert either a defined force or voltage to manipulate the mirror's shape. This allows for real-time adjustments to the wavefront, facilitating precise corrections to aberrations and distortions.

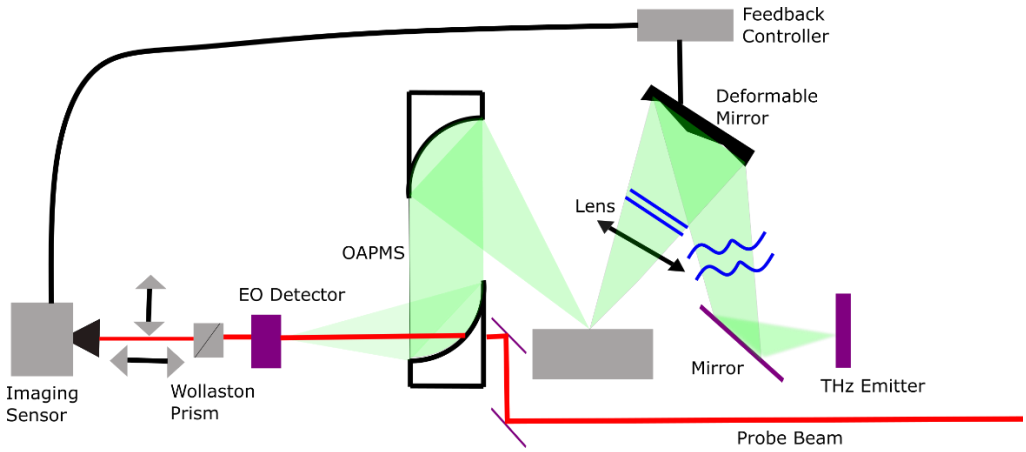

Figure 3: Conceptual view of THz optical set up with deformable mirror and closed loop control feedback for dynamic wavefront correction.

OBJECTIVES

1. Optical modelling with Zemax to optimize spectrometer design and employ finite element methods for simulating the deformable mirror device.
2. Tailoring deformable mirror (DM) device for terahertz frequencies, utilizing either a segmented or continuous mirror membrane (determined by the findings of objective 1), featuring an electrically conductive coating and standard actuator mechanisms.
3. Testing and validity of adaptive control: integration of DM into a pulsed THz time domain reflection geometry for developing calibration methods to ensure a distortion free system. The objective is to incorporate feedback from the control loop system and verify that the deformable mirror does not introduce aberrations.
4. Characterize battery cells for structural defects across three main manufacturing stages (in collaboration with Warwick manufacturing group): electrode coating (thickness 50-200μm), pressing, and stacking. Cross-compare THz data with white light interferometry; also available at the University of Warwick.

5. Utilize stage controllers to simulate manufacturing environment and capture battery images from various angles and implement 3D image reconstruction algorithms for comprehensive analysis.

OUTCOMES

1. Deformable mirror devices tailored to work for low-frequency THz range.
2. Direct wavefront sensing and aberration correction for a pulsed-THz system.
3. Automatic feedback response of wavefront shape and adaptive control of deformable mirror surface.
4. 3D image reconstruction of battery back with categorization of structure defects inspected using the developed technology.
5. Correlation of THz data with battery performance indicators to optimize the manufacture process.

REFERENCES

1. Battery 2030: Resilient, sustainable, and circular, McKinsey & Company
2. The Cost Benefits of Investing in Solutions to Reduce Battery Waste and Scrappage in Gigafactories, 2023, Hitachi High Technologies
3. Guillet, Jean Paul, Benoît Recur, Louis Frederique, Bruno Bousquet, Lionel Canioni, Inka Manek-Hönninger, Pascal Desbarats, and Patrick Mounaix. "Review of terahertz tomography techniques." Journal of Infrared, Millimeter, and Terahertz Waves 35 (2014): 382-411.
4. Sun, Qiushuo, Yuezhi He, Kai Liu, Shuting Fan, Edward PJ Parrott, and Emma Pickwell-MacPherson. "Recent advances in terahertz technology for biomedical applications." Quantitative imaging in medicine and surgery 7, no. 3 (2017): 345.
5. Chopra, Nishtha, and James Lloyd-Hughes. "Optimum optical designs for diffraction-limited terahertz spectroscopy and imaging systems using off-axis parabolic mirrors." Journal of Infrared, Millimeter, and Terahertz Waves 44, no. 11 (2023): 981-997.
6. Chopra, Nishtha, Justas Deveikis, and James Lloyd-Hughes. "Active THz beam shaping using a one-dimensional array of photoconductive emitters." Applied Physics Letters 122, no. 6 (2023).
7. Deveikis, Justas, and James Lloyd-Hughes. "Multi-pixel photoconductive emitters for the controllable generation of azimuthal and radial terahertz beams." Optics Express 30, no. 24 (2022): 43293-43300.
8. Eichenberger, Michael, Flavio Giorgianni, Nick Sauerwein, Carlo Vicario, and Christoph P. Hauri. "Deformable mirror for wavefront shaping of infrared radiation." Optics Letters 43, no. 9 (2018): 2062-2065.
9. Brossard, Mathilde, Jean-François Sauvage, Mathias Perrin, and Emmanuel Abraham. "Terahertz adaptive optics with a deformable mirror." *Optics Letters* 43, no. 7 (2018): 1594-1597.

EXECUTIVE SUMMARY

Development of $PtSe_2$ Surface-Enhanced Raman Spectroscopy (SERS) Thin Films for the Detection of Vector-borne Viruses

Dr. Phoebe Nicole G. Perez, *S&T Fellow*
Department of Science and Technology, Bicutan, Taguig, Philippines

Exacerbated by the compounding impacts of climate change and rapid urbanization, increased disease transmission and morbidity due to vector-borne viruses present a pressing global challenge. Dengue (DENV), Zika (ZIKV), and Chikungunya (CHIKV) are among the most threatening vector-borne diseases causing significant health and economic burdens, particularly in the Southeast Asia region. Worldwide, they comprise 17% of all infectious diseases and lead to 700,000 deaths annually. Among the three, Dengue is the most prevalent, causing substantial morbidity and mortality worldwide. Transmitted by the Aedes mosquito, one of the most powerful transmitters of arboviruses, about 4 billion people are at risk due to the vector's presence in 129 countries, including the Philippines. This translates to an estimated 96 million symptomatic cases and 40,000 deaths worldwide

Current diagnostic tools lack the ability to easily identify different virus serotypes, hindering effective management and surveillance efforts. This project leverages optics and photonics to develop an innovative solution to this health gap. By utilizing Raman spectroscopy and two-dimensional (2D) materials, this study aims to develop platinum diselenide ($PtSe_2$) Surface-Enhanced Raman Spectroscopy (SERS) thin films capable of accurately detecting and serotyping vector-borne viruses through the identification of optical biomarkers from DENV, ZIKV, and CHIKV. This approach offers several advantages, including rapid and precise identification of viral strains, which is essential for targeted treatment interventions and proactive outbreak control.

The three pivotal outcomes of this project contribute in the field of biomedical optics and disease diagnostics. First, this study expands the application of 2D transition-metal dichalcogenides (TMDs) for biomedical optics applications. Second, through the enhancement of the Raman signal of vector-borne viruses, this research elevates the capabilities of Raman spectroscopy, facilitating more accurate and nuanced diagnosis, with potential implications for prognosis, of vector-borne diseases. Finally, this project aims to establish a compelling complementary proof-of-concept for an ideal diagnostic tool for vector-borne diseases.

The impact of this research aligns with several Sustainable Development Goals such as SDG 3 (Good Health and Wellbeing), SDG 10 (Reduced Inequalities), SDG 11 (Sustainable Cities and Communities), and SDG 17 (Partnerships for the Goals). Socially, this research enhances disaster preparedness, lays the groundwork for future diagnostic tools, and benefits low-resource settings such as the Philippines. Economically, it aids in prognostication and reduces overtreatment costs while bolstering global health security against pandemics.

Through this project, the diagnosis and management of vector-borne diseases will be improved and would contribute to the global efforts in combating these illnesses. This innovative approach has the potential to revolutionize disease surveillance and control strategies, ultimately reducing the burden of vector-borne diseases on vulnerable populations worldwide.

PROJECT PROFILE	
Title: Development of $PtSe_2$ Surface-Enhanced Raman Spectroscopy (SERS) Thin Films for the Detection of Vector-borne Viruses	
Category: Health	
Applicant: Phoebe Nicole G. Perez, Ph.D.	
Institution: Department of Science and Technology (DOST)	**Contact Information**: phoebenicoleperez@gmail.com / pgperez@pchrd.dost.gov.ph

LITERATURE REVIEW

Vector-borne viruses have long been integrated with human history and societies, either as part of a current, emerging, or re-emerging infection. Recently, niche expansion of the vectors, as the arthropods colonize new habitats, allowed for the significant spread of the disease affecting larger populations worldwide [1]. This is attributed to a combination of factors, exacerbated by climate change, such as deforestation, urbanization, and increased air travel, all contributing to uncontrolled vector populations [2]. Furthermore, viral pathogens and other microbial symbionts contribute to vector host phenotypic plasticity affecting the structure and dynamics of disease outbreaks and future potential epidemics/pandemics. With the decline of public health services and the absence of efficient vector-control programs, many countries continue to experience a rise in cases of vector-borne diseases [3].

Global and Local Burden of Vector-borne Diseases

Vector-borne diseases cause significant morbidity among people of different ages, resulting in loss of income and increased healthcare costs. Worldwide, they comprise 17% of all infectious diseases and lead to 700,000 deaths annually. Among the different arboviral vector-borne diseases, Dengue is the most prevalent. Transmitted by the *Aedes* mosquito, one of the most powerful transmitters of arboviruses, about 4 billion people are at risk due to the vector's presence in 129 countries, including the Philippines. This translates to an estimated 96 million symptomatic cases and 40,000 deaths worldwide [3]. Other arboviral diseases include Chikungunya fever, Zika fever, and Japanese encephalitis, which were all detected previously in the Philippines. While the pandemic has dampened the number of cases in recent years, there has been a considerable increase in the number of cases in the Philippines between 2021 and 2022 (Table 1). There is also a 1.85✕ increase in the number of deaths from Dengue infections between 2021 and 2022 (Table 2).

Table 1. Cases of vector-borne diseases from 2015 to September 2022 in the Philippines (DOH data)

Cases	2015	2016	2017	2018	2019	2020	2021	2022*
Dengue	214,149	220,138	152,158	249,396	437,089	88,595	79,592	173,233
Chikungunya		6,346	2,756	2,900	1,138	157	93	509
Japanese Encephalitis	3	205	13	175	137	126	110	83
Zika	-	56	17	1	2	1	-	1

Table 2. Deaths from vector-borne diseases from 2015 to September 2022 in the Philippines (DOH data)

Deaths	2015	2016	2017	2018	2019	2020	2021	2022*
Dengue	651	1,093	811	1,241	1,681	357	286	528
Chikungunya		1	-	1	-	-	-	-
Japanese Encephalitis	-	14	1	7	5	-	4	2
Zika	-	1	-	-	-	-	-	-

Current gaps in the Clinical Management of Vector-borne Diseases (DENV, ZIKV, CHIKV) in the Philippines

Dengue virus (DENV) is a single-stranded, RNA virus under the genus *Flavivirus,* systematically classified in the family Flaviviridae. It has four distinct serotypes, all of which were endemic in the Philippines with varying frequencies of molecularly validated

sequences for the past 60 years. Diagnosis of Dengue viral infection is mostly based on reported symptoms and physical examination. It presents after 5 - 7 days of incubation, defined in three stages: febrile, critical, and convalescent [4]. Dengue patients may present as an asymptomatic, mild, or severe flu-like illness and are typically self-limiting. However, the case-fatality rate can be as high as 20% in the absence of early diagnosis and/or treatment. Severe outcomes such as dengue hemorrhagic fever (DHF) or dengue shock syndrome have been the focus of serotype association studies but serotype-to-clinical manifestations have relatively limited correlation studies [5]. Studies have shown that one of the strongest risk factors for developing severe outcomes is when a person gets infected sequentially and/or concurrently by different types of dengue fever [6]. Presently, there are no diagnostic tools used easily in the clinical setting that can detect the presence of different dengue serotypes.

Another endemic *Flavivirus* species, Zika Virus, (ZIKV) is actively transmitted in the Philippines as well. Unlike DENV, ZIKV infection's epidemiological data is very sparse (e.g. serological prevalence) and remains geographically limited, arising from sporadic outbreaks being reported [7]. The cases are generally presented as mild, although the symptoms are estimated to occur 3 - 14 days from exposure. Zika viral infection during pregnancy could result in microcephaly and other congenital malformations, referred to as Congenital Zika syndrome [8]. Serological assays widely used for monitoring these *Flavivirus* species (ZIKV and DENV) had low specificity arising from the cross-reactivity of the antibodies (i.e. IgG) or low sensitivity ascribed from the time-dependent antigen or antibody abundance [7].

The third vector-borne virus transmitted by infected *Aedes* species in the Philippines is Chikungunya virus (CHIKV). Chikungunya presents mainly as fever and polyarthralgia and is managed symptomatically, although chronic arthritis is the most common and severe complication [9].

Raman Spectroscopy as a Diagnostic Tool for Vector-Borne Diseases

Raman spectroscopy is a vibrational spectroscopy technique based on the inelastic scattering of the photons. Through this technique, the vibrational, rotational, and low-frequency modes of molecules can be investigated [10-11]. When a monochromatic light, such as a laser, hits a material and interacts with its molecules, the scattered light could either have a frequency the same as that of the incident light (Rayleigh scattering) or a slightly different frequency from the incident light (Raman scattering). This change in frequency, called a *Raman shift*, is due to the vibrational and rotational properties of the material [10]. Note that these Raman shifts, measured in wavenumbers (cm^{-1}) are independent of the excitation wavelength and are purely due to the intrinsic properties of the material. It is commonly used for fingerprinting the composition of materials since different molecules have a unique spectral signature [12]. Thus, Raman spectroscopy is often used to identify the chemical composition of materials.

Because of the ability of Raman spectroscopy to determine the molecular vibration of materials without being destructive, it has also been used to study biological samples [10]. One of the advantages of this spectroscopic technique over others is its ability to avoid interference from the water molecules of biological samples due to its virtual transparency in Raman [11]. Water, which is the major component in biological samples, has negligible Raman scattering. With technological advancement in recent years, the use of Raman spectroscopy for viral detection has revitalized. Viral identification is done by determining the viral component and/or the antibodies elicited from the immune response [13]. Compared to RT-PCR, it is much more cost-efficient since it does not require expensive reagents, assays, and kits. Moreover, Raman spectroscopy only requires minimal sample volume. Also, it requires less time as it has simpler processing steps (no need for additional labels or probes).

There are relatively few studies utilizing a regular Raman spectroscopy set-up for vector-borne viruses. One study compared the Raman spectrum of normal blood from the Dengue-infected blood. Their Raman spectra show that there are suppressed peaks present in the normal blood and had additional peaks at different frequencies [12, 14]. Compared with NS1, IgG, and IgM serology tests, it was found that results from Raman spectroscopy have better specificity and sensitivity [14-15]. Ultimately, these studies did not probe the different serotypes of the Dengue virus. However, Raman spectroscopy has been proven that it can differentiate between strains of the same viral species with a minimal viral titer of 50 plaque-forming units per µL [16].

Since the initial symptoms of ZIKV and DENV are similar, a study used surface-enhanced Raman spectroscopy (SERS) to distinguish ZIKV and the dengue NS1 protein [17]. SERS is a modified Raman spectroscopy technique that takes advantage of the near-field effect. This occurs when a metal is irradiated at the metal's plasmonic resonance and generates a strong local electromagnetic field which would result in the enhancement of the Raman scattering at the surface. In the published study, they successfully used a multiplexed SERS-based immunoassay using 1,2-BPE and 4-MBA as Raman reporter “nanotags" to distinguish the ZIKV and DENV NS1. However, this study did not report the actual spectrum of the Zika virus as well as its associated peaks.

There have been no reports yet on the Raman spectrum of the Chikungunya virus. The closest report on it in literature is as a negative control for a SERS probe designed to detect West Nile Virus (WNV) and DENV [18].

None of the enumerated literature above has correlated the results of the Raman experiments to the clinical outcomes. Thus, the results of this study will be able to address the current gaps not only in the Raman spectroscopy of vector-borne viruses but also in the diagnosis and management of diseases caused by these viruses. Furthermore, accurately identifying the Raman spectrum of these viruses in terms of changes in intensity, and appearance/disappearance of new peaks during the course of illness can be valuable information in predicting severe outcomes in the future. However, this goal will be more attainable with the fabrication of SERS substrates that can further strengthen the Raman signal from the viruses.

2D transition-metal dichalcogenides for biomedical SERS application

One of the reasons for the low number of published literatures on the use of Raman spectroscopy for viruses is the weak Raman signal of ZIKV and CHIKV. A solution is to deposit the viruses first onto a SERS substrate to strengthen its Raman signal.

Surface-enhanced Raman spectroscopy (SERS) is surface-sensitive biosensing method that amplifies the molecular vibration spectra by many orders of magnitude when the molecule is near metallic surfaces [19]. The enhancement effect of SERS is primarily due to the interplay between the electromagnetic and chemical effects [20]. The electromagnetic effect stems from the localized electromagnetic field near plasmonic nanoparticles or rough surfaces due to surface plasmon resonances (SPRs). Meanwhile, the chemical effect occurs as a result of the interaction between the substrate and absorbed molecules through processes like charge transfer and the mixing of molecular orbitals with electronic states.

Two-dimensional (2D) materials such as transition metal dichalcogenides (TMDs), black phosphorus, and hexagonal boron nitride (h-BN) has been gaining interest since the discovery of graphene in 2004 due to their high uniformity, chemical stability, biocompatibility, controllable doping, and ease of fabrication which is highly advantageous for SERS applications [21]. While significant advancements have been made in utilizing 2D materials for high-performance SERS substrates, the practical utilization of this technique, especially for biomedical applications, is still in its nascent phase. A particular avenue that

can be explored to advance the practical application of 2D TMDs SERS substrates is by further probing its biocompatibility to advance biomedical diagnostics, such as medical testing, identifying biomarkers, and imaging, with emphasis on enhancing sensitivity and specificity [21].

Among TMDs, $PtSe_2$ is relatively new and less studied. It is a Group 10 layered TMD with a calculated interlayer distance of 5.08 Å. The platinum (Pt) atom is sandwiched between two selenium (Se) atom layers and forms a 1T-phase with lattice parameters (a and b) of 3.73 Å [22]. In bulk form, it is a type-II Dirac semimetal but in a few layers form, it becomes a semiconductor [23-24]. Like with other TMDs, $PtSe_2$ also has a tunable band gap which can be controlled by implementing strain, chemical doping, applying electrical field, or changing the layer thickness [23]. In addition, $PtSe_2$ is one of the few 2D materials that is proven to be air-stable [25]. First-principles calculations proved that the layer-dependent SERS tunability of $PtSe_2$ is directly related to the interlayer interaction [26]. Currently, no specific research studies are focusing on $PtSe_2$ as a SERS substrate for virus detection. However, in the field of 2D materials in general, SERS applications for virus detection are an active area of research. Thus, not only will this proposed study address an important health issue but it will also address a current knowledge gap in the field of material science.

PROBLEM STATEMENT/OBJECTIVE

Problem Statement

- **Health issue**: Lack of a diagnostic tool that combines viral identification with serotyping and clinical surveillance and is capable of mass testing
- **Solution**: To develop a complementary optical accessory of a spectroscopy-based diagnostic tool for vector-borne diseases relevant to the Southeast Asia region
  Note: The applicant has an ongoing study that focuses on determining the Raman signature of vector-borne viruses. This proposed study on the other hand will develop a thin film to enhance the Raman signal detected from the vector-borne viruses. Moreover, this will improve Raman spectrum data as an input for the reference database for optical biomarkers of vector-borne viruses.

Objective

General: To develop platinum diselenide ($PtSe_2/Al_2O_3$) Surface-Enhanced Raman Spectroscopy thin films for the detection of vector-borne viruses

Specific:

- To fabricate few layer $PtSe_2$ with optimized thickness on Al_2O_3 using chemical vapor deposition
- To characterize the properties of $PtSe_2/Al_2O_3$ thin films using SEM, XRD, and Raman Spectroscopy
- To obtain the Raman spectrum of Dengue, Zika, and Chikungunya virus deposited on $PtSe_2/Al_2O_3$ thin films; and
- To compare these with the Raman spectrum from the viruses deposited on regular glass slides and commercially available SERS slides

OUTLINE OF TASKS / WORKPLAN

TARGET ACTIVITIES	YEAR 1				YEAR 2			
	Q1	Q2	Q3	Q4	Q1	Q2	Q3	Q4
Hiring of research personnel	■	■						
Procurement of materials and equipment	■	■						
Training of project team		■						
Fabrication and optimization of $PtSe_2/Al_2O_3$ thin films			■	■	■	■		

Characterization of $PtSe_2/Al_2O_3$ thin films								
Raman experiment on viruses deposited on glass slides								
Raman experiment on viruses deposited on SERS slides								
Raman experiment on viruses deposited on $PtSe_2/Al_2O_3$ thin films								
Data analysis								

OUTCOME(S)

- Expansion on the use of two-dimensional (2D) transition-metal dichalcogenides (TMDs) materials for biomedical optics application
- Enhancement of the Raman signal of vector-borne viruses and consequently, improvement of the capability of Raman spectroscopy for the diagnosis (and potential prognosis) of vector-borne diseases
- Proof-of-concept of an ideal diagnostic tool for vector-borne diseases that combines viral identification with serotyping and clinical surveillance while still being easy to use for low-resource settings

IMPACT

Sustainable Development Goals (SDGs) Addressed:
SDG 3: Good Health and Wellbeing, *SDG 10: Reduced Inequalities*, *SDG 11: Sustainable cities and communities*, *SDG 17: Partnerships for the goals*

Social Impact

- Results from this study will complement the ongoing work on the use of Raman spectroscopy as a diagnostic tool that can help prevent severe outcomes of dengue and lessen mortality of dengue fever. Consequently, this improves the Philippines' disaster preparedness for outbreaks.
- Moreover, this lays the groundwork for a future project that will further look at the clinical adaptability of using optical biomarkers as an alternative diagnostic tool which can lessen the burden for healthcare workers and facilities.
- Once proven, this study can also be extended to test other vector-borne viruses from other Southeast Asian countries

Economic Impact

- This will also strengthen the ongoing proof-of-concept study, which will be a jump-off point for a more extensive study on the use of Raman spectroscopy as a prognostication tool for dengue in the future. The prognosticating ability will prevent cases of overtreatment, which will lessen the burden on use of government resources especially during dengue outbreaks. In turn, the diagnostic test will lessen the financial burden of unnecessary admissions for patients who could be managed at home.
- Infectious vector-borne diseases have the potential to cause pandemics which not only pose a threat to human life but also to the global economy. Thus, early detection mechanisms must be deployed and easily accessible to the public for better monitoring and tracking.

REFERENCES

1. Weaver SC, Charlier C, Vasilakis N, Lecuit M. Zika, chikungunya, and other emerging vector-borne viral diseases. Annual Review of Medicine. 2018 Jan 29; 69:395-408.

2. Porras MF, Navas CA, Marden JH, Mescher MC, De Moraes CM, Pincebourde S, Sandoval-Mojica A, Raygoza-Garay JA, Holguin GA, Rajotte EG, Carlo TA. Enhanced heat tolerance of viral-infected aphids leads to niche expansion and reduced interspecific competition. Nat Comm. 2020 Mar 4;11(1184): 1-9
3. World Health Organization. Vector-borne Diseases: 2 March 2023 [Internet]. World Health Organization. 2023 [cited 3 April 2023]. Available from: https://www.who.int/news-room/fact-sheets/detail/vector-borne-diseases
4. Centers for Disease Control and Prevention [Internet]. Dengue Clinical Presentation. 2021 [updated 2023 April 13; cited 2023 April 1] Available from <https://www.cdc.gov/dengue/healthcare-providers/clinical-presentation>
5. Suppiah J, Ching SM, Amin-Nordin S, Mat-Nor LA, Ahmad-Najimudin NA, Low GK, Abdul-Wahid MZ, Thayan R, Chee HY. Clinical manifestations of dengue in relation to dengue serotype and genotype in Malaysia: A retrospective observational study. PLoS Negl Trop Dis. 2018 Sep 18;12(9):e0006817.
6. Kliegman R. Stanton B. St Geme J. W. Schor N. F. Behrman R.E. & Nelson W.E. (2020). Nelson textbook of pediatrics (Edition 21).
7. Biggs JR, Sy AK, Brady OJ, Kucharski AJ, Funk S, Tu YH, Reyes MA, Quinones MA, Jones-Warner W, Ashall J, Avelino FL, Sucaldito NL, Tandoc AO, Cutiongco-de la Paz EMC, Capeding MRZ, Padilla CD, Hibberd ML,. Hafalla JCR. Serological Evidence of Widespread Zika Transmission across the Philippines. Viruses. 2021 Jul 23;13(8):1441
8. World Health Organization. [Internet] Zika virus. 2018 [updated 2022 Dec 8; cited 2023 April 1] Available from <https://www.who.int/news-room/fact-sheets/detail/zika-virus>
9. Sy AK, Saito-Obata M, Medado IA, Tohma K, Dapat C, Segubre-Mercado E, Tandoc III A, Lupisan S, Oshitani H. Molecular characterization of chikungunya virus, Philippines, 2011–2013. Emerg Infect Dis. 2016 May;22(5):887-890.
10. Lukose J, Barik AK, Mithun N, Pavithran S, George SD, Murukeshan VM, Chidangil S. Raman spectroscopy for viral diagnostics. Biophysical Reviews. 2023 Apr 10:1-23.
11. Němeček D, Thomas Jr GJ. Raman spectroscopy of viruses and viral proteins. In Frontiers of Molecular Spectroscopy 2009 Jan 1 pp. 553-595. Elsevier.
12. Khan S, Ullah R, Saleem M, Bilal M, Rashid R, Khan I, Mahmood A, Nawaz M. Raman spectroscopic analysis of dengue virus infection in human blood sera. Optik. 2016 Feb 1;127(4):2086-2088.
13. Ramoji A, Pahlow S, Pistiki A, Rueger J, Shaik TA, Shen H, Wichmann C, Krafft C, Popp J. Understanding viruses and viral infections by biophotonic methods. Translational Biophotonics. 2022 Mar;4(1-2):e202100008.
14. Khan S, Ullah R, Khurram M, Ali H, Mahmood A, Khan A, Ahmed M. Evaluation of Raman spectroscopy in comparison to commonly performed dengue diagnostic tests. Journal of Biomedical Optics. 2016 Sep 1;21(9):095005-1 - 095005-4.
15. Mahmood T, Nawaz H, Ditta A, Majeed MI, Hanif MA, Rashid N, Bhatti HN, Nargis HF, Saleem M, Bonnier F, Byrne HJ. Raman spectral analysis for rapid screening of dengue infection. Spectrochimica Acta Part A: Molecular and Biomolecular Spectroscopy. 2018 Jul 5;200:136-142.
16. Yang Y, Xu B, Murray J, Haverstick J, Chen X, Tripp RA, Zhao Y. Rapid and quantitative detection of respiratory viruses using surface-enhanced Raman spectroscopy and machine learning. Biosensors and Bioelectronics. 2022 Dec 1;217:114721.
17. Sánchez-Purrà M, Carré-Camps M, de Puig H, Bosch I, Gehrke L, Hamad-Schifferli K. Surface-enhanced Raman spectroscopy-based sandwich immunoassays for multiplexed detection of Zika and Dengue viral biomarkers. ACS Infect Dis. 2017 Oct 13;3(10):767-776.
18. Paul AM, Fan Z, Sinha SS, Shi Y, Le L, Bai F, Ray PC. Bioconjugated gold nanoparticle based SERS probe for ultrasensitive identification of mosquito-borne viruses using Raman fingerprinting. J Phys Chem C. 2015 Oct 15;119(41):23669-23675.
19. Hegde, S. S., & Bhat, B. R.. Dengue detection: Advances and challenges in diagnostic technology. Biosensors and Bioelectronics: X, 10, 100100. https://doi.org/10.1016/j.biosx.2021.100100 Materials Today Physics 18 (2021) 100378
20. Tang, X., Hao, Q., Hou, X., Lan, L., Li, M., Yao, L., Zhao, X., Ni, Z., Fan, X., & Qiu, T. (2024). Exploring and engineering 2D transition metal dichalcogenides toward Ultimate SERS performance. Advanced Materials. https://doi.org/10.1002/adma.202312348
21. W. Jiang, X. Wang, Y. Chen, G. Wu, K. Ba, N. Xuan, Y. Sun, P. Gong, J. Bao, H. Shen, T. Lin, X. Meng, J. Wang, and Z. Sun, "Large-area high quality $PtSe_2$ thin film with versatile polarity", InfoMat 1(2), 260–267 (2019).
22. Y. Wang, L. Li, W. Yao, S. Song, J. T. Sun, J. Pan, X. Ren, C. Li, E. Okunishi, Y.-Q. Wang, E. Wang, Y. Shao, Y. Y. Zhang, H. Yang, E. F. Schwier, H. Iwasawa, K. Shimada, M. Taniguchi, Z. Cheng, S. Zhou, S. Du, S. J. Pennycook, S. T. Pantelides, and H.-J. Gao, "Monolayer $PtSe_2$, a New Semiconducting Transition-Metal-Dichalcogenide, Epitaxially Grown by Direct Selenization of Pt", Nano Lett. 15(6), 4013–4018 (2015).
23. Y. Zhao, J. Qiao, Z. Yu, P. Yu, K. Xu, S. P. Lau, W. Zhou, Z. Liu, X. Wang, W. Ji, and Y. Chai, "High-Electron-Mobility and Air-Stable 2D Layered $PtSe_2$ FETs", Adv. Mater. 29(5), 1604230 (2017).
24. M. Hilse, K. Wang, and R. Engel-Herbert, "Growth of ultrathin Pt layers and selenization into $PtSe_2$ by molecular beam epitaxy", 2D Mater. 7(4), 045013 (2020).
25. Li, M., Gao, Y., Fan, X., Wei, Y., Hao, Q., & Qiu, T. (2021). Origin of layer-dependent SERS tunability in 2D transition metal dichalcogenides. Nanoscale Horizons, 6(2), 186–191. https://doi.org/10.1039/d0nh00625d

Executive Summary for [**Category: Health**]

Compact Computational Flat-Optical Bronchoscopes for Image-guided Cancer Therapies Under Respiratory Deformation of Lungs

Praneeth Chakravarthula
cpk@cs.unc.edu, UNC Chapel Hill, Department of Computer Science

The proposal aims at developing ultra-thin and compact bronchoscopes using nanophotonic meta-optics. The proposed work will allow for a thin design with decreased tip length and increased working channel of the bronchoscope enabling unprecedented small size and improved imaging capabilities for early lung cancer detection.

Problem Statement and Objectives

Over 200,000 new cases of lung cancer are diagnosed annually in the United States alone, resulting in about 150,000 deaths, making lung cancer the most lethal of all forms of cancer. Only 1 in 6 lung cancers are diagnosed at an early stage and over half are diagnosed with distant metastasis. For effective and early diagnosis, adequate and representative biopsy sample collection is the key which will help in better management and improve patient outcomes. However, accessing inner nodules of the lung is challenging due to the large size of the bronchoscope (~3.5mm diameter and 1.2mm working channel) and thick non-agile camera modules compared to the bronchial airways of the lungs. Adding to this, the lungs deform intraoperatively due to respiratory motion making it further difficult to visualize the lesions towards the periphery of the lung. Given that existing solutions do not address this problem and a standard scope can only reach up to 4-5th generation of bronchi – in a typical 23 generation bronchial tree of lung – we aim to develop an ultra-thin and compact bronchoscope based on computationally designed flat meta-optical elements that will significantly reduce the size while still allowing for full color real-time imaging and guided therapies.

Impact of Proposed Research

The development and implementation of thin bronchoscopes will have a transformative impact on respiratory medicine. The ultra-thin meta-optical cameras will not only shrink the size and increase the agility of the device, but will also increase the working channel to allow for integration with biopsy needles for real-time guidance during biopsies. The reduced rigid tip length of the proposed bronchoscope, from replacing thick compound lenses with thin flat metalens, allows for enhanced maneuverability, facilitating smoother navigation through narrow and tortuous ducts with minimized patient discomfort and risk of complications. By reaching peripheral lung regions more effectively, the proposed design can enable more extensive visualization and sampling of lesions that were previously challenging to access, resulting in higher diagnostic yield and more accurate staging of lung cancer. Furthermore, integrating with the computational optimization techniques will improve image resolution thereby improving real-time guidance during procedures. Overall, the proposed research can significantly advance respiratory medicine and interventional pulmonology, enhancing patient outcomes.

A Proposal to Optica Foundation Challenge Program [**Category: Health**]

Compact Computational Flat-Optical Bronchoscopes for Image-guided Cancer Therapies Under Respiratory Deformation of Lungs

Praneeth Chakravarthula
cpk@cs.unc.edu
UNC Chapel Hill, Department of Computer Science
Chapel Hill, NC 27599-3175

Abstract

Bronchoscopy is a crucial minimally invasive diagnostic and therapeutic tool in respiratory medicine allowing direct visualization and sampling of the airways for the evaluation and management of various lung conditions. The size of bronchoscopes directly impacts the patient's comfort and tolerability during the procedure. A thinner and less rigid bronchoscope enables higher agility, larger accessibility including the peripheral pulmonary areas, and induce less stress on the surrounding tissues, especially when the lung is deforming during respiration. The size of the imaging optics poses a major limitation in miniaturization of the bronchoscope as well as increasing the size of the working channel for procedures, including taking cancer biopsy samples. Moreover, the size of the bronchoscope limits diagnostic and therapeutic approaches only to the central pulmonary regions, reaching only up to fourth-order bronchi in the best case.

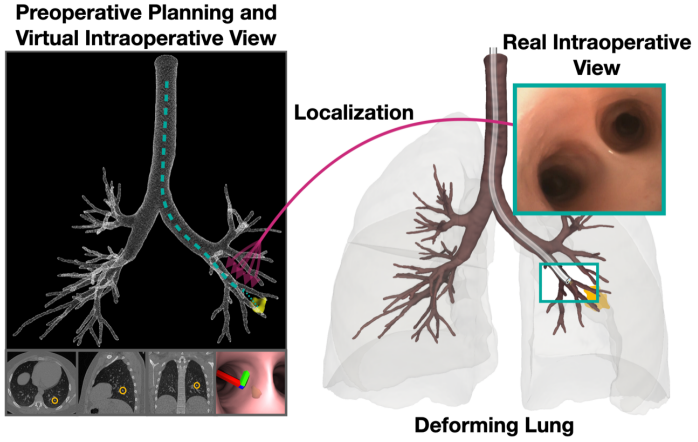

Figure 1. During bronchoscopy, a physician deploys a bronchoscope through the airways (right) to target a suspicious lung nodule (yellow) for biopsy or treatment, from a reference generated from the reconstruction of a preoperative CT scan (left).

In this project, we aim to use meta-optics to drastically miniaturize imaging optics while achieving similar functionalities with significantly reduced size. We propose an inverse-designed meta-optic that will be computationally optimized and combined with a coherent fiber bundle to achieve an imaging device that will enable at least 60% reduction over traditional imaging optics used in bronchoscopes. The size of the meta-optic lens will be miniaturized to about 1mm in diameter and under 2mm in rigid tip length compared to a few centimeters of tip length in standard bronchoscopes. This will allow for significantly improved maneuverability into higher order (at least up to ninth order) peripheral bronchi while maintaining image quality to visualize pulmonary airways. We will build an experimental prototype bronchoscope and demonstrate full color real-time video capture.

Problem Statement and Objectives

Over 200,000 new cases of lung cancer are diagnosed annually in the United States alone, resulting in about 150,000 deaths, making lung cancer the most lethal of all forms of cancer [1]. Only 1 in 6 lung cancer cases are diagnosed at an early stage and over half are diagnosed with

distant metastasis. For effective and early diagnosis, adequate and representative biopsy sample collection is the key which will help in better management and improve patient outcomes. However, accessing inner nodules of the lung is challenging due to the large size of the bronchoscope compared to the bronchial airways of the lungs. Adding to this, the lungs deform intraoperatively due to respiratory motion making it further difficult to visualize the lesions towards the periphery of the lung. Given that existing solutions do not address this problem and a standard 5.9 mm scope[1] can only reach up to 4th generation of bronchi – in a typical 23 generation bronchial tree of lung – we aim to develop a compact bronchoscope based on computationally designed flat meta-optical elements that will significantly reduce the diameter as well as the rigid tip length of the bronchoscope and increase the working channel while still allowing for full color real-time imaging and guided therapies.

Description of Proposed Work and Expected Outcomes

We aim to reduce the footprint of the imaging optics in the bronchoscope by replacing traditional bulky imaging lens stack with computational flat-optical metalenses. Conventional bronchoscopes, and endoscopes in general, use a bulky stack of refractive optical elements that are designed to reduce the aberrations and maximize the image quality, see Figure 2. However, the size of these optical elements result in thicker imaging scopes with rigid tips, fundamentally limiting the device agility, especially within smaller ducts such as higher order bronchial branches. Solutions that reduce the rigid tip length and compact the scope are in fact urgently needed.

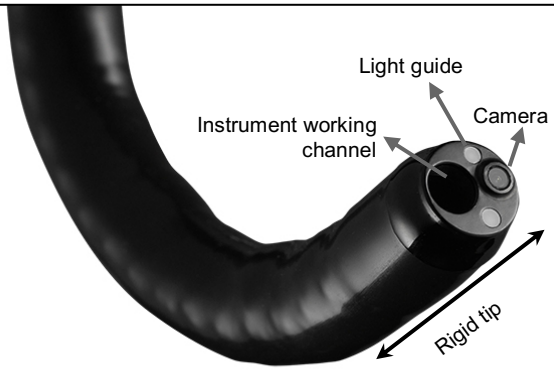

Figure 2. Standard 5.9mm Therapeutic Bronchoscope. The imaging optics restricts the size and flexibility of the bronchoscope, limiting the diagnosis only to the central airways, up to third or fourth order pulmonary nodules.

Flat meta-optics is an emerging technology that enables creating miniaturized optical elements using subwavelength nanophotonic structures that allow precise control over the behavior of light, such as its propagation, polarization, phase and amplitude. Meta-optics are composed of arrays of nanoscale scatterer elements that interact with light in unconventional ways. Such ultrathin flat optics not only dramatically shrink the size of traditional optics but can also enable functionalities that were not achievable previously, such as bending light at sharp angles, focusing light into subwavelength spots, extending depth-of-field and creating artificial optical phenomena, all on a single surface. However, meta-optics traditionally suffer from strong aberrations (both chromatic and Seidel) making large field-of-view and full-color imaging challenging. As such, a full-color meta-optic endoscope for 400-700 nm spectrum with acceptable field-of-view, depth-of-field and a small enough aperture has not yet been achieved to the best of our knowledge.

[1] Fujifilm EB-580 T Therapeutic Bronchoscope

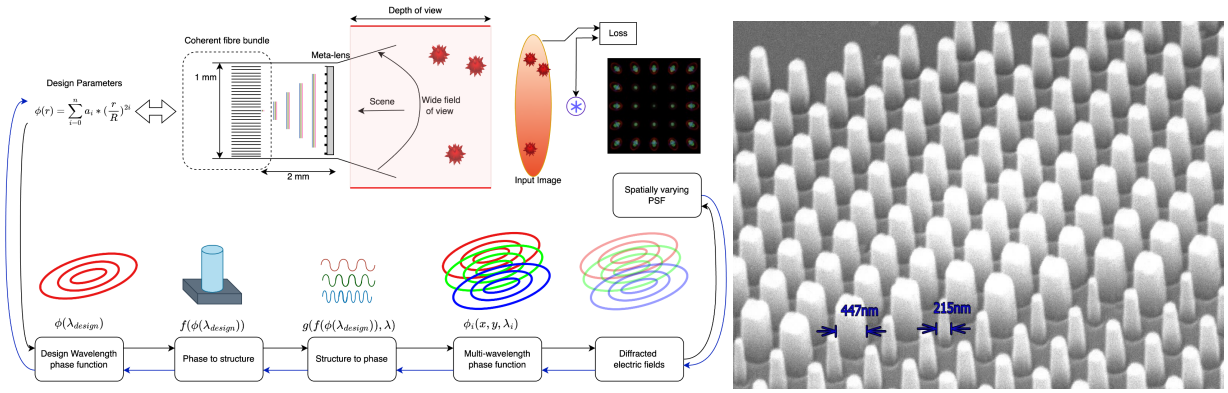

Figure 3. Overview of the metalens design pipeline (Left). We circumvent computational FDTD methods via differentiable fast approximation of RCWA which allows us to perform gradient-based optimization. A scanning electron microscope (SEM) image of a fabricated test metalens is shown on the right.

In this proposal, we aim to achieve an inverse-designed 1mm meta-optic, optimized to capture full-color scenes in the visible spectrum in real-time. The metalens will be designed in conjunction with a coherent fiber bundle of 1mm diameter, keeping the overall size of the bronchoscope imaging area and the rigid tip length to the minimum, and significantly increasing its working channel (from 1.2mm to ~2mm) as well as the flexibility to access higher-order peripheral bronchi of the lung. To this end, we will build fully differentiable forward models, some via learned deep neural networks, to model the wave effects of nano scatterers on the metalens and optimize for the metalens phase as an optimization parameter to minimize any aberrations under broadband illumination.

Differentiable modeling for metasurface optics.

We will build deep learning models for efficiently determining the optical response of the metalens-based imaging system in the bronchoscope as a function of the design parameters (e.g. tip length, incident wavelength, nano scatter shape). Specifically, we will learn the imaging response as

$$y = f(x, p),$$

where y is the PSF of the optical system obtained via wave propagation method f such as angular spectrum method, x is the input wavefront, and p denote the system design parameters. Imaging optics usually deviate from the paraxial regime where the imaging system can be described by a single, spatially invariant PSF. We will fully quantify chromatic and Seidel aberrations (coma, distortion, astigmatism, spherical), and compute spatially varying PSFs as

$$y(\theta) = f(x(\theta), p),$$

where θ is the angle of incidence for the incoming wavefront.

Modeling the millions of sub-wavelength scatterers on a meta-surface is challenging and requires full electromagnetic simulation to accurately model the wave effects of meta-optic. Traditionally, metasurfaces are simulated using finite-difference time-domain methods which result in high computational complexity, making them impractical for optimization-based inverse-design of metasurfaces beyond a few micrometers in aperture. Therefore, we will use rigorous coupled-wave analysis (RCWA) over several nanostructure sizes and build a differentiable proxy mapping function using deep neural networks to approximate the effects of nano

structures during the meta-optic design. This technique will allow for faster differentiable simulation. Specifically, we will approximate the phase response of the metasurface as

$$\phi(\lambda) = h(g(\phi(\lambda_{design})), \lambda),$$

where g is a function that converts the wavefront at the design wavelength λ_{design} into a metasurface nanostructure and h is a function that determines the phase response at an arbitrary wavelength λ for a given nano-structure design. Both g and h are built as fast and fully differentiable deep neural networks, closely approximating RCWA techniques. An overview of the pipeline for designing the flat meta-optic is illustrated in Figure 3. Once designed, we will fabricate the metalens and combine it with a thin coherent fiber bundle to complete a thin bronchoscope for evaluation. Preliminary simulation of imaging through coherent fiber bundles (with traditional imaging lens) is shown in Figure 4.

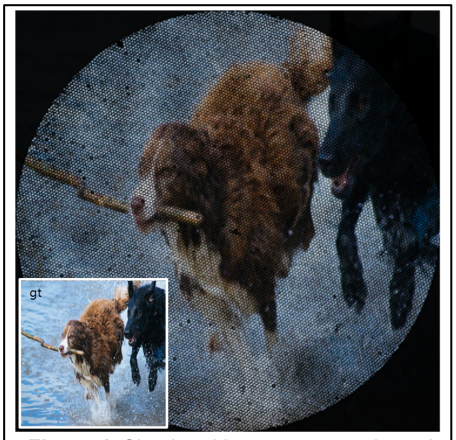

Figure 4. Simulated image as seen through a coherent fiber bundle. Inset shows groundtruth image.

Evaluation Plan

We will analyze the optical performance of the proposed meta-optic bronchoscope both quantitatively via its modulation transfer function (MTF[2]) and qualitatively by comparing it with existing standard bronchoscopes. For qualitative comparison, we first plan to conduct a comparison of images that are displayed on an OLED screen and images that are captured with the newly designed metalens fiber optic imager and the in-built camera of an off-the-shelf bronchoscope. Next, we plan to insert the metalens fiber-optic imager into the working channel of an existing bronchoscope, Ambu Scope 5 Broncho[3], and compare the image quality of the airways within the lungs. For this, we will collaborate with Prof. Ron Alterovitz at UNC Chapel Hill who has extensive experience with operating bronchoscopes on experimental lungs and conducting clinical trials on real pig and human lungs.

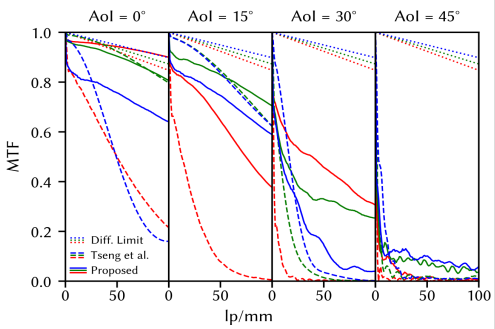

Figure 5. The calculated MTF for various angle of incidence (AoI). Thick solid lines correspond to the diffraction limit. Dashed lines correspond to calculated MTF curves for Tseng et al.[1]. Full thin lines correspond to the meta-optic proposed in this work.

We have already conducted a few preliminary evaluations in simulation for the proposed approach for designing the metalens-based bronchoscope, optimized for broadband illumination across the visible spectrum. Our preliminary results suggest that the metalens with 1mm aperture will achieve an FOV of 45 degrees and reduce the tip length significantly, down to 2mm, compared to a few centimeters in standard 5.9mm bronchoscope. A comparison of simulated MTFs of a metalens design (without fiber bundle) relative to diffraction limited PSF and best prior work is shown in Figure 5.

[2] MTF is the ability to transfer contrast at a given spatial frequency (resolution) from object to the sensor.
[3] https://www.ambuusa.com/endoscopy/pulmonology/bronchoscopes/product/ascope-5-broncho

Impact of Proposed Research

The development and implementation of thin bronchoscopes will have a transformative impact on respiratory medicine. The ultra-thin meta-optical cameras will not only shrink the size and increase the agility of the device but will also increase the working channel to allow for integration with biopsy needles for real-time guidance during biopsies, offering improved diagnostic capabilities and therapeutic interventions. The reduced rigid tip length of the proposed bronchoscope allows for enhanced maneuverability, facilitating smoother navigation through narrow and tortuous ducts with minimized patient discomfort and risk of complications. By reaching peripheral lung regions more effectively, the proposed thinner bronchoscope promises to enable more extensive visualization and sampling of lesions that were previously challenging to access, resulting in higher diagnostic yield and more accurate staging of lung cancer. Furthermore, integrating with the computational optimization techniques will improve image resolution thereby improving real-time guidance during procedures. Overall, the proposed research can significantly advance respiratory medicine and interventional pulmonology, enhancing patient outcomes.

Prior Work

Solutions explored for thin endoscopy involve lensless and computational imaging with single fibers [2-4] or coherent fiber bundles [5-8]. However, these approaches are often restricted by short working distances and vulnerability to bending and twisting of the optical fibers, hindering real-time image capture. Additionally, research has been conducted on optimizing and fabricating compact optical elements, including 3D printed elements, directly on fibers [10] or freeform mirror optics for side-viewing endoscopes [11]. While these alternatives offer high optical performance, the scalability of 3D printed or freeform optical elements remains a challenge, particularly for bronchoscopy, where disposable optics are preferred to prevent cross-contamination between patients. Meta-optics [12,13], on the other hand, not only dramatically shrink the size of traditional optics, but also can combine multiple functionalities in a single surface [14,15]. Moreover, flat meta-optics are compatible with high-volume semiconductor manufacturing technologies [16,17] and can create cheap disposable optics.

References

[1] Katsis et al: "Bronchoscopic biopsy of peripheral pulmonary lesions in 2020: a review of existing technologies." Journal of Thoracic Disease. 2020.

[2] Caramazza et al: "Transmission of natural scene images through a multimode fiber." Nature Communications, 2019.

[3] Liu et al: "All-fiber high-speed image detection enabled by deep learning." Nature Communications 2022.

[4] Wang et al: "High-speed all-Fiber micro-imaging with large depth of field." Laser Photonics 2022.

[5] Shin et al: "A minimally invasive lens-free computational microendoscope." Science Advances 2019.

[6] Badt and Katzl: "Real-time holographic lensless micro endoscopy through flexible fibers via fiber bundle distal holography." Nature Communications 2022.

[7] Orth et al: "Optical fiber bundles: ultra-slim light field imaging probes." Science Advances 2019.

[8] Choi et al: "Flexible-type ultrathin holographic endoscope for microscopic imaging of unstained biological tissues." Nature Communications 2022.

[10] Gissibl et al: "Two-photon direct laser writing of ultracompact multi-lens objectives." Nature Photonics 2016..

[11] Li et al: "Ultrathin monolithic 3D printed optical coherence tomography endoscopy for preclini- cal and clinical use." Light Science and Applications 2020.

[12] Yu and Capassol: "Flat optics with designer metasurfaces." Nature Materials 2014.

[13] Chen et al: "Principles, functions, and applications of Optical Meta-Lens" Advanced Optical Materials 2021.

[14] Munley et al: "Inverse-designed meta-optics with spectral-spatial engineered response to mimic color perception." Advanced Optical Materials 2022.

[15] Piccardo et al: "Roadmap on multimode light shaping" Advanced Optical Materials 2022.

[16] Colburn et al: "Broadband transparent and CMOS-compatible flat optics with silicon nitride metasurfaces." Optical Materials Express 2018.

[17] Zhang et al: "High-Efficiency, 80 mm aperture Metalens Telescope." Nano Letters 2023.

Next-generation High-precision Surgical Laser Technology

PI: Dr. Qiang Fu **Category: Health**

Abstract: Lasers are already routinely used for medical treatment in almost every modern hospital. Specifically, in the field of high-precision surgery such as eye surgery, the primary tools are generally ultraviolet lasers and near-infrared femtosecond lasers. The use of ultraviolet lasers involves ablation that relies on the scission of chemical bonds through photochemical processes, which can pose mutagenic risks to patients. Meanwhile, femtosecond laser cutting employs multi-photon ionization; while precise, its limited ablation efficiency makes it less suitable for broader high-precision surgical applications, such as in neurosurgery. Given these constraints, there is a pressing need for safer and more efficient laser technology for high-precision surgeries. Mid-infrared (MIR) lasers, which offer highly localized and purely thermal ablation processes, are a promising alternative.This project is devoted to the development of a new generation of mid-infrared laser scalpel which will sow the seeds for the replacement of current high-precision surgery technologies, offering unprecedentedly flexible and precise cutting with exceptional sub-single-cell collateral ablation damage margins (<5 μm). This advance is driven by cutting-edge MIR laser (optical parametric oscillator, OPO) and hollow-core fiber (HCF) technology. This project offers practical solutions capable of substantially reducing the likelihood of patients suffering from the side effects associated with traditional surgical lasers, which include excessive wounds, the formation of large scars and potential mutagenic effects. Importantly, this proposal will be centered upon needs in the fields of eye surgery and neurosurgery, which are areas of high global health importance and demand. This technology will enable remarkably unimpaired and accurate tissue ablation from the outside and deep into the body, providing better disease control, and leading to a higher likelihood of successful health outcomes.

Challenges and Innovations: Although MIR laser radiation at wavelengths of 6.1 or 6.45 μm has proven to offer much less ablation collateral effects than other wavelengths, no such laser sources are generally used in surgeries due to lack of both practical laser sources and robust power delivery systems. Compared to gigantic scientific free-electron-lasers and low-power quantum-cascade-lasers, compact pulsed OPOs are a promising solution, but current 6-6.5 μm designed OPOs offer limited power (≤1.5 W) and poor control on pulse properties (duration, shape, repetition rates), together these are inadequate for optimized surgical ablation outcomes.

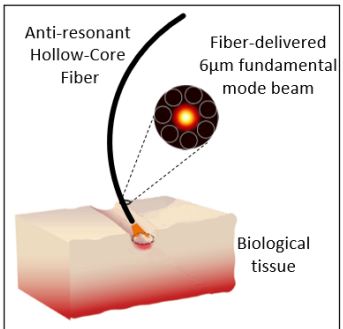

Proposed new mid-infrared laser scalpel for high-precision surgery

A fiber beam delivery system is vitally important for surgical lasers to enhance system robustness and flexibility, allow sharing of expensive laser sources, and application for minimally invasive surgery. Traditional MIR fibers have many limitations, e.g. low-damage-threshold (soft-glass fibers), mechanical rigidity (metallic HCF), and complex fabrication (Omniguide HCFs). Emerging anti-resonant HCFs (AR-HCFs) have compatibility with standard fiber fabrication techniques and extraordinary properties, i.e. low cost, scalability to long lengths, high mechanical durability, high damage threshold, and low nonlinearity/dispersion, with potential for low loss at 6-6.5 μm for surgical applications.

This project delivers high-power pulse-tailorable 6-6.5 μm light from a new electronically-controlled MIR OPO, guided by novel AR-HCFs, suitable for next-generation laser surgery.

Future Directions and Impact: This project aligns with the OPTICA Foundation Challenge call's Health theme, specifically under "New Therapeutic Laser." Integrating OPO and AR-HCF technologies, this project will help address the global biological graft tissue shortage for corneal transplant surgery and enhance the preservation of neurological tissues in neurosurgery, thereby improving patient outcomes and offering significant economic benefits. In this project, my research team will develop a handheld laser scalpel, and future designs will incorporate features compatible with endoscopic instruments to increase versatility across different surgical settings. We will deliver a surgical laser prototype and refine it for specific surgeries. Additionally, we will manage intellectual property to enhance licensing opportunities and pursue clinical validation to ensure the prototype's medical safety and efficacy. The OPTICA Foundation Challenge will serve as a stepping stone to establish a specialized photonics research team dedicated to next-generation high-precision surgery, aiming to set new standards in laser surgery, revolutionize the field, and transform surgical practices and outcomes.

Case for Support: Next-generation High-precision Surgical Laser Technology

Problem Statement and Objectives

Despite significant advancements in medical laser technology, current surgical tools still exhibit substantial limitations in spatial resolution and side effects. In specialized areas such as ophthalmic surgery and neurosurgery, current laser systems present challenges: ultraviolet lasers carry mutagenic risks and femtosecond lasers, though precise, are inefficient and unsuitable for handheld operations. Additionally, photothermal laser systems such as CO_2 lasers, while efficient and free of genetic risks, do not substantially lessen tissue damage compared to traditional scalpels and electrosurgical bipolar devices. This inability to minimize tissue damage compromises patient recovery and prolongs hospital stays, resulting in the continued dominance of electrical/mechanical tools. These traditional tools, although cost-effective, lead to tissue wastage in cornea transplant surgeries and inadequate preservation of critical brain tissues in neurosurgical procedures - both areas with high clinical demand and significant societal impact. Moreover, the need for advanced laser technology extends beyond healthcare into sectors such as communication, sensing, and manufacturing, where innovative laser and fiber technologies could drive substantial advancements.

This project aims to meet the critical demand for a safe, highly efficient laser tool for high-precision surgery by developing a novel mid-infrared (MIR) laser system. The proposed technology focuses on building a fiber-laser-pumped high-power optical parametric oscillator (OPO) that operates at wavelengths of 6-6.5µm, capable of producing laser beams with tailorable pulse parameters for minimal collateral tissue damage. Utilizing anti-resonant hollow-core fibers (AR-HCFs), the laser system will flexibly and efficiently emit near-diffraction-limited beams, suitable for both handheld and minimally invasive surgical applications. The objectives of this project are multifaceted:

(a) To engineer a high-power (average power >50 W; peak power >100 kW) 2-µm fiber laser with adjustable temporal characteristics as a robust pump laser system.
(b) To develop an OPO with high frequency conversion efficiency (>10%) for optimal MIR output.
(c) To achieve <1 dB/m loss in silica-based AR-HCFs and optimize the fiber power delivery system for precise, fundamental-mode output at the point of use.
(d) To construct an ablation testbed for precise targeting and preservation of biological tissues.
(e) To integrate these innovations into a compact surgical laser prototype for demonstration and validation, thereby expediting clinical translation.

Literature Review and Methodology

The goal of this project is to develop a novel 6-6.5µm pulse-structure-tailorable surgical laser which can achieve unprecedented ablation outcomes, i.e., removal of a defined amount of material efficiently and with minimal impact on surrounding and collateral tissues.

MIR lasers hold special promise for tissue ablation due to the absence of mutagenic risk, high absorption, and thus small penetration length (defining ablation resolution in depth, typically <10µm [1]). Current MIR surgical lasers, e.g., CO_2 gas lasers, rely on strong water absorption [1-3], shown to be non-ideal in achieving minimal collateral damage [2]. Moreover, they generate continuous-wave or long-pulses (many nanoseconds or longer) and thus lead to large regions of collateral damage (>30µm-width [4]), limiting ablation resolution (in width).

In the MIR, 6.1 and 6.45µm wavelengths, coinciding with the amide I and II absorption bands of protein, respectively [1,2], have been shown to be the optimal wavelengths to minimize collateral damage. This is because energy coupled into the protein matrix causes conformational changes which reduce the structural integrity of tissue allowing for tissue removal with much less collateral damage [5-6]. So far, pioneering surgical studies at such wavelengths have focused on free-electron laser (FEL, predominantly at the Vanderbilt FEL centre [7-9], which possesses the world's only FEL healthcare integration system). FELs are major scientific facilities due to their wholly impractical footprint and high price (hundreds of million pounds). Quantum cascade lasers (QCLs) are potentially an alternative, however, their low peak power (<<1kW) prevents their use in high-precision ablation [10-11]. In contrast, OPOs offer a promising practical solution as efficient nonlinear frequency

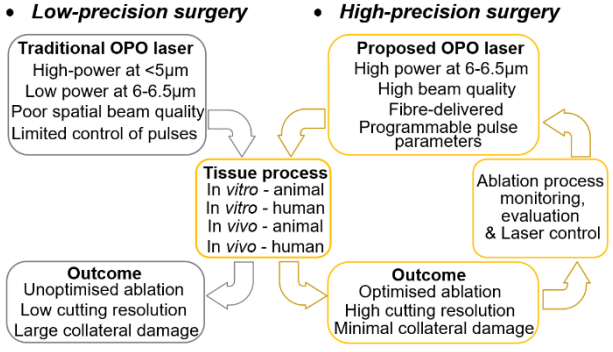

converters. They provide both wide MIR wavelength tuneability and powerful pulsed output. Although the OPO is an established technology [12-14], few works have focused on 6-6.5µm generation for tissue ablation [15-18]; all are based on bulk-laser-pumped OPOs, which involve high maintenance costs and produce relatively low beam quality (partially due to the poor-beam-quality of the pumps used). High beam quality is needed to enable small and selective tissue ablation. Critically, these OPOs also have low-power outputs (≤1.5W) which limit the ablation efficiency [19], and poor pulse duration control options, leading to sub-optimal collateral damage/ablation outcomes [20-23].

To overcome the limitations of traditional OPOs, the first fiber-laser-pumped temporal-controllable 6-6.5µm OPO is proposed here. It offers high power (>5W), near-diffraction-limited beams and remarkable temporal pulse control, achieved by electronically tailoring the pump pulses and tactfully designing the OPO cavity for the target 6-6.5µm wavelengths. The OPO characteristics can be conveniently adjusted and optimised after monitoring and evaluation of the ablation process and hence will be capable of providing optimised/required ablation outcomes.

For beam transport, fiber delivery systems are greatly preferable to free-space beam delivery or modified articulated arms, providing: enhanced system flexibility (surgeon-friendly, for endoscopic use) and reliability (fewer beam perturbations), better beam quality at focus, laser placement far from the operating theatre, sharing of expensive laser sources, and support of a safer and less cluttered operating environment [24]. As mentioned in the executive summary, options for single-mode fiber operating at 6-6.5µm are restricted. Omniguide fibers are promising and have gained a solid footing in surgery using CO_2 lasers operating at 10.6-µm [3,24-25]. However, the maximum fiber length and performance at 6-6.5µm wavelengths are limited by their challenging fabrication processes where at least two thermo-mechanically compatible, high refractive-index contrast materials must be identified and drawn down to fiber while reliably maintaining a multilayer structure with micrometer dimensions [25]. By contrast, this project will employ novel silica-based AR-HCFs, which are non-toxic, biocompatible, mechanically robust, highly damage resistant, and produced in long lengths. Light transmission in an air-core minimizes the transmission losses and undesired nonlinearities at high power, allowing their use for 6-6.5µm single-mode beam transmission.

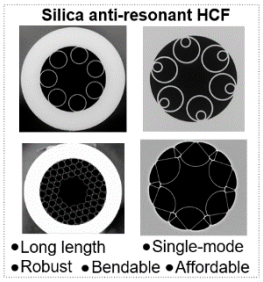

The laser system will be especially conducive to various tissue ablation investigations and high-precision surgical applications, e.g., cornea keratoplasty and brain tissue incisions.

Research Programme: The adjacent figure shows highly interlinked work packages. It highlights:

- The combination of work packages required to deliver this proposal.
- The need for continuous interactions between/across multiple work packages.
- The importance of integration/development of laser treatment methodology.
- The work direction for future clinical validation and evaluation.

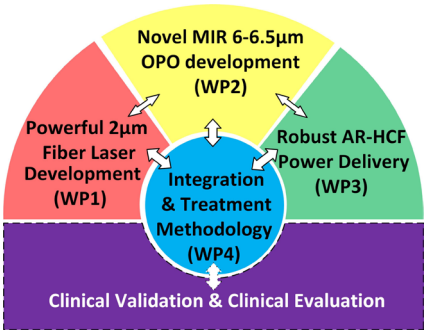

WP1: Short-pulsed 2-µm fiber laser systems with remarkable control of power and temporal characteristics. As an OPO pump source, a compact, maintenance-free, high-beam-quality fiber laser will be designed and built (not achievable for traditional bulk pump lasers). It will employ a holmium-doped-fiber master oscillator power amplifier (MOPA) configuration seeded by a 2.05-µm gain-switched laser diode. The MOPA consists of 3-4 amplifier stages to enable average/peak power scaling to 50-W/100-kW. The MOPA output will be near-diffraction-limited, linearly-polarised, and have a narrow spectral linewidth (<3.5 nm) to facilitate efficient pumping of the OPO (WP2). The MOPA temporal properties will be accurately driven/controlled by an arbitrary waveform generator and engineered to work in the picosecond or sub-nanosecond regimes with great flexibility in pulse duration, pattern, shape, and repetition rate. The temporal characteristics of the MOPA will dictate those of the proposed OPO which can be adjusted to achieve optimal ablation. For small collateral damage, "cold" photomechanical ablation is typically desirable [1,26], and requires short pulse durations, e.g. <3.1ns for corneas at 6.1µm [16].

The all-fiberized high-power 2.05-µm laser with unprecedented temporal control will be developed for the 1st time. I have gained all the experience needed (throughout my PhD research) to develop it.

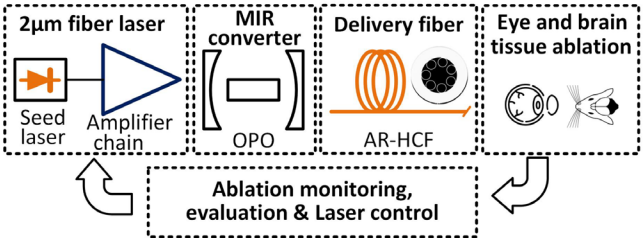

WP2: Tuneable MIR OPO laser covering the target 6-6.5 μm wavelength band. Driven by the estimated threshold peak powers for soft tissue ablation of ~1 kW (fluence ~1 J/cm^2 for nanosecond pulses [1,16,26], reducing with shorter pulses), a >10-kW-peak-power MIR OPO will be built in this project pumped by the fiber laser developed in WP1, providing flexible 6-6.5 μm tuneability and high beam quality output. The nonlinear crystal is a key element for OPO design; here I will employ zinc-germanium-phosphide (ZGP) crystal with large nonlinear coefficient (75 pm/V), high damage threshold (55.6 MW/cm^2 at 1 μm, 10 ns), good thermal conductivity and good mechanical properties. Using phase-matching technique, the OPO wavelength can be accurately tuned (by tuning crystal angle from 53.6° to 54.4°) between 6 to 6.5 μm. To scale the peak power to the 10 kW level, I will employ novel OPO designs invented by my previous works at Optoelectronics Research Centre (ORC), UK: burst-mode-pumping cavities [27] or fiber-feedback-cavities [28].

This unique OPO development requires cutting-edge short-pulsed MIR OPO design and implementation skills. I have been an experienced researcher in this area for >5 years [29,30].

WP3: Delivery of high-power MIR laser pulses. In this proposal, we plan to develop a power delivery system based on silica AR-HCF. The fibers will be fabricated in specialty fiber drawing cleanrooms, in collaboration with the team led by Prof. Xin Jiang, a leading specialist in HCFs at the Russell Centre for Advanced Lightwave Science (Philip Russell Centre). We will optimize key structural parameters of the AR-HCF, such as core sizes, number of tubes, membrane thickness, and tube gaps. These optimizations will build on state-of-the-art designs that I developed during my previous works at the ORC. The aim is to achieve an AR-HCF with a transmission loss of <1 dB/m and an overall delivery system insertion loss of <3 dB over a meter-scale power delivery. The robust AR-HCFs developed will be specifically used to deliver fundamental-mode MIR pulses within the 6-6.5 μm range. This capability will be employed for the 1st time to investigate the ablation of biological tissues. Furthermore, with support from Han's Laser Technology, a leading domestic industrial laser company, we will engineer a practical bench-top ablation laser system with a distally designed handpiece to facilitate use during tissue ablation tests proposed in WP4.

AR-HCF technology is a cutting-edge and rapidly evolving field. My previous contributions have led to the development of two state-of-the-art MIR hollow-core fibers specifically at wavelengths of 4.5-6 μm, as documented in references [31] and [32].

WP4: Tissue treatment methodology development and integration of laser system. We will systematically investigate tissue ablation in vitro. This research will be conducted in collaboration with biological partners at the College of Life Sciences and Medicine, Shenzhen University. After monitoring and precise evaluation, we will adjust various laser parameters such as wavelength, power, pulse duration/structure, and exposure time. These parameters, initially developed in WP2 and WP3, will be optimized to achieve optimal ablation outcomes. Detailed studies will be carried out to understand ablation phenomena across different tissue types, including selective ablation capabilities and performance in/around fluid-filled areas (cerebrospinal fluid in brain surgery). This will help evaluate the practicality of the laser system in diverse clinical scenarios. Outcomes from these experiments will be benchmarked against traditional mechanical ablation techniques, such as the use of a scalpel (eye surgery) and bipolar electrocautery (neurosurgery). Emphasis will be placed on the ablation of animal eye and brain tissues, setting the stage for progression from post-mortem human tissue studies to in vivo applications and, ultimately, clinical trials. As part of our long-term engagement strategy, we will organize focus groups with clinicians to observe and assess the technology, and to study relevant patient cohorts that meet the necessary clinical criteria.

Overall, my unique expertise in fiber lasers, OPOs, and AR-HCFs uniquely positions our team to lead this pioneering project.

Reference list:

[1] Vogel, et al, Chemical Reviews **103**(2), 577-644 (2003). https://doi.org/10.1021/cr010379n

[2] Vodopyanov, John Wiley & Sons, 2020. https://doi.org/10.1002/9781119074557.ch7

[3] Ryan, Journal of Neurosurgery JNS **112**(2), 434 (2010). https://doi.org/10.3171/2009.7.JNS09356

[4] Serebryakov, et al, J. Opt. Technol. **82**(12), 781-788 (2015). https://doi.org/10.1364/JOT.82.000781
[5] Edwards, Nature 371(6496), 416-419 (1994). https://doi.org/10.1038/371416a0
[6] Edwards, et al, Commercial and Biomedical Applications of Ultrafast and Free-Electron Lasers 184-193 (2002). https://doi.org/10.1117/12.461378
[7] Edwards, Review of scientific instruments **74**(7), 3207 (2003). https://doi.org/10.1063/1.1584078
[8] Joos, et al, Ophthalmic Technologies VI 89-92 (1996). https://doi.org/10.1117/12.240051
[9] Shah, et al, Lasers in Surgery and Medicine **39**(7), 589 (2007). https://doi.org/10.1002/lsm.20531
[10] Huang, et al, Ophthalmic technologies XXII 167-172 (2012). https://doi.org/10.1117/12.908468
[11] Hashimura, et al, Journal of Innovative Optical Health Sciences **07**(03), 1450029 (2014). https://doi.org/10.1142/S1793545814500291
[12] Dunn, Science **286**(5444), 1513-1517 (1999). http://doi.org/10.1126/science.286.5444.1513
[13] Petrov, Prog. in Quantum Electronics **42**, (2015).https://doi.org/10.1016/j.pquantelec.2015.04.001
[14] Brian,Tunable laser applications. CRC Press, 2016. 17-142. https://doi.org/10.1201/b19508
[15] Edwards, Commercial and Biomedical Applications of Ultrafast and Free-Electron Lasers 194-200 (2002). https://doi.org/10.1117/12.461379
[16] Mackanos, Lasers in Surg. and Med. **39**(3), 230-236 (2007). https://doi.org/10.1002/lsm.20461
[17] Stoeppler, Laser Physics **22**(6), 1095-1098 (2012). https://doi.org/10.1134/S1054660X12060114
[18] Lv, et al, Opt. Lett. 47(6), 1359-1362 (2022). https://doi.org/10.1364/OL.446336
[19] Edwards, Laser & Photon. Rev. **3**(6), 545-555 (2009). https://doi.org/10.1002/lpor.200810063
[20] Mackanos, IEEE J. Sel. Top. Quant. **18**(4), 1514(2012).https://doi.org/10.1109/JSTQE.2012.2188501
[21] Kim et al, J. Biomed. Opt. 6(3), (2001). https://doi.org/10.1117/1.1381561
[22] Vogel, Medical Laser Application **17**(1), 15-20 (2002). https://doi.org/10.1078/1615-1615-00040
[23] Venugopalan, IEEE Trans. on Biomed. Eng. **38**(10), 1049 (1991). https://doi.org/10.1109/10.88452
[24] Wang, Current Pharm. Biotec. **11**(4), 384 (2010). http://dx.doi.org/10.2174/138920110791233271
[25] Tao, et al, Adv. in Opt. and Photon. **7**(2), 379-458 (2015). https://doi.org/10.1364/AOP.7.000379
[26] Franjic, et al, Opt. Express **17**(25), 22937-22959 (2009). https://doi.org/10.1364/OE.17.022937
[27] Wu, OSA Continuum **3**, 2741 (2020). https://doi.org/10.1364/OSAC.400213
[28] Wu, et al, Opt. Lett. **47**(14), 3600-3603 (2022). https://doi.org/10.1364/OL.461118
[29] Fu, et al, Opt. Express **28**(4), 5741 (2020). https://doi.org/10.1364/OE.380189
[30] Fu, et al, Opt. Express **28**(22), 32540 (2020). https://doi.org/10.1364/OE.402360
[31] Fu, et al, Opt. Lett. 47(20), 5301-5304 (2022). https://doi.org/10.1364/OL.473230
[32] Fu, et al, CLEO Europe, (2023). http://doi.org/10.1109/CLEO/Europe-EQEC57999.2023.10231907

Impact and Beneficiaries

(a) In laser surgery, patients will benefit from having much lower side effects, better health outcomes, and shorter hospital stays which in turn improves their quality of life and lead to great economic impact. (b) In ophthalmic surgery, there is a significant global shortage of corneal graft tissues with only one available cornea for every 70 needed, and the newly developed laser tool can potentially solve this problem by reducing tissue wastage while allowing multiple corneal transplant recipients to benefit from a single eye donor. (c) In open brain surgery, a significant portion of removed brain/tumor tissues is typically unsuitable for further medical investigation or research, which are in high demand. The laser tool will be used for high-precision tissue removal, effectively preserving most of the tissues obtained from surgical cases. This enhanced preservation could potentially alleviate the critical shortage of living tissue samples in brain tissue banks. (d) Apart from healthcare area, free space communication, sensing, industrial/additive manufacturing, and remote detection will be greatly benefited by the new MIR laser and fiber technology. (e) In academic area, researchers will benefit significantly from the knowledge/data presented in high-profile journals and conferences.

Outcome and Ambition

The primary outcome of this OPTICA Foundation Challenge is the development of a cutting-edge MIR laser prototype, utilizing advanced 6-6.5μm laser and fiber technologies. Funded by the OPTICA Foundation, this project aims to revolutionize laser surgery by introducing transformative technology that enhances surgical precision, thereby improving patient outcomes, reducing hospital stays,

ensuring safer surgical environments, and advancing medical research, particularly in neuroscience. I plan to lead a dynamic, DEI-friendly research team dedicated to high-precision surgery, tackling critical issues such as surgical side effects, and achieving breakthroughs in reducing tissue wastage and damage. Throughout this initiative, I will enhance my academic standing by presenting our findings at conferences and fostering collaborations across academic and industrial sectors, while actively seeking further grant funding (see Timeline, T8). This award will provide the essential skills and resources to pioneer laser and fiber technologies in high-precision laser surgery. Over the next two years, my team, which includes 2 PhDs and a postdoc, will focus on developing a robust laser system designed for precise tissue ablation, setting new benchmarks in the field of medical surgery.

Host Institution and Collaboration

The project, co-hosted by the Center for Biomedical Photonics (CBP) and the Key Laboratory of Laser Engineering at Shenzhen University, is well-equipped with cutting-edge laser and fiber optic instruments essential for developing high-precision surgical laser technology. As an experienced HCF researcher, I will utilize my fiber design expertise alongside the Philip Russell Centre's fabrication facilities to produce specialized fibers tailored for this project. Under the leadership of Prof. Junle Qu, an OPTICA Fellow specializing in photonics imaging, we will extend the CBP's focus to include therapeutic laser applications, filling a crucial gap in its capabilities. Collaborations with the School of Life Sciences and Medicine at Shenzhen University and Han's Laser Technology will provide vital biological insights and ensure industrial applicability. This unique combination of advanced research and strategic partnerships positions us to lead in pioneering surgical laser technology.

Risk Assessment and Mitigation Strategies

The risks associated with WP1 and WP2 are low, leveraging my expertise and support from the host institution, with regular reviews planned to ensure alignment and efficiency. WP3 faces a medium risk of higher-than-expected fiber losses; we will mitigate this by increasing the laser's power budget and adjusting designs for greater loss tolerance. WP4 could experience delays due to insufficient animal tissue supplies, which we will address by closely coordinating with our biomedical partner and identifying alternative sources. Equipment failures, particularly the fiber drawing tower, pose a medium risk to facility-dependent tasks; we will counteract this by utilizing alternative equipment available at the Philip Russell Center's spin-off company- iFiber Optoelectronics Technology. In addition, the risk of human resource shortages due to partners or PhD students withdrawing will be mitigated by developing a broader collaborator network and establishing contingency plans for task redistribution and new recruitments to maintain project continuity.

Exploitation

The technology developed in this project offers broad healthcare applications, including as an ablation tool in ophthalmic, neurosurgical, and cancer treatments. We will conduct a pilot study on targeted patient cohorts, such as those needing keratoplasty or brain cancer interventions, utilizing clinical criteria like OCT, MRI, and X-ray to guide trial ablations in a safe, well-equipped environment. Moreover, the project will investigate additional applications such as MIR gas sensing, in collaboration with academic and industrial partners. Throughout the OPTICA Foundation Challenge, we will evaluate the commercial viability of the medical laser, tailoring its design for key market sectors and involving focus groups of clinicians and industry partners for feedback and rapid knowledge transfer. We will also perform a preliminary health economic analysis to highlight the technology's financial benefits. Intellectual property arising from this project will be diligently managed for patenting and licensing, leveraging the University's robust IP procedures and the Center for Biomedical Photonics at Shenzhen University's expertise in commercializing innovations.

Dissemination and Public Engagement

I will globally disseminate the outcomes of this project through publications in open access OPTICA journals like Optica, Biomedical Optics Express, and Optics Letters as well as in other high-prestigious journals such as Science Advances and Nature Photonics. Additionally, I will present our findings at international conferences, including CLEO, High Brightness Congress, and SPIE Photonics West, making the research accessible via my university's digital repository. Actively engaged in public outreach, I will participate in science festivals and conduct educational programs in local schools to foster an interest in photonics. As Chair of the "Lasers in Manufacturing" and Committee Member of the "Therapeutic Laser Application" technical groups at OPTICA, I will organize webinars and sessions that showcase practical laser applications, aiming to attract and cultivate new talent in the field.

A quantum information processor based on a high-finesse ring-resonator including a nanofiber cold-atom light-matter interface

Category: Information

Executive summary

Targeted Challenge

Engineering strong coupling between propagating photons and isolated quantum emitters is a crucial prerequisite for the transmission and processing of optically encoded quantum information, as well as for revealing novel quantum phenomena. Unfortunately, the interaction between light and most quantum emitters is typically weak. Indeed, even when tightly focusing a photon on a single trapped atom, the probability the two interact is in practice very low. For this reason, in the last decades, various strategies to enhance photon-atom coupling have been developed. In *cavity quantum electrodynamics* (QED), atoms are placed between highly reflective mirrors, allowing photons to bounce back and forth, thereby increasing the interaction probability. Instead, in *waveguide QED*, photons propagate through nanophotonic structures, that allow one to obtain stronger coupling than in free space and enable interactions with multiple atoms. Both cavity and waveguide quantum electrodynamics often lack single-atom control and addressability. This limitation is addressed by an emerging paradigm that employs *arrays of atoms trapped in optical tweezers*, offering unprecedent control over atomic internal and external degrees of freedom.

Proposed project

The ambitious goal of this project is to demonstrate a novel quantum system that combine advantages of cavity and waveguide QED with the single-atom control offered by arrays of optical tweezers. This system will consist of a high-finesse all-fiber ring-resonator including a so-called optical nanofiber (i.e., glass fiber 100 times thinner than a human hair). An ensemble of up to hundred neutral atoms will be trapped about 300 nm away from the nanofiber surface by shining an array of optical tweezers towards the nanofiber surface. The resulting system will allow us to explore a novel regime of light-matter coupling: it will operate in the single-atom strong coupling regime of cavity QED (cooperativity, $C > 1$), while maintaining a very high single-pass optical depth (optical depth, $OD > 1$), a rare combination required for the demonstration of novel protocols for quantum information processing. Furthermore, being entirely based on standard single-mode fiber, the proposed system will seamlessly integrate into any current or future fiber networks.

Intended outcomes

The proposed system will be capable of experimentally implementing quantum protocols that are beyond the capabilities of any existing platform. As an example, within the context of this proposal, we will demonstrate that it can operate as a photon sorter, i.e., a device that is able to decompose a coherent light pulse into its Fock state components. Such a device represents a "holy grail" in the field of quantum optics, as it would receive a classical input (i.e., a laser pulse) and deterministically produce a highly non-classical state of light as an output, a very desirable operation in quantum information processing.

A quantum information processor based on a high-finesse ring-resonator including a nanofiber cold-atom light-matter interface

Literature Review

Investigating the interaction between photons and quantum emitters has unveiled some of the most counterintuitive phenomena of quantum physics. While these discoveries are fascinating in their own right, they also pave the way for groundbreaking *quantum technologies* that simply cannot be matched by *classical devices*. However, the interactions between individual photons and isolated quantum emitters are generally weak and thus probabilistic. To harness the full potential of quantum mechanics, it is essential to engineer artificial systems, in which this interaction is strongly enhanced and therefore **deterministic**.

Historically, one of the most successful approaches developed for this purpose relied on placing the quantum emitters within the mirrors of a high-finesse optical cavity [1]. In **cavity quantum electrodynamics** (QED), the photon-emitter interaction strength is enhanced by the number of cavity roundtrips that the photon makes before being lost into the environment. An important figure of merit for cavity QED setups is the cooperativity parameter, defined as: $C=g^2/(\kappa\,\gamma)$, where g is the coupling rate between the emitters and the cavity, κ is the cavity loss rate and γ is the spontaneous decay rate of the emitters. Most of the applications in quantum information processing require operations in the **single-atom strong-coupling regime**, meaning $C > 1$ [1].

A complementary and more recent approach is offered by the rapidly growing field of **waveguide QED** [2, 3], in which quantum emitters are coupled to photons propagating in nanophotonic structures. Not only does this allow to achieve interaction strengths between a propagating photon and a single quantum emitter significantly stronger than in free space [1], but due to the low propagation loss of current nanophotonic devices, each propagating photon can interact equally strongly with a large number (i.e., hundreds or more) of successive emitters over long propagation distances.

It is important to note that in both cavity and waveguide electrodynamics it is typically not possible to individually address and control each quantum emitters, a feature that is highly desirable for quantum information processing. This capability has been pioneered by recent experiments, in which large ensembles of atoms are trapped using **arrays of optical tweezers** [4], and that are therefore quickly becoming a leading platform for quantum computation and simulation.

A logical question to address is whether the different advantages offered by these approaches of enhancing and controlling photon-atom interactions could **combined** to reach completely unexplored regimes of light-matter coupling (see Fig.1). Despite years of effort and notable attempts, current nanophotonic platforms have only achieved strong coupling with a few emitters coupled to nanophotonic waveguides via optical tweezers [5, 6], or to couple thousands of emitters to the same cavity mode, but in the weak-coupling regime [7, 8].

Over the past few years, we have also risen to this challenge, by demonstrating a platform able to **bridge the fields of cavity and waveguide QED**, consisting of an all-fiber ring-resonator containing an optical nanofiber, i.e., a glass fiber 100 times thinner than a human hair [8, 9, 10]. This configuration permits to interface

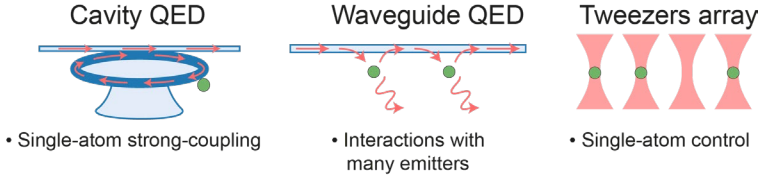

Fig. 1. Cavity QED, waveguide QED, and optical tweezer arrays each offer unique advantages. Combining these technologies could enable the exploration of new regimes of light-matter interaction.

thousands of cold atoms with photons propagating in the ring-resonator via the evanescent field of the optical nanofiber. This has been rather successful, allowing us to study the collective radiative dynamics of large ensembles of waveguide-coupled quantum emitters [9, 10] and the transition regime between cavity and waveguide QED, including its related non-Markovian dynamics [8].

Problem Statement/Objectives

Envisioned platform

In this project we aim to experimentally demonstrate a **novel hybrid nanophotonic system** for processing optically encoded quantum information. This system will **combine** (i) the **strong all-to-all interactions** typical of cavity QED, (ii) the **long interaction lengths** of waveguide QED and (iii) the **single-atom control** demonstrated with optical tweezers arrays. The envision platform is shown schematically in Fig. 2 and consists of a **high-finesse ring-resonator** containing an optical **nanofibre**. A **1D array of optical tweezers** will be used to trap a large ensemble of laser-cooled atoms about 300 nm away from the nanofiber surface. The key idea behind this configuration is to employ the nanofiber to allow a single propagating photon to interact strongly with each of the hundreds of trapped atoms, while the high-finesse ring-resonator will further enhance their coupling strength. The resulting cavity QED system will operate in the single-atom strong coupling regime, i.e., $C > 1$, for each of the hundred trapped atoms. Finally, the tweezers array will allow each of the trapped atoms to be addressed individually, allowing their internal state to be prepared and their relative distance to be precisely controlled.

An exciting feature of the proposed system is that it will operate in the **single-atom strong coupling regime** ($C > 1$), while maintaining a very high **single-pass optical depth** ($OD > 1$), a rare combination required for the experimental realization of **novel quantum protocols** [2]. As an example, in the context of this proposal, we will demonstrate the predicted but not yet measured photon number dependent group delay in vacuum induced transparency (VIT) [11, 12]. This protocol would lead to the temporal separation of a coherent light pulse into its Fock state components, leading to the demonstration of an **all-fiber photon sorter** (see Fig. 2), a highly sought-after device in quantum information processing.

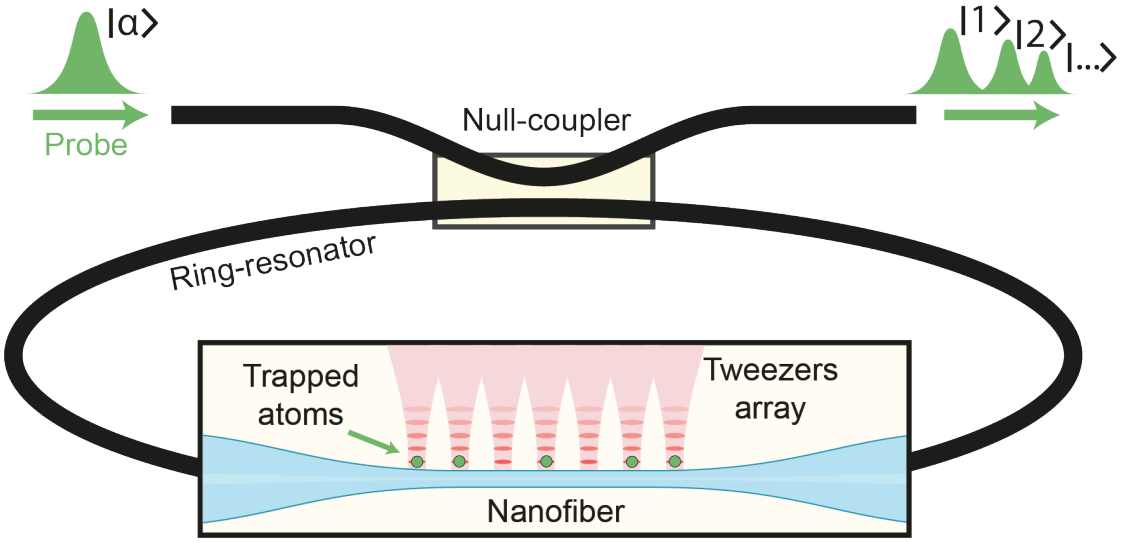

Fig. 2. The envision platform consists of an all-fiber, high-finesse ring-resonator containing an optical nanofiber. A 1D array of optical tweezers is used to trap up to a hundred laser-cooled atoms close to the nanofiber surface. This system will be used to demonstrate photon sorting, i.e., the temporal separation of a coherent light pulse into its Fock-state components (green-shaded pulses).

Another important feature of the proposed system is that, since it is completely based on standard single-mode optical fibers, it could be seamlessly integrated in fibers networks with very low insertion loss, a highly desirable characteristic for applications in quantum information processing and quantum networks, where photon loss should be avoided at all costs. Possible applications in this direction include the generation of non-classical states of light [13] and realization of photon-photon quantum gates [14].

Objectives

The following objectives (Objs.) will be pursued:

Obj.1: Demonstration of a **novel nanophotonic system**, consisting of large ($N > 100$) ensemble of optically trapped and individually addressable atoms, in which strong all-to-all interactions are engineered via coupling to the optical mode of a nanofiber-based high-finesse ring-resonator.

Obj. 2: Prove the potential of this platform by demonstrating novel quantum effects **beyond** the capabilities of **existing systems**. As an example, we will experimentally demonstrate that our system can operate as a **photon sorter**, i.e., it is able to deterministically separate in time the photon number components of a laser pulse. This protocol is based on the phenomenon of vacuum induced transparency and requires operations in an extreme regime of cavity QED, which, remarkably, can be accessed using our system.

Main elements of the proposal and preparatory work

I acknowledge that the proposed project is ambitious given the time and budget constraints of this call. However, considerable preparatory work has been carried out by our group over the last few years and I am convinced that we will be able to achieve our goals by the end of the project. In the following, I will discuss in more detail the main elements of the proposal, including our preliminary results.

Nanofiber cold-atoms interface and high-finesse ring cavities

Coupling large atomic ensembles to optical nanofibers is the specialty of our group, which pioneered this technique a little over 10 years ago. In particular, this project will take place in the so-called NanoFiRe Lab in the group of Prof. Rauschenbeutel at the Humboldt University in Berlin. This lab hosts a recently build cold atoms experiment in which laser-cooled cesium atoms are coupled to an optical nanofiber integrated into all-fiber ring-resonator [8, 9, 10]. Previously, technical limitations prevented us from reaching the single-atom strong coupling regime, primarily due to the high-loss (around 10% round-trip loss, corresponding to a finesse $F \approx 60$) resulting from the need of integrating commercially available tunable fiber couplers in our setup. Recently, in our self-built fiber post-processing rig we developed the fabrication of so-called **null-couplers** [15], in which the light coupling ratio can be controlled by launching acoustic waves propagating along the coupler waist. Importantly, null-couplers feature very low insertion loss (about 1%) and also allow for different couplings ratios for two orthogonal polarizations, a feature crucial for the demonstration of photon sorting. We have already demonstrated in our lab that using such couplers ring-resonator can be built with a finesse $F > 300$, which is more than enough to reach the single-atom strong coupling regime.

Trapping of atoms via tweezers arrays

Ensembles of laser-cooled atoms are typically trapped in the evanescent field of a nanofiber using nanofiber-guided laser beams [16]. This method, which is routinely used in our group, requires about 20 mW of nanofiber-guided light. As the nanofiber is placed in ultra-high vacuum, this leads to an increase in the temperature of the nanofiber of several hundred degrees. We have observed experimentally that when the nanofiber is integrated into a ring resonator, its temperature increase causes very fast and very large fluctuations of the resonator modes, making it very difficult to perform further experiments.

For this reason, for this project we will instead trap the atoms by shining towards the nanofiber an array of optical tweezers. When the tweezer beam hits the nanofiber, it forms a standing wave close to nanofiber due to the interference of the incident and the reflected lights. This creates optical traps for laser cooled atoms approximately 300 nm from the nanofiber surface. This technique has already been demonstrated for the trapping of up to three atoms in the evanescent field of nanophotonic structures [17] (and for a single atom with optical nanofibers [5]). Taking advantage of the enormous progress in experimental techniques for manipulating large arrays of atoms in free space [4], we aim at extending this technique in the field of waveguide QED and demonstrated up to hundred nanofiber-coupled atoms. We note that compared to free-space tweezers for, e.g., quantum computing, several experimental details are considerably simpler in our case. For example, due to waveguide mediated infinite-range interactions, in our case, there is no not need to bring the atoms very close together to achieve strong interactions, nor is it critical to be able to rearrange them to form defect-free ensembles. We note that this technique requires overall a much higher power (>1 W see Timeline) with respect to the traditional nanofiber-based trapping via guided modes. Nonetheless, the light glass overlap in the case of tweezers is several orders of magnitude smaller than for propagating fields and as a consequence, we do not expect any instability in the cavity modes.

Finally, I would like to mention that, while our group has extensive experience with single tweezers for laser-cooled atoms [18], we have not yet attempted to operate large (i.e., hundreds) optical tweezers simultaneously. For this reason, I plan to spend three months (August to October 2024) in the group of **Prof. Jeff Thompson** at **Princeton University**, one of the world leaders in this field, to familiarize myself with these experimental methods. I have already secured funding for this research stay through the "Strategic Partnership Program" of the Humboldt University of Berlin.

Outcomes

The most immediate outcome of this project will be the experimental demonstration of a protocol for quantum information processing that is beyond the capabilities of any existing platform. We will realize a **photon sorter**. The latter refers to a device that is able to separate a laser pulse into its photon number components (see Fig. 2). Such a device represents a "holy grail" in the field of quantum optics, as it would take a classical input (i.e., a laser pulse) and deterministically produce a highly non-classical state of light as an output, a very desirable operation in quantum information processing [19, 20].

Around a decade ago, it was predicted that this could be realized using vacuum induced transparency (VIT) in ensembles of cold atoms [11, 12, 20]. VIT is a coherent effect analogue to electromagnetically induced transparency (EIT), in which the control beam is replaced by a quantized cavity mode (Fig. 3(a)). As observed in standard EIT, also VIT allows one to open a transparency window in an opaque medium for a probe field and to slow-down its propagation by tailoring its group velocity (see Fig. 3(b)). This occurs due to a temporary transfer of the photon excitation from the probe field to the cavity mode. In VIT the width of the transparency window as well as the

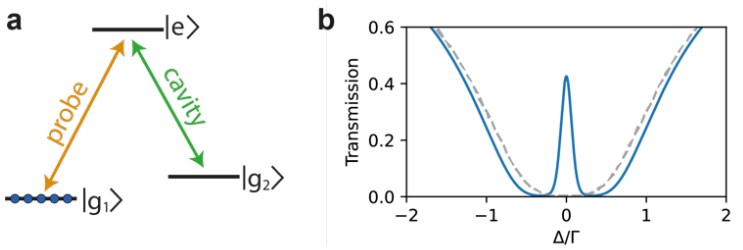

Fig. 3. (a) Λ-type energy level scheme required for VIT. In our implementation we will use the following internal states of Cs: $|g_1\rangle = |6S_{1\backslash 2}, F=3\rangle$, $|g_2\rangle = |6S_{1\backslash 2}, F=4\rangle$ and $|e\rangle = |6P_{3\backslash 2}, F=4\rangle$. (b) Calculated VIT spectrum (blue line) for an ensemble of atoms coupled to a nanofiber ring-resonator. The coupling to the cavity allows to open a transparency window into an otherwise opaque medium. The gray line indicated the single-pass transmission without the cavity. This calculation has been performed assuming the realistic parameters: single pass OD = 5 and single-atom cooperativity C = 6.3.

group velocity of the probe beam depend on the number of photons in the cavity mode, which in turn is determined by the number of photons initially present in the probe pulse. For this reason, the different photon-number components of the probe field will experience different group velocities and can be separated in time. To observe this phenomenon, one has to satisfy two conditions: (i) single-pass optical depth, OD > 1 and (ii) single-atom cooperativity C > OD [12]. Notably, these very stringent conditions can be easily met for the system in this proposal.

Impact

This proposal has several **novel elements**, each of which is likely to have a **major impact** on the fields of quantum optics and quantum information processing.

Waveguide-coupled tweezer arrays would enable the first-ever demonstration of a waveguide QED system with over 100 individually addressable emitters. This remarkable result would not only advance quantum information processing but also open up unprecedented opportunities to study **collective radiative dynamics**, such as **superradiance** and **subradiance**, in large ensembles of emitters [9, 10].

The **trapping of atoms** in an **all-fibre resonator** in the single-atom strong coupling regime will have a major impact on fundamental studies of quantum optics and in particular on the study of **non-Markovian quantum systems**. In fact, the low optical loss of optical fibers allows for the creation of exceptionally long cavities (up to several tens of meters), where the round-trip time can be comparable to or exceed the excited state lifetime of the emitters. In this case, the feedback provided by the cavity is not instantaneous, i.e., the cavity acts as a non-Markovian reservoir. Although we have conducted initial measurements in this direction [8], we have not yet reached the single-atom strong coupling regime, limiting our ability to fully investigate the quantum properties of this system. I would like to emphasize that such an experimental setup is unprecedented at optical frequencies.

Finally, there is no doubt that the experimental demonstration of **photon sorting**, discussed above, would represent a ground-breaking milestone for quantum information processing.

References

[1] A. Reiserer et al., Rev. Mod. Phys., 87, 1379-1418 (2015)
[2] D. Chang et al., Rev. Mod. Phys., 90, 031002 (2018)
[3] A.S. Sheremet et al., Rev. Mod. Phys., 95, 015002 (2023)
[4] A.M. Kaufman et al., Nat. Phys., 17, 1324-1333 (2021)
[5] K. Nayak et al., Phys. Rev. Lett., 123, 213602 (2019)
[6] T. Đorđević et al., Science, 373, 1511-1514 (2021)
[7] S. K. Ruddell et al., Optica, 4, 576 (2017)
[8] D. Lechner et al., Phys. Rev. Lett., 131, 103603 (2023)
[9] R. Pennetta et al., Phys. Rev. Lett., 128, 073601 (2022)
[10] R. Pennetta et al., Phys. Rev. Lett. 128, 203601 (2022)
[11] H. Tanji-Suzuki et al., Science, 333, 1266-1269 (2011)
[12] G. Nikoghosyan et al., Phys. Rev. Lett., 105, 013601 (2010)
[13] A. S. Prasad et al., Nat. Phot., 14, 719 (2020)
[14] B. Hacker et al., Nature, 536, 193-196 (2016)
[15] T. Birks et al., Journ. Light. Tech., 14, 11 (1996)
[16] E. Vetsch et al., Phys. Rev. Lett., 104, 203603 (2010)
[17] A. Goban et al., Phys. Rev. Lett., 115, 063601 (2015)
[18] L. Masters et al., Nat. Phot., Nature Photonics 17, 11 (2023)
[19] F. Yang, et al., Phys. Rev. Lett., 128, 213603 (2022)
[20] N. Lauk et al., Phys. Rev. A, 93, 063818 (2016)

Name of the project: Developing a portable and low-cost device using dynamic light scattering for Rotavirus detection in environmental and drinking water
Category: Environment & Health

Problem Statement:

- 500k children <5 years, and >50k more aged 5-9 die due to diarrhea each year
- 37% of these preventable deaths are due to Rotavirus
- Current detection systems are based on polymerase chain reaction (PCR), genetic sequencing, and SEM, which are expensive, require infrastructure, expensive consumables, highly skilled human resources, and in overall aren't practical for wide-scale deployment in resource-limited settings where they are actually needed.

Proposed Solution: Develop a low-cost, reagent-less, highly portable, Dynamic Light Scattering (DLS) based detection device for rapid detection of rotavirus in water. Pilot experiments with bench-top setup show that we can detect 4000 U/ml live attenuated rotavirus from Rotarix oral vaccine in water.

Features of the target device:

- Should be portable (⌀3cm, length 12cm, <250g), low-cost (~$100 in materials), user-friendly (minimal training required), no reagents required

Real world applications:

- Surveillance of environmental and/or drinking water in resource-limited settings, identify fecal contamination, prevent water-borne diseases transmitted by oral-fecal route

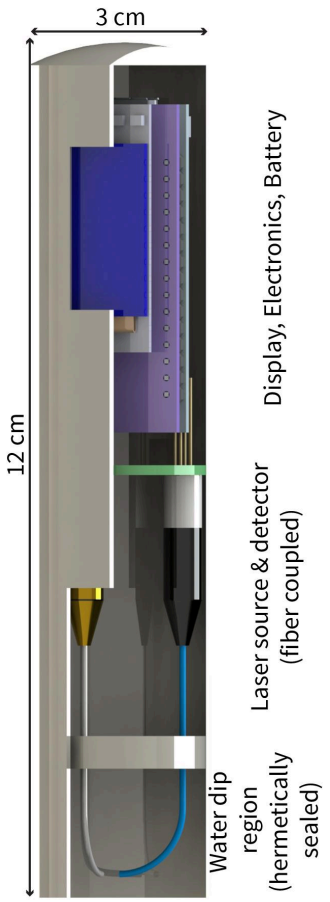

Fig: Design of the proposed system, showing different components

Project outcomes:

- Research, development and related publications in context of using DLS to detect rotavirus particles, focusing on particularly on required sensitivity and specificity
- Understanding of diffusion characteristics of rotavirus particles and their clusters
- Development of a prototype device, reaching alpha testing stage in partnership with local governmental and non-governmental stakeholders in water supply systems
- Foster local research and innovation ecosystem in a developing country, providing research opportunity to solve important global problems

Long-term Impact:

- Reduce infant mortality by at least 50k/ year in developing countries, including Nepal
- Develop methods that can be translated for detecting other kinds of waterborne viruses eg. hepatitis, norovirus etc
- Ensure resilient economic development by promoting and investing in research, innovation & manufacturing capabilities in Nepal

Collaborators: Prof. Daniele Faccio (U of Glasgow, DLS expert)

Developing a portable and low-cost device using dynamic light scattering for Rotavirus detection in environmental and drinking water

Literature Review:
Nearly 500,000 children under the age of 5, and 50,000 more aged 5-9 died due to diarrhea in 2022 (most recent available data) [1]. The vast majority of these deaths are in the low income countries in the world. Nearly 37% of these preventable deaths are attributed to rotavirus infections [2] in spite of the availability of vaccines for almost two decades. Even in the USA, up to 70,000 hospitalizations and 60 deaths are attributed to rotavirus infections. This data underscores the need for enhanced surveillance and proper water-treatment. Prevalent techniques for detection of rotavirus in water are based on polymerase chain reaction (PCR), gene sequencing and SEM – all of which are very challenging for deployment even in well-resourced areas, and particularly infeasible in resource-limited settings. Diagnostic enzyme immunoassay kits are only available to confirm infection with sufficiently high viral load or reactive proteins. Rapid and low-cost technologies to detect rotavirus in water, while important for the whole world, have become critical to save lives in the neediest parts of the world. In order to rapidly increase the surveillance capabilities to prevent these deaths, in this project I will use Dynamic Light Scattering (DLS) based techniques to develop a low-cost, rapid, reagentless, and portable device to detect rotavirus or their clusters in water.

Rotaviruses themselves are 55-70 nm in size [3]. They can also form vesicle cloaked clusters, whose sizes range up to hundreds of nanometers, and are emerging pathogens in water [4]. These vesicle cloaked clusters of rotavirus are of particular concern, because they are difficult to disinfect from the environment with conventional techniques such as chlorination, and can even remain in the environment for up to 16 weeks [4]. Commercial systems using DLS can detect particles up to 1 nm in size, and researchers have demonstrated the viability of using DLS to detect virus clusters already [5, 6]. However, these expensive commercial systems are economically infeasible to scale in developed countries, let alone deploy in the scale needed in low-resource settings. The low-cost and portable device I aim to develop in this project will be used to detect rotavirus in drinking and environmental waters, which will allow communities as well as local governments to take appropriate steps towards preventing spread.

Proposed Solution:
We have developed a simple and low-cost system (currently benchtop) to detect rotavirus particles that can be packaged and implemented in a resource-limited setting [7]. This system used a 5 mW, 532 nm laser, a widely available SMF-28 fiber, a photodiode, a transimpedance amplifier, and inexpensive microcontroller (Fig. 1). This system can currently detect 4000 U/ml live attenuated rotavirus from Rotarix oral vaccine (Fig. 2) in 10 minutes. We are working towards integrating all of these components into a portable prototype (Fig 3). The device will cost less than $100 in components, the size will be comparable to a standard glue-stick (30 mm x 120 mm), and will perform tests in under 10 minutes.

As Fig. 2 shows our pilot results, where the peaks correspond to virus particles that can be identified based on deviation outside of a noise threshold. Detection events were observed

for all virus concentrations from 125 kU/ml to 4 kU/ml but were not observed in the pure water.

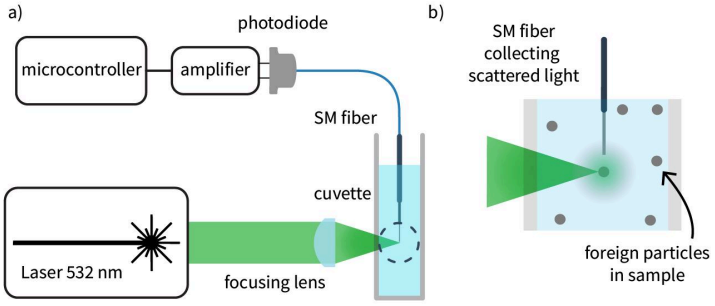

Fig. 1: a) Schematic of the DLS-based system used in the experiments. b) Detail showing fiber collecting scattered light.

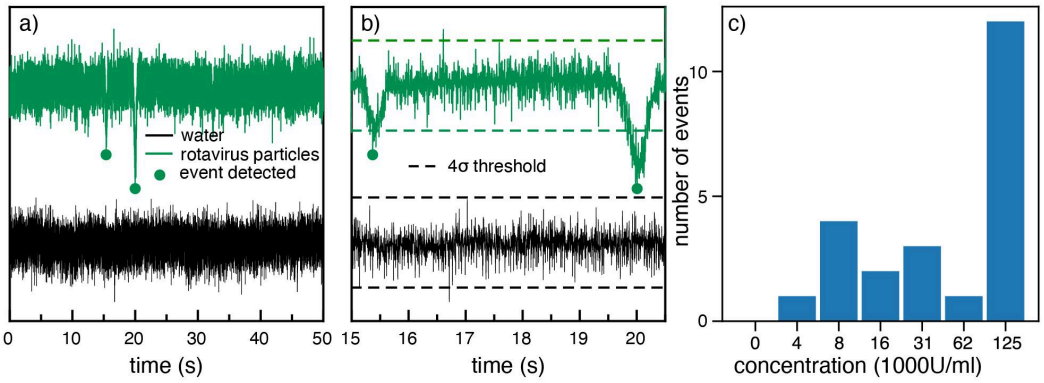

Fig. 2: a) Signals of water and 4x diluted Rotarix vaccine, with detected peaks in arbitrary units, b) Zoomed in version of Fig. 3a to show detail, along with the threshold value, c) Number of events detected by our system in 10 mins for different concentrations of virus particles.

I have been involved in community-engaged co-development of low-cost water surveillance systems for E. coli for the past 5 years [8-12]. Based on my past interactions, different stakeholders in the water system (consumers, water-user communities, regulators, etc.) prefer a portable dip-in system not-requiring any specific technical know-how. Therefore our goal is to develop a simple, low-cost dip-in system as depicted in Fig. 3.

Key Challenges and Objectives:

Challenge 1: A water sample may contain a wide array of foreign particles of different sizes and origins. It is imperative to get rid of the majority of unwanted particles prior to testing for viral particles using my method.

Objective 1: Develop a low-cost method to remove particles that interfere with DLS measurement.

I will start with a basic syringe filtration technique, using commonly available 220 nm syringe membrane filters. A 220 nm filter will remove all the particles (eg. most of the bacteria, silt, etc.) but should allow the rotavirus particles (along with many other virus particles and small molecules). I will try filters of smaller pore-sizes only if needed, as they are more expensive and require higher pressure from a machine.

Fig 3: Conceptual device showing intended use model

Challenge 2: The DLS method will only give me the approximate particle size, it does not tell me if the particle is a rotavirus, or some other particle.

Objective 2: Improving specificity of the DLS method to detect rotavirus. It is well-known that DLS-based technique can identify particle size by measurement of Diffusion coefficient $D = \frac{k_B T}{6\pi\eta r}$. Here, k_B is the Boltzmann constant, T is the temperature, η is the viscosity of water, and r is the particle size (radius for spherical particle). As rotavirus particles or their clusters are known to have specific shape, size and mass, I expect to obtain these specific characteristics of the particles from the measured signal shown in Fig. 2(b). For example, the average mass $\bar{m}$ of the particle can be quantified using the mean squared velocity $\bar{v^2}$ of the particle using the equipartition theorem: $\frac{1}{2}\bar{m}\ \bar{v^2} = \frac{1}{2}k_B T$

Similarly, I also expect to use Langevin dynamics of the particles in the presence of an optical force field, which I had investigated in the context of spectroscopy [12]. Based on the information obtained from several physical parameters, I also intend to use machine learning, which has provided 21% improvement in specificity in the context of fluorescence sensing [10].

Challenge 3: Literature suggests that 100-1000 rotavirus particles are enough to cause an infection. This sets the ideal sensitivity target to <100 particles in 50 ml (a single serving for an infant). Although this level of sensitivity is not possible with any existing technology, without using concentrative steps, I set this goal for this project as I believe that it should be possible using DLS technique.

Objective 3: Enhance sensitivity of the DLS method to detect <100 rotavirus particles/50 ml. Conventionally, concentrative steps using >20 liters of water are used to enhance sensitivity. While this strategy will be my fall-back, I intend to enhance the sensitivity using optical methods. I will explore the use of a cuvettes with reflecting mirrors (so that the effect of a single particle is amplified by multiple reflections), using several SMF-28 fibers at different locations of the probed sample volume, using multimode fibers along a CMOS camera so that a larger volume is probed at once.

Objective 4: Miniaturized dip-in alpha-product development, and validation with real-world samples outside the lab environment. A miniaturized dip-in alpha-product, as envisaged in Fig. 3, is my goal. I expect this objective to be constrained by the boundary conditions set by the outcomes of the previous objectives (specificity and sensitivity). However, with my >10 years of experience in opto-mechanical hardware and software design and validation, I am confident to fulfill this objective. I have a demonstrated track record [8-10] of taking a benchtop system to a portable (10x reduction in weight and size), low-cost (15x reduction in cost) version of the device. That portable device focused on detecting bacterial contamination in drinking water, and is now entering the commercialization phase. I am now turning towards real-time detection of rotavirus that has remained elusive in spite of causing 37% of infant deaths. With the benchtop system already showing promise in our pilot experiments for detecting rotavirus, we now move towards taking that to build a more sensitive, more specific, smaller, portable, and lower cost system.

In the final device I hope to use a fiber-coupled laser, and a fiber-coupled detector, the respective driver and amplifier would then be connected to a commercially available

microcontroller, which will perform the measurement and display it on a screen. Based on the measurement, it would also indicate via traffic-light LED. In the case when we need to increase specificity by using machine learning techniques, the device can connect to a server that runs the machine learning algorithm (if needed), using readily available GSM sim-card modules. The device casing will be made of ABS plastic for durability. Validation experiments for the envisaged alpha product will compare the sensitivity and specificity with PCR-based methods on environmental water from 100-200 sources.

Objective 5: **Further development, funding, etc.**
The Optica Challenge funding will support initial prototype development. In order to take this solution to the people, we would need more funding, for which we can apply to grants that support impact ventures like this. Specifically, I will seek support from USAID and UKAID that are known to support the planned activities. I also expect that accelerators and investors in the network Optica/Optica Foundation could also be helpful.

Outcomes

- Publications regarding:
  - specific diffusion behavior of the rotavirus particles, as they are found in the water distribution system and the environment, which will help their detection using techniques such as DLS
  - optical methods for enhancing sensitivity to detect 100 rotavirus particles in 100 ml sample
  - simple and low-cost method for sample preparation for DLS measurements
  - these publications will also help translate detection of other virus particles (eg. hepatitis, norovirus, etc.) and other liquid medium
- Enhanced partnerships:
  - with local governments and local community for co-development of a dip-in system
    - Lubhu Tallo Dobhan Water Supply Community (Partnership agreement signed)
    - Tarakeshwor Municipality (Partnership agreement signed)
  - with the group of Prof. Daniele Faccio (University of Glasgow), with whom we have been collaborating on this project
- TRL-6 prototype of a dip-in system to detect rotavirus and their clusters
  - designs, relevant patents
  - route for further development and impact
- Personal and institutional development

Long-term impact:

- **Better surveillance method for water-borne viruses in general**. Currently no realtime method exists to detect virus particles in environmental or drinking water. Although I will exclusively focus on rotavirus in this project, the outcomes from this project will be useful for surveillance of many other viruses (eg. hepatitis, norovirus, etc.), in many other liquid mediums (eg. serum). Successful completion of this project is likely to have immense impact in the academic and scientific community, industries, and society.
- **Saving lives in developing countries.** Assuming that only 25% of the rotavirus infections are reduced due to the real-time detection method we have developed, it will help save almost 50,000 infant lives per year in developing countries. Low-cost and reagentless properties of the proposed method is particularly helpful to facilitate implementation and achieve the stated 25% reductions in the infections.

- **Supporting industrialization and R&D ecosystem in Nepal.**

Immediate impact:

- **R&D opportunities and training to the local students and scientists**
  Projects like these also provide a platform for students and recent graduates to develop the basics of research skills and work in the country they call home. We have trained nearly 50 scientists at our institute, who would likely not have had any opportunity to learn and research in the field of optics and photonics in Nepal. This project will help me continue developing necessary laboratory infrastructure, provide R&D opportunities and training to the local students and scientists, and inspire many potential future leaders to work in optics, biophotonics, physics, and research in general.
- **Personal level: grow as a leader in Optics**
  Receiving the Optica Challenge Prize will enable me to not only solve one of the most pressing issues in the developing countries, it will allow me to continue to grow as a leader in cutting edge scientific research, development and innovation, in spite of extremely limited resources we have in Nepal.

Finally, as we highlighted in our recent comment in Nature Reviews: Methods and Primers, support from international collaborators, and funding from organizations like Optica is instrumental in nurturing the nascent research ecosystem that we have here in Nepal [11]. Projects like the proposed one give opportunities, and confidence, for scientists and engineers in low resource countries to create a positive, and lasting societal impact.

References

[1] United Nations Inter-agency Group for Child Mortality Estimation, Levels and Trends in Child Mortality, Report 2023.
[2] Tate, JE., et al., 2008 estimate of worldwide rotavirus-associated mortality in children younger than 5 years before the introduction of universal rotavirus vaccination programmes: a systematic review and meta-analysis. The Lancet infectious diseases 12.2 (2012).
[4] Zhang, M, et al., Vesicle-Cloaked Rotavirus Clusters Are Environmentally Persistent and Resistant to Free Chlorine Disinfection. Environmental science & technology (2022).
[5] Kondylis, P, et al., Analytical techniques to characterize the structure, properties, and assembly of virus capsids. Analytical chemistry (2018).
[6] Makra, I, et al., A method based on light scattering to estimate the concentration of virus particles without the need for virus particle standards. MethodsX (2015).
[7] Dahal, A.,..., **Maharjan, R.** et al., Low-cost Dynamic Light Scattering to Detect Rotavirus Particles in Drinking Water. Submitted to Frontiers in Optics + Laser Science (2024).
[8] **Maharjan, R**., et al., A Case for Optics-based Microbial Risk Assessment of Potable Water. CLEO (2024).
[9] Waiba, P.,..., **Maharjan, R.,** et al., RealtimeWAS: A Low-Cost, Portable Device for Real-time Detection of Fecal Contamination in Drinking Water. FM5G.3, FIO+LS. (2023).
[10] **Maharjan, R**., et al., Improving Detection of Fecal Contamination in Water Using Machine-Learning-Assisted Fluorescence Spectra Analysis, AM4A.1 Applied Industrial Spectroscopy (AIS) at Optica Sensing Congress. Munich (2023)
[11] **Maharjan, R**., Thapa, A., Rajbhandari, P., and Dhakal, A., “Research institutes from nest eggs: challenges and the way forward,” Nat Rev Methods Primers 4, 3 (2024).
[12] Sharma, R.,…, **Maharjan, R.**, et al., Distinguishing chemically similar particles in a complex environment via modulated field spectrometry, Opt. Continuum 2, 303-311 (2023)

Mesoporous Photonic Chip for identification of Protein (MPCiP)

Roman Zakoldaev, UiT The Arctic University of Norway

Health Challenge

Imagine a megapolis where waste removal systems cease to function - the resulting buildup would lead to a major health crisis. Similarly, in Alzheimer's disease, the accumulation of **misfolded protein** amyloid-β ($A\beta_{42}$) in the brain contributes to the formation of cellular plaques which gradually disrupts nerve cells and tissues, causing a cognitive decline (Figure 1). Qualitative and quantitative label-free assessment of amyloid proteins in human blood represents unmet and unique opportunity for **early detection** of the disease.

In clinical settings, doctors currently use costly and time-consuming fluorophore-based immunoassays. A **faster and label-free** alternative is **Raman spectroscopy (RS),** which uses light to discriminate between protein monomers and oligomers. However, conventional RS setups application is hindered by its high limit of detection and the bulkiness of the equipment.

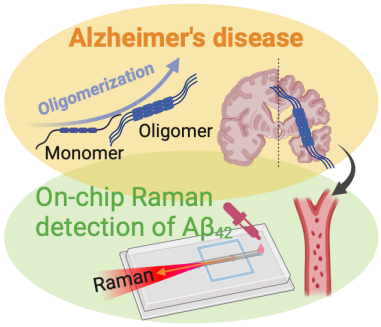

Figure 1. Tracking Alzheimer's Progression: amyloid-β monomers evolve into oligomers, contributing to brain damage. On-chip Raman spectroscopy for early detection of these biomarkers in blood.

Photonics Challenge

Recent developments in on-chip waveguide interferometers, bi-modal waveguides and other diagnostic photonics sensors have proven their feasibility for point-of-care biosensing. Yet, existing biosensors often rely on fluorescent labels or perform indirect measurements through intensity change, leading to issues like false positives and diagnosis delay. To overcome these challenges, I propose a photonics biosensing platform that includes a novel waveguide design to enhance proteins RS. Despite this potential, according to currently available literature, there are no clear arguments why **there has been limited** exploration of waveguide-coupled RS for protein analysis. This represents a **significant gap** in the field, which my project aims to address.

This project **aims** to develop and validate an ultra-sensitive photonics biosensing platform for waveguide-coupled Raman spectroscopy of misfolded proteins at nanomolar concentration, outlining a new era for time-resolved on-chip protein analysis.

Outcomes

A new type of waveguide biosensors will be developed to distinguish protein monomers/oligomers at nM level paving the way for early diagnosis of Alzheimer's disease. The single-step waveguide fabrication will be developed. The biosensor prototype will be presented at an Optica conference.

Impact

For medical institutions, the biosensor offers a new method for real-time detection and analysis of structural changes in proteins. Once the biosensor is approved for amyloids, it can be easily calibrated for other biomarkers.

Future prospects

Combination the biosensor with microfluidics will enable protein separation and purification for early diagnosis from blood samples. Furthermore, the platform will serve as a research platform for enhancing our understanding of chronic metabolic pathologies, as well as a validation platform for drug-dependent protein folding / unfolding kinetics to select available treatment options.

Mesoporous Photonic Chip for identification of Protein (MPCiP)

Roman Zakoldaev, UiT The Arctic University of Norway

Introduction

The human brain with its billions of neurons can be compared with a densely populated city. In this neural metropolis, the waste accumulation poses a functional threat to vital brain structures, specifically the entorhinal cortex and hippocampus. **Misfolded** amyloid-β **proteins** ($A\beta_{42}$) building up inside the entorhinal cortex and hippocampal intercellular spaces are considered as a defining characteristic of **Alzheimer's disease**[1] (Figure 1, a). While amyloid monomers themselves are not inherently harmful, their aggregation into oligomers marks a turning point towards harming neuron viability.

Recent research found that amyloid oligomers present in blood and in cerebrospinal fluid of patients[2] suffering from Alzheimer's disease. Yet, **the challenge lies** in the lack of efficient, reliable, and accessible methods for structural study and early detection of amyloids[3]. Current bioanalytical methods used in clinical research are those using fluorophores like immunoassays, or label-free methods such as cryogenic electron microscopy, nuclear magnetic resonance spectroscopy, circular dichroism spectroscopy. In ideal world, endogenous protein structures are studied *without* introducing any labels, which can diverge proteins from their natural, endogenous state[4]. However, in clinical settings, application of these label-free methods is limited because of their unavailability, high operational demands, and a lack of sufficient standardisation[5].

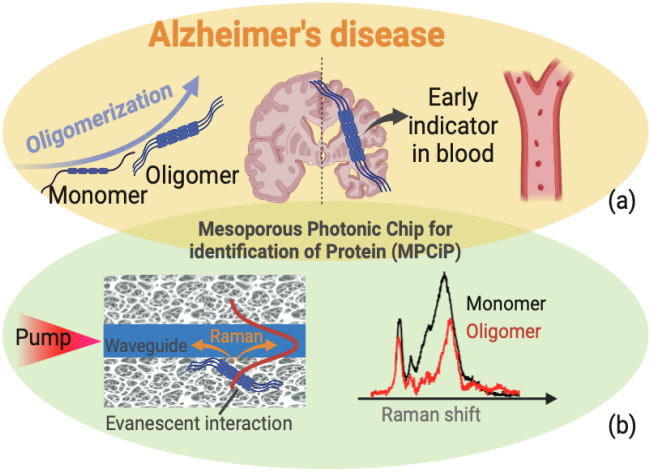

Figure 1 Graphical representation of Alzheimer's disease early biomarkers as oligomerization of amyloid-beta proteins (a) and their spectroscopic identification with the proposed photonic chip (b).

Raman spectroscopy (RS) allows label-free qualitative and quantitative analyses of proteins[6], offering insights into protein conformation and chemical bonding changes[7]. Researchers from EMPA[2] have concluded that RS of red blood cells could potentially be used for a clinically relevant Alzheimer's disease diagnostic tool. The fundamental limitation for conventional RS is its low signal efficiency, which corresponds to a **high limit of detection (LoD)**. For example, the LoD of RS of amyloid-beta proteins in a conventional Raman setup is around 100 μM, whereas clinics require a detection limit as low as 10 nM[8].

Surface Enhanced Raman Spectroscopy (**SERS**) applied in conventional Raman setups increases the biomolecule signal to the desired LoD[9]. This amplification is achieved by binding proteins to plasmonic nanostructures periodically arranged on the chip surface. Upon laser radiation, these structures generate an intense electromagnetic field, significantly amplifying the Raman signal. This technique shows promise in single molecule detection[9] and DNA analysis[10]. Subsequently, SERS was integrated into a microfluidic chip[11], which enabled precise detection of $A\beta_{42}$ down to nM level. However, this setup still requires bulky laboratory equipment around the microfluidic chip, presenting a **significant barrier** to achieving compact, chip-scale diagnostic devices suitable for on-site clinical applications.

Photonics technologies such as Waveguide Enhanced Raman Spectroscopy (**WERS**) suggest a way to make sensors more efficient while keeping them compact. WERS utilizes the evanescent[12] interaction - a phenomenon where light travels along a waveguide core and interacts with molecules

located in proximity, amplifying a signal up to 10^8. This approach promises a seamless transition from laboratory settings to point-of-care diagnostic tools. However, it is still challenging to concentrate sufficient targeted biomolecules in the evanescent field of the waveguide without introducing bioreceptors, such as antibodies, which cause stability issues and non-specific binding.

State-of-the-Art in WERS, Mesoporous Material

Recent research from Ghent University[13] demonstrated a promising solution for WERS by integrating a waveguide with a mesoporous SiO_2 layer, demonstrating a 600-fold enhancement in the Raman signal. Given the proven effectiveness of mesoporous SiO_2 materials in hosting proteins[14], and SiO_2 waveguides maintain low background signal within the amyloid's fingerprint region[15]. This material has the potential to be used in protein hosting, detection and analysis. Despite this potential, according to currently available literature, there are no clear arguments why **there has been limited** exploration of on-chip RS for protein analysis. This represents a **significant gap** in the field, which my project aims to address. To overcome these challenges, I propose the photonic chip that combines waveguides with mesoporous materials to enhance proteins analysis.

2. Problem Statement and Project Plan

The primary **objective** of this project is to develop and validate a **Mesoporous Photonic Chip for Identification of misfolded Proteins (MPCiP)**, which will be then calibrated to analyze amyloid oligomerization with expected nanomolar sensitivity.

Chip design and principle.

The MPCiP is constructed using a mesoporous-cladded waveguide fabricated within a mesoporous silica substrate by laser writing process. The waveguide directs the laser light through this porous layer, where interaction with protein occurs evanescently, producing and collecting the Raman signal (Figure 1,b). The output signal provides real-time information on protein structure changes and its monomers/oligomers concentration.

To improve the LoD to nanomolar level, mesoporous material is used for protein confinement, combined with WERS. Although the presence of pores can cause light scattering and suppress the evanescence field, maintaining a balance between the pore size (< 30 nm) and porosity (20-50 %) will result in a. relatively highly transparent optical material (transmission > 85%, l > 500 nm[16]).

Among waveguide fabrication methods, direct laser writing stands out due to its simplicity as it requires only one step to inscribe a waveguide into optical materials. However, existing laser technologies provide **only relatively high-contrast waveguides, which presents a gap in the field**. WERS requires waveguides both with high-contrast and high-confinement. In this project, the use of UV laser sources aims to achieve both high resolution and high contrast of the waveguides, a combination demonstrated for the first time.

I propose to complete the project in 18 months (6 quarters), executing 3 work packages (WPs) according to the following workflow. This workflow images are based on preliminary results or from references, outlining the expected outcomes (Figure 2).

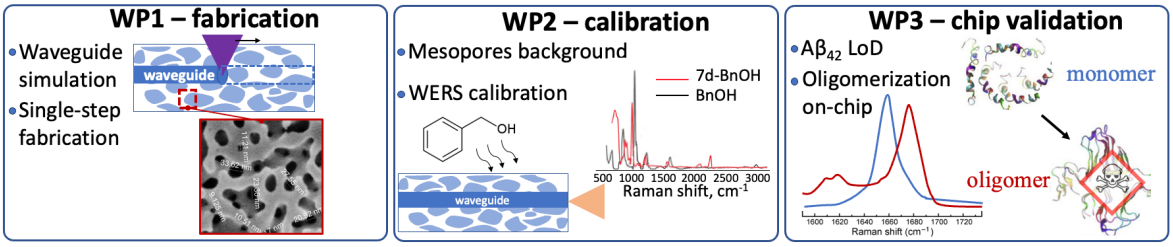

Figure 2. Illustration of the workflow with key results for each WP

WP1: Development of waveguides in mesoporous material

Objective: Design and fabricate waveguides within a mesoporous silicate material (pores size < 30 nm) using ultraviolet (UV) laser technology[15]. The waveguides will be designed for TM single-mode to maximize evanescent field penetration into the surrounding mesoporous material, enhancing sensitivity through interaction with immobilized proteins, which are confined in mesopores.

Tasks and Methodology: (**T1.1**) Use Lumerical FDTD simulation software to design waveguides considering possibilities of UV laser technology. The simulation will ensure the ability of waveguides to support a single-mode operation and assess how well the evanescent field is confined within mesoporous material. (**T1.2**) Waveguide fabrication is planned in a close collaboration with Dr. J.C. Gates[15] (University of Southampton, UK) using UV laser technology, achieving the lateral waveguide resolution of 0.5-2.0 μm. The laser-induced densification process collapses the pores within the mesoporous material, creating a refractive index contrast between the densified waveguide core (n~1.45) and un-densified cladding (n~1.15)[17]. (**T1.3**) Test the fabricated waveguides for optical losses and single mode operation.

Milestone (M1): Mesoporous-cladded waveguides are fabricated and tested.

WP 2: Waveguide-coupled Raman spectroscopy: calibration

Objective: Calibrate the waveguides by analyzing Raman signal from the background and immobilized standard analytes.

Tasks and Methodology: (**T2.1**) Use a confocal Raman microscope at UiT to record background Raman spectra (550 – 2000 cm^{-1}, resolution 1 cm^{-1}) on commercial mesoporous samples such as porous glass Vycor, and/or layers produced by flame hydrolysis deposition (J.C. Gates[15]). This step aims to analyze and determine the optimal pore size/volume ratio that results in a smooth Raman background signal, free from high-frequency features. Important to start this task before the fabrication process to select suitable materials. (**T2.2**) Perform waveguide-coupled Raman measurements at UiT (setup of Prof. O.G. Hellesø[15]). The setup will involve exciting Raman by coupling 660/785 nm laser radiation into waveguides. The captured signal will be filtered through a long-pass filter, then directed to a spectrometer (Teledyne Princeton, IsoPlane SCT320). This step will determine if in-line coupling is possible. The calibration of fabricated waveguides will include detecting benzyl alcohol (BnOH) and its denatured form (d7-BnOH) to identify sharp peaks[18]. A MSc student will be enrolled for this WP.

Milestones (M2): The waveguide is calibrated, and MPCiP is ready for protein analysis.

WP 3: MPCiP analysis of amyloid-β monomers and oligomerization

Objective: Investigate the oligomerization process of commercially available $A\beta_{42}$ by immobilizing it in the MPCiP and analyzing changes in Raman spectra with the focus on amide bands.

Tasks and Methodology: (**T3.1**) Assess mesoporous materials to decide if additional chemical treatment is needed to enhance surface wettability (see Risks), improving the immobilization of amyloid monomers. This task in combination with T2.1 should start at the beginning of the project to make a *decision* about suitable mesoporous material before the fabrication step. (**T3.2**) Conduct waveguide-coupled Raman spectroscopy of immobilized $A\beta_{42}$ (Sigma-Aldrich*) in MPCiP to differentiate monomers and determine the LoD by testing varying concentrations (10^{-4} M to 10^{-9} M). Verify these concentrations using Amyloid beta 42 Human ELISA Kit (Thermofisher). (**T3.3**) Study the oligomerization process of amyloids within MPCiP by inducing changes through heating or pH adjustments. Monitor shifts in the amide I band from 1658 cm^{-1} to 1670 cm^{-1} during protein oligomerization, as linked to disease pathology[8]. Analyze the amide III region (1200 - 1300 cm^{-1}) for insights into secondary structures and side-chain interactions. For spectral analysis, use principal

*Commercially available Amyloid β Protein Fragment 1-42

component analysis (PCA) or for handling complex/noisy data, apply a deep learning model developed at UiT[19].
Milestone (M3): MPCiP is validated for differentiate between amyloid $A\beta_{42}$ monomers and oligomers and determining their concentration.

Timing of the work plan, Gantt Chart makers for 6 quarters (18 months):

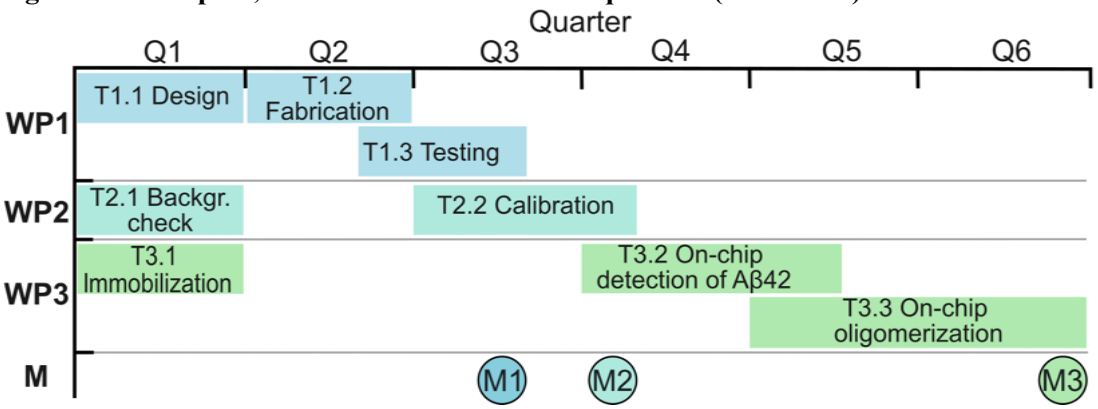

Risks and contingency plan:
Design and fabrication risk (level 2/5): There can be challenges in achieving the desired waveguide geometry (**T1.1**). To mitigate them, UV laser settings (repetition rate, power density and scanning speed) will be refined. If low evanescent field penetration into mesoporous material (low confinement), I will consider diffused or ridged waveguide types, which can be produced using photolithography available at Dr. Gates facilities. This serves as a backup plan, but my priority is to develop single-step laser fabrication of waveguides.
Low Raman signal (level 2/5): During the development of waveguides (**T1.1**), I will adjust the mesoporous structure in terms of porosity or pore size to enhance Raman signal strength. The effectiveness of these modifications will be assessed through Raman signal registration at the calibration phase (**T2.1**). Depending on the results, I might employ in-line or back-coupling for MPCiP.
Protein immobilization in MPCiP (level 3/5): To improve protein immobilization in mesoporous (**WP3**), I will find the "sweet" spot: (i) amyloids will bind to internal porous surface without any extra treatment; (ii) porous surface can be chemically activated with functional hydrophobic or hydrophilic groups to facilitate protein attachment; (iii) peptide decoration, which acts as recognition ligands for amyloids, will be used to improve the specificity of the sensor; This *decision* will be made in the beginning of the project after considering results from T2.1 and T3.1.
Infrastructure and budget. UiT is well-equipped with the necessary scientific instruments to support both experimental and simulation tasks. Most of the budget will be allocated towards purchasing optics and optomechanics for the fabrication step; mesoporous materials; proteins; verification ELISA kits.

3. Outcomes
Each project WP will result in immediate outcomes and deliverables (D). After simulation and waveguide fabrication (**WP1**), **single-step laser method** for inscribing high-confinement waveguides within mesoporous materials will be made into a patent, using the formal disclosure of invention (DOFI) (**D1**). Right after, project results will be presented at Optica conference: Laser Congress (**D2**).

Calibration of mesoporous-cladded waveguide Raman spectroscopy of standard analytes (**WP2**), suggesting a new platform for the on-chip sensing. The results will be submitted to open-access journal *Optics letters* with preliminary title "Low-loss, high-confinement mesoporous-cladded waveguides for small molecules Raman spectroscopy" (**D3**).

The MPCiP, **validated** for amyloid protein analysis, will differentiate between monomers and oligomers, offering qualitative insights crucial for early diagnosis of Alzheimer's disease. The results will be presented at Optica conference: Biophotonics Congress (**D4**), and further the manuscript will be prepared *Biomedical Optics Express* with preliminary title "Label-free study of amyloid $A\beta_{42}$ oligomerization process on photonic chip" (**D5**).

Communication is aimed to bridge the barriers between science and non-experts via *Optica chapter** events at UiT. Key results of the project will be presented in social media (Research Gate, LinkedIn) and newsletter platforms (forskning.no).

The connection of outcome and deliverables presented in Table 1.

Table 1

WP	Outcome	Deliverable	Quartel
1	Single-step laser method for waveguides inscribing	DOFI (D1)	2
		Conference (D2)	3
2	Calibrated mesoporous-cladded waveguide	Paper submission (D3)	4
3	MPCiP Analysis of $A\beta_{42}$	Conference (D4)	5
		Paper submission (D5)	6

4. Impact

Scientific impact*:*

The MPCiP will serve as a **new platform** for medical and biochemical communities to detect and analyze protein structural changes; detection of early bioindicators of Alzheimer's disease. Once MPCiP is approved for amyloids, it can be easily calibrated for other biomarkers, small molecules, such as glutathione, which recently has been considered as an indicator of Alzheimer's disease[19].

Economic impact:

The market value for chronic disease management is, unfortunately, constantly growing. For **Alzheimer's disease**, the projected market size by 2033 is **30.8 billion dollars****. As a diagnostic tool, the MPCiP biosensor will capture a significant share of this market.

Technological impact:

Insights gained from studying the **oligomerization** process of amyloid-β will enhance understanding of Alzheimer's pathology and lead to new approaches in disease treatment. The developed UV laser method **simplifies** the production processes by reducing reliance on cleanroom environments, thereby lowering operational costs and suggesting availability.

Societal impact:

The project supports the United Nations' Sustainable Development Goals***, particularly those related to health and well-being (Subgoal 3.4) and innovation (Subgoal 9.5). By enhancing the understanding of diseases like Alzheimer's, the MPCiP contributes to global health advancements. The project will contribute to upgrading scientific and technological capabilities globally, offering accessible technologies that can enhance research and development across diverse regions.

Impact on personal career development:

The project will significantly enhance my expertise in practical biosensing and increase my visibility within the scientific community. Project performance will lead to multiple first-author papers, facilitating my entry into a multidisciplinary field. In the long term, the results will serve as a foundation for securing additional funding and establishing my own research team. Further, to improve LoD of MPCiP and compactness by application of **deep learning** approach and **peptide decoration** of mesopores.

---

* https://site.uit.no/arcticoptica/

** https://www.towardshealthcare.com/insights/alzheimers-therapeutics-market-sizing

*** https://sdgs.un.org/goals

References:

1. Blennow, K., Hampel, H., Weiner, M., & Zetterberg, H. (2010). Cerebrospinal fluid and plasma biomarkers in Alzheimer disease. *Nature Reviews Neurology*, *6*(3), 131-144. https://doi.org/10.1038/nrneurol.2010.4
2. Nirmalraj, P. N., Schneider, T., & Felbecker, A. (2021). Spatial organization of protein aggregates on red blood cells as physical biomarkers of Alzheimer's disease pathology. *Science advances*, *7*(39), eabj2137. https://doi.org/10.1126/sciadv.abj2137
3. Housmans, J. A., Wu, G., Schymkowitz, J., & Rousseau, F. (2023). A guide to studying protein aggregation. *The FEBS journal*, *290*(3), 554-583. https://doi.org/10.1111/febs.16312
4. Jadavi, S., Dante, S., Civiero, L., Sandre, M., Bubacco, L., Tosatto, L., ... & Diaspro, A. (2023). Fluorescence labeling methods influence the aggregation process of α-syn in vitro differently. *Nanoscale*, *15*(18), 8270-8277. https://doi.org/10.1039/D2NR05487F
5. Lee, J. C., Kim, S. J., Hong, S., & Kim, Y. (2019). Diagnosis of Alzheimer's disease utilizing amyloid and tau as fluid biomarkers. *Experimental & molecular medicine*, *51*(5), 1-10. https://doi.org/10.1038/s12276-019-0250-2
6. Cameron, J. M., Bruno, C., Parachalil, D. R., Baker, M. J., Bonnier, F., Butler, H. J., & Byrne, H. J. (2020). Vibrational spectroscopic analysis and quantification of proteins in human blood plasma and serum. In *Vibrational Spectroscopy in Protein Research* (pp. 269-314). Academic Press. https://doi.org/10.1016/B978-0-12-818610-7.00010-4
7. Ruggeri, F. S., Habchi, J., Chia, S., Horne, R. I., Vendruscolo, M., & Knowles, T. P. (2021). Infrared nanospectroscopy reveals the molecular interaction fingerprint of an aggregation inhibitor with single Aβ42 oligomers. *Nature Communications*, *12*(1), 688. https://doi.org/10.1038/s41467-020-20782-0
8. Zhu, W., Wang, Y., Xie, D., Cheng, L., Wang, P., Zeng, Q., ... & Zhao, Y. (2018). In situ monitoring the aggregation dynamics of amyloid-β protein Aβ42 in physiological media via a Raman-based frequency shift method. *ACS Applied Bio Materials*, *1*(3), 814-824. https://doi.org/10.1021/acsabm.8b00257
9. Kneipp, K., Wang, Y., Kneipp, H., Perelman, L. T., Itzkan, I., Dasari, R. R., & Feld, M. S. (1997). Single molecule detection using surface-enhanced Raman scattering (SERS). *Physical review letters*, *78*(9), 1667. https://doi.org/10.1103/PhysRevLett.78.1667
10. Barhoumi, A., Zhang, D., Tam, F., & Halas, N. J. (2008). Surface-enhanced Raman spectroscopy of DNA. *Journal of the American Chemical Society*, *130*(16), 5523-5529. https://doi.org/10.1021/ja800023j
11. Bai, S., Ren, X., Obata, K., Ito, Y., & Sugioka, K. (2022). Label-free trace detection of bio-molecules by liquid-interface assisted surface-enhanced Raman scattering using a microfluidic chip. *Opto-Electronic Advances*, *5*(10), 210121-1.
12. Ettabib, M. A., Marti, A., Liu, Z., Bowden, B. M., Zervas, M. N., Bartlett, P. N., & Wilkinson, J. S. (2021). Waveguide enhanced Raman spectroscopy for biosensing: A review. *ACS sensors*, *6*(6), 2025-2045. https://doi.org/10.1021/acssensors.1c00366
13. Liu, Z., Zhao, H., Baumgartner, B., Lendl, B., Stassen, A., Skirtach, A., ... & Baets, R. (2021). Ultra-sensitive slot-waveguide-enhanced Raman spectroscopy for aqueous solutions of non-polar compounds using a functionalized silicon nitride photonic integrated circuit. *Optics Letters*, *46*(5), 1153-1156. https://doi.org/10.1364/OL.416464
14. Hudson, S., Cooney, J., & Magner, E. (2008). Proteins in mesoporous silicates. *Angewandte Chemie International Edition*, *47*(45), 8582-8594. https://doi.org/10.1002/anie.200705238
15. Jensen, M. N., Gates, J. C., Flint, A. I., & Hellesø, O. G. (2023). Demonstrating low Raman background in UV-written SiO 2 waveguides. *Optics Express*, *31*(19), 31092-31107. https://doi.org/10.1364/OE.498795

16. Bykov, E. P., Zakoldaev, R. A., Andreeva, N. V., Shishkina, A. S., Yandybaeva, Y. I., & Andreeva, O. V. (2022). Production of nanoporous silicate matrices—problems of optical homogeneity. *Journal of Optical Technology*, *89*(3), 161-168. https://doi.org/10.1364/JOT.89.000161
17. Yang, P., Wirnsberger, G., Huang, H. C., Cordero, S. R., McGehee, M. D., Scott, B., ... & Stucky, G. D. (2000). Mirrorless lasing from mesostructured waveguides patterned by soft lithography. *Science*, *287*(5452), 465-467.
18. Ettabib, M. A., Bowden, B. M., Liu, Z., Marti, A., Churchill, G. M., Gates, J. C., ... & Wilkinson, J. S. (2023). Grating-incoupled waveguide-enhanced Raman sensor. *Plos one*, *18*(8), e0284058. https://doi.org/10.1371/journal.pone.0284058
19. Jensen, M. N., Guerreiro, E. M., Enciso-Martinez, A., Kruglik, S. G., Otto, C., Snir, O., ... & Hellesø, O. G. (2024). Identification of extracellular vesicles from their Raman spectra via self-supervised learning. *Scientific reports*, *14*(1), 6791. https://doi.org/10.1038/s41598-024-56788-7
20. Roy, R. G., Mandal, P. K., & Maroon, J. C. (2023). Oxidative stress occurs prior to amyloid Aβ plaque formation and tau phosphorylation in Alzheimer's disease: Role of glutathione and metal ions. *ACS Chemical Neuroscience*, *14*(17), 2944-2954. https://doi.org/10.1021/acschemneuro.3c00486

Wafer-scale, transfer-free hetero-integrated photonic circuits using confined growth of single-crystalline 2D materials – Summary

Sang-Hoon Bae, Washington University in St. Louis

The integration of two-dimensional (2D) materials for on-chip photonic applications has attracted immense research interest, thanks to their prominent optoelectronic attributes and the unprecedented degrees of freedom to create heterogeneous integrated photonic layouts and van der Waals (vdW) heterostructures without the lattice-matching constraints that apply to heteroepitaxy. Abundant useful properties are shown in 2D materials of graphene and transition metal dichalcogenides (TMDs), encompassing vital optical functionalities from light emission, modulation, photodetection, and nonlinear optics. However, most reported 2D-materials-based integrated photonic devices to date still largely remain lab demonstrations, far faltering the surging vision of practical 2D-photonics commercialization in real-word.

Before fledging into fully viable technology, 3 long-standing challenges exist for integrated photonics based on 2D materials. (1) Most reported devices use transferred 2D materials. This is because substrates that are suitable for 2D material growth (such as sapphire) cannot be directly used for integrated optical applications (typically require thick SiO_2 BOX layer). Consequently, 2D materials are later transferred to prefabricated photonic templates such as waveguides and micro-cavities using PMMA or metal handler after growth. However, the transfer process inevitably induces residues and defects (cracks, holes, wrinkles) to 2D that significantly deteriorate material optical property and performance. Transfer of delicate 2D films is also incompatible with standard foundry mass-production process. (2) Lack of robust scalable synthesis method of high-quality 2D materials, especially 2D TMDs. Conventional mechanical exfoliation and transfer approaches can produce 2D flakes with high quality, but it remains a trial-and-error process with heavy labor work and extremely low yield. For scalable manufacture methods such as chemical vapor deposition (CVD), it was an open challenge to obtain controlled monolayer-by-monolayer (ML) single-crystalline uniform 2D material growth over wafer-scale, especially for 2D TMDs. (3) Due to the above two reasons, currently reported works are still restrained to single-device demonstration of 2D materials.

Here we propose a novel strategy to simultaneously solve the abovementioned issues, by providing a transfer-free approach to fabricate integrated 2D photonic devise at wafer-scale with high robustness, high throughput, and low-cost. The proposed project will be based on our modified CVD on patterned thin HfO_2/SiO_2 substrates that have judiciously engineered growth pockets to spatially confine the nucleation of 2D materials. Using this confined CVD method with spatial growth selectivity, we have priorly successfully achieved single-crystalline 2D TMD (WSe_2, MoS_2) controlled growth (ML, bilayer/BL, and BL 2D vdW heterostructures) on sapphire or HfO_2/Si templates. Here, we will use optical substrates (2 μm-thick SiO_2/Si) deposited with very thin (< 10 nm) HfO_2 to realize integrated photonic applications including 2D TMD (WSe_2, MoS_2) or quasi-2D metal-halide perovskites-based waveguide-integrated photodetectors and 2D ML-TMDs-based optical modulators. The growth patterns will be re-designed for optical devices followed by re-optimized confined CVD growth conditions. Compared to conventional Si or SiN photonic platforms that either necessitate 2D transfer or can hardly realize good waveguide quality on 2D, we propose a new hybrid bottom-up nanofabrication strategy, by using SU-8 polymer waveguides to directly make the as-grown 2D monolayers into integrated photonic devices without any layer transfer. This method completely solved the residue and defect problems in conventional approaches. The SU-8 polymer waveguides also have the benefit of low-loss (~2 dB/cm), low-cost, and easy-to-fabrication.

Wafer-scale hetero-integrated photodetectors array will be demonstrated without 2D transfer, by first doing confined CVD of ML 2D WSe_2 and/or MoS_2, followed by aligned photolithography and metal lift-off for electrodes and e-beam lithography (EBL) for SU-8 waveguides with high responsivity. Dual confined CVD of ML TMD will be developed to form 2D/HfO_2/2D structure to electrically modulate the absorption of the 2D material for broadband (visible to near infrared) integrated optical modulators. A proof-of-concept demonstration of scalable integrated 2D photonic nano-system with 2D modulators and photodetectors will be delivered as well, following the research steps/schedules detailed in proposal. By simultaneously solving the prior outstanding challenges in 2D integrated photonics community, we envisage this transfer-free scalable strategy to integrate single-crystalline 2D monolayers to photonic chip can offer a crucial leap towards the practical commercialization of 2D photonics into a viable and worthy technology.

Wafer-scale, transfer-free hetero-integrated photonic circuits using confined growth of single-crystalline 2D materials

1. Literature Review and Motivation

The heterogeneous integration of functional optical materials has not only proven a backbone in prototyping massive optoelectronic applications with excellent performance, but also a driving engine to explore novel nanophotonic phenomena in diverse heterostructures[1]. Featured with broad bandwidth and ultrafast speed, photonic integrated circuits (PIC) are poised to circumvent the electrical bottleneck in integrated electronics, relying on a wide spectrum of devices such as lasers, optical modulators, and photodetectors[2]. However, despite the successes of silicon (Si) and silicon nitride photonics, single material platform still has varying intrinsic shortcomings that can hardly meet the increasing demand for and multifunctional high-performance PIC devices[2]. Moreover, conventional heteroepitaxy approaches to this end involve stringent lattice-matching requirements, severely limiting the available choices of hetero-integrated photonic devices.

Featured with van der Waals (vdW) surfaces, two-dimensional (2D) materials as transferrable vdW building blocks showcasing unprecedented degrees of freedom to integrate and mix with arbitrary photonic templates without lattice-matching constraints[1,3]. These atomically thin materials have attracted tremendous research interest in the photonics and optoelectronics, owing to their intriguing and salient optoelectronic attributes[4,5]. Including graphene[6], transition-metal dichalcogenides (TMDs), black phosphorus (BP), hexagonal boron nitride (h-BN), and emergent candidates like quasi-2D halide perovskites[7], a big family of 2D materials show abundant optical functionalities, covering light emission, modulation, detection, and nonlinear optics. Various endeavors have thus been devoted to incorporating 2D materials to optical waveguides to develop high-performance integrated photonic devices. For instance, graphene-transferred Si waveguides are used to develop optical polarizers, and integrated optical amplitude or phase modulators[8] with broad optical bandwidth. All-optical graphene plasmonic switches are also proposed with ultrafast operation speed and low power consumption[9]. Compared to graphene that lack an electronic bandgap, 2D BP and TMDs are more promising for active photonic applications such as nano-lasers[10], amplifiers, and photodetectors with miniaturized device footprint and excellent CMOS compatibility. Besides graphene, broadband photo-detectors were also demonstrated with high responsivity and wide bandwidth using BP[11], or 2D TMDs[12]. They can also be assembled into artificial vdW heterostructures with diverse designer photonic structures for drastically enhanced light-matter interactions.

2. Problem Statement/Objectives

Despite prior exciting progress on 2D integrated photonics, most proposed 2D-integrated devices remain lab explorations, making real-word practical products still a distinct vision[5]. For nearly the last two decades since the debut of graphene, intensive efforts have been put in 2D material synthesis and 2D-photonics integration optimization at large-scale to prototype new functional devices. Nevertheless, **significant progress towards commercialization of 2D material-based technology is still largely elusive**.

Large-scale graphene monolayers were successfully synthesized via chemical vapor deposition (CVD)[5]. However, to make functional integrated photonic devices, the graphene sheets need to be transferred to prefabricated optical waveguides made of, for instance, Si or silicon nitride[8,13]. The PMMA- or metal-handlers-based 2D transfer process will inevitably induce polymer residues and defects like wrinkles or cracks, which can crucially deteriorate device performance[6]. In terms of 2D TMDs-based optical applications, the majority of previous demonstrations rely on exfoliated flakes[12-14], because the growth of continuous 2D TMD monolayers over wafer-scale is still challenging. Although mechanical exfoliations can produce 2D flakes with the best quality for on-chip lasers, modulators[15], and photodetectors[12], it remains a trial-and-error heavy labor work with very small-sized, irregular-shaped 2D film and extremely low yield[1,5]. Even with the perspectives of robotics-aided film exfoliation, the 2D transfer-based approaches still require precise control over the delicate 2D films well-aligned to target photonic structures and it unavoidably induces defects on 2D with degraded device performance and rising cost,

faltering most current research far away from robust and scalable mass-production required in 2D commercialization[1].

To summarize, currently **3 outstanding challenges exist** in 2D-materials-based integrated photonics. **(1) Lack of robust and high-throughput 2D material growth method** with high material quality over wafer-scale. **(2) Reliance of 2D film transfer** that inevitably induce material defects and transfer residues. **(3) Lack of system level demonstration of 2D-based integrated photonic chips**, as current papers majorly centered on only single device. For the first challenge, the realization of single-crystalline 2D monolayers (such as 2D TMDs and h-BN, except graphene) continuous over wafer-scale is still under investigation. This is mainly because kinetic control of few atomic monolayers has proven extremely challenging, caused by 3 critical issues: (i) monolayer-by-monolayer 2D material growth, (ii) single-crystalline 2D material growth, and (iii) 2D materials growth at a wafer-scale. So far, a few reports have tried to address one among the three issues. However, no single report has been made to tackle all three at the same time, although 2D commercialization becomes possible only after all issues are solved. Monolayer single-domain TMDs were grown on laser-pre-damaged areas, but this method cannot realize 2D heterostructures in wafer-scale due to the unconfined growth scheme, low laser-scanning yield, and damaged bottom seedings[16]. Large-scale layer-by-layer growth of 2D heterostructures were also reported, by with poly-crystalline 2D quality of compromised performance[17]. For the second challenge, transfer-free heteroepitaxy was explored to grow MoTe2 on arbitrary surfaces[18]. However, except certain single-crystalline substrates, most photonic templates, especially the post-fabricated optical waveguides and cavity structures are not suitable for 2D material growth, leading to drastically deteriorated 2D material quality. Moreover, the demonstrated 2D TMDs remains bulk (>10 layers), the extraordinary optoelectronic properties of 2D TMDs only reveal at a few monolayers[4]. For the reported growth of bulk 2D TMDs, they are no longer direct bandgap material, losing the suitability for most active optoelectronic applications[1]. For the third challenge, MIT researchers have proposed chalcogenide glass-on-graphene as a handy platform to make various integrated photonic devices of modulators, photodetectors, and polarizers[19]. However, it still remains discrete device level demonstration and drawbacks of graphene transfer is still necessitated.

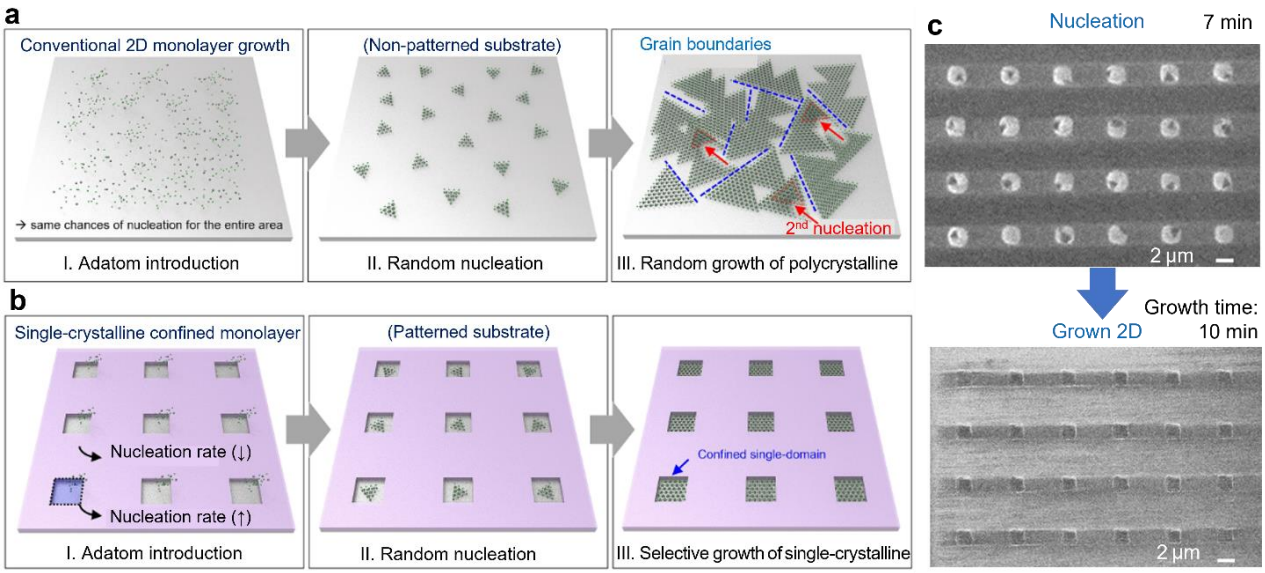

Figure 1. (a) Conventional CVD yields uniform polycrystalline 2D films with grain boundaries. (b) Confined CVD for location-selective single-domain 2D material synthesis strategy. (c) SEM of grown WSe_2 with verified 100% single-domain 2D monolayers on sapphire pockets with prefabricated a-SiO_2 trenches.

Objectives (proposed research): Here we propose a transfer-free and scalable approach to produce single-crystalline 2D material monolayers, bilayers, and their heterostructures via engineered CVD on judiciously pre-patterned optical substrates with designed growth pockets. This approach can make a **remarkable leap towards practical commercialization of 2D integrated photonics by simultaneously**

solving all the three challenges above: **(1)** highly robust confined CVD growth of single-crystalline 2D materials for low-cost foundry mass-production. **(2)** Direct and controlled layer-by-layer growth of 2D monolayers on arbitrary pre-defined locations and on almost arbitrary industrial wafers. **(3)** Capable of making 2D-based integrated photonic systems with excellent process compatibility by modified device fabrication process. We will focus on integrated photonic devices and circuity based on 2D semiconductors such as 2D TMDs (e.g., WSe_2, MoS_2) and 2D metal halide perovskites for on-chip photodetectors and optical modulators, as compared to graphene, wafer-scale growth of 2D TMDs with monolayer and single-crystallinity is still an open challenge with greater impact. The objectives above will be made reality based on the following three crucial technologies that we have already successfully achieved.

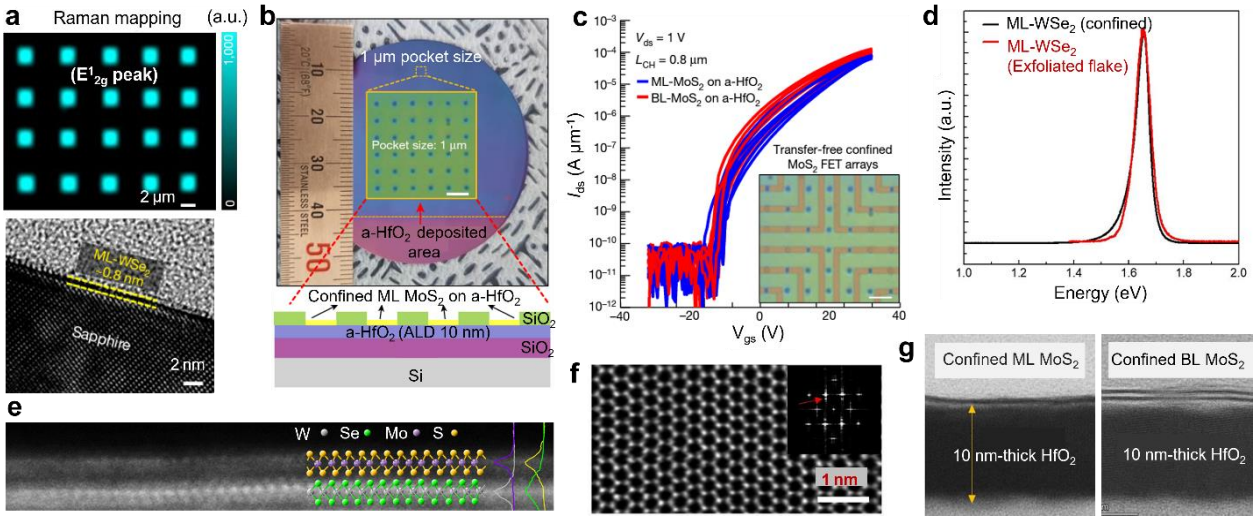

Figure 2. (a) Raman mapping & TEM of confined monolayer (ML) WSe_2 on sapphire. (b) Photo & schematic of confined growing ML-TMD on HfO_2-covered SiO_2/Si substrate. (c) Measured electrical I-V curve made by confined grown ML-bilayer (BL) MoS_2. (d) Photoluminescence spectra of confined grown ML-WSe_2 and exfoliated WSe_2 flakes. (e) and (f) HAADF-STEM of confined-grown WSe_2/MoS_2 vdW heterostructures, and ML-single-crystal WSe_2 on HfO_2. (g) Cross-sectional STEM of ML & BL MoS_2 grown on patterned HfO_2.

(i) Wafer-scale layer-by-layer controlled epitaxy of single-crystal 2D materials by geometrically confined CVD. In our previous work[1,20] (Nature 614, 88-94, 2023), we have solved multiple critical issues including monolayer-by-monolayer growth controllability (both homo- and hetero-structures) with single crystallinity at pre-designated locations in wafer-scale. Compared with conventional CVD that yields spatially ununiform (hybrid with 0~2 monolayers) polycrystalline 2D materials (**Fig. 1a**), crystalline sapphire substrates (c-plane Al_2O_3) patterned by deposited amorphous SiO_2 mask are applied as CVD growth templates. As the binding energies of the 2D adatoms on a-SiO2 is significantly higher than c-Al_2O_3, nucleation will preferably take place at the predefined growth pockets (i.e. c-Al_2O_3 substrate without SiO_2 coverage). The first set of nuclei is thus geometrically confined to predesignated locations (**Fig. 2b**). By judiciously controlling the growth pocket size (2~10 μm) and growth time, uniform single-crystalline 2D WSe_2 monolayers are formed (before starting the 2nd layer nucleation).

(ii) Monolayer-controllable non-epitaxial single-crystal 2D TMD growth on amorphous oxides by geometrically confined CVD. Despite the excellent 2D material quality realized on patterned c-sapphire, the substrate is not suitable for integrated photonic applications. On-chip integrated photonic devices typically require waveguide structures, such as Si-on-insulator, with thick buried low-index oxides (like SiO_2) to avoid leakage of guided electromagnetic waves[2]. Therefore, to realize a transfer-free method to fabricate 2D PICs, we need to directly growth 2D monolayers on optical templates with thick SiO_2 layer. Leveraging ALD HfO_2-covered oxide layers, growth selectivity is theoretically confirmed by density functional theory (DFT) calculations[20] and experimentally verified by Raman mapping (**Fig. 2a**), XPS, and AFM characterizations[20]. Single-domain controlled growth of monolayer (ML) to bilayer (BL) MoS_2 on a-HfO_2/ SiO_2/Si optical substrate (**Fig. 2b**) is experimentally verified with excellent optoelectronic

properties (**Figs. 2b & 2c**), even comparable to mechanically exfoliated ML 2D TMD flakes (**Fig. 2d**). The primal single-crystallinity of the ML, BL, and vdW heterostructures of WSe_2 and MoS_2 are also verified by the High-angle annular dark-field STEM images (**Figs. 2e-2g**)[20].

(iii) Modified hybrid bottom-up fabrication process of 2D integrated photonic devices. Instead of growing 2D on prefabricated structures like optical waveguides and resonators[18], which have massive fabrication-induced defects and contained interfaces, we propose forming high-quality ML 2D materials first by confined CVD. Then proceed with electrical contact fabrication and lastly do the waveguide (WG) fabrication (**Figs. 3a, 3b**) via e-beam lithography (EBL). This approach does not necessitate any 2D material transfer and consists of all-standard nanofabrication processes compatible for scalable manufacture at foundry with reduced cost. We have tested the fabrication of various SU-8 photonic structures (**Fig. 3c**) with low optical loss, such as the SU-8 polymer micro-ring resonator with quality factor Q~8×10^4 (**Fig. 3d**). The SU-8 polymer waveguides are beneficial with low optical loss, moderate refractive index, low-cost, and can be formed directly after EBL and development without involving expensive etching tools like RIE towards practical commercialization.

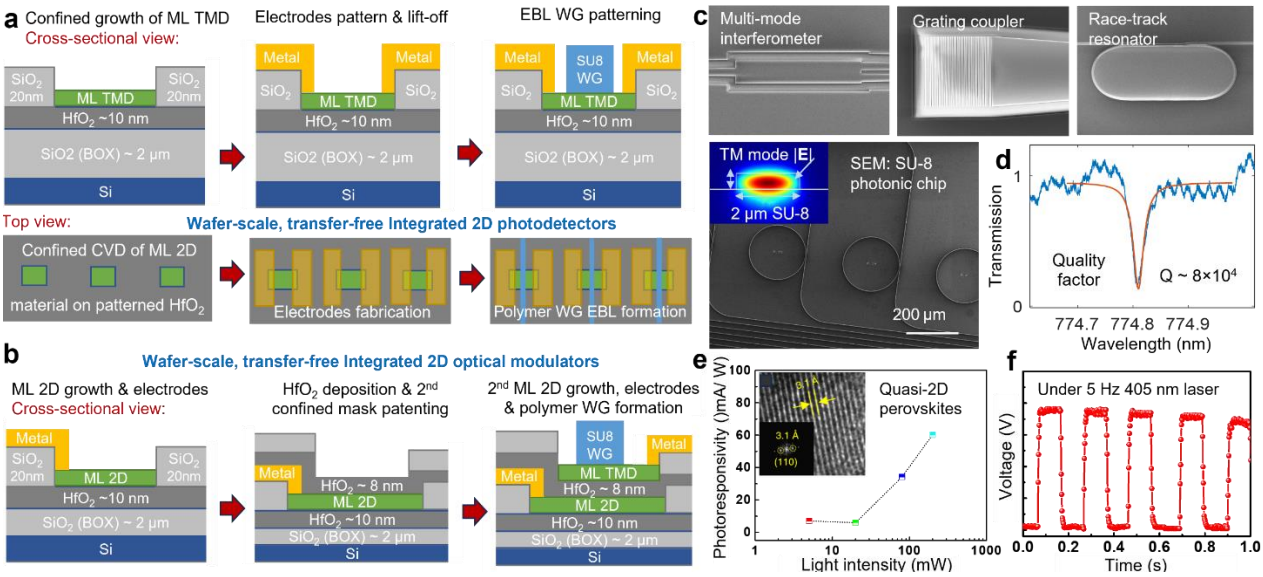

Figure 3. (a) and (b) Modified hybrid fabrication method for waveguide-integrated 2D photodetectors and modulators respectively. (c) SEM of various photonic components made by SU-8 polymer photonics. Inset: simulated |**E**| distribution of TM_{00} mode in a 2×0.6 µm SU-8 waveguide. (d) Transmission spectrum of a SU-8 micro-ring. (e), (f) Photo-responsivity of crystalline quasi-2D perovskite film. Inset: perovskite STEM image.

3. Outline of tasks/Work Plan

Tasks & milestones: We target the following 2D-integrated devices/systems. **(1)** Transfer-free, scalable fabrication of waveguide-coupled integrated photodetectors will be demonstrated levering confined-CVD-grown ML~BL WSe_2 or MoS_2, by following fabrication steps shown in **Fig. 3a**. **(2)** scalable fabrication of integrated optical amplitude or phase modulators based on confined CVD ML 2D TMDs (**Fig. 3b**). **(3)** A proof-of-concept demonstration of integrated photonic system with integrated optical modulators and photodetectors on the same photonic chip.

To realize the targets above, the following tasks will be addressed. **(T1) Optimized HfO_2 deposition and SiO_2 growth pattern design for optical applications**. Firstly, in our previous work, a-HfO_2 was deposited on ~ 30 nm thin SiO_2 substrate. To realize integrated optical waveguides without substrate light leakage, we will firstly optimize the atomic layer deposition (ALD) of ultra-flat a-HfO_2 on SiO_2 (2 µ-thick)/Si substrate. Also, our prior confined growth pocket size and pattern design were for electronic applications of 2D (**Fig. 2**): the growth pockets for 2D were too small in size (~ 2×2 µm) and too dense for optical applications. For integrated photonic devices such as modulators, lasers, and photodetectors, the desired size of ML 2D material (same as the growth pocket size) would be around 4~20 µm depending on applications. The spacing of the growth pockets is also desired to be larger to accommodate

electrodes and avoid the evanescent coupling between adjacent waveguides[1,6]. Thus, we will re-design the growth pattern (the growth condition will be also changed) to guarantee high-quality monolayer (ML) 2D TMD growth first. Then further optimize the confined CVD condition to target ML~BL 2D TMD (WSe_2) with low multi-domain portion to even single-crystalline quality. **(T2) Dual-layer confined growth of ML 2D materials**. After achieving Task (T1), the proposed 2D integrated photodetectors can be realized by all standard process of photolithography, e-beam evaporate of Pt/Au electrodes, metal lift-off, and EBL process without challenge (**Fig. 3a**). However, for modulators, capacitor structures need to be formed in order to electrically tune the carrier density/optical absorption of the 2D materials[15,19]. Thus, after the 1st confined growth, we will ALD HfO_2 as the spacing layer, followed by 2nd patterning of SiO_2 growth mask for 2nd confined CVD. **(T3) Confined growth of quasi-2D metal-halide perovskite (PVSK) & system optimization**. Besides 2D WSe_2 and MoS_2, we will also test confined CVD of 2D PVSK (**Figs. 3e, 3f**) for photodetection and laser applications. System optimization of photonic chip with 2D modulators & detectors will also be performed.

Schedule: **Month 1**: Optimize ALD HfO_2; Design confined growth mask pattern for optical applications.
Month 2-4: Optimize confined CVD growth condition for ML 2D WSe_2 on $HfO_2/SiO_2/Si$ with new patterns.
Month 4-5: Integrated 2D photodetectors array fabrication and optical measurement.
Month 5-8: Dual-layer confined growth of ML 2D WSe_2 or MoS_2 (with $2D/HfO_2/2D$ capacitor structure).
Month 9-10: Integrated optical modulators based on dual-ML 2D TMD and SU-8 polymer waveguides.
Month 10-12: Integrated 2D photonic chip with 2D modulator & photodetector: fabrication & measurement.

4. Outcomes and Impact

By implementing the tasks above, we embody an exciting leap towards the commercialization and advancement of 2D materials-based integrated photonics. A potentially revolutionary paradigm can be established by using confined CVD growth of ML single-crystalline 2D materials (TMDs, PVSK) for wafer-scale, transfer-free 2D integrated photonic devices manufacture with excellent quality, which simultaneously solving three previously long-standing challenges (2D quality, transfer issues, and system integration) in 2D integrated photonics society. We will demonstrate broadband integrated 2D photodetectors from 500 nm to 1 μm (responsivity > 0.3 $A \cdot W^{-1}$), broadband 2D modulators from visible to near infrared (> 5 GHz bandwidth), and proof-of-principle integrated 2D photonic chip via low-loss (~2 dB/cm) SU-8 waveguides with light modulation and photodetection, opening a new avenue for practical 2D hetero-integrated photonics towards commercialization to viable technology.

References

1. Meng, Y. et al. Photonic van der Waals integration from 2D materials to 3D nanomembranes. Nature Reviews Materials, doi:10.1038/s41578-023-00558-w (2023).
2. Tran, M. et al. Extending the spectrum of fully integrated photonics. Nature 610, 54–60 (2022).
3. Liu, Y., et al. Van der Waals integration before and beyond 2D materials. Nature 567, 323-333, (2019).
4. Xia, F., et al, A. Two-dimensional material nanophotonics. Nature Photonics 8, 899-907, (2014).
5. Kong, W. Path towards graphene commercialization from lab to market. Nat. Nanotechnol. 14, 927 (2019).
6. Romagnoli, M. et al. Graphene-based integrated photonics for next-generation datacom and telecom. Nature Reviews Materials 3, 392-414, (2018).
7. Ricciardulli, A. G., at al. Emerging perovskite monolayers. Nature Materials 20, 1325-1336 (2021).
8. Sorianello, V. et al. Graphene-Si phase modulators with gigahertz bandwidth. Nat. Photon. 12, 40-44 (2018).
9. Ono, M. et al. Ultrafast and energy-efficient all-optical switching with graphene-loaded deep-subwavelength plasmonic waveguides. Nature Photonics 14, 37-43 (2020).
10. Li, Y. et al. Room-temperature continuous-wave lasing from monolayer molybdenum ditelluride integrated with a silicon nanobeam cavity. Nature Nanotechnology 12, 987-992 (2017).
11. Youngblood, N., et al. Waveguide-integrated black phosphorus photodetector with high responsivity and low dark current. Nature Photonics 9, 247-252 (2015).

12. Maiti, R. et al. Strain-engineered high-responsivity MoTe2 photodetector for silicon photonic integrated circuits. Nature Photonics 14, 578-584 (2020).
13. Sun, Z., et al. Optical modulators with 2D layered materials. Nature Photonics 10, 227-238 (2016).
14. Sung, J. et al. Room-temperature continuous-wave indirect-bandgap transition lasing in an ultra-thin WS2 disk. Nature Photonics 16, 792-797 (2022).
15. Datta, I. et al. Low-loss composite photonic platform based on 2D semiconductor monolayers. Nature Photonics 14, 256-262 (2020).
16. Li, J. et al. General synthesis of 2D van der Waals heterostructure arrays. Nature 579, 368-374 (2020).
17. Jin, G. et al. Heteroepitaxial vdW semiconductor superlattices. Nature Nanotechnology 16, 1092 (2021).
18. Pan, Y. et al. Heteroepitaxy of semiconducting 2H-MoTe2 thin films on arbitrary surfaces for large-scale heterogeneous integration. Nature Synthesis 1, 701-708 (2022).
19. Lin, H. et al. Chalcogenide glass-on-graphene photonics. Nature Photonics 11, 798-805 (2017).
20. Kim, K. et al. Non-epitaxial single-crystal 2D material growth by geometrical confinement. Nature (2023).

References (Full-editable by Endnote)

1 Meng, Y. *et al.* Photonic van der Waals integration from 2D materials to 3D nanomembranes. *Nature Reviews Materials*, doi:10.1038/s41578-023-00558-w (2023).
2 Tran, M. *et al.* Extending the spectrum of fully integrated photonics. *Nature* **610**, 54–60 (2022).
3 Liu, Y., Huang, Y. & Duan, X. Van der Waals integration before and beyond two-dimensional materials. *Nature* **567**, 323-333, doi:10.1038/s41586-019-1013-x (2019).
4 Xia, F., Wang, H., Xiao, D., Dubey, M. & Ramasubramaniam, A. Two-dimensional material nanophotonics. *Nature Photonics* **8**, 899-907, doi:10.1038/nphoton.2014.271 (2014).
5 Kong, W. *et al.* Path towards graphene commercialization from lab to market. *Nature Nanotechnology* **14**, 927-938, doi:10.1038/s41565-019-0555-2 (2019).
6 Romagnoli, M. *et al.* Graphene-based integrated photonics for next-generation datacom and telecom. *Nature Reviews Materials* **3**, 392-414, doi:10.1038/s41578-018-0040-9 (2018).
7 Ricciardulli, A. G., Yang, S., Smet, J. H. & Saliba, M. Emerging perovskite monolayers. *Nature Materials* **20**, 1325-1336 (2021).
8 Sorianello, V. *et al.* Graphene–silicon phase modulators with gigahertz bandwidth. *Nature Photonics* **12**, 40-44 (2018).
9 Ono, M. *et al.* Ultrafast and energy-efficient all-optical switching with graphene-loaded deep-subwavelength plasmonic waveguides. *Nature Photonics* **14**, 37-43 (2020).
10 Li, Y. *et al.* Room-temperature continuous-wave lasing from monolayer molybdenum ditelluride integrated with a silicon nanobeam cavity. *Nature Nanotechnology* **12**, 987-992 (2017).
11 Youngblood, N., Chen, C., Koester, S. J. & Li, M. Waveguide-integrated black phosphorus photodetector with high responsivity and low dark current. *Nature Photonics* **9**, 247-252, doi:10.1038/nphoton.2015.23 (2015).
12 Maiti, R. *et al.* Strain-engineered high-responsivity MoTe2 photodetector for silicon photonic integrated circuits. *Nature Photonics* **14**, 578-584, doi:10.1038/s41566-020-0647-4 (2020).
13 Sun, Z., Martinez, A. & Wang, F. Optical modulators with 2D layered materials. *Nature Photonics* **10**, 227-238 (2016).
14 Sung, J. *et al.* Room-temperature continuous-wave indirect-bandgap transition lasing in an ultra-thin WS2 disk. *Nature Photonics* **16**, 792-797, doi:10.1038/s41566-022-01085-w (2022).
15 Datta, I. *et al.* Low-loss composite photonic platform based on 2D semiconductor monolayers. *Nature Photonics* **14**, 256-262, doi:10.1038/s41566-020-0590-4 (2020).
16 Li, J. *et al.* General synthesis of two-dimensional van der Waals heterostructure arrays. *Nature* **579**, 368-374, doi:10.1038/s41586-020-2098-y (2020).

17 Jin, G. *et al.* Heteroepitaxial van der Waals semiconductor superlattices. *Nature Nanotechnology* **16**, 1092-1098, doi:10.1038/s41565-021-00942-z (2021).

18 Pan, Y. *et al.* Heteroepitaxy of semiconducting 2H-MoTe2 thin films on arbitrary surfaces for large-scale heterogeneous integration. *Nature Synthesis* **1**, 701-708, doi:10.1038/s44160-022-00134-0 (2022).

19 Lin, H. *et al.* Chalcogenide glass-on-graphene photonics. *Nature Photonics* **11**, 798-805, doi:10.1038/s41566-017-0033-z (2017).

20 Kim, K. S. *et al.* Non-epitaxial single-crystal 2D material growth by geometrical confinement. *Nature* (2023).

Executive Summary:

Quantum-enhanced optical learning machine

Category: Information

Saroch Leedumrongwatthanakun
saroch.l@psu.ac.th
Division of Physical Science, Faculty of Science, Prince of Songkla University, Thailand

The pressing demand for information processing systems with high-bandwidth, high-speed, and energy-efficient capabilities is of considerable significance in the current information era. This has driven the development of alternative computing architectures over the recent decades including analog computing, neuromorphic computing, reservoir computing, extreme learning machines, and quantum computing. Among those, recent progress in optical computing has demonstrated positive results, indicating an efficient way to perform optical neural networks with a sensing capability. In parallel, the research area of quantum metrology has shown the improvement of high sensitivity on diverse optical instruments as well-established examples of gravitational wave detections and many configurations of quantum imaging and spectrometry. One of the experiments is known as the nonlinear SU(1,1) interferometer, proposed in 1986 by Yurke *et al.,* which has garnered significant attention thanks to its presence of sub-shot-noise sensitivity, even in the presence of external loss and a possibility to extend to multimode. Despite the advancements in such classical optical computing and quantum metrology, fundamental questions about the feasibility of exploiting optical quantum effects for information processing and machine learning remain open.

Our research proposal aims to address this challenge by investigating the capability of a quantum optical platform for simultaneously sensing and performing a pattern recognition task. We propose the development of an optical apparatus - the "*quantum-enhanced optical learning machine*". It consists of a cascade of multimodal optical parametric amplifiers, interspersed with a linear optical circuit and reconfigurable optical phase arrays. One layer of the optical machine is the reconfigurable multimode nonlinear SU(1,1) interferometer. We aim to explore the intricate interference between signal and idler radiations in the cascade setting. By implementing linear optical circuits, one can adjust the relative phases between the optical pump, signal, and idler fields of spatial modes of optical parametric amplifiers; hence enabling us to control the de/amplification and quantum correlation of parametric downconversion light in the circuit. Using the quantum effect, we aim to show the feasibility study of the high sensitivity of phase imaging beyond the standard quantum limit. Moreover, the learning capability and trainability of the optical machine will be investigated to estimate the potential and limitations of the machine in terms of measurement sensitivity, expressibility, and trainability. With those successes, we aim to showcase an application of the optical machine for simultaneous sensing and performing pattern recognition tasks.

The outcomes of the research project could have a far-reaching impact on our understanding of the role of the quantum effect presented in cascaded OPAs on simultaneously sensing and information processing with a possibility to address the global demand in sensing and computing.

Quantum-enhanced optical learning machine

Saroch Leedumrongwatthanakun, saroch.l@psu.ac.th
Division of Physical Science, Faculty of Science, Prince of Songkla University, Thailand
Category: Information

The collection of vast amounts of data has become primary, driven by our recognition of the immense potential in extracting and learning valuable information through AI-driven algorithms. Such knowledge could help enrich our quality of life and deepen our understanding of nature. The global demand for data storage and traffic as well as information processing via electronic computers has consequently increased. To meet the escalating requirements of training larger AI models, a transition towards more parallel processing using Graphics and Tensor Processing Units has been realized. The progression leads to even more acceleration in the demand for computations and necessitates the development of more efficient computing hardware capable of large-scale data processing while minimizing energy consumption and latency. Addressing these challenges, our research proposal aims to investigate the capability of an alternative quantum optical platform for sensing and information processing. This platform is based on a reprogrammable sequence of optical parametric amplifiers, linear optical circuits, and reconfigurable phase arrays that can encode classical information. The project offers a potential way for advancing quantum optical information processing with the possibility of overcoming the limitations of conventional electronic computing.

Literature Review

The development of diverse computing architectures has regained attention over the recent decades as the quest for alternative information processing units has been rapidly increasing. Examples include analog computing, neuromorphic computing, reservoir computing, extreme learning machines, and quantum computing [Wetzstein2020, Marković2020, Shastri2021].

Light is a good candidate for such computing paradigms because of its advantages in high bandwidth, high speed, low energy consumption, and low latency [Hamerly2019, Wetzstein2020]. As such, many researchers and startups have been advancing optical platforms both in bulk and integrated optics in many directions [Lin2018, Cao2022, Cartlidge2023]. For instance, in terms of energy consumption, an optical neural network has been shown to use less than 1 photon per multiplication to obtain about 90% accuracy on handwritten-digit classification [Wang2022]. In terms of high speed and large bandwidth, the recent development of the optical parallel convolutional processing unit has demonstrated 11 trillion operations per second, enabling the convolution of images with 2.5×10^5 pixels [Xu2020]. Besides, the idea based on large-scale optical random reservoir computing demonstrated the ability to predict spatiotemporal signals of chaotic systems [Rafayelyan2020].

Despite the recent progress in optical computing, the incorporation of nonlinearity, a pivotal resource in deep neural networks, is the major problem and has been long considered commonly to be the main drawback of optical computing due to the high energy requirement of a nonlinear optical process [Farhat1985, Shen2017, Hughes2018, Wang2023]. Nevertheless, recent advancements have demonstrated promising results, for example, by harnessing multiple scattering processes [Xia2023, Yildirim2023]. Besides, nonlinear activations can also be implemented instantaneously using homodyne detections [Chen2023].

In parallel, the emergence of quantum machine learning (QML) has opened a compelling avenue of research. In this context, our interest is in a specific scenario wherein a part of an information processing unit operates using quantum effects. The quantum devices are typically used to process a computationally difficult subroutine and/or learn from classical data. We here referred to such a device as a *quantum-enhanced learning machine.* Various models of such machines have been proposed, for example, variational quantum circuits and quantum Boltzmann machines [Cerezo2021, Amin2018, Mitarai2018, Steinbrecher2019]. To my knowledge, the questions about the advantages and performance of quantum-enhanced

learning machines, in comparison to classical counterparts, are still unclear and continue to be actively investigated.

Addressing challenges such as encoding large-scale classical information into a quantum system, and evaluating the learning capacity, trainability, and expressivity have been key areas of research [Schuld2022]. Additionally, the implementation of the quantum-enhanced learning machine within an optical platform remains in its infancy, with significant potential for our future understanding and development of an efficient measurement device that can spontaneously measure and process the data.

In our recent works, the implementation of programmable linear optical circuits using complex scattering processes was successfully demonstrated [Goel2024]. The circuit is utilized for the controllability of two-photon interferences [Leedumrongwatthanakun2020] as well as for the certification of high-dimensional entanglements [Goel2024]. Furthermore, our programmable optical circuit, known as the multi-plane light conversion device, was effectively utilized to achieve quantum state discrimination in high dimensions [Goel2023]. These results showcase the potential of our programmable optical circuit for manipulating entangled qudits, offering exciting possibilities to extend the implementation of quantum information processing beyond a traditional qubit-based quantum circuit.

Building upon these advancements and our expertise on the OPA in the low gain, we introduce the apparatus of the *quantum-enhanced optical learning machine* to tackle the problem. This machine is a reconfigurable optical circuit capable of generating high-dimensional entangled states from a cascade of multimodal optical parametric amplifiers (OPAs), interspersed with a linear optical circuit and reconfigurable optical phase array. The idea is to generalize the traditional multimodal nonlinear SU(1,1) interferometer [Yurke1986, Frascella2019] to the cascade and reconfigurable configuration. In the standard multimodal nonlinear SU(1,1) interferometer, the application is on wide-field phase imaging with sub-shot-noise sensitivity, even in the presence of external optical loss [Frascella2019]. Here, instead of an object placed in between OPAs, the optical circuit is used to change a basis of *d*-mode signal and idler fields, while an object (or classical information encoded on the optical phase arrays) is placed on the idler fields. The Sagnac configuration is used to obtain phase stability of the cascade of OPAs. Besides, the quantitative complementary metal-oxide-semiconductor (qCMOS) camera is used to detect the optical signals.

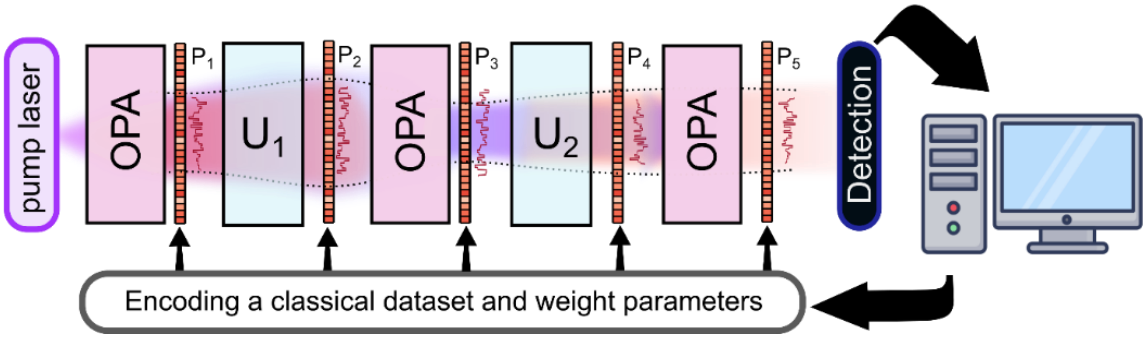

Figure.1 The conceptual schematic of quantum-enhanced optical learning machine: It consists of a series of high-dimensional entangled light sources generated from the optical parametric amplification (OPA) process, a linear circuit, U_i, and reconfigurable optical phase arrays P_i. The optical phase arrays, implemented by a spatial light modulator (SLM), are used to encode classical data and weight parameters onto the optical circuit where all pump, signal, and idler fields are manipulated to control de/amplification process in the cascade OPAs. In practice, the Sagnac loop is used to implement the cascade of OPAs.

Leveraging the programmability of spatial light modulators, we gain the manipulation over the relative complex amplitudes of the optical pump, signal, and idler fields. This enables the control of noiseless de/amplification and quantum correlation of the cascade OPAs. In the first step of the project, we wish to utilize the manipulation of the quantum effect to measure a sub-shot-noise image of the phase profile using the cascade OPAs. The theoretical and numerical developments for the setting of the cascaded OPAs are also investigated in order to provide an optimal design for the optical experiment, namely OPA gain, and the number of spatial entangled modes. In the second step, the learning capability and trainability of the quantum-enhanced optical learning machine are studied by using statistical learning theory. At this step, the method of encoding weighting parameters and the linear optical circuit is designed and implemented. This allows us to estimate the potential and limitations of the machine in terms of measurement sensitivity and the capability of learning. With those successes, we aim to finally showcase the application of the machine for simultaneous sensing and performing pattern recognition tasks. The project opens an avenue of quantum metrology in more complicated scenarios and might pave the way for implementing a decentralized quantum edge device.

Problem Statement/Objective

Can the quantum effect presented in the cascade of multimodal optical parametric amplifiers (OPAs), interspersed with a linear optical circuit and reconfigurable optical phase array (object) be used as a resource in sensing and information processing? If yes, why so?

Outcomes

1. Experimental demonstration of sub-shot-noise measurement of phase profile using the cascade of optical parametric amplifiers.
2. Underlying physics of the quantum-enhanced optical learning machine that is used as a resource for both sensing and computing.
3. Understanding the learning capability and trainability of the optical machine.
4. Training one graduate student
5. At least two publications

Impact

The research project holds the potential to have an impact on various aspects of information processing and artificial intelligence. If successful, the proposed investigation could lead to several significant advancements. It could contribute to our broader scientific understanding of quantum phenomena, that occur in the cascade of multimodal optical parametric amplifications, interspersed with a linear optical circuit. This control of amplifications and quantum correlation over multiple optical modes allows us to engineer a quantum state, particularly for sensing applications. For instance, it facilitates quantum-enhanced widefield imaging and a generation of high-dimensional multipartite entangled states for multiple observers.

We anticipate that the phenomena can be exploited for optical computing, the findings may put forward the understanding of a quantum resource used in computing and the role of quantum measurements, i.e., the interface of the hybrid quantum(optic)/classical(electronic) information encoding. If true, the practical utility of the proposed optical machine in large-scale real-world data classifications and predictions could have far-reaching implications.

Overall, the impact of the research proposal could lead to significant advancements in optical computing, quantum-enhanced technologies, and artificial intelligence, paving the way for a more efficient approach to large-scale information processing in the modern era.

References

[Amin2018] Amin, M. H., Andriyash, E., Rolfe, J., Kulchytskyy, B., & Melko, R. (2018). *Quantum Boltzmann Machine*. *Physical Review X*, **8**(2), 021050.

[Cao2022] Cao, H. and Eliezer, Y., (2022). Harnessing disorder for photonic device applications. *Applied Physics Reviews*, **9**(1), p.011309.

[Cartlidge2023] Cartlidge, E. (January 2023) Optics & Photonics News - Photonic Computing for Sale. p.26-33.

[Cerezo2021] Cerezo, M., Arrasmith, A., Babbush, R., Benjamin, S. C., Endo, S., Fujii, K., McClean, J. R., Mitarai, K., Yuan, X., Cincio, L., & Coles, P. J. (2021). Variational quantum algorithms. *Nature Reviews Physics*, **3**(9), 625–644.

[Chen2023] Chen, Z., Sludds, A., Davis, R., Christen, I., Bernstein, L., Ateshian, L., Heuser, T., Heermeier, N., Lott, J. A., Reitzenstein, S., Hamerly, R., & Englund, D. (2023). Deep learning with coherent VCSEL neural networks. *Nature Photonics*, **17**(8), 723–730.

[Farhat1985] Farhat, N. H., Psaltis, D., Prata, A., & Paek, E. (1985). Optical implementation of the Hopfield model. *Applied Optics*, **24**(10), 1469.

[Feldmann2021] Feldmann, J., Youngblood, N., Karpov, M., Gehring, H., Li, X., Stappers, M., Gallo, M. L., Fu, X., Lukashchuk, A., Raja, A. S., Liu, J., Wright, C. D., Sebastian, A., Kippenberg, T. J., Pernice, W. H. P., & Bhaskaran, H. (2021). Parallel convolutional processing using an integrated photonic tensor core. *Nature*, **589**(7840), 52–58.

[Frascella2019] Frascella, G., Mikhailov, E. E., Takanashi, N., Zakharov, R. V., Tikhonova, O. V., & Chekhova, M. V. (2019). Wide-field SU(1,1) interferometer. *Optica*, **6**(9), 1233.

[Goel2023] Goel, S., Tyler, M., Zhu, F., Leedumrongwatthanakun, S., Malik, M., & Leach, J. (2023). Simultaneously Sorting Overlapping Quantum States of Light. *Physical Review Letters*, **130**(14), 143602.

[Goel2024] Goel, S., Leedumrongwatthanakun, S., Valencia, N. H., McCutcheon, W., Tavakoli, A., Conti, C., Pinkse, P. W. H., & Malik, M. (2024). Inverse design of high-dimensional quantum optical circuits in a complex medium. *Nature Physics*, **20**(2), 232–239.

[Hamerly2019] Hamerly, R., Bernstein, L., Sludds, A., Soljačić, M., & Englund, D. (2019). Large-Scale Optical Neural Networks Based on Photoelectric Multiplication. *Physical Review X*, **9**(2), 021032

[Hughes2018] Hughes, T. W., Minkov, M., Shi, Y., & Fan, S. (2018). Training of photonic neural networks through in situ backpropagation and gradient measurement. *Optica*, **5**(7), 864.

[Leedumrongwatthanakun2020] Leedumrongwatthanakun, S., Innocenti, L., Defienne, H., Juffmann, T., Ferraro, A., Paternostro, M., & Gigan, S. (2020). Programmable linear quantum networks with a multimode fibre. *Nature Photonics*, **14**(3), 139–142.

[Lin2018] Lin, X., Rivenson, Y., Yardimci, N. T., Veli, M., Luo, Y., Jarrahi, M., & Ozcan, A. (2018). All-optical machine learning using diffractive deep neural networks. *Science*, **361**(6406), 1004–1008.

[Marković2020] Marković, D., Mizrahi, A., Querlioz, D., & Grollier, J. (2020). Physics for neuromorphic computing. *Nature Reviews Physics*, **2**(9), 499–510.

[Mitarai2018] Mitarai, K., Negoro, M., Kitagawa, M., & Fujii, K. (2018). Quantum circuit learning. *Physical Review A*, **98**(3), 032309.

[Rafayelyan2020] Rafayelyan, M., Dong, J., Tan, Y., Krzakala, F. and Gigan, S., (2020). Large-scale optical reservoir computing for spatiotemporal chaotic systems prediction. *Physical Review X*, **10**(4), p.041037.

[Schuld2022] Schuld, M., & Killoran, N. (2022). Is Quantum Advantage the Right Goal for Quantum Machine Learning? *PRX Quantum*, **3**(3), 030101.

[Shastri2021] Shastri, B.J., Tait, A.N., Ferreira de Lima, T., Pernice, W.H., Bhaskaran, H., Wright, C.D. and Prucnal, P.R., (2021). Photonics for artificial intelligence and neuromorphic computing. *Nature Photonics*, **15**(2), pp.102-114.

[Shen2017] Shen, Y., Harris, N. C., Skirlo, S., Prabhu, M., Baehr-Jones, T., Hochberg, M., Sun, X., Zhao, S., Larochelle, H., Englund, D., & Soljačić, M. (2017). Deep learning with coherent nanophotonic circuits. *Nature Photonics*, **11**(7), 441–446.

[Steinbrecher2019] Steinbrecher, G. R., Olson, J. P., Englund, D., & Carolan, J. (2019). Quantum optical neural networks. *Npj Quantum Information*, **5**(1), 1–9.

[Wang2022] Wang, T., Ma, S.-Y., Wright, L. G., Onodera, T., Richard, B. C., & McMahon, P. L. (2022). An optical neural network using less than 1 photon per multiplication. *Nature Communications*, **13**(1), 123.

[Wang2023] Wang, T., Sohoni, M. M., Wright, L. G., Stein, M. M., Ma, S.-Y., Onodera, T., Anderson, M. G., & McMahon, P. L. (2023). Image sensing with multilayer nonlinear optical neural networks. *Nature Photonics*, **17**(5), 408–415.

[Wetzstein2020] Wetzstein, G., Ozcan, A., Gigan, S., Fan, S., Englund, D., Soljačić, M., Denz, C., Miller, D. A. B., & Psaltis, D. (2020). Inference in artificial intelligence with deep optics and photonics. *Nature*, **588**(7836), 39–47.

[Xia2023] Xia, F., Kim, K., Eliezer, Y., Shaughnessy, L., Gigan, S., & Cao, H. (2023). Deep Learning with Passive Optical Nonlinear Mapping. arXiv: 2307.08558.

[Xu2020] Xu, X., Tan, M., Corcoran, B., Wu, J., Boes, A., Nguyen, T. G., Chu, S. T., Little, B. E., Hicks, D. G., Morandotti, R., Mitchell, A., & Moss, D. J. (2020). 11 TOPS photonic convolutional accelerator for optical neural networks. *Nature*, **589**(7840), 44–51.

[Yildirim2023] Yildirim, M., Dinc, N. U., Oğuz, I., Psaltis, D., & Moser, C. (2023). Nonlinear Processing with Linear Optics. arXiv: 2307.08533.

[Yurke1986] Yurke, B., McCall, S. L., & Klauder, J. R. (1986). SU(2) and SU(1,1) interferometers. *Physical Review A*, **33**(6), 4033–4054.

Executive Summary

Fabrication-free ultra-thin optical vortex generator

Category: Information

PI: Sejeong Kim, Department of Electrical and Electronic Engineering, University of Melbourne, Australia.

The project aims to address the rapidly increasing global demand for data transmission capacity, which is projected to grow 60-fold over the next decade. This surge necessitates the development of technologies beyond 5G and 6G. One promising solution involves deploying orbital angular momentum (OAM) modes. While OAM modes can be generated using commercially available tools such as spiral phase plates, Q-plates, and spatial light modulators, these tools tend to be bulky. Integrated photonics-based OAM generators, utilising metasurfaces or annular grating ring structures, have shown potential, but they require expensive and time-consuming electron beam lithography.

This project proposes an innovative approach to generating optical vortices using 2D materials. The method builds on a theoretical foundation published in 2003, which has not yet been experimentally explored to create an OAM generator for integrated photonics. The concept involves light with spin angular momentum (SAM) interacting with an anisotropic medium, where some portion of the light converts to the opposite handedness. During this process, the transmitted beam gains OAM to preserve total angular momentum. Since this process relies solely on the interaction between SAM and the medium, it eliminates the need for nanofabrication, significantly reducing costs and easing scalability. This project leverages the giant birefringence discovered in various 2D materials and will likely demonstrate a thin optical vortex generator that can be easily transferred onto various substrates. This project aims to demonstrate a fabrication-free, 2D-material-based OAM generator, achieve large-scale (> cm to wafer-scale) OAM generation, and develop an ultra-thin (<100 nm) OAM generator. These objectives will enhance the practicality, scalability, and integration of OAM technology.

The successful completion of this project depends on several key factors. Firstly, PI Kim, as a co-first author, played a pivotal role in the paper that reported the generation of optical vortices from liquid crystals by constructing the optical setup necessary to observe spiral arms and fork patterns. Secondly, her research lab is well-equipped with essential tools, including a supercontinuum laser capable of supporting experiments at wavelengths between 410 nm and 2.4 μm, and a spatial light modulator (SLM) for creating optical vortex with various topological charges. Additionally, PI Kim can commit 0.2 full-time equivalent (FTE) of her time to this project. Importantly, her group has recently observed optical vortex generation from hexagonal boron nitride, providing a solid foundation for this proposed work.

The outcome of this project will demonstrate a groundbreaking method for creating an OAM generator with a small footprint that is also readily available at wafer scale. This project has the potential to revolutionize optical vortex generation, significantly impacting fields such as data communication and imaging. It will advance research on 2D materials with giant birefringence, potentially leading to new applications in optical technologies. The results will be published in peer-reviewed journals and patented, ensuring substantial contributions to both scientific knowledge and practical applications.

Title: Fabrication-free ultra-thin optical vortex generator

PI: Sejeong Kim, University of Melbourne

< Literature Review >

1. Introduction

The exponential growth in demand for data transmission is expected to increase the required capacity by 60-folds in 10 years.[1] To meet this stringent requirement, researchers are currently investigating orbital angular momentum (OAM) as a potential solution for future technology beyond 5G and 6G.

Optical vortices are light waves characterised by helical phase fronts carrying OAM. The field emerged in 1989 with the discovery of vortex solutions and has been extensively studied over the previous three decades.[2] Throughout this period, optical vortices have found practical applications across various areas other than optical communications, including quantum technology, optical tweezers, microscopy, and imaging. This project will demonstrate an innovative optical vortex generator that does not require nanofabrication. The conventional methods used to create OAM are explained below, and the theoretical groundwork of the proposed work is on page 2.

2. OAM generation methods

There are various methods to create optical vortices, summarised below. One common and intuitive approach is using a **Spiral Phase Plate**. The spatially varying thickness of the plate induces spatially varying phase front of light, as shown in Fig. 1. This figure illustrates the creation of an optical vortex with a topological charge (l) of 1, where l indicates the number of twists the light makes in one wavelength. Spiral phase plates are now commercially available from many optics companies, such as Edmund Optics. These plates have recently regained attention in the research domain due to the advances in 3D-printing techniques, which enable creation of micro-sized spiral phase plates on various substrates, including optical fibres. However, once created, the plate can only generate a fixed topological charge.

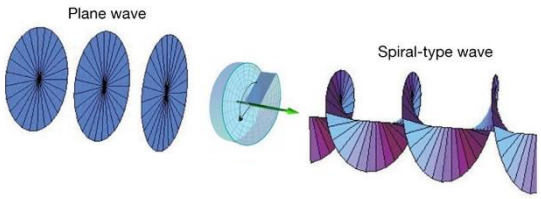

Figure1. Spiral phase plate creating OAM.

A **Spatial Light Modulator** (SLM) is an alternative method for creating optical vortices. An SLM consists of a 2D array of liquid crystal pixels that controls the phase of reflected beams. While it is more expensive than spiral phase plates, it offers the capability to generate any topological charge and allows for fast switching between different topological charges. SLMs are commercially available from various companies, including Santec and HOLOEYE. Despite fast switching and suitability for many free-space applications, miniaturising SLMs poses a challenge.

Metasurfaces offers a promising avenue in this respect. In 2011, a groundbreaking demonstration showcased phase control of light using antenna arrays (Fig. 2a), thereby overcoming the constraint of standard optical components that rely on gradual phase accumulation along the optical path.[3] Since then, metasurface-based OAM manipulation studies have yielded numerous advances, with recent designs showcasing multiplexed manipulation of OAM.[4] Another on-chip solution for generating an OAM beam involves the use of angular grating structures (Fig. 2b).

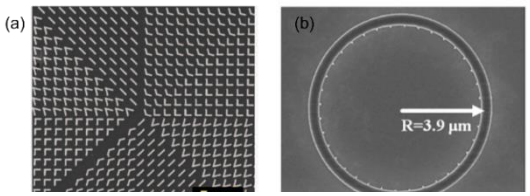

Figure2. OAM generation using (a) metasurface and (b) angular grating.

So far, these on-chip solutions necessitate electron beam lithography to define nano-sized structures.

< Problem Statement and Objectives >

To be compatible with the existing optical communication platforms, a compact device with small-footprint for OAM manipulation is necessary. Metasurface and angular grating-dressed micro rings are being investigated as potential candidates; however, they both require sophisticated nanofabrication involving electron-beam lithography to create nano-sized features. This need for precise nanofabrication is not only costly but also a bottleneck for scaling up. Scalable, low-cost solutions that can be integrated on chips or with fibre are crucial for practical OAM applications.

This project proposes a fabrication-free OAM-generator that can be used for both on-chip and large-scale applications. In this work, we investigate a propagating circularly polarised beam in anisotropic media that converts to the opposite handedness and gains OAM. The aims of this project are to:

1) Demonstrate a fabrication-free, 2D-material-based OAM generator;
2) Achieve large-scale (> cm to wafer-scale) OAM generation;
3) Develop an ultra-thin (<100 nm) OAM generator.

< Project plans >

PI Kim has already obtained preliminary data (page 4) that is the foundation of this proposal. Detailed aims are included in the 'Optica Foundation Challenge Timeline Template'.

< Feasibility and Capability >

1. Theoretical work

In the theoretical prediction paper published in 2003,[5] the authors mathematically derived that a circularly polarised paraxial beam propagating along the optical axis of an anisotropic medium can acquire OAM. Simply put, the input beam experiences spatially varying effective refractive indices when travelling through an anisotropic medium, causing some portion of the beam to convert to circularly polarised light (CPL) with opposite handedness. Now consider the conservation law of the total angular momentum, J, which is the sum of spin angular momentum (SAM), σ, and orbital angular momentum l. The initial beam with right-handed CPL has a total angular momentum of +1, with SAM corresponding to 1 and OAM corresponding to 0. The total angular momentum in the output beam with the opposite handedness must be conserved to +1, thus the beam should contain OAM corresponding to 2 as

$$J = \sigma + l: \quad (before)\ 1 = 1 + 0 \rightarrow (after)\ 1 = -1 + 2.$$

Now, the question is the efficiency of this conversion process. Simulation results predict that with sufficient propagation length, this conversion can reach nearly 50%.[5] The first experimental validation was reported in 2020.[6] This work utilized 5-mm-thick c-cut β-BaB_2O_4 (BBO) crystal and experimentally demonstrated that the outcoming second harmonic generated beam carries additional optical vortex charge (Fig. 3).

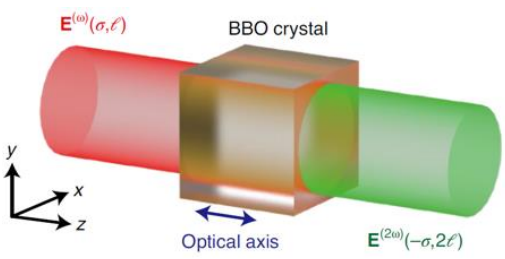

Figure3. Illustration showing the output beam gains OAM

2. Giant birefringence in 2D materials

The giant birefringence of 2D materials plays a central role in the proposed research. Prior to the discovery of 2D materials, conventional birefringent materials widely used included liquid crystals, with their Δn typically smaller than 0.1 and at best 0.2. Apart from liquid crystal, a well-known crystallin birefringent material is BBO, which has Δn corresponding to 0.12. In 2019, we measured and reported refractive indices from crystalline hBN, revealing a large birefringence ($\Delta n \sim 0.3$) for transparent materials (Fig 4. left).[7] Subsequently, intensive searches for giant optical anisotropy among natural and artificial materials have been pursued (Fig. 4 middle), revealing MoS_2 has exceptional birefringence, followed by hBN and $BaTiS_3$.[8] Recently, this investigation has been expanded to encompass a wider variety of 2D materials, with the wavelength window range extended to the far mid-IR.[9] This research will employ hBN, MoS_2, and $BaTiS_3$ to generate optical vortices. The choice of material is not limited and might include different 2D materials.

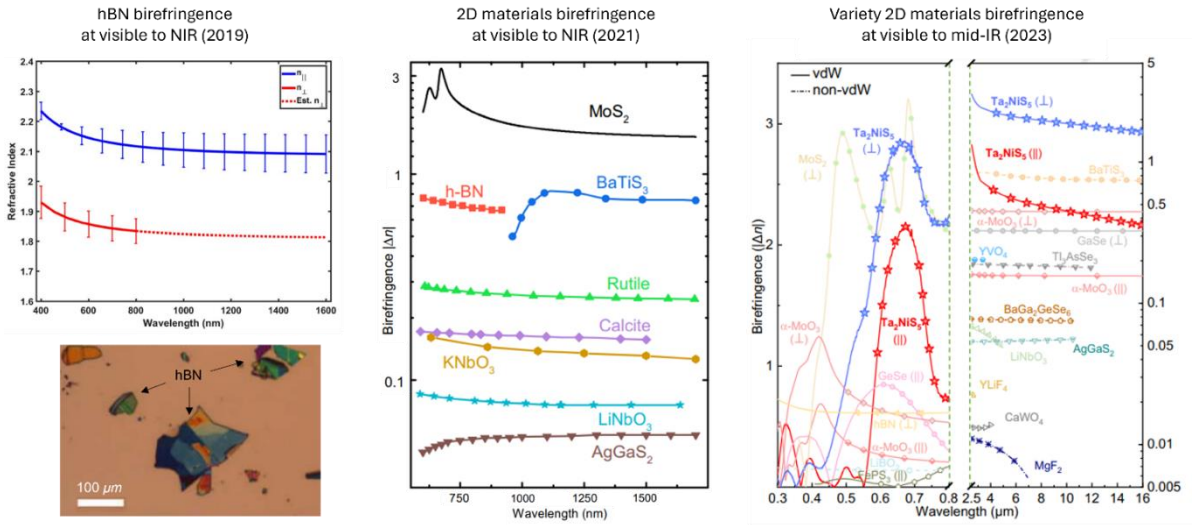

Figure 4. Giant birefringence from various 2D materials.

3. PI's capability

The successful completion of this project relies on several key factors. Firstly, PI Kim authored the paper that observed optical vortex generation from liquid crystal.[10] As a co-first author of the paper, she constructed the optical setup to observe spiral arms and fork patterns. Secondly, her research lab is equipped with essential equipment, including a supercontinuum laser, enabling optical vortex generation experiments at any wavelength between 410 nm to 2.4 μm, and a spatial light modulator (SLM) capable of creating any optical vortex charge number necessary to impose OAM to the incident beam. Finally, PI Kim has the time availability to commit 0.2 full-time equivalent (FTE) of her time. As a new PI of the lab, if successful, this will mark the first external funding for her research, with one PhD student dedicated to the project. Additionally, there are external collaborators involved, including Dr Haejun Jung (Hanyang University), A/Prof Nanfang Yu (Columbia University), and Prof Junsuk Rho (POSTECH). Most importantly, PI Kim's group has recently made progress in observing preliminary results, increasing the likelihood of achieving the proposed ambitious-yet-feasible aims.

4. Preliminary results

Material selection is one of the key aspects of our experiment. We opted for hBN due to its significant birefringence and transparency at the visible and near-IR (NIR) wavelength range. Being a wide bandgap material with a band edge absorption at the UV region of 6 eV, it maintains low optical loss from the visible spectrum and above. The finite-difference time-domain (FDTD) simulation is conducted with the incident Gaussian beam (from left to right) carrying no OAM ($l = 0$) propagating through the anisotropic medium of hBN. In Fig. 5(a), only the intensity of the LCP beam is displayed, while Fig. 5(b) shows the simulation result for the RCP component. In a homogeneous medium, the initial polarisation state, i.e., LCP in this case, remains fixed throughout propagation, resulting in zero intensity in the RCP intensity map. However, in an anisotropic medium, polarisation alterations induce the opposite handedness, as shown in Fig. 5(b), i.e., the RCP is created in the medium.

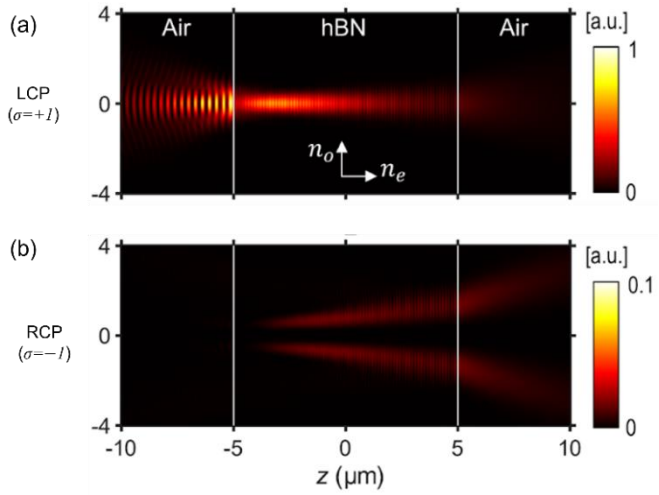

Figure 5. Intensity map of (a) LCP and (B) RCP when the light propagates from left to right.

We experimentally verified the generation of the optical vortex from the hBN flake. The flake shown in Fig. 6(a) is thicker than typical mechanically exfoliated ones because the flake, as purchased, was placed on the glass, i.e., we skipped the sticky tape exfoliation to obtain sufficient propagation length for the initial verification. A 593 nm laser was focused onto hBN using an objective lens (40×) and transmitted light was collected through a second objective lens (50×). The incident beam is LCP, while the transmitted beam contains both RCP and LCP. Only the RCP beam is imaged in Fig. 6(b), showing the doughnut beam intensity profile, confirming phase singularity at the centre.

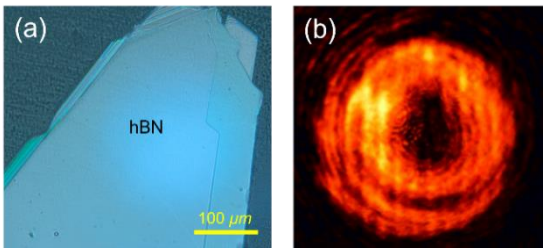

Figure 6. (a) Optical microscope image of a hBN flake. (b) CCD image of optical vortex.

< Outcomes >

This project will create a groundbreaking method of creating optical vortices using 2D materials. The outcomes of this project include innovation in multiple aspects. Firstly, it offers a novel solution for generating micro optical vortices on a chip. The method leverages the significant birefringence of 2D materials and their interaction with the spin angular momentum of light. This method creates optical vortices in a simple, and nanofabrication-free manner. Secondly, the project will likely result in the world's simplest vortex generator, which is easily scalable in both quantity and size. The size of this vortex generator is determined solely by the size of the material, allowing for even wafer-scale vortex generators using CVD growth technique. While CVD growth of many 2D materials remains challenging, it is advancing rapidly across various fields. Fortunately, high-quality CVD-grown hBN samples have been demonstrated by our collaborator. Additionally, the project will develop ultra-thin optical vortex generators. The findings will be published in peer-reviewed journals, and key discoveries will be

patented. The project will test various 2D materials and will find the best materials for optical vortex generation for visible and NIR applications.

< Impact >

As the demand for data capacity continues to rise annually to support high-speed video streaming and multidata, it is crucial to advance beyond 5G and 6G technologies. To meet this growing demand, achieving high data rates and spatial multiplexing is essential. The success of this project will significantly impact the miniaturization and cost reduction of OAM generators. Given that OAM has applications beyond data communication, such as in imaging, the project's outcomes will benefit various disciplines. Additionally, this work will significantly advance research on 2D materials. The extremely large birefringence of 2D materials has only recently been experimentally measured and reported, and this project will be among the first to leverage this property.

References

(1) Doohwan, L.; Hirofumi, S.; Yasunori, Y.; Takayuki, Y.; Takana, K.; Hiroshi, H. Toward terabit-class wireless transmission: OAM multiplexing technology. *NTT Technical Review* **2019**, *17* (5), 34-39.
(2) Coullet, P.; Gil, L.; Rocca, F. Optical vortices. *Optics Communications* **1989**, *73* (5), 403-408.
(3) Yu, N.; Genevet, P.; Kats, M. A.; Aieta, F.; Tetienne, J.-P.; Capasso, F.; Gaburro, Z. Light propagation with phase discontinuities: generalized laws of reflection and refraction. *science* **2011**, *334* (6054), 333-337.
(4) He, G.; Zheng, Y.; Zhou, C.; Li, S.; Shi, Z.; Deng, Y.; Zhou, Z.-K. Multiplexed manipulation of orbital angular momentum and wavelength in metasurfaces based on arbitrary complex-amplitude control. *Light: Science & Applications* **2024**, *13* (1), 98.
(5) Ciattoni, A.; Cincotti, G.; Palma, C. Circularly polarized beams and vortex generation in uniaxial media. *JOSA A* **2003**, *20* (1), 163-171.
(6) Tang, Y.; Li, K.; Zhang, X.; Deng, J.; Li, G.; Brasselet, E. Harmonic spin–orbit angular momentum cascade in nonlinear optical crystals. *Nature Photonics* **2020**, *14* (11), 658-662.
(7) Rah, Y.; Jin, Y.; Kim, S.; Yu, K. Optical analysis of the refractive index and birefringence of hexagonal boron nitride from the visible to near-infrared. *Optics letters* **2019**, *44* (15), 3797-3800.
(8) Ermolaev, G.; Grudinin, D.; Stebunov, Y.; Voronin, K. V.; Kravets, V.; Duan, J.; Mazitov, A.; Tselikov, G.; Bylinkin, A.; Yakubovsky, D. Giant optical anisotropy in transition metal dichalcogenides for next-generation photonics. *Nature communications* **2021**, *12* (1), 854.
(9) Feng, Y.; Chen, R.; He, J.; Qi, L.; Zhang, Y.; Sun, T.; Zhu, X.; Liu, W.; Ma, W.; Shen, W. Visible to mid-infrared giant in-plane optical anisotropy in ternary van der Waals crystals. *Nature Communications* **2023**, *14* (1), 6739.
(10) Son, B.; Kim, S.; Kim, Y. H.; Käläntär, K.; Kim, H.-M.; Jeong, H.-S.; Choi, S. Q.; Shin, J.; Jung, H.-T.; Lee, Y.-H. Optical vortex arrays from smectic liquid crystals. *Optics express* **2014**, *22* (4), 4699-4704.

Executive summary

Non-fundamental vibrational refractive index mapped spectroscopy for complete hypoxia assessment in nascent life

Optica foundation challenge - Health

Shree Krishnamoorthy, Tyndall National Institute, University College Cork, Ireland
shree.krishnamoorthy@tyndall.ie

Unmet need: Nascent life: the moments before birth during labour to first week of life, remains the most precarious. Two in every thousand babies suffer aftereffects of difficulties in breathing during labour or pre-term hypoxia and die. While tremendous progress has been made since 1990s in improving neonatal care, WHO recognizes that the unaddressed challenge is due to poor monitoring methods of the babies in clinics currently, including urgent Every Child Alive campaign with target date of 2030.

An early, and continuous, monitoring of hypoxia-related distress (e.g. using spectroscopy) would be a disruptive change in proactive clinical care for nascent life.

One of the barriers for technology is the ability to measure biomarkers non-invasively in a biological aqueous medium in 1350-2500 nm wavelength ranges using conventional spectroscopy at relevant tissue depths of 1-2 mm.

Addressing the challenge: **NoVIXS (**Non-fundamental vibrational refractive index mapped spectroscopy) project, will demonstrate a novel spectroscopic technique, that will enable monitoring hypoxic distress continuously without breaching the skin. The spectroscopy technique developed in **NoVIXS** will be the first ever to measure refractive index differences in the **aqueous biophantoms** across a large wavelength range of **1450-1650 nm up to 1 mm depth**.

Non-fundamental vibrations of different molecular bonds of water and biomarkers relevant to hypoxia are present as broad absorption bands spanning 10s of nm wide in different parts of the long-wavelength near infrared (LW-NIRS) region within 1350-2500 nm. All the vibrational modes together present themselves as a fingerprint of the biomarker of interest. When light of frequency that falls within the absorption peak interacts with the molecules, it experiences absorption and change in refractive index compared to frequencies outside the band. Traditional spectroscopic techniques rely on the intensity of light detected outside the sample suffer from low photon numbers due to high background absorption from water in biological tissues. Dispersion-based spectroscopy is on the other hand designed for measuring only in gaseous samples within narrow wavelength bands. Thus, there is a gap in spectroscopic method that - 1) is suitable for biomarkers with spectral fingerprints that span a large wavelength region and, 2) measures in aqueous samples with large background absorptions, addressing both will allow for monitoring onset of hypoxia effectively in nascent life.

In **NoVIXS** project of novel spectroscopy technique to measure a refractive-index in aqueous medium with depths relevant to measuring in human tissue will be conceptualized and demonstrated. The technique exploits the change in relative phase of light caused by change in refractive index due to the biomarker's spectral signatures. The proposed technique uses modulated lasers that access multiple spectral regions of a biomarker. The different regions modify the light according to the spectral signature of the biomarker. A novel detection system extracts the slight differences in the signal at the different wavelengths completing the biomarker fingerprint.

Impact: Towards addressing the grand challenge of monitoring hypoxia in nascent life in clinics **NoVIXS** takes the first step of transforming of the core spectroscopy technique. **NoVIXS** will enable development of devices for effective measurement the biomarkers related to hypoxia in human tissue in 1350-2500 nm wavelength region without drawing a single drop of blood.

Non-fundamental vibrational refractive index mapped spectroscopy for complete hypoxia assessment in nascent life

Optica foundation challenge - Health

Shree Krishnamoorthy, Tyndall National Institute, University College Cork, Ireland
shree.krishnamoorthy@tyndall.ie

Summary: NoVIXS (non-fundamental vibrational refractive index mapped spectroscopy) takes a first step towards building a device to monitor hypoxia in nascent babies. In this NoVIXS proposal a novel laser-based spectroscopy technique to measure a relative refractive-index profile, is both conceptualized and demonstrated [IDF-1]. The proposed spectroscopy technique will be adopted into a clinically relevant device to measure biomarkers related to hypoxia in human tissue as the project matures [IDF -2]. My current postdoctoral work focuses on developing a device to assess hypoxia that measures lactate using light and in a non-invasive manner. However, currently there are no devices that measure other clinical gold standards of hypoxia through human tissue without taking a physical sample.

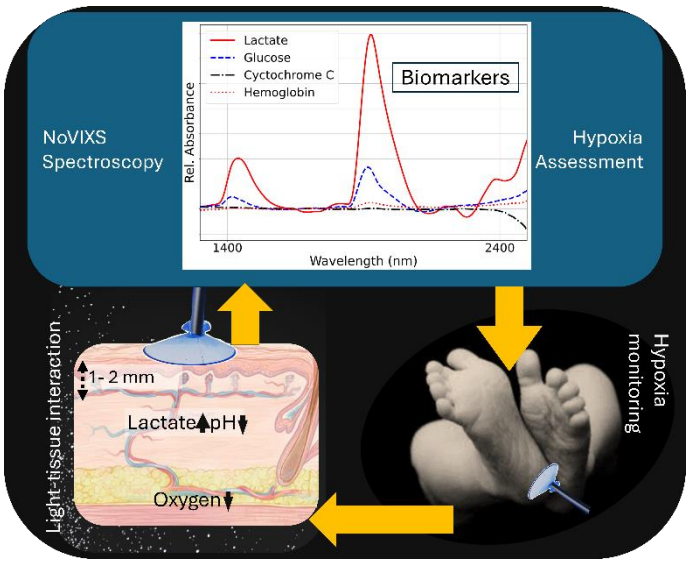

Figure 1: NoVIXS assesses hypoxia using optical spectroscopy in a non-invasive and continuous manner in a baby's heel.

It would be a major step forward if a technique to assess hypoxia in any human tissue without pricking the human skin were developed with impact across a wide range of medical applications. The novel aspect of the proposed work is to develop a spectroscopy technique and transform non-invasive spectroscopy. The novel technique developed in NoVIXS would allow rapid, accurate and non-invasive continuous measure of biomarkers, compared to current invasive and slow techniques that require blood or tissue to be drawn and subsequently analysed.

There are two key objectives required to deliver this ambitious project, 1) measure multiple hypoxia biomarkers simultaneously in a non-invasive manner without compromising on accuracy, and 2) to achieve this challenging measurement through high optical spectral resolutions over a large spectral region which are made possible by the novel spectroscopy technique developed in NoVIXS.

Why, and why now: Nascent life: the moments before birth, during labour and the first week of life, remains the most precarious. Two in one thousand babies suffer the aftereffects of difficulties in breathing during labour, or pre-term hypoxia, and die. While tremendous progress has been made since 1990s in improving neonatal care, the World Health Organization recognizes that this unaddressed challenge is due to poor monitoring methods of the babies in clinics as a part of urgent Every Child Alive campaign with target date of 2030 [3,4]. An early, and continuous, monitoring of hypoxia-related distress (e.g. using spectroscopy) is missing and would be a disruptive change in the current clinical care for nascent life.

The current gold standard for hypoxia assessment in a foetus and a new-born are based on discretionary measurement of lactate and pH levels at a systemic level. This currently requires drawing capillary blood during the course of measurement from the fetus, or the newborn, with a small prick from the capillary bed 1-2 mm below the skin. The blood draw and subsequent measurement in a blood gas analyser is performed using fetal blood sampling or a heel prick technique [5,6].

There are obvious shortcomings: the sampling is physically invasive, needs 20 mins between measurements, and cannot be done repeatedly and regularly (multiple times) without hurting the baby. Further, as per current practice they are performed as per clinicians' discretion if issues are suspected.

i.e., current practices are one-off passive monitoring and diagnostic tools, but are incapable of constant proactive measurement for early warning. Clearly, there is an unmet need for a continuous hypoxia monitoring method that covers the nascent stages of life from labour to the first week of life.

It should be said that alternative, non-invasive methods have also been developed for general patients and can be found in the literature and in clinical practise, as possible synergistic sources of information as outlined in Table 1.

For feasible hypoxia assessment, the spectroscopic method would need light to penetrate deep (> 2 mm) into aqueous samples and be capable of measuring all spectroscopic regions of a biomarker in a wide spectroscopic band.

Table 1: Potential of current technologies to assess hypoxia non-invasively in clinics.

Method	***Invasive? (Yes/No)***	***Hypoxia biomarkers (lactate/ pH)?***	***In aqueous medium?***	***Sample depth [mm]***	***Continuous? (Yes/No)***	***Summary***
Blood gas analyser [7]	Yes	**Lactate, pH**	**Yes**	**≥ 2**	No	Current clinical standard
Wearable sensor [8,9]	**No**	Lactate, pH	Yes	0	Yes	Hydrogel based sweat sensing needs sample in contact.
IR absorption [10]	N/A	Lactate, pH	No	0.003	No	FTIR based in 6000 nm band, dry samples
NIR absorption [11]	**No**	Lactate	Yes	≤0.5	**Yes**	LW-NIR using FT-NIR
CLaDS [12]	**No**	N/A	No	For gases	**Yes**	Dispersion spectroscopy gases
Spatially offset Raman [13]	**No**	Lactate, pH	Yes	< 1	**Yes**	Can only detect strong Raman signals at these separations.
NoVIXS [1,2]	**No**	**Lactate, pH**	**Yes**	**≥ 2**	**Yes**	NoVIXS's novel technique

It is evident that current technological solutions are unfit for the clinical standards [14,15,16]. The NoVIXS project will develop a new "technological" paradigm to address the urgent matter of hypoxia assessment in nascent life. NoVIXS will develop first-ever non-invasive, continuous, reagent-free hypoxia assessment using a novel spectroscopy technique. Hence the need for NoVIXS.

Problem statement and Objective:

In NoVIXS, a novel spectroscopic method will be developed to capture relative refractive-index profile with 10 kHz spectral resolution in a 100 MHz range around a non-fundamental vibration mode of water between 1450-1650 nm at a depth of 1 mm in an aqueous phantom. Which will be achieved as following objectives are realized:

Objective 1: Capture differential refractive index profile from aqueous samples of 1 mm - Benchtop system will be developed and used to capture the differential refractive index profile in aqueous samples of 1 mm thickness (Aim 3, M2, D2, month 24) based on the light-tissue model (Aim 4, M3, month 18).

Objective 2: Relative refractive index profile captured with high spectral resolution of 10 kHz in a 100 MHz band - Develop and demonstrate experimentally a fiber-based bench-top spectroscopy setup to provide resolution of 10 kHz (Aim 1, M1 month 12) using a combination of novel source in 1450-1650 nm band and corresponding phase-sensitive detector with a 10 kHz resolution in 100 MHz band around the laser light (Aim 2, D1, month 24).

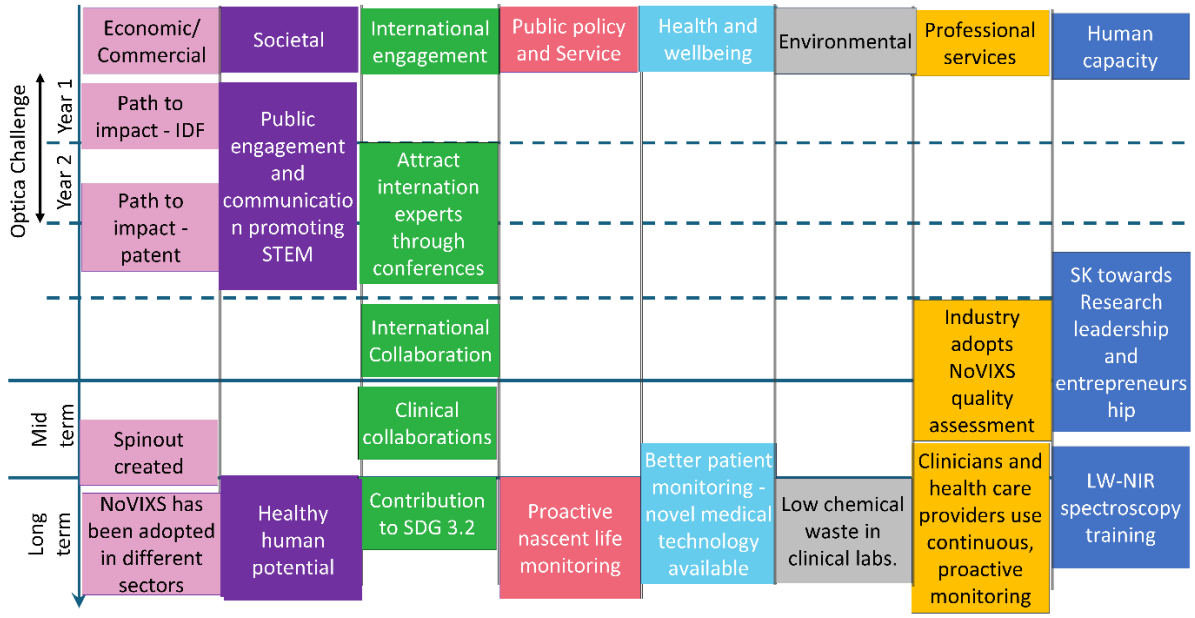

Figure 2: Complete impact map of NoVIXS project.

Mission and outcome:

Each baby deserves to go home.
With NoVIXS, each baby has a chance to go home.

Expected advances in biomarker measurement:

1. Non-invasive, prick-less hypoxia biomarker assessment from human tissue at a depth of 2 mm.
2. Development of a reagent-free, accurate hypoxia assessment with multiple biomarkers.

Expected advances in spectroscopy:

1. Optical spectroscopy with high spectral resolution of 10 kHz over 50 nm band.
2. Measurement in aqueous samples of thickness 2 mm in optical regions with limited light propagation namely long-wavelength near infrared (LW-NIR) range of 1350-2500 nm.

Impact: To enable mission of NoVIXS, the concepts and technology developed within this project and subsequent research and development will be honed into a fully matured product. This impact statement highlights a few aspects of this vision, and the overall impact is outlined in Figure 2.

Societal - NoVIXS project aims to be impactful in the real-world as it is inspired by a clinically relevant problem of monitoring of nascent life (UN SDG 3.2, WHO - Every Child Alive). The true societal impact would be when each new-born baby goes home healthy with quality clinical care with NoVIXS. During the course of this project, I will be actively involved in education and public engagement activities (Education & Public Engagement in Science and Research (tyndall.ie)) and keep the public informed and engaged through platforms like LinkedIn (shree-krishnamoorthy) and YouTube.

Economic and Commercial – Envision that every labour and neonatal wards are fitted with continuous hypoxia monitoring developed through NoVIXS Co., a spin-out. In this scenario the developed spectroscopy technique may also be licenced to other industries like pharma, food etc. To realize this impact - two IDFs have been filed with the UCC TTO for patent after POC has been obtained in year 2 of NoVIXS, initiating the spin-out of NoVIXS Co. This will generate revenue, employment and intellectual property through the project.

Human capacity – In the long-term Ireland would develop a workforce specialized on non-invasive health monitoring using LW-NIR spectroscopy. This would be initiated by my own learning in the short-term. In the mid- and long-term, hands-on research training and development for students through talks, course modules in BioPhotonics within the UCC's Biomedical course (under development) and through the summer schools like BIGGS (2026 onwards) (BIGSS - University of Galway) and BioPhotonics summer school in Hven - 2027 (Frontpage (biop.dk)). I am on my distinct, independent research path by establishing collaborations, access to mentors and international academic and industrial networks. I

am now advancing my career towards a fully funded investigator by securing own independent funding (ERC Starting grant (‘27), Royal Society University Fellowship(‘26), Optica Deutsch (‘29), SPIE-Franz Hillenkamp (‘28) and Horizon Europe fundings (Pillar 1, ERC – ’27, Pillar 2 health cluster – ’29, Pillar 3 – Innovative Europe – ’30)) and publications as senior author in peer-reviewed journals (ACS Photonics, JBO, Spectrachemica Acta, Applied Spectroscopy etc.). I would be upskilling myself through the range of professional and leadership training opportunities (Optica Level Up, 2025, Optica Innovation School 2026). I will also connect and search leadership communities by being active in different societies and networks (Tyndall Early Career Researchers’ Network (TEC-Net), Optica, IEEE sensor, SPIE memberships and technical groups).

References:

[1] Krishnamoorthy, S. “STIR spectroscopy technique” UCC Ref No. for STIR IDF is UCC-24-017.
[2] Krishnamoorthy, S. “NASCENT - long-wavelength Near infrAred optical Signals for Continuous non-invasivE Nascent life well-being moniToring” UCC Ref No. for the IDF is UCC-24-019.
[3] WHO report Levels and trends in child mortality (2021).
[4] UNICEF, Every Child Alive, URL- https://www.unicef.org/reports/every-child-alive, (2018), accessed on 10th April, 2024.
[5] Malin, Gemma L., Rachel K. Morris, and Khalid S. Khan. "Strength of association between umbilical cord pH and perinatal and long-term outcomes: systematic review and meta-analysis." BMJ 340 (2010).
[6] McCall, R. E., and C. M. Tankersley. "Phlebotomy Essentials, edition." (2007).
[7] Couck, Pedro, et al. "Preliminary performance evaluation of blood gas analyzers." Clinical Chemistry and Laboratory Medicine (CCLM) 44.8 (2006): 1030-1034.
[8] NajafiKhoshnoo, S., Kim, T., Tavares-Negrete, J.A., Pei, X., Das, P., Lee, S.W., Rajendran, J. and Esfandyarpour, R., "A 3D Nanomaterials-Printed Wearable, Battery-Free, Biocompatible, Flexible, and Wireless pH Sensor System for Real-Time Health Monitoring." Advanced Materials Technologies 8, no. 8 (2023): 2201655.
[9] Rockley Photonics. Real-time, non-invasive biomarker sensing on the wrist. (2021), accessed on 10th April, 2024.
[10] Kozari, E., et al. "Infrared and NMR spectroscopic fingerprints of the asymmetric H7+ O3 complex in solution." ChemPhysChem 22.8 (2021): 716-725.
[11] S. Krishnamoorthy et al., “Beyond Oxygen In-vivo Long-wavelength Near Infra-red Spectroscopy for Hypoxia Assessment”, Hot Topixx, ECBO, ES2B. 1, Optica Publishing Group (2021).
[12] Nikodem, M., et al. "Chirped lasers dispersion spectroscopy implemented with single-and dual-sideband electro-optical modulators." Optics Express 21.12 (2013): 14649-14655.
[13] Nicolson, F., Kircher, M.F., Stone, N. and Matousek, P., 2021. Spatially offset Raman spectroscopy for biomedical applications. Chemical Society Reviews, 50(1), pp.556-568.
[14] Zourabian, Anna, et al. "Trans-abdominal monitoring of fetal arterial blood oxygenation using pulse oximetry." Journal of biomedical optics 5.4 (2000): 391-405.
[15] S. Krishnamoorthy, et al. "Non-invasive continuous hypoxia assessment in intra-partum fetus through long wavelength near infrared spectroscopy." Photonic Instrumentation Engineering X. Vol. 12428. SPIE, (2023).
[16] Cummins, Gerard, et al. "Sensors for fetal hypoxia and metabolic acidosis: a review." Sensors 18.8 (2018): 2648.

Compact laser-plasma very high-energy electron (VHEE) accelerator for cancer therapy

Executive summary - Health

According to World Health Organisation, cancer is a leading cause of death worldwide, accounting for nearly 10 million deaths in 2020, or almost one in six deaths. Roughly 60% of cancer patients receive radiation therapy, which is effective at causing remission in specific cancers. More than 90% of radiotherapy, however, is currently performed using megaelectron volt (MeV) X-rays. These sources are highly detrimental as their radiation severely harms healthy tissues on its way while reaching the deep tumor. By contrast, the use of very-high-energy electrons provides a much more uniform dose deposition depth, which could significantly reduce the harmful impact of the radiation on healthy tissues. Protecting healthy tissue is critical to the patient's recovery; thus, using energetic electrons could be a game changer for cancer radiotherapy. The challenge lies in the machinery needed to produce electrons in the energy range of hundreds of MeV suitable for deep tumor treatment. Machines that achieve such energetic electrons with conventional radio-frequency technology are considerably more complex, large, and expensive than the widely used photon guns used to produce MeV photons for standard X-ray radiotherapy. Therefore, access to high-quality radiotherapy for deep tumors is very limited in many parts of the world, especially in low- and middle-income countries.

This project aims to experimentally demonstrate a proof-of-principle of compact laser-plasma accelerator that delivers high-energy electrons up to 100 MeV at a kilo-Hertz (kHz) repetition rate. The accelerator utilizes laser pulses with energies in the few-millijoule range and durations in the few-femtosecond range to generate and propel a plasma structure known as a wakefield. While this technology has already shown promise in achieving compact accelerators, it still encounters certain inherent limitations. One significant limitation is the disparity between the group velocity of the laser in the plasma and the relativistic electron bunch, which moves near the speed of light. Consequently, the faster electrons surpass the acceleration structure created by the wake, resulting in a termination of their acceleration. This limitation, known as "dephasing," constrains the maximum energy that can be attained by the electron bunches generated by the accelerator.

Optically shaping the driver laser in space and time at the focus will allow control of the dynamics of laser-plasma acceleration, mitigating the dephasing that limits the final electron energy. I aim to increase the electron energy by one order of magnitude compared to the current state-of-the-art kHz laser-plasma accelerators using the same driver-laser parameters. This source's unique beam properties, high energy, narrow energy spread, and high dose and dose rate will allow for the developing of next-generation radiotherapy treatments with precise dose control.

With current laser technology, the final size of this accelerator could be no larger than an optical table, making it cheap and accessible to many hospitals around the world. Moreover, a radiotherapy unit based on such technology could fit into a truck. This mobility and cost-effectiveness can allow this technology to permeate the economic and geographical periphery. This access will stand in contrast to techniques like proton beam therapy, whose massive sophistication and cost limit its use to the best-funded and most central cancer centers.

In conclusion, the development of this novel laser-plasma electron source technology, which relies on precise optical laser sculpting in space and time, offers promising prospects. It not only enables the creation of innovative and cost-effective radiotherapy sources but also unlocks opportunities for high-energy, high repetition rate table-top electron sources. This advancement holds the potential to drive significant advancements in medicine, biology, chemistry, and physics, which could lead to groundbreaking discoveries and transformative breakthroughs.

Proposal: Compact laser-plasma very high-energy electron (VHEE) accelerator for cancer therapy

Introduction

In a laser-plasma accelerator (LPA) [ESL09], an intense ultrashort laser pulse is focused on gas, causing ionization and forming a plasma (Fig. 1: Left). The laser pulse along the focus can be visualized as a flying sphere with a diameter of several microns. As the "laser sphere" moves, it expels electrons from the optical axis, creating a plasma wake or cavity-free region (Fig. 1: Right). Within this cavity, electric fields of remarkable magnitude, three orders of magnitude greater than those in standard radio-frequency (RF) accelerators, are generated. As a result, LPAs can accelerate electrons to energies as high as hundreds of MeV within a few millimeters. Conventional accelerators would require tens of meters to achieve the same electron energies.

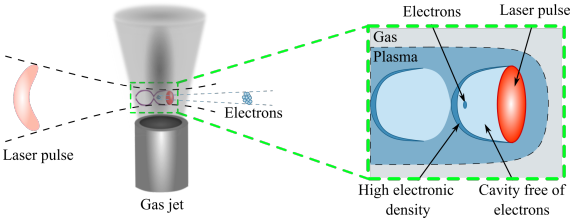

Figure 1: Left: Concept of a laser-plasma accelerator. Right: Zoomed region of the wake formation and electron acceleration.

The clear advantage of LPA is its substantial reduction in the facility's size and cost. In addition, the intrinsic properties of the LPA-generated electron bunches, such as durations of several femtoseconds (fs) and lateral dimensions on the order of a micron, have advantages over bunches obtained in conventional accelerators.

Many experiments are currently dedicated to pursuing laser-plasma acceleration of electrons to GeV energies. These efforts hope to use LPA to drive advanced light sources such as free electron lasers and as a new paradigm for the next generation of linear colliders for high-energy physics. Such experiments rely on petawatt scale laser systems that are large-scale lab facilities that operate, at best, at repetition rates on the order of one Hertz (Hz). Many high-impact societal applications, however, do not require such high-energy electrons. Radiotherapy of deep tissues, for example, needs electron beams with energies of around one hundred MeV. New near-single-optical-cycle duration, millijoule (mJ), kHz repetition rate lasers promise to deliver electrons at such energies. These laser systems are particularly attractive due to their tabletop size and competitive cost. The compact nature of this technology enables a radiotherapy unit to be housed within a truck, offering enhanced mobility and cost-effectiveness. This advantageous feature allows the technology to reach economic and geographical peripheries that previously lacked access to advanced radiotherapy treatments. In contrast to expensive and highly sophisticated techniques such as proton beam therapy, which are predominantly limited to well-funded and centrally located cancer centers, this technology has the potential to provide broader accessibility to effective cancer treatment.

Electron beams from LPAs have unique properties: they provide femtosecond electron bunches and dose rates as high as 10^8 Gy/s, compared to 10 Gy/min for conventional radiotherapy. Therefore, LPA could enable the study of the effect of extreme dose rates on ionizing radiation toxicity. Practically, this means that LPAs could be used to study the effect of the temporal fractionation of the dose on tissues [Bay+19] – to study how tumoral tissues react to the way the dose is deposited temporally. Such studies are motivated by the recently discovered FLASH effect [Fav+14], which shows that a very fast delivery (<500 ms) of therapeutic doses reduces the toxicity of healthy tissues while preserving the radiobiological effects on the tumor. Therefore, this project's ultra-compact electron source is a very promising tool for exploring innovative protocols for treating cancer.

Literature Review

Only a few kHz repetition rate LPAs are currently operational globally and have emerged recently. The leading kHz rate LPAs typically accelerate electrons within the energy range of 5-15 MeV [Gué+17; Hui+22; Sal+21], with some reaching up to 50 MeV [Laz+23]. The impressive stability exhibited during hands-off operation over a long period [Rov+20] stands a testament to the maturity of kHz LPA technology and its readiness for use in real-world applications. High repetition rate sources of electrons in the range of 10 MeV are excellent devices for radiobiology experiments of thin samples *in-vitro* [Cav+21].

However, they are unsuitable for irradiation of deep tissue, as is the case with cancer treatment in human adults. LPA experiments operating at 1 Hz have demonstrated that acceleration to energies of around 120 MeV provides electrons that deposit radiation doses at penetration depths of interest for electron beam radiotherapy of deep-seated tumors [Lun+12]. Thus, to bring the stability and high average dose rate advantages of kHz LPA machines to cancer therapy, a boost of around one order of magnitude in electron energy is required.

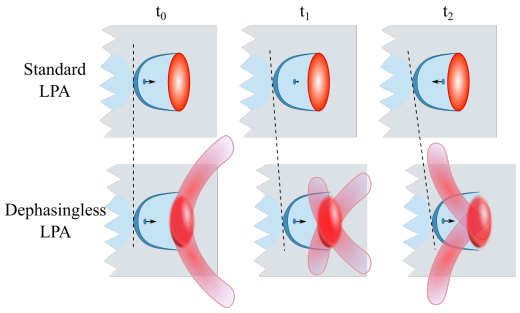

Figure 2: Top: Illustration of dephasing process LPA using a standard laser. Bottom: Illustration of dephasingless LPA with shaped laser. Arrows mark the acceleration direction of the electrons.

One of the processes which limit the maximal energy in LPAs is dephasing. In this process, trapped electrons reach the ion cavity's decelerating region in the cavity's forward part (Fig. 2: Top). It occurs because the laser group velocity in the plasma, and hence the cavity (or wakefield) velocity, are smaller than the electron beam velocity, which approaches (but never reaches) the speed of light.

I propose to mitigate the dephasing process by sculpting the laser in space and time along the focal depth. The laser front is shaped with special optics so that a focal spot "appears" due to constructive interference of the fronts coming from the sides (Fig. 2: Bottom). While the fronts have group velocities smaller than that of the electrons, the "appearance" velocity of the focal spot and hence the wake velocity could be matched with the velocity of the electrons. In this dephasingless LPA [Cai+20; Pal+20], electrons are accelerated during the whole process and gain much higher energy compared to standard LPA. According to a theoretical study [Cai+20], the expected electron energy for the project's laser parameters (3.4 fs, 2.5 mJ) is up to 200 MeV. This is an upper value with perfect beam shaping. Including possible optical aberrations, which cannot be corrected, and not having all freedom for shaping the laser in space and time, we will probably produce lower-energy electrons in the 50-100 MeV range.

Finally, this acceleration scheme can be combined with proven techniques for achieving high-quality mono-energetic bunches. Considering the practical and technical constraints, I propose developing a compact laser-plasma electron accelerator that delivers high-quality electrons up to 100 MeV at kHz. This significant energy gain would pave the way for groundbreaking tabletop experiments and applications benefiting cancer radiotherapy.

Problem Statement/Objectives

Main objective: Develop and obtain experimental proof-of-principle of a unique electron source that delivers high-quality mono-energetic electrons with energies up to 100 MeV at a kHz rate. The accelerator development will progress employing the following objectives, each covered by a Work Package (WP): WP1: Develop a theoretical foundation for dephasingless laser-plasma acceleration using few cycles, few mJ lasers at a kHz rate; WP2: Measure the intrinsic laser parameters and design an optical system for dephasingless acceleration, taking into account simulations/theory predictions (WP1); WP3: Design gas nozzles for the experiment considering simulations/theory predictions for the optimal density profiles. WP4: Ultimately obtain a working accelerator prototype, which delivers high-quality mono-energetic electrons with up to 100 MeV energy at a kHz rate.

Outline of tasks/Work Plan

To reach the desired kHz, 100 MeV monoenergetic electron source, three main components are required:

The laser which drives the acceleration of the electrons. The current research team and infrastructure at Laboratoire d'Optique Appliquée (France) possess expertise in developing and operating a TW-class laser system that delivers 2.5 mJ in 3.4 fs at kHz repetition rates [Oui+20]. This unique laser system, one of the few worldwide, is routinely used for kHz laser-plasma acceleration of stable electrons with MeV energy and picocoulomb charges. To achieve the desired pulse front curvature for dephasingless acceleration, I will implement a refractive beam shaper in the laser chain.

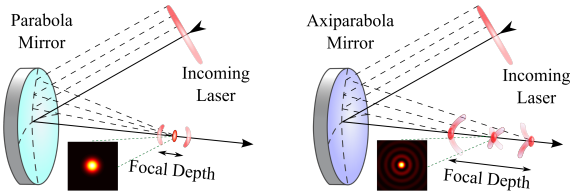

Figure 3: Left: Parabola mirror focuses rays to a single point, coupling spot size, and focal depth. Right: Axiparabola enables focusing rays from different radial positions to different focal planes, resulting in a small lateral spot and extended focal depth (quasi-Bessel beams).

The second ingredient needed to boost the energy of the electrons is a unique focusing optic that shapes the laser pulse at the focus to get more efficient acceleration. An ideal candidate is the aspherical reflective element known as the axiparabola (of which I am a co-inventor), which stretches the focal depth without increasing the lateral size of the beam [Sma+19; Oub+22]. This is done by generating quasi-Bessel beams, which are known for their diffraction-free features. The axiparabola effectively increases the acceleration length by focusing rays from different radial positions to different focal planes (Fig. 3: Right), while a standard parabolic mirror focuses all the rays to one point (Fig. 3: Left). The dynamics of the laser energy deposition on the optical axis are also critical, as the laser and trailing wake need to propagate at pace with the electrons in order to achieve efficient acceleration. The dynamics of the focal spot are controlled by manipulating the pulse front curvature before focusing on the axiparabola. With a curved front, the arrival time of different radial beam slices will be earlier than with a flat front, increasing the appearance velocity of the focal spot (Fig. 4). Together, this process is known as dephasingless acceleration. As shown in theoretical papers [Cai+20; Pal+20], the benefit of using such a method scales inversely with the pulse duration. Thus, significant energy gain is expected for the near-single-optical-cycle laser that will be used in this project. According to the theoretical models, we can expect up to 200 MeV electrons from the 2.5 mJ, 3.4 fs laser, while only 10-15 MeV have been achieved with standard parabolic focusing optics using a similar laser [Sal+21; Hui+22].

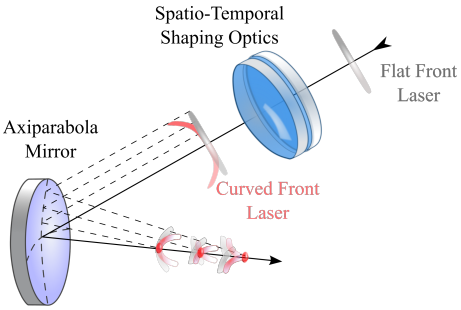

Figure 4: Spatiotemporal shaping optics initially transforms a flat (grey color) laser front to a curved one (rose color). It allows controlling the focal spot appearance velocity when used with an axiparabola. Curved fronts arrive faster to generate the necessary appearance velocity of the focal spot along the optical axis.

The final component of the project is the gas target. It is well known from LPA experiments that to achieve high-quality, monoenergetic electron beams; it is necessary to utilize controlled injection schemes. The main methods are (i) ionization injection which produces stable electrons with a broad spectrum (for the intermediate acceleration tests), and (ii) density gradient injection, which produces stable quasi-monoenergetic beams required for the ultimate goal of the project. Ionization injection is a relatively simple technique that requires only the installation of a particular gas mixture. Density gradient injection, meanwhile, requires precise shaping of the density of the gas target, achieved by specially designed supersonic nozzles. The group I work with has the expertise and academic collaborations to design and manufacture nozzles for the project [Rov+21].

The computational modeling for the WP1 phase will utilize Particle-in-Cell (PIC) simulations. In these simulations, the Maxwell equations for the electromagnetic field of the laser pulse are solved self-consistently with the equations of motion for macro-particles (ions and electrons) representing a large number of physical particles. First, I will introduce a quasi-Bessel laser beam into the code (M1.1). Then, I plan to introduce more complexity to the PIC simulation (M1.2) as the project progresses, bringing it closer to fully modeling the experimental conditions. The first simulation aims to obtain dephasingless acceleration in a uniform plasma. I will then model the plasma obtained from firing onto several standard supersonic nozzles (conical and slit nozzles), which I will use in the experiment (WP4). In parallel, I will work on a phenomenological theoretical model (M1.3), which will provide essential scalings (electron energy, charge, etc.) as a function of relevant input parameters of laser and plasma density.

To properly design the pulse shaping optics, I will measure the spectrally resolved wavefront of the experimental laser system (M2.1), using the recent technique I developed during my postdoc [Sma+24].

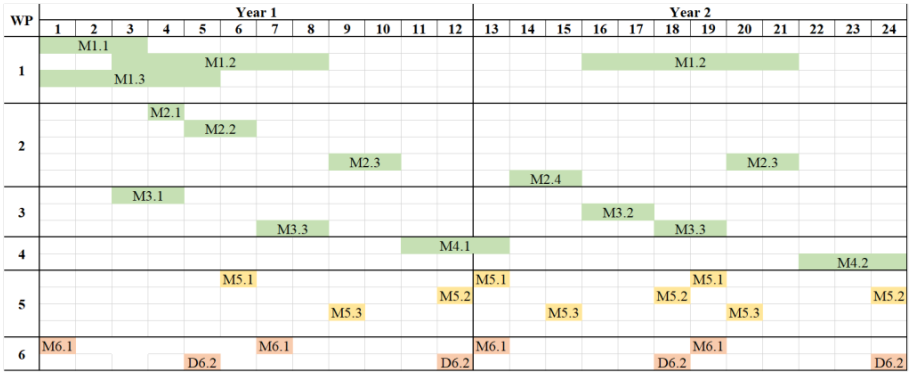

Figure 5: Gantt chart specifying the timing of the milestones (M) of the different work packages (WP), as well as the deliverables (D).

WP1	**Theory and simulations**
M1.1	Preparation for PIC simulations with shaped laser
M1.2	PIC simulations
M1.3	Analytical model development
WP2	**Optical design**
M2.1	Laser intrinsic properties measurements
M2.2	Optical design (spherical optics)
M2.3	Shaped beam measurement
M2.4	Optical design (aspherical/non-continous optics)
WP3	**Gas target design**
M3.1	Design a standard nozzle (conical or slit)
M3.2	Design a shock nozzle
M3.3	Interferometric gas/plasma density measurement
WP4	**Main experimental campaign**
M4.1	Phase-locked acceleration with spherical optics
M4.2	Phase-locked acceleration with **aspherical/non-continous** optics
WP5	**Exploration, dissemination and communication**
M5.1	Submit paper to Optica open-access journal
M5.2	Present results at Optica-organized symposium
M5.3	Lectures/workshops/seminars
WP6	**Project management**
M6.1	Meeting with the Optica Challenge Committee
D6.2	Progress report

Figure 6: Contents of the Work Packages, Milestones, and Deliverables.

Then using the OpticStudio ray tracing software, I will design an optical system that sculpts lasers in space and time (M2.2) as required by the simulations in WP1. The shaping optics consist of a spherical refractive doublet (or triplet) and the axiparabola. Experimentally, I will first measure the spatial properties of the axiparabola focal line by taking focal spot diagnostics at different points along the optical axis (M2.3). Using a spatiotemporal measurement technique [Sma+22] I developed in my doctorate, I will measure the energy distribution in space and its velocity over the interaction region in a vacuum (M2.4).

The gas target development is contained in WP3. The nozzles for the experiment will be designed using the computational hydrodynamic simulation software Ansys Fluent. First, I will design and manufacture standard conical and slit nozzles that provide nearly uniform axial density (M3.1). Then I will design more complicated, in terms of geometry, shocked nozzles (M3.2). For both cases, using an interferometric measurement device, I will measure the gas and plasma density of the nozzles that will be used in the experiment (M3.3).

The final experimental part of the project will be performed in ascending complexity during two primary campaigns. First, I will perform a dephasingless acceleration experiment with an axiparabola and a spherical refractive system using standard nozzles (M4.1). Then I will use a more advanced, aspheric refractive beam shaping system or non-continuous surface axiparabola (M4.2). Finally, in the same campaign, I will use a specially designed shock nozzle to accelerate and achieve a quasi-monoenergetic electronic beam (M4.2).

I emphasize the significance of communication and sharing of project outcomes. To address this, I have incorporated a specialized work package, WP5, which involves several activities. These include submitting papers to open-access journals, preferably Optica (M5.1), delivering lectures at Optica-organized symposiums (M5.2), as well as participating in other workshops and seminars (M5.3).

Lastly, the final work package, WP6, focuses on project management. This includes engaging in meetings with the Optica Challenge committee (M6.1) to provide updates on the project's progress and learn from the expertise of committee members. Regular progress reports (D6.2) will also be submitted to ensure effective project management.

Outcome(s)

In this project, I propose to develop a compact laser-plasma accelerator delivering very-high-energy electrons (up to 100 MeV electrons) at a kilo-Hertz (kHz) rate. I aim to increase the electron energy by

one order of magnitude compared to the current state-of-the-art kHz laser-plasma accelerators using the same driver-laser parameters.

Impact

Radiotherapy is one of the primary cancer treatments. The project will develop accelerators for more uniform and less toxic dose deposition radiotherapy sources. With current laser technology, the final size of this accelerator could be no larger than an optical table, making it cheap and accessible to many hospitals around the world. The technology developed in the project can also be used in many other societal applications. It includes medical and industrial screening with X-rays that are a secondary outcome of the acceleration and innovative sterilization in which fast electrons kill off all bacteria and parasites in food products or medical equipment but do not cause any harm to vital properties of the irradiated substance or package.

Particle accelerators are essential tools in modern science and technology. They are used in medical and commercial applications but also for scientific research. In this project, I will demonstrate a proof of concept of a compact electron accelerator. I will use intricate sculpting of laser pulses in space and time to boost the resultant electron energy to 100 MeV, one order of magnitude greater than the state-of-the-art LPAs operating at kHz rates. Once implemented, these compact and affordable accelerators and their associated technology will boost advances in biology, chemistry, and physics research.

References

[ESL09] E. Esarey, C. B. Schroeder, and W. P. Leemans. "Physics of laser-driven plasma-based electron accelerators". In: *Rev. Mod. Phys.* 81 (3 Aug. 2009), pp. 1229–1285.

[Lun+12] O. Lundh et al. "Comparison of measured with calculated dose distribution from a 120-MeV electron beam from a laser-plasma accelerator". In: *Medical Physics* 39.6Part1 (2012), pp. 3501–3508.

[Fav+14] V. Favaudon et al. "Ultrahigh dose-rate FLASH irradiation increases the differential response between normal and tumor tissue in mice". In: *Science Translational Medicine* 6.245 (2014), 245ra93–245ra93.

[Gué+17] D. Guénot et al. "Relativistic electron beams driven by kHz single-cycle light pulses". In: *Nature Photonics* 11.5 (May 2017), pp. 293–296.

[Bay+19] E. Bayart et al. "Fast dose fractionation using ultra-short laser accelerated proton pulses can increase cancer cell mortality, which relies on functional PARP1 protein". In: *Scientific Reports* 9.1 (July 2019), p. 10132.

[Sma+19] S. Smartsev et al. "Axiparabola: a long-focal-depth, high-resolution mirror for broadband high-intensity lasers". In: *Opt. Lett.* 44.14 (July 2019), pp. 3414–3417.

[Cai+20] C. Caizergues et al. "Phase-locked laser-wakefield electron acceleration". In: *Nature Photonics* 14.8 (Aug. 2020), pp. 475–479.

[Oui+20] M. Ouillé et al. "Relativistic-intensity near-single-cycle light waveforms at kHz repetition rate". In: *Light: Science & Applications* 9.1 (Mar. 2020), p. 47.

[Pal+20] J. P. Palastro et al. "Dephasingless Laser Wakefield Acceleration". In: *Phys. Rev. Lett.* 124 (13 Mar. 2020), p. 134802.

[Rov+20] L. Rovige et al. "Demonstration of stable long-term operation of a kilohertz laser-plasma accelerator". In: *Phys. Rev. Accel. Beams* 23 (9 Sept. 2020), p. 093401.

[Cav+21] M. Cavallone et al. "Dosimetric characterisation and application to radiation biology of a kHz laser-driven electron beam". In: *Applied Physics B* 127.4 (Mar. 2021), p. 57.

[Rov+21] L. Rovige et al. "Symmetric and asymmetric shocked gas jets for laser-plasma experiments". In: *Review of Scientific Instruments* 92.8 (Aug. 2021), p. 083302.

[Sal+21] F. Salehi et al. "Laser-Accelerated, Low-Divergence 15-MeV Quasimonoenergetic Electron Bunches at 1 kHz". In: *Phys. Rev. X* 11 (2 June 2021), p. 021055.

[Hui+22] J. Huijts et al. "Waveform Control of Relativistic Electron Dynamics in Laser-Plasma Acceleration". In: *Phys. Rev. X* 12 (1 Feb. 2022), p. 011036.

[Oub+22] K. Oubrerie et al. "Axiparabola: a new tool for high-intensity optics". In: *Journal of Optics* 24.4 (Mar. 2022), p. 045503.

[Sma+22] S. Smartsev et al. "Characterization of spatiotemporal couplings with far-field beamlet cross-correlation". In: *Journal of Optics* 24.11 (Oct. 2022), p. 115503.

[Laz+23] C. M. Lazzarini et al. *50 MeV electron beams accelerated by a terawatt scalable kHz laser*. 2023.

[Sma+24] S. Smartsev et al. "Simple few-shot method for spectrally resolving the wavefront of an ultrashort laser pulse". In: *Opt. Lett.* 49.8 (Apr. 2024), pp. 1900–1903.

Proposal Title: Revolutionizing Cancer Detection: Compact Fiber Technology for Machine-Learning Driven Endoscopic Hyperspectral Imaging

PI: Stephanos Yerolatsitis, Cyprus University of Technology, s.yerolatsitis@cut.ac.cy

Category: Health

Global Challenge: Cancer remains a leading cause of mortality and morbidity worldwide, with respiratory and gastrointestinal (GI) cancers, which can be detected optically, accounting for over 40% of all malignancies globally. Early detection of these cancers is critical as it significantly improves treatment outcomes, survival rates, and can even lead to full recovery. However, current early detection rates are low due to limitations in existing diagnostic tools, highlighting an urgent need for more accurate, accessible, and less invasive cancer-detecting methods.

Project Objective and Relationship to the Global Challenge: This proposal aims to address the critical global challenge of early cancer detection by developing an advanced endoscopic hyperspectral imaging platform using novel optical fiber technology. This innovation also aligns with the Optica Foundation Challenge by enhancing medical diagnostics and leveraging photonics to **advance biomedical imaging**, improving healthcare outcomes. By integrating machine learning algorithms with hyperspectral imaging, this project endeavors to provide a minimally-invasive, accurate diagnostic tool for early cancer detection in the respiratory and GI tracts.

Project Capability and Application: The primary objective is to develop a **thin, flexible, high-resolution fiber probe for endoscopic hyperspectral imaging** based on a novel photonic approach. This approach involves precisely engineering the geometry of the fiber probe and employing post-processing techniques to enhance the spectral working range. This will enable, for the first time, real-time, precise endoscopic tissue characterization across multiple wavelengths, facilitating early detection and classification of lung and GI cancers. This advancement will empower clinicians to detect cancer earlier and develop more effective treatment strategies based on cancer stage, classification, and response to treatment.

Key capabilities include:

- **Minimally-Invasive Diagnostics:** Developing a flexible, bespoke fiber probe with a diameter of less than 1 mm, capable of navigating complex anatomical regions with high resolution (less than 3 μm) and a field of view greater than 400 μm.
- **Enhanced Imaging and Classification:** Enabling, for the first time, endoscopic hyperspectral imaging (visible-to-NIR) combined with machine learning for real-time, high-accuracy cancer detection and classification through a novel photonic method that integrates multiple wavelengths simultaneously, exponentially increasing the amount of collected information.
- **Versatility and Integration:** Ensuring compatibility with existing endoscopic systems, enabling widespread clinical adoption.
- **Cost-Effective:** Developing reusable fiber probes that reduce costs.

Impact of the Award: The award will support collaboration with experts in the USA (CREOL, University of Central Florida), Cyprus (Cyprus University of Technology), and Germany (University Medicine Greifswald), facilitating the fabrication and testing of the advanced fiber technology required to validate this groundbreaking approach. The successful implementation of this project will revolutionize cancer diagnostics by providing clinicians with a powerful endoscopic tool for early detection and accurate characterization of cancer lesions. By pushing the boundaries of medical photonics, this project will also pave the way for future innovations in diagnostics and treatment, solidifying the role of optical technologies in modern healthcare.

Revolutionizing Cancer Detection: Compact Fiber Technology for Machine-Learning Driven Endoscopic Hyperspectral Imaging

Despite ongoing efforts to improve prevention, detection, and treatment, cancer remains a leading cause of mortality and morbidity worldwide. According to Globocan, there were almost 19.3 million new cancer cases and 10 million new deaths in 2020 alone [1]. Respiratory and gastrointestinal (GI) cancers, which can be detected optically, account for more than 40% of all malignancies in the world [1]. Early detection of these types of cancer can substantially improve treatment outcomes, survival rates, and even promote full recovery. For example, the five-year survival rate for early-stage lung cancer can be up to 62.8%, compared to less than 8.2% for advanced-stage lung cancer [2]. In the case of GI cancer, early diagnosis and endoscopic treatment can result in a 99% disease-specific five-year survival rate without the need for radiochemotherapy, while end-stage diagnosis is associated with a poor prognosis, with less than 10% of patients surviving beyond five years [3]. Unfortunately, early detection rates for both lung and GI cancer are very low, both in developed countries and areas with limited resources [4]. Therefore, there is a pressing need for the development of more accurate, approachable, and minimally invasive cancer-detecting methods. We aim to revolutionize diagnostic healthcare by developing a novel endoscopic optical fiber system to accurately diagnose and characterize early-stage cancer lesions with a particular focus on the respiratory and GI tracts.

Accurate cancer classification is crucial in understanding the behavior of cancer cells, predicting disease progression, guiding treatment decisions, and even enabling curation. Lung cancer comes with multiple subtypes, each with its unique genetic mutations and histological characteristics [5]. Low-dose CT scans, the current standard for lung cancer screening, are not foolproof and can result in significant false-negative outcomes, particularly in the early stages of the disease or in cases where nodules are small or located in difficult-to-image areas. Furthermore, similar challenges exist in the diagnosis and management of GI cancers, where diverse subtypes and intricate tumor biology necessitate improved diagnostic tools and treatment strategies to optimize patient care and outcomes. Although, fiber optic-based techniques, predominantly employed in GI cancers, offer endoscopists the ability to observe, biopsy, and perform therapeutic interventions, their large diameter and limited flexibility present challenges in reaching anatomically difficult-to-access areas. Additionally, as these fiber probes employ traditional RGB channels for imaging, they capture only a limited amount of information about the lesion's characteristics, frequently leading to misdiagnosis. Machine learning (ML) techniques are increasingly being applied to endoscopic imaging, promising to enhance diagnostic accuracy and refine treatment approaches in both respiratory and GI contexts. In this respect, commercial companies have taken initial steps to introduce ML algorithms, such as deep learning, to support endoscopists and improve diagnostic accuracy [6]. Despite these advancements, utilizing additional wavelengths of light can significantly aid in the detection and characterization of lesions.

Problem Statement: Our research proposal aims to revolutionize the field of cancer diagnosis by developing **an innovative platform for endoscopic hyperspectral imaging** based on **state-of-the-art optical fiber technology**. These next generation of endoscopic tools will provide a **minimally-invasive approach** to accurately diagnose and characterize early-stage cancer lesions with a particular focus on the respiratory and GI tracts, as shown in Figure 1. Additionally, our novel fiber technology enables the simultaneous collection of wavelengths outside the RGB channels, while the sub-millimeter fiber probe's size allows endoscopic access to remote locations, driving exponential change in precision with increased channels. By integrating **advanced ML algorithms**, our platform will enhance the diagnostic accuracy and characterization of lesions, leveraging the rich data obtained from hyperspectral imaging.

Figure 1: Conceptual illustration - sub-millimeter bespoke fiber-based platform designed to navigate endoscopically and examine suspected malignancy lesions.

Hyperspectral imaging is an advanced imaging technique that captures and processes information from a broad spectrum of wavelengths and offers intricate insights into the anatomical, chemical, and biological composition of tissue [7], [8], [9]. This enables the detection of subtle differences between cancerous and normal tissue that are not visible with conventional imaging methods, i.e. using only RGB channels. This technique can also be used for cancer classification [10]. Figure 2 illustrates an example that highlights the differences between hyperspectral and RGB imaging. Currently, there are no commercially available hyperspectral endoscopic imaging systems. Conventional endoscopic imaging fibers [11], which consist of thousands of cores where each core corresponds to a pixel on the camera, operate only within a limited range of wavelengths, thereby restricting their use primarily to RGB channels. Beyond the RGB range, the resolution of these multicore fibers rapidly degrades due to two distinct factors: increased core-to-core coupling at longer wavelengths, and the cores becoming large compared to the wavelength of the light at shorter wavelengths. Due to their limited operational wavelength range, conventional imaging fibers are not suitable for hyperspectral imaging. This limitation results in clinicians being unable to capture the full range of information for accurate tissue characterization.

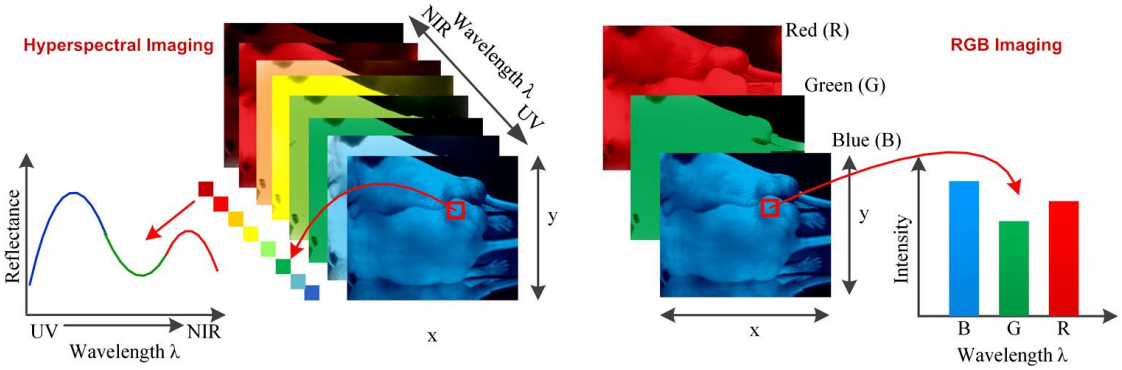

Figure 2: Comparison between hyperspectral and RGB imaging techniques. Hyperspectral imaging is a three-dimensional dataset of a two-dimensional image on each wavelength, spanning the UV to NIR spectrum. RGB image only has three image bands corresponding to red, green, and blue wavelengths. Adapted from B. Fei et al., [8] (CC-BY 4.0).

The main aim of the proposal is to develop innovative fiber technology to enhance the resolution capabilities of fiber bundles. This advancement will enable endoscopic hyperspectral imaging for the first time while ensuring the fiber's outer diameter remains compact and suitable for

endoscopic procedures. This technology will allow for the simultaneous acquisition of multiple wavelengths of light across the entire **visible and near-infrared spectrum**, facilitating real-time, accurate tissue characterization. The realization of this technology involves precisely engineering the geometry of the multicore fiber. Post-processing techniques, such as local tapering [12], [13], induce controlled coupling between the otherwise uncoupled fiber cores within selected regions of interest. When this tapered region is used as the input for the light, it transforms the phase and amplitude information of the input light from the sample into solely amplitude information at the output. By analyzing the relationship between the input light and the light distribution at the proximal end of the fiber bundle, we can reconstruct high-resolution images across a broad range of wavelengths using a reduced set of output data. This innovative approach serves as a form of computational imaging, where hyperspectral light from the distal sample is coupled into the fiber and then redistributed as intensities to the individual cores of the fiber bundle. Reconstructing an image becomes simpler when the phase of the light is not considered. Additionally, as the controllable coupling only occurs in a short region of the fiber—while the rest consists of uncoupled cores similar to a multicore fiber—the proposed fiber remains insensitive to performance changes due to bending. ML algorithms will be employed to analyze and train the fiber platform. This analysis is only required once; the trained model can then be applied to subsequent imaging procedures. Figure 3 illustrates a concept design of the platform.

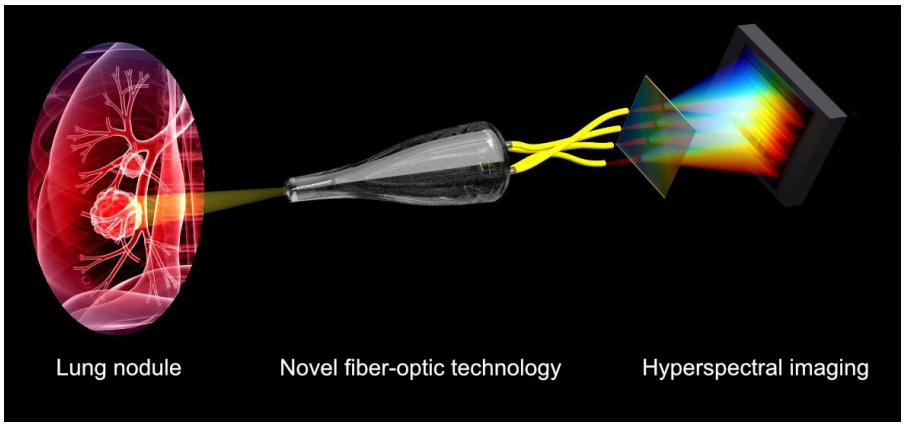

Figure 3: Concept design. By using novel fiber-optic technology combined with ML-driven hyperspectral imaging, we can inspect small nodules and those located in difficult-to-image areas. This approach will revolutionize early cancer detection

Given the principal investigator's (PI) expertise in fiber fabrication and post-processing [13] and biomedical device development and testing [14], this proposal has three main **aims**:

1. Fabricate and post-process the proposed fiber.
2. Use ML algorithms and a labeled data approach, to train the fiber bundle.
3. Validate its performance using biological samples.

We will initially conduct high-fidelity simulations to determine the optimal fiber geometry for our application. This process will specify the number and position of the cores, influencing the **final diameter** of the multicore fiber probe (<1 mm), its **field of view** (>400 μm), and its achievable **resolution** (<3 μm). To fabricate the fiber, I will collaborate with experts at the University of Central Florida (UCF) and visit their facilities for development (**Aim 1**). Given its proposed outer diameter, this novel fiber probe will be highly flexible and significantly thinner—**at least four times smaller than current technologies**—making it ideal for examining lesions in hard-to-reach locations and seamlessly integrating with other fiber technologies, thereby increasing its potential uses. To examine the lesion of interest, the proposed fiber probe can be inserted through a scope's working channel or a needle, making it versatile and suitable for use in a variety of clinical settings. For real-time hyperspectral imaging, we can use a diffraction grating to disperse the light from the individual proximal fiber cores and collect multiple wavelengths simultaneously with a high-

resolution camera. Combining the information from all the collected wavelengths of light allows for the reconstruction of a real-time high-resolution 3D image. An experimental system will be developed at the Cyprus University of Technology (CUT). In addition, any post-processing of the fiber probe will also be performed at CUT. In collaboration with experts at CUT, we will deploy ML algorithms to train the model (**Aim 2**). Finally, in collaboration with experts at the University Medicine Greifswald, we will validate the fiber probe using biological samples (**Aim 3**).

Impact: We envision a fiber-based optical system that not only provides clinicians with real-time imaging but also leverages actionable outcomes from ML algorithms (such as deep learning or YOLO [10]) to identify and label abnormal areas. This technology can be combined with optical and/or chemical dyes, enabling the visualization of specific cellular structures or molecular targets, such as cancer biomarkers [15]. By overlaying the information emitted by the dyes, which is typically in a different set of wavelengths compared to the tissue response, onto the reconstructed 3D image, we can take full advantage of our system's capabilities and obtain even more comprehensive information about the targeted area. Depending on the application, these chemical dyes can be administered via the endoscope, injected into the targeted area, or inhaled to target non-invasively specific lung areas. This groundbreaking fiber-based platform offers a vast amount of information and represents a significant advancement in technology, as there are currently no commercially available endoscopic probes that offer similar capabilities.

This cutting-edge fiber-based system can revolutionize lung and gastrointestinal (GI) cancer detection and treatment. Its ability to detect cancer earlier, especially in hard-to-reach areas, has immense potential for improving patient outcomes. By accurately diagnosing and characterizing early-stage cancer lesions, this platform can empower clinicians to develop more effective treatment strategies based on the cancer stage and classification. In addition, its real-time imaging and ML algorithms will offer quick and precise diagnoses, significantly reducing the time needed for diagnosis and treatment. The platform can provide two significant advantages over existing technologies: it can reduce the risk of false-negative outcomes and can decrease significantly the need for unnecessary biopsies by enabling targeted sampling of the region of interest. The probe can also be used before or during surgery or endoscopic intervention to identify the margins of a tumor or lesion. It is important to highlight that these novel fiber-based probes can be sterilized and reused, making them more cost-effective. Furthermore, this platform can be used in an outpatient setting, reducing the need for hospitalization and costly procedures. The minimally invasive nature of the fiber probe will enable clinicians to re-examine cancer lesions during therapy, providing real-time feedback on the efficacy of the treatment and guiding decision-making. Integrating hyperspectral and time-of-flight imaging techniques allows the reconstruction of hyperspectral 3D images that contain spectral information at different depths [16]. This capability would be valuable for clinicians as it would facilitate the identification of cancer margins.

This proposal focuses on cancer detection in the respiratory and GI tracts. The miniaturization of the proposed fiber probe can readily extend this technology to the examination of other types of cancer, including those located in challenging-to-access regions, such as the bile duct and pancreatic duct, one of the most malignant tumors. Its versatility and ability to integrate seamlessly with other fiber technologies make this platform a game-changer in cancer detection and treatment, with the potential to **transform the way we approach cancer care.**

Outcomes: In this proposal, we will fabricate and post-process the proposed fiber to establish the optimal geometry and post-processing optimization. We then envision training the fiber bundle using ML algorithms using a labelled data approach, and finally validating its performance using a biological sample. This validation will be the basis for future **ex-vivo tests** followed by **in-patient studies**. The award of this prize will grant the PI the necessary time, funds, and freedom to

validate this concept taking hyperspectral imaging to the pinnacle of practical and usable imaging technology. This award will also broaden the PI's research network through travel to key collaborators. This aspect is vital to the proposal, as completing certain parts of the project requires travel to the USA (for fiber fabrication) and Germany (for testing the fiber on a biological sample). The unique flexibility of this prize's funding offers an unmatched opportunity to complete this research, which other funding sources cannot guarantee. Furthermore, this prize will enable the PI to enhance his skills and expertise in emerging areas of photonics. Additionally, this award will support this critical initial demonstration, enabling the exploitation of this technology either by applying for further grants and/or creating a start-up company. The global market for endoscopic diagnostic tools is substantial and growing, with the endoscopic devices market projected to reach $37.63 billion in 2024 and $51.7 billion by 2029 [17]. With a clear plan for validation, commercialization, and funding, we are confident in the potential of our platform to make a significant impact in the field of medical diagnostics, as outlined in Table 1.

Table 1: Scientific, Economic and Societal Outcomes

Scientific Outcomes	
Sci1. Advancements in Medical Imaging	• Development of new advanced photonic technologies in medical imaging • Enabling endoscopic hyperspectral imaging for the first time • Enhanced understanding of cancer biology and progression
Sci2. Novel Fiber Optic Development	• Exploring new ways to control the behavior of light • Developing new diagnostic and therapeutic tools
Economic Outcomes	
Eco1. Market Potential and IP Generation	• Creation of new IP and patents • Significant market potential for a startup company in medical diagnostics and treatment technologies
Eco2. Cost Savings in Healthcare & Efficient Resource Utilization	• Lower overall healthcare costs due to earlier diagnosis and treatment monitoring using this fiber probe • Improved patient management and treatment outcomes
Societal outcomes	
Soc1. Enhanced Early Cancer Detection	• Increased survival rates due to early diagnosis • Improved patient quality of life through less invasive procedures
Soc2. Wider Access to Advanced Diagnostics	• Greater access to high-quality diagnostics • Reduced healthcare disparities

This research proposal proposes the development of a cutting-edge platform for endoscopic hyperspectral imaging based on state-of-the-art optical fiber technology, which will revolutionize the field of cancer detection. Hyperspectral imaging offers intricate insights into the tissue's chemical and structural composition, enabling the detection of subtle differences between cancerous and normal tissue that are not visible with conventional imaging methods. Our platform can provide high-resolution 3D images with ML techniques for real-time cancer detection and classification. The reduced size and high flexibility of our fiber probe make it ideal for examining lesions in hard-to-reach locations and enable seamless integration with other fiber technologies, increasing its potential uses. In addition to its diagnostic benefits, the fiber-based platform we are developing has the potential to be more cost-effective than traditional diagnostic methods. This research proposal has the potential to revolutionize cancer diagnosis, paving the way for earlier and more precise detection and thereby improving treatment outcomes for cancer patients. We are confident that this innovative approach, coupled with the cutting-edge technologies we employ, **will transform the field of medical diagnostics and contribute significantly to the fight against cancer.**

References:

[1] J. Ferlay *et al.*, “Cancer statistics for the year 2020: An overview,” *International Journal of Cancer*, vol. 149, no. 4, pp. 778–789, 2021, doi: 10.1002/ijc.33588.

[2] “Cancer of the Lung and Bronchus - Cancer Stat Facts,” SEER. Accessed: Apr. 29, 2024. [Online]. Available: https://seer.cancer.gov/statfacts/html/lungb.html

[3] H. Suzuki *et al.*, “High rate of 5-year survival among patients with early gastric cancer undergoing curative endoscopic submucosal dissection,” *Gastric Cancer*, vol. 19, no. 1, pp. 198–205, Jan. 2016, doi: 10.1007/s10120-015-0469-0.

[4] N. Hawkes, “Cancer survival data emphasise importance of early diagnosis,” *BMJ*, vol. 364, p. l408, Jan. 2019, doi: 10.1136/bmj.l408.

[5] W. D. Travis, “Pathology of Lung Cancer,” *Clinics in Chest Medicine*, vol. 32, no. 4, pp. 669–692, Dec. 2011, doi: 10.1016/j.ccm.2011.08.005.

[6] “Endoscopy CAD system | ENDO-AID | Welcome to the AI Future in Endoscopy.” Accessed: May 20, 2024. [Online]. Available: https://www.olympus.co.uk/medical/en/Products-and-solutions/Products/Product/ENDO-AID.html

[7] M. Halicek, H. Fabelo, S. Ortega, G. M. Callico, and B. Fei, “In-Vivo and Ex-Vivo Tissue Analysis through Hyperspectral Imaging Techniques: Revealing the Invisible Features of Cancer,” *Cancers (Basel)*, vol. 11, no. 6, p. 756, May 2019, doi: 10.3390/cancers11060756.

[8] B. Fei *et al.*, “Label-free reflectance hyperspectral imaging for tumor margin assessment: a pilot study on surgical specimens of cancer patients,” *J Biomed Opt*, vol. 22, no. 8, p. 086009, Aug. 2017, doi: 10.1117/1.JBO.22.8.086009.

[9] G. Lu and B. Fei, “Medical hyperspectral imaging: a review,” *JBO*, vol. 19, no. 1, p. 010901, Jan. 2014, doi: 10.1117/1.JBO.19.1.010901.

[10] H.-Y. Huang, Y.-P. Hsiao, A. Mukundan, Y.-M. Tsao, W.-Y. Chang, and H.-C. Wang, “Classification of Skin Cancer Using Novel Hyperspectral Imaging Engineering via YOLOv5,” *Journal of Clinical Medicine*, vol. 12, no. 3, Art. no. 3, Jan. 2023, doi: 10.3390/jcm12031134.

[11] J. M. Stone, H. a. C. Wood, K. Harrington, and T. A. Birks, “Low index contrast imaging fibers,” *Opt. Lett., OL*, vol. 42, no. 8, pp. 1484–1487, Apr. 2017, doi: 10.1364/OL.42.001484.

[12] D. Choudhury *et al.*, “Computational optical imaging with a photonic lantern,” *Nat Commun*, vol. 11, no. 1, p. 5217, Oct. 2020, doi: 10.1038/s41467-020-18818-6.

[13] T. A. Birks, I. Gris-Sánchez, S. Yerolatsitis, S. G. Leon-Saval, and R. R. Thomson, “The photonic lantern,” *Adv. Opt. Photon., AOP*, vol. 7, no. 2, pp. 107–167, Jun. 2015, doi: 10.1364/AOP.7.000107.

[14] “Sub millimetre flexible fibre probe for background and fluorescence free Raman spectroscopy - Yerolatsitis - 2021 - Journal of Biophotonics - Wiley Online Library.” Accessed: Jan. 05, 2024. [Online]. Available: https://onlinelibrary.wiley.com/doi/full/10.1002/jbio.202000488

[15] Y. Zhang, G. Zhang, Z. Zeng, and K. Pu, “Activatable molecular probes for fluorescence-guided surgery, endoscopy and tissue biopsy,” *Chem. Soc. Rev.*, vol. 51, no. 2, pp. 566–593, Jan. 2022, doi: 10.1039/D1CS00525A.

[16] A. D. Griffiths *et al.*, “Multispectral time-of-flight imaging using light-emitting diodes,” *Opt. Express, OE*, vol. 27, no. 24, pp. 35485–35498, Nov. 2019, doi: 10.1364/OE.27.035485.

[17] “Endoscopy Devices Market - Size, Share & Growth Trends.” Accessed: May 20, 2024. [Online]. Available: https://www.mordorintelligence.com/industry-reports/global-endoscopy-devices-market-industry

Ultra-fast 3D-image-based cell sorting based on photonic computing

Category: Health & Information

Abstract: There is a growing global demand for high-throughput, high-resolution, and affordable cell sorting technology in biomedical research and healthcare settings. However, current technologies, which use digital image processing methods, are hampered by tradeoffs between speed and resolution. Optical processing can extract pertinent image information without capturing the full digital image, thus circumventing the fundamental speed limit imposed by digital processing. We aim to leverage this unique advantage to develop an optical-computing-based cell sorter that can analyze multimodal morphological information faster and more cost-effectively than traditional methods. This is especially crucial for applications that require real-time feedback, high-volume screening, or high sensitivity to rare cell types, such as tissue biopsies and early cancer detection. Our proposal aims to address the challenge of improving point-of-care diagnostics and surgical outcomes through developing high-speed, high-sensitivity, artificial intelligence (AI)-powered biosensors based on cutting-edge research of optical computing.

Background: Recent advancements in photonic computing have sparked strong interest in exploring their real-world applications. Originally developed as a special-purpose analog computing platform, photonic processors excel at processing machine-learning data, especially for signals that already exist in the optical domain. When used as computational image sensors, these optical processors can nonlinearly compress images even before any light detection or signal digitization. This unique advantage of optical processing – analyzing image data without capturing the image – allows optical processors to surpass digital image processing in its fundamental limit in latency and throughput.

Processing images in the optical domain offers tremendous opportunities for biomedical imaging, where traditional techniques often encounter significant data bottlenecks from processing vast volumes of image data. By bypassing these bottlenecks, optical processors have the potential to push the boundaries of the efficiency, speed, and sensitivity of high-throughput biomedical assays, making them especially suitable for applications that require real-time feedback, such as point-of-care diagnostics and surgical operations.

Problem Statement: In this proposal, **we aim to address the challenge of improving the speed and quality of point-of-care diagnostics and surgical operations by developing a high-sensitivity AI-enhanced biosensor**, **empowered by the latest advancements in optical information processing**. We focus on a specific type of biosensor, flow cytometry cell sorters, which are widely applied in both fundamental biomedical research and clinical surgical operations. Traditional fluorescence-activated cell sorting technologies, while reliable, capture limited information about cell morphology. State-of-the-art image-based cell sorting (ICS) technologies offer improved morphological insights but are hampered by a fundamental trade-off between speed and resolution. In other words, despite the great demand for more precise cell sorters, these ICS systems are not fast enough and tend to be expensive. The primary goal of this proposal is to develop an ICS system that leverages nonlinear optical pre-processing to enable ultra-fast, high-resolution cell sorting without the need to capture full-resolution images.

Outcomes and Impacts: The proposed system will utilize a nonlinear multilayer optical neural network as its core technology, enabling direct operation on the light field scattered or fluorescence signals emitted by cells. The novelty of our approach is to use optical processing as the primary means to carry out AI algorithms for cell morphology analysis. This approach allows for substantial improvements in speed and resolution over existing ICS technologies. We aim to develop a platform capable of analyzing high-resolution, three-dimensional, and multi-modality image information, including fluorescence and label-free phase imaging. The system will be able to sort cells based on morphology at speeds exceeding 100 kHz, with a correspondingly low latency, which represents 10-100x speed improvement compared to current state-of-the-art ICS systems. The successful development of this novel ICS system will have a profound impact on both clinical diagnostics and biomedical research, and will be transformative in applications such as immunotherapies, tissue biopsies, and early cancer diagnosis.

Ultra-fast 3D-image-based cell sorting based on photonic computing

Literature Review

Recent advancements in photonic computing [1-7] have sparked excitement in their real-world applications. Originally developed as a special-purpose analog computing platform, photonic processors excel in their ability to process machine-learning data, especially for signals that already exist in the optical domain. When used as computational image sensors, these optical processors can nonlinearly compress images even before any light detection or signal digitization [8]. This unique advantage of optical processing advantage [9] – analyzing image data without capturing the image – allows optical processors to surpass digital image processing in latency and throughput.

The ability to process images in the optical domain is particularly promising for biomedical imaging, where traditional techniques often encounter significant data processing bottlenecks due to vast volumes of image data. By bypassing these bottlenecks, optical processors have the potential to push the boundaries of the efficiency, speed, and sensitivity of high-throughput biomedical assays, making them especially suitable for applications that require real-time feedback, such as point-of-care diagnostics and surgical operation.

In this proposal, we focus on developing a computational image sensor for image-based cell sorting (ICS) in flow cytometry, a technique with broad applications in both fundamental biomedical research [10] and clinical diagnostics [11]. Cell sorting is a perfect use case for optical processing: in a typical experiment, cells moving in a flow channel need to be classified at ~1-ms latency and a throughput rate of 100,000 cells per second, generating gigabytes of data per second if they are imaged. Traditional fluorescence-activated cell sorting technologies, while reliable, capture limited information about cell morphology. This limitation is a significant barrier in applications involving phenotypic heterogeneity, cell cycles, and the detection of rare cell types. Current ICS technologies offer improved morphological insights but are hampered by a fundamental trade-off between speed and resolution. This proposal builds upon the foundational work in nonlinear optical processing by our group and peers [8, 13-15], and aims to overcome the limitations of traditional ICS techniques by applying new techniques from optical computing.

Problem Statement/Objective

There is a growing global demand for high-throughput, high-resolution, and affordable cell sorting technology in biomedical research and healthcare settings. However, current technologies, which use digital image processing methods, are hampered by tradeoffs between speed and resolution. In this proposal, **we aim to address the challenge of improving the speed and quality of point-of-care diagnostics and surgical operations by developing a high-sensitivity artificial intelligence-enhanced biosensor**, **empowered by the latest advancements in optical information processing**.

The primary objective of this proposal is to develop an ICS system that leverages nonlinear optical pre-processing to enable ultra-fast, high-resolution cell sorting without the need to capture full-resolution images. This addresses the Health and Information categories of the Optica Foundation Challenge to develop new, innovative and more efficient technology solutions for the medical community.

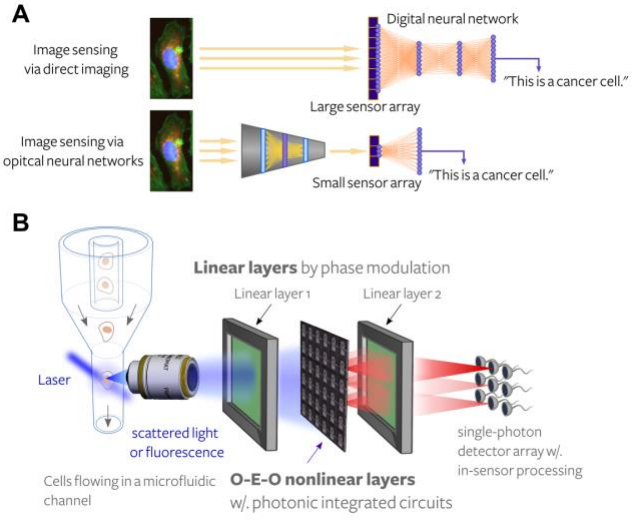

Figure 1. A nonlinear optical image sensor as an ultra-fast image-based cell sorter. (A) Illustration of how optical pre-processing helps to circumvent the information bottleneck commonly encountered in image sensing. (B) Drawing of a cell sorting device based on nonlinear optical processing of light field scattered off the cell.

In traditional ICS, cells are digitally imaged and then classified based on shape and structure (Figure 1A, top). This process presents several challenges for high-speed operations. Regardless of the image formation method, there is a fundamental trade-off between the signal-to-noise ratio and acquisition speed (exposure time) of the image. This becomes particularly problematic when trying to capture high-resolution images at a high speed. Moreover, these high-resolution digital images require a significant amount of digital electronic resources for storing, transporting, and processing of the data, which in turn puts a practical limit on how fast the cells can be classified. Additionally, imaging fast-moving cells in a flow channel often requires sophisticated imaging techniques [16-18], high-speed detectors, and complex post-processing methods. These requirements significantly increase both the complexity and the cost of ICS systems.

To address the problems encountered by conventional ICS systems, we propose removing the need to acquire any digital image. Instead, we will use optical operations to directly process the light field emitted or scattered from cell bodies to extract their morphological features. These features can be read out as the light intensity incident on a small array of fast photodetectors (Figure 1A, bottom). Our prior works have shown that with a nonlinear optical neural network, it is possible to reduce the dimension of cell images by 400 times in the optical domain, while still preserving competitive cell classification accuracy. Based on this principle, optical processing can bypass the bandwidth and signal-to-noise limitations inherent to traditional imaging schemes, thus providing a more efficient method to sort cells based on their morphological features. In addition, the high image compression ratio further allows us to classify cells based on their 3D morphology, which far exceeds the bandwidth limit of naïve imaging schemes, thus elimintating the ambiguity caused by 2D cell images. For example, certain types of cell organelles look similar when projected to a 2D image [10], and it may be helpful to image them from multiple perspectives to better distinguish between them. Being able to better identify and distinguish between types of cell organelles can have important clinical implications, such as identifying rare cells, or measuring responses to drug treatment. In addition, the proposed ICS system based on optical computing will also redcue the engineering cost compared to state-of-the-art ICS systems. While the complexity of optical setups will remain similar, we propose to use optical operations to offload computation from digital image processors, thus significantly reducing the size, and more importantly, the cost of photodetector arrays and digital processors for on-demand image processing.

Outcome(s)

The proposed system will utilize a nonlinear multilayer optical neural network [8] as its core technology, enabling direct operation on the light field scattered or fluorescence signals emitted by cells. This approach allows for substantial improvements in speed and resolution over existing ICS technologies. While the principle of optical processing remains the similar as our foundational work [8], we will adopt a brand-new design that is more compact, scalable, and better tailored to the specific needs of cell sorters (for example, to optimize the design of the systems to better accommodate the geometry of flow channels and the typical size of the cells). The outcome of this project will be a prototype ICS system capable of:

- Sorting cells based on morphology at speeds exceeding 100 kHz, significantly faster than current state-of-the-art ICS systems.
- Achieving high-resolution 3D and multi-modality imaging, including fluorescence and label-free phase imaging.
- Demonstrating superior precision in cell sorting, including the ability to identify rare or previously unrecognized cell types.
- Besides using more traditional technologies, such as liquid-crystal based spatial light modulators and free-form optics, we plan to use our platform as a testbed for emerging technologies, such as custom designed metasurfaces for hyperspectral image sensing, and integrated photonic chips for real-time near sensor processing.

Based on the technical specifications described above, we plan to demonstrate the utilities of this new technology in a broad array of biomedical applications, with suitable collaborators. For example, we will work with collaborators at Max Planck Institute to apply the high precision and throughput rate of our invention to improve tumor excision surgeries. Our improved ICS system will enable us to ensure sufficient margins around tumor resection sites by rapidly classifying cells dissociated from tissue biopsies and detecting the presence of rare, or even unrecognized cell types, which could indicate trace amounts of cancer cells. By achieving an event rate exceeding 100 kHz, we will be able to screen tissue 100 times faster than existing technologies [11]. Speed enhancement is crucial for this application since it allows real-time point-of-care feedback to surgeons to improve surgical outcomes.

Impacts

The successful development of this ICS system will have a profound impact on both clinical diagnostics and biomedical research. Clinically, it will enable rapid, label-free, and real-time examination of tissue margins during tumor removal surgeries, substantially improving patient care by reducing procedure times and increasing the accuracy of cancer detection. In the broader context of biomedical research, the system will enhance capabilities in single-cell sequencing, immunotherapy, and the early detection of cancer or rare cells in blood samples, among other applications. By providing access to detailed 3D morphological data at unprecedented speeds, this technology has the potential to catalyze significant advancements across multiple fields of study and application.

Timeline and Work Plan

Year 2024:

- **Q1-Q2:** Develop a software pipeline for simulating light diffraction and *in silico* training of the optical-computing-based cell sorter (**Aim 1**)
    - Simulation of multiple scattering of light field across a 3D cell volume of inhomogeneous refractive index with a differentiable physical model.
    - Simulation of the training of optical hardware with backpropagation.
    - Benchmark the performance of the trained system against linear optical classifiers to show the merit of nonlinear optical processing.
- **Q3-Q4:** Design, construct, and test the optical setup of the cell sorter (**Aim 2**)

Year 2025:

- **Q1-Q2:** Investigation of different methods for *in situ* training of the optical setup [19-21] (**Aim 3**).
    - Develop training methods that will allow the cell sorter to adapt to different cell types and applications, and potentially investigate on unsupervised learning methods for recognizing rare cell types.
- **Q3-Q4:** Real-cell sorting experiments in flow channels (**Aim 4**).
    - Demonstrate the capacity in biologically/clinically relevant studies in collaboration with collaborators at Max Planck Institute.

References

[1] Wetzstein, G., Ozcan, A., Gigan, S., Fan, S., Englund, D., Soljačić, M., ... & Psaltis, D. Inference in artificial intelligence with deep optics and photonics. Nature 588, 39-47 (2020).

[2] Xu, X., Tan, M., Corcoran, B., Wu, J., Boes, A., Nguyen, T. G., ... & Moss, D. J. 11 TOPS photonic convolutional accelerator for optical neural networks. *Nature* **589**, 44-51 (2021).

[3] Feldmann, J., Youngblood, N., Karpov, M., Gehring, H., Li, X., Stappers, M., ... & Bhaskaran, H. Parallel convolutional processing using an integrated photonic tensor core. *Nature* 589, 52-58 (2021).

[4] Huang, C., Fujisawa, S., de Lima, T. F., Tait, A. N., Blow, E. C., Tian, Y., ... & Prucnal, P. R. A silicon photonic–electronic neural network for fibre nonlinearity compensation. *Nature Electronics* **4**, 837-844 (2021).

[5] Ashtiani, F., Geers, A. J., & Aflatouni, F. An on-chip photonic deep neural network for image classification. *Nature* **606**, 501-506 (2022).

[6] Chen, Z., Sludds, A., Davis III, R., Christen, I., Bernstein, L., Ateshian, L., ... & Englund, D. Deep learning with coherent VCSEL neural networks. *Nature Photonics* **17**, 723-730 (2023).

[7] Xu, Z., Zhou, T., Ma, M., Deng, C., Dai, Q., & Fang, L. Large-scale photonic chiplet Taichi empowers 160-TOPS/W artificial general intelligence. *Science* **384**, 202-209 (2024).

[8] Wang, T., Sohoni, M. M., Wright, L. G., Stein, M. M., Ma, S. Y., Onodera, T., ... & McMahon, P. L. Image sensing with multilayer nonlinear optical neural networks. *Nature Photonics* **17**, 408-415 (2023).

[9] McMahon, P. L. The physics of optical computing. *Nature Reviews Physics* **5**, 717-734 (2023).

[10] Schraivogel, D., Kuhn, T. M., Rauscher, B., Rodríguez-Martínez, M., Paulsen, M., Owsley, K., ... & Steinmetz, L. M. High-speed fluorescence image–enabled cell sorting. *Science* **375**, 315-320 (2022).

[11] Soteriou, D., Kubánková, M., Schweitzer, C., López-Posadas, R., Pradhan, R., Thoma, O. M., ... & Guck, J. Rapid single-cell physical phenotyping of mechanically dissociated tissue biopsies. *Nature Biomedical Engineering* **7**, 1392-1403 (2023).

[12] Israel, Y., Reynolds, J. L., Klopfer, B. B., & Kasevich, M. A. Continuous wave multi-pass imaging flow cytometry. *Optica* **10**, 491-496 (2023).

[13] Yildirim, M., Dinc, N. U., Oguz, I., Psaltis, D., & Moser, C. Nonlinear Processing with Linear Optics. *arXiv preprint:2307.08533* (2023).

[14] Xia, F., Kim, K., Eliezer, Y., Shaughnessy, L., Gigan, S., & Cao, H. Deep Learning with Passive Optical Nonlinear Mapping. *arXiv preprint:2307.08558* (2023).

[15] Wang, H., Hu, J., Baek, Y., Tsuchiyama, K., Joly, M., Liu, Q., & Gigan, S. Optical next generation reservoir computing. *arXiv preprint: 2404.07857* (2024).

[16] Lei, C., Kobayashi, H., Wu, Y., Li, M., Isozaki, A., Yasumoto, A., ... & Goda, K. High-throughput imaging flow cytometry by optofluidic time-stretch microscopy. *Nature protocols* **13**, 1603-1631 (2018).

[17] Li, Y., Mahjoubfar, A., Chen, C. L., Niazi, K. R., Pei, L., & Jalali, B. Deep cytometry: deep learning with real-time inference in cell sorting and flow cytometry. *Scientific reports* 9, 11088 (2018).

[18] Wu, J. L., Xu, Y. Q., Xu, J. J., Wei, X. M., Chan, A., Tang, A. H., ... & Tsia, K. K. Ultrafast laser-scanning time-stretch imaging at visible wavelengths. *Light: Science & Applications* **6**, e16196-e16196 (2017).

[19] Wright, L. G., Onodera, T., Stein, M. M., Wang, T., Schachter, D. T., Hu, Z., & McMahon, P. L. Deep physical neural networks trained with backpropagation. *Nature* **601**, 549-555 (2022).

[20] Momeni, A., Rahmani, B., Malléjac, M., Del Hougne, P., & Fleury, R. Backpropagation-free training of deep physical neural networks. *Science* **382**, 1297-1303 (2023).

[21] Bandyopadhyay, S., Sludds, A., Krastanov, S., Hamerly, R., Harris, N., Bunandar, D., ... & Englund, D. Single chip photonic deep neural network with accelerated training. *arXiv preprint:* 2208.01623 (2022).

Executive Summary: Advancing toward precision medicine approaches in biomedical imaging using label-free microscopy, spatial -omics, and artificial intelligence (Health)

The Challenge: Recent years have seen the explosion of "precision medicine" techniques in healthcare – approaches that tailor treatment and management of disease to individual patient's genetic makeup, environmental exposures, and lifestyle. These methods are particularly valuable in the context of cancer, which can be a highly heterogeneous disease with different phenotypes, each of which may call for a completely different treatment strategy. Cancer is undisputedly a major global health challenge: it is one of the leading worldwide causes of death and over 40% of the human population is estimated to develop cancer in their lifetime. Utilizing precision medicine techniques to tailor cancer treatment has enabled significantly increased survival and quality of life for cancer patients. However, without tools to effectively identify and classify cancer phenotypes, the promise of precision medicine is left unrealized - both patients and clinicians are left with few treatment options, having to fall back to general surgery and/or chemotherapy, which can carry significant mortality and morbidity. Unfortunately, while precision medicine approaches for treatment and drug screening have advanced, methods for identifying disease phenotypes have lagged, relying on extremely costly assays of molecular biomarkers, various histopathological analyses, or -omic sequencing. Therefore, until the development of more accessible techniques for patient-specific disease classification and subtyping, the significant advancements in precision medicine for therapeutics will be unrealized for much of the global population. ***The challenge we propose to address is the need for rapid, inexpensive, tumor phenotyping and label-free staining.*** Successfully developing this approach could bridge the gap to implementing precision medicine therapeutics in global populations, impacting millions, while simultaneously enhancing gold standard technologies in pathology.

Proposed Project (Health Category): The main objective of this project is to develop a novel approach using label-free microscopy, spatial -omics, and artificial intelligence to enable rapid, inexpensive, and accurate estimation of clinically relevant biomarkers. This main objective directly leads to two impactful downstream applications: (1) to enable point-of-care disease phenotyping for patient-specific diagnostics, and (2) to enhance pathology techniques by providing "label-free staining" and spatial mapping of biochemical markers. While biomedical image classification for disease detection is a common area of research, the field has yet to develop robust and generalizable methods for more nuanced classification challenges such as phenotyping. Our group has demonstrated that co-registering genetic sequencing information with label-free imaging modalities can be used to effectively subtype tissues *at a similar level of accuracy to sequencing*, but without the high cost or lengthy experimental time required for -omic experiments. We have also shown that utilizing this data alongside artificial intelligence methods can also be used for spatially mapping gene expression markers using label-free imaging alone, suggesting that *this methodology could be an effective approach to "label-free staining" of tissues* – utilizing optical microscopy methods as a proxy to histopathological staining. While other works have also investigated artificial intelligence for label-free staining, this has so far been limited to labeling tissues for individual proteins or general chromogenic stains such as Hematoxylin and Eosin, which only captures a small piece of information about the tissue. Utilizing recent advancements in spatial transcriptomics, our approaches integrate the entire human transcriptome, enabling understanding of mechanistic biological changes not limited to simple abundance or binary expression. Therefore, *our work could represent a major breakthrough toward precision medicine approaches in biomedical imaging to enable patient-specific disease phenotyping, and more broadly, enhanced pathology*. In Aim 1, we will use spatial transcriptomics and label-free optical imaging to generate co-registered spatial maps of the human transcriptome. Aims 2-3 will focus on defining causative relationships between optical and -omic markers, and developing artificial intelligence models to perform tissue subtyping and label-free staining.

Intended Outcomes: Through this project, we will deliver a completely novel approach to tissue phenotyping and label-free histopathological staining. Unlike current methods, our approach will be scalable, highly repeatable, rapid, and has the potential for *in vivo* application. The project will break new ground in precision medicine approaches in biomedical imaging. By exploring the fundamental mechanisms dictating light-tissue interactions at the genetic scale, the techniques we develop can be applied broadly in biomedical imaging, revolutionizing our ability to understand tissue and disease development at a microscope scale.

Advancing toward precision medicine approaches in biomedical imaging using label-free microscopy, spatial -omics, and artificial intelligence

1. Problem Statement / Objective

"Precision medicine" in healthcare has become increasingly popular in the last decade – this refers to approaches that tailor therapeutic strategies to specific disease phenotypes and individual patient's genetic makeup, environmental exposures, and lifestyle.[1] These methods are particularly valuable in the context of cancer, which can be a highly heterogeneous disease with different phenotypes, each of which may call for a completely different treatment strategy. Cancer is a major health challenge globally, as one of the leading worldwide causes of death and with over 40% of the human population estimated to develop cancer in their lifetime.[2] Utilizing precision medicine techniques to tailor cancer treatment has enabled significantly increased survival and quality of life for cancer patients. However, without tools to effectively identify and classify cancer phenotypes, the promise of precision medicine is left unrealized - both patients and clinicians are left with few treatment options, having to fall back to general surgery and/or chemotherapy, which can carry significant mortality and morbidity. Unfortunately, while precision medicine approaches for treatment and drug screening have advanced, parallel methods for identifying disease phenotypes have lagged, relying on extremely costly assays of molecular biomarkers, various histopathological stains, or -omic sequencing. Therefore, until the development of more accessible techniques for patient-specific disease classification and phenotyping, the significant advancements in precision medicine for therapeutics and disease management will be unrealized for much of the global population.

Label-free biomedical imaging (LBI) represents a powerful tool that could bridge the gap to precision medicine techniques for disease phenotyping. LBI exploits natural sources of optical contrast to provide understanding of biological processes and alterations that may occur during disease onset.[3] There are a variety of popular LBI methods that target different sources of endogenous contrast including those related to metabolism (autofluorescence, fluorescence lifetime), structure (polarization and second harmonic generation), and biochemistry (Raman), among others. By leveraging natural sources of contrast, LBI obviates the need for external contrast agents, making it particularly attractive for point of care applications such as disease screening and diagnosis where toxicity and patient safety is paramount. Another area where LBI shows great promise is enhancing histopathology through "label-free staining,"[4] which is a critical tool for disease phenotyping. Standard histopathology employs contrast agents to bind to specific markers of interest. This requires extensive development of specific antibodies and protocols for each marker, which often are not quantitative and only assess binary expression. Identifying biomarkers for disease phenotyping in histopathology is another area where technology based on LBI could make significant impact.

In this proposal, we seek to develop novel precision medicine techniques for rapid, inexpensive, and accurate cancer phenotyping using a combination of spatial sequencing, LBI, and artificial intelligence. This main objective directly leads to two impactful downstream applications (Figure 1): (1) *rapid, point-of-care optical tumor phenotyping for patient-specific diagnostics*, and (2) *enhanced pathology techniques by providing "label-free staining" and spatial mapping of biochemical markers*. This work could represent a breakthrough toward precision medicine approaches in biomedical imaging to enable patient-specific phenotyping, and more broadly, enhanced pathology.

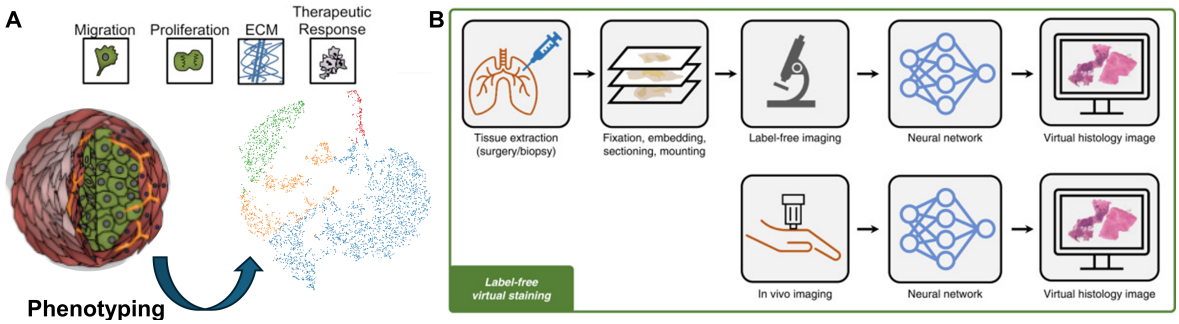

Figure 1: Our proposal aims to develop precision medicine techniques using label-free biomedical imaging for (A) tissue phenotyping into clinically relevant categories to guide precision medicine therapeutics, and (B) quantitative label-free staining for spatially estimating abundance of biological markers (Figure B reproduced from [3]).

2. Impact

The potential impact of this work cannot be understated: The successful completion of this work would break new ground in biomedical imaging in the context of precision medicine, with the wider potential to revolutionize our clinical approaches to disease treatment and management. Our proposal focuses on optical phenotyping for pancreatic cancer – the seventh leading cause of cancer death globally, with less than 15% overall 5-year survival rate.[5] Pancreatic cancer is highly heterogeneous, with some extremely aggressive disease subtypes, and other subtypes that are semi-benign, where patients can live over 15 years without major issues arising.[6] Optical phenotyping could greatly improve our ability to treat and manage pancreatic cancer by defining and detecting these subtypes, leading to faster and more accurate precision medicine treatment and therapeutics. More importantly, while our proposal focuses on pancreatic cancer, our approach could be generalized to any disease that could be targeted with precision medicine approaches. Given that many cancers exhibit heterogeneous behavior, rapid, point-of-care phenotyping could be broadly impactful across the cancer continuum. Beyond this, our advancements in label-free staining for enhanced pathology are relevant beyond cancer and could be generalized to interrogate a variety of biomarkers, augmenting our technological capabilities both in basic science research, and clinical application.

Demonstrating and leveraging the relationship between LBI and genetic pathway regulation / gene expression would mark a significant step toward the PI's long-term research goal to develop label-free, precision, biomedical imaging technologies, and would provide the basis for pursuing funding through larger NIH and NSF research grants to further develop this technology toward clinical application. Due to the non-trivial risks in the initial development of these approaches, the proposed project may be difficult to fund from other sources, making this award a perfect fit. As described in the Personal Statement of the CV, the PI is well positioned to complete this work – he possesses a strong background in optical imaging, computational analysis, and genomics, as well as leading an interdisciplinary team at a premier institution for optical sciences.

3. State of the Art and Literature Review

3.1 Label-free biomarker identification for disease phenotyping

Identifying biomarkers using LBI has been the subject of research efforts for several decades. Perhaps the most common application is diagnosis and screening: a vast amount of research work has focused on identifying disease-specific imaging biomarkers to enable early detection and diagnosis. Examples of this include early detection of gastrointestinal cancers, diagnosis of skin cancer, and assessing plaques in the coronary arteries, among a myriad of other applications.[7] While there is often a high level of accuracy in classifying tissue types using label-free imaging, these efforts rarely connect the source of optical contrast with a true biological mechanism. In other words, most works will correlate label-free contrast with a specific tissue type but fail to understand precisely what tissue alterations lead to the detected label-free contrast. As such, the generalizability of these studies is severely limited beyond the specific dataset or tissue type that was assessed.

Other efforts focus on collecting specific types of label-free contrast that are well understood. Examples in the context of cancer include blood oxygenation via spectral imaging, measuring collagen organization and abundance through second harmonic generation, and metabolic markers through fluorescence lifetime imaging (FLIM). These approaches have the advantage of leveraging known sources of contrast connected to the "hallmarks" of cancer. However, like the case of simple tissue classification, the specific biological mechanisms dictating these imaging features is still not fully understood – many different genetic pathways may lead to alterations in the metabolic behavior, vasculature, and extracellular matrix variations, and current research has failed to connect the relationship between the genetic regulation and LBI contrast. Different types of cancer, and even different phenotypes of a specific cancer (such as pancreatic cancer), can exhibit completely different genetic regulation behavior, leading to the vast disease heterogeneity that we observe.[6] This implies that these general sources of LBI contrast are not necessarily relevant or useful for all patients, which ultimately decrease the sensitivity and specificity of the technologies. With a more precise understanding of the connection between genetic regulation and LBI contrast, not only could the significant patient-to-patient variability be addressed, but it could also be possible to tease out the specific tissue interactions at play to enable "optical phenotyping," for example, where tissue could be assessed for metastatic potential and proliferative ability rapidly and cost effectively using LBI.

3.2 Artificial intelligence for label-free staining

Since the recent explosion of artificial intelligence in biomedical imaging, several groups have aimed to develop techniques for label-free staining.[8] The advantages to such an approach are myriad: histopathological staining is used broadly and can be time intensive, costly, difficult to quantify, and can lack robust reproducibility. The ability to generate analogs to histopathological stains using LBI would be transformative to the field by enabling rapid, low-cost, reproducible, and quantitative measurements of specific biomarkers. Generally, histopathological staining is based on binding specific chemicals or antibodies to biomarkers of interest. These biomarkers often are implicated in light-tissue interactions, and therefore LBI can be used to map out the abundance of these markers. For example, researchers have shown that using autofluorescence images, a neural network can be trained to generate histological stains such as Hematoxylin & Eosin (H&E), which bind to the cell nuclei and cytoplasm respectively. This approach has also been shown to be able to estimate expression of specific proteins such as PanCK (epithelial marker) or Ki-67 (measure of proliferation).[3] While these works are groundbreaking as a proof of concept, they only scratch the surface of what could be possible. These approaches so far have used individual stains as ground truth for training the AI algorithms. While this allows for a direct input-to-output pipeline, a major limitation of this approach is that it does not allow for understanding potential cross correlation between expression of different proteins, and only allows mapping a limited set of proteins at once, given that only a few different stains can be multiplex simultaneously. Furthermore, it remains to be seen which LBI modalities may have the highest predictive ability for different biomarkers. These outstanding challenges must be addressed in order to realize the true potential of label-free staining.

3.3 Preliminary work completed by the PI's team

In contrast to the techniques above, the proposed approach directly addresses limitations in both biomarker identification for optical phenotyping with LBI, as well as label-free staining, by leveraging the recently developed technology of spatial -omics. In our previous work with pancreatic cancer, we demonstrated the methodology to acquire and co-register autofluorescence and FLIM images, as well as a full spatial transcriptomic dataset acquired using the 10X Visium system (**Figure 2A, B**).[9] With this co-registered dataset, we first investigated the regulation of the genetic pathways corresponding to the Warburg effect, the transition of cancer cells to using anaerobic glycolysis for energy production. This transition varies the abundance of metabolites NADH and FAD, which have distinct fluorescence spectra and can be measured in the "optical redox ratio." We showed that the up-regulation of the pathways implicated in the Warburg effect were directly correlated with the optical

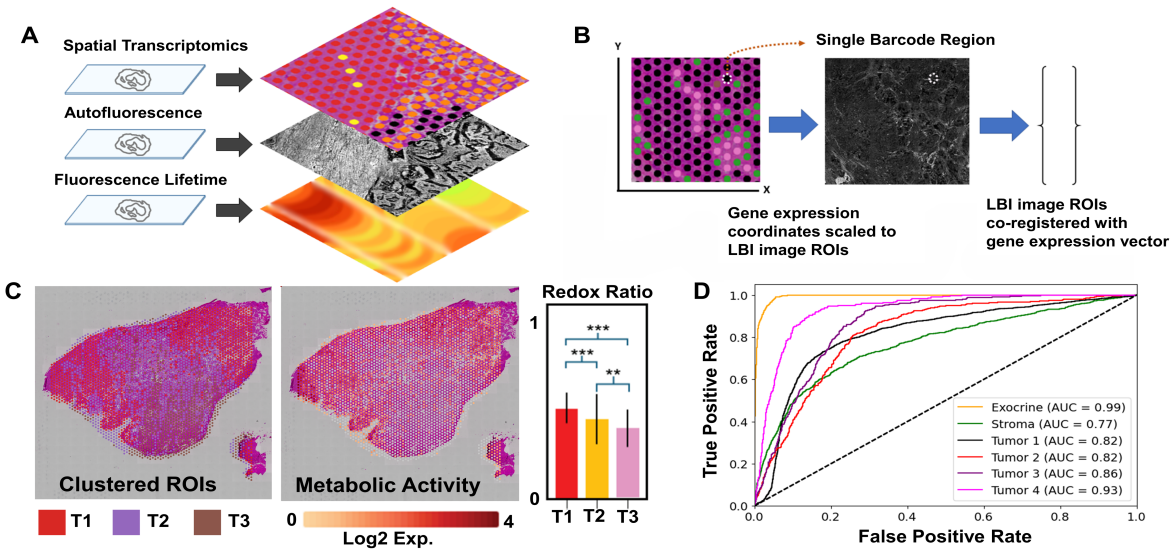

Figure 2: (**A ,B**) Our prior work has enabled us to develop methods for acquiring and co-registering spatial transcriptomics and LBI images. With this, we showed (**C**) correlation between metabolic pathways implicated in the Warburg effect, and the optical redox ratio, as well as the ability to (**D**) effectively phenotype tissues using LBI images.

redox ratio measured through LBI (**Figure 2C**). To our knowledge, we are the first to show this direct connection between the optical redox ratio and an actual biological mechanism related to the Warburg effect – other works simply have correlated abundance of NADH and FAD to the redox ratio but have not explained the underlying mechanism dictating the variation in these metabolites. Next, we utilized the spatial transcriptomics signatures to cluster tissues into different clinically-relevant phenotypes. We built a random forest classifier using our LBI images and showed that we could "optically phenotype" our samples to high accuracy, demonstrating the feasibility of the approach (**Figure 2D**). Finally, we evaluated the ability to perform label-free, quantitative staining by building a regression model using LBI modalities to predict the expression of different biomarkers, in which we were able to achieve over 80% accuracy in predicting the expression values for specific transcripts. While these preliminary results are extremely promising, several challenges remain to fully realize the potential of our approach. Namely, it is critical to broaden our patient cohort to investigate intra and inter-patient heterogeneity, as well as to integrate other LBI modalities beyond autofluorescence and FLIM to explore relationships between different LBI contrast mechanisms and genetic regulation, and finally it is necessary to develop artificial intelligence methods to define these complex interactions in order to achieve rapid and high accuracy optical phenotyping and label-free staining.

4. Proposed Solution: Leveraging artificial intelligence to define optic-omic relationships

Building on our promising work, this proposal is focused on addressing the outstanding challenges above in order to push LBI toward precision medicine approaches. We first will broaden our dataset to a diverse range of 16 pancreatic cancer patients, enabling us to more thoroughly analyze intra- and inter-patient heterogeneity. This will allow us to evaluate the sensitivity, specificity, and generalizability of the relationships between LBI and genetic regulation. In doing so, we will also generate a dataset including a broader representation of LBI modalities – autofluorescence and FLIM, as well as Raman spectroscopy and polarization. By including additional sources of contrast, we anticipate the ability to form connections between a wider range of genetic pathway alterations. Using this dataset, we will implement causal statistical methods to attempt to define optic-omic interactions indicating which genetic pathways are most influential in defining LBI contrast. Finally, we will develop custom deep learning models to perform the two objectives of (1) optical tumor phenotyping, and (2) label-free staining. **Figure 3** shows a conceptual outline of the three aims required to achieve these goals in the proposed work, and the **Timeline** document provides more detail.

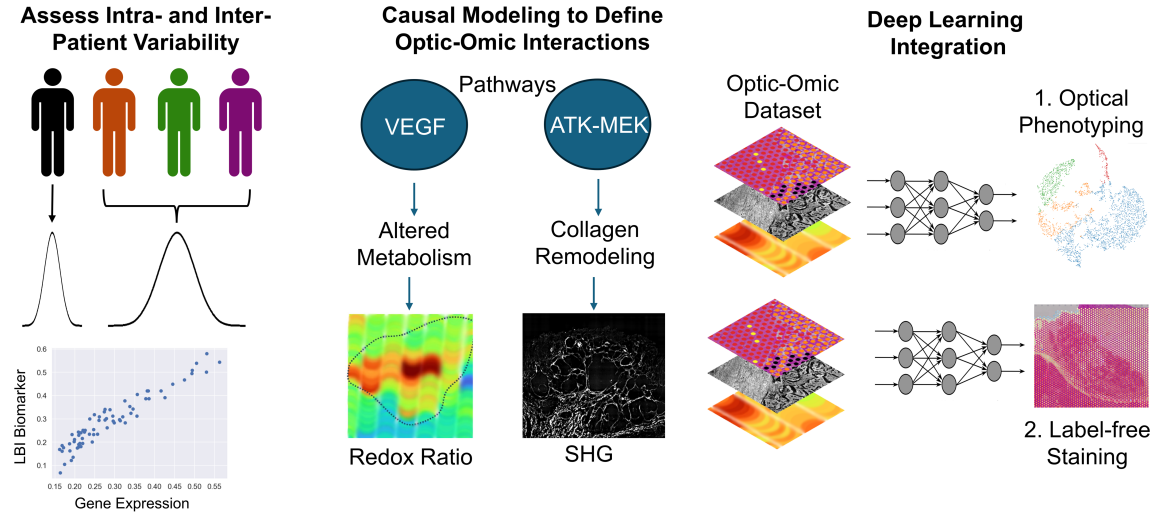

Figure 3: The proposal will focus on three aims: (1) acquiring our optic-omic dataset for a diverse patient population to assess intra- and inter- patient variability, (2) implementing casual statistical modeling to define optic-omic interactions, and (3) integrating deep learning models for performing optical phenotyping and label-free staining using LBI images.

5. Expected Outcomes

Please refer to the **Timeline** document for detailed description of the work completed in each Aim, and the timeline through the award period. The expected outcomes are shown below.

Aim 1 (Months 1-6): Generate co-registered spatial transcriptomics and label-free optical microscopy dataset for patient cohort to investigate intra- and inter-patient variability. In this aim, we anticipate generating a co-registered optic-omic dataset for 16 patients comprised of (1) full spatially resolved human transcriptome; (2) multispectral autofluorescence microscopy images; (3) fluorescence lifetime images (FLIM), spatially resolved (4) Raman spectroscopy, and (5) Mueller Matrix polarization microscopy. In this dataset, there will be over 64,000 discrete data points, where each point contains a full transcriptomic signature and the corresponding 100-micron x 100-micron field of view in each imaging modality. Using linear mixed-effects models, we will establish the intra- and inter-patient variability of our LBI markers, and correlations with transcriptomic signatures.

Aim 2 (Months 6-12): Define causal optic-omic relationships using statistical modeling. From this aim, we will demonstrate a novel and robust approach to biomarker identification and validation through causal statistical modeling.[10] Our approach will enable us to elucidate underlying genetic mechanisms that lead to variations in LBI contrast. Using this approach, we will validate standard LBI sources of contrast such as the optical redox ratio and metabolites identified through FLIM and Raman, before broadening to define causal mechanisms behind and angiogenesis and collagen network disruptions measured through polarization and SHG. This approach will be novel and generalizable beyond the modalities we use here, having potential for broad impact on the field.

Aim 3 (Months 12-18): Develop AI models for label-free subtyping and virtual staining. From this aim, we will develop two novel artificial intelligence models. The first will enable rapid optical phenotyping of tissues to identify clinically relevant disease phenotypes based on LBI modalities alone. Through this we will be able to identify which LBI modalities have the highest diagnostic relevance for potential future *in vivo* application. The second model will break new ground in label-free staining by enabling us to generate transcriptomic signatures and measures of genetic pathway regulation using LBI modalities, significantly improving over existing work to estimate singular protein abundance.

Taken together, these outcomes will lay the foundation for the PI to make groundbreaking advancements in the development of LBI technologies. Next steps will include broadening these techniques to other diseases and tissues, in addition to assessing the feasibility of collecting relevant LBI markers *in vivo* for point-of-care tumor phenotyping. Funding will be pursued through federal agencies including the NSF CAREER and the NIH through R21 or R01 mechanisms.

6. Conclusion

Cancer represents one of the largest global health challenges we are presently facing. Precision medicine is revolutionizing our ability to treat and manage this heterogeneous disease in a patient-specific and more accurate manner, but parallel approaches to identify disease phenotypes to enable precision medicine therapeutics is lacking. Our proposal focuses on addressing this gap by developing precision medicine techniques for optical phenotyping using label-free biomedical microscopy, spatial -omics, and artificial intelligence. Through this work, we will lay the foundation for developing label-free, rapid, and inexpensive technologies for identifying disease phenotypes, understanding the biological mechanisms dictating label-free biomedical imaging contrast, and creating novel approaches for label-free staining to enhance pathology. Ultimately, these advancements could lead to major improvements in our ability to treat and manage cancer by providing a robust approach to identifying and defining disease phenotypes, leading to precision medicine therapeutic action.

References

1. Akhoon N. Precision Medicine: A New Paradigm in Therapeutics. Int J Prev Med. 2021 Feb 24;12:12. doi: 10.4103/ijpvm.IJPVM_375_19.
2. American Cancer Society. Lifetime Probability of Developing (2017-2019) or Dying (2018-2020) from Cancer (Cancer Facts & Figures 2024 Supplemental Data). 2024.
3. Bai B, et al. Deep learning-enabled virtual histological staining of biological samples. Light Sci Appl. 2023 Mar 3;12(1):57. doi: 10.1038/s41377-023-01104-7.
4. Shaked, NT, et al. Label-free biomedical optical imaging. Nat. Photon. 17, 1031–1041 (2023). https://doi.org/10.1038/s41566-023-01299-6
5. American Cancer Society. Cancer Facts & Figures 2024. Atlanta: American Cancer Society; 2024.
6. Torres C, Grippo PJ. Pancreatic cancer subtypes: a roadmap for precision medicine. Ann Med. 2018 Jun;50(4):277-287. doi: 10.1080/07853890.2018.1453168. Epub 2018 Mar 22.
7. Waterhouse DJ, et al A roadmap for the clinical implementation of optical-imaging biomarkers. Nat Biomed Eng. 2019 May;3(5):339-353. doi: 10.1038/s41551-019-0392-5.
8. Kreiss, L., Jiang, S., Li, X. et al. Digital staining in optical microscopy using deep learning - a review. PhotoniX 4, 34 (2023). https://doi.org/10.1186/s43074-023-00113-4
9. Knapp T, et al. Validation of label-free optical imaging markers of pancreatic cancer using spatial transcriptomics. Proc. SPIE 12854 2024, 1285407. https://doi.org/10.1117/12.2691452
10. Pearl J. An introduction to causal inference. Int J Biostat. 2010 Feb 26;6(2):Article 7. doi: 10.2202/1557-4679.1203.

Inverse-designed energy-efficient nonlinear photonic multi-channel neural network

Asst. Prof. Uğur Teğin, Koç University, utegin@ku.edu.tr, Category: Information & Environment

As transistor counts plateau, current computing architectures with memory-access bottlenecks face limitations resulting in high power consumption on data-intensive tasks. An energy-efficient, high-speed, and scalable alternative computing paradigm is necessary to advance our civilization. As an alternative approach, optical computing, an analog computing paradigm, has been around for decades and is closely following developments in data science and AI (G. Wetzstein et al. **Nature** 588.7836, 2020). However, photonic neural networks suffered from fundamental challenges like redundant electro-optic connections and a lack of versatile nonlinearities with low power consumption in a scalable and small form factor. Utilizing spatiotemporal nonlinear dynamics in multimode fibers, scalable optical nonlinear computing has been demonstrated for machine learning applications (U. Teğin et al., **Nature Computational Science**,1.8, 2021). Although, this study presents a promising platform with all-optical complex nonlinearity, a pulsed laser with kW peak powers, and bulky optical components needed to create nonlinear dynamics.

To revolutionize photonic neural networks and optical computing technologies, developing all-optical nonlinear computing that is low-energy, fast, compact, and reliably manufacturable is crucial. We propose an energy-efficient nonlinear photonic neural network designed through inverse methods to achieve this goal, enabling multi-channel computing. Our approach features an integrated nonlinear optical computing architecture using multimode silicon nitride waveguides and includes inverse-designed units to manipulate light propagation, facilitating the training of photonic neural networks. The spatiotemporal nonlinear Schrödinger equation governs the nonlinear spatiotemporal propagation in these silicon nitride waveguides, with the inverse-designed control units inducing mode mixing between the waveguides.

Our innovative solution leverages **spatiotemporal nonlinear dynamics, integrated optics, and inverse design**, offering three key features:

1. Strong Nonlinear Optical Computing with Low Power Consumption: Silicon nitride's high material nonlinearity (n2) and the effective nonlinearity of waveguides (γ) result in 5000 to 7000 times greater nonlinearity than optical fibers depending on the waveguide geometry. This makes multimode silicon nitride waveguides highly effective for spatiotemporal nonlinear optical computing with continuous wave lasers, enabling strong all-optical nonlinear computing with just a few watts.

2. Small-Footprint Scalable Nonlinear Photonic Neural Network: Our technology uses waveguide modes to nonlinearly process optical information. These modes, acting as channels, couple linearly and nonlinearly. The high refractive index of silicon nitride allows for small-area multimode optical waveguides, facilitating high-resolution data processing and scalable optical computing. Our solution offers a small footprint and scalability by increasing the number of modes with increasing propagation area or decreasing the operation wavelength, significantly enhancing the effectiveness of integrated photonic computing.

3. High-Performance Multi-Channel Optical Computing with Inverse Design: Utilizing an inverse design approach, our solution incorporates mode mixing units for training photonic neural networks. By further implementing an inverse-designed wavelength division multiplexing unit, we propose an advance wavelength-selective optical computing with different paths to achieve multi-channel photonic neural network design. It creates a versatile platform that integrates various optical computing architectures into a single design.

The framework introduced by our inverse-designed energy-efficient nonlinear photonic multi-channel neural network has the potential to provide extreme utility in diverse areas of application. This approach provides compelling evidence that inverse-designed integrated platforms can be utilized for various geometries for task-oriented applications.

Inverse-designed energy-efficient nonlinear photonic multi-channel neural network

Asst. Prof. Uğur Teğin, Koç University, utegin@ku.edu.tr

1. Literature review

Artificial neural networks are ideal applications for analog computing platforms due to being notoriously robust against noise and resilient to imperfections [1]. Among analog computing frameworks, optics perform computation intrinsically by offering fundamental operations like Fourier transform, matrix multiplication, and convolution with passive optical elements [2,3]. Thus, it has a rich history closely following the evolution of data processing and AI (see Fig. 1) [4-6].

Starting with the optical implementation of the Hopfield network [7], photonic neural networks emerged. To mimic the artificial neural networks in digital form, dynamics nonlinear crystals are utilized to have active control for training the optical setup [8]. However, interest in custom optical hardware declined in the 1990s because the technology required for the optoelectronic implementation of nonlinear activation functions was not yet fully developed, and the challenge of managing analog weights made it difficult to control extensive optical networks reliably.

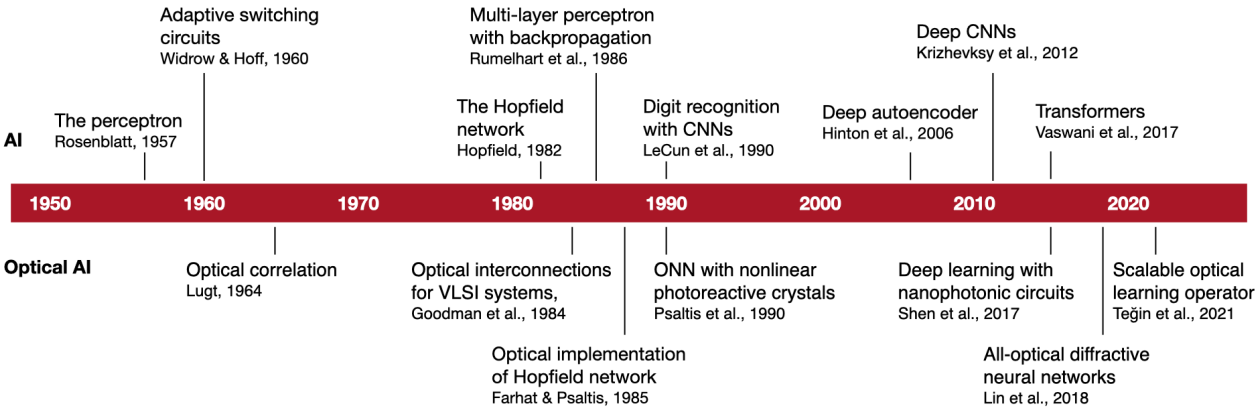

Figure 1: Timeline of artificial intelligence and selected related optical and photonic implementations

The introduction of neuromorphic computing methods in the 2000s, such as reservoir computing and extreme learning machines, show a way to overcome the training issues in optical computing by offering fixed yet nonlinear hidden layers [9,10]. This bioinspired solution renewed interest in optical neural networks and various delay-based optical systems are utilized for optical computing [11]. However, photonic neural networks lacked strong all-optical nonlinear connections to reach similar performance levels with their digital counterparts. **Here, we would like to emphasize that the nonlinear connections are essential to high performance computing in AI.** Nonlinear computing performs dimensionality expansion to the dataset and/or create clustering between the related data samples [12]. One of the many fruits of my PhD studies at EPFL is the demonstration of nonlinear computing with complex spatiotemporal nonlinear dynamics in multimode fibers for optical computing and creating a powerful, scalable, and nonlinear photonic neural network. This study earned recognition with a cover feature in Nature Computational Science and media attention, including The Economist [13]. Although this study presents excellent machine learning performance and all-optical nonlinear computing, a pulsed laser with kW peak powers is needed to create nonlinear dynamics. A low-energy, fast, small-footprint, reliably manufacturable nonlinear optical computing will be a helpful building block for photonic neural networks.

In the field of integrated optics, silicon nitride has emerged as a promising platform for nonlinear optics due to its relatively low two-photon absorption, wide transparency window, and high optical damage threshold [14,15]. With remarkable improvements in fabrication methods, such as the introduction of the photonic Damascene process, ultra-low loss silicon nitride structures with micron-level thicknesses become feasible [16]. Over the last decade, these advantages have made silicon nitride waveguides and resonators ideal for applications in frequency comb generation [17], and optical signal processing [18]. Furthermore, inverse design became an interesting direction in micro and nanophotonics. It is a computational approach to designing optical devices by specifying desired performance outcomes and using algorithms to determine the

optimal structure or material configuration to achieve those outcomes [19,20]. Although this method contrasts with traditional intuition-based design processes, it provides remarkable performance for broad tasks, such as wavelength multiplexers, mode multiplexing, couplers, and on-chip sensors [21-24]. By topology optimization and machine learning to explore a vast design space, inverse design in nanophotonics enables the creation of highly efficient, compact, and often unconventional photonic devices. Recent numerical and experimental studies demonstrate that linear scattering-based inverse-designed integrated optical units can perform matrix multiplication and optical computing [25,26]. Such developments present improvements over computer-assisted diffractive neural networks, which have limited applications to THz optics in bulk form [27,28].

2. Problem statement / Objectives

In today's data-driven world, the rising demand for computing power, fueled by machine learning and data-heavy applications, poses a significant challenge. Modern AI technologies use enormous amounts of power. Training advanced language models such as GPT-3 can consume as much energy as charging 13,000 electric cars from scratch [29]. Likewise, the high power consumption of AI technologies limits the operation of trained neural networks to cloud computing. Along with the slowdown in Moore's Law, seen in the stagnation of transistor counts on microchips, AI's computational power demands highlight the need for a more sustainable and efficient approach to computing. This new approach should provide a scalable computational power and minimize environmental impact.

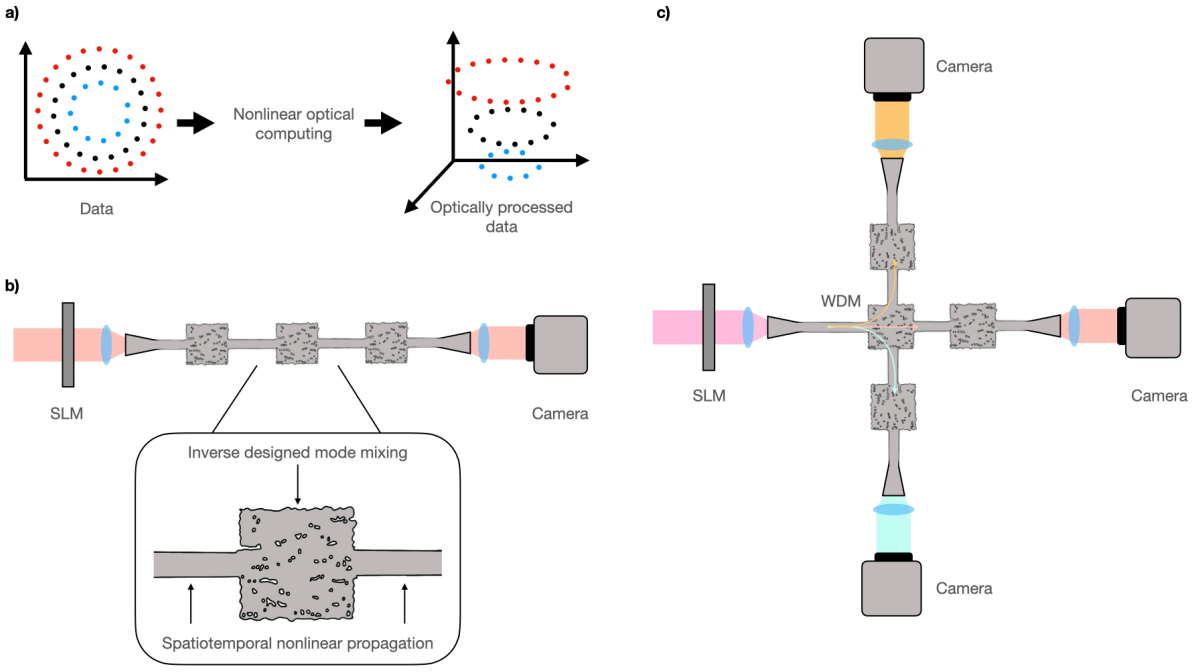

Figure 2: (a) Illustration on the impact of nonlinear optical computing, (b) the inverse-designed energy-efficient nonlinear photonic neural network, and (c) its multi-channel architecture.

Optical computing has significant speed, efficiency, and high parallelism potential as a paradigm shift in computation. All-optical strong nonlinear connections are essential to perform nonlinear information processing to realize optical counterparts of the artificial neural networks. So far, state-of-the-art performances with nonlinear optical computing have been achieved via high-power ultrafast lasers and bulky fiber optical systems [12].

To revolutionize the field of photonic neural networks and optical computing technology, low-energy, fast, small-footprint, reliably manufacturable all-optical nonlinear computing is essential. We propose the inverse-designed energy-efficient nonlinear photonic neural network to realize this goal, which can branch out as multi-channel computing. We design an integrated nonlinear optical computing architecture with multimode silicon nitride waveguides and incorporate inverse-designed units to shape light propagation to train photonic neural networks. As illustrated in Fig. 2, the spatiotemporal nonlinear Schrödinger equation governs nonlinear spatiotemporal propagation in silicon nitride wide waveguides, and the inverse-designed control units create mode mixing between the waveguides. This mode mixing behavior of the inverse-designed units provides us

control over the nonlinear propagation of the information-carrying light. During the design process, we favor the high optical computing performances for benchmark datasets (Fashion MNIST, CIFAR-10, COVID-19 X-Ray, etc.), thus optimizing the topology of these units to provide trained photonic neural networks. We expect to reach at least 90% test accuracy for the selected datasets and aim for less than 50 W power consumption. Such power consumption is more than an order of magnitude less than GPUs for AI applications.

Our innovative technology combines the benefits of spatiotemporal nonlinear dynamics, integrated optics, and inverse design, offering three key features:

I. Strong nonlinear optical computing with low power consumption: In addition to silicon nitride's high material nonlinearity (n_2), the effective nonlinearity of a waveguide (γ) is significantly high due to its inverse proportionality to the effective propagation area. Depending on the waveguide geometry, it results in 5000 to 7000 times more effective nonlinearity. Thus, multimode silicon nitride waveguides and structures offer spatiotemporal nonlinear dynamics with orders of magnitude higher nonlinearities than optical fibers. Such a nonlinear optical platform opens a path to create spatiotemporal nonlinear dynamics with continuous wave lasers. Our novel design enables us to perform strong all-optical nonlinear computing with few watts.

II. Small-footprint scalable nonlinear photonic neural network: This innovative technology utilizes the waveguide modes to decompose and process optical information. These waveguide modes operate as channels, and in addition to linear coupling due to imperfections, they nonlinearly couple with each other. The high refractive index of silicon nitride provides multimode optical waveguides with small areas, which helps us to process high-resolution data and scale our optical computing platform. Unlike other integrated optical computing schemes, our novel solution is scalable with the number of modes that can increase the effective area and/or decrease the operation wavelength. Offering an intrinsic small footprint with integrated optics yet being scalable is one of the groundbreaking features of our inverse-designed energy-efficient nonlinear photonic multi-channel neural network. Furthermore, due to the high effective nonlinearity of the proposed material, propagation length decreases in favor of small-footprint photonic computing.

III. High-performance multi-channel optical computing with inverse design: Our innovative technology can branch out into multi-channel photonic neural network designs. Powered by the inverse design approach, we incorporate mode mixing units to train photonic neural network architectures for the aforementioned benchmark datasets. By incorporating an inverse-designed wavelength division multiplexing, we propose to perform wavelength-selective optical computing with different paths to achieve multi-channel photonic neural network design. Depending on the wavelength of the information-carrying light, the wavelength division multiplexing unit steers the propagation direction to the designated trained photonic neural network path. It creates a versatile platform to combine different optical computing architectures into a single design.

3. Outline of tasks / Work Plan

WP 1 - Design and simulation

Goal: WP1 aims to perform numerical studies to design the photonic neural network architecture and provide an in-depth understanding of spatiotemporal nonlinear information processing in candidate structures.

Over the years, we have developed expertise in optical waveguide and nonlinear optics simulation tools using the beam propagation method (BPM) and semivectorial finite difference method. They perform intensive calculations with GPU parallelization and deliver the most realistic modeling of spatiotemporal nonlinear propagation of light and modal analysis of the waveguides. In this work package, we will develop a numerical tool by incorporating commonly used inverse design tools (SPINS, Tidy3D, etc.) and our nonlinear optics simulations to realize our innovative architecture. Our efforts will focus on designing edge couplers, multimode silicon nitride waveguides, and inverse-designed mode mixing units. An illustration of a single photonic neural network and its multi-channel implementation are presented in Fig. 2.

We will perform numerical studies to explore various geometries to optimize waveguide parameters and laser power to achieve the best optical computing performances. Since the waveguide parameters affect the number of information channels (modes) and the effective

nonlinearity with the area where the light travels, we must fine tune these parameters for best performances. Here, we would like to emphasize that the waveguide will provide spatiotemporal nonlinear propagation governed by the spatiotemporal nonlinear Schrödinger equation and the inverse-designed sections along the propagation will be utilized to increase the performance of the photonic neural networks. Furthermore, by combining several photonic neural networks designed for particular wavelengths via inverse-designed wavelength division multiplexing, we will design and numerically study the photonic multi-channel neural network.

WP 2 - Fabrication and characterization

Goal: WP2 aims to fabricate and characterize candidate photonic neural network structures and perform their tests before machine learning studies.

In this work package, we will fabricate and experimentally test the candidate photonic neural network designs determined by the numerical studies on WP1. With layout software such as L-Edit and K-Layout, we will develop the waveguide patterns to be used in the fabrication process. Based on the fabrication capabilities of N2star (Koç University Nanofabrication and Nanocharacterization Center), we have expertise in designing and developing low-loss silicon nitride waveguides at our university. We will follow the standard and matured techniques for waveguide fabrication involving vapor deposition, lithography, and etching. Since we want to develop multimode waveguides, our task is relatively easy, and our goal is to fabricate large cross-sections. Inverse-designed control units can be processed during these fabrication steps with adequate feature sizes [30]. However, we can use e-beam lithography techniques if necessary. During and after fabrication processes, we will perform cross-sections and related characterizations. Our optical tests will involve coupling and propagation loss measurements, spectral broadening, and spatial changes under linear and nonlinear light propagation.

	Year I				Year II			
	Q1	Q2	Q3	Q4	Q1	Q2	Q3	Q4
WP 1 - Design and simulation								
Task 1.1: Integrated waveguide and inverse design								
Task 1.2: Beam propagation simulations								
WP 2 - Fabrication and characterization								
Task 2.1: Fabrication of candidate structures								
Task 2.2: Physical and optical characterizations								
WP 3 - Photonic neural network performance tests								
Task 3.1: ML studies and benchmarks								
Task 3.2: ML studies with multi-channel photonic NNE								

Figure 3: Gantt chart for the project which is organized through 3 work packages (WP), each with 2 tasks. ML stands for machine learning and NNE stands for neural network.

WP 3 - Photonic neural network performance tests

Goal: WP3 aims to experimentally realize the single and multi-channel photonic neural networks.

In this work package, the inverse-designed energy-efficient nonlinear photonic neural networks (single and multi-channel) designed in WP1 and fabricated in WP2 will be integrated into an optical setup illustrated in Fig. 2. At the input of the waveguide, due to the slab geometry of the waveguide, we will utilize cylindrical lenses or Powell lenses to fill the edge coupler effectively. Our preliminary numerical studies suggest that an asymmetric waveguide improves the nonlinear connection between higher- and low-order modes. We anticipate that such an interaction can enhance performance in machine learning studies. Initially, we will employ a digital decision layer to link optical information to labels. We selected commonly used machine learning datasets (Fashion MNIST, CIFAR-10, and COVID-19 X-Ray) to benchmark the performance of our inverse-designed energy-efficient nonlinear photonic neural network architecture. For each dataset we

expect to offer at least 90% test accuracy. We will explore the design cases to remove the digital decision layer to perform all-optical computing. Furthermore, we will also test the photonic multi-channel neural network in this work package. It will perform as a wavelength-dependent trained photonic neural network, and for different wavelength regimes, the architecture will provide inference on different machine learning tasks.

4. Outcome(s)

This project will demonstrate that a task-oriented, inverse-designed multi-channel photonic neural network platform can simultaneously achieve multiple tasks with energy efficiency and high accuracy. Our novel design offers all-optical nonlinear connections with small footprints and continuous wave lasers. The project's innovative approach will profoundly impact various application areas in photonics by offering high-performance and scalable integrated optical computing.

By employing wavelength-dependent computation paths, the project will illustrate how multiple tasks can be performed together in a small form factor. This approach provides compelling evidence that inverse-designed integrated platforms can be utilized for various geometries for task-oriented applications.

Additionally, this research will pave the way for future development of different object-oriented programming platforms through inverse design. The project will also show that commonly used machine learning datasets can be processed with high accuracy and low energy consumption on scalable integrated neural network platforms. This efficiency makes the platform an excellent candidate for implementing complex machine learning models and performing various learning tasks simultaneously.

Moreover, the project's outcomes will highlight the potential of photonic neural networks for completely integrated forms since the laser source and the sensors are operating with integrated optical technologies. By providing robust solutions for complex, multi-task operations, our novel research will advance energy-efficient nonlinear optical computing technologies and their integration into practical applications.

5. Impact

The framework introduced by our inverse-designed energy-efficient nonlinear photonic multi-channel neural network has the potential to provide extreme utility in diverse areas of application. Information processing with the photonic neural network can be energy-efficiently realized as long as data can be encoded as phase/amplitude objects (thanks to the spatial light modulator in Fig. 2), which means data of different modalities (images, text, etc.) can be processed at the same time. As such, optical counterparts of multi-channel deep learning networks [31] trained on conventional digital hardware can be developed thanks to our platform, filling a research gap where optics has not been fully explored as a means for multi-channel learning.

The proposed photonic neural network's versatility and energy efficiency imply a competitive advantage for deployment in industry and consumer products. On the industry side, the inherent parallelism offered by optics and enhanced by our design of wavelength-selective optical computing paths indicates an AI accelerator scheme, which will help us tackle complex problems ranging from optimization to workplace automation. Adopting a consumer perspective, the small energy footprint of our inverse-designed photonic neural network means that it can be readily adapted to consumer products without a significant resource overhead, either as a component or a separate device.

The framework described above is also well-suited to quantum optics applications, where silicon nitride-based waveguides are being developed to take advantage of quantum supremacy [32,33]. With extensions to our design, on-chip scalable and fault-tolerant photonic quantum computers can be engineered. In addition, complex media, e.g., fibers where mode mixing is observed, is a strong candidate where both quantum optics and our inverse-designed photonic neural network can be harnessed [34].

References

[1] Liu, Mengchen, et al. "Analyzing the noise robustness of deep neural networks." 2018 IEEE Conference on Visual Analytics Science and Technology (VAST). IEEE, 2018.
[2] McAulay, Alastair D. Optical computer architectures: the application of optical concepts to next generation computers. John Wiley & Sons, Inc., 1991.
[3] Goodman, Joseph W. Introduction to Fourier optics. Roberts and Company publishers, 2005.
[4] Wetzstein, Gordon, et al. "Inference in artificial intelligence with deep optics and photonics." Nature 588.7836 (2020): 39-47.
[5] Goodman, Joseph W., et al. "Optical interconnections for VLSI systems." Proceedings of the IEEE 72.7 (1984): 850-866.
[6] Miller, D. A. B., et al. "Novel hybrid optically bistable switch: The quantum well self-electro-optic effect device." Applied Physics Letters 45.1 (1984): 13-15.
[7] Farhat, Nabil H., et al. "Optical implementation of the Hopfield model." Applied optics 24.10 (1985): 1469-1475.
[8] Abu-Mostafa, Yaser S., and Demetri Psaltis. "Optical neural computers." Scientific American 256.3 (1987): 88-95.
[9] Jaeger, Herbert, and Harald Haas. "Harnessing nonlinearity: Predicting chaotic systems and saving energy in wireless communication." science 304.5667 (2004): 78-80.
[10] Huang, Guang-Bin, Qin-Yu Zhu, and Chee-Kheong Siew. "Extreme learning machine: theory and applications." Neurocomputing 70.1-3 (2006): 489-501.
[11] Van der Sande, Guy, Daniel Brunner, and Miguel C. Soriano. "Advances in photonic reservoir computing." Nanophotonics 6.3 (2017): 561-576.
[12] Teğin, Uğur, et al. "Scalable optical learning operator." Nature Computational Science 1.8 (2021): 542-549.
[13] Bertics, A. “Artificial intelligence and the rise of optical computing” https://www.economist.com/science-and-technology/2022/12/20/artificial-intelligence-and-the-rise-of-optical-computing.
[14] Blumenthal, Daniel J., et al. "Silicon nitride in silicon photonics." Proceedings of the IEEE 106.12 (2018): 2209-2231.
[15] Gaeta, Alexander L., Michal Lipson, and Tobias J. Kippenberg. "Photonic-chip-based frequency combs." nature photonics 13.3 (2019): 158-169.
[16] Pfeiffer, Martin Hubert Peter, et al. "Photonic damascene process for low-loss, high-confinement silicon nitride waveguides." IEEE Journal of selected topics in quantum electronics 24.4 (2018): 1-11.
[17] Okawachi, Yoshitomo, et al. "Octave-spanning frequency comb generation in a silicon nitride chip." Optics letters 36.17 (2011): 3398-3400.
[18] Lacava, Cosimo, et al. "Si-rich silicon nitride for nonlinear signal processing applications." Scientific reports 7.1 (2017): 22.
[19] Molesky, Sean, et al. "Inverse design in nanophotonics." Nature Photonics 12.11 (2018): 659-670.
[20] So, Sunae, et al. "Deep learning enabled inverse design in nanophotonics." Nanophotonics 9.5 (2020): 1041-1057.
[21] Wiecha, Peter R., et al. "Deep learning in nano-photonics: inverse design and beyond." Photonics Research 9.5 (2021): B182-B200.
[22] Piggott, Alexander Y., et al. "Fabrication-constrained nanophotonic inverse design." Scientific reports 7.1 (2017): 1786.
[23] Su, Logan, et al. "Nanophotonic inverse design with SPINS: Software architecture and practical considerations." Applied Physics Reviews 7.1 (2020).
[24] Piggott, Alexander Y., et al. "Inverse design and demonstration of a compact and broadband on-chip wavelength demultiplexer." Nature photonics 9.6 (2015): 374-377.
[25] Hughes, Tyler W., et al. "Wave physics as an analog recurrent neural network." Science advances 5.12 (2019): eaay6946.
[26] Nikkhah, Vahid, et al. "Inverse-designed low-index-contrast structures on a silicon photonics platform for vector–matrix multiplication." Nature Photonics (2024): 1-8.
[27] Lin, Xing, et al. "All-optical machine learning using diffractive deep neural networks." Science 361.6406 (2018): 1004-1008.
[28] Mengu, Deniz, et al. "Misalignment resilient diffractive optical networks." Nanophotonics 9.13 (2020): 4207-4219.
[29] L. Ulrich, “GM bets big on batteries: A new $2.3 billion plant cranks out Ultium cells to power a future line of electric vehicles,” IEEE Spectr. 57(12), 26–31 (2020)

[30] Yang, Ki Youl, et al. "Multi-dimensional data transmission using inverse-designed silicon photonics and microcombs." Nature communications 13.1 (2022): 7862.
[31] Ngiam, Jiquan, et al. "Multimodal deep learning." Proceedings of the 28th international conference on machine learning (ICML-11). 2011.
[32] Bourassa, J. Eli, et al. "Blueprint for a scalable photonic fault-tolerant quantum computer." Quantum 5 (2021): 392.
[33] Taballione, Caterina, et al. "8× 8 reconfigurable quantum photonic processor based on silicon nitride waveguides." Optics express 27.19 (2019): 26842-26857.
[34] Goel, Suraj, et al. "Inverse design of high-dimensional quantum optical circuits in a complex medium." Nature Physics (2024): 1-8.

Name: Development of low excess noise, ultra-high resolution, spectral domain OCT system through the development of low intensity noise, incoherent fiber Supercontinuum source.

Category: Health.

Problem: Excess intensity noise of broadband optical sources, such as supercontinuum (SC), used for spectral domain (SD) ultra-high resolution (UHR) Optical Coherence Tomography (OCT) forms the fundamental limitation to achieve shot-noise limited detection. The consequence of this is to lose the capability of early-stage detection of pathologies in ophthalmology, cardiology, cancer diagnosis etc. Existing solutions require either non-standard, complex, bulky sub 50 femtosecond pulse width, shot noise limited pump laser designs, and complex, patent protected optical fiber designs to generate low excess intensity noise supercontinuum. Such methods further elevate the cost and complexity of the already expensive (>100000$) UHR OCT systems that currently are limited to high-income developed countries. Further, the existing solutions fail if there is a small amount of intensity noise (0.5-1%) of pump (which is true with many practical pump lasers) used for SC generation.

Our Solution: The goal is to develop a low excess noise (ideally shot noise limited) UHR SD OCT system based on low intensity noise, incoherent fiber supercontinuum (SC) source. This will be achieved by following the essential requirements of low intensity noise SC generation. They are: 1) Low intensity noise of the pump that generates SC and 2) Low quantum noise amplification in the SC generated. Besides, both the above requirements should be met in a cost-efficient manner. This will be achieved, a) by developing, in-house, a low noise, continuous wave (CW) fiber-based pump laser, and b) by using standard off-the shelf telecom optical fibers for SC generation as shown in figure.

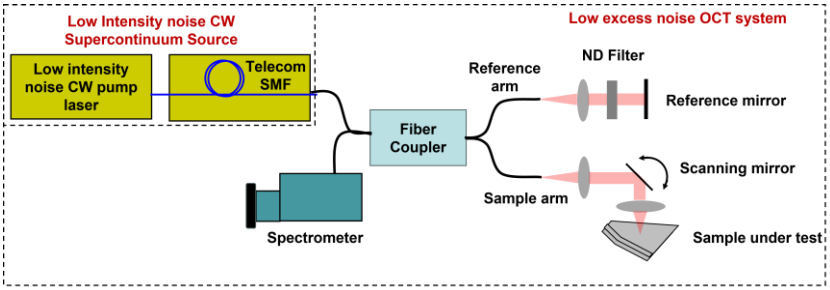

Figure: Schematic of proposed low excess noise SD UHR OCT system

Unique features: CW natures of the pump enable low quantum noise amplification (unlike femtosecond laser pumped SC generated), and the low intensity noise nature enables low intensity noise of the SC generated. Both CW pump and telecom fiber make the system cost-efficient by atleast an order of magnitude compared to the existing systems (based on complex, pulsed pump and, patent protected photonic crystal fibers), without compromising the excess noise performance of OCT. Same technique can be readily transferable to low intensity noise SC generation in other nonlinear optical fiber types such as photonic crystal fibers, highly nonlinear fibers etc., depending on the wavelength region of interest.

Outcomes: Publications and patents on these new methods for low noise nonlinear frequency generation to generate widely tunable wavelength and broadband SC sources in various nonlinear optical fiber media. Tabletop prototypes of low intensity noise widely tunable wavelength, broadband SC sources, and low excess noise OCT system. Technology transfer to a private Indian company for the first realization of UHR OCT system in India. Trained graduate students in research areas of fiber lasers, nonlinear fiber optics and OCT.

Impact: The proposed OCT system enables early-stage detection of multiple diseases in various categories of healthcare diagnostics such as Ophthalmology, Dermatology Cardiology etc. Due to the cost-efficient nature, the developed technology provides wide accessibility of UHR OCT technology to billions of underserved populations in low income developed countries. The SC source developed when used for other low-coherence interferometric applications such as contact-less, non-destructive testing and inspection of processes parameters in industrial manufacturing, oil, and gas sensing, can increase the signal to noise ratio, resolution, acquisition speed and sensitivity.

Development of low excess noise, ultra-high resolution, spectral domain OCT system through the development of low intensity noise, incoherent fiber Supercontinuum source.

1. Literature Review

Optical Coherence Tomography (OCT) uses low-coherence interferometry (LCI) technique to obtain cellular level resolution, 3D images of biological tissues in a non-invasive manner [1]. It is used in diagnosis of many diseases like Glaucoma, Skin cancer, Diabetic retinopathy, Coronary artery stenosis etc. [2]. Among various OCT modalities, Spectral/Fourier domain OCT (SD OCT) is most prevalent due to its higher sensitivity and image acquisition speeds [3]. Figure 1 shows the typical schematic of an SD OCT system. The achievable axial resolution of SD-OCT is inversely related to the spectral bandwidth of the source. Latest developments in the broadband optical sources with more than octave spanning bandwidth (called Supercontinuum), enabled SD-OCT to achieve ultra-high resolution (UHR-OCT) of few µm corresponding to a single cell dimension [4].

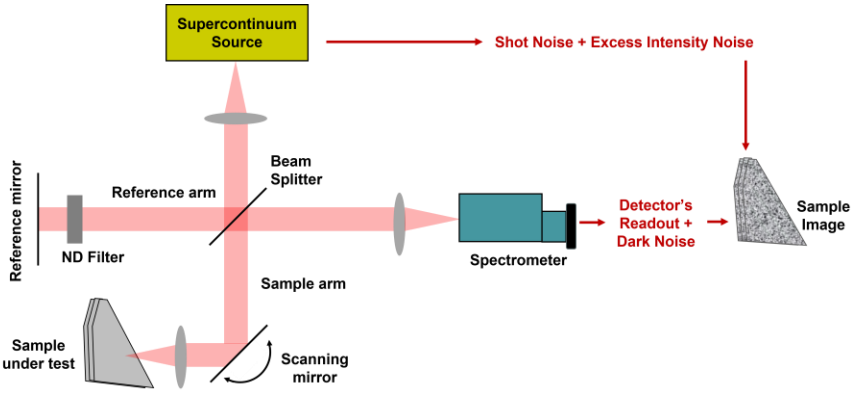

Fig. 1. Schematic of ultra-high resolution, spectral domain OCT system showing different components and noise sources.

A crucial figure of merit for an OCT system is the signal to noise ratio, (SNR). Signal corresponds to the detected spectral interference and is proportional to product of backscattered and reflected optical powers from SUT and the reference mirror. The noise corresponds to the background detected power. The noise degrades the achievable visibility of the spectral interference and hence the contrast of images. This significantly inhibits the early-stage detection of the diseases. As shown in figure 1, multiple noise sources originating from the input broadband source, and the detector, contribute to the SNR of OCT images. The goal of every OCT system is to achieve shot-noise limited detection [5], i.e., the noise in the detected image is limited by the fundamental random nature of detected photons, with negligible contribution from the noise of the detector and the optical source.

Towards this goal, OCT systems with bulky, expensive, cryogenically cooled superconducting, and high-internal gain photo detectors were demonstrated to avoid dark noise at low reference optical power levels [6]. On the other hand, the use of low-bandwidth sources such as super luminescent diodes (SLDs), can also achieve shot-noise limited OCT due to negligible excess intensity noise of SLDs [4]. However, owing to UHR capability and the availability of multiple spectral bands, SC sources are highly attractive to OCT systems. But the excess intensity noise arising from the SC source dominates the noise of detector in OCT images. This is due to various nonlinear optical processes involved in SC generation mechanism [7]. Therefore, there is a compromise between achieving UHR and the shot-noise limited detection in OCT imaging systems.

	Reference publication	Fiber Type	Pump Choice	Limitations
Anomalous Dispersion Regime	J M Dudley et al. Rev. Mod. Phy., (2006),	Standard Photonic Crystal Fiber (PCF)	<50fs shot noise limited pump lasers	**Non-standard, complex pump laser designs - Expensive**
Normal Dispersion Regime	A M Heidt et al., Optica, (2022)	PCFs with Low (<7ps^2/km), flat Dispersion profile	Standard Mode Locked (100fs – <1ps), shot noise limited pump lasers	**Non-standard, Complex, Research grade, patents protected fiber (PCF) designs - Expensive**

Fig. 2. Summary of current low excess noise SC generation methods in anomalous and normal dispersion regimes.

This has triggered a lot of research activity in the development of low excess intensity noise SC sources for OCT [8]. The methods, summarized in figure 2, include use of very short pulse (<50fsec) pump sources for SC generation in anomalous dispersion standard photonic crystal fibers (PCFs) [8], and the use of normal dispersion (ANDi) PCFs with low and flat dispersion profiles over a broad wavelength range for ANDi SC generation [9].

2. Problem Statement and Objective

The primary limitations of the existing low excess intensity noise UHR OCT systems shown in figure 2 are:

1. In anomalous dispersion, the pump pulse widths needed for low-noise, coherent SC generation are of sub 50fs [8]. Such non-standard pump lasers require complex, bulky designs and hence are expensive.
2. In normal dispersion, the fibers needed must have low (<7ps^2/km) [9], flat dispersion profiles. Such fibers require complex dispersion engineered refractive index profiles making them expensive and they are still in research phase with patents protection.
3. The above methods utilize seeded incoherent nonlinear optical processes in anomalous dispersion and coherent nonlinear optical processes in normal dispersion to obtain coherent and low-noise SC [8]. However, for OCT, only low-noise and low-coherence of SC is needed.
4. Further, it was shown that with small excess intensity noise of the pump source (~1%), the above SC generation methods completely fail due to pump noise induced SC de-coherence and noise amplification [10,11].
5. However, J. R. Taylor et. al, in 2004 demonstrated that the use of continuous-wave (CW) pump source rather than femtosecond pulsed pump for SC generation can significantly reduce intensity noise level of SC to the input pump noise level (unlike 50dB amplified intensity noise of femtosecond pulse pumped SC) due to low peak power (10s watts), Raman Soliton nature of the SC generated [12].

Therefore, what is desirable for low excess noise OCT system is

1. A CW pump source, but with ideally zero intensity noise (shot-noise limit) for low intensity noise SC generation.
2. A standard, conventional off the shelf optical fibers (e.g, SMF28e) for SC generation.
3. A low noise detection mechanism. This can be achieved with standard off-the-shelf spectrometers.

Therefore, the primary objective of this proposal is to develop a low excess noise (ideally shot noise limited) OCT system. The has been divided into subobjectives detailed below.

3. Work Plan/Tasks

3.1. Development of low excess intensity noise pump source for SC generation

In this objective, we aim to achieve wavelength tunable from 1µm to 1.5µm, low excess intensity noise (ideally shot noise limited) fiber laser with ~50W of optical power. This enables SC generation in standard telecom fibers with zero dispersion wavelength (ZDW) at 1.3µm and highly nonlinear fibers (HNLFs) with ZDW at 1.5µm. To achieve this, we will use the widely known tunable wavelength cascaded Raman fiber lasers architecture [13-15] shown in figure 3.

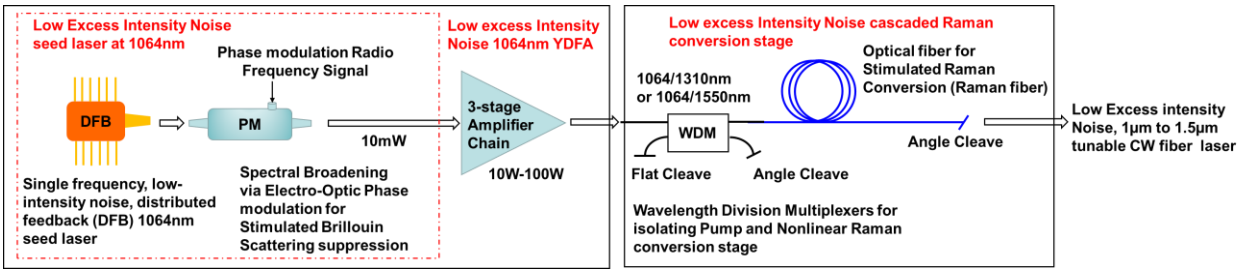

Fig. 3. Schematic of Tunable wavelength low excess intensity noise CW fiber laser.

A low excess intensity noise, ~100W class Ytterbium doped fiber amplifier (YDFA) based on multistage amplification of shot-noise limited, phase modulated single frequency distributed feedback (DFB) seed laser will be developed and used for pumping cascaded Raman conversion stage. This enables low excess intensity noise Raman fiber laser from 1µm to 1.5µm [15]. Theoretical/Numerical investigation will be performed to study and optimize the intensity noise performance.

3.2. Development of low excess intensity SC source

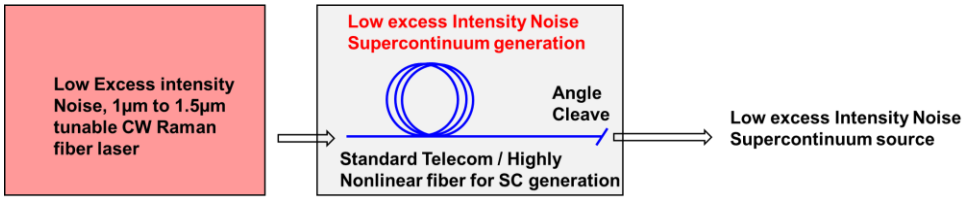

Fig. 4. Schematic of low excess intensity noise SC source

In this objective, the above developed tunable, low excess intensity noise Raman fiber laser will be utilized as pump for SC generation in telecom or HNLF optical fibers as shown in figure 4. The target optical bandwidth and relative intensity noise (RIN) of SC source are >300nm (1300 – 1700nm) and <-120dBc/Hz (0 – 10MHz RF frequencies). The >300nm optical bandwidth ensures UHR of ~1µm and <-120dBc/Hz RIN ensures low excess noise of OCT images. Theoretical/numerical investigations will be performed to optimize the RIN of SC generation.

3.3. Development of low excess noise UHR SD OCT system

In the final objective, low excess noise, UHR OCT system will be developed by utilizing the low excess intensity noise SC source developed above along with standard OCT components as shown in figure 5.

The noise performance will be evaluated by acquiring OCT images of various phantoms and will be compared with existing research grade and commercial OCT systems.

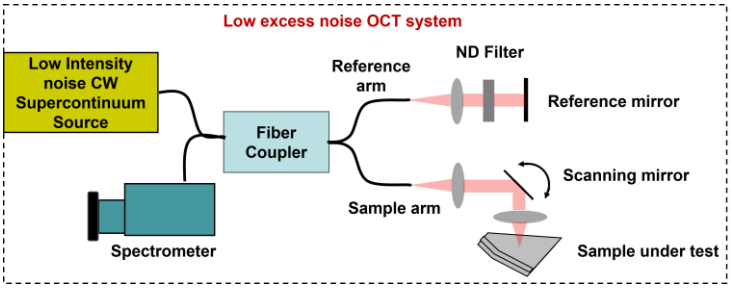

Fig. 5. Schematic of low excess noise UHR OCT system

Theoretical and Numerical analysis of SNR performance evaluation of the OCT system and the images will be performed.

Below is the summary of all the objectives with timelines to achieve the goal of this project.

Task	1-6 mos.	7-12 mos.	13-18 mos.	19-24 mos.
1. Development of low excess intensity noise, 50W class, 1-1.5µm tunable wavelength Raman fiber laser	■	■		
1.1. Purchase of all the components necessary for low excess intensity noise YDFA	■			
1.2. Purchase of components necessary for Raman conversion	■			
1.3. Development of low excess intensity noise, 100W class phase modulated single frequency YDFA		■		
1.4. Development of YDFA pumped tunable Raman fiber laser		■		
1.5. Theoretical and Numerical analysis of RF phase modulation schemes for RIN optimization of Raman fiber lasers	■	■		
2. Development of low excess intensity noise SC source using the above tunable Raman fiber laser.			■	
2.1. Purchase of components necessary for SC generation	■			
2.2. Theoretical and Numerical analysis of RF phase modulation schemes for RIN optimization of SC generation.			■	■
3. Development of low excess noise OCT system using the above SC source.				■
3.1. Purchase of components of OCT system except the optical source		■		
3.2. OCT experiments on the tissue phantoms using the above system				■
3.3. Theoretical and Numerical analysis of SNR performance evaluation of the OCT system and the images obtained			■	■

4. Intended Outcomes

1) Publications/Patents on low excess noise continuous wave (CW) tunable Raman fiber lasers based on low noise YDFAs.

2) Publications/Patents on low excess noise CW SC generations methods in conventional optical fibers.
3) Publications/Patents on the developed OCT system and its performance enhancements.
4) Protype of low excess noise, low-cost UHR OCT system using the developed SC source.
5) Transfer of this technology to an Indian company, Innovation Imaging Technologies Pvt Ltd (IITPL), for realization of the first UHR OCT system in India.
6) Trained graduate students with skills in fiber lasers analysis, design and development, nonlinear fiber optics etc. to either take industry or academic jobs.

5. Impact

(1) Research: It disseminates new knowledge and techniques on CW, low-noise nonlinear frequency generation through SC and it's RIN properties which has been least considered in the literature.
(2) Technology: It develops fiber-based low excess noise CW tunable wavelength and SC sources, low-complex, shot-noise limited OCT system for early-stage detection of many pathologies. Due to its low-cost nature, it enables wide accessibility of UHR OCT to billions of underserved populations in low-income, developing countries.

6. References

1. J. Fujimoto and E. Swanson, "The development, commercialization, and impact of optical coherence tomography," Invest. Ophthalmol. Visual Sci. 57(9), OCT1–OCT13 (2016).
2. Ali S, Gilani SBS, Shabbir J et al. Optical coherence tomography's current clinical medical and dental applications: a review, F1000Research 2021, 10:310 (https://doi.org/10.12688/f1000research.52031.1)
3. Johannes F. de Boer, Rainer Leitgeb, and Maciej Wojtkowski, "Twenty-five years of optical coherence tomography: the paradigm shift in sensitivity and speed provided by Fourier domain OCT [Invited]," Biomed. Opt. Express 8, 3248-3280 (2017).
4. A. Unterhuber, B. Považay, K. Bizheva, B. Hermann, H. Sattmann, A. Stingl, T. Le, M. Seefeld, R. Menzel, M. Preusser, H. Budka, C. Schubert, H. Reitsamer, P. K. Ahnelt, J. E. Morgan, A. Cowey, and W. Drexler, "Advances in broad bandwidth light sources for ultrahigh resolution optical coherence tomography," Phys. Med. Biol. 49, 1235–1246 (2004).
5. D. S. S. Rao, M. Jensen, L. Grüner-Nielsen, J. T. Olsen, P. Heiduschka, B. Kemper, J. Schnekenburger, M. Glud, M. Mogensen, N. M. Israelsen, and O. Bang, "Shot-noise limited, supercontinuum based optical coherence tomography," Light Sci. Appl. 10, 133 (2021).
6. Fathipour, V., Schmoll, T., Bonakdar, A. et al. Demonstration of Shot-noise-limited Swept Source OCT Without Balanced Detection. Sci Rep 7, 1183 (2017).
7. K. L. Corwin, N. R. Newbury, J. M. Dudley, S. Coen, S. A. Diddams, B. R. Washburn, K. Weber, and R. S. Windeler, "Fundamental amplitude noise limitations to supercontinuum spectra generated in a microstructured fiber," Appl. Phys. B 77, 269–277 (2003).
8. J. M. Dudley, G. Genty, and S. Coen, "Supercontinuum generation in photonic crystal fiber," Rev. Mod. Phys. 78, 1135–1184 (2006).
9. Benoît Sierro, Pascal Hänzi, Dirk Spangenberg, Anupamaa Rampur, and Alexander M. Heidt, "Reducing the noise of fiber supercontinuum sources to its limits by exploiting cascaded soliton and wave breaking nonlinear dynamics," Optica 9, 352-359 (2022).
10. N. R. Newbury, B. R. Washburn, K. L. Corwin, and R. S. Windeler, "Noise amplification during supercontinuum generation in microstructure fiber," Opt. Lett. 28, 944-946 (2003).
11. Etienne Genier, Patrick Bowen, Thibaut Sylvestre, John M. Dudley, Peter Moselund, and Ole Bang, "Amplitude noise and coherence degradation of femtosecond supercontinuum generation in all-normal-dispersion fibers," J. Opt. Soc. Am. B 36, A161-A167 (2019).
12. C. J. S. de Matos, S. V. Popov, and J. R. Taylor, "Temporal and noise characteristics of continuous-wave-pumped continuum generation in holey fibers around 1300nm", Appl. Phys. Lett. 85, 2706-2708 (2004).
13. V. R. Supradeepa, Y. Feng, and J. W. Nicholson, "Raman fiber lasers," J. Opt. 19, 023001 (2017).
14. Y. Feng and L. Zhang, "High power Raman fiber lasers" in Raman Fiber Lasers, Berlin, Germany:Springer, 2017.
15. Rashmita Deheri, Sarthak Dash, V. R. Supradeepa, and V. Balaswamy, "Cascaded Raman fiber lasers with ultrahigh spectral purity," Opt. Lett. 47, 3499-3502 (2022).

PROJECT NAME: Direct Subjective Refraction. CATEGORY: Health.

We receive about 80% of information about the world through our eyes, making vision the most important sense for humans. And not only that, but a clear image must reach our retina. **Refractive errors** (myopia, hyperopia, astigmatism, presbyopia) affect up to 67% of the global population and 100% over 50 years. Furthermore, preventable refractive error affects 1 billion people worldwide, representing the 1st cause of visual impairment and the 2nd cause of visual loss according to WHO (UN), with dramatic consequences at social and economic levels and, impacting life quality for people. The evaluation of refractive error is the basic piece of information about the state of the eye and is the main test performed in eyecare clinics worldwide. The gold standard method for diagnosis is called **subjective refraction** and consists of identifying different letters through different lenses until achieving the best combination of lenses providing the best visual acuity. This traditional approach is highly variable (0.27 D), time-consuming (>6 minutes), and is affected by accommodation.

We have developed a new method called **Direct Subjective Refraction (DSR)**, which uses a tunable lens to create fast and periodic defocus changes that, combined with the chromatic aberration of the eye and a bichromatic stimulus, creates a chromatic flicker perception which is minimum when the patient is perfectly compensated. The task of the patient in the DSR method is minimizing the chromatic flicker. We showed that the DSR task is easy, barely requires supervision (clinicians explain the task and patients perform it autonomously), decreases measurement time by 5x, and increases precision by 2x compared to the traditional method**.** Besides, it can help to standardize the measurement of refractive error by removing the need for letters (different alphabets) and extending it to the illiterate population.

First clinical measurements have shown the potential of the new method and have allowed us to acquire invaluable feedback from the clinicians, the final user. The DSR method brings **a revolution to the eyecare community** as the first subjective method that provides a prescription without identifying letters. The high precision and low measurement time make SureVision a potential candidate for replacing current paradigms, as their advantages overpass current devices and improve all the agents involved: patients, clinicians, clinics, and manufacturers.

The main goal of this project is to **provide definitive evidence and increase the scientific knowledge of the Direct Subjective Refraction method and expand the applications** of this novel method. In summary, the main activities that will be performed are: 1) build various optical setups to measure different features of the visual function while performing the DSR task; 2) design and perform psychophysical experiments to increase the scientific knowledge of the DSR method; 3) perform engineering efforts to add other functionalities to the current DSR optical system; and 4) perform measurements to increase the clinical evidence of the benefits of the DSR method.

In IO-CSIC the project has been developed since the conception of the idea to the implementation and the proof of concept in patients.

- Facilities that have evolved ad-hoc for the development of the project in software and hardware.
- The research group has created and established robust international networks of collaborators with different expertise like University of Pennsylvania, University of Rochester, Complutense University of Madrid, and University of Granada.
- Our institution relies on protocols and committees to ensure the regulation in terms of responsible and ethical research.

In the long term, the project will be highly transformative, as it will represent a **disruptive method** to measure the refractive error. Increasing the clinical and scientific confidence in the fast and accurate prescription obtained with the Direct Subjective Refraction method would create a positive impact in the community, generating value, and a return on the investment to society. Therefore, the successful completion of the OPTICA Challenge project will bring a positive impact on the community at large, healthcare, economic growth, preventable blindness, and well-being in general, aligned with the Sustainable Development Goals (3, 8, and 10) of the United Nations.

LITERATURE REVIEW

We receive about 80% of the world's information through our eyes, making vision the most important sense for humans[1]. Not only that, but a clear image must reach our retina. **Refractive error** is the visual condition in which light is not properly focused on the retina, resulting in blurred vision and the need for external compensation to be able to focus. Prescription evaluation is probably the most common eye exam procedure in which doctors measure the refractive error of the eye. Refractive errors are classified as myopia, hyperopia, astigmatism, and presbyopia. It affects 67% of the world's population and 100% of people over the age of 50, resulting in more than 4 billion people using some form of vision correction. This number is expected to increase due to the aging population and the rise in myopia, which is expected to reach 50% of the population by 2050[2]. Furthermore, preventable refractive errors affect 1 billion people worldwide, representing the 1st cause of visual impairment and the 2nd cause of vision loss according to the World Health Organization, with dramatic social and economic consequences and impact on people's quality of life. Although it is not a fatal disease, it is highly disabling if not diagnosed and corrected, and it progressively reduces people's quality of life. Therefore, the determination of refractive error is a critical aspect of eye care. Not only does it guide the prescription of corrective lenses, but it also serves as a fundamental means of obtaining basic information about the condition of the patient's eyes, such as emmetropia, moderate or high myopia or hyperopia, and more. This preliminary assessment often precedes several other ophthalmic procedures.

Refractive error can be diagnosed in several ways. It can be evaluated **objectively** by measuring some features of the optical system of the eye (surface curvature, axial length, optical aberrations, among others). In recent years, there have been many advances in these technologies, and the measurements generally require very little time. However, clinicians consider this measurement to be a starting point for the subjective measurement rather than a definitive measurement[3]. **The subjective** evaluation uses a process called **subjective refraction**, which requires the patient to identify different letters through different lenses while the clinician asks questions about the preference of one lens over another.

Subjective refraction is a **time-consuming** procedure. It entails, for each patient's eye, the full dedication of a well-trained eye care professional for **>6 minutes**[4], and can be much more in some patients. For many eye care practitioners, subjective refraction is a significant part of their daily workload. The limited presence of optometrists stands as a primary factor contributing to non-corrected refractive errors in developing regions, creating a bottleneck within eye care services. Time limitations in optometry practice restrict the extent of comprehensive eye examinations and visual tests. The **variability** of traditional subjective refraction is high **(around ±0.28D)**[3] and it is closely related to the constraints in measurement time to be reported. These errors are significant, as reported by several authors[5,6,7]. In summary, although the visual system can adapt, accurate prescriptions are still needed for comfortable and precise vision.

Accommodation, the ability of the eye to change the focusing position, has a strong influence on the subjective refraction procedure. During the procedure, accommodation can be activated and can typically result in overcorrection of myopia or undercorrection of hyperopia, especially in young subjects, where the accommodative response is fully functional. To reduce the effects of accommodation, the most used method is the **fogging** technique, which consists of adding positive power (myopic defocus that cannot be compensated by the eye's accommodation) to blur the letter test and then decreasing this addition in small steps. Although this technique is effective in reducing the influence of accommodation, it involves a long detour in the evaluation, which increases the measurement time and thus the patient's fatigue.

---

[1]. Hutmacher F. Why Is There So Much More Research on Vision Than on Any Other Sensory Modality? Front Psychol. 2019 Oct 4;10:2246. doi: 10.3389/fpsyg.2019.02246.

[2].Holden BA, Fricke TR, Wilson DA et al. Global Prevalence of Myopia and High Myopia and Temporal Trends from 2000 through 2050. Ophthalmology. 2016; 123:1036-42

[3]. Elliott DB. Clinical Procedures in Primary Eye Care, 3rd edition. Clin Exp Optom. 2008;91:496-497.

[4] Rodriguez-Lopez, Dorronsoro. Beyond traditional subjective refraction. Current Opinion in Ophthalmology. 3(3), 228-234 (2022).

[5] Atchison DA, Schmid KL, Edwards KP, et al. The effect of under and over refractive correction on visual performance and spectacle lens acceptance. Ophthalmic Physiol Opt. 2001;21(4):255–61.

[6] Bist J, Kaphle D, Marasini S, Kandel H. Spectacle non-tolerance in clinical practice – a systematic review with meta-analysis. Ophthalmic Physiol Opt. 2021;41(3):610–22.

[7] Freeman CE, Evans BJW. Investigation of the causes of non-tolerance to optometric prescriptions for spectacles. Ophthalmic Physiol Opt. 2010;30(1):1–11.

PROBLEM STATEMENT/OBJECTIVE

Over the years, efforts have been made to enhance efficiency by developing objective techniques that eliminate the subjective and iterative nature of traditional methods. Modern objective refraction instruments, many of which are open-field, wavefront-based, portable, or combined with keratometry, has become widespread in clinics. However, objective autorefractors are not considered to yield results that are directly interchangeable with subjective refraction. Instead, they serve as a valuable starting point for the subjective refraction procedure[2,3].

Attempts have been made to introduce new technologies aimed at simplifying the traditional method, such as Vision-R 800T (Essilor), i.Scription (Zeiss), Chronos (Topcon), NidekTS-610 (Nidek), Netra (EyeNetra), Easee eye test (Easee), VARS (VmaxVision), EyeRefract (Visionix), and VAO (Voptica)[3]. These instruments offer certain advantages such as automation, self-refraction, or a combination of subjective and objective techniques. However, these instruments are based on variations of the traditional subjective refraction, and, while they bring some improvements, they are still subject to the intrinsic limitations and constraints associated with the traditional method of identifying letters or minimizing blur.

In the Institute of Optics from CSIC (Madrid, Spain), we have developed a new method to evaluate the refractive error called **Direct Subjective Refraction (DSR)**, which uses a disruptive working principle based on the use of quick defocus changes in combination with a bichromatic stimulus (made of blue and red components) to create a chromatic flicker. In short, the quick change in defocus produces a flicker perception of the stimulus, which affects more to blue components when the subject is myopic, to red components where is hyperopic, and it is minimal in the best prescription. This video shows the working principle. Therefore, the task of the subject in this method is to minimize the flicker, being the **first subjective method that does not use the letter identification** of the traditional method to find the refractive error. We have shown that this method **reduces measurement time by 5x** (from 6 to 1.2 minutes) and **increases repeatability** (from ±0.28 to ±0.17 D) compared to the traditional method[8]. The improvement of this method is explained because **the accommodation response barely influences**, which stays in a fixed position due to the impossibility of following the fast defocus change, largely eliminating the main issue of the traditional method. Besides, it is an **autonomous** procedure as patients can perform it by themselves (previous explanation of the task by the clinician). Another advantage of the DSR resides in the elimination of letters to evaluate the refractive error. The use of a flicker-minimization task instead of the letter-identification task is a way of standardizing the evaluation due to the use of different alphabets in different parts of the world and at the same time could increase access to the evaluation for the illiteracy population.

The DSR method was developed during the PhD thesis of the Project Leader, Victor Rodriguez Lopez[9]. A pilot study was carried out to test the proof-of-concept in 25 volunteers. It was proved that the DSR method is much faster (<1 minute) and more repeatable (±0.17 D) than the traditional method. Besides, the method was extended to provide a full prescription (both the spherical equivalent and the amount of astigmatism)[8] and its robustness against different stimuli configurations has been confirmed[10].

On the other hand, the prevalence of myopia in the population is increasing and becoming a true epidemic. The main hypothesis that justifies this increase is defocus in the periphery of the retina. In ocular development, peripheral defocus plays an important role in the emmetropization of the eye, i.e. the process of eye growth to adjust the optical power and the retinal plane. Emmetropization is controlled by peripheral defocus to determine whether the eye will grow or not. However, in myopic eyes, the presence of peripheral defocus stimulates abnormal eye growth and results in increased myopia. Characterizing peripheral defocus can help develop compensations that consider the entire prescription, foveal and peripheral. Traditional subjective refraction in the periphery is not possible because the resolution is very low due to the low sampling of ganglion cells in the peripheral areas of the retina. This is a major limitation in myopia monitoring. However, the chromatic flicker of Direct Subjective Refraction activates different neural pathways focused on temporal change and motion detection, which are more accurate than the spatial

---

[8] V. Rodríguez-Lopez, A. Hernandez, C. Dorronsoro. Defocus flicker deactivates accommodation. Biomed. Opt. Exp (2023) https://doi.org/10.1364/BOE.486466. Biomedical Optics Express 14, 3654-3670 (2023).

[9] V. Rodríguez-Lopez. Perception of static and dynamic blur for developing clinical instrumentation in optometry and ophthalmology. PhD in Biomedical Sciences and Technologies. Defended 25th November 2022.

[10] V. Rodríguez-Lopez, C. Sanchez-García, E. Esteban-Ibañez, N. Arejita, C. Dorronsoro. Robustness of the Direct Subjective Refraction method. Association for Research in Vision and Ophthalmology Conference (ARVO) New Orleans, 2023

resolution pathways. Therefore, Direct Subjective Refraction offers new opportunities for peripheral refractive error measurement for better monitoring of myopia progression and the development of personalized optical compensations.

To date, many **scientific contributions** have been produced:

- 5 contributions to ARVO Annual Meetings (2019 -hot topic, among the 5% best contributions of the conference over 12.000-; 2021; 2023; and 2 to 2024), the most important conference in ophthalmology and vision science, and 2 more to other important international meetings in visual science (Biophotonics Eye Research Conference 2023; Spanish National Optics Conference 2024).
- 3 invited talks in American-European Congress of Ophthalmic Surgery (AECOS) 2023 (in person), Young Researchers in Biophotonics Winter Meeting 2024 (online), and Optica Vision & Color Summer Data Blast Session organized by Optica (online).
- 3 papers published in high-impact journals: 1) *Beyond Traditional Subjective Refraction*, Current Opinion in Ophthalmology, 2) *Defocus flicker deactivates accommodation* in Biomedical Optics Express and 3) *The spatiotemporal defocus sensitivity function* in Biomedical Optics Express.
- 1 PhD thesis[8].
- 1 patent (P190451ES, CSIC owner) was filled on 4th March 2019 and accepted on 7th April 2021, and PCT extended to Europe, the US, and Japan.
- 5 Master's Thesis.

The main goal of this project is to increase the scientific knowledge and evidence of the Direct Subjective Refraction method and to expand the applications of this novel method. In summary, the main activities that will be performed are: 1) building different optical setups to measure different features of visual function while performing the DSR task (Figure 1); 2) designing and performing psychophysical experiments to increase the scientific knowledge of the DSR method and the robustness of the measurement; 3) engineering efforts to add other functionalities to the current DSR system; 4) carrying out clinical measurements to increase the scientific evidence of the benefits of the DSR method.

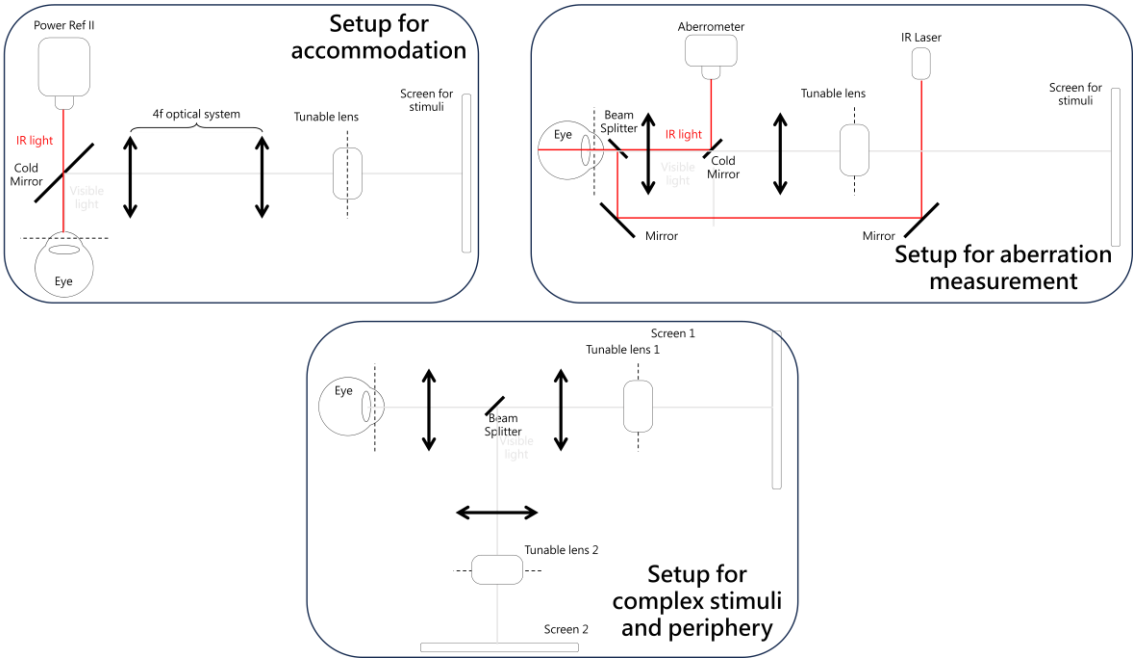

Figure 1. Setups planned to achieve the project goals. See the Work Plan Timeline for more information.

OUTCOME(S)

The disruptive nature of the technology makes Direct Subjective Refraction the first subjective method that does not use letter identification as its working principle, like the traditional method, but chromatic flicker minimization. The research has a high impact on fundamental aspects of the optical and perceptual mechanisms of vision, with direct application to the most common clinical test used to evaluate ocular health. Impacts are expected in the following areas: (1) understanding of the perceptual consequences of rapid

defocus changes for different chromatic channels, luminance levels, and pupil size, among other conditions, (2) optimization of the Direct Subjective Refraction task, (3) build various optical setups to measure different features of the visual function while performing the DSR task, (4) extension of the Direct Subjective Refraction method to other measurements such as peripheral refraction, (5) clinical validation of Direct Subjective Refraction.

The main expected outcomes are:

- 2-3 scientific papers in high-impact journals (Optica, Eye, Biomedical Optics Express, Journal of Vision, Ophthalmology, Current Biology, Nature Communications, among others).
- 1 patent application protecting the novel optical system, growing the family patent of the method, and considering PCT extension to other regions of interest.
- Incorporation of 1 junior engineer for carrying out the engineering developments described in the work plan.
- Foster collaborations with international highly reputed laboratories (Johannes Burge de Burge Lab, University of Pennsylvania, Philadelphia, USA, Brian Vohnsen de Vohnsen Lab, University of Dublin, Ireland, and Marcos Lab, University of Rochester, Rochester, USA).
- Explore collaborations with international leader companies in Ophthalmic Optics (Essilor International, Johnson & Johnson, Alcon Research Labs, Advanced Medical Optics, Indizen Optical Technologies), most of them with previous collaborations with the research group.
- Participation in international conferences: Annual Meeting of the Association for Research in Vision and Ophthalmology, European Society of Cataract & Refractive Surgeons, American Society of Cataract & Refractive Surgeons, OPTICA-Frontiers in Optics, SPIE-Photonics West, or Visual and Physiological Optic meeting; all of them previously attended by the fellow or other team members.

IMPACT

Direct Subjective Refraction is a technology that enables a fast and accurate evaluation of refractive errors, significantly reducing measurement time while increasing precision. It represents a turning point in the way vision has been evaluated in the last decades, with the potential for transforming not only the eyewear industry but also society as a whole. As mentioned before, novel methods are mainly modifications of the traditional method and therefore maintain their disadvantages. This method is the first that uses a different subjective approach to provide a prescription, minimization of chromatic flicker.

All agents involved are benefited:

- **For patients**. Reduces fatigue and measurement time associated with obtaining the prescription, providing an accurate prescription in a very short time. The suitability of the new method will increase access to a simple prescription for patients who currently do not have it. The patient can benefit from both more time to obtain a more complete visual exam as well as obtaining a *premium* prescription.
- **For clinicians**. It reduces measurement time, allowing them to use that extra time to perform more tests in a complete visual exam or to measure more patients while providing a very accurate prescription.
- **For clinics**. It improves overall efficiency and can pay back in a very short time the improvements that DSR provides, both in more accurate or *premium* prescriptions, as well as using the time savings on more patients or more vision tests.
- **For lens manufacturers**. Reduce returns by having a more accurate prescription. In addition, the current minimum lens pitch is ±0.25 D in most cases. DSR stimulates technological progress by promoting the possibility of more accurate lens manufacturing.
- **Screening companies and NGOs** could benefit from the advantages of DSR, as it provides an accurate and autonomous prescription with portable and accessible equipment.

Furthermore, DSR has a potentially significant impact on the eyewear industry. The high precision of the DSR method can lead to a reduction in the number of returns and exchanges, thereby reducing waste and CO_2 footprint and improving the sustainability of the industry. Additionally, the customization can provide the opportunity for more innovative and personalized eyewear designs, catering to individual needs.

The project has a strong relationship with the **Sustainable Development Goals** of the United Nations, mainly with Goal 3 (Good health and well-being), 8 (Decent work and economic growth), and 10 (Reduced inequalities). From the ethical perspective, the project will be carried out in accordance with ethical standards for research, national and EU regulations and will be submitted to CSIC's Ethical Committee for approval.

As a summary, increasing the scientific evidence of the DSR method and a potential transfer of the technology to society will be highly transformative, revolutionizing how refractive error is measured with a disruptive approach. It will also serve as an incentive for the ophthalmic industry, as more precise prescriptions will require new expertise and resources. The scientific and clinical progress expected from this project will produce a positive impact on the community at large, healthcare, economic growth, preventable blindness, and well-being in general, aligned with the Sustainable Development Goals of the United Nations.

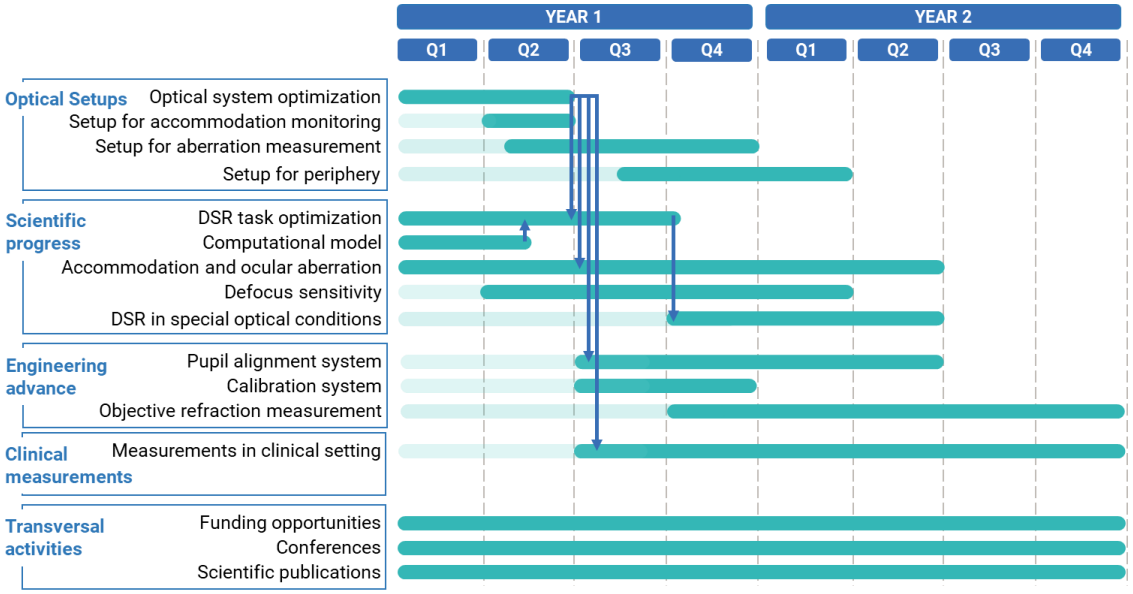

Figure 2. Gantt Chart of activites planned during the project.

TARGETING RETINA MICROVASCULATURE TO IDENTIFY THE LINK BETWEEN DIABETES AND NEURODEGENERATIVE DISEASES (VASCULINK)

GROUND-BREAKING NATURE OF THE PROJECT

The VASCULINK proposes a novel multimodal methodology for the use of photonic technologies in the diagnosis of diabetes mellitus (DM) complications and the development of related dementia, in particular Alzheimer's disease (AD).

In this study, my unique experience in the field of various modern optical imaging techniques and my biomedical background will be used to answer the question of how DM and AD are related, as well as to provide evidence that the eye retina can act as a target for early diagnosis of both pathological conditions. A novel retinal imaging tool will be developed that combines structural and functional retinal imaging techniques, including laser speckle contrast, fluorescence lifetime, hyperspectral and polarization imaging. The Project aims to provide a groundbreaking characterization of retina vasculature in DM and AD, for the first time establishing how cerebral microvasculature and metabolic parameters are altered in these diseases.

KEY CONCEPT AND RESEARCH OBJECTIVES

The Project has **two main scientific challenges (SC)**. The first scientific challenge **SC1** is: **What is the link between DM and AD?** Dementia, in particular AD, and DM are two diseases that are growing at an alarming rate among the world's population. The link between AD and DM has recently been the subject of close study by specialists. Observation of DM patients showed that they were 2 times more likely than other subjects to develop AD for 15 years. These patients were 1.75 times more likely to develop other types of dementia. Among the scientific community, it is increasingly common to find the opinion that AD is the “third type” of diabetes.

Cognitive impairment and dementia associated with DM can be mediated through vascular factors, including primarily the development of microangiopathy. Many studies have focused on altering insulin signaling in the brain as a possible mechanism for the link between AD and DM, but researchers have paid much less attention to the direct effect of vascular dysfunction on the pathogenesis of AD. Vascular problems can contribute to the development of inflammation and oxidative stress in the brain, which in turn can lead to damage to neurons and contribute to the development of AD.

Thus, although the relationship between DM and AD is obvious, it is complex, multicomponent and requires detailed study. At the same time, there are a limited number of instrumental methods that would allow a comprehensive study of the effect of vascular complications of DM on the development of AD.

In this regard, a second scientific challenge **SC2** is: **How to evaluate the development of DM and AD at an early-stage?** It is known the retina and the brain have the same embryological origin. They both originate from the neural tube. Thus, the retina is the only part of the central nervous system that can be noninvasively visualized by optical methods with subcellular resolution and used as “a window into the brain”. Recent studies have shown that people with DM and AD may experience structural and functional changes in the retina. These changes may include thinning of the retinal nerve fiber layer and changes in the retinal blood vessels (changes in stiffness, vessel caliber, branching structure, and fractal dimension). Also, the toxic beta-amyloid peptide (Aβ) was found in the retina of people with AD.

Thus, retinal imaging has the potential as a non-invasive and cost-effective method for detecting early signs of diabetes and dementia and may also make it possible to trace the link between these two pathological conditions.

In this Project, I propose the development of a multimodal optical system that would allow the first time to study a number of parameters of retinal tissue (morphology and stiffness of the vessels, blood velocity and oxygenation, metabolic activity, AGE and Aβ accumulation) *in vivo* and find patterns associated with the development of DM and AD. The Project work program includes ambitious but achievable goals. It has been developed using the track record of my multidisciplinary achievements in biomedical engineering, biophotonics, cell biology, and clinical studies and the unique research environment and world-renowned experts at the Host.

TARGETING RETINA MICROVASCULATURE TO IDENTIFY THE LINK BETWEEN DIABETES AND NEURODEGENERATIVE DISEASES (VASCULINK)

PROBLEM STATEMENT/OBJECTIVE

Dementia and diabetes mellitus (DM) are two diseases that are growing at an alarming rate among the world's population. According to the GBD 2019 Dementia Forecasting Collaborators study, the number of people with dementia alone will increase from 57M cases worldwide in 2019 to 153M cases in 2050. In addition, by 2040, this category of diseases will become the second most common cause of death in developed countries. At the same time, Alzheimer's disease (AD) accounts for 60-70% of cases. According to the International Diabetes Federation, the problem of high-quality diagnosis and effective treatment of DM is also one of the most acute in modern healthcare. In 2021, there were 537M patients with DM in the world, and by 2045, this number is projected to increase to 783M. DM is one of the ten deadliest diseases with an annual mortality rate of over 1M.

AD and DM have recently been the subject of close study by specialists. Observation of DM patients showed that they were 2 times more likely than other subjects to develop AD for 15 years. These patients were 1.75 times more likely to develop other types of dementia [*Ott A. et al., Diabetes mellitus and the risk of dementia: The Rotterdam study, Neurology 53, 1937 (1999); Yaffe K. et al., Diabetes, impaired fasting glucose, and development of cognitive impairment in older women, Neurology 63, 658 (2004)*]. Among the scientific community, it is increasingly common to find the opinion that AD is the “third type” of diabetes.

There are many common pathogenetic mechanisms underlying both diseases: insulin resistance, hyperinsulinemia, chronic hyperglycemia, acute hypoglycemic episodes, inflammation, dyslipidemia, oxidative stress, mitochondrial dysfunction, etc. Cognitive impairment and dementia associated with DM can also be mediated through vascular factors, including primarily the development of microangiopathy. Many studies have focused on altering insulin signaling in the brain as a possible mechanism for the link between AD and DM, but researchers have paid much less attention to the direct effect of vascular dysfunction on the pathogenesis of AD. Vascular problems can contribute to the development of inflammation and oxidative stress in the brain, which in turn can lead to damage to neurons and contribute to the development of AD. Although the toxic beta-amyloid peptide (Aβ) was first isolated from the blood vessels of the brain of patients with Alzheimer's disease, the contribution of pathological changes in the vascular tissue of the brain to the disease has not been sufficiently studied.

Thus, although the relationship between diabetes mellitus and AD is obvious, it is complex, multicomponent and requires detailed study.

At the same time, there are a limited number of instrumental methods that would allow a comprehensive study of the effect of vascular complications of DM on the development of AD. Modern technologies of *in vivo* examination of brain vessels are limited by CT angiography, which, in addition to radiation exposure, is associated with the use of contrast agents. Technologies for detecting Aβ and tau protein pathology in AD using positron emission tomography (PET) of the brain or cerebrospinal fluid (CSF) studies are limited due to their high cost, technical complexity, invasiveness of procedures and the need to use radioactive indicators. Thus, the identification of alternative, more accessible technologies and biomarkers of preclinical manifestations of DM and AD and their relationship can accelerate understanding of the pathogenesis of both diseases, facilitate screening and risk stratification, and ultimately help in the discovery, development and testing of new treatments or preventive therapies in clinical trials.

It is known the retina and the brain have the same embryological origin. They both originate from the neural tube. Thus, the retina is the only part of the central nervous system that can be noninvasively visualised by optical methods with subcellular resolution and used as “a window into the brain”.

Recent studies have shown that people with diabetes and AD may experience structural and functional changes in the retina. These changes may include thinning of the retinal nerve fibre layer and changes in the retinal blood vessels (changes in stiffness, vessel calibre, branching

structure, and fractal dimension). Also, the pathological Aβ protein was found in the retina of people with AD.
Thus, retinal imaging has the potential as a non-invasive and cost-effective method for detecting early signs of diabetes and dementia, and may also make it possible to trace the link between these two pathological conditions.
In this Project, Dr. Dremin proposes the development of a multimodal optical system that would allow the first time to study a number of parameters of retinal tissue *in vivo* and find patterns associated with the development of DM and AD (see **Fig. 1**).

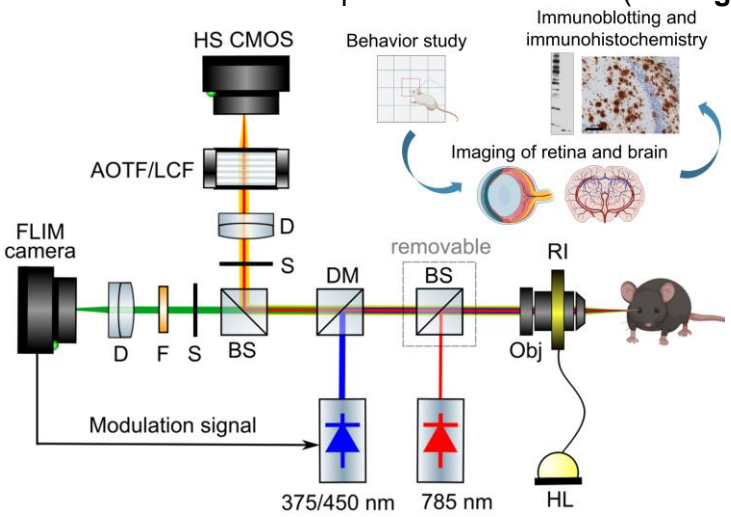

Fig. 1. *Simplified optical scheme of the proposed diagnostic sytem and the main concept of the Project. D, doublet; F, emission filter; S, shutter; BS, beamsplitter; DM, dichroic mirror; RI, ring illuminator; HL, halogen lamp; AOTF, acousto-optic tunable filter; LCF, liquid crystal filter; HS CMOS, high-speed camera; 375/450 nm, fluorescence excitation lasers; 785 nm, laser for LSCI.*

In this study, the unique experience of Dr. Dremin in the field of various modern optical imaging techniques and his biomedical background will be used to answer the question of how DM and dementia (in particular AD) are related, as well as to provide evidence that the retina can act as a target for early diagnosis of both pathological conditions. A novel retinal imaging tool will be developed that combines structural and functional retinal imaging techniques, including laser speckle contrast, fluorescence lifetime, hyperspectral and polarization imaging.
At the same time, these goals are related to the problems of physiology and data processing. One of the most important tasks will be the interpretation of data obtained from animal models and the development of experimental protocols that will directly compare the state of the vessels of the brain and retina and translate the results into the language of human physiology, which will ensure the transfer of technology into clinical practice.
The project aims to provide a groundbreaking characterisation of retina vasculature in DM and AD, for the first time establishing how cerebral microvasculature parameters are altered in these diseases. Dr. Dremin envisages achieving the following **research objectives** (RO):

RO1. Development of a novel multimodal retina imaging system. Achieving this RO will allow us to obtain a new diagnostic system for comprehensive and deep analysis of vascular and metabolism parameters of retinal tissue.
RO2. Technique verification on phantoms and cell cultures. To achieve this goal, various retina-mimicking phantoms will be developed. Phantom calibration, as well as verification of sensitivity to metabolic shifts in retinal cell cultures, will make it possible to obtain a system ready for clinical testing.
RO3. Study of the microvasculature (morphology, stiffness, blood velocity, oxygenation, etc.), the metabolic activity, as well as AGE and Aβ accumulation in the retina and brain in a mouse model of DM (streptozotocin-induced) and AD (5xFAD). A comparison of the recorded characteristics will confirm the hypothesis that the retina may indeed be “a window into the brain”. As a result, this will allow us to study the relationship of DM complications with the development of AD, as well as demonstrate a new tool for early diagnosis of these diseases.

Partners of the Project:
Internal collaboration at Aston University: Prof. Rhein Parri, neuroscience; Prof. James Wolffsohn, optometry; Dr. Srikanth Bellary, endocrinology.
External academic collaborations: Prof. Andrey Abramov, cell physiology and neuropathology (UCL); Assoc. Prof. Merce Masana, neuroscience (University of Barcelona).
Industrial collaboration: Occuity Ltd., optometry (UK).

LITERATURE REVIEW

Currently, there are a number of methods for *in vivo* retinal examination, namely fundus photography, optical coherence tomography of retinal morphology and angiography associated with the introduction of contrast agents. None of these methods can provide information about the dynamics and regulation of blood flow, vascular stiffness, oxygenation and metabolism of tissues and the accumulation of AGEs and Aβ. At the same time, changes in these parameters may be directly related to the development of both diseases. The development of next-generation computing technologies, such as artificial intelligence and deep learning algorithms, can further expand the potential of imaging the retina with a large amount of data as a promising tool and source of biomarkers for DM and AD, especially for people at the preclinical stage of both diseases.

Modern optical imaging techniques can be successfully used for a detailed analysis of the state of microvasculature and the metabolism of retinal tissues.

Fluorescence life-time measurement

Registration and analysis of fluorescence intensity and lifetime will provide information on the chemical composition and metabolism of retinal tissues through the determination of endogenous fluorophores such as nicotinamide adenine dinucleotide (NADH), flavin adenine dinucleotide (FAD), collagen, lipofuscin, etc. The two essential metabolic cofactors, NADH and NADPH, are required for energy production and antioxidant defence, respectively, and are generated in distinct pathways of glucose metabolism. Even though both NADH and NADPH can be measured by autofluorescence, these cofactors have a similar spectrum and cannot be separated by simple measurement of fluorescence intensity. Measuring the fluorescence lifetime opens up completely new possibilities [*J. Lakowicz, Principles of fluorescence spectroscopy, Springer, Boston, MA, 954 (2006)*]. However, the use of this technology for the study of whole organisms is still in its infancy. Moreover, to date, there have been no studies of metabolic changes in glucose metabolism directly in tissue *in vivo*. Recently, Dr. Dremin demonstrated the possibility of such measurements [*E. Potapova et al., Detection of NADH and NADPH levels in vivo identifies shift of glucose metabolism in cancer to energy production, FEBS J. (2024)*]. Thus, the technology proposed in this project to assess NADH and NADPH cofactor levels in retina tissues for the first time will help to understand the underlying glucose utilisation processes at DM and AD development.

DM hyperglycemia causes not only a malfunction of the vascular endothelium but also the general glycation of proteins with the formation of advanced glycation end-products (AGE) [*P. Gkogkolou, M. Bohm, Advanced glycation end products: key players in skin aging?, Derm. Endocrinol., 4(3), 259 (2012)*], which are responsible for the development of various DM complications, including retinopathy, and may be a factor in the development of dementia. It is known that the accumulation of AGE increases the intensity of autofluorescence of various biological tissues [*E. Gerrits et al., Skin autofluorescence: a tool to identify type 2 diabetic patients at risk for developing microvascular complications, Diabetes Care, 31(3), 517 (2008)*], which has also been shown in the works of the Applicant [*V. Dremin et al., Multimodal optical measurement for study of lower limb tissue viability in patients with diabetes mellitus, J. Biomed. Opt. 22(8), 085003 (2017)*]. Thus, the use of FLIM will make it possible to track both the accumulation of AGE in retinal tissues and the change in the fluorescence lifetime of the associated forms of NADH and FAD during protein glycation.

In this study, it is planned to use the latest advances in the development of frequency-domain FLIM cameras [*E. Potapova et al., Endofluorescence imaging of murine hepatocellular carcinoma cell culture by fluorescence lifetime microscopy with modulated CMOS camera, J. of Biomedical Photonics & Eng. 8(1), 010303 (2022)*]. One major advantage of frequency-domain FLIM over popular time-domain FLIM techniques, such as time-correlated single photon counting, is acquisition speed, making frequency-domain an ideal technique for real-time clinical application, as well as measuring rapid cellular processes.

Laser speckle contrast imaging

Laser speckle contrast imaging (LSCI), as a method of full-scale visualisation of blood flow dynamics with high temporal resolution, is implemented by wide-field illumination of the tissue

surface with a red or near-infrared (NIR) coherent light source and registration of the resulting speckle pattern by a camera [*A. Sdobnov et al., advances in dynamic light scattering imaging of blood flow, Laser Photonics Rev. 18(2), 2300494 (2023)*]. This method is closest to widespread use in clinical ophthalmology, although it still has a wide potential for development and improvement. The use of a high-speed (high-frame) camera will make it possible to implement a multi-exposure approach for quantifying the distribution of blood flow velocities in the retina. Unlike the tissues of the skin or brain, the retina is an excellent object for calculating the absolute values of blood flow velocity in individual vessels. Algorithms for time-frequency analysis of speckle contrast images will be developed to analyse the mechanisms of blood flow regulation, including the determination of cardiac pulse wave to calculate vascular stiffness [*D. Postnov et al., Cardiac pulsatility mapping and vessel type identification using laser speckle contrast imaging, Biomed. Opt. Express. 9(12), 6388 (2018)*]. This task will be solved using modern time series wavelet analysis approaches a great contribution to the development of which was previously made by the Fellow [*N. Golubova et al., Time-frequency analysis of laser speckle contrast for transcranial assessment of cerebral blood flow, Biomed. Signal Process. Control. 85, 104969 (2023); I. Mizeva et al., Wavelet analysis of the temporal dynamics of the laser speckle contrast in human skin, IEEE Trans. Biomed. Eng. 67(7), 1882–1889 (2019)*]. This approach will also significantly improve the contrast of blood vessels compared to the standard speckle contrast calculation method. Also, the use of time-frequency analysis will allow us to identify artefacts of eye movement and take this information into account when processing data.

Hyperspectral imaging

The analysis of the chromophore content, which allows the assessment of blood filling and oxygenation of the retina, can be performed using the hyperspectral imaging method providing a three-dimensional data array (hyperspectral cube of data), which includes spatial information (2D) about the object, supplemented with spectral information (1D) for each spatial coordinate. This technology is actively used in various fields of medical science, including endocrinology [*E. Zharkikh et al., Biophotonics methods for functional monitoring of complications of diabetes mellitus, J. Biophotonics 13(10), e202000203 (2020)*], and it has recently been shown that the spectral characteristics of diffuse reflection of the retina can vary greatly with the development of AD [*X. Hadoux et al., Non-invasive in vivo hyperspectral imaging of the retina for potential biomarker use in Alzheimer's disease, Nat. Commun. 10, 4227 (2019)*]. Currently, the use of the Fabry-Perot microinterferometer or acousto-optic and liquid crystal filters in conjunction with compact CMOS/CCD cameras makes it possible to design portable hyperspectral systems that can be easily deployed in clinical conditions.

However, despite the widespread use of hyperspectral technologies e.g. in the field of remote sensing, their clinical applicability is still in its early stages and requires in-depth scientific research. Since hyperspectral images contain hundreds of bands, they cannot be analysed by visual inspection, instead algorithms should be developed to extract meaningful information from images. Machine Learning and Pattern Recognition based methods can be very successful for this purpose, as they are able to automatically learn the relationship between the spectrum captured at each pixel of the image and the information that is desired to be extracted. Recently, Dr. Dremin has developed an approach based on neural network fitting, which allows to restore information about blood content and saturation in biological tissues in real time with high accuracy [*V. Dremin et al., Skin complications of diabetes mellitus revealed by polarized hyperspectral imaging and machine learning, IEEE Trans. Med. Imaging 40(4), 1207 (2021); E. Zherebtsov et al., Hyperspectral imaging of human skin aided by artificial neural networks, Biomed. Opt. Express 10, 3545 (2019)*]. This technique can be easily adapted for retinal tissue measurements.

Polarization measurements

As various pathologies progress in the tissue, significant changes occur in the content and organisation of collagen and cellular morphology. These changes lead to modifications of the scattering and birefringent properties of tissues, which can be detected using polarimetric optical methods [*C. He et al., Polarisation optics for biomedical and clinical applications: a*

review, Light Sci. Appl. 10, 194 (2021)]. Tissue aging and accumulation of AGEs also affect their polarization properties, as illustrated by Applicant in his previous studies [*V. Dremin et al., Incremental residual polarization caused by aging in human skin, J. Biomed. Opt. 29(5), 052912 (2023); V. Dremin et al., Skin complications of diabetes mellitus revealed by polarized hyperspectral imaging and machine learning, IEEE Trans. Med. Imaging 40(4), 1207 (2021)*]. Moreover, it has recently been shown that the Aβ accumulation in brain tissues also changes their polarization properties [*M. Borovkova et al., Screening of Alzheimer's disease with multiwavelength Stokes polarimetry in a mouse model, IEEE Trans. Med. Imaging 41(4), 977 (2022)*]. Thus, monitoring the polarization of retinal tissues can undoubtedly be a valuable tool for establishing a link between the development of DM and AD.
A hyperspectral imaging channel can be easily adapted to carry out these measurements. The tissues will be illuminated with linearly polarised light, and the corresponding optical elements in the detection path will allow recording co- and cross-polarized images relative to the incident light [*V. Dremin et al., Incremental residual polarization caused by aging in human skin, J. Biomed. Opt. 29(5), 052912 (2023)*]. Additionally, the possibility of integrating modern compact polarization cameras into the system, which provide the ability to analyse a wide range of polarimetric characteristics, can be considered.

OUTCOMES

The Project aims to develop a novel approach to the diagnosis and monitoring of DM and AD complications beyond the state-of-the-art. Understanding the relationship between DM and AD can help in developing strategies for the prevention and treatment of both diseases.
With the help of VASCULINK, this connection will be investigated and the transition from new hypotheses and technologies to real mechanisms, diagnosis and treatment will be ensured. In particular, VASCULINK will make a breakthrough in understanding the role of vascular parameter changes in DM and AD, which will provide a new treatment goal and allow the introduction of a new diagnostic method. Thus, this project will become the basis for large-scale inter-center clinical trials, through which it will be possible to predict and prevent the development of dementia in patients with DM. One of the main obstacles in the development of treatments for DM and dementia is their not fully understood etiopathogenesis. Given the insufficiency or even lack of effective ways to treat these diseases, the search for fundamentally new diagnostic methods and therapeutic targets will lead to the production of new compounds that can become the basis for the development of medicines.

IMPACT

If successful, the results of the Project will be of significant importance for healthcare (medical early diagnostics and monitoring), which, in turn, may have a high social impact in the next 5-10 years. This Project will allow the Dr. Dremin to become a highly qualified link between science and clinical medicine. In the future, the Project results will aid clinicians in accurate diagnosis and disease management, increasing positive patient outcome. Devices will improve the quality of clinical assessments as well as potential treatments through increased diagnostics speed, ultimately increasing the quality of life for the patient population with DM and AD. Project results will provide clinicians with a compact, reliable, fast, easy to use and relatively inexpensive tool to monitor the status of patients constantly. Such a tool is currently necessary in medical sectors around the world and presents itself as an as-yet unseen non-invasive device to help clinicians. Furthermore, the successful implementation of this Project could have significant and lasting effects on clinics Globally. The approach offered by a novel ophthalmological tool can provide unprecedented levels of care within the clinic. Diagnosis could be speed up and treatment periods can be accurately tailored to unique needs of the patient through objective assessment. This will ultimately improve patients' health condition and significantly lowering healthcare costs, with obvious advantages for both patients and health care services. It is very likely that, being used as a platform, the proposed method would pave the way for further research in various relevant strategically important areas, including oncology, dermatology, label-free biosensing, etc. Therefore, this Project will benefit numerous academic groups worldwide, working in the areas of biophotonics, laser and sensing systems, biomedical engineering, clinical research, advanced signal processing, etc.

Executive Summary of Proposal:

Intelligent high-throughput super-resolution imaging platform for precise diagnosis and treatment of rare diseases

Dr. Weisong Zhao (weisongzhao@hit.edu.cn)
Early-Career Member of Optica
Professor, School of Instrumentation Science and Engineering
Harbin Institute of Technology, China

According to the current medical records, approximately 10,000 rare diseases exist globally. However, due to the small number of patients and limited information for each rare disease, medical expertise is rare; knowledge is scarce; and research is limited. Many rare diseases cannot be accurately diagnosed, and the development of treatment drugs is difficult and costly. Therefore, there is a strong demand for precise diagnosis and treatment of rare diseases. Based on current research, researchers speculate that the phenotypes of genetic rare diseases caused by specific gene mutations are strong, and if suborganelle structures, dynamics, and functions can be observed more carefully at the subcellular level, their pathogenic mechanisms may be discovered.

By offering unprecedented levels of detail and clarity in imaging cellular structures and molecular interactions, super-resolution (SR) microscopy enables researchers to unravel the intricate mechanisms underlying these rare genetic disorders, shrinking the required medical sample size. Its high resolution and sensitivity empower scientists to observe subtle changes at the subcellular level, shedding light on disease progression, identifying potential therapeutic targets, and ultimately paving the way for more effective treatments.

In this proposal, we will construct an intelligent high-throughput bioimaging platform by integrating of ultrafast SIM imaging system with high-throughput SR reconstruction module. Our ultrafast live-cell SIM for 564 Hz temporal resolution and is compatible with all fluorescence labels. Furthermore, our developed intelligent high-throughput super-resolution algorithm achieves a fourfold resolution improvement over the diffraction limit, with a resolution of up to 60nm, enabling the observation and analysis of fine subcellular structures. The intelligent biological imaging platform allows for automated, real-time imaging, meeting the demands of subcellular dynamics research. This provides a powerful experimental platform for the diagnosis, treatment research, and drug development of rare diseases.

Beyond that, the intelligent high-throughput bioimaging platform represents a transformative tool for advancing our understanding of cell biology and accelerating the development of new treatments for a wide range of diseases. Its integration of cutting-edge imaging technologies and automation features promises to revolutionize the field of bioimaging and propel scientific discovery forward into new frontiers.

Intelligent high-throughput super-resolution imaging platform for precise diagnosis and treatment of rare diseases

Dr. Weisong Zhao (weisongzhao@hit.edu.cn)
Early-Career Member of Optica
Professor, School of Instrumentation Science and Engineering
Harbin Institute of Technology, China

1. Background

According to the current medical records, approximately 10,000 rare diseases exist globally. However, due to the small number of patients and limited information for each rare disease, medical expertise is rare; knowledge is scarce; and research is limited. For example, Hemophilia A (HA) is an inherited bleeding disorder, which is caused by a deficiency in coagulation factor VIII (FVIII)[1]. Prophylactic FVIII replacement therapy is recommended for severe and some moderate HA patients, in order to transform the bleeding phenotype from severe to non-severe. The major concerns of current therapy for HA are the development of FVIII inhibitors and the need for frequent injections due to the short half-life time of drugs[2]. Besides, patients face significant risks of developing complications[3]. Delving into the etiology of rare diseases and developing more effective disease treatment drugs remain challenging tasks for biomedical researchers.

By offering unprecedented levels of detail and clarity in imaging cellular structures and molecular interactions[4,5,6], SR microscopy enables researchers to unravel the intricate mechanisms underlying these rare genetic disorders. Its high resolution and sensitivity empower scientists to observe subtle changes at the subcellular level[7,8], shedding light on disease progression, identifying potential therapeutic targets, and ultimately paving the way for more effective treatments[9] **(Fig. 1a)**. In the realm of rare diseases where understanding is often limited and treatment options are scarce, SR microscopy stands as a transformative tool, offering hope for improved diagnostics, targeted therapies, and enhanced patient outcomes[10].

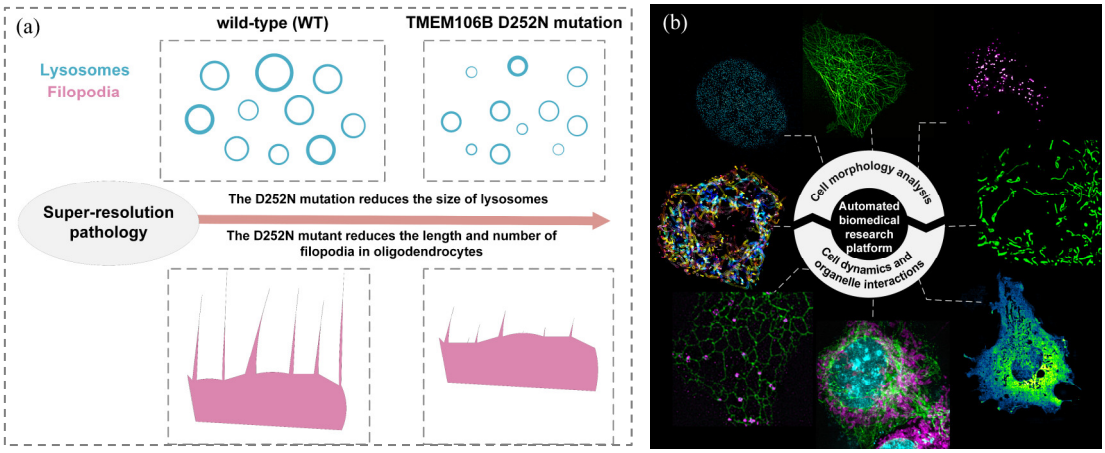

Fig1. An overview of super-resolution pathology and the algorithm-enhanced SIM for biomedical research. a) fundamentals of super-resolution pathology; b) algorithm-enhanced SIM super-resolution imaging results.

Structured illumination microscopy (SIM) has been widely used in live-cell imaging studies due to its fast imaging speed, low phototoxicity, and minimal photobleaching effects. However, it suffers from the limitation of relatively low resolution. Combining super-resolution reconstruction algorithms can further enhance the spatiotemporal resolution of structured illumination microscopy, enabling long-term imaging of live cells and facilitating the visualization of subcellular structures and dynamics in living cells[11] (**Fig. 1b**). Overall, the intelligent high-throughput super-resolution imaging platform is of paramount significance for enhancing both automated resolution and real-time imaging of live cells, which is the major motivation of this proposal. The intelligent biological imaging platform provides powerful tools for studying the pathogenic mechanisms and diagnosis/treatment methods of rare genetic diseases. It has many unexplored possibilities for revolutionizing current SR imaging for cell biology and biomedical research.

2. Statement of problem, objectives, and method

The major problems that we aim to solve are real-time observation of dynamic activities in living cells at the subcellular scale. Scientifically, the sparse deconvolution algorithm[11] can enhance the resolution of SIM microscopy to 60nm, enabling detailed observation of subcellular structures. However, with multiple constraints involved, the use of sparse deconvolution requires step-by-step parameter adjustment. The parameter tuning is tricky and requires prior knowledge. Moreover, because of the inevitable photobleaching effect, the SNR will vary over time in long-term live-cell imaging, leading to different optimal parameters even in the same dataset. These complexities of use essentially restrict the method dissemination and high-throughput application.

Our proposed solution is to utilize a deep-learning engine to extract the pattern of parameter selections in a high-dimensional representation, enabling parameter-free and real-time sparse deconvolution reconstruction. Inputting raw SIM images with the optimally reconstructed images as ground-truth, the deep neural networks (DNNs) will automatically learn the complex expressions of low-to-high resolution transformations. Then, the well-trained DNNs can be frozen for direct SR reconstructions. This non-iterative form of reconstruction with the graphics processing unit (GPU) acceleration has the potential to achieve real-time SR imaging.

The overall technical route is shown in **Fig. 2**. First, we construct an ultrafast interference-based SIM system to acquire 9-frame structural illumination images. Utilizing parameter solving and linear equation separation of high and low-frequency components, followed by stitching to obtain extended spectral components, we then employed classical SIM reconstruction algorithms for inverse filtering to achieve SR-SIM images with double resolution. Subsequently, to further enhance the signal-to-noise ratio, contrast, and resolution, we applied our parameter-free sparse solution deconvolution algorithm, achieving a fourfold improvement in resolution beyond the diffraction limit. At this stage, leveraging the sparse solution deconvolution algorithm combined with deep learning networks, we pre-trained an intelligent SR reconstruction network and then pruned it into a lightweight model for acceleration. Finally, this frozen model will be integrated into the imaging system as a post-processing step.

By integrating of ultrafast SIM imaging system with real-time SR reconstruction module, we construct an intelligent bioimaging platform. There are several advantages of our platform.

First, our platform has contained all the advantages of ultrafast live-cell SIM for 564 Hz temporal resolution and is compatible with all fluorescence labels. Second, the spatial resolution is automatically doubled from 120 nm of SIM to 60 nm without parameter-tuning. Last, the SR reconstructions are in real-time, and this feature is particularly valuable for live-cell imaging. Using this platform, biologists can dissect the sub-organelle interactions in real-time without training or specific experience. We expect our smart platform to break the stereotype that SR microscopes are all difficult to use, making SR imaging easier.

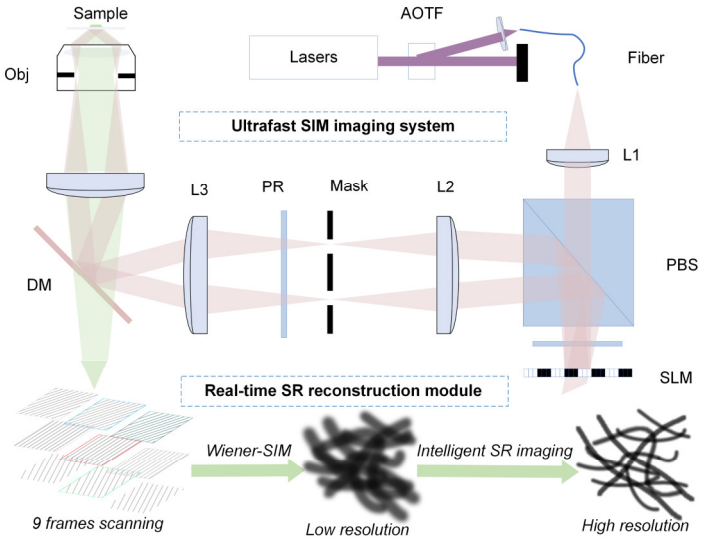

Fig 2. Intelligent real-time SR platform. PBS: polarization beam splitter; AOTF: acousto-optic tunable filters; HWP: half wave-plate; DM: dichroic mirror; SLM: spatial light modulator; PR: polarization rotator; L1–L5: lenses; Obj: Objective.

3. Outline of Work Plan

3.1 Optical setup of ultrafast SIM

The SIM system is based on a commercial inverted fluorescence microscope (IX83, Olympus) equipped with a TIRF (total internal reflection fluorescence) objective (100×/1.7 HI oil, APON, Olympus) and a multiband dichroic mirror (DM) as shown in **Fig. 2**[11]. In short, the output light from a polarization-maintaining single-mode fiber is collimated by an objective lens (L1) and diffracted by the pure phase grating that consists of a polarizing beam splitter (PBS), a half-wave plate and the SLM (3DM-SXGA, ForthDD). The diffraction beams are then focused by another achromatic lens (L2) onto the intermediate pupil plane, where a carefully designed stop mask is placed to block the zero-order beam and other stray light and to permit passage of ±1 ordered beam pairs only. To maximally modulate the illumination pattern, a home-made polarization rotator is placed after the stop mask. Next, the light passes through another lens (L3) and a tube lens (L4) to focus on the back focal plane of the objective lens, which interferes with the image plane after passing through the objective lens. Emitted fluorescence is collected by the same objective passed through a DM, an emission filter, and another tube lens (L5). Finally, the emitted fluorescence is split by an image splitter before being captured by an ultrafast sCMOS camera (Flash 4.0 V3, Hamamatsu, Japan).

With encoded high-frequency information from the nine acquired raw images, we use a Wiener-SIM reconstruction to achieve a twofold resolution improvement. Subsequently, the

Wiener-SIM image is further processed by the Sparse deconvolution to fulfill a fourfold resolution improvement for 60 nm resolution SR imaging. To collect feature-rich enough data for training, we systematically perform the experiments for various organelles, including actin, microtubules, caveolin, lysosome, OMM/IMM, ER (endoplasmic reticulum), lipid droplet, and so on, under different SNRs. Such a data pool will effectively guide the DNNs to learn the authentic representation of the Sparse deconvolution while preventing the over-fitting effects.

3.2 Real-time SR reconstruction method

We first apply sparse deconvolution to further boost SNR, contrast, and resolution, fulfilling the 4fold resolution improvements against diffraction-limit. At this stage, the parameters of sparse deconvolution are all selected by experts with the step-by-step protocol. By collecting SR images of different organelles under different SNRs, the generative adversarial network with multi-scale discriminators (PatchGAN) is employed to learn the transformation from the SIM image to its corresponding Sparse-SIM image (**Fig. 3**). Then, we pre-trained the SR reconstruction network and pruned it to a lightweight model for acceleration. Finally, this frozen model will be integrated into the imaging system as a postprocessing step.

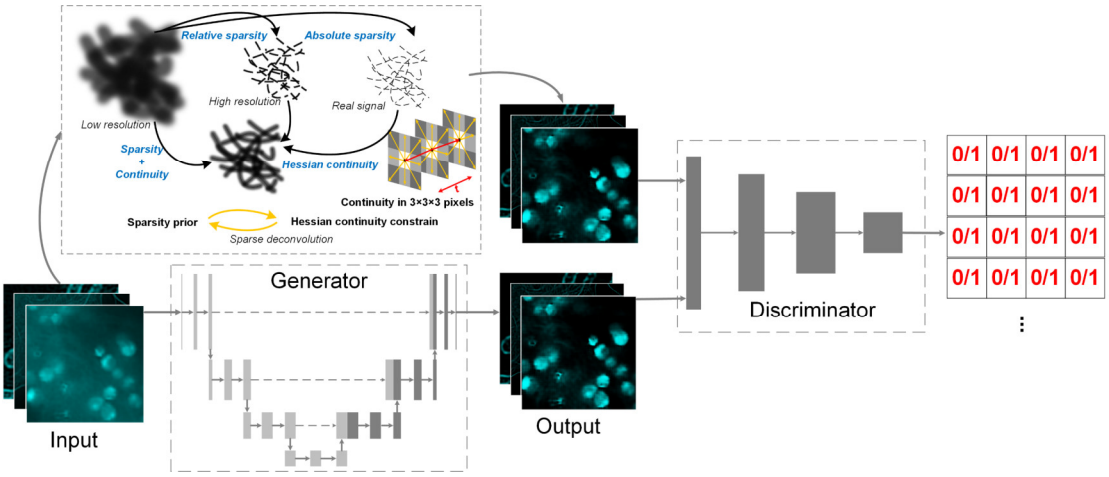

Fig 3 Real-time super-resolution imaging architecture

3.3 Integration of Intelligent high-throughput SR-SIM platform

The pre-trained model will be pruned to compress the models to run with significantly reduced energy cost and inference time. Since this compression removes redundant information, the prediction accuracy could even increase after pruning and it can also reduce the potential over-fitting effects. Then, with optimization of the linear and non-iterative Wiener-SIM reconstruction on a high-performance GPU, we further enable real-time SIM reconstructions. Integrated with the subsequent learning-based inference, we construct a fully automatic bioimaging platform that enables 60 nm spatial resolution with 30 Hz real-time imaging speed (containing acquisition, reconstruction, and saving time).

4. Outcome(s)

In this proposal, we will develop a fully automatic bioimaging platform that integrates high-throughput SR-SIM imaging, high-speed data collection, and real-time analysis. Specific outcomes and deliverables include:

(1) A high-throughput SR-SIM platform with 60 nm resolution and 30 Hz frame rate. The SR imaging platform enables real-time dynamic observation of subcellular structures

and life processes.

(2) More than 2 high-impact publications (targeted in Optica and other journals);

(3) One optical scientist to be trained.

5. Impact

In summary, this proposal represents a transformative tool for integrating cutting-edge imaging technology and automation features. Specifically, we will construct an intelligent high-throughput SR-SIM imaging platform for automatic bioimaging with a resolution of 60 nm and a real-time imaging speed of 30 Hz. The intelligent biological imaging platform allows for automated, real-time imaging, meeting the demands of subcellular dynamics research. This provides a powerful experimental platform for the diagnosis, treatment research, and drug development of rare diseases.

6. Reference

1. Fischer, Kathelijn, and Rolf Ljung. Primary prophylaxis in haemophilia care: guideline update 2016. ***Blood Cells, Molecules, and Diseases*** **67** 81-85(2017).
2. Yanan, Z. et al. Phosphatidylserine positive microparticles improve hemostasis in in-vitro hemophilia A plasma models. ***Scientific Reports*** **10**, 7871 (2020).
3. Zekavat, Omid Reza, et al. Abnormal frequency of the memory B cell subsets and plasmablasts in patients with congenital severe hemophilia A: correlation with "Inhibitor" formation. ***Blood Research*** **59,** 1-8(2024).
4. Schermelleh, L. et al. Super-resolution microscopy demystified. ***Nature Cell Biology*** **21**, 72-84 (2019).
5. Xu, K., Zhong, G. & Zhuang, X. Actin, spectrin, and associated proteins form a periodic cytoskeletal structure in axons. ***Science*** **339**, 452-456 (2013).
6. Szymborska, A. et al. Nuclear pore scaffold structure analyzed by super-resolution microscopy and particle averaging. ***Science*** **341**, 655-658 (2013).
7. Lawo, S., Hasegan, M., Gupta, G.D. & Pelletier, L. Subdiffraction imaging of centrosomes reveals higher-order organizational features of pericentriolar material. ***Nature Cell Biology*** **14**, 1148-1158 (2012).
8. Mennella, V. et al. Subdiffraction-resolution fluorescence microscopy reveals a domain of the centrosome critical for pericentriolar material organization. ***Nature Cell Biology*** **14**, 1159-1168 (2012).
9. Maria, A. et al. Bridging live-cell imaging and next-generation cancer treatment. ***Nature Reviews Cancer*** **23**, 731-745(2023).
10. Shijia, X. et al. Superresolution live-cell imaging reveals that the localization of TMEM106B to filopodia in oligodendrocytes is compromised by the hypomyelination-related D252N mutation. ***Science China Life Sciences*** **66**, 1858-1868(2023).
11. Weisong, Z. et al. Sparse deconvolution improves the resolution of live-cell super-resolution fluorescence microscopy. ***Nature Biotechnology*** **40**, 606–617 (2022).

Executive Summary

Title: Development of a low-cost, portable device for human brain blood flow and function measurements

Cerebral blood flow (CBF) is an important biomarker for brain health. Alterations in CBF are closely associated with serious clinical conditions such as stroke, traumatic brain injury, and Alzheimer's disease. Stroke, for instance, is the second leading cause of death globally according to World Health Organization, and monitoring CBF in the acute phase is crucial for guiding treatment within the critical 6-9 hours post-stroke treatment window. Besides clinical applications, CBF can also be utilized to measure brain function for applications such as stress level monitoring, or brain-computer interfaces. Existing methods to measure CBF include functional magnetic resonance imaging (fMRI) and transcranial doppler ultrasound (TCD). However, these techniques are costly and require high technical expertise to operate. A global challenge is the lack of a method for everyday monitoring of CBF, particularly in areas with limited resources. An ideal solution will be a low-cost, non-invasive, portable system that can be used at home and easily carried to various communities.

Our goal is to develop a device that can be readily used at home for everyday CBF monitoring, similar to oximeters which has been conveniently used to measure oxygen saturation. Optical methods serve as perfect candidates to accomplish such a task. Diffuse correlation spectroscopy (DCS) is an optical method that has been established to measure CBF in the past two decades. However, traditional DCS has relatively low signal-to-noise ratio (SNR), restricting the achievable depth sensitivity. Consequently, the scalp, rather than the brain, contributes primarily to the measured blood flow in DCS. DCS also uses relatively expensive (>$10,000) single photon avalanche diode (SPAD) as detectors, thus making it financially challenging for wide adoptions. Recently, we have proposed to use a fiber-based speckle contrast optical spectroscopy (SCOS) to measure human CBF. SCOS uses relatively low-cost complementary metal–oxide–semiconductor (CMOS) cameras as detectors. We have demonstrated that the performance of SCOS can surpass that of DCS systems in terms of SNR by *at least one and up to two orders of magnitude* at a high measurement rate of ~50 Hz with much lower cost detectors (~$500). Our current prototype SCOS system, however, utilizes lenses and bulky cameras which need to be mounted on an optical table in a laboratory environment. Therefore, the development of the next generation miniaturized SCOS system is key to extend its utility for everyday monitoring of brain health. We propose to miniaturize the SCOS system to construct a more portable and wearable device that measures CBF non-invasively in real time. This will be done by pursuing three specific aims:

Aim 1: Design the hardware for the miniaturized SCOS device. We will remove the lenses in both the illumination and detection side of the prototype SCOS system to improve wearability while maintain a similar level of performance.

Aim 2: Develop the software for real time displaying of brain hemodynamics and function. We will connect the CMOS detector to a mini-computer and develop the software for real time data processing and display.

Aim 3: Conduct pilot human brain CBF measurements during a cognitive task (n=10). This will demonstrate the application of the miniaturized SCOS for human brain function measurements.

This successful completion of this project will provide a CBF monitor that can be use without any specialized training. The portability and affordability will make it an ideal solution for global health care, especially in rural areas where the access to medical resources, e.g. MRI scanner, is limited. It will also motivate the development of future generations of SCOS devices that feature wireless connections to tablets and cellphones. These will shape the future of everyday recording of human brain health that responds to the stated goal of the *Health* category of *Optica Foundation Challenge* that calls for "*new, innovative and affordable technology solutions*". The design of the hardware and software to sense optical speckle changes for decoding brain dynamics also responds to the *Information* category of "*Exploring new optical sensing technologies to improve various parameter monitoring capabilities*".

Literature Review

Cerebral blood flow (CBF) is an important biomarker of brain health, as it regulates oxygen delivery to the brain and removes metabolic waste such as carbon dioxide. Alterations in CBF correlate with serious clinical conditions such as stroke[1,2], traumatic brain injury[3], and Alzheimer's disease[4,5]. Stroke, for instance, is the second leading cause of death globally, responsible for 11% of total deaths according to World Health Organization. Monitoring CBF in the acute phase of stroke is crucial for guiding treatment within the critical 6-9 hours post-stroke treatment window. CBF also provides information about brain function[6–9] that can be used to monitor mental health, such as assessing stress levels, and in other applications including brain-computer interfaces. Therefore, monitoring CBF is important for clinical applications as well as physiology and cognitive neuroscience studies. A major global challenge, however, is the lack of a convenient method for everyday monitoring of CBF, especially in regions with limited resources. The state-of-the-art technique is functional magnetic resonance imaging (fMRI), but it is a physically large and expensive machine, which limits its use to well-resourced medical centres. Transcranial doppler ultrasound is another method to measure CBF in clinics. But like fMRI, it is also relatively costly and requires specialized training to operate. An ideal solution will be a low-cost, non-invasive, portable device that can be easily used and carried outside of the clinic and into communities with limited resources.

Optics offers a convenient way to non-invasively and continuously monitor CBF that cannot be accomplished with other techniques such as positron emission tomography and arterial spin labelling fMRI. When a scattering sample, for instance, red blood cells flowing in a blood vessel, is illuminated by coherence light, speckle patterns with grainy appearances of bright and dark regions will arise from the interference of the light waves, as illustrated in Fig. 1. A speckle pattern is very sensitive to changes in the scattering sample, and is often referred to as the fingerprint of the scattering medium[10]. Therefore, analysis of the changes in the speckle pattern can provide valuable information of the scattering particles, which can be used to determine, for instance, the speed of red blood cells. Diffuse correlation spectroscopy (DCS) is an optical method that exploits the dynamics of speckle patterns to measure blood flow and decode CBF[11]. In DCS, coherence light is launched at one position on the surface of the sample/brain and a detector is placed at another position to collect reemitted light with intensity $I(t)$ that changes over time due to speckle fluctuations. A blood flow index (BFi) is obtained from the decorrelation time τ_c of the intensity auto-correlation function $g_2(\tau) = \langle I(t)I(t+\tau)\rangle / \langle I(t)\rangle^2$. The depth of the measurement is determined by the source-detector separation (SDS). At a larger SDS distances, the penetration depth of the light signal is deeper, but the collected photon flux is smaller, resulting in poorer signal to noise ratio (SNR). Traditional DCS has relatively low SNR, therefore limiting the achievable SDS to only ~20 mm; at this distance, the main

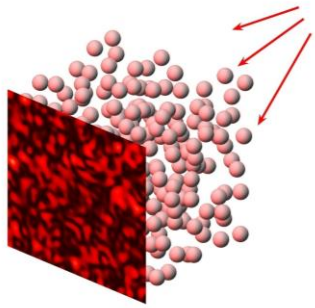

Figure 1. Speckle pattern. Speckle pattern (the squared pattern) arises from the interference of light waves (red arrows) scattered by the scattering particles (pink spheres). The speckle pattern acts as the "fingerprint" of the scattering system.

Abbreviations: ***BFi*** blood flow index; **CBF** cerebral blood flow; **CBV** cerebral blood volume; **CMOS** complementary metal–oxide–semiconductor; **$CMRO_2$** cerebral metabolic rate of oxygen; **CrCP** critical closing pressure; **DCS** diffuse correlation spectroscopy; **fMRI** functional magnetic resonance imaging; **fNIRS** functional near infrared spectroscopy; **ICP** intracranial pressure; **OD** optical density; ROI region of interest; **SCOS** speckle contrast optical spectroscopy; **SDS** source-detector separation; **SNR** signal to noise ratio.

contribution to the measured blood flow arises from the scalp instead of the brain for adults, i.e., the brain-to-scalp sensitivity is low[12]. Thus, DCS is limited in clinical usage and is not feasible for brain function measurements in adults for applications such as mental workload measurements and brain-computer interfaces. It also has relatively low acquisition rate (<10 Hz), which is not desired when high temporal resolution is preferred. Additionally, DCS requires costly (~$10,000) single photon avalanche diodes as detectors, financially limiting its wide adoption for everyday use. Further miniaturizing DCS systems is also challenging due to the relatively large size of the detectors available in the market. A new optical method that can achieve lower cost, higher SNR and acquisition rate, better portability, and wearability, while also maintaining the advantages of DCS including non-invasiveness, robustness, and convenience in use will be ideal for everyday monitoring of human CBF and mental health.

Problem Statement/Objective

We aim to develop a device that can be used at home for everyday monitoring of human CBF and mental health. Recently, we have developed a fiber-based speckle contrast optical spectroscopy (SCOS) system to non-invasively measure human CBF. Similar to DCS, SCOS also utilizes the speckle patterns to decode blood flow information. In SCOS, the spatial speckle contrast K defined as $K = std(I)/\langle I \rangle$, measured with a particular camera exposure time T_{exp}, is calculated, where $std(I)$ is the standard deviation and $\langle I \rangle$ is the average of the spatial speckle pattern intensity as shown in Fig. 1[13]. Unlike DCS, SCOS can also conveniently measure optical density (OD), defined as $OD = log_{10}(I(0)/I(t))$, which is linearly related to cerebral blood volume (CBV). The contrast K is directly related to τ_c measured in DCS[14]. At large camera exposure times $T_{exp} \gg \tau_c$, the blood flow index (BFi) can be defined as BFi= $1/\tau_c$ = $1/K^2$ which quantifies the variations of CBF. We have already built a first-generation SCOS system (Fig. 2a, b) and demonstrated measurements of human CBF as well as OD at a large SDS of 33 mm[15,16] for the first time. We simultaneously collected SCOS and DCS measurements and demonstrated a more than 10X improvement of SNR at a much higher measurement rate (~50 Hz) as compared to traditional DCS systems. As show in Fig. 2c, the cardiac pulse measured on the human forehead at a SDS of 25 mm is much cleaner and more consistent for SCOS than DCS. Unlike DCS which requires costly single photon counting devices, SCOS utilizes relatively low-cost (~$100-$500) complementary metal-oxide semiconductor (CMOS) cameras as detectors. All these features make SCOS a perfect candidate for the task of

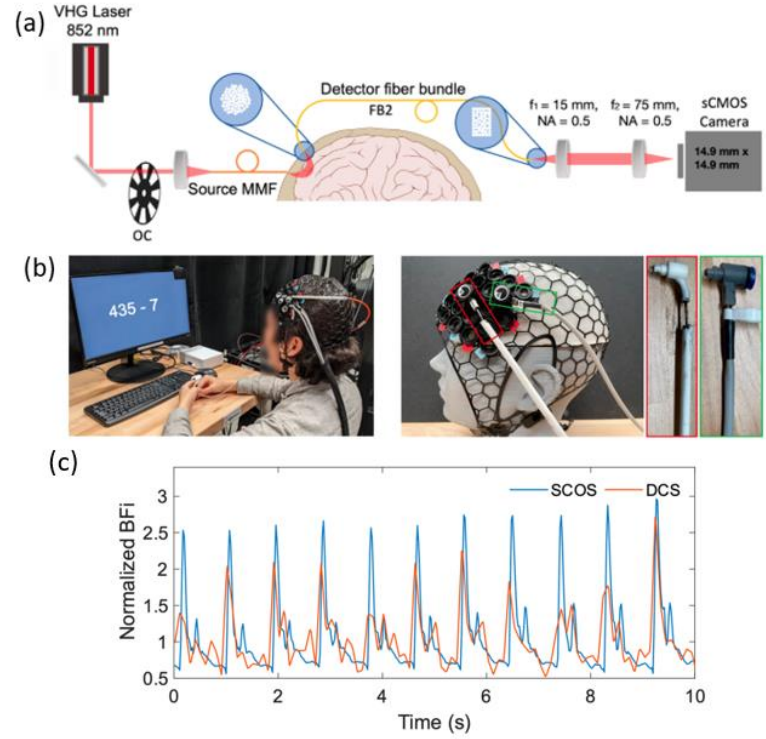

Figure 2. Demonstration of SCOS measurements. (a) Schematic of our existing first-generation SCOS system. (b) Demonstration of the fiber placement on the subject's head for brain CBF measurements. (c) Comparison of SCOS and DCS for measurements of the cardiac waveforms of the blood flow index (BFi). OC: optical chopper; MMF: multi-mode fiber; NA: numerical aperture.

everyday monitoring of CBF. However, our first-generation SCOS system utilizes lenses and bulky cameras such that it needs to be mounted on an optical table in a laboratory environment. Therefore, the development of the next generation miniaturized SCOS system is key to extend its utility for everyday monitoring of brain health.

We propose to miniaturize the SCOS system and construct a second-generation, more portable and wearable device that non-invasively measures CBF and CBV in real time. This will be achieved by advancing three aims: (1) Design the hardware for the miniaturized SCOS device by removing the lenses in the optical path. Instead of using a bulky camera, we will use a low-cost, light weight, board level housing CMOS detector (Basler daA1920-160um, 2.3 MP, 160 fps, $289) to be placed directly on the subject's head. (2) Develop software for real time display of brain hemodynamics. CBF and CBV time traces will be calculated and displayed on the monitor in real time. (3) Conduct pilot human brain function measurements during a cognitive task (n=10) to show CBF changes due to brain activation.

Outcome

Upon completion of the above-mentioned aims, we will have developed the next-generation SCOS device capable of measuring and displaying human brain CBF and CBV in real time. The schematic of the system is shown in Fig. 3. We will use a CMOS sensor to collect light directly on the subject's head. We will still use a fiber for the light source, but we will also explore using low-cost laser diodes that are safe to be directly attached on the head. The CMOS sensor and light source fiber will both be secured to a wearable headband. The data will be transmitted to a mini computer and CBF, CBV time traces will be calculated and displayed on the monitor in real time. To operate, the headband with the CMOS sensor and light source attached will be secured to the subject's forehead. The operator, or subject, can then use the recording software to select their desired recording parameters (e.g., duration of the recording, frame rate, etc.) and start recording CBF and CBV signals. If time permits, we also aim to provide additional physiological measures, including heart rate, intracranial pressure (ICP), and critical closing pressure (CrCP, or zero flow pressure) as other options to be calculated in the software[17]. Some of these additional parameters would require connecting to another device, such as a Finapres Nova device (Finapres Medical Systems, Netherland), to measure arterial blood pressure[17]. We will provide the software interface to integrate these devices but will ensure that the SCOS device can also be used alone. The laser source, the mini-computer, and the monitor will be contained in a box (~20×15×10 cm^3) with a fan to dissipate heat, which makes it convenient to carry the system outside of the laboratory environment. In the future, after completing the hardware and software development described in the three aims above, we will also develop a stress assessment procedure to measure the brain function in the prefrontal cortex[18], to aid in monitoring mental health. In short, the successful completion of this project will establish a second-generation, low-cost, easy-to-use device for human CBF measurements, making monitoring CBF as easy as measuring blood oxygen levels with fingertip oximeters.

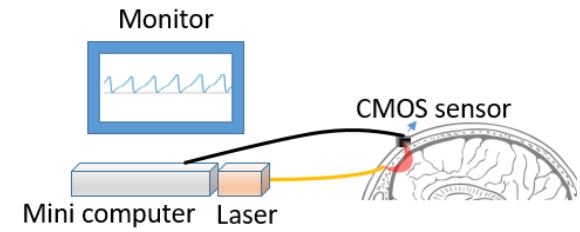

Figure 3. The schematic of the miniaturized SCOS system.

Impact

This miniaturized SCOS device will provide an easy, non-invasive method for continuous monitoring of human CBF and CBV, serving as biomarkers for brain health. The use of low-cost CMOS sensors makes it a more affordable solution compared to fMRI, which is the state-of-the-art method to measure brain hemodynamics, as well as DCS, which is the existing optical technique to measure human CBF clinically. Preliminary results (Fig. 2) have already demonstrated the great potential of SCOS to achieve a much higher SNR (more than 10 times) and deeper tissue penetration compared to DCS[16]. Potential and important clinical

applications include monitoring the ICP and CBF for patients suffering from medical conditions as shock, stroke, cerebral edema, or traumatic brain injury, where the cerebral autoregulation can be impaired leading to cerebral hyperperfusion, hypoperfusion, and ischemia. The portability of the miniaturized SCOS device also makes it an ideal solution for global health care, especially in rural areas. It can also serve as a tool to longitudinally monitor brain health, as changes in CBF and CBV have been suggested to be early indications of mild cognitive impairment or Alzheimer's disease[19], and mental health, such as giving warnings of fatigue, sleepiness, and high stress levels when driving[20].

The success of this project will also motivate the development of future generations of the SCOS devices. Our current plan is as follows: For the third generation SCOS device, we will integrate SCOS with functional near infrared spectroscopy (fNIRS)[21] to also measure oxy- and deoxy-hemoglobin, and calculate the cerebral metabolic rate of oxygen ($CMRO_2$). This can be done by including a second wavelength (650 nm) channel in the SCOS device to measure ODs at both wavelengths. The advantage of developing a SCOS-fNIRS system is that ODs can be measured by SCOS without requiring additional detectors, while DCS-fNIRS systems, for instance, require separate detectors for CBF and OD measurements. The fourth generation SCOS device will feature measurements for a larger area, or even the full head, by implementing a multi-channel system to improve spatial resolution. Brain activation maps can then be reconstructed[22,23] from the multi-channel measurements for applications such as brain-computer interfaces. This will look similar to an newly developed, whole head fNIRS system as shown in Fig. 4 to provide all the hemodynamic parameters over a large area for monitoring of the whole brain. The fifth generation SCOS device will be a helmet or cap with built-in light sources and detectors. Wireless communications will be utilized using tablets or cell phones for easier recording and display. Besides these technological developments, we aim to further reduce the price of the device by exploring even lower cost laser diodes (~$20 e.g. Thorlabs L780P010) and cell phone cameras in the future, which will enable mass production of the product and improve its affordability for widespread use.

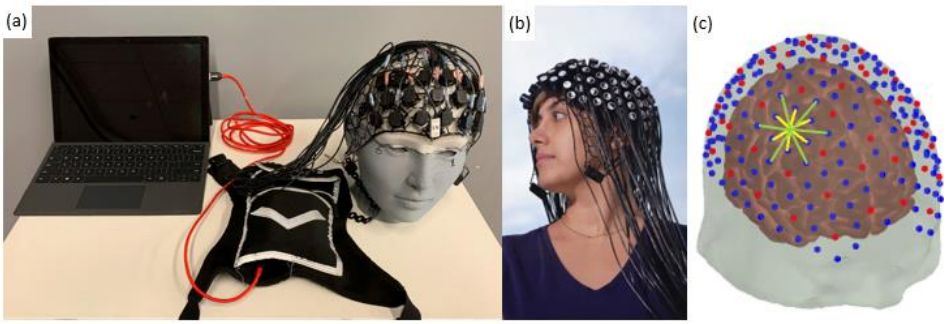

Figure 4. **Existing wearable whole head fNIRS system at Boston University.** This system has been used for cognitive neuroscience studies**.** (a) Existing NinjaNIRS21 system with 8 sources and 12 detectors and control unit backpack. (b) Whole head NinjaCap with NIRx NSP2 system. (c) High-density optode montage (sources in red, and detectors in blue).

In addition to the focus on brain health monitoring in this project, the SCOS device can also be modified and used to monitor the health of other organs such as kidney or skin. Vasculature and blood flow are deeply affected in many of the major health-related questions of the century, including cancers, cardiovascular diseases, neuro-vascular diseases and diabetes. Therefore, a convenient and affordable way to measure blood flow will benefit human health tremendously.

In summary, the development of the SCOS device will open up new opportunities to monitor brain health, detect disease that affects brain hemodynamics, and assess the effectiveness of treatments. It does not require special training to use, allowing easy implementation in clinics or in patients' homes. It can also be easily carried to communities that have limited access to medical resources such fMRI scanners. Therefore, this proposal responds to the stated goal of the *Health* category of the *Optica Foundation Challenge* that calls for "*innovative and*

affordable technology solutions" for the medical community, especially those with limited resources. The design of the hardware and software to sense optical speckle changes to decode brain dynamics also responds to the *Information* category of "*Exploring new optical sensing technologies to improve various parameter monitoring capabilities*".

References

1. Bandera, E. *et al.* Cerebral Blood Flow Threshold of Ischemic Penumbra and Infarct Core in Acute Ischemic Stroke. *Stroke* **37**, 1334–1339 (2006).
2. Leigh, R., Knutsson, L., Zhou, J. & van Zijl, P. C. Imaging the physiological evolution of the ischemic penumbra in acute ischemic stroke. *J. Cereb. Blood Flow Metab.* **38**, 1500–1516 (2018).
3. Bouma, G. J. & Muizelaar, J. P. Cerebral blood flow, cerebral blood volume, and cerebrovascular reactivity after severe head injury. *J. Neurotrauma* **9 Suppl 1**, S333-348 (1992).
4. Korte, N., Nortley, R. & Attwell, D. Cerebral blood flow decrease as an early pathological mechanism in Alzheimer's disease. *Acta Neuropathol. (Berl.)* **140**, 793–810 (2020).
5. Cruz Hernández, J. C. *et al.* Neutrophil adhesion in brain capillaries reduces cortical blood flow and impairs memory function in Alzheimer's disease mouse models. *Nat. Neurosci.* **22**, 413–420 (2019).
6. Durduran, T. *et al.* Diffuse optical measurement of blood flow, blood oxygenation, and metabolism in a human brain during sensorimotor cortex activation. *Opt. Lett.* **29**, 1766–1768 (2004).
7. Jaillon, F., Li, J., Dietsche, G., Elbert, T. & Gisler, T. Activity of the human visual cortex measured non-invasively by diffusing-wave spectroscopy. *Opt. Express* **15**, 6643–6650 (2007).
8. Li, J. *et al.* Transient functional blood flow change in the human brain measured noninvasively by diffusing-wave spectroscopy. *Opt. Lett.* **33**, 2233–2235 (2008).
9. Liu, W. *et al.* Fast and sensitive diffuse correlation spectroscopy with highly parallelized single photon detection. *APL Photonics* **6**, 026106 (2021).
10. Goodman, J. W. Statistical Properties of Laser Speckle Patterns. in *Laser Speckle and Related Phenomena* (ed. Dainty, J. C.) 9–75 (Springer, Berlin, Heidelberg, 1975). doi:10.1007/978-3-662-43205-1_2.
11. Durduran, T. & Yodh, A. G. Diffuse correlation spectroscopy for non-invasive, micro-vascular cerebral blood flow measurement. *NeuroImage* **85**, 51–63 (2014).
12. Zhou, W. *et al.* Functional interferometric diffusing wave spectroscopy of the human brain. *Sci. Adv.* **7**, eabe0150.
13. Valdes, C. P. *et al.* Speckle contrast optical spectroscopy, a non-invasive, diffuse optical method for measuring microvascular blood flow in tissue. *Biomed. Opt. Express* **5**, 2769–2784 (2014).
14. Boas, D. A. & Dunn, A. K. Laser speckle contrast imaging in biomedical optics. *J. Biomed. Opt.* **15**, 011109 (2010).
15. Zilpelwar, S. *et al.* Model of dynamic speckle evolution for evaluating laser speckle contrast measurements of tissue dynamics. *Biomed. Opt. Express* **13**, 6533–6549 (2022).
16. Kim, B. *et al.* Measuring human cerebral blood flow and brain function with fiber-based speckle contrast optical spectroscopy system. *Commun. Biol.* **6**, 1–10 (2023).
17. Wu, K. C. *et al.* Validation of diffuse correlation spectroscopy measures of critical closing pressure against transcranial Doppler ultrasound in stroke patients. *J. Biomed. Opt.* **26**, 036008 (2021).
18. Al-Shargie, F. *et al.* Mental stress assessment using simultaneous measurement of EEG and fNIRS. *Biomed. Opt. Express* **7**, 3882–3898 (2016).
19. Zhang, H. *et al.* Cerebral blood flow in mild cognitive impairment and Alzheimer's disease: A systematic review and meta-analysis. *Ageing Res. Rev.* **71**, 101450 (2021).
20. Chuang, C.-H. *et al.* Brain Electrodynamic and Hemodynamic Signatures Against Fatigue During Driving. *Front. Neurosci.* **12**, (2018).

21. Ferrari, M. & Quaresima, V. A brief review on the history of human functional near-infrared spectroscopy (fNIRS) development and fields of application. *NeuroImage* **63**, 921–935 (2012).
22. Dehghani, H., White, B. R., Zeff, B. W., Tizzard, A. & Culver, J. P. Depth sensitivity and image reconstruction analysis of dense imaging arrays for mapping brain function with diffuse optical tomography. *Appl. Opt.* **48**, D137–D143 (2009).
23. Boas, D. A. & Yodh, A. G. Spatially varying dynamical properties of turbid media probed with diffusing temporal light correlation. *JOSA A* **14**, 192–215 (1997).

Expanding light storage capacity via chiral photon-phonon Brillouin interaction

(OPTICA Foundation Challenge 2024, category: Information)

Xinglin Zeng, Max Planck institute for the science of light, xinglin.zeng@mpl.mpg.de

Challenges: In the information network, despite the rapid transmission speeds of data, there exists a critical necessity to buffer or store optical signals, which enables computers to decompose tasks into subtasks within the nodes of optical networks and address them individually. Employing all-optical storage shows advantageous, as alternatives like electro-optic control impose bandwidth and speed limitations. The stimulated Brillouin scattering (SBS) effect presents a promising avenue for all-optical controlled information storage and through this effect, an optical information can be resonantly stored to acoustic phonons and subsequently retrieved out. This concept has been demonstrated to store the amplitude, phase and frequency, showing rapid information retrieval and frequency-selective operation.

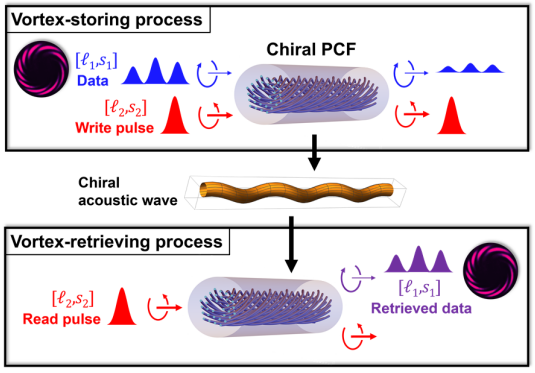

Fig. 1. Brillouin light storage of vortex states

In the last decade, there has been widespread utilization of spatial channels to increase optical communication capacity. However, **the spatial channels have not yet been exploited so far in the light storage** because of three bottleneck problems: 1. **Mode crosstalk** exists in most optical fibers; 2. Multimode Brillouin scattering **efficiency is quite low** in most optical fiber; 3. The scattered modes are **difficult to be detected** due to various noises. These three challenges severely constrain the development of optoacoustic light storage technology to the next generation.

Capabilities and outcomes: To address these challenges, **we propose a new light storage technique for spatial information based on the chiral photon-phonon Brillouin interaction in twisted photonic crystal fibers (PCF).** By engineering the fiber structure, it is possible to form strongly guiding cores in the PCF, permitting tight confinement of sound and light with close to 100% overlap while robustly preserving vortex states. Recently, we have achieved significant milestones on the observation of efficient intervortex chiral SBS in the twisted PCF. Motivated by the results, in this project, we will: 1. optimize the fiber parameters and fabricate a new twisted PCF that is suitable for vortex light storage; 2. demonstrate the storage of single or multiple circular polarization and vortex states in the twisted PCF. **We aim to develop the next generation light storage that can store all physical dimensions of optical wave.**

Impact: This project could not only enable new light storage technique for spatial information, but also lead to new breakthroughs in many other fields: 1. the vortex light storage could facilitate the development of **all-optical network** and control the flow of data in the optical buffers or routers; 2. the efficient multi-dimensional chiral SBS that produces spiral flexural waves might be useful to realize the **full-vectorial optical fiber sensing**; 3. the light storage on multiple vortex modes might enable manipulation of quantum states separately and boost **all-optical processing in quantum domain**.

Expanding light storage capacity via chiral photon-phonon Brillouin interaction

(Category: Information)

Applicant: Xinglin Zeng
Max Planck institute for the science of light
xinglin.zeng@mpl.mpg.de

1. Background and Literature Review

An information network consists of nodes where information is generated, processed and routed. Despite the high-speed data transmission, there is a critical need to buffer or store optical signals, which allows computers to break a task down into sub-tasks in the nodes of optical networks and solve them individually. It is beneficial to do light storage with all-optical techniques because other approaches such as electro-optic control limit the bandwidth and are constraint in terms of speed. The stimulated Brillouin-Mandelstam scattering (SBS) effect, a third-order nonlinear effect linking optical and acoustic waves, offers promising approach for all-optical controlled information storage [1]. The optical information is resonantly transferred to a coherent acoustic phonon via SBS effect and then transferred back to the optical domain by a delayed optical retrieval pulse. The concept was demonstrated to preserve amplitude and phase [2], frequency [3] and a temporal series of pulses [4], showing a number of merits such as high-speed coherent information access, frequency selective operation, and in-memory computing capabilities [5].

Over the past decade, there has been extensive utilization of spatial channels (polarization states and optical modes) to enhance optical communication capacity [6] and this technology is becoming a promising transmission method in data centers [7] and quantum communication systems [8]. **However, the storage and retrieval of polarization states and spatial information have not yet been carried out so far because of three bottleneck problems**:

a. In most optical fibers, the **crosstalk** between eigenmodes can easily occur;
b. The Brillouin scattering of higher-order modes has **lower efficiencies** than that of the fundamental modes in most optical fiber;
c. The scattered modes and polarization states are **difficult to be detected** due to the noises coming from Rayleigh scattering, Fresnel reflections and so on.

The recent advent of twisted photonic crystal fiber (PCF), which can robustly preserve circular polarization and vortex states, has made the SBS of structured optical waves possible. During my postdoctoral research at Max Planck institute for the science of light (MPL), I collaborated with Prof. Philip Russell and Prof. Birgit Stiller, conducted a series of researches on the multi-dimensional SBS in twisted PCF. By engineering the fiber structure, it is possible to form strongly guiding wavelength-scale glass cores in the PCF, permitting tight confinement of sound and light in a small area, with close to 100% overlap. This makes PCF more preferable than normal step-index circular fibers for Brillouin optoacoustic study. **We have developed an air-filled chiral PCF capable of providing large optoacoustic coefficient between chiral photons and acoustic phonons, which enables efficient amplification, isolation, inter-modal conversion and frequency conversion of vortex states [9-12]** (part of the

results are shown in Fig. 1). Those solid results confirm that multi-dimensional chiral SBS of low crosstalk and high efficiency is possible in optical fiber, and motivate us to address the bottleneck problems of light storage. Therefore, in this proposal, I plan to study the light storage of circular polarization states and vortex modes with chiral photon-phonon forward Brillouin interaction in twisted PCF.

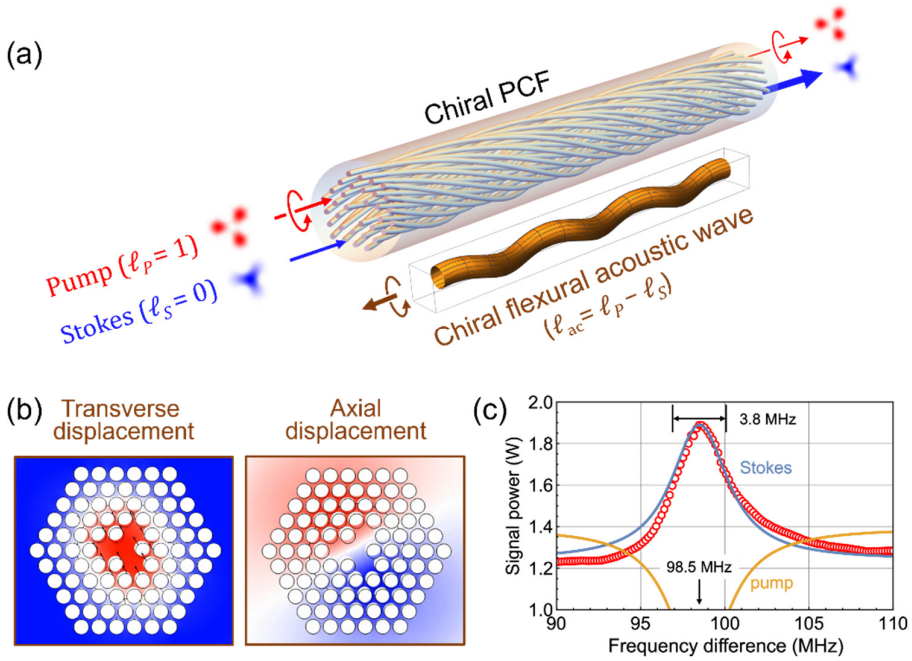

Fig. 1. (a) Conceptual view of chiral forward Brillouin scattering. The power of vortex-carrying pump wave can be efficiently transferred to Stokes wave during scattering, while the chiral acoustic phonons is generated. The circular arrows indicate the direction of azimuthal phase progression and the straight arrows indicate propagation direction. (b) Numerically calculated chiral acoustic wave at one instant in time. (c) Experimental measurement of Stokes power as a function of pump-Stokes frequency.

2. Objective

The goal of this project is to experimentally demonstrate the storage (writing and reading) of circular polarization and vortex states into traveling chiral acoustic waves. The concept will be demonstrated in chiral PCF with a large air-filling fraction, which allows for stable guidance of circular-polarized vortex modes and strong optoacoustic interaction simultaneously.

Within this project, we plan to address the following three sub-objectives:

a. Fabricating a suitable chiral PCF for efficient chiral photon-phonon interaction
We will fabricate a chiral PCF that can support chiral forward Brillouin interaction of sufficiently high efficiency to enable vortex states light storage.

b. The storage of single circular polarization and vortex states in the chiral PCF
We will demonstrate the storage of single circular polarization and vortex states, based on the inter-polarization and intervortex chiral forward Brillouin scattering in the twisted PCF.

c. The storage of multiple vortex states in chiral PCF
The last sub-objective is also most challenging part: Storing and retrieving multiple signals in the same time. Each signal is encoded with different circular polarization state or vortex modes.

The concept is illustrated in Fig. 2. In the storage process, the incoming vortex-carrying optical data pulse is transferred to a chiral flexural acoustic wave by using a co-propagating vortex-carrying write pulse. Both data and write pulses have different vortex modes. Following this interaction, the information originates from the data pulse resides solely within the acoustic domain. After an interval of tens of nanoseconds, in the read-out process, a read pulse interacts with the chiral flexural acoustic wave, transferring the information back to the optical domain. Under the mediation of chiral acoustic wave, not only amplitude, phase and frequency information are preserved, but also the polarization and spatial information (in this case, vortex states).

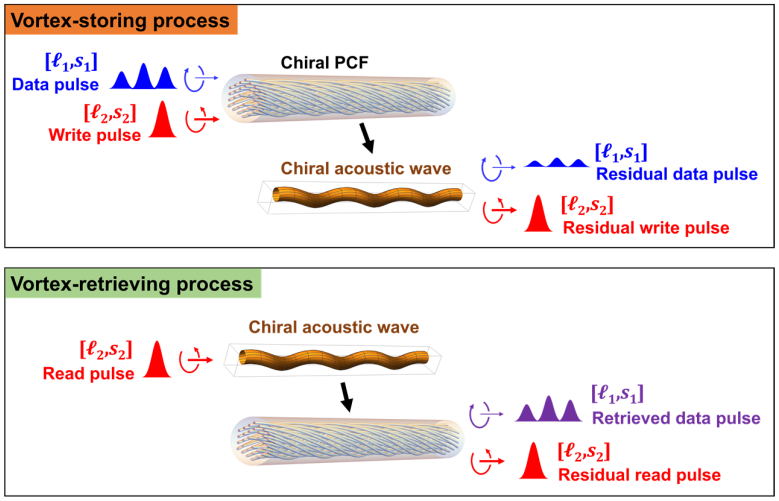

Fig. 2. The principal of optoacoustic storage of vortex states with chiral forward Brillouin scattering.

Fig.3 shows schematic diagram of spatial information light storage experiment, which includes information writing/reading and detection. In the following section, I will list the challenges that this project may have, with some possible solutions.

Problem 1: In contrast to the general light storage of amplitude or phase that is based on the longitudinal plane wave in backward SBS, the light storage of spatial information has to use the structured acoustic waves, which in most cases come from forward SBS. However, the efficiency of forward SBS is much weaker than that of backward SBS, which then makes the spatial light storage challenging.

Possible solutions:

a. Optimizing the structure of chiral PCF. Specifically, optimizing the air-filling fraction of PCF structure and the core size, to tightly confine the acoustic and optical modes in the fiber with close to 100% optoacoustic overlap. Thanks to the world-class PCF drawing facilities in MPL, we have obtained several chiral PCFs with significant optoacoustic efficiency [12]. However, the light storage experiment requires even larger efficiency and therefore more optimization.

b. Using chalcogenide soft-glass as fiber material. The Brillouin gain would be some 100 times higher if chalcogenides (As_2Se_3 or As_2S_3) [13] were used instead of silica. However, there might also be another challenging when drawing chiral PCF with such material: the soft glass is more brittle than the silica glass. One solution is to first draw the non-chiral chalcogenides PCF and then twist it by post-processing.

Problem 2: It is challenging to detect the spatial mode profiles of retrieved data because: 1. the parasitic noises such as Rayleigh scattering, Fresnel reflections and spontaneous backward Brillouin scattering affect the signal-to-noise ratio (SNR); 2. the retrieved data pulses are very close in time (typically ~100 ns that corresponds to the acoustic lifetime in the forward Brillouin scattering) to the original data pulses.

Possible solutions:

a. Utilizing the lock-in detection scheme to measure only the desired signal pulses while get rid of the noises.
b. Using a near-field raster scanning system to spatially resolve the retrieved data. The system will contain a PC-controlled fiber raster scanning stage, narrowband filter and signal detection equipment (in our case, the oscilloscope). The near field distributions of retrieved data pulses, which contains aforementioned noises and temporally close to the original data pulses, can be collected pixel by pixel by the raster scanning stage. The pulse area at each pixel will be recorded by the oscilloscope and the whole mode profile will be reconstructed by offline-processing based on the area values of all pixels.

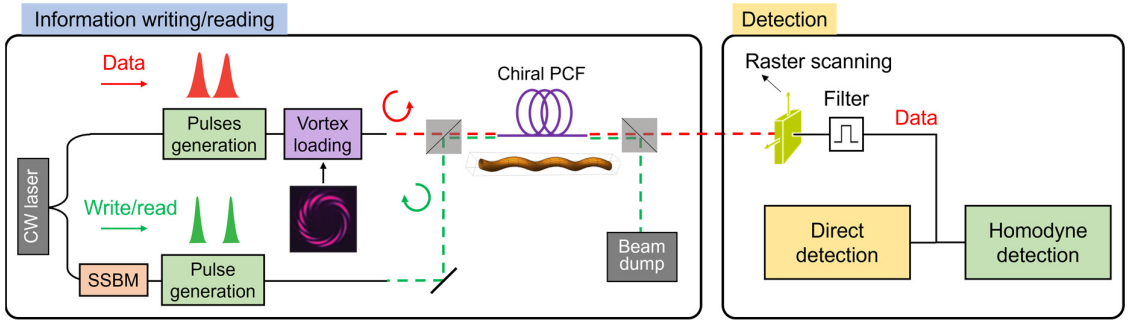

Fig.3. Experimental setup for the Brillouin light storage with spatial information (vortex states)

At last, this project will benefit from strong support provided by the MPL. This support includes access to the fiber-drawing facilities, extensive expertise and state-of-the-art equipment that includes a wide range of characterization tools, from pulse generation to spatial mode analysis.

3. Outcomes

New chiral PCF of high intervortex optoacoustic efficiency: Working with fiber fabrication team in MPL, I aim to obtain a new chiral PCF with large air-filling fraction (>0.8), short twist period (<5 mm) and small core size (<2 μm).
Storage of spatial information in chiral PCF: Demonstrating the storage of circular polarization and vortex states (single state and multiple states) in chiral PCF. Besides spatial information, the amplitude, frequency and phase will also be stored.
Publications: During the period of project, I target to achieve 1-2 journal publications and submit at least 2 conference papers.
Training students: One or two master students will be actively involved in the project, receiving comprehensive training in the field of intermodal SBS and light storage.
Collaborations: This project will continue to bridge collaboration between myself, Prof. Birgit Stiller, Prof. Philip Russell. Birgit Stiller is an expert in the field of Brillouin scattering and light storage research. Philip Russell is the inventor of the photonic

crystal fibers and an expert on twisted PCFs and chiral photonics. Therefore, I will benefit from an excellent research environment at my institute. The progress and innovation in the field will be accelerated through joint projects and knowledge exchange.

4. Impact

This project will not only provide insight into the physics of intervortex chiral SBS and enable next generation light storage for spatial information, but also have impact on a number of topics:

a. All-optical network
   The vortex-Brillouin light storage technique could facilitate the development of optical switches and routers, which can efficiently control the flow of data in the all-optical network without the need for electronic conversions.
b. Vectorial optical sensing
   The chiral Brillouin scattering produces spiral flexural acoustic wave, which might be capable of interacting with external 3D variation in the environment and facilitate the realization of full-vectorial optical fiber sensing.
c. Quantum communications
   The light storage on multiple vortex modes might boost all-optical processing in the quantum domain. It might enable manipulation of certain states separately and make parallel processing of a multi-dimensional state possible.
d. Chiral physics
   More fundamentally, this chiral phonons-mediated light storage can open up new perspectives on many fundamental researches such as topological photonics, non-Hermitian physics and other chirality-related phenomena.

Reference

[1] Z. Zhu, D. J. Gauthier, and R. W. Boyd, Science **318**, 1748–1750 (2007).
[2] M. Merklein, B. Stiller, K. Vu, S. J. Madden, and B. J. Eggleton, Nat Commun **8**, 574 (2017).
[3] B. Stiller, M. Merklein, K. Vu, P. Ma, S. J. Madden, C. G. Poulton, B. J. Eggleton, APL Photonics **4**, 040802 (2019).
[4] B. Stiller, K. Jaksch, J. Piotrowski, M, Merklein, M, K. Schmidt, K. Vu, P. Ma, S. Madden, M. J. Steel, C. G. Poulton, and B. J. Eggleton, npj Nanopho. **1**, 5 (2024).
[5] S. Becker, Dirk Englund, and Birgit Stiller, Nat. Commun. **15**, 3020 (2024).
[6] B. J. Puttnam, G. Rademacher, and R. S. Luís, Optica **8**, 1186-1203 (2021).
[7] M. Fiorani, M. Tornatore, J. Chen, L. Wosinska, and B. Mukherjee, J. Opt. Commun. Netw. **9**, A143-A153 (2017).
[8] A. Mair, A. Vaziri, G. Weihs, and A Zeilinger, Nature **412**, 313–316 (2001).
[9] X. Zeng, W. He, M. H. Frosz, A. Geilen, P. Roth, G. K. L. Wong, P. St.J. Russell, and B. Stiller, Photon. Res. **10**, 711-718 (2022).
[10] X. Zeng, P. St.J. Russell, C. Wolff, M. H. Frosz, G. K. L. Wong, and Birgit Stiller Science Advances. **8**, eabq6064 (2022).
[11] X. Zeng, P. St.J. Russell, Y. Chen, Z. Wang, G. K. L. Wong, P. Roth, M. H. Frosz, and B. Stiller, Laser Photonics Rev. **17**, 2202277 (2023).
[12] X. Zeng, P. St.J. Russell, and B. Stiller, arXiv:2401.09155.
[13] C. Fortier, J. Fatome, S. Pitois, Opt. Express **16**, 9398-9404 (2008).

Color Centers in Silicon Photonics for Quantum Networking and Computation

PI: Xueyue Zhang, Columbia University, zhang.xueyue@columbia.edu

Global Challenges in Information

The burgeoning global demand for secure and efficient information transfer presents significant challenges, as traditional networks face increasing threats from eavesdropping and disruptions. Quantum networks herald a new era of **communication security, protected by fundamental laws of quantum mechanics**. Additionally, these networks are vital for connecting modular quantum computers, addressing problems beyond the reach of classical computing through **large-scale distributed quantum computing**. The cornerstone of these networks is the quantum repeater, which facilitates the long-distance propagation of quantum information at high rates. Color centers emerge as a leading solution for these repeaters due to their ability to interface with flying photons and maintain long-lived spin states as quantum memory.

Although color centers are the backbone of metropolitan-scale quantum network demonstrations, current prototypes are limited to a few nodes with a low entanglement generation rate. Challenges with the most developed diamond color centers include **significant loss** from necessary frequency conversions for long-range transmission and **the difficulties of large-scale diamond device manufacturing**.

Furthermore, **photonic quantum computing using silicon photonics**, despite significant investments approaching a billion dollars, is hindered by the **lack of efficient spin-photon interfaces**, which are crucial for generating high-fidelity photonic resource states in a deterministic manner.

Solution and Capability

We aim to address these challenges using **color centers in silicon**, leveraging the mature infrastructure of silicon photonics and electronics. We focus on T centers—a carbon-hydrogen defect—that operate within the telecom-O-band at 1326 nm and feature electron and nuclear spins with coherence times of up to 2 seconds. The **major limitation** of T centers is the large optical linewidth compared to the lifetime-limited linewidth, which prohibits efficient interaction with photonic structures. The homogeneous linewidth, dominated by thermal phonon-induced relaxation, is especially harmful since feedback or postselection-based protocols cannot mitigate this effect. The direct solution of lowering the temperature is not cost-effective and adds complexity: it is impractical for deploying high-end cryostats every 10 km to house a quantum repeater.

We propose to leverage the unique capabilities of silicon photonic devices to engineer the local environment for T centers. Our modeling suggests that a **thermal linewidth reduction of more than two orders of magnitude is attainable** without lowering the operating temperature. Our team has deep expertise in T center creation, photonic crystal cavity integration, and measurement. In the 24-month project, we will (1) develop measurement protocols to accurately probe the thermal linewidth in regular devices, (2) design devices with optimal parameters for reducing the thermal linewidth, and (3) fabricate the integrated device on commercial silicon-on-insulator (SOI) wafers.

Impact

This solution will significantly enhance the **feasibility and scalability of quantum networks and photonic quantum computing**. By approaching a lifetime-limited homogeneous linewidth for T centers, we expect to **reach new levels of cooperativity in silicon photonics**. This advancement not only opens the door to next levels of light-matter interaction for high-fidelity single-photon gates and entanglement generation but also accelerates the deployment of quantum networks worldwide, promising a new era of ultra-secure and precise global communication.

Color Centers in Silicon Photonics for Quantum Networking and Computation

PI: Xueyue Zhang, Columbia University, zhang.xueyue@columbia.edu

Literature Review and Introduction

Classical networks are the vital force that connects the world together and drives the information revolution. Recently, the concept and prototypes of **quantum networks** (Fig. 1a) have emerged as our control over quantum systems has reached unprecedented levels [1]. Unlike classical networks, quantum networks use principles like the non-cloning theorem to ensure **absolute security against eavesdropping** [2]. Additionally, distributing remote entanglement among quantum nodes offers valuable tools for **precision measurements and quantum sensor networks** [3–5].

Similar to optical interconnects tackling bottlenecks in modern data centers, local quantum networks or quantum links show great potential for **scaling quantum processors**. Scaling monolithic quantum processors for practical computing tasks is extremely challenging. Thus, creating smaller, reliable quantum processing modules and linking them in a quantum network may provide the ultimate solution [6, 7].

Telecom-band photons in optical fibers are optimal to minimize propagation loss, as demonstrated by decades of advancements in optical communication. Additionally, quantum repeaters [8] are essential between distant nodes to exponentially enhance the success probability of establishing remote entanglement. As natural candidates for quantum repeaters, color centers provide optical transitions to interface with flying photons and long-lived quantum spins for entanglement swapping protocols. Notably, mature platforms using diamond color centers have been demonstrated in multi-node [9] or metropolitan-scale quantum networks [10]. However, these color centers do not operate in the telecom band, and diamond presents challenges for nanofabrication and device integration. Moreover, the high cost of quality diamond impedes the large-scale deployment of diamond-based quantum repeaters.

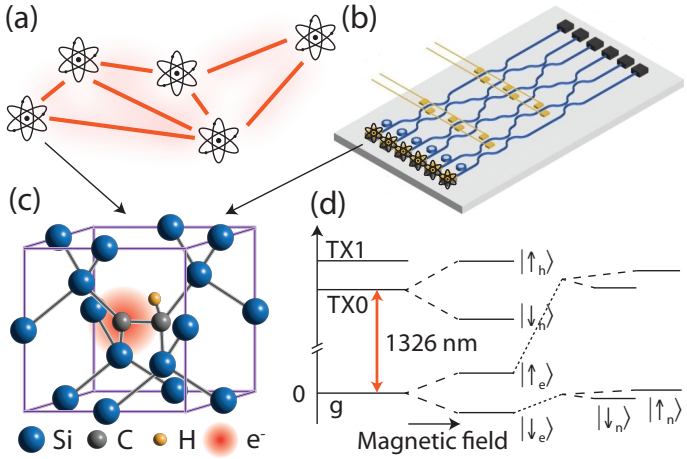

Figure 1: (a) Quantum network schematics. (b) Schematics of silicon photonics based manufacturable optical quantum computing. Figure adapted from Dr. Galan Moody. (c) T center atomic structure. (d) T center level structure showing the optical ground and excited states (TX0 and TX1) on the left and the electron and nuclear spin under magnetic field on the right.

Besides quantum networks, **quantum computing** [11] presents another information revolution with even broader impact on **cyber-security, materials/chemistry modeling, and pharmaceutical discoveries. Optical quantum computing** [12], particularly through silicon photonics (Fig. 1b), stands out as a manufacturable platform that leverages existing semiconductor foundries [13]. This approach has recently attracted nearly a billion dollars in global investment. However, a critical challenge remains: generating high-fidelity photonic resource states [14–16]. Current methods based on nonlinear optics, are probabilistic and difficult to scale, creating a significant bottleneck. In addition, the lack of an efficient spin-photon interface in silicon photonics hinders the deterministic generation of resource states from quantum emitters.

To address the challenges in quantum networking and computation, we focus on **color centers**

in silicon, utilizing the **mature silicon photonics platform for easier integration with photonic and electronic components**. Among the silicon color centers, T centers (Fig. 1c)–a carbon-hydrogen defect–show promise for quantum network applications. The T centers' transition lies in the telecom-O-band at 1326 nm (Fig. 1d), and their electron and nuclear spins serve as quantum memories. Initially studied in the 1980s [17–19], T centers have only recently been explored for quantum information, exhibiting desirable properties such as a 1 µs optical lifetime, 2 ms electron spin coherence, and over 2 s nuclear spin coherence [20, 21]. These attributes position T centers as effective quantum repeater nodes. With research still in its early stages [22–26], there are significant opportunities to further explore T centers' properties and their integration with sophisticated silicon-based technologies.

Problem Statement and Objectives

The primary limitation of T centers is their large optical linewidth, around 1-2 GHz at 4 K [20, 21], which is significantly broader than the desired lifetime-limited linewidth of approximately 160 kHz for T centers in bulk silicon. This four orders of magnitude mismatch poses significant challenges for efficient photon coupling, crucial for achieving high-fidelity spin readout, spin-photon entanglement, and photon gates controlled by the emitter. Addressing this requires both an increase in the lifetime-limited linewidth and a reduction in the total linewidth. Incorporating T centers into photonic crystal cavities has recently achieved an order of magnitude increase [22, 23, 25, 26] in the lifetime-limited linewidth thanks to the Purcell enhancement.

Reducing the total linewidth, however, is more complex. Part of the total linewidth arises from spectral diffusion due to charge environment fluctuations near the T center [21]. Incorporating emitters into PN junctions–a technique proven in silicon carbide [27]–has shown potential to nearly eliminate this issue. Alternatively, since spectral diffusion is typically slow, post-selection or feedback-based control could also mitigate its effects [28].

The linewidth hard to mitigate comes from rapid transitions between the TX0 excited state and the TX1 second excited state, mediated by thermal phonons [20] (Fig.1c). The transition frequency between TX1 and TX0 is 427 GHz (or 1.76 meV), while the thermal energy at 4 K corresponds to 83 GHz. At this temperature, the number of thermal phonons capable of driving the TX1-TX0 transition is significant, and the thermally induced linewidth increases exponentially with temperature, as confirmed by recent measurements [20]. This thermal-limited linewidth is calculated to be below 1 MHz at 1 K but rises exponentially to around 200 MHz at 4 K (Fig.2a). Our photoluminescence experiment using an below-bandgap laser (Fig. 2b) demonstrated higher TX1 population with increasing laser power causing a higher local temperature.

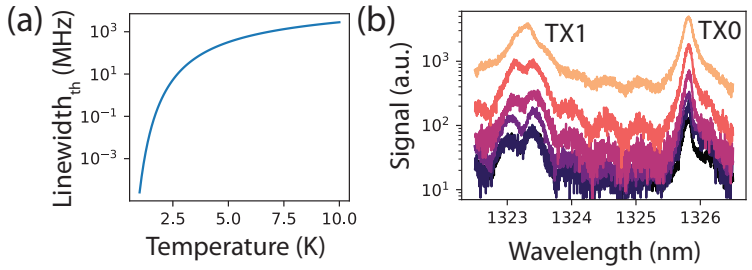

Figure 2: (a) Thermal linewidth vs. local temperature. (b) Measured TX1 and TX0 optical transitions with increasing optical power in a below-bandgap photoluminescence experiment. Lighter color represents higher power.

A brute-force approach to reduce this thermal linewidth is cooling the T center samples in a 1-K cryostat. However, 1-K cryostats require more advanced cryogenic technology, making them less cost-effective and space-efficient. Considering the goal to commercialize these quantum repeater nodes and deploy them every 10 km, it's essential to find solutions that effectively reduce the linewidth at 4 K or higher temperatures.

Instead of focusing solely on temperature, our proposal aims to engineer the TX1-TX0 splitting

frequency, which significantly influences the thermal linewidth [29, 30]. Early spectroscopy studies of T centers in bulk silicon indicate that the TX1-TX0 splitting is a function of local strain [19, 31]. The impact of strain on this splitting depends on the strain's orientation relative to the silicon crystal directions. For example, strain along the (100) direction can substantially increase the TX1-TX0 splitting by about 943 THz per unit strain for a subensemble of T centers, offering a practical method to adjust the splitting frequency.

Our ultimate goal is to overcome the linewidth limitations of operating T centers at easily achievable cryogenic temperature leveraging (1) this unique tuning knob provided by solid state systems to control TX1-TX0 splitting and (2) the mature microelectromechanical (MEMS) technology in silicon. To realize this goal, we outline our objectives as concrete steps:

- Develop the measurement setup and protocols to probe the thermal limited linewidth as a function of temperature.
- Design the optics and MEMS structures to optimize large controllable strain at the T center location.
- Fabricate the integrated device and measure the TX1-TX0 transition frequency and the thermal limited linewidth at various strain levels.

Plans and Outcomes

Measuring Thermal Limited Linewidth

To eliminate the influence of spectral diffusion, we need to measure the homogenous linewidth of a T center, which is dominated by the thermal linewidth. Previous spectroscopy work studying the temperature-dependent linewidth uses either bulk ^{28}Si to minimize spectral diffusion [20] or spectral hole burning to probe the homogeneous linewidth for ensembles of T centers [32]. However, the bulk measurements are not compatible with device characterization, and the ensemble measurement also introduces difficulties in analyzing individual T centers in their unique local strain and optical environment.

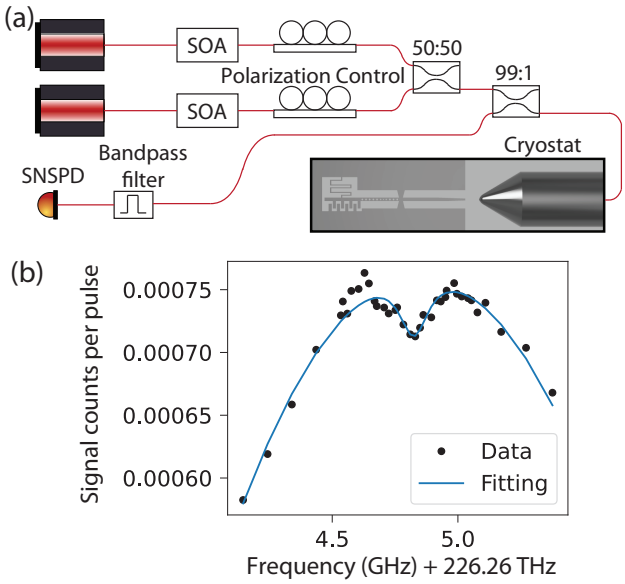

Figure 3: (a) Measurement setup schematics for hole burning and two-tone expereiments. SOA: semiconductor optical amplifier. SNSPD: superconducting nanowire single-photon detector. The numbers represents the beam splitter ratio. (b) Preliminary hole burning result for a single cavity enhanced T center.

Dr. Zhang has built a measurement setup for cavity-enhanced T center at UC Berkeley. She is also developing the measurement protocols to probe the homogenous linewidth for a single T center integrated in photonic crystal cavity using hole burning techniques and two-tone correlation measurement. The preliminary hole burning results (Fig. 3b) have shown the homogeneous linewidth of a single T center around 100 MHz at 3.8 K and increases considerably at 4.3 K.

To achieve the objectives in this proposal, we will build an upgraded setup (Fig. 3a) at Columbia University to expand the capability of these measurements. The setup will center around a cryostat that provides access to a wide range of temperatures to study the thermal linewidth and its strain dependency. For high coupling efficiency, we will use a lensed fiber to excite and collect signals

from the T centers.

We will use both the hole burning protocol and the two-tone correlation protocol developed by Dr. Zhang to probe the thermal limited linewidth. These complimentary measurements will be first developed and benchmarked on a device without external strain.

MEMS and Integrated Photonics Device Design

The key design target for the device is achieving the large strain needed to reduce the thermal-limited linewidth at 4 K. According to Fermi's golden rule, increasing the TX1-TX0 splitting E_a influences the thermal linewidth in two aspects [29]. One is the increase of the density of state that grows polynomially. The other is the thermal occupancy of the phonon modes that is exponentially suppressed by the Bose-Einstein distribution. At 4 K, our calculation shows that the exponential suppression dominates for E_a around the zero-strain value (Fig. 4a), meaning strain engineering is a feasible path to reduce thermal linewidth. Using the large strain dependency of 943 THz per strain in (100), a strain larger than 5.8×10^{-4} is capable of increasing E_a to 978 GHz (Fig. 4b) and reducing the thermal linewidth to 1 MHz (Fig. 4c), which is below the lifetime-limited linewidth of 1.7 MHz given 100 ns of cavity-enhanced optical lifetime.

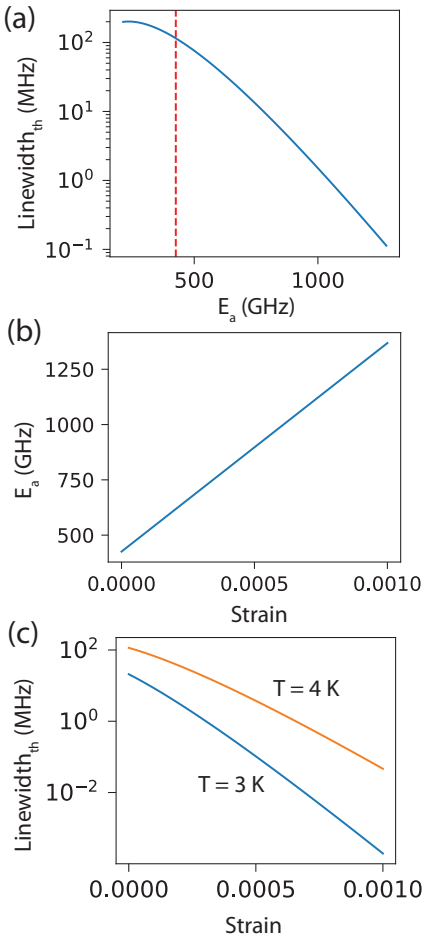

Figure 4: (a) Thermal linwidth vs. TX0-TX1 transition frequency. The dashed line marks the zero-strain value. (b) TX0-TX1 transition frequency vs. strain. (c) Thermal linewidth vs. strain at 4 K and 3 K.

In order to achieve tunable strain in the system, we will design a suspended comb drive structure, which is commonly used in the MEMS community, using commercially available silicon on insulator (SOI) substrate (Fig. 5a). The two combs are attached to separate electrodes to control the electrostatic force between them. One of the comb is rigidly defined on the silicon membrane and the other comb drive is connected to the silicon photonic waveguide where T centers reside. The second comb is attached to the main silicon membrane with a spring to provide a restoration force. The silicon beam is also connected to the main membrane with a tether to provide structural support and an anchor for the MEMS structure. We will use COMSOL to simulate the strain available in such a structure and determine the key parameters for the MEMS structure, including the comb pitch and period, maximum actuation length, and the position of the tether.

The integrated photonics design mainly involve a photonic crystal cavity and the taper coupler (Fig. 5a). The photonic crystal cavity has an extended number of Bragg mirrors at the side of comb drive to prevent loss from proximity of metalic electrodes on the comb drive. The inverse taper will gradually adapt the silicon waveguide mode to the air mode matching the Gaussian profile of the lensed fiber. We will perform FDTD or FEM simulation to determine the key dimensions of the design.

Device Fabrication and Testing

We will start from the commercially available SOI wafer and send out for ion implantation with commercial implanters such as Innovion. After the carbon implantation, we will perform a thermal annealing at 900^{o}C to repair the silicon lattice damage and send out for hydrogen implantation.

The following fabrication steps will be performed locally in the Columbia Nano Institution (CNI) and is shown in Fig. 5b. All the silicon structures inluding the MEMS and the photonic components will be defined by reactive ion etch (RIE). Then we will perform a rapid thermal annealing at 300^{o}C to facilitate the creation of T centers. The electrodes for the MEMS combs are defined after the annealing to avoid diffusion of metal into silicon. Following the metal patterning, we release the sacrificial oxide layer and the device is ready.

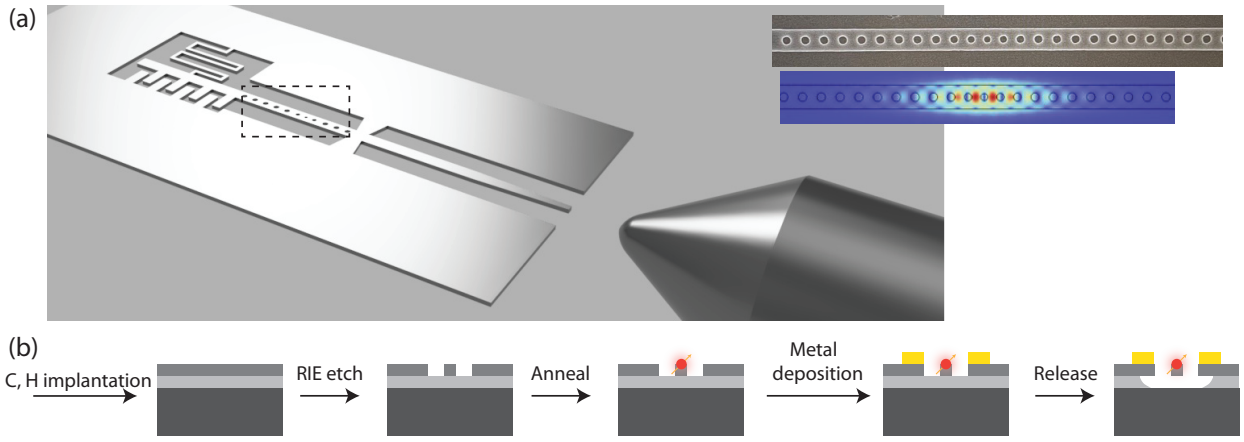

Figure 5: (a) Schematics of the proposed device (not to scale) coupled with a lensed fiber. The inset shows an SEM image of a photonic crystal cavity and its FEM simulation. (b) Fabrication flow after ion implantation. The spin sign represents T centers.

Finally, we will cool down the device in the cryostat and measure the TX1 and TX0 levels as a function of applied voltage using photoluminescence, as shown in Fig. 2b. Employing the COMSOL strain simulation, we can extract the strain sensitivity of these levels. We will measure the thermal linewidth with increasing applied voltage and compare it with theoretical predictions in Fig. 4c.

Impact

Achieving a lifetime-limited homogeneous linewidth for T centers represents a **significant milestone for silicon color centers**. By using post-selection or feed-forward protocols to mitigate spectral diffusion [28], we could achieve a **cooperativity of 1 or higher in silicon photonics** for the first time. This breakthrough positions T centers as strong competitors for quantum repeater nodes, alongside other leading platforms such as diamond and silicon carbide color centers, as well as rare earth ions. The advantage of silicon photonics lies in its compatibility with foundry manufacturing, quality control, and integration with other components—key factors in large-scale quantum node deployment and accelerating quantum network coverage.

The availability of sophisticated silicon photonic structures makes the realm of high cooperativity particularly appealing. Efficient light-matter interaction will facilitate photon-mediated interactions between emitters in advanced platforms like **topological photonic systems** [33] and **metamaterials** [34]. Most significantly, utilizing mature, low-loss components in silicon photonics will enable high-fidelity single photon gates [35] and the generation of resource states [36], paving the way towards the holy grail of **optical quantum computing** [12].

Furthermore, this proposal marks the first step towards incorporating mechanical degrees of freedom and MEMS structures into silicon quantum emitters, opening extensive possibilities for **hybrid quantum systems**.

References

[1] Stephanie Wehner, David Elkouss, and Ronald Hanson. "Quantum internet: A vision for the road ahead". In: *Science* 362.6412 (2018). ISSN: 0036-8075. DOI: 10.1126/science.aam9288.

[2] C. H. Bennett and G. Brassard. "Quantum cryptography: Public key distribution and coin tossing". In: *Proceedings of IEEE International Conference on Computers, Systems and Signal Processing*. Vol. 175. New York, 1984, p. 8.

[3] Rodney Van Meter. *Quantum networking*. John Wiley & Sons, 2014.

[4] Daniel Gottesman, Thomas Jennewein, and Sarah Croke. "Longer-Baseline Telescopes Using Quantum Repeaters". In: *Physical Review Letters* 109.7 (2012), p. 070503. ISSN: 0031-9007. DOI: 10.1103/physrevlett.109.070503. eprint: 1107.2939.

[5] P. Kómár et al. "A quantum network of clocks". In: *Nature Physics* 10.8 (2014), pp. 582–587. ISSN: 1745-2473. DOI: 10.1038/nphys3000. eprint: 1310.6045.

[6] C. Monroe and J. Kim. "Scaling the Ion Trap Quantum Processor". In: *Science* 339.6124 (2013), pp. 1164–1169. ISSN: 0036-8075. DOI: 10.1126/science.1231298.

[7] Sergey Bravyi, Oliver Dial, Jay M. Gambetta, Darío Gil, and Zaira Nazario. "The future of quantum computing with superconducting qubits". In: *Journal of Applied Physics* 132.16 (2022), p. 160902. ISSN: 0021-8979. DOI: 10.1063/5.0082975. eprint: 2209.06841.

[8] Koji Azuma et al. "Quantum repeaters: From quantum networks to the quantum internet". In: *arXiv* (2022). DOI: 10.48550/arxiv.2212.10820. eprint: 2212.10820.

[9] M. Pompili et al. "Realization of a multinode quantum network of remote solid-state qubits". In: *Science* 372.6539 (2021), pp. 259–264. ISSN: 0036-8075. DOI: 10.1126/science.abg1919. eprint: 2102.04471.

[10] C. M. Knaut et al. "Entanglement of nanophotonic quantum memory nodes in a telecom network". In: *Nature* 629.8012 (2024), pp. 573–578. ISSN: 0028-0836. DOI: 10.1038/s41586-024-07252-z. eprint: 2310.01316.

[11] David P. DiVincenzo. "Quantum Computation". In: *Science* 270.5234 (1995), pp. 255–261. ISSN: 0036-8075. DOI: 10.1126/science.270.5234.255.

[12] Jeremy L. O'Brien. "Optical Quantum Computing". In: *Science* 318.5856 (2007), pp. 1567–1570. ISSN: 0036-8075. DOI: 10.1126/science.1142892. eprint: 0803.1554.

[13] Koen Alexander et al. "A manufacturable platform for photonic quantum computing". In: *arXiv* (2024). eprint: 2404.17570.

[14] Robert Raussendorf and Hans J. Briegel. "A One-Way Quantum Computer". In: *Physical Review Letters* 86.22 (2001), pp. 5188–5191. ISSN: 0031-9007. DOI: 10.1103/physrevlett.86.5188.

[15] N. Yoran and B. Reznik. "Deterministic Linear Optics Quantum Computation with Single Photon Qubits". In: *Physical Review Letters* 91.3 (2003), p. 037903. ISSN: 0031-9007. DOI: 10.1103/physrevlett.91.037903. eprint: quant-ph/0303008.

[16] Michael A. Nielsen. "Optical Quantum Computation Using Cluster States". In: *Physical Review Letters* 93.4 (2004), p. 040503. ISSN: 0031-9007. DOI: 10.1103/physrevlett.93.040503. eprint: quant-ph/0402005.

[17] N. S. Minaev and A. V. Mudryi. "Thermally-induced defects in silicon containing oxygen and carbon". In: *physica status solidi (a)* 68.2 (1981), pp. 561–565. ISSN: 0031-8965. DOI: 10.1002/pssa.2210680227.

[18] E Irion, N Burger, K Thonke, and R Sauer. "The defect luminescence spectrum at 0.9351 eV in carbon-doped heat-treated or irradiated silicon". In: *Journal of Physics C: Solid State Physics* 18.26 (1985), p. 5069. ISSN: 0022-3719. DOI: 10.1088/0022-3719/18/26/018.

[19] A.N. Safonov, Edward C. Lightowlers, and Gordon Davies. "Carbon-Hydrogen Deep Level Luminescence Centre in Silicon Responsible for the T-Line". In: *Materials Science Forum* 196-201 (1995), pp. 909–914. ISSN: 0255-5476. DOI: 10.4028/www.scientific.net/msf.196-201.909.

[20] L Bergeron et al. "Silicon-Integrated Telecommunications Photon-Spin Interface". In: *PRX Quantum* 1.2 (2020). DOI: 10.1103/prxquantum.1.020301. eprint: 2006.08793.

[21] Daniel B. Higginbottom et al. "Optical observation of single spins in silicon". In: *Nature* 607.7918 (2022), pp. 266–270. ISSN: 0028-0836. DOI: 10.1038/s41586-022-04821-y.

[22] Lukasz Komza*, Xueyue Zhang*, Yu-Lung Tang, Zihuai Zhang, and Alp Sipahigil. "Reconfigurable photonic crystal cavity arrays for multiplexed spin-photon interfaces in silicon". In: *Bulletin of the American Physical Society* (2024).

[23] Lukasz Komza*, Xueyue Zhang*, Yu-Lung Tang, Hanbin Song, and Alp Sipahigil. "Frequency multiplexed emission from cavity-enhanced T centers". In: *CLEO: Fundamental Science*. Optica Publishing Group. 2024, FTu3I–3.

[24] Hanbin Song*, Xueyue Zhang*, Yiyang Zhi, Lukasz Komza, and Alp Sipahigil. "Integrated Platform for Spin-Photon Interfaces in Silicon". In: *CLEO: Fundamental Science*. Optica Publishing Group. 2024, FTu3I–2.

[25] Fariba Islam et al. "Cavity-Enhanced Emission from a Silicon T Center". In: *Nano Letters* 24.1 (2024), pp. 319–325. ISSN: 1530-6984. DOI: 10.1021/acs.nanolett.3c04056. eprint: 2310.13808.

[26] Adam Johnston, Ulises Felix-Rendon, Yu-En Wong, and Songtao Chen. "Cavity-coupled telecom atomic source in silicon". In: *arXiv* (2023). eprint: 2310.20014.

[27] Christopher P. Anderson et al. "Electrical and optical control of single spins integrated in scalable semiconductor devices". In: *Science* 366.6470 (2019), pp. 1225–1230. ISSN: 0036-8075. DOI: 10.1126/science.aax9406. eprint: 1906.08328.

[28] V. M. Acosta et al. "Dynamic Stabilization of the Optical Resonances of Single Nitrogen-Vacancy Centers in Diamond". In: *Physical Review Letters* 108.20 (2012), p. 206401. ISSN: 0031-9007. DOI: 10.1103/physrevlett.108.206401. eprint: 1112.5490.

[29] Kay D Jahnke et al. "Electron–phonon processes of the silicon-vacancy centre in diamond". In: *New Journal of Physics* 17.4 (2015), p. 043011. DOI: 10.1088/1367-2630/17/4/043011. eprint: 1411.2871.

[30] Srujan Meesala et al. "Strain engineering of the silicon-vacancy center in diamond". In: *Physical Review B* 97.20 (2018), p. 205444. ISSN: 2469-9950. DOI: 10.1103/physrevb.97.205444. eprint: 1801.09833.

[31] Chloe Clear et al. "Optical transition parameters of the silicon T centre". In: *arXiv* (2024). eprint: 2405.07144.

[32] A DeAbreu et al. "Waveguide-integrated silicon T centres". In: *Optics Express* 31.9 (2023), p. 15045. DOI: 10.1364/oe.482008. eprint: 2209.14260.

[33] Mohammad Hafezi, Sunil Mittal, J Fan, A Migdall, and JM Taylor. "Imaging topological edge states in silicon photonics". In: *Nature Photonics* 7.12 (2013), pp. 1001–1005.

[34] Isabelle Staude and Jörg Schilling. "Metamaterial-inspired silicon nanophotonics". In: *Nature Photonics* 11.5 (2017), pp. 274–284.

[35] L.-M. Duan and H. J. Kimble. "Scalable Photonic Quantum Computation through Cavity-Assisted Interactions". en. In: *Physical Review Letters* 92.12 (2004). ISSN: 0031-9007, 1079-7114. DOI: 10.1103/physrevlett.92.127902. eprint: quant-ph/0309187. URL: https://link.aps.org/doi/10.1103/PhysRevLett.92.127902.

[36] Hannes Pichler, Soonwon Choi, Peter Zoller, and Mikhail D. Lukin. "Universal photonic quantum computation via time-delayed feedback". en. In: *Proceedings of the National Academy of Sciences* 114.43 (2017), pp. 11362–11367. ISSN: 0027-8424, 1091-6490. DOI: 10.1073/pnas.1711003114. eprint: 1702.02119. URL: http://www.pnas.org/lookup/doi/10.1073/pnas.1711003114.

High-Performance On-Chip Gas Sensing with Optical Neural Networks

PI: Yaojing Zhang, The Chinese University of Hong Kong, Shenzhen,
yaojingzhang@cuhk.edu.cn

Optica Foundation Challenge Category: Environment

Global warming caused by greenhouse gases is a major concern of the people of the world. High-precious monitoring of greenhouse gases is thus indispensable. Benefiting from the high-density integration, optical gas sensors have been widely used for gas detection. Most optical gas detection mainly replies on the linear absorption of the gas into the light source, which suffer from drawbacks of limited sensitivities. On the contrary, gas sensors based on optical nonlinearities can break this limitation. Silicon photonics is known to be compatible with complementary metal oxide semiconductor (CMOS) fabrication process, yielding the low-cost manufacturability using high-yield 300-mm wafers and large-scale integration of silicon chips. Our previous work on widely tunable Raman lasers has advantages of narrow linewidth and cover wide wavelengths from 1240 to 1680 nm (Nature Communications 13, 1-8 (2022)). In addition, microresonator-based frequency combs also offer similar advantages of narrow linewidth and wide comb wavelength range. With the rapid development of machine learning, silicon based artificial neural network technology is beginning to be applied to gas sensing in various complex environments. The applicant will develop on-chip gas sensors, integrating them with on-chip neural networks to monitor various greenhouse gases, thus developing High-performance on-chip gas sensing with optical neural networks.

The proposed project aims to leverage the capabilities of advanced silicon photonics to develop high-performance on-chip gas sensors. Our approach integrates widely tunable Raman lasers, microresonator-based frequency combs, and silicon-based artificial neural networks (ANNs) to achieve unprecedented sensitivity and specificity in gas detection. This capability is crucial for monitoring greenhouse gases in diverse environmental conditions. The developed on-chip gas sensors can be deployed for continuous monitoring of greenhouse gases in the atmosphere. They can be used in fixed stations or mobile units to track environmental pollution levels and contribute to climate change studies. Industries can utilize these sensors to monitor and control emissions of greenhouse gases, ensuring compliance with environmental regulations. The high sensitivity and selectivity of the sensors make them ideal for detecting low concentrations of harmful gases in industrial processes. In addition, integrating these sensors into smart building systems can enhance air quality monitoring and management. They can detect and alert about harmful gas concentrations, contributing to healthier living and working environments. By combining cutting-edge silicon photonics with AI-driven neural networks, this project aims to deliver a transformative solution for high-precision, scalable, and cost-effective gas sensing, addressing critical needs in environmental monitoring and various industrial applications.

Proposal: High-Performance On-Chip Gas Sensing with Optical Neural Networks

1. Literature Review

Internet of Things (IoT) is experiencing unprecedented rapid development. The use of wearables and smart homes in people's lives is gradually increasing. Smart sensors are also an important part of it, including the sensor arrays and machine learning techniques for signal processing [1]. As we know, global warming is a phenomenon of rising temperatures due to an increase in greenhouse gases. This rise in temperature leads to an increase in extreme weather, such as droughts, floods and hurricanes. Here, we will focus on the development of smart gas sensors and further implement them for detecting greenhouse gases. Linear absorption sensors are the commonly used and follow the Beer-Lambert Law. Cavity structures can further employ to enhance their sensitivities [2-4]. However, linear absorption sensors usually sacrifice sensitivity at smaller sample concentrations to obtain high sensitivity at larger concentrations [5]. Intracavity sensors are alternative approaches. One method is to utilize an intracavity gain medium that is brought close to the laser threshold to achieve high sensitivity [6]. However, the spontaneous radiation from the laser can limit the sensitivity of such sensing systems and is not that stable [6]. Optical parametric oscillators have none of these limitations. They have low spontaneous emissivity and broadband gain. Thus, the ideal candidates for gas sensors [7].

Nowadays, silicon and silicon nitride (Si_3N_4) are major platforms for photonic integrated circuits. For silicon, it has the reasons behind its dominance of microelectronics: scalability, the pathway to low-cost manufacturing enabled by using high yield 300 mm wafers, and availability of open foundries leveraging on complementary metal-oxide-semiconductor (CMOS) processing. Important progress has recently been made in silicon-based Raman lasers, where we have realized resonant modes with at least one high quality factor in each free spectral range by proposing a new resonator design mechanism. Based on this mechanism, we have designed a resonator that maintains more than one million high quality factors in the 440 nm wavelength range and further realized a Raman laser with a wavelength range tunable down to 516 nm, which is the largest tuning range of Raman lasers to date [8]. In addition to this, Raman lasers have the important advantage of a narrow linewidth [9-12]. Si_3N_4 has an additional advantage of no nonlinear absorption and been widely used for frequency combs [13]. And the frequency combs also feature with narrow linewidth. Therefore, both Raman laser and frequency combs have potential use for gas sensors. In recent years, machine learning has been developing rapidly, and artificial neural network technology is beginning to be applied to gas sensing in a variety of complex environments [14]. However, until now, on-chip optical neural network (ONN) integrated with on-chip devices have not been well investigated.

2. Problem Statement and Objective

2.1 Problem Statement

Currently, the field of smart gas sensors needs to further improve detection accuracy, reduce device size and energy consumption. For optical gas detectors, traditional optical gas detectors rely mainly on linear absorption of a light source and their detection sensitivity is inversely proportional to the concentration of the gas sample. Therefore, they are often suitable for detecting gas samples with low sensitivities. Integrated nonlinear photonics relies on nonlinear effects, like in platforms of silicon and Si_3N_4, which can enable the generation of photons for lasing and frequency combs for and high-resolution spectroscopy. For the optically pumped laser, stimulated Raman scattering is a useful approach, allowing wavelength conversion and extending the optical output wavelength range beyond the pump laser and Raman lasing linewidth is very narrow. Frequency combs as a revolutionary technology are well known for enabling the generation of equally spaced comb lines for optical metrology, biological imaging, and

high-coherent communications. Thus, optical nonlinearity is expected to break through the limitation of linear absorption of traditional optical gas detectors, and utilize its advantages of narrow linewidth, high accuracy, high coherence, and broadband tunability to enhance light-substance interactions, which can be used to improve the sensitivity of gas detection. Further integrated with on-chip ONN can increase the integration degree and reduce the power consumption.

2.2 Overview of objectives

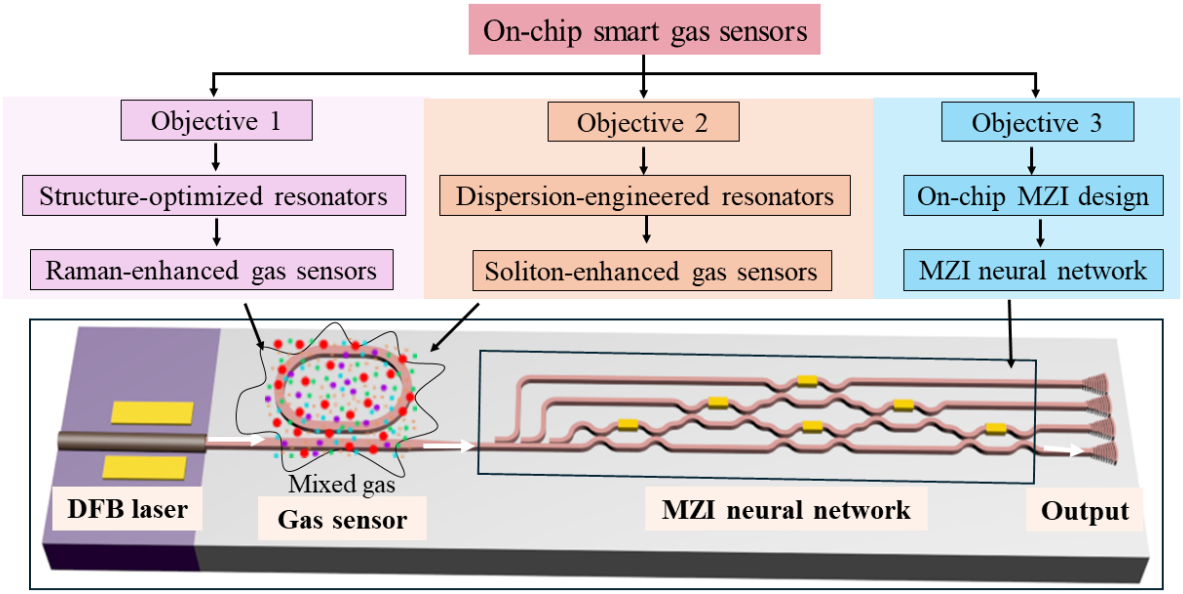

Fig. 1 Schematic of proposed on-chip smart gas sensor system, including three key objectives.

The applicant's proposed work on integrated smart gas sensors consists of three main components: a semiconductor laser to generate pump light, an on-chip optical gas sensor to detect the gas sample, and an on-chip neural network to perform pattern recognition of the detected signals, as shown in Fig. 1. In this case, the semiconductor laser generates pump light, which then enters the on-chip gas sensor through butt coupling. Finally, a neural network is used for training and learning to build a decision rule model, and the accuracy and performance of the test model is evaluated through testing. The on-chip neural network will consist of cascaded Mach–Zehnder interferometer (MZI) interferometer units for arbitrary matrix transformation. For on-chip gas sensors, the applicant intends to develop two devices as shown in Fig. 2: a silicon-based Raman-enhanced gas sensor and a soliton-enhanced gas sensor, to study the mechanism of the two optical nonlinear effects, Raman scattering and soliton frequency comb, on the enhancement of gas molecule detection. The applicant will investigate the influence of device structure on the detection of gas molecules based on the two integrated platforms of silicon-based and silicon-nitride, respectively, and obtain the design scheme of device structure. It is proposed to first start from Lambert's Beer law and combine the nonlinear Schrödinger equation to generate Raman laser and optical frequency combs to reveal the mechanism of optical nonlinearity for enhanced gas detection. Then, the time-domain finite-difference method is used to simulate and calculate the intrinsic modes and mode-field distributions in the structure of the optical resonator, to study the influence of the device structure on the Raman laser and optical frequency comb, and then to reveal the influence of the device structure on the gas detection law. Finally, combined with the on-chip neural network, the mode recognition of multiple gases detected is carried out to realize the development of high-precision intelligent on-chip optical gas sensors.

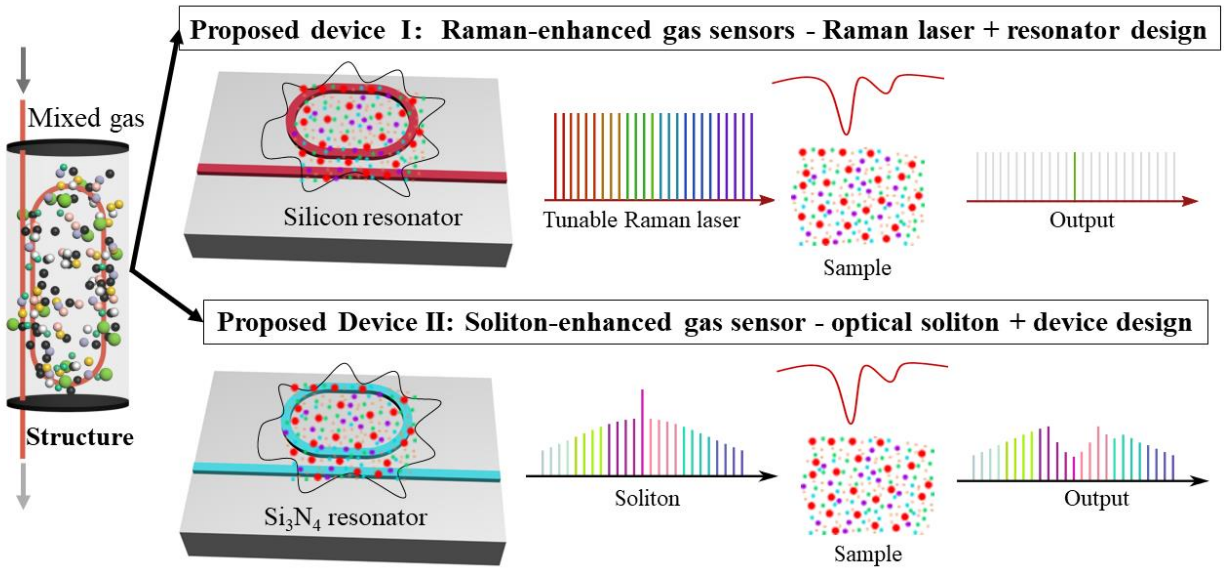

Fig. 2 Schematic of two proposed on-chip gas sensors.

2.3 Innovation objectives

Depending on the targeted on-chip smart gas sensors, this project will have three objectives. This proposal will mainly work on silicon and Si_3N_4 platform since they are compatible with the CMOS fabrication process. The applicant has rich experience in photonic experiments, which will benefit the realization of each objective, including device design, experimental setups, and optical measurements. The proposed devices will provide new scientific insights into using integrated photonics for developing Raman-enhanced gas sensors, soliton-enhanced gas sensors, and on-chip ONN. The success of each objective has the potential to generate high scientific and technological impact. That is, Raman-enhanced gas sensors can lead to novel silicon devices and high-precise gas sensing. The soliton-enhanced gas sensors have potentials to arise new approach for gas sensing, novel Si_3N_4 devices, and the high-sensitivity gas sensing. The on-chip ONN can yield compact footprint and novel model to further improve the performance of the devices and signal analysis. The realization of each objective has the potential for the development of future commercial products.

Objective 1: Raman-enhanced gas sensors

Silicon-based Raman lasers based on the Raman effect have the advantages of wavelength extension, broadband tunability, narrow linewidth, high compatibility and high integration. A large wavelength range of continuous wavelength tuning can be realized by adjusting the wavelength of the laser's pump source, and the linewidth is usually <100 Hz. For Raman lasers, Raman lasers can be generated with a frequency shift of 15.6 THz from the pump light by designing a silicon-based resonator structure and then inputting pump light into the resonator when the Raman gain is larger than the microcavity loss. At the same time, the silicon-based Raman laser can be seamlessly integrated with conventional silicon-based optoelectronic integrated circuits and fabricated using existing silicon-based microelectronic processing technology and equipment, which can reduce fabrication costs and improve integration, and this compatibility contributes to the development of compact and efficient integrated photonic systems. The applicant's proposed silicon-based Raman-enhanced gas sensors are based on its work of realizing broadband tunable Raman lasers based on silicon-based resonators, and taking advantage of the narrow linewidth and broadband tunability of Raman lasers, the applicant is to further study the mechanism of Raman laser-enhanced gas sensing and the physical mechanism of the corresponding device structure to realize high-precision gas detection for the purpose of applying them to the detection of greenhouse gases.

Objective 2: Soliton-enhanced gas sensors

Optical frequency combs based on four-wave mixing can generate equally spaced optical pulse comb lines by pumping light through the input, which have high coherence and narrow linewidths and have important applications in communications. The generation and application of integrated optical frequency combs has been a hot spot of integrated optics. The applicant's proposed microcavity soliton enhanced gas sensor is based on its work of realizing a dark pulse frequency comb based on a Si_3N_4 resonator, designing the dispersion of the Si_3N_4 resonator, which in turn generates high-coherence solitons, and researching the mechanism of soliton enhanced gas sensing and the corresponding physical mechanism of the device structure to realize high-precision gas detection.

Objective 3: On-chip ONN

A neural network consists of neurons, each of which receives and summarizes signals from the previous layer, compares the weighted sum to a threshold, and generates an output using an activation function. This output is passed on to the next layer of neurons as an input to the next layer of neurons. The connections between neurons are made by synapses, each of which has an associated weight that is used to regulate the degree of influence of the input signal. During the training phase the system adjusts the weights of the synapses by using algorithms such as backpropagation to enable the neural network to learn the features and patterns of the input data and produce the desired output. Once training is complete the neural network system can be used to perform complex tasks such as pattern recognition. On-chip artificial neural networks are a hot research topic because of their high degree of integration, real-time processing capability and low power consumption. It can realize a large number of neurons and connections on a single chip, thus achieving a high degree of hardware integration, which in turn improves the performance and efficiency of the system. At the same time, the on-chip neural network has a strong real-time processing capability, which can quickly process and respond to the input data, and is suitable for application scenarios with high real-time requirements. In real life, there are multiple complex gases in the atmosphere, and accurately detecting each gas component is a challenge. For achieving this goal of multiple gas detection, the applicant proposes to carry out an on-chip neural network system consisting of cascaded Mach-Zönder interferometer units to perform pattern recognition, i.e., model training and model validation, of gas molecules detected in on-chip gas sensors, so as to achieve high-precision detection of different gas molecules.

3. Outcomes

- **The outcome of our proposal is expected to be a prototype of a compact and <u>the first</u> full-integrated smart gas sensor. The on-chip gas sensor will be several orders of magnitude reduction in size and weight.**
- **Full-integrated** system with laser sources, modulators, MZI network, grating array, and photodetector.
- The state-of-art on-chip ONN for sample pattern recognition with model training and model validation.
- The produced intellectual property (IP) from the project will be managed to follow the IP rules and the policies. The university will support and evaluate any IP output for possible patent applications and seek for possible licensing strategies with industrial partners for commercial products.
- Commercializing our proposed optical applications will take a step towards on-chip smart gas sensors processing. The relevant IP outcomes will also be considered for patents or other ways of licensing to industrial companies for commercial products.

4. Impact

4.1 Credibility of the measures to enhance the career perspectives and skills development

The project will enable the applicant well equipped with comprehensive scientific skills and new abilities in conducting research and leading a research group in my career. This project highly extends my previous research background and enables me to open new research directions in using integrated photonics for practical applications. Particularly, this project will allow me to gain skills in designing different types of resonators, generating Raman lasing and optical frequency combs, and research experience with on-chip gas sensors. The proposed on-chip optical applications can also highly contribute to driving progress in integrated systems on photonic chips for commercial products. My leadership through supervising PhD students will be continued to improve. The research experience will enrich my research diversity. This research project will be a great chance for me to enhance my career as an assistant professor in a university.

4.2 Suitability and quality of the measures to maximize expected outcomes and impacts

The scientific outputs from the project mainly have three ways to expand the influence of the project: (i) attend international conferences for oral presentations or poster exhibitions, like Conference on Lasers and Electro-Optics (CLEO), CLEO Pacific Rim, CLEO Europe, European Conference on Integrated Optics (ECIO), and Frontiers in Optics; (ii) upload open-access pre-prints for timely access by the scientific community of arXiv.org, and Zenodo.org; (iii) publish results on high-impact, open-access, and peer-reviewed journals in Optica Publishing. The latest research outcomes will be posted on my group website at Chinese University of Hong Kong, Shenzhen, and through social media like Facebook, LinkedIn, and Twitter for a wider audience.

4.3. The magnitude and importance of the project's contribution to the expected scientific, societal and economic impacts

4.3.1 Scientific and technological impacts

This proposal includes three independent objectives, each of which is expected to have significant scientific and technological impacts. Since the three objectives employ integrated resonators and on-chip MZI, the common technological impacts will be in terms of small footprint, and low power consumption. For scientific impacts, the first objective of realizing the frequency comb spectroscopy is promising for the next generation of bio-sensing benefitting from the precious comb source. The technological impact will reflect in the design of the resonator and the new approach for dark comb generation in the NIR regime. The second objective of the optical gyroscopes will bring the scientific impact to achieve integrated gyroscopes with high sensitivities and low power consumption. The proposed device design will present a well-designed structure for inducing mode differences for symmetry breaking. The last objective on the application of the optical isolator can have a scientific impact by proposing a new approach to gain large isolation between counterpropagating light waves. The technological impact would also be from the carefully engineered device structure for more possible applications.

4.3.2 Economic and societal impacts

Each objective has the potential for new products that can benefit society. In particular, the first objective of the Raman-enhanced gas sensors with enhanced responsivity will have a societal impact in tracking environmental pollution levels and facilitating climate change research. the second objective of soliton-enhanced gas sensors with high sensitivities has significance for detecting low concentrations of harmful gases in industrial processes. The third objective on on-chip ONNs can be useful for optical communications and can enable novel types of PICs. The three objectives together are crucial for monitoring greenhouse gases in diverse environmental conditions. The developed on-chip gas sensors can be deployed for continuous monitoring of greenhouse gases in the atmosphere.

References

[1] S. Feng, F. Farha, Q. Li, Y. Wan, Y. Xu, T. Zhang, and H. Ning, Sensors **19**, 3760 (2019).
[2] B. Bernhardt *et al.*, Nat. Photonics **4**, 55 (2010).
[3] M. A. Reber, Y. Chen, and T. K. Allison, Optica **3**, 311 (2016).
[4] M. J. Thorpe, K. D. Moll, R. J. Jones, B. Safdi, and J. Ye, Science **311**, 1595 (2006).
[5] R. M. Gray, M. Liu, S. Zhou, A. Roy, L. Ledezma, and A. Marandi, arXiv preprint arXiv:2301.07826 (2023).
[6] V. M. Baev, T. Latz, and P. E. Toschek, Appl. Phys. B **69**, 171 (1999).
[7] D. D. Arslanov, M. Spunei, J. Mandon, S. M. Cristescu, S. T. Persijn, and F. J. Harren, Laser Photonics Rev. **7**, 188 (2013).
[8] Y. Zhang, K. Zhong, X. Zhou, and H. K. Tsang, Nat. Commun. **13**, 3534, 3534 (2022).
[9] M. A. Ferrara and L. Sirleto, Micromachines **11**, 330 (2020).
[10] B.-B. Li, W. R. Clements, X.-C. Yu, K. Shi, Q. Gong, and Y.-F. Xiao, Proc. Natl. Acad. Sci. **111**, 14657 (2014).
[11] Ş. K. Özdemir *et al.*, Proc. Natl. Acad. Sci. **111**, E3836 (2014).
[12] P.-J. Zhang, Q.-X. Ji, Q.-T. Cao, H. Wang, W. Liu, Q. Gong, and Y.-F. Xiao, Proc. Natl. Acad. Sci. **118** (2021).
[13] S. Zhang, T. Bi, I. Harder, O. Ohletz, F. Gannott, A. Gumann, E. Butzen, Y. Zhang, and P. Del'Haye, Laser Photonics Rev., 2300642 (2023).
[14] J. Frazão, S. I. Palma, H. M. Costa, C. Alves, A. C. Roque, and M. Silveira, Sensors **21**, 2854 (2021).

Executive Summary

Skin color-bias-free oximeter

Oximeters, one of the most used optical medical devices for measuring blood oxygen saturation levels, show inaccurate results based on the color of the skin. This inaccuracy disproportionately affects people of color and deprives them of supplemental oxygen in times of dire need. In this work, we plan to develop a skin color-bias-free oximeter that provides accurate measurements irrespective of skin color.

An adequate level of oxygen in the body is essential for our survival. Typically, an optical pulse oximeter is used to measure the oxygen content in the blood. If pulse oxygenation drops below 92%, supplemental oxygen is administered. Hence, it is critical to ensure the oximeter reading is accurate. Occult hypoxemia is an urgent situation where even if the arterial oxygen saturation (measured with blood gas analysis) drops below 88%, pulse oximeters, nonetheless, show an oxygen saturation of 92 to 96%. In this scenario, the patient does not receive supplemental oxygen. Depending on the severity and duration, hypoxemia can lead to mild symptoms or lead to death. In a study on COVID-19 patients, researchers at the University of Michigan observed 11.7% occurrences of occult hypoxemia in black patients compared to 3.6% of white patients. This inaccuracy has devastating consequences – being unaware of the oxygen deficiency, caregivers do not administer oxygen therapies to patients needing supplemental oxygen, putting specific populations from minority backgrounds (Black, Latinx, and Native American) at disproportionately higher risk.

In the fundamental design, oximeters rely on light absorption in skin, blood, and tissue. A calibration curve is used, which correlates light absorption to oxygen saturation. The calibration depends on skin color. For example, if the calibration was taken from volunteers with lighter skin colors, the results would be erroneous for patients with darker skin colors. In this work, we plan to design and demonstrate a skin-color-sensitive oximeter, which will provide insights into the user's skin color and blood oxygen levels. In Aim 1, we will create new analytical and empirical calibration curves used in oximeters. These new calibration curves will be developed using well-established skin color characterization scales, namely, the Fitzpatrick classification system, von Luschan chromatic scale, and the Monk scale. We hope to reduce measurement inaccuracies with the proposed design by intelligently selecting an appropriate calibration curve, using a combination of artificial intelligence algorithms and optical sensors. In Aim 2, we will develop an intelligent oximeter using two oximeter sensors on a stretchable substrate capable of simultaneous transmission- and reflection-mode oximetry. Hence, we will use that to select the correct calibration curve of the oximeter based on skin color. In Aim 3, for validation, we will run a validation study with 50 subjects at the USC Center for Advanced Lung Disease, representing the whole skin color spectrum. In Aim 4, we will work with USC Keck Medicine Department of Family Medicine and the Race Equity, Diversity, and Inclusion Council at USC. Our efforts will raise awareness among medical professionals and affected communities about the limitations of current devices.

The project to develop a skin color-bias-free oximeter aligns perfectly with the Optical Foundation Challenge in Health by innovatively using optical technology to address a critical and pervasive health disparity. This initiative proposes advanced optical sensors for a dual-mode oximeter that adapts to skin color, improving accuracy and equity in medical diagnostics. By addressing the documented inaccuracies in oximetry across different skin colors, the project not only advances technology but also champions the cause of equitable health solutions.

Oximeters are the most used optical medical device and they must remain accurate for everyone. Clinical administration of oxygen is usually adjusted by observing the blood oxygen content of patients using a pulse oximeter. If oxygen falls below a certain threshold, supplemental oxygen is provided to the patients [1]. Therefore, oximeters must provide accurate results. If higher oxygen saturation is reported than what is actual, patients will not receive supplemental oxygen due to the measurement error, which will result in hypoxemia [2]. **Depending on the severity and duration, hypoxemia can lead to mild symptoms or lead to death.** Mild symptoms include headaches and shortness of breath. In severe cases, hypoxemia can interfere with heart and brain function. It can lead to a lack of oxygen in the body's organs and tissues, which is called hypoxia.

In the simplest form, oximeters use two wavelengths of light, typically red and near-infrared (NIR) to measure a person's oxygenation. The pulse oxygenation value is computed by measuring the absorption ratio at these two wavelengths (Fig. 1a). Here, the light is transmitted through the skin, and transmission-mode absorption is taken into account. Since pulse oximetry is a ratiometric measurement, a simple calibration curve relates light attenuation to the oxygen content [4]. **If this calibration is taken from people with lighter skin colors, the results will be erroneous for people with darker skin colors, and vice versa. This racial bias is a documented problem in oximeters [5, 6], putting specific populations from minority backgrounds at disproportionately higher risk.** During the COVID-19 pandemic, researchers at the University of Michigan have observed that black patients with low arterial oxygen saturation were demonstrating higher SpO_2 in pulse oximeters [3]. Some of these patients did not receive supplemental oxygen just because their SpO_2 was recorded higher (92-96%) as opposed to their actual low arterial oxygen saturation (<88%) [3]. **This is a fundamental problem with the current pulse oximeters, where racial bias is built into the hardware** (Fig. 1b).

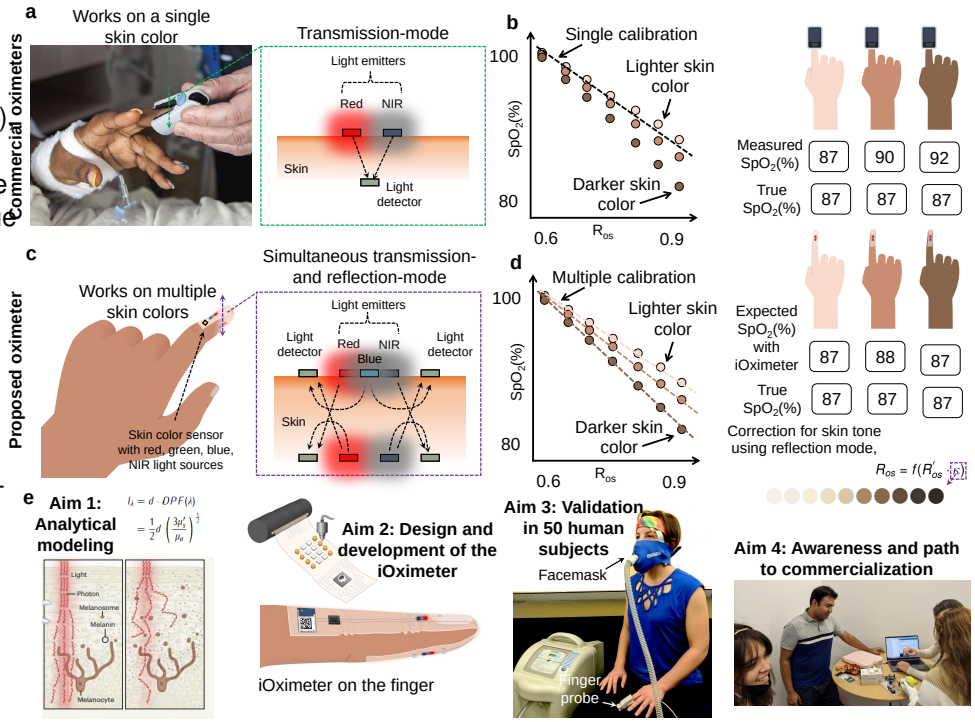

Figure 1: Current and proposed oximeter designs. (**a**) Transmission-mode oximeter that is calibrated for a single skin color. No skin pigment information can be captured using the existing sensor. (**b**) Since sensor calibration is performed based on a single skin type, the oximeter's error gets amplified when used on other skin types. 5% SpO_2 error in dark skin is shown based on data by Sjoding et al. [3]. (**c**) Proposed oximeter design for both transmission and reflection modes. Both oxygenation and skin color information can be captured with this design. An additional sensor (blue light) is added for accurate skin color sensing. (**d**) Since the sensor captures skin color information, calibration can be adjusted for multiple skin colors with a skin color correction factor (κ). (**e**) The aims of the study include analytical modeling (Aim 1), design and development of the oximeter (Aim 2), validation in a clinical setting on 50 participants (Aim 3), and raising awareness regarding the bias in oximetry (Aim 4).

A consensus of "observed racial bias in oximetry" is seen in the literature bolstering the study performed by the Michigan group during COVID-19. Bickler et al. found at 60-70% SaO_2, SpO_2 overestimated SaO_2 (bias +/- SD) by 3.56 +/- 2.45% (n = 29) in darkly pigmented subjects, compared with 0.37 +/- 3.20% (n = 58) in lightly pigmented subjects ($P < 0.0001$) [5]. Feiner et al. also came to the same conclusion of

biased measurements when monitoring patients with saturations below 80%, especially those with darkly pigmented skin [7]. In a recent larger study, Valbuena et al. found in 30,039 pairs of SpO_2-SaO_2 readings, the occurrences of occult hypoxia were 2.7% in white patients compared to 12.9% in black patients [8]. **Reasons for this racial bias are not well comprehended and potentially enabled by limitations in existing regulatory oversight [9]. Unfortunately, attempts to understand and solve this problem remained very small.**

In this work, we propose a simultaneous transmission- and reflection-mode oximeter, which will carry both oxygenation and skin color information (Fig. 1c). In this sensor design, light emitters and detectors are placed on both sides of the tissue – with this topology, transmitted and reflected lights can be captured. **Oxygenation information will be encoded in both measurements, while the reflection-mode measurement will provide skin color information. Another accurate measurement of the skin color can be performed using a dedicated optoelectronic sensor [10]**. Consequently, it is possible to adjust the calibration curve based on the skin color information measured in the reflection mode (Fig. 1d). Furthermore, We will provide the origins of bias in oximetry with analytical and empirical insights by undertaking the design and development of the new oximeter. In addition, we will conduct validation in a clinical setting with 50 participants and work on raising awareness regarding the bias in oximetry (Fig. 1e).

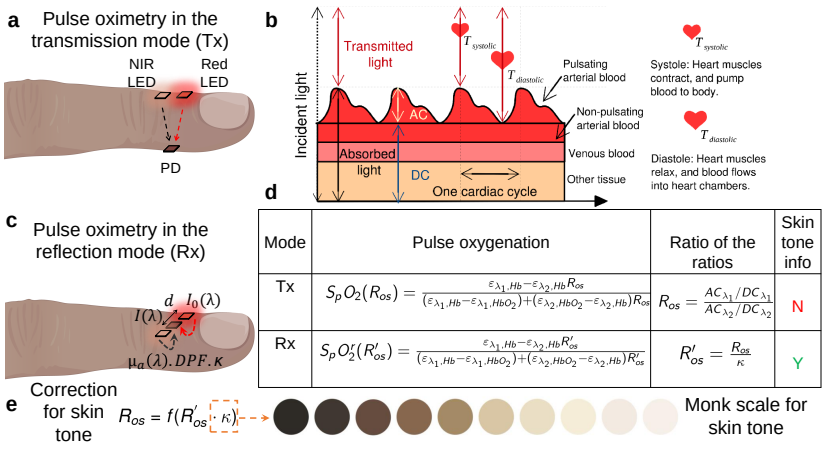

Figure 2: Analytical models of oximetry. (**a-b**) In the transmission mode, LEDs are placed on one side, and the PD is placed on the other side of the tissue. Light passes through bone, tissue, non-pulsating arterial and venous blood, and arterial blood. Once this signal is obtained from two different wavelengths of light, the ratio of the ratios (R_{os}) is calculated and correlated to SpO_2. In the transmission mode, no skin color information is captured by the device. (**c**) In the reflection mode, LEDs and PD are placed on the same side. (**d**) Here, the ratio of the ratios captures skin color information in the form of $R'_{os} = \frac{R_{os}}{\kappa}$. (**e**) We will correlate κ to the existing skin color scales.

To understand the limitations of current oximeters, it is essential to explore the inner workings of the existing pulse oximeters. We will compare analytical models in transmission and reflection modes, and outline the required study to include analytical and empirical models that can handle multiple skin colors. A pulse oximeter uses light attenuation in the transmission mode to quantify SpO_2. In transmission mode pulse oximetry, light from LEDs is directed into the top of the finger, and the transmitted light is sensed at the bottom of the finger with a photodetector (Fig. 2a-b). Here, $R_{os} = \frac{AC_{\lambda_1}/DC_{\lambda_1}}{AC_{\lambda_2}/DC_{\lambda_2}}$, is the ratio of pulsatile (AC) to stationary (DC) signals at the two wavelengths in the transmission-mode and κ provides insight into the skin type (Fig. 2c). When both the transmission and reflection-mode operations are performed simultaneously, oxygenation and skin color information is gathered in a single shot, which is impossible while operating only in the transmission mode (Fig. 2d). In addition, the calibration curve can be changed based on the skin color correction factor κ (Fig. 2e).

Previous experience with oximetry: **Dr. Khan extensively worked on oximetry during his PhD and developed five different types of oximeters, namely, organic transmission-mode oximeter [11], organic refection-mode oximeter [12], organic reflectance oximeter array [13], multichannel PPG sensors [14], and an ambient-light oximeter [15].** Our fundamental and applied research on developing flexible biophotonic sensors led to the first demonstration of a pulse oximeter based on organic semiconductors [11], and the first flexible reflectance oximeter array (ROA) composed of printed OLEDs and OPDs [13]. All these experiences will play a vital role in developing the proposed iOximeter.

Tasks:

Aim 1: Analytical and empirical models of light propagation through different skin colors in pulse oximeters.

In order to comprehend the constraints of current oximeters, it is crucial to delve into the internal mechanisms of these existing pulse oximeters. We will conduct a comparative analysis of analytical models employed in both transmission and reflection modes. Furthermore, we will outline the necessary investigation, encompassing both analytical and empirical models capable of accommodating various skin tones. In pulse oximetry's transmission mode, SpO_2 is quantified by assessing light attenuation. In this mode, LEDs emit light into the upper part of the finger, and a photodetector at the bottom of the finger captures the transmitted light (Fig. 2a-b). Oxygen saturation (SpO_2) is calculated using Eq. 1. Here, $\varepsilon_{\lambda_1,Hb}$ and $\varepsilon_{\lambda_2,Hb}$ are the molar absorptivity of deoxy-hemoglobin at red and NIR wavelengths. Similarly, $\varepsilon_{\lambda_1,HbO_2}$ and $\varepsilon_{\lambda_2,HbO_2}$ are the molar absorptivity of oxy-hemoglobin at red and NIR wavelengths.

$$SpO_2(R_{os}) = \frac{\varepsilon_{\lambda_1,Hb} - \varepsilon_{\lambda_2,Hb} R_{os}}{(\varepsilon_{\lambda_1,Hb} - \varepsilon_{\lambda_1,HbO_2}) + (\varepsilon_{\lambda_2,HbO_2} - \varepsilon_{\lambda_2,Hb}) R_{os}} \tag{1}$$

An empirical correction is required to overcome the limitations of Beer-Lambert's Law in scattering tissue. Interesting to note that in the transmission mode, none of the factors in the equation relates to skin color. On the contrary, in the reflection mode, a similar model can be established with one difference where the ratio term contains a contribution from differential path length factor (DPF) and skin color (S). Both of these can be coupled in a single term that we define as skin color correction factor, $\kappa = \frac{DPF_{\lambda_1}}{DPF_{\lambda_2}} \cdot S$ that is measurable if we perform transmission and reflection-mode oximetry simultaneously. Therefore, the ratio of the ratios in the reflection mode can be expressed as, $R'_{os} = \frac{R_{os}}{\kappa}$.

Here, $R_{os} = \frac{AC_{\lambda_1}/DC_{\lambda_1}}{AC_{\lambda_2}/DC_{\lambda_2}}$, is the ratio of pulsatile (AC) to stationary (DC) signals at the two wavelengths in the transmission-mode and κ provides insight into the skin type (Fig. 2c). **When both the transmission and reflection-mode operations are performed simultaneously, oxygenation and skin color information is gathered in a single shot, which is impossible while operating only in the transmission mode (Fig. 2d).**

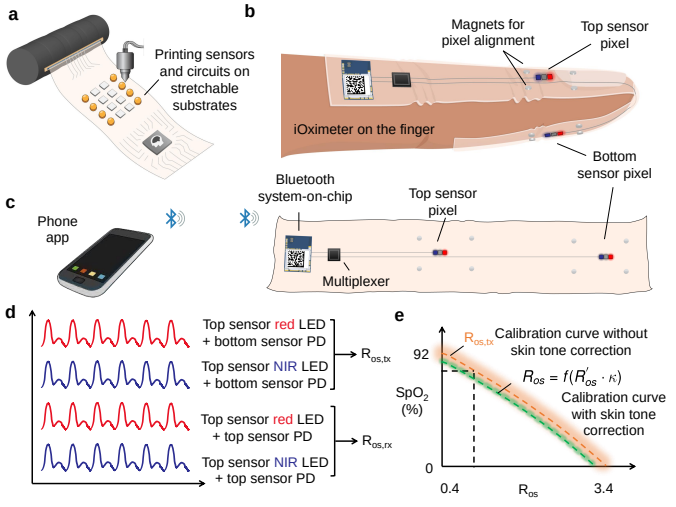

Figure 3: Design and fabrication of the iOximeter. (**a**) The sensor will be fabricated on a stretchable substrate using printing techniques. (**b-c**) The iOximeter is placed on top of a finger. Two oximeter pixels are used, which are connected to a Bluetooth system-on-chip using an I2C multiplexer. Data is wirelessly transmitted to a phone. (**d**) Data collection strategies: transmission-mode data collection using the top red and NIR LEDs and the bottom PD, and reflection-mode data collection using the top LEDs and PD. (**e**) After capturing the skin color factor, the oximeter intelligently chooses the correct calibration curve for the user.

For including the skin color in the model, we will use the Fitzpatrick, VL, and Monk scales to obtain skin color information from each participant. We will follow the study protocol by open oximetry (https://openoximetry.org/study-protocols/) and use Delfin Technologies, Ltd. SkinColorCatch to capture skin color information to demonstrate how the calibration curve changes based on the skin color correction factor κ (Fig. 2e).

Aim 2: Fabrication of iOximeter

We plan to build a custom wearable oximeter, which captures transmission and reflection mode data, and transmits that wirelessly to a phone. We will be printing conductive stretchable traces on an elastomeric substrate to connect various electronic components (Fig. 3a). Flexible and stretchable hybrid electronics is one of our primary expertise [16, 17, 18] – **we will design a soft, comfortable, wireless, band-aid-like iOximeter** (Fig. 3b).

To perform the simultaneous oximetry, we

will use two commercial oximeter sensor pixels (Maxim Integrated MAX86916). These are very small, 3.5mm x 7.0mm x 1.5mm. For streaming data from two sensor pixels, an Inter-Integrated Circuit (I2C) multiplexer will be used with a Nordic nRF52832 Bluetooth transceiver (Fig. 3b-c). We will use the red and NIR LEDs from the top pixel and the PD from the bottom for a transmission mode measurement. With the red and NIR LEDs from the top pixel and the PD from the top pixel, we will take the reflection mode measurement (Fig. 3d). **A similar approach can be utilized to take transmission- and reflection-mode measurements from the bottom side. Using the I2C mux, it is possible to stream data at 1kHz from the four channels, which is 250 Hz from each channel.** This sampling frequency is sufficient to resolve the PPG waveform and calculate SpO_2 and the skin color factor (κ). Once we capture κ, the obtained calibration curve from Aim 1 can be used to calculate the SpO_2 with a correction for skin color.

In our current prototype, the key three components of the iOximeter are seamlessly integrated into a single flexible PCB (Fig. 4). This design features a DC-DC boost converter, two low dropout regulators, nRF52832 BLE SOC, an optical sensor module with integrated LEDs and photodiode, and a dual channel analog front end with external LEDs and photodiodes. **The optical sensor module is equipped with four distinct LEDs (blue, green, red, IR), a photodiode with a broad spectral responsivity range (400nm - 1050nm), and a 19-bit ADC.** Communication with the MCU is established through the I2C protocol. This optical sensor primarily serves the purpose of skin color measurement. The analog front end accommodates two photodiodes for independent readings and provisions for three LEDs. This flexibility enables custom physical arrangements of LEDs and Photodiodes to implement the proposed topology. The proposed setup utilizes two high-speed, highly sensitive PIN photodiodes with enhanced sensitivity for visible light (350 to 1100nm). One functions as a transmittance mode PPG sensor, and the other as a reflectance mode PPG sensor, accompanied by a single dual-color emitting LED with peak wavelengths of 660nm and 940nm. The AFE communicates with the MCU over SPI.

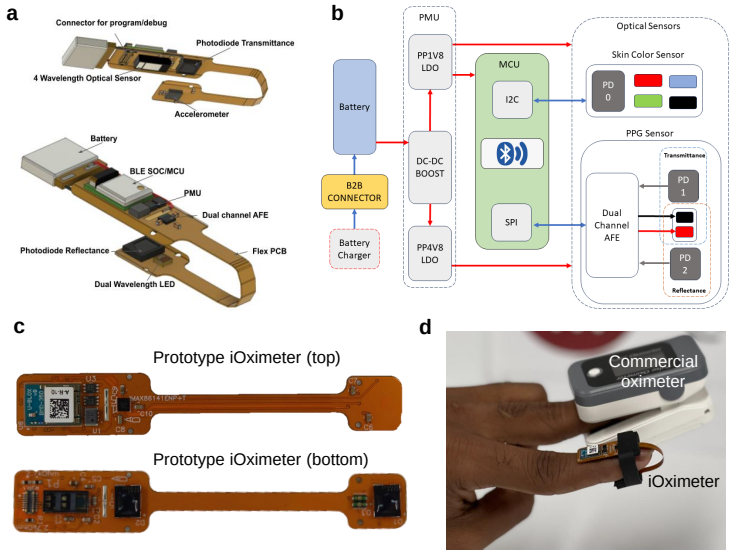

Figure 4: Current prototype of the iOximeter. (**a**) Design of the device showing DC-DC boost converter, two low dropout regulators, nRF52832 BLE SOC, and an optical sensor module with integrated LEDs and photodiode. (**b**) System block diagram of the iOximeter demonstrating how the sensor is operated and collects data. (**c-d**) Photographs of the device from top and bottom, and on a volunteer's finger. A commercial oximeter is shown for comparison (unpublished).

Aim 3: Validation of the iOximeter under controlled hypoxia.

In our preliminary testing, we collected data from 18 participants. We carefully reduced participants' oxygen concentration while simultaneously monitoring SpO_2 and PPG data from both commercial and our sensors. The altitude generator was used for the controlled oxygen concentration changes. Drawing in ambient air, the generator filtered a portion of oxygen, directing it through tubing into a mask worn by participants. The chamber knob adjustments allowed control of oxygen concentration within the safe range of 100% to 92%, monitored by a commercial pulse oximeter. Concurrently, our sensor collected transmitted mode IR and red PPG data during this controlled change in oxygen saturation.

Fig. 5a-b illustrates the variation of IRdc/Reddc and Redac/IRac derived from PPG data for different oxygen saturations for 18 participants (6 from each skin color group). Notably, for darker skin tones, the ratio of DC components is large while for AC components it's the opposite. This can be conferred from Eq. 10. For darker skin color, the ratio of the probability of successful photon (k) will be large as more photons from red LED will be absorbed in darker skin color. Moreover, increased concentrations of melanin have

an exponential impact(w). Together, these factors contribute to distinct ratio changes across different skin tones. As commercial pulse oximeters are reported to overestimate oxygen saturation in diverse skin tones, particularly for lower oxygen saturation levels, we employed the experimental data from Fig. 5a-b (100% to 96%). The extracted parameters are presented in Fig. 5d. Fig. 5a reveals that a decrease in SpO2 results in an increase in the ratio of DC components. The analytical model elucidates this negative slope observed in our study. **Interestingly, there is a decrease in slope from lighter to darker skin tone. This infers that, due to the increase of melanin in darker skin tone absorption coefficient becomes dominant, and reduced scattering decreases. This leads to the decrease of optical path length traveled by the photon resulting in the decrease of slope (u)** . Fig. 5c predicts the ratio of dc and ac components of the PPG data for oxygen saturation ranging from 100% to 88% across three skin tones. Utilizing these predicted data, it shows the SpO2 vs ROS for various skin tones. It is evident that as the saturation level decreases, variations in SpO_2 vs ROS become more pronounced among diverse skin tones. **Notably, for lighter skin tones at 88% saturation, skin tone-02 and skin tone-03 are predicted to be 86.7% and 82.3%, resulting in errors of 1.3% and 5.7%, respectively. This dataset needs to be increased to n=50 human participants to confirm our results. The Optica support will allow us to establish our findings.**

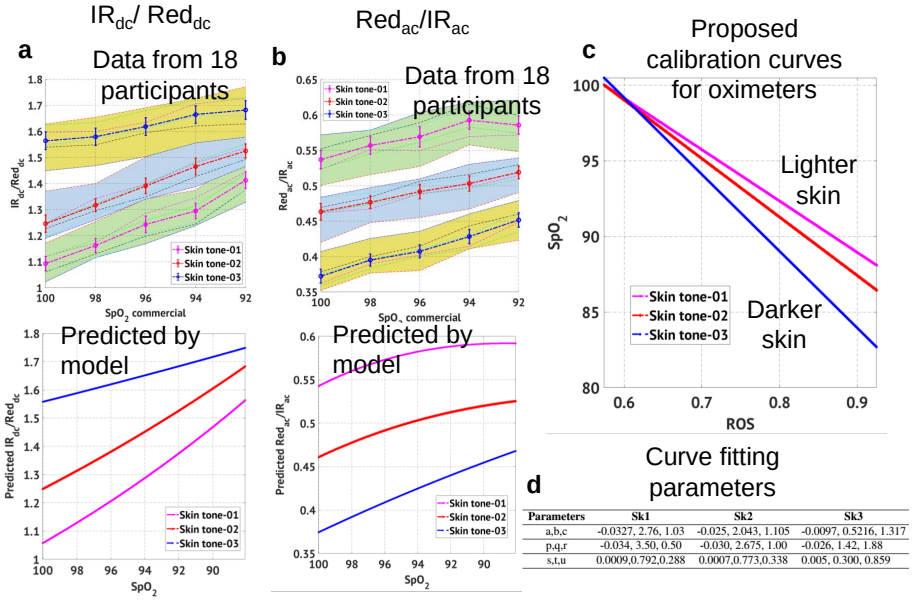

Parameters	Sk1	Sk2	Sk3
a,b,c	-0.0327, 2.76, 1.03	-0.025, 2.043, 1.105	-0.0097, 0.5216, 1.317
p,q,r	-0.034, 3.50, 0.50	-0.030, 2.675, 1.00	-0.026, 1.42, 1.88
s,t,u	0.0009,0.792,0.288	0.0007,0.773,0.338	0.005, 0.300, 0.859

Figure 5: Preliminary results show a clear bias in oximetry results based on skin color. (**a**) IRdc/Reddc derived from PPG data for different oxygen saturation (top), and predicted by our model (bottom). (**b**) Redac/IRac derived from PPG data for different oxygen saturation (top), and predicted by our model (bottom). (**c**) New calibration curves show SpO2 has a dependency on skin color. (**d**) Variables calculated from the experimental data for use in the analytical model (unpublished).

Aim 4: Creating awareness

Pulse oximetry data from 30 years ago suggest dark pigments in the skin cause overestimation of SpO_2 [19]. Unfortunately, that problem still exists, and only because of COVID-19 this quarter-century-old problem is getting the attention it deserves. Hence, creating awareness about the limitations of current oximeters and the potential of skin-color-sensitive oximeters is vital to address healthcare disparities ensuring that it reaches healthcare providers and communities, particularly those serving underrepresented minority populations, and ultimately achieves widespread accessibility and impact. We will partner with USC **Keck Medicine's Family Medicine Department and the Race Equity, Diversity, and Inclusion Council (REDI Council) in Population and Public Health Sciences** to raise awareness among healthcare professionals and communities about current device limitations and the potential of skin-color-sensitive oximeters to address these disparities.

A positive outcome from this work will have a broad impact on health equity. Currently, oximeters are the only available tool for measuring oxygenation in many parts of the world. The described bias in the oximeter is disproportionately hurting people of color. Hence, it is critical to solve this problem. Moreover, this work sheds light on the gap that currently exists in the medical device field in terms of racial bias [20, 21, 22]. **We hope this work will encourage similar exploratory studies in medical devices and patient care where bias is evident or hidden**. Also, we want to train the next-generation problem solvers to question existing standards, dig deep to discover the problem, and improve the methods or pave the pathway for innovation.

References

[1] R. Murphy, K. Mackway-Jones, I. Sammy, P. Driscoll, A. Gray, R. O'Driscoll, J. O'Reilly, R. Niven, A. Bentley, G. Brear, et al. Emergency oxygen therapy for the breathless patient. Guidelines prepared by North West Oxygen Group. *Emergency Medicine Journal*, 18(6):421–423, 2001.

[2] R. Rodríguez-Roisin and J. Roca. Mechanisms of hypoxemia. *Intensive care medicine*, 31(8):1017–1019, 2005.

[3] M. W. Sjoding, R. P. Dickson, T. J. Iwashyna, S. E. Gay, and T. S. Valley. Racial bias in pulse oximetry measurement. *New England Journal of Medicine*, 383(25):2477–2478, 2020.

[4] J. G. Webster. *Design of pulse oximeters*. Crc Press, 1997.

[5] P. E. Bickler, J. R. Feiner, and J. W. Severinghaus. Effects of skin pigmentation on pulse oximeter accuracy at low saturation. *The Journal of the American Society of Anesthesiologists*, 102(4):715–719, 2005.

[6] Z. Vesoulis, A. Tims, H. Lodhi, N. Lalos, and H. Whitehead. Racial discrepancy in pulse oximeter accuracy in preterm infants. *Journal of Perinatology*, 42(1):79–85, 2022.

[7] J. R. Feiner, J. W. Severinghaus, and P. E. Bickler. Dark skin decreases the accuracy of pulse oximeters at low oxygen saturation: the effects of oximeter probe type and gender. *Anesthesia & Analgesia*, 105(6):S18–S23, 2007.

[8] V. S. Valbuena, S. Seelye, M. W. Sjoding, T. S. Valley, R. P. Dickson, S. E. Gay, D. Claar, H. C. Prescott, and T. J. Iwashyna. Racial bias and reproducibility in pulse oximetry among medical and surgical inpatients in general care in the Veterans Health Administration 2013-19: multicenter, retrospective cohort study. *BMJ*, 378, 2022.

[9] O. E. Okunlola, M. S. Lipnick, P. B. Batchelder, M. Bernstein, J. R. Feiner, and P. E. Bickler. Pulse oximeter performance, racial inequity, and the work ahead. *Respiratory Care*, 67(2):252–257, 2022.

[10] J. Kim, G. A. Salvatore, H. Araki, A. M. Chiarelli, Z. Xie, A. Banks, X. Sheng, Y. Liu, J. W. Lee, K.-I. Jang, et al. Battery-free, stretchable optoelectronic systems for wireless optical characterization of the skin. *Science Advances*, 2(8):e1600418, 2016.

[11] C. M. Lochner, Y. Khan, A. Pierre, and A. C. Arias. All-organic optoelectronic sensor for pulse oximetry. *Nature Communications*, 5(1):1–7, 2014.

[12] D. Han, Y. Khan, J. Ting, S. M. King, N. Yaacobi-Gross, M. J. Humphries, C. J. Newsome, and A. C. Arias. Flexible Blade-Coated Multicolor Polymer Light-Emitting Diodes for Optoelectronic Sensors. *Advanced Materials*, 29(22):1606206, 2017.

[13] Y. Khan, D. Han, A. Pierre, J. Ting, X. Wang, C. M. Lochner, G. Bovo, N. Yaacobi-Gross, C. Newsome, R. Wilson, et al. A flexible organic reflectance oximeter array. *Proceedings of the National Academy of Sciences*, 115(47):E11015–E11024, 2018.

[14] Y. Khan, D. Han, J. Ting, M. Ahmed, R. Nagisetty, and A. C. Arias. Organic multi-channel optoelectronic sensors for wearable health monitoring. *IEEE Access*, 7:128114–128124, 2019.

[15] D. Han, Y. Khan, J. Ting, J. Zhu, C. Combe, A. Wadsworth, I. McCulloch, and A. C. Arias. Pulse oximetry using organic optoelectronics under ambient light. *Advanced Materials Technologies*, 5(5):1901122, 2020.

[16] Y. Khan, A. Thielens, S. Muin, J. Ting, C. Baumbauer, and A. C. Arias. A new frontier of printed electronics: flexible hybrid electronics. *Advanced Materials*, 32(15):1905279, 2020.

[17] Y. Khan, M. Garg, Q. Gui, M. Schadt, A. Gaikwad, D. Han, N. A. Yamamoto, P. Hart, R. Welte, W. Wilson, et al. Flexible hybrid electronics: Direct interfacing of soft and hard electronics for wearable health monitoring. *Advanced Functional Materials*, 26(47):8764–8775, 2016.

[18] A. Abramson, C. T. Chan, Y. Khan, A. Mermin-Bunnell, N. Matsuhisa, R. Fong, R. Shad, W. Hiesinger, P. Mallick, S. S. Gambhir, et al. A flexible electronic strain sensor for the real-time monitoring of tumor regression. *Science Advances*, 8(37):eabn6550, 2022.

[19] L. A. Jensen, J. E. Onyskiw, and N. Prasad. Meta-analysis of arterial oxygen saturation monitoring by pulse oximetry in adults. *Heart & lung*, 27(6):387–408, 1998.

[20] M. W. Sjoding, S. Ansari, and T. S. Valley. Origins of Racial and Ethnic Bias in Pulmonary Technologies. *Annual Review of Medicine*, 74, 2022.

[21] D. R. Williams and R. Wyatt. Racial bias in health care and health: challenges and opportunities. *JAMA*, 314(6):555–556, 2015.

[22] E. K. Webb, J. A. Etter, and J. A. Kwasa. Addressing racial and phenotypic bias in human neuroscience methods. *Nature Neuroscience*, 25(4):410–414, 2022.

Integrated Quantum Dot Lasers for High-Performance Optical Neural Networks on a Silicon Photonics Platform

The rapid growth of *artificial intelligence (AI)*-driven services has created an unprecedented demand for compute capacity and speed. However, this surge is accompanied by a parallel increase in power consumption [>60 kWh per rack in extremely-dense AI workloads], as well as capital (CapEx) and operational (OpEx) expenditures [$154 billion globally on AI services in 2023]. The rate of progress in electronic hardware, doubling every 18 months, lags behind the doubling of machine learning computational demands every 3.5 months, resulting in a widening gap between compute requirements and hardware capacities.

This proposal seeks to bridge this gap by leveraging advanced optical technologies for AI systems. Specifically, it introduces a co-designed hardware and software solution for **a fully integrated optical neural network (ONN) using a silicon photonic integrated circuit (PIC).** By employing *heterogeneous integration* technology and utilizing *Intel's silicon photonics platform*, the project aims to integrate multi-channel *quantum dot (QD) lasers* into an optimized crossbar-based ONN hardware architecture. This approach is poised to surpass the capabilities of traditional electronic architectures in terms of speed, power efficiency, and parallel processing capabilities.

Key Development Tracks:

1. Quantum Dot Lasers for Heterogeneous Integration: This track focuses on developing robust, energy-efficient on-chip QD mode-locked lasers (MLLs) capable of generating optical frequency combs for wavelength division multiplexing (WDM) ONNs. Objectives include reducing cavity losses, lowering laser thresholds, achieving multi-wavelength emission, maximizing operating temperatures, increasing optical power, and leveraging the lower linewidth enhancement factor of QDs to enable an isolator-free system.
2. Co-optimization of Architecture and Algorithms for Integrated ONN: The ONN is designed for high efficiency and parallelism, utilizing a compliant architecture of microring resonator (MRR) crossbars and multi-wavelength optical channels generated by on-chip QD lasers. Efforts here aim to minimize the design's footprint, reduce crosstalk, and develop an ONN algorithm that accomplishes complex tasks with minimal parameters. This includes incorporating hardware-aware training and model lightweighting techniques to optimize algorithms for hardware adaptability.
3. Fully Integrated PIC and Optoelectronic Co-packaging System: This track involves developing a fully integrated PIC and optoelectronic co-packaging system with QD lasers *on a single silicon wafer*, eliminating the need for additional optical interfaces. Electrical components will be flip-chip packaged with the PIC to shorten transmission lengths, aiming to achieve high compute density, ultra-low energy efficiency, and low computational latency, and extend scalability using optical network-on-chip (ONoC) strategies.

Initial validation has demonstrated a recognition accuracy of 91.313% on the MNIST dataset with only 536 model parameters at high-speed (37 GHz) using Intel's standard 65 nm CMOS process line. By incorporating on-chip non-volatile memory and multi-cores scale-out framework, we project our hardware to theoretically increase in computing density by 70 times compared to Google's TPU electronic accelerator while reducing power consumption by 1000 times. Ultimately, the fabricated **QD MLL device and ONN system** will be optimized and fine-tuned for **co-integration** using state-of-the-art **heterogeneous integration** technology into a **holistic and isolator-free PIC** as a compact and efficient System on Chip (SoC). This transformative development is expected to unlock significant advancements in energy efficiency, sustainability, and scalability and create new commercialization opportunities. Moreover, it promises substantial **global socioeconomic impacts, especially in the Middle East**. This region stands to benefit immensely from the deployment of advanced photonics and AI technologies, aligning with economic diversification strategies and fostering a technologically proficient workforce, propelling the region toward a sustainable and innovative future.

Integrated Quantum Dot Lasers for High-Performance Optical Neural Networks on a Silicon Photonics Platform

I. Background and Literature Review

The advent of artificial intelligence (AI)-driven services has triggered an unprecedented increase in demand for processing capability and energy efficiency[1]. A prime example is the phenomenal growth of ChatGPT, which now boasts a staggering 175 billion parameters. Consequently, the cost of inference using ChatGPT-3 is tenfold higher than that of a standard search on conventional search engines like Google[2]. Industry estimates reveal that daily operating costs can reach up to $700,000[3]. These astonishing figures merely scratch the surface as the complexity and size of AI models continue to expand. While the computational demand of machine learning (ML) doubles every 3.5 months, advancements in electronic hardware, such as transistor density, clock speed, and power efficiency, lag behind with a doubling rate of approximately 18 months. This widening gap between the escalating compute demands, and the limited capacities of electronic hardware has emerged as a critical bottleneck in AI progress.

In this context, there is a rekindled interest in custom hardware designed to accelerate matrix-vector multiplication (MVM), a key operation that dominates modern AI models by constituting over 80% of their workloads. *Optical neural networks (ONNs)* provide a promising alternative by leveraging the inherent properties of photons, including ultra-high bandwidth and processing frequency (>100GHz), ultra-low power consumption (sub-pJ/bit), and high parallelism through additional dimensions of division multiplexing[4]. Among the various platforms, *silicon (Si) photonics* stands out due to its compatibility with complementary metal–oxide–semiconductor (CMOS) manufacturing and high-density integration capacity, making it an ideal candidate for hardware implementation of ONNs. Currently, mainstream ONN Si-based hardware solutions include cascaded Mach-Zehnder interferometers (MZIs) and wavelength division multiplexing (WDM)-based microring resonator (MRR) arrays. While the former remains a more established architecture, it suffers from higher computational complexity of $O(n^2)$ and requires a drastically larger area[5]. In contrast, the directly mapped MRR architecture offers a more efficient solution with high parallelism and a smaller footprint, and has gained traction since the "broadcast-and-weight (B&W)" scheme was pioneered by Tait *et al.* in 2014[6]. However, the scalability of the B&W solution is limited due to the inevitable internal loop waveguide design. Consequently, attention has shifted to the crossbar configuration, which ensures high parallelism within a compact area, enhances scalability, and represents the most desirable large-scale ONN architecture. In 2021, Feldmann *et al.* achieved state-of-the-art ONN hardware that integrated non-volatile memory with an MRR crossbar, enabling trillions of multiply-accumulate operations per second[7]. However, their solution still relied on an off-chip laser co-packaged with a discrete optical comb, leading to substantial coupling losses. To further enhance system performance and fulfill the computational acceleration demands of edge devices, the development of **a fully integrated ONN hardware with an on-chip laser remains an essential objective.**

To overcome the inherent limitation of the indirect bandgap of Si for efficient on-chip light sources, our former team spearheaded a pioneering *heterogeneous integration process*. This groundbreaking technique enabled the seamless integration of InP-based quantum well (QW) material for light generation with Si waveguides for light guiding. By constructing III-V devices on Si with lithographically precise alignment to Si waveguides via wafer-scale processing, mass production of Si photonics-based optical modules was achieved within a decade through collaboration with Intel, generating revenue exceeding $1 billion. Ongoing efforts, spearheaded by the applicant, Dr. Yating Wan, focus on device design and process optimization to replace InP-based QW epitaxial material with GaAs-based *quantum dot (QD)* epitaxial material through the cooperation with the *Intel® Research Center*. This strategic endeavor holds immense promise for improving performance and reducing costs by incorporating QD active regions, which offer benefits such as lower threshold currents, higher temperature stabilities, and, most importantly, *much-reduced sensitivity to reflections that obviates the need for bulky and costly isolators*[8].

II. Problem Statement and Objectives

In addressing the critical challenges associated with on-chip light sources and the AI computational bottleneck, our proposal aims to co-design hardware and software for a **fully integrated ONN Si photonic integrated circuit** (PIC). Leveraging **heterogeneous integration technology** and **Intel's Si photonics platform,** this project will **integrate multi-channel QD lasers** with an optimized **crossbar-based ONN hardware architecture** that exceeds the capabilities of traditional electronic architectures in terms of speed, power efficiency, and parallel processing capabilities. This stands in stark contrast to the bulky off-chip solution that requires substantial power consumption (approximately 2dB+6dB) for coupling and modulation alone.

To achieve this, we will develop **robust, energy-efficient on-chip QD mode-locked lasers (MLLs)** capable of generating optical frequency combs for WDM ONNs. These lasers will be optimized to meet several key metrics. *Firstly*, we will focus on reducing losses in the cavity and lowering laser thresholds below 200 A/cm^2 to maximize energy efficiency. *Secondly*, we will achieve multi-wavelength emission by integrating multi-wavelength QD lasers on Si and progressing towards fixed 50 or 100 GHz channel spacing, with a channel count > 8 and power-per-line > 0 dBm. *Thirdly*, we will strive to maximize operation temperature by leveraging the 3D confinement and the large conduction band offset of InAs/GaAs QDs. Building upon our previous achievement of 120°C operation[9], we aim to further increase this parameter to >150°C through epi and device design optimization. *Fourthly*, drawing upon our previous achievement of reaching 185 mW continuous-wave optical power, we aim to achieve even higher optical power values by enhancing the gain region bonded on Si and minimizing the optical loss and series resistance via the optimization of structural and epitaxial designs, fabrication processes, and contact metallization. *Finally*, we will address the issue of laser sensitivity to reflections by leveraging the lower linewidth enhancement factor of QDs (0.4) compared to quantum QWs (approximately 4). Our group has previously demonstrated no sensitivity to reflection even with 100% off-chip feedback in Fabry-Perot lasers, and we aim to replicate this result in the QD MLLs.

In parallel, the **ONN will be designed and optimized for high efficiency and high parallelism** to fully leverage the advantages of the on-chip MLL solution. We have chosen a compliant architecture of MRR crossbar as an MVM accelerator, incorporating a hardware-software co-design approach to improve computational density and energy consumption. *Firstly*, we aim to minimize the design's footprint and reduce crosstalk (both thermal and inter-channel) through simulation-based verification of individual device structure and system-level functionality. Our objective is to achieve a compact, high-precision hardware design with predicted performance parameters and packaging requirements. *Secondly*, we will develop an ONN algorithm that accomplishes tasks as complex as feasible with the minimum number of parameters to ensure effective acceleration on edge devices. We will utilize training tools such as light weighting, noise perception, and quantization to further improve the generality and accuracy of the model on large datasets. *Thirdly*, we will fabricate and characterize the designed ONN chip, followed by comprehensive evaluation of the fully integrated optoelectronic hardware. *Thereafter*, the fabricated **QD MLLs and ONN chip will be heterogeneously integrated into a single package** confining all optical signals. This integration will enhance efficiency, stability, and scalability while eliminating unnecessary coupling and modulation losses (>8 dB) associated with external sources, endowing our circuits with unprecedented advantages in terms of cost, size, weight, and power (cSWaP).

III. Research Plan and Outcomes

The research plan for this project consists of three core tracks encompassing design, simulation, fabrication, co-integration, and characterization.

Track 1: Design and fabrication of QD lasers for heterogeneous integration. Our previous works provided initial demonstrations of integrated QD lasers on the Si-on-insulator (SOI) platform with exceptional performance. QD gain medium embraces multiple favorable material properties over QW counterpart, such as low transparency current density, excellent optical gain thermal stability, inhomogeneous dot size-resulted wide spectral gain bandwidth, low relative intensity noise, and large tolerance to material/process defects and optical feedback. Through the low-loss evanescent coupling of the laser light to a Si waveguide, we successfully developed heterogeneous-integrated on-chip QD lasers with a threshold current of 4 mA, an SMSR of 60 dB, a fundamental linewidth of 26 kHz, and a

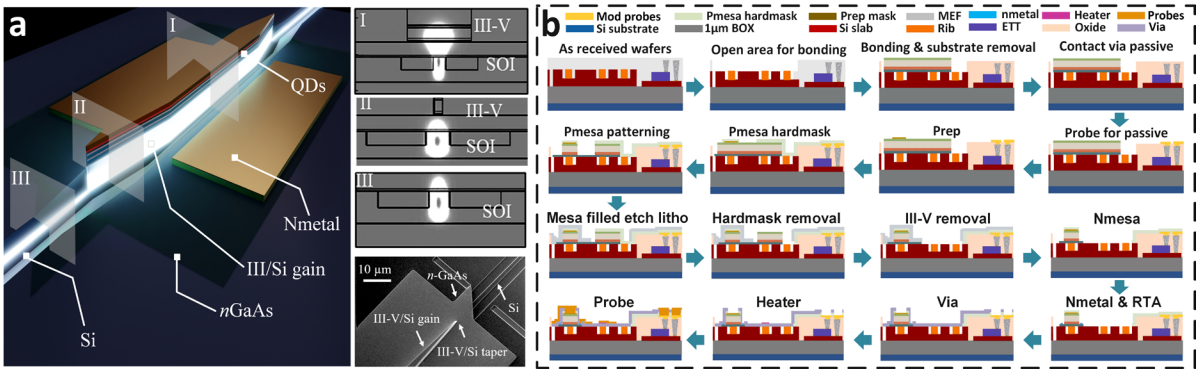

Fig. 1 (a) Schematic of a heterogeneously integrated QD laser. (b) Process design to heterogeneously integrate the QD gain elements with the ONN PIC.

3-dB bandwidth of 13 GHz[8]. Building upon this foundation, we will now focus on on-chip integration of *high-quality frequency combs using QD MLLs*. The unique broadband gain profiles and inhomogeneous broadening effects of QDs enable the engineering of MLLs to generate comb emissions with varying mode spacings. This characteristic is crucial to realizing compact and efficient sources of WDM signals in the ONN MVM implementation. Fig. 1a shows a schematic of the laser evanescently coupled to low-loss Si waveguides. The critical goals in the *laser design* include optimizing the saturable absorber length, the electrical isolation distance, and the Sagnac loop mirror design. *Testing* will focus on extracting relevant characteristics for computing applications, including bandwidth, relative intensity noise (RIN), timing jitter, and total transmission capacity. Fig. 1b outlines the proposed *process flow* for the heterogeneous integration platform. Critical steps include post-wafer-bonding process to accommodate the prefabricated Si structures and protective measures to mitigate potential damage to the Si waveguides. To achieve this, we will implement a more restrictive mesa dry

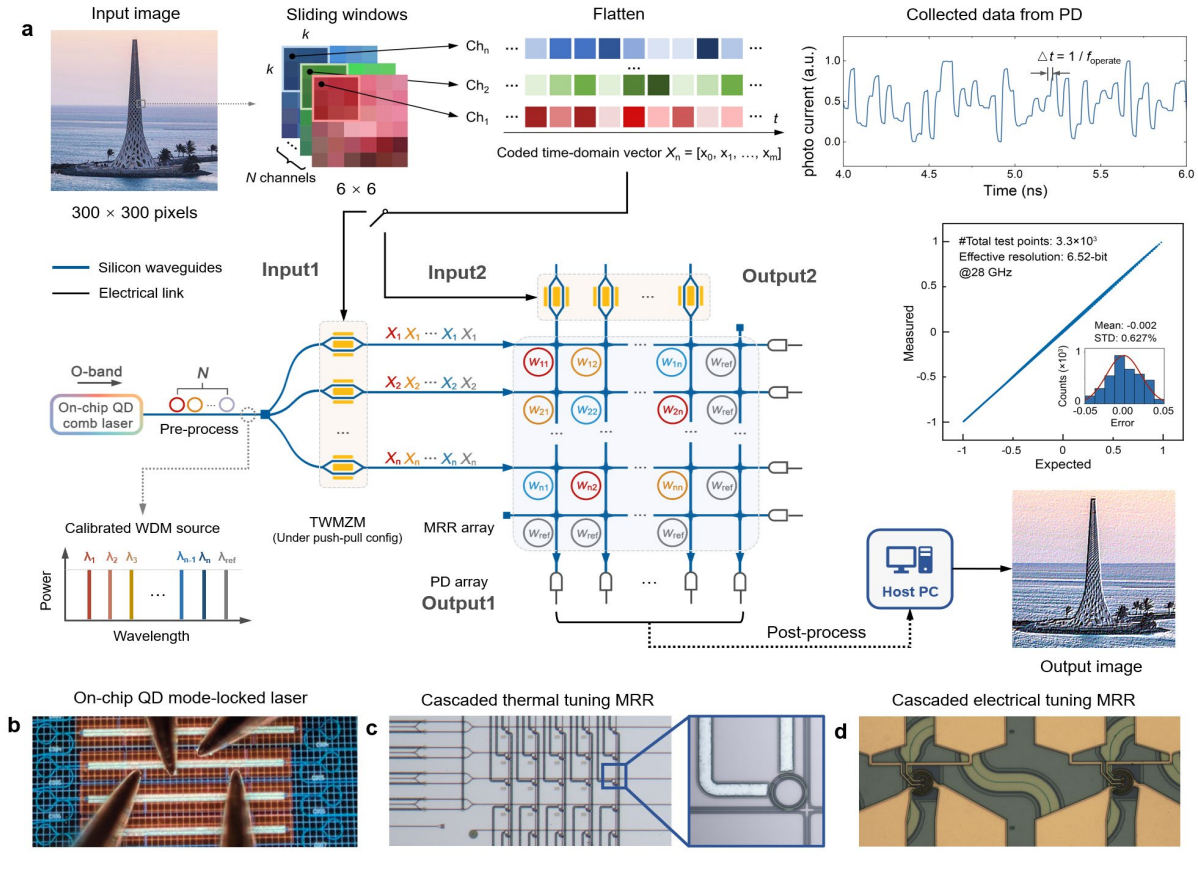

Fig. 2 (a) Typical workflow and expected precision of PCU. Photo of fabricated (b) On-chip mode-locked laser, (c) cascaded thermal tuning MRRs, (d) cascaded electrical tuning MRRs.

etch area and introduce a wet mesa filled etch step to selectively remove excess III–V materials near the protective oxides safeguarding the Si devices. Substrate removal conditions will be thoroughly investigated to ensure proper preservation of Si devices while maintaining high bonding strength and yield.

Track 2: Co-optimization of architecture and algorithms for heterogeneously integrated ONN. To compliment the compact physical footprint of heterogeneously integrated MLLs, we developed a photonic computing unit (PCU) functioning as a tensor core. This core utilizes a compact and scalable MRR crossbar to facilitate MVM operations. Fig. 2a illustrates the typical workflow of our PCU for an image convolution task. In this process, the input image is segmented into multiple vectors by channels and converted into time-domain voltage sequences. These sequences are broadcasted by Mach-Zehnder modulators (MZMs) into multi-wavelength optical channels generated by our on-chip MLL and then processed by the MRR array for multiplications. The resulting signals are aggregated by photodetectors, converted back to the electrical domain for post-processing, and output. After device-level optimization tailored for a heterogeneous integration platform, we developed a complete opto-electronic link model. We verified the MVM functionality of the PCU and achieved a system precision above 6-bit. Following our device-to-architecture designs, the first run of individual photonic components has all been fabricated using Intel's standard 65 nm CMOS process line (Fig. 2b-d). We are poised to commence the experimental measurements on these devices and will fine-adjust process parameters based on the feedback to achieve an optimal performance.

To better meet the demands of edge devices, we have optimized traditional algorithms for hardware adaptability. Here, we proposed a standardized algorithm optimization strategy for PCU. This strategy incorporates a hardware-aware training framework and a model lightweighting scheme. In our framework, we constructed a real hardware noisy and low bit-precision training environment. Further integrating various model compression techniques, including pruning and weight-sharing, a lightweight and deploy-robust model can be obtained. Finally, we introduced the knowledge distillation approach to enhance the accuracy of model tasks. A large pre-trained network serves as the teacher model, with our hardware-adapted model acting as the student. Both models receive the same input, and after recognition, the teacher model produces a soft label. This label, representing distilled knowledge, is transferred to the student model, enabling it to emulate the teacher's behavior and enhance accuracy. The effectiveness of our strategy has been preliminarily confirmed, achieving 95.03% accuracy on the MNIST dataset with only 943 parameters. Upon determining the optimal array size for a single PCU, we can apply this established strategy to train a tailored, hardware-friendly ONN model.

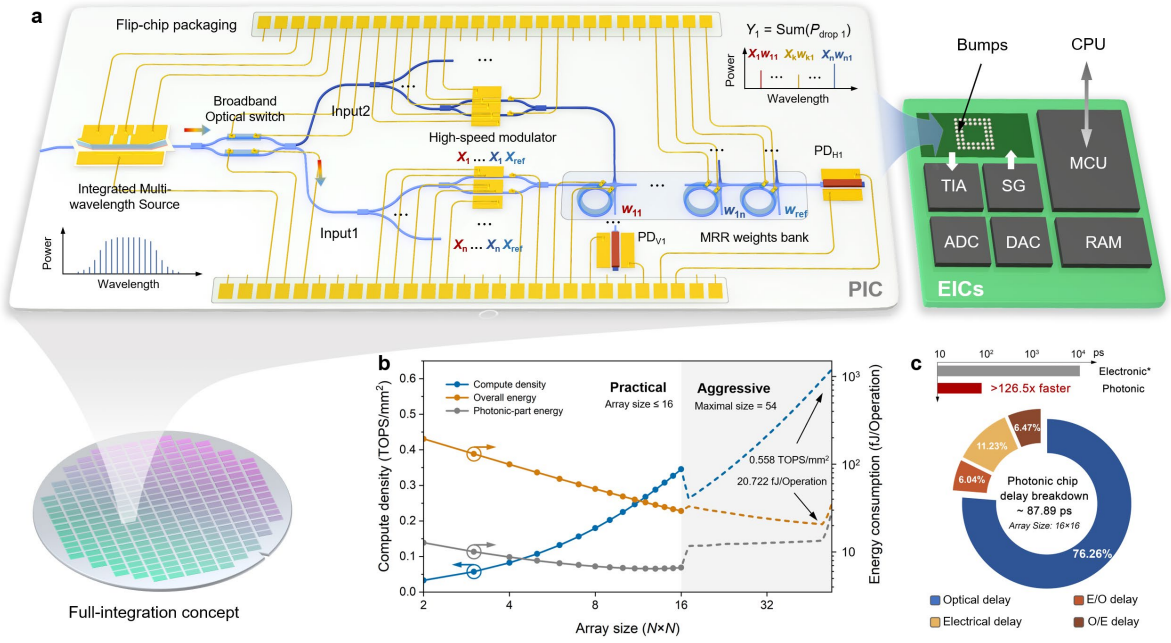

Fig. 3 (a) Conceptual drawing of the complete opto-electronic co-packaged system. (b) Expected system computational performances. (c) Total computing latency (array size: 16×16).

Track 3: Development of fully integrated PIC and optoelectronic co-packaging system. After completing the co-optimization between devices, architecture, and algorithms, we will develop the entire optoelectronic hybrid system, as depicted in Fig. 3a. Supported by our on-chip lasers, the PIC chip can be fully co-integrated on a single silicon wafer. Thanks to this co-integration, there is no need for any additional optical interface, which significantly simplifies the co-packaging with advanced electronic integrated circuits (EICs). The necessary electrical components including signal generators (SGs), trans-impedance amplifier (TIAs), analog/digital convertors (ADCs/DACs), random access memory (RAM) and microcontroller unit (MCU), which are planned to be flip-chip packaged with the PIC to shorten the transmission lengths. Moreover, due to the elimination of optical packaging gap (127 μm) restrictions, the MRR grid size can also be greatly reduced. Under a typical operating speed of 28 GHz, we estimated the system's potential performance across different array sizes, as shown in Fig. 3b. By improving the MRR's Q-factor and voltage operation precision, supported by a single laser, a system compute density as high as 0.558 TOPS/mm^2 with an ultra-low energy efficiency of 20.722 fJ/Operation can be achieved. Considering a realistic scale scenario, the computational latency for a 16×16 array is less than 100 ps, which is 126.5 times lower than that of a comparable advanced electrical computing system. Further leveraging the optical network-on-chip (ONoC) scaling-out strategy, feasible due to on-chip laser integration, a multi-core parallel computing system can be realized, offering ultra-high computing throughput comparable to the most advanced commercial products currently available.

IV. Significance and Potential Impact

Successful development of this proposal can solve the efficiency and bandwidth capacity bottlenecks of electronic-based AI systems as well addressing the impending need for continued feasible scaling.

Revolutionizing AI's Energy Footprint: AI's meteoric rise in technology is both a boon and a challenge. The computational demand, especially in data centers, is growing exponentially. Extreme-density AI workloads now push power consumption up to 60 kW per rack[12]. To contextualize, traditional web hosting servers hover around 100 W per rack. Data centers consumed a staggering 400 billion kWh globally in 202136, with an added 86% average due to active cooling and power distribution losses[13]. By harnessing optical components, there's potential to slash power consumption by up to 75%. Based on preliminary results and by further leveraging on-chip non-volatile memory and our large-scale ONoC^2 framework, we project our hardware to theoretically increase in *computing density by 70 times compared to Google's TPU electronic accelerator*, while *reducing power consumption by 1000 times*. This breakthrough has the potential to revolutionize AI acceleration and enable more efficient and scalable data center architectures.

Commercialization Potential: Heterogeneously integrated on-chip lasers, initially developed in a university lab (where the applicant conducted 5-year Postdoc research), have been successfully commercialized within a decade and have since generated *over $1 billion in revenue* by Intel[14]. However, the current packaging limitations pose challenges in accommodating bulky, lossy, expensive, and complex optical isolators. Our approach utilizes QD lasers, which, due to their small loss enhancement factor, eliminate the need for bulky optical isolators, presenting a more compact and efficient solution. The realization of *fully integrated ONN modules with on-chip QD lasers* could spur patent innovations and the creation of startups, enhancing scalability and manufacturability prospects for larger wafer sizes up to 300 mm.

Global Socioeconomic Impacts in the Middle East: AI is set to dominate the tech sector with global expenditures projected to reach $154 billion by 2023[15], a rate more than four times that of overall IT spending during the same period[16]. The proposed AI system implementation could drastically cut costs and transform a wide array of industries, including autonomous driving, healthcare, telecommunications, and entertainment. Currently, *the Middle East* is at a crucial turning point. Traditionally seen as behind in innovation and technological advancement, the region now stands to gain substantially from the digital revolution. With strategic economic diversification efforts aimed at reducing reliance on oil and gas, its high concentration of young, tech-savvy individuals, and significant internet and mobile device usage, there is a fertile ground for advancing this research and fostering cross-sector collaboration in this region. Supporting integrated photonics and AI technologies, the Middle East can catalyze significant economic and ecological benefits, steering towards a future that is sustainable, innovative, and at the forefront of technological progress.

References

1. Shastri, B. J. *et al.* Photonics for artificial intelligence and neuromorphic computing. *Nature. Photonics* **15**, 102–114 (2021).
2. Dastin, J. *et al.* For tech giants, AI like Bing and Bard poses billion-dollar search problem, *Reuters* (2023).
3. Mok, A. ChatGPT could cost over $700,000 per day to operate. Microsoft is reportedly trying to make it cheaper. *Business Insider* (2023).
4. Feng, C. *et al.* A Compact Butterfly-Style Silicon Photonic–Electronic Neural Chip for Hardware-Efficient Deep Learning. *ACS Photonics* **9**, 3906–3916 (2022).
5. Zhang, H. *et al.* An optical neural chip for implementing complex-valued neural network. *Nature Communications* **12**, 457 (2021).
6. Tait, A. N., *et al.* Broadcast and Weight: An Integrated Network For Scalable Photonic Spike Processing. *Journal of Lightwave Technology* **32**, 3427–3439 (2014).
7. Feldmann, J. *et al.* Parallel convolutional processing using an integrated photonic tensor core. *Nature* **589**, 52–58 (2021).
8. Wan, Y. *et al.* High Speed Evanescent Quantum-Dot Lasers on Si. *Laser & Photonics Reviews* **15**, 2100057 (2021).
9. Shang, C. *et al.* Perspectives on Advances in Quantum Dot Lasers and Integration with Si Photonic Integrated Circuits. *ACS Photonics* **8**, 2555–2566 (2021).
10. Sun, J. *et al.* A 128 Gb/s PAM4 Silicon Microring Modulator With Integrated Thermo-Optic Resonance Tuning. *Journal of Lightwave Technology* **37**, 110–115 (2019).
11. Van Campenhout, J. *et al.* Silicon Photonics for 56G NRZ Optical Interconnects. in *2018 Optical Fiber Communications Conference and Exposition (OFC)* 1–3 (2018).
12. Su, L. Plenary: Innovation for the next decade of compute efficiency. (2023).
13. Hintemann, R. & Hinterholzer, S. *Data centers 2021: Data center boom in Germany continues - Cloud computing drives the growth of the data center industry and its energy consumption*. (2022).
14. Gazettabyte. *Intel details its 800-gigabit DR8 optical module* (2021).
15. Shirer, M. Worldwide Spending on AI-Centric Systems Forecast to Reach $154 Billion in 2023. (2023).
16. NRDC. *Data Center Efficiency Assessment* (2014).

Tbps Multi-Dimensional Optical Fiber Interconnects by Integrated Photonic Processors

The explosive growth of global data traffic, particularly due to artificial intelligence applications in recent years, has driven researchers and engineers to develop optical interconnects capable of carrying more digital data while more efficiently than ever before. By leveraging technologies such as wavelength-division multiplexing, polarization-division multiplexing, and high-speed multi-level modulation formats, the data capacity of optical fibers has already been substantially improved. The industry has already invested considerable efforts towards achieving 1.6 Tbps and 3.2 Tbps short-reach optical transceivers. However, **the spatial dimension of optical fiber, especially the orthogonal fiber modes, remains untapped in the industry**, despite mode-division multiplexing (MDM) being long envisioned as potential technology for overcoming the capacity limit of optical fibers. Although various multi-dimensional and world-record transmission demonstrations utilizing few-mode fibers (FMF) have been reported in recent years, challenges such as cost, complexity, power consumption, and latency have hindered its integration into applications. Therefore, the **key challenge identified in this project** is how to implement multi-dimensional fiber communication technology on a broader scale to permit continued data traffic growth.

Two major challenges are associated with incorporating mode dimension into multi-dimensional optical fiber communications, including **(1)** the need for a low-loss, low-cost and scalable mode (de)multiplexers for optical fibers; **(2)** concern on the high-power, high-speed, and high-latency electronic digital signal processing to descramble mixed signals due to inter-modal crosstalk. To tackle this issue, we propose a scalable approach utilizing photonic integration and photonic computing acceleration is this proposal.

Previously, we have developed an efficient multichannel optical I/O device which can bridge the photonic chip with few-mode fibers directly, while supporting launching of eight data lanes in different orthogonal polarizations and modes. We have also reported mode unscrambling for few-mode fibers using integrated optical mesh on the silicon photonics platform. **In this proposal**, we plan to keep investigating and improving the coupling efficiency between the fiber and photonic chip using multi-dimensional optical I/O, to further increase system power budget margin. Furthermore, we propose to use the high-speed integrated optical transceivers with reconfigurable optical mesh, consisting of Mach-Zender interferometers to perform the optical multiple-in multiple-out (MIMO) processing. The integrated optical mesh for optical signal processing can be placed between the multi-dimensional optical I/O and high-speed silicon photonic transceivers. The integrated optical mesh will be appropriately configured to perform singular value decomposition. The high-speed optical transceivers can therefore be activated to achieve a one-by-one mode mapping between the transmitter side and the receiver side for mode-division multiplexing fiber communications. To achieve a total data rate of more than Tbps, all dimensions including mode, polarization, and wavelength can be utilized. For example, assume a single lane rate of 100Gbps is employed, three fiber modes and four wavelength channels can be used to easily reach a total data rate of about 1.2Tbps. **The proposed project will combine our expertise** in designing low-loss passive silicon photonic devices, high-speed silicon photonics transceivers, and high-capacity fiber optic communications.

The research outcomes of this project are prototypes of photonic integrated devices and circuits built for Tbps multi-dimensional optical fiber communications. We are seeking to break the communication bandwidth limit through the incorporation of additional physical dimensions inside optical fibers, while reducing associated power consumption and cost needed. Leveraging the well-established Si CMOS infrastructure and process, the proposed research project has the potential to solve the challenges of exponential growth in global data traffic and associated power consumption.

Tbps Multi-Dimensional Optical Fiber Interconnects by Integrated Photonic Processors

Asst. Prof. Dr. Yeyu Tong,
Early-Career Member of Optica, yeyutong@hkust-gz.edu.cn
The Hong Kong University of Science and Technology (Guangzhou)

I. Literature Review

The rapid expansion of global data traffic, recently particularly driven by artificial intelligence applications, has pushed researchers and engineers to design optical interconnects which can carry more digital data, while more efficiently than before. Through the utilization of wavelength-division multiplexing, polarization-division multiplexing, and high-speed multi-level modulation formats, the data-carrying capacity of optical fibers has been enhanced significantly. The industry is already making strides towards achieving 1.6 Tbps and 3.2 Tbps optical transceivers. Nevertheless, the spatial dimension of optical fiber, such as orthogonal fiber modes, remains unutilized in the industry, despite mode-division multiplexing (MDM) being long considered as a potential technology for breaking the capacity limit of optical fibers [1–4]. While various multi-dimensional and world-record transmission demonstrations using few-mode fibers (FMF) have been reported in labs in recent years [5,6], it is undeniable that factors such as cost, complexity, power consumption, and latency have impeded its integration into volume applications. Previous experiments have highlighted the significant potential of adding the spatial dimension into optical fiber communications [5–8], thus the key question now is when and how this multi-dimensional fiber communications will be implemented on a broader scale.

The main challenges associated with MDM in optical fibers include (1) Lack of low-cost, low-loss, and scalable mode (de)multiplexers. Previous reported mode multiplexers include bulk optics such as phase plates or multi-plane light conversion (MPLC), and 3D waveguides using fiber photonic lanterns or laser inscription [9]. Low insertion loss and have been realized while supporting different higher-order fiber modes. In addition to the serial manufacturing process for making the mode multiplexers, researchers also came up with ideas of using CMOS-compatible silicon photonics integration platform to realize mode multiplexing for fiber while supporting mass production [10–18]. However, the number of mode channels and the insertion loss are still limited, due to the different mode field profiles in circular-core optical fibers and planar waveguides. In the past few years, we and a few other groups around the world have reported efficient and multi-dimensional I/O devices between the few-mode fibers and silicon photonic integrated circuits. Although good insertion loss around –6dB can be obtained for eight linearly polarized (LP) fiber modes [18], a lower insertion loss is still necessary considering the link power budget. (2) Concern on fiber modal crosstalk and signal mixing. Unlike the frequency domain, where selective bandpass filters can be employed to eliminate inter-channel crosstalk, the spatial dimension is more susceptible to inter-modal crosstalk during transmission, such as fiber bending, stress, or even mechanical misalignment of fiber splices. While such signal mixing can be mitigated through the use of coherent communication and electronic digital signal processing (DSP), concerns arise due to the need for high-speed, high-power, and high-latency digital matrix operations. Additionally, the dimensionality of the DSP equalizer would rapidly expand with the inclusion of more spatial channels. To solve this issue, photonic computing acceleration gets attention, where matrix transformation can be performed optically by propagating through a reconfigurable optical mesh with extremely low time latency [19–21]. We and a few other groups reported mode unscrambling for few-mode fibers using integrated optical mesh [20,22,23]. By placing the mode unscrambling processor unit between the high-speed silicon photonic transceivers [24] at the transmitter side and receiver side, the mode dimension of optical fibers can be incorporated for future high-capacity optical communications.

References - *Prior relevant results from the applicant are highlighted in the reference list.*

1. B. J. Puttnam, G. Rademacher, and R. S. Luís, "Space-division multiplexing for optical fiber communications," Optica, OPTICA 8, 1186–1203 (2021).
2. D. J. Richardson, J. M. Fini, and L. E. Nelson, "Space-division multiplexing in optical fibres," Nature Photonics 7, 354–362 (2013).
3. P. J. Winzer, "Making spatial multiplexing a reality," Nature Photonics 8, 345–348 (2014).
4. N. Bozinovic, Y. Yue, Y. Ren, M. Tur, P. Kristensen, H. Huang, A. E. Willner, and S. Ramachandran, "Terabit-Scale Orbital Angular Momentum Mode Division Multiplexing in Fibers," Science 340, 1545–1548 (2013).
5. M. Van Den Hout, G. Di Sciullo, G. Rademacher, R. S. Luís, B. J. Puttnam, N. K. Fontaine, R. Ryf, H. Chen, M. Mazur, D. T. Neilson, P. Sillard, F. Achten, J. Sakaguchi, C. Antonelli, C. Okonkwo, and H. Furukawa, "273.6 Tb/s Transmission Over 1001 km of 15-Mode Fiber Using 16-QAM C-Band Signals," in 2023 OFC.
6. G. Rademacher, B. J. Puttnam, R. S. Luís, T. A. Eriksson, N. K. Fontaine, M. Mazur, H. Chen, R. Ryf, D. T. Neilson, P. Sillard, F. Achten, Y. Awaji, and H. Furukawa, "Peta-bit-per-second optical communications system using a standard cladding diameter 15-mode fiber," Nat Commun 12, 4238 (2021).
7. H. Chen, W. Zhou, and **Y. Tong**, "Towards Tbps single-λ interconnect by a multimode integrated optical I/O on silicon for few-mode fibers," in OFC 2024, top-scored, p. M3B.2.
8. H. Wang, J. Ai, Z. Ma, S. Ramachandran, and J. Wang, "Finding the superior mode basis for mode-division multiplexing: a comparison of spatial modes in air-core fiber," AP 5, 056003 (2023).
9. N. K. Fontaine, J. Carpenter, S. Gross, S. Leon-Saval, Y. Jung, D. J. Richardson, and R. Amezcua-Correa, "Photonic Lanterns, 3-D Waveguides, Multiplane Light Conversion, and Other Components That Enable Space-Division Multiplexing," Proceedings of the IEEE 110, 1821–1834 (2022).
10. A. M. J. Koonen, H. Chen, H. P. A. van den Boom, and O. Raz, "Silicon Photonic Integrated Mode Multiplexer and Demultiplexer," IEEE Photonics Technology Letters 24, 1961–1964 (2012).
11. Y. Ding, H. Ou, J. Xu, and C. Peucheret, "Silicon Photonic Integrated Circuit Mode Multiplexer," IEEE Photon. Technol. Lett. 25, 648–651 (2013).
12. B. Wohlfeil, G. Rademacher, C. Stamatiadis, K. Voigt, L. Zimmermann, and K. Petermann, "A Two-Dimensional Fiber Grating Coupler on SOI for Mode Division Multiplexing," IEEE Photonics Technology Letters 28, 1241–1244 (2016).
13. Y. Lai, Y. Yu, S. Fu, J. Xu, P. P. Shum, and X. Zhang, "Compact double-part grating coupler for higher-order mode coupling," Optics Letters 43, 3172–3175 (2018).
14. **Y. Tong**, W. Zhou, X. Wu, and H. K. Tsang, "Efficient Mode Multiplexer for Few-Mode Fibers Using Integrated Silicon-on-Insulator Waveguide Grating Coupler," IEEE Journal of Quantum Electronics 56, 2019.
15. W. Shen, J. Du, J. Xiong, L. Ma, and Z. He, "Silicon-integrated dual-mode fiber-to-chip edge coupler for 2 × 100 Gbps/lambda MDM optical interconnection," Opt. Express, OE 28, 33254–33262 (2020).
16. T. Watanabe, B. I. Bitachon, Y. Fedoryshyn, B. Baeuerle, P. Ma, and J. Leuthold, "Coherent few mode demultiplexer realized as a 2D grating coupler array in silicon," Opt. Express 28, 36009 (2020).
17. K. Y. Yang, C. Shirpurkar, A. D. White, J. Zang, L. Chang, F. Ashtiani, M. A. Guidry, D. M. Lukin, S. V. Pericherla, J. Yang, H. Kwon, J. Lu, G. H. Ahn, K. Van Gasse, Y. Jin, S.-P. Yu, T. C. Briles, J. R. Stone, D. R. Carlson, H. Song, K. Zou, H. Zhou, K. Pang, H. Hao, L. Trask, M. Li, A. Netherton, L. Rechtman, J. S. Stone, J. L. Skarda, L. Su, D. Vercruysse, J.-P. W. MacLean, S. Aghaeimeibodi, M.-J. Li, D. A. B. Miller, D. M. Marom, A. E. Willner, J. E. Bowers, S. B. Papp, P. J. Delfyett, F. Aflatouni, and J. Vučković, "Multi-dimensional data transmission using inverse-designed silicon photonics and microcombs," Nat Commun 13, 7862 (2022).
18. W. Zhou, Z. Zhang, H. Chen, H. K. Tsang, and **Y. Tong**, "Ultra-compact and efficient integrated multichannel mode multiplexer in silicon for few-mode fibers," Laser & Photonics Reviews, 18, 2300460, 2024.
19. D. A. B. Miller, "Self-configuring universal linear optical component [Invited]," Photon. Res., 1, 1–15 2013.
20. A. Annoni, E. Guglielmi, M. Carminati, G. Ferrari, M. Sampietro, D. A. Miller, A. Melloni, and F. Morichetti, "Unscrambling light—automatically undoing strong mixing between modes," Light: Science & Applications 6, e17110 (2017).
21. W. Bogaerts, D. Pérez, J. Capmany, D. A. B. Miller, J. Poon, D. Englund, F. Morichetti, and A. Melloni, "Programmable photonic circuits," Nature 586, 207–216 (2020).
22. K. Lu, Z. Chen, H. Chen, W. Zhou, Z. Zhang, H. K. Tsang, and **Y. Tong**, "Empowering high-dimensional optical fiber communications with integrated photonic processors," Nature Communications, 15, 3515, 2024.
23. R. Tang, R. Tanomura, T. Tanemura, and Y. Nakano, "Ten-Port Unitary Optical Processor on a Silicon Photonic Chip," ACS Photonics 8, 2074–2080 (2021).
24. **Y. Tong**, Z. Hu, X. Wu, S. Liu, L. Chang, A. Netherton, C.-K. Chan, J. E. Bowers, and H. K. Tsang, "An experimental demonstration of 160-Gbit/s PAM-4 using a silicon micro-ring modulator," IEEE Photonics Technology Letters 32, 125–128 (2019).

II. Problem Statement/Objective

The objective of this project is to investigate and explore Tbps optical fiber communications utilizing multiple dimensions including wavelength, polarization, and mode, leveraging silicon photonic integration platform and optical signal processing. To integrate the mode dimension into the high-capacity optical fiber communications, two key problems should be solved to unlock the potential of mode-division multiplexing technology.

(1) Efficient multi-dimensional chip-to-fiber I/O device

Although bulk optics technology and laser inscribed waveguides can be used to realize efficient mode multiplexers for few-mode fibers, due to benefits of low-cost and high-volume production using photonic integration, direct bridging of the few-mode fibers with the photonic integrated circuits has been explored in recent years via diffraction gratings and edge nanotapers, as depicted in Figure 1a. However, it is challenging to maintain high coupling efficiency while supporting high-dimensional optical I/O. Figure 1b summarizes the number of spatial channels and the experimental chip-to fiber coupling efficiencies reported in recent works [10–18]. By using 2D grating coupler, eight fiber LP modes can be selectively excited with peak efficiencies around –6dB [18]. It is worthwhile to mention that the single-mode optical I/O via edge coupling in the current silicon photonic transceivers, a chip-to-fiber coupling efficiency of about –1dB is feasible. Therefore, it is necessary to improve the coupling efficiency for the multi-dimensional optical I/O, to satisfy the link power budge requirements.

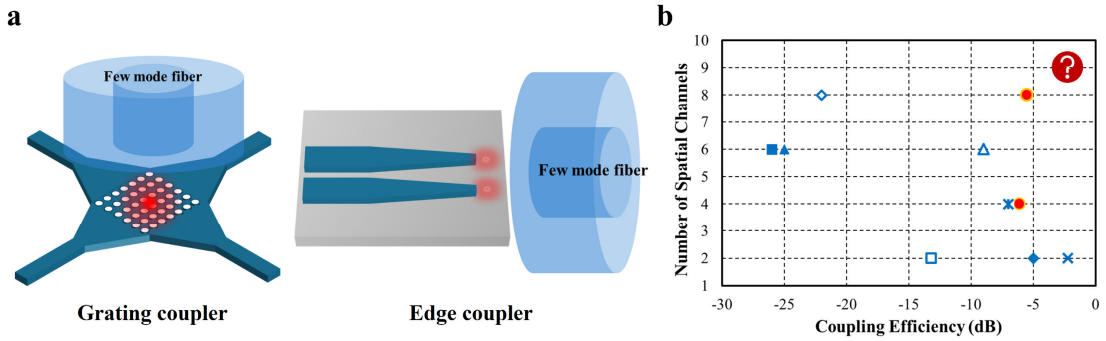

Figure 1. **a** Schematic diagram of the multi-dimensional chip-to-fiber I/O by diffraction gratings and edge nanotapers supporting more than one spatial channel. **b** Comparison of figure-of-merits, including the number of spatial channels (including polarization) and experimental chip-to-fiber loss, for multi-dimensional optical I/O in recent years for few-mode fibers [10–18]. The work done by the applicant is highlighted with red dots [14,18].

(2) Integrating optical singular value decomposition into optical transceivers

To utilize the mode dimension in optical fiber communication system, mode scrambling induced signal mixing must be tackled to achieve one-by-one mode mapping between the transmitter side and receiver side. However, when light travels through a circular-core FMF, mode mixing is inevitable due to rotational symmetry and mode degeneracy. In addition, inter-modal coupling can also easily be triggered by fiber non-uniformity, sharp bending, or misalignment of fiber splices. Therefore, mode descrambling must be included in the communication system. In this proposed project, a Mach-Zehnder interferometer (MZI) based reconfigurable optical processor is utilized to perform the optical signal processing, as depicted by Figure 2a. The dimensionality of optical mesh can be improved by cascading the tunable MZIs according to the matrix decomposition scheme shown in Figure 2b. Relying on two unitary matrices and a diagonal matrix, according to singular value decomposition (SVD), optical multiple-input multiple-output (MIMO) processing can be utilized to retrieve the mixed modes after

fiber transmission and the high-dimensional optical I/O. Integrated optical mesh can thus be used with optical transceivers to incorporate the mode dimension into optical fiber communication.

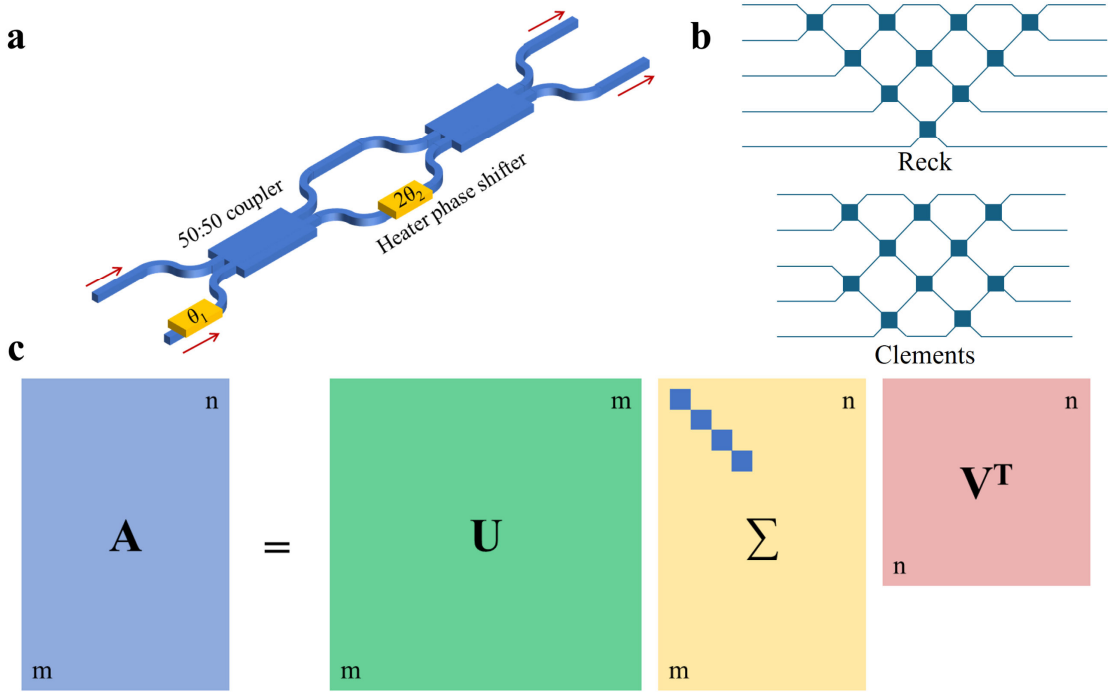

Figure 2. **a** Unitary matrix transformation by integrated coherent Mach-Zehnder interferometer (MZI), using heater based optical phase shifters. **b** Matrix decomposition by Reck and Clements scheme, where each square represents a tunable 2×2 MZI. **c** Singular value decomposition of an m×n complex matrix A, where U is an m×m complex unitary matrix, Σ is an m×n diagonal matrix, V is an n×n complex unitary matrix.

III. Outline of tasks/Work Plan

Based on our exploration of the multi-dimensional optical I/O for few-mode fibers and optical signal processing for mode descrambling, we propose to develop Tbps optical fiber communication system utilizing multiple dimensions including wavelength, polarization, and mode, by silicon photonic integrated circuits as depicted in Figure 3a. The FMF is available in our lab purchased from *OFS*. The photonic chip can be manufactured by commercial silicon photonics foundries according to our design. The proposed project includes three tasks: (1) Improve coupling efficiency of the multi-dimensional optical I/O on silicon for FMFs, including wavelength, polarization, and mode. A new design based on diffraction gratings or nanotapers is needed. For the first method based on diffraction gratings, the chip-to-fiber directionality must be enhanced. If edge coupling is adopted, mode field patten and size matching are important. (2) Design MZI-based reconfigurable optical mesh for mode descrambling according to the number of spatial channels incorporated. Bandwidth span of optical mesh and optical I/O should also be evaluated to decide the number of wavelength channels and channel spacing to be used. (3) Design the optical transceiver unit consisting of electro-optical modulators and photodiodes. Figure 3b shows an example using a ring modulator and a germanium-on-silicon photodiode available in most silicon photonics foundry process design kits. Ring modulator is proposed as it can work for selective wavelength channel without wavelength multiplexers. The wavelength demultiplexers can also adopt ring-cavity based filters in the optical transceiver unit. To achieve a total data-carrying capacity of more than Tbps, the number of data lanes and the number of multiplexed channels can be optimized when designing the high-speed silicon photonic transceivers.

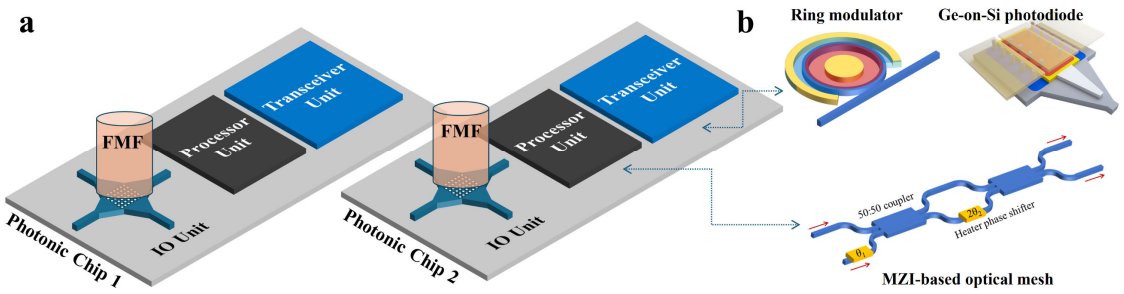

Figure 3. **a** Schematic diagram of mode-multiplexed optical fiber communications with integrated photonic processors and transceivers. **b** Insets of silicon photonic ring-modulators and germanium-on-silicon photodiode used in the transceiver unit, and Mach-Zehnder interferometer (MZI) based optical mesh employed in the processor unit.

IV. Outcome(s)

The research outcomes of this project are prototypes of photonic integrated devices and circuits built for Tbps multi-dimensional optical fiber communications. The few-mode fiber will be used and directly bridged with the photonic chip via a low-loss and multi-dimensional optical I/O, which can incorporate the dimensions including wavelength, polarization, and mode. We will experimentally demonstrate (1) efficient multi-dimensional optical I/O between the photonic chip and few-mode fibers. (2) integrated reconfigurable optical mesh to undo the mode mixing. (3) Tbps per fiber optical communications utilizing integrated high-speed transceivers and multiple dimensions of the few-mode fiber. This program will allow us to combine our expertise in designing novel passive chip-to-fiber I/O devices, as well as high-speed transceivers on silicon, and optical fiber communication demonstrations. We will address and evaluate the specific issues of using photonic integrated circuits for high-dimensional fiber optic communications, including lower-loss optical I/O devices for optical fibers, optical MIMO based mode descrambling, and Tbps optical communications employing the various multiplexing dimensions and integrated high-speed optical transceivers. Through this proposed research project, we should be able to identify the full potentials and possible limitations of utilizing the photonic integration and photonic computing acceleration approach, for unlocking the multi-dimensional optical fiber communication systems.

V. Impact

The results of this project will advance high-capacity optical fiber communications. We are seeking to improve the communication bandwidth through the incorporation of additional physical dimensions, while reducing associated power consumption and cost. Our goal is to establish the feasibility of a Tbps multi-dimensional fiber communication system by photonic integration and optical signal processing, which can potentially be a low-cost, low-power, and low-latency solution. First of all, the proposed multi-dimensional optical I/O device will combine the photonic functions including coupling and multiplexing, enabling an efficient, multi-channel bridge between the optical fiber and the photonic chip. Furthermore, integrating the on-chip processor unit into the communication system will facilitate low-power and low-latency optical signal processing for mode unscrambling before photodetection, eliminating the need for power-intensive and high-speed digital equalizers. Therefore, the photonic integrated circuits in this research project will not only enable efficient conversion between the fiber modes and in-plane waveguide modes, but also providing optical signal processing and optical transceivers on the same silicon photonic chip. Leveraging the well-established Si CMOS infrastructure and process, our proposed approach will drive optical technologies to address the challenges of exponential growth in global data traffic and associated power consumption.

Executive Summary

Conformal Chiral Metasurfaces with Tailored Near-fields for Pharmaceutical Analysis

Introduction: Chirality is a fundamental property of molecules, and their enantiomers can exhibit critical differences in their chemical and physical properties. Many pollutants, such as pesticides and pharmaceuticals, contain chiral compounds with enantioselective degradation and toxicities. Pharmaceutical residues, though largely unregulated in environmental monitoring, are now identified as "compounds of emerging concern." Therefore, detecting and distinguishing between different enantiomers while retaining local environmental contexts is crucial for assessing their potential impact. Light serves as a label-free tool capable of probing the transfer of charge and energy at molecular scales. However, their signals are often weak due to the large mismatch between the detection wavelength and the dimensions of molecular bonds. As a result, achieving maximized chiral responses with customized spatial and temporal properties remains a long-standing challenge.

Objective: Our research objectives are to *develop chiral nanophotonic sensors with customized near-field properties for high-resolution, label-free pharmaceutical analysis.* Nanophotonic structures have been shown to effectively confine electromagnetic energy at nanoscale, offering a surface-functionalized interface for enhanced energy coupling. The key to the enhanced near-field interaction lies in the excitation of optical resonances, which lays the foundation for most nanophotonic studies. Despite its profound role, the pathway to designing nanostructures that specifically support the desired near-field resonances remain largely unexplored. To address the challenge, we propose a new design framework to explicitly create near-field optical resonances with customized chiral properties (Figure, left). This approach enables surface-functionalized interfaces to effectively mediate the responses of chiral analytes. To increase the interacting surface area, we will suspend the nanostructures within a flexible substrate using a universal polymer-assisted transfer technique. This technique allows for conformal integration with analytes of unconventional form factors (Figure, right).

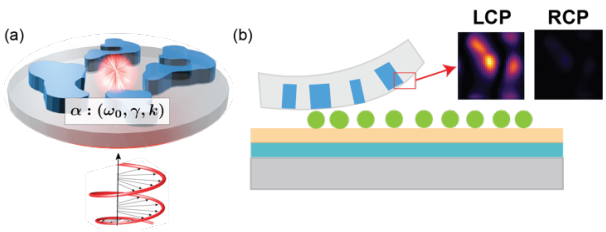

Figure. A schematic of a nanophotonic chiral sensor with customized near-fields.

Capability and impact: The technology could be adapted for label-free, high-throughput chiral imaging and spectroscopy for in-situ pharmaceutical analysis. The chiral-optical near-field properties can be tailored to align with a broad range of molecular fingerprints, enabling the assessment of environmental pollutants across diverse ecosystems. Furthermore, the customized chiral near-field enhancement will streamline processes for high-throughput enantiomer separation and enable the analysis of enantiospecific toxicity and degradation. This will also aid in the development of chiral photocatalysis for driving enantioselective photoreactions and synthesizing optically pure compounds. Lastly, the CMOS compatibility and compact footprint of the nanophotonic sensors provide a route to transform the technology from a laboratory tool to large-scale, heterogeneous integrated systems on an industrial scale.

Proposal

1. Literature Review

Chirality, exemplified by nonsuperimposable mirror images like left and right hands, is a fundamental property observed in molecules ranging from atomic to macroscopic scales. This spatial asymmetry at the molecular level results in enantiomers—molecules that typically exhibit distinct chemical and biological properties. This phenomenon is critical in a variety of pharmaceutical compounds, such as metoprolol and propranolol, which exhibit enantioselective degradation and toxicity[1]. In environmental monitoring, pharmaceuticals remain unregulated, but their residues in the environment are now recognized as "compounds of emerging concern". This is due to their potential to cause significant impacts on human health and ecosystems, even at very low concentrations[2]. Therefore, monitoring and distinguishing these enantiomers is essential for accurately assessing their environmental impact and ensuring the safety of ecosystems.

Despite the importance of enantioselective analysis, it remains challenging to detect and separate chiral molecules from the mixed compound. Due to their enantioselective interactions with light, chiral-optical effects have been observed and can be utilized for the quantitative, label-free, and nondestructive assessment of enantiomers. However, chiral light–matter interactions are typically weak due to the scale mismatch between the detection wavelength and the dimensions of molecular bonds, especially when tiny concentrations of substances are present. This results in reduced efficacy in the detection and quantification of pharmaceutical pollutants, thus limiting the ability to trace key enantiomeric molecules that contribute to environmental contamination.

Metasurfaces composed of nanoscale elements have enabled new regimes of light-matter interaction, offering unprecedented flexibility to manipulate the near-field and free-space properties of light. The key to this versatility stems from the excitation of resonances, which provide two important advantages: (1) enhanced light-matter interaction and (2) geometrical tunability. Through proper engineering of nanostructures, near-field light-matter interactions can be significantly enhanced, employing tailored spatial and temporal properties, making them highly suitable for sensing applications. Previous studies have explored various configurations of meta-atoms for detecting non-chiral materials. Representative demonstrations include employing high-quality-factor (Q) resonators supporting bound states in the continuum (BIC) for ultrasensitive detection of molecular fingerprints[3]. These structures have a clear first-principles basis that allows for rational customization of high-Q resonances. However, extending the design flexibility to planar induced chirality remains a challenging and actively explored field. From first-principles analysis, the conditions for inducing planar chirality require[4]: (1) symmetry breaking involving mirror and N-fold (N>2) rotational symmetry, and (2) supporting coplanar electric and magnetic moments within the device plane. These physical requirements are challenging to meet due to nontrivial physical requirements that lack a direct geometric solution. To fully leverage the resonance-enhanced chiral responses for pharmaceutical analysis, **it is crucial to streamline the design workflow so as to directly satisfy the aforementioned requirements.** This advancement is also scientifically intriguing and can benefit a variety of applications, including quantum photonics, sensing, imaging, and communication.

2. Problem Statement/Objective

To date, most planar chiral metasurfaces are designed through rational schemes based on physical intuition, which involves carefully engineered geometries to support spin-dependent resonant dynamics. Various meta-atom configurations have been investigated to resonantly enhance chiral light-matter interaction. These include Kerker metasurfaces supporting fundamental modes[5] and nonlocal metasurfaces induced by quasi-BIC[6]. Despite the progress, the field enhancements achieved are predominantly **volumetric and confined within the nanostructures**. As a result, chiral analytes are not directly accessible to the energy hotspots, leading to reduced detection sensitivity. Furthermore, the conventional approaches lack a generalized pathway for maximizing chiral optical responses, since they typically rely on empirical evidence to suggest a starting geometry, followed by exhaustive parameter sweeps. This approach is notably time-consuming and inefficient, especially for chiral structures where significant numbers of geometrical parameters are involved. It is, therefore, important to develop **a direct pathway to maximize chiral responses with customized spatial and temporal properties**.

As resonant behavior remains crucial for nontrivial optical responses, a promising yet unexplored approach is to directly target the near-field dynamics and perform explicit mode engineering tailored to chiral responses. However, the engineering of resonances is challenging due to the lack of rigorous correlations between near-fields and structural parameters. To overcome the limitations of analytical knowledge, a natural solution is to transform the design task into an optimization problem using inverse design[7]. These strategies treat the design task as the maximization of a desired Figure of Merit (FOM), followed by using computational algorithms to explore the design space. These methods relax the requirement for physical intuition and result in significantly higher FOMs than the rational design schemes. To date, most inverse-design methods have focused on defining far-field responses as the FOM, aiming to maximize device efficiencies such as beam deflection, focusing, and splitting (Fig. 1 left). Here, to the best of our knowledge, *we are the first to propose applying near-field resonances as the FOMs to enable non-trivial chiral responses (Fig. 1 right)*. By applying this new design paradigm, **our research objectives are to develop a generalized framework to (1)** streamline the design framework to achieve planar-induced chirality with customized near-field properties, **(2)** fabricate conformal metasurfaces for optimum integration with chiral analytes, and **(3)** apply chiral sensors for in-situ, high-throughput, and nondestructive pharmaceutical analysis.

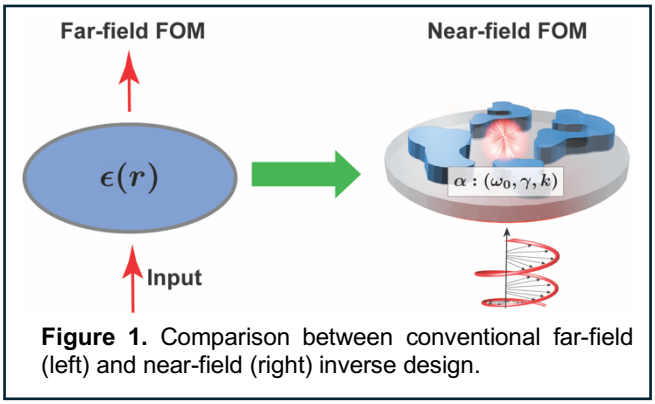

Figure 1. Comparison between conventional far-field (left) and near-field (right) inverse design.

3. Outcomes

3.1 Near-field engineering for planar induced chirality

The proposed strategy is expected to achieve planar induced chirality with maximized chiral responses. As stated in the first section, the requirements for inducing planar chirality involve prescribed symmetry considerations and modal dynamics. These requirements are straightforward to meet using the near-field design paradigm: the *N*-fold rotational symmetry

can be broken by specifying spin-dependent modes; namely, the modes are exclusively induced by circularly polarized light of a specific handedness. For the requirement involving coplanar electric and magnetic moments, an out-of-plane dipole mode can be specified as an objective function, which in turn satisfies the non-orthogonal coplanar condition. The FOM for engineering resonant behavior is the local density of states (LDOS), corresponding to the power emitted by a point-dipole source placed at the location of interest. The intensity of the dipole source can be maximized to exhibit strong LDOS through an adjoint variable method[8], leading to the creation of near-field resonances with tailored frequencies, spins, and decay rates.

A schematic of the design concept is illustrated in Fig. 2a. We specify a vertical electric dipole source in the metasurface plane as the FOM, which is engineered to be induced only upon left circular polarization (LCP) while remaining unexcited upon right circular polarization (RCP). Fig. 2b shows the optimized geometric profile, revealing a structure that breaks mirror and *N*-fold rotational symmetry. The spin-dependent mode behaviors are further illustrated in the electric field distributions (Fig. 2b, middle), showing more than 1000:1 intensity contrast between LCP and RCP incidence. To validate its chiral optical effect, we evaluate the far-field responses of the optimized chiral metasurface. *Importantly, the field enhancement occurs on top of the structures, as shown in the side view of the field distribution (Fig. 2b, right), allowing analytes to directly access the enhanced interaction area for ultrasensitive sensing*. Fig. 2c shows the transmittance spectrum for both LCP and RCP, demonstrating a narrowband circular dichroism at the resonant wavelength with a Q-factor significantly higher than the rationale design schemes[5]. It can thus be seen that the proposed method enables planar induced chirality beyond the capability of first-principles analysis.

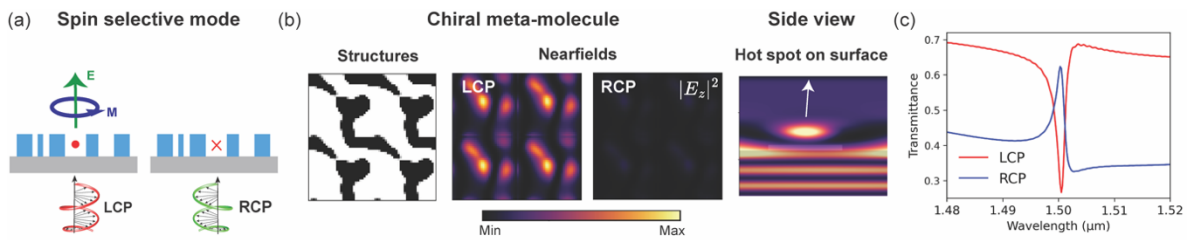

Figure 2. Planar chiral metasurfaces with customized near-field profiles. (a) Design implementation for chiral metasurfaces, which are designed to support spin-selective vertical electric dipole resonance. (b) Top view of the optimized chiral structures and electric field distributions of the chiral modes, showing large spin-decoupled mode excitations. Side view shows the field enhancement occurs on top of the structures. (c) Transmittance spectrum showing high-Q, narrowband circular dichroism.

3.2 Fabrication of chiral metasurfaces

In the proposed research, freeform chiral metasurfaces will be fabricated using standard CMOS-compatible processes. In brief, a thin layer of amorphous silicon will be grown on a fused silica substrate using plasma-enhanced chemical vapor deposition. The metasurface patterns with nanoscale features will be defined using electron beam lithography, followed by hard mask deposition and reactive ion etching. UNC Charlotte's Optoelectronic and Optical Device Fabrication Facility hosts 4,000 square feet of cleanroom space, where we have utilized the resources to develop mature processes for fabricating dielectric metasurfaces. Fig.3a shows the scanning electron microscope image of the chiral structures fabricated at the home institute, showing precisely defined curvilinear features that closely

resemble the design in Fig. 2b. To increase the surface interacting area with analytes, we propose to transfer the chiral nanostructures onto a flexible substrate. We have previously developed a universal polymer-assisted transfer technique to enable large-area, defect-free transfer of high-aspect-ratio nanostructures[9]. The fabrication process involves defining metasurfaces on a thin germanium layer that serves as a sacrificial layer, followed by encapsulating the patterns with polydimethylsiloxane (PDMS). The metasurface layer is then released by dissolving the germanium sacrificial layer. Fig. 3b shows the optical image of the transferred metasurface, which will preferentially interact with chiral substances because of an increased surface area between molecules and chiral evanescent fields, leading to enhanced sensitivity (Fig. 3c). *This method not only ensures the defect-free transfer of freestanding metasurfaces, but also broadens the conventional scope of metasurface substrates beyond bulky and rigid planar form factors*.

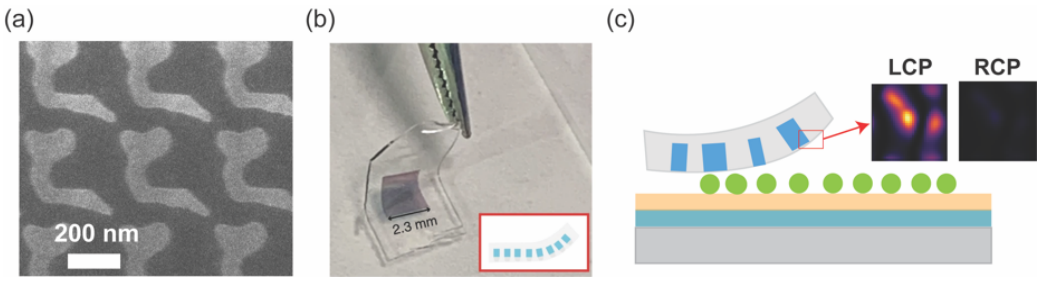

Figure 3. (a) Scanning electron microscope image of the fabricated chiral metasurface. (b) Optical image of the flexible metasurface embedded in a thin layer of polymer. (c) The suspended layer facilitates conformal coating with analytes to enhance the interaction area.

3.3 Chiral sensor for pharmaceutical analysis

The fabricated chiral sensors will be utilized for imaging-based spectrometerless fingerprint detection of selected environmental pollutants. We will leverage CMOS-compatibility processes to pattern densely packed arrays of chiral sensors on a single chip to form a barcode matrix, offering a compact and inexpensive solution for in-situ, label-free ultrasensitive detection of chiral compounds. A schematic of the barcode technique is shown in Fig. 4. A large-scale sensor matrix is patterned on a single chip, with each matrix element designed to target a specific molecular absorption signature and chirality $(\omega, \pm)$, where ω and $\pm$ denote frequency and spin, respectively. The conformal covering of the metasurfaces with chiral analytes causes a pronounced change in the imaged intensity due to the spatial overlap between the molecules with the enhanced chiral near-fields. The absorption signatures are converted in a 2D spatial map that serves as a barcode to identify the molecular type and chirality in arbitrary mixed compositions.

The readout of the barcode images will be processed through linear decomposition to retrieve the detailed compositional information. For nonlinear molecular dynamics, neural network-based algorithms could be employed for analyzing complex kinetics and chemical reactions. The barcoding chiral sensor will be applied for enantioselective environmental analysis of pharmaceuticals. To test the effectiveness and sensitivity of the technology, a wide range of pharmaceuticals, including analgesics, β-receptor antagonists, and antidepressants, will be tested to analyze their enantiospecific profiles.

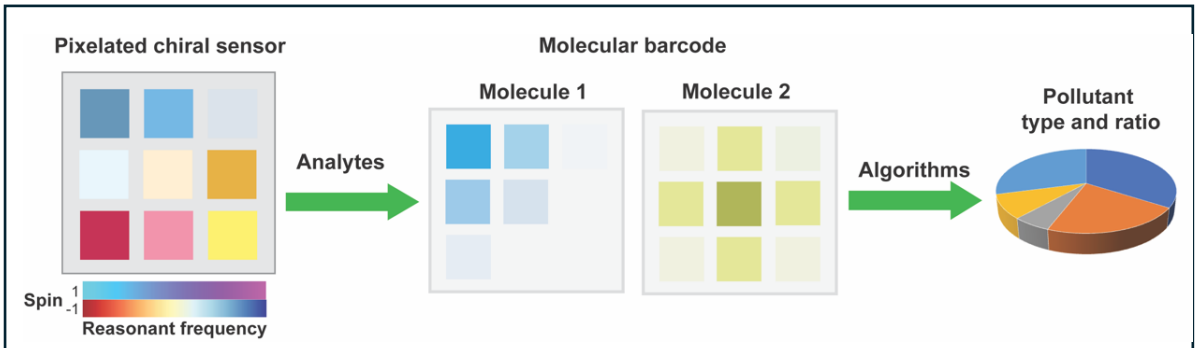

Figure 4. Barcoding chiral sensor for pharmaceutical analysis. Schematic of the proposed chip-based barcoding sensor consisting of chiral metasurfaces designed to target specific resonant frequencies and spins (left). Molecular fingerprints are converted into 2D absorption maps (middle), which can be used to identify the molecular types and their enantiospecific properties (right).

4 Impact

The proposed research presents significant advancements to chiral sensing from both fundamental and application aspects, and they include:

Ultrasensitive pharmaceutical analysis: The proposed project represents a major technical advancement in pharmaceutical analysis through novel design and experimental efforts. (1) Design-wise, we developed a generic framework to tailor the chiral near-fields, allowing the field enhancement to effectively overlap with chiral molecules. (2) Experimentally, we developed a unique transfer technique to incorporate the metasurfaces on a flexible substrate for conformal integration. These methods extend the compatibility with enantiomers exhibiting unconventional form factors, allowing for technology adaptation in diverse environmental settings. This further facilitates the transition from lab-scale research to practical, field-tested pharmaceutical analysis. Furthermore, the proposed barcoding sensor presents a promising method to analyze enantiospecific properties in mixed chiral compounds, offering a compact solution for in-situ, high-throughput, and nondestructive pharmaceutical analysis.

Standardized workflow to achieve planar-induced chirality: The proposed research tackles the long-standing challenge of achieving planar induced chirality from a perspective of near-field inverse design. This offers a generic pathway to streamline the design workflow of nontrivial metasurfaces, allowing researchers from various interdisciplinary fields to bridge the knowledge gap and deploy the proposed optimization-based framework to design high-Q metasurfaces for diverse sensing applications.

Broad impacts in photochemistry: Controlling near-fields at the nanoscale has significant implications for photochemistry, particularly in developing chiral photocatalysis for catalyzing enantioselective photoreactions and synthesizing optically pure compounds[10]. The proposed research provides a versatile tool to precisely tailor the near-field distribution around the chiral photosensitizer, allowing the reaction conditions to be finely tuned for high enantiomeric excess, improved efficiency, and selective activation.

References

1. Ma, R., Qu, H., Wang, B., Wang, F. & Yu, G. Widespread monitoring of chiral pharmaceuticals in urban rivers reveals stereospecific occurrence and transformation. *Environ Int* **138**, 105657 (2020).
2. Ziylan, A. & Ince, N. H. The occurrence and fate of anti-inflammatory and analgesic pharmaceuticals in sewage and fresh water: treatability by conventional and non-conventional processes. *J Hazard Mater* **187**, 24–36 (2011).
3. Tittl, A. *et al.* Imaging-based molecular barcoding with pixelated dielectric metasurfaces. *Science (1979)* **360**, 1105–1109 (2018).
4. Zhu, A. Y. *et al.* Giant intrinsic chiro-optical activity in planar dielectric nanostructures. *Light Sci Appl* **7**, 17158 (2018).
5. Solomon, M. L., Hu, J., Lawrence, M., García-Etxarri, A. & Dionne, J. A. Enantiospecific optical enhancement of chiral sensing and separation with dielectric metasurfaces. *ACS Photonics* **6**, 43–49 (2018).
6. Shi, T. *et al.* Planar chiral metasurfaces with maximal and tunable chiroptical response driven by bound states in the continuum. *Nat Commun* **13**, 4111 (2022).
7. Molesky, S. *et al.* Inverse design in nanophotonics. *Nature Photonics* vol. 12 659–670 Preprint at https://doi.org/10.1038/s41566-018-0246-9 (2018).
8. Lalau-Keraly, C. M., Bhargava, S., Miller, O. D. & Yablonovitch, E. Adjoint shape optimization applied to electromagnetic design. *Opt Express* **21**, 21693 (2013).
9. Zhou, Y., Zheng, H., Kravchenko, I. I. & Valentine, J. Flat optics for image differentiation. *Nat Photonics* **14**, 316–323 (2020).
10. Solomon, M. L. *et al.* Nanophotonic platforms for chiral sensing and separation. *Acc Chem Res* **53**, 588–598 (2020).

Multiplexed and Continuous Monitoring of Metabolites using High-Q Metasurfaces and Modular DNA Aptamer Probes for Chronic Stress Management

Optica Foundation Challenge: Health

PI: Dr. Yuanwei Li, Stanford University, Stanford, CA, USA

Challenge: *Chronic stress* is a burgeoning global health issue, impacting nearly one-third of the population with severe consequences including mental disorders, cardiovascular diseases, and hormonal imbalances. Current methods, such as ultra-performance liquid chromatography-mass spectrometry, for detecting stress-related biomarkers are limited by the need for bulky, expensive equipment and lengthy processing times, hindering timely and effective stress management. Furthermore, alternative methods like fluorometric assays and enzyme-linked immunosorbent assays struggle with low sensitivity and throughput, especially when dealing with complex biological fluids like sweat. Furthermore, existing technologies often do not support the simultaneous detection of multiple biomarkers, essential for comprehensive stress assessment. There is a pressing need for more accessible, accurate, and rapid technology to enable continuous monitoring of multiple stress-related metabolite biomarkers, such as adenosine, dopamine, oestradiol, and cortisol, to facilitate immediate and personalized therapeutic interventions.

Proposed project: This proposal aims to develop an innovative, *portable biosensing* platform capable of *multiplexed and continuous* monitoring of metabolite biomarkers related to chronic stress in sweat. Utilizing cutting-edge nanophotonic technology, the platform integrates dielectric metasurfaces, termed very-large-scale integrated high-Q nanoantenna pixels (VINPix), with spherical nucleic acids (SNAs) and innovative split aptamer designs, to provide rapid, sensitive, quantitative, and simultaneous detection of adenosine, dopamine, oestradiol, and cortisol. Specifically, this approach employs a hybrid-attachment strategy where part of the split aptamer is attached to the SNA plasmonic nanoparticle core and another part to the dielectric VINPix. The attachment of SNAs to the VINPix upon metabolite binding, coupled with localized electromagnetic hotspots, significantly amplifies optical scattering intensity changes that correlate to biomarker concentrations. This dielectric-plasmonic sandwich setup significantly boosts detection specificity and sensitivity. Furthermore, the dense array of VINPix (over *5 million* VINPix are patterned per square centimeter; equivalent to over 31,000 96-well plates), combined with the application of microfluidic techniques, acoustic bioprinting, or photochemistry, allows for the simultaneous and continuous detection of *thousands of sensors* targeting various metabolites.

Intended outcomes: By leveraging advanced nanophotonic technology and novel molecular recognition designs, this sensor promises to monitor adenosine, dopamine, oestradiol, and cortisol continuously, sensitively, and quantitatively. At the project conclusion, we will have demonstrated a VINPix system with modular aptamers on the surface that selectively target metabolites, such as adenosine, dopamine, oestradiol, and cortisol; successfully achieved quantitative detection of these biomarkers, with a lower limit of detection in the *picomolar range* within *20 minutes* of sweat sample introduction; and demonstrated a VINPix sensor system prototype with integrated microfluidics, designed for the continuous and multiplexed monitoring of these metabolites in sweat.

Looking forward, given the widespread impact of chronic stress on global health, this technology has the potential to revolutionize how individuals *monitor their physiological states and manage stress-related conditions*. By enabling continuous, non-invasive monitoring of metabolite biomarkers in sweat, the technology will provide crucial insights into the physiological manifestations of stress, enhancing our fundamental understanding of its impacts on human health. In the long term, this technology could lead to significant advancements in personalized health monitoring and proactive health management, potentially reducing stress-related illnesses and improving quality of life through early detection and management. Additionally, the platform's *scalability and adaptability* for detecting other biomarkers, including proteins, ions, and microRNA, could lead to its application in various medical diagnostic and therapeutic areas.

Literature Review and Problem Statement

Chronic stress is a prevalent issue affecting nearly one third of the global population[1], leading to numerous health complications, including mental health disorders, cardiovascular diseases, immune dysfunction, and hormonal imbalances like irregular menstrual cycles[2,3]. Effective management of stress requires not only understanding its physiological, psychological, and neurochemical impacts but also developing tools for early detection and intervention. Metabolites, including adenosine, dopamine, oestradiol, and cortisol, are critical biomarkers for monitoring stress due to their roles in physiological and psychological stress responses[4]. Continuous monitoring of these biomarkers simultaneously using portable devices can significantly enhance the accuracy and timeliness of stress monitoring, facilitating precise, immediate, and personalized therapeutic interventions.

Existing technologies for biomarker detection in biological fluids face significant limitations. Current standard practices, including ultra-performance liquid chromatography-mass spectrometry (UPLC-MS)[5,6], although accurate, are hampered by the need for bulky equipment, high costs, slow processing times, and low throughput, making them impractical for continuous monitoring. Alternative methods like fluorometric assays and enzyme-linked immunosorbent assays (ELISA)[7,8] suffer from low sensitivity, susceptibility to fluorophore degradation, and low-throughput, particularly challenging given the low biomarker concentrations typically found in biological fluids, especially sweat[9]. Furthermore, existing technologies often do not support the simultaneous detection of multiple biomarkers, essential for comprehensive stress assessment.

The Dionne Lab has pioneered the development of high-Q dielectric metasurfaces[10–13], evidenced by our numerical models, fabrication protocols, and spectroscopic characterization. We have also applied these metasurfaces as refractive index sensors for DNA based on hybridization[13]. Furthermore, our most recent work has miniaturized these long biperiodic resonant nanoantennas into finite sized pixels by incorporating reflective photonic crystal mirrors at their ends, termed very-large-scale integrated high-Q nanoantenna pixels (VINPix)[14]. This miniaturization enhances the resonator site density to *10 million/cm*^{2}. These VINPix arrays have recently been utilized for the detection of proteins and environment DNA, incorporating microfluidic reagent delivery systems.

Objectives

To address the urgent need for technological advancements that provide immediate health insights and empower individuals to manage stress proactively through timely interventions, we propose a novel portable sensor technology. This technology is capable of multiplexed and continuous monitoring of metabolite biomarkers related to chronic stress, including adenosine, dopamine, estradiol, and cortisol, in sweat. Specifically, this platform leverages resonant silicon nanophotonic antennas, termed very-large-scale integrated high-Q nanoantenna pixels (VINPix)[14]. These VINPix will be functionalized with modular DNA aptamer probes and integrated with plasmonic nanoparticles to rapidly, quantitatively, sensitively, continuously, and accurately detect these metabolite biomarkers. A separate miniaturized light source and camera will detect optical scattering intensity changes that correlate to biomarker concentrations.

Our approach is **significant** since it will facilitate easily deployable, quantitative, and readily modifiable personal monitoring of multiple metabolite biomarkers - particularly those relevant to chronic stress-induced diseases (e.g., adenosine, dopamine, oestradiol, and cortisol). Notably, our assay promises several **innovative advantages** compared to existing diagnostics: 1) continuous monitoring by taking advantages of microfluidics and achieving rapid results in < *20* minutes. 2) An extremely low limit of detection, owing to the high-Q chips' laser-sharp scattering spectra and the amplification of scattering changes by plasmonic nanoparticles. 3) facile modification of the assay surface functionalization for new host biomarkers. 4) By relying on nanopatterned Si, we capitalize on the low-cost and scalable fabrication of established high-throughput CMOS fabrication processes. 5) Fluorescent tagging or secondary antibodies are not required; therefore, the chip is the "disposable/universal reagent". 6) Massive multiplexing is possible on a single chip, owing to the "free-space" illumination of the densely packed arrays of resonators combined with our innovative bioprinting and photochemistry-induced functionalization techniques. 7) Minimal training for use is needed, unlike mass spectroscopy which requires a lab technician or health care professional.

Our **final goal** is the development of a portable (handheld), rapid, and quantitative sensor that supports the simultaneous and continuous monitoring and detection of multiple biomarkers in sweat, significantly improving the utility and comprehensiveness of stress assessments. Specifically, our goal can be accomplished by fulfilling the following **objectives**:

1. Develop Novel Split Aptamer Design for Enhanced Biomarker Detection: Utilize innovative split aptamer DNA sequences that undergo structural changes upon binding to target metabolites, thereby creating a dynamic detection environment. This design aims to significantly enhance biomarker detection by increasing both the sensitivity and specificity of the assay.

2. Integrate VINPix with Spherical Nucleic Acids (SNAs) for Ultrasensitive and Robust Detection (**Fig. 1**): Attach split aptamers to SNA nanoparticle cores and resonant silicon nanophotonic antennas (VINPix) to establish an ultrasensitive sandwich detection mechanism. SNAs are 3D nanostructures consisting of nucleic acids that are densely functionalized and oriented spherically around a nanoparticle core. The DNA aptamers on metasurfaces and SNAs interact with target analytes, forming a secondary DNA structure that localizes SNAs and analytes on dielectric metasurfaces. This creates localized electromagnetic hotspots due to dielectric-plasmonic coupling, amplifying resonance shifts linked to biomarker concentrations and causing a visible color change indicating biomarker presence. This dual-attachment method enhances detection sensitivity and reliability by concentrating biomarkers in localized enhanced electric fields, promising a lower detection limit compared to traditional assays.

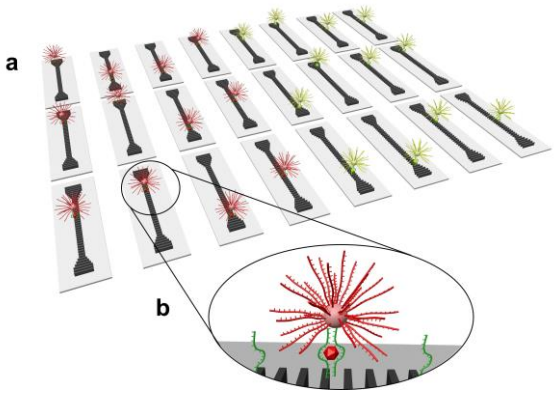

Fig. 1. a, A schematic view of high-Q metasurface arrays for small molecule sensing, facilitated by SNAs. b, A magnified view highlighting the interactions between small molecules and DNA aptamers.

3. Employ Acoustic Bioprinting or Photochemistry for Extensive Multiplexing: Use acoustic and inkjet bioprinting technologies to deposit molecular probes on metasurfaces with high precision (~15-micron resolution), and photochemistry to achieve even finer reaction resolution (~1 micron) for functionalizing distinct resonators with different split DNA aptamers. This allows for the multiplexed detection of metabolites on a single chip, with up to *hundreds to thousands* of sensors detected simultaneously (over *5 million* VINPix are patterned per square centimeter; equivalent to over 31,000 96-well plates).

4. Facilitate Continuous Monitoring with Integrated Microfluidic System: Integrate metasurfaces with a microfluidic system that supports continuous monitoring by collecting and analyzing sweat in real-time. This system leverages the direct optical signals from the silicon structures for rapid and accurate biomarker detection, with acquisition times as low as 200 milliseconds, and eliminates the need for fluorescent tagging, thereby reducing costs and reagent requirements.

Outcomes

The anticipated outcomes of this proposal include: 1) **a VINPix system with modular molecular probes** on the surface that selectively target metabolites. 2) **Quantitative detection** of adenosine, dopamine, oestradiol, and cortisol, with a lower limit of detection (LLOD) in the *picomolar range* within *20 minutes* of sweat sample introduction. And 3) **Multiplexed and continuous monitoring** of metabolites in sweat. The societal impact of these outcomes is profound, potentially reducing the prevalence and severity of stress-related health issues across diverse populations.

1. A VINPix system with modular molecular probes that selectively target metabolites.

1.1. Design and synthesis of modular probes that selectively target metabolites

1.1.1 Synthesis and selectivity of aptamers for metabolite detection

We have identified DNA aptamer sequences that directly recognize oestradiol, dopamine, cortisol, and adenosine respectively using in vitro solution-phase systematic evolution of ligands by exponential

enrichment. The solution dissociation constant of these aptamers will be determined via competitive fluorescence assays. We will demonstrate the selectivity of the aptamers for the target versus chemically related, biologically relevant nontargets. We will investigate target-induced changes in aptamer secondary structural motifs using circular dichroism spectroscopy. Upon target association, the aptamers should show spectral shifts and changes in intensity in the major positive band, which suggests conformational changes upon metabolite binding.

1.1.2 Aptamer stability under pH, salt, and temperature variations

The aptamers' stability will be tested under varying conditions like pH, salt, and temperature to ensure consistent performance in real-world applications. Moreover, the melting temperature (T_m) of aptamer-target analyte binding will be measured using UV absorbance spectroscopy to understand the stability and strength of the binding interaction. A higher melting temperature generally indicates a stronger and more specific interaction. By measuring T_m, we will determine the optimal condition range under which the aptamer functions best for biosensing. We will also study how the T_m changes under different conditions, providing insights into the binding stability, affinity, and specificity of the aptamer for its target.

1.2. Chip surface functionalization with probes

1.2.1 Protocols for stable attachment of aptamer probes to VINPix

Self-assembled monolayers will be formed on metasurfaces, which enable the creation of dense, consistent, and well-organized arrays of probe molecules. We applied a covalent salinization technique to the metasurfaces. Subsequently, the alkene groups present in the monolayer underwent a targeted reaction with DNA aptamer probes via click chemistry. To minimize non-specific binding of metabolites to the sensor surfaces, surface passivation and surface chemistry modification strategies will be used.

1.2.2 Protocols for stable attachment of aptamer probes to plasmonic Au nanospheres

Au nanospheres were functionalized with spit aptamers using a salt-aging strategy. First, 3'-propylthiol-terminated aptamers were incubated with dithiothreitol at room temperature to cleave the disulfide end. Afterwards, the aptamers were added to the Au nanosphere suspensions in phosphate buffer. Finally, NaCl solution was added to the solution until it reached the targeted final salt concentration.

1.3. Selective functionalization of probes on VINPix using bioprinting or photochemistry

1.3.1 Selective probe attachments using bioprinting or photochemistry

First, bioprinting will be used to achieve selective functionalization of different probes on metasurfaces. Our acoustic bioprinter will be upgraded for the rapid dispensing of picoliter droplets containing DNA aptamer probes. The acoustic printing parameters will be varied to regulate the size and directionality of the printed microdroplets, optimizing for positioning accuracy and throughput. Alternatively, we will harness photochemistry to precisely control the selective attachment of probes with enhanced resolution for densely multiplexed detection. A UV-LED will be used to selectively expose certain areas of the resonators, facilitating the targeted attachment of aptamer probes to specific locations on the resonators. These methods ensure precise and location-specific functionalization, critical for multiplexed detection.

1.3.2 Evaluate the binding uniformity and cross-reactivity of immobilized probes

To evaluate the cross-reactivity of the probes, fluorescence imaging will be used to characterize the VINPix metasurfaces that have been selectively functionalized with different fluorophore-labeled aptamers. To verify the uniformity and reproducibility of aptamer binding, we will utilize a combination of techniques including fluorescent tagging, electron microscopy, and atomic force microscopy.

2. Quantitative detection of metabolites with a LLOD in the picomolar range within 20 minutes of sweat sample introduction.

2.1. Detection of synthetic metabolites at various concentrations in buffer solutions

2.1.1 Establish a clear correlation between the concentration of the targets and the resonance shifts

We will use aqueous PBS solutions that contain synthetic molecules at various concentrations. When target molecules are introduced into the system, they bind with aptamers on the metasurfaces and SNAs. This interaction causes the analytes and SNAs to localize on the resonators, thereby changing the refractive index of the resonator's surrounding environment. It should be detectable as changes in optical scattering intensity upon the binding of target small molecules and SNAs, within a rapid timeframe of

less than 20 minutes. The concentration of adenosine, dopamine, oestradiol, and cortisol solutions will be further diluted (from mM to aM) to determine a LLOD.

2.1.2 Create calibration procedures for quantifying metabolite concentrations

We will establish a clear correlation between the concentration of the target molecules and the resonance shifts observed in the system, and therefore establish a quantitative testing methodology. Specifically, aqueous PBS solutions that contain synthetic molecules at various concentrations and SNAs are introduced to the biosensor. The scattering signals of the metasurfaces are measured, indicative of metabolite and SNA binding. The lower the concentrations of the target substance, the smaller resonance shifts in the resonant wavelength. We determine the calibration curve by assessing the biosensor's response to a series of standard solutions at varying concentrations. From this calibration curve, we will establish the linear range, which in turn defines the dynamic range of the biosensor.

2.1.3 Comparative analysis between the full aptamer approach and the SNA split aptamer strategy

We will compare the detection performance of the two types of DNA aptamers to refine the overall detection strategy. Split aptamer/SNA system will offer two key advantages: 1) Enhanced sensitivity and selectivity: the presence of target biomarkers catalyzes the binding of SNAs to metasurfaces, triggering remarkedly increased resonance shifts. This effect is also magnified by electromagnetic hotspots between the SNAs and metasurfaces, improving detection sensitivity and enabling precise molecule identification. 2) Visual biomarker detection: the SNA attachment on the high-Q metasurfaces results in a visible color change of the metasurfaces, providing a visual signature of the biomarkers' presence. This visual cue simplifies detection, ideal for point-of-care testing, eliminating the need for complex instruments.

2.2. Detection of adenosine, dopamine, oestradiol, or cortisol in artificial sweat and actual sweat

Known amounts of metabolites will be spiked into the synthetic sweat samples. Actual sweat will be collected using sweat collection systems or absorption pads. We will evaluate and compare the interaction rates between our biosensor and its target metabolite analytes in artificial and actual sweat. By introducing the target analyte at a predefined concentration, we capture the spatial-spectral frames for a rapidly sweeping wavelength range around the resonance wavelength of VINPix. We then extract the resonance shift for each resonator cluster from these images at designated time intervals. From this kinetic data, we can determine the association and dissociation rates, and the equilibrium dissociation constant, providing valuable insights into the binding kinetics of our system and time to detection. We aim to achieve a picomolar LLOD for adenosine, dopamine, oestradiol, and cortisol in sweat. Achieving such a high degree of sensitivity is imperative for stress management and related early disease detection and monitoring, particularly in conditions where biomarker concentrations in sweat are exceptionally low in early stages.

3. Multiplexed and continuous monitoring of metabolites in sweat

3.1 Multiplexed detection of metabolites on one chip for vital health metrics

To analyze real-time concentrations of adenosine, dopamine, estradiol, and cortisol in a person's sweat for interpreting stress-related diseases, specific ratios between these biomarkers are informative: 1) Ratio of Cortisol/Dopamine: An increased ratio may indicate elevated stress or anxiety levels. Higher cortisol relative to dopamine can suggest that the body is in a prolonged state of stress, which might lead to burnout or depression. 2) Ratio of Estradiol/Cortisol: This ratio is useful in understanding stress impacts in the context of hormonal balance. A lower ratio may suggest an inadequate protective response to chronic stress, particularly relevant in studying stress differences between genders. 3) Ratio of Adenosine/Cortisol: A lower ratio might indicate poor stress recovery or chronic stress situations, as the calming effects are overwhelmed by stress response mechanisms.

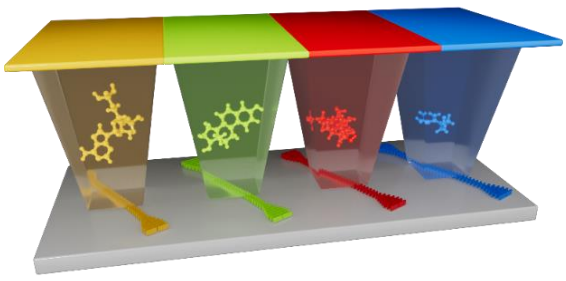

Fig. 2 Scheme showing the multiplexed detection of metabolites on a single chip.

By combining the VINPix sensor array with advanced bioprinting or photochemistry techniques, we can achieve high-fidelity, high-density, and spatially precise functionalization of modular probes on

metasurfaces. This integration allows for the simultaneous detection of metabolites on a single chip (**Fig. 2**), thereby streamlining the measurement process and improving the efficiency of monitoring these biomarkers and their ratios. This capability is important for stress monitoring and the early detection and management of related diseases, enhancing diagnostic accuracy and patient care.

To assess the assay's specificity and efficiency, synthetic metabolite targets corresponding to each probe type will be introduced to our sensor individually. We will then conduct spectral imaging to link spatially dependent resonant shifts with the binding of specific probe-target pairs. Furthermore, we plan to label metabolites of interest with fluorophores emitting at different wavelengths and employ fluorescence microscopy to validate the spatially multiplexed and sequence-specific binding on our platform. Moreover, we will determine the sensitivity, limit of detection, dynamic range, reproducibility, and time-to-result, and compare between our metasurface-based detection system and parallel standard laboratory tests like ELISA and mass spectrometry. We expect to achieve similar or even better sensitivity, accuracy, and specificity compared to mass spectrometry and ELISA, while significantly reducing the time required for detection and enabling multiplexing capabilities.

3.2 Continuous monitoring by integrating microfluidics systems with VINPix

Finally, our project strives to continuously monitor these metabolites in sweat. This will be achieved by integrating metasurfaces with a microfluidic system that includes a reaction chamber and specifically designed inlets and outlets for efficient sweat collection (**Fig. 3**). These features ensure that the sweat is directed seamlessly from the collection points to the reaction chamber where the metasurfaces, equipped with specific sensors for each metabolite, perform continuous and simultaneous quantitative analysis. To ensure robust monitoring, the system will utilize capillary action coupled with micro-pump technology to draw sweat through the microfluidic channels. This approach guarantees a constant flow of samples across the reactive metasurfaces, thus enabling real-time biomarker detection. The metasurfaces within the reaction chamber are designed with high specificity and sensitivity towards targeted metabolite biomarkers. These metasurfaces will be functionalized with specific aptamers that bind selectively to these metabolites, facilitating their detection and quantification through changes in optical signals. The resulting system will be capable of continuous, simultaneous, and quantitative measurements of key metabolite biomarkers, providing important health metrics. This integration is a significant step forward in health monitoring and provides an important value inflection point for our technology, especially for monitoring and management of chronic stress.

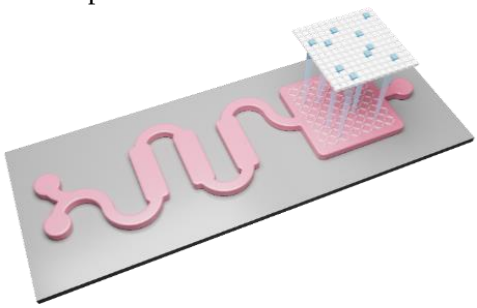

Fig. 3 Continuous and multiplexed monitoring by integrating metasurfaces with microfluidics.

Impact

This proposal outlines the development of an innovative, portable sensor technology for the multiplexed and continuous monitoring of key metabolite biomarkers related to stress. By leveraging advanced nanophotonic technology and novel molecular recognition designs, this sensor promises to monitor adenosine, dopamine, oestradiol, and cortisol continuously, sensitively, and quantitatively. Looking forward, this technology has the potential to revolutionize how individuals monitor their physiological states and manage stress-related conditions. By providing real-time, precise biomarker data, users can receive immediate feedback on their stress levels and hormonal balance, enabling proactive health management. The successful integration of this technology into consumer health devices could open new markets and drive widespread adoption of personalized health monitoring tools. Additionally, the platform's scalability and adaptability for detecting other biomarkers, including proteins, ions, and microRNA, could lead to its application in various medical diagnostic and therapeutic areas.

References

[1] N. Salari, A. Hosseinian-Far, R. Jalali, A. Vaisi-Raygani, S. Rasoulpoor, M. Mohammadi, S. Rasoulpoor, B. Khaledi-Paveh, *Global. Health* **2020**, *16*, 57.

[2] N. Schneiderman, G. Ironson, S. D. Siegel, *Annu. Rev. Clin. Psychol.* **2005**, *1*, 607.

[3] S. Cohen, D. Janicki-Deverts, W. J. Doyle, G. E. Miller, E. Frank, B. S. Rabin, R. B. Turner, *Proc. Natl. Acad. Sci.* **2012**, *109*, 5995.

[4] M. J. Nunes, C. M. Cordas, J. J. G. Moura, J. P. Noronha, L. C. Branco, *Sport. Med. - Open* **2021**, *7*, 8.

[5] P. L. Wood, *Neuropsychopharmacology* **2014**, *39*, 24.

[6] H. G. Gika, G. A. Theodoridis, J. E. Wingate, I. D. Wilson, *J. Proteome Res.* **2007**, *6*, 3291.

[7] S. B. Nimse, M. D. Sonawane, K.-S. Song, T. Kim, *Analyst* **2016**, *141*, 740.

[8] E. L. Snapp, in *Methods Anal. Golgi Complex Funct.* (Eds.: F. Perez, D. J. B. T.-M. in C. B. Stephens), Academic Press, **2013**, pp. 195–216.

[9] W. Gao, S. Emaminejad, H. Y. Y. Nyein, S. Challa, K. Chen, A. Peck, H. M. Fahad, H. Ota, H. Shiraki, D. Kiriya, D.-H. Lien, G. A. Brooks, R. W. Davis, A. Javey, *Nature* **2016**, *529*, 509.

[10] M. Lawrence, D. R. Barton, J. Dixon, J.-H. Song, J. van de Groep, M. L. Brongersma, J. A. Dionne, *Nat. Nanotechnol.* **2020**, *15*, 956.

[11] E. Klopfer, M. Lawrence, D. R. I. I. I. Barton, J. Dixon, J. A. Dionne, *Nano Lett.* **2020**, *20*, 5127.

[12] J. Dixon, M. Lawrence, D. R. Barton, J. Dionne, *Phys. Rev. Lett.* **2021**, *126*, 123201.

[13] J. Hu, F. Safir, K. Chang, S. Dagli, H. B. Balch, J. M. Abendroth, J. Dixon, P. Moradifar, V. Dolia, M. K. Sahoo, B. A. Pinsky, S. S. Jeffrey, M. Lawrence, J. A. Dionne, *Nat. Commun.* **2023**, *14*, 4486.

[14] V. Dolia, H. B. Balch, S. Dagli, S. Abdollahramezani, H. C. Delgado, P. Moradifar, K. Chang, A. Stiber, F. Safir, M. Lawrence, J. Hu, J. A. Dionne, *arxiv* **2023**.

Portable lab-on-a-chip devices with integrated fluorescent sensors for rapid analysis of metabolite biomarkers

The challenge. Metabolites are intermediate or end products of metabolism, produced by enzymatic reactions in cells and subsequently released into biofluids. Altered cell metabolism is associated with many diseases, such as cancer, neurodegenerative disorders, and liver diseases, making metabolites valuable biomarkers for diagnosis, prognosis, and health monitoring. However, the analysis of metabolite biomarkers often relies on sophisticated instrumentation such as mass spectrometry (MS) and nuclear magnetic resonance (NMR), or enzymatic assays in chemistry or clinical laboratories. These methods can be resource-intensive and involve long turnaround times. In developing countries or regions with limited resources, this can result in delayed or absent testing for disease diagnostics. Moreover, long waiting times for test results can delay treatment decisions for urgent cases, such as sepsis in intensive care units (ICUs). Therefore, there is a critical need for rapid analysis of metabolite biomarkers.

Proposed research. Fluorescence detection is a popular optical modality for molecular analytics due to its high sensitivity, simplicity, ease of operation, and suitability for integration into portable instrumentation. We propose leveraging fluorescence detection for rapid and user-friendly metabolite analysis through the development of lab-on-a-chip devices with integrated fluorescent protein (FP)-based sensors. These devices will offer several advantages: low cost, portability, and low sample consumption inherent to lab-on-a-chip technology, along with rapid response (in 1 min), high specificity and straightforward one-pot reactions provided by FP-based sensors.

This project will focus on *two metabolite biomarkers, lactate and pyruvate, in saliva samples*, given their crucial roles in the prognosis of sepsis and cancer, respectively. In Aim 1, we will develop off-chip optical assays for the quantification of lactate and pyruvate. We have developed a one-pot assay for rapid quantification of lactate in saliva using a fluorescent lactate sensor. We will extend these efforts to develop a new fluorescent pyruvate sensor and corresponding detection assay. In Aim 2, the assays will be integrated into a lab-on-a-chip device, preferably through the immobilization of the sensors on micropillar arrays, to enable rapid on-chip detection. In Aim 3, we will develop a sample-to-answer analyzer, which will consist of an inexpensive fluorescence imager utilizing a smartphone camera as the detector, paired with image data analysis software to provide quantification results. The validation of these quantification results will be compared to those obtained using gold standard methods.

Expected outcomes. We anticipate that the proposed research will yield a *high-performance fluorescent sensor for pyruvate* and reliable one-pot off-chip quantification assays for both lactate and pyruvate. These assays will be capable of analyzing metabolite biomarkers in biofluids within a wet chemistry lab setting. Building on these assays, we expect to create a *portable sample-to-answer analyzer* comprising a lab-on-a-chip device, a fluorescence imager, and automated analysis software. This analyzer will feature unmatched simplicity, affordability, and rapid turnaround times, enabling analysis of metabolite biomarkers in diverse settings, such as hospitals and pharmacies.

Impact. The successful demonstration of the lactate and pyruvate analyzer represents a significant milestone toward developing a deployable rapid metabolite testing device for health monitoring and clinical applications. It will lay the foundation for our future collaborations with hospitals to explore the potential of the devices, such as *tracking salivary lactate to predict and monitor sepsis and measuring salivary pyruvate to prognosticate oral cancer*. This advancement will equip healthcare systems and physicians with new tools for early diagnosis and treatment. Importantly, the strategies used to develop these metabolite detection sensors, assays, and devices can be generalized to enable quantitative analyses of a diverse array of metabolite biomarkers in various biofluids for broad health-related applications. Similar to the widespread use of COVID test strips and glucometers, these portable tools will be easily distributable and globally accessible, facilitating metabolite monitoring on a national or even global scale.

Portable lab-on-a-chip devices with integrated fluorescent sensors for rapid analysis of metabolite biomarkers

1. Literature Review

Metabolite biomarkers. Metabolites are intermediate or end products of metabolism, produced by enzymatic reactions within cells and subsequently released into biofluids. Altered cell metabolism is associated with many diseases[1,2], making metabolites valuable biomarkers for diagnosis, prognosis and health monitoring. There is significant focus on small-molecule metabolites, including amino acids and organic acids. For instance, researchers have found significantly elevated blood glutamate levels in patients with major depressive disorder[3], while citrate concentrations have been linked to cancers and liver diseases[4].

Pyruvate and Lactate. Pyruvate and lactate are key products of glycolysis[5]. In this process, glucose is broken down by a series of enzymes in the cytoplasm, converting it into pyruvate. Most pyruvate is then transported into the mitochondria to fuel the tricarboxylic acid (TCA) cycle, which produces adenosine triphosphate (ATP), the primary energy source for cells. Under conditions such as low oxygen levels, pyruvate does not enter the mitochondria for oxidation. Instead, it is directly reduced to lactate, catalyzed by lactate dehydrogenase, in a process called anaerobic glycolysis[6]. Notably, the accumulation of lactate in the tissue microenvironment is indicative of inflammatory diseases and cancer[7].

Health and clinical relevance. Studies have shown that lactate concentration can surge up to tenfold in saliva and blood within minutes after intense exercise, making salivary lactate a crucial indicator of physiological status[8]. Furthermore, altered levels of lactate and pyruvate are associated with various diseases. For instance, a study found a fourfold increase in lactate levels relative to pyruvate in hemodynamically unstable patients with septic or cardiogenic shock[9]. Cancerous cells exhibit an increased rate of glycolysis, resulting in elevated pyruvate levels. Researchers found that patients with oral cancer have altered pyruvate levels in both saliva and serum[10].

Analytical strategies. Traditionally, metabolite analysis has heavily relied on sophisticated instrumentation such as mass spectrometry (MS) and nuclear magnetic resonance (NMR)[11], or enzymatic assays[12]. While MS and NMR are powerful tools capable of analyzing a broad spectrum of metabolites, they necessitate meticulous sample preparation (e.g., extraction, derivatization), specialized expertise for operation, and complex data analysis. For targeted monitoring of specific metabolites, these instruments may be overly complex and resource-intensive. In contrast, enzymatic assays, although not requiring large instrumentation, involve multiple liquid handling steps, demanding skilled operators with specialized knowledge in wet chemistry. Moreover, these assays involve the use of various reagents, including enzymes, substrates, cofactors, and energy molecules, which contribute to elevated manufacturing costs.

Fluorescent protein (FP)-based sensors. These optical sensors are recombinant protein molecules that incorporate an analyte recognition domain and a fluorescent reporter domain[13]. Analyte binding modulates the photophysical properties of the reporter domain, leading to a change in fluorescence signal. While FP-based sensors have been widely adopted for cellular imaging of ions and metabolites, their potential in diagnostics has not been fully explored. These sensors exhibit rapid response time, typically within seconds, which contrasts with the extended reaction time of enzymatic assays, often exceeding one hour. They also feature a straightforward one-pot reaction that eliminates the need for cofactors, substrates, and energy molecules. Compared to conventional methods, FP-based sensors offer unmatched simplicity, affordability, and rapid turnaround time.

Lab-on-a-chip devices. Lab-on-a-chip (also known as microfluidic) technology has rapidly advanced alongside the growing capabilities of nanofabrication[14]. These devices utilize microscale features on polymer or glass substrates to manipulate fluids, enabling tasks such as separation, dilution, mixing, and chemical reactions. Integrated with optical or electrical detectors, they allow for efficient molecular

detection for sample analysis. Characterized by low sample consumption, high automation, and portability, lab-on-a-chip devices have emerged as a major source of innovation for biochemical analysis across diverse fields such as healthcare, environmental monitoring, and food safety.

2. Problem Statement/Objectives

The analysis of metabolite biomarkers for health monitoring and clinical applications often relies on chemistry or clinical laboratories, which can be resource-intensive and involve long turnaround time. These resources may be scarce in developing countries and regions, resulting in delayed or absent testing for disease diagnostics. Moreover, long waiting time can lead to delayed treatment decisions for urgent cases, such as sepsis in intensive care units (ICUs). Therefore, rapid analysis of metabolite biomarkers is critically needed. In response to this need, we propose the development of portable lab-on-a-chip devices with integrated FP-based sensors for rapid and user-friendly metabolite detection. This project will focus on quantification of two representative metabolite biomarkers, lactate and pyruvate, in saliva samples using fluorescent sensors, establishing a foundation for future expansion to other metabolites.

3. Approach

Aim 1. Assay development using fluorescent sensors for lactate/pyruvate analysis off chip.

We plan to first develop assays for lactate and pyruvate analysis using the latest FP-based lactate sensor, eLACCO2.1[15] (Fig. 1a), and a new pyruvate sensor to be engineered.

Lactate detection. The purified eLACCO2.1 sensor exhibits a 15-fold signal increase upon exposure to 10 mM lactate, with a dissociation constant of 1.9 mM, and shows a strong response within the physiological range of salivary lactate (0.2-2 mM). These characteristics of eLACCO2.1 have been successfully reproduced in our lab (Fig. 1b). Although some FP-based sensors exhibit a sigmoidal relationship between signal and concentration changes, eLACCO2.1 demonstrates excellent linearity below a 0.2 mM threshold (Fig. 1c), making it ideal for quantification purposes if the sample is appropriately pre-diluted. To quantify lactate in saliva, we have tested two strategies: standard addition and external calibration. Our quantification result indicates 0.21 mM (by standard addition) and 0.24 mM (by external calibration) lactate in pooled saliva samples, consistent with the literature[16]. While the matrix effect of ions and biomolecules in the saliva sample can pose challenges to measurement accuracy, our fluorescence signals in diluted saliva samples suggest negligible impact on the sensor's intensity and sensitivity (Fig. 1c, d). We plan to validate our quantification results by

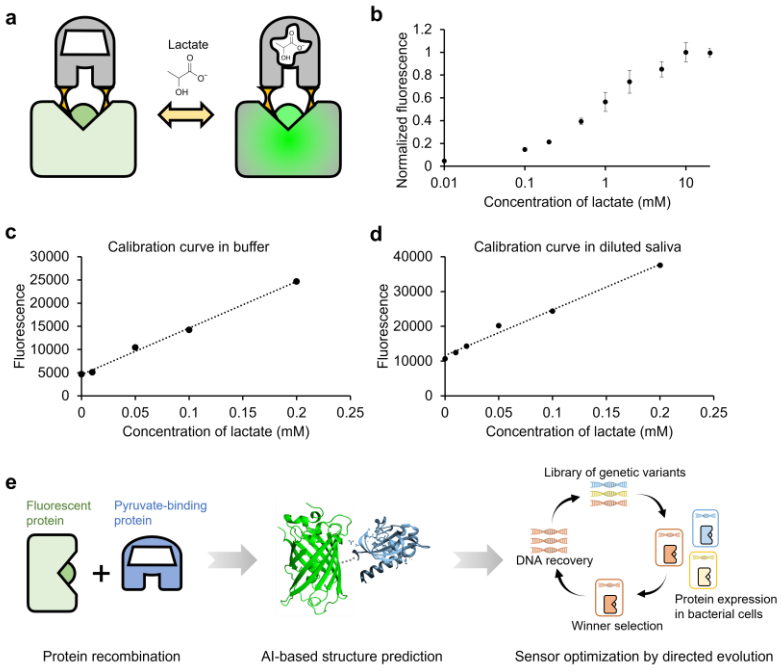

Fig. 1. Metabolite detection assays. (a) Schematic representation of fluorescent lactate sensor eLACCO2.1. (b) Titration curve of purified lactate sensor. (c) (d) Linear calibration curve in buffer and 4x diluted saliva samples. (e) Developing a high-performance fluorescent pyruvate sensor through protein engineering strategies.

comparing them with those obtained from gold standard methods such as enzymatic assays and mass spectrometry.

Pyruvate detection. Unlike the large responsiveness of eLACCO2.1, current fluorescent pyruvate sensors exhibit a signal increase of no more than 2.5-fold in response to pyruvate concentration change[17,18]. This limited signal change can compromise quantification accuracy, making it more susceptible to experimental variations. Therefore, we propose to develop a new pyruvate sensor with enhanced responsiveness (higher sensitivity) through protein engineering strategies, including protein recombination, structure prediction, and directed evolution (Fig. 1e). These strategies have proven effective in engineering high-performance FP-based sensors in our previous work to improve the responsiveness of a citrate sensor from 0.2-fold to 9-fold[19]. Building on our established process of iterative mutagenesis and screening[20], we will create libraries of genetic mutants of the pyruvate sensor, express them in bacterial cells, and measure the responsiveness (fluorescence with and without pyruvate) using a plate reader. The most promising mutant selected from each round of screening will be used for the next round of protein evolution. We aim to achieve an optimized pyruvate sensor with >10-fold responsiveness after 10 rounds of directed evolution.

The dissociation constant of the existing pyruvate sensors is between 0.07-0.48 mM, which is optimal for quantifying salivary pyruvate, as the physiological range of pyruvate in saliva is 0.05-0.5 mM according to the Human Metabolome Database. Although a slight change in the dissociation constant may occur during the protein engineering process, it is not likely to affect its effectiveness in quantification. The optimized pyruvate sensor will be purified, characterized in buffer solutions, and used to quantify pyruvate in saliva samples, following a protocol similar to the one described above for the lactate sensor eLACCO2.1. The sensing domains used in both eLACCO2.1 and the new pyruvate sensor are highly specific, responding exclusively to their target analyte and not to other metabolites with similar chemical structures.

Aim 2. Integration of the assays into lab-on-a-chip devices.

Once the off-chip quantification results for lactate and pyruvate are validated against gold standard methods, the assays will be integrated into lab-on-a-chip devices. We will explore two different integration strategies: with and without immobilization of the sensors.

Micropillar device with sensor immobilization. We will leverage micropillar arrays fabricated through hot embossing microfabrication on cyclic olefin polymers[21]. The micropillars will be surface functionalized via oxygen plasma treatment, followed by grafting with (3-aminopropyl)triethoxysilane (APTES) to enable covalent protein attachment using glutaraldehyde as a cross-linker (Fig. 2a). This method, successfully used for immobilizing antibodies for immunoassays[22], will now be adapted to attach purified FP-based sensors, eLACCO2.1 and the pyruvate sensor.

To confirm the successful immobilization of the sensors, fluorescence on the micropillar surfaces will be measured using a fluorescence microscope. The immobilization protocol will be optimized for maximum covalent bonding efficiency by varying parameters such as plasma treatment duration, concentrations of the cross-linker and sensor, and incubation time. The fluorescence signals of the immobilized sensors will be evaluated in the presence and absence of their target metabolites (lactate or pyruvate) to confirm their responsiveness (Fig. 2b). Previous studies have shown that eLACCO2.1 remains functional when immobilized on cell surfaces[15], suggesting the robustness of the sensor. To further mitigate risks, a flexible peptide will be fused to the N-terminal of the sensors to enhance their mobility post-immobilization, preventing potential distortion. Chambers containing sensor-functionalized micropillars will be filled with PBS or MOPS buffers to prevent denaturation and loss of function of the sensors. The devices will be sealed to minimize evaporation and stored at 4°C to maintain protein functionality for extended periods. Typically, purified sensors can be stored in a refrigerator for a couple of months, and the storage stability of the device and assay will be thoroughly evaluated. Because of the nature of reversible binding, sensors immobilized

on micropillars can be regenerated by washing off the metabolites (Fig. 2c), allowing for multiple uses and potentially enhancing sustainability.

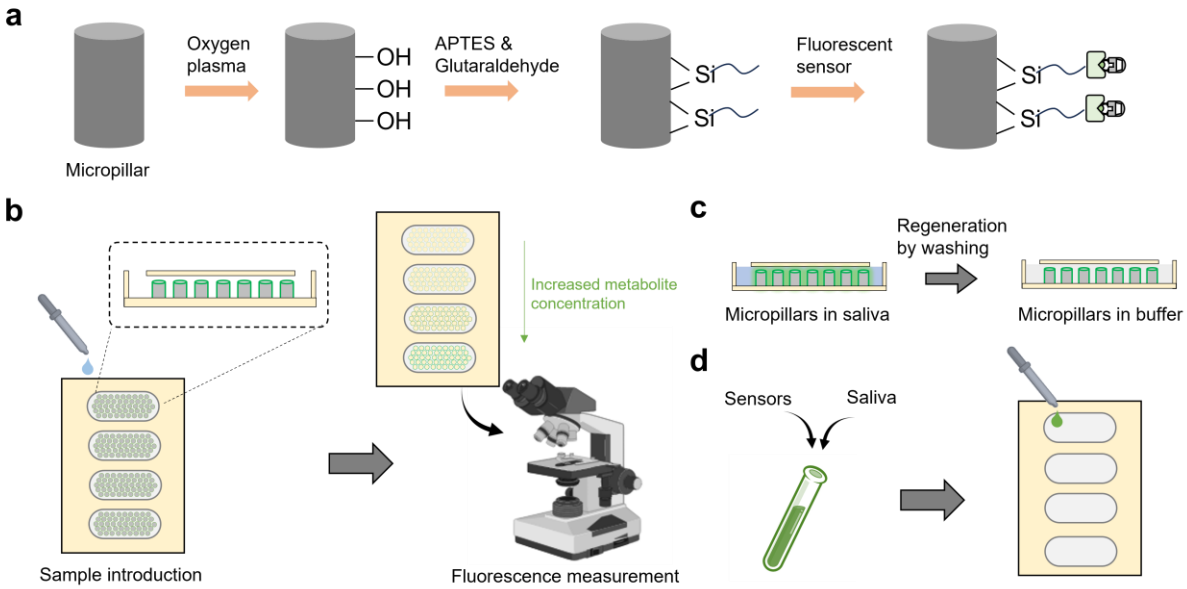

Fig. 2. (a) Immobilization of the sensors on a micropillar. (b) Schematic representation of sample loading and imaging of micropillar array devices. (c) Regeneration of micropillar arrays for multiple use. (d) Integration of the sensors on chip without immobilization.

Device without sensor immobilization. An alternative strategy for sensor integration is to use sensors without immobilization. In this approach, purified sensors in buffer will be mixed with saliva samples and transferred to a microchamber within a thermoplastic device for fluorescence detection under a microscope (Fig. 2d). Given that the sensors remain in a mobile format, we anticipate they will exhibit sensitivity comparable to that observed in our off-chip assays. While the sensors in this device cannot be regenerated for multiple uses due to their inseparability after mixing, this approach has a higher likelihood of success.

Aim 3. A sample-to-result analyzer for analyzing saliva samples.

To develop a sample-to-result analyzer, we will design a portable and cost-effective fluorescence detection system equipped with optics and a smart phone for capturing fluorescence images (Fig. 3a). An image analysis program, including functionalities such as segregation of micropillar arrays, background subtraction, and intensity measurement, will be created using software like ImageJ or MATLAB. A graphical user interface will be developed to enable end users to easily analyze the image data.

Similar to the off-chip assays, the standard addition method will be used to spike the sample, generating a calibration curve to quantify lactate or pyruvate (Fig. 3b). The lab-on-a-chip device will have multiple detection

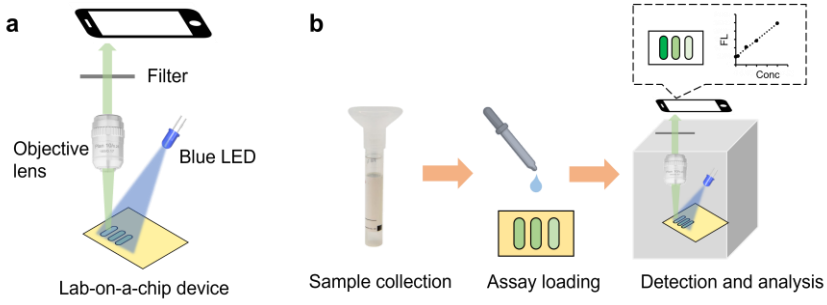

Fig. 3. Sample-to-result analyzer. (a) Optical setup of the fluorescence detection system. (b) Workflow of metabolite analysis using the analyzer.

chambers for measuring samples spiked with standard solutions. Replicated experiments will be conducted either on a single device or multiple devices, depending on whether micropillar arrays are used.

The validation of the developed analyzer will be conducted by analyzing saliva samples from a small group of healthy individuals (e.g., a sample size of 20). First, saliva samples will be spiked with lactate and pyruvate to create artificial high-concentration samples. These spiked samples, along with non-spiked saliva, will be quantified using our analyzer to assess its accuracy. Second, since lactate levels are known to elevate substantially after exercise[8], saliva samples will be collected from the group both before and after exercise for analysis. Parallel analyses using enzymatic assays or mass spectrometry will be performed to compare and validate the results obtained from our analyzer.

4. Outcomes

We anticipate that the proposed research will yield a high-performance fluorescent sensor for pyruvate and reliable one-pot off-chip quantification assays for lactate and pyruvate. These assays will be capable of analyzing metabolite biomarkers in saliva and potentially other biofluids in a wet chemistry lab setting. Based on the developed assays, we expect to establish an innovative portable and user-friendly analyzer. This analyzer will include a lab-on-a-chip device, a fluorescence detector for signal readout, and automated analysis software, enabling sample-to-answer analysis of metabolites and deployment in various settings, including hospitals and pharmacies, beyond traditional clinical and chemistry labs.

5. Impact

The successful demonstration of the lactate and pyruvate analyzer represents a significant milestone toward developing a deployable rapid metabolite testing device for health monitoring and clinical applications. We will continue to explore the potential of the devices through collaboration with the University Health Network, Canada's largest hospital network. This includes tracking salivary lactate to predict and monitor sepsis in patients and measuring salivary pyruvate to prognosticate oral cancer. This advancement will empower the healthcare system and physicians with new tools for early diagnosis and treatment.

Furthermore, the strategies used to develop metabolite detection sensors, assays and devices will be generalized to enable the detection of a diverse array of metabolite biomarkers in various biofluids, not just saliva samples. Similar to the widespread use of COVID test strips and glucometers, these portable tools will be easily distributable and globally accessible, facilitating metabolite monitoring on a national or even global scale.

6. References

1. Yang M, Soga T, Pollard PJ. Oncometabolites: Linking altered metabolism with cancer. *Journal of Clinical Investigation*. 2013;123(9). doi:10.1172/JCI67228
2. Sangar V, Eddy JA, Simeonidis E, Price ND. Mechanistic modeling of aberrant energy metabolism in human disease. *Front Physiol*. 2012;3 OCT. doi:10.3389/fphys.2012.00404
3. Inoshita M, Umehara H, Watanabe SY, et al. Elevated peripheral blood glutamate levels in major depressive disorder. *Neuropsychiatr Dis Treat*. 2018;14. doi:10.2147/NDT.S159855
4. Iacobazzi V, Infantino V. Citrate-new functions for an old metabolite. *Biol Chem*. 2014;395(4). doi:10.1515/hsz-2013-0271
5. Bar-Even A, Flamholz A, Noor E, Milo R. Rethinking glycolysis: On the biochemical logic of metabolic pathways. *Nat Chem Biol*. 2012;8(6). doi:10.1038/nchembio.971
6. Granchi C, Bertini S, Macchia M, Minutolo F. Inhibitors of Lactate Dehydrogenase Isoforms and their Therapeutic Potentials. *Curr Med Chem*. 2010;17(7). doi:10.2174/092986710790416263

7. Li X, Yang Y, Zhang B, et al. Lactate metabolism in human health and disease. *Signal Transduct Target Ther*. 2022;7(1). doi:10.1038/s41392-022-01151-3
8. Yan P, Qin C, Yan Z, Chen C, Zhang F. Can salivary lactate be used as an anaerobic biomarker? *PeerJ*. 2023;11. doi:10.7717/peerj.15274
9. Levy B, Sadoune LO, Gelot AM, Bollaert PE, Nabet P, Larcan A. Evolution of lactate/pyruvate and arterial ketone body ratios in the early course of catecholamine-treated septic shock. *Crit Care Med*. 2000;28(1). doi:10.1097/00003246-200001000-00019
10. Bhat M, Prasad KVV, Trivedi D, Rajeev B, Battur H. Pyruvic acid levels in serum and saliva: A new course for oral cancer screening? *Journal of Oral and Maxillofacial Pathology*. 2016;20(1). doi:10.4103/0973-029X.180955
11. Letertre MPM, Dervilly G, Giraudeau P. Combined Nuclear Magnetic Resonance Spectroscopy and Mass Spectrometry Approaches for Metabolomics. *Anal Chem*. 2021;93(1). doi:10.1021/acs.analchem.0c04371
12. Balss J, Pusch S, Beck AC, et al. Enzymatic assay for quantitative analysis of (d)-2-hydroxyglutarate. *Acta Neuropathol*. 2012;124(6). doi:10.1007/s00401-012-1060-y
13. Nasu Y, Shen Y, Kramer L, Campbell RE. Structure- and mechanism-guided design of single fluorescent protein-based biosensors. *Nat Chem Biol*. 2021;17(5). doi:10.1038/s41589-020-00718-x
14. Pattanayak P, Singh SK, Gulati M, et al. Microfluidic chips: recent advances, critical strategies in design, applications and future perspectives. *Microfluid Nanofluidics*. 2021;25(12). doi:10.1007/s10404-021-02502-2
15. Nasu Y, Aggarwal A, Le GNT, et al. Lactate biosensors for spectrally and spatially multiplexed fluorescence imaging. *Nat Commun*. 2023;14(1). doi:10.1038/s41467-023-42230-5
16. Tékus É, Kaj M, Szabó E, et al. Comparison of blood and saliva lactate level after maximum intensity exercise. *Acta Biol Hung*. 2012;63(SUPPL. 1). doi:10.1556/ABiol.63.2012.Suppl.1.9
17. Arce-Molina R, Cortés-Molina F, Sandoval PY, et al. A highly responsive pyruvate sensor reveals pathway-regulatory role of the mitochondrial pyruvate carrier MPC. *Elife*. 2020;9. doi:10.7554/eLife.53917
18. Harada K, Chihara T, Hayasaka Y, et al. Green fluorescent protein-based lactate and pyruvate indicators suitable for biochemical assays and live cell imaging. *Sci Rep*. 2020;10(1). doi:10.1038/s41598-020-76440-4
19. Zhao Y, Shen Y, Wen Y, Campbell RE. High-Performance Intensiometric Direct- And Inverse-Response Genetically Encoded Biosensors for Citrate. *ACS Cent Sci*. 2020;6(8). doi:10.1021/acscentsci.0c00518
20. Zhao Y, Lee S, Campbell RE, Lin MZ. Directed Evolution of a Genetically Encoded Bioluminescent Ca2+ Sensor. In: ; 2023. doi:10.3390/iecb2023-14563
21. Geissler M, Malic L, Morton KJ, et al. Polymer Micropillar Arrays for Colorimetric DNA Detection. *Anal Chem*. 2020;92(11). doi:10.1021/acs.analchem.0c00830
22. Geissler M, Ponton A, Nassif C, et al. Use of Polymer Micropillar Arrays as Templates for Solid-Phase Immunoassays. *ACS Appl Polym Mater*. 2022;4(8). doi:10.1021/acsapm.2c00163

Name: Laser-Microwave Dual-Modality Remote Sensing Powered by Laser Dynamics

Yuxi Ruan, University of Wollongong, Australia

Category: Information

Challenge: Multi-modality sensing represents a promising technological advancement, integrating information from diverse sensing modalities to greatly enhance environmental understanding and perception. Realizing the full potential of multi-modality sensing introduces new challenges in the design of multi-sensor systems and signal processing.

This project focuses on laser-microwave dual modality remote sensing, which find wide applications in environment monitoring, disaster sensing, and more. Current laser-microwave dual-modality sensing systems comprise two separate sub-systems: a laser sensing module and a microwave sensing module, which work independently from both signal generation and processing, thus present two notable problems:

- Independent optical and microwave sub-systems leads to bulky, heavy and costly sensing systems with high energy consumption. It also results in the requirement of cumbersome calibration, alignment and data synchronization.
- There is a lack of principled signal processing framework for fusion of sensing modalities. The fusion currently is performed in ad-hoc ways at data level to extract sensing information. The synergy between the modalities is not fully exploited due to the lack of "interaction" between the two modalities.

3. The category selected: This project will redefine laser-microwave dual-modality sensing by developing a unified system powered by a laser-dynamics, resulting in the next generation of laser-microwave sensing techniques with significantly enhanced sensing capability. The project falls into the area of 'Information' and aligns with "Exploring new optical sensing technologies to improve various parameter monitoring capabilities" (item 10)

4. Capability, Intended Outcomes and Impact

Capability: I, together with my colleagues, have been working in the field of the proposed project extensively. We have pioneered the sensing technologies by laser with optical feedback (Laser-OF) for achieving high sensitivity, large range and compact system (refer to my publications in my CV). My recent work (Y. Ruan, et al, "Achieving high sensing resolution using a Microwave Photonic Signal generated by a laser diode with a control cavity," Optics and Lasers in Engineering, vol. 158, 2022) has shown that microwave modulated optical signal can be generated by operating a laser at period-one dynamic state. These open a door for realizing next generation dual-modal sensing. The proposed project will be conducted in 'Sensing, Communications and Control Laboratory' at the University of Wollongong, where I have been working since my PhD study. The research lab will provide both optical and electrical devices, and elements for the relevant experimental investigation.

Intended outcomes:

- Generate a tunable dual-frequency laser by laser dynamics induced by external feedback, and an innovative design to generate photonic microwave signals for achieving radar function with tunable step frequency and wide bandwidth
- Implement ***a unified system*** for laser-microwave dual-modality sensing, enabling future on-chip implementation with small size, light weight and high power efficiency.
- Achieving synergy in laser-microwave sensing by developing an optimal framework for fusing modalities ***at the signal level***.

Impact: This project expects to generate new knowledge in dual-modality sensing system realization, resulting in cutting-edge techniques to unlock the full capabilities of laser-microwave sensing. The application of these advanced sensing technologies in environmental monitoring can help mitigate the economic impact of natural disasters by enabling faster response times and more effective resource allocation. Socially, the enhanced ability to monitor and respond to environmental hazards can bolster community resilience and safety.

Project Title: Laser-Microwave Dual-Modality Remote Sensing Powered by Laser Dynamics

1. Literature Review

Multi-modality sensing represents a promising technological advancement, integrating information from diverse sensing modalities to greatly enhance environmental understanding and perception [1]. This project focuses on laser-microwave dual modality remote sensing, where the microwave signal is generated by optical configuration. This research is in the area of microwave photonics (MWP). MWP has emerged as one of the most active and exciting research areas, bringing together the worlds of optoelectronics and microwave engineering, opening a door for numerous promising applications in advanced sensing, internet of things, 5G, etc [2, 3]. Sensing and measurement technologies will be revolutionized in both theory and applications due to the introduction of MWP to the area.

Regarding laser-microwave dual-modality sensing system, a typical example, as illustrated in Fig. 1, exemplified by integrated Lidar-Radar setups. Lidar and Radar have been demonstrated to be most effective tools for detecting natural disasters and realizing auto-vehicles. However, both technologies grapple with issues related to their expensive deployment. Each comes with its own limitations. Lidar faces attenuation issues in moist convection while Radar doesn't match Lidar's resolution. Therefore, the fusion of Lidar and Radar emerges as a promising solution. Most current fusion system comprise two separate sub-systems: a laser sensing module and a microwave sensing module, which work independently , i.e., the two sensing signals are generated respectively by laser system and radar system [4, 5] . *The reliance on two independent optical and microwave sub-systems brings to bulky, heavy and costly sensing systems with high energy consumption*, constraining its applicability in platforms such as drones and satellites. It also results in the requirement of cumbersome calibration, alignment and data synchronization, which are critical for fusion.

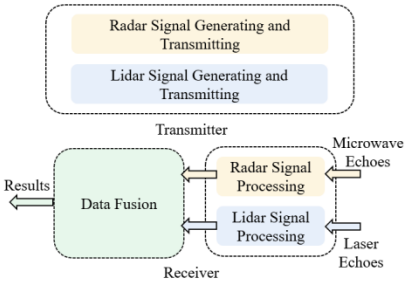

Fig. 1: Conventional integrated lidar and radar.

The echo signals are processed separately, before the fusion is performed in ad-hoc ways at data level to extract sensing information [6, 7]. Such signal processing *is often non-optimal, and the synergy between the two sensing modalities is not fully exploited due to the lack of "interaction" between the two modalities*. So, the sensing capability and performance fall short of the full potential of dual modality sensing.

This project aims to redefine laser-microwave dual modality sensing by unifying laser and microwave sensing modalities in both system implementation and signal processing. I, together with my colleagues, have been working in the field of the proposed project extensively. We have explored the sensing technologies by laser with optical feedback (Laser-OF) for achieving high sensitivity, large range and compact system. Laser-OF has been recognized as a promising non-contact sensing technology due to its merits of minimum part-count scheme, low cost in implementation and ease in optical alignment. Numerous efforts have been devoted to exploring theories and applications of such sensing technology, and a multitude of applications have been reported, including the measurement of displacement, velocity, distance, acoustics, etc [8]. The systems are conventionally based on semiconductor lasers (SL). Recent years, the lasers employed have been extended to THz lasers, leading to a variety of promising THz applications to imaging, materials analysis, etc [9]. In existing laser-OF sensing techniques, the laser operates at its steady state.

What if a laser is pushed to operate beyond the steady state? This question was first explored by me together with my research partners. We experimentally discovered that the capability of laser-OF sensing can be greatly enhanced when making a laser work at higher dynamic states, e.g., period-one (P1) [10-13]. We observed that, in this case, the laser intensity is modulated by a waveform in microwave frequencies. Furthermore, we also discovered that, by making a laser operate at quasi-period

(QP), a photonic microwave signal with step frequency characteristics can be generated, and the microwave signal can be flexibly controlled. These discoveries open a new door for realizing Dual-Modality laser-microwave sensing and make it possible to generate and control both laser and photonic microwave signals with wide dynamic range. Further more, using a common core Laser-OF configuration for generating the two sensing signals and removing the need of external electrical-optical modulator and RF synthesisers, enables the system potential to be implemented on a single chip.

2. Problem Statement/Objectives

2.1 Problems

Realizing the full potential of multi-modality sensing introduces new challenges in the design of multi-sensor systems and signal processing. Current laser-microwave dual-modality sensing systems comprise two separate sub-systems: a laser sensing module and a microwave sensing module, which work independently from both sensing signal generation and echo signal processing, thus present two notable problems:

- *The reliance on two independent optical and microwave sub-systems* contributes to bulky, heavy and costly sensing systems with high energy consumption, constraining its applicability in platforms such as drones and satellites. It also results in the requirement of cumbersome calibration, alignment and data synchronization, which are critical for fusion.
- The receiver uses a two-stage process: after separate lidar and radar signal processing, the *fusion of sensing modalities is performed heuristically at the data level*. There is a lack of principled signal processing framework for fusion. The two-stage process is often non-optimal, and the synergy between the modalities is not fully exploited due to the *lack of "interaction" between the two modalities*. So, the sensing capability and performance fall short of the full potential of dual modality sensing.

2.2 Objectives

Aiming to solve above two problems, a unified design structure for laser-microwave sensing system is proposed in this project, as depicted in Fig. 2. We will redefine the system from both dual-modality sensing signal generation and their echoes processing. Its specific objectives include:

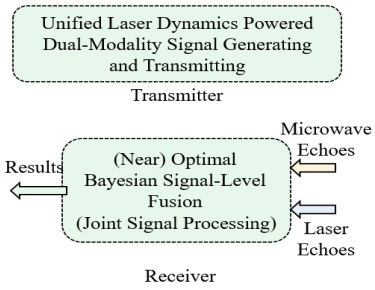

Fig. 2 : Unified laser-microwave sensing system.

- Developing a unified sensing system capable of concurrently generating and controlling laser and microwave sensing signals, enabling potential on-chip implementation distinguished by compact size, lightweight, and exceptional power efficiency.
- At the signal level, developing a optimal theoretical framework for fusing modalities, achieving synergy in laser-microwave sensing. Practical signal processing methods will be designed to unlock the full capabilities of multi-modality sensing.
- Investigating its sensing applications

3. Outline of tasks/Work Plan

The research tasks are defined as below to answer above questions. The applicant Ruan will lead the project team consisting of a Research Assistance (RA), A/Prof Yanguang YU and A/Prof Qinghua Guo, the team members are all from the research lab arranged for this project in the University of Wollongong (UoW), Australia.

We propose a unified dual-modality signal generating and transmission based on laser dynamics. The schematic system architecture is shown as Fig 3., composed of four primary blocks: laser dynamics shaped tunable dual-frequency (DF) generator, frequency-modulated laser sensing function, photonic microwave sensing function and optical domain information processing.

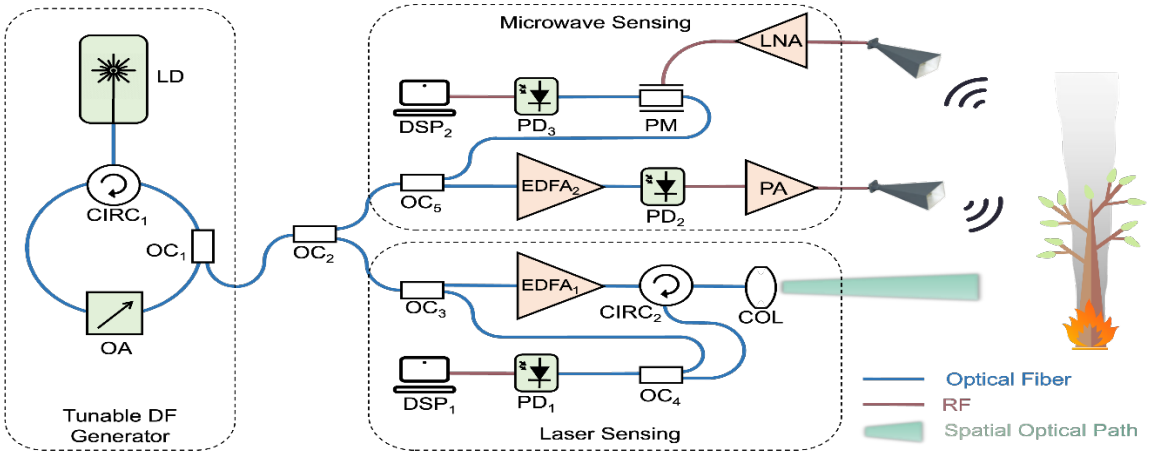

Fig. 3 Schematic of the Unified laser Dynamics Powered Dual-Modality Signal Generating and Transmission LD: Laser Diode; CIRC: Circulator; OA: Optical Attenuator; OC: Optical Coupler; DSP: Digital Signal Processor; PD: Photodetector; PM: Phase Modulator; EDFA: Erbium-doped Fiber Amplifier; PA: Power Amplifier; LNA: Low-noise Amplifier; COL: Fibre Collimator; RF: Radio Frequency

The DF generator is the core for generating dual-modality sensing signals. A laser diode (LD) with external feedback (e.g. optical feedback-OE) is employed for the generator. An LD with OF exhibits rich dynamics and has been found various applications. Our preliminary works show that an LD operating at specific dynamic regions can produce a DF spectrum and have a stepped-frequency (SF) characteristic. This will enable us to achieve:

- Generating a DF spectrum with opposing instantaneous frequency shifts, enhancing laser sensing e.g Lidar's detection capabilities.
- Producing an SF signal spanning a broad microwave range, catering to the remote sensing e.g. Radar function.

Above idea will enable use of the same optical configuration to achieve both laser and photonic microwave sensing functionalities with compact structure, allowing simultaneously exploitation of their complementary characteristics for remote sensing to greatly enhance sensing performance.

3.1 Task 1: DF based FMCW laser sensing (Ruan, Yu and RA)

This is to develop a design method (both hardware and software) for DF based FMCW Lidar. The feature of the opposing frequency shift in DF can reduce detection error caused by laser nonlinearity, atmospheric turbulence, and speckle noise.

We firstly study block 1 on tunable DF generator. Here, a 905nm wavelength laser diode (LD) is leveraged, given its frequent use in commercial Lidar systems. External optical injection allows this LD to function across varied dynamic statuses. Through our preliminary efforts, we've discerned that specific dynamic regions enable a dual-frequency (DF) spectrum from a singular mode LD. We've also identified a stepped-frequency (SF) characteristic in certain dynamic areas. Our comprehensive study aims to:

- Generate dual frequencies with opposing instantaneous frequency shifts, enhancing laser sensing (e.g. Lidar's detection) capabilities through a tunable DF.

The frequency tuning in the DF generator are managed by LD system parameters (e.g. injection optical strength and injection current), this tunning approach makes the system compactness feasible without external electrical-optical modulators to be involved.

As an example of laser sensing, we'll assess the lidar function offered by the system, the detection performance will be evaluated both theoretically and practically. As illustrated in right bottom block (named Laser sensing) of Fig 3, the DF based FMCW light generated is split into two beams by OC_3.

One beam serves as a reference, while the other beam, after EDFA1, CIRC2 and the telescope, transmit to a target. The combined light from the reference and returning beams is processed by DSP1, revealing target distance, velocity and other target relevant parameters.

3.2 Task 2: Photonic microwave sensing functionality and Optical domain processing (Ruan, Yu and RA)

A joint-control method for the system parameters (injection optical strength, cavity length and injection current) will be developed to linearly shift the DF in an opposing manner. This will allow the LD with OF to produce a modulated photonic microwave (PMW) signal, suitable for microwave sensing functions across a broad tuning range. In particular, SF characteristics will be developed to enhance the microwave bandwidth to achieve high performance radar function.

The right upper block (named Microwave Sensing) in Fig. 3 elaborates on the radar function offered by the proposed system. The adjusted DF optical signal reaches OC_5, after $EDFA_2$, PD_2 and power amplification (PA), an microwave signal with frequency modulated and step frequency feature is broadcasted.

The inbound microwave signal modulates the reference light's optical phase after the LNA. This optical domain processing (ODP) design can enhance the speed of information processing and reduces the DSP burden.

The following theory and experiment studies will be conducted:

- Investigate the rules for selecting system parameters when operating the laser with OF at period windows to generate a step frequency signal with a minimal noise floor.
- Develop an approach for the step control to implement a Step Frequency Photonic Radar (SFPR), this will need to develop a joint modulation method for the LD related parameters.
- Investigate the performance of the SFPR system in various scenarios to evaluate its effectiveness in range resolution and unambiguous range.
- Simulation and experiments on imaging application by the proposed SFPR design.
- Regarding the ODP unit, an optical phase modulator module for signal mixing will be developed, and a real-time optical Fourier-transform block for spectral analysis will be implemented. This ODP processing unit not only facilitates rapid information processing but also alleviates the load and reduce cost on DSP.

3.3. Task 3 Develop a Machine-learning based design algorithm for DF generator (Ruan assisted by a PhD student)

A LD with OF operating in a period windows dynamic state contributes a new implementation architecture for photonic microwave systems. However, designing such a laser system to generate frequency-modulated microwave sensing signals through traditional Lang-Kobayashi (L-K) equations requires extensive computational effort to derive the system control parameters (SCP), making real-time adjustment of the SCP impossible in cases where it is needed. In task 3, we aim to develop an effective design approach based on machine learning. A feedforward neural network (FNN), in conjunction with a gradient descent algorithm, is employed to fast and accurately ascertain the SCP, offering a solution readily applicable in the system design. Both simulation and experiment will be conducted to validate the proposed approach.

3.4 Task 4: Probabilistic Framework for Optimal Fusion at Signal-Level (Ruan and Guo)

We propose to perform the fusion at signal level with a probabilistic framework. As shown in Fig. 4 (also the notations), we formulate the fusion as finding the a posteriori probability (marginal) of the sensing parameters $p(\theta \mid \tau_L, \tau_M)$, thereby the estimate of the parameters can be obtained. This provides not only the optimal estimates (fusion) but also estimation uncertainty. Although this is the best performance we can achieve, the direct implementation requires high dimensional integration of

$p(\theta,\theta_L,\theta_M|\tau_L,\tau_M)$, which is challenging. Fortunately, the probabilistic framework opens a door for the use of powerful yet low complexity inference techniques including Guo's (my current research partner) unitary approximate message passing (UAMP) [14] and hybrid message passing on factor graph [15], so that near-optimal performance can be achieved with low cost. The other attractiveness of the probabilistic framework is its flexibility, allowing a unified algorithmic implementation regardless signal representations of laser and microwave modalities and parameter constraints that depend on concrete applications.

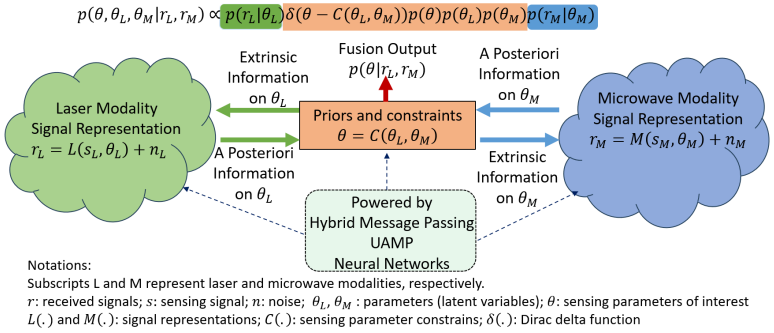

Fig. 4: Modality synergy with turbo interaction (iteration).

4. Outcome(s)

1) A novel technique is proposed to generate a tunable dual-frequency (DF) laser by using a semiconductor laser (SL) with external optical feedback. This will enable a DF based FMCW Lidar source to be implemented for simultaneously range and velocity with high resolution and robustness to atmospheric turbulence.

2) An innovative design is proposed for achieving photonic Radar. By jointly adjusting the SL associated parameters to tune the DF shifted in opposite direction, which enables the SL to produce a modulated laser intensity with tunable modulation frequency. This DF feature empowers the laser to generate a photonic microwave signal used for Radar functionalities over a wide tuning spectrum. Additionally, the SL with a stepped-frequency (SF) characteristic will further enhance the Radar signal bandwidth.

3) An optimal framework is developed for fusing modalities at the signal level. Practical signal processing implementation will be designed to unlock the full capabilities of multi-modality sensing.

4) An innovative scheme is designed to create a laser-microwave dual-modality sensing system, where a laser serves as both DF chirped laser source and microwave source. The two signal sources are generated by the SL dynamics without the need of external electrical-optical modulator and RF synthesizers. They share the same core hardware configuration, which allows a compact system solution and thus greatly reduces system complexity and cost. Machine learning based design for determining the system parameter are developed.

5. Impact

This project expects to generate new knowledge in Dual-Modality sensing system realization, resulting in cutting-edge laser-microwave sensing techniques to unlock the full capabilities of laser-microwave dual modal sensing. The application of these advanced sensing techniques in environmental monitoring, such as wildfire sensing, can help mitigate the economic impact of natural disasters by enabling faster response times and more effective resource allocation. Environmentally, improved sensing capabilities can contribute to better management of diverse ecosystems, aiding in the conservation of biodiversity and the protection of natural resources. Socially, the enhanced ability to monitor and respond to environmental hazards can bolster community resilience and safety, particularly in rural and remote areas prone to bushfires and other environmental risks.

6. REFERENCES

1. Yang, R., Zhang, W., Tiwari, N., Yan, H., Li, T., & Cheng, H. (2022). Multimodal sensors with decoupled sensing mechanisms. Advanced Science, 9(26), 2202470.
2. J. Capmany and D. Novak, "Microwave photonics combines two worlds," *Nature photonics,* vol. 1, no. 6, p. 319, 2007.
3. D. Marpaung, J. Yao, and J. Capmany, "Integrated microwave photonics," Nature Photonics, vol. 13, no. 2, pp. 80-90, 2019/02/01 2019, doi: 10.1038/s41566-018-0310-5.
4. Y. Jin et al., "Radar and Lidar Deep Fusion: Providing Doppler Contexts to Time-of-Flight Lidar," in IEEE Sensors Journal, vol. 23, no. 20, pp. 25587-25600, 15 Oct.15, 2023, doi: 10.1109/JSEN.2023.3313093.
5. L. Wang et al., "Multi-Modal and Multi-Scale Fusion 3D Object Detection of 4D Radar and LiDAR for Autonomous Driving," in IEEE Transactions on Vehicular Technology, vol. 72, no. 5, pp. 5628-5641, May 2023, doi: 10.1109/TVT.2022.3230265.
6. Y. Li, J. Deng, Y. Zhang, J. Ji, H. Li and Y. Zhang, " EZFusion : A Close Look at the Integration of LiDAR, Millimeter-Wave Radar, and Camera for Accurate 3D Object Detection and Tracking," in IEEE Robotics and Automation Letters, vol. 7, no. 4, pp. 11182-11189, Oct. 2022, doi: 10.1109/LRA.2022.3193465.
7. R. Ravindran, M. J. Santora and M. M. Jamali, "Camera, LiDAR, and Radar Sensor Fusion Based on Bayesian Neural Network (CLR-BNN)," in IEEE Sensors Journal, vol. 22, no. 7, pp. 6964-6974, 1 April1, 2022, doi: 10.1109/JSEN.2022.3154980.
8. T. Taimre, M. Nikolić, K. Bertling, Y. L. Lim, T. Bosch, and A. D. Rakić, "Laser feedback interferometry: a tutorial on the self-mixing effect for coherent sensing," Adv. Opt. Photon., vol. 7, no. 3, pp. 570-631, 2015/09/30 2015.
9. P. Dean, A. Valavanis, J. Keeley, K. Bertling et al., "Terahertz imaging using quantum cascade lasers—a review of systems and applications," Journal of Physics D: Applied Physics, vol. 47, no. 37, p. 374008, 2014/08/28 2014.
10. **Y. Ruan**, B. Liu, Y. Yu, J. Xi, Q. Guo, and J. Tong, "High sensitive sensing by a laser diode with dual optical feedback operating at period-one oscillation," Applied Physics Letters, vol. 115, no. 1, p. 011102, 2019.
11. B. Nie, **Y. Ruan**, Y. Yu, Q. Guo, J. Xi, and J. Tong, "Period-One Microwave Photonic Sensing by a Laser Diode With Optical Feedback," Journal of Lightwave Technology, vol. 38, no. 19, pp. 5423-5429, 2020.
12. B. Liu, **Y. Ruan**, Y. Yu, Q. Guo, J. Xi, and J. Tong, "Modeling for optical feedback laser diode operating in period-one oscillation and its application," Optics Express, vol. 27, no. 4, pp. 4090-4104, 2019/02/18 2019.
13. **Y. Ruan**, Y. Yu, B. Liu, Q. Guo, J. Xi, and J. Tong, "Achieving high sensing resolution using a Microwave Photonic Signal generated by a laser diode with a control cavity," Optics and Lasers in Engineering, vol. 158, p. 107171, 2022.
14. M. Luo, Q. Guo, M. Jin, Y. C. Eldar, et. al., "Unitary Approximate Message Passing for Sparse Bayesian Learning," in IEEE Transactions on Signal Processing, vol. 69, 2021.
15. H. Kang, J. Li, Q. Guo, M. Martorella, E. Giusti and J. Cai, "Robust Interferometric ISAR Imaging With UAMP-Based Joint Sparse Signal Recovery," in IEEE Transactions on Aerospace and Electronic Systems, vol. 59, no. 4, Aug. 2023.

Executive Summary

Proposal Title: Coupling Mechanics, Physiology, and Spectroscopy in Skin: Advancements in Non-Invasive Diagnostics

1. **Global Challenge Addressed:** The proposal seeks to tackle significant challenges in non-invasive medical diagnostics and emotional state assessments through advanced optics and photonics. Despite the existing advancements in healthcare technologies, there is a critical need for improved non-invasive methods that can offer quicker, more accurate health diagnostics and emotional assessments without the discomfort or risks associated with invasive techniques.
2. **Relationship Between Challenge and Project:** This project directly addresses these challenges by developing a comprehensive understanding of the skin's biomechanical, physiological, and spectroscopic responses to various conditions. The focus is on integrating these responses using cutting-edge hyperspectral imaging (HSI) and advanced computational models to monitor and analyze skin health and emotional states more accurately than currently possible.
3. **Selected Categories:** The proposal fits within the categories of Biomedical Optics and Biophotonics, given its emphasis on utilizing photonics technologies to probe biological tissues non-invasively. It also intersects with Computational Optics by employing complex algorithms and models to interpret the vast amount of data obtained from hyperspectral imaging.
4. **Capability and Application:** The project leverages hyperspectral imaging combined with mechanical testing of the skin to capture detailed spectral data that reflects underlying physiological changes, such as blood flow or emotional flushing. By applying comprehensive mechanical-physiological-spectroscopic models, the project can predict and analyze skin's behavior under various states, enhancing diagnostic processes and emotional analysis. This method promises to significantly improve the detection and monitoring of skin-related health issues, such as skin cancer or systemic diseases manifesting with skin symptoms, and to refine the understanding of emotional responses in a medical or psychological context.

Title: Investigation of the Mechanical-Physiological-Spectroscopic Coupling Mechanisms in In Vivo Skin and Its Applications in Emotion Expression

Applicant: Zongze Huo
Institution: School of Mechanical Engineering, Tianjin University

Application Date: May 20, 2024

Literature Review:

1.1 Scientific Significance of Skin Research

Skin, the largest organ of the human body, acts as the first line of defense and a vital indicator of health and emotional states. Its complex structure serves multiple biological functions including protection, regulation, and sensation. Advances in biomechanics, physiology, and spectroscopy have deepened our understanding of skin's intricate properties and its interactions with light, which include reflection, transmission, and absorption. These interactions are pivotal for assessing health metrics such as blood oxygen saturation and blood flow. Current technologies, however, often analyze mechanical and optical behaviors separately, without a holistic understanding of their interrelated effects.

The reflectance spectrum of skin provides extensive information about the body's condition. Emotional changes, for example, visibly alter the skin's spectral response—illustrated by expressions like "flushed with laughter" or "paled with fright." This spectral variability serves as a critical dimension in emotional state assessments. The skin's layered structure—comprising the epidermis, dermis, and subcutaneous tissue—contributes distinctively to its optical characteristics. Interactions between light and skin components like cells, blood vessels, and pigments cause various phenomena such as reflection, scattering, and absorption.

Research has proposed models to decode these interactions for better expression recognition and health monitoring. Gotardo et al. introduced a static appearance model considering hemoglobin levels and wrinkle depth, enhancing our grasp of facial expressions. Benitez-Quiroz et al. have utilized machine learning to correlate skin tone and blood flow with facial expressions, evidencing how emotions can modify spectral signatures. Furthermore, technologies like infrared imaging and photoacoustic tomography have enabled deeper insights into skin’s physiological changes under emotional stimuli.

However, the integration of mechanical, physiological, and spectroscopic data remains underexplored, especially in how these factors collectively influence skin's optical response. Such an understanding is crucial for advancing non-invasive diagnostic methods and for developing more sophisticated models that reflect the skin’s dynamic nature.

1.2 Research Landscape and Future Directions

Internationally, significant strides have been made in quantifying the biomechanical properties of skin, such as elasticity and viscoelasticity. Yet, the research integrating these mechanical properties with physiological responses, particularly through spectroscopic methods, is still nascent. The adoption of hyperspectral imaging technology in conjunction with machine learning is beginning to bridge the gap between skin condition diagnostics and expression analysis. This multidisciplinary approach is less prevalent in domestic research, which often focuses more narrowly on skin disease diagnostics without incorporating comprehensive spectroscopic and mechanical analyses.

The combination of hyperspectral imaging with biomechanical models opens new avenues for understanding the skin’s behavior under various conditions. Hyperspectral imaging (HSI) has particularly revolutionized our ability to detect and analyze subtle changes in skin, providing a powerful

tool for medical diagnostics and health screenings, like detecting skin cancer or monitoring skin lesions. As we continue to explore these interactions, the full potential for skin's spectral data in health monitoring and emotional analysis remains largely untapped. Moving forward, research will benefit from a more integrated approach that combines these diverse fields to enhance our understanding of skin's complex responses and to develop better diagnostic and therapeutic tools.

Objective:

This research aims to elucidate the intricate coupling mechanisms of mechanical strain, physiological changes, and spectroscopic responses in human skin. The objective is to develop an integrated mechanical-physiological-spectroscopic model to predict and analyze the skin's behavior under various emotional and physiological states, thus enhancing the diagnostic capabilities and understanding of skin health.

Research Content:

2.1 Research Methods

Hyperspectral Imaging Analysis: Utilize Hyperspectral Imaging (HSI) technology to acquire spectral data of the skin under various physiological and deformation states. This technology provides rich spectral information, aiding in the precise observation and analysis of skin changes.

In Vivo Skin Mechanical Testing: Conduct in vivo mechanical tests on the skin by applying controlled mechanical strain and controlling wrist grip strength to induce skin deformation, simulating different skin states such as stretching or compression, and capturing the spectral response of the skin under mechanical deformation.

Theoretical Model Development and Parameter Inversion: Develop a mechanical-physiological-spectroscopic theoretical model to simulate and predict the spectral response of the skin under specific mechanical stresses and blood conditions. The model will integrate Kubelka-Munk theory with hyperelastic models to establish connections between skin reflectance spectra and parameters like strain and physiological conditions.

The model will link physical parameters such as skin layer thickness, melanin content, blood content, and oxygen saturation. By adjusting parameters, the model can be applied to different physiological conditions of the skin. Based on the developed mechanical-physiological-spectroscopic coupling response model, perform inverse analysis of skin parameters.

Emotion Induction Experiments: Conduct emotion induction experiments based on psychological theories to capture the facial skin deformation and reflectance spectrum under different emotional states. Analyze the impact of emotional states on physical parameters such as skin layer thickness, melanin content, blood content, and oxygen saturation using the reflectance spectrum and previously developed theoretical models.

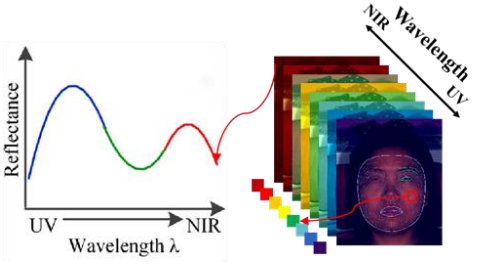

Figure 1: Schematic of the 3D Spectral Data Field Model

2.2 Technical Roadmap

By establishing a multi-field coupling model and combining hyperspectral-mechanical experimental measurements, characterize multiple mechanical, physiological, and spectroscopic parameters of in vivo skin. This reveals the laws of spectral response under the coupled action of mechanical deformation and physiological changes, thereby providing a theoretical basis for research based on skin reflectance spectrum and typical applications in non-contact emotional analysis. The key content's technical roadmap is shown in the diagram.

2.3 Feasibility Demonstration

Technical Support and Equipment Availability: HSI technology and related mechanical testing equipment planned for this study have been widely used in the fields of medicine and biomechanics. The maturity and reliability of these technologies provide a solid foundation for precise measurements of skin spectral responses. The experimental devices planned for use, including hyperspectral cameras and skin loading devices, are mature products, ensuring the feasibility of the experiments and accuracy of the data.

Theoretical Model Support: This research relies on classical spectroscopic theories, such as the Kubelka-Munk theory and Monte Carlo simulations, which have been widely applied in the spectral analysis of biological tissues and have been extensively validated in skin spectral analysis. Additionally, the theoretical models planned in this project will incorporate mechanical properties such as hyperelasticity and anisotropy, further enhancing the scientific validity and applicability of the models.

Research Foundation: The applicant's research group has a long-standing foundation in spectroscopic mechanics research. The applicant has accumulated research experience in related fields and has achieved certain research outcomes, having published research papers as the first author in journals like Optics and Laser Technology, Biomedical Optics Express, and Experimental Mechanics, and applied for three national invention patents as the first student applicant. The applicant has received awards such as the ICATM2024 World Mechanics Congress Student Support Award and has been invited by the Optical Society of America to give a keynote speech at Engineer Week 2024, demonstrating the capability to tackle various technical and scientific challenges that may arise in the research.

2.4 Potential Problems and Solutions

2.4.1 Unverified Relationship Between Deformation and Reflectance Spectrum: Although theoretically it is believed that deformation of skin and other soft materials affects their spectral characteristics, especially the reflectance spectrum, this effect has not been sufficiently verified experimentally. Deformation may cause changes in the spatial arrangement of internal microstructures, such as collagen fibers and elastic fibers, thus affecting light scattering and absorption behaviors. However, specific experimental research on this phenomenon is currently very limited.

Solution: Experimental Verification of Deformation's Impact on the Reflectance Spectrum Using HIS. Use a hyperspectral imaging (HSI) system to mechanically load the skin under controlled conditions. Apply varying degrees of stretching and compression to simulate various physical deformation scenarios that skin may encounter in daily life. Before and after loading, collect comprehensive skin spectral data using the HSI system. Pay special attention to skin areas known to have different physiological conditions, such as areas with higher blood volume or different pigment deposition. Analyze changes in the skin's reflectance spectrum before and after loading, identifying specific wavelength patterns of spectral changes that may be directly related to the physical deformation of the skin. Use statistical methods to verify the correlation between deformation and spectral changes to ensure that the observed changes are caused by mechanical deformation and not by other incidental

factors.

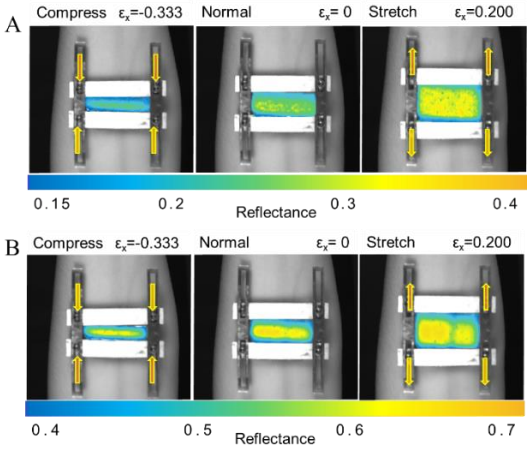

Figure 2. Hyperspectral images of the spectral response of forearm skin under stretch and compression in two wavelength ranges: (A) 400-500 nm and (B) 850-1000 nm.

2.4.2 Unclear Coupling Mechanisms of Mechanics, Physiology, and Spectroscopy: The reflectance spectrum of in vivo skin is determined by both mechanical and physiological properties. While there has been considerable research on physiological parameters, there is a lack of quantitative studies considering skin's mechanical performance and in vivo experimental data, as well as a lack of theoretical formulas for mechanically modulating the reflectance spectrum.

Solution: Research on the Coupling Mechanisms of Skin Mechanics-Physiology-Spectroscopy.

Facial expressions accompany changes in the skin's reflectance spectrum. The project will combine studies on skin mechanical properties and multispectral imaging technology to deeply explore the mechanical-spectroscopic behavior of human skin. Building on the existing research of the research group, the skin surface strain will be introduced into the dynamic reflectance model of the skin. By using hyperspectral imaging (HSI) along with skin reflectance spectrum models, capture the changes in skin microcomponents under deformation. The project intends to measure changes in skin components such as blood volume fraction and hydration under strain using non-contact spectroscopic technology, revealing the coupling mechanisms between skin physiological components and skin layer deformation.

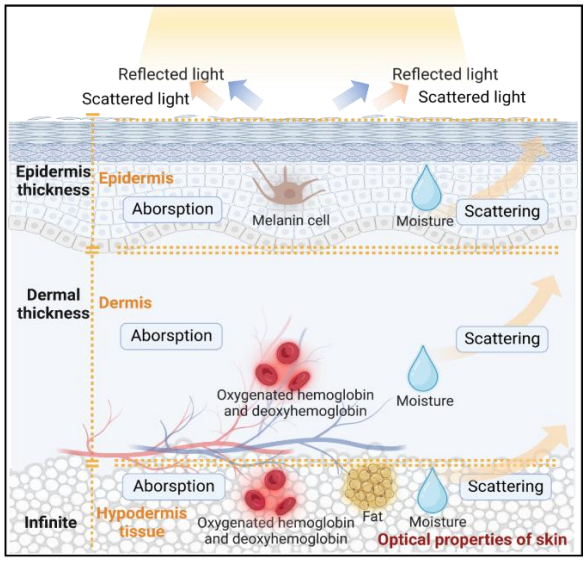

Figure 3. Schematic representation of the compositions and the optical properties of the skin.

2.4.3 Unknown Mechanisms of Emotional States on Skin Reflectance Spectrum and Skin

In the typical applications of the mechanics-physiology-spectroscopy coupling response model, there is a lack of research on the mechanisms by which emotional states affect the skin's reflectance spectrum and the skin itself.

Solution: Collection and Analysis of Spectral Features and Skin Parameters Under Different Emotional States. A hyperspectral camera is used to measure the three-dimensional spectral information of facial skin under the influence of different emotions, obtaining the spectral distribution of the skin at different wavelengths under various emotional states. Based on the proposed theoretical model, invert the changes in skin parameters under different emotional states. Construct a skin reflectance physiological spectrum map as shown in the figure.

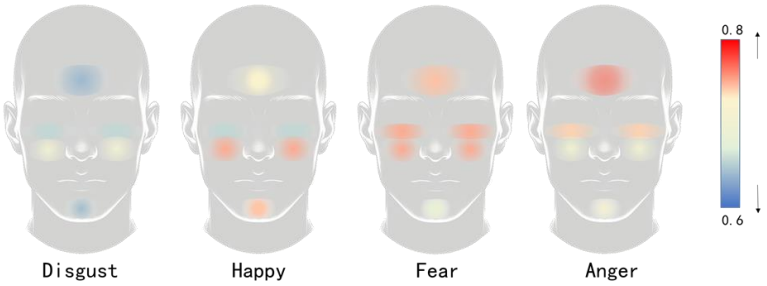

Figure 4: Skin Reflectance Physiological Spectrum Map (Color changes indicate changes in blood content in the dermis)

Outcomes:

1. Establishment of a validated theoretical model for the mechanical-physiological-spectroscopic responses of skin.
2. Development of non-invasive diagnostic tools for health monitoring based on the refined understanding of skin’s spectral responses.
3. Publication of findings in peer-reviewed journals, contributing to the scientific community’s understanding of skin dynamics.

Impact:

The expected advancements in skin research will revolutionize the approach towards non-invasive diagnostics, allowing for early detection of dermatological diseases, monitoring of physiological changes, and assessment of treatment efficacy. Additionally, the project will provide significant insights into the emotional states’ effect on skin properties, pioneering new methodologies in psychological studies and emotional analytics.

Silicon photonic integrated circuits for high-sensitivity greenhouse gas monitoring

Climate change is posing a formidable challenge to global ecosystems and human societies. Rising temperatures and increased frequency of extreme events such as hurricanes and droughts are among the observable impacts. **In 2023, the concentrations of the three main greenhouse gases, namely, carbon dioxide (CO_2), methane (CH_4), and nitrous oxide (N_2O) have reached the historical record and are expected to keep increasing in 2024**. In response to the escalating challenges, the need for high-sensitivity greenhouse gas monitoring and early warning has become increasingly urgent. While great progress has been made in gas sensors, the implement of miniaturized gas sensors with high sensitivity, long lifetime, and working ability in complex environments still faces great challenges. Silicon photonics, with the advantages of strong light-matter interaction, high integration density and inherent compatibility with complementary metal-oxide semiconductor (CMOS) technology, offers a promising avenue for the development of ultra-compact, cost-effective, and highly sensitive on-chip greenhouse gas monitoring systems.

Here, we propose to build a **photonic integrated circuit** (PIC) on silicon photonic platform, as illustrated in Fig 1, incorporating the key components of a supercontinuum light source, suspended nanomembrane silicon (SNS) microring resonator (MRR) sensor, and an integrated spectrometer for **high-sensitivity greenhouse gas sensing**.

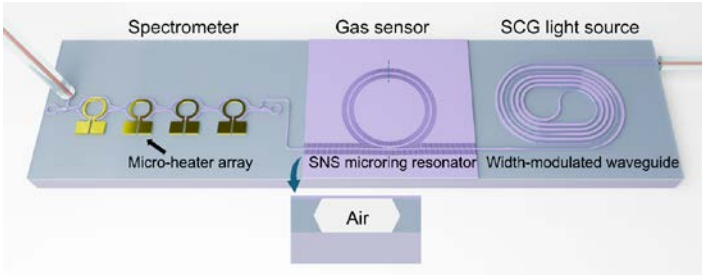

Fig 1 Schematic of the proposed PIC for greenhouse gas monitoring, including supercontinuum light source, SNS MRR gas sensor, and on-chip spectrometer.

Targeting for a flat supercontinuum light source, we propose a width-modulated silicon waveguide featuring interleaved normal and abnormal dispersion region connected by tapers for effective dispersion engineering. The on-chip gas sensor will be implemented using an SNS MRR. The deep-subwavelength waveguide thickness allows for a large confinement factor of light in the air, enhancing light-gas interaction while simultaneously reducing overlap with the waveguide sidewall, thereby minimizing waveguide loss and improving the quality factor of the MRR for high-sensitivity gas sensing. The spectral signal measurement will be conducted by using a high-resolution speckle spectrometer, which employs a cascaded Mach-Zehnder Interferometer (MZI) network to facilitate light forward propagation and interference. Additionally, on-chip loop mirrors, MRRs are incorporated into the MZI network to introduce distinctive excess phase delays. By driving the micro-heater array, multiple effective physical channels can be achieved and thus expand the spectrum measurement range.

By successfully fabricating and implementing the PIC, we anticipate achieving a flattened supercontinuum spectrum spanning from 1.5 μm to 2.8 μm, that covers the featured absorption peaks of CH_4, N_2O, and CO_2. The development of SNS MRR with enhanced quality and confinement factor is expected to enable a greenhouse gas detection limit of <100 ppm. Moreover, by leveraging the speckle spectrometer for spectrum reconstruction, this project will enable the gas absorption spectra measurement with <0.1 nm spectral resolution, facilitating the precise identification and quantification of greenhouse gases. Ultimately, these outcomes are poised to catalyze the implementation of integrated systems with **both the footprint and cost reduced by several orders of magnitude compared with the conventional optical gas sensors**, which holds profound implications for climate change mitigation, environmental sustainability, and societal well-being.

Silicon photonic integrated circuits for high-sensitivity greenhouse gas monitoring

I. Literature Review

Climate change is posing a formidable challenge to global ecosystems and human societies [1]. Rising temperatures and increased frequency of extreme events such as hurricanes, floods, and droughts are among the observable impacts. **In 2023, the concentrations of the three main greenhouse gases, namely, carbon dioxide (CO_2), methane (CH_4), and nitrous oxide (N_2O) have reached the historical record and are expected to keep increasing in 2024** [2]. In response to the escalating challenges posed by climate change, the need for high-sensitivity greenhouse gas monitoring, data collecting, and early warning has become increasingly urgent. While great progress has been made in gas sensors, the implement of miniaturized gas sensors with high sensitivity, long lifetime, and working ability in complex environments still faces great challenges. The current gas sensors can generally be divided into two categories: electrical gas sensors and optical gas sensors. The electrical gas sensors feature the advantages of high accuracy and low cost, but they typically suffer from the moderate adaptability, short lifetime, and sensitivity to environments, such as the humid and corrosive environment [3]. The optical gas sensors utilize the specific absorption peaks of gas molecules to detect the type and concentration of the gases by measuring and analyzing the infrared absorption peaks, as shown in Fig 1, and thus own the advantage of good adaptability, long lifetime and robustness to environment [4]. However, the current optical gas sensors typically have moderate sensitivity, large footprint and high cost.

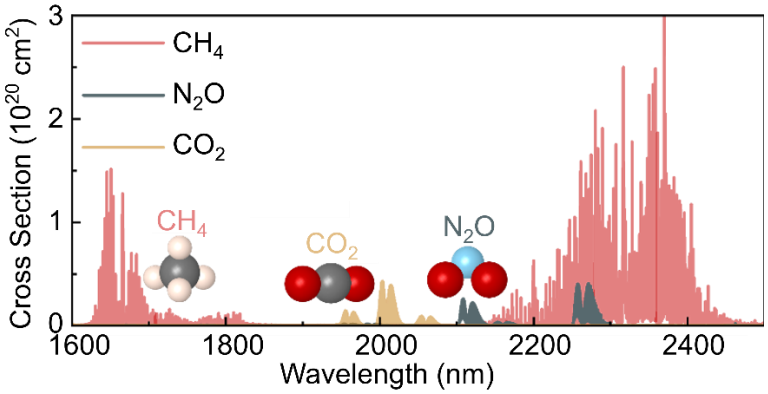

Fig 1 Featured absorption peaks of the greenhouse gasses at the infrared wavelength band.

Silicon photonics, with the advantages of strong light-matter interaction, high integration density and inherent compatibility with complementary metal-oxide semiconductor (CMOS) technology [5], offers a promising avenue for the development of ultra-compact, cost-effective, and highly sensitive optical gas sensors [6]. Recent advancements have leveraged photonic integrated devices featuring diverse waveguide structures on various material platforms, as evidenced in Table 1, to enhance the sensitivity of greenhouse gas detection. However, their typical limit of detection (LoD) is on the order of 100 ppm. **The improvement in LoD remains a formidable challenge, due to the enduring trade-off between waveguide confinement factor and propagation loss** [7], as one of the main causes of waveguide loss is the scattering on the waveguide sidewalls, when the optical mode interacts with the waveguide sidewall roughness arisen from the lithography and etching fabrication process [8]. Expanding the waveguide dimension emerged as an effective approach to mitigate the waveguide loss by minimizing optical mode-waveguide sidewall overlap [9], but concurrently compromises waveguide confinement, thereby attenuating light interaction with surrounding gas molecules.

Table 1 Current implementations of on-chip gas sensors.

Year	Waveguide structure	Platform	Gas type	LoD (ppm)	Ref
2008	Slot microring resonator	Silicon	C_2H_2	--	[10]
2011	Photonic crystal slot waveguide	Silicon	CH_4	100	[11]
2016	Microring resonator	Silicon with PHMB*	CO_2	20	[12]
2017	Spiral waveguide	Silicon	CH_4	100	[13]
2018	Straight waveguide	Germanium-silicon	CH_4	366	[14]

*PHMB: guanidine polymer derivative, exhibits reversible refractive index change upon absorption and release of CO_2 molecules.

Our recent study demonstrated the efficacy of a suspended nanomembrane silicon (SNS) resonator for highly sensitive CO2 gas sensing at the 2 μm wavelength band, successfully overcoming the conventional trade-off between resonator quality factor and waveguide confinement[15]. However, the gas sensing system still relies on an external continuous-wave tunable laser for spectrum measurement, making the gas monitoring system bulky and expansive. **One approach to tackle the issue is to use integrated spectrometers along with on-chip broadband source instead of the tunable laser source**. While previous research has demonstrated progress in on-chip supercontinuum generation (SCG) [16] and high-resolution spectrometers [17, 18], the monolithic integration of an SCG source and spectrometer for gas sensing still encounters the challenges of limited sensitivity due to the spectral power density nonuniformity of SCG [19], the moderate sensitivity of spectrometers [20], and the absence of high-sensitivity on-chip sensors.

II. Problem statement / Objective

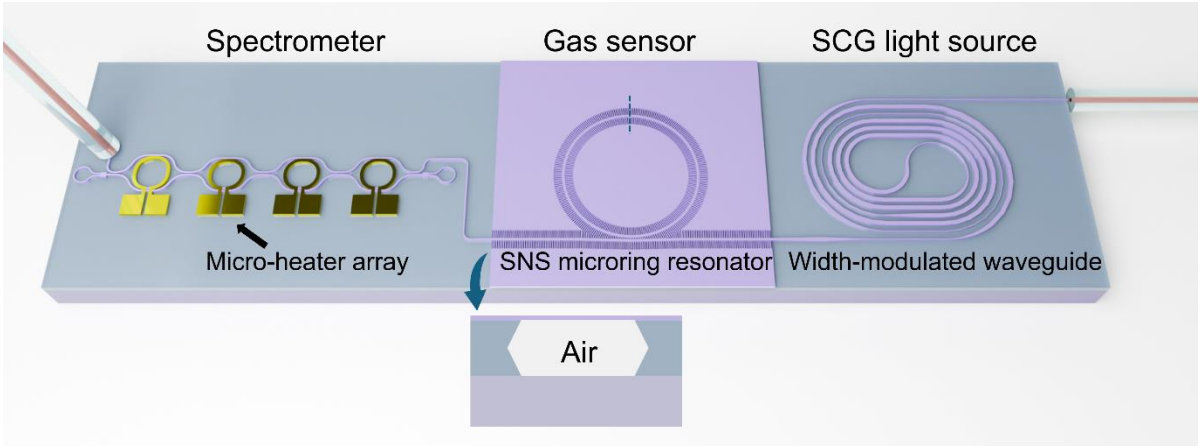

Fig 2 Schematic of the proposed photonic integrated circuit for greenhouse gas monitoring.

To address the challenge of limited sensitivity in gas monitoring, our proposal entails the development of a photonic integrated circuit (PIC) on silicon photonic platform, as shown in Fig 2, incorporating the key components of an SCG light source, SNS microring resonator sensor, and an integrated spectrometer.

SCG light source

To flatten the spectral power density of SCG, we propose a width-modulated silicon waveguide featuring interleaved normal and abnormal dispersion region connected by tapers

for effective dispersion engineering. Initial simulations show a flattened SCG spectrum spanning from 1.5 μm to 2.8 μm when pumped by a 2-μm sub-picosecond (300 fs) pulse laser, as shown in Fig. 2(a). While the simulation results demonstrate effective spectrum broadening and uniform spectral power density, the experimental implementation of supercontinuum generation (SCG) remains challenging, as waveguide fabrication quality and accuracy impact waveguide loss and dispersion, subsequently affecting soliton fission and dispersive wave generation. In this project, we will focus on the experimental implementation of a flat SCG by pumping the proposed width-modulated silicon spiral waveguide with a sub-picosecond pulse laser at 2 μm.

SNS microring resonator sensor

The on-chip gas sensor will be implemented using an SNS microring resonator (MRR) with a 70 nm waveguide thickness. We have recently explored the potential of guiding and manipulating light in the deep subwavelength regime. The ultra-thin waveguide thickness allows for a large confinement factor of light in the air, enhancing light-gas interaction while simultaneously reducing overlap with the waveguide sidewall, thereby minimizing waveguide loss. The SNS waveguide can theoretically achieve an 80% confinement factor, and initial experimental results show a high-quality factor of 3×10^5 for the SNS MRR at 2 μm wavelength, as illustrated in Fig. 2(b) and (c). This high-quality factor can enhance gas monitoring sensitivity through either refractive index sensing, by tracking the resonance wavelength shift, or gas absorption sensing, by measuring the extinction ratio variation of the resonance with increasing absorption loss. While we have initially demonstrated CO_2 gas sensing using an SNS MRR, the device's adaptability for detecting all greenhouse gases remains challenging. One solution is to develop the SNS MRR across different wavelength bands to cover the specific absorption peaks of various greenhouse gases.

Integrated spectrometer

The spectral signal measurement will be conducted using a high-resolution speckle spectrometer. Unlike dispersive spectrometers that rely on one-to-one spectral-to-spatial mapping [21], the speckle spectrometer employs a complex photonic circuit to generate a wavelength-dependent speckle pattern, which serves as a fingerprint for spectrum reconstruction [22]. The high spectral resolution of a speckle spectrometer typically depends on the rapid decorrelation of the speckle pattern with wavelength, achieved through the interference of light with large optical path length differences in a coherent network with extended dispersive optical paths. Here we propose using a cascaded Mach-Zehnder Interferometer (MZI) network to facilitate light forward propagation and interference. Additionally, on-chip loop mirrors are designed to enable backward light propagation, thereby increasing the optical path length. Microring resonators (MRRs) are incorporated into the MZI network to introduce distinctive excess phase delays around the resonance wavelengths. Micro-heaters above each MRR control the path length difference and the speckle pattern, allowing for the creation of multiple effective physical channels, which determine the spectrum measurement range of the spectrometer. Our preliminary experimental findings demonstrate the speckle spectrometer can be used to measure the absorption spectrum of CH_4 gas, as shown in Fig. 2(d). Unlike universal integrated spectrometers, this project aims to tailor speckle spectrometers to match the center wavelength and linewidth of greenhouse gas absorption peaks, thereby improving gas monitoring efficiency.

In short, the objective of the project is to monolithically integrate the SCG source, the gas sensor and the speckle spectrometer to form a photonic integrated circuit for high-sensitivity greenhouse gas monitoring. Additionally, we seek to develop an efficient spectrum reconstruction algorithm to accurately retrieve the gas absorption spectrum, enabling precise determination of the types and concentrations of greenhouse gases.

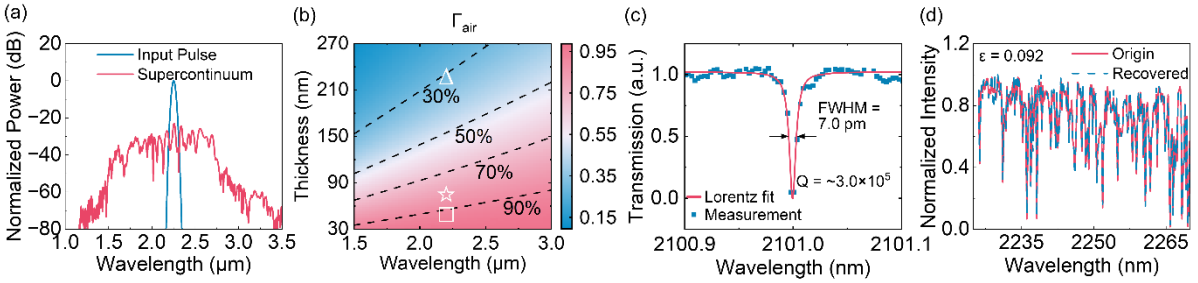

Fig 2 Initial simulation and experimental results of the different components used in the photonic integrated circuit. (a) Simulated SCG by using a width-modulated silicon waveguide. (b) Simulated confinement factor of the SNS waveguide with different waveguide thicknesses. (c) Experimental transmission spectrum of the SNS MRR. (d) Experimental measurement of the CH_4 absorption spectrum by using the speckle spectrometer.

III. Outcomes

Through the integration of the SCG light source, SNS resonator gas sensor, and speckle spectrometer into a photonic integrated circuit, the project aims to revolutionize the sensitivity, compactness, and efficiency of greenhouse gas monitoring systems. By successfully fabricating and implementing the width-modulated silicon waveguide for dispersion engineering, we anticipate achieving a flattened supercontinuum spectrum spanning from 1.5 μm to 2.8 μm. This advancement will successfully address the challenge of spectral power density variation and significantly enhance the signal-to-noise ratio (SNR) of the system, thereby improving detection sensitivity. Moreover, the development of SNS waveguides and MRRs with enhanced quality factor and confinement factor holds the promise of unprecedented levels of sensitivity in gas sensing, enabling the detection of greenhouse gases with remarkable precision. Furthermore, by leveraging the speckle spectrometer for spectrum reconstruction, we expect to obtain high-resolution gas absorption spectra, facilitating the precise identification and quantification of greenhouse gases. Ultimately, these outcomes are poised to catalyze the implementation of integrated systems for high-sensitivity greenhouse gas monitoring, thereby playing a pivotal role in climate change mitigation and environmental stewardship efforts.

IV. Impact

The impact of this project transcends mere technological advancement, as it holds profound implications for climate change mitigation, environmental sustainability, and societal well-being. By advancing the greenhouse gas monitoring technology, this initiative is poised to fill a critical gap in our capacity to accurately track and comprehend the complexities of climate change dynamics. The development of a compact, high-sensitivity photonic integrated circuit for gas sensing offers the promise of vastly improving our ability to identify and quantify greenhouse gases with precision, thereby facilitating early detection of environmental threats and informing targeted mitigation efforts. Furthermore, the integration of these advanced sensing capabilities into environmental monitoring networks has the potential to bolster resilience against climate-related disasters and safeguard vulnerable communities on a global scale. Moreover, by furnishing policymakers, researchers, and industries with actionable data on greenhouse gas emissions, this project has the potential to galvanize the adoption of more efficacious climate change mitigation strategies, thus propelling us toward a more sustainable and resilient future for generations to come.

References:

1. Kotz, M. et al. The economic commitment of climate change. *Nature* **628**, 551-557 (2024).
2. Esper, J. et al. 2023 summer warmth unparalleled over the past 2,000 years. *Nature* (2024).
3. Barandun, G. et al. Challenges and Opportunities for Printed Electrical Gas Sensors. *ACS Sensors* **7**, 2804-2822 (2022).
4. Hodgkinson, J. & Tatam, R.P. Optical gas sensing: a review. *Measurement Science and Technology* **24**, 012004 (2013).
5. Shekhar, S. et al. Roadmapping the next generation of silicon photonics. *Nature Communications* **15**, 751 (2024).
6. Hänsel, A. & Heck, M.J.R. Opportunities for photonic integrated circuits in optical gas sensors. *Journal of Physics: Photonics* **2**, 012002 (2020).
7. Kim, D.-G. et al. Universal light-guiding geometry for on-chip resonators having extremely high Q-factor. *Nature Communications* **11**, 5933 (2020).
8. Shi, Y. et al. Investigation on roughness-induced scattering loss of small-core polymer waveguides for single-mode optical interconnect applications. *Optics Express* **28**, 38733-38744 (2020).
9. Stern, B. et al. Battery-operated integrated frequency comb generator. *Nature* **562**, 401-405 (2018).
10. Robinson, J.T. et al. On-chip gas detection in silicon optical microcavities. *Optics Express* **16**, 4296-4301 (2008).
11. Lai, W.-C. et al. On-chip methane sensing by near-IR absorption signatures in a photonic crystal slot waveguide. *Optics Letters* **36**, 984-986 (2011).
12. Mi, G. et al. Silicon microring refractometric sensor for atmospheric CO2 gas monitoring. *Optics Express* **24**, 1773-1780 (2016).
13. Tombez, L. et al. Methane absorption spectroscopy on a silicon photonic chip. *Optica* **4**, 1322-1325 (2017).
14. Liu, Q. et al. Mid-infrared sensing between 5.2 and 6.6 μm wavelengths using Ge-rich SiGe waveguides [Invited]. *Optical Materials Express* **8**, 1305-1312 (2018).
15. Guo, R. et al. High-Q silicon microring resonator with ultrathin sub-wavelength thicknesses for sensitive gas sensing. *Applied Physics Reviews* **11**, 021417 (2024).
16. Kuyken, B. et al. Mid-infrared to telecom-band supercontinuum generation in highly nonlinear silicon-on-insulator wire waveguides. *Optics Express* **19**, 20172-20181 (2011).
17. Redding, B. et al. Compact spectrometer based on a disordered photonic chip. *Nature Photonics* **7**, 746-751 (2013).
18. Zhang, Z. et al. Tandem Configuration of Microrings and Arrayed Waveguide Gratings for a High-Resolution and Broadband Stationary Optical Spectrometer at 860 nm. *ACS Photonics* **8**, 1251-1257 (2021).
19. Lau, R.K.W. et al. Octave-spanning mid-infrared supercontinuum generation in silicon nanowaveguides. *Optics Letters* **39**, 4518-4521 (2014).
20. Hadibrata, W. et al. Compact, High-resolution Inverse-Designed On-Chip Spectrometer Based on Tailored Disorder Modes. *Laser & Photonics Reviews* **15**, 2000556 (2021).
21. Zhang, Z. et al. Integrated scanning spectrometer with a tunable micro-ring resonator and an arrayed waveguide grating. *Photonics Research* **10**, A74-A81 (2022).
22. Zhang, Z. et al. Compact High Resolution Speckle Spectrometer by Using Linear Coherent Integrated Network on Silicon Nitride Platform at 776 nm. *Laser & Photonics Reviews* **15**, 2100039 (2021).